TRANSACTIONS

OF THE

AMERICAN SOCIETY

OF

CIVIL ENGINEERS

(INSTITUTED 1852)

VOLUME 126, PART II

1961

Edited by the Executive Secretary, under the direction of the Committee on Publications.

Reprints from this publication, which is copyrighted, may be made on condition that the full title, name of author, title of publication, page reference (or paper number), and date of publication by the Society are given.

NEW YORK
PUBLISHED BY THE SOCIETY
1961

ENGIN.
TA
1
.A526
v.126
pt.2

Copyright 1962 by the AMERICAN SOCIETY OF CIVIL ENGINEERS

NOTE—The Society is not responsible for any statement made or opinion expressed in its publications.

CONTENTS, VOL. 126, PART II

PAGE

LIGHT WOOD TRUSSES
By R. F. Luxford 1
Discussion:
By E. George Stern 35
David Countryman 36
R. F. Luxford 37

TOOLS AND TECHNIQUES FOR DEWATERING
By Byron J. Prugh 38

STRUCTURAL ENGINEERING ASPECTS OF NUCLEAR POWER PLANTS
By Lewis L. T. Au and Edward Y. W. Tsui 53

DESIGN PRESSURE FOR A REACTOR CONTAINMENT VESSEL
By John A. Bailey 77

SOME BASIC CONCEPTS IN MATRIX STRUCTURAL ANALYSIS
By Frank R. Berman 87

REINFORCED CONCRETE SHEAR WALL ASSEMBLIES
By Jack R. Benjamin and Harry A. Williams 114

CONSTRUCTION OF THE MORRISON BRIDGE
By R. D. Bane 146

EPOXY RESIN FOR STRUCTURAL REPAIR OF CONCRETE PAVEMENT
By Wilson L. Davis and Eugene Pinkstaff 154

MINIMUM COST DESIGN OF LARGE SUPPORT RINGS
By Kenneth P. Buchert 170

RATIONALE FOR DETERMINING DESIGN WIND VELOCITIES
By A. G. Davenport 184

MATRIX ANALYSIS OF PLANE RIGID FRAMES
By Fernando Venancio Filho 214

STATIC TENSION TESTS OF COMPACT BOLTED JOINTS
By Robert T. Foreman and John L. Rumpf 228

PRELIMINARY ANALYSIS OF CONTINUOUS GABLE FRAMES
By James W. Gillespie and Jan J. Tuma 255

CONCRETE ADDITION TO CELLULAR SHEET PILE SHIPWAY
By John W. Irvine and Richard F. Gaston 270

ANALYSIS OF CURVED GIRDERS
By H. H. Fickel 280

PAGE

LONG REINFORCED CONCRETE COLUMNS: A SYMPOSIUM
ULTIMATE STRENGTH OF HINGED COLUMNS
By Bengt Broms and I. M. Viest 309
Discussion:
By G. C. Ernst 339
J. J. Hromadik 340
T. Jumikis and A. S. Hall 345
Bengt Broms and I. M. Viest 346
ULTIMATE STRENGTH ANALYSIS OF RESTRAINED COLUMNS
By Bengt Broms and I. M. Viest 348
DESIGN
By Bengt Broms and I. M. Viest 367
Discussion:
By J. G. MacGregor and C. P. Siess 385
Phil M. Ferguson 391
Bengt Broms and I. M. Viest 397
TORSIONAL ANALYSIS OF SUSPENSION BRIDGE TOWERS
By Frank Baron and Anthony G. Arioto 401
ENGINEERING EDUCATION AND THE CONSTRUCTION INDUSTRY
By C. H. Oglesby and John W. Fondahl 428
Discussion:
By Paul F. Keim 443
Theodore B. Appel, Jr. 444
Henry G. Howard 445
C. H. Oglesby and John W. Fondahl 446
DISTRIBUTIONS OF EXTREME WINDS IN THE UNITED STATES
By H. C. S. Thom 450
Discussion:
By J. Lieblein 463
H. C. S. Thom 466
CHARTS FOR DESIGN OF REINFORCED CONCRETE COLUMNS
By W. H. Gardner, Jr., and Donald H. Kline 467
Discussion:
By George B. Begg, Jr. 479
James R. Krusling 480
W. H. Gardner, Jr., and Donald H. Kline 480
BUCKLING OF ONE-STORY FRAMES AND BUILDINGS
By John E. Goldberg 482
CONSTRUCTION OF ROCKY REACH HYDROELECTRIC PROJECT
By W. N. Evans and J. H. Boyd 516
SIMPLY SUPPORTED CORNER PLATE
By Mario G. Salvadori and H. C. Reggini 537
TEST OF A RIVETED PLATE GIRDER WITH A THIN WEB
By Desi D. Vasarhelyi, Jim C. Taylor, Naresh C. Vasishth and Chia-Yao Yuan 550
MATRIX FORMULATION OF FOLDED PLATE EQUATIONS
By A. C. Scordelis 579
STATISTICAL AND ECONOMIC ANALYSIS OF A BIDDING TREND
By Marvin Gates 601

PAGE

LOAD DISTRIBUTION OF DIAPHRAGMS IN I-BEAM BRIDGES
By BENJAMIN C. F. WEI 624

VENTILATED BUILDING FOUNDATIONS IN GREENLAND
By ROGER H. WILLIAMS 657

DISCUSSION:
By John A. Pihlainen 664
Roger H. Williams 666

LESSONS OF COLLAPSE OF VANCOUVER 2ND NARROWS BRIDGE
By A. HRENNIKOFF 668

DISCUSSION:
By Kuang-Han Chu 685
Robert Dannemann 685
A. Hrennikoff 688

RIVETS AND HIGH-STRENGTH BOLTS: A SYMPOSIUM

COUNCIL RESEARCH
By E. J. RUBLE 694

STRENGTH IN TENSION
By WILLIAM H. MUNSE, KENNETH S. PETERSEN, AND EUGENE CHESSON, JR. 700

DISCUSSION:
By Richard T. Douty 719
W. R. Penman and Ethan F. Ball 726
William H. Munse, Kenneth S. Petersen, and Eugene Chesson, Jr. 727

BEHAVIOR OF BEAM-TO-COLUMN CONNECTIONS
By WILLIAM H. MUNSE, WYATT G. BELL, AND EUGENE CHESSON, JR. 729

FATIGUE TEST OF JOINTS OF HIGH-STRENGTH STEEL
By NORMAN G. HANSEN 750

EFFECTS OF FABRICATION TECHNIQUES
By DESI D. VASARHELYI, SAID Y. BEANO, RONALD B. MADISON, ZUNG-AN LU, AND UMSEH C. VASISHTH 764

INSTALLATION AND TIGHTENING OF BOLTS
By ETHAN F. BALL AND J. J. HIGGINS 797

DISCUSSION:
By Alfred Zweig 807
M. Zar 808
William H. Munse 808
Raymond Archibald 809
Ethan F. Ball and J. J. Higgins 809

HIGH-STRENGTH BOLTS ON MACKINAC BRIDGE
By JOHN W. KINNEY 811

DESIGN CONSIDERATIONS FOR FATIGUE IN TIMBER STRUCTURES
By WAYNE C. LEWIS 821

DISCUSSION:
By Paul G. Fluck 829
Floyd E. Schneider 829
Wayne C. Lewis 830

PAGE
IMPACT OF COMPUTERS ON ENGINEERING EDUCATION
BY GORDON P. FISHER 832
DISCUSSION:
By William A. Boe 841
Francis E. Swain 842
Warner Lansing 844
Gordon P. Fisher 845
DYNAMIC EFFECTS OF EARTHQUAKES
BY RAY W. CLOUGH 847
DISCUSSION:
By Clarence J. Derrick 864
George W. Housner 868
A. A. Eremin 871
John A. Blume 872
Ray W. Clough 874
LONG SPAN PRESTRESSED CONCRETE FOLDED PLATE ROOFS
BY JOHN C. BROUGH, JR., AND B. H. STEPHENS, JR. 877
DISCUSSION:
By A. A. Eremin 899
John C. Brough, Jr., and B. H. Stephens, Jr. 900
DESIGN OF PRESTRESSED CONCRETE BEAMS BY COMPUTER
BY JOSEPH J. BONASIA 901
DISCUSSION:
By Richard J. Newson 928
Joseph J. Bonasia 928
INFLUENCE OF PARTIAL BASE FIXITY ON FRAME STABILITY
BY THEODORE V. GALAMBOS 929
DISCUSSION:
By Eugene Guillard 952
Joseph W. Appeltauer and Thomas A. Barta 953
Theodore V. Galambos 963
DISCONTINUITY STRESSES IN BEAMS ON ELASTIC FOUNDATIONS
BY JOSEPH PENZIEN 970
DISCUSSION:
By R. S. Alwar 996
Joseph Penzien 997
GENERALIZATION OF THE SUCCESSIVE APPROXIMATIONS METHOD
BY PANAGIOTIS D. MOLIOTIS 998
DISCUSSION:
By Pering-Fei Gou 1036
Panagiotis D. Moliotis 1040

Page

RESEARCH ON FIRE RESISTANCE OF PRESTRESSED CONCRETE
By Hubert Woods.................................... 1041

Discussion:
By V. Paschkis.................................... 1052
Hubert Woods.................................... 1053

PROPERTIES OF STEEL AND CONCRETE AND THE BEHAVIOR OF STRUCTURES
By George Winter.................................... 1054

Discussion:
By Ralph L. Barnett.................................... 1083
Lester H. Gabriel.................................... 1084
Henry J. Cowan.................................... 1086
Oliver G. Julian.................................... 1086
A. Zaslavsky.................................... 1090
Paul Zia.................................... 1091
George Winter.................................... 1095

REVIEW OF RESEARCH ON COMPOSITE STEEL-CONCRETE BEAMS
By Ivan M. Viest.................................... 1101

Discussion:
By W. J. Jurkovich.................................... 1121
J. C. Chapman.................................... 1123
Ivan M. Viest.................................... 1123

WIND FORCES ON STRUCTURES
Final Report of the Task Committee on Wind Forces of the Committee on Loads and Stresses of the Structural Division, ASCE.... 1124

FOUNDATION INSTALLATION REQUIRING RECHARGING OF GROUND WATER
By James D. Parsons.................................... 1199

FOREWORD

ASCE TRANSACTIONS, 1961, Part II, contains, nominally, all papers published in the Journals of the Construction and Structural Divisions, Proceedings of the American Society of Civil Engineers. The following papers were not included in this part because discussion was not complete when the volume was closed:

JOURNAL OF THE CONSTRUCTION DIVISION

February 1960

Fundamentals of Arctic Blasting
by Clifton W. Livingston (Proc. Paper 2355)[a]

Field Office Bookshelf
Progress Report of the Committee on Publications of the Construction Division (Proc. Paper 2357)[c]

Polyvinyl Acetate and Portland Cement Mortars
by Robert T. Howe (Proc. Paper 2358)[a]

Control of Ground Water in Excavations
by W. F. Swiger (Proc. Paper 2359)[a]

May 1960

Photographic Analysis for Construction Operations
by John W. Fondahl (Proc. Paper 2483)

November 1960

Soil Freezing to Reconstruct a Railway Tunnel
by George J. Low (Proc. Paper 2639)

Simple Rules for Hot and Cold Weather Concreting
by John J. Manning (Proc. Paper 2661)

JOURNAL OF THE STRUCTURAL DIVISION

January 1960

Orthogonal Gridworks Loaded Normally to Their Planes
by Ignacio Martin and Jose Hernandez (Proc. Paper 2344)[a]

Summary of the Activities of the Column Research Council
by Bruce G. Johnston (Proc. Paper 2345)[b]

Continuous Girder Bridge with Variable Moment of Inertia
by Sabri Sami (Proc. Paper 2346)[b]

The Shell Vault of the Exposition Palace, Paris
by Nicolas Esquillan (Proc. Paper 2347)[b]

Stability Considerations in the Design of Steel Plate Girders
by Charles E. L. Massonnet (Proc. Paper 2350)[b]

New Aspects Concerning Inelastic Instability of Steel Structures
by Bruno Thurlimann (Proc. Paper 2351)[b]

February 1960

Effective Length of Framed Columns
by Thomas C. Kavanagh (Proc. Paper 2363)[b]

March 1960

Italian Arch Dam Design and Model Confirmation
by Guido Oberti (Proc. Paper 2410)[b]

April 1960

Effect of Floor Systems on Pony Truss Bridges
by Robert M. Barnoff and William G. Mooney (Proc. Paper 2436)[b]

May 1960

Bar-Chain Method for Analyzing Truss Deformation
by S. L. Lee and P. C. Patel (Proc. Paper 2477)

June 1960

Stability Problems of Compressed Steel Members and Arch Bridges
by Georg Wastland (Proc. Paper 2512)[b]

Design of Welded Aluminum Structures
by H. N. Hill, J. W. Clark, and R. J. Brungraber (Proc. Paper 2528)

July 1960

Limit Design of Reinforced Concrete Beams
by D. T. Wright and C. Berwanger (Proc. Paper 2541)

Secondary Stresses in Parallel Wire Suspension Cables
by Thomas Alan Wyatt (Proc. Paper 2542)

Various Instability Modes of the Fixed Base Column
by D. A. Sawyer (Proc. Paper 2544)

Dynamic Response of Elasto-Plastic Frames
by Joseph Penzien (Proc. Paper 2545)

Method for Analysis of Multibeam Bridges
by John E. Duberg, Narbey Khachaturian, and Raul E. Fradinger (Proc. Paper 2552)

Basic Column Strength
by Lynn S. Beedle and Lambert Tall (Proc. Paper 2555)[b]

Lateral Buckling of Beams
by J. W. Clark and H. N. Hill (Proc. Paper 2559)[b]

August 1960

Strength of Welded Aluminum Columns
by R. J. Brungraber and J. W. Clark (Proc. Paper 2581)[b]

September 1960

Test on a 120-ft-Span Prestressed Concrete Beam
by G. D. Base and R. E. Rowe (Proc. Paper 2608)

October 1960

Freezing and Thawing Effects on Prestressed Concrete
by M. J. Gutzwiller and F. E. Musleh (Proc. Paper 2633)

Flow Graphs in Structural Analysis
by Kurt H. Gerstle (Proc. Paper 2634)

November 1960

Use of Continuity-Factor and Final Position
by Yon-Sun Chou (Proc. Paper 2637)

Corrected Deflection Theory of Suspension Bridges
by John Szidarovsky (Proc. Paper 2638)

Principle of Virtual Work in Structural Analysis
by Frank Di Maggio (Proc. Paper 2643)

Load Distribution in Composite Girder-Slab Systems
by G. Hondros and J. G. Marsh (Proc. Paper 2645)

Shear Diaphragms of Light Gage Steel
by Arthur H. Nilson (Proc. Paper 2650)

December 1960

Stress Analysis of Rigid Frame Bridges with Inclined Legs
by Shih-Yuan Cheng (Proc. Paper 2668)

Movements of a Cable Due to Changes in Loading
by James Michalos and Charles Birnstiel (Proc. Paper 2674)

Concepts of Structural Safety
by C. B. Brown (Proc. Paper 2678)

Periods of Framed Buildings for Earthquake Analysis
by Mario G. Salvadori and Ewald Heer (Proc. Paper 2680)

Tentative Recommendations for the Design and Construction of Composite Beams and Girders for Buildings
Progress Report of the Joint ASCE-ACI Committee on Composite Construction (Proc. Paper 2692)[c]

Structural Model Analysis by Means of Moire Fringes
by A. J. Durelli and I. M. Daniel (Proc. Paper 2693)

In the foregoing list, the symbol [a] denotes a paper cleared for publication in the Journals prior to December 1, 1959, which will not be published in the Transactions. The symbol [b] is used to signify papers that were part of Symposia that were not completed in time to publish the entire group in Transactions. The symbol [c] represents a committee report that will not be included in Transactions.

AMERICAN SOCIETY OF CIVIL ENGINEERS

Founded November 5, 1852

TRANSACTIONS

Paper No. 3090

LIGHT WOOD TRUSSES

By R. F. Luxford[1]

With Discussion by Messrs. E. George Stern;
David Countryman; and R. F. Luxford

SYNOPSIS

This paper enters into a consideration of lightweight wood trusses to be used in construction that utilizes light framing. The paper reports on tests run on glued and nailed light trusses with varying span and slope. Conditions of load and environment are varied and test readings made. The conclusions reached from these tests concern the relative value of glued and nailed trusses and the advantages of each.

INTRODUCTION

The use of lightweight wood trusses is becoming of increasing importance in house and other light frame construction. There are a number of reasons for this, including the following:

1. The exterior walls and roof can be erected without the placement of any interior walls. Thus, the interior becomes one large, unobstructed area for further work.
2. The entire ceiling and walls can be finished as one unit without interruption of partitions. If dry-wall construction is used, sheets as large as 4 ft by 12 ft can be installed uncut. The finish floor also can be laid over the en-

---

Note.—Published essentially as printed here, in November, 1958, in the Journal of the Structural Division, as Proceedings Paper 1839. Positions and titles given are those in effect when the paper or discussion was approved for publication in Transactions.

[1] Engr., Forest Products Lab., Forest Service, U.S. Dept. of Agric., Madison, Wis.

tire area without the cutting and fitting necessary when partitions are in place.

3. Roof trusses offer complete flexibility for utilization of interior space. This means that, in later years, partitions can be moved to meet changed living requirements without affecting the structural stability of the house.

4. Large unobstructed areas conforming to the present trend toward open planning are more easily obtained.

5. The house can be more quickly enclosed when trusses are used than when conventional rafter-and-joist construction is used.

6. Truss construction requires less material, that reduces the cost of the house.

SCOPE OF INVESTIGATION

Lightweight wood trusses now in common use are usually of nailed construction. When adequately designed and well manufactured, they give good service. Glued trusses, however, offer some advantages, such as a saving in materials and added stiffness, as compared to nailed trusses. Therefore, special emphasis has been given to glued trusses in this work.

Several series of tests were made. They included:

1. Glued or nailed trusses of W Type with 17-ft span and 5-in-12 slope. Some were subjected to severe atmospheric conditions before being tested.
2. Nailed trusses of W type with 24-ft span and 5-in-12 slope.
3. Glued trusses of W type with 26-ft span and 3-in-12 slope.
4. Glued trusses of W and king-post types with 32-ft span and 2-in-12 slope.
5. Glued trusses of box-beam type with 32-ft span and 1-in-12 slope.

GENERAL CONSIDERATIONS

In these experiments, all structural members of the trusses were in the same plane and hence, free of the eccentricity at the joints that occurs when the structural members are lapped--as is frequently done when bolts, split rings, and nails are used. Trusses built by this method of construction also have the advantage of easy stacking for storage or transportation. Another advantage is that joints in ceiling material need not be staggered because of lapped chord members.

In general, the gusset plates were of the same size on opposite sides of a joint. This also eliminates some eccentricity that will occur when gusset plates of different sizes are used on the two sides of a joint.

For the standard nailed joint, nails used were of sufficient length to extend through both gusset plates and the central members. This type of nailing is commonly used because it is more economical than nailing from both sides. This means that the nails are acting in double shear, and a few tests were made to determine what might be expected.

The plywood gusset plates were so cut and placed that the grain of the main truss members and that of the face ply of the gusset plate were as nearly parallel as possible. Because exact parallelism is not always possible, some rolling shear will occur between glued gusset plates and the main structural members when the truss is loaded. Rolling shear may also occur between adjacent plies of the plywood gusset plate. A few exploratory tests were made with the grain of the face ply either perpendicular or parallel to the grain of a 2- by 4-inch piece simulating a truss joint.

SINGLE-JOINT ASSEMBLY TESTS

Face Grain of Plywood at Right Angles to Applied Load.—One assembly used for tests to ascertain the effects of nonparallelism of grain of adjacent members in glue joints consisted of 2 pieces of plywood 5 in. by 12 in. in size attached to a nominal 2-in. by 4-in. piece 12 in. in length. The face grain of the plywood was at right angles to the applied load. The pieces were either nailed or glued to the wide faces of the 2-by-4 at its midlength, as shown in Fig. 1. For the nailed assembly, 8 eightpenny nails were used that were long enough to penetrate the central member and both gusset plates. The nails were not clinched, and no space was left between the members. In the glued assemblies, the pressure necessary to set the glue was applied with clamps.

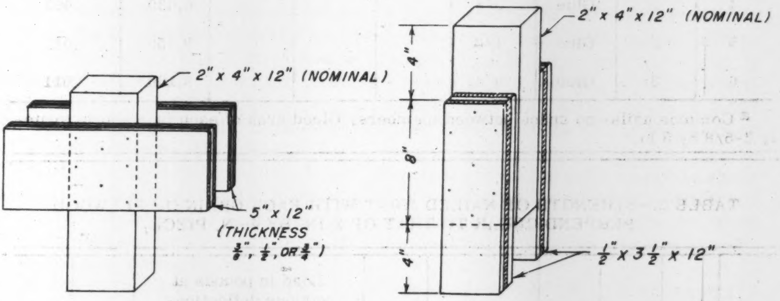
2" x 4" x 12" (NOMINAL)
5" x 12" (THICKNESS $\frac{3}{8}$", $\frac{1}{2}$", OR $\frac{3}{4}$")
2" x 4" x 12" (NOMINAL)
4"
8"
4"
$\frac{1}{2}$" x 3 $\frac{1}{2}$" x 12"

FIG. 1.—TYPES OF SPECIMENS FOR EXPLORATORY NAIL-JOINT TESTS, USING PLYWOOD PLATES

A well made glue joint is a very effective means of joining two pieces of wood, and its ultimate strength is developed at very small slippage. A nailed joint can also be designed to give satisfactory service; some slippage must take place, however, before the nails come into good bearing, and considerable slippage occurs at maximum load.

Table 1 gives results on specimens consisting of 3/8-in., 1/2-in., and 3/4-in. Douglas-fir plywood glued to nominal 2-in. by 4-in. Douglas-fir, with the face grain of the plywood at right angles to that of the 2-by-4's. The plywood of the three thicknesses was not matched. The glued area on each side was about 3-5/8 in. by 5 in. in size, or a total for both sides of about 36 sq in. The results showed considerable variation for the three thicknesses. That may have been due to variation in the quality of the material, to variation in the thickness of the outer ply used in plywood of the different thicknesses, or to a combination of these variables. Even the lowest maximum load value for a glue joint, 6,630 lb, equals a glue strength of about 185 psi. Hence, very few square inches

TABLE 1.—STRENGTH OF NAILED AND GLUED JOINTS WITH FACE GRAIN OF PLYWOOD PERPENDICULAR TO THAT OF 2-IN. BY 4-IN. PIECE

Line	Number of tests	Attachment[a]	Thickness of plywood gusset plate, inches	Load in pounds at various deflections			Maximum load, pounds	Maximum deflection, inches
				0.010-in. deflection	0.015-in. deflection	0.020-in. deflection		
1	3	8 8d nails	3/8	1,730	2,020	2,240	4,200	0.240
2	3	8 8d nails	1/2	2,100	2,420	2,640	4,430	.222
3	3	8 10d nails	3/4	2,400	2,700	3,080	6,160	.370
4	3	Glue	3/8				6,630	.003
5	3	Glue	1/2				9,750	.011
6	3	Glue	3/4				8,160	.011

[a] Common nails—no space between members. Glued area of each face approximately 3-5/8 by 5 in.

TABLE 2.—STRENGTH OF NAILED JOINT WITH FACE GRAIN OF PLYWOOD PERPENDICULAR TO THAT OF 2-IN. BY 4-IN. PIECE

Line	Number of tests	Attachment[a]	Space between members, inches	Placement of nails	Shear	Load in pounds at various deflections				Maximum load, pounds	Maximum deflection, inches
						0.010-in. deflection	0.015-in. deflection	0.020-in. deflection	Average		
1	3	7-8d	None	All one side	Double	1,965	2,225	2,435	2,210	4,000	0.168
2	3	7-8d	0.027	↕	Single	730	840	940	837	2,750	.477
3	3	7-8d	.027		Double	1,320	1,565	1,755	1,550	3,420	.177
4	3	7-8d	.027	4 one side, 3 other side	do	1,590	1,860	2,025	1,825	4,035	.280
5	3	1-8d	.027		Single	118	137	147	134		
6	3	1-8d	.027		Double	210	240	270	240		
RATIOS											
Line 3 to line 1						0.67	0.70	0.72	0.70	0.85	1.06
Line 3 to line 2						1.81	1.86	1.87	1.85	1.25	.37
Line 4 to line 2						2.18	2.21	2.16	2.18	1.47	
Line 4 to line 3						1.20	1.19	1.15	1.18		1.58
Line 2 to line 5						6.2	6.1	6.4	6.3		
Line 3 to line 6						6.3	6.5	6.5	6.5		

[a] Common nails.

of glue area would be needed to develop adequate joint strength for lightweight roof trusses.

The accompanying deflection was very small--about 0.01 in. At this small deflection, a nailed joint developed less than one-half its ultimate strength, as shown in Table 1. Even at maximum load, the nailed joint is much lower in strength than the glue joint, and the accompanying deflection is at least 20 times greater. Only those loads causing relatively small slips, from 0.010 in. to 0.020 in., need be considered for truss design, because large slippage would permit greater deflection of a truss than is desirable for service.

Face Grain of Plywood Parallel to Applied Load.—Other exploratory tests of nailed joints were made with the load, the face grain of plywood, and the face grain of structural members, all of which were parallel.

The assembly consisted of two pieces of 1/2-in.-thick plywood 3-1/2 in. by 12 in. in size attached to a nominal 2-in. by 4-in. piece 12 in. in length. The plywood was attached to the wide faces of the 2-by-4 for a distance of 8 in. and extended 4 in. beyond one end of it to simulate a pair of splice plates, as shown in Fig. 1.

For most of the tests, a 0.027-in. space was left between the plywood and the solid members to simulate the small separation of the parts of a truss resulting from shrinkage during service. The slight separation causes an appreciable reduction in holding power, because considerable force is necessary to overcome friction in a tight joint. A comparison of the values in line 3 with those in line 1 of Table 2 shows that a multiple-nail joint with a space of 0.027 in. between the plywood and the solid member has only about 70% of the strength of a tight miltiple-nail joint.

Nails in double shear sustain loads about twice those for nails in single shear at small deflections. As the loads approach maximums, however, the efficiency of nails in double shear is only about 125% of that of nails in single shear. When the comparison is based on tests of individual nails, similar results are obtained, as shown in Fig. 2.

If 1/2 of the nails subjected to double shear are driven into one side and 1/2 into the other, their efficiency at small slips is more than double that of nails in single shear, as shown by the ratios of values for lines 4 and 2 in Table 2. At maximum load the ratio is only about 1-1/2 to 1.

The relative efficiency of a joint with multiple nailing is lower than that of a joint with a single nail, whether the comparison be based on nails in single or double shear. For a joint with 7 nails, the relative efficiency per nail is about 90% of that for a joint with a single nail, as shown by values in lines 2, 3, 5, and 6 of Table 2.

CONSTRUCTION OF TRUSSES

Douglas-fir lumber was used in these tests. Most of it was comparable to the construction grade.[2] This grade has an assigned working stress of 1,500 psi over the center 1/3 of the length of the piece. Because the stress in the chords of a truss is, in general, uniform throughout the length of the members, the material was regraded so that the construction grade limitations applicable to defects in the center one-third of the length were applied to the entire length. The plywood for the gusset plates was commercial, exterior-type Douglas-fir.

---

[2] "Standard Grading and Dressing Rules for Douglas Fir," Rule Book 15, West Coast Lumbermen's Assoc., March 15, 1956.

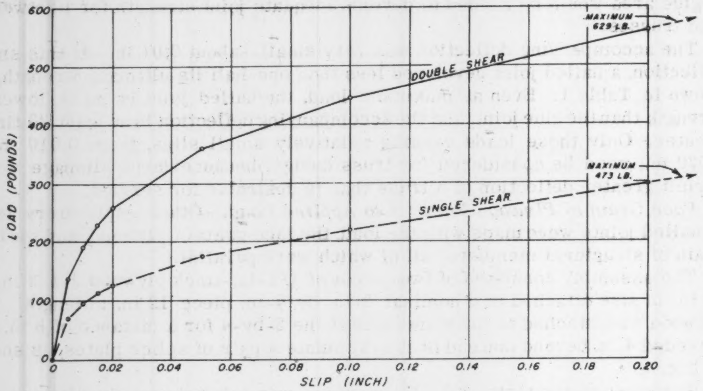

FIG. 2.—COMPARISON OF NAIL-HOLDING POWER OF COMMON NINEPENNY NAILS IN DOUBLE AND SINGLE SHEAR

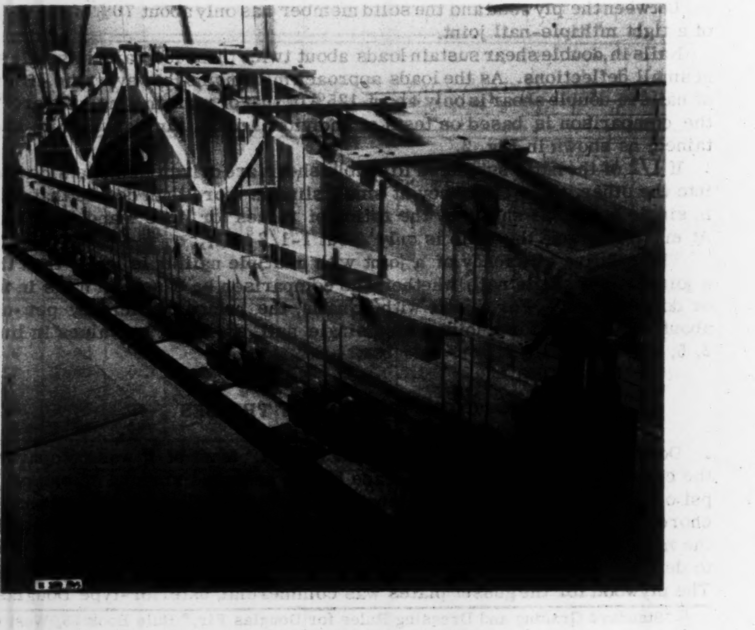

FIG. 3.—TRUSS READY FOR TEST

A resorcinol type of glue was used whenever gusset plates were glued to the trusses to eliminate the possibility of glue failures during subsequent exposure of certain trusses to both high and low relative humidities. During the setting of the glues, pressure was applied with either clamps or nails, as detailed elsewhere in this report.

The glue was spread on both the truss members and the gussets, and a closed-assembly period of 5 min to 10 min was allowed between spreading of the glue and during the subsequent 5-day curing period was maintained at between 70° F 1,000 sq ft of joint area. The temperature of the room at the time of gluing and during the subsequent 5-day curing period was maintained at between 70° and 80° F.

Most of the trusses were of the W type. The trusses were so designed that the distance between truss points of the lower chord was 1/3 of the span, and the joint in the upper chord divided the chord length into 2 equal parts.

TESTING PROCEDURE

The earlier tests of trusses were made by means of dead loads placed on platforms suspended at various points along the upper chords with a constant ceiling load hung from the lower chord.

Later, equipment for readily applying and removing load was secured and used for a number of trusses. This equipment, designed especially for the testing of trusses, applies the load through a system of cables and sheaves, as shown in Fig. 3. The cables were loaded by means of a variable-speed winch. The load was measured at each reaction by means of a calibrated load cell. Lateral movement or buckling of the truss was resisted by restraining members that were fitted over the top chords and were attached to a rigid wood frame.

In general, three runs were made on each truss. The first run was made by loading the truss at appropriate increments until its design load was reached. The dials, stationed at truss points and midway between truss points along the upper and lower chords, were read at each load increment. After the design load was reached, the load was removed and the dials were read again to record the set, or residual deflection. The second run was made in a similar manner but was carried to 2-1/4 or 2-1/2 times design load. The load was again removed and residual deflections read. Finally, the truss was loaded to failure, its deflection being read at each load increment.

RESULTS

W Truss with 17-Ft Span and 5-in-12 Slope.—It is well known that a carefully made glue joint is a very efficient joint immediately after manufacture. Not so well established is what may happen to the glued joints of a truss during the high and low relative humidities that may prevail during service.

One purpose of this investigation was to determine the effect of high and low relative humidity on glued joints in a completed truss under load. Because both high and low humidities could most easily be obtained in one of the laboratory's dry kilns, the length of these trusses was limited by the kiln dimensions. A truss of 17-1/2-ft length with a 5-in-12 slope was chosen and tested over a 17-ft span.

The type and dimensions of the truss are illustrated in Fig. 4. The framing members were 2-by-4's (1-5/8 by 3-5/8 in cross section), and the sizes of the nailed gusset plates are those used by a commercial fabricator. The number of ninepenny nails placed in double shear is based on the assumption that

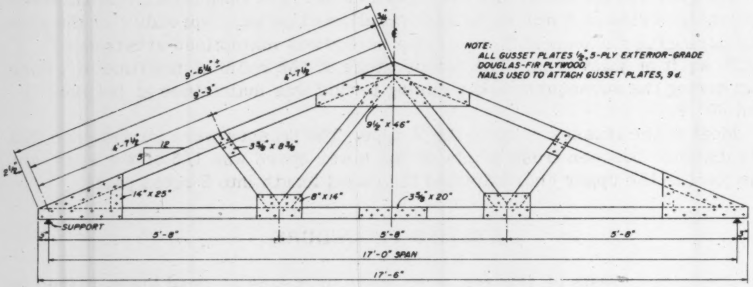
3¼"
℄
9'-6¼" ±
9'-3"
4'-7½"
4'-7½"
12
5
2½"
9½" x 46"
3⅝" x 8⅝"
14" x 25"
8" x 14"
3⅝" x 20"
SUPPORT
3"
5'-8"
5'-8"
5'-8"
3"
17'-0" SPAN
17'-6"

NOTE:
ALL GUSSET PLATES ½", 5-PLY EXTERIOR-GRADE DOUGLAS-FIR PLYWOOD.
NAILS USED TO ATTACH GUSSET PLATES, 9 d.

FIG. 4.—W TRUSS SHOWING PLYWOOD GUSSET PLATES OF THE SIZES USED BY A COMMERCIAL FABRICATOR

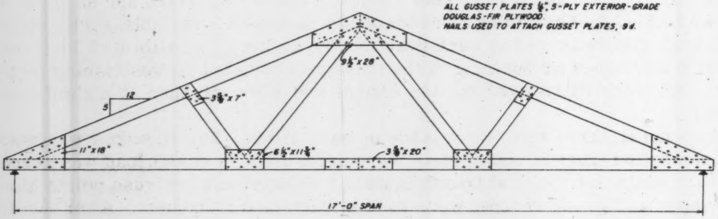
9½" x 28"
12
5
3⅝" x 7"
11" x 18"
6½" x 11⅝"
3⅝" x 20"
17'-0" SPAN

NOTE:
ALL GUSSET PLATES ½", 5-PLY EXTERIOR-GRADE DOUGLAS-FIR PLYWOOD.
NAILS USED TO ATTACH GUSSET PLATES, 9 d.

FIG. 5.—W TRUSS WITH PLYWOOD GUSSET PLATES SOMEWHAT REDUCED IN SIZE FROM THOSE SHOWN IN FIG. 4, EXCEPT AT CENTER OF LOWER CHORD

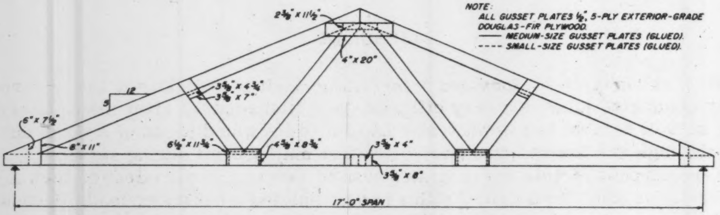
2⅝" x 11½"
4" x 20"
12
5
3⅝" x 4⅝"
3⅝" x 7"
6" x 7½"
8" x 11"
6½" x 11⅝"
4⅝" x 8⅝"
3⅝" x 4"
3⅝" x 8"
17'-0" SPAN

NOTE:
ALL GUSSET PLATES ½", 5-PLY EXTERIOR-GRADE DOUGLAS-FIR PLYWOOD.
—— MEDIUM-SIZE GUSSET PLATES (GLUED).
---- SMALL-SIZE GUSSET PLATES (GLUED).

FIG. 6.—W TRUSS WITH PLYWOOD GUSSET PLATES GLUED TO FRAMING MEMBERS

each nail will withstand about 180 lb of load with only 0.01 in. of slip. Fig. 5 shows a nailed truss with somewhat smaller gusset plates but the same number of nails.

The size of the gusset plates for glued trusses can be considerably smaller than for nailed trusses because of the greater efficiency of the glued joint. The two sizes of gusset plates used are shown in Fig. 6. The net glue area for each joint made with medium and small gusset plates is shown in Table 3. Clamps were used for applying pressure during the glue-curing period.

A graphical analysis of the stresses for design and 2-1/4 times design load is shown in Fig. 7. While a nailed joint is not truly a pin-connected joint, for a practical analysis, it was considered acting as such. These stresses are given in Table 4.

The number of nails used and the glue area for each joint are in about the proportion indicated by the stress analysis.

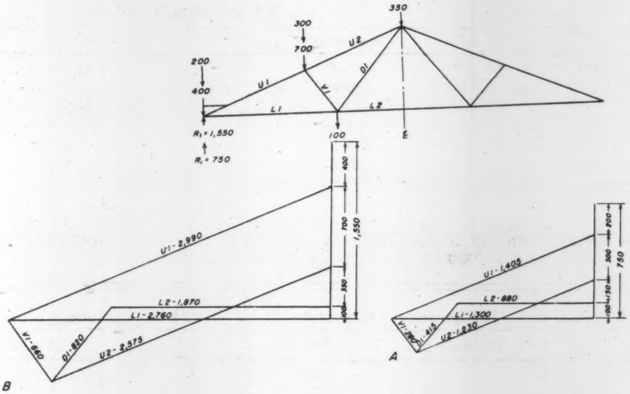

FIG. 7.—GRAPHICAL ANALYSIS OF STRESSES IN 17-1/2 FT W TRUSS ON A 17-FT SPAN

The primary failure of all nailed trusses was at the center of the lower chord. There was a gradual separation of the plywood gusset plates from the central member. The plywood plate on the side with the nail points protruding separated more rapidly than that holding the nailheads (Fig. 8). There was considerable pulling of the nailheads into the plywood.

The glued trusses failed at different joints in the truss. In all glued trusses, failures occurred in the face ply of the gusset plate, adjacent to the central member, or between that face ply and second ply as a rolling shear. There was no glue failure even after the trusses were exposed to low and high relative humidities. Fig. 9 shows a typical failure in the lower chord, that is a shearing failure with some tension parallel-to-grain failure.

A representative load-deflection curve for a nailed truss is shown in Fig. 10. The deflection values apply to the center of the lower chord. There was gradual slipping of the nails even at low loads. At a design roof load of 1,200 lb (35 psf), the deflection was about 0.13 in., and after release of load the deflection was about 0.05 in. Similarly, at 2-1/4 times design load, the deflection was about 0.48 in. and the residual deflection was about 0.34 in. In other words, after releasing the roof load equal to 2-1/4 times design load, about 3/4 of the deflection remained. The action of a glued joint is quite different, as shown in Fig. 11. After applying and releasing the design roof load and also after applying and releasing 2-1/4 times the design roof load, no residual deflection was apparent.

Fig. 12 shows average load-deflection curves for 3 nailed (Nos. 1, 2, and 3) and 3 glued (Nos. 8, 9, and 10) trusses when the load was applied in continuing increments until failure occurred. The 3 nailed and 3 glued trusses were of similar construction. Although there was some variation in behavior among the 3 glued trusses and also among the 3 nailed trusses, the 2 groups were much more dissimilar in behavior. The glued trusses showed considerably less deflection at low loads, and at failure their deflection was still relatively small. When failure did occur, it was sudden and complete. The nailed trusses, on the other hand, showed considerable deflection at low loads. At a load of 1,200 lb, equal to a design roof load of 35 psf, the deflection of the glued truss was 0.04 in. and that of the nailed truss, 0.08 in. This difference continued to increase until, at failure, the deflection of the nailed truss was more than 4 times that of the glued truss, although the maximum load was only about 3/4 as great.

TABLE 3.—GLUED JOINT AREAS OF W TRUSSES

Member	Glued joint, square inches	
	Medium	Small
U-1	25.3	12.0
U-2	20.0	6.8
L-1	40.0	27.0
L-2	14.5	7.3
V-1	8.2	3.6
D-1	12.6	5.3

TABLE 4.—STRESSES FROM GRAPHIC ANALYSIS OF A W-TYPE ROOF TRUSS WITH 5-IN-12 SLOPE FOR A 17-FT SPAN, 2-FT SPACING

Member	Design load,[a] in pounds		2-1/4 design load,[b] in pounds	
	Tension	Compression	Tension	Compression
U-1		1,405		2,990
U-2		1,230		2,575
L-1	1,300		2,760	
L-2	880		1,870	
V-1		280		660
D-1	415		820	

[a] Ceiling, 300 lb, or 8.8 psf roof, 1,200 lb, or 35.3 psf.
[b] Ceiling, 300 lb, or 8.8 psf roof, 2,800 lb, or 82.4 psf.

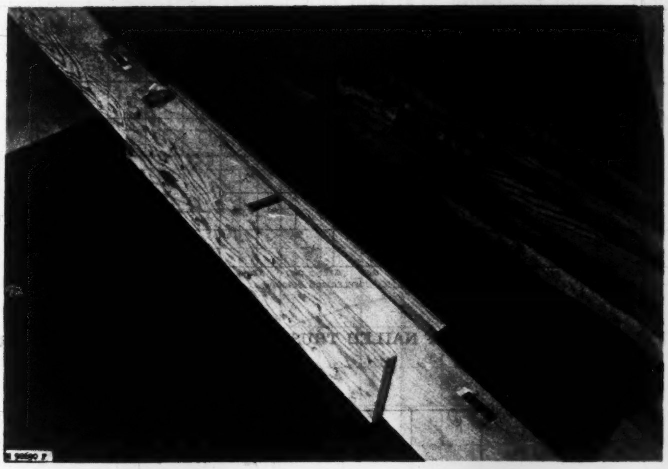

FIG. 8.—LOWER-CHORD FAILURE IN NAILED TRUSS

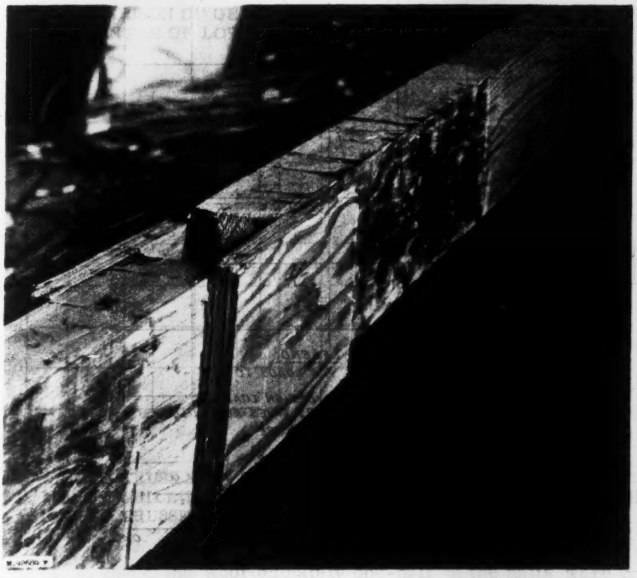

FIG. 9.—LOWER-CHORD FAILURE IN GLUED TRUSS

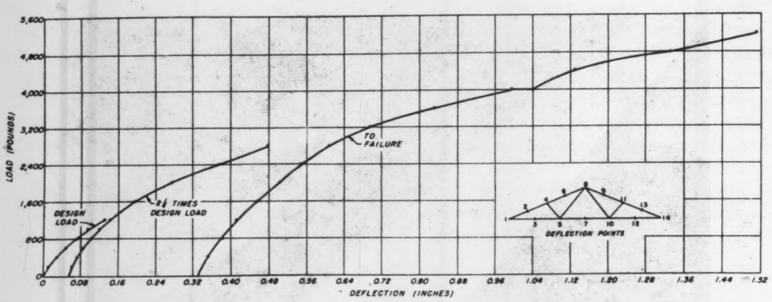

FIG. 10.—DEFLECTION OF NAILED TRUSS AT CENTER OF LOWER CHORD (TRUSS NO. 1)

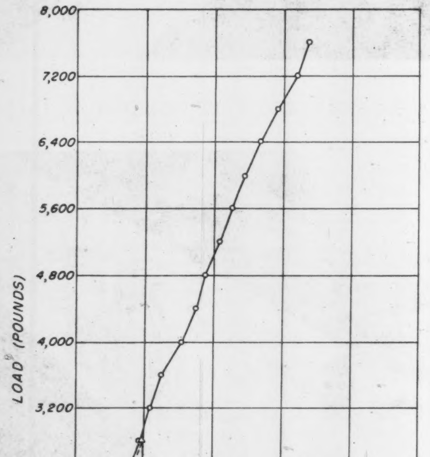

FIG. 11.—DEFLECTION OF GLUED TRUSS AT CENTER OF LOWER CHORD (TRUSS NO. 8)

In addition to comparing the relative merits of glued and nailed trusses, some variables within each group were also considered, as shown in Table 5. For truss No. 5, the same size and number of nails were used as for control trusses Nos. 1, 2, and 3, but approximately one-half of the nails were driven from each side. As shown in Table 6, truss No. 5 deflected somewhat less than the average of the control trusses. The maximum load was also greater—200 psf as compared to 161 lb for the control trusses.

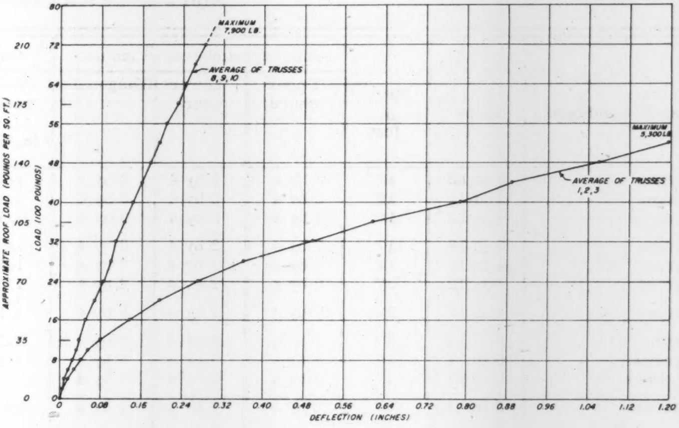

FIG. 12.—COMPARISON OF DEFLECTION OF GLUED AND NAILED TRUSSES AT CENTER OF LOWER CHORD

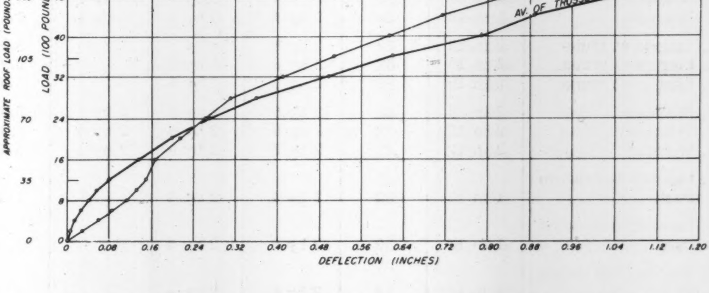

FIG. 13.—NAILED TRUSS NO. 4 EXPOSED TO HIGH AND LOW RELATIVE HUMIDITY WHILE UNDER DESIGN LOAD, COMPARED TO UNEXPOSED NAILED TRUSSES

TABLE 5.—DESCRIPTION OF

Truss No. and type	Slope	Span, in feet	Size of members, in inches			Gusset
			Upper chord	Lower chord	Diagonals	Thickness, in inches
1, W truss	5 in 12	17	2 by 4	2 by 4	2 by 4	1/2
2, W truss	5 in 12	17	2 by 4	2 by 4	2 by 4	1/2
3, W truss	5 in 12	17	2 by 4	2 by 4	2 by 4	1/2
4, W truss	5 in 12	17	2 by 4	2 by 4	2 by 4	1/2
5, W truss	5 in 12	17	2 by 4	2 by 4	2 by 4	1/2
6, W truss	5 in 12	17	2 by 4	2 by 4	2 by 4	1/2
7, W truss	5 in 12	17	2 by 4	2 by 4	2 by 4	3/8
8, W truss	5 in 12	17	2 by 4	2 by 4	2 by 4	1/2
9, W truss	5 in 12	17	2 by 4	2 by 4	2 by 4	1/2
10, W truss	5 in 12	17	2 by 4	2 by 4	2 by 4	1/2
11, W truss	5 in 12	17	2 by 4	2 by 4	2 by 4	1/2
12, W truss	5 in 12	17	2 by 4	2 by 4	2 by 4	1/2
13, W truss	5 in 12	24	2 by 4	2 by 4	2 by 4	1/2
14, W truss	5 in 12	24	2 by 4	2 by 4	2 by 4	1/2
15, rafter-and-joist construction	4 in 12	26	2 by 6	2 by 10		
16, W truss	3 in 12	26	2 by 4	2 by 4	2 by 4	1/2
17, W truss	3 in 12	26	2 by 4	2 by 4	2 by 4	1/2
18, W truss	3 in 12	26	2 by 4	2 by 4	2 by 4	1/2
19, W truss	3 in 12	26	2 by 4	2 by 4	2 by 4	1/2
20, W truss	3 in 12	26	2 by 4	2 by 4	2 by 4	1/2
21, king-post truss	2 in 12	32	2 by 6	2 by 6		5/8
22, king-post truss	2 in 12	32	2 by 6	2 by 6		5/8
23, king-post truss	2 in 12	32	2 by 6	2 by 6		5/8
24, W truss	2 in 12	32	2 by 6	2 by 6	2 by 4	5/8
25, W truss	2 in 12	32	2 by 6	2 by 6	2 by 4	5/8
26, W truss	2 in 12	32	2 by 6	2 by 6	2 by 4	5/8
27, tapered box-beam truss	1 in 12	32	2 by 4	2 by 4		1/2
28, tapered box-beam truss	1 in 12	32	2 by 6	2 by 4		1/2
29, tapered box-beam truss	1 in 12	32	2 by 6	2 by 4		1/2

LIGHTWEIGHT WOOD TRUSSES

plates	Joints					Weight of truss, in pounds	Variable moisture exposure
Size	Glued		Nailed				
	Kind	Pressure	Common nail, Penny	Clinched	Nailed from		
Large			9	No	1 side		No
do			9	No	1 side		No
do			9	No	1 side		No
do			9	No	1 side	88.0	Yes
do			9	No	2 sides	97.2	No
Fairly Large			9	No	1 side	81.4	No
Large			8	No	1 side		No
Small	Resorcinol	Clamps					No
do	↕	↕					No
do							No
Medium						76	Yes
Small						69.5	Yes
a			10	Yes	1 side	112	No
a			10	Yes	1 side	114	No
			12	No	1 side		No
b	Resorcinol	Nails	4	No	2 sides		No
b	↕	↕	4	No	2 sides		No
b			4	No	2 sides		No
b			4	No	2 sides		No
b			4	No	2 sides		No
c			5	No	2 sides	215	No
c			5	No	2 sides	196	No
c			5	No	2 sides	189	No
d			5	No	2 sides	196	No
d			5	No	2 sides	196	No
d			5	No	2 sides	199	No
			6	No	2 sides	215	No
			6	No	2 sides	238	No
			6	No	2 sides	267	No

[a] See Fig. 15. [b] See Table 8. [c] See Fig. 25. [d] See Fig. 26.

TABLE 6.—RESULTS OF TESTS OF

Truss No.	Roof loads[a] and deflections					
	Design roof load				2-1/4 or 2-1/2 times	
	Load, psf	Deflection			Load, psf	
		Actual, inches	Deflection/ span ratio	Residual, inches		Actual, inches
1	35.3	0.132	1/1,550	0.055	82.4	0.478
2	35.3	.029	1/7,040	.005	82.4	.275
3	35.3	.075	1/2,720	.029	82.4	.330
Av.	35.3	.079	1/2,580	.026	82.4	.361
4	35.3	.151	1/1,350	.014	82.4	.311
5	35.3	.063	1/3,240	.019	82.4	.280
6	35.3	.082	1/2,490	.021	82.4	.361
7	35.3	.110	1/1,850	.033	82.4	.428
8	35.3	.023	1/8,880	.000	82.4	.080
9	35.3	.019	1/10,740	.007	82.4	.060
10	35.3	.070	1/2,920	.013	82.4	.160
Av.	35.3	.037	1/5,520	.002	82.4	.100
11	35.3	.049	1/4,160	.001	82.4	.116
12	35.3	.063	1/3,240	.013	82.4	.159
13	35.5[b]	.149	1/1,930	.011	81.5[b]	.317
14	52.0[b]	.209	1/1,370	.028	115.0[b]	.520
15	40.0	.970	1/320	.085		
16	40.0	.340	1/920	.011	100	.880
17	40.0	.425	1/730	.035	100	1.110
18	40.0	.365	1/850	.019	100	.930
19	40.0	.254	1/1,230	.000	100	.716
20	40.0	.303	1/1,030	.041	100	.701
Av.	40.0	.337	1/930	.021	100	.867
21	40.0	.270	1/1,420	.000	100	.710
22	40.0	.310	1/1,240	.030	100	.750
23	40.0	.320	1/1,200	.020	100	.790
Av.	40.0	.300	1/1,280	.017	100	.750
24	40.0	.550	1/700	.030	100	1.490
25	40.0	.480	1/800	.040	100	1.240
26	40.0	.510	1/750	.060	100	1.420
Av.	40.0	.513	1/750	.043	100	1.383
27	40.0	1.24	1/310	.210	100	3.330
28	40.0	1.07	1/360	.030	100	2.640
29	40.0	.91	1/420	.000	100	2.300

[a] For trusses Nos. 1 to 12, inclusive, ceiling load of 8.8 psf. For trusses Nos. 13

[b] Includes 10-lb dead roof load.

LIGHTWEIGHT WOOD TRUSSES

at center of lower chord						
design roof load		Maximum roof load			Maximum recorded deflection	
Deflection			Deflection			
Deflection/ span ratio	Residual, inches	Load, psf	Actual, inches	Deflection/ span ratio	Load, psf	Deflection, inches
1/430	0.338	153	1.51	1/140		
1/740	.133	153	1.07	1/190		
1/620	.187	176			165	1.12
1/560	.219	161	1.24	1/160		
1/660	.107	165	1.04	1/200		
1/730	.140	200			140	.85
1/560	.170	175			130	.69
1/480	.135	118	.59	1/350		
1/2,550	.000	224	.271	1/750		
1/3,400	.003	260	.304	1/670		
1/1,280	.018	212	.371	1/550		
1/2,040	.005	232	.315	1/650		
1/1,760	.003	165	.240	1/850		
1/1,280	.021	118	.215	1/950		
1/910	.000	149[b]	1.049	1/270		
1/550	.114	248[b]	1.975	1/150		
		85	1.70	1/180		
1/350	.033	100	.88	1/350		
1/280	.105	128	1.48	1/210		
1/340	.052	134	1.33	1/230		
1/440	.016	154	1.20	1/260		
1/450	.037	148	1.16	1/270		
1/360	.049	133	1.21	1/260		
1/540	.010	188	1.25	1/310		
1/510	.060	167	1.20	1/320		
1/490	.040	177	1.23	1/310		
1/510	.037	177	1.23	1/310		
1/260	.060	158	2.34	1/160		
1/310	.100	165	2.04	1/190		
1/270	.110	157	1.80	1/210		
1/280	.090	160	2.06	1/190		
1/120	.350	137	4.80	1/80		
1/150	.070	130	3.40	1/110		
1/170	.040	151	3.60	1/110		

and 14, ceiling load 9.4 psf.

There was some question as to whether gusset plates of the size used for the nailed joints were actually necessary, especially at joints other than at the center of the lower chord. Hence, in truss No. 6, all gusset plates were reduced in size except at the center of the lower chord. The comparative sizes are shown in Figs. 4 and 5. At low loads the deflection was slightly greater, but thereafter the deflection was even less than for the control trusses. The maximum load was somewhat greater for truss No. 6 than for the control trusses. The failure occurred at the center of the lower chord, at which no reduction in size of gusset plate was made. Apparently some saving could be made in the amount of plywood used for gusset plates.

In truss No. 7, the gusset plates had the same area as the control trusses but were 3/8 in. thick compared to the 1/2 in. thickness of the controls. This reduction in thickness of gusset plates definitely increased the deflection for given loads and also decreased the maximum load. As shown in Table 6, the maximum load was 118 psf compared to an average of 161 psf for the control trusses. The pulling of the heads of the nails into the 3/8-in. plywood was more pronounced than it was in the 1/2-in. plywood gusset plates.

Humidity exposure.—One nailed truss and two glued trusses were exposed to two cycles of high and low humidity before test. One cycle consisted of exposing the trusses to 80% relative humidity for 30 days and then to 20% relative humidity for 30 days. The range in moisture content was from 15% to 7%. The length of exposure was not long enough to bring the moisture content of the wood trusses into equilibrium with the prevailing humidity. During the conditioning period, the trusses were loaded to a design load equal to a roof load of approximately 35 psf and to a ceiling load of 9 psf.

At the end of the humidity exposures, nailed truss No. 4 showed some separation of plywood gusset plates from the main member. The glued trusses showed no visible effect.

The separation of the plywood plates from the central members apparently caused an increase in deflection for loads up to 1,600 lb, equivalent to a roof load of about 45 psf. This load is somewhat above the usual design roof load. At approximately 2,400 lb, the deflection was the same as for the control trusses, and beyond that the deflection was even less than for the control trusses (Fig. 13).

The control trusses of glued construction, Nos. 8, 9, and 10, exhibited little difference among themselves up to 2-1/4 times design load, whether the plywood gusset plates were medium or small in size. There was some question, however, as to whether the size of gusset plates might have some effect after subjecting the glued trusses to both low and high humidity. Fig. 14 shows load-deflection curves for the average of the glued control trusses, for truss No. 11 with medium-size gusset plates, and for truss No. 12 with small-size gusset plates. The sizes of gusset plates are shown in Fig. 6. Apparently, better behavior is obtained for medium-size gusset plates. The deflections for given loads with medium-size gusset plates are not greatly different from those for the controls, although the maximum load for truss No. 11 is only about 70% that of the controls but still equal to the nailed truss.

When truss No. 12 with the small gusset plates was subjected to both high and low relative humidity, it was apparently considerably affected by this exposure. The deflection at a load of 1,200 lb, equivalent to a design roof load of 35 psf, was about 1-1/2 times that of the glued control trusses. The maximum load was approximately one-half that of the controls but was still several

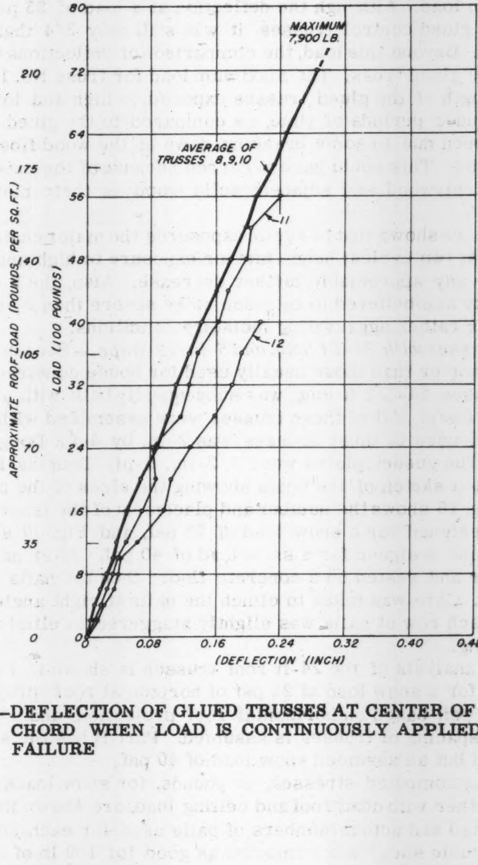

FIG. 14.—DEFLECTION OF GLUED TRUSSES AT CENTER OF LOWER CHORD WHEN LOAD IS CONTINUOUSLY APPLIED UNTIL FAILURE

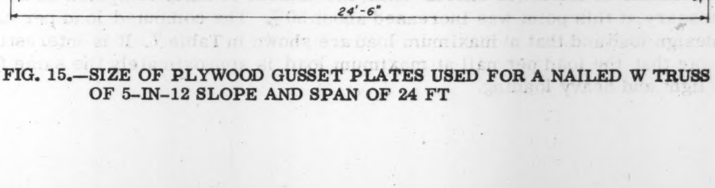
12
5
12"x40
3⅜"x 8⅜"
13"x 22"
8"x 14"
3⅜"x 26"
24'-0"
24'-6"

FIG. 15.—SIZE OF PLYWOOD GUSSET PLATES USED FOR A NAILED W TRUSS OF 5-IN-12 SLOPE AND SPAN OF 24 FT

times the design load. Although the deflection at a load of 35 psf was greater than that of the glued control trusses, it was still only 3/4 that of the nailed control trusses. Beyond this load, the comparison of deflections was even more favorable for the glued truss. The maximum load for truss No. 12 was 118 psf. The lower strength of the glued trusses exposed to high and low relative humidity for extended periods of time, as compared to the glued controls, may possibly have been due to some breaking down of the wood fiber directly behind the glue joint. This could have occurred because of the unequal shrinking and swelling of plywood and adjacent solid wood as their moisture content changed.

Other tests have shown that in cyclic exposures the major changes frequently occur in the first two cycles; hence further exposure to high and low humidity might not cause any appreciable further decrease. Also, the 2 cycles of high and low humidity are believed to be much more severe than 2 seasons of service, even under rather aggravating moisture conditions.

Nailed W Trusses with 24-Ft Span and 5-in-12 Slope.—Because the 17-1/2-ft trusses were shorter than those usually used for house construction, a second group of W trusses, 24-1/2 ft long, was subsequently built with a slope of 5-in-12 for strength tests. All of these trusses were assembled with nails.

The material used in these trusses was 2-in. by 4-in. Douglas-fir of the 1,450f grade. The gusset plates were 1/2-in., 5-ply Douglas-fir of exterior type. Fig. 15 is a sketch of the truss showing the sizes of the plywood gusset plates used. Fig. 16 shows the number and placement of the tenpenny nails used for the truss designed for a snow load of 25 psf, and Fig. 17 shows the joint details for a truss designed for a snow load of 40 psf. After nailing the truss was turned over and rested on a concrete floor; then the nails were clinched with a hammer. Care was taken to clinch the nails at right angles to the grain of the wood. Each row of nails was slightly staggered to eliminate a possible cause of splitting.

A graphical analysis of the 24-ft roof trusses is shown in Fig. 18. Part A is the analysis for a snow load of 25 psf of horizontal roof projection, a dead roof load of 10 psf, based on horizontal roof projection, and a ceiling load of 10 psf. A 2-ft spacing of trusses is assumed. Part B has the same dead roof and ceiling load but an assumed snow load of 40 psf.

The resulting computed stresses, in pounds, for snow loads of both 25 psf and 40 psf, together with dead roof and ceiling load, are shown in Table 7, along with the computed and actual numbers of nails used for each joint. Each tenpenny nail in double shear was computed as good for 180 lb of design load including an increase of 15% for short-time loading. The formula used for computing the load per nail in shear was

$$P = K D^{3/2} \quad \ldots\ldots\ldots\ldots\ldots\ldots\ldots \quad (1)$$

For Douglas-fir, K = 1,375. The diameter D of tenpenny common nails is 0.148 in. Then

$$P = (1{,}375)\ (0.148)^{3/2}\ (1.15)\ (2) = 180 \text{ lb}$$

The 17-ft nailed roof trusses previously discussed all failed at the splice at the center of the lower chord. Thus, the number of nails computed as being necessary at this point was increased about 50%. The computed load per nail at design load and that at maximum load are shown in Table 7. It is interesting to note that the load per nail at maximum load is approximately the same for the light and heavy loading.

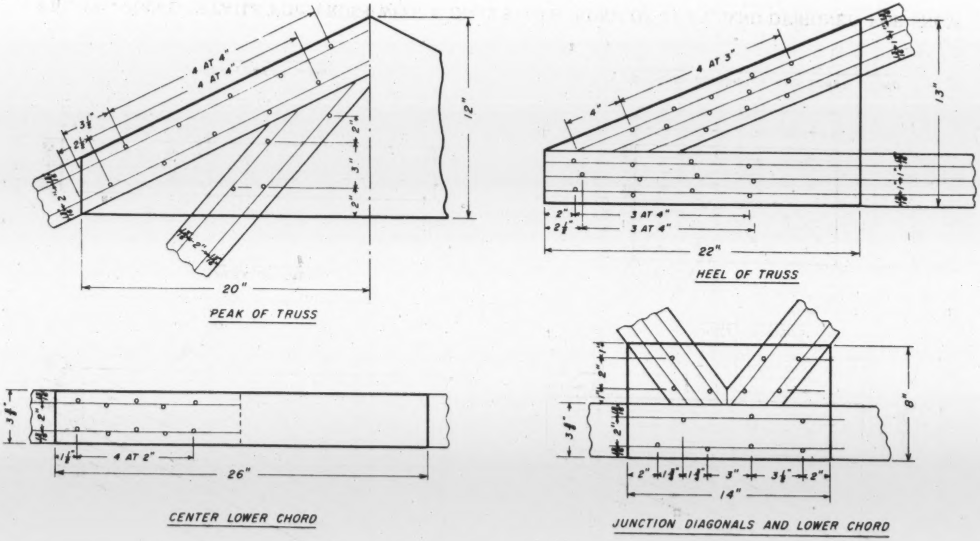
4 AT 4"
4 AT 4"
3½"
2¼"
2"
3"
2"
12"
20"
4 AT 3"
4"
13"
3 AT 4"
3 AT 4"
2"
2¼"
22"
3⅝"
2"
1⅝"
4 AT 2"
26"
8"
2"
2"
1½"
1½"
3"
3½"
2"
14"

PEAK OF TRUSS

HEEL OF TRUSS

CENTER LOWER CHORD

JUNCTION DIAGONALS AND LOWER CHORD

FIG. 16.—JOINT DETAILS FOR TRUSS WITH 5-IN-12 SLOPE, SPAN OF 24 FT, AND DESIGNED FOR SNOW LOAD OF 24 PSF

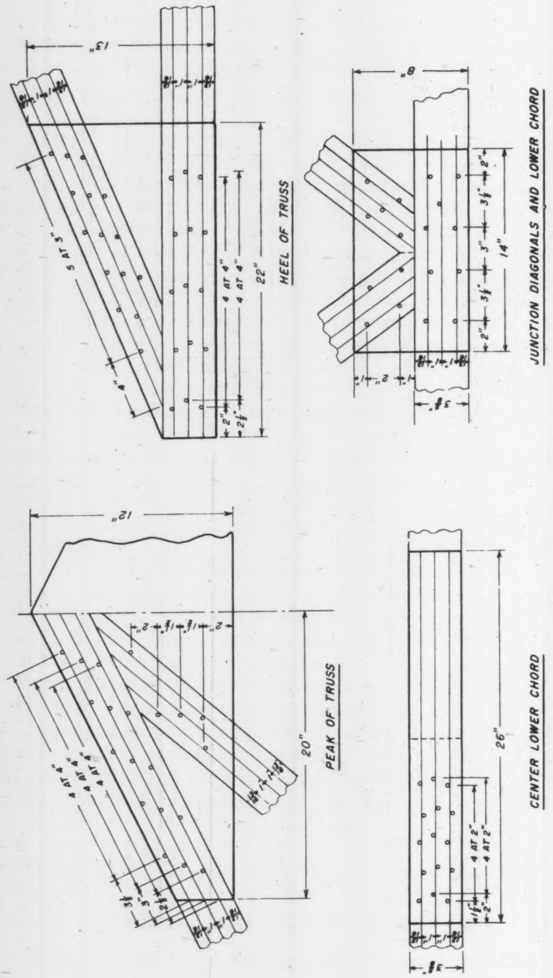
HEEL OF TRUSS
13"
5 AT 3"
4"
4 AT 4"
4 AT 4"
22"
2"
2½"
JUNCTION DIAGONALS AND LOWER CHORD
8"
14"
2"
3¼"
3"
3¼"
2"
3⅝"
PEAK OF TRUSS
12"
20"
4 AT 4"
4 AT 4"
4 AT 4"
3½"
3"
2½"
CENTER LOWER CHORD
26"
4 AT 2"
4 AT 2"
1½"
2"
3⅝"

FIG. 17.—JOINT DETAILS FOR TRUSS WITH 5-IN-12 SLOPE, SPAN OF 24 FT, AND DESIGNED FOR SNOW LOAD OF 40 PSF

TABLE 7.—DATA FOR W ROOF TRUSS WITH 24-FT SPAN AND 5-IN-12 SLOPE

Member	Stress, in pounds, for		Nailing schedule,[a] number of nails				Load per nail, in pounds			
	Light roof load[b]	Heavy roof load[c]	Light load		Heavy load		Design load		Maximum load[d]	
			Re-quired	Used	Re-quired	Used	Light roof load	Heavy roof load	Light roof load	Heavy roof load
U-1	-2,060	-2,700	11.5	12	15.0	15	172	180	720	860
U-2	-1,790	-2,320	10.0	10	12.9	15	179	155	750	740
L-1	+1,910	+2,500	10.6	12	13.9	15	159	167	670	800
L-2	+1,270	+1,650	7.0	10	9.2	15	127	110	530	530
V-1	-403	-570	2.3	3	3.2	4	135	142	570	680
D-1	+610	+770	3.4	4	4.3	5	152	154	640	740

[a] Lateral resistance 180 lb for tenpenny, clinched nail in double shear.

[b] Load per square foot; roof, 25 lb live plus 10 lb dead; ceiling, 10 lb.

[c] Load per square foot; roof, 40 lb live plus 10 lb dead; ceiling, 10 lb.

[d] Based on ratio of maximum to design loads, considering roof loads only. Light roof load $\frac{7,100}{1,700} = 4.2$. Heavy roof load $\frac{11,900}{2,500} = 4.8$.

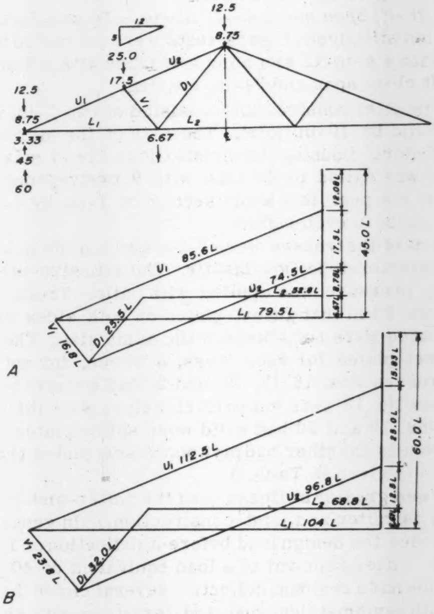
12.5
8.75
12
5
25.0
17.5
U2
D1
12.5
8.75
U1
V1
L1
L2
3.33
45
60
6.67
℄
U1 85.6L
U2 74.5L
L2 52.8L
L1 79.5L
D1 25.5L
V1 16.8L
12.08L
17.5L
8.75L
6.67L
45.0L
A
U1 112.5L
U2 96.8L
L2 68.8L
L1 104 L
D1 32.0L
V1 23.8L
15.83L
25.0L
12.5L
6.67L
60.0L
B

FIG. 18.—GRAPHICAL ANALYSES FOR W TRUSS WITH 5-IN-12 SLOPE AND SPAN OF 24 FT

The deflections and residual deflections at the center of the lower chord for snow loads of both 25 psf and 40 psf are given in Table 6.

At a design snow load of 25 psf, the deflection at the center of the lower chord of truss No. 13 was only 1/1,930 of the span. For truss No. 14, designed for a snow load of 40 psf, the deflection was only 1/1,370 of the span. Even at 2-1/4 times design load, the deflections were small and much less than the usual deflection requirement of 1/360 of the span at the design load. The two trusses differed only in the number of nails used.

Load-deflection curves based on deflection at the center of the lower chord for the truss designed for snow loads of 25 psf and 40 psf are shown in Figs. 19 and 20. Curves for design load, 2-1/4 times design load, the maximum load are shown. The curves show some residual deflection. The ceiling load and weight of weighing platforms, however, had not been removed when the residual deflection was read. If adjustment is made for deflection caused by these loads, as was done in Table 6, the residuals are much smaller.

Truss No. 13, designed for a snow load of 25 psf, failed when the long diagonal split at the nails that joined it to the lower chord, as shown in Fig. 21. There was some bending of the nails and opening at the center of the lower chord previous to failure, as shown in Fig. 22. This also occurred in truss No. 14, that was designed for a snow load of 40 psf. The principal failure in the truss designed for a snow load of 40 psf was splitting of the upper chord between the heel and the first joint, as shown in Fig. 23. This was preceded by some lateral buckling of the upper chord.

W Trusses with 26-Ft Span and 3-in-12 Slope.—To compare nailed rafter-and-joist construction with glued trusses, tests were conducted on a rafter-and-joist construction with a 4-in-12 slope and a W truss with a 3-in-12 slope, both designed for a 26-ft clear span and 24-in. spacing.

The rafter-ceiling joist construction consisted of two 2-in. by 6-in. rafters and a continuous 2-in. by 10-in. joist. The size of the members was in accordance with the Federal Housing Administration table of maximum allowable spans. Each rafter was nailed to the joist with 9 twelvepenny common nails. They were nailed at the peak to a short section of 1-in. by 8-in. ridge board with 2 twelvepenny nails in each rafter.

All main members of the trusses were 2-by-4's, and the gusset plates were of 1/2-in., 5-ply, exterior-type Douglas-fir. The adhesive used was a resorcinol resin. Gluing pressure was applied with nails. Truss No. 16 differed from Nos. 17 through 20 in that gusset plates on both sides were not used at all joints and when used were not always of the same size. The amount of plywood used for gusset plates for each truss, however, did not differ greatly. The diagonals of trusses Nos. 16, 17, 19, and 20 had square-cut ends, whereas the diagonals of truss No. 18 were cut to fit closely against the upper and lower chords. Trusses Nos. 19 and 20 had solid wood splice plates at the center of the lower chord, whereas the other had plywood gusset plates throughout. More detailed information is given in Table 8.

The trusses showed greater stiffness than the rafter-and-joist construction (Fig. 24). (No. 15 is rafter and joist construction.) In general, the trusses carried more than twice the design load before a deflection of 1/360 of the span occurred (Table 6). After removal of a load equivalent of 40 psf, the rafter-and-joist construction had a residual deflection several times that of the trusses.

Truss No. 16, with asymmetrical gusset plates on opposite sides of its joints, failed at a lower load than the other trusses. Trusses Nos. 19 and 20, with

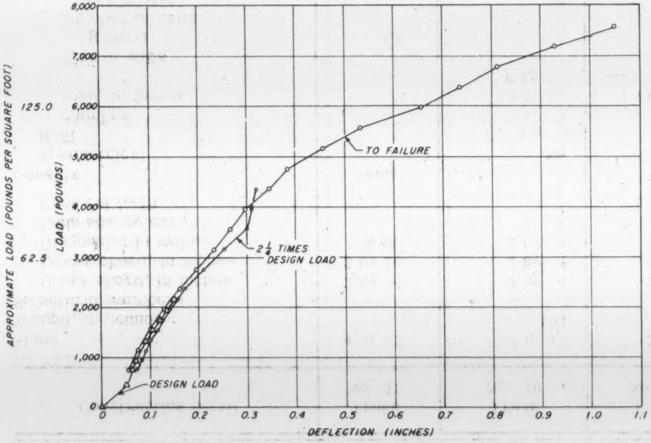

FIG. 19.—DEFLECTION AT CENTER OF LOWER CHORD FOR VARIOUS INCREMENTS OF LOAD ON A NAILED TRUSS WITH 5-IN-12 SLOPE AND SPAN OF 24 FT, DESIGNED FOR A SNOW LOAD OF 25 PSF

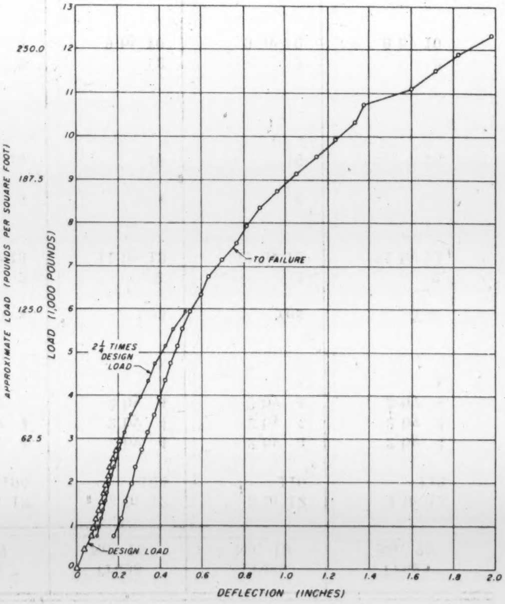

FIG. 20.—DEFLECTION AT CENTER OF LOWER CHORD FOR VARIOUS INCREMENTS OF LOAD ON A NAILED TRUSS OF 5-IN-12 SLOPE AND WITH A SPAN OF 24 FT, DESIGNED FOR A SNOW LOAD OF 40 PSF

TABLE 8.—CONSTRUCTION DETAILS OF RAFTER AND TRUSSES

Construction detail	Truss No. 15	Truss No. 16	Truss No. 17	Truss No. 18	Truss No. 19	Truss No. 20
Slope	4 in 12	3 in 12	3 in 12	3 in 12	3 in 12	3 in 12
Weight, in pounds		104	100	104	110	112
Structural members						
Upper chord, in inches	2 by 6	2 by 4	2 by 4	2 by 4	2 by 4	2 by 4
Lower chord, in inches	2 by 10	2 by 4	2 by 4	2 by 4	2 by 4	2 by 4
Diagonals, in inches	None	2 by 4	2 by 4	2 by 4	2 by 4	2 by 4
Ends square cut		x	x		x	x
Ends cut to fit				x		
Gussets	None					
Symmetrical		No	Yes	Yes	Yes	Yes
Heel						
Number		2	2	2	2	2
Size, in inches		15 by 33 6 by 12	11 by 13	11 by 13	11 by 13	11 by 13
Size of nails (penny)	12	4	4	4	6	6
Number of nails per gusset		36 16	16	16	16	16
Number of nails at joint	9					
Peak						
Number		2	2	2	2	2
Size, in inches		12 by 15 3-5/8 by 15	9 by 10	9 by 10	9 by 10	9 by 10
Size of nails (penny)	12	4	4	4	6	6

Number of nails per gusset		6 16 12	18	18	18	18
Number of nails at joint	4					
Short diagonal-top chord						
Number	None	1	2	2	2	2
Size, in inches		3-1/2 by 7	3-1/2 by 10	3-1/2 by 10	3-1/2 by 10	3-1/2 by 10
Size of nails (penny)		6	6	6	6	6
Number of nails per gusset		8	8	8	8	8
Short diagonal-long diagonal-bottom chord						
Number	None	1	2	2	2	2
Size, in inches		10 by 10	8 by 10	8 by 10	8 by 10	8 by 10
Size of nails (penny)		4	4	4	6	6
Number of nails per gusset		14	14	14	14	14
Bottom chord splice						
Number	None	2	2	2	2	2
Size, in inches		4 by 24	4 by 24	4 by 24	4 by 24	4 by 24
Size of nails (penny)		6	6	6	6	6
Number of nails per gusset		12	12	12	12	12

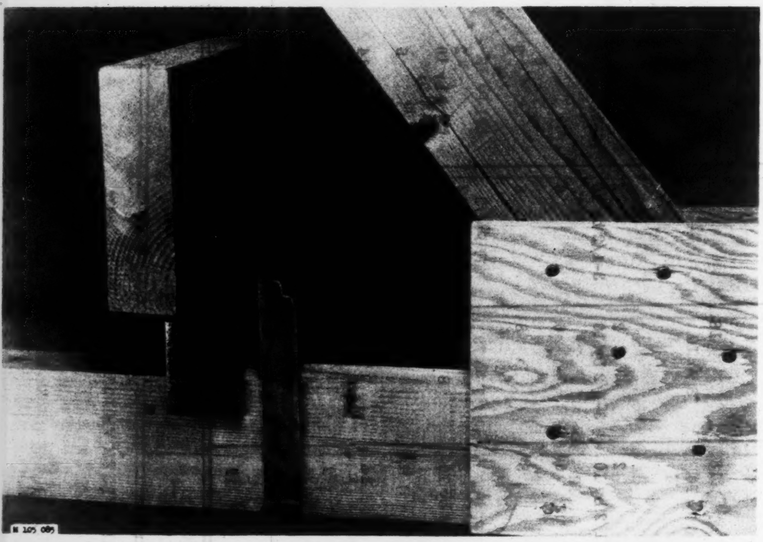

FIG. 21.—TRUSS WITH 5-IN-12 SLOPE, 25 PSF SNOW LOAD

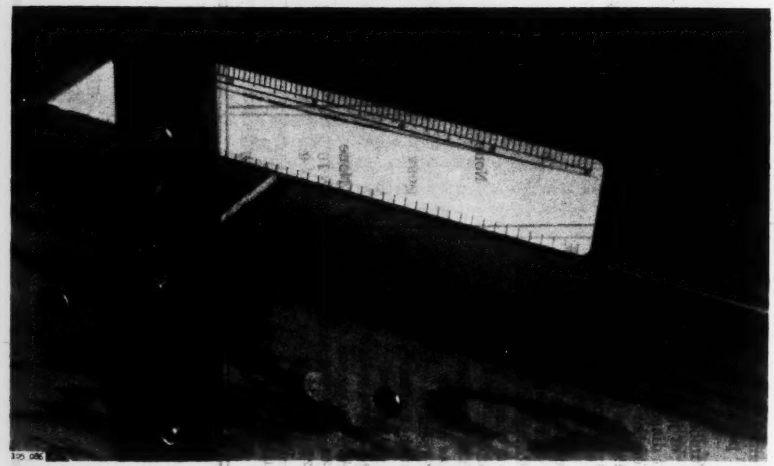

FIG. 22.—CENTER JUNCTION OF LOWER CHORD

solid wood tie plates for the lower chord, failed at higher loads than the other trusses.

Trusses show considerable superiority over rafter-and-joist construction.

King-Post and W Trusses with 32-Ft Span and 2-in-12 Slope.—It was felt that, in addition to the experiments with W trusses of 17-ft, 24-ft, and 26-ft spans and with slopes of 5-in-12 and 3-in-12, trusses of longer spans and lower slopes should also be tested. Therefore, both king-post and W trusses of 32-ft span and 2-in-12 slope were included in this experiment.

The king-post and W trusses consisted of 2-in. by 6-in. members and 5/8-in.-thick plywood for gusset plates, except at the center of the lower chord at which solid wood splice plates were substituted. A resorcinol-resin glue was used, and pressure was applied with nails. Details of construction for the king-post truss are given in Fig. 25 and those for the W trusses in Fig. 26.

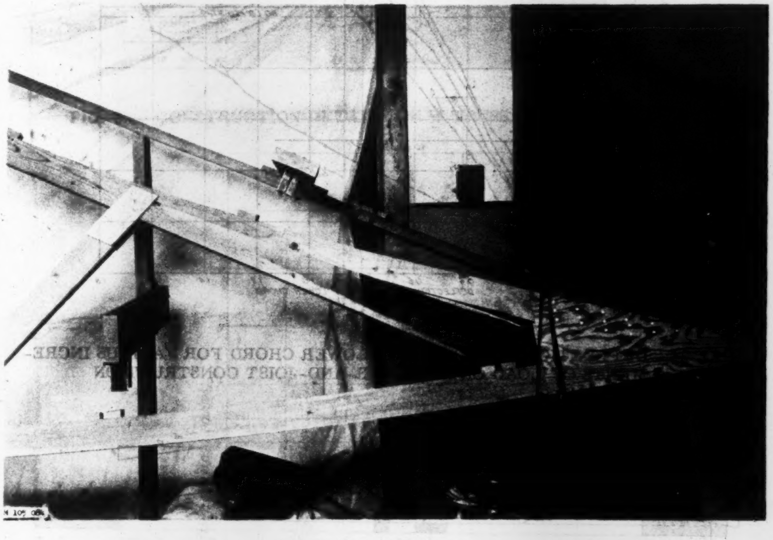

FIG. 23.—TRUSS WITH 5-IN-12 SLOPE, 40 PSF SNOW LOAD

Both the king-post (Nos. 21, 22, and 23) and W trusses (Nos. 24, 25, and 26) sustained loads well above the design load before a deflection of 1/360 of the span at the center of the lower chords was reached (Table 6, Figs. 27 and 28). Both types sustained loads about 4 times as great as the design roof load of 40 psf. The residual deflections of all trusses were very small immediately after removal of the design load and also after removal of 2-1/2 times the design load.

The W trusses failed because rolling shear developed in the plywood of the peak gusset plates, as shown in Fig. 29. The king-post trusses failed in bend-

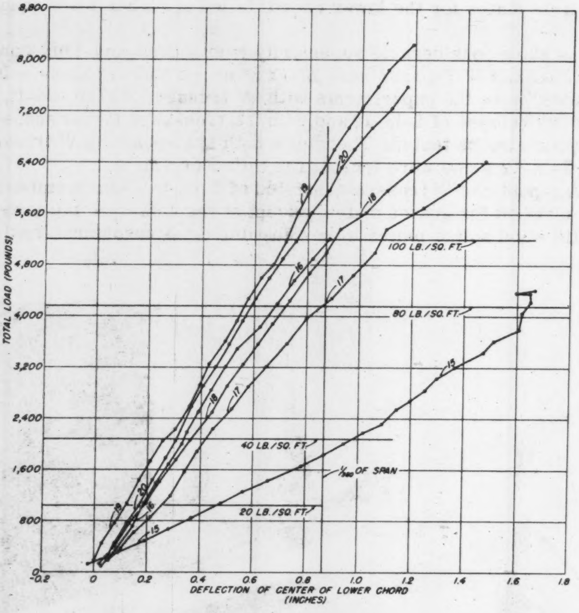

FIG. 24.—DEFLECTION AT CENTER OF LOWER CHORD FOR VARIOUS INCREMENTS OF LOAD ON A RAFTER-AND-JOIST CONSTRUCTION

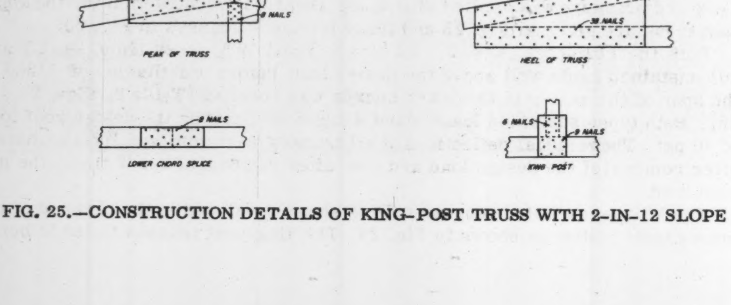
12
2
12" x 80"
2" x 6"
2" x 4"
1" x 6" x 18" SOLID WOOD SPLICE PLATE
8" x 12"
19¼" x 48"
2" x 6"
2'4"
16'4"
32'8"
23 NAILS
8 NAILS
PEAK OF TRUSS
NAILS ARE IN 3 ROWS SPACED ABOUT 4" APART EDGE MARGIN ¾"
38 NAILS
38 NAILS
HEEL OF TRUSS
8 NAILS
LOWER CHORD SPLICE
6 NAILS
9 NAILS
KING POST

FIG. 25.—CONSTRUCTION DETAILS OF KING-POST TRUSS WITH 2-IN-12 SLOPE

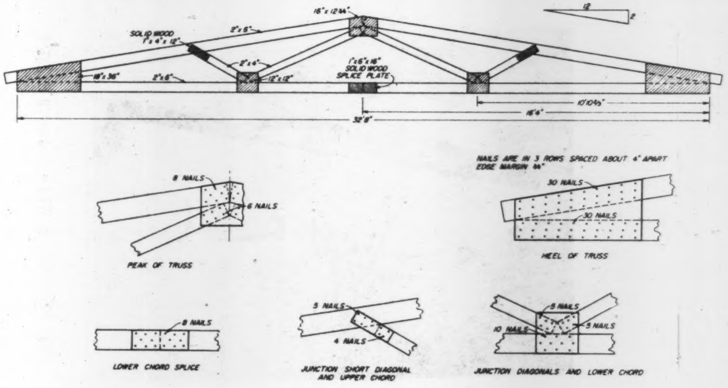
16" x 12¾"
12
2
SOLID WOOD
1" x 4" x 12"
2" x 6"
2" x 4"
18" x 36"
2" x 6"
12" x 12"
1" x 6" x 16"
SOLID WOOD
SPLICE PLATE
10'10⅘"
16'4"
32'8"
8 NAILS
6 NAILS
PEAK OF TRUSS
NAILS ARE IN 3 ROWS SPACED ABOUT 4" APART
EDGE MARGIN ¾"
30 NAILS
30 NAILS
HEEL OF TRUSS
8 NAILS
LOWER CHORD SPLICE
5 NAILS
4 NAILS
JUNCTION SHORT DIAGONAL AND UPPER CHORD
5 NAILS
10 NAILS
5 NAILS
JUNCTION DIAGONALS AND LOWER CHORD

FIG. 26.—CONSTRUCTION DETAILS OF W TRUSS WITH 2-IN-12 SLOPE

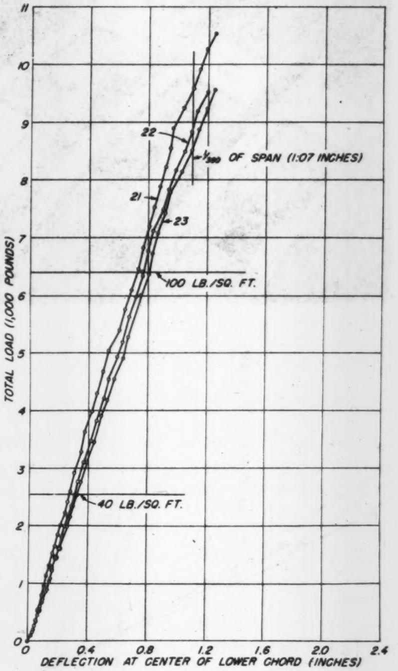

FIG. 27.—DEFLECTION AT CENTER OF LOWER CHORD FOR VARIOUS INCREMENTS OF LOAD ON A KING-POST TRUSS WITH 2-IN-12 SLOPE AND 32-FT SPAN

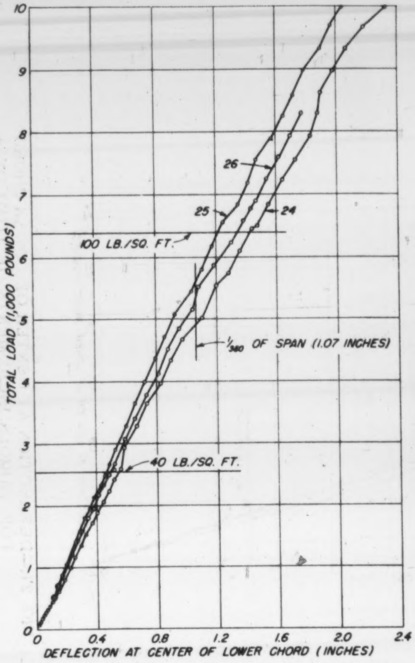

FIG. 28.—DEFLECTION AT CENTER OF LOWER CHORD FOR VARIOUS INCREMENTS OF LOAD ON W TRUSSES WITH 2-IN-12 SLOPE AND SPAN OF 32 FT

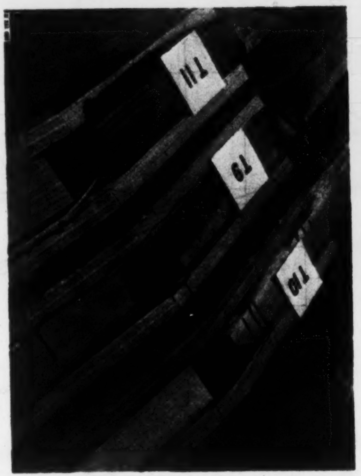

FIG. 29.—ROLLING SHEAR FAILURE

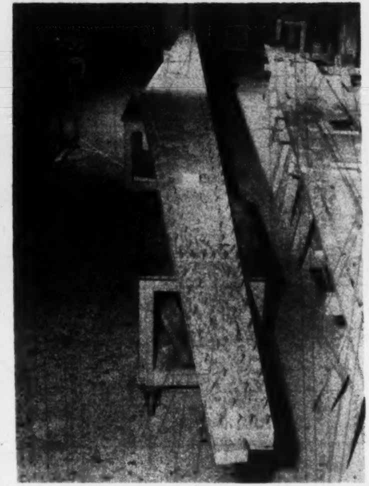

FIG. 30.—TRUSS WITH 1-IN-12 SLOPE

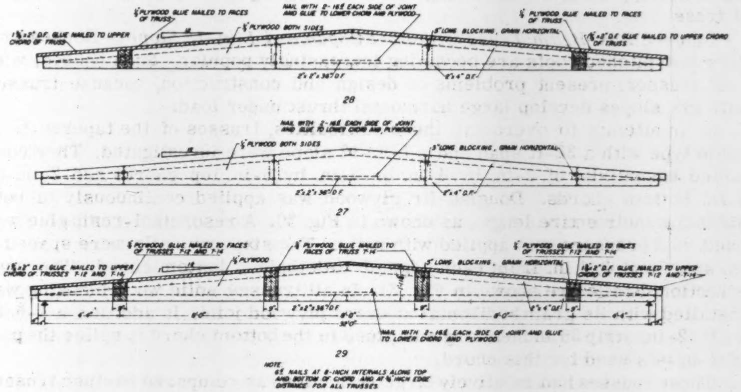
⅜" PLYWOOD GLUE NAILED TO FACES OF TRUSS
NAIL WITH 2-16d EACH SIDE OF JOINT AND GLUE TO LOWER CHORD AND PLYWOOD
1⅝"x2" D.F. GLUE NAILED TO UPPER CHORD OF TRUSS
⅜" PLYWOOD BOTH SIDES
12
1
5" LONG BLOCKING, GRAIN HORIZONTAL
2"x2"x36" D.F.
2"x4" D.F.
28
27
⅜" PLYWOOD GLUE NAILED TO FACES OF TRUSSES T-12 AND T-14
⅜" PLYWOOD
⅜" PLYWOOD GLUE NAILED TO FACES OF TRUSS T-14
1⅝"x2" D.F. GLUE NAILED TO UPPER CHORD OF TRUSSES T-12 AND T-14
9"
4'-4"
8'-0"
32'-0"
NAIL WITH 2-16d EACH SIDE OF JOINT AND GLUE TO LOWER CHORD AND PLYWOOD
29
NOTE
6d NAILS AT 8-INCH INTERVALS ALONG TOP AND BOTTOM OF CHORD AND AT ¾ INCH EDGE DISTANCE FOR ALL TRUSSES

FIG. 31.—CONSTRUCTION DETAILS OF NAIL-GLUED TRUSSES OF 1-IN-12 SLOPE AND 32-FT SPAN

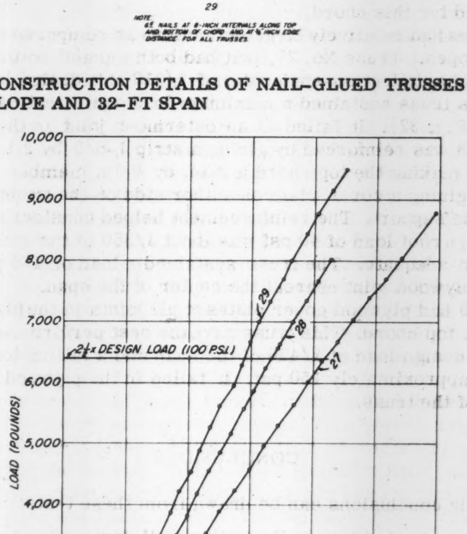

FIG. 32.—DEFLECTION AT CENTER OF LOWER CHORD FOR VARIOUS INCREMENTS OF LOAD ON NAIL-GLUED TRUSSES WITH 1-IN-12 SLOPE AND SPAN OF 32 FT

ing of the upper chord, indicating a need for high-grade material for this type of truss.

Tapered Box-Beam Truss with 32-Ft Span and 1-in-12 Slope.—Houses with very low-pitched roofs are becoming increasingly popular. Such houses, with roof trusses, present problems of design and construction, because trusses with low slopes develop large horizontal thrust under load.

In an attempt to overcome these difficulties, trusses of the tapered box-beam type with a 32-ft span and a 1-in-12 slope were investigated. They consisted essentially of 2-in. by 4-in. or 2-in. by 6-in. top chords and 2-in. by 4-in. bottom chords. Douglas-fir plywood was applied continuously on both sides for their entire length, as shown in Fig. 30. A resorcinol-resin glue was used, and pressure was applied with nails. The sixpenny nails were spaced 8 in. apart and 3/4 in. from each edge of both top and bottom chord. The construction details are shown in Fig. 31. In all trusses, solid wood blocking was installed with its grain horizontal at every plywood joint. In addition, a 1-5/8-in. by 2-in. strip 36 inches long was glued to the bottom chord to splice the pair of 2-by-4's used for this chord.

These trusses had relatively large deflections as compared to other trusses with steeper slopes. Truss No. 27, that had both top and bottom chords made of 2-by-4's, had a deflection-span ratio of 1/310 at a design load of 40 psf of roof load. This truss sustained a maximum load equivalent to 137 psf of roof load (Table 6, Fig. 32). It failed at an outermost joint in the plywood face.

Truss No. 28 was reinforced by gluing a strip 1-5/8 by 2 in. in size on the top chord, thus making the top chord a 2-in. by 6-in. member. It was further reinforced by gluing a cover plate on either side of the truss at the plywood joint nearest the support. The reinforcement helped considerably, and the deflection at design roof load of 40 psf was about 1/360 of the span. This is usually considered adequate. The truss sustained a load of 130 psf, and failure occurred at a plywood joint nearest the center of the span.

Truss No. 29 had plywood cover plates at all joints in the plywood faces and a 2-in. by 6-in. top chord. This truss gave the best performance of the 3, with a deflection at design load of 1/420 of the span and a failing load equivalent to a roof load of approximately 150 psf. It failed in the plywood face about 6 ft from one end of the truss.

CONCLUSIONS

The following conclusions can be drawn from these tests:

1. The tests reported here indicate that well designed and well constructed nailed trusses with a slope of 4-in-12 or greater should give adequate service.
2. Glued trusses, because of their rigid joints, are much stiffer than nailed trusses.
3. Glued trusses show little increase in deflection even when carrying near-maximum loads, whereas nailed trusses will deflect considerably under similar conditions.
4. Glued trusses show some loss in stiffness and considerable loss in maximum load from exposure to cycles of high and low relative humidity. Nailed trusses are less affected.
5. The ease with which high rigidity and strength can be obtained in glued joints makes glued trusses particularly suitable for trusses with low slopes.

6. Because the strength of a glued truss is entirely dependent on the efficiency of the glued joints, only those glues that will perform satisfactorily under adverse atmospheric conditions are recommended.

DISCUSSION

E. GEORGE STERN,[3] **M. ASCE.**—The studies performed at the United States Forest Products Laboratory were limited, in that they covered only 28 trussed rafters of certain slopes, assembled with plywood gusset plates, resorcinol-resin glue, or common wire nails. Hence, the conclusions drawn from these tests must be restricted to the cases investigated.

It is stated that well designed and well constructed nailed trusses with a slope of 4-in-12 or greater should give adequate service, although (1) only nailed trussed rafters with a slope of 5-in-12 were investigated and (2) nailed trussed rafters with slopes of 2-in-12, 3-in-12, and 4-in-12 were found to perform extremely satisfactorily by other investigators during their extensive studies. Furthermore, the statement is made that the rigidity and strength of glued joints makes glued trusses particularly suitable for trusses with low slopes. On the other hand, (1) nailed trusses of low slopes were not included in the described tests, (2) the tested glued trussed rafters were found to be much more rigid than required under most severe service conditions, and (3) extremely rigid, nailed trussed rafters with low as well as high rafter slopes have been tested and are in use throughout the country.

It is conceded that the nailed trussed rafters described in the paper were assembled with common wire nails, whereas the nailed trussed rafters that proved to provide such outstanding service are assembled with improved nails, that is, hardened high-carbon-steel, helically threaded nails or with inserted, nailed-on, bent-over or toothed metal plates of various types that are commercially available today.

The author observed that some trussed rafters failed because of rolling shear developed in the plywood gusset plates. This type of failure can be observed if the plywood is fastened with glue that, of necessity, provides only a surface bond along the contact areas. If, on the other hand, nails are used to fasten the plywood gusset plates firmly, the loads are transmitted through the depth of the plywood and lumber. Then, rolling shear cannot take place. In the first case, the glue was stronger than the plywood. In the latter case, the plywood is strengthened by the nails that fasten the plywood.

Other failures were observed because of the fact that the use of common wire nails resulted in joint failure due to lumber splitting and nail bending. The use of the more slender and stiffer, hardened high-carbon-steel nails would probably have prevented such failures on the basis of experience available with these improved nails.

It was interesting to note that; (1) nails in double shear sustain loads about twice those for nails in single shear at small deflections, that is, at design load, and (2) if one-half of the nails subjected to double shear are driven into one side and one-half into the other, their effectiveness at small slips, that is, at design load, is even more than double that of nails in single shear. These findings are significant, insofar as some United States building codes do not allow nails in double shear to transmit twice the load of nails in single shear under any circumstances, because the effectiveness of nails in double shear beyond the design load increases at a lesser rate than the effectiveness of nails in single shear.

---

[3] Earle B. Norris Research Prof. of Wood Const., Virginia Polytechnic Inst., Blacksburg, Va.

The presented test data are significant because they provide valuable information. They are possibly of greatest value when used as a basis of comparison with data obtained for other trussed rafters in commercial use or under development.

DAVID COUNTRYMAN.[4]—Mr. Luxford's paper presents valuable evidence on the structural adequacy of an important type of member. It is probably safe to say that more than a million similar light wood trusses are already in service in this country.

The tests generally indicate excellent performance for these members with high stiffness and load-carrying factors. Also, the beneficial effects of using glue are obvious. Even when the gussets in Truss Nos. 8, 9, and 10 were cut down to an absurdly low glue area, the ultimate load was still 6-1/2 times the design value. This is an indication that present plywood working stresses in rolling shear are conservative.

For example, the computed ultimate rolling shear stresses for member U-1 of the heel joint gussets of these trusses, from data in Tables 3 and 4, averages 380 psi; this compares with a recommended design stress in rolling shear of 34 psi for plyscord. The use of this working stress would evidently indicate gussets of a size only slightly smaller than those of Truss No. 11, that successfully resisted variable moisture exposures.

These particular trusses were assembled using clamps for pressure gluing. A very practical aspect of this whole subject is whether or not reliable members can be obtained if the joints are nail-glued. It has been argued that nails do not provide enough pressure to draw wood members together into close contact. This may indeed be the case for an assembly consisting of layers of 2-in. lumber. However, because the plywood is relatively flexible, it can be more readily drawn to conformity with the lumber by the nails.

That this method is successful is demonstrated by the fact that no glue failure was noted in any of the 14 trusses assembled with nail-gluing, although failures did occur in rolling shear in the plywood gussets themselves, in certain cases, showing that the joints were highly stressed.

Further, a report by the Small Homes Council at the University of Illinois at Urbana, Ill., of tests on similar trusses, states that no failures occurred in the glued joints, although the plywood gussets were nail-glued. This agency recommends nails or staples for the gluing of these members.

In a discussion of this paper, the fine performance of the nailed trusses should not be overlooked. These members are not so exacting to build as those that are glued. They can be readily site-fabricated in the open, even during unfavorable weather. The lumber need not be dry, and they can be erected as soon as they are made.

As shown by Truss Nos. 13 and 14, 10d nails can be spaced as close as 2 in. in three lines by 2-by-4's, although with such close spacing, some care should be taken not to aline them with the grain.

---

[4] Engr., Douglas Fir Plywood Assoc., Tacoma, Wash.

The preliminary joint tests on nails in double shear showed that stiffness is increased considerably, but only about 25% is added to the ultimate strength. However, it should be noted that this low increase in strength applied only when the nail is too short to clinch, as these were.

Some tests conducted by the Douglas Fir Plywood Association,[5] on matched specimens on 3/8 in., 1/2 in., and 5/8 in. plywood with 10d and 12d common nails, nailed green and tested after seasoning, showed these nails in double shear averaged 2.2 times their single shear strength, providing the point protruded at least 3/8 in. and was clinched perpendicular to the load direction.

The joints fabricated in Truss Nos. 13 and 14 were of this type. Based on allowing twice the usual design load per nail, because they were placed in double shear, these trusses still sustained about five times their design load, with excellent stiffness factors. Failure occurred in the lumber chords before the full nail joint strength was developed.

Throughout Mr. Luxford's paper, a deflection limitation of 1/360th of the span is noted as acceptable. It is the writer's understanding that this deflection limitation generally applies to floor members, or to members supporting plastered construction. A deflection of 1/240th of the span for roof members not supporting plaster is perhaps more generally accepted. If this were not the case, then the conventional rafter and joist construction tested would not qualify for its design load of 40 psf.

R. F. LUXFORD.[6]—In Mr. Stern's discussion, he emphasizes the use of hardened high-carbon steel helically threaded nails. While trusses have been built using hardened threaded nails, a discussion of their merits is beyond the scope of this paper. Practice has demonstrated that perfectly satisfactory wood trusses can be designed and built using either glue or common nails for attaching gusset plates.

In general, the writer is in agreement with the statements made by Mr. Countryman. While he states that lumber need not be dry for nailed trusses, Mr. Countryman might well agree that a better truss would result by the use of dry lumber.

---

[5] Laboratory Bulletin 54-A, Douglas Fir Plywood Assoc., Tacoma, Wash.

[6] Engr., Forest Products Lab., Forest Service, U.S. Dept. of Agric., Madison, Wis.

AMERICAN SOCIETY OF CIVIL ENGINEERS
Founded November 5, 1852
TRANSACTIONS

Paper No. 3094

TOOLS AND TECHNIQUES FOR DEWATERING

By Byron J. Prugh,[1] M. ASCE

SYNOPSIS

The paper undertakes a description and comparison of the use of present day dewatering tools including conventional wellpoints; high-lift systems with ejectors, submersible or turbine pump units; sand drains; and grout curtain walls. Construction job examples of the use of contemporary dewatering tools are given.

INTRODUCTION

The foreword to a recent handbook[2] on dewatering started out with the phrase, "The science of wellpointing is still an inexact science". The statement may be extended to include all dewatering. But while dewatering is still an inexact science, constant progress has been made in the analysis of soil properties and in procedures for estimating the volume of water to be expected for the dewatering and/or pressure relief of construction excavations. Concurrently with the development of new analytical procedures, the tools used in dewatering and pressure relief systems have been improved and new installation techniques devised. The term tools refers to the equipment and procedures being used to successfully dewater construction excavations.

A dewatering and/or pressure-relief system must be economically evaluated from three specific cost factors:

1. Initial cost of equipment, either rental or purchase.
2. Installation and subsequent removal of the equipment.
3. The operation of the system after installation.

Note.—Published essentially as printed here, in February, 1960, in the Journal of the Construction Division, as Proceedings Paper 2356. Positions and titles given are those in effect when the paper or discussion was approved for publication in Transactions.

[1] Research Dir., Moretrench Corp., Rockaway, N. J.

[2] Moretrench Handbook, April 1958, (Private printing and distribution).

Ironically enough, the first item covering the rental or purchase of the equipment (and transportation) is usually the smallest of the three cost items, yet the equipment cost is often used as a comparative basis in evaluating dewatering systems rather than the overall costs. The latter, which include the installation-operation of the system, would provide a more realistic basis. A contractor often finds that while the rental or purchase cost of equipment is small, the total cost to install that particular system and to operate it for the life of the job far exceeds his original estimate. His purchasing agent has scored a "cost of equipment" reduction, overlooking the engineering and operational factors. On an equal volume basis, several small gasoline pumps will rent for less than one large diesel pump. This apparent saving is reversed when fuel, maintenance, and operating labor costs are considered.

DEWATERING EQUIPMENT COVERS CONSIDERABLE RANGE

Dewatering equipment falls into several broad categories. A multitude of the smaller shallow jobs such as manholes, catch basins, small pipelines, tank pits, etc., or rock and semi-impervious excavations, are done by "open pumping", using either diaphragm or self-priming centrifugal type pumps with the proper utilization of auxiliary devices such as underdrains, filter blankets and sumps. Most foundation engineers discourage open pumping in the vicinity of bearing foundations due to the loosening of the soil by upward water movement. Unless drainage ditches surround the area with deep collecting sumps, the loosening of soil caused by the upward water flow may cause settlement of the completed structure.

The second major dewatering system is the so-called "conventional wellpoint system". Based on the total job dewatering costs, wellpoint systems are generally cheaper than any other method. This holds true even on deep excavations where multi-stage wellpoint installations are used. Each stage of a conventional wellpoint system consists of the wellpoints, usually 1-1/2 in. or 2 in. pipe size, collecting main or "header pipe", discharge piping and wellpoint pumps which consist of centrifugal pumps continuously primed with vacuum pumps.

With proper design, wellpoint pumps may be centrally located. Perhaps the chief advantage of the wellpoint system is its versatility. Soil conditions may not be fully revealed in the original borings and when unexpected dewatering conditions develop, the wellpoint system can be readily adapted to it. Wellpoints can be added in weak locations, additional pump capacity can be supplied and wellpoint screens can be raised or lowered with a minimum of difficulty. Header and discharge pipe can be jobs which are relocated to accommodate construction activities.

Wellpoint innovations of the last decade are now standard in wellpoint design such as: the interconnecting and hydraulic design of several wellpoint stages, at different elevations, to allow one large centralized pump location; the installation of the wellpoint screens in pervious rock formations such as disintegrated mica schist or sandy limestone, by rotary drills or holepunchers; and the use of wellpoints in the consolidation of compressible fine grained soils, or the stabilization of fine grained soils.[3]

Wellpoints may be of any overall length, especially in pressure relief systems where the screen location is governed by the location of the Aquifer. Up to 70 ft or 80 ft overall wellpoints have been installed using the one third or two point methods of lifting into a vertical position. One of the fundamental limitations of a conventional wellpoint system is the available suction lift per stage which falls between 15 ft and 25 ft, depending upon the design. Therefore, certain types of construction, usually[4] deep excavations with limited physical dimensions (such as tunnels, small deep pits, deep city buildings, etc.) sometimes require the use of the third major dewatering system, temporarily called by the writer, "high lift systems". A "high lift system" employs a pump device in the bottom of a large diameter well screen which removes the suction lift limitation.

---

[3] "Stabilization of an Ore Pile by Drainage," by K. Terzaghi and R. B. Peck, Proceedings, ASCE, Vol. 83, SM1, January, 1957.

All of the deep wellpoint or high lift methods may have a vacuum applied to the casing and through the well screen to the soil. Vacuum application greatly increases the ground water yield from the soil to the well but it simultaneously reduces the capacity of the pumping devices by reducing the available net positive suction head. This vacuum application distinguishes the high lift system from the conventional type of deep well installation which depends on gravity drawdown alone. Pumping equipment for high lift systems is normally of a design intended for water supply installations where the well yield exceeds the pump capacity. On the other hand, in dewatering, the pump capacity must always exceed the well yield and there results a "water-starved" condition which can damage conventional water supply equipment unless precuations are taken.

High lift systems are also applicable to soil consolidation over large areas where a large drawdown and/or partial vacuum application to the underside of a compressible layer is desired. Both types of installations are usually governed by physical rather than economical considerations, and considerable technical knowledge is necessary. Each job must be individually designed. The design of a high lift system should be made by a competent engineer or firm to obtain the maximum efficiency at the lowest cost. Three of the major high lift pump devices are:

Water Ejectors or Eductors.—This is a relatively low cost unit allowing the high lift screens to be spaced closer together at reasonable cost. Individual ejectors have a range of from 5 gpm to 60 gpm. They require the use of two parallel headers, one as a pressure supply, the second as a collecting main. The collecting main discharges through a large vented tank which serves to store water for priming the system. Of great importance is the sizing of the correct ejector to the yield of the wellpoint screen. The motive force is water under pressure with a supply yield ratio of 1:1 or 1.2:1, which actually more than doubles the normal horsepower required to pump a certain gallonage of water from the ground. Even with the optimum sizing of ejectors, the efficiency is only approximately one-third of a centrifugal pump.

For any type of economical operation, ejector nozzles and throats must be changed after the initial pumpdown to obtain reasonable efficiency. For example, as wellpoint yield drops off after prolonged pumping, the ejector internals should be changed to reduce the power input proportionally. Change of internals should also be made if individual pumping tests reveal incorrect sizing of ejector for the ground water yield to the well screen.

Because of power considerations, the maximum practical capacity of an ejector operated high lift system is 1,500 gpm to 2,000 gpm, This usually limits

---

[4] Liberal use of word "usually" is necessary to avoid arguments due to exceptions in all phases of dewatering.

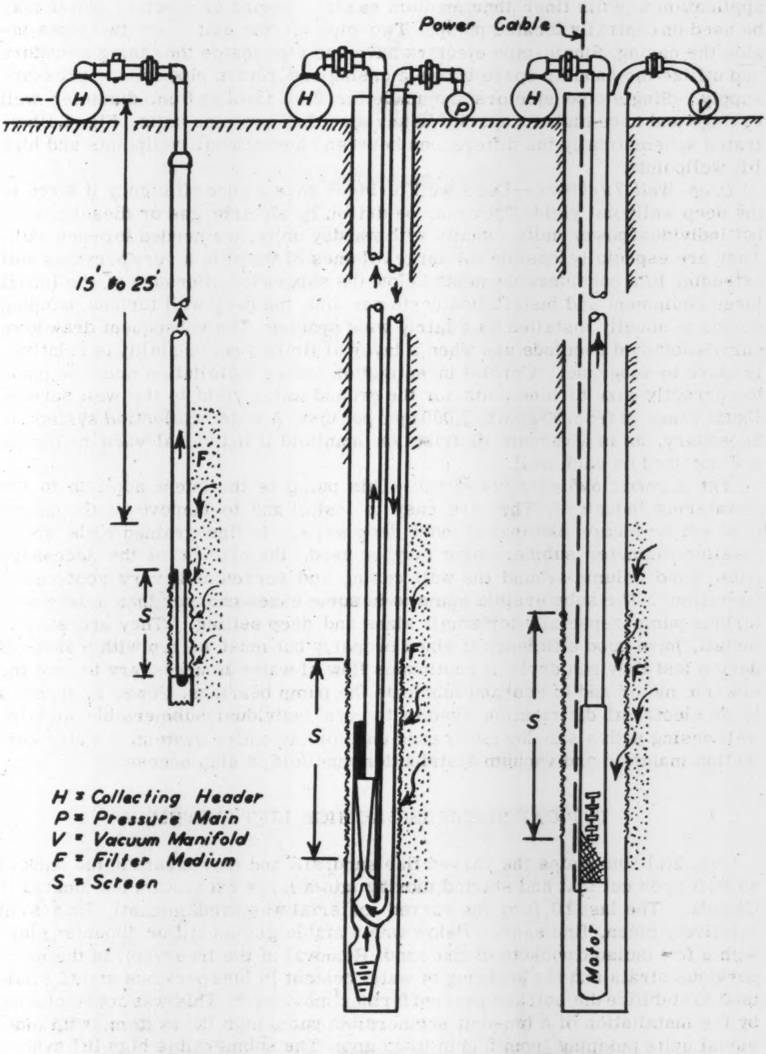
Power Cable
H
H
P
H
V
15' to 25'
F
S
S
F
S
Motor
H = Collecting Header
P = Pressure Main
V = Vacuum Manifold
F = Filter Medium
S = Screen
WELLPOINT
2" or 1½"
SELF-JETTING
EJECTOR
2" to 8"
DOUBLE PIPE
SUBMERSIBLE
4" to 12"

FIG. 1

application to soils finer than medium sands. Engine or electric power may be used on centrally located pumps. Two-pipe ejector units have two pipes inside the casing. Single-pipe ejectors have one pipe inside the casing as return and utilize the annular space between casing and return pipe for the pressure supply. Single pipe ejectors are made for 2 in. through 6 in. diameter well casings and have higher capacity in any size than two pipe units. Fig. 1 illustrates schematically the differences between conventional wellpoints and high lift wellpoints.

Deep-Well Turbines.—Deep-well turbines have a good efficiency if sized to the deep wellpoint yield. They may be driven by electric, gas or diesel power, but individual power units, usually with standby units, are needed for each well. They are especially feasible for large volumes of water in a very pervious soil extending to a considerable depth below the subgrade. Because of the initial large equipment and installation costs per unit, the deep well turbine pumping device is usually installed on a fairly wide spacing. The subsequent drawdown curves obtained preclude use when a layer of limited permeability is relatively close to subgrade. Careful investigation before installation must be made to correctly size turbine units for the ground water yield to the well screen. Usual range is from 50 gpm to 2,000 gpm per unit. A water collection system is necessary, as is a vacuum distribution manifold if individual vacuum pumps are not used on each well.

The Electric Submersible Pump.—This pump is the latest addition to the dewatering industry. They are easy to install and to remove as the casing need not be plumb like that of most deep wells. In fine-grained soils where smaller diameter submersibles may be used, the placing of the necessary filter sand column around the well casing and screen is a very economical operation. The submersible pump is in some cases cheaper than a deep well turbine pump especially for small sizes and deep setting. They are easy to install, have good efficiency if sized properly but must be run with a shut-off device lest they run dry. A continuous flow of water is necessary to cool the electric motor and to cool and lubricate the pump bearings. Power is supplied by an electrical distribution system to each individual submersible high lift well casing with a standby generating unit for the entire system. A water collection manifold and vacuum distribution manifold is also necessary.

TYPICAL SUBMERSIBLE HIGH LIFT SYSTEM

Fig. 2(a) illustrates the varved fine sand, silt and clay layers in the bank of an 80 ft open cut that had started moving into a large excavation job located in Canada. The last 10 ft of the varved material was predominantly layers of relatively clean, fine sand. Below was a stable glacial till or "boulder clay" with a few isolated pockets of fine sand. Removal of the free water in the more pervious strata and the lowering of water content in less pervious strata would tend to stabilize the soil and prevent further movement. This was accomplished by the installation of a ten-unit submersible pump high lift system, with individual units pumping from 5 gpm to 50 gpm. The submersible high lift system lowered the ground water from the original level of 20 ft below ground surface to 60 ft over a horizontal distance of 770 ft.

Fig. 2(b) shows an 80 ft long, 12 in. diameter casing being jetted and driven into position by a 100 ft holepuncher. A high lift well screen with riser pipe and the correct filter medium is placed inside this 12-in. installation casing

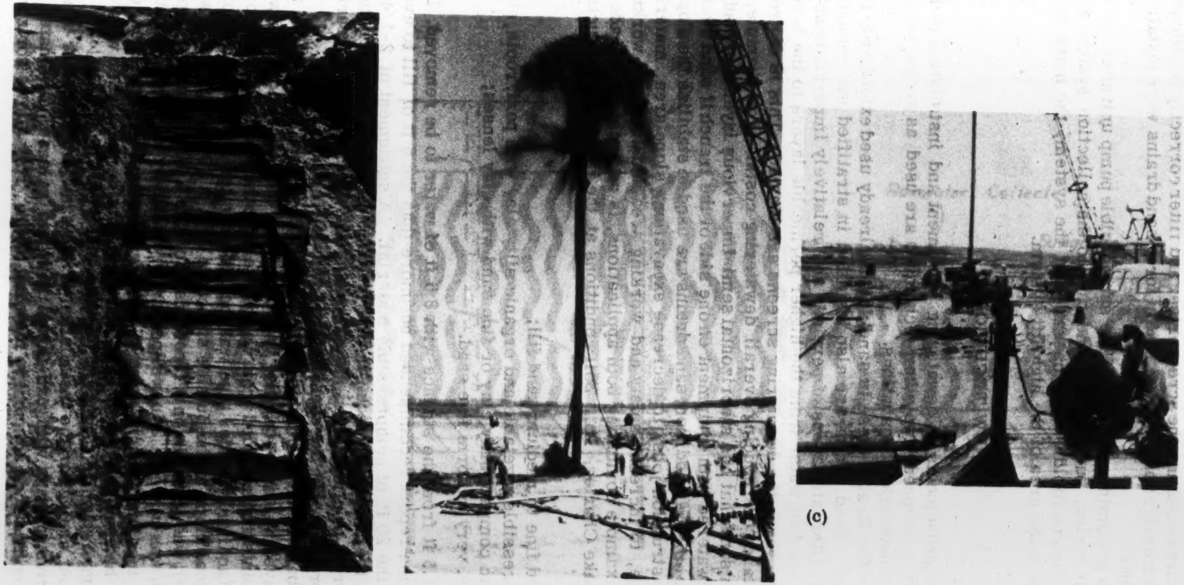

(a) (b) (c)

FIG. 2

which is then withdrawn leaving the screen, riser and filter correctly positioned in the ground. Piezometers and approximately forty sand drains were installed in a similar manner.

Fig. 2(c) shows preliminary testing of the submersible pump unit after being placed in the well casing, but before connecting to the collection system and vacuum distribution manifold. Upon operation of the system, the mass soil movement ceased in the area of the high lift system.

NEW TECHNIQUES

Besides the improvements in dewatering equipment and installation techniques previously mentioned, two other techniques are used as supplemental aids to dewater construction excavations.

Sand Drains.—The first of these is sand drains already used extensively for soil consolidation. Sand drains are also installed in stratified or laminated soils that contain alternate layers of pervious and relatively impervious soil. The sand drains conduct water from the higher permeable layers to the lower permeable layers where the dewatering screens are located. This is of great economic importance in reducing overall dewatering costs. For example, a pipeline trench in sand that has a horizontal semi-impervious layer above subgrade, may be dewatered with equipment on one side of the trench if sand drains are placed on the other. In addition, sand drains are used to stabilize the slopes (or banks) of construction jobs, to decrease excavation, slope area, material handling distance, to increase safety and working area and to better working conditions. An example combining both applications, is an excavation made in a swamp near Lake Charles, La. Soil conditions at the time of construction were:

6 ft of dredged fine to medium sand fill;
20 ft of compressible vegetable and organic silty clay with peat, roots, etc.;
4 ft of medium compact silty clay or fine sand with clay lenses;
20 ft of dense, very uniform fine sand.

Subgrade was 14.5 ft from the surface with 8.5 ft of water to be removed. The original foundation report recommended not more than the 6 ft of fill to avoid shear action in the 20 ft of compressible material. A settlement of 2-1/4 ft was expected in the compressible layer in 2 yr due to the 6 ft of fill. Structure was to be supported on piles driven into the dense fine sand. Structure bearing design was no problem, but the construction excavation was.

Dewatering, bank stabilization and reduction of excess pore pressures in the compressible layer was accomplished by surrounding the excavation area with 38 ft long wellpoints that extended from water level into the dense, very uniform fine sand layer (aquifer). Header pipe was located at water level with a 2 horizontal to 1 vertical slope to the outside structure line. A 39 ft long casing with teeth (bog cutter), was jetted in on 5 ft centers to create a 10 in. diameter hole, in each of which was placed a 2 in. wellpoint surrounded by a uniform medium sand as a filter medium. Three rows of sand drains were also installed, one 15 ft inside the header, the others 15 ft and 30 ft outside the header with the sand drains staggered on 15 ft centers in each row. (Fig. 3).

Use of a jetted casing for the installation of the sand drains rather than a conventional driven casing with end closed with flap release, eliminates the "smear" or remolded zone adjacent to the sand drain. This allows horizontal

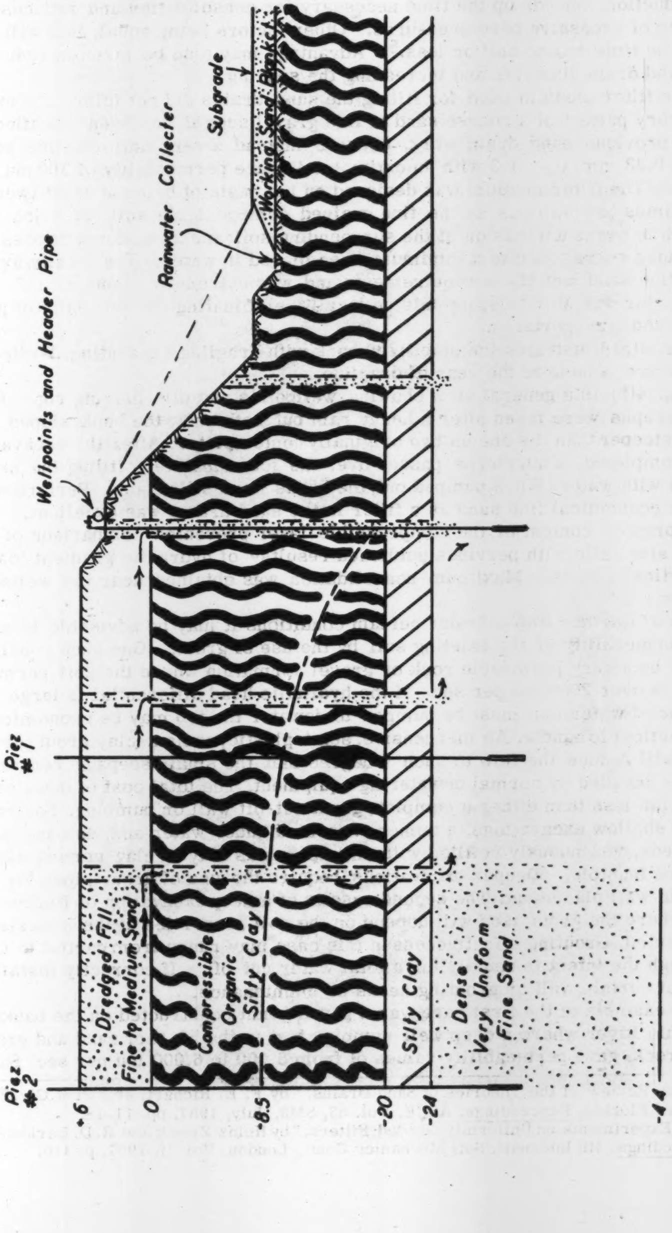
Wellpoints and Header Pipe
Rainwater Collecter
Subgrade
Working Sand Blanket
Piez #1
Piez #2
+6
0
-8.5
-20
-24
-44
Dredged Fill
Fine to Medium Sand
Compressible
Organic
Silty Clay
Silty Clay
Dense
Very Uniform
Fine Sand

FIG. 3.—SAND DRAINS AND WELLPOINTS

permeability or flow to approach that of the normal ground rather than undergo reduction, speeds up the time necessary for consolidation and reduces the buildup of excessive pore pressures. Other factors being equal, this will reduce the time to one half or less.[5] Advantage may also be taken in reducing the sand drain diameter and increasing the spacing.

The filter medium used for filling the sand drains did not follow the usual arbitrary pattern of a coarse sand to fine gravel such as has been specified on most previous sand drain work, but was instead a very uniform fine sand, $D_{50} = 0.23$ mm, $U_c = 1.3$ with an estimated inplace permeability of 300 mu per second. The filter medium was designed on the basis of being at least twenty-five times as pervious as the fine grained compressible soil; of being fine enough to prevent intrusion of the surrounding soil; and as uniform as possible to reduce segregation to a minimum when placed in water. The locally available fine sand met these requirements and was extremely economical. The contractor was able to scoop this up locally, eliminating the necessity of purchase and transportation.

Fig. 4(a) illustrates the stabilized bank with dragline excavating. Wellpoint pumps are visable to the rear of dragline.

Fig. 4(b) is a general view showing wellpoints and pile driving rig. Both photographs were taken after a heavy rain but both show the bank slopes that were steeper than the one on two originally contemplated. After the excavation was completed, a hurricane passed over the job completely filling the excavation with water. When pumped out, the banks were still stable. Performance of the economical fine sand as a filter in the sand drains was excellent. The high organic content of the compressible layer prevented comparison of the grain size ratio with pervious published results[6] of hydraulic gradient losses in vertical filters. Maximum consolidation was obtained near the wellpoint header.

Grout Curtain Wall.—Under certain conditions it may be advisable to alter the permeability of the existing soil by the use of grout. One such condition would be a very permeable rock or gravel formation where the soil permeability is over 2000 mu per sec. If the hydraulic head differential is large, the volume of water that must be pumped to dewater the job may be economically impractical to handle. An inexpensive, semi-plastic, cement-clay grout curtain wall will reduce the flow to such a degree that the small seepage remaining may be handled by normal dewatering equipment. The total cost of dewatering being far less than either a complete grout cut-off wall or pumping. For relatively shallow excavations, a trench excavated under water and, as excavation proceeds, continuously refilled with an impervious clay or clay-cement slurry may be feasible. Deeper excavations require the use of grout pipes for the curtain wall placement. The second case is of a deep excavation of limited extent where the grout used will depend on the soil properties of the material to be grouted. Grouting effectiveness in this case may range from partial to total although the intent is usually for a total water cut-off. If correctly installed, a grout curtain wall or grouting needs no maintenance.

An example of the first case was a power plant constructed on the banks of the Ohio River where a deep well pumping test in the 50 ft of sand and gravel over rock, gave permeability values of from 5,000 to 6,000 mu per sec. Sandy

---

[5] "A Review of the Theories of Sand Drains," by F. E. Richart, Jr., Prof.Civ.Eng., Univ. of Florida, Proceedings, ASCE, Vol. 83, SM3, July, 1957, pp. 11-18.

[6] "Experiments on Uniformly Graded Filters," by Heinz Zweck and R. D. Daridenkoff, Proceedings, 4th Internatl. Soil Mechanics Conf., London, Vol. II, 1957, p. 410.

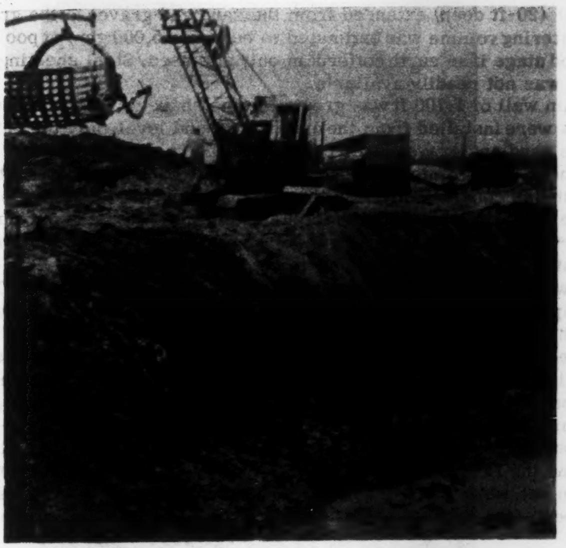

(a)

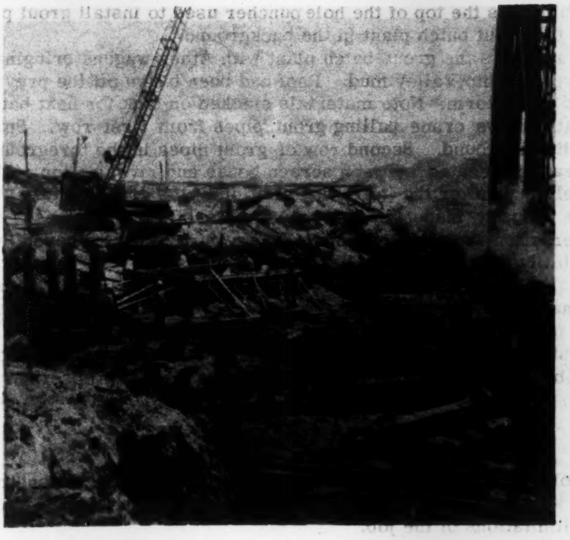

(b)

FIG. 4

clay (loam) (20-ft deep) extended from the sand and gravel to the ground surface. Dewatering volume was estimated to be from 15,000 gpm at pool to 50,000 gpm at flood stage if an earth cofferdam only was used. Steel sheeting was suggested but was not readily available.

A curtain wall of 1,700 ft was grouted in the shape of a U". While the 70 ft grout pipes were installed from the original ground level, only the entire thickness of the sand and gravel layer overlaying the rock, varying from 20 ft to 50 ft in thickness, was grouted for a vertical surface area of approximately 50,000 sq ft. Cost was considerably less than a single row of steel sheet piling. Despite some installational errors, including one hole in the grout curtain wall you could "drive a truck through", the volume of water pumped was reduced to approximately 30% of the minimum expected.

There were roughly, 800,000 gal of grout pumped in through 10,000 lineal ft of grout pipe or some 16 gal per sq ft of curtain wall. This is equivalent to a wall 5 ft thick based on a 40% porosity. A conservative average of 30,000 gal was pumped per shift which required the use of approximately 4 tons per hr of dry material. Grout was mixed in batches of 4,000 gal in two alternately used flocculation tanks. Pumping was at the rate of from 75 gpm to 200 gpm.

An admixture of certain salts and dyes was added to the cement-clay grout which imparted color so that mixtures could be readily identified, strength increased and the flocculation and set times could be varied. The cement-clay grout when set, while semi-plastic, has no thixothropic properties as exhibited by pure bentonite grouts. After setting it will not move under hydrostatic pressure.

Fig. 5(a) shows typical stratified soil ranging from coarse sand to well graded sand and gravel to uniform medium gravel.

Fig. 5(b) shows the top of the hole puncher used to install grout pipes, grout pipes and the grout batch plant in the background.

Fig. 6(a) shows the grout batch plant with Athey wagons bringing material through typical Ohio Valley mud. Roof had been blown off the previous day in a rain and wind storm. Note materials stacked on tank for next batch.

Fig. 6(b) shows crane pulling grout pipes from first row. Spilled grout shows white on ground. Second row of grout pipes in the foreground was not used. Crane is located between screen house and river on top of dyke. Approximately 2 yr after the initial installation of the grout curtain wall, it was able to be visually inspected to determine its effectiveness as a dewatering aid. Observation was made when the dyke was partially removed, eliminating any possibility of a silt blanket over the river bottom.

Fig. 7(a) shows a test pit dug by a floating rig on the river 12 ft away. Major pumping had stopped in the area and water level was being held 10 ft below river some 200 ft from test pit by pumping equipment yet the test pit is dry 8 ft at this spot. Grout penetrated 3 ft into coarse sand, 6 ft to 10 ft into openwork gravel.

Fig. 7(b) shows a cross section through the test pit with observed conditions.

CONCLUSIONS

1. Tools and methods to be considered when designing a construction dewatering system primarily depend on the soil properties at the site and the physical limitations of the job.

2. Overall dewatering costs should be considered rather than one item, such as rental of dewatering equipment. By altering the dewatering method

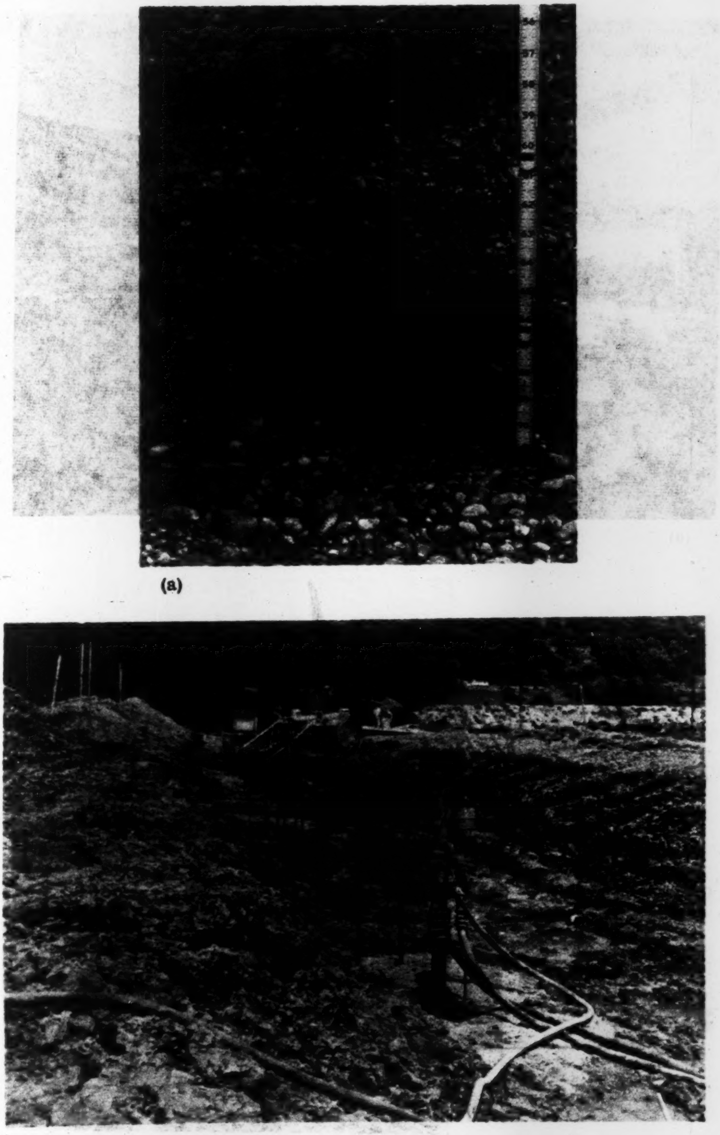

(a)

(b)

FIG. 5

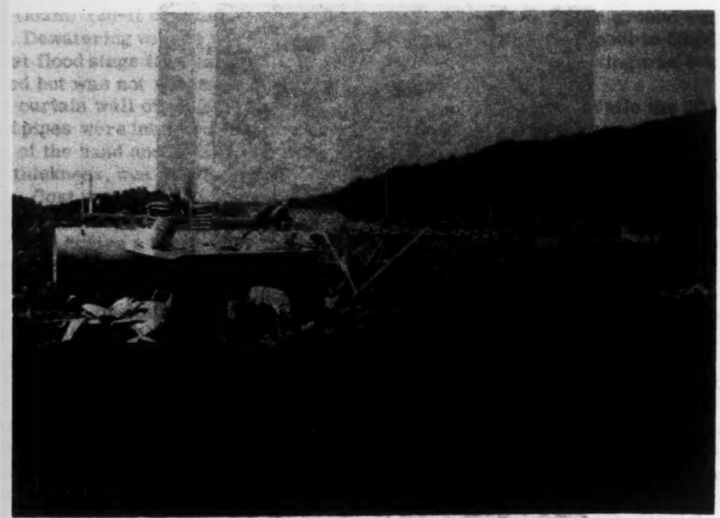

(a)

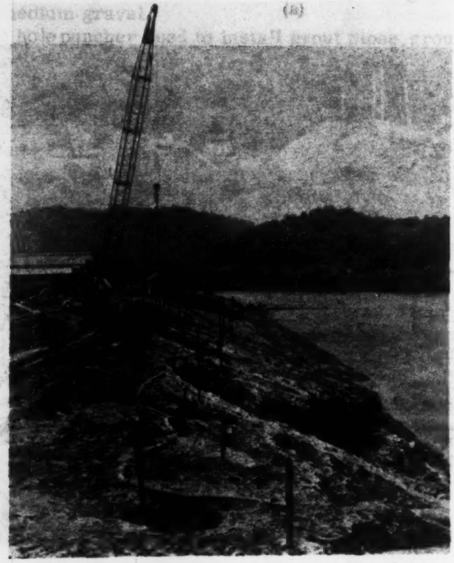

(b)

FIG. 6

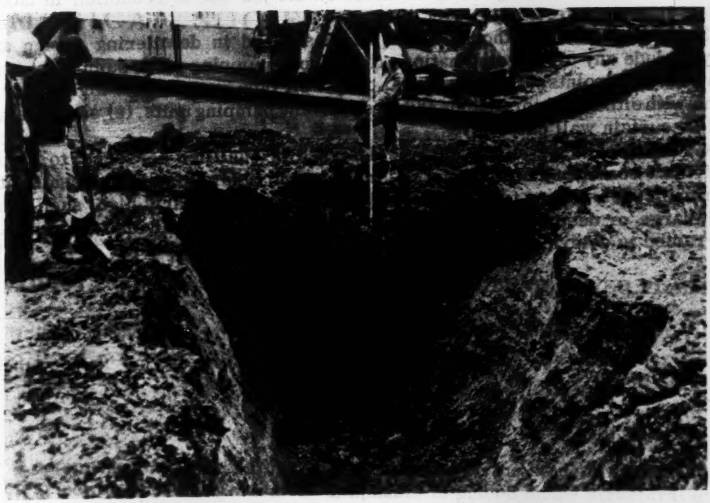

(a)

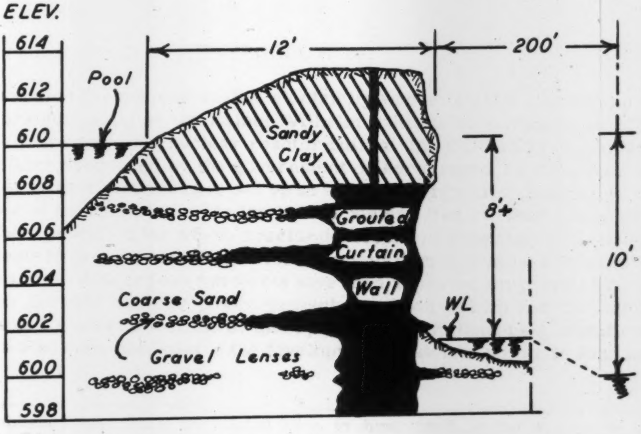

ELEV.
614
612
610
608
606
604
602
600
598
12'
200'
Pool
Sandy Clay
Grouted
Curtain
Wall
8'+
10'
Coarse Sand
WL
Gravel Lenses

(b)

FIG. 7

and tools, overall savings may be made on the job due to reduction in labor, excavation or materials.

3. All tools and methods should be considered in dewatering design and may include any of, or combinations of, (a) open pumping from sumps, (b) conventional wellpoints, (c) conventional deep well type pumping, (d) high lift systems with either ejector, submersible or turbine pumping units, (e) sand drains, and (f) curtain wall cut-offs.

4. All dewatering jobs should be designed by qualified personnel to fit the individual conditions of that particular job and to obtain maximum results at a minimum cost. Where total dewatering costs are particularly high, such as on very large or deep excavations, extensive engineering analysis in advance is warranted to determine the most suitable and economic method.

AMERICAN SOCIETY OF CIVIL ENGINEERS
Founded November 5, 1852
TRANSACTIONS

Paper No. 3096

STRUCTURAL ENGINEERING ASPECTS OF NUCLEAR POWER PLANTS

By Lewis L. T. Au[1] and Edward Y. W. Tsui,[2] Fellows, ASCE

SYNOPSIS

A comprehensive description and discussion of the structural features of nuclear power plants is presented. Emphasis is placed on the structural engineering aspects which depart from conventional power systems. Stress analyses in reactor pressure vessels with supports under various loading conditions as well as temperature gradients are critically reviewed. The effect of dynamic forces and wind on structures is also examined.

INTRODUCTION

The foundation for nuclear-fueled electricity was established by the splitting of an uranium atom at the Kaiser Wilhelm Institute of Germany, in 1938, and by the first controlled nuclear reactor built at the University of Chicago, in 1942. Either sponsored by the government or encouraged by the power industry, most large countries have set up an atomic energy organization for the development of nuclear power. In the United States, five nuclear power projects have been installed for a 5-yr reactor development program. Ten nuclear power projects have been established for the power demonstration reactor program. Also, five nuclear power projects have been approved for private license applications and one nuclear power project has been set up for the armed forces. Table 1 shows the outline of these projects. Simultaneously, significant efforts have also been recorded in the development of atomic power in England,

---

Note.—Published essentially as printed here, in June, 1960, in the Journal of the Structural Division, as Proceedings Paper 2509. Positions and titles given are those in effect when the paper or discussion was approved for publication in Transactions.

[1] Structural Engr., Steinman, Boynton, Gronquist, and London, New York, N.Y.

[2] Research Engr., Missile and Space Div., Lockheed Aircraft Corp., Sunnydale, Calif.

TABLE 1.—NUCLEAR POWER PLANTS IN THE UNITED STATES

Program	Sponsor	Location	Reactor Type	Fuel	Gross Electric Power, in mw	Plant Cost, in dollar million	Operating Date
Five Year Reactor Development	AEC & Atomic International	Santa Susana, Calif.	Sodium graphite	2.8% of U-235	6.0	10	July, 1957
	AEC	Lemont, Ill.	Boiling water	Slightly enriched U-235	4.5	17	Dec., 1956
	AEC	Oak Ridge, Tenn.	Aqueous homogeneous	Uranyl sulfate in heavy water	2.0	.47	1956
	AEC	Arco, Idaho	Fast breeder	Highly enriched U & U-238	15.0	40	1958
	AEC & Duquense Light Co.	Shippingport, Pa.	Pressurized water	Highly enriched U & CO_2	60.0	55	1957
Power Demonstration Reactor	Yankee Atomic Elec. Co.	Rowe, Mass.	Pressurized water	2.7% U-235	134.0	35	1958
	Atomic Power Development Asso.	Detroit, Mich.	Fast breeder	20% U-235	100.0	55	1959
	Consumers Public Power Dist.	Beatrice, Neb.	Sodium graphite	1.8% U-235	75.0	25	1958
	City of Orlando, Fla.	Orlando, Fla.	Liquid metal fueled	Highly enriched U-Bi solution	25-40	21-33	1960-1961
	City of Piqua, Ohio	Piqua, Ohio	Organic moderated	3% U-235	12.5	6	1960
	City of Holyoke, Mass.	Holyoke, Mass.	Gas-cooled	3% U-235	15.0	7	1960-1961
	Chugach Elec. Asso.	Anchorage, Alaska	Sodium cooled	2.0% U-235	10.0	8	1961
	Wolverine Elec. Corp.	Hersey, Mich.	Homogeneous	Enriched U	10.0	4	1959
	University of Fla.	Gainesville, Fla.	Pressurized water	30-40% U-235	2.0	2	1959
	Penn. Power & Light Co. & Westinghouse Elec. Co.		Homogeneous		70-150	108	1963
Private Corporations	Pacific Gas & Elec. Co. & G.E.	San Francisco Bay, Calif.	Boiling water	Enriched UO_2	5.0		1957
	Consolidated Edison Co.	Buchanan, N.Y.	Pressurized water	90% U-235 THO	236.0	55	1959
	Commonwealth Edison Co. & Nuclear Power Group, Inc.	Dresden, Ill.	Boiling water	1.1% U-235	180.0	45	1960
	Penn Power & Light Co.	Pa.	Homogeneous	U in liquid form	15.0		1962
	Elk River Rural Coop. Power Asso.	Elk River, Minn.	Boiling water	Natural U U-235 spikes	22.0	7	1960
Armed Forces	U.S. Army	Ft. Belvo River, Va.	Pressurized water	Slightly enriched U	2.0		Apr., 1957

France, Russia, and some other countries. Table 2 shows the corresponding projects being carried out by the British and French. After a brief review of these works, it is obvious that the progress of the nuclear power industry is rapidly accelerating. On the other hand, the conventional power plants will find their ultimate in capacity and fuel supply. It can be expected that the development of the nuclear power plants will attain its full swing in the near future.

Unfortunately, this new development presents many new problems to structural engineers. The major problems are created primarily from radioactivity and heat transfer. Other problems are the planning of structures to accommodate the new facilities and special equipment, and finding appropriate materials to perform various functions in order to provide structural supports, protect personnel safety, supply channels for the passage of the heat transfer medium, etc. Besides, if the plant site is located in an active earthquake zone, the most probable seismic force to be used in the design of the reactor and other special structures also presents an interesting problem. These structural features will be discussed after a comparison between the conventional and nuclear power plants.

COMPARISON OF CONVENTIONAL AND NUCLEAR POWER PLANTS

The difference between a conventional and a nuclear power plant may be briefly outlined as follows: (a) in fuel—coal versus uranium, (b) in equipment—furnace versus reactor, and (c) in reaction—chemical versus nuclear. Fig. 1 shows a schematic view of each type of power plant.

In a steam plant, burning of coal in a furnace produces heat which is delivered to the boiler to generate steam for the turbo-generator where mechanical energy is changed to electrical energy (Fig. 2). Whereas in a nuclear plant, fissioning of uranium atoms in the reactor produces heat which, in turn, is conveyed to the heat exchanger through a cooling system. The heat exchanger then generates steam for the production of electricity. Fig. 3 shows the general layout of the Calder Hall Nuclear Power Station.

The burning of fuel is a chemical reaction which involves changes in arrangement of electrons of atoms or molecules. This change is very small, only one-third of a billionth of coal mass converts to heat or 1 lb of coal produces 13,000 Btu, for example.

Fissioning of atoms is a nuclear reaction which involves changes in arrangement of neutrons, protons, and electrons of atoms as well. As a consequence, a part of the mass is missing that actually changes to a tremendous amount of energy according to Einstein's formula:

$$E = 9 \times 10^{20} M \quad \ldots\ldots\ldots\ldots\ldots\ldots \quad (1)$$

in which E is energy, in ergs, and M is mass, in grams.

For example,[3] when an U-235 atom captures a neutron to split to Zr-90 and Nd-144, it can be shown that the energy released is approximately 182^{mev}. Assuming 10% efficiency, should 1 lb of U-235 be fissioned, the energy released would be about 248,000 x 13,000 Btu, which is approximately 250,000 times more than that produced by burning 1 lb of coal.

If one neutron from the first fission be captured by another uranium atom, the process can continue in a chain reaction. This reaction, however, will

---

[3] "Introduction to Nuclear Engineering," by F. A. Fohnman, Univ. of Colorado, 1953.

TABLE 2.—NUCLEAR POWER PLANTS

Authority	Location	Reactor Type	Fuel	Gross Electric Power, in MW	Plant Cost, in dollar million	Operating Date
			(a) British			
U.K. AEA	Calder Hall, Cumberland 2 Identical	Thermal heterogeneous	Natural uranium	130 Total net	42-56	1956-1957
	Calder Hall 2 Chapelerous Dumfries-Shire 2	Thermal heterogeneous	Natural uranium	200 Total net		1959-1960
U.K. CEA	Bradwell, Essex 2 Identical	Thermal heterogeneous	Natural uranium	300	100-117	1960-1961
	Berkeley, Gloucestershire 2 Identical	Thermal heterogeneous	Slightly enriched uranium	275 Total net	68-88	1957
	Hinkley Point, Somerset 2 Identical	Thermal heterogeneous	Natural uranium	500 net	168	1961
	Trawsfynydd, Merionethshire, Wales			500		1962
Scotland Elec. Board	Hunterston, Ayrshire, Scotland	Thermal meterogeneous	Natural uranium	320	104	
	Ulster N. Ireland			150	70	1963-1964
			(b) French			
G1	Marcoule	Gas-cooled, graphite moderated	Natural uranium	5.75	20	Sept., 1956
G2	Marcoule	Gas-cooled, graphite moderated	Natural uranium	47.7	30	1958
G3		Gas-cooled, graphite moderated	Natural uranium	47.7	30	1958
EDF-1	Avoine (near Chinon)	Gas-cooled, graphite moderated	Natural uranium	60.0	40	1959

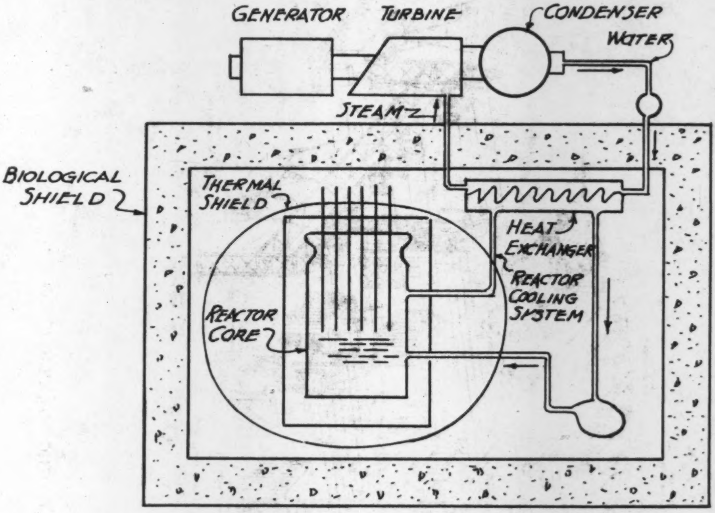
GENERATOR
TURBINE
CONDENSER
WATER
STEAM
BIOLOGICAL SHIELD
THERMAL SHIELD
HEAT EXCHANGER
REACTOR COOLING SYSTEM
REACTOR CORE

NUCLEAR

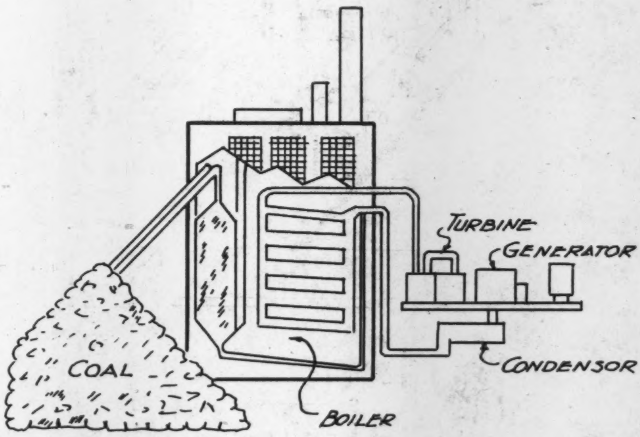
TURBINE
GENERATOR
CONDENSOR
COAL
BOILER

CONVENTIONAL

FIG. 1.—POWER PLANTS

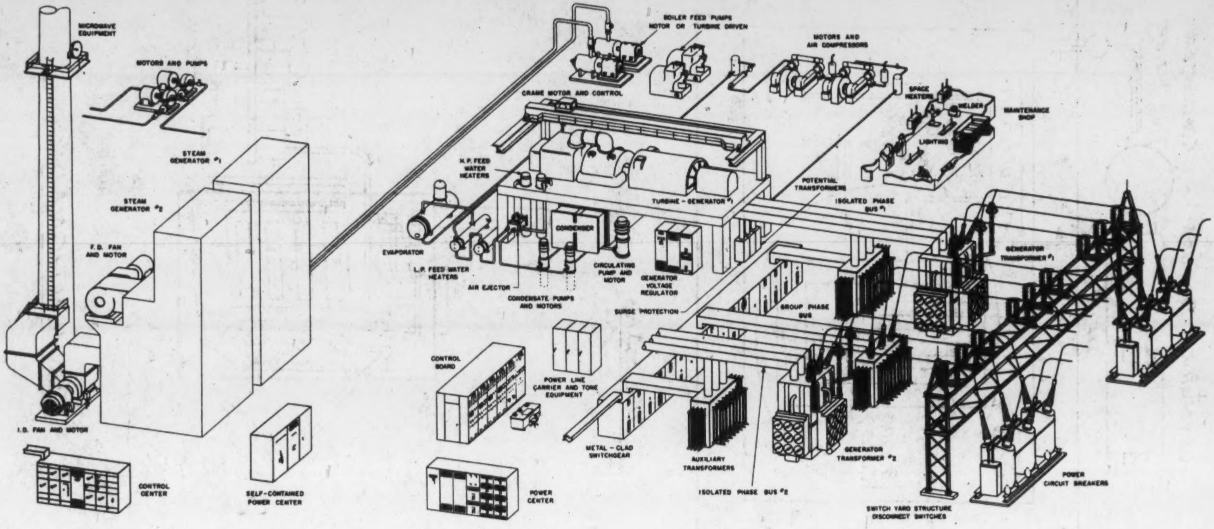
MICROWAVE EQUIPMENT
MOTORS AND PUMPS
STEAM GENERATOR #1
STEAM GENERATOR #2
F.D. FAN AND MOTOR
I.D. FAN AND MOTOR
CONTROL CENTER
SELF-CONTAINED POWER CENTER
BOILER FEED PUMPS MOTOR OR TURBINE DRIVEN
CRANE MOTOR AND CONTROL
MOTORS AND AIR COMPRESSORS
SPACE HEATERS
WELDER
MAINTENANCE SHOP
LIGHTING
H.P. FEED WATER HEATERS
EVAPORATOR
L.P. FEED WATER HEATERS
AIR EJECTOR
CONDENSER
CONDENSATE PUMPS AND MOTORS
CIRCULATING PUMP AND MOTOR
GENERATOR VOLTAGE REGULATOR
TURBINE - GENERATOR #1
POTENTIAL TRANSFORMERS
ISOLATED PHASE BUS #1
GENERATOR TRANSFORMER #1
SURGE PROTECTION
GROUP PHASE BUS
CONTROL BOARD
POWER LINE CARRIER AND TONE EQUIPMENT
POWER CENTER
METAL - CLAD SWITCHGEAR
AUXILIARY TRANSFORMERS
ISOLATED PHASE BUS #2
GENERATOR TRANSFORMER #2
SWITCH YARD STRUCTURE DISCONNECT SWITCHES
POWER CIRCUIT BREAKERS

FIG. 2.—TYPICAL STEAM DRIVEN ELECTRIC POWER STATION

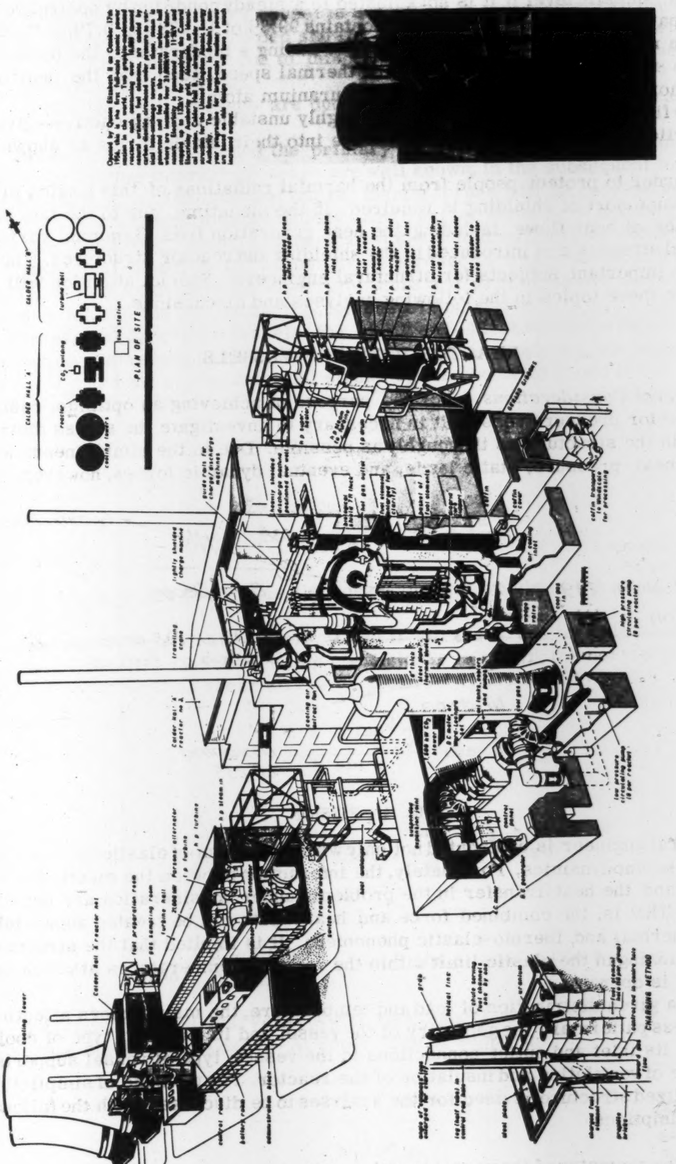
cooling tower
Calder Hall 'A' reactor no. 1
travelling crane
Parsons alternator
turbine hall
CALDER HALL 'A'
CALDER HALL 'B'
reactor
cooling towers
turbine hall
PLAN OF SITE
CHARGING METHOD

FIG. 3.—CALDER HALL NUCLEAR POWER STATION

reach a fantastic level if it is not adjusted to a steady condition by control rods, When natural uranium is used, which contains 99.3% of U-238 and 0.7% of U-235, a chain reaction can be established only by adding a moderator to the fuel mixture to slow down the fast neutrons to thermal speed, such that the neutrons have more chance to hit and capture the uranium atoms.

The fission products themselves are highly unstable and radioactive—giving off particles and energy until they evolve into their stable forms as shown in Fig. 4.

In order to protect people from the harmful radiations of this fission process, some sort of shielding is required. In the meantime, due to the fact that all kinds of heat flows, including the heat generation from Gammas, various thermal stresses are introduced in the shielding and reactor structures. These are the important subjects for structural engineers. Special attention will be given to these topics in the following analyses and discussions.

REACTOR PRESSURE VESSELS

General Considerations.—For the purpose of achieving an optimum design of a reactor pressure vessel, it is necessary to investigate the stress distribution in the structure as thoroughly as possible. Due to the simultaneous action of heat, pressure, static loads, and eventual dynamic forces, however, the structural engineer is confronted not only with a problem of elasticity, but also one of thermodynamics. Fortunately, the interaction between the elastic deformation and the heat transfer in the problems under consideration are usually small. That is, the combined force and heat inputs can be treated separately as isothermal and thermo-elastic phenomena. It is implied that the structure is functioning in the elastic limit within the range of temperatures at which the reactor is operated.

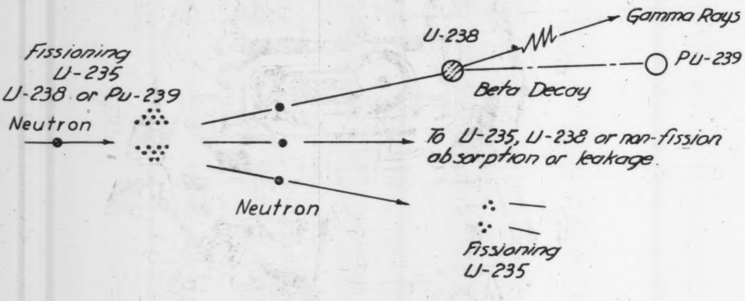

FIG. 4.—FISSION

For a given distribution of load and temperature, the main factors affecting the stress pattern are the geometry of the vessel and its support; type of coolant and its inlet and outlet connections to the vessel; type of vessel supports; and type of ventilation and insulation of the reactor. For the sake of simplicity, an idealized structure is used for the analyses to be discussed, with the following assumptions:

1. The geometry of the vessel is either spherical or a combination of hemispheres and cylinders.

2. The reactor pressure vessel is supported by cylindrical skirts.
3. The reactor is gas cooled and the weight of coolant is negligible.
4. The local stresses due to miscellaneous connection and ligament restraints are not considered.
5. The thermal stresses are due to steady state temperature gradients.

Primary Stresses.—Since the primary or membrane stresses in the shell introduced by the internal pressure are well known, in the subsequent material only those due to dead load and lateral inertia forces will be considered. According to the assumptions previously cited, reactor structures may be grouped into two categories; namely, spherical vessels and cylindrical vessels with hemispherical heads. As far as membrane stresses are concerned, it is further assumed that loads such as moderator core and grid structure are directly carried down to the foundation through supporting skirts.

Stresses in Spherical Vessels (Fig. 5). Case I—Stresses due to Dead Load.—Assuming the vessel is supported all around at an angle ϕ_0, the meridianal stress σ_ϕ and the circumferential stress σ_θ can be determined by

$$\sigma_\phi = \frac{-\,a\,w}{h\,(1+\cos\phi)} \quad \dots\dots\dots\dots\dots\dots \quad (2)$$

and

$$\sigma_\theta = \left(\frac{1}{1+\cos\phi} - \cos\phi\right)\frac{a\,w}{h} \quad \dots\dots\dots\dots \quad (3)$$

in which a, h, w are the radius, thickness, and unit weight of the shell, respectively.

Stresses in Spherical Vessels. Case II—Stresses due to Lateral Seismic Force.—Assuming that the seismic coefficient c is known, the normal stresses σ_ϕ and σ_θ as well as shear stress $\sigma_{\theta\phi}$ can be determined by

$$\sigma_\phi = \frac{c\,w\,a\,\tan^2\frac{\phi}{2}}{h\sin\phi}\cos\theta \quad \dots\dots\dots\dots \quad (4)$$

$$\sigma_\theta = -\,\frac{c\,w\,a}{h}\left(\sin\phi + \frac{\tan^2\frac{\phi}{2}}{\sin\phi}\right)\cos\theta \quad \dots\dots\dots\dots \quad (5)$$

and

$$\sigma_{\theta\phi} = \frac{c\,w\,a\sin\theta}{h\sin^3\phi}\left(-2 + 2\cos\phi + \sin^2\phi\cos\phi\right) \quad \dots\dots \quad (6)$$

Stresses in Cylindrical Vessels with Hemispherical Heads (Fig. 6). Case I—Stresses due to Dead Loads.—At upper edge of support:

$$\sigma_\phi = -\,\frac{a\,w\left(1 - \cos\phi_0 + K\right)}{h\sin^2\phi_0} \quad \dots\dots\dots\dots \quad (7)$$

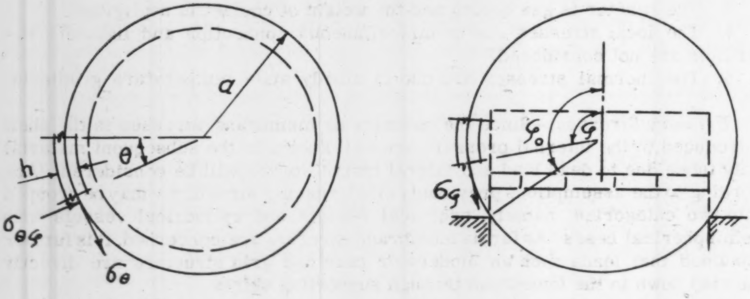
a
θ
h
σθφ
σθ
φ₀
φ
σφ

(a) PLAN (b) PROFILE

FIG. 5.—SPHERICAL VESSEL

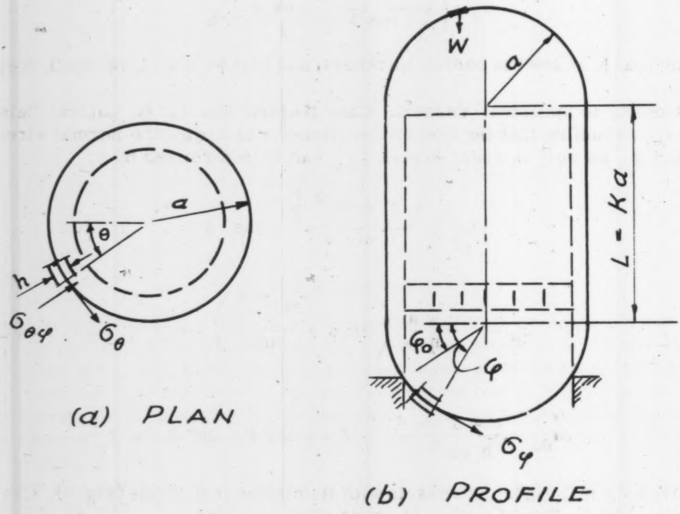
a
θ
h
σθφ
σθ
W
a
L = Ka
φ₀
φ
σφ

(a) PLAN (b) PROFILE

FIG. 6.—CYLINDRICAL VESSEL WITH HEMISPHERICAL HEADS

and

$$\sigma_\theta = \left(\frac{1 - \cos \phi_0 + K}{\sin^2 \phi_0} - \cos \phi_0 \right) \frac{a\ w}{h} \tag{8}$$

At lower edge of support:

$$\sigma_\phi = \frac{a\ w}{h\left(1 + \cos \phi_0\right)} \tag{9}$$

and

$$\sigma_\theta = -\left(\frac{1}{1 + \cos \phi_0} - \cos \phi_0 \right) \frac{a\ w}{h} \tag{10}$$

Stresses in Cylindrical Vessels with Hemispherical Heads. Case II—Stresses due to Lateral Seismic Force.—At the upper edge of support:

$$\sigma_\phi = \frac{a\ c\ w \cos \theta}{h \sin^3 \phi} \left[K \left(\frac{K}{2} + \sin \phi \right) + (1 - \cos \phi)^2 \right] \tag{11}$$

$$\sigma_\theta = \frac{-\ a\ c\ w \cos \theta}{h} \left\{ \sin \phi + \frac{1}{\sin^3 \phi} \left[K \left(\frac{K}{2} + \sin \phi \right) + (1 - \cos \phi)^2 \right] \right\} \tag{12}$$

$$\frac{\partial \sigma_{\theta\phi}}{\partial \theta} - \sigma_\theta \cos \phi + \frac{\partial \sigma_\phi}{\partial \phi} \sin \phi + \sigma_\phi \cos \phi - c\ a\ w\ h \sin \phi \cos \phi \cos \theta = 0 \tag{13}$$

and

$$\left(\sigma_{\theta\phi}\right)_{\theta = 0} = 0 \tag{14}$$

Eqs. 4 through 6 can also be used for the evaluation of stresses at the lower edge of support.

Discontinuity Stresses.—The bending stresses at the junction A of the skirts and spherical vessel due to uniform internal pressure will be analyzed. The same method of approach may be applied for other configurations of vessels. It is assumed that the thickness of the vessel and skirt elements is constant (Fig. 7).

When the difference of the radii of the sphere and skirts is not large, line A-A' of the deformed structure (Fig. 7(b)) may be considered to be horizontal.

Now if E and ν are Young's modulus and Poisson's ratio, respectively, then

$$\lambda_i = \left[3\left(1 - \nu^2\right) / a_i^2\ h_i^2 \right]^{\frac{1}{4}} \tag{15}$$

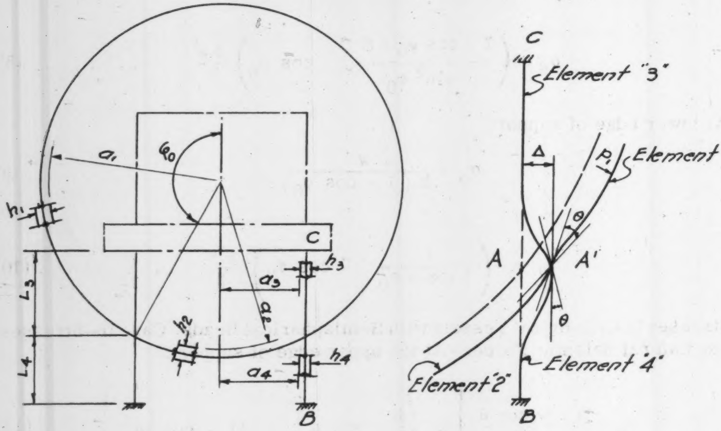
C
Element "3"
Δ
P_1
Element "1"
a_1
φ_0
h_1
θ
C
h_3
A
A'
L_3
a_3
a_2
h_2
θ
L_4
h_4
a_4
Element "4"
Element "2"
B
B

(a) PROFILE (b) DEFLECTED JOINT

FIG. 7.—DETERMINING DISCONTINUITY STRESSES

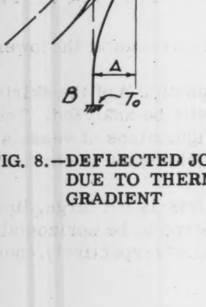
C
C'
θ
θ
A
A'
T_1
Δ
B
T_0

FIG. 8.—DEFLECTED JOINT DUE TO THERMAL GRADIENT

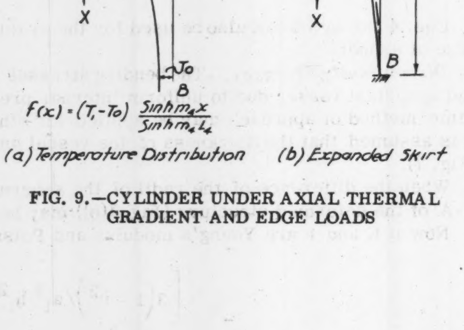
T_1
A'
f(x)
A
T(x)
X
T_0
B
$f(x) = (T_1 - T_0)\,\frac{\sinh m_4 x}{\sinh m_4 L_4}$
Δ
M_4
A'
θ_4
A
W
θ_0
θ
L_4
X
B

(a) Temperature Distribution (b) Expanded Skirt

FIG. 9.—CYLINDER UNDER AXIAL THERMAL GRADIENT AND EDGE LOADS

$$\beta_i = \left[3\left(1-\nu^2\right)\left(a_i/h_i\right)^2\right]^{\frac{1}{4}} \quad \ldots\ldots\ldots\ldots\ldots \quad (16)$$

and

$$D_i = E\ h_i^3/12\left(1-\nu^2\right) \quad \ldots\ldots\ldots\ldots\ldots \quad (17)$$

in which a_i and h_i are the radius and thickness of the element i, respectively. Also, if Δ_0 is the unrestricted horizontal component of displacement of joint A due to internal pressure P_i, then

$$\Delta_0 = \left\{p_i\ a_i^{\ 2}\left(\frac{1-\nu}{2}\right)/E\ h_i\right\}\ \sin\left(\pi-\phi_0\right) \quad \ldots\ldots\ldots \quad (18)$$

in which Δ and θ are the horizontal translation and rotation of joint A, M_i and Q_i are the moment and shear in element i per unit length, and ϕ_0 is the meridianal angle of joint A.

The moments M_i and shears Q_i are related to the unknowns Δ and θ as follows: For the spherical elements (i = 1,2):

$$\frac{2\ \beta_i\ a_i\ \sin^2\phi_0}{E\ h_i}\ Q_i + \frac{2\ \beta_i^{\ 2}\ \sin\phi_0}{E\ h_i}\ M_i = \Delta_0 - \Delta \quad \ldots\ldots \quad (19)$$

and

$$\frac{2\ \beta_i^{\ 2}\ \sin\phi_0}{E\ h_i}\ Q_i + \frac{4\ \beta_i^{\ 3}}{E\ a_i\ h_i}\ M_i = \theta \quad \ldots\ldots\ldots\ldots \quad (20)$$

For the cylindrical skirts (i = 3,4):

$$\frac{1}{2\ \lambda_i^{\ 3}\ D_i}\ Q_i + \frac{1}{2\ \lambda_i^{\ 2}\ D_i}\ M_i = \Delta \quad \ldots\ldots\ldots\ldots \quad (21)$$

and

$$\frac{1}{2\ \lambda_i^{\ 2}\ D_i}\ Q_i + \frac{1}{\lambda_i\ D_i}\ M_i = \theta \quad \ldots\ldots\ldots\ldots \quad (22)$$

Eqs. 19 through 22 may be solved for M_i and Q_i in terms of Δ and θ which, in turn, may be expressed in known parameters λ_i, β_i, D_i, etc. from the following simultaneous equilibrium equations of joint A:

$$\sum_{i=1}^{4} M_i = 0 \quad \ldots\ldots\ldots\ldots\ldots\ldots \quad (23)$$

and

$$\sum_{i=1}^{4} Q_i = 0 \quad \ldots\ldots\ldots\ldots\ldots\ldots \quad (24)$$

Consequently, the stress in any element i is given by

$$\sigma_i = \frac{6\ M_i}{h_i^{\ 2}} \quad \ldots\ldots\ldots\ldots\ldots\ldots \quad (25)$$

Thermal Stresses.—Let us consider the same structure as that treated previously (Fig. 7). The stresses in the elements at the junction A due to functional and linear thermal gradients along the axis of the bottom skirt will be analyzed separately. It is assumed that the temperature inside the vessel is uniform, and gradients through the thickness as well as along the meridian of the vessel shell are negligibly small.

In the subsequent material T_1 and T_0 are the temperatures at points A and B of the bottom skirt, respectively; θ is the rotation of joint A; θ_0 denotes the unrestricted rotation at A of the bottom skirt due to linear or functional thermal gradient; Δ is the free horizontal thermal expansion of the vessel, including the top skirt (AC) due to $T_1 - T_0$; α represents the coefficient of thermal expansion; H_i and k_i are the film coefficient and thermal conductivity, respectively;

$$m_i = \sqrt{2\ H_i / k_i\ h_i} \quad \ldots\ldots\ldots\ldots\ldots\ldots \quad (26)$$

and

$$A_i = E\ h_i\ \alpha\ \left(T_0 - T_1\right) / D_i\ a_i \quad \ldots\ldots\ldots\ldots \quad (27)$$

Referring to Fig. 7(a) and 8, it can be shown that the moment and shear for each element at joint A are functions of the rotation θ:

For the Spherical Sections (i = 1,2)

$$M_i = \frac{E\ h_i\ a_i}{4\ \beta_i^{\ 3}}\ \theta \quad \ldots\ldots\ldots\ldots\ldots \quad (28)$$

and

$$Q_i = \frac{-\ E\ h_i}{2\ \beta_i^{\ 2}\ \sin\phi_0}\ \theta \quad \ldots\ldots\ldots\ldots\ldots \quad (29)$$

For the Top Skirt (i = 3)

$$M_i = D_i\ \lambda_i\ \theta \quad \ldots\ldots\ldots\ldots\ldots\ldots \quad (30)$$

and

$$Q_i = -\ 2\ D_i\ \lambda_i^{\ 2}\ \theta \quad \ldots\ldots\ldots\ldots\ldots\ldots \quad (31)$$

For the Bottom Skirt (i = 4)—Case A—Functional Thermal Gradient.—If a cylinder of constant thickness is subjected to an axial thermal gradient and edge loads as shown in Fig. 9, the basic differential equation for the horizontal translation w is

$$\frac{d^4w}{dx^4} + 4\ \lambda_i^{\ 4}\ w = A_i\ \frac{\sinh m_i\ x}{\sinh m_i\ L_i} \quad \ldots\ldots\ldots \quad (32)$$

It can be shown that the general solution of Eq. 32 is

$$w = \frac{e^{-\lambda_i x}}{2 \lambda_1^3 D_i} \left[\lambda_i M_i \left(\sin \lambda_i x - \cos \lambda_i x \right) - Q_i \cos \lambda_i x \right]$$

$$+ \frac{A \sinh m_i x}{\left(m_i^4 + 4 \lambda_i^4 \right) \sinh m_i L_i} \quad \ldots\ldots\ldots\ldots\ldots\ldots \quad (33)$$

At joint A

$$(w)_{x = 0} = - \frac{1}{2 \lambda_i^3 D_i} \left(\lambda_i M_i + Q_i \right) = 0 \quad \ldots\ldots\ldots \quad (34)$$

and

$$\left(\frac{dw}{dx} \right)_{x = 0} = \frac{2 \lambda_i M_i + Q_i}{2 \lambda_i^2 D_i} + \frac{A_i m_i}{\left(m_i^4 + 4 \lambda_i^4 \right) \sinh m_i L_i} = \theta \quad \ldots\ldots \quad (35)$$

The simultaneous equations (Eqs. 34 and 35) yield

$$M_i = 2 \lambda_i D_i \left(\theta - \frac{A_i m_i}{\left(m_i^4 + 4 \lambda_i^4 \right) \sinh m_i L_i} \right) \quad \ldots\ldots \quad (36)$$

and

$$Q_i = - 2 \lambda_i^2 D_i \left(\theta - \frac{A_i m_i}{\left(m_i^4 + 4 \lambda_i^4 \right) \sinh m_i L_i} \right) \quad \ldots\ldots \quad (37)$$

For the Bottom Skirt (i = 4)—Case B—Linear Thermal Gradient.—If the temperature gradient is constant, say

$$T_x = T_1 - \left(T_1 - T_0 \right) x / L_i \quad \ldots\ldots\ldots\ldots\ldots \quad (38)$$

the non-homogeneous part of Eq. 32 becomes

$$E h_i \alpha \left(T_1 - T_0 \right) x / D_i a_i L_i \quad \ldots\ldots\ldots\ldots\ldots \quad (39)$$

After performing similar mathematical manipulation as that in Case A,

$$M_i = 2 \lambda_i D_i \left[\theta - \frac{\alpha a_i}{L_i} \left(T_1 - T_0 \right) \right] \quad \ldots\ldots\ldots \quad (40)$$

and

$$Q_i = - 2 \lambda_i^2 D_i \left[\theta - \frac{\alpha a_i}{L_i} \left(T_1 - T_0 \right) \right] \quad \ldots\ldots\ldots \quad (41)$$

Consequently, the angle of rotation θ can be determined from the equilibrium condition $\Sigma M_i = 0$ at joint A, which gives

$$\theta = \frac{\lambda_4 \; D_4}{\sum\limits_{i=1}^{2} \frac{E \, h_i \, a_i}{4 \, \beta_i^3} + \sum\limits_{i=3}^{4} \lambda_i \, D_i} \; \theta_0 \; . \; . \; . \; . \; . \; . \; . \; . \; . \; . \; . \; (42)$$

in which

$$\theta_0 = \frac{A_4 \quad m_4}{\left(m_4^4 + 4 \, \lambda_4^4\right) \sinh \, m_4 \; L_4} \; . \; . \; . \; . \; . \; . \; . \; . \; . \; . \; . \; (43)$$

for case A, and

$$\theta_0 = \frac{\alpha \; a_4}{L_4} \left(T_1 - T_0\right) \; . \; . \; . \; . \; . \; . \; . \; . \; . \; . \; . \; . \; . \; . \; (44)$$

for case B.

For skirts of equal thickness, Eq. 42 reduces to

$$\theta = \frac{\theta_0}{2 + \sum\limits_{n=1}^{2} \frac{E \, h_i \, a_i}{4 \, \beta_i^3 \, \lambda_4 \, D_4}} \; . \; . \; . \; . \; . \; . \; . \; . \; . \; . \; . \; . \; . \; . \; . \; (45)$$

***Seismic Shears.*—The main factors affecting the dynamic response of reactor structures against earthquake are the damping capacity and the rigidity of the structure. Unfortunately, due to the fact that the available data concerning the recorded ground motions in the active earthquake zones are still meager, structural designers are confronted with a difficult problem of how to select a forcing function for the dynamic analysis of the type of structures under consideration. In the absence of a practical code, a design criterion has been proposed which was based on 50% of the recorded acceleration of the 1940 El Centro earthquake.[4] The results are shown in Fig. 10, which give the base shear as functions of the undamped period and fraction of equivalent viscous critical damping capacity of the structure. In the case of gas-cooled reactor structures, the undamped period T can be approximately determined by**

$$T = 0.32 \sqrt{\Delta} \; . \; . \; . \; . \; . \; . \; . \; . \; . \; . \; . \; . \; . \; . \; . \; . \; . \; (46)$$

in which T is the undamped period, in seconds, and Δ is the horizontal deflection, in inches, at the centroid or modulator core due to the total weight of the reactor structure acting horizontally. Hence, if the approximate damping factor is known, the maximum probable base shear of the system can be interpolated from Fig. 10.

BIOLOGICAL SHIELDING

***Design Procedure.*—Since the alpha and beta particles are usually absorbed inside the reactor pressure vessel, the main purpose of shielding is to intercept**

---

[4] "Aseismic Design of Structures by Rigidity Criterion," by E. Y. W. Tsui, Proceedings, ASCE, Vol. 85, No. ST2, February, 1959.

and absorb the neutrons and gammas to such an extent that the radiation outside the shield is reduced to a harmless level. In general, the principal factors affecting the design of shields are the source of the radiation, the physical requirements as to size and layout of the shield, the attenuating rate of the materials used, and human tolerance to radiation. In order to design an effective shield, the following procedure is recommended:

1. Determination of the intensity and location of radiation sources inside the shield and the allowable radiation level outside the shield, both when the power plant is in operation and when it is shut down.

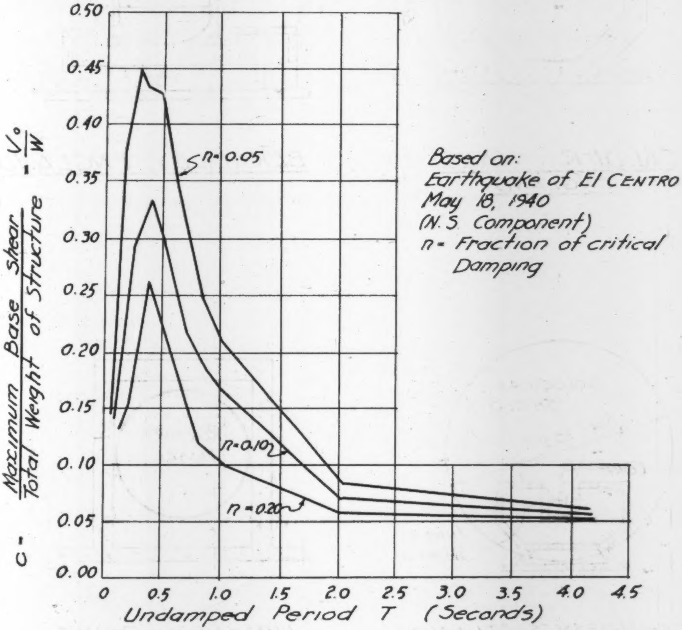

FIG. 10.—ACCELERATION SPECTRA FOR DAMPED ONE-MASS STRUCTURES

2. Based on the physical requirements of the structure, shields may be divided into three basic types: (a) unit shields for reactor and its components, (b) compartment shields for isolation of the reactor from the coolant system, and (c) shadow shields for certain locations of unusual exposure (Fig. 11).

3. Lead, iron or steel, aluminum, high density concrete, and water have all been used as shielding materials. The proper choice, however, depends on the physical and shielding properties, availability and the cost of the material.

4. Shield thickness is then determined from the source strength, the absorptive power of the material, and the level of human tolerance. It should be

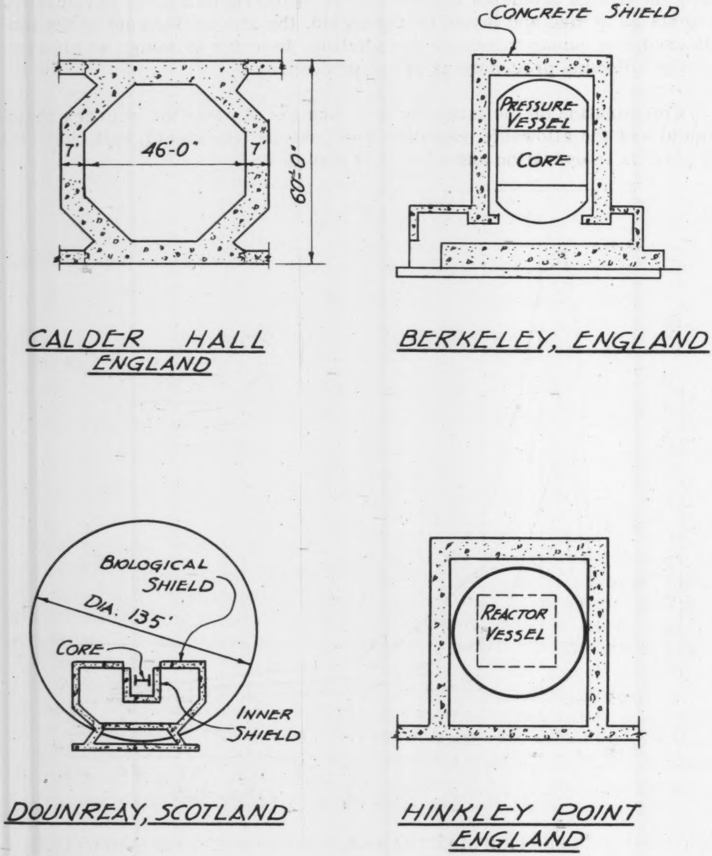
7'
46'-0"
7'
60'-0"
CONCRETE SHIELD
PRESSURE VESSEL
CORE
BIOLOGICAL SHIELD
DIA. 135'
CORE
INNER SHIELD
REACTOR VESSEL

CALDER HALL ENGLAND

BERKELEY, ENGLAND

DOUNREAY, SCOTLAND

HINKLEY POINT ENGLAND

FIG. 11.—SHIELD

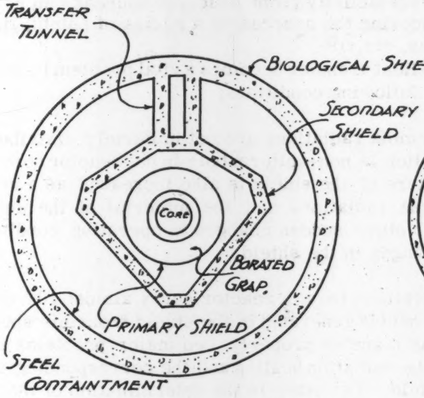
TRANSFER TUNNEL
BIOLOGICAL SHIELD
SECONDARY SHIELD
CORE
BORATED GRAP.
PRIMARY SHIELD
STEEL CONTAINTMENT

ENRICO FERMI, DETROIT MICH.

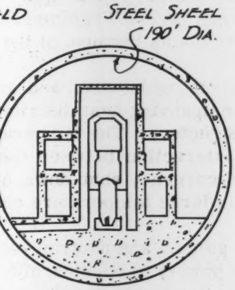
STEEL SHEEL 190' DIA.

DRESDEN, ILL.

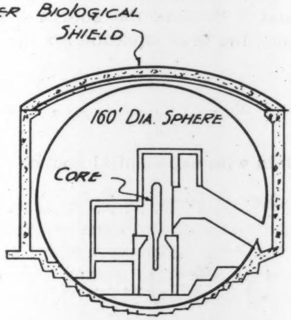
OUTER BIOLOGICAL SHIELD
160' DIA. SPHERE
CORE

INDIAN PT., N.Y.

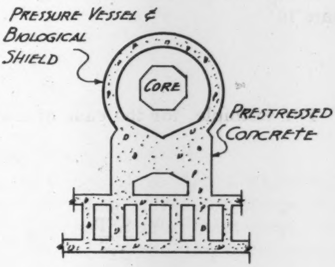
PRESSURE VESSEL & BIOLOGICAL SHIELD
CORE
PRESTRESSED CONCRETE

G-2, FRANCE

SKETCHES

noted that the contribution of radioactivity from different sources can be approximately computed by considering the sources as a series of points, lines, disks, cylinders, cones, spheres, etc.[5,6]

Thermal Stress Problems.—Heat transfer becomes a vital problem in nuclear power plants because of the following conditions:

1. Since the neutron and gamma radiations are not uniformly distributed, the accompanying heat distribution is non-uniform both in the reactor core and in the structure. The temperature of the shield is also increased as a result of the interaction between these radiations and the material of the shield.
2. Emergency shut-down or other sudden changes in operating conditions result in large temperature changes in the shield.

The gamma and neutron radiations from a reactor carry almost 10% of the reactor power, so considerable heat is generated in the shield from this source. In order to provide for the heat transfer properly, two major problems must be solved. One is to calculate the radiation heating and the corresponding temperature distribution of the shield. The other is the determination of thermal stresses in the shield due to this heat input.

The general heat equation is

$$C\ \delta \frac{\partial T}{\partial t} = \frac{\partial}{\partial x}\left(K \frac{\partial T}{\partial x}\right) + \frac{\partial}{\partial y}\left(K \frac{\partial T}{\partial y}\right) + \frac{\partial}{\partial z}\left(K \frac{\partial T}{\partial z}\right) + S \quad \ldots . (47)$$

in which K is the thermal conductivity, T denotes temperature, t is time, C represents specific heat, δ is density, and S denotes the source strength.

In the case of one-dimensional heat flow, the heat equation for the steady state is[7]

$$S + K \frac{d^2T}{dx^2} = 0 \quad \ldots\ldots\ldots\ldots (48)$$

For example, for the case of a slab shield with exponential source

$$S = S_0\ e^{-\Sigma x} \quad \ldots\ldots\ldots\ldots (49)$$

$$\frac{d^2T}{dx^2} = -A\ e^{-\Sigma x} \qquad \left(A = \frac{S_0\ \Sigma}{K}\right) \ldots\ldots\ldots (50)$$

$$\frac{dT}{dx} = \frac{A}{\Sigma}\ e^{-\Sigma x} + C_1 \quad \ldots\ldots\ldots\ldots (51)$$

and

$$T = -\frac{A}{\Sigma^2}\ e^{-\Sigma x} + C_1\ x + C_2 \quad \ldots\ldots\ldots (52)$$

in which Σ is the macroscopic cross section or absorption coefficient of the material and S_0 is the total heat incident on the surface.

---

[5] "Radiation Shielding," by B. T. Price, C. C. Horton and K. T. Spinney, 1957.

[6] "Reactor Shielding Design Manual," by T. Rockwell, McGraw-Hill Book Co., Inc., New York, 1956.

[7] "Introduction to Nuclear Engineering," by R. Stephenson, McGraw-Hill Book Co., Inc., New York, 1957.

The constants C_1 and C_2 can be solved from the appropriate boundary conditions. For example, if the temperature at the inside and outside faces of shield is zero, then T = 0 for x = 0 and $x = x_0$; where x_0 is the thickness of shield.

Eq. 51 yields

$$C_1 = \frac{A}{x_0\, \Sigma^2} \left(e^{-\Sigma x} - 1 \right) \ldots\ldots\ldots\ldots\ldots \quad (53)$$

and

$$C_2 = \frac{A}{\Sigma^2} \ldots\ldots\ldots\ldots\ldots\ldots\ldots \quad (54)$$

The maximum temperature can be obtained from the condition that

$$\frac{dT}{dx} = 0 \ldots\ldots\ldots\ldots\ldots\ldots\ldots \quad (55)$$

or

$$K_{Tmax} = \frac{1}{\Sigma} \ln \left(\frac{\Sigma K_0}{1 - e^{-\Sigma K_0}} \right) \ldots\ldots\ldots\ldots \quad (56)$$

When x_0 becomes large, the following approximations may be used:

$$K_{Tmax} \doteq \frac{K_0}{6} \ldots\ldots\ldots\ldots\ldots \quad (57)$$

and

$$T_{max} \doteq \frac{3}{4} \frac{I_0}{\Sigma K} \ldots\ldots\ldots\ldots \quad (58)$$

in which I_0 is the effective incident radiation energy on shield.

Other parameters directly related to the temperature distributions in the shields are heat transfer coefficient for pressure drop in reactor, temperature rise in the center of reflector, cooling requirements after shut-down, etc.[8]

In case of steady heat flow, thermal stresses arise from two basic temperature distributions, namely, linear and functional.

For linear temperature distribution, the thermal moment required to prevent the rotation of the ends of a fixed beam or a section of a wall is

$$M = E\ I\ \alpha\ \Delta T/x_0 \ldots\ldots\ldots\ldots\ldots \quad (59)$$

in which E I is the flexural rigidity of the member, $\alpha\ \Delta T$ denotes the thermal expansion, and x_0 is the structure thickness.

The moment distribution method can be used to solve the thermal problems in rigid frames. First, apply Eq. 59 to find the fixed end moments corresponding to the average temperature difference. Then, distribute the unbalanced joint moments until a condition of equilibrium is established.

---

[8] "Research Reactors," by U. S. Atomic Energy Commission, McGraw-Hill Book Co., Inc., New York, 1956.

For a non-linear temperature distribution, a moment-temperature analogy, as suggested[9] by H. S. Davis, may be applied, since the differential equations

$$\frac{dM^2}{dK^2} = - w(x) \quad \dots\dots\dots\dots\dots\dots \quad (60)$$

and

$$\frac{d^2T}{dx^2} = - A\ e^{-\Sigma K} \quad \dots\dots\dots\dots\dots\dots \quad (61)$$

are similar.

Other factors which influence the strength and stability of shield structures are fatigue due to cyclic temperature variations, creep, thermal buckling, etc. These factors are related to the properties of the shield materials at high temperatures, strain rate, deflection, stress concentration, corrosion and the geometry of the structure.[10]

OTHER STRUCTURAL FEATURES

Reactor Containment.—To prevent damage and casualty due to failure of the reactor or leakage in the coolant circuit, there has been some endeavor made to ventilate the contaminated atmosphere through filters or absorbers such as in the Oak Ridge air cooled X-10 pile and in the Brookhaven National Laboratory air cooled research reactor. However, a containment must enclose these two parts or portions thereof. The accidental gases and radioactive vapor which leak out will, thus, be trapped and held by the containment shell.

Various factors are involved in the design of the containment. The most important ones are:

1. Gas volume, pressure, and temperature under normal operation or when caused by accident.
2. Loadings including dead load, live load, snow, wind, seismic, etc.
3. Requirements of existing and future codes; the usual recommendation being API 620 or the ASME code.
4. Air locks for equipment and personnel.
5. The size, shape, foundations and structural supports for the containment.

Some examples of containments and their characteristics have been listed by C. Robert McCullough.[11] Items including design pressure, exclusion radius, volume dimensions, and leakage are also mentioned.

Drainage.—Drainage is an important item in the design of any power plant. It safeguards foundations; controls and removes both surface and ground water; and disposes of fuel wastes. Because radioactive rays are present in the wasted materials, the drainage system of a nuclear power plant has its special problems. These wastes are dangerous as soon as they come out from the reactor and the contamination may spread to the ground and nearby streams. Consequently, they must be carefully neutralized as much as possible and disposed of with extreme caution. In some cases, low-point outlets have been eliminated from reactor vessels and fuel-element storage tanks in order to prevent accidental draining.

---

[9] "Thermal Considerations in the Design of Concrete Structure for Shielding Atomic Power Plants," by H. S. Davis, A. I. Ch. E., 1958.

[10] "Thermal Stresses," by B. E. Gatewood, McGraw-Hill Book Co., Inc., New York, 1957.

[11] "The Experience in the U. S. with Reactor Operation and Reactor Safeguard," by C. Robert McCullough, Table IV.

Deflection and Vibration Problems.—There are two major vibration problems in a power plant, namely, the forced vibration of the turbo-generator pedestal and induced vibration of stack due to steady wind. In order to keep the structure stable, resonant vibration should be avoided.

Since the pedestal is basically a space frame subjected to both static and dynamic loads in three dimensions, most of these loads are acting eccentrically with respect to the center line of the structural members. Accurate analysis is quite involved and tedious. A practical approach is to consider the structure as two-dimensional bents in both longitudinal and transverse directions and analyze each of them separately. A recommendation has been made that the maximum deflection for the main members to be limited to 0.02 in. Ordinarily, this severe limitation of the deflection will result in a fundamental natural frequency of the member higher than that of the operating frequency of the generator. However, a very careful study must be made in each particular case. Shear deflection should be taken into account in the heavy horizontal member. It has been suggested[12] that the natural frequency of the parts and of the assembly as a whole should not fall in the range between one-half to two times the forcing frequency. The German Bureau of Standards recommended in 1954, that the difference between the two frequencies should not be less than 20%. For a simple beam with mass assumed concentrated at its center, the fundamental frequency is given by

$$f = 187.7/\sqrt{D} \quad \ldots\ldots\ldots\ldots\ldots\ldots \quad (62)$$

in which f is the natural frequency in revolutions per minute, and D is the maximum static deflection, in inches.

In practice, the turbine pedestal should be isolated from other structures. Thin slabs, thin walls, cantilever brackets and free-standing columns should always be avoided.

Resonant vibration of stacks can be induced by a steady wind if the von Karman vortex frequency of the stream is equal to the natural frequency of the structure. The former can be approximately computed by

$$f = S\ V/D \quad \ldots\ldots\ldots\ldots\ldots\ldots \quad (63)$$

in which f is the vortex frequency, in cycles per second, V denotes wind velocity, in feet per second, D is the stack diameter, in feet, and S represents the Strouhal number (≈ 0.19).

The fundamental bending frequency of unlined stack may be computed roughly by the following empirical formula:[13]

$$f = D(3{,}040\ t + 2{,}520)h^2 \quad \ldots\ldots\ldots\ldots\ldots \quad (64)$$

---

[12] "ALCOA Structural Handbook," Aluminum Company of America, Pennsylvania, 1956.

[13] "The Vibration of Steel Stacks," by W. L. Dickey and G. S. Woodruff, Transactions, ASCE, Vol. 121, 1956.

in which t is the thickness of stack, in inches, and h denotes the equivalent height, in feet.

While the breathing frequency or the frequency of the stack vibrating as a ring is given by

$$f = 24{,}500\ t/r^2 \qquad (65)$$

in which t and r are the thickness and radius of stack, in inches.

Unfortunately, there is a wide variation in wind velocity in each locality, and the selection of the critical velocity becomes a problem for the experienced engineer.

ACKNOWLEDGEMENTS

The writers wish to thank Mr. J. R. Anderson, P. E., Civil Engineering Design Dept. of EBASCO Services, Inc. for his valuable suggestions and recommendations.

APPENDIX.—READING REFERENCES

---

1. "Theory of Plates and Shells," by S. Timoshenko, McGraw-Hill Book Co., Inc., New York, 1940, pp. 351-362.
2. "Earthquake Stresses in Spherical Domes and in Cones," by E. P. Popov, Proceedings, ASCE, Vol. 82, No. ST3, May, 1956.
3. "Supporting Skirts for Reactor Pressure Vessels," by R. Hicks, The Engineer, August, 1957, pp. 256-258.
4. "Beams on Elastic Foundations," by M. Hetenyi, The University of Michigan Press, Ann Arbor, 1946, pp. 32-37.
5. "Nuclear Power Engineering," by H. C. Schwenk and R. H. Shannon, McGraw-Hill Book Co., Inc., New York, 1957.

AMERICAN SOCIETY OF CIVIL ENGINEERS

Founded November 5, 1852

TRANSACTIONS

Paper No. 3097

DESIGN PRESSURE FOR A REACTOR CONTAINMENT VESSEL[a]

By John A. Bailey[1]

SYNOPSIS

The basis for selection of the magnitude of the reactor accident against which the containment vessel must provide protection is discussed and a limiting accident is analyzed. A numerical example is shown and generalized curves are included.

INTRODUCTION

Containment vessels are placed around water-cooled power reactors as a final barrier to the uncontrolled release of fission products, which could conceivably result from a severe reactor accident. While it is necessary to consider severe accidents in the design of containment vessels it should be noted that the precautions taken in design and operation make a containment-requiring accident very remote.

If a large amount of thermal energy is released and/or generated in a containment-requiring reactor accident and if there is no certain method of isolating the radioactive fission products, (both generally the case, at present) the containment vessel must also withstand the effects of this energy release or generation. One of the most obvious effects is the rise of internal pressure in the containment vessel.

The factors governing this pressure rise in water-cooled and moderated reactors are analyzed herein and a method is presented for calculating the enclosure pressures which could result from a reactor or primary coolant system

---

Note.—Published essentially as printed here, in February, 1960, in the Journal of the Structural Division, as Proceedings Paper 2382. Positions and titles given are those in effect when the paper or discussion was approved for publication in Transactions.

[1] Atomic Power Equipment Department, General Electric Company, San Jose, California.

rupture accident. The design of the containment vessel is limited by the most severe accident for which it is required to design and so it is only the major accidents which will be considered.

THE PRESSURE-VOLUME RELATIONSHIP

Mechanism of Pressure Rise.—Since most water-cooled reactors operate at high pressures, a primary system rupture of any significant size would release liquid and/or vapor at a very rapid rate. Initially, the air around the break would be displaced by the escaping liquid and vapor. Mixing of air and vapor would follow shortly, with the two tending toward thermal equilibrium with each other. Some energy would probably be transferred to the air and vapor from the hot vessel or primary piping and some energy would be absorbed by cooler structural masses and equipment (including the containment-vessel wall). Any energy generated by chemical or nuclear processes would be released either during or after the accident. The peak internal pressure to which a given enclosure may be subjected is the result of the following competing rates of energy transfer into and out of the media within the enclosure:

1. Rate of energy release from the reactor vessel;
2. Rate of heat transfer to and from structural and equipment masses in the enclosure; and
3. Rate and timing of additional energy generation (chemical or nuclear).

Rate of Energy Release.—The rate of energy release from a primary system rupture would be a function of the size, location, and geometry of the break, the initial condition of the primary fluid, and the pressure into which the fluid discharges. For a given reactor and plant design the initial primary coolant conditions are confined to a relatively small range. The normal internal enclosure pressure is usually approximately at atmospheric level.

A break at a high elevation in the system would be more likely to permit partial vaporization of liquid within the vessel with the resulting discharge of a liquid-vapor mixture. A rupture near the bottom of the primary system would result in discharge of a mixture which would be primarily liquid. The equilibration of the liquid would probably occur mostly outside the reactor vessel or primary system. In the latter case the discharge rate per unit area of break would be higher. Rupture of a line connecting the reactor and steam drum or heat exchanger could permit the discharge from both sides of the break if it were a complete severance. A smooth rounded hole, such as that resulting from the severance of a vessel inlet pipe near a nozzle into the vessel, could have a higher discharge coefficient than a jagged square-edge break.

Perhaps the most difficult determination is that of the maximum break size. For a pipe break, obviously, there is a maximum flow area, but in the case of a vessel it is difficult to select the largest size primary system break which must be considered in containment design. It should be emphasized that the precautions taken in reactor and plant design and operation make any containment-requiring accident extremely remote. When considering cases of this degree of remoteness it is quite difficult to assess the "relative remoteness" of other occurrences which could have an effect on the accident.

One method of avoiding this problem is to assume, as has been done subsequently, that no energy is transferred into or out of the liquid, vapor, or gas during the process of equilibration. This makes the value of peak pressure independent of the discharge rate from the rupture.

Heat Transfer During Pressure Rise.—With weight rates of flow from a break in the region of 1,000 to 10,000 lb per sec per sq ft of flow area, the elapsed time between system rupture and peak pressure could, in the worst cases, conceivably be on the order of 1 sec or less. The inherent peak-pressure-reduction capability of a normal plant design could be negligibly small over this period of time. Moreover some considerable masses of metal are at temperatures above the final equilibrium temperature within the enclosure. Unless there is special equipment designed to reduce the pressure peak, it is questionable that any significant credit can be taken for this effect in any accident involving a large system rupture. Conversely any significant heat transfer from hot vessel walls or fuel during the pressure rise seems unlikely.

Additional Energy Contributions.—Should the accident be accompanied by a nuclear excursion there would be additional energy present in the system which could raise the peak pressure. A similar effect could be produced by any chemical reaction such as a metal-water reaction. A chemical reaction occurring after loss of water, for example, would probably not affect the first pressure peak but might cause a second peak whose magnitude would again be governed by the relative rates of energy transfer into and out of the thermodynamic media within the enclosure.

Dynamic Effects.—It is conceivable that a very rapid or nearly instantaneous rupture could generate pressure waves which could result in enclosure pressures above those calculated for thermal equilibrium. This could only be caused by an extremely rapid and large rupture which would seem unlikely in a reactor vessel and primary system in which the steel is generally in the temperature range where any failure would be of a ductile type. Moreover the primary system is usually surrounded by shielding material which would attenuate and partially contain any shock waves which might be generated.

An Analytical Model.—It can be seen that a rigorous analysis including all the possible variations in mechanisms and sequences would be a tremendously involved undertaking and when completed might not necessarily offer the degree of assurance required that the calculated peak pressure would not be exceeded in an actual accident. One way of avoiding the uncertainty of balancing the various energy transfer rates against each other is to make the conservative assumption that the equilibration of liquid, vapor, and air (with themselves) is accomplished in the complete absence of any energy losses. Any additional energy contributions which were concurrent with the rupture would be included. This would result in a conservative value of peak enclosure pressures. Following the peak pressure, energy losses could be included in the analysis as well as any delayed energy contributions. Any secondary pressure peaks could thus be calculated.

It is necessary to examine any secondary pressure peaks in order to establish their magnitude relative to the first peak. One type of accident which could possibly produce a secondary pressure peak higher than the initial peak predicted by the model, would be a rupture accident followed by a delayed metal-water reaction with all the energy being added only to the air and vapor. In this case the absence of heat absorption by vaporization of water could make the pressure-producing effect of the energy greater than in the case where water is vaporized. The presence of massive shielding around the reactor greatly reduces the rate at which any subsequently generated heat could be transferred to the air and vapor. Because of this and the difficulty of getting any significant metal-water reaction, the model chosen is believed to be conservative.

ANALYSIS OF THE PRESSURE-VOLUME RELATIONSHIP

The following analyzes the specific situation of a rupture accident in which it is assumed that:

1. Equilibration of liquid, vapor, and air (with themselves) occurs adiabatically with respect to structural masses within the enclosure;
2. No additional energy contributions are made after initial equilibration;
3. There are no significant dynamic effects; and
4. Air follows the perfect-gas relation and has a constant heat capacity.

Air at low temperatures follows the perfect-gas relation so the amount of air in the enclosure, W_a, is

$$W_a = \frac{P_{a1} V_{a1}}{R_a T_{a1}} \quad \ldots\ldots\ldots\ldots\ldots (1)$$

in which P_{a1} and T_{a1} are the initial air pressure and temperature within the enclosure, R_a represents the gas constant, and V_{a1} is the enclosure free volume. The free volume is taken as that volume into which the air and water vapor are free to expand. If atmospheric moisture is considered, the partial pressure of the moisture, P_{m1}, and the amount of moisture, W_{m1}, may be found from an assumed value of initial relative humidity, ϕ:

$$P_{m1} = \phi P_{g1} \quad \ldots\ldots\ldots\ldots\ldots (2)$$

in which P_{g1} is the saturation pressure for water vapor at the chosen ambient air temperature, T_{a1}, and may be found in steam tables. The total internal enclosure pressure, P_{t1}, which is probably very close to atmospheric pressure is equal to the sum of the air and water vapor partial pressures, so the initial air pressure, P_{a1}, is given by

$$P_{a1} = P_{t1} - P_{m1} \quad \ldots\ldots\ldots\ldots\ldots (3)$$

Assuming that the moisture behaves as though it were a perfect gas, the weight of moisture initially in the air, W_{m1}, is

$$W_{m1} = \frac{P_{m1} V_{a1}}{R_m T_{m1}} \quad \ldots\ldots\ldots\ldots\ldots (4a)$$

or

$$W_{m1} = \frac{V_{a1}}{V_{m1}} \quad \ldots\ldots\ldots\ldots\ldots\ldots\ldots \text{(4b)}$$

in which

$$V_{m1} = \frac{R_m T_{m1}}{P_{m1}} \quad \ldots\ldots\ldots\ldots\ldots\ldots\ldots \text{(4c)}$$

The value of P_{m1} is found from Eq. 2 and $T_{m1} = T_{a1}$, an assumed value. As an alternate method, the initial moisture specific volume, V_{m1}, may be evaluated by

$$V_{m1} = \phi v_{g1} \quad \ldots\ldots\ldots\ldots\ldots\ldots\ldots \text{(5)}$$

where ϕ is assumed, as in Eq. 2, and v_{g1} is the specific volume of saturated vapor at the initial ambient temperature, $T_{a1} = T_{m1}$. After the accident and thermal equilibrium, both air and water vapor occupy that portion of the enclosure and reactor vessel volume not filled with liquid water and the total internal enclosure pressure is the sum of the two partial pressures. It follows then that the sum of the liquid and vapor volumes is equal to the combined volumes of the reactor vessel and the enclosure free volume:

$$V_{w1} + V_{a1} = W_w (1-x)\, v_{f2} + (x\, W_x)\, V_{g2} \quad \ldots\ldots\ldots\ldots \text{(6)}$$

in which W_w is the total amount of liquid and vapor (if any) within the primary system before the accident. That portion of the original contents of the primary system, W_w, which is vapor at equilibrium after the accident is x. There is no physical difference in the terminal condition, between moisture which was originally in the air, W_{m1}, and that portion of the primary system water which is vapor upon equilibration, x W_w. Solving Eq. 6 for the vaporized portion of the primary system water, x, gives the following:

$$x = \frac{\dfrac{W_{a1} + V_{w1}}{W_w} - \dfrac{W_{m1}}{W_w} (v_{g2} - v_{f2})}{v_{fg2}} \quad \ldots\ldots\ldots\ldots \text{(7)}$$

Since $W_w = V_{w1}/ v_{w1}$, where v_{w1} is the initial equivalent specific volume of the primary system fluid in whatever proportions the liquid and vapor may be mixed, and $W_{m1} = V_{a1}/ v_{m1}$, Eq. 7 may be rewritten as

$$x = \frac{V_{w1} \left[\dfrac{V_{a1}}{V_{w1}} \left(1 - \dfrac{v_{g2}}{v_{m1}} \right) + 1 \right]}{v_{fg2}} = v_{f2} \quad \ldots\ldots\ldots \text{(8)}$$

The initial primary fluid specific volume, v_{m1}, and initial enclosure moisture specific volume are functions of the assumed conditions before the accident. The terminal specific volumes (v_{f2}, v_{fg2}, and v_{g2}) are functions of the conditions existing after the accident. The ratio of enclosure free volume to primary system volume, V_{a1}/V_{w1}, is a design variable.

Since this idealized equivalent of an actual thermodynamic process is a nonflow, constant-volume process, the energy balance is written as

$$Q = U_2 - U_1 \quad \ldots\ldots (9)$$

in which U_1 is the total internal energy of the media before the accident, U_2 denoted the corresponding value after release and equilibration of the primary water, and Q is the net energy contribution to the system from nuclear and/or chemical, heat generation, if any. Breaking down U_1 and U_2 into their component parts, Eq. 9 may be written as

$$\begin{aligned} Q = [&W_w (u_{f2} + x u_{fg2}) + W_{m1} u_{g2} + W_a u_{a2}] \\ &- (W_w u_{w1} + W_{m1} + u_{m1} + W_a u_{a1}) \quad \ldots\ldots (10) \end{aligned}$$

Note that u_{w1} is the equivalent specific internal energy of the entire primary system fluid in whatever proportions the liquid and vapor may be mixed. Rearranging and substituting

$$u_{a2} - u_{a1} = c_v (T_{a2} - T_{a1}) \quad \ldots\ldots (11)$$

$$\begin{aligned} Q = &W_w (u_{f2} + x u_{fg2} - u_{w1}) + W_{m1} (u_{g2} - u_{m1}) \\ &+ W_a C_v (T_{a2} - T_{a1}) \quad \ldots\ldots (12) \end{aligned}$$

Using W_a (from Eq. 1), W_w, W_{m1}, and taking the original amount of energy in the primary fluid as

$$U_{w1} + W_w u_{w1} = \frac{V_{w1}}{V_{w1}} u_{w1} \quad \ldots\ldots (13)$$

Eq. 10 may be written as

$$\begin{aligned} \frac{Q}{U_{w1}} = &\frac{V_{a1}}{V_{w1}} \frac{v_{w1}}{v_{m1}} \frac{u_{g2} - u_{m1}}{u_{w1}} + \frac{P_a v_{m1} c_v}{R_a u_{w1}} \frac{T_{a2}}{T_{a1}} - 1 \\ &+ \frac{u_{f2} + x f_{g2}}{u_{w1}} - 1 \quad \ldots\ldots (14) \end{aligned}$$

Note that Eq. 14 applies as long as the amount of heat added does not exceed that which would cause vaporization of all the primary water; this is usually the case. The volume occupied by air after the accident is very nearly equal to that before so

$$P_{a2} = \frac{T_{a2}}{T_{a1}} P_{a1} \quad \ldots\ldots\ldots\ldots\ldots\ldots \quad (15)$$

Eq. 15 neglects the slight increase in air volume resulting from the vaporization of some of the circulating water. Assuming thermal equilibrium, the terminal air temperature, T_{a2}, is equal to the saturation temperature corresponding to the vapor pressure within the enclosure after the accident. The total internal pressure, P_{t2}, is

$$P_{t2} = P_{a2} = P_{m2} \quad \ldots\ldots\ldots\ldots\ldots\ldots \quad (16)$$

in which P_{m2} is the vapor partial pressure after equilibration.

After initial conditions have been assumed and a value placed on the net energy contribution, Q, there are five variables:

1. Final media temperatures, $T_{a2} = T_{m2}$;

2. Final vapor pressure, P_{m2};

3. Final air pressure, P_{a2};

4. Final total enclosure pressure, P_{t2}; and

5. Vaporized portion of the primary fluid, x.

There are five functional relationships:

(a) Eq. 8, x in terms of the final vapor pressure P_{m2} and temperature T_{m2} (through the steam-table values of v_{f2}, v_{fg2}, v_{g2});

(b) Eq. 14, x in terms of the final vapor pressure P_{m2} and temperature, $T_{m2} = T_{a2}$ (through steam table values of u_{f2}, u_{fg2}, and u_{g2});

(c) Eq. 15, final air pressure P_{a2} in terms of final air temperature, $T_{a2} = T_{m2}$;

(d) Steam tables, vapor partial pressure P_{m2} in terms of vapor temperature, T_{m2}; and

(e) Eq. 16, total enclosure pressure P_{t2} in terms of air and vapor partial pressures.

Because of the nature of the equations and functional relationship provided by steam tables, an explicit solution for P_{t2} and is not possible. It is necessary to assume a value of P_{m2} and solve Eqs. 8 and 14 for a value of x which results in the proper value of Q/U_{w1}. Eqs. 15 and 16 yield the total internal enclosure pressure.

In order to generalize the analysis somewhat, Eq. 8 and 14 are arranged to use the ratio of enclosure free volume to primary system volume, V_{a1}/V_{w1}. For given initial conditions and net energy contribution, Q/U_{w1}, a curve of enclosure pressure, P_{t2}, and a function of V_{a1}/V_{w1} can be plotted.

The results of this analysis are shown in Figs. 1 and 2 assuming that the entire primary system is filled with saturated liquid. The internal enclosure pressure is shown as a function of initial primary system coolant conditions, the ratio of enclosure free volume to primary system volume, V_{a1}/V_{w1}, and the ratio of net energy contribution to initial internal energy, Q/U_{w1}. For a given initial primary coolant condition the plot of enclosure pressure, P_{t2}, against volume ratio, V_{a1}/V_{w1}, nearly linear on a logarithmic grid and, as expected, the relationship is an inverse one.

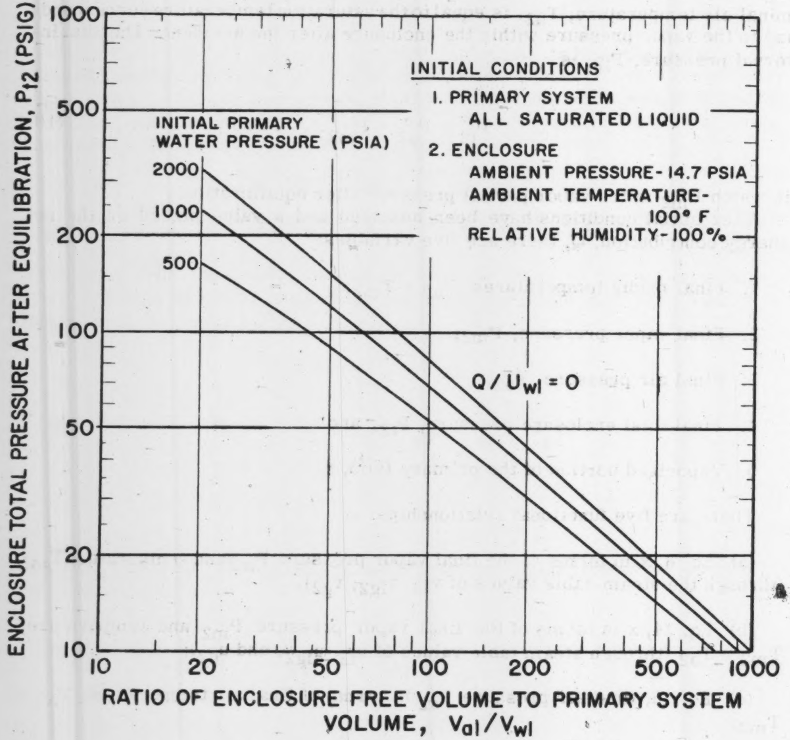

FIG. 1.—ENCLOSURE PEAK PRESSURE FOLLOWING PRIMARY SYSTEM RUPTURE, $Q/U_{w1} = 0$

INFLUENCE OF THE PRESSURE-VOLUME RELATIONSHIP ON ENCLOSURE DESIGN

Generally a design criterion states that the enclosure design pressure must equal or exceed that peak pressure which could result from an accident of a given severity. The enclosure designer has then a certain latitude in balancing enclosure free volume against design pressure. On large containment vessels code restrictions and fabrication limitations may limit the acceptable range of volume and pressure values. Within these limitations the choice of enclosure size may be primarily an economic one.

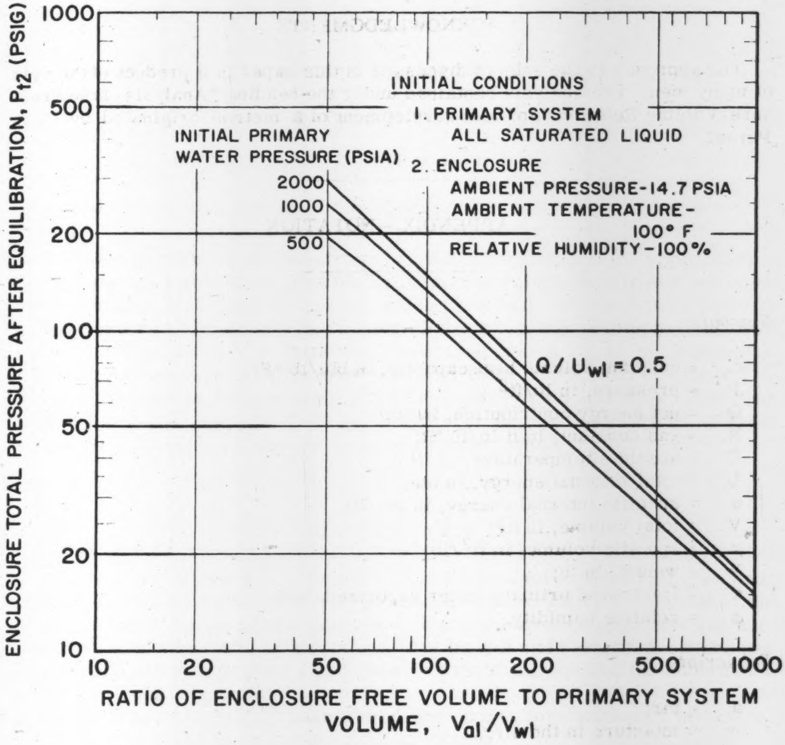

FIG. 2.—ENCLOSURE PEAK PRESSURE FOLLOWING PRIMARY SYSTEM RUPTURE, $Q/U_{w1} = 0.5$

FUTURE DEVELOPMENT

The expense of placing containment vessels around nuclear power plants is quite high. Considerable thought, analysis, and testing is being carried on to find methods of reducing enclosure costs. One system now under consideration for reducing peak enclosure pressure encloses the reactor vessel in a chamber vented to the enclosure through a pool of water. The water would condense the escaping vapor, thus reducing the peak enclosure pressure. It has a further advantage of trapping a portion of fission products which might be released. The success of such a system in reducing the pressure peak depends on being able to place a reasonable limitation on break size, for there could be no such effect if the release of all of the primary coolant were instantaneous or nearly so.

ACKNOWLEDGMENTS

The approach to the subject discussed in this paper is a product of the work of many men. The analysis contained under the heading "Analysis of the Pressure-Volume Relationship" is a development of a method originated by C. A. Pursel.

APPENDIX.—NOTATION

Symbols

c_v = constant volume heat capacity, in btu/lb °F;
P = pressure, in lb/ft^2
Q = net energy contribution, in btu;
R = gas constant, in ft lb/lb °R;
T = absolute temperature, in °R;
U = total internal energy, in btu;
u = specific internal energy, in btu/lb;
V = total volume, in ft^3;
v = specific volume, in ft^3/lb;
W = weight, in lb;
x = fraction of primary water vaporized; and
ϕ = relative humidity.

Subscripts

a = air;
m = moisture in the air;
t = total;
w = primary water;
1 = initial condition;
2 = terminal condition;
f = property of the saturated liquid;
g = property of the saturated vapor; and
fg = property of change upon vaporization.

AMERICAN SOCIETY OF CIVIL ENGINEERS
Founded November 5, 1852
TRANSACTIONS

Paper No. 3116

SOME BASIC CONCEPTS IN MATRIX STRUCTURAL ANALYSIS

By Frank R. Berman[1]

SYNOPSIS

The development of the electronic digital computer and the application of matrix algebra has made it possible for the structural engineer to analyze complex or highly redundant structures which previously had been prohibitive to analyze by the hand method of calculation. Papers recently written have utilized either the "flexibility" or "stiffness" matrix approach. It is the purpose of this paper to point out the common origin of these methods in energy and to discuss procedures for calculating the total energy of a structure. The concept of the "total" structure will be considered. Applications include analysis of a truss with elastic supports and a continuous beam.

INTRODUCTION

The analysis of complex or highly redundant structures which had been prohibitive to analyze by hand calculation became a possibility as a result of the development of the electronic computer. Furthermore, the application of matrix theory to structural analysis was then logical and permitted the concise formulation of large problems and control of the data required for submission to the electronic computer.

Many writers (2,4-20)[2] have shown the matrix formulation of structural theory and its application to structural problems.

Note.—Published essentially as printed here, in August, 1960, in the Journal of the Structural Division, as Proceedings Paper 2582. Positions and titles given are those in effect when the paper or discussion was approved for publication in Transactions.

[1] Cons. Engr., Huntington, N. Y.

[2] Numerals in parentheses refer to corresponding items in Appendix II.

In this country, S. Levy's (3) application in 1947 of the strain energy theory to a complex aircraft structure was presented in matrix form by R. L. Bisplinghoff and A. L. Lang (8). W. Lansing and L. B. Wehle (10), P. H. Denke (13), R. W. Clough (17), B. Klein (18), H. C. Martin (19), Turner (21), and many others (2,16) have likewise made noteworthy contributions.

In Europe, B. Langefors (7, 9, 12), starting with the tensor concepts of G. Kron (1), independently pioneered in the matrix formulation of structural theory. Papers by H. Falkenheimer (5) and others (6, 15) followed. Probably the most comprehensive and thorough treatment of energy methods in matrix and non-matrix form is that given by J. H. Argyris (15).

The concept of energy is the starting point of the paper, but first we will note a superposition relationship that we will need for our work.

SUPERPOSITION OF DEFLECTIONS

Given a structure in the plane acted upon by a set of forces P_1, P_2, P_3 in equilibrium with reaction forces R_1, R_2, and R_3 (Fig. 1), we assume that linearity and the law of superposition apply. Thus, if Δ_1 is the deflection in the direction of P_1 we can write

$$\Delta_1 = \delta_{11} P_1 + \delta_{12} P_2 + \delta_{13} P_3 \quad \ldots\ldots\ldots\ldots (1)$$

We can generalize Eq. 1 for a set of forces P_1, P_2, . . . P_n with the result

$$\Delta_i = \delta_{i1} P_1 + \delta_{i2} P_2 + \ldots \delta_{ii} P_i + \ldots \delta_{in} P_n \quad \ldots\ldots (2)$$

or in matrix form

$$\left\{ \Delta_i \right\} = \left[\delta_{ij} \right] \left\{ P_j \right\} \quad \ldots\ldots\ldots\ldots\ldots\ldots\ldots (3)$$

We recognize in Eq. 3 that $\left[\delta_{ij} \right]$ is the matrix of influence deflection coefficients which in the literature is also known as a "flexibility" matrix.

We can now examine the basic concept of strain energy.

STRAIN-ENERGY CONCEPT

Consider the axially compressed bar, shown in Fig. 2. If we define the strain energy as the work done by the applied force, P_1, in shortening the bar by the amount, Δ_1, we can write, noting that P_1 builds up from zero to its final value of P_1,

$$U = \frac{1}{2} P_1 \Delta_1 \quad \ldots\ldots\ldots\ldots\ldots\ldots\ldots (4)$$

Now let us generalize Eq. 4. Consider the linear elastic planar structure given in Fig. 3. The loads P_1, P_2, . . . P_n, shown acting, are in equilibrium and include both the applied loads and their reactions. If we measure all deflections with respect to an arbitrary set of orthogonal axes (shown as x, y axes), we have the deformed shape of the structure as shown in Fig. 3.

If we define the strain energy as the work done by all the applied forces P_1, P_2, . . . P_n in deforming the structure and noting that all the forces increase

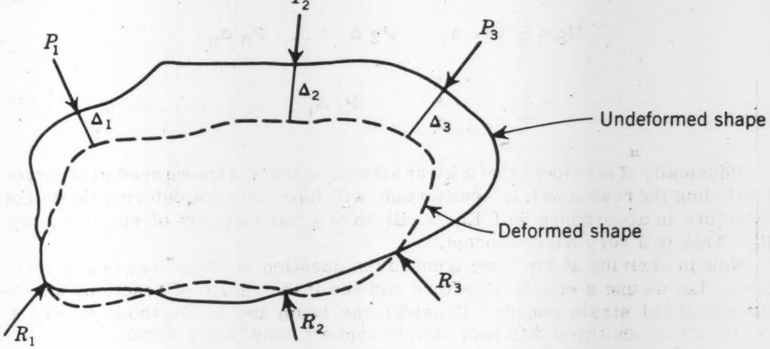
P_1
P_2
P_3
Δ_1
Δ_2
Δ_3
Undeformed shape
Deformed shape
R_1
R_2
R_3

FIG. 1

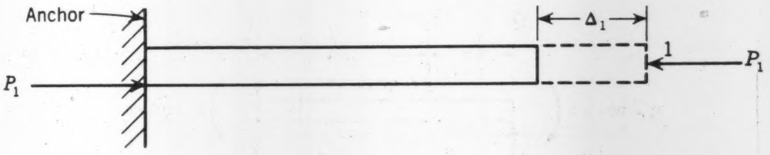
Anchor
Δ_1
1
P_1
P_1

FIG. 2

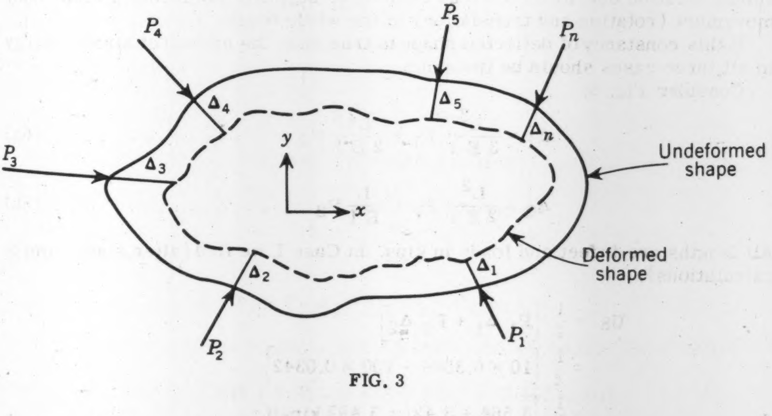
P_4
P_5
P_n
Δ_4
Δ_5
Δ_n
P_3
Δ_3
y
x
Undeformed shape
Deformed shape
Δ_2
Δ_1
P_2
P_1

FIG. 3

from zero to their final values, we can write for the total strain energy, U_S,

$$U_S = \frac{1}{2}\left(P_1 \Delta_1 + P_2 \Delta_2 + \ldots P_n \Delta_n\right)$$

$$= \frac{1}{2} \sum_{i=1,2,\ldots n} P_i \Delta_i \qquad \ldots\ldots\ldots\ldots\ldots\ldots \text{(5)}$$

Physically it is evident that a given structure under a known system of forces (including the reactions), in equilibrium, will have only one deformed state and therefore in accordance with Eq. 5 will have a fixed amount of strain energy, U_S. This is a very basic concept.

Now in arriving at Eq. 5 we ignored the question of which forces are reactions. Let us use a simple structure and see if the choice of reactions affects the amount of strain energy. Consider the beam and loads shown in Fig. 4. We will study three different simple support conditions; namely,

(1) Case I - Cross section at ⓐ is clamped.
(2) Case II - Cross section at ⓒ is clamped.
(3) Case III - Cross section at ⓑ is clamped.

Consider first the deflected shapes. Fig. 5 shows the probable shapes for the different cases.

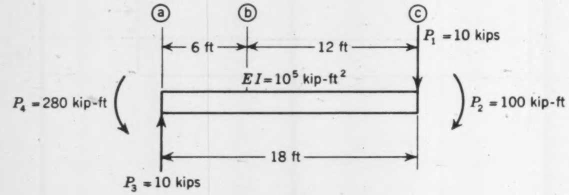

FIG. 4

In all three cases the deflected shapes are the same. The difference in absolute location due to the various choices of supports is merely a rigid body movement (rotation and translation) of the whole beam.

If this constancy of deflected shape is true, then the amount of strain energy in all three cases should be the same.

Consider Fig. 6;

$$\Delta_1 = \frac{L^3}{3EI} P_1 + \frac{L^2}{2EI} P_2 \qquad \ldots\ldots\ldots\ldots\ldots \text{(6a)}$$

$$\Delta_2 = \frac{L^2}{2EI} P_1 + \frac{L}{EI} P_2 \qquad \ldots\ldots\ldots\ldots\ldots \text{(6b)}$$

All lengths are in feet and loads in kips. In Case I, we find (after some simple calculations),

$$\begin{aligned} U_S &= \frac{1}{2}\left[P_1 \Delta_1 + P_2 \Delta_2\right] \\ &= \frac{1}{2}\left[10 \times 0.3564 + 100 \times 0.0342\right] \\ &= \frac{1}{2}\left[3.564 + 3.42\right] = 3.492 \text{ kip-ft} \end{aligned}$$

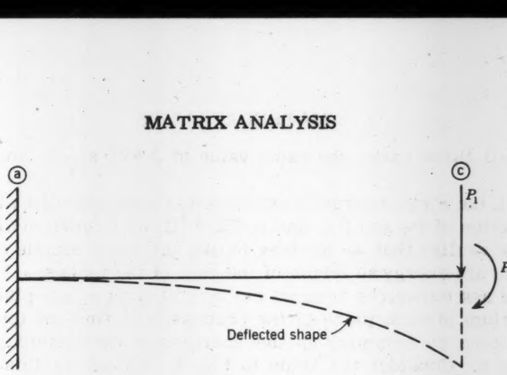
ⓐ
ⓒ
P_1
P_2
Deflected shape

(*a*) CASE I

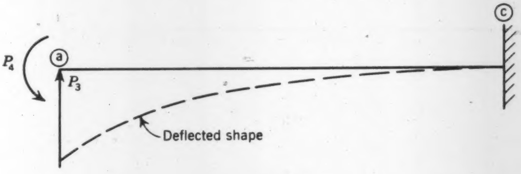
ⓒ
ⓐ
P_4
P_3
Deflected shape

(*b*) CASE II

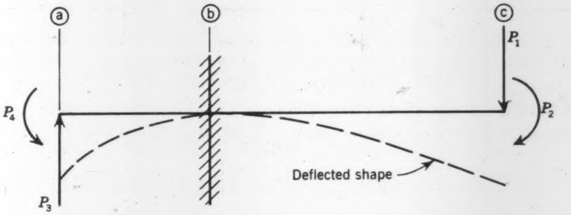
ⓐ
ⓑ
ⓒ
P_1
P_4
P_2
Deflected shape
P_3

(*c*) CASE III

FIG. 5

In Case II, we find

$$
\begin{aligned}
U_S &= \frac{1}{2}\left[P_3\,\Delta_3 + P_4\,\Delta_4\right]\\
&= \frac{1}{2}\left[-0.2592 \times 10 + 280 \times 0.0342\right]\\
&= \frac{1}{2}\left[-2.592 + 9.576\right] = 3.492 \text{ kip-ft}
\end{aligned}
$$

In Case III, we find

$$
\begin{aligned}
U_S &= \frac{1}{2}\left[P_1\,\Delta_1 + P_2\,\Delta_2 + P_3\,\Delta_3 + P_4\,\Delta_4\right]\\
&= \frac{1}{2}\left[10 \times 0.1296 + 100 \times 0.0192 - 10 \times 0.0432 + 280 \times 0.0150\right]\\
&= \frac{1}{2}\left[1.296 + 1.92 - 0.432 + 4.20\right] = 3.492 \text{ kip-ft}
\end{aligned}
$$

We see in all three cases the same value of 3.492 kip-ft for the total strain energy, U_S.

In Case I, the strain energy is expressed as a function of P_1 and P_2; in Case II, as a function of P_3 and P_4; and in Case III, as a function of P_1, P_2, P_3 and P_4. We now realize that we are free to use any set of simple supports and express the strain energy in terms of the rest of the forces.

Next, we ask ourselves "can we cut up a structure into pieces, maintaining the equilibrium of each piece in the process, and find the total energy of the uncut structure by summing up the energies of the individual pieces?" The answer is yes. Consider the beam in Fig. 4. Let us cut this beam into three pieces, maintaining the equilibrium of each piece by applying equilibrating forces, as shown in Fig. 7.

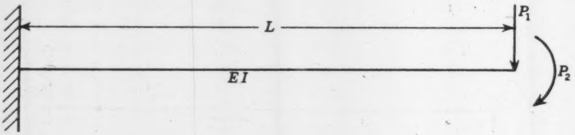

FIG. 6

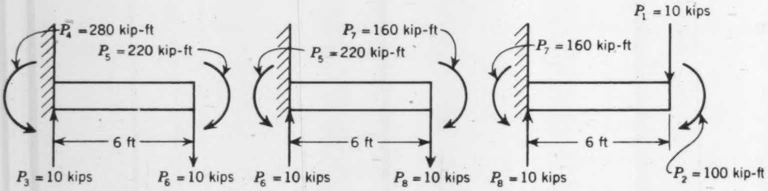

P_4 = 280 kip-ft
P_5 = 220 kip-ft
6 ft
P_3 = 10 kips
P_6 = 10 kips
P_7 = 160 kip-ft
P_5 = 220 kip-ft
6 ft
P_6 = 10 kips
P_8 = 10 kips
P_1 = 10 kips
P_7 = 160 kip-ft
6 ft
P_8 = 10 kips
P_2 = 100 kip-ft

PIECE 1 PIECE 2 PIECE 3

FIG. 7

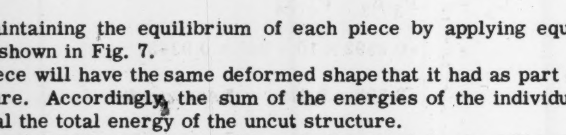

P_1
P_2
a
b
c
R_1
R_2
R_3

FIG. 8

Each piece will have the same deformed shape that it had as part of the uncut structure. Accordingly, the sum of the energies of the individual pieces should equal the total energy of the uncut structure.

Each piece, for illustration, is clamped along its left edge. Using formulas similar to Eqs. 6, we find for piece 1:

$$\begin{aligned} U_1 &= \frac{1}{2}\left[P_6\,\Delta_6 + P_5\,\Delta_5\right] \\ &= \frac{1}{2}\left[+10 \times 0.0468 + 220 \times 0.0150\right] \\ &= 1.884 \text{ kip-ft} \end{aligned}$$

For piece 2:

$$\begin{aligned} U_2 &= \frac{1}{2}\left[P_7\,\Delta_7 + P_8\,\Delta_8\right] \\ &= \frac{1}{2}\left[+\,160 \times 0.0114 + 10 \times 0.0360\right] \\ &= 1.092 \text{ kip-ft} \end{aligned}$$

For piece 3:

$$\begin{aligned} U_3 &= \frac{1}{2}\left[P_1\,\Delta_1 + P_2\,\Delta_2\right] \\ &= \frac{1}{2}\left[10 \times 0.025 + 100 \times 0.0078\right] \\ &= 0.516 \text{ kip-ft} \end{aligned}$$

The total energy U_S is given by

$$\begin{aligned} U_S &= U_1 + U_2 + U_3 \\ &= 1.884 + 1.092 + 0.516 \\ &= 3.492 \text{ kip-ft} \end{aligned}$$

which checks our previous calculation of the total strain energy.

Thus, we see that we can break up a structure into convenient units. We can select any group of reactions or simple supports for each piece. Before we proceed with the matrix formulation of theory incorporating the preceding concepts, let us consider for a moment what we mean by the total structure.

CONCEPT OF THE "WHOLE" STRUCTURE

Traditionally, the structural engineer has concentrated his analysis efforts on the superstructure. Noting that interaction with the foundation does influence the stress and displacements within the superstructure in the cases of yielding supports and indeterminate reactions, it is logical to include the foundation with the superstructure calling this combination the "whole" structure. This is tantamount to saying that all elements that may contribute to the total energy of the system should be included in the "whole" structure.

Consider the two-span beam on elastic supports shown in Fig. 8.

To show the inclusion of the foundation, we redraw Fig. 8 with the results shown in Fig. 9.

The foundation member, shown in Fig. 9, has the same elastic effects (that is, elastic support movements) at the beam supports as specified in the original problem. If in Fig. 8 the support at a settled an amount S due to a given value of R_1, then the foundation member shown in Fig. 9, would displace the same amount S at a due to the same value R_1, acting upon the foundation member at a. The simple reactions shown at point o are those necessary for equilibrium of the external forces, such as P_1 and P_2. The addition of the foundation member now places the support forces R_1, R_2 and R_3 in the category of internal forces. Point o, selected as the point of application of the "whole" structure reactions, is the arbitrary origin of a set of axes that neither translates nor rotates (and therefore the reactions do not contribute to the energy).

In Fig. 10, we have separated the superstructure from the foundation to facilitate the calculation of the total energy, U_T.

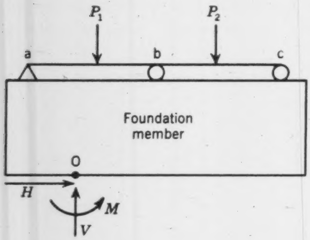

FIG. 9

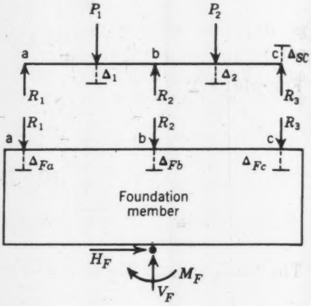

FIG. 10

We can write the energy U_S for the superstructure as

$$U_S = \frac{1}{2}\left[P_1\,\Delta_1 + P_2\,\Delta_2 + R_3\,\Delta_{SC}\right] \quad \ldots\ldots\ldots\ldots \quad (7)$$

and the energy of the foundation member, U_F, as

$$U_F = \frac{1}{2}\left(R_1\,\Delta_{Fa} + R_2\,\Delta_{Fb} + R_3\,\Delta_{Fc}\right) \quad \ldots\ldots\ldots\ldots \quad (8)$$

The total energy of the "whole" structure, U_T, is then given by

$$U_T = U_S + U_F \quad \ldots\ldots\ldots\ldots\ldots\ldots \quad (9)$$

Now let us proceed with the matrix formulation of theory beginning with energy expressions.

MATRIX FORMULATION OF ENERGY AS A FUNCTION OF LOADS

The matrix formulation of strain energy as a function of loads resulting in Eq. 21 (to be presented subsequently) has been covered elsewhere (8-10) and is repeated here both for completeness and to illustrate the fundamental concepts given in this paper.

We consider a "whole" structure acted upon by a set of forces (including reactions), P_S. Now we break the structure up into k convenient parts, maintaining the equilibrium of each part in the process by the addition of appropriate equilibrating forces at the cuts.

If each piece is considered to be in equilibrium under its own set of forces (including its reactions), P_{ki}, then we can express the energy of a typical piece, U_k, as

$$U_k = \frac{1}{2} \sum_{i = 1,\, 2,\, \ldots\, i} P_{ki}\,\Delta_{ki} \quad \ldots\ldots\ldots\ldots\ldots \quad (10)$$

where Δ_{ki} is the deflection of the P_{ki} load. The energy of the whole system, U_T, is the sum of the individual energies and is given by

$$U_T = U_1 + U_2 + \ldots U_k = \sum_{k=1,2,k} U_k \quad \ldots\ldots\ldots (11)$$

In matrix form we can rewrite Eq. 10 as

$$\left[U_k\right] = \frac{1}{2}\left[P_{ki}\right]\left\{\Delta_{ki}\right\} \quad \ldots\ldots\ldots\ldots\ldots\ldots (12)$$

If we use Eq. 3 in Eq. 12, employing appropriate notation, we have as a result

$$\left[U_k\right] = \frac{1}{2}\left[P_{ki}\right]\left[\delta_{kij}\right]\left\{P_{kj}\right\} \quad \ldots\ldots\ldots\ldots\ldots\ldots (13)$$

Eq. 13 expresses the strain energy of piece k as a function of the forces, P_{ki}, acting upon it. In Eq. 13, $\left[P_{ki}\right]$ is a row matrix the the transpose of $\left\{P_{kj}\right\}$. The term $\left[\delta_{kij}\right]$ is the matrix of flexibilities for piece k.

Now let us take a statically indeterminate structure under the action of applied loads, P_A. If we make the structure statically determinate by the selection of certain redundants, P_x, and consider the "whole" structure, that is, include the foundation, then we can write the total energy as

$$U_T = \frac{1}{2}\left[P_x \;\vdots\; P_A\right]\left[\begin{array}{c:c} \delta_{xy} & \delta_{xB} \\ \hdashline \delta_{Ay} & \delta_{AB} \end{array}\right]\left\{\begin{array}{c} P_y \\ \hdashline P_B \end{array}\right\} \quad \ldots\ldots\ldots\ldots (14)$$

The use of partitioning here is to separate the redundant forces from the given applied loads acting upon the original structure. Eq. 14 is the desired equation for the total energy. Let us see how we may obtain the total energy by breaking up the statically determinate structure into k parts (including the foundation), and then summing up the energies of the individual parts as indicated by Eq. 11.

Starting with a typical k piece, we note that the loads, P_{ki}, acting upon the piece can be expressed in terms of the redundants, P_x, and the applied loads, P_A, acting upon the given structure; thus,

$$\left\{P_{ki}\right\} = \left[a_{kix} \;\vdots\; a_{kiA}\right]\left\{\begin{array}{c} P_x \\ \hdashline P_A \end{array}\right\} \quad \ldots\ldots\ldots\ldots\ldots (15)$$

where the partitioned [a] represents the required coefficients expressing the P_{ki} in terms of the P_x and P_A loads. If we now use Eq. 15 in Eq. 13 we get for each k piece

$$\left[U_k\right] = \frac{1}{2}\left[P_x \;\vdots\; P_A\right]\left[a_{kix} \;\vdots\; a_{kiA}\right]^T\left[\delta_{kij}\right]\left[a_{kjy} \;\vdots\; a_{kjB}\right]\left\{\begin{array}{c} P_y \\ \hdashline P_B \end{array}\right\} \quad \ldots\ldots (16)$$

where $[\;\;]^T$ stands for the transpose matrix. If we now use Eq. 16 in Eq. 11 we have as a result

$$\left[U_T\right] = \frac{1}{2}\left[P_x \;\vdots\; P_A\right]\sum_k\left(\left[a_{kix} \;\vdots\; a_{kiA}\right]^T\left[\delta_{kij}\right]\left[a_{kjy} \;\vdots\; a_{kjB}\right]\right)\left\{\begin{array}{c} P_y \\ \hdashline P_B \end{array}\right\} \ldots (17)$$

Let us now examine the expression

$$\left[\begin{array}{c:c} a_{kix} & a_{kiA} \end{array}\right]^T \left[\delta_{kij}\right] \left[\begin{array}{c:c} a_{kjy} & a_{kjB} \end{array}\right] \quad \ldots\ldots\ldots\ldots (18)$$

which appears in Eqs. 16 and 17. The term $\left[\delta_{kij}\right]$ is the matrix of influence deflection or flexibility coefficients for piece k in terms of the P_{ki} forces acting upon that piece. To transform these coefficients into coefficients in terms of the P_x and P_A forces acting upon the statically determinate structure we carry out the classical transformation given in Expression 18 which is of the form

$$[A]^T [B] [A] = [C] \quad \ldots\ldots\ldots\ldots\ldots\ldots \; 19$$

where $[B]$ is a symmetrical matrix; $[C]$, the result will be symmetrical, automatically.

Carrying out the triple matrix multiplication called for in Expression 18 results in

$$\left[\begin{array}{c:c} a_{kix} & a_{kiA} \end{array}\right]^T \left[\delta_{kij}\right] \left[\begin{array}{c:c} a_{kiy} & a_{kjB} \end{array}\right] = \left[\begin{array}{c:c} \delta_{kxy} & \delta_{kxB} \\ \hdashline \delta_{kAy} & \delta_{kAB} \end{array}\right] \quad \ldots\ldots\ldots (20)$$

which is the matrix of flexibilities for piece k in terms of the P_x and P_A forces. Using Eq. 20 in Eq. 17 we see that the total energy is given by

$$\left[U_T\right] = \frac{1}{2}\left[\begin{array}{c:c} P_x & P_A \end{array}\right] \left(\sum_k \left[\begin{array}{c:c} \delta_{kxy} & \delta_{kxB} \\ \hdashline \delta_{kAy} & \delta_{kAB} \end{array}\right]\right) \left\{\begin{array}{c} P_y \\ \hdashline P_B \end{array}\right\} \quad \ldots\ldots\ldots (21)$$

Eq. 21 indicates a basic procedure for the determination of the total strain energy as the summation of the flexibilities of the individual parts expressed in terms of the redundants, P_x, and the given applied forces, P_A. The theory given by Eq. 20 would be used to transform the flexibilities given in terms of forces acting upon the k part into flexibilities in terms of P_x and P_A.

For an alternate procedure for evaluating the total energy, U_T, consider the summation of the triple products given in Eq. 17. We can write the triple product as

$$\sum_k \left[\begin{array}{c:c} a_{kix} & a_{kiA} \end{array}\right]^T \left[\delta_{kij}\right] \left[\begin{array}{c:c} a_{kjy} & a_{kjB} \end{array}\right] = [a]^T \left[\delta_k\right] [a] \ldots\ldots (22)$$

where $\left[\delta_k\right]$ is the diagonal block matrix

$$\left[\delta_k\right] = \begin{bmatrix} \delta_{1ij} & & & & & \\ & \delta_{2ij} & & & & \\ & & \delta_{3ij} & & & \\ & & & \delta_{4ij} & & \\ & & & & \ddots & \\ & & & & & \delta_{kij} \end{bmatrix} \quad \ldots\ldots\ldots\ldots\ldots\ldots (23)$$

and $[a]^T$ is the transpose of $[a]$ where $[a]$ is given by

$$[a] = \begin{bmatrix} a_{1jy} & a_{1jB} \\ a_{2jy} & a_{2jB} \\ a_{3jy} & a_{3jB} \\ a_{4jy} & a_{4jB} \\ \vdots & \vdots \\ a_{kjy} & a_{kjB} \end{bmatrix} \quad \ldots\ldots\ldots\ldots\ldots\ldots \quad (24)$$

Matrix $[a]$ is the array of coefficients expressing the forces acting upon the pieces (such as bar forces) in terms of the redundants P_x and applied forces P_A. Having set up the $[\delta_k]$ and $[a]$ matrices, we use Eq. 22 with the result

$$[a]^T \left[\delta_k\right][a] = \left[\begin{array}{c|c} \delta_{xy} & \delta_{xB} \\ \hline \delta_{Ay} & \delta_{AB} \end{array}\right] \quad \ldots\ldots\ldots\ldots\ldots \quad (25)$$

Eq. 25 is used in Eq. 14 which is the expression for the total energy, U_T. It is to be noted that the size of matrices developed in building up the $[\delta_k]$ and $[a]$ matrices, in accordance with the foregoing theory in practice, is minimized by various packing or condensing techniques.

DEFLECTIONS AND THE METHOD OF LEAST WORK

If the total energy of a linear elastic structure is expressed as a function of one or more P_i loads, then using the well-known differential relation of Castigliano

$$\frac{\partial U_T}{\partial P_i} = \Delta_i \quad \ldots\ldots\ldots\ldots\ldots\ldots\ldots\ldots \quad (26)$$

we can find the deflection at P_i in the direction of P_i. Furthermore, if the P_i loads are taken as the redundants P_x, then $\Delta_x = 0$ in the usual case (keeping in mind, we are using the "whole" structure concept) and Eq. 26 becomes

$$\frac{\partial U_T}{\partial U_x} = 0 \quad \ldots\ldots\ldots\ldots\ldots\ldots\ldots \quad (27)$$

which is known as the Least Work Theorem of Castigliano.

Applying Eq. 27 to a statically indeterminate structure whose total energy is given by Eq. 14 we find

$$\left\{\frac{\partial U_T}{\partial P_x}\right\} = \{0\} = \left[\delta_{xy} \;\vdots\; \delta_{xB}\right] \left\{\begin{array}{c} P_y \\ \hline P_B \end{array}\right\} \quad \ldots\ldots\ldots\ldots\ldots \quad (28)$$

Eq. 28 is the matrix form of the equations of consistent deflection, known as the Maxwell-Mohr Equations. Solution of the x equations given by Eq. 28 yields for the redundants

$$\left\{P_y\right\} = -\left[\delta_{xy}\right]^{-1}\left[\delta_{xB}\right]\left\{P_B\right\} = [D]\left\{P_B\right\} \qquad (29)$$

Eq. 29 expresses the redundant P_x (or P_y) in terms of the applied forces P_A (or P_B).

Stresses.—If we set up a matrix [J]

$$[J] = \left[\frac{D}{I_A}\right] \qquad (30)$$

then to find the forces acting upon the pieces of structure, we have

$$\left\{P_i\right\} = [a]\ [J]\left\{P_B\right\} \qquad (31)$$

To find any desired stresses within the original structure, we first find these stresses in terms of the redundants, P_x, and applied loads, P_A, thus

$$\{S\} = \left[b_x \,\vdots\, b_A\right]\left\{\begin{array}{c} P_x \\ \hdashline P_A \end{array}\right\} \qquad (32)$$

where [b] is the matrix of coefficients expressing the stresses, S, in terms of the redundants and loads. Use of Eq. 30 in Eq. 32 gives the desired result for, S,

$$\{S\} = \left[b_x \,\vdots\, b_A\right][J]\left\{P_A\right\} \qquad (33)$$

Deflections.—To find deflections at the applied loads, P_A, we apply Eq. 26 to the expression for the total energy given by Eq. 14, to result in

$$\left\{\frac{\partial U_T}{\partial P_A}\right\} = \left\{\Delta_A\right\} = \left[\delta_{Ay} \,\vdots\, \delta_{AB}\right]\left\{\begin{array}{c} P_y \\ \hdashline P_B \end{array}\right\} \qquad (34)$$

In Eq. 34 the deflections $\{\Delta_A\}$ are expressed in terms of the redundants and applied loads. To find the deflections as a function of the applied loads only, we use Eq. 30 in Eq. 34 getting

$$\left\{\Delta_A\right\} = \left[\delta_{Ay} \,\vdots\, \delta_{AB}\right][J]\left\{P_B\right\} \qquad (35)$$

Eq. 35 is the desired result.

Flexibilities.—It should be noted that the flexibility coefficients for the original structure (in terms of the applied loads only) is given by

$$\left[\delta_{AB}\right] = \left[\delta_{Ay} \,\vdots\, \delta_{AB}\right][J] \qquad (36)$$

We see from the foregoing that Eq. 14 for the total energy, U_T, of the "whole" structure is the fundamental equation and the matrix contained in (21); namely,

$$\left[\begin{array}{c:c} \delta_{xy} & \delta_{xB} \\ \hdashline \delta_{Ay} & \delta_{AB} \end{array}\right]$$

is the key in the solution of the stresses and displacements in a structural problem.

To illustrate the theory and basic concepts, we will carry out two problems, the first involving a statically determinate truss on elastic supports and the second involving a continuous beam on unyielding supports.

PROBLEM 1

Given the statically determinate truss on elastic supports, shown in Fig. 11, it is desired to obtain the influence deflection coefficients for the truss, including the elasticity of the foundation. Basic data, including bar stresses for one kip values of the P loads, are given in Table 1. Values of the reactions R_1, R_2 and R_3 for one kip values of the loads are given in Table 2.

The flexibility coefficients, representing the elasticity of the foundation, are given in Table 3. It is to be noted that since the modulus of elasticity, E, is assumed constant at 30,000 ksi, it does not appear in any of these coefficients (or, in other words, all deflections are multiplied by E). We will drop the E in all subsequent formulation, and then in the final result reinsert it. For example, the deflection at R_2, Δ_{R_2} (in feet), is given as

$$E\,\Delta_{R_2} = 21.8081\,R_2 + 16.2851\,R_3 \quad \ldots\ldots\ldots\ldots \quad (37)$$

Let us now draw the "whole" structure (Fig. 12).

We will designate the energy of the superstructure by U_S and that of the foundation by U_F. The basic procedure to obtain the total energy U_T (and therefore our answer) follows three steps (noting that no redundants exist in this problem):

(1) The truss is considered to be broken up into the nine basic bars making up the truss. These are the k pieces cited previously. The energy, U_S, is obtained using the alternate procedure which essentially consists of setting up one matrix incorporating all the flexibilities of the 9 bars as indicated by Eq. 23 and then finding the energy, U_S.

(2) The energy, U_F, of the foundation is found from Eq. 16 using the matrix flexibility of the foundation which essentially is Table 2.

(3) The total energy, U_T, is found using the procedure indicated in Eqs. 11 and 21 and is given by

$$U_T = U_S + U_F \quad \ldots\ldots\ldots\ldots\ldots\ldots \quad (38)$$

The answer to our problem is the flexibility matrix, used to define the total energy, U_T. This matrix will yield deflections relative to absolute reference axes located at point o in Fig. 12.

Step 1.—Using the data in Table 1, the flexibility matrix $\left[\delta_k\right]$ given by Eq. 23 is

$$\left[\delta_k\right] = \begin{bmatrix} 1.748 & & & & & & & & \\ & 1.748 & & & & & & & \\ & & 1.748 & & & & & & \\ & & & 1.748 & & & & & \\ & & & & 1.512 & & & & \\ & & & & & 1.512 & & & \\ & & & & & & 1.512 & & \\ & & & & & & & 2.867 & \\ & & & & & & & & 2.867 \end{bmatrix} \quad \ldots\ldots\ldots \quad (39)$$

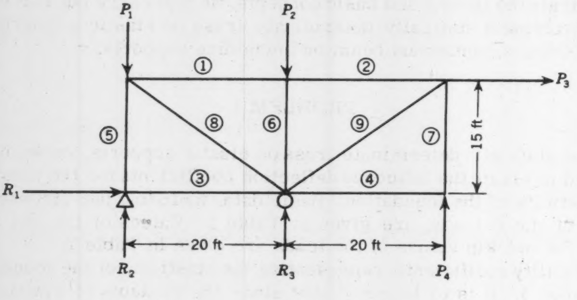
P1
P2
①
②
P3
⑤
⑧
⑥
⑨
⑦
15 ft
③
④
R1
20 ft
20 ft
R2
R3
P4

FIG. 11

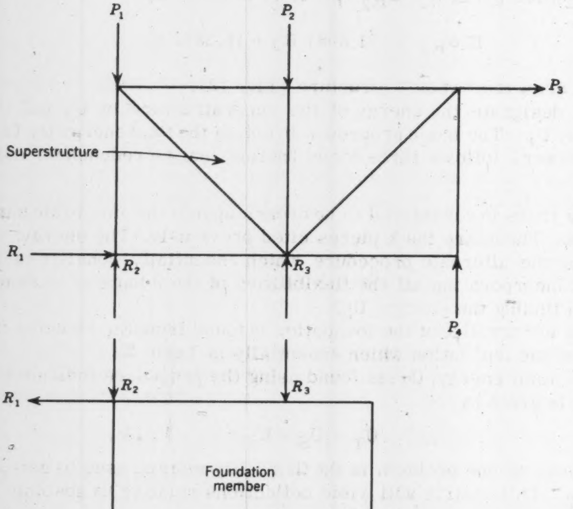
P1
P2
P3
Superstructure
R1
R2
R3
P4
R2
R3
R1
Foundation member
H_F
O
M_F
V_F

FIG. 12

TABLE 1.—BAR DATA AND STRESSES

Bar No. (1)	L, in ft (2)	A, in sq in. (3)	L/A (4)	Bar Stresses[a] for			
				P_1 = 1 kip (5)	P_2 = 1 kip (6)	P_3 = 1 kip (7)	P_4 = 1 kip (8)
1	20	11.44	1.748	0	0	+1	-1.33333
2	20	11.44	1.748	0	0	+1	-1.33333
3	20	11.44	1.748	0	0	+1	0
4	20	11.44	1.748	0	0	0	0
5	15	9.92	1.512	-1	0	+0.75	-1
6	15	9.92	1.512	0	-1	0	0
7	15	9.92	1.512	0	0	0	-1
8	25	8.72	2.867	0	0	-1.25	+1.66667
9	25	8.72	2.867	0	0	0	+1.66667

[a] A plus (+) sign denotes tension

TABLE 2.—REACTIONS

Reactions (1)	Reactions for			
	P_1 = 1 kip (2)	P_2 = 1 kip (3)	P_3 = 1 kip (4)	P_4 = 1 kip (5)
R_1	0	0	-1	0
R_2	+1	0	-0.75	+1
R_3	0	+1	+0.75	-2

TABLE 3.—FOUNDATION FLEXIBILITIES

Deflection at (1)	Due to		
	R_1 = 1 kip (2)	R_2 = 1 kip (3)	R_3 = 1 kip (4)
R_1	0.24295	0	0
R_2	0	21.8081	16.2851
R_3	0	16.2851	18.1925

Note that the first row (and first column) corresponds to bar ①, etc. The term δ_k is a diagonal matrix. The flexibility of an axially loaded bar is given by the value of L/AE for the bar.

The matrix $[a]$ given in Eq. 24, expressing the bar stresses in terms of the applied loads P_1, P_2, P_3 and P_4, is set up using the data in Table 1 and is

$$[a] = \begin{bmatrix} 0 & 0 & +1 & -1.33333 \\ 0 & 0 & +1 & -1.33333 \\ 0 & 0 & +1 & 0 \\ 0 & 0 & 0 & 0 \\ -1 & 0 & +0.75 & -1 \\ 0 & -1 & 0 & 0 \\ 0 & 0 & 0 & -1 \\ 0 & 0 & -1.25 & +1.66667 \\ 0 & 0 & 0 & +1.66667 \end{bmatrix} \quad \ldots\ldots\ldots\ldots\ldots \quad (40)$$

Note in $[a]$ the first column corresponds to P_1, etc., and the first row to bar ①, etc.

The value of U_S is given by

$$U_S = \frac{1}{2}\begin{bmatrix} P_1 & P_2 & P_3 & P_4 \end{bmatrix}\begin{bmatrix} \delta_S \end{bmatrix}\begin{Bmatrix} P_1 \\ P_2 \\ P_3 \\ P_4 \end{Bmatrix} \quad \ldots\ldots\ldots\ldots\ldots \quad (41)$$

where

$$\begin{bmatrix} \delta_S \end{bmatrix} = [a]^T \begin{bmatrix} \delta_k \end{bmatrix} [a] \quad \ldots\ldots\ldots\ldots \quad (42)$$

Performing the operations called for in Eq. 42, we find $\begin{bmatrix} \delta_S \end{bmatrix}$ given by

$$\begin{bmatrix} \delta_S \end{bmatrix} = \begin{bmatrix} +1.512 & 0 & -1.134 & +1.512 \\ 0 & +1.512 & 0 & 0 \\ -1.134 & 0 & +10.5742 & -11.7682 \\ +1.512 & 0 & -11.7682 & +25.1669 \end{bmatrix} \quad \ldots\ldots\ldots \quad (43)$$

Note the symmetry of the result. Again the first row and first column refers to the load P_1, etc.

Step 2.—Using the data contained in Table 3, we can write the foundation flexibility matrix as

$$\begin{bmatrix} \delta_{kF} \end{bmatrix} = \begin{array}{c} \\ R_1 \\ R_2 \\ R_3 \end{array} \begin{array}{c} \begin{array}{ccc} R_1 \quad\quad & R_2 \quad\quad & R_3 \end{array} \\ \begin{bmatrix} 0.24295 & 0 & 0 \\ 0 & 21.8081 & 16.2851 \\ 0 & 16.2851 & 18.1925 \end{bmatrix} \end{array} \quad \ldots\ldots\ldots\ldots \quad (44)$$

The row and column designations are shown in (δ_{kF}) to emphasize that these flexibilities are in terms of R_1, R_2, and R_3. We need to express them in terms of P_1, P_2, P_3, and P_4, and for this purpose we set up a transformation matrix which expresses the R's in terms of the P's.

This is done using Table 2, to result in

$$[a_F] = \begin{array}{c} \\ R_1 \\ R_2 \\ R_3 \end{array} \begin{array}{c} \begin{array}{cccc} P_1 & P_2 & P_3 & P_4 \end{array} \\ \left[\begin{array}{cccc} 0 & 0 & -1 & 0 \\ +1 & 0 & -0.75 & +1 \\ 0 & +1 & +0.75 & -2 \end{array}\right] \end{array} \quad \ldots\ldots\ldots\ldots\ldots \quad (45)$$

The row and column designations are shown to indicate the relationship of the R's to the P's.

Now the energy of the foundation, U_F, can be written as

$$U_F = \frac{1}{2} \left[R_1 \; R_2 \; R_3\right] \left[\delta_{kF}\right] \begin{Bmatrix} R_1 \\ R_2 \\ R_3 \end{Bmatrix} \quad \ldots\ldots\ldots\ldots\ldots \quad (46)$$

If we express the R's in terms of the P's by

$$\begin{Bmatrix} R_1 \\ R_2 \\ R_3 \end{Bmatrix} = [a_F] \begin{Bmatrix} P_1 \\ P_2 \\ P_3 \\ P_4 \end{Bmatrix} \quad \ldots\ldots\ldots\ldots\ldots\ldots\ldots \quad (47)$$

then using Eq. 47 in Eq. 46, and noting Eq. 45, we have the energy in terms of P_1, P_2, and P_3, thus

$$U_F = \frac{1}{2} \left[P_1 \; P_2 \; P_3 \; P_4\right] \left[\delta_F\right] \begin{Bmatrix} P_1 \\ P_2 \\ P_3 \\ P_4 \end{Bmatrix} \quad \ldots\ldots\ldots\ldots \quad (48)$$

where

$$\left[\delta_F\right] = \left[a_F\right]^T \left[\delta_{kF}\right]\left[a_F\right] \quad \ldots\ldots\ldots\ldots\ldots \quad (49)$$

Carrying out Eq. 49 we find

$$\left[\delta_F\right] = \left[\begin{array}{cccc} 21.8081 & 16.2851 & -4.14225 & -10.7621 \\ 16.2851 & 18.1925 & 1.43055 & -20.0999 \\ -4.14225 & 1.43055 & 4.17960 & -7.00335 \\ -10.7621 & -20.0999 & -7.00335 & 29.4377 \end{array}\right] \quad \ldots \quad (50)$$

Step 3.—The total strain energy U_T is given by Eq. 38, and is equal to

$$U_T = \frac{1}{2} \left[P_1 \; P_2 \; P_3 \; P_4\right] \left[\delta_P\right] \begin{Bmatrix} P_1 \\ P_2 \\ P_3 \\ P_4 \end{Bmatrix} \quad \ldots\ldots\ldots\ldots \quad (51)$$

where

$$\left[\delta_P\right] = \left[\delta_S\right] + \left[\delta_F\right] \quad \ldots\ldots\ldots\ldots\ldots \quad (52)$$

and using Eqs. 43 and 49 in Eq. 52, we have (at this point we reinsert E)

$$E\left[\delta_P\right] = \begin{array}{c} \\ P_1 \\ P_2 \\ P_3 \\ P_4 \end{array} \begin{array}{c} \begin{array}{cccc} P_1 & P_2 & P_3 & P_4 \end{array} \\ \left[\begin{array}{cccc} 23.3201 & 16.2851 & -5.2762 & -9.2501 \\ 16.2851 & 19.7045 & 1.4306 & -20.0999 \\ -5.2762 & 1.4306 & 14.7538 & -18.7716 \\ -9.2501 & -20.0999 & -18.7716 & 54.6046 \end{array}\right] \end{array} \quad \ldots \quad (53)$$

The term $E\left[\delta_P\right]$ given by Eq. 53 is our desired result. The P row and column designations are shown for purposes of identification.

PROBLEM 2

Given the three-span continuous beam on unyielding supports and under the loading shown in Fig. 13, it is desired to find all the reactions. In Fig. 13 A' is the area effective in resisting shear.

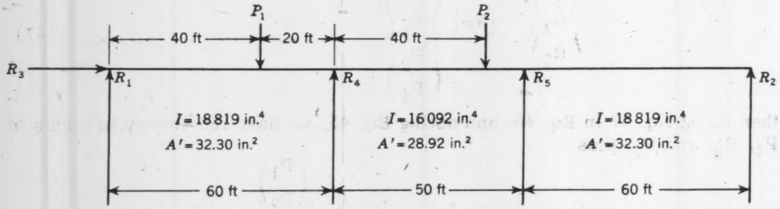

FIG. 13

This structure is statically indeterminate to the second degree. Furthermore, the horizontal reaction, R_3, is equal to zero and can be ignored in this problem.

The solution logically follows six steps:

(1) Selection of a statically determinate structure.

(2) Break-up of the structure into k parts.

(3) Calculation of the total energy using a matrix combining the flexibilities of the individual parts.

(4) Expression of the total energy in terms of the applied loads and redundants acting upon the statically determinate structure.

(5) Solution for the redundants.

(6) Evaluation of the reactions as functions of the applied loads.

Step 1.—The reactions R_1 and R_2 are selected as the redundants. The statically determinate structure, therefore, has R_1, R_2, P_1, and P_2 acting upon it.

Step 2.—Fig. 14 shows the break up of the structure into three parts lettered A through C. The required equilibrating forces are shown in Fig. 14. It should be noted that the structure is cut just to the left and right of the loads P_1 and P_2. Section A is clamped at its right end, section B at the cross section at R_4, and section C at the cross section at R_5.

If we consider the joints (points) upon which P_1 and P_2 act as pieces of structure, they do not contribute to the energy calculation at this step, since the strain energy of a point is equal to zero.

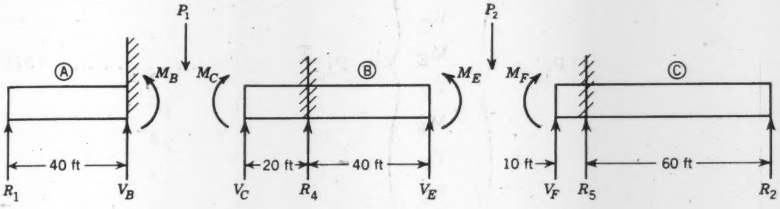

FIG. 14

Step 3.—The flexibilities for a simple cantilever acted upon at the free end by a moment, M, and a transverse force, V, are known to be

$$\delta_{MM} = \frac{L}{E\,I} \quad \ldots\ldots\ldots\ldots\ldots\ldots \quad (54a)$$

$$\delta_{MV} = \delta_{VM} = \frac{L^2}{2\,E\,I} \quad \ldots\ldots\ldots\ldots\ldots \quad (54b)$$

and

$$\delta_{VV} = \frac{L^3}{3\,E\,I} + \frac{k\,L}{A'\,G} \quad \ldots\ldots\ldots\ldots\ldots \quad (54c)$$

where in the expression for δ_{VV} the effect of shear, $\frac{k\,L}{A'\,G}$, is included. If deflections, δ, are to be in feet, Eqs. 54 become (noting E is a constant and k is equal to 1.0 for I shapes),

$$E\,\delta_{MM} = 144\frac{L}{I} \quad \ldots\ldots\ldots\ldots\ldots \quad (55a)$$

$$E\,\delta_{MV} = E\,\delta_{VM} = 144 \times \frac{L^2}{2\,I} \quad \ldots\ldots\ldots\ldots \quad (55b)$$

and

$$E\,\delta_{VV} = 144 \times \frac{L^3}{3\,I} + 2.5 \times \frac{L}{A'} \quad \ldots\ldots\ldots\ldots \quad (55c)$$

In Table 4 are listed the flexibilities calculated in accordance with Eqs. 55. The term E will drop out of the calculations. Accordingly, we will ignore it for simplicity.

The total energy, U_T, can be written as

$$U_T = \frac{1}{2}\left[P_i\right]\left[\delta_{ij}\right]\left\{P_j\right\} \quad \ldots\ldots\ldots\ldots\ldots \quad (56)$$

where

$$\left\{P_j\right\} = \left\{\begin{matrix} R_1 \\ M_C \\ V_C \\ M_E \\ V_E \\ M_F \\ V_F \\ R_2 \end{matrix}\right\} = \left[P_i\right]^T \quad \dots\dots\dots\dots\dots\dots \quad (57)$$

and, using Table 4,

$$\left[\delta_{ij}\right] = \begin{bmatrix} 166.335 & & & & & & & \\ & 0.153037 & 1.53040 & & & & & \\ & 1.53040 & 21.953 & & & & & \\ & & & 0.357942 & 7.15884 & & & \\ & & & 7.15884 & 194.360 & & & \\ & & & & & 0.089485 & 0.44743 & \\ & & & & & 0.44743 & 3.8473 & \\ & & & & & & & 555.570 \end{bmatrix} \quad \dots \quad (58)$$

The row (and column) designations correspond to the designations of the rows given for $\left\{P_j\right\}$ in Eq. 57.

TABLE 4.—FLEXIBILITY COEFFICIENTS

Section (1)	Forces (2)	$E\ \delta_{MM}$ (3)	$E\ \delta_{MV}$ (4)	$E\ \delta_{VV}$ (5)
A	R_1	–	–	166.335
B	M_C, V_C	0.153037	1.53040	21.953
	M_E, V_E	0.357942	7.15884	194.360
C	M_F, V_F	0.089485	0.44743	3.8473
	R_2	–	–	555.570

Step 4.—To express the total energy, U_T, in terms of the forces acting upon the statically determinate structure, we write the transformation

$$\left\{P_j\right\} = \left[a_{jy} \,\vdots\, a_{jB}\right] \left\{\begin{array}{c} P_Y \\ \hline P_B \end{array}\right\} \quad \dots\dots\dots\dots\dots \quad (59)$$

Using the equations of static equilibrium and putting the sections together, we can obtain [a] by setting up the matrix product

$$[a] = \left[a_{jy} \,\vdots\, a_{jB}\right] = \left[b_{jk}\right]\left[C_{ky} \,\vdots\, C_{kB}\right] \quad \ldots\ldots\ldots\ldots \quad (60)$$

where

$$\left[b_{jk}\right] = \begin{array}{c|ccccc|} & R_5 & R_1 & R_2 & P_1 & P_2 \\ \hline R_1 & & +1 & & & \\ M_C & & +40 & & & \\ V_C & & +1 & & -1 & \\ M_E & +10 & & +70 & & \\ V_E & +1 & & +1 & & -1 \\ M_F & +10 & & +70 & & \\ V_F & -1 & & -1 & & \\ R_2 & & & +1 & & \\ \hline \end{array} \quad \ldots\ldots\ldots\ldots \quad (61)$$

and

$$\left[C_{ky} \,\vdots\, C_{kB}\right] = \begin{array}{c|cccc|} & R_1 & R_2 & P_1 & P_2 \\ \hline R_5 & +1.2 & -2.2 & -0.4 & +0.8 \\ R_1 & +1 & & & \\ R_2 & & +1 & & \\ P_1 & & & +1 & \\ P_2 & & & & +1 \\ \hline \end{array} \quad \ldots\ldots\ldots\ldots \quad (62)$$

In both Eqs. 61 and 62 the row and column designations are shown for identification of elements.

Calculating [a] by Eq. 60 we can express the total energy, U_T, in terms of the forces as the statically determinate structure by using Eq. 60 in Eq. 59 and then Eq. 59 in Eq. 56 with the result

$$U_T = \frac{1}{2}\left[P_x \,\vdots\, P_A\right]\left[\begin{array}{c|c} \delta_{xy} & \delta_{xB} \\ \hline \delta_{Ay} & \delta_{AB} \end{array}\right]\left\{\begin{array}{c} P_y \\ \hline P_B \end{array}\right\} \quad \ldots\ldots\ldots\ldots \quad (63)$$

with

$$\left[\begin{array}{c|c} \delta_{xy} & \delta_{xB} \\ \hline \delta_{Ay} & \delta_{AB} \end{array}\right] = [a]^T \left[\delta_{ij}\right] [a]$$

$$= \begin{array}{c|cc|cc|} & R_1 & R_2 & P_1 & P_2 \\ \hline R_1 & +1098.72 & +262.23 & -264.21 & +42.953 \\ R_2 & +262.23 & +1098.71 & -87.410 & +64.429 \\ \hline P_1 & -264.21 & -87.410 & +82.301 & -14.318 \\ P_2 & +42.953 & +64.429 & -14.318 & +10.237 \\ \hline \end{array} \quad \ldots \quad (64)$$

Step 5.—The redundants are given by

$$\left\{P_y\right\} = -\left[\delta_{xy}\right]^{-1}\left[\delta_{xB}\right]\left\{P_B\right\} = [D]\left\{P_B\right\} \quad \ldots\ldots\ldots \quad (65)$$

Carrying out the operations indicated in Eq. 65, we find

$$\begin{Bmatrix} R_1 \\ R_2 \end{Bmatrix} = -\left[\delta_{xy}\right]^{-1}\left[\delta_{xB}\right]\begin{Bmatrix} P_1 \\ P_2 \end{Bmatrix} = \begin{bmatrix} 0.234865 & -0.026614 \\ 0.023501 & -0.052288 \end{bmatrix}\begin{Bmatrix} P_1 \\ P_2 \end{Bmatrix} \quad \ldots\ldots \quad (66)$$

Step 6.—To find the reactions in terms of P_1 and P_2, we form the matrix

$$[J] = \left[\frac{D}{I_2}\right] = \begin{array}{c|cc|} & P_1 & P_2 \\ R_1 & 0.234865 & -0.026614 \\ R_2 & 0.023501 & -0.052288 \\ P_1 & +1 & \\ P_2 & & +1 \end{array} \quad \ldots\ldots\ldots\ldots \quad (67)$$

We can express the reactions in terms of the redundants and the applied loads thus,

$$\begin{Bmatrix} R_1 \\ R_2 \\ R_4 \\ R_5 \end{Bmatrix} = [g]\begin{Bmatrix} R_1 \\ R_2 \\ P_1 \\ P_2 \end{Bmatrix} \quad \ldots\ldots\ldots\ldots\ldots\ldots \quad (68)$$

with

$$[g] = \begin{array}{c|cccc|} & R_1 & R_2 & P_1 & P_2 \\ R_1 & +1 & & & \\ R_2 & & +1 & & \\ R_4 & -2.2 & +1.2 & +1.4 & +0.2 \\ R_5 & +1.2 & -2.2 & -0.4 & +0.8 \end{array} \quad \ldots\ldots\ldots\ldots \quad (69)$$

Then our desired results are given by

$$\begin{Bmatrix} R_1 \\ R_2 \\ R_4 \\ R_5 \end{Bmatrix} = [g]\,[J]\begin{Bmatrix} P_1 \\ P_2 \end{Bmatrix} \quad \ldots\ldots\ldots\ldots\ldots\ldots \quad (70)$$

Carrying out the indicated operations

$$\begin{Bmatrix} R_1 \\ R_2 \\ R_4 \\ R_5 \end{Bmatrix} = \begin{bmatrix} +0.23486 & -0.02661 \\ +0.02350 & -0.05229 \\ +0.91150 & +0.19581 \\ -0.16986 & +0.88310 \end{bmatrix} \begin{Bmatrix} P_1 \\ P_2 \end{Bmatrix} \qquad \ldots\ldots\ldots\ldots \quad (71)$$

we have our actual answers.

This is as far as we will go in our discussion of the strain energy in terms of loads. We should, for completeness, consider the formulation of strain energy in terms of the displacements which define the deformed shape of the structure. In so doing we will develop the basic formulae and theory which, in its application, is known in the literature as the "method of stiffness" or the "stiffness" matrix approach.

SUPERPOSITION OF FORCES

Consider in Fig. 2, the axially loaded bar anchored at its left end. The cross sectional properties are constant.

We can write

$$\Delta_1 = \delta_{11} P_1 \qquad \ldots\ldots\ldots\ldots\ldots\ldots \quad (72)$$

where δ_{11} is the flexibility coefficient. The inverse relationship is

$$P_1 = \frac{1}{\delta_{11}} \Delta_1 = k_{11} \Delta_1 \qquad \ldots\ldots\ldots\ldots\ldots \quad (73)$$

where k_{11} is the stiffness coefficient. In the same manner that we define δ_{11} as the deflection at 1 due to a unit value of P_1, we can define k_{11} as the force at 1 due to a unit value of Δ_1.

We can generalize this concept using Fig. 1, and superimpose the forces, writing for any force, P_i,

$$P_i = k_{i1} \Delta_1 + k_{i2} \Delta_2 + \ldots k_{ij} \Delta_j \qquad \ldots\ldots\ldots \quad (74)$$

where the k's are the stiffness coefficients. In matrix form Eq. 74 can be written as

$$\left\{ P_i \right\} = \left[k_{ij} \right] \left\{ \Delta_j \right\} \qquad \ldots\ldots\ldots\ldots\ldots\ldots \quad (75)$$

where $\left[k_{ij} \right]$ is known as the stiffness matrix. The subscripts i and j have the same range. The equations given by Eq. 75 are analogous to those given by Eq. 3. Substitution of Eq. 3 into Eq. 73 requires

$$\left[k_{ij} \right] \left[\delta_{ji} \right] = [I] \qquad \ldots\ldots\ldots\ldots\ldots\ldots \quad (76)$$

which indicates that $[\delta]$ is the inverse of $[k]$.

STRAIN ENERGY AS A FUNCTION OF DISPLACEMENTS

Fig. 15 is an outline of a simply supported pin-connected truss. The 13 horizontal and vertical arrows shown represent the joint displacements that can take place when the truss deforms. Obviously, if these 13 deflections were known, we would know the deformed shape of the truss. These, then, are the 13 deflection parameters defining the strain energy of the truss.

Let us assume that forces act in the direction of these 13 deflections. The 13 arrows shown thus represent forces and displacements. If we call the deflections Δ_i and the forces P_i where i has the range 1 to 13, we can write for the total strain energy

$$U_T = \frac{1}{2} \sum_{i = 1,\ 2,\ -\ -\ 13} P_i \ \Delta_i \quad \ldots\ldots\ldots\ldots\ldots \quad (77)$$

or in matrix form

$$\left[U_T\right] = \frac{1}{2}\left[P_i\right]\left\{\Delta_i\right\} \quad \ldots\ldots\ldots\ldots\ldots\ldots \quad (78)$$

Using Eq. 75 in Eq. 78 we have as a result

$$\left[U_T\right] = \frac{1}{2}\ \left[\Delta_i\right]\left[k_{ij}\right]\left\{\Delta_j\right\} \quad \ldots\ldots\ldots\ldots\ldots \quad (79)$$

Note the similarity of Eq. 79 with Eq. 13.

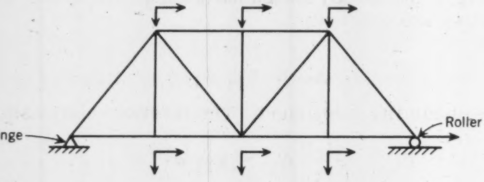

FIG. 15

In our study of strain energy as a function of the loads, we demonstrated that we could select any set of simple reactions, break up the structure into pieces, add the flexibilities of the pieces, and then obtain the total energy or sum the energies of the individual pieces. Space does not permit us to consider the same questions when strain energy is a function of displacements. Suffice it to say that we can do all these things except that in place of flexibilities we have stiffness and in place of loads we are dealing with displacements.

We can apply another of Castigliano's theorems, namely,

$$\frac{\partial U_T}{\partial \Delta_i} = P_i \quad \ldots\ldots\ldots\ldots\ldots\ldots \quad (80)$$

to the expression for the total strain energy given by Eq. 79 with the result

$$\left\{P_i\right\} = \left[k_{ij}\right]\left\{\Delta_j\right\} \quad \ldots\ldots\ldots\ldots\ldots\ldots \quad (81)$$

The $\{P_i\}$ are the forces acting at the points at which the deflections are considered acting. In an actual problem, no forces may be acting at some of these points or joints. To complete our formulation therefore, let us partition $\{P_i\}$ into two groups, as follows,

$$\left\{P_i\right\} = \left\{\begin{array}{c} P_A \\ \hline 0 \end{array}\right\} \quad \ldots\ldots\ldots\ldots\ldots\ldots \quad (82)$$

where P_A represents those forces (or moments) that exist. Applying the same grouping to the Δ's we can rewrite Eq. 81 in the partitioned form

$$\left\{\begin{array}{c} P_A \\ \hline 0 \end{array}\right\} = \left[\begin{array}{c|c} k_{AB} & k_{An} \\ \hline k_{mB} & k_{mn} \end{array}\right] \left\{\begin{array}{c} \Delta_B \\ \Delta_n \end{array}\right\} \quad \ldots\ldots\ldots\ldots\ldots \quad (83)$$

in which the subscripts m and n refer to the points or joints where forces (or moments) are equal to zero.

We could continue and develop the detailed formulas used in the "method of stiffnesses" but as we are primarily concerned with the basic concept of energy, we shall stop at this point; there are, however, several papers (16, 19, 22) which deal with the theory and application of the "method of stiffnesses."

CONCLUSIONS

We have examined the concept of strain energy and have noted that it has a constant value for a given structure subjected to a set of forces in equilibrium. We have seen how we can obtain the total energy by breaking the structure up into convenient units, using arbitrary supports, and have shown the formulas for the solution of statically indeterminate structures. Two applications were then carried out. A similar investigation of strain energy expressed in terms of displacements was carried to a point where we could satisfy ourselves that earlier observations were applicable. We also discussed the inclusion of the foundation in our concept of the "whole" structure.

ACKNOWLEDGMENTS

The writer wishes to express his appreciation to the Fairchild Astrionics Division, Wyandanch, N. Y., for their material support and encouragement. He is particularly indebted to Douglas Craven and the staff of the Publications and Photography Departments of FAD for their assistance in the preparation of this paper.

APPENDIX I.—NOTATION

Symbols and notation used in this paper are given below. Notation clearly defined in the text is not shown here:

$[\;]$ = brackets denoting a rectangular matrix;

$\{\;\}$ = column matrix;

$[\;]^T$ = transpose of a matrix;

$[I_n]$ = unit matrix of order n;

$[\delta]$ = flexibility matrix;

$[k]$ = stiffness matrix;

δ_{ij} = influence deflection coefficient; deflection in direction of $i^{\underline{th}}$ load due to a unit value of the $j^{\underline{th}}$ load; and

k_{ij} = influence stiffness coefficient; spring constant; force in the $i^{\underline{th}}$ direction due to unit value of deflection in $j^{\underline{th}}$ direction.

Subscripts

x,y used to denote any redundant P_x, P_y. x and y have the same range of numbers, being used interchangeably.

m,n used to denote any applied load P_m, P_n. Same range of numbers or loads, being used interchangeably. Note n is used also for unit matrix.

APPENDIX II.—REFERENCES

1. "Tensor Analysis of Networks," by G. Kron, John Wiley and Sons, Inc., New York, 1939.
2. "Matrix Methods of Analysis Applied to Wing Structures," by V. P. Jensen, Douglas Aircraft Co. Report E. S. 6480, January, 1944.
3. "Computation of Influence Coefficients for Aircraft Structures with Discontinuities and Sweepback," by S. Levy, Journal of the Aeronautical Sciences, Vol. 14, No. 10, October, 1947, pp. 547-560.
4. "The Partitioning of Matrices in Structural Analysis," by S. U. Benscoter, Journal of Applied Mechanics, Vol. 15, No. 4, December, 1948, pp. 303-307.
5. "Le Calcul Systematique des Caracteristiques Elastiques des Systemes Hyperstatiques," by H. Falkenheiner, La Recherche Aeronautique, No. 17, France, September-October, 1950.
6. "On an Application of Matrix Calculus to the Theory of Frames," by T. Poschl, Ing.-Arch., Vol. 19, No. 1, 1951, pp. 69-74.
7. "Structural Analysis of Sweptback Wings by Matrix Transformation," by B. Langefors, SAAB Airc. Co., Linkoping T. N. 3, 1951.
8. "Some Results of Swept-back Wing Structural Studies," by A. L. Lang, and R. L. Bisplinghoff, Journal of the Aeronautical Sciences, Vol. 18, No. 11, November, 1951, pp. 705-717.
9. "Analysis of Elastic Structures by Matrix Transformation with Special Regard to Semimonocoque Structures," by B. Langefors, Journal of the Aeronautical Sciences, Vol. 19, No. 7, July, 1952, pp. 451-458.
10. "A Method of Reducing the Analysis of Complex Redundant Structures to a Routine Procedure," by L. B. Wehle, and W. Lansing, Journal of the Aeronautical Sciences, Vol. 19, No. 10, October, 1952, pp. 677-684.
11. "Structural Analysis and Influence Coefficients for Delta Wings," by S. Levy, Journal of the Aeronautical Sciences, Vol. 20, No. 7, July, 1953, pp. 449-454.

12. "Exact Reduction and Solution by Parts of Equations for Elastic Structures," by B. Langefors, SAAB Tech. Notes 24, SAAB Aircraft Co., Linkoping, Sweden, 1953.

13. "Matrix Structural Analysis," by P. H. Denke, presented at the Second National Conf. of Applied Mechanics, Ann Arbor, Mich., June, 1954.

14. "Solving Highly Complex Elastic Structures in Easy Stages," by G. Kron, Journal of Applied Mechanics, Vol. 22, No. 2, June, 1955, pp. 235-244.

15. "Energy Theorems and Structural Analysis," by J. H. Argyris, Aircraft Engineering, Vol. XXVI, October, 1954, p. 343; November, 1954, p. 383; and Vol. XXVII, February, 1955, p. 42, March, 1955, p. 80, April, 1955, p. 125, and May, 1955, p. 145.

16. "Stiffness and Deflection Analysis of Complex Structures," by Turner, Clough, Martin, and Topp, Journal of the Aeronautical Sciences, Vol. 23, No. 9, September, 1956, pp. 805-823.

17. "Matrix Analysis of Beams," by R. W. Clough, Proceedings, ASCE, Vol. 84, No. EM1, January, 1958.

18. "A Simple Method of Matrix Structural Analysis," by B. Klein, Journal of the Aeronautical Sciences, Vol. 24, No. 1, January, 1957, pp. 39-46.

19. "Truss Analysis by Stiffness Considerations," by H. C. Martin, Transactions, ASCE, Vol. 123, 1958, pp. 1182-1194.

20. "The Use of a Transformation Chain in Matrix Structural Analysis," by F. R. Berman, Conf. Papers of the ASCE, Conf. on Electronic Computation, November, 1958.

21. "Large Deflections of Structures Subjected to Heating and External Loads," by Turner, Dill, Martin, and Melosh, Journal of the Aero/Space Sciences, Vol. 27, No. 2, February, 1960, pp. 97-106, 127.

22. "Digital Computation for Stiffness Matrix Analysis," by J. S. Archer, Transactions, Vol. 125, 1960.

AMERICAN SOCIETY OF CIVIL ENGINEERS

Founded November 5, 1852

TRANSACTIONS

Paper No. 3117

REINFORCED CONCRETE SHEAR WALL ASSEMBLIES

By Jack R. Benjamin,[1] M. ASCE, and Harry A. Williams,[2] F. ASCE

SYNOPSIS

This paper gives the results of an investigation of one-story and two-story reinforced concrete shear wall assemblies. Tests were made on four one-story models with parallel shear walls connected by a reinforced concrete diaphragm. Loads were applied to the diaphragm, and three separate diaphragm tests were then made. Following these tests, two one-story specimens with face walls were tested. Finally, two two-story models were tested.

Theoretical studies were made for all tests and practical design approximations are suggested.

INTRODUCTION

This paper is concerned with a part of the investigation of strength and behavior of shear walls conducted between 1951 and 1956 at Stanford University, Calif. Other parts of the investigations have been previously published.[3,4,5]

Note.—Published essentially as printed here, in August, 1960, in the Journal of the Structural Division, as Proceedings Paper 2566. Positions and titles given are those in effect when the paper or discussion was approved for publication in Transactions.

[1] Prof. of Struct. Engrg., Stanford Univ., Stanford, Calif.

[2] Prof. of Civ. Engrg., Stanford Univ., Stanford, Calif.

[3] "The Behavior of One-Story Reinforced Concrete Shear Walls," by Jack R. Benjamin and Harry A. Williams, Transactions, ASCE, Vol. 124, 1959, pp. 669-708.

[4] "The Behavior of One-Story Brick Shear Walls," by Jack R. Benjamin and Harry A. Williams, Proceedings, ASCE, Vol. 84, ST4, 1958.

[5] "Behavior of One-Story Reinforced Concrete Shear Walls Containing Openings," by Jack R. Benjamin and Harry A. Williams, Journal, ACI, No. 5, Vol. 30, 1958, pp. 605-618.

The behavior of individual shear walls can be predicted within engineering accuracy.[3,4,5] Structures containing assemblies of shear walls connected by floor and roof diaphragms are most complex in their behavior. The investigations reported herein were designed to study the basic problems in the prediction of over-all structural response to lateral loads caused by blast. The conclusions apply equally well to wind and earthquake loads.

Three types of simple model structures were studied. These models were of approximately one-quarter scale. They did not correspond to any actual structures but, rather, were used to investigate various theoretical approaches to the problem. The mathematical studies considered these models as structures in themselves. While some scale effect may occur in translating the results to full-size structures, it is believed that such influences will be within the normal variations encountered with shear wall structures.

Four one-story parallel walled structures without face walls were tested. These were designated as specimens SD-2 to SD-5, inclusive. Model SD-2 contained two walls and a connecting diaphragm, and models SD-3, 4, and 5 had three parallel walls, also with connecting diaphragms. Three separate diaphragm tests were made in addition to determine the diaphragm properties.

Following these tests, two one-story specimens with face walls were tested. Model SD-6 had two identical shear walls, and specimen SD-7 had three different shear walls. Loads were applied to the diaphragm in such a manner as to produce large torsional forces. The influence of foundation distortion was studied extensively.

Finally, two two-story models were tested. These specimens, SD-8 and SD-9, were identical except for loading. Model SD-8 was loaded symmetrically, and model SD-9 eccentrically. These models had three walls in each story and no face walls.

EXPERIMENTAL PROCEDURES

All models were partially precast flat on the floor. The precast elements were then assembled in the testing jig and the remaining elements cast in place. In general, all walls were precast and all diaphragms were cast in place. All assemblies were tested in a specially designed shear jig. A model under test is shown in Fig. 1. Three individual diaphragms were tested in a 200,000-lb testing machine.

Type I portland cement was used in the concrete mix with a small amount of additive to improve workability. Precast elements were generally cured for one or two weeks before final assembly. Tests were conducted when the cast-in-place concrete was at a strength of approximately 3,000 psi. The precast elements were then at a concrete strength of approximately 3,800 psi at the time of test. All reinforcing consisted of structural or intermediate grade steel.

The assemblies were loaded at the diaphragm level using calibrated hydraulic jacks. Dynometers were provided at the hold-downs. The particular construction details and test procedures will be described subsequently.

ONE-STORY PARALLEL WALL STRUCTURES

Four one-story models with parallel shear walls were tested. Model SD-2 had two shear walls, while the others, SD-3, 4, and 5, each had three walls. Three individual shear walls, SD-1a, b, and c, were tested first as control specimens.

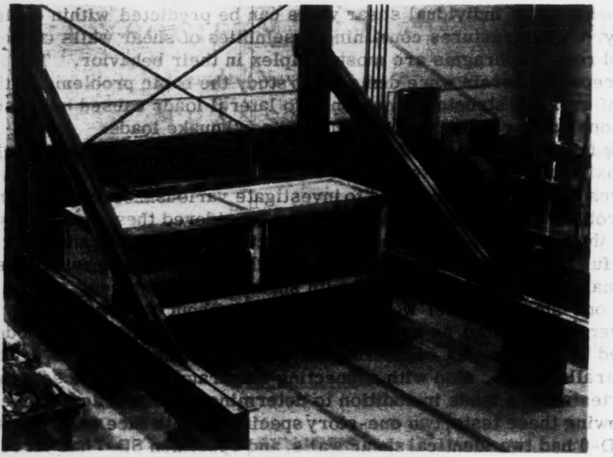

FIG. 1.—SHEAR JIG WITH SPECIMEN SD-5 UNDER TEST.

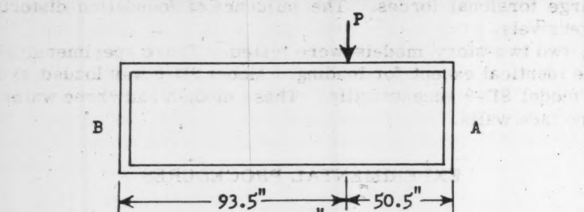
P
B
A
93.5"
50.5"
144"
48"
V
A-36.75"
B-36.25"
V
T
T
A-42"
B-42.5"
DIAPHRAGM
4-#6
COLUMNS
4-#4
#2 @ 5" c/c each way
WALLS-4"
DIAPHRAGM-5"
2"
4"
#2 Ties @
5" c/c.

FIG. 2.—TYPICAL SECTIONS. SPECIMEN SD-2.

The investigation of Model SD-2 had two purposes. The first was to see whether a torsional couple resulting from shear wall warping had negligible influence on the diaphragm, as one would expect. The second was to determine whether roof diaphragms and shear walls behave in a similar manner.

Test results and approximate theoretical computations both showed that the torsion could be neglected. Diaphragm crack patterns, deflection measurements, and general behavior indicated that, theoretically, shear walls and diaphragms can be treated in a similar manner.

Three one-story assemblies, each having three parallel walls, A, B, and C, were then tested. Wall and diaphragm elements were the same as for SD-2, Fig. 2, and the finished model appeared as in Fig. 1. Equal forces, P/2, were applied to the diaphragms midway between the walls as shown by the hydraulic jack locations in the photograph.

The theoretical rigidities of the walls and diaphragms were computed on the assumption that the steel could be neglected and the concrete was uncracked. Each wall then had a rigidity of $R = 0.980\ E$ kips per in. of deflection. Each diaphragm segment had a rigidity of $D = 0.174\ E$ kips per in.

If the foundation is infinitely rigid, the effective wall rigidities are equal. However, the testing apparatus deforms, changing the effective wall rigidities. Symmetry indicates that the two end walls, A and C, will have identical rigidities. However, wall B will have a smaller rigidity than the end walls due to testing apparatus-distortion. If the shear in a wall is V, and P is the total applied load, the solution for end wall shear is

$$\frac{V_A}{P} = \frac{0.188 + \frac{D}{R_B}}{1 + \frac{2D}{R_B} + \frac{D}{R_A}} \quad \cdots\cdots\cdots\cdots\cdots\cdots \quad (1)$$

Also,

$$V_A = V_C, \quad V_B = P - 2\,V_A \quad \cdots\cdots\cdots\cdots\cdots \quad (2)$$

Specimen SD-3 failed prematurely at a tie-down. Results are not shown but the data emphasized that great variations in the tie-down force occurred due to the initial load take-up. The center wall carried almost no load up to an applied load of 20 kips. The wall cracking was typical. The diaphragm did not crack.

Assembly SD-4 differed from SD-3 in that the tie-down column rods were changed to No. 4 bars to eliminate further tie-down failure. The test of SD-3 showed that center wall B was slow to pick up load, probably because jig distortion allowed both horizontal movement and rotation of the foundation of this wall. To control the horizontal movement for SD-4, an adjustable wedge was placed at the horizontal foundation reaction point of wall B. As the test proceeded, the foundation movement of B relative to A and C was measured. Then the wedge was used to force the three walls into line. The foundation rotation of B relative to A and C was also measured. Then the tie-down rod nuts were adjusted to make the foundation rotation of wall B the average of that of A and C. The net result of all of the adjusting was to approximately insure that the foundations of the walls moved together.

Ultimate failure of specimen SD-4 occurred at the junction of the tension beam of the diaphragm and wall C. Failure was complete as a result of concrete and bond failure at the pour joint despite extensive doweling through this area.

The load-deflection and tie-down force curves are given in Fig. 3. The test procedure is evident in the tie-down force curves where the forces varied at each load as the center wall was adjusted. Individual wall and diaphragm load-deflection curves are given in Figs. 4 and 5. Shear walls cracked in the usual diagonal pattern.

The one striking feature of the experimental data is that the tie-down force curves are, essentially, continuous straight lines in both the cracked and uncracked regions. The slope does not change as individual elements crack and no load redistribution due to cracking is apparent.

When the experimental results are compared with the theoretical prediction based on a rigid foundation, the correlation is not good. If walls A and C are assumed to have a theoretical rigidity of 0.98 E, the effective rigidity of wall B can be computed. Using an average value of $V_A/P = 0.31$ from the experimental curves, R_B is found to be 0.37 E. Computations show the jig to be less than 10% as rigid as the shear walls. The effective value of R_B of 0.37 E is reasonable considering the large influence of small errors in adjustment.

After trying to adjust the movement of wall B of SD-4, it was decided to test assembly SD-5 without such adjustment but rather to carefully measure all such movements. SD-5 was identical to SD-4 except that wall A had three times as much panel steel. Thus the elastic rigidities would remain identical but their cracked rigidities would differ.

The test of SD-5 proceeded very well up to an applied load of 84 kips when the joint between wall C and the diaphragm failed completely. Wall load-deflection curves are shown in Fig. 6. The curves show a greater cracked rigidity for wall A than for walls B and C. The relationship between individual wall shears and total applied load is given in Fig. 7. Note the constancy of slope from elastic through the cracked range. The variations in wall rigidities were insufficient to affect the shear distribution.

The relative shear distribution computed from theoretical wall rigidities and measured foundation movements agreed with that found experimentally, within the limits of experimental accuracy. Very small errors in measurement have a large influence on the computations because of the very large rigidity of the shear walls and diaphragms.

DIAPHRAGM TESTS

The tests of assemblies SD-2 to SD-5 inclusive produced very little reliable information as to diaphragm rigidity and strength. The rigidity information was of doubtful value because of the scatter of experimental data coupled with the fact that the desired component of diaphragm shear was not measured directly. Hence, three separate diaphragms, identical to those used for SD-2 to SD-5, were tested in various ways.

ONE STORY ASSEMBLIES WITH FACE WALLS

Two assemblies were tested with solid face walls front and rear. The assembly, SD-6, had two identical shear walls. The design is shown in Fig. 8. Load was applied eccentrically to the diaphragm in order to place significant torsional shears in the face walls.

The addition of face walls, for which the concrete was placed integrally with the transverse shear walls, greatly complicates and changes the theoretical

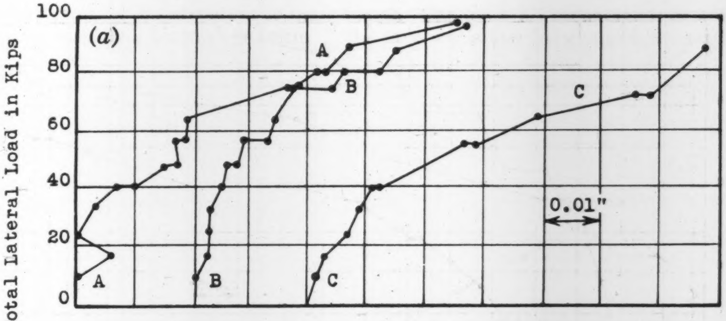

FIG. 3(a).—LOAD-DEFLECTION CURVES FOR SHEAR WALLS. SPECIMEN SD-4.

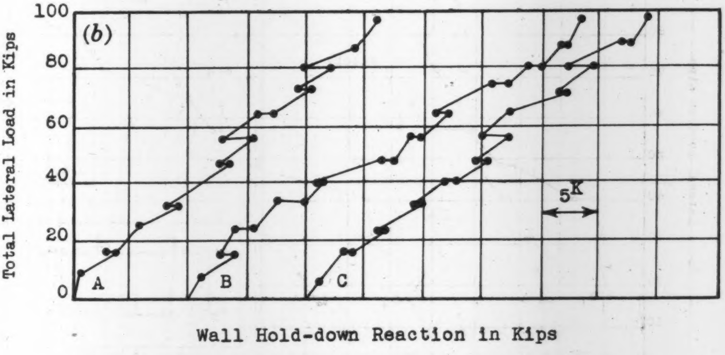

FIG. 3(b).—APPLIED LOAD VS. WALL HOLD-DOWN REACTIONS. SPECIMEN SD-4.

analysis. Consider the simple box type two-wall structure, having solid face walls, as shown in Fig. 9. Assume that the foundation is elastically supported but that the soil modulus is less at wall A than at wall B. Replace P by a force

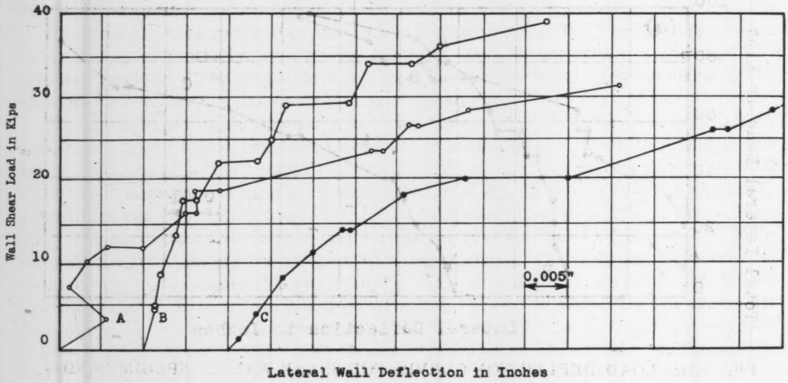

FIG. 4.—WALL SHEAR LOAD VS. WALL DEFLECTION. SPECIMEN SD-4.

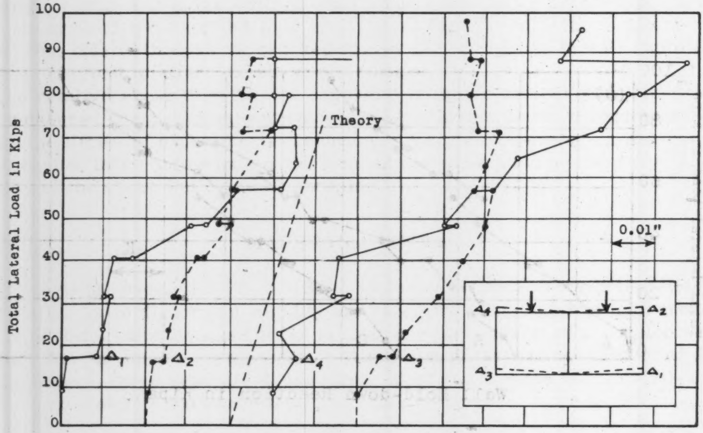

FIG. 5.—LOAD-DEFLECTION CURVES FOR DIAPHRAGM. SPECIMEN SD-4.

P on the center line and a torsional couple. Now separate the problem into three parts:

1. Direct translation of the diaphragm.
2. Foundation distortion.
3. Torsion of the assembly.

First consider only direct translation of the diaphragm without rotation and without foundation movement. The foundation is assumed to be infinitely stiff.

The structure is symmetrical and both shear walls are identical. Each transverse shear wall then carries half of the total load, P. The two horizontal reactions, F_A and F_B, are equal to $\frac{P}{2}$. The face walls have no shear stress and no distortion in the direction of their length. The over-all structure then acts as a vertical-box cantilever beam. The face walls are flanges and the walls A and B, two identical webs. If simple theory is used, the face walls are essentially stressed only by bending while the end walls carry the shear.

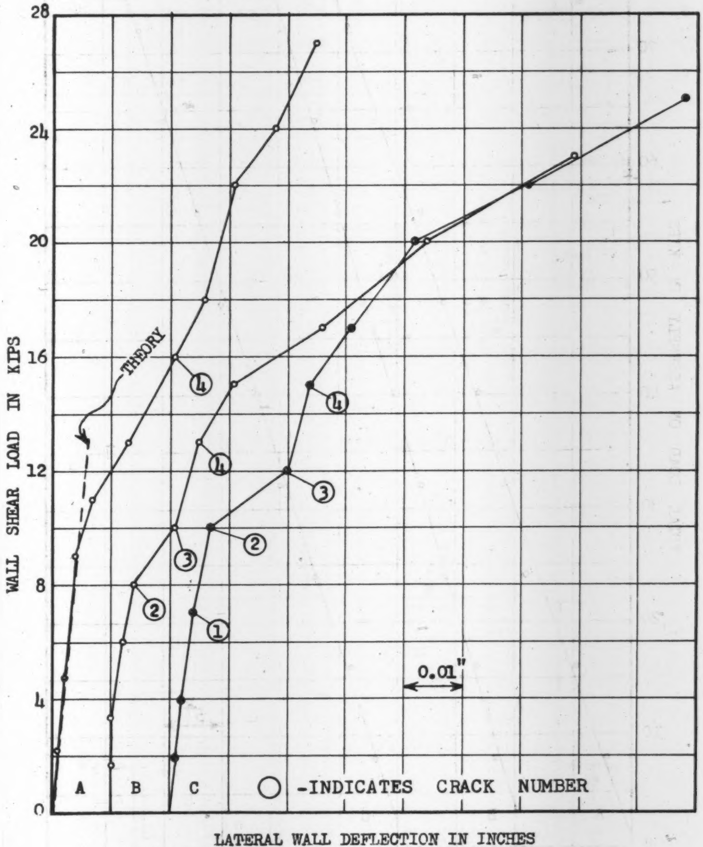

FIG. 6.—LOAD-DEFLECTION CURVES FOR SHEAR WALL. SD-5.

Note that this solution is quite different from that obtained if the walls are not connected. If walls C and D are not placed integrally with A and B, they do not act as flanges of a beam but as separate cantilever beams in themselves. Thus the bending rigidity of the assembly is greatly reduced if the face walls

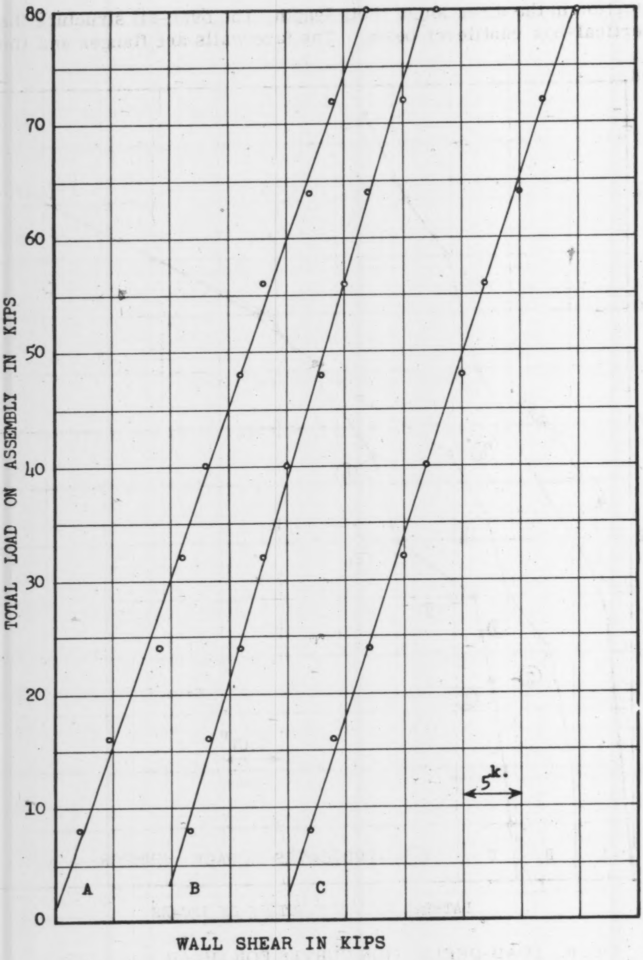

FIG. 7.—APPLIED LOAD VS. WALL SHEAR. SD-5.

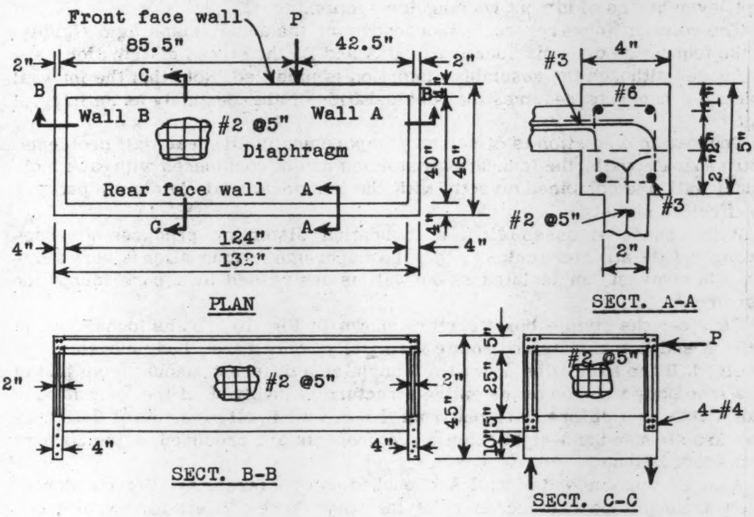
Front face wall
P
85.5"
42.5"
2"
2"
C
B
B
Wall B
Wall A
#2 @5"
Diaphragm
40"
48"
Rear face wall
A
A
C
4"
4"
124"
132"
4"
4"
PLAN
4"
#3
#6
1"
2"
2"
5"
#3
#2 @5"
2"
SECT. A-A
2"
#2 @5"
2"
4"
4"
SECT. B-B
5"
25"
45"
5"
10"
P
#2 @5"
4-#4
SECT. C-C

FIG. 8.—SPECIMEN SD-6 DETAILS.

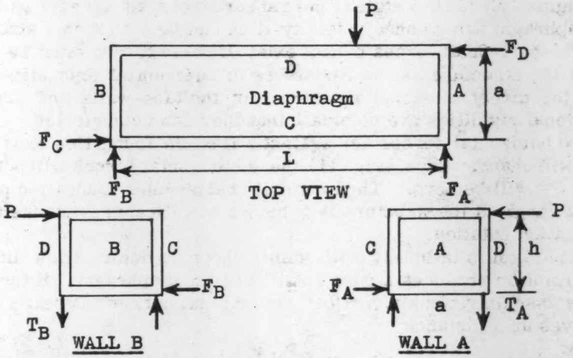
P
F_D
D
B
Diaphragm
A
a
C
F_C
L
F_B
TOP VIEW
F_A
P
D
B
C
F_B
T_B
WALL B
P
C
A
D
h
F_A
a
T_A
WALL A

FIG. 9.—FORCES ACTING ON TWO-WALL BOX SPECIMEN SD-6.

are not connected to the end walls while the shearing rigidity is not greatly influenced by this assumption. With separate walls, the end walls act as vertical cantilever beams of almost rectangular section.

The solution for stresses is independent of the actual diaphragm rigidity. If the foundation deforms identically at A and B, the stress distributions are unchanged although the assembly distortion is modified. Note that the integral placing of concrete requires the consideration of the assembly as an integral unit.

Foundation distortion is of primary importance in all shear wall problems. With separate walls, the foundation distortion can be considered with each individual wall and combined directly with the individual wall rigidity to produce an effective rigidity.

With connected assemblies, a foundation distortion produces stresses throughout the structure unless either the diaphragm or foundation is very flexible. In contrast, an isolated shear wall is unstressed by a pure foundation movement.

Consider the simple box structure shown in Fig. 10. If the foundations of walls A and B translate and rotate identically, only a free body movement is involved. If the foundation of wall A translates a different amount from that of B, a free body rotation of the entire structure is involved. If the foundation of wall A rotates a different amount from that of wall B, all elements of the structure are stressed and eight reaction components are produced at the corners of the foundation.

Assume that one end of wall A is pushed up by a force, P_F. Vertical forces of equal magnitude are necessary at the other three corners for equilibrium. For simplicity assume P_F produces uniform shear stress, $\frac{P_F}{2\,t\,h}$, in the wall panels framing into each corner. Thus each end and face wall panel is subjected to a uniform shear stress. The horizontal forces, $\frac{P_F\,a}{2\,h}$ and $\frac{P_F\,L}{2\,h}$, are now necessary for equilibrium of the shear walls and the face walls, respectively. The diaphragm is placed in a state of pure shear stress, as were the wall panels.

If the diaphragm has no shear rigidity, it cannot be placed in a state of pure shear and the horizontal forces cannot exist. If these forces must be zero, P_F is zero and the structure has no resistance to differential foundation rotation other than the direct torsional resistance of the face walls and diaphragm. These torsional rigidities are so small that they can be neglected. Furthermore, if the horizontal forces act against a flexible foundation material, the foundation will change shape, (Fig. 11), these horizontal forces will not be produced, and P_F will be zero. The originally rectangular foundation plan must remain a rectangle if the structure is to have a significant resistance to differential foundation rotation.

If the diaphragm is infinitely stiff against shearing deformation, differential foundation rotation produces a pure rotation of the diaphragm. If the vertical edges of the assembly remain vertical, the original corner where P_F was first applied moves up a distance

$$\delta = \frac{P_F\,a}{2\,h\,t\,G} \quad \text{. (3a)}$$

or

$$\delta = \frac{P_F\,L}{2\,h\,t\,G} \quad \text{. . . . . (3b)}$$

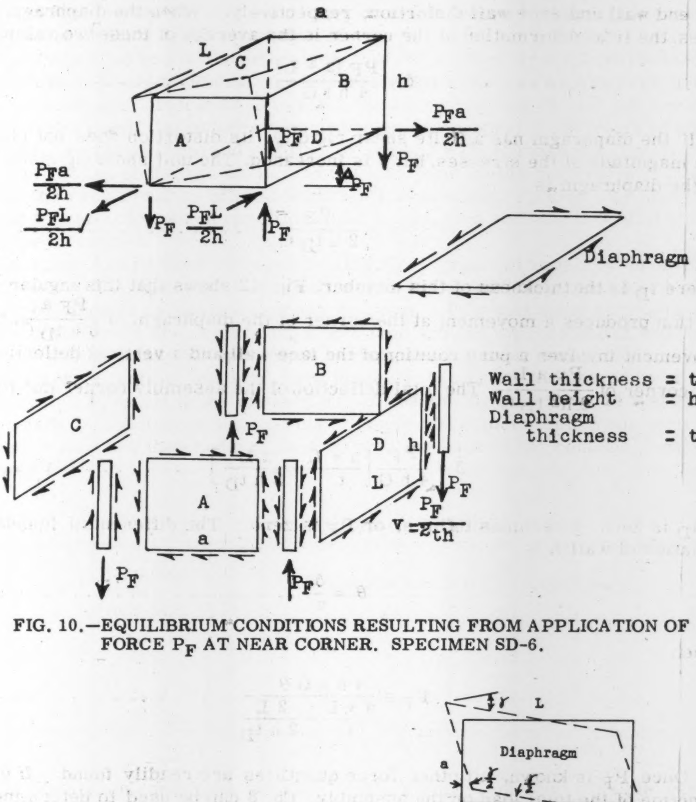
a
L
C
B
h
$\frac{P_F a}{2h}$
A
P_F
D
P_F
P_F
$\frac{P_F a}{2h}$
$\frac{P_F L}{2h}$
P_F
$\frac{P_F L}{2h}$
P_F
Diaphragm
B
C
P_F
D
h
L
A
a
P_F
P_F
$V = \frac{P_F}{2th}$
P_F
P_F
Wall thickness = t
Wall height = h
Diaphragm thickness = t_D

FIG. 10.—EQUILIBRIUM CONDITIONS RESULTING FROM APPLICATION OF FORCE P_F AT NEAR CORNER. SPECIMEN SD-6.

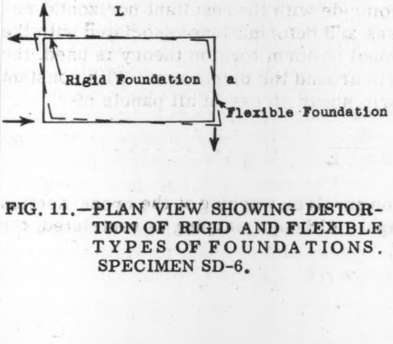
L
Rigid Foundation
a
Flexible Foundation

FIG. 11.—PLAN VIEW SHOWING DISTORTION OF RIGID AND FLEXIBLE TYPES OF FOUNDATIONS. SPECIMEN SD-6.

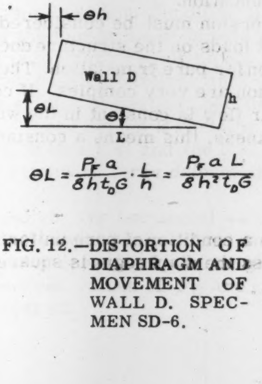
γ
L
Diaphragm
a
$\frac{\gamma}{2}$
$\frac{\gamma}{2}$
$\frac{\gamma}{2} \cdot \frac{a}{2} = \frac{\gamma a}{4} = \frac{P_F a}{8 h t_D G}$
θh
Wall D
h
θL
θ
L
$\theta L = \frac{P_F a}{8 h t_D G} \cdot \frac{L}{h} = \frac{P_F a L}{8 h^2 t_D G}$

FIG. 12.—DISTORTION OF DIAPHRAGM AND MOVEMENT OF WALL D. SPECIMEN SD-6.

for end wall and face wall distortion, respectively. When the diaphragm rotates, the final deformation at the corner is the average of these two values or

$$\delta = \frac{P_F\,(a + L)}{4\,h\,t\,G} \quad \ldots\ldots\ldots\ldots\ldots\ldots \quad (4)$$

If the diaphragm has a finite shear rigidity, its distortion does not change the magnitude of the stresses, but δ is increased. The unit shearing distortion in the diaphragm is

$$\gamma = \frac{P_F}{2\,h\,t_D\,G} \quad \ldots\ldots\ldots\ldots\ldots\ldots \quad (5)$$

where t_D is the thickness of this member. Fig. 12 shows that this angular distortion produces a movement at the corner of the diaphragm of $\frac{P_F\,a}{8\,h\,t_D\,G}$. This movement involves a pure rotation of the face wall and a vertical deflection at its corner of $\frac{P_F\,a\,L}{8\,h^2\,t_D\,G}$. The total deflection of the assembly corner due to P_F is

$$\delta = \frac{P_F}{4\,h\,G}\left[\frac{a + L}{t} + \frac{a\,L}{2\,h\,t_D}\right] \quad \ldots\ldots\ldots\ldots\ldots \quad (6)$$

If t_D is zero, δ becomes infinite, or P_F is zero. The differential foundation rotation of wall A is

$$\theta = \frac{\delta}{a} \quad \ldots\ldots\ldots\ldots\ldots\ldots\ldots \quad (7)$$

Then

$$P_F = \frac{4\,h\,a\,G\,\theta}{\frac{a + L}{t} + \frac{2\,L}{2\,h\,t_D}} \quad \ldots\ldots\ldots\ldots\ldots\ldots \quad (8)$$

Once P_F is known, all other force quantities are readily found. If θ is a function of the total load on the assembly, Eq. 8 can be used to determine the direct relationship between P_F and the total assembly load. Evidently, the angle θ will depend on the characteristics of the supporting soil and the type of foundation.

Torsion must be considered if the line of action of the resultant of the applied loads on the structure does not coincide with the resultant horizontal reaction for pure translation. The stresses and deformations associated with the torsion are very complex. If conventional uniform torsion theory is used, the shear flow is constant in the wall panels around the diaphragm. With constant thickness, this means a constant uniform shear stress in all panels of

$$v = \frac{T}{2\,a\,t\,L} \quad \ldots\ldots\ldots\ldots\ldots\ldots\ldots \quad (9)$$

Such a condition of pure uniform torsion involves warping of the cross-section unless the diaphragm is square in shape. Although warping is restricted, the deformations involved are so small they do not in themselves preclude the application of uniform torsion theory.

Specimen SD-6 was tested extensively in order to prove or disprove the theory previously presented. Because considerable difficulty was experienced in the instrumentation of models SD-2 to SD-5, the entire instrumentation was revised for this specimen. Gages were mounted on an independent steel frame so as to measure the translation and rotation of the end wall foundations, the translation of the top of the end walls, and the load point on the diaphragm. In addition, the rectalinearity of the foundation was checked. Jacking was provided so that this or any desired condition could be obtained and also face wall shear could be measured.

Tie-down forces were measured using SR-4 gages on specially made tie-down rods. The horizontal end-wall reactions at the kick beam were also measured directly by jacks and pressure gages. This was necessary because the tie-down forces are derived from both face and end wall instead of end wall alone as with previous SD specimens having parallel shear walls only.

Three proof tests at low load were made first to check the operation of the equipment. After all items checked within reasonable accuracy, 14 test runs were made at 5 different load levels. Loads were increased from zero to maximum load and then reduced back to zero for each of the conditions shown in Table 1.

TABLE 1.—CONDITIONS OF LOADING

Series	Maximum Load, in Kips	Foundation Condition for Test Runs			
		I	II	III	IV
A	16	1	2	3	4
B	24	5	6	7	
C	40	8	9	10	
D	64	11	12	13	
E	96	14			

The foundation conditions listed in Table 1 represent four possible variations in foundation movement. In Condition I, the foundation was kept rectangular at all times. The foundation diagonals were measured at each load level and sufficient force F_D, (Fig. 9), was applied by jacking to make both diagonals change length the same amount in the same direction. Condition II was similar to Condition I. The changes in length of the foundation diagonals were measured under these conditions. Condition III is for zero F_D, or no shear in the face walls. Finally, Condition IV is the other possible statical limit when F_A equals zero. The latter condition was only studied at one load because of the danger of severely damaging the structure. Load Series E contains only one test because the ultimate load was reached in this test and the test was extended to include post-ultimate behavior with attendant large deformations. Thus Test 14 differs from the other 13.

Typical test data are shown in Figs. 13, 14, and 15. The horizontal wall reactions F_A and F_B are shown in Figs. 13 and 14 respectively. The dashed lines were computed. Note that both increasing and decreasing loads are given. The walls were cracked in this range. The observed values of F_D are given in Fig. 15 for tests 11 and 12. F_D was zero in test 13.

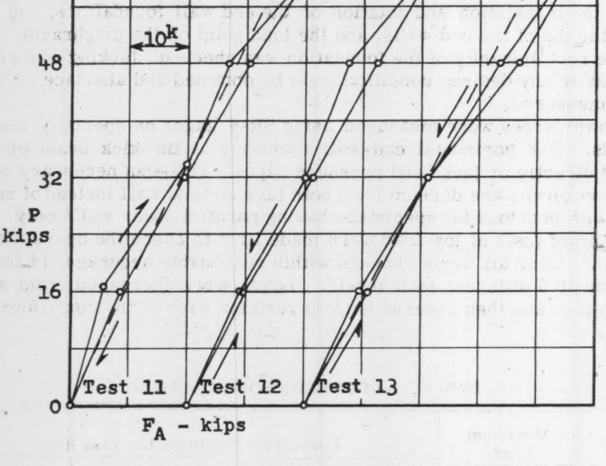

FIG. 13.—APPLIED LOADS VS. SHEAR IN WALL. SPECIMEN SD-6.

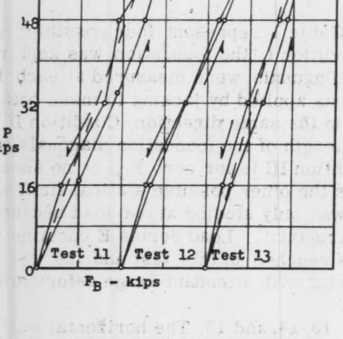

FIG. 14.—APPLIED LOAD VS. SHEAR IN WALL B. SPECIMEN SD-6.

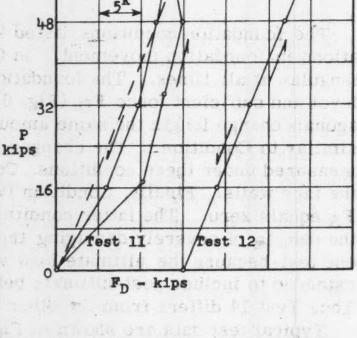

FIG. 15.—APPLIED LOAD VS. SHEAR IN WALL D. SPECIMEN SD-6.

With uniform torsion theory,

$$F_A = 0.58\ P - 18000\ \frac{a}{h}\ \theta \quad \text{(10a)}$$

$$F_B = 0.42\ P + 18000\ \frac{a}{h}\ \theta \quad \text{(10b)}$$

and

$$F_D = 0.24\ P + 18000\ \frac{L}{h}\ \theta \quad \text{(10c)}$$

The measured differential rotations, θ, were highly variable and nonlinear. The probable experimental errors are of the same magnitude as the measured quantities. After lengthy study, it was concluded that uniform torsion theory with no differential foundation rotation was the best solution.

The measured changes in length of the foundation diagonals are given in Fig. 16. The changes in length of the diagonals necessary to reduce the face wall shears by 50% from the rigid foundation values is seen to be very small. Thus, in practice, a small yielding of the soil may reduce the face wall shears appreciably.

The testing machine distortions were found to be very large compared to specimen distortions. Thus no deflection data are presented. Ultimate load was 72 kips and failure occurred in the upper portion of shear wall A. The relative wall shears carried by each resisting element again were not a function of cracking. Thus, wall A carried a constant proportion of the load for a given test condition regardless of the load or of the assembly disintegration.

The second face wall assembly, SD-7, differed considerably from SD-6. Details are shown in Fig. 17. Note that the three shear walls differ greatly from each other. Wall A contains a large opening, B has a solid, 2-in. panel, and C has a solid, 4-in. panel. The face walls and diaphragm are solid and similar to those of SD-6. The instrumentation was a duplicate of that used with SD-6 except that additional gages were necessary at the center wall. The horizontal wall reactions were measured directly by three hydraulic jacks. The resultant face wall shear and tie-down force at the center wall were also measured directly by hydraulic jacks. The end wall tie-down forces were measured with SR-4 gages on the tie-down rods.

The rotation of the foundation of each of the three walls was measured at each load level and that of the center wall was adjusted by jacking the tie-down until its foundation rotation was approximately the average of the end wall rotations. On the first test the three horizontal reaction jacks were continually adjusted, thus maintaining the ends of the foundations of the three walls in a straight line.

Two tests were made on this specimen. During the first test the procedure was as follows. A load was applied to the structure and then the face wall jack at point 1 (Fig. 17) was adjusted to bring the foundation back to a rectangular shape by making the changes in over-all lengths of the foundation diagonals equal and of the same sense. Then the center tie-down jack at point 3 was adjusted while the rectangularity of the foundation was maintained. A set of readings were then taken. After all items were recorded, the face wall shear was reduced to zero by releasing the jack at point 1 and the changes in length of foundation diagonals determined. All other items were also determined at this time. The face wall jack load was then re-applied, returning the specimen to its original condition. All items were again recorded. The specimen was then ready for an increase in load. This was continued up to a load of 70 kips at which time the entire load was removed.

The procedure for the second test was the same as for the first except that the face wall shear was not varied at each load point. The foundation remained rectangular at all times during this test. This test was maintained into the post-ultimate range. Some differential foundation rotation occurred during this test.

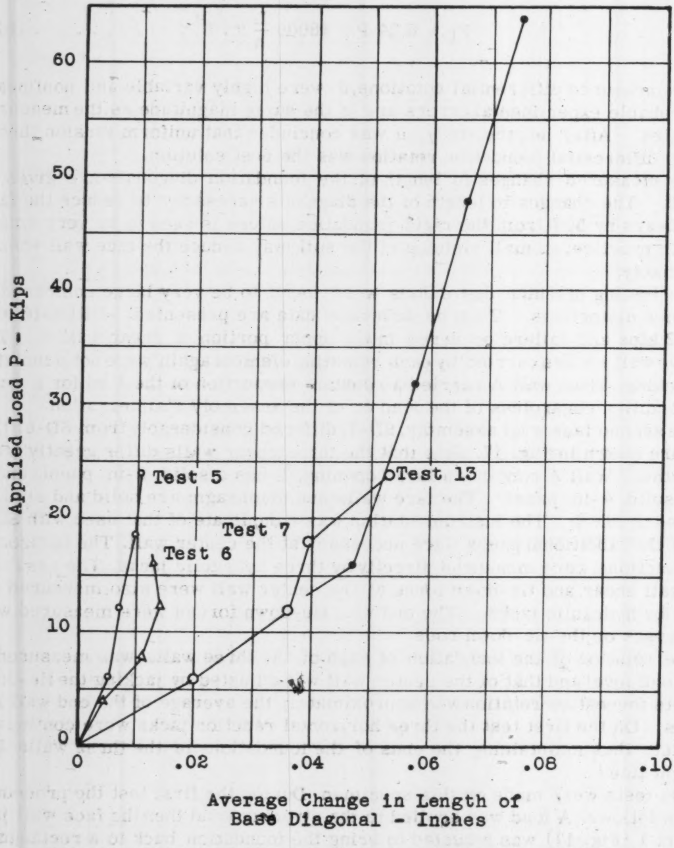

FIG. 16.—LOAD VS. BASE DIAGONAL CHANGES. SPECIMEN SD-6.

Photographs of specimen SD-7 are given in Fig. 18. For all these specimens, 93 kips was the maximum load. Fig. 18(a) is the rear face wall, Fig. 18(b) is the roof, Fig. 18(c) is wall A, Fig. 18(d) is wall B. Figs. 18(c) and (d) are for cycle 2. Wall C did not crack significantly. The loads at which the

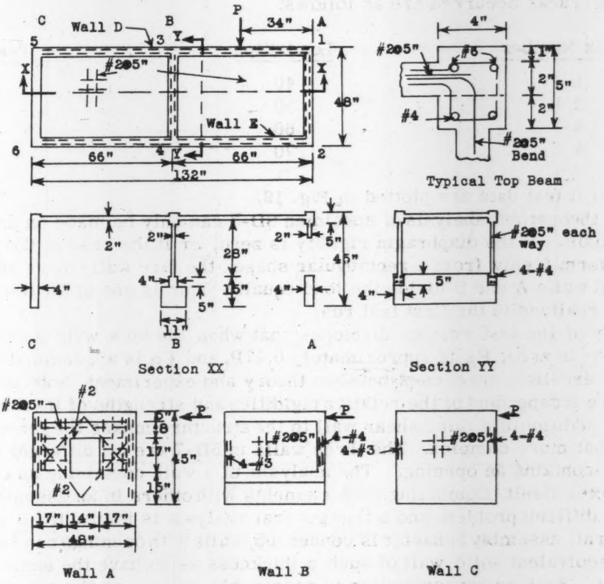
C
Wall D
B
P
34"
A
1
5
3
Y
X
#2@5"
X
48"
Wall E
6
4
Y
66"
66"
2
132"
4"
#2@5"
#6
1"
2"
5"
2"
#4
#2@5"
Bend
Typical Top Beam
2"
2"
4"
4"
28"
15"
5"
11"
2"
5"
45"
4"
#2@5" each way
4-#4
5"
4"
C
B
A
Section XX
Section YY
#2
#2@5"
2"
8
17"
45"
15"
#2
17"
14"
17"
48"
P
#2@5"
4-#4
4-#3
P
#2@5"
4-#4
4-#3
P
Wall A
Wall B
Wall C

FIG. 17.—DETAILS OF SPECIMEN SD-7.

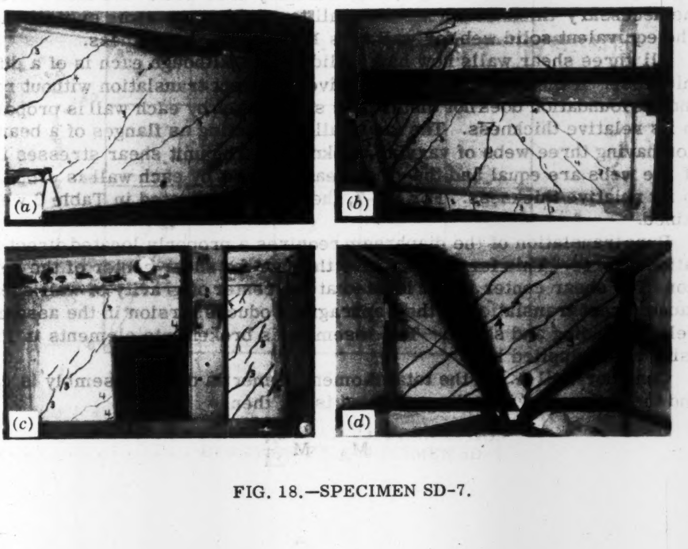

FIG. 18.—SPECIMEN SD-7.

various cracks occurred are as follows:

Crack Number	Load-Kips	Test Run
1	40	1
2	50	1
3	60	1
4	70	2

Typical test data are plotted in Fig. 19.

The theoretical analysis of specimen SD-7 can only be made on an approximate basis. If the diaphragm rigidity is zero, or if the base of the structure can deform freely from a rectangular shape, the face walls have zero shear load and walls A and B divide the load equally. This is one of the limiting conditions realized in the first test run.

Study of the test results discloses that when the face wall shear is made zero, F_C is zero, F_A is approximately 0.47P, and F_B is approximately 0.53P. This is excellent agreement between theory and experiment. Note that the results are independent of the relative rigidities and strengths of the shear walls.

The addition of a third shear wall to the structure makes the general theory somewhat more complex. The three walls in SD-7 are all different in design. Wall A contains an opening. The analysis of a wall containing an opening is complex in itself. Combining such elements with others in an assembly makes a most difficult problem and a true general analysis is impractical. Insofar as the overall assembly behavior is concerned, walls with openings can be replaced by an equivalent solid wall of such a thickness as to have the same effective rigidity. Such an approximation is reasonable as long as the actual wall can carry the forces involved without failure.

The equivalent solid wall for wall A is determined by first computing the rigidity of the actual wall including tributary face walls and then solving for the necessary thickness of a solid wall to produce the same overall rigidity. The equivalent solid web for wall A is 1.16 inches in thickness.

All three shear walls now have solid panels although each is of a different thickness. If the roof diaphragm is given a direct translation without rotation and the foundation does not distort, the shear taken by each wall is proportional to its relative thickness. The face walls are acting as flanges of a beam section having three webs of varying thickness. The unit shear stresses in each of the webs are equal and thus the shear carried by each wall is proportional to its relative thickness. For SD-7, the results indicated in Table 2 were obtained.

Pure translation of the diaphragm requires a properly located direct translational force. This force must pass through the shear center of the box section. The shear center is not located at the center of gravity of wall shear because direct translation of the diaphragm produces torsion in the assembly as well as bending and shear. The assembly is broken into elements in Fig. 20, using a unit applied load.

Consider wall A. If the total moment of inertia of the assembly is called I and the I of wall A including columns is I_A, then

$$M_A = M \frac{I_A}{\Sigma I} \quad \ldots\ldots\ldots\ldots\ldots\ldots \quad (11)$$

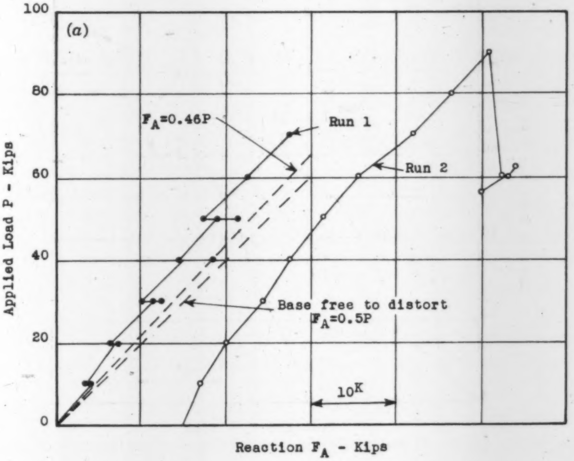

FIG. 19(a).—APPLIED LOAD VS. FOUNDATION REACTION F_A. SPECIMEN SD-7.

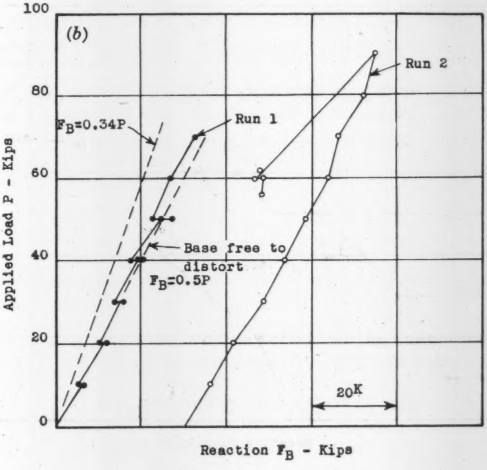

FIG. 19(b).—APPLIED LOAD VS. FOUNDATION REACTION F_B. SPECIMEN SD-7.

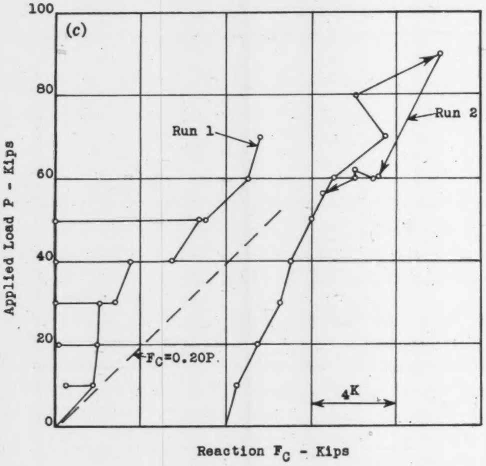

FIG. 19(c).—REACTION F_C VS. APPLIED LOAD. SPECIMEN SD-7.

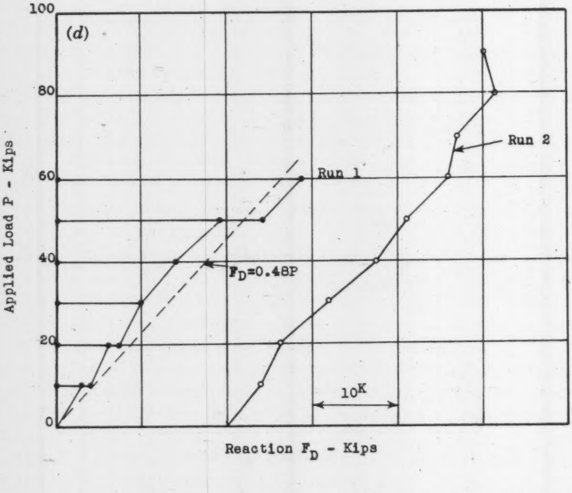

FIG. 19(d).—APPLIED LOAD VS. FOUNDATION REACTION F_D. SPECIMEN SD-7.

in which M = 28P, the total moment in the assembly at the foundation level. The following computations result if P = 1 kip:

Wall	I_{web}	I_{col}	Total	$I/\Sigma I$	$28\ I/\Sigma I$
A	6,200 in^4	15,500 $in.^4$	21,700 $in.^4$	0.068	1.9 kip in.
B	10,700	15,500	26,200	0.082	2.3
C			36,900	0.116	3.2
Face (Total D and E)			233,000	0.733	20.5
		$\Sigma I =$	317,800 $in.^4$		

Considering equilibrium of wall A;

$$(0.162)\ (28) = 44Q_A + 1.9$$

$$Q_A = 0.060 \text{ kips}$$

Wall C;

$$(0.559)\ (28) = 44Q_C + 3.2$$

$$Q_C = 0.283 \text{ kips}$$

The vertical force acting on each face-wall segment is equal to the moment divided by twice the center to center distance between them or

$$\frac{20.5}{(2)\ (44)} = 0.233 \text{ kips}$$

Now the vertical equilibrium of each face-wall segment can be completed. The face-wall segments are not now in moment equilibrium, thus requiring horizontal forces or shears applied top and bottom of the segment. For example, the front face-wall segment between walls A and B has a shear-force of Q_{AB}.

TABLE 2.—RESULTS FOR SD-7

Wall (1)	Thickness, in inches (2)	Relative Thickness (3)	Wall Shear (4)
A	1.16	0.162	0.162P
B	2	0.279	0.279P
C	4	0.559	0.559P
Total	7.16	1.000	1.000P

$$28Q_{AB} = (30)\ (0.173) - (30)\ (0.060)$$

$$Q_{AB} = 0.121 \text{ kips}$$

The other shears can be computed, yielding the values shown in Fig. 20. The forces exerted on the top of the wall assembly at the diaphragm level are shown at the bottom of Fig. 20.

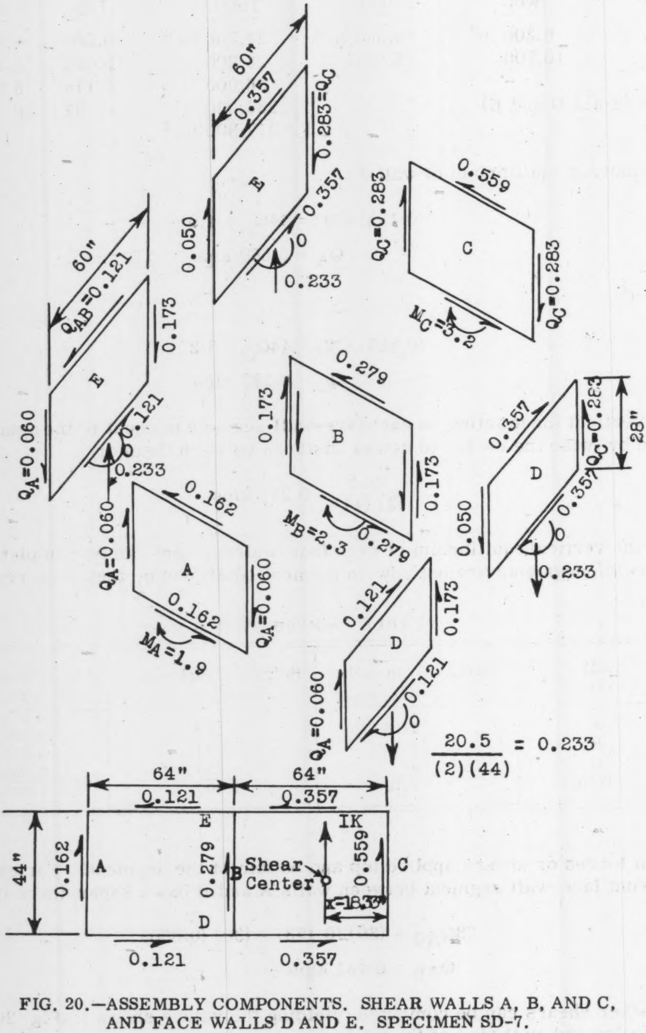
60"
0.357
0.283=Q_C
E
0.357
0.050
0
0.233
0.559
Q_C=0.283
C
Q_C=0.283
M_C=3.2
60"
Q_AB=0.121
0.173
E
Q_A=0.060
0.121
0.233
0.279
0.173
B
0.173
M_B=2.3
0.279
0.357
Q_C=0.283
28"
D
0.357
0.050
0.233
0.162
Q_A=0.060
A
Q_A=0.060
0.162
M_A=1.9
0.121
0.173
D
Q_A=0.060
0.121
0
20.5 / (2)(44) = 0.233
64"
64"
0.121
0.357
44"
0.162
A
E
0.279
B
D
Shear Center
IK
0.559
C
x=18.3"
0.121
0.357

FIG. 20.—ASSEMBLY COMPONENTS. SHEAR WALLS A, B, AND C, AND FACE WALLS D AND E. SPECIMEN SD-7.

The applied load must be so located as to produce this force pattern. Taking moments about wall C,

$$(1)(x) = (0.279)(64) + (0.162)(128) - (0.121 + 0.357)(44)$$

From which

$$x = 18.33 \text{ in.}$$

Thus the shear center is 18.33 in. from wall C.

Obviously it is impossible to develop practical equations giving the locations of the shear center for all possible wall arrangements. Box structures, however, must be considered in this manner or very poor results are obtained.

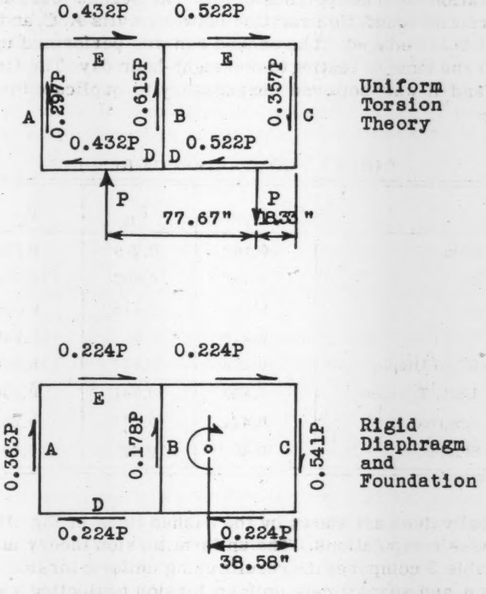
0.432P
0.522P
E
E
0.297P
0.615P
0.357P
A
B
C
0.432P
D
D
0.522P
P
P
77.67"
18.33"
Uniform
Torsion
Theory
0.224P
0.224P
E
0.363P
A
0.178P
B
C
0.541P
D
0.224P
0.224P
38.58"
Rigid
Diaphragm
and
Foundation

FIG. 21.—RESULTS OF TORSION ANALYSIS. SPECIMEN SD-7.

The actual load was applied to SD-7 midway between walls A and B. Thus, considerable torsion is induced in the structure. The torsional moment is then

$$P\left(\frac{64}{2} + 64 - 18.33\right) = 77.67P$$

The torsional analysis of this structure can be made on two different assumptions. First, if the diaphragm and foundation are flexible only to the point where uniform torsion theory can apply, the solution can be made using the uniform torsion approach from the theory of elasticity, Fig. 21. These forces are associated with a condition of pure shear in all walls. If all such deformation is concentrated in the roof diaphragm, the diagonals in each box element change length. The diagonals change length in the box between A and B approximately 3 x 10^{-9} in. per kip of load, and between B and C approximately 1 x 10^{-7} in. per kip of load. Such magnitudes are very small compared to those produced by even a nominal shear stress in the diaphragm. Thus, it is reasonable to expect uniform torsion theory to apply even though warping is not completely free.

If both diaphragm and foundations are infinitely rigid, warping is completely restricted, and only shearing distortion is considered in the walls. The forces shown in Fig. 21 would then result. Such a solution involves rotation about the center of gravity of wall thickness, or 38.58 in. from wall C. Comparison of values discloses that the two solutions differ greatly.

The first test on SD-7 was conducted so as to have the rotation of the foundation of all three walls essentially identical at all times. Thus differential foundation rotation need not be considered. The second test run, however, does involve differential foundation rotation between walls A, C, and B such that the shear on wall B is reduced. The second run was performed in this manner in order to limit the time of testing to one eight-hour day. The first run gave excellent data and it was believed unnecessary to duplicate this portion of the test.

TABLE 3.—COMPARISON OF RESULTS

	F_A	F_B	F_C	$F_D = F_E$
Direct Translation	0.162	0.279	0.559	-0.478
Uniform Torsion	0.297	0.062	-0.359	0.954
Rigid Diaphragm	0.363	0.178	-0.541	0.448
Approx. Unif. Torsion	0.279	0	-0.279	0.810
Translation + Rigid Diaph.	0.525	0.457	0.018	-0.030
Translation + Unif. Torsion	0.459	0.341	0.200	0.476
Translation + Approx. U.T.	0.441	0.279	0.280	0.332
Experimental Slopes	0.40	0.42	0.18	0.50

Theoretical values are shown by the dashed lines in Fig. 19, expressing the results of these computations. The uniform torsion theory method of solution was used. Table 3 compares the results using uniform torsion, rigid diaphragm and foundation, and approximate uniform torsion neglecting wall B. Values are for a unit load applied to the assembly. Average experimental slopes are given in Table 3 for comparison.

Comparison of theory and experiment shows that the best source of comparison is the value of F_D, the face wall shear. The rigid diaphragm solution, the first method shown above, is extremely poor while uniform torsion theory affords good correlation. The approximate uniform torsion theory solution, neglecting wall B, is reasonably good and much more practical than the more rigorous approach.

Studies of the two specimens, SD-6 and SD-7, showed the great influence of face walls on shear wall assemblies. The solution of box assemblies requires a complete re-evaluation of the theory. Modes of failure and general behavior are identical with those observed for individual wall and diaphragm elements.

TWO-STORY STRUCTURES WITHOUT FACE WALLS—SPECIMENS SD-8 AND SD-9

In general, multi-story shear wall assemblies cannot be analyzed as a group of one-story structures. However, with all stories loaded, the errors involved may be small. This problem was studied with two specimens, SD-8 and SD-9, which were identical in structure but subjected to different loadings. The specimen details are shown in Fig. 22. Model SD-8 was loaded uniformly with equal loads in each panel and the roof diaphragm load half that of the second-story diaphragm. Specimen SD-9 was loaded in the same manner but in only one panel so that the structure was subjected to torsion.

Photographs of the specimens under test are shown in Figs. 23, 24 and 25. The specimens were constructed by precasting the walls and then assembling them in the testing jig at which time the concrete for the diaphragms was placed. All concrete was of the same mix and had a strength of 3,000 psi or higher at the time of test. The instrumentation was revised for these specimens. The horizontal loads, P, were applied by hydraulic jacks. Horizontal wall shears, R, were measured directly by calibrated hydraulic jacks that were continuously adjusted to keep the wall foundations in a straight line. Tie-down forces were measured directly with jacks and foundation rotations were eliminated.

Loads were applied in small increments after which all jacks were adjusted and forces and deflections measured. A continuous static equilibrium check was maintained to control errors.

Two series of tests were made on SD-8. The first run involved increasing the load up to first crack and then decreasing it back to zero. The second test was carried into the post ultimate range. Test results for Specimen SD-8 are given in Fig. 26. Data for SD-9 are given in Fig. 27. Deflection results for this model were inconsistent.

These structures are statically indeterminate to the second degree. Elastic analyses were made in which both bending and shear deflection of walls and diaphragms were included. With Specimen SD-8 the two-story computations yield,

$$R_A = R_C = 0.39P; \; R_B = 0.22P; \; T_A = T_C = 0.34P.$$

These theoretical relationships are plotted along with the experimental results. Note the excellent agreement. If single-story theory is used to solve the same problem, assuming a rigid diaphragm in addition, the following results are found:

$$R_A = R_C = 0.43P; \; R_B = 0.14P; \; T_A = T_C = 0.36P; \; T_B = 0.12P.$$

While the differences in R_B are large, other variations are small. Thus the error involved in using single-story theory in this particular problem is not excessive.

Similar computations were made for specimen SD-9. The theoretical results are shown in Table 3 for comparison and the two-story theory results are shown by dashed lines in Fig. 27.

Note that the results of the approximate single-story analysis are essentially identical to the more exact results. Some conclusions can be drawn if the reasons for this virtual identity are investigated.

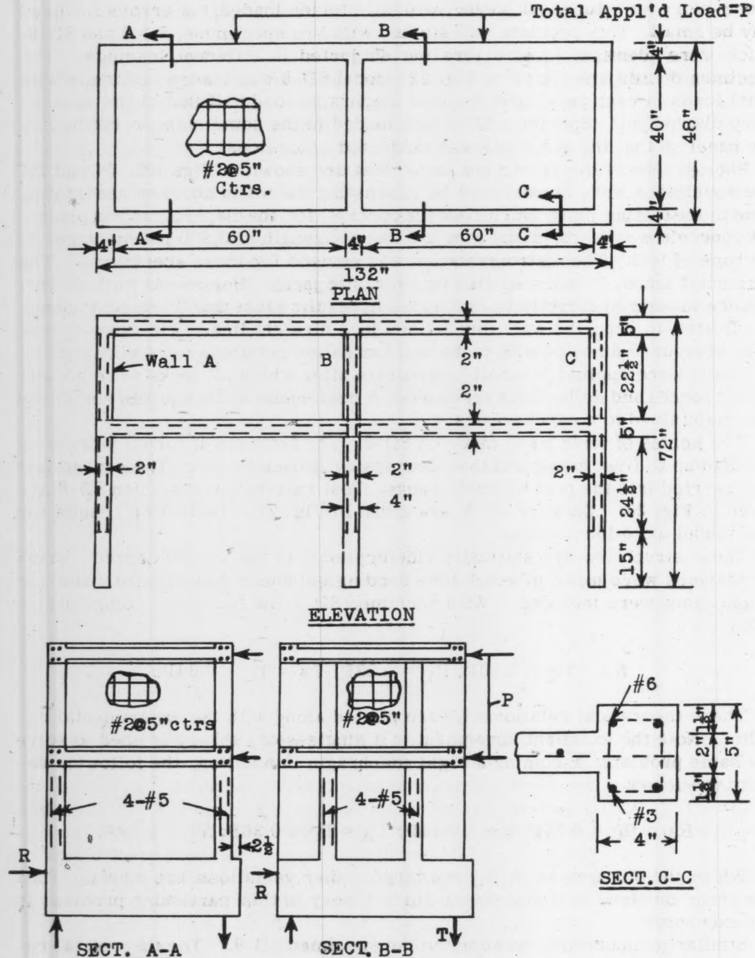
Total Appl'd Load=P
A
B
#2@5"
Ctrs.
C
A
60"
B
60"
C
4"
4"
4"
132"
PLAN
4"
40"
48"
4"
Wall A
B
C
2"
2"
5"
22½"
5"
72"
2"
2"
4"
2"
24½"
15"
ELEVATION
#2@5"ctrs
4-#5
2½
R
SECT. A-A
P
#2@5"
4-#5
R
T
SECT. B-B
#6
#3
1½"
2½"
5"
4"
SECT. C-C

FIG. 22.—DETAILS OF SPECIMENS SD-8 AND SD-9.

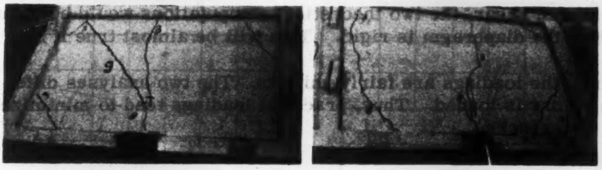

Top Face of Upper Diaphragm

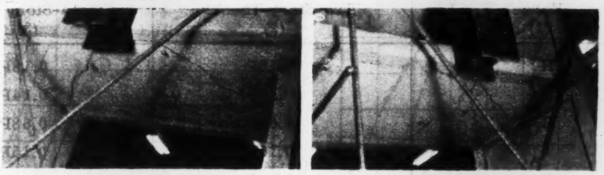

Bottom Face of Lower Diaphragm

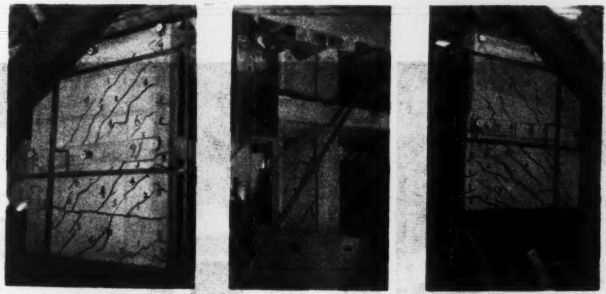

Wall A Wall B Wall C

FIG. 23.—CRACK PATTERN FOR SD-8 AT MAXIMUM LOAD.

FIG. 24.—SPECIMEN SD-9 IN JIG

First, a major source of deformation is shearing distortion. If all distortion was from shear, the two theoretical computations would be identical providing that the diaphragm is rigid. This will be almost true if face walls are added.

Second, the loadings are fairly uniform. The two analyses differ greatly if only one story is loaded. Thus, practical loadings tend to minimize the theoretical differences.

TABLE 4

Force (1)	Two-Story Theory (2)	Single-Story Theory (3)
R_A	0.18P	0.18P
R_B	0.14P	0.14P
R_C	0.68P	0.68P
T_A	0.16P	0.15P
T_B	0.10P	0.12P
T_C	0.58P	0.57P

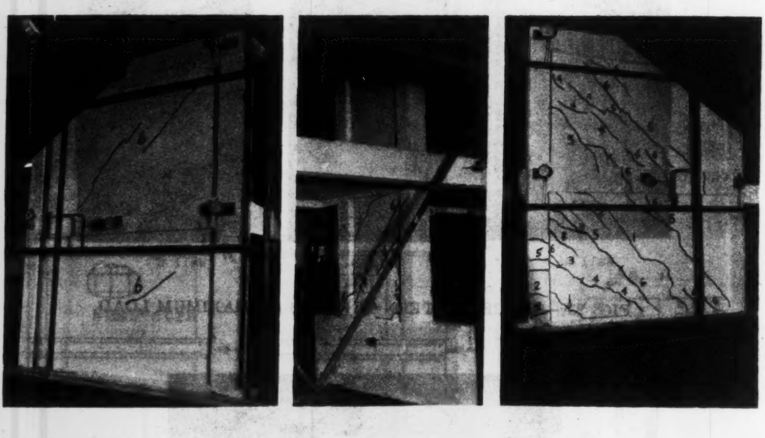

Wall A Wall B Wall C

FIG. 25.—COMPONENT WALLS AT ULTIMATE.

Finally, the structures are very rigid, making experimental errors large and the measured deflections of no real value in checking theory. With practical structures, items such as foundation distortion tend to invalidate complex analytical procedures. The best theoretical solution remains only a very rough estimate at best. If the entire SD series of specimens is studied as a whole, this is an inevitable conclusion.

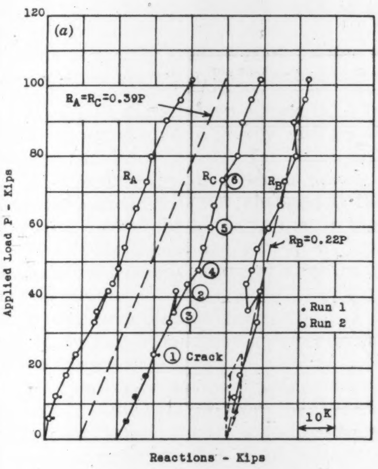

FIG. 26(a).—APPLIED LOAD VS. REACTIVE FORCES. SPECIMEN SD-8.

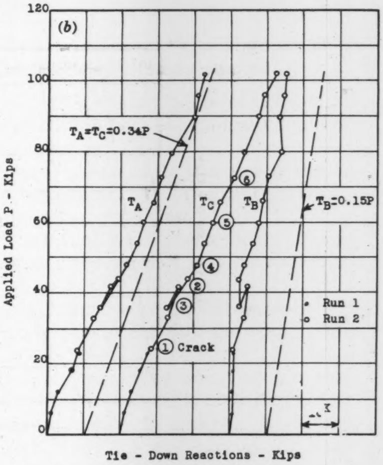

FIG. 26(b).—APPLIED LOAD VS. TIE-DOWN REACTIONS. SPECIMEN SD-8.

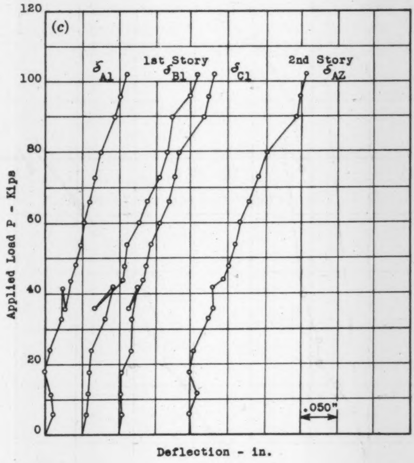

FIG. 26(c).—APPLIED LOAD VS. STORY DEFLECTION FOR SHEAR WALLS A, B, AND C. SPECIMEN SD-8.

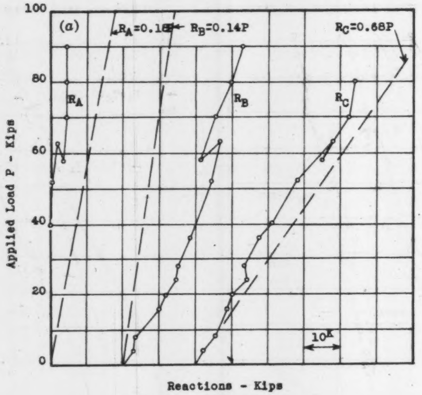

FIG. 27(a).—APPLIED LOAD VS. REACTIONS. SPECIMEN SD-9.

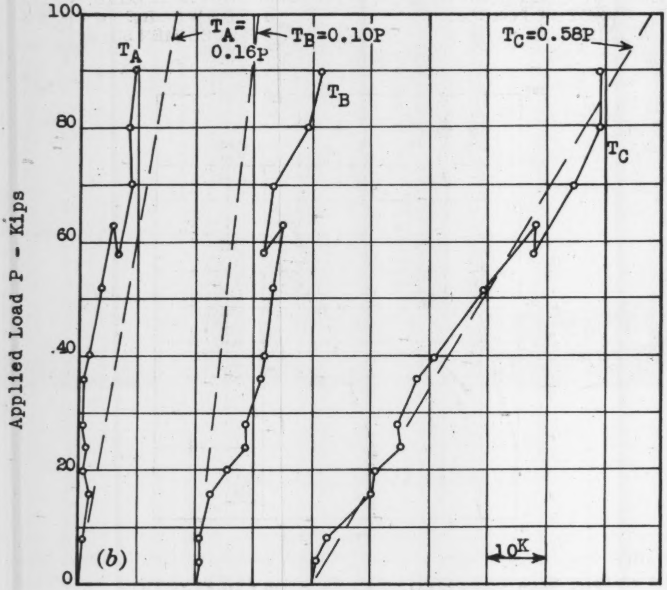

FIG. 27(b).—APPLIED LOAD VS. FOUNDATION TIE-DOWN FORCES. SPECIMEN SD-9.

CONCLUSIONS

The assembly studies made in this report yield several conclusions. These conclusions are obviously limited in scope by the specimens studied.

1. Force distribution among the elements of a shear wall assembly can be made by using elastic theory with good correlation between computed and observed results.
2. The distribution of shear among several shear walls that are in the uncracked condition is not changed as the elements crack. The distribution at ultimate load is the same as that in the uncracked condition.
3. Deformations are extremely small and not well predicted by theory. Foundation distortions are of vital importance although they may be very small in magnitude.
4. Uniform torsion theory yields a good solution. With closed sections providing the foundation limits, the deformation is consistent with the assumptions in the theory.
5. Two-story assemblies can be solved as two independent single-story structures using single-story theory and assuming an infinitely rigid diaphragm. This conclusion is limited to the structures studied. In general, if shearing distortion predominates in all walls and both structure and loading are regular, the structure can be analyzed using single-story theory. The errors in any one wall may be important but the overall analysis is reasonable and practical.

Instrumentation problems with shear wall assemblies limit experimental studies. The deformations are very small and the force distribution highly sensitive to rigidity variations. Considerable success was attained by closely controlling the foundation conditions by continuous jacking. The force distributions are then found at the expense of the deformations.

ACKNOWLEDGMENTS

The work reported in this paper was part of a project conducted at Stanford University, Stanford, Calif., during 1955-56 under Contract DA49-129-Eng-193 with the office of the Chief of Engineers, Department of the Army, Washington, D. C.

AMERICAN SOCIETY OF CIVIL ENGINEERS
Founded November 5, 1852
TRANSACTIONS

Paper No. 3118

CONSTRUCTION OF THE MORRISON BRIDGE

By R. D. Bane,[1] F. ASCE

SYNOPSIS

Late in 1958, Multnomah County completed a new bridge in Portland, Oregon, at a cost of over $13,000,000 to cross the Willamette River and to connect through extensive approaches to downtown streets. This article reports on the construction of the 760-ft river bridge and its approach systems.

The new Morrison Bridge over the Willamette River was opened to the traveling public in downtown Portland, Oregon, during May, 1958. Four months later the removal of the old Morrison Street Bridge from the site ended the 3-yr period required for construction of this modern bridge and approaches. This article presents a general description of the construction phase of the Morrison Bridge Project and discusses in detail a few selected features of construction.

Briefly, the project consists of a three-span river crossing, 760 ft in length, together with approach systems on each river bank. The river crossing has two deck truss approach spans and a double-leaf bascule span with a 220-ft clear horizontal opening. A six-lane roadway, 78 ft wide between curbs,

---

Note.—Published essentially as printed here, in May, 1960, in the Journal of the Construction Division, as Proceedings Paper 2482. Positions and titles given are those in effect when the paper or discussion was approved for publication in Transactions.

[1] Engr. of Special Assignments, Sverdrup and Parcel Engrg. Co., San Francisco, Calif.

with 5-ft sidewalks are provided on the river bridge. The west approaches span across three cross streets to accommodate traffic to and from the downtown area and major arterial streets. The east approach system, extending approximately 1,900 ft from the east river bank, has off and on connections to the nearby east industrial area and carries main bridge traffic on two three-lane, one-way, elevated approaches over five cross streets to connect with U.S. Highway 99E.

Late in 1955, the pier contractor mobilized marine equipment at the site for the river substructure units and proceeded with the driving and loading of test piles. Additional equipment and materials were soon assembled at the site by the contractor in preparation for construction of Pier 1, at the west bank, Piers 2 and 3 located in the center, and Pier 4, near the east bank of the river. Pier foundations were built one at a time to permit maximum reuse of cofferdam materials. The contractor made Piers 2, 3, and 4 easily accessible to workmen, equipment, and supplies by installing a timber trestle between Pier 2 and the east river bank. Pier 1 was within reach of land-based equipment on the west harbor wall.

Construction of Pier 2 (Figs. 1 and 2), below the surface of the river, was probably the most hazardous undertaking on the entire project. Briefly, this is how the contractor proceeded with the building of this deepest bascule pier:

The two lowest rings for the cofferdam's internal framing were assembled on a barge with considerable overhang along the sides of the barge. After the barge was floated to the pier location, steel guide piles were driven at each corner for suspending the framing rings. The barge was then partially filled with water and towed away from the suspended frame. Next, the two upper framing rings were assembled in place as the entire internal framing unit was slowly lowered into position. Z-32 steel sheet piles were driven around the frame to tip elevation of -80 and top elevation of +15, Portland Datum. El. 3.2 equals low-water elevation according to this datum. The sand and gravel in the cofferdam was excavated by clamshell bucket down to El. -75. One hundred fifty four 14-in. bearing piles, at 102 lb per ft, were driven to tip elevation of -119 inside the cofferdam limits. Piles were driven under water with a McKiernan-Terry 10S hammer which delivers 32,500 ft-lb of energy per blow. Next, a concrete seal course, 26 ft deep, was poured into the cofferdam. The 6,200 cu yd in this seal course were placed in 34 hr of continuous pouring. Transit-mix trucks delivered this concrete over the timber trestle to the pier site where it was conveyed by gravity to 9-in diameter tremies into the seal. After the seal course had been in place for 7 days, the water was pumped from within the cofferdam. Two 12-in., 125 hp, and two 10-in., 50 hp electric pumps were used in initial unwatering; but after drawdown was complete, one 10 in. pump easily discharged all run-in which was less than 2,000 gal per min. A 10-ft depth of concrete footing was next constructed within the dry confines of the cofferdam and then shaft construction proceeded. After shafts were built to El. 25 and forms were removed, pumping ceased and water rose to river level within the cutoff wall. Steel sheet piles were extracted and the internal bracing frame was removed and dismantled. No difficulty was experienced with the frame which was made up of 24-in WF walers, timber posts, and timber struts. In areas where struts passed through concrete shafts, steel beams were used and left in place. Cofferdams were constructed by a similar procedure for Piers 1, 3, and 4.

As each of the river piers was constructed above the level of the river, progress was accelerated and the work was vigorously pressed by the con-

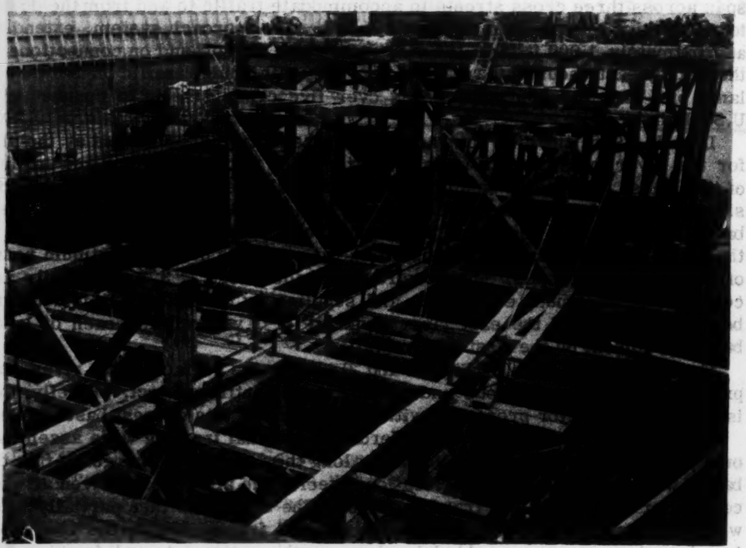

FIG. 1.—FRAMING IN COFFERDAM FOR BASCULE PIER 2

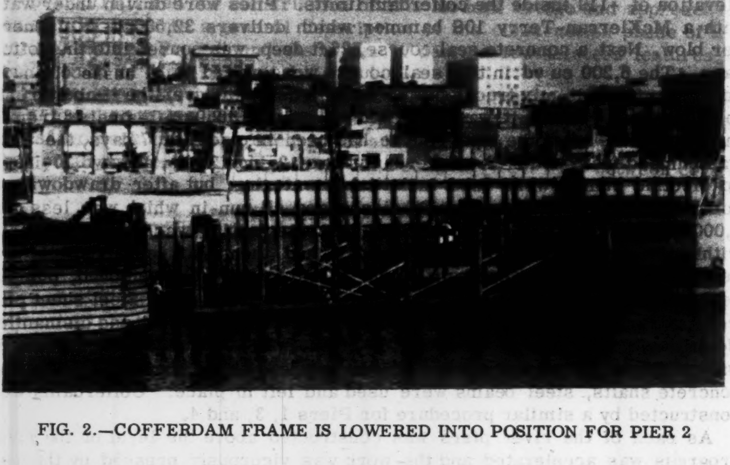

FIG. 2.—COFFERDAM FRAME IS LOWERED INTO POSITION FOR PIER 2

tractor until completion (Fig. 3). The river piers contract was completed slightly later than the specified date. However, the piers were ready to receive structural steel superstructure only 19 days later than originally required by the contract.

Nearly 60,000 cu yd of concrete were incorporated in various portions of bridge. Mixes at desired consistencies were designed in a commercial laboratory and adjusted in the field to meet conditions of placement. In general, test cylinders for mixes averaged at least 30% above minimum required strengths. Cement factors were always held to the specified minimum. Concrete aggregates were dredged from the Willamette River and stockpiled at a batching plant about 3 miles upstream from the project site. Transit mixers were used and the time of travel from batcher to the structure averaged 10 min. Two-way radio contact between plant dispatcher and trucks resulted in maintaining excellent control of consistency under all conditions of placement.

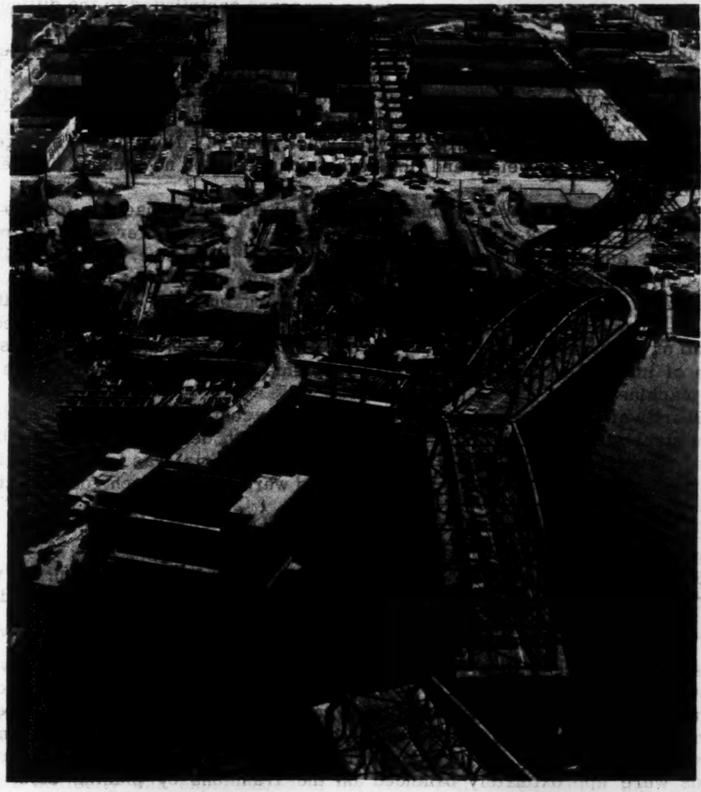

FIG. 3.—BRIDGE UNDER CONSTRUCTION WITH BASCULE PIER 3 IN FOREGROUND

Construction of the river piers was six months along in May, 1956, when contracts were awarded on the river superstructure and east approaches portions of the project. Two months later a contract for the west approaches was awarded. Progress on both east and west approaches proceeded approximately as anticipated, and each was ready for vehicular traffic on the specified contract dates. While the construction of the river spans may seem more spectacular, a relatively large part of the engineer's field forces' time was required in supervising the work on the approaches. The necessity of keeping streets open for the public and business concerns contributed to the difficulty of this work.

Substructure work on the approaches was completed according to schedule. During the foundation construction period, the all-welded girders were being fabricated for use as superstructure stringers. Stringers were yarded after fabrication, then transported to the bridge site on trucks and trailers. At the site, steel stringers were erected with truck cranes. None of the stringers exceeded 26 tons in weight and field erection presented no unusual problems or difficulty.

The contractor devised an unusual concrete-finishing machine for use on the straight-run deck of the east approaches. A Clary roller finishing machine was adapted to meet the job requirements. Rails were installed 42 ft apart to accurate elevations along the sides of the deck forms upon which the machine was operated. This modified finishing machine made the initial strike-off and finished the slab to the extent that only a skip float was needed ahead of the brooming operation. In consolidating the concrete mix, the usual type of internal vibrator was used to supplement the 9-in. vibrating pipe on the machine.

Shortly after the award of the superstructure contract was made, a nationwide steel strike resulted in a subsequent 6-month delay in receipt of fabricated structural steel at the site. Although this material was late in arriving, men and machinery worked such hours, and were used to such good effect on the superstructure, that it was possible to open the bridge to traffic only $2\frac{1}{2}$ months later than was originally scheduled.

Structural steel was fabricated in Gary, Ind., and Memphis, Tenn. It was unloaded in a Portland yard from railway freight cars, near a riverside dock about $\frac{3}{4}$ mile upstream from the bridge site. Bascule leaf members were hoisted into place with a 50-ton scow derrick after fabricated pieces were brought to the site on barges (Fig. 4). The leaves were erected in down position, starting at the counterweights and cantilevering from the trunnion beam toward the center of the span. Timber bents temporarily supported the counterweight frame from the pit floor until it was filled with concrete. Erection loads were approximately balanced on the trunnions by placing steel and counterweight concrete alternately. Side spans, each 90 ft wide by 207 ft long, and weighing 450 tons, were erected on barges at the riverside dock and floated into position as single units. Two 300-ton barges were used, one under each truss, using temporary falsework bents of proper height to meet the bridge seats. A portion of the end panel next to the shoreline was erected after each span was in exact position in order to allow for adequate clearance while floating into approximate position. Barges were then lowered by flooding with water and at the same time the spans were raised vertically on jacks. As barges came clear they were towed from the site.

Lightweight aggregate (expanded shale) was mixed in combination with medium fine river sand and $\frac{1}{4}$ in. pea gravel to produce concrete for side span decks with dry weight of 103 pcf. With a cement factor of 7 sacks per cu yd, specimen cylinders showed compressive strengths in excess of 2,900 psi for 7-day breaks and over 4,000 psi for 28-day breaks.

Experienced millwrights installed and adjusted all machinery for the bascule spans to exceptionally good field tolerances. Racks were each completely assembled in the manufacturer's plant in Portland, carefully inspected, and scribed with the pitch circle. Sections were then match-marked, disassembled, and shipped to the structural steel fabricator. Racks were shop-positioned to the truss assembly and holes for connection were drilled undersize in the truss members opposite those in the rack segments. This precaution allowed for a final adjustment in the field after erection was complete and counterweights were placed. Final adjustments in the field up to 3/16 in. were made on temporary erection bolts which were undersized, preparatory to reaming holes in the rack and truss to receive the full diameter of the specified turned bolts.

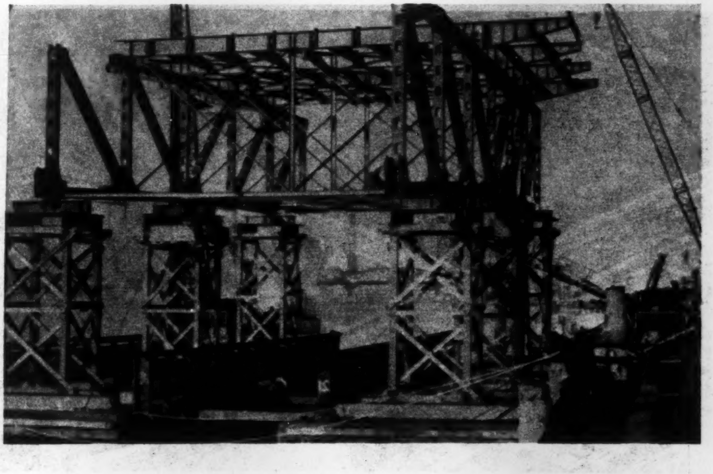

FIG. 4.—DECK TRUSS ON BARGES

No difficulty was experienced in the electrical check-out of the control system. A prescribed procedure was followed in adjusting the center of gravity of bascule leaves to the desired position near trunnion centerline. Changes in the number of portable counterweight blocks in the upper and lower counterweight galleries were used to make this adjustment.

Late in 1956, officials for the County decided to provide for a traffic detour across the Willamette during the latter 9 months of the project construction period. Otherwise, the conflict in alienment of the old and new bridge would have necessitated closing the crossing to the public during this period. This decision required the construction of a detour which utilized the adjacent

Morrison Street Bridge in place except for its east span which was angled to the upstream (Fig. 3). Traffic was routed from the east river bank around and under the approach spans to Water Avenue. Contract cost for building and maintaining the detour was $70,000. An average of 16,000 vehicles per day was accommodated over the old modified structure after the detour was opened to travel in June, 1957 (Fig. 5). The Morrison crossing was closed to vehicles a total of 6 days while the east end of the old east span was floated by barge to its new location and necessary end connections were being made.

Construction of the new Morrison Bridge was certainly well supervised by sidewalk superintendents. The proximity of the downstream sidewalk of the old bridge to the new work provided spectators with a veritable "seat in the front row." Observers gathered there daily to watch the bridge rise from the depths of the river to take its arched and graceful form across the water.

This bridge is the third to be built at this site. The first was a timber bridge built in 1883, and was the first bridge over the Willamette in Portland.

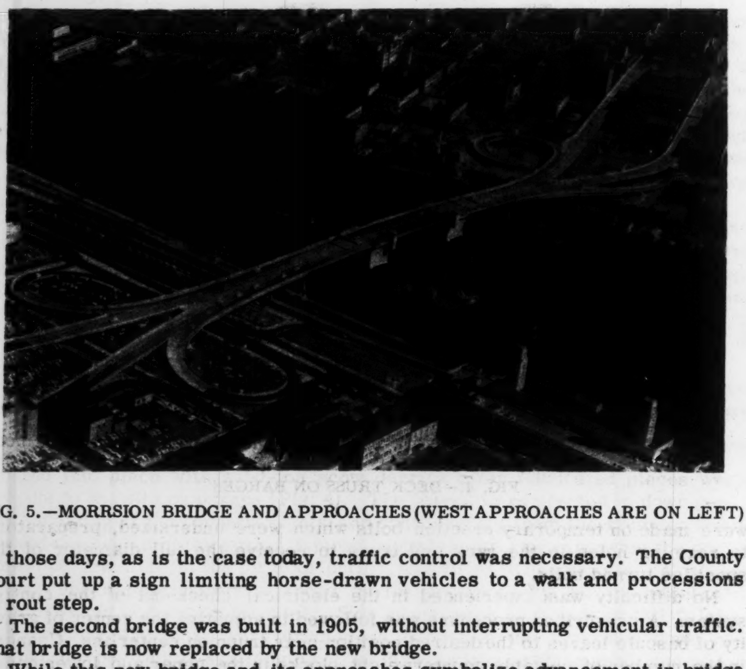

FIG. 5.—MORRSION BRIDGE AND APPROACHES (WEST APPROACHES ARE ON LEFT)

In those days, as is the case today, traffic control was necessary. The County Court put up a sign limiting horse-drawn vehicles to a walk and processions to rout step.

The second bridge was built in 1905, without interrupting vehicular traffic. That bridge is now replaced by the new bridge.

While this new bridge and its approaches symbolize advancement in bridge design, it, too, is destined to become obsolete. Perhaps this obsolescence will appear in the steel grid floor on the bascule span. Certainly an open floor would not be suitable to the suggested car of the future which glides along on air pads instead of wheels.

ACKNOWLEDGMENTS

Sverdrup and Parcel, Inc., and Moffatt, Nichol and Taylor, project design engineers, also supervised the construction for the sponsor, Multnomah County. Competitive bids for the work were received by the County and the four contracts were awarded as follows:

1. River Piers - Manson Construction and Engineering Co., $1,908,516. Awarded October, 1955.
2. River Superstructure - American Bridge Division, U.S. Steel Corp., $2,270,443. Awarded May, 1956.
3. East Approaches - Kuckenberg Construction Company, $2,971,571. Awarded May, 1956.
4. West Approaches - Donald M. Drake Company, $1,178,360. Awarded July, 1956.

AMERICAN SOCIETY OF CIVIL ENGINEERS

Founded November 5, 1852

TRANSACTIONS

Paper No. 3121

EPOXY RESIN FOR STRUCTURAL REPAIR OF CONCRETE PAVEMENT

By Wilson L. Davis,[1] M. ASCE, and Eugene Pinkstaff[2]

SYNOPSIS

This paper describes tests performed in the North Central Division Laboratory of the Corps of Engineers in formulating epoxy resins that will satisfactorily repair surface defects in portland cement concrete pavements, that will bond the hardened surfaces of concrete together, and that will bond new concrete to existing concrete. It describes also the field application of the resulting epoxy resins.

INTRODUCTION

In the program of concrete runway construction in the North Central Division of the Army Engineers there has developed a need for a suitable material to make economical structural repairs of concrete pavements. Epoxy type resin was evaluated for this purpose in the laboratory and found to function satisfactorily when tested under simulated field conditions. The resin was then used to repair surface defects, to bond two adjacent pavement slabs, and to bond new concrete slabs to existing concrete pavement. The following is a description of the testing and the application of the epoxy resin for structural concrete pavement repair.

Note.—Published essentially as printed here, in February, 1960, in the Journal of the Construction Division, as Proceedings Paper 2360. Positions and titles given are those in effect when the paper or discussion was approved for publication in Transactions.

[1] Chf. Soils and Materials Branch, U. S. Army Engr. Div., North Central, Chicago, Ill.

[2] Genl. Materials Engr., U. S. Army Engr. Div., North Central, Chicago, Ill.

EPOXY RESIN SYSTEM

The epoxy resin used was Epon 820.[3] This is a commercial liquid resin with an epoxide equivalent of 175-210, an average molecular weight of 350-400, and a viscosity at 25° C of 4,000-10,000 centipoises.[4] Since the epoxy resin is too brittle when cured alone for the desired use, it was flexiblized with Thiokol LP-3 (Thiokol Chemical Corp.). This is a long chain aliphatic liquid polymer containing disulfide links and reactive terminals. Thiokol LP-3 has a specific gravity of about 1.27 and a viscosity of from 7-12 poises.[5] The resin system was catalytically co-cured with DMP-10 (Rohm and Haas Co.) dimethyl amino methyl phenol) which is one of the more active tertiary amine catalysts. Its activity is such that it will effect a cure of an Epon 820-Thiokol LP-3 mixture at room temperature. Inert fillers were added, as subsequently indicated, to reduce the costs and to obtain desirable working properties. The gray color of the concrete pavement was nearly duplicated by adding titanium dioxide pigment to obtain a white opaque mixture, after which lamp black was added to obtain the desired shade of gray. For some applications the gray color would not be necessary since the cured resin would not be visible.[6]

Since the epoxy resin system cured without a flexiblizer tends to be brittle, and the addition of flexiblizer increases the percentage compressive strain, it seems obvious that for structural concrete pavement repair the amount of flexiblizer added to the epoxy resin should optimize strength versus flexibility of the cured resin system. It was therefore desirable to compare the percentage compressive strain of the resin formulations at a nominal compressive for concrete, such as 5,000 psi. The most desirable formulation was then the one that had a percentage compressive strain at 5,000 psi compressive stress that most nearly approached that of concrete, yet contained enough flexiblizer so that it did not exhibit any tendency to be brittle.

It should be noted that the number of tests were insufficient for a high degree of accuracy. The results are considered approximate but adequate. In addition, stress-strain properties of the resin are all that were tested. The remarkable resistance of the material to chemicals and water immersion has been quite well documented.[4]

The stress-strain properties of the cured resins were determined according to ASTM D 695-54, "Compressive Properties of Rigid Plastics." Test specimens were obtained by pouring the mixed resin into a cylindrical plastic mold whose dimensions were 3/4 in. by 1-1/2 in. long. After the most suitable resin system had been chosen using the criterion of optimizing strength versus flexibility, the resin was tested in the laboratory by repairing concrete beams that were broken in flexure. These tests were intended to duplicate field applications, and the results were compared with the unpatched strength of each beam. Three types of resin systems were tested, although basically they possessed much similarity. These were a liquid resin system, a mortar-type resin system, and a thixotropic-type resin system.

---

[3] Shell Chemical Corp., Technical bulletins, "Epon Resins," Feb., 1958; "Epon Resins For Structural Uses," April, 1957; "Recommendations For Handling Epon Resins And Auxiliary Chemicals In Manufacturing Operations," May, 1957.

[4] "Epoxy Resins, Their Applications and Technology," by Henry Lee and Kris Neville, McGraw - Hill Book Company, Inc., New York, 1957.

[5] Thiokol Chemical Corp., technical literature, "Thiokol Liquid Polymer / Epoxy Resin Casting Compounds," Sept., 1954, and "Thiokol Liquid Polymer / Epoxy Resin."

[6] "Epoxy Resins," by Irving Skeist, Reinhold Publishing Corp., New York, 1958.

LIQUID RESIN SYSTEM

The liquid resin system was intended to be suitable for application by pouring into vertical cracks of relatively narrow cross section compared to their depth. They would thus be inaccessible for the application of a resin patch except by this or a similar method of application. The specific problem that prompted the desire for such a material was to provide structural strength across a sawed contraction joint after a contraction crack had developed very close to the sawed joint. An example of this type of pavement failure is shown in Fig. 1. It was anticipated that in some instances one method of repair would be to patch the sawed joint and then to allow the adjacent crack to serve the function of the patched joint. This type of resin system could, of course, be adapted to repair a great variety of defective areas other than sawed contraction joints.

It was first experimentally determined that the amount of Thiokol LP-3 to be used for this purpose should be approximately 40 parts per hundred parts of Epon 820. Three mixes were then prepared in an attempt to obtain more compressive stress at a reduced compressive strain by reducing the amount of Thiokol LP-3 flexiblizer. Three mixes were prepared which contained LP-3 at 40, 35, and 30 parts per hundred of Epon 820. Otherwise they were the same. In Table 1(b) are the approximate results which were read directly from the stress-strain curves shown in Fig. 2(a).

From the standpoint of durability and impact resistance, 40 parts of Thiokol LP-3 would be the most desirable, providing its stress-strain characteristics were satisfactory for its intended use. At 30 parts of Thiokol LP-3, the cured system tends to be brittle. In both of the 30 parts compression specimens, cracking seemed evident at approximately 0.012 in. per in. compressive strain.

The proportions of the two container system for 40 parts of Thiokol LP-3 per hundred parts of Epon 820 are shown in Table 1(c).

In order to get an estimate of the amount of materials required for a particular application, it is necessary to know the number of pounds of each ingredient contained in each cubic foot of the cured resin. Since the resin cures at nearly constant volume, the quantities of the materials used constitute the quantity of the cured resin. The amount of each ingredient in 1 cu ft of the cured resin for 40 parts of Thiokol LP-3 is shown in Table 1(d).

In order to determine the usefulness of the resin system for the purpose for which it was intended, concrete flexural beams were mended with the resin in order to simulate the field conditions. Also smooth ends of two concrete beams which had been used for field flexural tests were joined together with a 1/4 in. wide patch over their entire cross section. This is shown in Fig. 3. In all five flexural beams 6 in. by 6 in. in cross section were cast with a simulated dummy joint. The mold used was 36 in. long. The flexural strength of the unpatched end was used as a direct comparison with the strength of the patched end. The simulated dummy joint was 1/4 in. wide by 1-1/2 in. deep. This was a patch of 25% of the depth of the beam. A photograph of a patched simulated dummy joint is shown in Fig. 4. Three of the patched joints were broken in simulated compression, that is, the joint was next to the applied load. Two were broken in simulated tension, that is, the joint was directly over the applied load but on the opposite side of the beam. Unfortunately the concrete was obviously of inferior quality. This did not nullify the results of the tests, however, since the strength of the patched section was compared with the strength of the unpatched section of the same beam. The results of the flexural tests are summarized in Table 2.

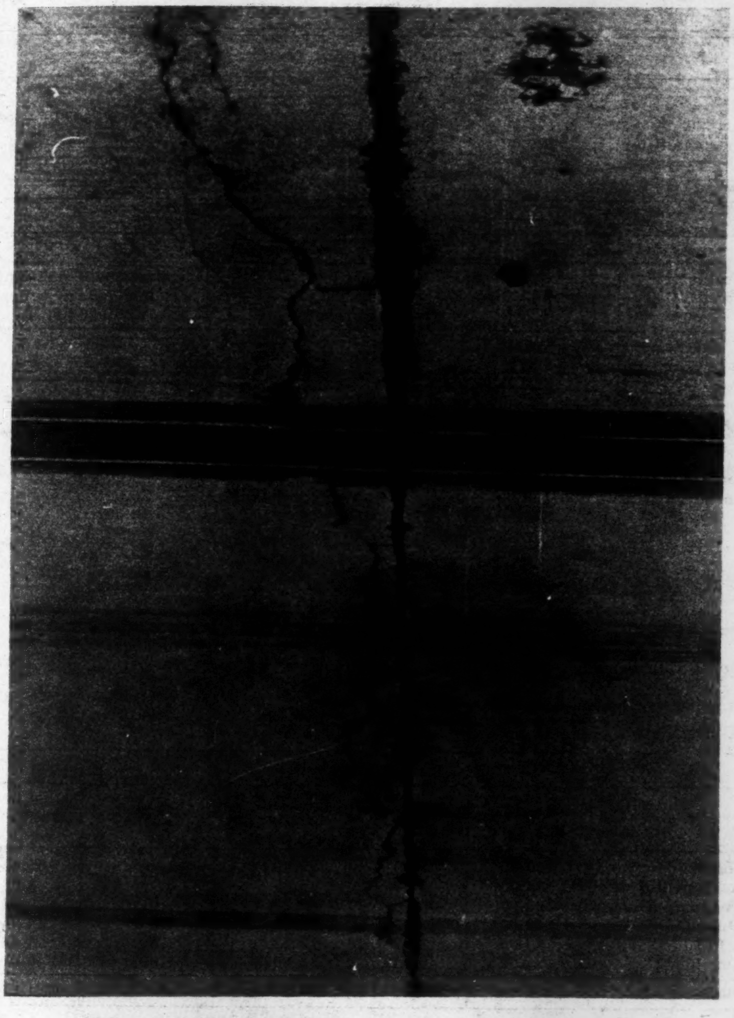

FIG. 1.—PAVEMENT FAILURE NEAR CONTRACTION JOINT

TABLE 1.—LIQUID RESIN SYSTEM

(a) Composition

A:		B:	
Epon 820	100.00 gm.	Thiokol LP-3	X gm.
Limestone filler	120.00	Titanium dioxide	25.00
		DMP-10	10.00
		Lamp black	.02

(b) Stress-Strain Properties

Grams of Thiokol LP-3	5-day air cure		
	Approximate peak compressive stress, in psi	Approximate % strain at peak compressive stress	Approximate % strain at compressive stress of 5,000 psi
40	8,400	6.2	3.1
35	8,370	4.6	1.2
30	8,210	2.0	0.9

(c) Proportions

A:		B:	
Epon 820	100.00 gm	Thiokol LP-3	40.00 gm
Limestone filler[a]	120.00	Titanium dioxide	25.00
	220.00 gm	DMP-10	10.00
		Lamp black	.02
			75.02 gm

$$\frac{A}{B} = \frac{220.00}{75.02} = \frac{2.9326}{1}$$

Specific gravity = 1.665 Density = 103.9 lb per cu ft

$$\text{Specific volume} = \frac{\text{ft.}^3}{103.9\ \text{lb}} = 0.0096\ \text{cu ft per lb}$$

Percentage filler = 49.2%

Pot life, limit of pourability = 40 plus min

(d) Itemized Quantities

Item	Weight, in grams	Weight, in %	Weight % x density, lb per cu ft	Unit cost $/lb	Cost per cu ft of resin
Epon 820	100.00	33.90	35.22	1.58	$55.65
Titanium dioxide	25.00	8.47	8.80	0.43	3.78
Limestone filler	120.00	40.68	42.27	0.01[c]	0.42
Thiokol LP-3	40.00	13.56	14.09	1.06	14.94
DMP-10	10.00	3.39	3.52	1.82	6.41
Lamp black	.02	0.007	0.0073	1.00	0.01
Totals	295.02	100.007	103.9073		$81.21

$$\$/\text{lb} = \frac{\$81.21}{103.91\text{b/w ft.}} = 0.782\ \$/\text{lb}$$

[a] Commercial limestone dust such as that used in asphalt pavements. [b] Approximate small lot unit costs. The cost per cubic foot of resin will be considerably reduced in larger quantities. [c] Limestone filler is assumed to cost $0.01 per lb.

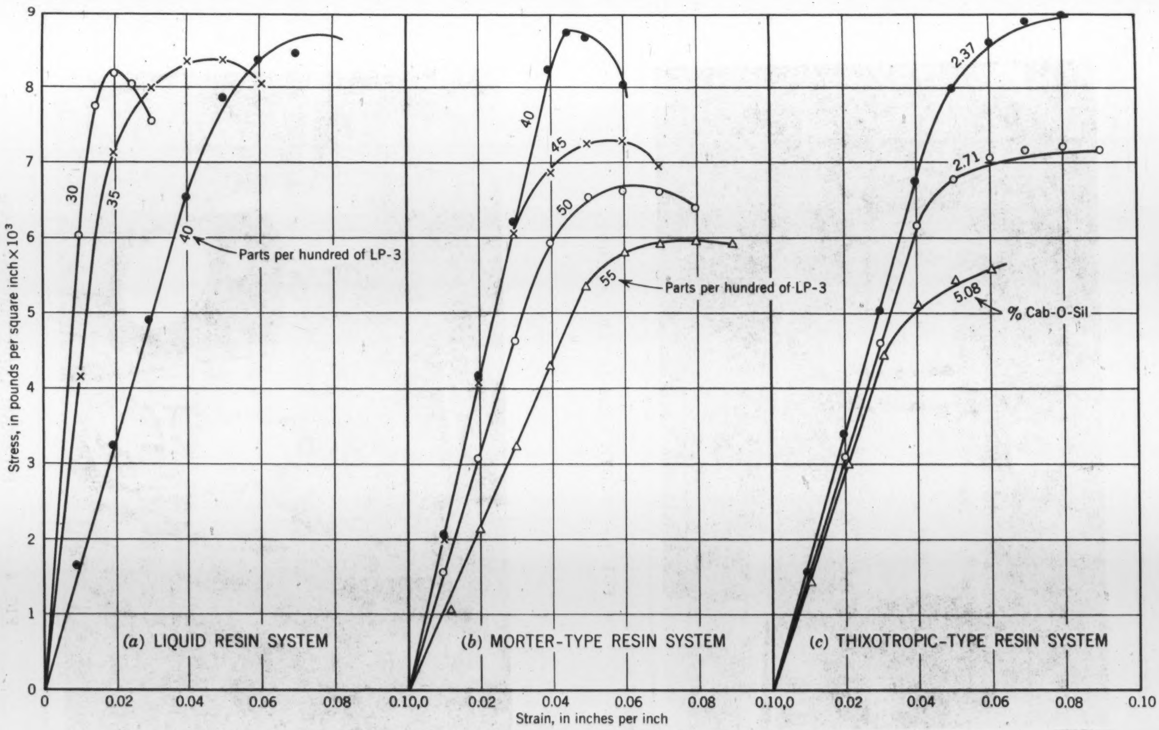
Stress, in pounds per square inch × 10³
0
1
2
3
4
5
6
7
8
9
30
35
40
Parts per hundred of LP-3
40
45
50
55
Parts per hundred of LP-3
2.37
2.71
5.08
% Cab-O-Sil
(a) LIQUID RESIN SYSTEM
(b) MORTER-TYPE RESIN SYSTEM
(c) THIXOTROPIC-TYPE RESIN SYSTEM
0
0.02
0.04
0.06
0.08
0.10,0
0.02
0.04
0.06
0.08
0.10,0
0.02
0.04
0.06
0.08
0.10
Strain, in inches per inch

FIG. 2

FIG. 3.—SMOOTH ENDS AFTER PATCHING

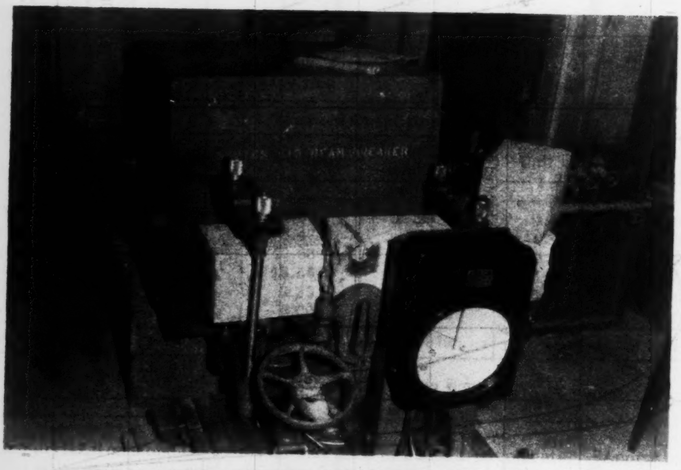
BEAM BREAKER

FIG. 4.—PATCHED BEAM AND BEAM BREAKER

TABLE 2.—FLEXURAL STRENGTH TESTS

Flexural strength, unpatched and, in psi	Flexural strength, patched end, in psi	Remarks[a]
(a) Liquid Resin System		
548 (Average of 4)		Age: 16 days; type III cement; 7 days moist cure
	Compression 555 (Average of 3) Tension 534 (Average of 2)	Simulated 1/4 in. by 1 1/2 in. dummy contraction joints, patched with 40 parts per hundred LP-3. Age: 15 days type III cement; 7 days moist cure. Resin: 5 days air cure.
	717	Smooth end patch 1/4 in. wide over entire cross section, patched with 40 parts per hundred LP-3. Resin: air cured 6 days.
(b) Mortar-Type Resin System		
717 (Average of 2)		Concrete: 7 days moist cure, 11 days air cure; type III cement.
	792 (Average of 2)	1/2 in. by 3 in. by 8 in. ellipsoid. Beam moist cured, 7 days and air cured 11 days. Resin: air cured 5 days.
	667 (Average of 2)	1 1/2 in. by 3 in. by 8 ellipsoid. Same cure as above.
	667	Smooth end patch 1/4 in. wide over entire cross section. Resin air cured 5 days.
(c) Thixotropic-Type Resin System		
717 (Average of 2)		Concrete: 7 days moist cure, 11 days air cure; type III cement.
	658	New concrete and resin: moist cured 5 days; new beam cast against fractured faces.
	842	New concrete and resin: moist cured 7 days; new beam cast against fractured faces.
	867	Same cure as above. Cast smooth faces.

[a] Bond failure negligible in all tests.

MORTAR-TYPE RESIN SYSTEM

The mortar-type resin system was essentially a trowelable mixture and was intended to be suitable for repairing horizontal areas of relatively large cross section compared to their depth, especially aggregate "pop outs" and spalled areas in concrete pavement. The mix was sufficiently viscous to be placed on the usual pavement grade without flowing from place.

The filler used was mortar sand conforming to ASTM C 144-52 T, "Aggregate for Masonry Mortar". Colloidal uncompressed silica was used as a thickening agent to improve the working properties and prevent settling of the sand. Titanium dioxide and lamp black were again used to obtain the desired color. Because of the mortar sand this blend is rather difficult to mix and handle.

The resin system is essentially the same as that described under the liquid resin system intended for pour application. The only difference is a filler modification which provides more desirable working properties for this type of application and also results in a cost reduction. The cured resin system was tested in compression after a 5-day air cure. The most suitable mixes tested are summarized in Table 3(a). The stress-strain properties were taken from the stress-strain curves shown in Fig. 2(b).

The mix containing 45 parts of Thiokol LP-3 was deemed the most suitable since it most nearly optimized durability and impact resistance versus stiffness and strength.

The suitability of the material for structural surface repair such as "pop outs" in concrete pavements was determined by flexural beam tests. Three 6 in. by 6 in. by 36 in. flexural test beams were cast. After the concrete had attained its initial set, areas were dug from the concrete to form surfaces that approximated the shape of ellipsoids. These areas then simulated "pop outs" that had formed in the field. These are shown in Fig. 5. Two ellipsoids were formed with dimensions of approximately 3 in. x 8 in. x 1/2 in. deep, and two were formed with dimensions of approximately 3 in. x 8 in. x 1-1/2 in. deep. They were formed 8 in. long to insure that the beam broke through the resin in the center 6-in. span. The beams were then moist cured for 7 days and air cured for 6 days before patching. The "pop out" areas were then patched with the mix containing 45 parts of Thiokol LP-3 per hundred of Epon 820. After the resin had air cured for 5 days, the patched beams were all broken with the patched area in compression, that is, with the load applied next to the patched surface. Also two smooth ends were mended together from a beam that had previously been used for field flexural tests. The results are shown in Table 2.

The proportions of the two container system containing 45 parts of Thiokol LP-3 per hundred parts of Epon 820 are shown in Table 3(c). The quantity of each of the ingredients per cubic foot of cured resin is shown in Table 3(d).

THIXOTROPIC-TYPE RESIN SYSTEM

The thixotropic resin system was tested for bonding new concrete to old concrete surfaces. It was originally tested to determine its suitability for bonding a freshly placed 10 in. concrete slab to an existing 10 in. concrete pavement. The mix was essentially of the same composition as the liquid resin system containing 40 parts of Thiokol LP-3 per hundred of Epon 820. Sufficient Cab-O-Sil thickening and thixotropic agent was substituted for the limestone filler to optimize the flow properties versus the stress-strain properties.

TABLE 3.—MORTAR-TYPE RESIN SYSTEM

(a) Composition

A:		B:	
Epon 820	100.00 gm.	Thiokol LP-3	X gm.
Mortar sand	260.00	DMP-10	10.00
Cab-O-Sil	8.00	Titanium dioxide	25.00
Lamp black	.02	Cab-O-Sil	2.00

(b) Stress-Strain Properties

Grams of Thiokol LP-3	5-day air cure		
	Approximate peak compressive stress, in psi	Approximate % strain at peak compressive stress	Approximate % strain at compressive stress of 5,000 psi
40	8,800	4.6	2.4
45	7,280	5.6	2.4
50	6,680	6.0	3.2

(c) Proportions

A:		B:	
Epon 820	100.00 gm	Thiokol LP-3	45.00 gm.
Mortar sand	260.00	DMP-10	10.00
Cab-O-Sil[a]	8.00	Titanium dioxide	25.00
Lamp black	.02	Cab-O-Sil	2.00
	368.02 gm		82.00 gm

$\frac{A}{B} = \frac{368.02 \text{ gm}}{82.00 \text{ gm}} = \frac{4.488}{1}$ Specific gravity = 1.8665 $\frac{\text{gm}}{\text{cc}}$

Density = 116.5 lbs per cuf ft

Percentage filler = 65.67%

Specific volume = $\frac{\text{cu ft}}{116.5 \text{ lb}}$ = 0.0086 cu ft per lb

Pot life, limit of workability = 50 plus min

(d) Itemized Quantities

Item	Weight, in grams	Weight, in %	Weight % x density, lb per cu ft	Unit cost $/lb	Cost per cu ft of resin
Epon 820	100.00	22.22	25.89	1.58	$40.91
Mortar sand	260.00	57.78	67.31	0.01	0.67
Cab-O-Sil	10.00	2.22	2.59	1.32	3.42
Lamp black	0.02	0.004	0.005	1.00	0.005
Thiokol LP-3	45.00	10.00	11.65	1.06	12.35
DMP-10	10.00	2.22	2.59	1.82	4.71
Titanium dioxide	25.00	5.56	6.48	0.43	2.79
Totals	450.02	100.004	116.51		64.86

$\$/\text{lb} = \frac{64.86 \ \$/\text{w ft}}{116.5 \ \text{lb}/\text{w ft}} = 0.56 \ \$/\text{lb}$

---

[a] Uncompressed silica.

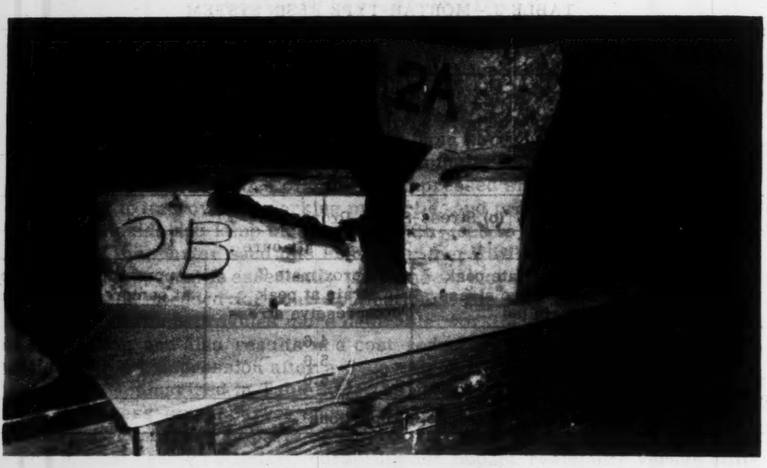

FIG. 5.—SIMULATED "POP OUTS" AFTER REPAIRING AND BREAKING

FIG. 6.—BEAM WITH BREAK BETWEEN TWO PATCHED SECTIONS

The most suitable mixes of this type tested for structural bonding between existing and freshly placed concrete pavement are summarized in Table 4(b). The stress-strain properties were taken from the graph shown in Fig. 2(c).

The mix containing 8 grams or 2.71% of the total mix of Cab-O-Sil thickening and thixotropic agent was deemed the more suitable since it had less tendency to sag and flow when spread 1/8 in. thick on a vertical concrete surface. This is shown in Fig. 7.

The suitability of the material for bonding new concrete to old concrete surfaces was tested by casting freshly mixed concrete next to hardened concrete beams that had been coated with the resin to form a layer approximately 1/8 in. thick. Two beams were cast next to old beams with fractured faces, and one beam was cast next to an old beam with a smooth surface. All the beams, both old and new, contained the same concrete mix. This was one containing 7.8 sacks of high early strength cement and 39 gal of water per cubic yard of concrete. Photographs of the flexural beams are shown in Fig. 7. The beams were patched with the mix containing 2.71% of Cab-O-Sil. The results of the flexural tests are shown in Table 2. As noted in the table the beams were moist cured until tested.

The proportions of the two container system containing 40 parts of Thiokol LP-3 per hundred of Epon 820 and with Cab-O-Sil constituting 2.71% of the total mix are shown in Table 4(c). The quantity of each of the ingredients per cubic foot of cured resin is shown in Table 4(d).

APPLICATION OF EPOXY RESIN FOR STRUCTURAL CONCRETE PAVEMENT REPAIR

The structural defects in concrete pavement consisted, for the most part, of either vertical cracks (Fig. 1), that usually occurred near a sawed contraction joint and effectively extended through the width and depth of the pavement, or surface defects of various sizes. These were usually either aggregate "pop outs" or torn areas that were the result of the joint sawing operation.

One method of repairing the vertical cracks consisted of removing a section of pavement extending for a distance of 5 ft from the sawed joint, after which a new section was placed with a joint being provided between the new and old pavement. The joint was subsequently filled with epoxy resin to bond one end of the new slab to the existing pavement. The other end of the new section was cast next to the old concrete with the fractured face of the pavement furnishing the necessary interlock for load transfer across the joint thus formed. The application of the resin is shown in Fig. 8. The resin was mixed in 35-lb batches. During this particular application the weather was wet and cool with an average temperature of approximately 40° F and an average relative humidity of approximately 95% and with intermittent precipitation. The joint was dried with a blow torch and heated slightly before pouring the resin. The resin will reportedly form a good bond through only a very thin water film. To conserve material and to provide heat other than that caused by the reaction, the joint was poured approximately one-half full of resin after which it was displaced with warm 1/2 in. to No. 4 concrete aggregate to the pavement surface. After the resin had set, the joint was troweled to grade with the thixotropic resin system, if this were necessary. The procedure was an emergency expedient and expensive. It is elaborated upon because it illustrates an unusual resin application. A better method consisted of applying the thixotopic type resin system to the existing slab before placing the new slab. The resin then cured as the concrete set.

TABLE 4.—THIXOTROPIC-TYPE RESIN SYSTEM

(a) Composition

A:		B:	
Epon 820	100.00 gm	Thiokol LP-3	40.00 gm
Cab-O-Sil	X	Titanium dioxide	25.00
Limestone filler	112.0	DMP-10	10.00
		Lamp black	.02

(b) Stress-Strain Properties

Grams of Cab-O-Sil	5-day air cure		
	Approximate peak compressive stress, in psi	Approximate % strain at peak compressive stress	Approximate % strain at compressive stress of 5,000 psi
7 (2.37% of total mix)	9,000	8.0	2.9
8 (2.71% of total mix)	7,120	7.0	3.2
15 (5.08% of total mix)	5,600	6.0	3.8

(c) Proportions

A:		B:	
Epon 820	100.00 gm	Thiokol LP-3	40.00 gm
Limestone filler	112.00	DMP-10	10.00
Cab-O-Sil	8.00	Titanium dioxide	25.00
	220.00 gm	Lamp black	0.02
			75.02 gm

$$\frac{A}{B} = \frac{220.00\ \text{gm}}{75.02\ \text{gm}} = \frac{2.9326}{1} \qquad \text{Specific gravity} = 1.562\ \frac{\text{gm}}{\text{cc}}$$

Density = 97.469 lb per cu ft

Percentage filler = 49.16%

Percentage Cab-O-Sil thixotropic agent = 2.71%

$$\text{Specific volume} = \frac{\text{cu ft}}{99.467\ \text{lb}} = 0.010\ \frac{\text{cu ft}}{\text{lb}}$$

Pot life, limit of applicability to vertical surface = 1 1/2 plus hr

(d) Itemized Quantities

Item	Weight, in grams	Weight, in %	Weight % x density, lb per cu ft	Unit cost $/lb	Cost per cu ft of resin
Epon 820	100.00	33.90	33.04	1.58	$52.20
Cab-O-Sil	8.00	2.71	2.64	1.32	3.48
Limestone filler	112.00	37.97	37.00	.01	.37
Thiokol LP-3	40.00	13.56	13.22	1.06	14.01
Titanium dioxide	25.00	8.47	8.26	.43	3.55
DMP-10	10.00	3.39	3.30	1.82	6.01
Lamp black	.02	.007	.007	1.00	.007
Totals	295.02	100.007	99.467		79.63

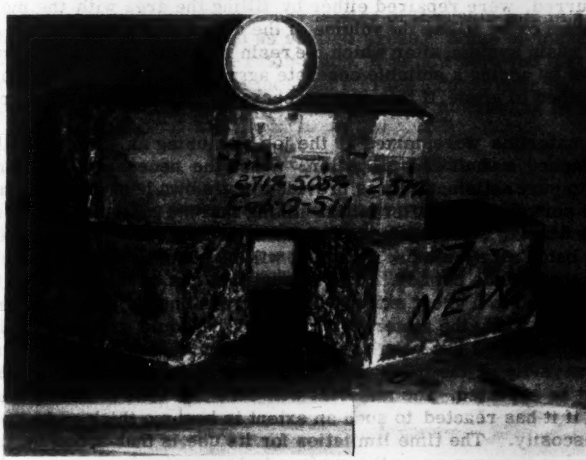
2717-5087
2376
Cal-0-511
NEW

FIG. 7.—OLD AND NEW CONCRETE THAT HAD BEEN BONDED WITH THIXOTROPIC-TYPE RESIN SYSTEM

FIG. 8.—JOINING TWO EXISTING SLABS

The surface defects, such as torn areas or areas in which aggregate "pop outs" had occurred, were repaired either by filling the area with the mortar type resin system or by filling the volume of the defective area about one-half with the liquid resin system, after which the resin was displaced to the surface of the pavement by adding a suitable concrete aggregate. Finally the repaired area was smoothed to grade, if this were necessary, with the thixotropic resin system.

The resin materials were mixed at the job site using an electric drill to which was attached a shaft and propeller. Since the necessary heat for the resin system to cure satisfactorily is provided by its own heat of reaction, the pot life, or the period of time after initial mixing that the material can be utilized, will depend on the amount mixed. For the same surrounding temperature, the larger the batch size the more heat that will be generated by the reaction and hence the shorter the pot life. The amount that can be mixed at one time will therefore depend to a great extent on the surrounding air temperature and on how soon after mixing the material is placed. The liquid system containing 40 parts of Thiokol LP-3 has been used in 35-lb batches as previously mentioned. The severity of the batch size limitation is therefore not nearly as great as might be expected. The material will cure and bond to nearly its full strength even if it has reacted to such an extent to become thick or to greatly increase in viscosity. The time limitation for its use is that it can be satisfactorily placed in the area or on the surface to be repaired.

The resin materials, especially the Epon 820 and DMP-10, should be regarded as strong skin irritants. They should be mixed in good ventilation. Neither the materials nor the fumes should be allowed to come into contact with the skin or clothing.

Cores were taken through the joints that were filled with the liquid resin and through the joints between the old and new concrete where thixotropic-type resin was used. Visual examination of these cores indicated that an excellent job had been obtained, there was no evidence in any of the cores of bond failure. In one core from a poured joint there was evidence of what must have been a loose piece of concrete that had not been removed from the edge of the old pavement. However, the resin had penetrated the crack and completely surrounded the loose particle so that in the core it was firmly bonded in place.

Four cores from the poured type of joints and two cores from the joints where new concrete was placed directly against the resin were sent to the Ohio River Division Laboratory of the Corps of Engineers for testing. Corresponding cores were taken within 5 ft of the joint at each location and these were also shipped to the laboratory for testing. All cores were subjected to the tensile splitting test as described in a paper by Sven Thaulow entitled "Tensile Splitting Test and High Strength Concrete Test Cylinders" published in the American Concrete Institute Journal, Jan., 1957. Three of the four cores from the poured joints had higher tensile splitting strength than the corresponding cores from the concrete near the joint. The fourth core had a tensile splitting strength of 70 psi less than its corresponding core. One of the two cores taken from joints where the new concrete was placed directly against the resin had a tensile splitting strength of 80 psi more than the corresponding core from concrete near the joint, while the other core had a tensile splitting strength of 50 psi less than its corresponding core.

The pavement was placed in service 7 days after being repaired. This was in the late fall. The pavement was in service during the winter months. The following spring, approximately 4 months after being repaired, an inspection was made of the repaired areas. The repaired joints were functioning satisfactorily. The only evidence of any failure of the resin was in a few small sections that had been repaired as spalled areas. Some of these showed a bond failure along the edge of the resin patch. It is now believed that these locations were not only spalls but also included a crack located near the saw-cut and the edge of the spall. These cracks were probably functioning as active joints.

ACKNOWLEDGMENTS

The tests herein described were conducted by the North Central Division of the Army Corps of Engineers. The permission granted by the Chief of Engineers to publish this information is appreciated.

AMERICAN SOCIETY OF CIVIL ENGINEERS
Founded November 5, 1852
TRANSACTIONS

Paper No. 3122

MINIMUM COST DESIGN OF LARGE SUPPORT RINGS

By Kenneth P. Buchert,[1] F. ASCE

SYNOPSIS

There is suggested a method of design for large support rings. The method proposes that the outer flange plate of the ring can be eliminated on various sections of the ring without materially affecting the ring stresses. Significant savings in the fabrication cost of the ring can thus be realized.

INTRODUCTION

Support rings of the type shown in Fig. 1 have been used extensively in recent years to support the weight of penstocks, tanks, large ducts, wind tunnels, and other structures.

Herman Schorer has presented[2] a method for the design of supports for large pipelines. The method proposed was to use a constant-moment-of-inertia support ring welded to the shell, which, in turn, was supported at the ends of its horizontal diameter to support the pipe. In recent years, larger and larger lines have been designed and built, many using support rings. These rings often consist of a web member welded to the shell and a flange member welded to the web. For relatively small pipes, sometimes the flange member has been eliminated and only a web member is used. For very large pipes or ducts, double, triple, and sometimes quadruple webs and multiple flanges have

---

Note.—Published essentially as printed here, in May, 1960, in the Journal of the Structural Division, as Proceedings Paper 2473. Positions and titles given are those in effect when the paper or discussion was approved for publication in Transactions.

[1] Genl. Supervisor, Design Engrg., Consol. Western Steel Div., U. S. Steel Corp., Los Angeles, Calif.

[2] "Design of Large Pipe Lines," by Herman Schorer, Transactions, ASCE, Vol. 98, 1933, pp. 101-191.

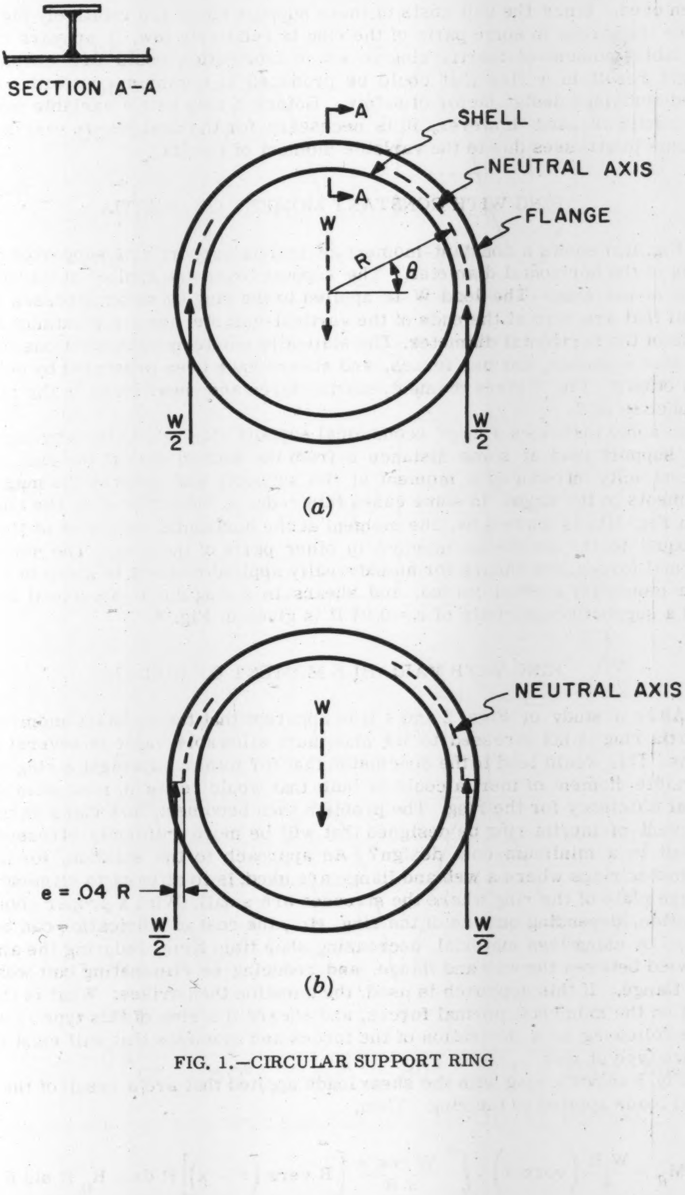
SECTION A-A
A
A
SHELL
NEUTRAL AXIS
FLANGE
W
R
θ
W/2
W/2
(a)
NEUTRAL AXIS
W
e = .04 R
W/2
W/2
(b)

FIG. 1.—CIRCULAR SUPPORT RING

been used. Since the unit costs of these support rings are relatively high and since the stress in some parts of the ring is relatively low, it appears that a variable-moment-of-inertia ring in which fabrication costs are considered might result in a ring that could be produced at minimum cost with a given predetermined design factor of safety. Before a ring with a variable moment of inertia is used, however, it is necessary for the designer to evaluate the change in stresses due to the variable moment of inertia.

RING WITH CONSTANT MOMENT OF INERTIA

Fig. 1(a) shows a constant-moment-of-inertia support ring supported at the ends of the horizontal diameter. The support loads are applied at the neutral axis of the ring. The load W is applied to the ring by shear stresses in the shell that are zero at the ends of the vertical diameter and are maximum at the ends of the horizontal diameter. The statically indeterminate solutions for the bending moments, normal forces, and shears have been presented by Schorer and others. Fig. 2 gives moment, normal force and shear force in the ring as a function of θ.

In some instances a more economical support ring can be built by applying the support load at some distance e from the neutral axis of the ring. This eccentricity introduces a moment at the supports and reduces the maximum moments in the rings. In some cases this reduces the stresses in the ring. If e in Fig. 1(b) is made 0.04, the moment at the horizontal diameter of the ring is equal to the maximum moment in other parts of the ring. The moments, normal forces, and shears for an externally applied moment is given in Fig. 3. The moments, normal forces, and shears in a ring due to a vertical load W and a support eccentricity of e = 0.04 R is given in Fig. 4.

RING WITH VARIABLE MOMENT OF INERTIA

After a study of Figs. 2 and 4 it is apparent that the constant-moment-of-inertia ring is not stressed to its maximum allowable value in several locations. This would lead to the conclusion that for minimum weight a ring with a variable moment of inertia could be built that would result in maximum structural efficiency for the ring. The problem then becomes: How can a variable-moment-of-inertia ring be designed that will be more uniformly stressed and result in a minimum-cost design? An approach to the solution, for large-diameter rings where a web and flange are used, is to attempt to eliminate the flange plate of the ring where the stresses are small. With a proper choice of location, depending on size of the ring, etc., the cost of fabrication can be reduced by using less material, decreasing shop fitup time, reducing the amount of weld between the web and flange, and reducing or eliminating butt welds in the flange. If this approach is used, the question then arises: What is the effect on the moments, normal forces, and shears if a ring of this type is used? The following is a derivation of the forces and moments that will exist in the above type of ring.

Fig. 5 shows a ring with the shear loads applied that are a result of the vertical loads applied to the ring. Then,

$$M_\theta = \frac{W\,R}{4}\left(\text{vers}\ \theta\right) - \int_0^\theta \frac{W \cos x}{\pi R}\left[R\ \text{vers}\left(\theta - x\right)\right] R\,dx - H_0\,R \sin\theta\ .\ .\ (1)$$

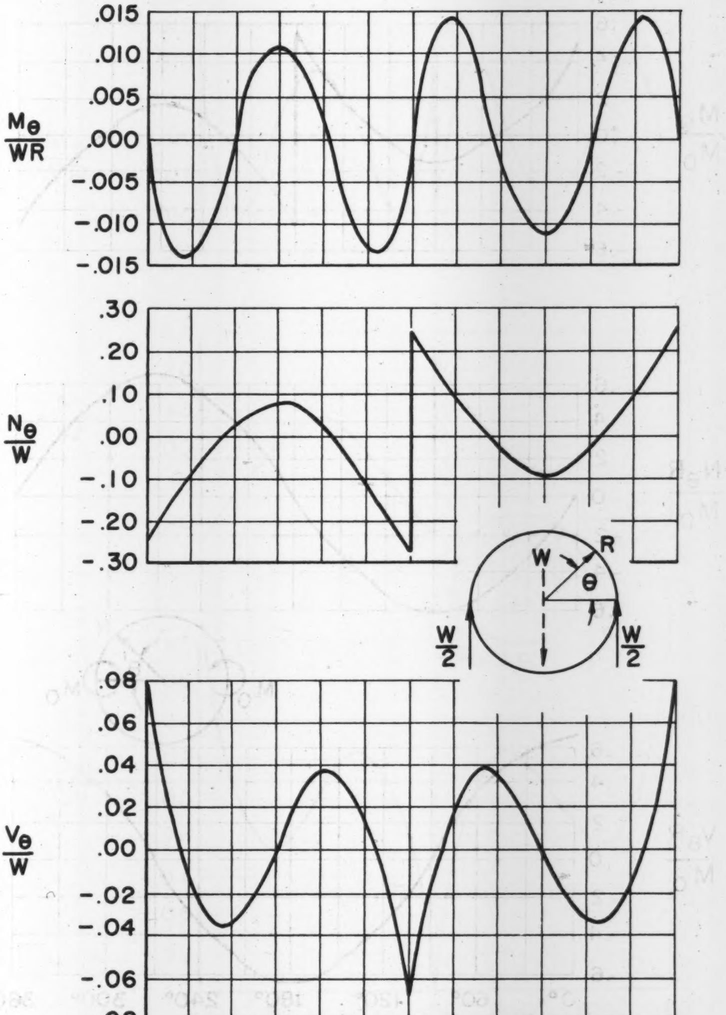

FIG. 2.—SUPPORT RING WITH SUPPORT LOAD APPLIED AT NEUTRAL AXIS

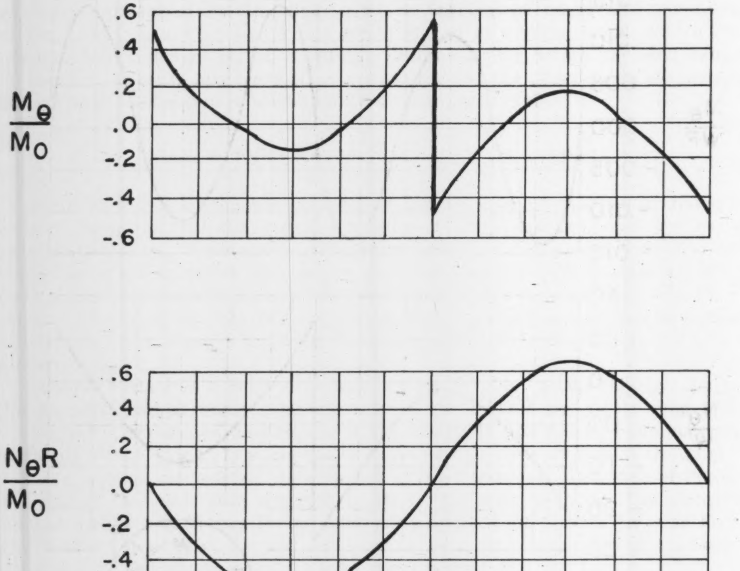

FIG. 3.—SUPPORT RING WITH APPLIED EXTERNAL MOMENT AT EXTREMETIES OF A HORIZONTAL DIAMETER.

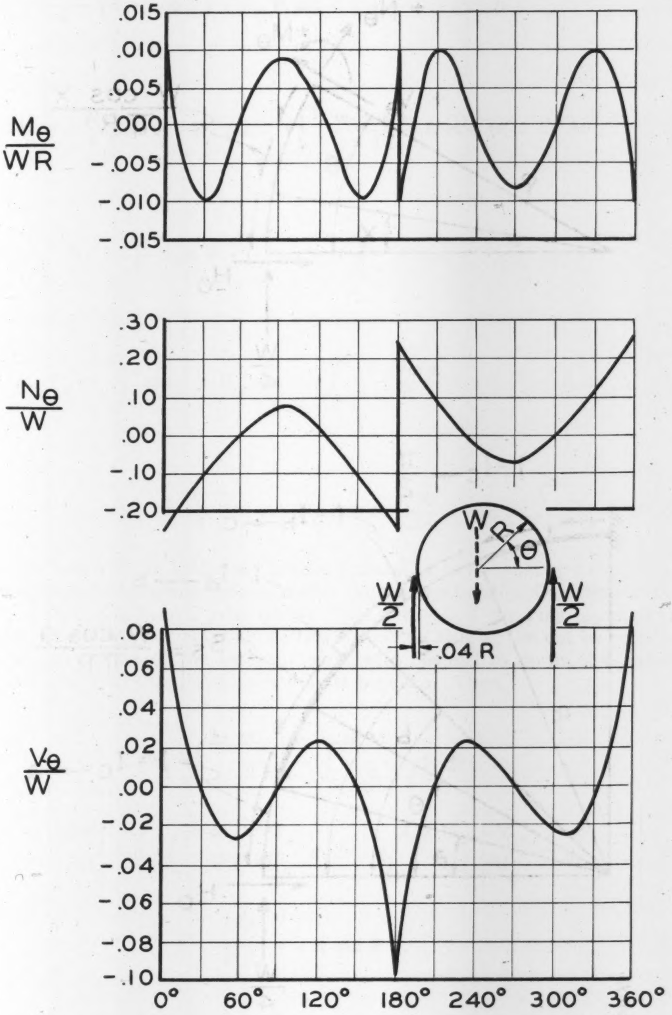

FIG. 4.—SUPPORT RING WITH SUPPORT LOAD APPLIED ECCENTRIC TO NEUTRAL AXIS

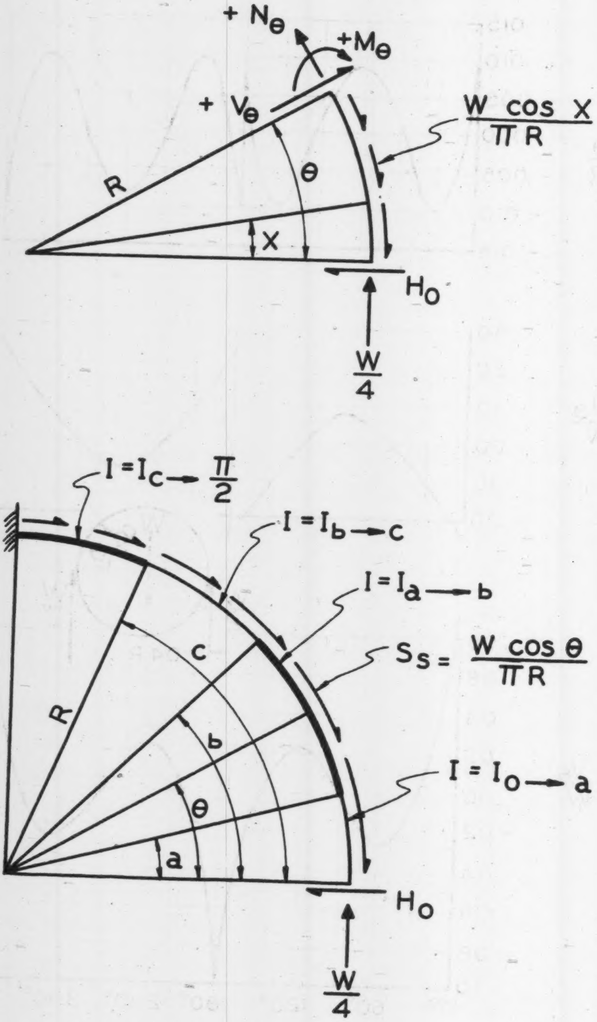
+ N_θ
+M_θ
+ V_θ
$\frac{W \cos X}{\pi R}$
R
θ
X
H_o
$\frac{W}{4}$
$I = I_c \to \frac{\pi}{2}$
$I = I_b \to c$
$I = I_a \to b$
$S_s = \frac{W \cos \theta}{\pi R}$
c
R
b
θ
a
$I = I_o \to a$
H_o
$\frac{W}{4}$

FIG. 5.—SUPPORT RING WITH APPLIED LOADS

or

$$M_\theta = \frac{W R}{4}\left(1 - \cos\theta\right) - H_0 R \sin\theta + \frac{W R}{2\pi} \theta \cos\theta - \frac{W R}{\pi} \frac{\sin\theta}{2} \quad . . (2)$$

and

$$N_\theta = - \frac{W}{4} \cos\theta - H_0 \sin\theta + \int_0^\theta \frac{W \cos x}{\pi R} R \cos(\theta - x)\, dx \quad . . . . . (3)$$

or

$$N_\theta = -\frac{W}{4} \cos\theta - H_0 \sin\theta + \frac{W}{2\pi} \theta \cos\theta + \frac{W}{2\pi} \sin\theta \quad . . . . . (4)$$

and

$$V_\theta = -\frac{W}{4} \sin\theta + H_0 \cos\theta + \int_0^\theta \frac{W \cos x}{\pi R} R \sin(\theta - x)\, dx \quad . . . . (5)$$

or

$$V_\theta = - \frac{W}{4} \sin\theta + H_0 \cos\theta + \frac{W}{2\pi} \theta \sin\theta \quad . . . . (6)$$

Since the force H_0 is statically indeterminate, it is necessary to apply one of the principles of indeterminate structures to solve for H_0. One method that can be used is Cantigliano's principle of least action. If the ring is cut at the horizontal diameter, the relative deflection of the ring at the cut is zero, or the partial derivative of the internal work with respect to H_0 must equal the relative deflection at this point, hence must be zero. Then,

$$W_i = \int_0^{2\pi} \frac{M_\theta^{\ 2}\, ds}{2 E I} \int_0^{2\pi} \frac{M_\theta^{\ 2}}{2 E I} R\, d\theta \quad . . . . (7)$$

$$\frac{\partial W_i}{\partial H_0} = 0 = \int_0^{2\pi} \frac{M_\theta}{E I} \frac{\partial M_\theta}{\partial H_0} R\, d\theta = 4\int_0^{\pi/2} \frac{M_\theta}{E I} \frac{\partial M_\theta}{\partial H_0} R\, d\theta \quad . . . . (8)$$

$$\frac{\partial M_\theta}{\partial H_0} = - R \sin\theta \quad . . . . (9)$$

$$\frac{\partial W_i}{\partial H_0} = 0 = \int_{0,a,b,c}^{a,b,c,\pi/2} \left[\frac{W}{4\,I} (1 - \cos\theta) - \frac{H_0}{I} \sin\theta + \frac{W}{2\,\pi\,I}\,\theta \cos\theta - \frac{W}{2\,\pi\,I} \sin\theta \right] \sin\theta \, d\theta = \left\{ \frac{W}{4\,I} (-\cos\theta) - \frac{W}{4\,I} \left(\frac{\sin^2\theta}{2} \right) - \left(\frac{H_0}{I} + \frac{W}{2\,\pi\,I} \right) \left(\frac{\theta}{2} - \frac{\sin\theta \cos\theta}{2} \right) + \frac{W}{16\,\pi\,I} (\sin 2\,\theta - 2\,\theta \cos 2\,\theta) \right\}_{0,a,b,c}^{a,b,c,\pi/2} \ldots\ldots\ldots\ldots (10)$$

in which I is considered to be different from $\theta = 0$ to a, $\theta =$ a to b, etc. For this particular solution I is constant from $\theta = 0$ to a, $\theta =$ a to b, etc.

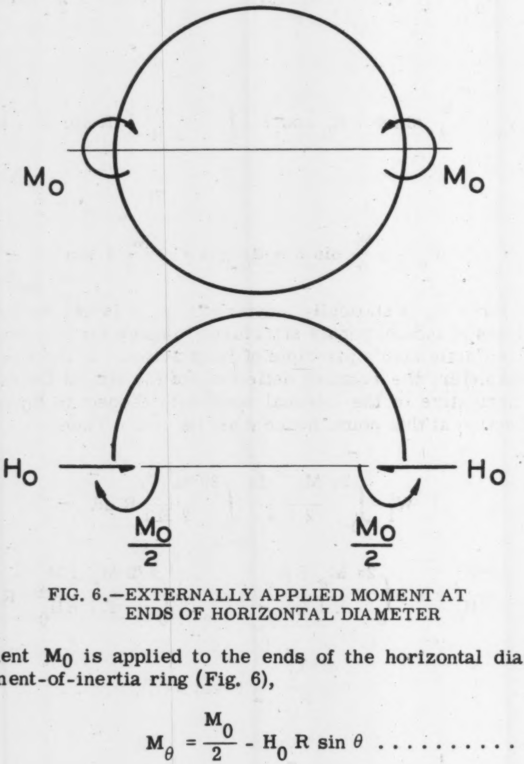

FIG. 6.—EXTERNALLY APPLIED MOMENT AT ENDS OF HORIZONTAL DIAMETER

If a moment M_0 is applied to the ends of the horizontal diameter of a variable-moment-of-inertia ring (Fig. 6),

$$M_\theta = \frac{M_0}{2} - H_0 R \sin\theta \ldots\ldots\ldots\ldots\ldots (11)$$

$$\frac{\partial W_i}{\partial H_0} = 0 = \int_0^{2\pi} \frac{M_\theta^{\,2}\, ds}{2\,E\,I} = \int_0^{2\pi} \frac{M_\theta}{E\,I} \frac{\partial M_\theta}{\partial H_\theta} R \, d\theta \ldots\ldots\ldots (12)$$

$$\frac{\partial M_\theta}{\partial H_0} = - R \sin \theta \quad \ldots\ldots\ldots\ldots\ldots\ldots \quad (13)$$

$$\frac{\partial W_i}{\partial H_0} = 0 = 4\int_0^{\pi/2} \frac{1}{I}\left(\frac{M_0}{2} - H_0 R \sin \theta\right) R \sin \theta \; d\theta$$

$$= \left\{ \frac{1}{I}\left[\frac{M_0}{2}\,(- \cos \theta) - H_0 R \left(\frac{\theta}{2} - \frac{\sin \theta \cos \theta}{2}\right)\right]\right\}_{0,a,b,c}^{a,b,c,\pi/2} \quad \ldots \quad (14)$$

in which I is a variable as before.

COMPARISON OF FORCES AND MOMENTS

With the basic equations derived previously, it is possible to determine the effect on the moments, normal forces, and shears of varying the geometry of the ring. After examining Fig. 2 and 4, an arbitrary selection of ring geometry was made as follows:

$$a = 5^0,\ b = 50^0,\ \text{and}\ c = 65^0$$

The value of H_0 for these values of a, b, and c and for ratios of moments of inertia of the ring, with a flange and without a flange, of 1, 3, and 6 were calculated. The results are as follows:

Ratio of Moment of Inertia	Value of H_0
1	0.07958 W
3	0.07964 W
6	0.07967 W

Since the values of H_0 are so nearly alike, the values of the moments, normal forces, and shears will be, for practical design purposes, the same for the ratios of moments of inertia given.

PARTIALLY FILLED PIPE

In some cases support rings are designed relatively close together and the pipe carries a fluid whose specific gravity is significant. In such cases it is sometimes necessary to investigate the stresses in a ring under partially full conditions because the stresses for the partially full condition sometimes exceed those for the full or full and pressurized condition. The basic equations for this condition were summarized by Schorer.[2] It should be noted in the equations that follow that the stresses in a ring under the half-full condition are considerably less when the eccentricity of the supports is zero than when eccentricity exists. Therefore, the designer must carefully evaluate whether or not to build eccentricity into the ring. Schorer gave the following conservative formulas for the half-full condition (the notation used has been changed to conform to that of the writer):

$$M = \frac{W}{2}\frac{R}{\pi}\left[\frac{2\,r}{\pi\,R} - \frac{\pi}{4}\left(1 + \frac{e}{r}\right) + \left(\frac{5}{4} - \frac{r}{R} + \frac{e}{R}\right)\sin\theta\right] \quad \ldots\ldots\ (15)$$

for the upper quadrants of the ring where W is the load assuming a full pipe and

$$M = \frac{W}{2}\ \frac{R}{\pi}\left[\frac{2\,r}{\pi\,R} + \frac{\pi}{4}\left(1 + \frac{e}{R}\right) + \left(\frac{1}{4} + \frac{r}{R} + \frac{e}{R}\right)\sin\theta + \left(\frac{3\,\pi}{2} - \theta\right)\cos\theta\right] \quad \ldots\ (16)$$

for the lower quadrants. It should be pointed out that the foregoing results are conservative; the normal force in the ring is only one-half of that for a full pipe, and the direct stress due to pressure is zero.

EXAMPLE

The following will illustrate one method of how a variable-moment-of-inertia ring could result in cost savings:

Design Criteria
Diameter of Duct = 18 ft
Thickness of Pipe = 5/8 in.
Load on Support Ring = 400 kips
Design Pressure = 42 psig
Service = Air
Allowable Stress in Ring = 12,650 psi = $\frac{P}{A} + \frac{N_\theta}{A} + \frac{M_\theta C}{I}$
Allowable Length of Shell Acting with Ring = 0.78 $\sqrt{r\,t}$ on each side of web of ring

Consider a ring similar in detail to that shown in Fig. 1 with a $\frac{1}{2}$ in. by 12 in. web and a $\frac{1}{2}$ in. by 10 in. flange and with the eccentricity of the supports zero. The section properties of the ring will be A = 19.3 in.^{2}, I = 579.in.^{4}, c_o = 7.33 in., and c_i = 5.80 in. where c_o and c_i are the distances from the neutral axis to the outside of the ring and to the inside of the ring, respectively. Fig. 7(a) gives the stresses on the outer and inner flanges of the ring. Note that the stresses are high in only two places in the ring.

Consider the possibility of removing the $\frac{1}{2}$ in. by 12 in. flange plate in the region of $\theta = 0^0$ to 5^0, $\theta = 50^0$ to 55^0, etc., around the ring. The properties of the ring where the flange is removed are A = 14.3 in.^{2}, I = 213 in.^{4}, c_o = 9.31 in., and c_i = 3.32 in. Since the stresses are relatively high in the region of $\theta = 0$ to -5^0 and $\theta = 180^0$ to 185^0, the flange should not be removed in this area or the details of the support connection should reinforce this portion of the ring. The resulting ring will not be symmetrical about the horizontal axis and, therefore, is not exactly the same as the ring that was analyzed previously. However, the same conclusions regarding the relatively constant value of H_0 will apply in this case. One method of qualitatively justifying this conclusion is that those portions of the ring that contribute very little to the total work done by the internal stresses in the ring can be changed considerably without a significant effect on the value of H_0. Using this reasoning, the value

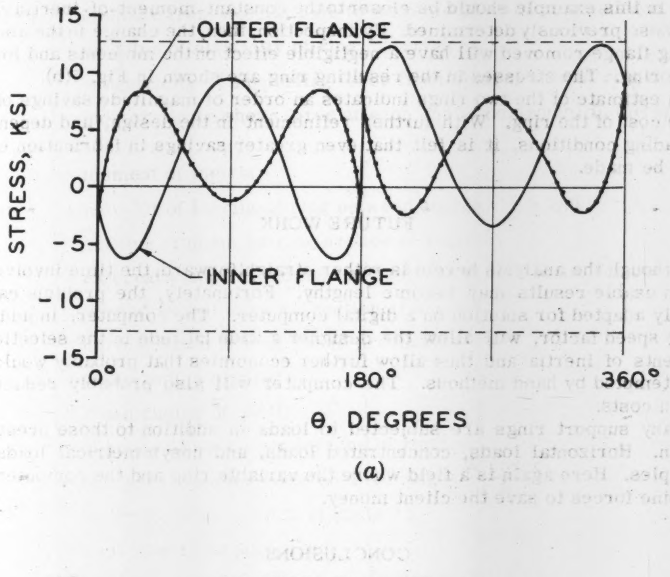

FIG. 7.—STRESSES IN SUPPORT RING

of H_0 in this example should be closer to the constant-moment-of-inertia value than those previously determined. By inspection, then, the change in the amount of ring flange removed will have a negligible effect on the moments and forces in the ring. The stresses in the resulting ring are shown in Fig. 7(b).

An estimate of the two rings indicates an order of magnitude savings of 10% in the cost of the ring. With further refinement in the design, and depending on loading conditions, it is felt that even greater savings in fabrication costs could be made.

FUTURE WORK

Although the analysis herein is rather straightforward, the time involved to obtain usable results may become lengthy. Fortunately, the problem can be readily adapted for solution on a digital computer. The computer, in addition to the speed factor, will allow the designer a wide latitude in the selection of moments of inertia and thus allow further economies that probably would not be attempted by hand methods. The computer will also probably reduce the design costs.

Many support rings are subjected to loads in addition to those presented herein. Horizontal loads, concentrated loads, and unsymmetrical loads are examples. Here again is a field where the variable ring and the computer can combine forces to save the client money.

CONCLUSIONS

A method has been presented which can be used to obtain more economical designs of support rings for large pipe or ducting. It is found that by eliminating the flange in large rings a significant savings will result in the cost of fabrication of the ring, and the stresses in the ring will be within predetermined allowable values. By a judicious choice of places where the flanges are eliminated, it is possible to use the same design moments, normal forces, and shears in the ring as would be used with a constant moment of inertia ring. It appears possible by the use of digital computers to obtain still further economies in the design of support rings and also to analyze many conditions or combinations of loading.

ACKNOWLEDGMENTS

The writer wishes to acknowledge his indebtedness to John A. Dosier for checking the equations and calculations and to those people in the United States Steel Corporation who presented suggestions during the preparation of this paper.

APPENDIX.—NOTATION

The following notation has been used in this paper:

A = cross-sectional area of ring and effective portion of shell;

a, b, c = angles between horizontal axis of ring and point on ring where moment of inertia changes;

c_o or c_i = distance from neutral axis to extreme fiber of ring section;
E = modulus of elasticity of ring material;
e = eccentricity of supporting force from neutral axis of ring section;
H_0 = indeterminate shear force at each end of horizontal diameter (Fig. 5);
I = moment of inertia;
$I_{a \rightarrow b}$ = moment of inertia of ring between angles $\theta = a$ and $\theta = b$;
M_θ = bending moment on ring section at angle θ;
M_0 = externally applied moment at each end of horizontal diameter;
N_θ = normal (hoop) force on section at angle θ;
P = normal force in ring due to pressure;
R = mean radius of ring;
r = mean radius of shell;
s = distance along circumference of ring;
S_s = unit shear loading from shell to ring = $\frac{W \cos x}{\pi R}$;
V_θ = shear force on section at angle θ;
W = total load to be supported;
W_i = internal strain energy of ring under load;
x = angle between horizontal diameter and point on ring; and
θ = angular location of section under analysis.

AMERICAN SOCIETY OF CIVIL ENGINEERS
Founded November 5, 1852
TRANSACTIONS

Paper No. 3123

RATIONALE FOR DETERMINING DESIGN WIND VELOCITIES

By A. G. Davenport[1]

SYNOPSIS

This paper first justifies the use of the "extreme wind velocity averaged over a mile or minute" as a "basic design wind velocity" in preference to absolute peak velocities which cannot be considered independently of the size of the structure, and of the dynamic response of anemometer, structure, and structural materials.

An attempt is, then, made to show from published records that reasonably systematic relationships exist between the ground roughness (as characterized by such general qualitative descriptions as "city," "treed countryside," and "open prairie") and both the magnitude of the extreme wind velocities near the ground and its rate of increase with height. This allows approximate estimates of the ratio of surface velocity to gradient velocity to be made. By these means, independent sets of anemometer records taken at locations differing in surface roughness can be compared.

By further introducing the extreme value theory a method is suggested whereby these sets of records may be numerically related taking into account the relative ground roughness, the number of years of record, the quality and consistency of the records, and the height of the anemometer. This process assists in minimizing the systematic errors which are often introduced into individual anemometer records.

Some published extreme-value data for the British Isles are analyzed according to the described procedure and an example is given illustrating how design wind velocities can be determined in a manner which takes into account

---

Note.—Published essentially as printed here, in May, 1960, in the Journal of the Structural Division, as Proceedings Paper 2475. Positions and titles given are those in effect when the paper or discussion was approved for publication in Transactions.

[1] Univ. of Bristol, England, formerly with the Div. of Bldg. Research, Natl. Research Council, Ottawa, Canada.

the important influence of surface roughness, the variability of useful life of different structures, and the risks involved if the wind velocity is exceeded.

INTRODUCTION

One of the principal loads acting on above-ground engineering structures is that due to the wind. Its accurate determination, therefore, is of fundamental importance in deciding what degree of safety and economy can be achieved in such a structure.

Formerly, it was common practice to design structures to resist the highest wind ever recorded by the instruments then in use. Although this did provide a sort of yardstick from which design wind loads could be estimated, it was unreliable and subject to the difficulty that most meteorological records will eventually be broken. A longer period of record increased the chances of recording a very high wind velocity. Another problem was that instruments which responded rapidly to fluctuations in wind speed tended to indicate higher velocities than those which were more sluggish. In other known instances, the highest wind had unfortunately blown away the instrument and the crucial information was lost.

All these difficulties tended to throw the problem of determining design wind velocities into the lap of the statistician who, from the records of several years, could estimate the probability of a given wind velocity recurring. Such are the vagaries of climate that the structural engineer can never hope for information much more certain than this.

Further problems emerge from other considerations. Because the velocity of the wind is continually fluctuating, recorded peak velocities will depend largely on the sensitivity of the anemometer. The pressures exerted on a structure will also fluctuate, leading to dynamic amplification of the actual stresses in the structure. This dynamic amplification, as well as being dependent on the intensity and power of the fluctuations, will also depend on the size and shape of the structure (as they will determine the rate of build-up of gust pressures) and on the response of the structure and its constituent materials to dynamically applied loads. The dynamic amplification will vary, therefore, with the size and flexibility of the structure.

For these reasons, wind loads are perhaps best considered in terms of a steady, applied force, independent of the structure's shape, size, and dynamic characteristics, together with a coefficient denoting the amplification which can arise through the interaction of the superimposed pressure fluctuations and the structure's dynamic response. The resolving of this coefficient, however, which is similar in many respects to the "earthquake problem," is not discussed herein.

This paper is confined to the determination of what will be termed the basic design wind velocity, which corresponds to the extreme sustained wind velocity giving rise to the steady component of the pressure. It is, therefore, an average velocity and the determination of a suitable averaging interval forms part of this discussion.

An attempt is made, also, to determine how records from a wide variety of anemometers of differing exposures and periods of record may be related to one another, thereby minimizing the systematic errors which may arise in the records due to anemometer siting and to the improvement of their overall reliability. This requires that cognizance be taken of the important influence of surface roughness both on the magnitude of the surface velocities and on the increase of velocity with height. Combining these results with the extreme-value theory leads to an exploratory method through which basic design wind velocities of given probability of occurrence may be predicted for locations of differing surface roughness.

STRUCTURE OF NATURAL WIND

The wind is caused by the atmospheric pressure differentials which rise over the surface of the earth. The acceleration produced by these pressure differentials is accompanied by other components of acceleration known as the geostrophic acceleration, due to the curvature and rotation of the earth, and the centripetal acceleration. The resultant of these accelerations produces a motion in the free air, unaffected by friction near the surface, which is parallel to the lines of equal barometric pressure (known as isobars). The velocity of the free air is known as the gradient velocity.

Under steady state conditions the gradient velocity can be determined directly if the latitude, the radius of curvature of the isobars, and the pressure gradient (or spacing of the isobars) are known (1).[2] For zones of cyclonic winds (associated with a low pressure system and with storms and high winds) the gradient velocity V_G is given by

$$V_G = r\,w \sin\lambda \left[\sqrt{\frac{\frac{dp}{dN}}{\rho\, r\, w^2 \quad \sin^2 \lambda} + 1} \;-\; 1 \right] \quad . \; . \; . \; . \; . \; . \; . \; . \; (1)$$

in which r is the radius of curvature of isobars, w denotes the rotational speed of the earth; λ is the latitude, dp/dN represents the pressure gradient, and ρ is the density of the air. Eq. 1 lends itself ideally to simple nomographic solution, as shown by W. J. Humphreys (1), and the gradient velocity may be estimated directly from isobar charts. Accurate estimates of gradient velocity, however, are difficult to obtain unless the grid of meteorological stations measuring surface pressures is close.

The velocity of the gradient wind is, however, attained only at heights around 1,000 ft to 2,000 ft above the ground. Closer to the ground, the wind is retarded by the frictional forces and obstructions at the surface and the virtual stresses produced by the vertical exchange of momentum by turbulence; its direction, then, is no longer parallel to the isobars. Turbulence also causes rapid fluctuations in the velocity of a wide range of frequencies and amplitudes. The velocity of the wind at lower levels, therefore, is usefully expressed in terms of its mean speed and the deviations from this velocity.

The time or distance interval over which the mean is averaged depends on the purpose for which the wind velocity is to be used.

Choice of a Suitable Averaging Interval.—In determining basic wind velocities for the design of structures certain fundamental considerations determine what averaging interval is most appropriate. These may be stated as follows:

1. The interval should coincide, as far as possible, with some natural periodicity of the wind.

---

[2] Numerals in parentheses refer to corresponding items in Appendix I.

2. The interval should be "long" compared to both (a) the natural frequency of the structure, and (b) the response time of the instrument; in this way there will be no dynamic interaction between the structure and fluctuations in the mean wind; measured wind velocities will be independent of the instruments response.

3. The interval should be short enough to record the "peaks" of severe storms.

4. The interval should correspond to a body of air of sufficient size to envelop completely a structure and its vortex regions.

The "mile of wind" or the "minute of wind" both represent suitable, if not optimum, intervals for measuring high-wind velocities for purposes of structural design. Both these intervals satisfy the foregoing conditions for reasons now discussed:

1. By means of auto-correlation coefficients, Durst (2) found that in storm winds a major group of eddies, thermal in origin, had a wavelength of about 4,000 ft to 6,000 ft, corresponding closely to the mile interval or the minute interval in winds of 60 mph.

2. a. The natural period of most structures is of the order of 0.1 sec to 3 sec (3), with that for the Empire State Building of 8.14 sec (4). With the damping present in most structures, fluctuations corresponding to one mile in extreme winds would have infinitesimal dynamic action.

b. R. H. Sherlock and M. B. Stout (5), referring to the response time of commercial anemometers, wrote in 1937, "that because of the inertia of moving parts of the instruments the records could only be accepted as accurate if they were averaged over 10 seconds or more." Thus, even at 150 mph, the mile of wind (or the minute of wind) satisfies the second requirement.

3. The mile of wind also represents a body of air far larger than most structures, so that static pressures at least equivalent to this average speed can be anticipated.

4. The mile of wind will be of sufficiently short duration to record the peak of a sudden severe local thunderstorm or squall.

These arguments, justifying the use of the extreme mile or minute of wind as basic design velocities, are endorsed further in that the mile of wind has been recommended for use in the United States (where records are available for many years) as the basis for design wind velocities and the minute of wind in the British Isles.[3]

Increase of Velocity with Height: Influence of Surface Roughness and Stability.—One of the most important factors to be considered is the increase of this mean wind velocity with height; a corollary to this is the retarding effect of the surface friction on the wind velocity nearer the surface.

---

[3] Since writing this, the existence of a gap in the energy spectrum of wind speed, centered at a frequency of about 1 cycle per hr, appears to have been established by Van der Hoven (Journal of Meteorology, Vol. 14, 1957, pp. 160-164). This, together with the results from a recent study at the University of Bristol, of over 100 spectra of strong winds now suggests that reliable predictions of the turbulence at higher frequencies (necessary in predicting maximum wind loads) can be made from the average wind speed taken over a longer period, such as one hour. In many countries climatological records of mean hourly wind velocities are more readily available. The discussion that follows applied equally to these mean hourly wind-speeds as well as to those averaged over a rather shorter period.

Various empirical, semi-empirical, and theoretical formulas have been derived to represent the variation of wind velocity with height. Three of the more familiar forms are the spiral, logarithmic, and exponential profiles. For structural purposes, the exponential or power law profile has been used most widely because of its simplicity. It can be stated as

$$V_z = k\, z^{1/\alpha} \quad \ldots\ldots\ldots\ldots\ldots\ldots \quad (2)$$

where V_z is the velocity at height z above ground, and k and α are constants.

By suitable choice of exponent, Eq. 2 can be made to correspond closely over a considerable range to the other forms of profile which are less empirical. The power law is applicable only in the layer extending from the ground up to the height at which the gradient velocity is first attained (usually in the range of 1,000 ft to 2,000 ft). Above this height, the wind velocity may be regarded as constant.

D. Brunt (6) has noted that "If the variation of wind with height be represented by a lower law z^p it is found that p is increased by an increase in either roughness or stability" (z being the height above ground). Here Brunt refers specifically to a range of heights above approximately 10 m (33 ft), the height being of interest to structural engineers.

An attempt is now made to evaluate these influences of stability and surface roughness on first, the rate of increase of mean velocity with height; and second, the magnitude of the mean surface velocity. Both of these values are of prime importance in estimating basic design wind velocities for structures.

Stability.—The stability of a storm is measured by the lapse rate or rate of temperature variation with height. In storm winds of long duration, in which turbulence causes thorough mixing, the lapse rate near the ground is invariably close to the adiabatic which corresponds to a state of natural stability (7,8). Rudolf Geiger (9) has stated that this condition is generally attained at velocities greater than 6 m per sec (13 mph). Observations of hurricanes Edna (1954) and Ione (1955) off the New England coast, reported by Edwin Kessler (10), apparently confirm the general assertion that the stability of mature and large-scale storms, whether of the tropical or extra-tropical variety, is close to being neutral.

Exceptions may be found, however, in severe local storms such as thunderstorms and frontal squalls (and perhaps in larger storms such as hurricanes in their early incipient stages, before full maturity is reached) which are notably unstable, where air near the ground is warmer than that aloft. As a consequence of this instability, extreme thermal interchange takes place between the air near the surface and the faster moving upper air which is unretarded by friction near the surface. Under circumstances of extreme instability, the value of the exponent $1/\alpha$ may attain the limiting value of zero, corresponding to zero increase in velocity with height. At Agra, Barkat Ali (11) measured an exponent of 0.02 (1/50) in very unstable conditions and O. G. Sutton (7) suggests a value of 1/100.

From these remarks the following general inferences may be drawn with regard to the effects of stability on the profile:

a. Severe local storms, such as thunderstorms or frontal squalls, are extremely unstable and so the increase of mean velocity with height is very small; the frictional characteristics of the ground surface may have almost negligible effects on the velocity profile.

b. Large-scale mature storms of either tropical or extra-tropical description exhibit nearly neutral stability with no marked tendency for violent thermal interchange; the dominating influence on the velocity profile in these storms is not the stability but the surface roughness.

Surface Roughness.—The important question now arises as to how great an effect surface roughness has on the wind velocity profile in large-scale mature storms which are probably the most important. In comparison with the vast amount written in engineering papers on this general subject, scant attention has been given to this particular question. It appears to be of paramount importance in the accurate evaluation of wind velocities.

It should first be emphasized that what is referred to by the term "surface roughness" is neither the shielding due to individual obstacles nor the orographic effects influencing the airflow in mountain regions, but the cumulative statistical drag effect of many obstructions on the wind. The surface roughness, therefore, is characterized by the density, size, and height of the buildings, trees, vegetation, rocks, etc., on the ground, around, and over which the wind must flow; it will be a minimum over the ocean and a maximum in a large city.

For years the measurement of wind-velocity profiles has been of interest in the fields of meteorology, aviation, agriculture, and wind power as well as in civil engineering. Information has now accumulated from which it is possible to evaluate the influence of the surface roughness on the wind velocity profile.

In Table 1, the exponents $1/\alpha$ corresponding to the accumulated experimental results of a number of observers are shown on a comparative basis and the corresponding power law profiles plotted in Fig. 1. The records from which these exponents and equivalent power-law curves are derived are given in the Appendix. Where the results were not explicitly stated as a power law, it was found that, in each case, a power law could be closely fitted to the records with only small deviations. It should be noted that the records refer specifically to mean velocity profiles prevailing above a height of 30 ft in strong winds, over flat ground surface at lapse rates which, if not explicitly stated, from the nature of the storms studied presumably could not have differed greatly from the adiabatic. The records, therefore, are homogeneous except that the nature of the ground roughness and the aggregate nature of obstructions vary widely, from the smooth surface of the sea to the rough obstructed surface of a large city.

The exponent of the power law increase is seen to vary between 1/10.5 and 1, depending only on the surface roughness characteristics. It is seen that Curves 1 to 9 have exponents lying between 1/10.5 and 1/5.9 and, in each case, the surrounding terrain was characteristically flat and open. The average for the observations taken on land lies close to 1/7 which is a familiar exponent found at the boundaries of pipes and wind tunnels in which mechanical turbulence predominates and the fluid is neutrally stable. The exponents of Curves 12 to 16 lie between 1/5 and 1/2.8 and average 1/3.5. For these curves the terrain corresponded to the rougher characteristics of treed and wooded farmland, towns, scrub trees, etc. Curves 17, 18 and 19 are derived from records obtained in large cities (Copenhagen, Paris and New York) which probably represent conditions of extreme surface roughness; the corresponding exponents are 1/2.1 and 1/1.6. For all the curves (except 10 and 11 which are probably not typical of level country) the value of the exponent is seen to increase in a

TABLE 1.—INFLUENCE OF SURFACE ROUGHNESS ON VALUES OF THE EXPONENT $1/\alpha$ IN THE POWER-LAW VARIATION OF MEAN WIND VELOCITY WITH HEIGHT UNDER CONDITIONS OF STRONG WIND OR ADIABATIC LAPSE RATE BETWEEN HEIGHTS OF 30 FT AND 1,000 FT

Curve No.	Source	Location	Upper Limit of Investigation, in feet	Description of Terrain in Site Locality	$\frac{1}{\alpha}$	Remarks
1	Goptarev	Caspian Sea (off Apsheron Penin.)	166	Coastal waters of inland sea	$\frac{1}{10.5}$	
2	Juul	Masnedsund, Denmark	182	Flat shore on "Ocean of Small Islands"	$\frac{1}{8.3}$	
3	Scrase	Salisbury Plain, England	43	Open grassland without hedgerows or trees	$\frac{1}{7.7}$	
4	Wing	Ballybunion, Ireland	492	Flat treeless grassland, Atlantic Ocean 1/2 mile distant	$\frac{1}{7.4}$	
5	Sherlock	Ann Arbor, Michigan, U.S.A.	250	Open slightly rolling farm land	$\frac{1}{7}$	
6	Taylor	Salisbury Plain, England	-	Open grassland without hedgerows or trees	$\frac{1}{7}$	
7a	Giblett	Cardington, Beds., England	150	Open level agricultural land with only isolated trees	$\frac{1}{7.8}$	
7b	Frost	Cardington, Beds., England	350	Same as above	$\frac{1}{5.9}$	
7c	Frost	Cardington, Beds., England	1,000	Same as above	$\frac{1}{6.7}$	
8	Deacon	Sale, Victoria, Australia	503	Gently rolling grazing land with few trees	$\frac{1}{6.25}$	
9	Heywood	Leafield, Oxfordshire, England	313	Open fields divided by low stone walls and hedges	$\frac{1}{5.9}$	
10	Kamei	Japan	-	Rough coast	$\frac{1}{5}$	Observations not necessarily typical of level country
11	Wax	Orkney Islands	118	Flat topped grass hill, 1/3 mile inland from high cliff overlooking the sea	$\frac{1}{4.6}$	
12	Huss and Portman	Akron, Ohio, U.S.A.	352	Gently rolling country with many bushes and small trees	$\frac{1}{4.55}$	
13	Franckenberger and Rudloff	Quickborn, Germany	230	Relatively level meadow land but with numerous hedges and trees around the small fields	$\frac{1}{4.35}$	
14a	Smith	Upton, Long Island, N.Y., U.S.A.	410	Level country uniformly covered with scrub oak and pine to a height of 30 ft	$\frac{1}{4}$	Hurricanes Carol and Edna 1954:
14b	Panofsky	Upton, Long Island, N.Y., U.S.A.	410		$\frac{1}{3.85}$	
14c	U.S. Weather Bureau	Upton, Long Island, N.Y., U.S.A.	410		$\frac{1}{3.3}$	(fastest 1 min. mean speed)
14d	U.S. Weather Bureau	Upton, Long Island, N.Y., U.S.A.	410		$\frac{1}{2.9}$	(fastest 6 min. mean speed)
15	Kamei	Japan	-	Three Japanese towns	$\frac{1}{3}$	
16	Dines	Farnborough, England	1,650	Wooded and treed farm land	$\frac{1}{2.8}$	
17	Jensen	Copenhagen, Denmark	242	Centre of a large city	$\frac{1}{2.3}$	
18	Taylor	Paris, (Eiffel Tower)	900	Centre of a large city	$\frac{1}{2}$	
19	Rathbun	New York (Empire State Building)	1,263	Centre of a large city	$\frac{1}{1.6}$	

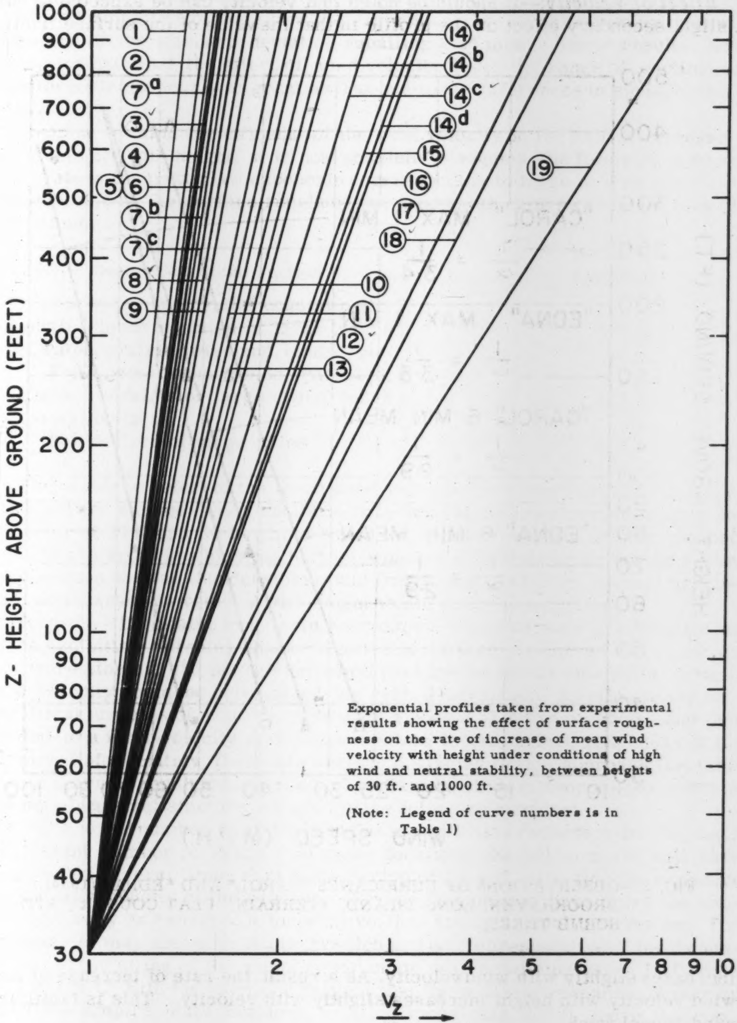

Exponential profiles taken from experimental results showing the effect of surface roughness on the rate of increase of mean wind velocity with height under conditions of high wind and neutral stability, between heights of 30 ft. and 1000 ft.

(Note: Legend of curve numbers is in Table 1)

FIG. 1.—EFFECT OF SURFACE ROUGHNESS ON RATE OF INCREASE OF MEAN VELOCITY WITH HEIGHT

manner which is remarkably consistent with the increase in the roughness of the terrain and the number of obstructions.

***Effect of Velocity.*—It should be noted that velocity can be expected to have a slight secondary effect on the profile in that the value of the surface friction**

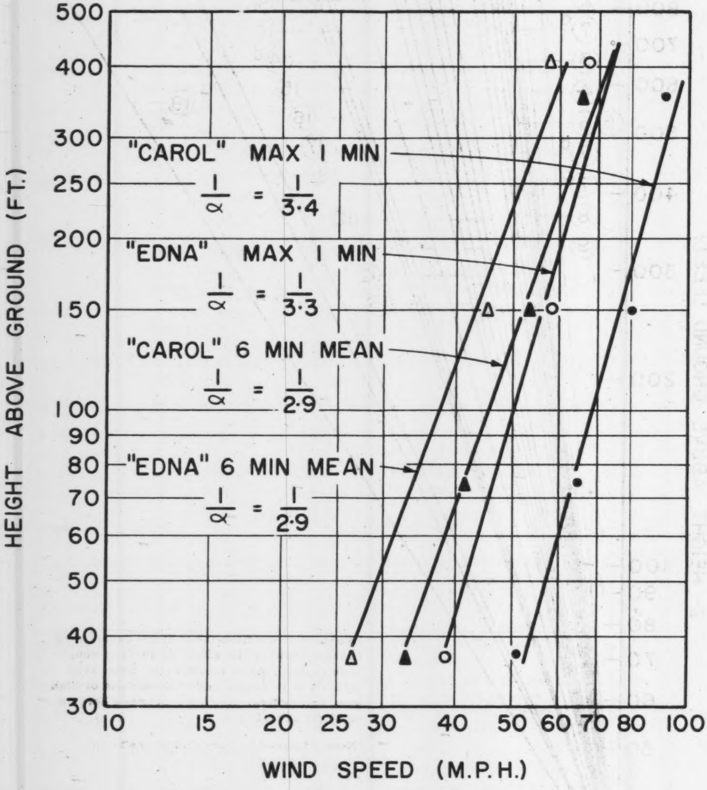

FIG. 2.—OBSERVATIONS OF HURRICANES "CAROL" AND "EDNA" (1954) AT BROOKHAVEN, LONG ISLAND. (TERRAIN: FLAT COUNTRY WITH SCRUB TREES)

increases slightly with wind velocity. As a result, the rate of increase of mean wind velocity with height increases slightly with velocity. This is familiar in wind-tunnel work.

Numerical evidence of the indirect influence of the velocity on the velocity-height relationship is furnished by G. F. Collins' investigations of nine storms (30), mainly at Brookhaven Laboratory, Long Island. He found (Fig. 2), by examining the 5-min mean velocities at different elevations up to 410 ft, that

the exponent of the power-law profile increased by approximately 0.02 for every 10-mph increase in surface wind velocity; at 50 mph the value being 0.27 (that is, 1/3.7) and the extrapolated value at 80 mph being 0.33 (1/3.0). These profiles, according to Collins, fitted the experimental records extremely well with the value of the standard deviation equalling 1.26 mph. These results, however, indicate that the effect of wind velocity (over the range of maxima encountered) is not nearly as great as that due to the differences in surface roughness.

Bearing in mind the influence of the wind velocity on the rate of increase of wind velocity with height, it is now possible to suggest the following approximate values for power law exponents corresponding to more or less qualitative descriptions of the surface roughness or aggregate nature of the surface obstructions:

Description of the Terrain	Power-Law Exponent
For open country, flat coastal belts, small islands situated in large bodies of water, prairie grassland, tundra, etc.	1/7
For wooded countryside, parkland, towns, outskirts of large cities rough coastal belts	1/3.5
For centers of large cities	1/2.5

These values refer to the mean wind velocity over level ground, to large-scale severe storms (which exhibit nearly neutral stability) and to heights between about 30 ft and the height at which the gradient velocity is first attained. If there are areas in which the highest probable velocities occur during severe local storms such as thunderstorms and frontal squalls (which seems improbable), no increase in velocity with height would seem appropriate.

Records.—If reliable long-term anemometer records were available for all areas exhibiting differing characteristics of surface roughness and incidence to severe storms, the discussion could perhaps be left at this point; a basic wind velocity could be determined for each geographical location based on a statistical analysis of wind records over a period of 40 yr or 50 yr, and then applied to a wind-velocity profile appropriate to the surface roughness of the vicinity. Unfortunately, there are serious obstacles to this approach (certainly, in a sparsely populated country such as Canada) since meteorological records are not always satisfactory enough for the following reasons:

Only a small number of stations in Canada will have records extending back a sufficient number of years. At some locations the anemometer will have been moved several times during the period of record, affecting the exposure and the homogeneity of the records. Severe storms may have blown the anemometer away or rendered it inoperative, thus losing crucial information. The anemometer may also give readings which are not representative of level country due to the siting of the anemometer on or near a building. Hugh L. Dryden and George C. Hill, for example, suggest that the well-exposed anemometer on top of the Empire State Building, situated more than 200 ft above the roof, reads 23% higher than the approaching flow, due to the presence of the building (31). If, at airports, anemometers were raised high enough to be free from the influence of the buildings they would present a hazard to aircraft. In winter, the period of worst storms, Dines anemometers sometimes clog with blowing snow. Ice accretions sometimes form on cup anemometers. Anemometer readings taken in mountains, in valleys, and on coastal cliffs are subject to orographic effects sometimes resulting in noticeably higher velocities.

All of these considerations add emphasis to Sherlock's (32) recommendation, shared by many others, that design velocities should be based "on a statistical analysis of wind records over a period of 40 to 50 years." Also the results obtained from the records of one station should be related to those from other neighboring stations by a suitable statistical method. Only in this way can spurious and systematic errors arising in the records of an individual station be minimized.

The next step, therefore, is to explore a suitable method whereby the accumulated records of all meteorological wind records might be correlated. Since it is not desirable to restrict the admissible records to those obtained from anemometers situated in "open level country" (this, in certain regions of Canada, for example, would decimate the available records), it is first necessary to investigate more fully the effects of surface roughness on the velocities measured near the surface over level ground.

It has already been noted that there is some height at which the influence of the ground friction transmitted upwards through eddy viscosity, has a negligible effect on the velocity of the wind as it responds to the pressure gradient. If the velocity at this height is denoted by V_G (the gradient velocity), and the height at which this velocity is first attained by z_G, then by reference to the power-law increase of velocity with height

$$V_z = V_G \left(\frac{1}{z_G}\right)^{1/\alpha} z^{1/\alpha} \quad \ldots\ldots\ldots\ldots\ldots \quad (3)$$

In order to determine the ratio of the velocity at height z above the ground to the gradient velocity, it is first necessary to determine values of z_G corresponding to the various surface roughness categories already discussed. An attempt is now made to do this on the basis of the pertinent experimental records that are available.

Examination of Sherlock's (16) investigations at Ann Arbor, Mich., indicates that for these conditions of flat open country, the value of z_G (the height at which the gradient velocity is first attained) is of the order of 900 ft. This value agrees reasonably well with that obtained by Taylor, at Salisbury Plain, (discussed by W. W. Pagon (17)) for similar terrain in which average values of z_G for strong winds were 1,250 ft in summer and 885 ft in winter. An approximate value of 900 ft, therefore, is chosen for the value of z_G in flat open country.

In large cities, Pagon (17), citing Taylor's studies at the Eiffel Tower in Paris, suggests a value of z_G for strong winds in a large city of 2,020 ft in summer and 1,420 ft in winter. An approximate average value of 1,700 ft is adopted for the present. The value of 1,300 ft is chosen for the intermediate conditions of rough wooded country. These values of z_G of 900 ft, 1,300 ft, and 1,700 ft (together with the appropriate exponents), corresponding to the three types of roughness conditions, give the three curves of Fig. 3.

It is not suggested at this stage that these curves are highly accurate. Indeed, the qualitative aspects of the problem do not permit great accuracy. It should be noted that in these curves the values of $1/\alpha$ are founded on a relatively greater amount of information than are the values of z_G; the errors involved in the latter, however, (which may differ by 200 ft) are of less consequence.

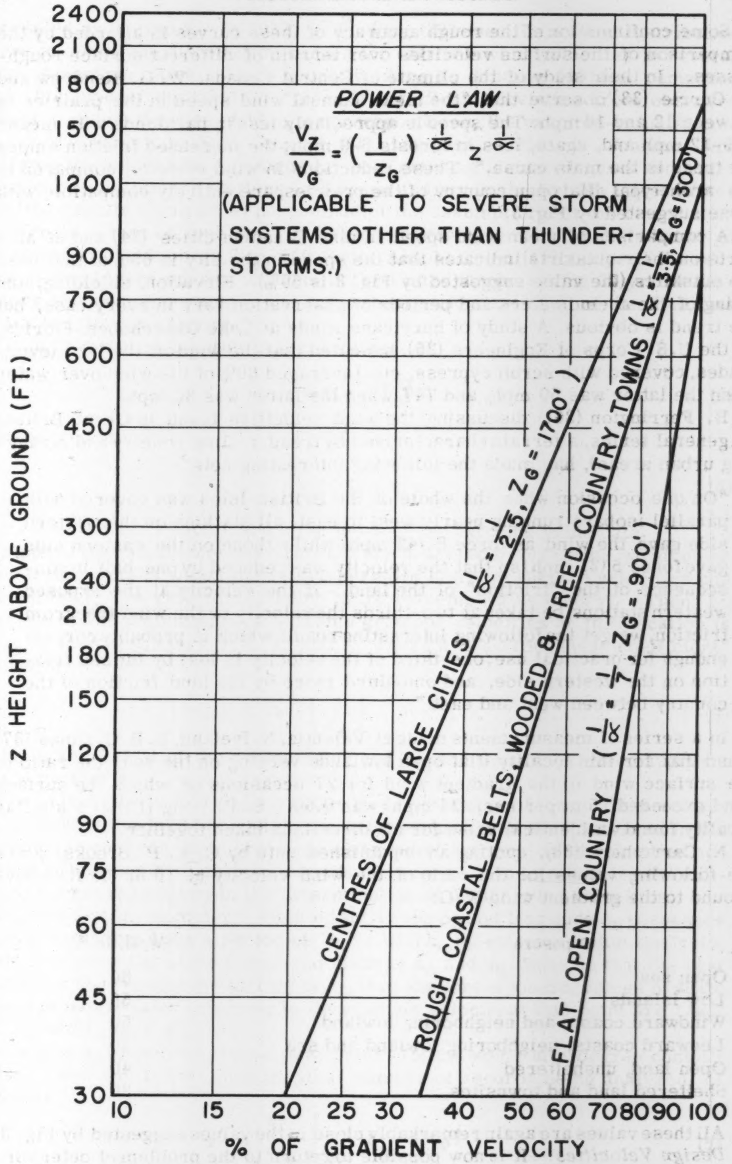

FIG. 3.—INCREASE OF VELOCITY WITH HEIGHT OVER LEVEL GROUND FOR THREE DIFFERENT TYPES OF SURFACE ROUGHNESS ACCORDING TO THE POWER LAW

Some confirmation of the rough accuracy of these curves is afforded by the comparison of the surface velocities over terrain of different surface roughnesses. In their study of the climate of Central Canada, W. G. Kendrew and D. Currie (33) observe that "the mean (annual wind speed in the prairies is between 12 and 16 mph. The speed is appreciably less in parklands with means of 9-12 mph and, again, less in forests 5-9 mph; the increased friction among the trees is the main cause." These reductions in wind velocity, compared to the archetypal flat open country of the prairies, are entirely compatible with those suggested by Fig. 3.

A comparison of mean wind speed in nine Canadian cities (34) and at airports on their outskirts indicates that the speed in the city is 65% of that near the outskirts (the value suggested by Fig. 3 is 59%). Elevation, shielding, and siting of the anemometers and periods of observation vary in every case, but the trend is obvious. A study of hurricane winds at Lake Okeechobee, Florida, by the U.S. Corps of Engineers (35), indicated that the wind off the land (everglades, covered with scrub cypress, etc.) averaged 60% of the wind over water when the latter was 50 mph, and 74% when the latter was 80 mph.

H. Ferrington (36), discussing the wind velocities found in Great Britain (in general terms, a terrain characterized by treed, rolling country and straggling urban areas), has made the following interesting note:

> "On one occasion when the whole of the British Isles was covered with parallel isobars running nearly west to east, all stations on the western side gave the wind as force 8 (42 mph) while those on the eastern side gave force 5 (21 mph) so that the velocity was reduced by one-half in consequence of the "friction" of the land. If the velocity at the exposed western stations be taken at two-thirds the velocity of the wind free from friction, we get the following interesting result which is probably correct enough for practical use; one-third of the velocity is lost by the sea friction on the western side, and one-third more by the land friction of the country between west and east."

In a series of measurements made at Valentia, N. Ireland, L. H. G. Dines (37) found that for this locality (flat open lowlands verging on the sea) the ratio of the surface wind to the gradient wind for 27 occasions on which the surface wind exceeded 15 m per sec, (34 mph) was 0.58. S. P. Wing (15) at a similar locality found an identical value for all directions taken together.

N. Carruthers (38), quoting an unpublished note by C. E. P. Brooks, gives the following values for the ratio of the wind velocity at 10 m (33 ft) above ground to the gradient wind W/G:

Exposure	W/G, in %
Open sea	60
Low islands	55
Windward coasts and neighboring lowland	50
Leeward coasts, neighboring lowland and sea	40
Open land, unsheltered	40
Sheltered land and townsites	30

All these values are again remarkably close to the values suggested by Fig. 3.

Design Velocities.—It is now possible to return to the problem of determining design velocities appropriate to different geographical regions. The prediction of probabilities and return periods of extreme wind velocities has been suggested many times. In 1932, S. P. Wing (39) used the normal distribution curve to obtain the distribution curves for extreme wind velocities in several large American cities. More recently, Arne L. Johnson (40) has remarked that this type of distribution "gives a significant deviation from observed values." Since the date of Wing's correspondence, the extreme-value distribution (due largely to E. J. Gumbel (41)) has been developed. Johnson, who analyzed the anemometer records for both extreme indicated gusts and hourly mileages at thirteen stations in Sweden and six in the British Isles, states that "the results obtained do not contradict the assumption that the distribution of extreme values of type No. 1 is in close agreement with the distribution of the actual wind velocities," (p. 119 (40)). Arnold Court (42) analyzed the records of twenty five weather stations in the United States, having 37 yr of satisfactory records, according to the same theory and states "all of the wind data seems to follow the theory."

This distribution function takes the form (41)

$$\phi(x) = e^{-e^{-y}} \quad \text{. . . . .} \quad (4)$$

The reduced variate

$$y = a(x - u) \quad \text{. . . . .} \quad (5)$$

where a is the scale factor and u the mode of the extreme value data.

Suppose that all anemometer records are analyzed to obtain the parameters a and u (in terms of which the return period of extreme surface velocities can be completely determined according to the extreme value theory). Then, an estimate of the distribution of extreme gradient velocities at this location is given by the parameters $1/k$, a, and k_u where k is a "roughness coefficient" defined by

$$k = \left(\frac{z_G}{z_A}\right)^{1/\alpha} \quad \text{. . . . .} \quad (6)$$

z_A being the height of the anemometer and z_G and $1/\alpha$ being given approximately by Fig. 3.

The object now is to try to correlate these estimates of the gradient velocities in order to reduce the systematic errors which may have occurred in the anemometer records, to improve the estimate of extreme-wind velocities occurring at stations with shorter periods of records, and to minimize the subjective elements involved in the determination of design-wind velocities.

Suppose that anemometer n situated at latitude ϕ_n and longitude λ_n possesses records extending back a period of N_n yr which, by extreme-value analysis, yields values for the scale factor and mode of a_n and u_n. Suppose that the best estimate of the "roughness factor" is k_n, then the corresponding values of scale factor and modal value referring to the gradient velocity at this point are $1/k_n$; $a_n = a'_n$ and $k_n u_n = u'_n$.

It is now assumed that these parameters follow some m^{th} degree contour surface (where m is less than the total number of records being analyzed) of the forms

$$a' = \sum_{j=0}^{m} \sum_{i=0}^{j} A_{ij} \lambda^{i} \phi^{j-i} \quad \text{. . . . .} \quad (7)$$

and

$$u' = \sum_{j=0}^{m} \sum_{i=0}^{j} B_{ij} \lambda^i \phi^{j-i} \quad \ldots\ldots\ldots\ldots\ldots (8)$$

The values of the coefficients A_{ij} and B_{ij} are now obtained by fitting the observed values to these surfaces by the method of least squares. This problem is one well suited to electronic computation. In fitting the values, it would be appropriate to weight them first, by the factor $\sqrt{N_n}$ which puts more reliance on the records of longer period and, second, by a factor Q determined unavoidably, by a subjective evaluation of the quality of the records, with regard to the siting of the anemometer, the number of times it has been moved, and the possible amplification effects of mountains, valleys, etc. For example, a first-class weather station, where the anemometer is situated on level ground away from shielding and has not been moved, might be given a weighting of 9 or 10 (out of a possible 10), whereas an anemometer situated close to the roof of a building, in a shielded area or in a valley, might be weighted by a factor of only 1 or 2. The least-squares process minimizes the errors in a' and u' due to the many causes cited, on the assumption that the weighted errors are normally distributed.

This process leads directly to the contours of a' and u' for the territory considered. If it is now desired to erect a structure at a certain location to last a period of T yr ($T > 10$) with a risk of q that the basic design wind velocity V will be exceeded within this time, the return period R of this wind velocity V is given by

$$R = \frac{-T}{\log_e (1 - q)} \approx \frac{T}{q} \text{ if q is small} \quad \ldots\ldots\ldots (9)$$

This represents a probability of 1/R. By extreme value theory, the value of the required gradient velocity

$$V_G = \frac{1}{a'} \left\{ - \log_e \left[- \log_e \left(1 - \frac{1}{R} \right) \right] \right\} + u' \quad \ldots\ldots\ldots (10)$$

where a' and u' are determined from the contours.

The values of the velocity nearer the surface corresponding to this gradient velocity are determined from Fig. 3 according to the appropriate roughness conditions.

If the structure is to be erected on a hill or in a valley, a suitable amplification factor should be used. Examples of these are given by Pagon (17) and P. C. Putnam (43). The only way to determine this will often be by actual observation of wind velocities at the site for a short period and then comparing their value with those at a nearby anemometer on level terrain.

In this way, it becomes possible to relate the "basic design wind velocity" for each structure to the roughness characteristics of the ground surrounding it, the anticipated span of the structures useful life, and the risks consequent on the design wind velocity being exceeded. Any system which does not take into account the wide variation in those factors which are to be encountered obviously does not permit either a full measure of safety or economy to be effected.

Extreme Wind Speeds Over the British Isles.—To study their practicality, the method and procedures described were applied to some extreme value data obtained by H. C. Shellard (Table 3). Of the forty eight stations whose anemograph records have been analyzed by Shellard, only those described in "The Gazetteer of British Meteorological Stations," (H.M.S.O., London, 1931), are referred to here since the essential site descriptions of the other stations are not available in published form and, in any case, consist largely of those stations with only short periods of record.

Values of U and 1/a were calculated from Shellard's values for the 'once in ten years' and 'once in a hundred years' extreme wind speeds and these are recorded in Table 3. These values were also checked against Shellard's original computation sheets, with his kind permission.

TABLE 2.—TYPES OF TERRAIN GROUPED ACCORDING TO THEIR AERODYNAMIC ROUGHNESS

Category	Description	$\frac{1}{\alpha}$	z_G
1	Very smooth surfaces: e.g. large expanses of open water; low unsheltered islands; tidal flats; lowlands verging on the sea	$\frac{1}{8.5}$	800
2	Level surfaces with only low, surface obstructions: e.g. prairie grassland; desert; arctic tundra	$\frac{1}{7.5}$	900
3	Level, or slightly rolling surfaces, with slightly larger surface obstructions: e.g. farmland with very scattered trees and buildings, without hedgerows or other barriers; wasteland with low brush or surface vegetation; moorland	$\frac{1}{6.5}$	1,000
4	Gently rolling, or level country with low obstructions and barriers: e.g. open fields with walls and hedges scattered trees and buildings	$\frac{1}{5.5}$	1,100
5	Rolling or level surface broken by more numerous obstructions of various sizes: e.g. farmland, with small fields and dense hedges or barriers; scattered windbreaks of trees, scattered two-story buildings	$\frac{1}{4.5}$	1,200
6	Rolling or level surface, uniformly covered with numerous large obstructions: e.g. forest, scrub trees, parkland	$\frac{1}{3.5}$	1,350
7	Very broken surface with large obstructions: e.g. towns; suburbs; outskirts of large cities; farmland with numerous woods and copses and large windbreaks of tall trees	$\frac{1}{3}$	1,500
8	Surface broken by extremely large obstructions: e.g. center of large city	$\frac{1}{2.5}$ - $\frac{1}{1.5}$	1,800

The roughness category of each station was assessed by comparing the photographs and descriptions of the anemometer stations given in the "Gazetteer" (op. cit.) with the descriptions given in Table 2. (These roughness categories for each station are given in Table 3). Knowing the roughness category and the height of the anemometer (z_A) the roughness factor (k_A) was found from Fig. 4, and recorded in Table 3. The anemometer height given in Table 3

TABLE 3.—ANALYSIS OF EXTREME MEAN HOURLY WIND SPEEDS OVER THE BRITISH ISLES[a]

Stations[b]	Lat. -N ° '	Long. ° '	Category	z_A (ft)	k_A	$\frac{1}{a}$	U (mph)	Established gradient with $k_A \times \frac{1}{a}$	Established gradient with $k_A \times U$ (mph)	Q	N	Wt. $\alpha Q\sqrt{N}$
Larwick	60 09	1 08W	2	39	1.65	5.30	56.4	8.75	93.1	7	24	3
Stornoway	58 11	6 21W	2	40	1.60	6.00	54.2	9.60	86.4	9	18	4
Tiree	56 32	6 55W	2	42	1.60	6.52	50.1	10.40	80.2	12	28	6
Aberdeen	57 10	2 06W	6	41	2.75	4.69	32.9	12.90	91.0	9	15	3
Eskdalemuir	55 19	3 12W	4	35	1.88	3.97	45.5	7.50	85.6	9	32	5
Aldergrove	54 39	6 13W	4	42	2.05	3.79	38.5	7.77	78.9	10	25	5
Pt. of Ayre	54 25	4 22W	1	40	1.50	5.21	47.7	7.82	71.6	11	19	5
Holyhead	53 19	4 37W	2	38	1.60	5.28	49.4	8.45	79.0	8	19	4
Southport	53 38	3 00W	2	33	1.65	5.02	48.3	8.28	79.7	12	42	8
Sealand	53 13	3 00W	4	42	1.80	4.41	40.8	7.94	73.4	10	19	4
Catterick	54 22	1 37W	4	33	1.90	6.80	35.4	12.92	67.3	10	10	3
Spurnhead	53 35	0 07E	1	34	1.55	3.58	48.5	5.24	75.2	13	29	7
Cranwell	53 02	0 30W	3	33	1.68	4.78	38.5	8.05	64.7	12	23	6
Birmingham	52 29	1 56W	7	118	2.40	4.06	34.2	9.75	82.0	10	31	6
Cardington	52 07	0 25W	3	135	1.40	6.06	42.9	8.48	60.1	12	23	6
Gorleston	52 35	1 43E	3	34	1.60	3.77	42.1	6.03	67.4	9	36	5
Felixstowe	51 37	1 20E	4	40	1.70	4.10	41.9	6.97	71.2	9	17	3
Shoeburyness	51 32	0 49E	4	89	1.57	4.49	44.9	7.05	70.5	10	29	5
Manston	51 21	1 21E	5	46	2.00	3.70	39.9	7.40	79.8	13	12	5
Kew Obs'vty	51 28	0 19W	8	75	2.75	2.42	29.7	6.65	81.7	7	24	3
Croydon	51 21	0 07W	7	105	2.15	4.26	37.4	9.16	80.5	9	23	4
Lympne	51 05	1 01E	4	48	1.75	3.72	42.7	6.51	74.7	10	27	5
Boscombe Down	51 10	1 45W	4	33	1.90	3.74	39.4	7.10	74.9	10	22	5
Calshot	50 49	1 18W	2	42	1.60	4.55	42.3	7.28	67.7	10	24	5
St. Ann's Hd.	51 41	5 11W	1	70	1.40	9.51	57.8	13.31	80.9	8	14	3
Scilly	49 56	6 18W	1	57	1.45	5.92	55.2	8.58	80.0	12	28	7
Lizard	49 57	5 12W	2	60	1.50	5.13	53.0	7.70	79.5	8	17	4
Pendennis	50 09	5 03W	3	42	1.65	4.30	58.2	7.10	96.0	7	20	3
Plymouth	50 22	4 08W	2	65	1.55	5.22	48.4	8.09	75.0	7	30	4

[a] Shellard, H. C., "Extreme Wind Speeds over Great Britain and Northern Ireland." Meteorological Magazine, vol. 87, Sept. 1958, pp. 257-265. [b] Stations are grouped according to general geographic locality.

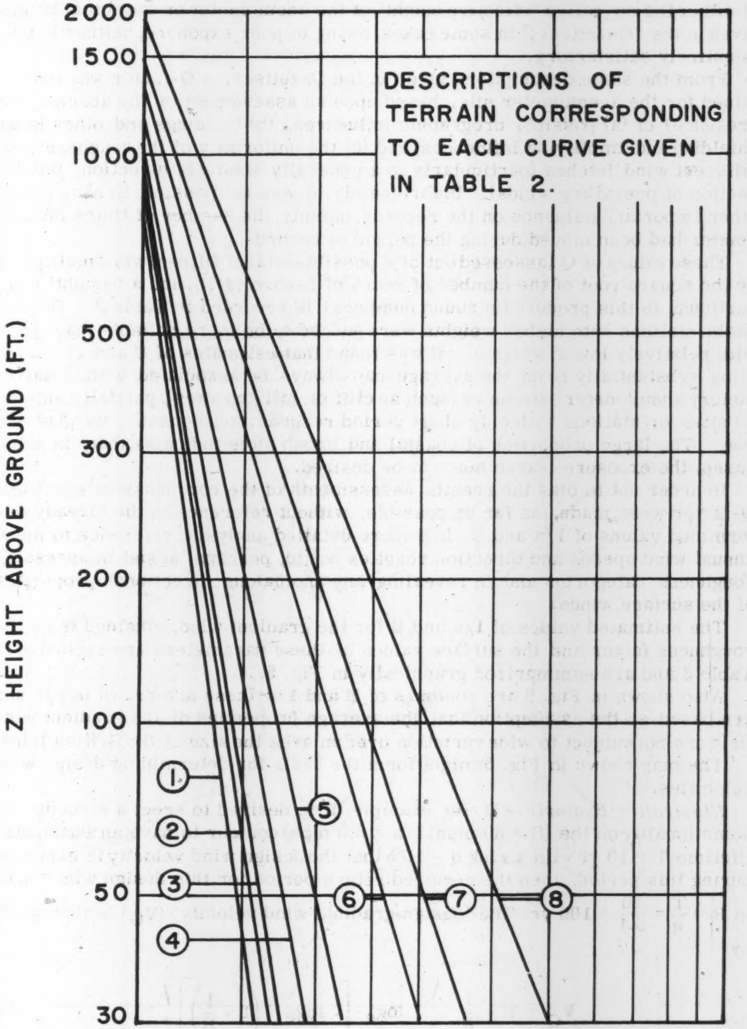

FIG. 4.—ROUGHNESS FACTORS (k_A) FOR DETERMINING THE RATIO OF GRADIENT TO SURFACE WIND SPEEDS OVER DIFFERENT TYPES OF TERRAIN

is either the so-called 'effective height' of the anemometer or the actual height given in the "Gazetteer;" in some cases, owing to poor exposure, neither height is entirely satisfactory.

From the same descriptions given in the Gazetteer, a Q-factor was determined for the anemometer site, based upon an assessment of the absence (or presence) of (a) possible orographic influences, (b) buildings and other local shielding and amplifying influences, and (c) the uniformity of the roughness for different wind fetches (particularly in a generally westerly direction, the direction of prevailing winds). Unfortunately, it was not possible to assess another important influence on the records, namely, the number of times the anometer had been moved during the period of record.

These values of Q (assessed out of a possible total of fifteen) were multiplied by the square root of the number of years of record $(\sqrt{N})$, and a 'weight' proportional to this product (in round numbers) is recorded in Table 3. On this basis, stations with higher weights were judged to be more reliable than those with relatively lower weights. It was found that estimates of U and 1/a deviating substantially from the average can always be associated with unsatisfactory anemometer exposures (such as cliff or hill-top sites), partially shielded sites, or stations with only short period records; consequently, weights are low. The large proportion of coastal and urban sites indicates that, in many cases, the exposure leaves much to be desired.

In order not to bias the results, assessments of the roughness category and Q-factor were made, as far as possible, without reference to the already determined values of 1/a and U. In a more detailed analysis, reference to mean annual wind speeds and direction rosettes would, perhaps, assist in assessing roughness categories and in revealing any anomalous directional properties of the surface winds.

The estimated values of 1/a and U for the gradient wind, obtained from the roughness factor and the surface values of these parameters are recorded in Table 3 and are summarized graphically in Fig. 5.

Also shown in Fig. 5 are contours of U and 1/a; these are drawn by eye and are based on the assumption that the average properties of the gradient wind field are not subject to wide variation over an area the size of the British Isles.

The map shown in Fig. 5 might form the basis for determining design wind velocities.

Illustrative Example.—If, for example, it is desired to erect a structure at some locality on the (U = 80 mph; 1/a = 8.0 mph) contour to have an anticipated lifetime T = 10 yr with a risk q = 10% that the design wind velocity is exceeded during this period, then the required return period for this design wind speed is $R = \frac{T}{q} = \frac{10}{0.1} = 100$ yr. The 'design gradient wind velocity' (V_G) is then given by

$$V_G = U + \frac{1}{a} \left\{ - \log_e \left[- \log_e \left(1 - \frac{1}{R} \right) \right] \right\} \quad \ldots\ldots\ldots \text{(11)}$$

$$= 80 + 8.0 \times 4.6$$

$$= 117 \text{ mph}$$

This, in fact, gives the extreme mean hourly velocity for the gradient wind. Recent unpublished information indicates that the mean minute wind velocity

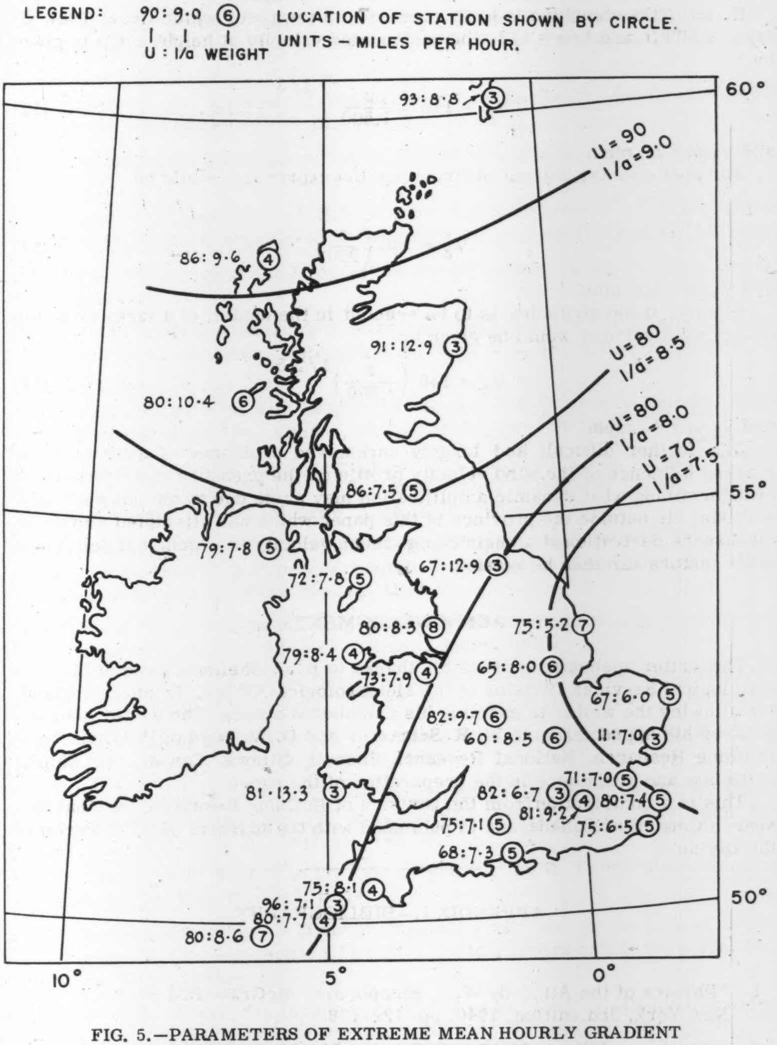
LEGEND: 90 : 9.0 ⑥ LOCATION OF STATION SHOWN BY CIRCLE.
U : 1/a WEIGHT UNITS – MILES PER HOUR.
60°
55°
50°
10°
5°
0°
U = 90
1/a = 9.0
U = 80
1/a = 8.5
U = 80
1/a = 8.0
U = 70
1/a = 7.5
93 : 8.8 ③
86 : 9.6 ④
91 : 12.9 ③
80 : 10.4 ⑥
86 : 7.5 ⑤
79 : 7.8 ⑤
67 : 12.9 ③
72 : 7.8 ⑤
75 : 5.2 ⑦
80 : 8.3 ⑧
79 : 8.4 ④
73 : 7.9 ④
65 : 8.0 ⑥
67 : 6.0 ⑤
82 : 9.7 ⑥
60 : 8.5 ⑥
11 : 7.0 ③
71 : 7.0 ⑤
81 · 13.3 ③
82 : 6.7 ③
81 : 9.2 ④
80 : 7.4 ⑤
75 : 7.1 ⑤
75 : 6.5 ⑤
68 : 7.3 ⑤
75 : 8.1 ④
96 : 7.1 ③
80 : 7.7 ④
80 : 8.6 ⑦

FIG. 5.—PARAMETERS OF EXTREME MEAN HOURLY GRADIENT WIND SPEED OVER THE BRITISH ISLES

(advocated in this report) is on the average 25% greater than this and so the extreme 'mean minute' speed is 117 x 1.25 = 146 mph.

If, now, the structure is to be erected in a town, for which (from Table 3) z_G is 1,500 ft and $1/\alpha = 1/3$, the design wind velocity at height z (ft) is given by

$$V_z = 146 \left[\frac{z}{1,500}\right]^{1/3} \qquad (12)$$

and $V_{100} = 59$ mph.

For open country without obstructions the expression would be

$$V_z = 146 \left(\frac{z}{900}\right)^{\frac{1}{7}} \qquad (13)$$

and $V_{100} = 106$ mph.

Finally, if the structure is to be erected in the center of a large city, the design wind velocity would be given by

$$V_z = 146 \left(\frac{z}{1,800}\right)^{1/2.5} \qquad (14)$$

and $V_{100} = 46$ mph.

The further difficult and largely unresolved problems of assessing the marked influence of the wind velocity profile on the pressure distribution, and of determining what dynamic amplification may arise due to the unsteady flow of gusts, lie outside the province of this paper which has attempted merely to discuss the derivation of a basic design mean velocity to which, it is felt, these other factors can then be related.

ACKNOWLEDGMENTS

The writer wishes to express his thanks to H. C. Shellard, Head of the Climatological Services Division of the Meteorological Office, London, England, for allowing the writer to examine his calculation sheets. The writer also expresses his appreciation to W. R. Schriever and D. W. Boyd of the Division of Building Research, National Research Council, Ottawa, Canada, for helpful criticism and assistance in the preparation of the paper.

This is a contribution from the Division of Building Research, National Research Council of Canada, and is published with the approval of the Director of the Division.

APPENDIX I.—BIBLIOGRAPHY

1. "Physics of the Air," by W. J. Humphreys, McGraw-Hill Book Co., Inc., New York, 3rd edition, 1940, pp. 129-136.

2. "Structure of Wind over Level Country," by M. A. Giblett, et al., Geophys. Mem. No. 54, Met. Office, London, 1932.

3. "Vibrations of Structures," by Franklin P. Ulrich and Dean S. Carder, Proceedings of Symposium on Earthquake and Blast, Los Angeles, Calif., June, 1952, p. 130.

4. "Wind Forces on a Tall Building," by J. Charles Rathbun, Transactions, ASCE, Vol. 105, 1940, pp. 1-41.

5. "Wind Structure in Winter Storms," by R. H. Sherlock and M. B. Stout, Journal of Aeronautical Sciences, Vol. 5, No. 2, December, 1937, pp. 53-61.

6. "Physical and Dynamical Meteorology," by D. Brunt, Cambridge Univ. Press, 2nd edition, 1952, p. 114.

7. "Atmospheric Turbulence," by O. G. Sutton, Methuen and Co., Ltd., 1949, p. 20.

8. "Relation of Gustiness to Other Meteorological Parameters," by I. I. Singer and M. E. Smith, Journal of Meteorology, Vol. 10, April, 1953, pp. 121-124.

9. "The Climate Near the Ground," by Rudolf Geiger, Harvard Univ. Press, 1950.

10. "Outer Precipitation Bands of Hurricane Edna and Ione," by Edwin Kessler, Bulletin of the Amer. Meteorological Soc., Vol. 38, No. 6, June, 1957, p. 335.

11. "Variation of Wind with Height," by Barkat Ali, Quarterly Journal, Royal Meteorological Soc., London, Vol. 58, 1932, pp. 285-288.

12. "Some Results of the Investigation of Gradients in the Vicinity of Oil-drilling Derricks," by N. P. Goptarev, Trudy Gosudarst venny. okeanograficheskу institut, Moscow, Vypusk 36, 1957, p. 128.

13. "Measuring Wind Velocities at Varying Heights Above Ground," by J. Juul, Organization for European Economic Co-operation, Final Report of working group No. 2, "Wind Power," 1954.

14. "Some Characteristics of Eddy Motion in the Atmosphere," by F. J. Scrase, Geophys. Mem. No. 52, Met. Office, London, 1930.

15. "Wind Pressures and the Design of Radio and High Transmission Towers," by S. P. Wing, Electrician, Vol. 87, No. 2250, July 1, 1921, pp. 6-10.

16. "Variation of Wind Velocity and Gusts With Height," by R. H. Sherlock, Transactions, ASCE, Paper 2553, 1953.

17. "Wind Velocity in Relation to Height Above Ground," by W. W. Pagon, Engineering News-Record, McGraw-Hill Book Co., Inc., New York, Vol. 114, No. 21, May 23, 1935, pp. 742-51.

18. "The Velocity Profile in the Lowest 400 Ft," by R. Frost, Meteorological Magazine, Vol. 76, 1947, p. 14.

19. "Micrometeorology, A Study of Physical Processes in the Lowest Layers of the Earth's Atmosphere," by O. G. Sutton, McGraw-Hill Book Co., Inc., New York, 1953, p. 238.

20. "Gust Variation with Height up to 150 Metres," by E. L. Deacon, Quarterly Journal, Royal Meteorological Soc., Vol. 81, London, 1955, p. 562.

21. "Wind Structure Near the Ground and its Relation to Temperature Gradient," by G. S. P. Heywood, Quarterly Journal, Royal Meteorological Soc., Vol. 57, London, 1931, p. 433.

22. "Studies on Natural Wind Pressure on Buildings and Other Structures," by I. Kamei, Building Research Inst. of Japan, Vol. 1, No. 16, March, 1955.

23. "An Experimental Study of Wind Structure with Reference to the Design and Operation of Wind Driven Generators," by M. P. Wax, British Electrical and Allied Ind. Res. Assoc., Tech. Report C/T114, 1956.

24. Daniel Guggenheim Airship Inst. Report No. 156, by P. O. Huss and D. J. Portman, Akron Univ., Ohio, 1949.

25. "Windmessungen an den Quickborner Funkmasten 1947-8," by E. Franckenberger and W. Rudloff, Met. Amt. für N. W. Deutsch, Hamburg, 1949.

26. Discussion of R. H. Sherlock's "Variation of Wind Velocity and Gusts with Height," by I. I. Singer and M. E. Smith, Transactions, ASCE, Vol. 118, 1953, p. 493.

27. "Survey of Meteorological Factors Pertinent to Reduction of Loss of Life and Property in Hurricane Situations," by U. S. Weather Bur., Nat. Hurricane Research Proj., Washington, D. C., Report no. 5, March, 1957.

28. "Statistical Properties of the Vertical Flux and Kinetic Energy at 100 Metres," by H. A. Panofsky, Pennsylvania State College, Mineral Industries Exp. Station, Div. of Meteorology, Scientific Report No. 2, 1953. (AFCRC Contract No. AF 19(604) -166).

29. "4th Report on Wind Structure," by J. S. Dines, Aeronautical Research Council, Reports and Memoranda, Report 1912-1913, London, pp. 310-330.

30. "Determining Basic Wind Loads," by G. F. Collins, Proceedings, ASCE, Vol. 81, November, 1955.

31. "Wind Pressure on a Model of the Empire State Building," by Hugh L. Dryden and George C. Hill, Journal of Research, Natl. Bur. of Standards, Vol. 10, 1933, pp. 493-523.

32. "The Nature of the Wind," by R. H. Sherlock, Proceedings, ASCE, Vol. 84, No. ST4, July, 1958.

33. "Climate of Central Canada," by W. G. Kendrew and D. Currie, Edmond Cloutier, Queen's Printer, Ottawa, 1955, p. 150.

34. "Climatic Summaries for Selected Meteorological Stations in Canada," by C. C. Boughner and M. K. Thomas, Vol. II, Dept. of Transport, Meteorological Division, Toronto, May, 1948, pp. 1-88.

35. "Characteristics of United States Hurricanes Pertinent to Levee Design for Lake Okeechobee, Fla.," by U. S. Weather Bur., Hydrometeorological Report, No. 32, 1954.

36. "Wind Loads on Buildings," by H. Ferrington, Structural Engineer, Vol. 21, No. 12, December, 1943, pp. 497-526; Vol. 22, No. 1, January, 1944, pp. 15-40.

37. "Comparison of Surface and Upper Winds at Valentia," by L. H. G. Dines, Professional Notes, Meteorological Office, London, Vol. 6, No. 83, 1938.

38. "Variations in Wind Velocity Near the Ground," by N. Carruthers, Quarterly Journal, Royal Meteorological Soc., Vol. 69, London, 1943, p. 291.

39. Discussion of "Wind Bracing in Steel Buildings," by S. P. Wing, Proceedings, ASCE, August, 1932, p. 1103.

40. "Strength Safety and Economical Dimensions of Structures," by Arne I. Johnson, Stockholm, Institutionem For Fyggnadsstatik Kunge Tekniska Hogskolan, No. 12, 1953.

41. "Statistical Theory of Extreme Values and Some Practical Applications," by E. J. Gumbel, Natl. Bur. of Standards, App. Maths. Series No. 33., Washington, D. C., 1954.

42. "Wind Extremes as a Design Factor," by Arnold Court, Journal of the Franklin Institute, Vol. 256, No. 1, July, 1953.

43. "Power From the Wind," by P. C. Putnam, Van Nostrand Book Co., New York, 1948.

44. "The Model-Law for Phenomena in Natural Wind," by M. Jensen, Ingeniøren, Internatl. Edition, Vol. 2, No. 4, Copenhagen, November, 1958, pp. 121-128.

APPENDIX II.—RECORDS OF WIND VELOCITY PROFILES

*1. GOPTAREV'S OBSERVATIONS

Location: Caspian Sea off Apsheron Peninsula
Terrain: Coastal waters of inland sea
Reference: 12

These observations taken at the site of offshore oil wells include many measurements of very strong winds. The average values for twenty seven occasions when the mean wind velocity (for 10 min) at 5.7 m (19 ft) above the sea exceeded 15 m per sec (approximately 34 mph) were as follows:

Height		Velocity	
meters	feet	m per sec	mph
5.7	19	16.80	37.8
15	50	19.30	43.3
27.3	91	20.07	45.2
50.6	168	20.57	46.5

2. JUUL'S OBSERVATIONS

Location: Masnedsund, Denmark
Terrain: Flat level coast of "ocean of small islands" (off sea wind)
Reference: 13

---

* Numbers refer to those given in Fig. 1 and Table 1.

Height		Velocity	
meters	feet	m per sec	mph
5	16.5	14.2	32
15	49.5	16.5	37
35	115.5	17.2	39
55	182.0	18.8	42

3. SCRASE'S OBSERVATIONS

Location: Salisbury Plain
Terrain: Open grass-covered plain
Reference: 14

Reported profile in adiabatic conditions given by power law with exponent of 0.13 (1/7.7). Wind measurements were made between heights of 3 m and 13 m (approximately 10 ft and 43 ft).

4. WING'S OBSERVATIONS

Location: Ballybunion, Ireland

Terrain: Low level plain. Atlantic Ocean $\frac{1}{2}$-mile beyond low level sand dunes.
Reference: 15

Height		Velocity	
meters	feet	m per sec	mph
4.5	15	10.7	24
92	300	14.3	32
149	492	15.6	35

(These records refer to curve '1' of Fig. 8 of Wing's paper "which is a curve which most of the high winds there very nearly approach," (p. 9, (15)).

5. SHERLOCK'S OBSERVATIONS

Location: Ann Arbor, Mich.
Terrain: Open farmland
Reference: 16

Fastest 1 min mean velocities

Height		Velocity	
meters	feet	m per sec	mph
15	50	19.9	44.5*
23	75	20.1	45 *
30	100	20.3	45.5*
38	125	21.0	47
46	150	21.2	47.5
53	175	21.7	48.5
61	200	21.7	48.5
76	250	24.1	54

---

* These values may be slightly higher than would otherwise be obtained because measurements were made near the brow of a slight rise.

6,18 TAYLOR'S OBSERVATIONS

These records were taken from Pagon's paper (17) in which Taylor's records are summarized in terms of the following Ekman spiral parameters.

		Cities	Open Country
θ		45^0	20^0
z_G (ft)	summer	2020	1250
	winter	1420	885

where θ = angle between directions of surface and gradient winds
z_G = height at which gradient velocity is first attained.

Taylor's experiments were conducted at Salisbury Plain and at the Eiffel Tower.

The Ekman spirals specified by the above parameters correspond closely with power laws with exponents of $\frac{1}{2}$ and 1/7 (for "cities" and "open country" respectively).

7a. GIBLETT'S OBSERVATIONS

Location: Cardington, England
Terrain: Large flat open airfield
Reference: 2

The ratio of wind velocities recorded by an anemometer at 150 ft to those at 50 ft under neutrally stable conditions and wind velocities in excess of 20 mph, was found to be 1.14 which corresponds to a power law increase with an exponent of 1/7.8.

N. B. Frost (18) has drawn attention to possible differences in exposure of the two anemometers used in this investigation which may account for the slight discrepancy between Giblett's results and Frost's.

7b, c. FROST'S OBSERVATIONS

Location: Cardington, England
Terrain: Flat open airfield

These were obtained from Sutton (19) (see also 18) who states:

> "Layers 5 - 400 ft and 4 - 1,000 ft have been investigated by R. Frost using instruments suspended from a captive balloon over the airfield at Cardington, Southern England. His results indicate that in these layers the profile can be represented by power laws in all conditions of temperature gradient. From a further examination of extended profiles from 4 - 1,000 ft, Frost concludes that the value of $\frac{1}{\alpha}$ (the power law exponent) in conditions of adiabatic lapse rate is .149 (1/6.7) which is very close to the value 1/7 (.142) occurring in the generally accepted power-law profile for the turbulent boundary layer of a flat plate in a wind tunnel."

In the experiments between the heights 4 ft and 400 ft (18), the average wind velocities from fifty seven separate observations for which the lapse rate was approximately adiabatic were as follows:

Height		Velocity	
meters	feet	m per sec	mph
1	4	3.57	7.98
9	30	5.02	11.26
24	80	6.04	13.51
46	150	6.60	14.79
107	350	7.70	17.23

(Corresponding exponent = $0.17 = \frac{1}{5.9}$)

8. DEACON'S OBSERVATIONS

Location: Sale, Victoria, Australia
Terrain: Gently rolling grazing land with very few trees
Reference: 20

Thirty-one successful observations were made of wind velocities greater than 20 mph at 40 ft and averaging 27.6 mph and the ratio of the velocities at different heights found to average at the following values:

Height		
meters	feet	$U_z/\overline{U}_{40}$
12	40	1
64	210	1.272
153	503	1.540

9. HEYWOOD'S OBSERVATIONS

Location: Leafield, Oxfordshire
Terrain: Open fields divided by low stone walls and hedges
Reference: 21 (and 20)

Deacon (20) states "In Heywood's Table 7 there are 38 observations with approximately adiabatic lapse rate and wind speed at 95 m (312 ft) greater than 8.5 m/sec (279 ft/sec) and these give a mean ratio $\overline{U}_{95}/\overline{U}_{12.7} = 1.40$."

10, 15. KAMEI'S OBSERVATIONS

These were obtained from the study of wind velocity profiles in three Japanese towns and, also, along the coast and represent summarized results (22). The power law exponents suggested by these studies were

1/3 in towns and
1/5 at the coast.

11. WAX'S OBSERVATIONS

Location: Costa Hill, Orkney Islands
Terrain: Rough coast, flat-topped hill, 1/3 mile inland from high cliff overlooking sea
Reference: 23

Height		Velocity	
meters	feet	m per sec	mph (100-sec mean)
17.7	58	19.5	43.7
26.8	88	20.9	46.8*
36.0	118	22.6	50.7

12. HUSS AND PORTMAN'S OBSERVATIONS

Location:	Akron, Ohio, U. S. A.
Terrain:	Gently rolling country with many bushes and small trees
Reference:	24 (and 20)

Deacon (20) states that "These authors evaluated $1/\alpha$ by least squares from 5 min mean velocities at 6 heights between 12 m and 107 m (39 ft and 350 ft). The 40 values for wind speeds greater than 9 m per sec (29.5 fps) at 50 m (164 ft) give a mean $\alpha = .219$ with a standard deviation of the individual values of 0.042."

13. FRANCKENBERGER AND RUDLOFF'S OBSERVATIONS

Location:	Quickborn (near Hamburg), Germany
Terrain:	Level meadowland with numerous hedges and trees around the small fields
Reference:	25 (and 20)

Deacon (20) states that the mean of twenty one observations of mean wind speeds at 70 m (230 ft) greater than 15 m per sec (49.2 fps) gives the following

Height		
meters	feet	$\overline{U}_z/\overline{U}_{10}$
10	33	1
30	99	1.285
70	230	1.508

14a. SMITH'S OBSERVATIONS

Location:	Brookhaven, Upton, Long Island, U. S. A.
Terrain:	Level country uniformly covered with scrub oak and pine
Reference:	26

Reported average exponent for thirteen winter storms was 0.25.

14b. PANOFSKY'S OBSERVATIONS

Location:	Brookhaven, Upton, Long Island, U. S. A.
Terrain:	Level country uniformly covered with scrub oak and pine
Reference:	28 (and 20)

Deacon (20) gives the following velocity ratios for conditions of wind at 91 m (298 ft) greater than 9 m per sec (29.5 fps).

---

* Average of two simultaneous readings of 46.1 and 47.5 mph.

Height		
meters	feet	$\overline{U}_z/\overline{U}_{10m}$
11	36	1.02
45	147	1.47
91	298	1.81
125	410	1.91

14c, d. U. S. WEATHER BUREAU OBSERVATIONS

Location: Brookhaven, Upton, Long Island, U. S. A.
Terrain: Level country uniformly covered with scrub oak and pine
Reference: 27

Records taken during hurricanes Edna and Carol (1954) are shown in Fig. 2.

16. DINES' OBSERVATIONS

Location: Royal Aircraft Establishment, Farnborough, England
Terrain: Treed and wooded farmland and fields
Reference: 29

Height		Velocity*	
meters	feet	m per sec	mph
50	165	7.2	16.2
100	330	8.9	20.0
150	495	10.4	23.4
200	660	11.4	25.6
250	825	12.2	27.4
300	990	12.9	29.0
400	1320	14.5	32.6
500	1650	15.6	35.1

17. JENSEN'S OBSERVATIONS

Location: Copenhagen, Denmark
Terrain: Center of a large city
Reference: 44

In Jensen's Fig. 1, the following observations are recorded.

Height z		
meters	feet	Velocity at height z m / Velocity at 100 m
34	111	.68
50	164	.75
74	242	.91

---

* Measured by balloons and theodolites: average of 25 experiments in which velocities > 10 m per sec.

19. RATHBUN'S OBSERVATIONS

Location: Center of New York City
Terrain: Heavily built up city
Reference: 4

Velocities for the storm of March 22, 1936 (the most severe recorded) were as follows:

	Height		Velocity	
	meters	feet	m per sec	mph
N. Y. City Met. Obs.	18.9	62	12.5	28
U. S. Weather Bureau	138	454	25.9	58
Empire State Building	385	1263	40.2	90

AMERICAN SOCIETY OF CIVIL ENGINEERS

Founded November 5, 1852

TRANSACTIONS

Paper No. 3124

MATRIX ANALYSIS OF PLANE RIGID FRAMES

By Fernando Venancio Filho[1]

SYNOPSIS

The problem of plane rigid frames is formulated in matrix form, using the principle of virtual work with displacements or forces as unknowns. The method is especially suitable for high speed digital computers.

INTRODUCTION

The matrix form of the equations of plane redundant structures by the displacement and force methods is derived following ideas developed by J. H. Argyris[2] and making an adaptation from the equations deduced by that author for plane structures composed of rigid joints and straight bars with constant transverse section. The extension of the method to structures with curved bars and/or variable transverse section is obvious and immediate. By the matrix formulation, one finds the joints equilibrium equations of the displacement method or the elastic compatibility equations of the force method. It will be seen, however, that for the structures analyzed, in terms of the matrix formulation, the displacement method has a great advantage over the force method. The equations are solved by matrix methods, the final results being in the form of a matrix of the internal forces at the ends of the bars.

Note.—Published essentially as printed here, in July, 1960, in the Journal of the Structural Division, as Proceedings Paper 2547. Positions and titles given are those in effect when the paper or discussion was approved for publication in Transactions.

[1] Asst. Prof., Structures Dept., Instituto Tecnológico de Aeronáutica São José dos Campos, São Paulo, Brasil.

[2] "Energy Theorems and Structural Analysis," by J. H. Argyris, part I, General Theory, Aircraft Engineering, Vol. 27, Nos. 2 and 3, February and March, 1955.

DISPLACEMENT METHOD

In this method the linear displacements x and y and the angular displacement θ of each joint are chosen as redundants.

Consider any bar ik of the structure, bounded by the joints i and k, Fig. 1. Let α_{ik} be the inclination from the bar axis in relation with the x axis and the system of orthogonal axis x' and y', the x' axis lying along the bar axes ik. Express the displacements of the joints i and k in the system x' y' in terms of the ones in the system xy:

$$\begin{bmatrix} \theta_1{}^{(ik)} \\ x_i'^{(ik)} \\ y_i'^{(ik)} \\ \theta_k{}^{(ik)} \\ x_k'^{(ik)} \\ y_k'^{(ik)} \end{bmatrix} = \begin{bmatrix} 1 & 0 & 0 & 0 & 0 & 0 \\ 0 & \cos\alpha_{ik} & \sin\alpha_{ik} & 0 & 0 & 0 \\ 0 & -\sin\alpha_{ik} & \cos\alpha_{ik} & 0 & 0 & 0 \\ 0 & 0 & 0 & 1 & 0 & 0 \\ 0 & 0 & 0 & 0 & \cos\alpha_{ik} & \sin\alpha_{ik} \\ 0 & 0 & 0 & 0 & -\sin\alpha_{ik} & \cos\alpha_{ik} \end{bmatrix} \begin{bmatrix} \theta_i \\ x_i \\ y_i \\ \theta_k \\ x_k \\ y_k \end{bmatrix} \quad ..(1)$$

Assume the whole structure to be composed of n/6 bars, then

$$[\Delta] = [a]\,[x] \quad \dots\dots\dots\dots\dots\dots \quad (2)$$

in which $[\Delta]$ is a column matrix whose n elements are the displacements $\theta_1{}^{(12)}$, $x_1'^{(12)}$, $y_1'^{(12)}$, $\theta_2{}^{(12)}$, $x_2'^{(12)}$, $y_2'^{(12)}$ . . . $\theta_i{}^{(ik)}$, $x_i'^{(ik)}$, $y_i'^{(ik)}$, $\theta_k{}^{(ik)}$, $x_k'^{(ik)}$, $y_k'^{(ik)}$ . . . of the joints of the bars 12, . . . ik . . . taken, respectively, in each bar axis system; [X] is a column matrix the p elements of which are the unknown displacements of each joint; consequently, [a] will be an (n x p) matrix, which, multiplied by [X], will result in $[\Delta]$. The matrix [a] has an aspect similar to the first matrix on the right hand side of Eq. 1. It depends only upon the geometry of the structure and it can be found by simple inspection. Geometrically, its elements are the joint displacements referred to the bar axes, due to unit joint displacements referred to the x, y axes. The internal forces $M_i{}^{(ik)}$, $F_{x_i'}{}^{(ik)}$, $F_{y_i'}{}^{(ik)}$, $M_k{}^{(ik)}$, $F_{x_k'}{}^{(ik)}$, $F_{y_k'}{}^{(ik)}$, Fig. 2, can now be expressed as functions of the displacements $\theta_i{}^{(ik)}$, $x_i'^{(ik)}$, $y_i'^{(ik)}$, $\theta_k{}^{(ik)}$, $x_k'^{(ik)}$, $y_k'^{(ik)}$, Fig. 3, and the external loads.

In fact, if l_{ik}, A_{ik}, and I_{ik}, are, respectively, the span, the area and the moment of inertia of the transverse section, and E is Young's Modulus of the material, the parts from these internal forces due to the joint displacements will be in order:

$$E\left(\frac{4\,I_{ik}}{l_{ik}}\ \theta_i^{ik} + \frac{6\,I_{ik}}{l^2_{ik}}\ y_i'^{(ik)} + \frac{2\,I_{ik}}{l_{ik}}\ \theta_k^{(ik)} - \frac{6\,I_{ik}}{l^2_{ik}}\ y_k'^{(ik)}\right)$$

$$E\left(\frac{A_{ik}}{l_{ik}}\ x_i'^{(ik)} - \frac{A_{ik}}{l_{ik}}\ x_k'^{(ik)}\right)$$

$$E\left(\frac{6\,I_{ik}}{l^2_{ik}}\ \theta_i^{(ik)} + \frac{12\,I_{ik}}{l^3_{ik}}\ y_i'^{(ik)} + \frac{6\,I_{ik}}{l^2_{ik}}\ \theta_k^{(ik)} - \frac{12\,I_{ik}}{l^3_{ik}}\ y_k'^{(ik)}\right)$$

$$E\left(\frac{2\,I_{ik}}{l_{ik}}\ \theta_i^{(ik)} + \frac{6\,I_{ik}}{l^2_{ik}}\ y_i'^{(ik)} + \frac{4\,I_{ik}}{l_{ik}}\ \theta_k^{(ik)} - \frac{6\,I_{ik}}{l^2_{ik}}\ y_k'^{(ik)}\right)$$

$$E\left(-\frac{A_{ik}}{l_{ik}}\ x_i'^{(ik)} + \frac{A_{ik}}{l_{ik}}\ x_k'^{(ik)}\right)$$

and

$$E\left(-\frac{6\,I_{ik}}{l^2_{ik}}\ \theta_i^{(ik)} - \frac{12\,I_{ik}}{l^3_{ik}}\ y_i'^{(ik)} - \frac{6\,I_{ik}}{l^2_{ik}}\ \theta_k^{(ik)} + \frac{12\,I_{ik}}{l^3_{ik}}\ y_k'^{(ik)}\right)$$

Calling $m_i^{(ik)}, f_{x_i'}^{(ik)}, f_{y_i'}^{(ik)}, m_k^{(ik)}, f_{x_k'}^{(ik)}, f_{y_k'}^{(ik)}$, the parts from $M_i^{(ik)}$, $F_{x_i'}^{(ik)}$, $F_{y_i'}^{(ik)}$, $M_k^{(ik)}$, $F_{x_k'}^{(ik)}$, $F_{y_k'}^{(ik)}$, due to the external loads, one can write under matrix form:

$$\begin{bmatrix} M_i^{(ik)} \\ F_{x_i'}^{(ik)} \\ F_{y_i'}^{(ik)} \\ M_k^{(ik)} \\ F_{x_k'}^{(ik)} \\ F_{y_k'}^{(ik)} \end{bmatrix} = E \begin{bmatrix} \frac{4\,I_{ik}}{l_{ik}} & 0 & \frac{6\,I_{ik}}{l^2_{ik}} & \frac{2\,I_{ik}}{l_{ik}} & 0 & -\frac{6\,I_{ik}}{l^2_{ik}} \\ 0 & \frac{A_{ik}}{l_{ik}} & 0 & 0 & -\frac{A_{ik}}{l_{ik}} & 0 \\ \frac{6\,I_{ik}}{l^2_{ik}} & 0 & \frac{12\,I_{ik}}{l^3_{ik}} & \frac{6\,I_{ik}}{l^2_{ik}} & 0 & -\frac{12\,I_{ik}}{l^3_{ik}} \\ \frac{2\,I_{ik}}{l_{ik}} & 0 & \frac{6\,I_{ik}}{l^2_{ik}} & \frac{4\,I_{ik}}{l_{ik}} & 0 & -\frac{6\,I_{ik}}{l^2_{ik}} \\ 0 & -\frac{A_{ik}}{l_{ik}} & 0 & 0 & +\frac{A_{ik}}{l_{ik}} & 0 \\ \frac{6\,I_{ik}}{l^2_{ik}} & 0 & -\frac{12\,I_{ik}}{l^3_{ik}} & -\frac{6\,I_{ik}}{l^2_{ik}} & 0 & \frac{12\,I_{ik}}{l^3_{ik}} \end{bmatrix} \begin{bmatrix} \theta_i^{(ik)} \\ x_i'^{(ik)} \\ y_i'^{(ik)} \\ \theta_k^{(ik)} \\ x_k'^{(ik)} \\ y_k'^{(ik)} \end{bmatrix} + \begin{bmatrix} m_i^{(ik)} \\ f_{x_i'}^{(ik)} \\ f_{y_i'}^{(ik)} \\ m_k^{(ik)} \\ f_{x_k'}^{(ik)} \\ f_{y_k'}^{(ik)} \end{bmatrix} \quad ...(3)$$

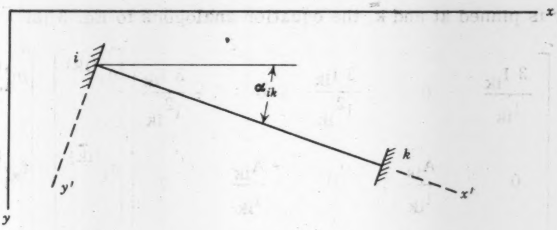
x
i
α_{ik}
k
y'
x'
y

FIG. 1

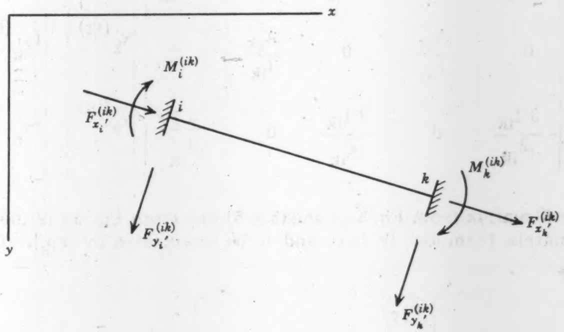
x
$M_i^{(ik)}$
$F_{x_i'}^{(ik)}$
i
$F_{y_i'}^{(ik)}$
k
$M_k^{(ik)}$
$F_{x_k'}^{(ik)}$
$F_{y_k'}^{(ik)}$
y

FIG. 2

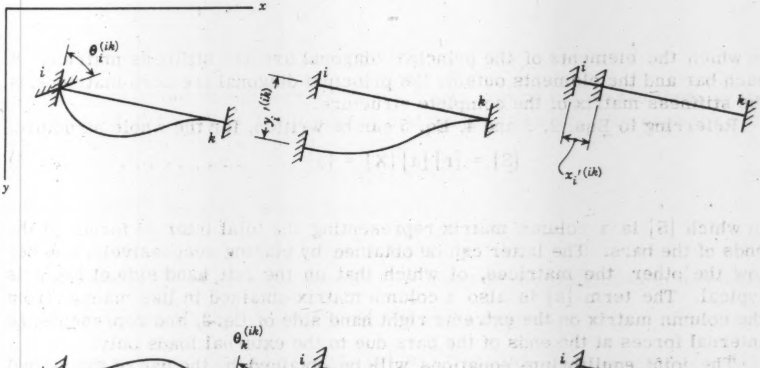
x
$\theta_i^{(ik)}$
i
k
$y_i'^{(ik)}$
$x_i'^{(ik)}$
y
$\theta_k^{(ik)}$
$y_k'^{(ik)}$
$x_k'^{(ik)}$

FIG. 3

If a bar is pinned at end k, the equation analogous to Eq. 3 is:

$$\begin{bmatrix} M_i^{(ik)} \\ F_{x_i'}^{(ik)} \\ F_{y_i'}^{(ik)} \\ F_{x_k'}^{(ik)} \\ F_{y_k'}^{(ik)} \end{bmatrix} = E \begin{bmatrix} \frac{3\,I_{ik}}{l_{ik}} & 0 & \frac{3\,I_{ik}}{l^2_{ik}} & 0 & -\frac{3\,I_{ik}}{l^2_{ik}} \\ 0 & \frac{A_{ik}}{l_{ik}} & 0 & -\frac{A_{ik}}{l_{ik}} & 0 \\ \frac{3\,I_{ik}}{l^2_{ik}} & 0 & \frac{3\,I_{ik}}{l^3_{ik}} & 0 & -\frac{3\,I_{ik}}{l^3_{ik}} \\ 0 & -\frac{A_{ik}}{l_{ik}} & 0 & \frac{A_{ik}}{l_{ik}} & 0 \\ -\frac{3\,I_{ik}}{l^2_{ik}} & 0 & -\frac{3\,I_{ik}}{l^2_{ik}} & 0 & \frac{3\,I}{l^3_{ik}} \end{bmatrix} \begin{bmatrix} \theta_i^{(ik)} \\ x_i'^{(ik)} \\ y_i'^{(ik)} \\ x_k'^{(ik)} \\ y_k'^{(ik)} \end{bmatrix} + \begin{bmatrix} m_i'^{(ik)} \\ f_{x_i'}^{(ik)} \\ f_{y_i'}^{(ik)} \\ f_{x_k'}^{(ik)} \\ f_{y_k'}^{(ik)} \end{bmatrix} \quad . . (3a)$$

The (6 x 6) matrix from Eq. 3 or the (5 x 5) one from Eq. 3a is the so called stiffness matrix from the ik bar, and it be designated by $\left[r_{ik}\right]$. The (n x n) matrix,

$$[r] = \begin{bmatrix} [r_{12}] & & \\ & \ddots\ [r_{ik}] & \\ & & \ddots \end{bmatrix} \quad . . . . (4)$$

in which the elements of the principal diagonal are the stiffness matrices of each bar and the elements outside the principal diagonal are zero matrices, is the stiffness matrix of the complete structure.

Referring to Eqs. 2, 3 and 4, Eq. 5 can be written, for the whole structure.

$$[S] = [r]\,[a]\,[X] + [s] \quad . . . . (5)$$

in which [S] is a column matrix representing the total internal forces at the ends of the bars. The latter can be obtained by placing successively, one below the other, the matrices, of which that on the left hand side of Eq. 3 is typical. The term [s] is also a column matrix obtained in like manner from the column matrix on the extreme right hand side of Eq. 3, and represents the internal forces at the ends of the bars due to the external loads only.

The joint equilibrium equations will be obtained by the use of the virtual work principle, in matrix form. Referring to a force system F_1, F_2 . . . F_n, represented by the column matrix:

$$[F] = \begin{bmatrix} F_1 \\ F_2 \\ \cdot \\ \cdot \\ \cdot \\ F_n \end{bmatrix} \quad \dots\dots\dots\dots\dots\dots\dots\dots \quad (6)$$

and to the displacements of its points of application in its directions, δ_1, δ_2 . . . δ_n, represented by the column matrix:

$$[\delta] = \begin{bmatrix} \delta_1 \\ \delta_2 \\ \cdot \\ \cdot \\ \cdot \\ \delta_n \end{bmatrix} \quad \dots\dots\dots\dots\dots\dots\dots\dots \quad (7)$$

the work from the F forces corresponding to the δ displacements can be expressed in matrix form as,

$$T = [\delta]^*[F] \quad \dots\dots\dots\dots\dots\dots\dots\dots \quad (8)$$

in which the matrix with (*) is the transpose matrix. In fact:

$$[\delta]^*[F] = \begin{bmatrix} \delta_1 & \delta_2 & \dots & \delta_n \end{bmatrix} \begin{bmatrix} F_1 \\ F_2 \\ \cdot \\ \cdot \\ \cdot \\ F_n \end{bmatrix} = F_1\,\delta_1 + F_2\,\delta_2 + \dots F_n\,\delta_n = T$$

The equilibrium conditions from the joints can be expressed then, by the vanishing of the work of the forces of matrix [S] from Eq. 5 through the displacements from matrix [a], Eq. 2, thus,

$$[a]^*[S] = 0 \quad \dots\dots\dots\dots\dots\dots\dots\dots \quad (9)$$

or, substituting from Eq. 5 the value of [S]:

$$[a]^*[r]\,[a]\,[X] + [a]^*[s] = 0 \quad \dots\dots\dots\dots\dots \quad (10)$$

The matrix [X] of the unknowns will be found by multiplying both members of Eq. 10 by $\left\{[a]^*[r]\,[a]\right\}^{-1}$, the reciprocal of $[a]^*[r]\,[a]$:

$$[X] = -\left\{[a]^*[r]\,[a]\right\}^{-1}[a]^*[s] \quad \dots\dots\dots\dots\dots \quad (11)$$

Substituting in Eq. 5 the value of [X] from Eq. 11, the problem of finding the internal forces at the ends of the bars is completely solved:

$$[S] = \left\{[E] - [r]\,[a]\left\{[a]^*[r]\,[a]\right\}^{-1}[a]^*\right\}[s] \quad \dots\dots\dots \quad (12)$$

in which [E] is the identity matrix.

From the perusal of Eq. 12, the following conclusions can be reached: (1) Matrix [S], giving the internal forces at the ends of the bars, is the solution of the problem and is obtained by matrix operations on matrices [r], [a] and [s], as indicated by Eq. 12; (2) Matrices [a] and [r] depend on the geometric and elastic properties of the structure, and matrix [s] depends on the external loads; (3) Once the matrix, which is to be multiplied by [s] in Eq. 12, is obtained, several cases of loading can be solved, simply by introducing the proper [s] matrix; (4) The order of the matrix $[a]^*[r]\,[a]$, which is the matrix to be inverted, is equal to p, the number of unknown displacements; (5) This form of attack of the problem is particularly suitable for the use of electronic digital computers. With a matrix interpretive program, the matrix operations indicated in Eq. 12 are conveniently performed.

Consider, as a simple application example, the structure in Fig. 4. Let all the bars have the same transverse section of moment of inertia I and the external loads as indicated. The bar extensions will be neglected so that it is not necessary to consider the area of the transverse section. The unknowns, in this problem, will be the rotations θ_2 and θ_4 of joints 2 and 4 and the horizontal sidesway δ.

Let, $X_1 = \theta_2$, $X_2 = \theta_4$, and $X_3 = \delta$.

Equation 2 will be, for this particular case:

$$\begin{bmatrix} \theta_1^{(12)} \\ \theta_2^{(12)} \\ y_2'^{(12)} \\ \theta_3^{(34)} \\ \theta_4^{(34)} \\ y_4'^{(34)} \\ \theta_2^{(24)} \\ \theta_4^{(24)} \end{bmatrix} = \begin{bmatrix} 0 & 0 & 0 \\ 1 & 0 & 0 \\ 0 & 0 & 1 \\ 0 & 0 & 0 \\ 0 & 1 & 0 \\ 0 & 0 & 1 \\ 1 & 0 & 0 \\ 0 & 1 & 0 \end{bmatrix} \begin{bmatrix} X_1 \\ X_2 \\ X_3 \end{bmatrix} \quad \dots\dots\dots\dots (13)$$

Equation 5 will be:

$$\begin{bmatrix} M_1^{(12)} \\ M_2^{(12)} \\ F_{y'_2}^{(12)} \\ M_3^{(34)} \\ M_4^{(34)} \\ F_{y'_4}^{(34)} \\ M_2^{(24)} \\ M_4^{(24)} \end{bmatrix} = EI \begin{bmatrix} \frac{4}{l_{12}} & \frac{2}{l_{12}} & -\frac{6}{l_{12}^2} & 0 & 0 & 0 & 0 & 0 \\ \frac{2}{l_{12}} & \frac{4}{l_{12}} & -\frac{6}{l_{12}^2} & 0 & 0 & 0 & 0 & 0 \\ -\frac{6}{l_{12}^2} & -\frac{6}{l_{12}^2} & \frac{12}{l_{12}^3} & 0 & 0 & 0 & 0 & 0 \\ 0 & 0 & 0 & \frac{4}{l_{34}} & \frac{2}{l_{34}} & -\frac{6}{l_{34}^2} & 0 & 0 \\ 0 & 0 & 0 & \frac{2}{l_{34}} & \frac{4}{l_{34}} & -\frac{6}{l_{34}^2} & 0 & 0 \\ 0 & 0 & 0 & -\frac{6}{l_{34}^2} & -\frac{6}{l_{34}^2} & \frac{12}{l_{34}^3} & 0 & 0 \\ 0 & 0 & 0 & 0 & 0 & 0 & \frac{4}{l_{24}} & \frac{2}{l_{24}} \\ 0 & 0 & 0 & 0 & 0 & 0 & \frac{2}{l_{24}} & \frac{4}{l_{24}} \end{bmatrix} \begin{bmatrix} 0 & 0 & 1 \\ 1 & 0 & 0 \\ 0 & 0 & 1 \\ 0 & 0 & 0 \\ 0 & 1 & 0 \\ 0 & 0 & 1 \\ 1 & 0 & 0 \\ 0 & 1 & 0 \end{bmatrix} \begin{bmatrix} X_1 \\ X_2 \\ X_3 \end{bmatrix} + \begin{bmatrix} 0 \\ 0 \\ -H \\ 0 \\ 0 \\ 0 \\ -\frac{p\,l_{24}^3}{12} \\ \frac{p\,l_{24}^3}{12} \end{bmatrix} \quad \dots (14)$$

The equilibrium condition, Eq. 10, will be:

$$\begin{bmatrix} 0&1&0&0&0&0&1&0 \\ 0&0&0&0&1&0&0&1 \\ 1&0&1&0&0&1&0&0 \end{bmatrix} E\,I \begin{bmatrix} \frac{4}{l_{12}} & \frac{2}{l_{12}} & -\frac{6}{l_{12}^2} & 0 & 0 & 0 & 0 & 0 \\ \frac{2}{l_{12}} & \frac{4}{l_{12}} & -\frac{6}{l_{12}^2} & 0 & 0 & 0 & 0 & 0 \\ -\frac{6}{l_{12}^2} & -\frac{6}{l_{12}^2} & \frac{12}{l_{12}^3} & 0 & 0 & 0 & 0 & 0 \\ 0 & 0 & 0 & \frac{4}{l_{34}} & \frac{2}{l_{34}} & -\frac{6}{l_{34}^2} & 0 & 0 \\ 0 & 0 & 0 & \frac{2}{l_{34}} & \frac{4}{l_{34}} & -\frac{6}{l_{34}^2} & 0 & 0 \\ 0 & 0 & 0 & -\frac{6}{l_{34}^2} & -\frac{6}{l_{34}^2} & \frac{12}{l_{34}^2} & 0 & 0 \\ 0 & 0 & 0 & 0 & 0 & 0 & \frac{4}{l_{24}} & \frac{2}{l_{24}} \\ 0 & 0 & 0 & 0 & 0 & 0 & \frac{2}{l_{24}} & \frac{4}{l_{24}} \end{bmatrix} \begin{bmatrix} 0&0&1 \\ 1&0&0 \\ 0&0&1 \\ 0&0&0 \\ 0&1&0 \\ 0&0&1 \\ 1&0&0 \\ 0&1&0 \end{bmatrix} \begin{bmatrix} X_1 \\ X_2 \\ X_3 \end{bmatrix}$$

$$+ \begin{bmatrix} 0&1&0&0&0&0&1&0 \\ 0&0&0&0&1&0&0&1 \\ 1&0&1&0&0&1&0&0 \end{bmatrix} \begin{bmatrix} 0 \\ 0 \\ -H \\ 0 \\ 0 \\ 0 \\ \frac{p\,l_{24}^2}{12} \\ \frac{p\,l_{24}^2}{12} \end{bmatrix} = 0 \quad \ldots\ldots\ldots\ldots\ldots \text{(15)}$$

After making the indicated operations there results:

$$E\,I\left(\frac{4}{l_{24}} + \frac{4}{l_{14}}\right)X_1 + E\,I\frac{2}{l_{24}}X_2 - E\,I\frac{6}{l_{12}^3}X_3 - \frac{p\,l_{24}^2}{12} = 0 \ldots \text{(16a)}$$

$$E\,I\frac{2}{l_{24}}X_1 + E\,I\left(\frac{4}{l_{34}} + \frac{4}{l_{24}}\right)X_2 - E\,I\frac{6}{l_{34}^2}X_3 + \frac{p\,l_{24}^2}{12} = 0 \ldots \text{(16b)}$$

and

$$-E\,I\frac{6}{l_{12}^2}X_1 - E\,I\frac{6}{l_{34}^2}X_2 + E\,I\left(\frac{12}{l_{12}^3} + \frac{12}{l_{34}^3}\right)X_3 - H = 0 \ldots \text{(16c)}$$

two joint and one sidesway equilibrium equations which could be obtained by the usual way.

FORCE METHOD

The matrix formulation by the force method can be made in a similar manner to the displacement method for structures in which it is convenient to take as redundants the bending moments at the ends of the bars, as in the continuous beam problem. The force method, nevertheless, shows its greatest potentiality when the so called group loadings are used and, in this case, the redundants are not, generally, bending moments at the ends of the bars.

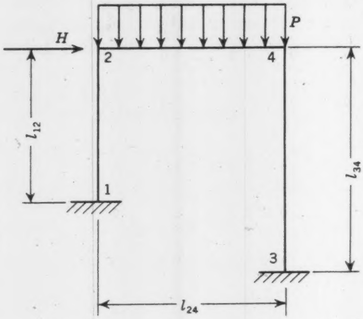

FIG. 4

Consider the continuous beam from Fig. 5, with constant transverse section area of moment of inertia I and with any vertical external load.

The basic statically determinate system will be obtained placing hinges on supports 2 and 3 and the redundants will be the bending moments in the beam at these supports. Thus,

$$\begin{bmatrix} M_1^{(12)} \\ M_2^{(12)} \\ M_2^{(23)} \\ M_3^{(23)} \\ M_3^{(34)} \\ M_4^{(34)} \end{bmatrix} = \begin{bmatrix} 0 & 0 \\ 1 & 0 \\ 1 & 0 \\ 0 & 1 \\ 0 & 1 \\ 0 & 0 \end{bmatrix} \begin{bmatrix} X_1 \\ X_2 \end{bmatrix} \quad \ldots\ldots\ldots\ldots\ldots (17)$$

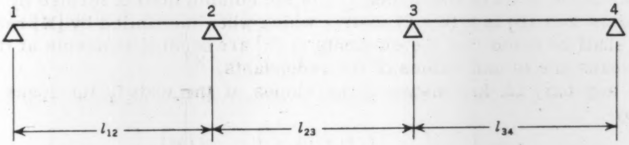
1
2
3
4
l_{12}
l_{23}
l_{34}

FIG. 5

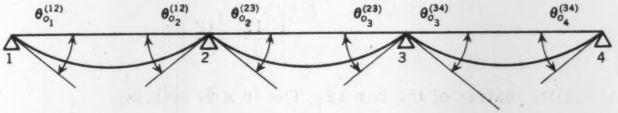
$\theta_{0_1}^{(12)}$
$\theta_{0_2}^{(12)}$
$\theta_{0_2}^{(23)}$
$\theta_{0_3}^{(23)}$
$\theta_{0_3}^{(34)}$
$\theta_{0_4}^{(34)}$
1
2
3
4

FIG. 6

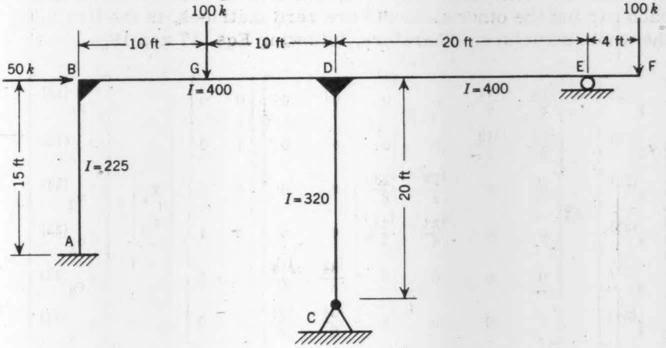
100 k
100 k
10 ft
10 ft
20 ft
4 ft
50 k
B
G
D
E
F
I = 400
I = 400
15 ft
I = 225
I = 320
20 ft
A
C

FIG. 7

or,

$$[M] = [b]\,[X] \quad \ldots\ldots\ldots\ldots\ldots\ldots (18)$$

in which [M] is the column matrix of six elements representing the bending moments at the ends of the spans; [X] is the column matrix formed by the two redundants and [b] is a (6 x 2) matrix which when multiplied by [X] results in [M]. It shall be noted that the elements of [b] are bending moments at the ends of the spans due to unit values of the redundants.

For any bar, 12, for instance, the slopes at the ends of the spans will be given by:

$$\begin{bmatrix} \theta_1^{(12)} \\ \theta_2^{(12)} \end{bmatrix} = \frac{1}{E\,I} \begin{bmatrix} \frac{l_{12}}{3} & \frac{l_{12}}{6} \\ \frac{l_{12}}{6} & \frac{l_{12}}{3} \end{bmatrix} \begin{bmatrix} M_1^{(12)} \\ M_2^{(12)} \end{bmatrix} + \begin{bmatrix} \theta_{o_1}^{(12)} \\ \theta_{o_2}^{(12)} \end{bmatrix} \quad \ldots . (19)$$

The matrix:

$$\left[f_{12}\right] = \frac{1}{E\,I} \begin{bmatrix} \frac{l_{12}}{3} & \frac{l_{12}}{6} \\ \frac{l_{12}}{6} & \frac{l_{12}}{3} \end{bmatrix} \quad \ldots\ldots\ldots\ldots\ldots (20)$$

is the flexibility matrix of the bar 12. The (6 x 6) matrix:

$$[f] = \begin{bmatrix} \left[f_{12}\right] & & \\ & \left[f_{23}\right] & \\ & & \left[f_{34}\right] \end{bmatrix} \quad \ldots\ldots\ldots\ldots\ldots\ldots (21)$$

in which the elements of the principal diagonal are the flexibility matrices of each bar and the other elements are zero matrices, is the flexibility matrix of the whole structure. Therefore, following Eqs. 17 and 19,

$$\begin{bmatrix} \theta_1^{(12)} \\ \theta_2^{(12)} \\ \theta_2^{(23)} \\ \theta_3^{(23)} \\ \theta_3^{(34)} \\ \theta_4^{(34)} \end{bmatrix} = \frac{1}{E\,I} \begin{bmatrix} \frac{l_{12}}{3} & \frac{l_{12}}{6} & 0 & 0 & 0 & 0 \\ \frac{l_{12}}{6} & \frac{l_{12}}{3} & 0 & 0 & 0 & 0 \\ 0 & 0 & \frac{l_{23}}{3} & \frac{l_{23}}{6} & 0 & 0 \\ 0 & 0 & \frac{l_{23}}{6} & \frac{l_{23}}{3} & 0 & 0 \\ 0 & 0 & 0 & 0 & \frac{l_{34}}{3} & \frac{l_{34}}{6} \\ 0 & 0 & 0 & 0 & \frac{l_{34}}{6} & \frac{l_{34}}{3} \end{bmatrix} \begin{bmatrix} 0 & 0 \\ 1 & 0 \\ 1 & 0 \\ 0 & 1 \\ 0 & 1 \\ 0 & 0 \end{bmatrix} \begin{bmatrix} X_1 \\ X_2 \end{bmatrix} + \begin{bmatrix} \theta_{o_1}^{(12)} \\ \theta_{o_2}^{(12)} \\ \theta_{o_2}^{(23)} \\ \theta_{o_3}^{(23)} \\ \theta_{o_3}^{(34)} \\ \theta_{o_4}^{(34)} \end{bmatrix} \quad \ldots\ldots (22)$$

in which the second part of the right hand side of Eq. 22, is a matrix formed by the slopes at the ends of the spans in the basic system, due to the external loads, Fig. 6.

Concisely, Eq. 12 can be written

$$[\theta] = [f]\,[b]\,[X] + \left[\theta_o\right] \quad \ldots\ldots\ldots\ldots\ldots (23)$$

The elastic compatibility equations at the supports can be formulated by the condition of the vanishing of the work of the bending moments of matrix [b], Eq. 18, through the slopes from $[\theta]$, Eq. 23:

$$[b]^*[f]\,[b]\,[X] + [b]^*\left[\theta_o\right] = 0 \ldots\ldots\ldots\ldots\ldots (24)$$

Multiplying both members by $\left\{[b]^*[f]\,[b]\right\}^{-1}$:

$$[X] = -\left\{[b]^*[f]\,[b]\right\}^{-1}[b]^*\left[\theta_o\right] \ldots\ldots\ldots\ldots (25)$$

The final solution will be found by substituting Eq. 25 in Eq. 18:

$$[M] = -[b]\left\{[b]^*[f]\,[b]\right\}^{-1}[b]^*\left[\theta_o\right] \ldots\ldots\ldots\ldots (26)$$

Eq. 24, when written out in full, gives the three moment equations of the given continuous beam. In fact,

$$\begin{bmatrix}0&1&1&0&0&0\\ \\ 0&0&0&1&1&0\end{bmatrix}\frac{1}{E\,I}\begin{bmatrix}\frac{l_{12}}{3}&\frac{l_{12}}{6}&0&0&0&0\\ \frac{l_{12}}{6}&\frac{l_{12}}{3}&0&0&0&0\\ 0&0&\frac{l_{23}}{3}&\frac{l_{23}}{6}&0&0\\ 0&0&\frac{l_{23}}{6}&\frac{l_{23}}{3}&0&0\\ 0&0&0&0&\frac{l_{34}}{3}&\frac{l_{34}}{6}\\ 0&0&0&0&\frac{l_{34}}{6}&\frac{l_{34}}{3}\end{bmatrix}\begin{bmatrix}0&0\\1&0\\1&0\\0&1\\0&1\\0&0\end{bmatrix}\begin{bmatrix}X_1\\ \\ X_2\end{bmatrix}$$

$$+\begin{bmatrix}0&1&1&0&0&0\\ \\ 0&0&0&1&1&0\end{bmatrix}\begin{bmatrix}\theta_{o_1}^{(12)}\\ \theta_{o_2}^{(12)}\\ \theta_{o_2}^{(23)}\\ \theta_{o_3}^{(23)}\\ \theta_{o_3}^{(34)}\\ \theta_{o_4}^{(34)}\end{bmatrix} = 0 \ldots\ldots\ldots\ldots (27)$$

After making the operations, the following moment equations are found:

$$\frac{1}{E\,I}\left(\frac{l_{12}}{3}+\frac{l_{23}}{3}\right)X_1 + \frac{1}{E\,I}\,\frac{l_{23}}{6}\,X_2 + \left(\theta_{o_2}^{(12)} + \theta_{o_2}^{(23)}\right) = 0 \ldots (28a)$$

and

$$\frac{1}{E\,I}\;\frac{l_{23}}{6}\;X_1 + \frac{1}{E\,I}\left(\frac{l_{23}}{3} + \frac{l_{34}}{3}\right)X_2 + \left(\theta_{o_3}{}^{(23)} + \theta_{o_3}{}^{(34)}\right) = 0 \;.\;.\;.\; (28b)$$

NUMERICAL EXAMPLE

Consider the structure[3] of Fig. 7. The influence of axial forces is neglected, as habitually. For computational convenience assume 2 E = 0.1.

Matrices [a], [r], and [s] are

$$[a] = \begin{bmatrix} 0 & 0 & 0 \\ 1 & 0 & 0 \\ 0 & 0 & 1 \\ 1 & 0 & 0 \\ 0 & 1 & 0 \\ 0 & 1 & 0 \\ 0 & 0 & 1 \\ 0 & 1 & 0 \end{bmatrix} \quad [r] = \begin{bmatrix} 3 & 1.5 & -0.3 & 0 & 0 & 0 & 0 & 0 \\ 1.5 & 3 & -0.3 & 0 & 0 & 0 & 0 & 0 \\ -0.3 & -0.3 & 0.04 & 0 & 0 & 0 & 0 & 0 \\ 0 & 0 & 0 & 4 & 2 & 0 & 0 & 0 \\ 0 & 0 & 0 & 2 & 4 & 0 & 0 & 0 \\ 0 & 0 & 0 & 0 & 0 & 2.4 & -0.12 & 0 \\ 0 & 0 & 0 & 0 & 0 & -0.12 & 0.006 & 0 \\ 0 & 0 & 0 & 0 & 0 & 0 & 0 & 3 \end{bmatrix} \quad [s] = \begin{bmatrix} 0 \\ 0 \\ -25 \\ -250 \\ 250 \\ 0 \\ -25 \\ 200 \end{bmatrix}$$

Matrix [a]*[r] [a] is

$$\begin{bmatrix} 7 & 2 & -0.30 \\ 2 & 9.4 & -0.12 \\ -0.30 & -0.12 & 0.046 \end{bmatrix}$$

The inverse of this matrix is $\left\{[a]^*[r]\,[a]\right\}^{-1}$

$$\begin{bmatrix} 0.20491 & -0.02746 & 1.26481 \\ -0.02746 & 0.11373 & 0.11754 \\ 1.26481 & 0.11754 & 30.29385 \end{bmatrix}$$

---

[3] "Digital Computation for Stiffness Matrix Analysis," by J. S. Archer, Proceedings, ASCE, Vol. 84, No. ST 6, October, 1958.

Finally matrix $[E] - [r]\,[a]\left\{[a]^*[r]\,[a]\right\}^{-1}[a]^*$ is

$$\begin{bmatrix}
1 & 0.07208 & 7.19105 & 0.07208 & 0.07645 & 0.07645 & 7.19105 & 0.07645 \\
0 & 0.76471 & 5.29384 & -0.23529 & 0.11764 & 0.11764 & 5.29384 & 0.11764 \\
0 & 0.01088 & 0.16769 & 0.01088 & -0.01294 & -0.01294 & -0.83231 & -0.01294 \\
0 & -0.76472 & -5.29432 & 0.23528 & -0.11762 & -0.11762 & -5.29432 & -0.11762 \\
0 & 0.29998 & -2.99978 & -0.29998 & 0.60000 & -0.40000 & -2.99878 & -0.40000 \\
0 & 0.21768 & 3.35317 & 0.21768 & -0.25885 & 0.74115 & 3.35317 & -0.25885 \\
0 & -0.01088 & -0.16766 & -0.01088 & 0.01294 & 0.01294 & 0.83234 & 0.01294 \\
0 & 0.08238 & -0.35262 & 0.08238 & -0.34119 & -0.34119 & -0.35262 & 0.65881
\end{bmatrix}$$

Multiplying this matrix by the external load matrix [s], matrix [S] will be:

$$[S] = \begin{bmatrix} M_1^{(12)} \\ M_2^{(12)} \\ F_{y_2}'^{(12)} \\ M_2^{(23)} \\ M_3^{(23)} \\ M_3^{(53)} \\ F_{y_3}'^{(53)} \\ M_3^{(34)} \end{bmatrix} = \begin{bmatrix} -343.17 \\ -152.93 \\ 8.07 \\ +152.97 \\ 294.98 \\ -338.56 \\ -8.07 \\ 43.50 \end{bmatrix}$$

AMERICAN SOCIETY OF CIVIL ENGINEERS

Founded November 5, 1852

TRANSACTIONS

Paper No. 3125

STATIC TENSION TESTS OF COMPACT BOLTED JOINTS

By Robert T. Foreman,[1] A.M. ASCE, and John L. Rumpf,[2] M. ASCE

SYNOPSIS

Static tension tests of large butt joints, fabricated from A7 steel and fastened with A325 bolts arranged in compact patterns, indicate that present design specifications are unduly conservative with respect to the shear strength of the bolts.

INTRODUCTION

Purpose.—The 1954 design specification[3] for use of high strength bolts, or the "substitution rule," as it might be designated, permits one A325 bolt to replace one A141 rivet (of the same nominal size) in structural designs. The basic properties of the parent materials of the high strength bolt and structural rivet suggested, from the outset, a superiority for the bolt, but, since this strength advantage had not been completely demonstrated by structural

---

Note.—Published essentially as printed here, in June, 1960, in the Journal of the Structural Division, as Proceeding Papers 2523. Positions and titles given are those in effect when the paper or discussion was approved for publication in Transactions.

[1] Research Engr., Bethlehem Steel Co., Bethlehem, Pa., Formerly Research Asst., Fritz Engrg. Lab., Lehigh Univ., Bethlehem, Pa.

[2] Research Instr., Fritz Engrg. Lab., Lehigh Univ., Bethlehem, Pa.

[3] "Specifications for Assembly of Structural Joints Using High Strength Steel Bolts," Research Council on Riveted and Bolted Structural Joints, February, 1954.

applications, the bolt has continued to be governed by the "one for one" specification.

Since the initial adoption of the present specifications, considerable information concerning the properties of the high-strength bolt has been obtained from laboratory tests at several universities in the United States. However, in the main, these investigations have been concerned with relatively small bolted connections. The research program at Lehigh University, Bethlehem, Pennsylvania, has had as its object—"to study the behavior, under static tension loads, of large plate joints connected with high strength bolts to determine if fewer bolts may be used than presently required by specification." The primary interest of the program is an investigation of the ultimate, or failure characteristics of bolted joints.

Scope.—The "Large Bolted Joints Project" consists of static tension tests of bolted joints using 7/8 in., 1 in., and $1\frac{1}{8}$ in. high strength bolts. Special investigations have been planned for butt joints, shingle-type joints, joints fabricated from ordinary structural steel and high strength steel, and the "unbuttoning" phenomenon of long joints. Eventually, the program will include the testing of bolted joints at loads in the vicinity of 5000 kips.

This report is concerned with the results of testing butt joints fabricated from structural plate and fastened with the previously mentioned sizes of A325 bolts arranged in compact patterns. A compact pattern, as used in this paper, is defined as a bolt group having values of g/d (gage to hole diameter ratios) and p/d (pitch to hole diameter ratios) of approximately 4, and a length not greater than 5 pitches.

In an attempt to illustrate the conservatism of the 1954 specification, the ratio of nominal net tensile stress in the plate to nominal shear stress on the bolt was chosen as the basic variable of the testing program. In the following discussion, this ratio is written as the quotient, T/S. A decrease in the T/S quotient corresponds to a decrease in the shearing areas provided, or an increase in the bolt shear stress. A list of the many possible variables encountered in a program of this nature is given in Table 1, with comments concerning the variables included in this investigation.

In all, the testing program included nine compact joints, six using 7/8 in. bolts, one using 7/8 in. rivets, one using 1 in. bolts, and one using 1 1/8 in. bolts. Being designed to fail at loads in the vicinity of 1800 kips the test specimens would be called full-scale structural joints.

Previous Research.—Much work has been done by other investigators on the topic of riveted and bolted joints. Even the briefest of summaries of all these investigations would be prohibitive. However, it is appropriate to mention two summaries whose chief similarity, to the tests being described, is the size of the test specimens.

In 1940, Davis, Woodruff, and Davis reported[4] on an extensive series of static tension tests of large riveted joints. These tests were conducted at the University of California, Berkeley, Calif., in connection with the design and construction of the San Francisco-Oakland Bay Bridge. Many of the findings can be applied to bolted joints as well as to riveted ones.

---

[4] "Tension Tests of Large Riveted Joints," by R. Davis, G. Woodruff and H. Davis, Transactions, ASCE, Vol. 105, 1940, pp. 1193-1245.

In March, 1959, Vasarhelyi and others reported[5] on the static-tension tests of two large bolted joints. Because of the capacity of the testing machine, it was not possible to rupture these specimens but slip characteristics were determined. Later, smaller joints were cut from the above specimens and these were tested to failure. The four joints noted had T/S ratios of approximately 1.00/0.75.

DESCRIPTION OF TEST JOINTS

A complete description of each of the nine compact test joints is presented in Table 2. All of the test specimens were fabricated as half of a butt joint, or what might be called a "double lap" joint, consisting of an inner or main plate made up of two pieces of 18 in. by 1 in. by 7 ft-1 in. steel plate, and two outer or lap plates that were the same size of steel plate. Plate of constant thickness was used in order to minimize the effect of variation in material properties.

TABLE 1

No.	Variable	In this investigation
1	Type of load	Static load only
2	Position of load	Axial load only
3	Temperature	Room temperature
4	Type of material	ASTM-A7 Steel
5	Type of joint	One-half butt joint
6	Number of plies	All four plies
7	Grip	All 4"
8	Length of joint	Varies from 2 pitches to 5 pitches
9	Pattern	Varied by omitting bolts; no staggering
10	Pitch	3 1/2" and 4"
11	Gage	3", 3 5/8", and 4 1/2"
12	T/S	Varied by omitting bolts
13	Faying surface	All mill sc[illegible] degreased
14	Size of hole	1/16" lar[illegible]an bolt diameter
15	Type of hole	All drille[illegible]
16	Hole alignment	Drilled through four plies
17	Fastener type	A 325 bolts and A 141 rivets
18	Fastener size	7/8", 1", and 1 1/8"
19	Tensioning method	Impact wrench, Turn-of-the-nut method
20	Bolt tension	Governed by half turn of nut

---

[5] "Effects of Fabrication Techniques on Bolted Joints," by D. D. Vasarhelyi, S. Y. Beane, R. B. Madison, Zung-An Lu and U. C. Vasishth, Proceedings, ASCE, Vol. 85, No. ST 3, March, 1959, pp. 71-116.

TABLE 2.—DESCRIPTION OF TEST JOINTS

	B1	B2	B3	B4	B5	B6	BR2	A3	G1
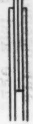	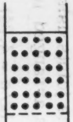	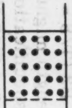	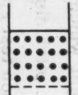	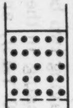	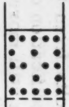	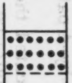	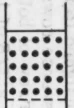	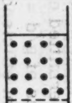	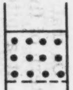
PLATE MATERIAL	MAIN PLATE : 2 Pls 18"x 1" ASTM—A7 LAP PLATES : 2 Pls 18"x 1" ASTM—A7								
NUMBER OF 7/8" A325 BOLTS	30	25	20	23	20	18	25—7/8" A141 Rivets	16—1"	12—1 1/8"
T:S RATIO	1:0.74	1:0.89	1:1.11	1:0.96	1:1.11	1:1.15	1:0.89	1:1.10	1:1.11
GAGE, g	3 5/8"	3 5/8"	3 5/8"	3 5/8"	3 5/8"	3"	3 5/8"	4 1/2"	4 1/2"
g/d	3.87	3.87	3.87	3.87	3.87	3.20	3.87	4.24	3.79
PITCH, p	3 1/2"	3 1/2"	3 1/2"	3 1/2"	3 1/2"	3 1/2"	3 1/2"	4"	4"
p/d	3.73	3.73	3.73	3.73	3.73	3.73	3.73	3.76	3.37

"d" is the diameter of the drilled hole

The first joints to be tested were those using 7/8 in. fasteners, or the "B" series, as they were designated. The first three of these specimens were designed on the basis of a progressively decreasing T/S ratio, beginning with the 1954 specification value of T/S = 1.00/0.75. On that basis, Joint B1 required thirty bolts for a T/S of 1.00/0.74. A pattern of five longitudinal lines at a gage of 3-5/8 in. and six transverse rows at a pitch of 3-1/2 in. was chosen as representing common spacings used in detailing practice. These dimensions produced a compact bolt group and permitted easy variation of the T/S ratio without major pattern changes. Values of g/d = 3.87 and p/d = 3.73 were within the range that produces greatest joint efficiencies.

The next two specimens, B2 and B3, were designed to increase the magnitude of the bolt shear stress by omitting transverse rows of bolts from the original pattern of B1. Omitting one transverse row of bolts for Joint B2 produced a 5-by-5 pattern of twenty-five bolts with a T/S of 1.00/0.89. Omitting a second transverse row of bolts produced the 5-by-4 pattern of twenty bolts in Joint B3 at a T/S of 1.00/1.11.

Test results of the first three specimens indicated the need for information on joint behavior at a T/S in the vicinity of 1.00/1.00. Joint B4 was fabricated at a T/S of 1.00/0.96 by omitting two bolts from the middle row of a 5-by-5 pattern similar to that of B2. This modification of the original close pattern suggested the design of B5 which used a still more "open" pattern, but reverted to the same T/S as Joint B3 (1.00/1.11). The bolt arrangement of B5 consisted of twenty bolts in a 5-by-5 pattern having two bolts missing in each of the second and fourth rows and one bolt missing in the middle row. Joint B6 was proportioned for the lowest T/S (1.00/1.15), and utilized the most compact pattern; 18 bolts in a 6-by-3 arrangement which reduced the gage to 3 in. (g/d = 3.20) but retained the original $3\frac{1}{2}$ in. pitch distance.

One riveted joint was designed as a comparison test specimen. The joint, designated BR2, was laid out exactly like Joint B2 (T/S = 1.00/0.89) so that a direct comparison of rivet strength to bolt strength might be made at a shear stress greater than presently allowed by rivet specifications.

Two test specimens were designed to use larger diameter bolts as a means of confirming the results obtained in tests of the joints using 7/8 in. fasteners. Joint A3 was fabricated with sixteen in. bolts arranged in a compact pattern of four longitudinal lines at a gage of $4\frac{1}{2}$ in. (g/d = 4.24) and four transverse rows at a pitch of 4 in. (p/d = 3.77). This arrangement produced a T/S of 1.00/1.10. Joint G1 utilized these same gage and pitch dimensions (but g/d = 3.79, p/d = 3.37) to place 12 - $1\frac{1}{8}$ in. bolts in a 4-by-3 pattern for a T/S of 1.00/1.11. Again, gage and pitch distances were in the range of those currently used in practice, and the corresponding values of g/d and p/d were such as to indicate efficient use of the plate material.

MATERIAL PROPERTIES

Plates.—The plate used was American Society for Testing Materials (ASTM) A7 structural steel, cut from universal mill plate (of the same heat), 18 in. by 1 in. and approximately 72 ft long. Two specimens were fabricated from each 72 ft plate after a representative piece of coupon material (18 in.

by 4 ft) was cut from the middle (Fig. 1). A comparison of actual to nominal dimensions of the plate material showed a variation of + 0.5% to - 2.0% in the gross area.

Coupons were machined from the 1 in. plate to standard dimensions[6] having a cross sectional area of approximately 1.5 sq in. at the reduced section over an 8 in. gage length. The specimens were tested in a 120 kip testing machine using the autographic strain recording device to obtain the stress-strain curve up to approximately the beginning of strain hardening. A cross head motion rate of 0.1 in. per min was used (ASTM permits 0.5 in. per min for an 8 in. gage length), while the automatic recorder was in operation, but after the recorder was disengaged the rate was increased to approximately 0.3 in. per min in order to decrease test time in the inelastic range. A typical stress-strain diagram is shown in Fig. 2.

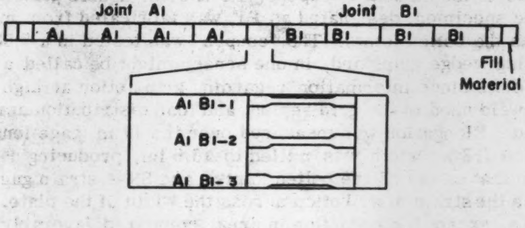

FIG. 1.—LOCATION OF COUPONS

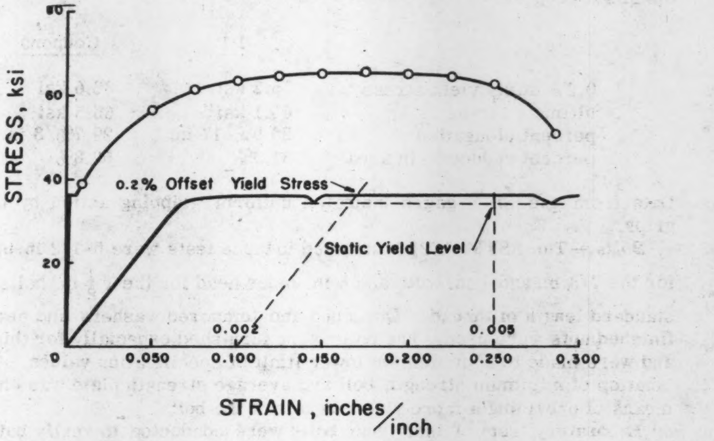

FIG. 2.—THE STRESS-STRAIN DIAGRAM
FOR PLATE MATERIAL

---

[6] "Standard Methods of Tension Testing of Metallic Materials," ASTM, ASTM E8-54T.

A summary of material properties is shown in Table 3. The average coupon yield stress is below the mill test value, but is above the minimum ASTM value of 33 ksi. Average coupon ultimate stress is approximately equal to the mill test value and is almost at the average ASTM value of 66 ksi. Variation in yield and ultimate stresses obtained in the laboratory compared to those obtained by mill tests has been explained by investigations[7] concerning the effect of strain rate on stress levels. Each coupon failure was typical of that for a ductile material.

In addition to the standard coupons, a full size, double plate "coupon" was tested. The specimen, designated as P1, was fabricated from material of the same heat as the bolted joints. The "coupon" was tested in a 5,000 kip testing machine using wedge grips and, in one sense, might be called a pilot test for the bolted joints since information regarding grip action at high loads, action of the seal weld used in the grip region, and load distribution across the plate was obtained. Elongation was measured over the 17 in. gage length of the reduced section (18 in. width was milled to 16.5 in., producing a "net" section greater than that of any of the bolted joints), and SR-4 strain gages were used to determine the strain distribution across the width of the plate. The material properties, except for reduction in area, compared favorably with those of the small coupons:

	P1	Coupons
0.2% offset yield stress	35.2 ksi	36.6 ksi
ultimate stress	65.1 ksi	65.5 ksi
percent elongation	26.5%/17 in.	29.7%/8 in.
percent reduction in area	31.0%	52.8%

Data from the SR-4 gages indicated uniform gripping action by the wedge grips.

Bolts.—The ASTM-A325 bolts used in these tests were 5-1/2 in. under head for the 7/8 in. and 1 in. bolts and 6 in. under head for the $1\frac{1}{8}$ in. bolts, and with standard length of thread. Quenched and tempered washers and heavy semi-finished nuts were used. The bolts were furnished especially for this project, and were made to approach the lower limit of specification values. The combination of minimum strength bolt and average strength plate was chosen as a means of providing a more rigorous test of the bolts.

Laboratory tests of individual bolts were conducted to verify bolt properties. Five bolts of each size were chosen at random as representative of each lot and pulled in direct tension in a 300 kip testing machine. All of the bolts satisfied the recommended proof load (PL) and ultimate load requirements specified by ASTM. The 7/8 in. bolts were closest to the desired minimum strength requirement, being an average 102% of the specified minimum ultimate load, while the 1 in. bolts were 106% and the $1\frac{1}{8}$ in. bolts were 114% of their respective minimum ultimate loads.

In conjunction with the verification of individual bolt properties, data relating load and elongation characteristics of each bolt were recorded. When

---

[7] "On the Yield Properties of Structural Steel Shapes," by L. Tall and R. L. Ketter, Fritz Lab. Report No. 220A.33, Lehigh Univ., Bethlehem, Pa., November, 1958.

TABLE 3.—RESULTS OF COUPON TESTS

Coupon Number	Static Yield Level psi	Avg. Static Yield Level psi	Yield Stress 0.2% Offset psi	Avg. Yield Stress 0.2% Offset psi	Ult. Tensile Stress psi	Avg. Ult. Tensile Stress psi	Elong. in 8" %	Avg. Elong. %	Reduct. in Area %	Avg. Reduct. in Area %
A1B1-1	32 800	34 800	41 500	38 500	74 000	68 500	30.4	30.3	54.4	51.5
-2	34 900		36 000		66 400		29.4		42.6	
-3	36 700		38 000		65 200		31.0		57.5	
A2B2-1	32 000	35 200	39 900	38 900	65 400	66 300	24.7	25.9	58.6	49.7
(G1) -2	36 600		38 500		68 800		23.1		34.3	
-3	37 000		38 400		64 700		30.0		56.3	
A3B3-1	32 800	34 200	33 400	34 300	64 700	65 800	31.7	28.6	58.8	48.6
-2	34 400		34 500		67 400		27.2		40.3	
-3	35 300		35 100		65 400		27.0		46.7	
A4B4-1	33 600	32 300	36 000	34 400	64 200	63 500	30.8	31.3	56.1	57.4
-2	29 300		31 500		61 100		32.5		58.0	
-3	33 900		35 600		65 300		30.5		58.1	
A5B5-1	34 400	33 900	36 800	36 000	65 200	64 300	29.9	31.1	55.1	56.8
-2	31 200		33 600		61 600		33.0		61.0	
-3	36 000		37 500		66 000		30.5		54.4	
A6B6-1	37 600	37 100	39 300	39 000	65 400	64 600	28.9	29.7	55.5	57.0
-2	34 200		36 300		62 200		31.2		58.7	
-3	39 500		41 500		66 100		29.1		56.7	
BR1BR2-1	33 700	33 500	35 700	35 300	64 700	65 400	30.7	30.0	55.3	48.7
-2	32 300		33 800		66 400		29.0		37.8	
-3	34 400		36 400		65 000		30.3		52.9	
Grand Avg.		34 400		36 600		65 500		29.7		52.8
Mill Test				40 700		65 000		28.0		

tested, each bolt was held at a 4 in. grip, the same length of grip used in the bolted joints, so that the load-elongation curve obtained by this procedure could be used as a calibration curve for determining the amount of internal tension of the bolts tightened in the large joint specimens. The average direct tension calibration curve for the 7/8 in. bolts is shown as the upper curve of Fig. 3. Curves for the 1 in. and $1\frac{1}{8}$ in. bolts were similar.

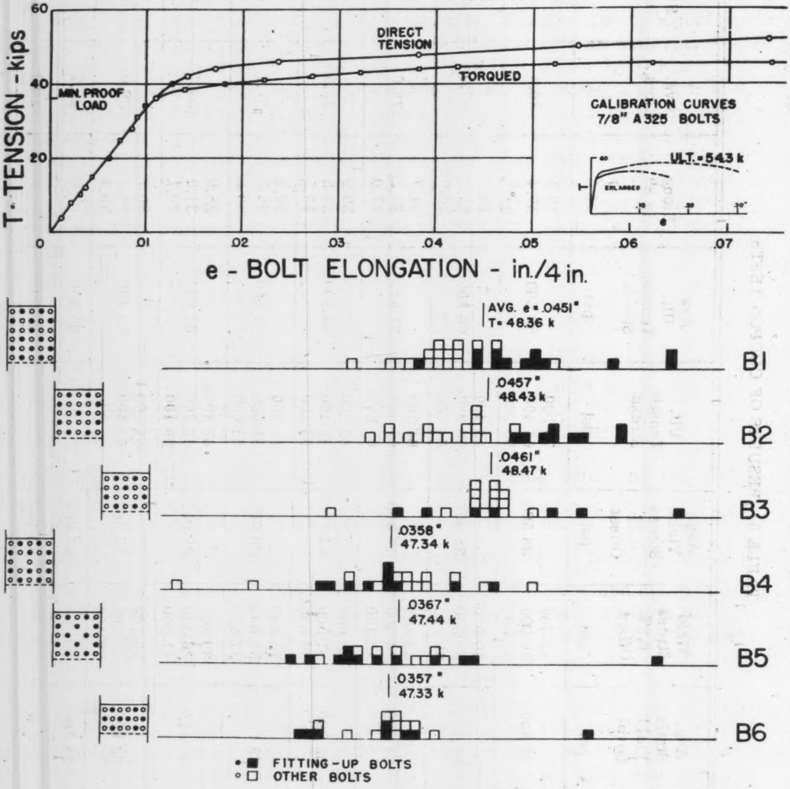

FIG. 3.—BOLT TENSION DISTRIBUTION

The lower curve of this same figure (Fig. 3) is the average calibration curve for 7/8 in. bolts as obtained for tension induced by impact torquing of the nut. Each of three bolts, chosen at random, was mounted at the 4 in. grip in a calibrator and tightened by torquing the nut in angular increments with a pneumatic impact wrench. Internal bolt load was measured by the calibrator's load cell, and bolt elongation was measured with a special extensometer.

The most important information obtained by these two different calibration procedures is not that there is a difference in the strength, but that in the region used, both methods produce a relatively "flat" load-elongation curve, a characteristic which facilitates the evaluation of total clamping force on a bolted joint. This matter is considered in detail under the section on bolt tensions.

Tests to determine the basic shear strength of single bolts were conducted by placing a bolt in a loading jig that produced double shear on the bolt when compressive loading was applied. Bolts were mounted in jigs with lubricated and non-lubricated faying surfaces, and were tensioned to various degrees of internal load. Bolts in the non-lubricated jigs failed at slightly higher loads indicating that friction carried a small but negligible part of the ultimate load. Internal tension had no effect on the value of ultimate shear stress. The average ultimate shear stress on the nominal area was approximately 80 ksi for the 7/8 in. and 1 in. bolts, and 84 ksi for the $1\frac{1}{8}$ in. bolts.

Rivets.—The rivets used in BR2, the comparison riveted joint, were formed from ASTM-A141 structural rivet steel. Standard coupons (0.505-in. diam) were machined from three manufactured rivets chosen at random, and were tested in tension. An average of the three tests showed a static yield level of 46.7 ksi and an ultimate stress of 54.6 ksi.

Shear tests of single rivets, shop driven in jigs with mill scale faying surfaces (similar to the shear tests of the high strength bolts), indicated an average value of nominal ultimate shear stress equal to 49.9 ksi.

FABRICATION OF TEST JOINTS

Shop Procedure for Bolted Joints.—The four pieces of plate used in the assembly of each joint were taken from the same rolling. The four corner holes of each joint assembly were sub-drilled and reamed for alignment. All remaining holes were drilled through the solid four plies of material while the plates were held in alignment by steel pins in the corner holes. All holes were $\frac{1}{16}$ in. larger than the nominal size of the fastener. Faying surfaces were cleaned of loose mill scale and burrs. Since the test specimens were actually one half of a butt joint, fill plates were required between the two outer plates in the gripping region. The fill plates were welded in place with a continuous 1/2 in. bead weld to insure a uniformity of wedge grip action under test and to prevent the falling of loose plate after joint failure. The gripping end of the inner plates was welded in a similar fashion. Joint assemblies were shipped with four temporary machine bolts in the corner holes.

Bolting-Up.—The bolting-up operation was conducted at Fritz Laboratory by the fabricator's field crew using their current field procedure for this type of work, namely, the "turn-of-nut" method.[8] Using this method, the amount of nut rotation required to produce the desired internal tension depends on the diameter of the bolt and the grip length. For the bolts used in these joints, the necessary rotation was one-half turn from the "snug" position.

When tightening joint B3, the standard tightening sequence was slightly modified so that information regarding the relaxation of fitting-up bolts might be obtained. After a pattern of fitting-up bolts had been selected and tightened the required half turn, these bolts were measured with the bolt extensometer to determine their change in length. The remaining bolts of the pattern were then tightened and the fitting-up bolts were measured to detect any relaxation due to the tightening of the neighboring bolts. The fitting-up bolts were checked or "touched-up" by attempting to turn the nut of each bolt with the impact wrench. The wrench operator decided by the "feel" of the wrench impacting whether further tightening was necessary. Some bolts required as much as an additional one-quarter turn while others did not require any additional tightening.

---

[8] "Installation and Tightening of High Strength Bolts," by E. F. Ball and J. J. Higgins, Proceedings, ASCE, Vol. 85, No. ST 3, March, 1959, pp. 117-131.

Measurements of the fitting-up bolts with the bolt extensometer showed a relatively small amount of relaxation when the neighboring bolts were tightened. The greatest relaxation noted was 0.0014 in. and this corresponded to a loss of approximately 4,400 lbs internal tension based on an average calibration curve. During the process of "touching-up" the fitting-up bolts, the bolt which had shown the greatest relaxation was one of those given another one-quarter turn, and this additional tightening more than restored the tension lost due to relaxation. The average internal bolt tension for all bolts, as determined from the calibration curves, was above the value required by the 1954 specifications.

The tightening sequence for the other joints followed the standard field procedure, differing from that of B3 in that no intermediate measurements of fitting-up bolts were recorded.

The elongations of all bolts used in the B-joints are plotted in Fig. 3 in the form of a histogram. From this, and the calibration curves plotted to the same abscissa, it is possible to read off the internal tension in each bolt.

Shop Procedure for Riveted Joint.—The fabrication of the comparison riveted joint, BR2, was carried out at the same time as the fabrication of Joints B4, B5, and B6, and in a similar manner. Holes were drilled through the four plies of material after the corner holes had been sub-drilled and reamed, and the plates fastened in position with four pins in the corner holes. The joint was then riveted according to ordinary shop riveting practice.

INSTRUMENTATION

Instrumentation of the test specimens included use of the following equipment:

1. Electric strain gages (SR-4) for measuring strains in the main and lap plates, within and outside the bolt pattern;
2. slide bar extensometer for measuring plate elongation between each transverse row of bolts;
3. dial gages (0.001 in.) for measuring slip between the main and lap plates at each transverse row of bolts; and
4. dial gages (0.001 in.) for measuring total elongation of the joint within the bolt pattern.

The instrumentation set-up was not identical for all tests, but was gradually developed as each completed test yielded additional information. Fig. 4 shows a typical instrumentation arrangement on one of the test joints (B2).

TEST PROCEDURE

All of the joints were loaded to failure in a 5,000 kip hydraulic testing machine, using flat wedge grips to apply the load. Fig. 5 shows one of the bolted joints mounted in the machine before testing. No special precautions were taken with alignment of the specimens. The general procedure was as follows:

1. The specimen was mounted in the test machine, fitted with the desired instrumentation, and partially enclosed with a protective screen at both faces;
2. "no-load" readings of all gages were recorded;
3. the specimen was gripped with a load of 100 kips, and "zero" readings of all gages were recorded;
4. load was applied in 100 kip increments until major slip was experienced, gages being read at each loading;
5. at major slip, the testing machine would drop load due to the sudden displacement and then stabilize at the lower value; gages were read after the stabilization;
6. load was applied in selected increments until the slip load was again reached, gages being read at each increment;
7. load was applied again in 100 kip increments, allowing time for stabilization at constant load in the inelastic range; this required about 10 min;
8. dial gages were removed and the working scaffold dismantled when a predetermined danger point was reached; and
9. load was applied to failure, reading SR-4 strain gages where possible.

TEST RESULTS

Bolt Tensions.—Values of individual bolt elongations for each of the "B" joints, as measured after completion of the bolting-up operation, are plotted along the horizontal scale of the bolt calibration curves of Fig. 3. The dark blocks represent elongations of fitting-up bolts that are indicated in the bolt patterns by solid circles. Although a considerable scatter of elongations is indicated, little difference in the individual values of internal bolt tension is found when the elongations are projected up to the calibration curves. The relatively constant values of bolt tension exist because the elongations occur at the "flat" portion of the bolt calibration curves. This same characteristic "flat" zone was found in calibrating the 1 in. and $1\frac{1}{8}$ in. bolts used in Joints A3 and G1. Since bolt tension was found to be constant regardless of the scatter in measured bolt elongations, an average value of bolt tension was obtained for each joint by entering the calibration curves with the respective average bolt elongation. To obtain the total clamping force for a given joint the value of average bolt tension was multiplied by the number of bolts in the pattern. This procedure produced the quantity that is referred to as "total initial clamping force," the clamping force that exists before load is applied to the specimen.

The effect of the "human element" upon scatter of bolt elongations may also be seen in Fig. 3. The average elongations for the first three specimens (B1, B2, B3) are quite different from the average elongations for the last three specimens (B4, B5, B6), although there is excellent agreement within the two separate groups. The difference found in the two groups is explained

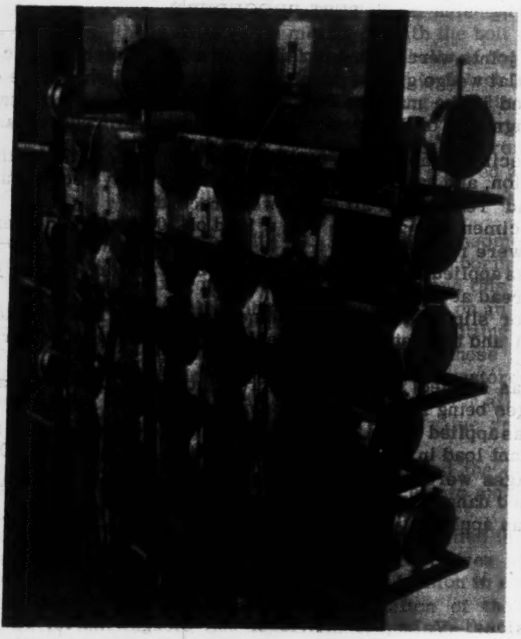

FIG. 4.—INSTRUMENTATION

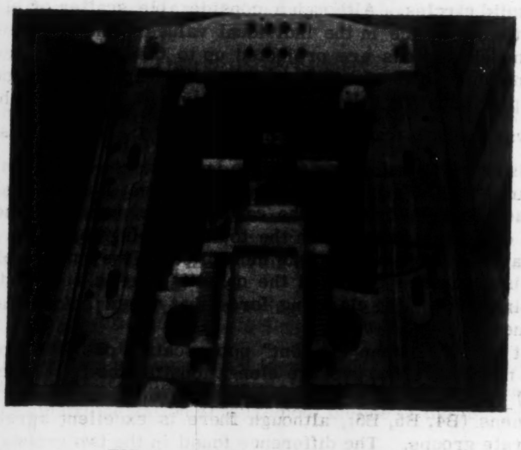

FIG. 5.—GENERAL TEST SET-UP

by the fact that the first three joints were bolted-up at the same time and by the same bolting crew, while the last three joints were bolted at a later time and by a different crew. All bolts were from the same lot and were tightened by the same procedure. The only variant in the two separate operations was the men who operated the equipment and their "feel" of the snugging and touch-up operations.

Prior to each tension test of a bolted joint all bolts within that joint were remeasured to determine if any change in length had occurred since the time of bolting-up. No change was noted after more than a ten-month lapse of time from the initial bolting-up date. No apparent loosening of the bolts was noted during this same period of time. Any large amount of relaxation of the bolts would affect the joint slip characteristics, particularly the "slip coefficient." However, no significant decrease in slip coefficient with lapse of time was suggested by the test data.

Joint Behavior Under Test.—A summary of test results is given in Table 4. During the early stages of each test, the joints experienced what has been called minor slip, characterized by a small decrease of testing machine load and a small increase in displacement as indicated by the slip and total elongation gages. Major slip occurred at some higher load and was easily distinguished by a characteristic resounding "bang" accompanied by a sudden and considerable decrease of load by the testing machine and an increase in displacement of the inner and outer plates equivalent to approximately the hole clearance.

As additional load increments were applied after major slip, periodic noises, sounding like a scraping or grating of the plate surfaces and accompanied by decreases of testing machine load of from 5 kip to 10 kip, were noted. This was believed to be caused by further slipping into complete bearing since, due to the artificial condition of dropping load created by the testing machine (in an actual structure the load would remain constant), the specimens were not initially forced to slip into full bearing at the major slip load, but experienced instead a partial slip. The slip region is indicated by the dashed lines of Fig. 7, a typical illustration of the load-elongation characteristics of a bolted joint (B2) and the comparison riveted joint (BR2). Fig. 7 is an enlargement of an area of Fig. 6.

Of the eight bolted joints tested, three resulted in plate failures and the remaining five failed either by shearing a single bolt or by shearing all bolts. Plate failures occurred when the T/S was from 1.00/0.74 to 1.00/0.96, while bolt failures were observed when the T/S was 1.00/1.10 or less. All bolt failures were initiated by failure of corner bolts, and consisted of shearing off, either at the bolt head end or the nut end, leaving the bolt shank in the hole. Similar fastener failures have been reported in tests of riveted joints[4] and in large bolted joints.[5] Two tests were stopped after the first corner bolt sheared so that plate and bolt deformations might be examined with the joints intact.

Although a bolt failure resulted when the T/S was in the neighborhood of 1.00/1.10 (See Table 4), the net section tensile stress at ultimate load was approximately equal to, and in some cases, greater than the corresponding coupon ultimate stress. Fig. 8 is a non-dimensional plot of the "efficiency" or degree to which each joint developed its corresponding coupon stress. It may be seen here that all of the fastener failure specimens (except the riveted joint) approach or exceed the horizontal line through point 1.00 which indicates full development of coupon ultimate strength. The short lines on each

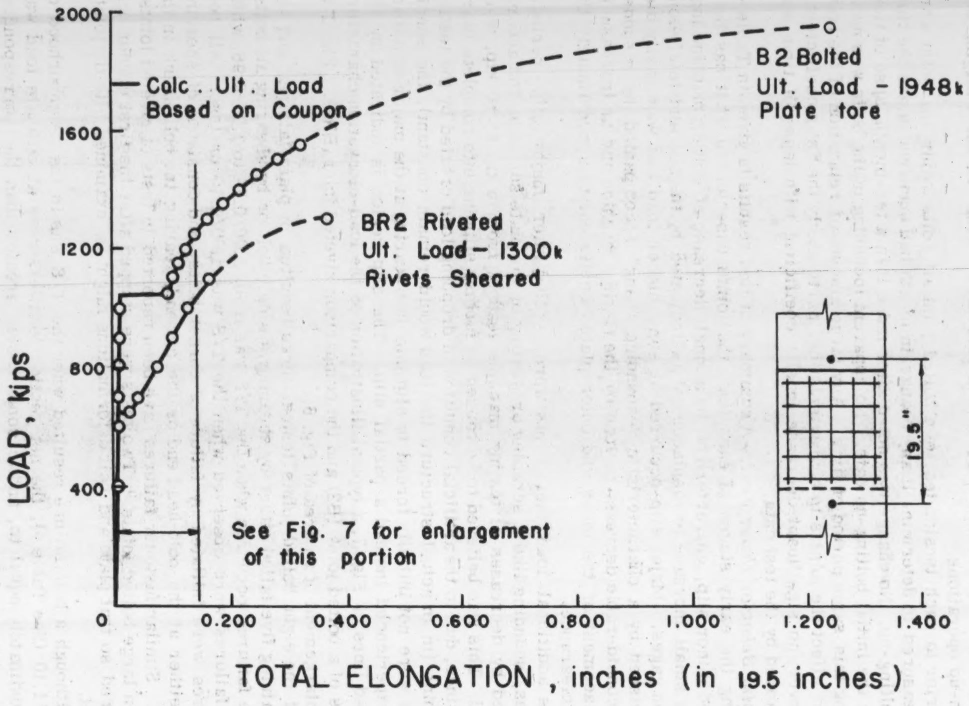

FIG. 6.—LOAD VS. TOTAL ELONGATION FOR JOINTS B2 AND BR2

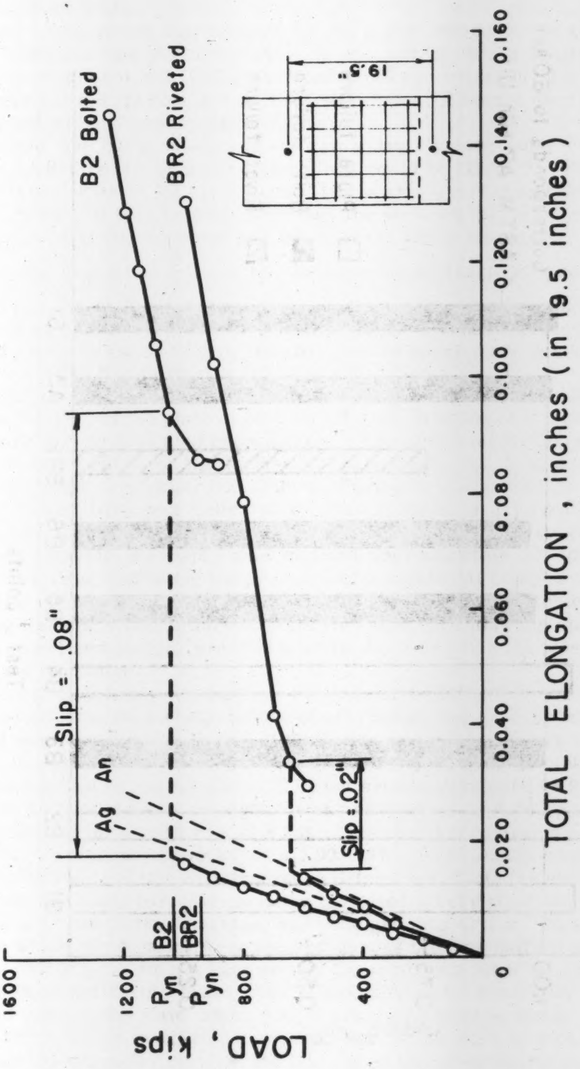

FIG. 7.—LOAD VS. TOTAL ELONGATION FOR JOINTS B2 AND BR2 (ENLARGED)

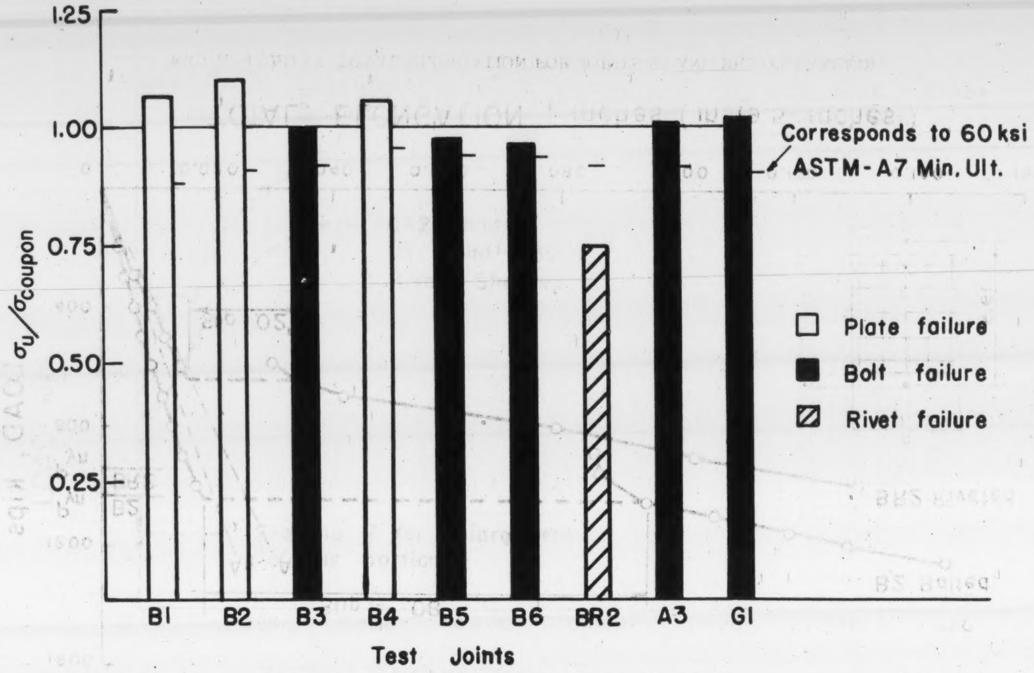

FIG. 8.—EFFICIENCY OF COMPACT JOINTS

bar indicate the level of the minimum ultimate stress of 60 ksi specified by ASTM-A7. All bolted joints developed more than this tensile stress on the net section of the plate.

In all tests except that of joint B3 (20 bolts) there was no distinction between ultimate and rupture loads. In the test of B3, a single corner bolt sheared off the nut end, and load dropped off approximately 100 kips. While load was being held constant at the lower value, a second corner bolt shear off the nut end and load dropped again.

As load was being re-applied the remaining eighteen bolts sheared simultaneously before the original failure load could be attained. Fig. 9, showing the sheared bolts of B3, is a typical representation of shear failure for the 7/8 in. bolts. It may be seen here that the shearing plane is not through the reduced area at the threaded end but is at the full shank area. For joints A3 (1 in. bolts) and G1 ($1\frac{1}{8}$ in. bolts) the commercial length of thread placed the thread run out at the shearing plane so that there may have been some reduced area effect. Values of ultimate shear stress reported in Table 4, ranged from 70 ksi to 75 ksi, (for bolt failure specimens) based on the nominal area. The bolt failure is shown in Fig. 10.

A typical plate failure may be seen in Fig. 11, the ruptured Joint B1. Notice the necking of the plate in both directions. Bending of the corner bolts in an inward direction is also recognizable. The additional transverse force due to the Poisson effect of the inelastic portion of the plate is undoubtedly the cause of premature corner bolt failure. Further evidence of this lateral force on the corner bolts was indicated by the corner hole deformation in plates from joints that failed by bolt shear. The original drilled holes were distorted to ellipses having the major axis inclined approximately 10° to the original centerline, thus, indicating the presence of a horizontal component of force on the bolts. A typical example of this hole distortion is presented in Fig. 12, showing the single bolt failure of Joint B5. Fig. 13 shows the amount of plate displacement and necking which existed in Joint B4 after the tensile failure of one of the lap plates.

The test of the only comparison riveted joint (BR2, $T/S = 1.00/0.89$) resulted in simultaneous shear failure of all rivets. The general behavior of the riveted joint was similar to that of the bolted joints. At rupture the shank and manufactured head of the rivets fell from the specimen, but the driven head remained lodged in one lap plate. The net section developed 48.9 ksi as compared to 64.6 ksi coupon strength for an "efficiency" of 0.76 as shown in Fig. 8. Ultimate shear stress was 43.3 ksi. This test demonstrates that the present (1960) rivet specifications $T/S = 1.00/0.75$ are not unduly conservative.

Plate Strains.—Strain distribution as determined from the data of the SR-4 gages and the slide bar extensometer indicated a very good alignment of the specimens in the testing machine, and good gripping action. Results of early tests in which SR-4 gages were located across the bolt pattern demonstrated that the unit strains did not vary across the joint from edge to edge.

In subsequent tests, gages were eliminated until eventually gages were mounted only on the plate edges with check gages spotted within the bolt pattern. Unit strains calculated from the pitch elongations as measured by the slide bar extensometer verified the findings of the SR-4 instrumentation. Although the measurements of the extensometer were not as fine (0.0001 in.) as those of the SR-4 gages, it was believed that the instrument would provide

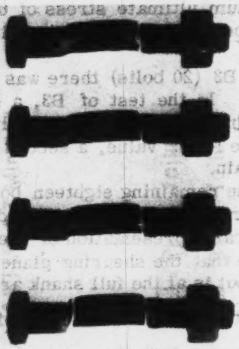

FIG. 9.—BOLT FAILURES OF JOINT B3

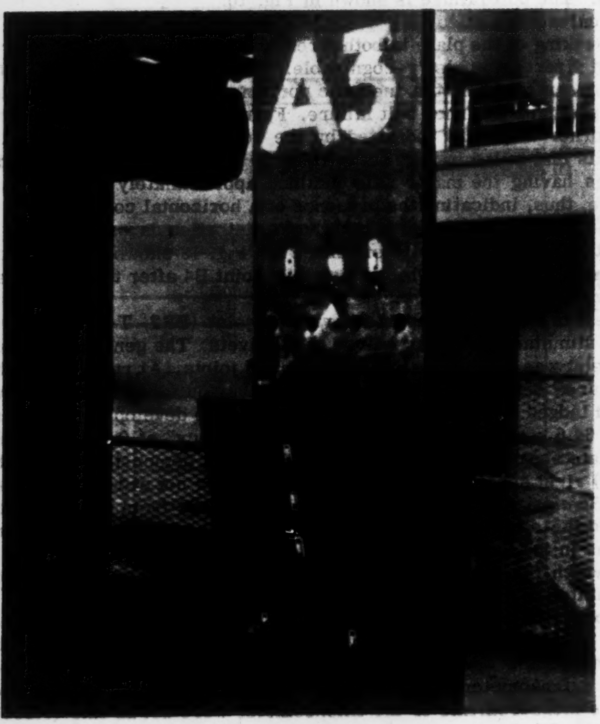

FIG. 10.—SHEAR FAILURE OF JOINT A3

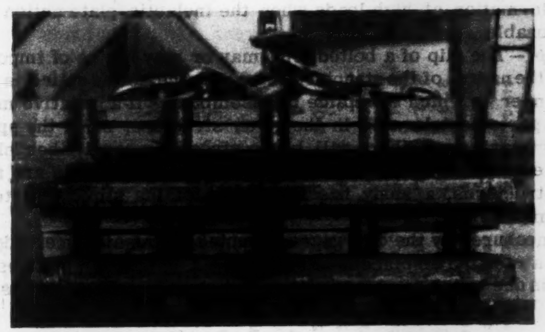

FIG. 11.—TENSILE FAILURE OF JOINT B1

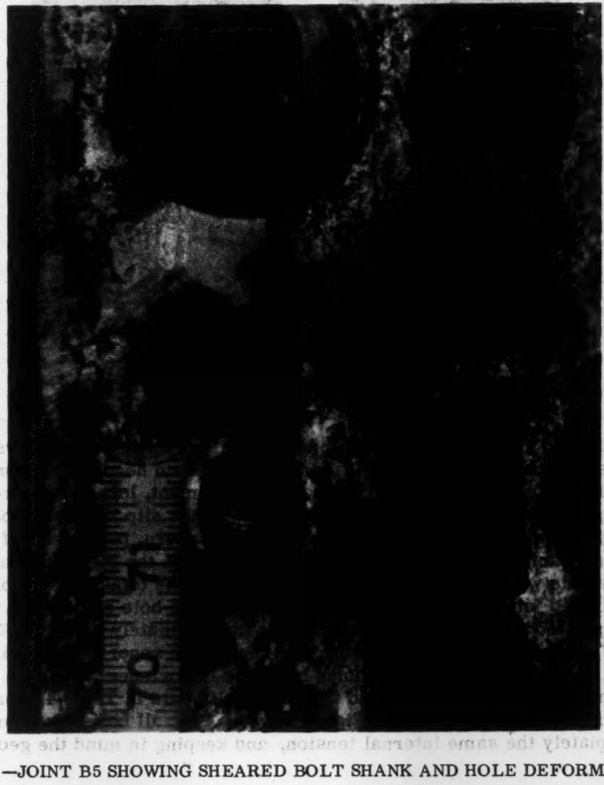

FIG. 12.—JOINT B5 SHOWING SHEARED BOLT SHANK AND HOLE DEFORMATION

valuable information at high loads when the inelastic plate action made SR-4 data questionable.

Joint Slip.—The slip of a bolted joint may or may not be of importance, depending on the nature of the structure for which the bolted splice is being used, and the manner in which the splice is assembled. If a relative movement of the mating parts is tolerable in the given structure, or if the splice is assembled in bearing and there will be no stress reversal, then slip is of no consequence. However, since the aforementioned conditions are not applicable to all structures, a study has been made of the slip characteristics for each specimen of the program.

Slip as measured by the dial gages, mounted on the specimen edges (Fig. 4), is actually a relative displacement between the main and lap plates. The displacement is due to the combined effect of the sliding of the plate surfaces and of elastic and inelastic plate strains between each row of fasteners. These plate displacements may be classified under two main headings; minor slip and major slip. Minor slip is a very small displacement, local in nature, and is caused primarily by differences in strains. Major slip is a large plate displacement occurring uniformly throughout the pattern, placing all of the fasteners in bearing or partial bearing as the result of the rigid body movement which results when surface friction is overcome. The total plate displacement for the bolted joints was 0.08 in., approximately the hole clearance, while for the one riveted joint this measurement was approximately 0.02 in. For structures in which a joint displacement of the magnitude reported here may not be allowed, the major slip load becomes of prime importance.

FIG. 13.—JOINT B4 AFTER FAILURE SHOWING SLIP AND NECKING OF MAIN PLATES

Major slip loads are presented with other slip data in Table 4. Considering the information obtained from Fig. 3 (namely that all bolts were torqued to approximately the same internal tension, and keeping in mind the geometry of

TABLE 4.—RESULTS OF JOINT TESTS

	UNITS	B1	B2	B3	B4	B5	B6	BR2	A3	G1
PATTERN		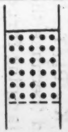	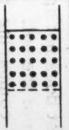	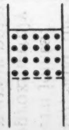	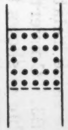	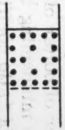	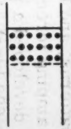	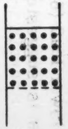	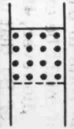	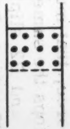
NUMBER OF 7/8" A 325 BOLTS		30	25	20	23	20	18	25-7/8" A 141 Rivets	16-1"	12-1 1/8"
NOMINAL GROSS AREA	sq in	36.0	36.0	36.0	36.0	36.0	36.0	36.0	36.0	36.0
NOMINAL NET AREA	sq in	26.6	26.6	26.6	26.6	26.6	24.8	26.6	27.5	26.5
NOMINAL SHEAR AREA	sq in	36.1	30.0	24.0	27.7	24.0	21.6	30.0	25.1	23.9
TENSION—SHEAR RATIO		1:0.74	1:0.89	1:1.11	1:0.96	1:1.11	1:1.15	1:0.89	1:1.10	1:1.11
SLIP LOAD	kips	1238	1047	911	850	609	673	654	843	920
NOMINAL BOLT SHEAR	ksi	34.3	34.9	38.0	30.7	25.4	31.2	21.8	33.6	38.5
TENSION ON NET SECTION	ksi	46.5	39.4	34.2	32.0	22.9	27.1	24.6	30.7	34.7
AVG. EXTENSION OF BOLTS	in	0.0451	0.0457	0.0461	0.0358	0.0367	0.0357		0.0317	0.0519
INITIAL CLAMPING FORCE	kips	1451	1211	970	1089	949	852		968	936
COEFFICIENT OF SLIP		0.427	0.432	0.469	0.390	0.321	0.395		0.435	0.491
ULTIMATE LOAD	kips	1956	1948	1750	1786	1680	1550	1300	1820	1798
NOMINAL BOLT SHEAR	ksi	54.2	64.9	72.9	64.5	70.0	71.8	43.3	72.5	75.2
TENSION ON NET SECTION	ksi	73.5	73.2	65.8	67.1	63.2	62.5	48.9	66.2	67.8
TYPE OF FAILURE		Tear at net section main plate	Tear at net section one lap plate	Shear of bolts	Tear at net section one lap plate	Shear of bolt	Shear of bolt	Shear of rivets	Shear of bolts	Shear of bolts
EFFICIENCY, THEORETICAL	%	73.9	73.9		73.9					
EFFICIENCY, TEST	%	79.3	81.6		78.1					
EFFICIENCY, NET	%	107.3	110.4		105.7					

the bolt patterns, one might explain the relative magnitudes of the slip loads as follows. For the first three joints, the major slip loads were in the ratio B1 > B2 > B3.

Because the slip load is dependent on total clamping force, that must depend on the number of bolts in the joint if each bolt develops the same internal tension, it would be expected that B3 slip before B2, and B2 slip before B1, because there were 20 bolts in B3, 25 bolts in B2 and 30 bolts in B1. Considering Joint B4, that had 23 bolts (three more than B3), it might be expected that the slip load would be slightly higher than that of B3. However, that was not the case. This same contradiction is seen in the data of B5 that used the identical number of bolts as in B3, but slipped at a much lower load (609 kips versus 911 kips). The explanation for these differences is suggested by a closer examination of the bolt patterns.

Joints B4 and B5 utilized what might be called "open" patterns, and for that reason probably did not obtain a uniform distribution of clamping force. Joint B6 presented the most compact pattern used, and actually developed a greater slip load than B5 that used two more bolts (673 kips versus 609 kips). A direct comparison of the slip characteristics (slip load, number of bolts) of Joints A3 and G1 to the B joints discussed previously would be misleading because larger diameter bolts were used. However, a comparison of "slip coefficients" shows that the closed patterns of A3 and G1 developed the same relative resistance to slip as the closed patterns of B1, B2, and B3. Converting the major slip loads to nominal shear stress on the bolts (Table 4) shows that the lowest shear stress was 25.4 ksi (for "open" pattern of B5), and the average shear stress was greater than 34.0 ksi for the closed pattern joints.

The riveted joint, BR2, slipped at a load that was approximately 60% of that developed by the comparable bolted joint, B2. This merely points to the fact that the clamping force of rivets is variable and at best does not approach the clamping force of A325 bolts tightened to one-half turn of the nut.

The "slip coefficient" has been chosen as a means of comparing relative resistance to slip. This number is defined by the equation $K = P_s/T_i$, in which K is the slip coefficient, P_s is one-half the major slip load (because there are two slip planes in a butt joint), and T_i is the total initial clamping force. The "coefficient" is actually a fictitious coefficient of friction, since it is obtained by taking the quotient of one-half the joint load at major slip, and the clamping force which existed before any load was applied to the joint. This procedure is similar to that in other investigations, but the misleading term, coefficient of friction, has been redesignated "slip coefficient."

Two values of slip coefficient may be calculated depending on which procedure of bolt calibration has been followed. For example, using the data of Joint B3, one value of initial bolt tension may be obtained from each of the calibration curves shown in Fig. 3. By entering the direct tension curve (upper curve) with the average bolt elongation (0.0461 in.) a clamping force of 48.5 kips per bolt or a total initial clamping force of 970 kips is obtained (48.5 kips per bolt times 20 bolts). Similarly, using the torqued calibration curve with the same value of bolt elongation, a clamping force of 45.0 kips per bolt or an average total initial clamping force of 900 kips is obtained. Major slip load for B3 was 911 kips therefore,

$$K_1 = \frac{911}{2 \times 970} = 0.469$$

$$K_2 = \frac{911}{2 \times 900} = 0.506$$

Both values are equally valid for expressing resistance to slip. Values of slip coefficient, reported in Table 4, are based on the first procedure (direct tension) since this is in line with the majority of published investigations concerned with slip in bolted joints. Values of slip coefficient for these tests (0.40) compare favorably with values of "nominal" coefficient of friction reported in other tests.[5,9]

Joint Elongation.—Fig. 6 shows a complete load-elongation curve for bolted joint B2 and the comparable riveted joint BR2. The B2 curve is representative in shape of this type of curve for other bolted joints but the total elongation at ultimate load varies according to whether a plate or bolt failure develops and, of course, depends on the length of the joint. Of more importance is the elongation of the joints in the elastic region.

In an effort to develop a technique for predicting elongation within a bolted joint of this type, it was decided to determine some "effective" area that, when used in the deflection formula, would result in a correct value for total joint elongation within the bolt pattern under elastic loading conditions. Area was chosen as the "effective" variable because in a given joint, P and L will be given, and an effective value of E might lead to confusion in design. The elongation formula was solved in terms of area and written in the form $A_{eff} = \frac{\Delta P}{\Delta e} \times \frac{L}{E}$, where $\Delta P/\Delta e$ is the slope of the experimental curve. In order to obtain the true slope defined by the experimental data, calculations were made according to the method of least squares. The calculated value of $\Delta P/\Delta e$ was then used to determine A_{eff}. The ratio A_{eff}/A_{gross} ranged from 1.25 to 1.01 for the bolted joints.

In no case was the effective area of the bolted specimen less than the gross area of the section. However, the effective area of the riveted joint was considerably less than gross area, and was only slightly greater than the actual net area. Because the only major difference between the bolted joints and the riveted joint was the magnitude of the clamping force, it seems reasonable to conclude that clamping force is the stiffening agent. It might, also, be concluded from this that in calculating the elastic elongation of a bolted joint, loaded in axial tension, reasonably accurate values would be obtained by using an effective area equal to the gross area of the main material, providing major slip does not occur. Elongations computed in this manner should be greater than those that would actually occur.

SUMMARY AND CONCLUSIONS

The following conclusions are based on the results of the static tension tests of the previously described compact, butt-type joints, fastened with 7/8 in., 1 in., and $1\frac{1}{8}$ in. A325 bolts, tightened by one-half turn of the nut.

---

[9] "Slip of Joints Under Static Loads," by R. A. Hechtman, D. R. Young, A. G. Chin and E. R. Savikko, Transactions, ASCE, Vol. 120, 1955, p. 1335.

Tension-Shear Ratio.—The 1954 specification[3] that calls for a T/S ratio = 1.00/0.75 is overly conservative for compact bolted joints under static loading (Table 4). Plate failures in the bolted joints at tension-shear ratios of 1.00/0.89 and 1.00/0.96 suggest a change to equal values of allowable stresses for tension and shear in joints of this type.

However, examination of the data from joints which failed by shear of bolts at values of T/S from 1.00/1.10 to 1.00/1.15 reveals that in all cases the net section had developed stresses greater than the minimum ultimate stress of 60 ksi. Since minimum strength bolts were used in these tests, a tension-shear ratio of 1.00/1.10 would provide a balanced design at ultimate load.

This conclusion is based on bolts for which the shearing plates cut through shank areas and not through threads. This ratio would correspond to an allowable shear stress of 22 ksi on the nominal area of the bolts when a tensile stress of 20 ksi is allowed on the net section of the plate. It is important to note that none of the bolted specimens experienced major slip at a nominal bolt shear less than 25.4 ksi, this being the value developed by the open pattern of Joint B5 which is not a recommended configuration.

Joint Slip.—The load at which a bolted joint slips into bearing is not only dependent upon the clamping force of the fasteners and the surface condition but, apparently, is also dependent upon the fastener pattern. Solid patterns (that is, no omitted bolts) in which the bolts were arranged in a compact group produced the best slip resistance.

Solid pattern compact joints with dry mill scale faying surfaces and with bolts tightened by the one-half turn of the nut will not slip below the working shear stress of 22 ksi suggested previously. The compact arrangement is also desirable from the point of view of least weight of material. The total plate displacement, or major slip, for a bolted joint with aligned holes places all bolts in bearing simultaneously, and is approximately equal to the hole clearance (Fig. 7). In large joints such as these there is no correlation between slip and yielding of the net section.

Joint Elongation.—A bolted joint stressed to the working load produces less total elongation than would be predicted for the solid plate material from which the joint was fabricated (Fig. 7). The stiffening agent is the high clamping force of the bolts. Estimates of total elongation for compact pattern joints (before slip occurs) may be obtained by using an effective stressed area equal to the gross section of the main material.

Bolt Tensions.—Internal bolt tensions obtained by the "turn-of-nut" method[8] are above the 1954 specification required bolt tension, and are of consistent magnitude, regardless of slight variations in the change of bolt length produced by tightening (Fig. 3). In the several months time that elapsed between bolting and testing of the joints, no change in bolt length or apparent loss of clamping was indicated. Loss of tension in fitting-up bolts caused by tightening neighboring bolts in the pattern was more than compensated by the "touching-up" procedure.

Plate Failures—Efficiency.—The three plate failure specimens each had a theoretical efficiency of 73.9%. The test efficiencies of these joints exceeded this by from 5% to 10%, giving net efficiencies of 105% to 110%. Stated in other terms, the maximum tensile stresses developed on the net section of the plate during test were 105% to 110% of the ultimate strength of the related coupon. This has been observed by other investigators when values of g/d have been favorable. In this case, g/d was 3.87, (Table 4).

Bolt and Rivet Failures—Fastener Efficiency.—In cases for which bolt shear was the criterion for failure, a corner bolt was always the first to fail. Average nominal bolt-shear stress at failure was 72.5 ksi, or approximately 90% of the ultimate shear stress found in tests of single bolts in double shear. Shearing occurred through full shank area or thru thread runout but not through any full thread areas.

The failure of the riveted joint, BR2, was a shear of all fasteners. Average nominal shear for the rivets of BR2 was 43.3 ksi, or approximately 87% of the ultimate shear stress found in tests of single rivets in double shear.

ACKNOWLEDGMENTS

The work reported on in this paper has been conducted at the Fritz Engineering Laboratory, Lehigh University, Bethlehem, Pa. William J. Eney is Director of the Laboratory and Head of the Department of Civil Engineering. Fabrication of the test joints was carried out at the Bethlehem Steel Co. fabricating shops in Bethlehem, Pa.

The tests and results reported herein form part of an investigation on large bolted joints sponsored, financially, by the Pennsylvania Department of Highways, and the United States Bureau of Public Roads, and guided by the Research Council on Riveted and Bolted Structural Joints.

The authors wish to express their sincere appreciation to Mr. Lynn S. Beedle who is serving as Director of the project; to the members of the advisory sub-committee, (E. J. Ruble, Chairman) for their helpful criticism; to the fabrication and erection departments of Bethlehem Steel Company, particularly Messrs. E. F. Ball, K. deVries, and J. J. Higgins for their aid in expediting the fabrication of the test specimens; to Mr. W. R. Penman and Mr. A. Schwartz of the Lebanon Plant of Bethlehem Steel Company for furnishing the bolts; and to Messrs. S. J. Errera, K. R. Harpel, and I. J. Taylor, and their staff at the Fritz Laboratory for their work in preparing the test set-up and instrumentation.

APPENDIX

A list of various terms and symbols as used in this report is given below with a brief definition or explanation:

T/S: Ratio of the tensile stress on the net section of plate to the shear stress on the nominal area of the fasteners.

g/d: Ratio of gage (transverse spacing) to the actual diameter of the hole in the plate.

p/d: Ratio of pitch (longitudinal spacing) to the actual diameter of the hole in the plate.

Proof Load (PL): A specified load at which permanent deformation of the bolt must not occur.

Direct Tension Load-Elongation Curve: Relation of internal bolt tension to bolt elongation. Determined by pulling a single bolt in static tension at a prescribed grip.

Torqued Load-Elongation Curve: Relation of internal bolt tension to bolt elongation. Determined by impact torquing the nut of a bolt which is held at a prescribed grip.

Skidmore-Wilhelm Calibrator: An instrument made up of a hydraulic load cell and a Bourdon gage which reads directly the amount of internal bolt tension induced by torquing. Used in the field to calibrate impact wrenches.

Total Initial Clamping Force: The force obtained by entering the load-elongation bolt calibration curve (Fig. 3) with the average elongation of a given bolt group, and multiplying the corresponding internal bolt load by the number of bolts in that group.

Coefficient of Slip: $K = P_s/T_i$, where P_s is one-half of the major slip load, and T_i is the total initial clamping force. Two values of K exist, depending on which curve of Fig. 3 is used to obtain the clamping force.

Fitting-up Bolt: A bolt used to draw the plies of plate material into firm contact before the remaining bolts of the pattern are tightened.

Snug: The expression used to describe the tightness of a bolt before beginning the turn of the nut. "Snug" is indicated by the impact wrench when impacting begins.

Required Bolt Tension: (According to 1954 specifications) Minimum required tension is equal to 90% of PL.

Minor Slip: Very small relative displacement of inner and outer plates of the test joint. Local in nature.

Major Slip: Sudden, large relative displacement of inner and outer plates of the test joint.

Theoretical Efficiency: Ratio of the net area to gross area of the plate.

Test Efficiency: Ratio of the maximum stress on the gross area of the test plate to the ultimate stress of the corresponding coupon.

Net Efficiency: Ratio of test efficiency to theoretical efficiency (or, ratio of the maximum stress on the net area of the test plate to the ultimate stress of the corresponding coupon).

AMERICAN SOCIETY OF CIVIL ENGINEERS

Founded November 5, 1852

TRANSACTIONS

Paper No. 3126

PRELIMINARY ANALYSIS OF CONTINUOUS GABLE FRAMES

By James W. Gillespie,[1] A. M. ASCE, and Jan J. Tuma,[2] F. ASCE

SYNOPSIS

Charts for the preliminary analysis of continuous gable frames are presented. The study is restricted to two, three, and four equal-span frames of constant cross section subjected to uniformly distributed loads. All relationships are based on the assumption of elastic deformation. Numerical examples are included.

INTRODUCTION

The design of continuous gable frames is a cut and trial procedure. The sizes of members, which cannot be found without knowing them first, must be assumed. Then the frame can be analyzed and redesigned in several trials, until a satisfactory solution is found.

To facilitate the selection of member sizes and to accelerate this process of successive approximations, algebraic formulas, based on the principle of elastic deformation, have been developed for single-span gable frames by A.

Note.—Published essentially as printed here, in April, 1960, in the Journal of the Structural Division, as Proceedings Paper 2444. Positions and titles given are those in effect when the paper or discussion was approved for publication in Transactions.

[1] Instr. in Civ. Engrg., Oklahoma State Univ., Stillwater, Okla.

[2] Prof. of Civ. Engrg., Oklahoma State Univ., Stillwater, Okla.

Kleinlogel,[3] K. Beyer,[4] R. Saliger,[5] Z. Bažant, et al,[6] A. Amerikian,[7] John D. Griffiths,[8] M. P. Korn,[9] and others.

For the analysis of continuous gable frames, algebraic formulas based on the principle of elastic deformation have been derived by Kleinlogel.[10]

Charts for the analysis of continuous gabel frames are presented herein. Two, three, and four equal-span frames of constant cross section subjected to uniformly distributed loads are considered. The bottoms of frames are assumed to be hinged and all dimensions are expressed in terms of the span and parameters α and β (Fig. 1).

All deformations are assumed to be elastic. The deformations due to normal forces and shearing forces are neglected. The sign convention of the slope-deflection method is introduced. The positive reactive moments and angular rotations are clockwise. The positive reactive forces are to the right and upward. The positive linear displacements are to the left.

The slope-deflection equations used in this study were formulated by A. Vasquez Pena[11] and F. Hedges.[12] The standard nomenclature is used throughout the paper. The meaning of special symbols is explained wherever they occur.

NOMENCLATURE

M_{ij} = Moment at i on member ij;

H_{ij} = Horizontal thrust at i on member ij;

V_{ij} = Shear at i on member ij;

α = Column parameter;

β = Gable height parameter;

γ = $\sqrt{1 + 4\beta^2}$;

θ_i = Angular rotation at i;

Δ_{ix} = Horizontal displacement at i;

Δ_{ijx} = Relative horizontal displacement $\Delta_{ix} - \Delta_{jx}$;

w = Intensity of load; and

Q_{ij} = Moment coefficient for M_{ij}.

---

[3] "Rigid Frame Formulas," by A. Kleinlogel, 1st. Amer. Edition, New York, 1952, pp. 329-338.

[4] "Statik Im Stahlbetonbau," by K. Beyer, 2nd Edition, Berlin, 1948, pp. 581-583.

[5] "Praktische Statik," by R. Saliger, 6th Edition, Wien, 1949, pp. 410-412.

[6] "Statika Stavebnich Konstrukci," by Z. Bazant, F. Klokner and K. Hruban, 7th Edition, Praha, 1953, pp. 214-216,220.

[7] "Analysis of Rigid Frames," by A. Amerikian, Washington, 1942, pp. 146-233.

[8] "Single Span Rigid Frames in Steel," by John D. Griffiths, AISC publication, New York, 1948, pp. 14-15,18.

[9] "Steel Rigid Frames Manual," by M. P. Korn, Ann Arbor, Mich., 1953, pp. 27-49.

[10] "Mehrstielige Rahmen," by A. Kleinlogel, Vol. II, 6th Edition, New York, 1948, pp. 97-184.

[11] "A Method of Analysis of Structures with Symmetrical Members," by A. Vasquez Pena, M.S. Report, Oklahoma State Univ. Library, Stillwater, Okla., 1955.

[12] "Moment Distribution in Frames with Bent Members," by F. Hedges, M.S. Report, Oklahoma State Univ. Library, Stillwater, Okla., 1956.

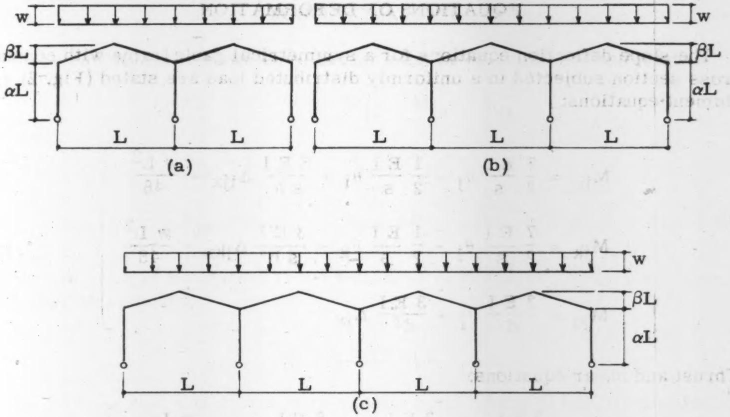
w
βL
αL
L
L
(a)
w
βL
αL
L
L
L
(b)
w
βL
αL
L
L
L
L
(c)

FIG. 1.–CONTINUOUS GABLE FRAMES

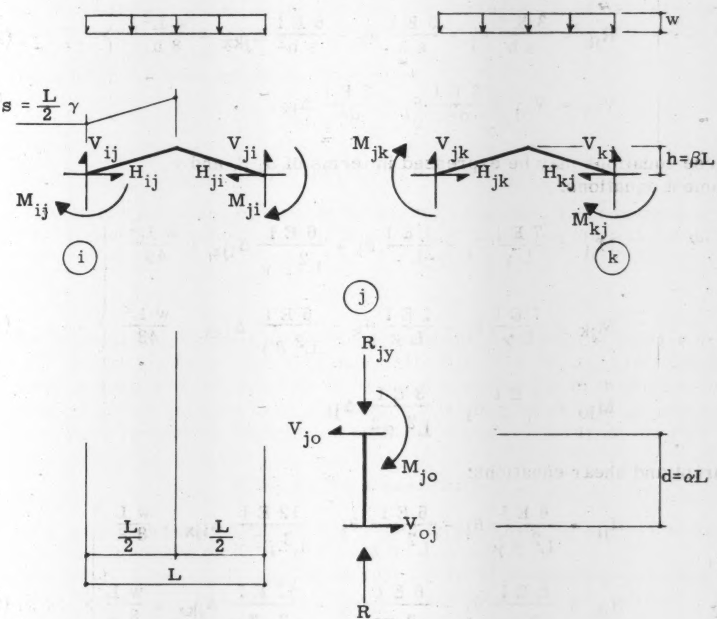
w
s = L/2 γ
V_ij
H_ij
M_ij
V_ji
H_ji
M_ji
i
M_jk
V_jk
H_jk
V_kj
H_kj
M_kj
h=βL
k
j
R_jy
V_jo
M_jo
V_oj
R_oy
o
d=αL
L/2
L/2
L

FIG. 2.–A TYPICAL JOINT

EQUATIONS OF DEFORMATION

The slope deflection equations for a symmetrical gable frame with constant cross section subjected to a uniformly distributed load are stated (Fig. 2) as:
Moment equations:

$$\left.\begin{aligned}
M_{ji} &= \frac{7}{2}\,\frac{E\,I}{s}\,\theta_j - \frac{1}{2}\,\frac{E\,I}{s}\,\theta_i + \frac{3\,E\,I}{s\,h}\,\Delta_{ijx} + \frac{w\,L^2}{48}\\
M_{jk} &= \frac{7}{2}\,\frac{E\,I}{s}\,\theta_j - \frac{1}{2}\,\frac{E\,I}{s}\,\theta_k - \frac{3\,E\,I}{s\,h}\,\Delta_{jkx} - \frac{w\,L^2}{48}\\
M_{jo} &= \frac{3\,E\,I}{d}\,\theta_j + \frac{3\,E\,I}{d^2}\,\Delta_{jx}
\end{aligned}\right\}\;\ldots\ldots\,(1a)$$

Thrust and shear equations:

$$\left.\begin{aligned}
H_{ji} &= \frac{3\,E\,I}{s\,h}\,\theta_i - \frac{3\,E\,I}{s\,h}\,\theta_j - \frac{6\,E\,I}{s\,h^2}\,\Delta_{ijx} + \frac{w\,L^2}{8\,h}\\
H_{jk} &= \frac{3\,E\,I}{s\,h}\,\theta_j - \frac{3\,E\,I}{s\,h}\,\theta_k - \frac{6\,E\,I}{s\,h^2}\,\Delta_{jkx} + \frac{w\,L^2}{8\,h}\\
V_{jo} &= V_{oj} = \frac{3\,E\,I}{d^2}\,\theta_j + \frac{3\,E\,I}{d^3}\,\Delta_{jx}
\end{aligned}\right\}\;\ldots\ldots\,(2a)$$

These equations may be expressed in terms of α, β, and γ.
Moment equations:

$$\left.\begin{aligned}
M_{ji} &= \frac{7\,E\,I}{L\,\gamma}\,\theta_j - \frac{1\,E\,I}{L\,\gamma}\,\theta_i + \frac{6\,E\,I}{L^2\,\beta\,\gamma}\,\Delta_{ijx} + \frac{w\,L^2}{48}\\
M_{jk} &= \frac{7\,E\,I}{L\,\gamma}\,\theta_j - \frac{1\,E\,I}{L\,\gamma}\,\theta_k - \frac{6\,E\,I}{L^2\,\beta\,\gamma}\,\Delta_{jkx} - \frac{w\,L^2}{48}\\
M_{jo} &= \frac{3\,E\,I}{L\,\alpha}\,\theta_j + \frac{3\,E\,I}{L^2\,\alpha^2}\,\Delta_{jx}
\end{aligned}\right\}\;\ldots\ldots\,(1b)$$

Thrust and shear equations:

$$\left.\begin{aligned}
H_{ji} &= \frac{6\,E\,I}{L^2\,\beta\,\gamma}\,\theta_i - \frac{6\,E\,I}{L^2\,\beta\,\gamma}\,\theta_j - \frac{12\,E\,I}{L^3\,\beta^2\,\gamma}\,\Delta_{ijx} + \frac{w\,L}{8\,\beta}\\
H_{jk} &= \frac{6\,E\,I}{L^2\,\beta\,\gamma}\,\theta_j - \frac{6\,E\,I}{L^2\,\beta\,\gamma}\,\theta_k - \frac{12\,E\,I}{L^3\,\beta^2\,\gamma}\,\Delta_{jkx} + \frac{w\,L}{8\,\beta}\\
V_{jo} &= V_{oj} = \frac{3\,E\,I}{L^2\,\alpha^2}\,\theta_j + \frac{3\,E\,I}{L^3\,\alpha^3}\,\Delta_{jx}
\end{aligned}\right\}\;\ldots\ldots\,(2b)$$

JOINT EQUATIONS

Three conditions of static equilibrium must be satisfied at each joint:

$$\sum M_j = 0 \quad \Big| \quad M_{ji} + M_{jo} + M_{jk} = 0 \qquad (3)$$

$$\sum F_{jx} = 0 \quad \Big| \quad -H_{ji} - V_{jo} + H_{jk} = 0 \qquad (4)$$

$$\sum F_{jy} = 0 \quad \Big| \quad V_{ji} - R_{jy} + V_{jk} = 0 \qquad (5)$$

In the case of rigid foundation at the bottom of each column, only joint Eqs. 3 and 4 may be considered.

MATRIX TABLE

The joint Eqs. 3 and 4 have been expressed in terms of Eqs. 1b and 2b for all joints of the two, three, and four span gable frames shown in Fig. 1. The results were recorded in three matrix tables each corresponding to one frame. In the formation of these matrices, the reoccurrence of certain groups of terms was noted. This phenomena is due to the nature of the frame and the slope-deflection equation.

The solution of these matrices in terms of

$$\alpha = 0.2, 0.4, 0.5, 0.6, 0.7, 0.8, 1.0$$

$$\beta = 0.1, 0.2, 0.3, 0.4, 0.5$$

is accomplished by means of the IBM 650 digital computer. The computer program is on file in the school of Civil Engineering, Oklahoma State University.

CHARTS

The deformation equivalents obtained from the IBM 650 output have been used for the calculation of moment coefficients Q's. The results are recorded graphically (Charts A-20, A-21, A-30 through A-33, and A-40 through A-44). The charts can be utilixed very efficiently if β has a value that is charted. Quite accurate results can be obtained by linear interpolation from the charts.

NUMERICAL EXAMPLES

Three numerical examples are introduced to illustrate the numerical procedure. All values are given in feet, kips, or kip-feet.

Example 1.—A two-equal-span gable frame (Fig. 3) is analyzed by means of Charts A-20 and A-21 and the results are compared with those obtained[13] by M. P. Korn and J. S. Kinney.

---

[13] "Steel Rigid Frames Manual-Analysis of Multispan Rigid Frames," by M. P. Korn and J. S. Kinney, Ann Arbor, Mich., 1953, pp. 59-65.

(a) Parameters:

$$\alpha = \frac{15}{40} = 0.375 \quad \Big| \quad \beta = \frac{10}{40} = 0.250 \qquad w\,L^2 = 3{,}200$$

(b) End moments:

From Charts	From Korn and Kinney
$M_{12} = -(0.0580)(3{,}200) = -185.60$	$M_{12} = -187.80$
$M_{21} = +(0.0663)(3{,}200) = +212.16$	$M_{21} = +215.40$

Example 2.—A three-equal-span gable frame (Fig. 4) is analyzed by means of Charts A-30 through A-33 and the results are compared with those of F. Hedges.[12]

(a) Parameters:

$$\alpha = \frac{20}{40} = 0.500 \qquad \beta = \frac{10}{40} = 0.250 \qquad w\,L^2 = 1{,}920$$

(b) End moments:

From Charts	From Hedges
$M_{12} = -(0.0605)(1{,}920) = -116.16$	$M_{12} = -116.60$
$M_{21} = +(0.0682)(1{,}920) = +130.94$	$M_{21} = +132.60$
$M_{20} = +(0.0020)(1{,}920) = +\ 3.84$	$M_{20} = +\ 3.00$
$M_{23} = -(0.0702)(1{,}920) = -134.78$	$M_{23} = -135.00$

Example 3.—A four-equal-span gable frame (Fig. 5) is analyzed by means of Charts A-40 through A-44, and the results are compared with those of J. J. Tuma et al.[14]

(a) Parameters:

$$\alpha = \frac{19}{40} = 0.475 \quad \Big| \quad \beta = \frac{6}{40} = 0.150 \quad \Big| \quad w\,L^2 = 1{,}216$$

---

[14] "Analysis of Frames with Curved and Bent Members," by J. J. Tuma, K. S. Havner and F. Hedges, Proceedings, ASCE, Vol. 84, No. ST 5, September, 1958, pp. 19-22.

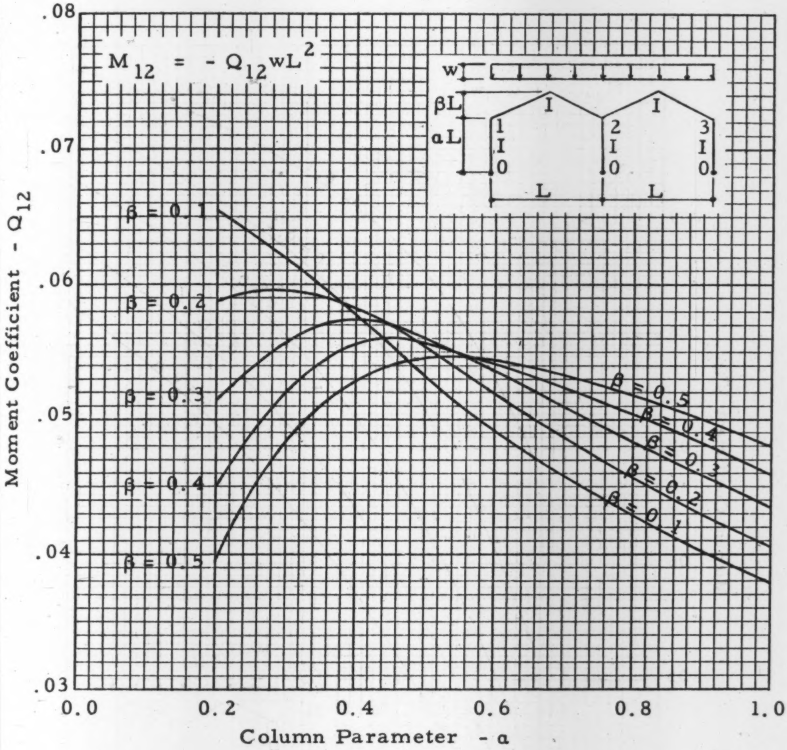

CHART A-20.—TWO-SPAN FRAME, BENT GIRDERS

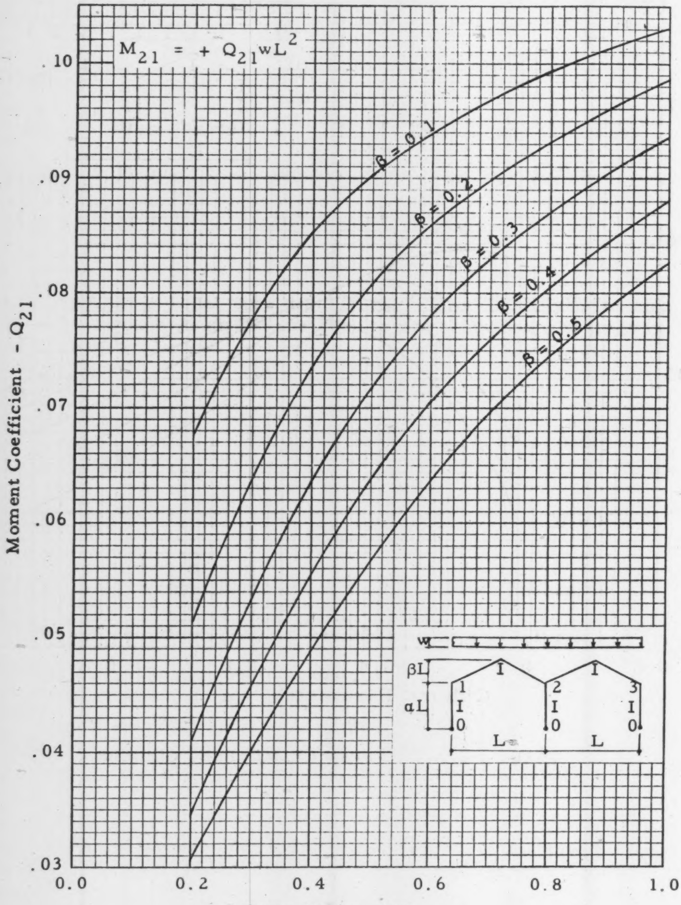

CHART A-21.—TWO SPAN FRAME, BENT GIRDERS

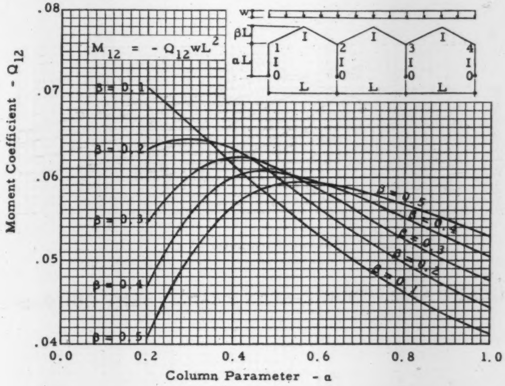

CHART A-30.—THREE-SPAN FRAME, BENT GIRDERS

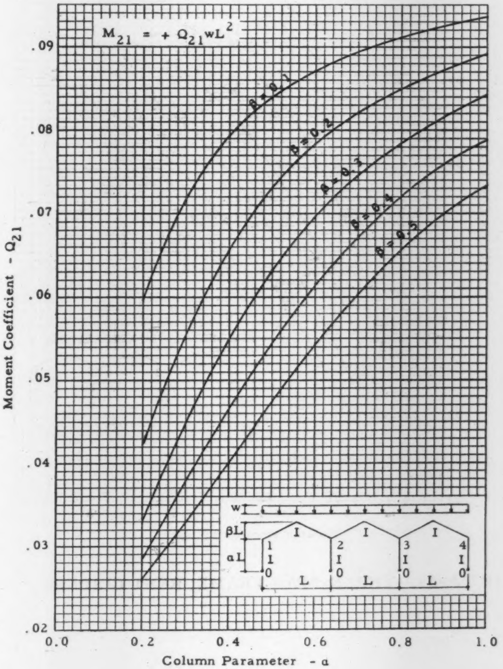

CHART A-31.—THREE-SPAN FRAME, BENT GIRDERS

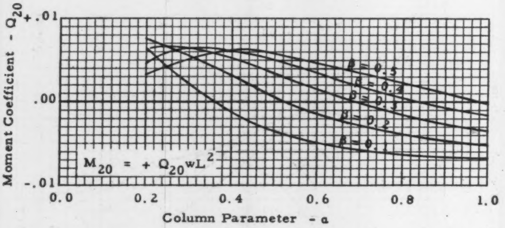

CHART A-32.- THREE-SPAN FRAME, BENT GIRDERS

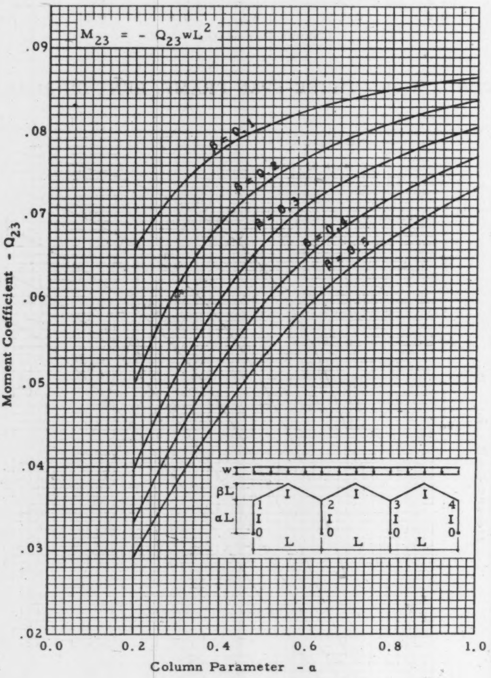

CHART A-33.—THREE-SPAN FRAME, BENT GIRDERS

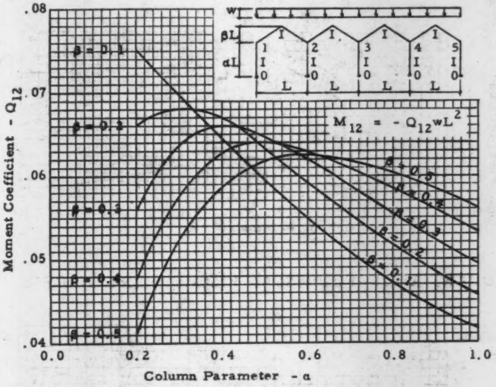

CHART A-40.—FOUR-SPAN FRAME, BENT GIRDERS

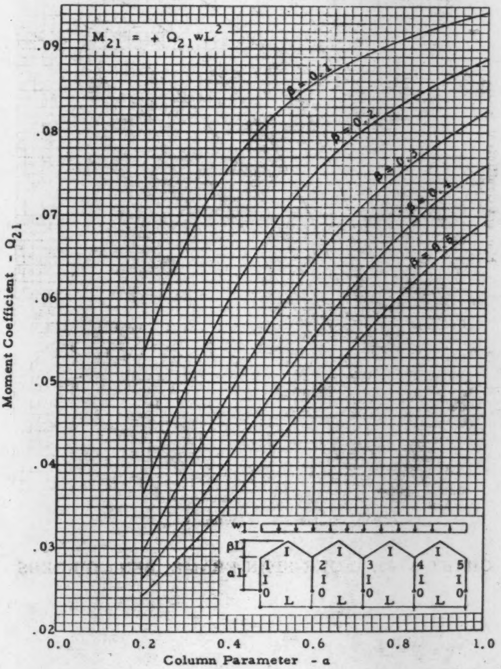

CHART A-41.—FOUR-SPAN FRAME, BENT GIRDERS

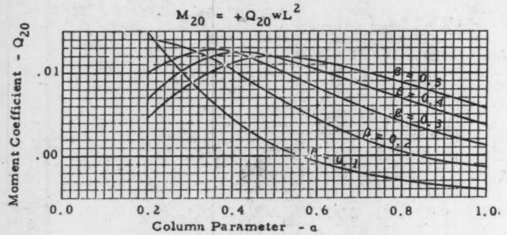

CHART A-42.—FOUR-SPAN FRAME, BENT GIRDERS

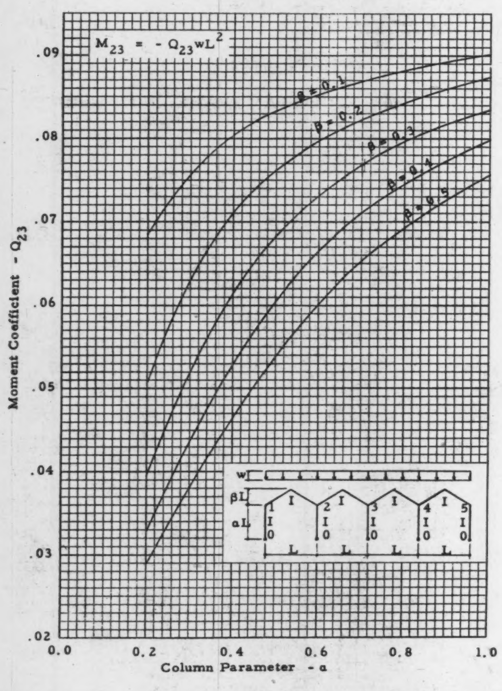

CHART A-43.—FOUR-SPAN FRAME, BENT GIRDERS

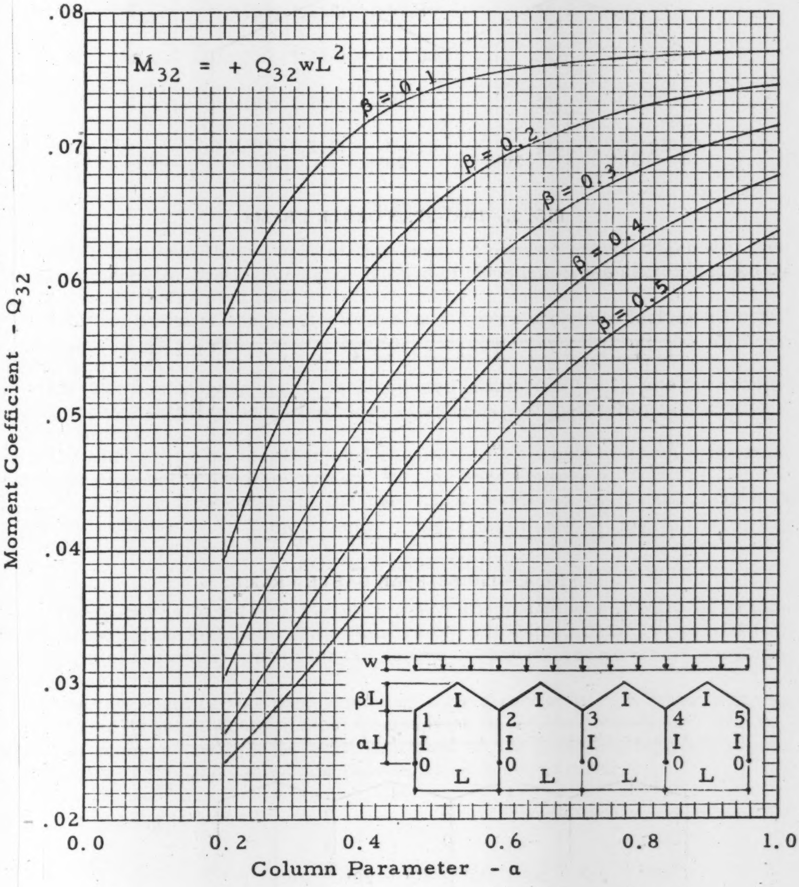

CHART A-44.—FOUR-SPAN FRAME, BENT GIRDERS

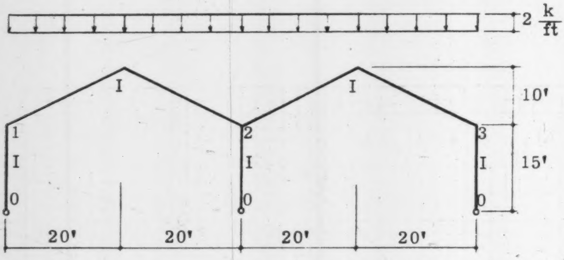
2 k/ft
I
I
10'
1
2
3
I
I
I
15'
0
0
0
20'
20'
20'
20'

FIG. 3.—TWO-SPAN GABLE FRAME

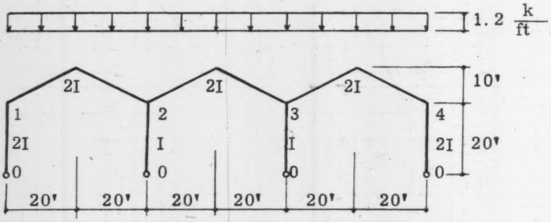
1.2 k/ft
2I
2I
2I
10'
1
2
3
4
2I
I
I
2I
20'
0
0
0
0
20'
20'
20'
20'
20'
20'

FIG. 4.—THREE-SPAN GABLE FRAME

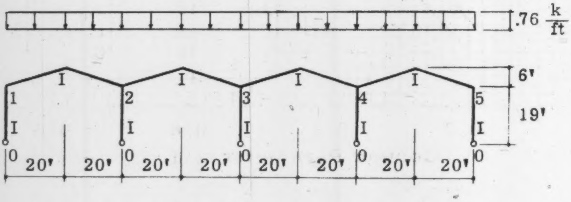
.76 k/ft
I
I
I
I
6'
1
2
3
4
5
I
I
I
I
I
19'
0
0
0
0
0
20'
20'
20'
20'
20'
20'
20'
20'

FIG. 5.—FOUR-SPAN GABLE FRAME

(b) End moments:

From Tables A-40 through A-44	From Tuma, et al
$M_{12} = -(0.0625)(1,216) = -76.00$	$M_{12} = -76.34$
$M_{21} = +(0.0739)(1,216) = +89.86$	$M_{21} = +89.73$
$M_{20} = +(0.0050)(1,216) = +\ 6.08$	$M_{20} = +\ 6.55$
$M_{23} = -(0.0789)(1,216) = -95.94$	$M_{23} = -96.27$
$M_{32} = +(0.0692)(1,216) = +84.15$	$M_{32} = +84.25$

SUMMARY

(1) It has been the purpose of this paper to present charts which will give end moments for continuous gable frames of constant cross section loaded by a uniformly distributed load.

(2) The limits of the parameters α and β were chosen to include all combinations of span length, column length, and gable height that are thought to be practical.

(3) The use of these charts is illustrated (Examples 1,2,3), and the results indicate that they can be utilized very effectively for the preliminary analysis of these frames.

(4) Similar charts for other load conditions, variations of spans, and cross sections are being prepared and will be published elsewhere.[16]

(5) For the final analysis the procedure developed by Tuma, et al[12] is recommended.

ACKNOWLEDGMENTS

This paper is based on a thesis by J. W. Gillespie[15] submitted to the graduate school of the Oklahoma State University, Stillwater, Okla., in partial fulfillment of the requirements for the degree of Master of Science in Civil Engineering.

The investigation was performed under the direction of J. J. Tuma, and was supported by the Robberson Steel Company of Oklahoma City, Okla. The reported moment coefficients were compiled on the IBM 650 electronic digital computer at the Oklahoma State University computing center.

---

[15] "Tables and Nomographic Charts for the Preliminary Analysis of Continuous Rigid Frames with Bent Members," by J. W. Gillespie, M.S. Thesis, Oklahoma State Univ. Library, Stillwater, Okla., 1958.

[16] "Charts for Preliminary Analysis of Continuous Gable Frames," by J. W. Gillespie, Oklahoma State University Engineering Experiment Station Publication, Stillwater (in preparation).

AMERICAN SOCIETY OF CIVIL ENGINEERS

Founded November 5, 1852

TRANSACTIONS

Paper No. 3129

CONCRETE ADDITION TO CELLULAR SHEET PILE SHIPWAY

By John W. Irvine,[1] F. ASCE, and Richard F. Gaston[2]

SYNOPSIS

A graving dock used as a shipway, and constructed of cellular sheet piling in the early days of World War II, has been lengthened 100 ft. The additional length was provided by sinking a reinforced concrete trapezoidal-shaped cofferdam with the aid of open dredged wells.

The opportunity for construction of the first nuclear powered aircraft carrier necessitated lengthening of submerged Shipway No. 11 at the Newport News Shipbuilding and Dry Dock Co., Newport News, Va.

In 1940-1943, in order to provide for the construction of major naval vessels (particularly aircraft carriers) the Newport News Shipbuilding and Dry Dock Co. constructed two adjoining shipways, the larger of which was Shipway No. 11 (1,000 ft long, 140 ft wide at the gate entrance, and 40 ft deep over the sill at mean high water). In this shipway there were constructed six LSTs which were launched simultaneously, and since that time, many aircraft carriers of the ESSEX Class, the MIDWAY Class, and later the FORRESTAL and RANGER.[3]

Note.—Published essentially as printed here, in May, 1960, in the Journal of the Construction Division, as Proceedings Paper 2493. Positions and titles given are those in effect when the paper or discussion was approved for publication in Transactions.

[1] Plant Engr., Newport News Shipbuilding and Dry Dock Co., Newport News, Va.

[2] Staff Supervisor, Plant Engrs. Dept., Newport News Shipbuilding and Dry Dock Co., Newport News, Va.

[3] "Shipways with Cellular Walls on a Marl Foundation," by M. M. FitzHugh, J. S. Miller and K. Terzaghi, Transactions, Vol. 112, 1947, p. 298.

The first nuclear powered aircraft carrier which is to be christened the ENTERPRISE, after its famous predecessor, which was also built at Newport News, was designed with its length greater than the 1,000 ft capacity of the shipway.

It was necessary, therefore, to lengthen the shipway and designs were made and plans drawn to increase the original effective length to 1,100 ft. Several methods of adding this additional length were investigated. Although the natural inclination was to continue the extension in cellular steel pile construction, there was the difficult problem of maintaining not only the stability of the present structure which depended on the interlocking cells, but also the adjacent shop buildings and equipment. It was, therefore, decided to adopt a plan using a concrete caisson.

Design plans and cost estimates were invited from the original builders of the shipway, in 1940, due to their familiarity with the site and ground conditions and after acceptance, work was commenced on April 28, 1958.

Prior to the contractor starting work, it was necessary to relocate all underground facilities in the area. This involved moving a sanitary sewer, storm sewer, 10 KVA cables, oxygen and propane gas lines, air, steam, fresh and salt water lines. The contractor only had to remove one foundation footing from an abandoned trestle, the roadway paving and the concrete wall and walkway across the head of the shipway.

When the caisson was first laid out, it was found that an existing 36-in. diameter deep-well, installed when the shipways were built, was out of plumb and would foul the cutting edge of the caisson before it reached plan grade. Therefore, the north-south axis of the caisson was moved 16 in. toward the east.

The caisson was unusual in some respects, as it was open on one side which had to be closed with a temporary timber bulkhead. It was 94 ft by 76 ft in area and 61 ft deep, from the cutting edge to the top of the capped wells. The site of the extension showing partial excavation preparatory to setting the steel cutting-edge is shown in Fig. 1.

The cutting edge, along the entire outside perimeter and along the longitudinal center line, consisted of two $\frac{1}{2}$ in. steel plates 18 in. wide, one vertical and the other inclined at a 45° angle, welded continuously and reinforced with 1-in. diameter reinforcing rods 4 ft long, with hooked ends, spaced at 12 in. center to center (Fig. 2). This cutting edge was fabricated by the Shipyard for the contractor.

The entire perimeter and the longitudinal center line was excavated to a depth of 6 ft and the cutting edge was set at El. 103.

While preparations were being made to set the cutting edge, the straight wall forms and the barrel forms (for the dredging wells) were being built in the bottom of Shipway No. 11. These forms were built 16 ft in height to handle the maximum concrete pour contemplated.

After placing the cutting edge, next came the first setting of the barrel forms. These were set with their bottoms at the original ground level, which was decked with scrap boards. This would be the top of the work chamber of the caisson. All excavation would be from this work chamber through the dredging wells (Fig. 3). Following the setting of the barrel forms the outside forms were set to enclose the first concrete pour which was 1,050 cu yd. This form-setting procedure was repeated four times, with two concrete pours being made before each shifting of forms. The total concrete in these eight pours was 6,760 cu yd.

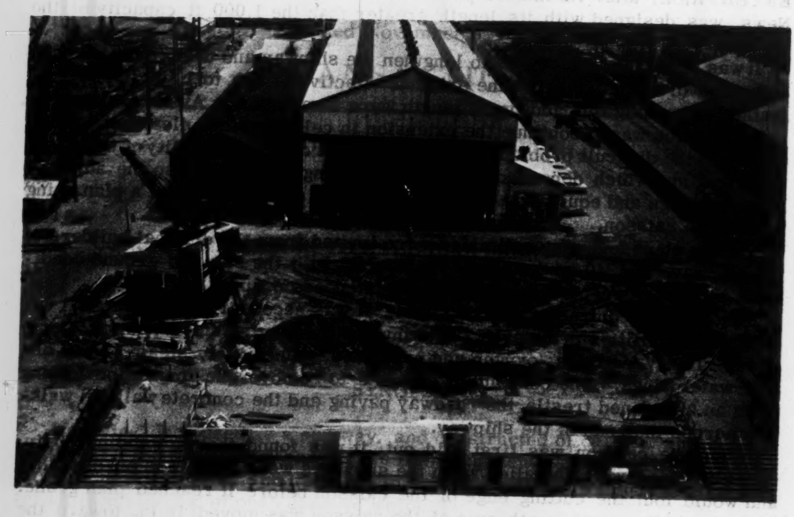

FIG. 1.—SITE OF SHIPWAY NO. 11

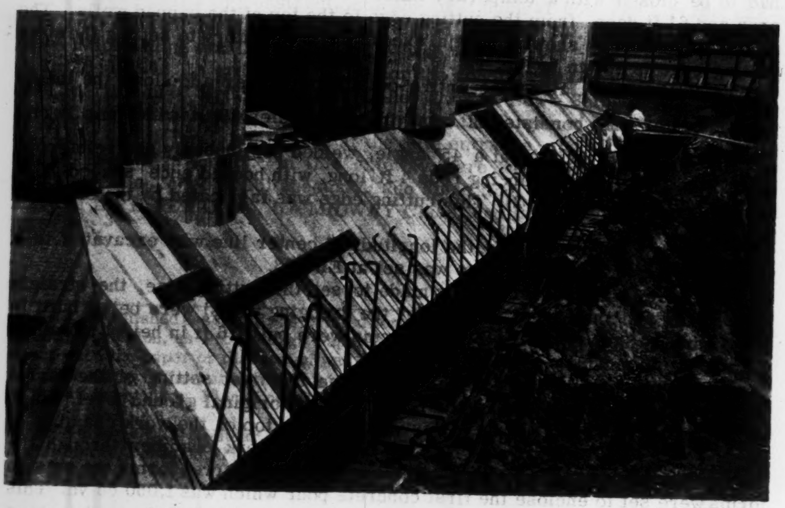

FIG. 2.—STEEL CUTTING EDGE

All concrete was transit-mixed and was transferred in place with six 2 cu yd bottom-dump buckets, handled by two whirler derricks, one each side of the shipway, track mounted for mobility. This set up and procedure worked satisfactorily and all succeeding pours were handled in this manner. Fig. 4 shows the initial slab completely formed ready for pouring, and Fig. 5 with the forms removed. Excavation has just begun in this photograph and cranes can be seen dropping earth into hoppers and awaiting trucks.

After pouring the first section of the caisson, and proper curing, excavastarted, working through the dredge wells with $1\frac{1}{2}$ yd heavy duty clam-shell buckets. When the wells were excavated to the approximate depth of the cutting edge, the areas between the wells then had to be broken out by hand excavation. The first 10 ft of excavation was hauled-in fill and was relatively easy to dig; however, below this level, blue marl was encountered. This is a sandy clay with some shells, and in the undisturbed state it is very hard. Hand picks, air spades, and water jets were all used to loosen this material but progress was so slow some other method had to be used. The contractor, with the Yard's permission, then resorted to the use of dynamite. A total of 6,545 sticks of 20% dynamite was used. In Fig. 6, the caisson has begun to take its completed shape. The first section has been added to the initial slab.

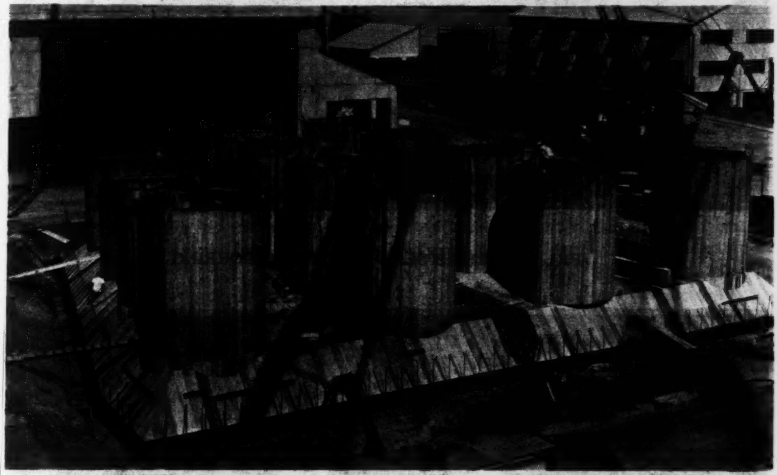

FIG. 3.—INITIAL SLAB WITH STEEL CUTTING EDGE

With the removal of the excavation under the caisson its sinking was accomplished by its dead weight. As each additional lift of approximately 16 ft was added the sinking became more uniform. Also, it involved the problem, where the marl was dry on the east side and wet on the west, of holding the caisson in a level plane. To check this feature, four caisson levelling gages—rubber hoses filled with water—with sight glasses at the four corners, were used. To control the level movement of the caisson the excavation was altered

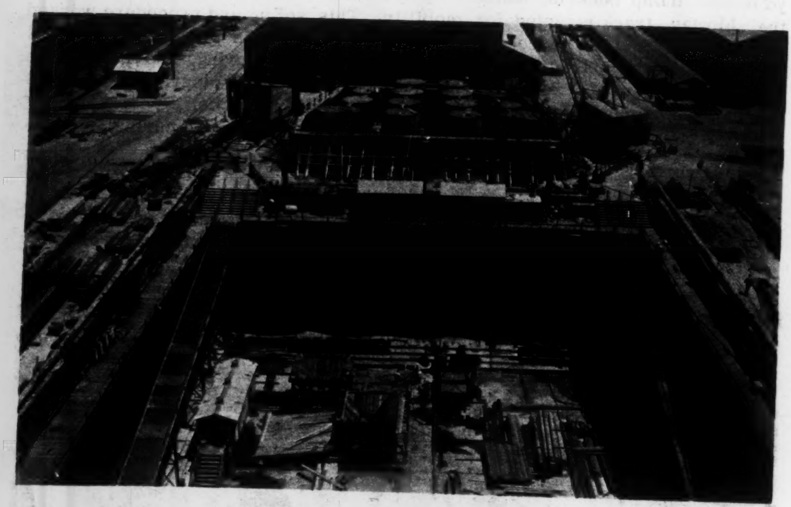

FIG. 4.—INITIAL SLAB READY FOR POURING

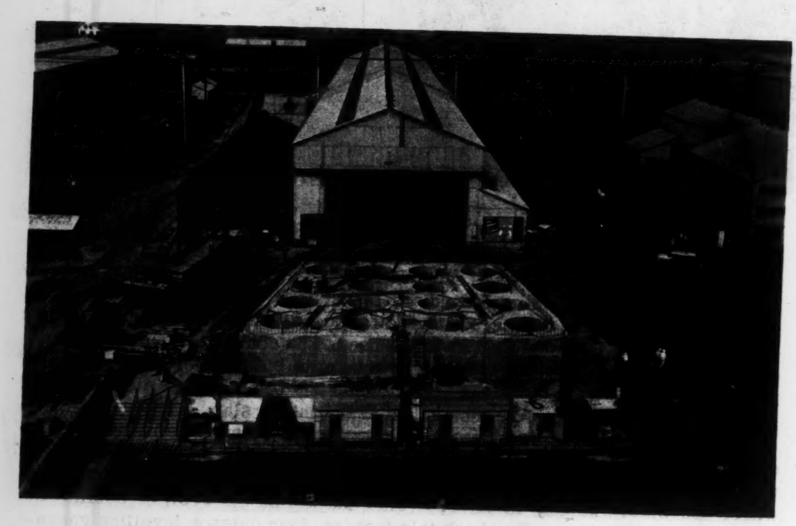

FIG. 5.—INITIAL SLAB WITH FORMS REMOVED

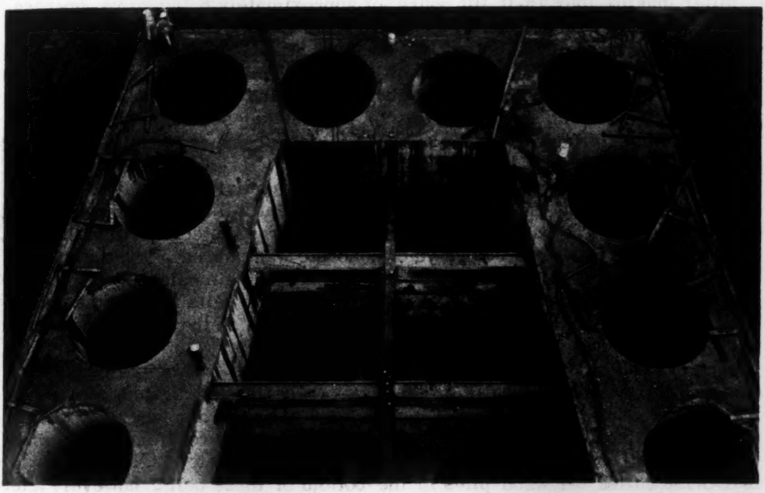

FIG. 6.—CAISSON TAKING SHAPE

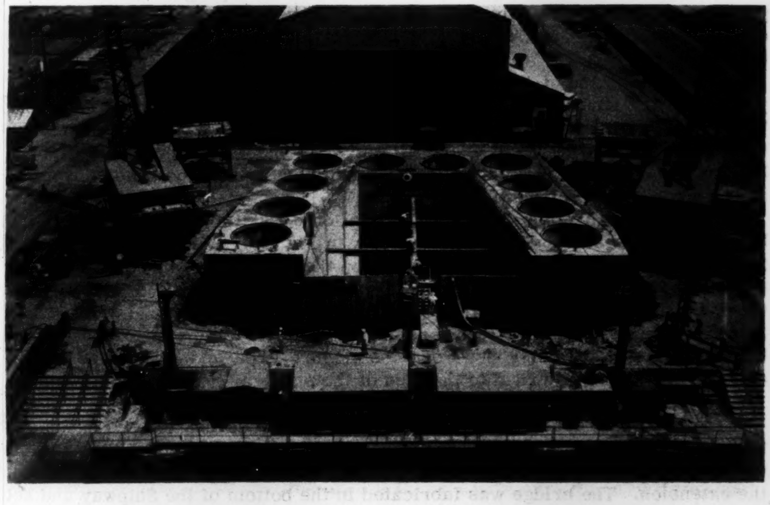

FIG. 7.—INTERIOR BRACING CONTINUES AS CAISSON GOES DOWN

from side to side and end to end with interior bracing inside, as shown in Fig. 7.

After making four 15-ft lift pours, of approximately 6,760 cu yd, preparations were made to clean out the work chamber and pour the seal. At this point a prolonged rainy spell set in. The caisson cutting edge having reached the plan grade at El. 40, began to settle more. This condition was caused by the excess rain and the fact that at about El. 40 the marl ran out and a layer of fine silty sand was encountered. To stop further settlement, the caisson was flooded and preparations made to use a high-pressure jet for cleaning out the work chamber under water.

After the work chamber was cleaned out, it was divided into four sections by the use of bagged gravel dams. One section at a time was poured by the tremie method. The pours were altered from corner to corner to maintain a level plane. A total of 1,395 cu yd of concrete was poured in the entire seal, making a total of 8,155 cu yd of concrete in the complete caisson.

With the caisson sealed at the bottom, the dredge wells around the outside were capped and sealed (Fig. 8). Work then started on the retaining walls on the top inside edge of the caisson.

The excavation of cells 81 and 85 followed, on each side of the planned opening in the end shipway wall. As these two cells were excavated, steel bracing was placed to prevent them from being disturbed or displaced. These two cells were excavated to El. 52, two of the 13 ft diameter well forms placed and the entire cell outside of the wells was filled with concrete (Fig. 9). The original plans called for wood piles in the bottom of these cells, however, after examination of the bottom it was decided they would not be necessary. During the process of placing the bracing in cells 81 and 85, the excavation of cells 82, 83, and 84 was commenced.

While the excavation of cells 82, 83, and 84 was in progress, steel sheet-pile closure walls were driven on each side between the caisson and the back of cells 81 and 85. This served as a back form and left in place for the closure concrete walls.

As the excavation of the three cells that were to be removed, progressed, the temporary timber bulkhead on the open end of the caisson was removed. Then the removal of the steel sheet pile began. It was necessary to remove these piles by splitting about every fifth or sixth sheet, burning them off at the bottom and lifting out in a group. Pulling individually was too time consuming and in some cases impossible.

Next, 188 wood piles, 36 ft long, a total of 6,280 lin ft were driven in the bottom of cells 82, 83, and 84, as shown in Fig. 10. The floor section was formed and poured in six sections, three on the caisson and three on cells 82, 83, and 84, fairing in the last pour with the existing shipway floor. Along with the pouring of the floor the closure wall between the caisson and cells 81 and 85 were brought up to El. 98. The retaining wall at the top was extended from the west edge of the caisson across the closure area and across the tops of cells 81 and 85 and returned to the side of the stairway leading to Shipway No. 11 (Fig. 11).

Of special interest is a portable bridge 22 ft wide across the end of the extension, as shown in Fig. 11. This bridge will enable traffic to continue to flow without having to cross the mainline railroad track which brushes the end of the extension. The bridge was fabricated in the bottom of the Shipway and set on seats previously cast in the top of the retaining walls. Forming and pouring this bridge completed all concrete work on the project.

FIG. 8.—CAISSON AT FINAL ELEVATION

FIG. 9.—RETAINING WALL ADDED

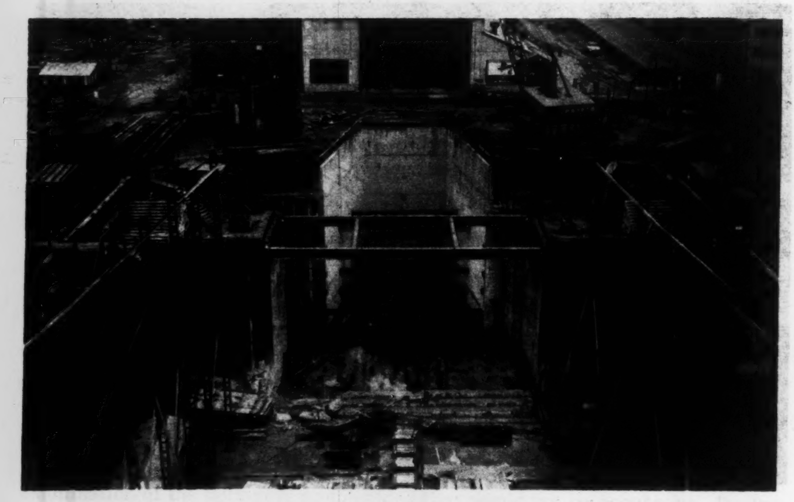

FIG. 10.—THREE CENTER CELLS REMOVED

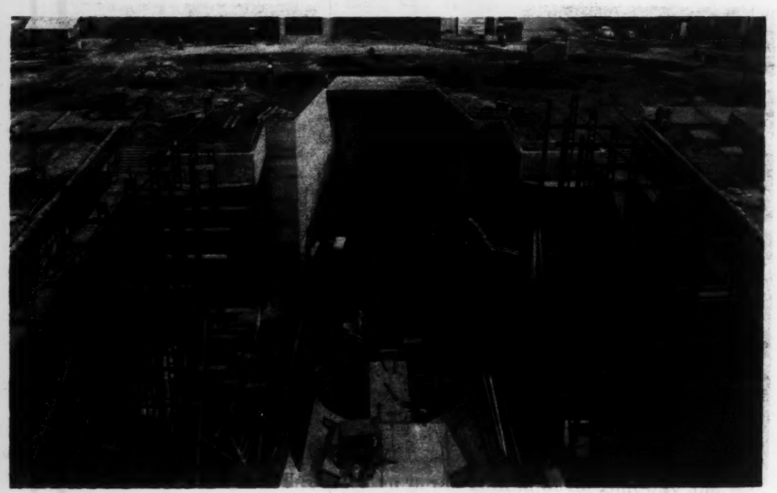

FIG. 11.—EXTENSION COMPLETED

The remaining work consisted of backfill, separating steel sheet pile, placing handrail, and dismantling and loading out equipment.

A total of 12,936.5 cu yd of concrete was used and it took the contractor 264 days of operation out of the 265 days in which they had originally estimated to complete the job.

AMERICAN SOCIETY OF CIVIL ENGINEERS

Founded November 5, 1852

TRANSACTIONS

Paper No. 3139

ANALYSIS OF CURVED GIRDERS

By H. H. Fickel[1]

SYNOPSIS

The derivation of influence lines for bending and torsional moments and shears on horizontally curved girders are presented herein. Solutions are given for simple and continuous spans. Diagrams are supplied showing the characteristic values of curved girders with constant moments of inertia. The effects of variable moments of inertia and also of the elasticity of the torsional supports are described.

INTRODUCTION

The statics of curved girders have been described by several writers[2] and various methods of analyses are known for loads in predetermined positions, as are commonly found in building construction.

The writer seeks to derive expressions for influence lines for simple and continuous spans. The conventional methods of one-dimensional structural analysis are used. Thereby, the theory is limited to structural members the length of which is great as compared with their other dimensions. The analytical significance of this is that the boundary conditions are fully satisfied only with respect to an ideal centerline. The same limitation however exists in the case of the straight girder for which the one-dimensional analysis has been fully accepted as giving satisfactory results.

In this connection the term "influence area" needs to be qualified. In the strict sense of the word, an influence area may be thought of as being the deformed surface of a two-dimensional structural member, such as a monolithic slab, under a specific load. However, owing to the simplifying assumptions of

---

Note.—Published, essentially as printed here, in September, 1959, in the Journal of the Structural Division, as Proceedings Paper 2164. Positions and titles given are those in effect when the paper or discussion was approved for publication in Transactions.

[1] Bridge Design Engr., Dept. of Highways, British Columbia, Canada.

[2] "The Analysis of Engineering Structures," by A. J. S. Pippard and J. F. Baker, Arnold, London, Third Edition, 1957.

the one-dimensional method, the influence areas referred to hereafter are surfaces such as would be formed, for example, by an infinite number of cross beams, rigidly attached to a girder, if this girder were subjected to deflections and rotations.

It is considered beyond the scope of this paper to deal with the stress analysis due to rotation or combined rotation and bending.

Notation.—The letter symbols adopted for use in this paper are defined where they first appear, in the illustrations or in the text, and are arranged alphabetically, for convenience of reference, in the Appendix.

SIMPLE SPAN CURVED GIRDERS

The Statically Determinate Primary System.—For a curved girder to be stable and statically determinate, there must exist a torsional restraint at one end. Such a system is shown in Fig. 1 and it shall be referred to as the primary system.

In practice, a simple span will have torsional restraints at both ends and therefore represent an indeterminate system with one redundant. For the analysis of this indeterminate system, the forces and displacements on the primary system must be known.

The sign convention used herein is as follows: vertical loads and reactions are positive if acting downward; shears are positive if acting upward on the left end of an element; bending moments are positive if creating tension in the bottom fiber; torsional moments are positive, if facing the end of a section, they turn clockwise; vertical forces in their positive direction will be represented in plan be circles; and bending and torsional moments will be represented by moment vectors such that looking in the direction of the arrow, the positive moment turns clockwise.

The term deflection shall mean vertical displacements which, if plotted along the girder, constitute the bending diagram. Deflections shall be positive in the downward direction. The term slope shall mean the angular displacement of the tangent to the bending diagram. The term rotation shall mean the rotational displacements about the longitudinal girder axis, which, if plotted along the girder, constitute the rotation diagram. Rotations shall be positive if the top flange of the girder rotates towards the center of curvature C.

Fig. 1 shows a general case of loading and the positive direction of the reactions. The external load P at the distance e from the girder centerline can be replaced by the load P and the torsional moment $T_p = P\ e$ as shown in dotted lines. The eccentricity e shall be positive if on the concave side of the girder. Since it is desired to obtain expressions for influence lines, only a unit load $P = 1$ will be considered. Consequently $T_p = e$. The effects of $P = 1$ and $T_p = e$ will first be considered separately. To distinguish between them, the symbols of the effects of $P = 1$ will be denoted by the superscript a and the symbols of the effects of $T_p = e$ by the superscript b. To indicate the effects of external loading on the primary system, their symbols will be given the subscript o. To indicate the effects of the redundant force on the primary system, their symbols will be given the subscript 1.

Finally the points of load application or the points at which displacements are computed will be denoted by ω and ω^1. The point for which an influence line is determined will be denoted by ρ and ρ^1.

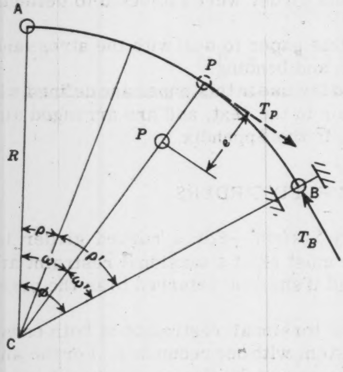
A
P
T_P
P
e
R
B
T_B
ρ
ρ'
ω
ω'
φ
C

FIG. 1.—GENERAL CASE OF LOADING AND THE POSITIVE DIRECTION OF THE REACTIONS

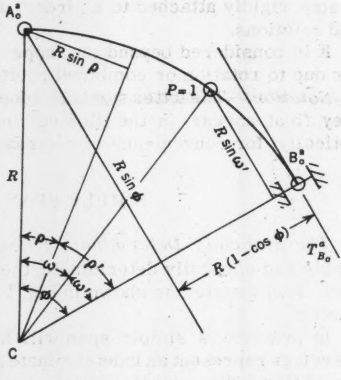
A°ₒ
R sin ρ
P=1
R sin ω'
Bₒᵃ
R
R sin φ
R (1 − cos φ)
T^a_{Bo}
ρ
ρ'
ω
ω'
φ
C

FIG. 2.—EQUILIBRIUM OF THE PRIMARY SYSTEM UNDER THE ACTION OF A VERTICAL FORCE

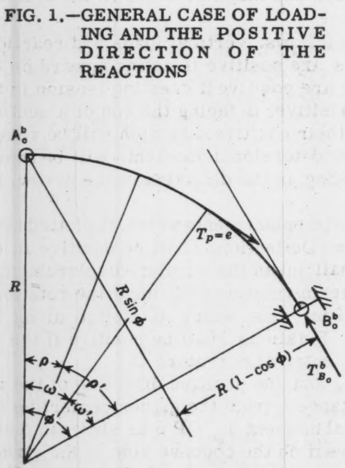
Aₒᵇ
T_P=e
R
R sin φ
Bₒᵇ
R (1 − cos φ)
T^b_{Bo}
ρ
ρ'
ω
ω'
φ
C

FIG. 3.—EQUILIBRIUM OF THE PRIMARY SYSTEM UNDER THE ACTION OF A TORSIONAL MOMENT

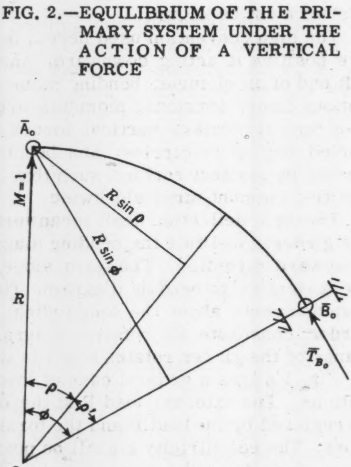
Āₒ
M=1
R sin ρ
R sin φ
R
B̄ₒ
T̄_{Bo}
ρ
ρ'
φ
C

FIG. 4.—EQUILIBRIUM OF THE PRIMARY SYSTEM UNDER THE ACTION OF A UNIT BENDING MOMENT APPLIED AT END A

In Fig. 2 consider the equilibrium of the primary system under the action of a vertical force on the girder centerline. By taking moments about the axis BC:

$$R \sin \omega^1 + A_o^a R \sin \phi = 0 \quad \ldots\ldots\ldots\ldots\ldots \quad (1)$$

hence

$$A_o^a = - \frac{\sin \omega^1}{\sin \phi} \quad \ldots\ldots\ldots\ldots\ldots\ldots\ldots \quad (2a)$$

and

$$B_o^a = \frac{\sin \omega^1}{\sin \phi} - 1 \quad \ldots\ldots\ldots\ldots\ldots \quad (2b)$$

By taking moments about the tangent to the girder in B

$$T_{B_o}^a - R\left(1 - \cos \omega^1\right) - A_o^a R (1 - \cos \phi) = 0 \quad \ldots\ldots\ldots \quad (3)$$

hence

$$T_{B_o}^a = R\left(1 - \cos \omega^1 - \frac{1 - \cos \phi}{\sin \phi} \sin \omega^1\right) \ldots\ldots\ldots \quad (4)$$

With the reactions known, the influence line equations for any point ρ are obtained. For shear they are

$$V_o^a = B_o^a = \frac{\sin \omega^1}{\sin \phi} - 1 \text{ (for } 0 \leq \omega \leq \rho) \quad \ldots\ldots\ldots \quad (5a)$$

and

$$V_o^a = - A_o^a = + \frac{\sin \omega^1}{\sin \phi} \text{ (for } \rho \leq \omega \leq \phi) \ldots\ldots\ldots\ldots \quad (5b)$$

and for bending moments

$$M_o^a = - B_o^a R \sin \rho^1 - T_{B_o}^a \sin \rho^1 \quad \ldots\ldots\ldots\ldots\ldots \quad (6)$$

which, after substituting Eqs. 2(b) and 4 and replacing ω^1 by $\phi - \omega$, becomes

$$M_o^a = R \frac{\sin \omega \sin \rho^1}{\sin \phi} \text{ (for } 0 \leq \omega \leq \rho) \quad \ldots\ldots\ldots \quad (7a)$$

and

$$M_o^a = - A_o^a R \sin \rho = R \frac{\sin \omega^1 \sin \rho}{\sin \phi} \text{ (for } \rho \leq \omega \leq \phi) \quad \ldots\ldots \quad (7b)$$

For torsional moments

$$T_o^a = T_{B_o}^a \cos \rho^1 - B_o^a R \left(1 - \cos \rho^1\right) \ldots\ldots\ldots\ldots \quad (8)$$

which after substituting Eqs. 2(b) and 4 and replacing ω^1 by $\phi - \omega$ becomes

$$T_o^a = R\left(1 - \frac{\cos \rho^1 \sin \omega}{\sin \phi} - \frac{\sin \omega^1}{\sin \phi}\right) \text{ (for } 0 \leq \omega \leq \rho) \ldots\ldots \quad (9a)$$

$$T_o^a = A_o^a R\,(1 - \cos \rho) = -R\,\frac{(1 - \cos \rho)}{\sin \phi}\,\sin \omega^1 \text{ (for } \rho \leq \omega \leq \phi) \,.\,.\, \text{(9b)}$$

Consider further the equilibrium of the primary system under the action of a torsional moment T_p using Fig. 3.
By taking moments about the axis BC

$$e \sin \omega^1 - A_o^b R \sin \phi = 0 \quad \ldots\ldots\ldots\ldots \text{(10)}$$

hence

$$A_o^b = \frac{\sin \omega^1}{R \sin \phi}\, e \quad \ldots\ldots\ldots\ldots \text{(11a)}$$

and

$$B_o^b = -A_o^b = -\frac{\sin \omega^1}{R \sin \phi}\, e \quad \ldots\ldots\ldots\ldots \text{(11b)}$$

By taking moments about the tangent of the girder in B

$$T_{B_o}^b - A_o^b R\,(1 - \cos \phi) - e \cos \omega^1 = 0 \quad \ldots\ldots\ldots\ldots \text{(12)}$$

hence

$$T_{B_o}^b = \left(\cos \omega^1 - \frac{1 - \cos \phi}{\sin \phi}\,\sin \omega^1\right) e \quad \ldots\ldots\ldots\ldots \text{(13)}$$

With the reactions known, the influence line equations for any point ρ are obtained. For shear they are

$$V_o^b = B_o^b = -\frac{\sin \omega^1}{R \sin \phi}\, e \text{ (for } 0 \leq \omega \leq \rho) \quad \ldots\ldots\ldots \text{(14a)}$$

and

$$V_o^b = -A_o^b = -\frac{\sin \omega^1}{R \sin \phi}\, e \text{ (for } \rho \leq \omega \leq \phi) \quad \ldots\ldots\ldots \text{(14b)}$$

and for bending moments

$$M_o^b = -B_o^b R \sin \rho^1 - T_{B_o}^b \sin \rho^1 \quad \ldots\ldots\ldots\ldots \text{(15)}$$

which after substituting Eqs. 11(b) and 13 and replacing ω^1 by $\phi - \omega$ becomes

$$M_o^b = \frac{-\sin \omega \sin \rho^1}{\sin \phi}\, e \text{ (for } 0 \leq \omega \leq \rho) \quad \ldots\ldots\ldots \text{(16a)}$$

and

$$M_o^b = -A_o^b R \sin \rho = -\frac{\sin \omega^1 \sin \rho}{\sin \phi}\, e \text{ (for } \rho \leq \omega \leq \phi) \quad \ldots\, \text{(16b)}$$

for torsional moments

$$T_o^b = T_{B_o}^b \cos \rho^1 - B_o^b R\left(1 - \cos \rho^1\right) \quad \ldots\ldots\ldots \text{(17)}$$

which after substituting Eqs. 11(b) and 13 and replacing ω^1 by $\phi - \omega$ becomes

$$T_o^b = \frac{\cos \rho^1 \sin \omega}{\sin \phi} + \frac{\sin \omega^1}{\sin \phi}\, e \text{ (for } 0 \leq \omega \leq \rho) \quad \ldots\ldots\ldots \text{(18a)}$$

and

$$T_o^b = A_o^b R\,(1 - \cos\rho) = \frac{1 - \cos\rho}{\sin\phi}\sin\omega^1 e \text{ (for } \rho \leq \omega \leq \phi) \; . \; . \; . \quad (18b)$$

Consider further the equilibrium of the primary system under the action of a unit bending moment applied at the end A (Fig. 4). The effects of this loading will be of interest in connection with the analysis of continuous curved girders in the subsequent sections.
By taking moments about BC

$$\cos\phi - \bar{A}_o R \sin\phi = 0 \quad . \; . \; . \; . \; . \; . \; . \; . \; . \; . \; . \; . \; . \; . \; . \quad (19)$$

hence

$$\bar{A}_o = \frac{\cos\phi}{R\sin\phi} \quad . \; . \; . \; . \; . \; . \; . \; . \; . \; . \; . \; . \; . \; . \; . \; . \; . \quad (20a)$$

and

$$\bar{B}_o = -\frac{\cos\phi}{R\sin\phi} \quad . \; . \; . \; . \; . \; . \; . \; . \; . \; . \; . \; . \; . \; . \; . \; . \quad (20b)$$

The shear at any point ρ is

$$\bar{V}_o = -\bar{A}_o = \bar{B}_o = -\frac{\cos\phi}{R\sin\phi} \quad . \; . \; . \; . \; . \; . \; . \; . \; . \; . \; . \; . \; . \quad (21)$$

The bending moment at any point ρ is

$$\bar{M}_o = \cos\rho - \bar{A}_o R \sin\rho = \cos\rho - \frac{\cos\phi}{\sin\phi}\sin\rho \quad . \; . \; . \; . \; . \; . \; . \quad (22)$$

The torsional moment at any point ρ is

$$\bar{T}_o = \bar{A}_o R\,(1 - \cos\rho) - \sin\rho = \frac{\cos\phi - \cos\rho^1}{\sin\phi} \quad . \; . \; . \; . \; . \; . \quad (23)$$

Finally it will be necessary to obtain expressions for the moment and shear distribution due to the redundant torsional end moment $T_A = X_1 = 1$ (Fig. 5).
By taking moments about BC:

$$\sin\phi - A_1 R \sin\phi = 0 \quad . \; . \; . \; . \; . \; . \; . \; . \; . \; . \; . \; . \; . \; . \quad (24)$$

hence

$$A_1 = \frac{1}{R} \quad . \; . \; . \; . \; . \; . \; . \; . \; . \; . \; . \; . \; . \; . \; . \; . \; . \; . \; . \quad (25a)$$

and

$$B_1 = \frac{-1}{R} \quad . \; . \; . \; . \; . \; . \; . \; . \; . \; . \; . \; . \; . \; . \; . \; . \; . \; . \quad (25b)$$

The shear at any point ρ is

$$V_1 = -A_1 = B_1 = \frac{-1}{R} = \text{constant} \quad . \; . \; . \; . \; . \; . \; . \; . \; . \; . \quad (26)$$

The bending moment at any point ρ is

$$M_1 = \sin\rho - A_1 R \sin\rho = 0 = \text{constant} \quad . \; . \; . \; . \; . \; . \; . \; . \; . \quad (27)$$

The torsional moment at any point ρ is

$$T_1 = \cos\rho + A_1 R (1 - \cos\rho) = 1 = \text{constant} \quad \text{. . . . . (28)}$$

The Simple Span With Rigid Torsional Restraints.—The analysis of the indeterminate system is based on the condition that no rotation can take place at the point of action of the redundant force.

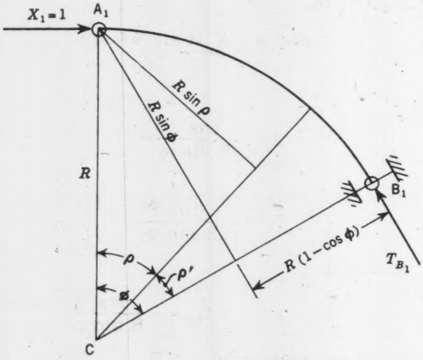

FIG. 5.—EQUILIBRIUM OF THE PRIMARY SYSTEM UNDER THE ACTION OF A UNIT TORSIONAL MOMENT APPLIED AT END A

If $\delta^a_{1\omega}$ is the girder rotation at the point of action of X_1 due to $P = 1$ at ω and δ_{11} is the girder rotation at the same point due to $X_1 = 1$, then to satisfy the boundary condition

$$\delta^a_{1\omega} + X^a_1\,\delta_{11} = 0 \quad \text{or} \quad X^a_1 = -\frac{\delta^a_{1\omega}}{\delta_{11}} \quad \text{. . . . . (29)}$$

The same reasoning applies in the case of external moments. If $e\,\delta^b_{1\omega}$ is the end rotation due to $T_p = e$, then

$$X^b_1 = -\frac{e\,\delta^b_{1\omega}}{\delta_{11}} \quad \text{. . . . . (30)}$$

By superposition the final value of X_1 is

$$X_1 = X^a_1 + X^b_1 = \frac{-\left(\delta^a_{1\omega} + e\,\delta^b_{1\omega}\right)}{\delta_{11}} \quad \text{. . . . . (31)}$$

With X_1 known, the effects of external loading on the indeterminate system can be given by

$$V = V_o^a + V_o^b + V_1\,X_1 \qquad \text{(32a)}$$

and

$$M = M_o^a + M_o^b + M_1\,X_1 \qquad \text{(32b)}$$

and generally for any desired effect

$$E = E_o^a + E_o^b + E_1\,X_1 \qquad \text{(32c)}$$

The magnitude of δ_{11} can be found by application of the principle of virtual work

$$\delta_{11} = \int_o^{\phi} M_1^2 \frac{ds}{E\,I} + \int_o^{\phi} T_1^2 \frac{ds}{N\,J} + \int_o^{\phi} V_1^2 \frac{ds}{N\,A} \qquad \text{(33)}$$

The third integral in the previous expression is negligibly small and will be omitted. Furthermore, by Eqs. 27 and 28 $M_1 = 0$ and $T_1 = 1$ hence

$$\delta_{11} = \int_o^{\phi} \frac{R\,d\rho}{N\,J} = \frac{R}{N\,J}\ \phi \qquad \text{(34)}$$

Eq. 31 represents the solution for a specific loading. However, since the derivation of influence lines rather than a specific solution is desired, $\delta_{1\,\omega}$ will be replaced by $\delta_{\omega\,1}$ in accordance with Maxwell's theorem. Then $\delta^a_{\omega\,1}$ is the function giving the deflections of the girder due to $X_1 = 1$ and $\delta^b_{\omega\,1}$ is the function giving rotations of the girder due to $X_1 = 1$.

To evaluate the $\delta_{\omega 1}$-line, consider an element ds as in Fig. 6(a). The rotation of the element ds is

$$d\alpha = \frac{T_1}{N\,J}\,ds = \frac{T_1}{N\,J}\ R\,d\rho \qquad \text{(35)}$$

As per Fig. 6(b), a positive rotation $d\alpha$ of the element ds causes the point ω to deflect by

$$d\delta_{\omega} = R\left[1 - \cos\left(\omega^1 - \rho^1\right)\right] d\alpha \qquad \text{(36)}$$

Disregarding for the present the boundary condition

$$\delta^a_{\omega\,1} = 0 \text{ for } \omega^1 = \phi,$$

$$\delta^a_{\omega\,1} = \frac{R^2}{N\,J}\int_o^{\omega^1} \left[1 - \cos\left(\omega^1 - \rho^1\right)\right] d\rho^1 = \frac{R^2}{N\,J}\left(\omega^1 - \sin\,\omega^1\right) \qquad \text{(37)}$$

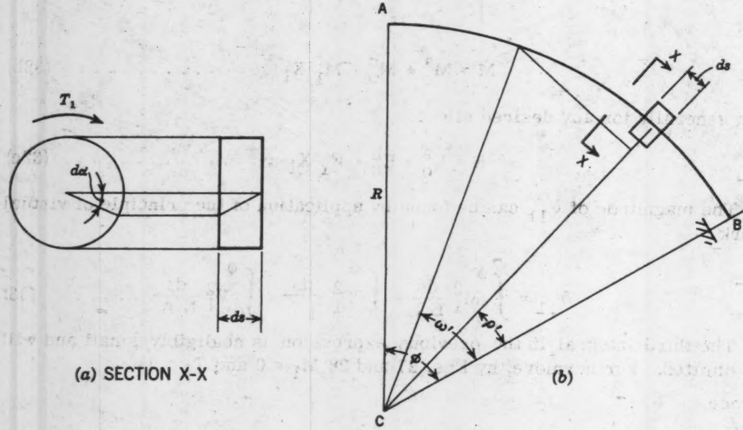
T₁
dα
ds
A
X
ds
X
R
B
ω'
ρ'
φ
C

(a) SECTION X-X

(b)

FIG. 6

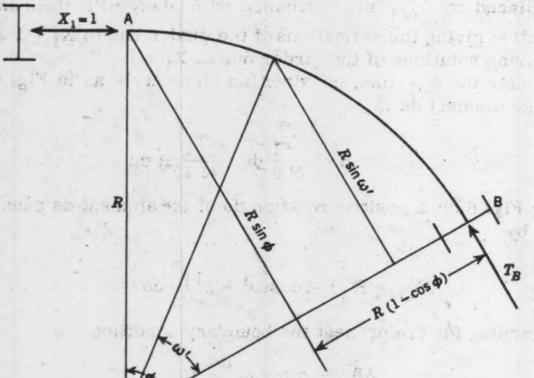
X₁ = 1
A
R
R sin φ
R sin ω'
B
T_B
R (1 − cos φ)
ω'
φ
C

FIG. 7.—PRIMARY SYSTEM WITH ELASTIC RESTRAINTS

In order to satisfy the previously mentioned boundary condition, the girder is rotated about the axis BC through an angle of $\frac{R^2}{N\,J}\,\frac{(\phi - \sin\phi)}{R\sin\phi}$ and the correction is applied to Eq. 37.

Thus

$$\delta^a_{\omega 1} = \frac{R^2}{N\,J}\left(\omega^1 - \sin\omega^1\right) - \frac{R^2}{N\,J}\left(\phi - \sin\phi\right)\frac{\sin\omega^1}{\sin\phi} \quad \ldots\ldots \quad (38)$$

from which

$$\delta^a_{\omega 1} = \frac{R^2}{N\,J}\left(\omega^1 - \phi\,\frac{\sin\omega^1}{\sin\phi}\right) \quad \ldots\ldots\ldots\ldots \quad (39)$$

The rotation diagram, that is the $\delta^b_{\omega 1}$-line, is determined by integrating the rotations of the elements as given by Eq. 35 and adding the rotational components of the deflections $\delta^a_{\omega 1}$ of Eq. 39. It will be noted that the $\delta^b_{\omega 1}$-line has been multiplied by the variable eccentricity e. Thereby the rotation diagram assumes the form of an extension to the bending diagram such that the sum of both represents the bending area

$$e\,\delta^b_{\omega 1} = \int_0^{\omega^1} d\alpha\, e - \frac{\delta^a_{\omega 1}}{R}\, e = \frac{R}{N\,J}\,\omega^1 e - \frac{R}{N\,J}\left(\omega^1 - \phi\,\frac{\sin\omega^1}{\sin\phi}\right) e \quad \ldots \quad (40)$$

and

$$e\,\delta^b_{\omega 1} = \frac{R}{N\,J}\,\phi\,\frac{\sin\omega^1}{\sin\phi}\, e \quad \ldots\ldots\ldots\ldots \quad (41)$$

By substituting Eqs. 34, 39, and 41 in Eq. 31, we obtain

$$X_1 = \frac{\sin\omega^1}{\sin\phi}\,(R - e) - \frac{\omega^1}{\phi}\,R \quad \ldots\ldots\ldots\ldots \quad (42)$$

By application of Eq. 32

$$A = A^a_o + A^b_o + A_1\,X_1 \quad \ldots\ldots\ldots\ldots \quad (43a)$$

which, with Eqs. 2, 11, 25 and 42 becomes

$$A = -\frac{\omega^1}{\phi} \quad \ldots\ldots\ldots\ldots \quad (43b)$$

and

$$B = -\frac{\omega}{\phi} \quad \ldots\ldots\ldots\ldots \quad (43c)$$

All the other effects are similarly obtained. The shears are

$$V = B = -\frac{\omega}{\phi} \quad (\text{for } 0 \leq \omega \leq \rho) \quad \ldots\ldots\ldots\ldots \quad (44a)$$

and

$$V = -A = \frac{\omega^1}{\phi} \quad (\text{for } \rho \leq \omega \leq \phi) \quad \ldots\ldots\ldots\ldots \quad (44b)$$

The bending moments are

$$M = \frac{\sin \omega \, \sin \rho^1}{\sin \phi} \, (R - e) \quad (\text{for } 0 \leq \omega \leq \rho) \quad \ldots\ldots\ldots \quad (45a)$$

and

$$M = \frac{\sin \omega^1 \, \sin \rho}{\sin \phi} \, (R - e) \quad (\text{for } \rho \leq \omega \leq \phi) \quad \ldots\ldots\ldots \quad (45b)$$

Torsional moments

$$T = -\frac{\sin \omega \, \cos \rho^1}{\sin \phi} \, (R - e) + \frac{\omega}{\phi} \, R \quad (\text{for } 0 \leq \omega \leq \rho) \quad \ldots\ldots \quad (46a)$$

and

$$T = \frac{\sin \omega^1 \, \cos \rho}{\sin \phi} \, (R - e) - \frac{\omega^1}{\phi} \, R \quad (\text{for } \rho \leq \omega \leq \phi) \quad \ldots\ldots \quad (46b)$$

Eqs. 43 to 46 represent influence areas as they contain the two variables ω and e.

The moment and shear distribution due to a unit end-bending moment as described previously will be of interest in connection with the analysis of the continuous curved girder.

If $\bar{\delta}_{1\omega}$ is the end rotation caused by the specific loading $M^L = 1$, then by Eq. 29

$$\bar{X}_1 = -\frac{\bar{\delta}_{1\omega}}{\delta_{11}} \quad \ldots\ldots\ldots\ldots\ldots\ldots\ldots \quad (47)$$

and by the principle of virtual work

$$\bar{\delta}_{1\omega} = \int_o^\phi \bar{M}_o \, M_1 \, \frac{ds}{E\,I} + \int_o^\phi \bar{T}_o \, T_1 \, \frac{ds}{N\,J} \quad \ldots\ldots\ldots\ldots \quad (48)$$

Which with Eqs. 22, 23, 27, and 28 becomes

$$\bar{\delta}_{1\omega} = \frac{R}{N\,J} \int_o^\phi \frac{\cos \phi - \cos \rho^1}{\sin \phi} \, d\rho^1 = \frac{R}{N\,J} \left(\frac{\cos \phi}{\sin \phi} \, \phi - 1 \right) \quad \ldots \quad (49)$$

so that with Eq. 34.

$$\bar{X}_1 = \frac{1}{\phi} - \frac{\cos \phi}{\sin \phi} \quad \ldots\ldots\ldots\ldots\ldots\ldots\ldots \quad (50)$$

Hence the effects of $M^L = 1$ are as follows: The shears are

$$V^L = \bar{V}_o + V_1 \, \bar{X}_1 = -\frac{1}{R\,\phi} \quad \ldots\ldots\ldots\ldots\ldots \quad (51a)$$

The bending moments are

$$M^L = \bar{M}_o + M_1 \bar{X}_1 = \cos \rho - \frac{\cos \phi^1}{\sin \phi} \sin \rho \quad \ldots\ldots\ldots \quad (51b)$$

The torsional moments are

$$T^L = \bar{T}_o + T_1 \bar{X}_1 = \frac{1}{\phi} - \frac{\cos \rho^1}{\sin \phi} \quad \ldots\ldots\ldots\ldots \quad (51c)$$

When the unit bending moment acts at the end B of the girder (instead of at A as in Fig. 4) the corresponding effects are as follows: The shears are

$$V^R = \frac{1}{R\,\phi} \quad \ldots\ldots\ldots\ldots\ldots\ldots \quad (52a)$$

The bending moments are

$$M^R = \cos \rho^1 - \frac{\cos \phi}{\sin \phi} \sin \rho^1 \quad \ldots\ldots\ldots\ldots \quad (52b)$$

The torsional moments are

$$T^R = -\frac{1}{\phi} + \frac{\cos \rho}{\sin \phi} \quad \ldots\ldots\ldots\ldots\ldots \quad (52c)$$

The Simple Span With Elastic Torsional Restraints.—The problem of the preceding section shall now be modified by assuming the torsional restraints to be elastic instead of rigid. It will also be assumed that both end restraints are of equal elasticity. This torsional elasticity may be defined by the rotation of the support due to a unit torsional moment. If this rotation is denoted by ξ then it will be convenient to write

$$\xi = k \frac{R\,\phi}{N\,J} \quad \ldots\ldots\ldots\ldots\ldots\ldots \quad (53)$$

The elasticity of the supports has no influence on the equilibrium of the modified primary system, that is the primary system with elastic restraints as shown in Fig. 7. For this reason Eq. 1 to 28 remain valid.

The rotation δ_{11} now is the sum of the girder rotation as given by Eq. 34 and the rotations of the supports A and B as given by Eq. 53. Thus

$$\delta_{11} = \frac{R\,\phi}{N\,J}\,(1 + 2\,k) \quad \ldots\ldots\ldots\ldots\ldots \quad (54)$$

Similarly the $\delta^a_{\omega 1}$-line is the sum of the girder deflections as given by Eq. 39 and the deflections caused by the rotation of support B. Disregarding the boundary condition $\delta^a_{\omega 1} = 0$ for $\omega^1 = \phi$, the positive rotation ξ at B causes each point ω to deflect by

$$\delta = \frac{R^2}{N\,J}\,k\,\phi\,\left(1 - \cos \omega^1\right) \quad \ldots\ldots\ldots\ldots \quad (55)$$

In order to satisfy the previously mentioned boundary condition, the girder is rotated about the axis BC so that the deflection of each point caused by the positive rotation ξ at B is

$$\delta = \frac{R^2}{N\,J}\,k\,\phi \left[\left(1 - \cos \omega^1\right) - (1 - \cos \phi)\,\frac{\sin \omega^1}{\sin \phi}\right] \quad \ldots\ldots \quad (56)$$

Hence, the complete $\delta^a_{\omega 1}$ - line is

$$\delta^a_{\omega 1} = -\frac{R^2}{N\,J}\,\phi\left[\frac{\sin\omega^1}{\sin\phi}\;(1 + k) + \frac{\sin\omega}{\sin\phi}\,k - \frac{\omega^1}{\phi} - k\right] \quad \ldots \text{(57)}$$

Similarly the $\delta^b_{\omega 1}$ - line is the sum of the girder rotations as given by Eq. 35 the rotation of the support B and the rotational component of the deflection $\delta^a_{\omega 1}$.

Thus

$$e\,\underset{-}{\delta}{}^a_{\omega 1} = \frac{R}{N\,J}\,\omega^1\;e + \frac{R}{N\,J}\,k\;\;\phi\;\;e - \frac{\underset{-}{\delta}{}^a_{\omega 1}}{R}\;\;e \quad \ldots\ldots\ldots \text{(58)}$$

or

$$e\,\underset{-}{\delta}{}^b_{\omega 1} = \frac{R\,\phi}{N\,J}\left[\frac{\sin\omega^1}{\sin\phi}\;\;(1 + k) + \frac{\sin\omega}{\sin\phi}\;\;k\right]e \quad \ldots\ldots\ldots \text{(59)}$$

Now by Eq. 31.

$$X_1 = \frac{\sin\omega^1}{\sin\phi}\;(R - e) - \frac{\omega^1}{\phi}R + \frac{k}{1{+}2\;k}\;R\left[\frac{\sin\omega\;-\;\sin\omega^1}{\sin\phi}\left(1 - \frac{e}{R}\right) - \;\frac{\omega - \omega^1}{\phi}\right] \ldots \text{(60)}$$

Further by application of Eq. 32 and with

$$U = \frac{\sin\omega\;-\;\sin\omega^1}{\sin\phi}\;\left(1 - \frac{e}{R}\;\;-\;\frac{\omega - \omega^1}{\phi}\right. \quad \ldots\ldots\ldots \text{(61)}$$

$$A = -\;\frac{\omega^1}{\phi}\;+\frac{k}{1{+}2\;k}\,U \quad \ldots\ldots\ldots\ldots\ldots\ldots \text{(62a)}$$

and

$$B = -\;\frac{\omega}{\phi} - \frac{k}{1{+}2\;k}\;U \quad \ldots\ldots\ldots\ldots\ldots\ldots \text{(62b)}$$

in which A and B represent the vertical reactions at these points.
The shears are

$$V = B\;\;(\text{for } 0 \leq \omega \leq \rho) \quad \ldots\ldots\ldots\ldots\ldots \text{(63a)}$$

and

$$V = -\;A\;\;(\text{for } \rho \leq \omega \leq \phi) \quad \ldots\ldots\ldots\ldots\ldots \text{(63b)}$$

The bending moments (with $M_1 = 0$) are

$$M = \frac{\sin\omega\;\sin\rho^1}{\sin\phi}\;\;(R - e)\;\;(\text{for } 0 \leq \omega \leq \rho) \quad \ldots\ldots\ldots \text{(64a)}$$

and

$$M = \frac{\sin\omega^1\;\sin\rho}{\sin\phi}\;(R - e)\;\;(\text{for } \rho \leq \omega \leq \phi) \quad \ldots\ldots\ldots \text{(64b)}$$

The torsional moments are

$$T = - \frac{\sin \omega \cos \rho^1}{\sin \phi} (R - e) + \frac{\omega}{\phi} R + \frac{k}{1+2\,k} R\,U \quad (\text{for } 0 \leq \omega \leq \rho) \,.\,.\, \text{(65a)}$$

and

$$T = \frac{\sin \omega^1 \cos \rho}{\sin \phi} (R - e) - \frac{\omega^1}{\phi} R + \frac{k}{1 + 2\,k} R\,U \quad (\text{for } \rho \leq \omega \leq \phi) \,.\,.\,.\,.\, \text{(65b)}$$

CONTINUOUS CURVED GIRDERS

General Outline Of Analysis.—By virtue of Maxwell's theorem, any influence line may be regarded as the bending line due to a specific loading. If, for example, a hinge is introduced at the support n of the continuous girder shown in Fig. 8 and the two ends meeting there are rotated so that an angle δ_{nn} is subtended by their tangents, then the ordinates of the resulting bending line divided by δ_{nn} are the ordinates of the influence line for $M_n = X_n$. Therefore

$$X_n = - \frac{\delta_{\omega n}}{\delta_{nn}} \,.\,.\,.\,.\,.\,.\,.\,.\,.\,.\,.\,.\,.\,.\,.\,.\,.\,.\, \text{(66)}$$

In order to find the bending line of the continuous curved girder, a new primary system is adopted. This new primary system consists of a series of simple curved girders. Each simple span is, in itself, an indeterminate system, but its statical properties are known from the analysis presented previously in this paper.

Fig. 9 demonstrats the notations to be used in this section. In this figure y_r^L is the ordinate of the bending line (or area) of span r due to M = 1 at its left end, y_r^R is the ordinate of the bending line (or area) of span r due to M = 1 at its right end, β_r is the slope of span r at the point of application of M = 1, γ_r is the slope of span r at the end opposite M = 1.

Assuming for the present that the slopes β_r and γ_r are known, the moments at the supports M_{rn} caused by the introduction of δ_{nn} at support n can be computed by means of the three-moment-equation. If these moments are then applied to the primary system as external loads, the resulting bending lines of the individual spans (Fig. 10) are identical with the desired bending line of the continuous girder of Fig. 8.

If, in addition, the functions y_r^L and y_r^R are known, then the bending line of any individual span r is

$$\delta_{\omega n} = y_r^L M_{(r-1)n} + y_r^R M_{rn} \,.\,.\,.\,.\,.\,.\,.\,.\,.\,.\,.\, \text{(67)}$$

Eq. 67 substituted in Eq. 66 furnishes the solution for the influence line X_n within the span r.

Finally, if at any span r the influence lines for X_{r-1} and X_r have been established, then any desired effect within this span is given by the superposition

$$E_r = E_{ro} + E_{r1}^L X_{r-1} + E_{r1}^R X_r \,.\,.\,.\,.\,.\,.\,.\,.\,.\,.\,.\,.\, \text{(68)}$$

The Statically Indeterminate Primary System.—For all relevant loading conditions, the effects on the primary system, that is on the simple span, have been previously presented.

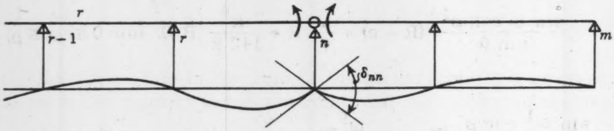
r
r − 1
r
n
m
δ_{nn}

FIG. 8

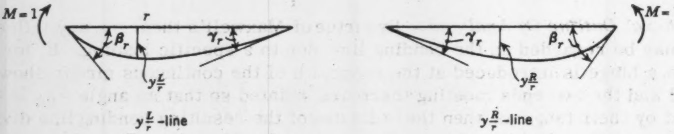
M = 1
r
β_r
γ_r
y_r^L
y_r^L-line
γ_r
β_r
M = 1
y_r^R
y_r^R-line

FIG. 9

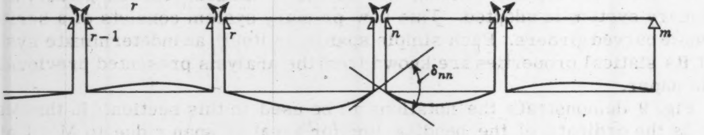
r
r − 1
r
n
m
δ_{nn}

FIG. 10.—BENDING LINE OF PRIMARY SYSTEM DUE TO THE REDUNDANT SUPPORT MOMENTS

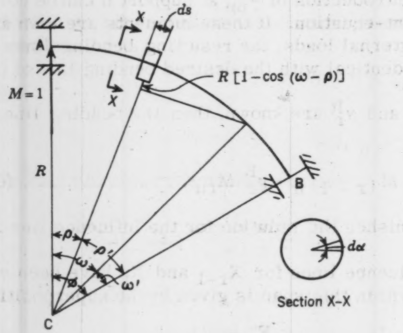
A
X
ds
X
R [1 − cos (ω − ρ)]
M = 1
R
B
ρ
ρ'
ω
ω'
φ
C
dα
Section X-X

FIG. 11

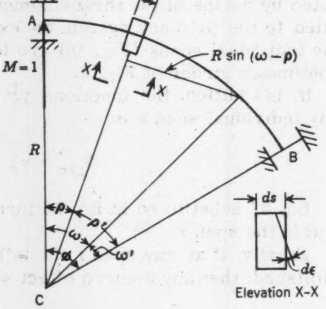
A
ds
R sin (ω − ρ)
M = 1
X
X
R
B
ρ
ρ'
ω
ω'
φ
C
ds
dε
Elevation X-X

FIG. 12

For ease of reference, Eqs. 44 through 52 are repeated herein with such new subscripts as to indicate their proper relation to the new primary system.

The effects E_{ro} caused by external unit loads in span r as follows: Shears are

$$V_{ro} = -\,\omega/\phi_r \quad (\text{for } 0 \leq \omega \leq \rho) \;\ldots\ldots\ldots\ldots \qquad (69a)$$

and

$$V_{ro} = \omega^1/\phi_r \quad (\text{for } \rho \leq \omega \leq \phi) \;\ldots\ldots\ldots\ldots \qquad (69b)$$

Bending moments are

$$M_{ro} = \frac{\sin\omega\,\sin\rho^1}{\sin\phi_r}\left(R_r - e\right) \quad (\text{for } 0 \leq \omega \leq \rho) \;\ldots\ldots \qquad (70a)$$

and

$$M_{ro} = \frac{\sin\omega^1\,\sin\rho}{\sin\phi_r}\left(R_r - e\right) \quad (\text{for } \rho \leq \omega \leq \phi) \;\ldots\ldots \qquad (70b)$$

Torsional moments are,

$$T_{ro} = -\,\frac{\sin\omega\,\cos\rho^1}{\sin\phi_r}\left(R_r - e\right) + \frac{\omega}{\phi_r}\,R_r \quad (\text{for } 0 \leq \omega \leq \rho) \;\ldots \qquad (71a)$$

and

$$T_{ro} = \frac{\sin\omega^1\,\cos\rho}{\sin\phi_r}\left(R_r - e\right) - \frac{\omega^1}{\phi_r}\,R_r \quad (\text{for } \rho \leq \omega \leq \phi) \;\ldots \qquad (71b)$$

The effects E^L_{r1} caused by a unit bending moment at the left end of span r as follows: The shears are

$$V^L_{r1} = -\,\frac{1}{R_r\,\phi_r} \;\ldots\ldots\ldots\ldots\ldots\ldots \qquad (72a)$$

The bending moments are

$$M^L_{r1} = \cos\rho - \frac{\cos\phi_r}{\sin\phi_r}\,\sin\rho \;\ldots\ldots\ldots\ldots \qquad (72b)$$

and the torsional moments are

$$T^L_{r1} = \frac{1}{\phi_r} - \frac{\cos\rho^1}{\sin\phi_r} \;\ldots\ldots\ldots\ldots\ldots \qquad (72c)$$

The effects E^R_{r1} caused by a unit bending moment at the right end of span r are as follows: The shears are

$$V^R_{r1} = \frac{1}{R_r\,\phi_r} \;\ldots\ldots\ldots\ldots\ldots\ldots \qquad (73a)$$

The bending moments are

$$M^R_{r1} = \cos \rho^1 - \frac{\cos \phi_r}{\sin \phi_r} \sin \rho^1 \quad \ldots\ldots\ldots\ldots \quad (73b)$$

and the torsional moments are

$$T^R_{r1} = - \frac{1}{\phi_r} + \frac{\cos \rho}{\sin \phi_r} \quad \ldots\ldots\ldots\ldots\ldots\ldots \quad (73c)$$

It will now be necessary to derive expressions for y^L_r, y^R_r, β_r and γ_r. For simplicity the subscript r will be omitted in the following derivations and also y shall represent y^L_r. The bending area is composed of the bending diagram y^a and e-times the rotation diagram y^b.

To evaluate the bending diagram of a simple span r due to a unit bending moment at its left end, that is, the y^a line, consider an element ds as in Figs. 11 and 12.

The slope of the element ds is

$$d\epsilon = \frac{M^L_1}{E\,I}\, R\, d\rho \quad \ldots\ldots\ldots\ldots\ldots\ldots\ldots\ldots \quad (74a)$$

The rotation of the element ds is

$$d\alpha = - \frac{T^L_1}{N\,J}\, R\, d\rho \quad \ldots\ldots\ldots\ldots\ldots\ldots\ldots \quad (74b)$$

From Figs. 11 and 12 the deflection of any point w is

$$y^a = - \int_o^\omega M^L_1 \frac{R^2}{E\,I} \sin(\omega - \rho)\, d\rho - \int_o^\omega T^L_1 \frac{R^2}{N\,J} \left[1 - \cos(\omega - \rho) \right] d\rho \quad \ldots \quad (75)$$

and with $E\,I / N\,J = \mu$

$$\frac{E\,I}{R^2}\, y^a = - \int_o^\omega M^L_1 \sin(\omega - \rho)\, d\rho - \mu \int_o^\omega T^L_1 \left[1 - \cos(\omega - \rho) \right] d\rho \quad \ldots\ldots \quad (76)$$

observing the boundary condition $y^a = 0$ for $\omega = \phi$ this integral becomes

$$\frac{E\,I}{R^2}\, y^a = \left(\frac{\phi \sin \omega}{2 \sin^2 \phi} - \frac{\omega \cos \omega^1}{2 \sin \phi} \right)(1 + \mu) + \left(\frac{\omega^1}{\phi} - \frac{\sin \omega^1}{\sin \phi} \right) \mu \quad \ldots\ldots \quad (77)$$

From the definition of end slopes it follows that

$$\beta = \frac{dy^a}{dR\,\omega} \text{ (with } \omega = 0) \quad \ldots\ldots\ldots\ldots \quad (78a)$$

and

$$\gamma = - \frac{dy^a}{dR\,\omega} \text{ (with } \omega^1 = 0) \quad \ldots\ldots\ldots\ldots \quad (78b)$$

hence, by differentiation

$$\frac{E\,I}{R\,\phi}\,\frac{dy^a}{dR\,\omega} = \left(\frac{\cos\omega}{2\sin^2\phi} - \frac{\omega\sin\omega^1}{2\,\phi\,\sin\phi}\right)(1+\mu) - \frac{\cos\omega^1}{2\,\phi\,\sin\phi}(1-\mu) - \frac{\mu}{\phi^2}\quad . \ . \ (79)$$

with $\omega = 0$

$$\frac{E\,I}{R\,\phi}\,\beta = \frac{1}{2\sin^2\phi}(1+\mu) - \frac{\cos\phi}{2\,\phi\,\sin\phi}(1-\mu) - \frac{1}{\phi^2}\,\mu \ . \ . \ . \ . \quad (80a)$$

with $\omega^1 = 0$

$$\frac{E\,I}{R\,\phi}\,\gamma = -\frac{\cos\phi}{2\sin^2\phi}(1+\mu) + \frac{1}{2\,\phi\,\sin\phi}(1-\mu) + \frac{1}{\phi^2}\,\mu \quad . \ . \ (80b)$$

The rotation diagram, that is the y^b line, is arrived at by integrating the rotations of the elements ds as given by Eq. 74(b) and adding the rotational components of the deflections y^a as given by Eq. 77

$$e\,y^b = e\int_o^{\omega} d\alpha - e\,\frac{y^a}{R} = -e\int_o^{\omega}\frac{T_1^L}{NJ}\,R\,d\rho - e\,\frac{y^a}{R} \ . \ . \ . \ . \ . \ . \ . \ . \quad (81)$$

which, on integration, becomes

$$e\,\frac{E\,I}{R^2}\,y^b = \left(\frac{\omega^1}{\phi} - \frac{\sin\omega^1}{\sin\phi}\right)\mu\,\frac{e}{R} - \frac{E\,I}{R^2}\,y^a\,\frac{e}{R} \ . \ . \ . \ . \ . \ . \ . \ . \quad (82)$$

Now by addition of Eqs. 77 and 82 the bending area becomes

$$\frac{E\,I}{R^2\,\phi^2}\,y = \left(\frac{\sin\omega}{2\,\phi\,\sin^2\phi} - \frac{\omega\cos\omega^1}{2\,\phi^2\sin\phi}\right)(1+\mu)\left(1-\frac{e}{R}\right)$$

$$+\left(\frac{\omega^1}{\phi^3} - \frac{\sin\omega^1}{\phi^2\sin\phi}\right)\mu \ . \ . \ . \ . \ . \ . \ . \ . \ . \ . \ . \ . \ . \ . \quad (83a)$$

This function shall be abbreviated for simplicity. Thus,

$$\frac{E\,I}{R^2\,\phi^2}\,y = \frac{E\,I}{R^2\,\phi^2}\,y_r^L = \Phi^L = a_y\,(1+\mu)\left(1-\frac{e}{R}\right) - b_y\,\mu \quad . \ . \ (83b)$$

in which

$$a_y = \left(\frac{\sin\omega}{2\,\phi\,\sin^2\phi} - \frac{\omega\cos\omega^1}{2\,\phi^2\sin\phi}\right); \quad b_y = \frac{\omega^1}{\phi^3} - \frac{\sin\omega^1}{\phi^2\sin\phi}$$

Because of symmetry, the bending area of a simple span r due to a unit bending moment at its right end is similar but opposite hand

$$\frac{E\,I}{R^2\,\phi^2}\quad y_r^R = \Phi^R \ . \ . \ . \ . \ . \ . \ . \ . \ . \ . \ . \ . \ . \ . \quad (83c)$$

Continuous Spans With Rigid Torsional Restraints.—The magnitude of the angle δ_{nn} introduced at a hypothetical hinge as described previously can be chosen arbitrarily without affecting the final results. It will be convenient to make $\delta_{nn} = -1/EI$. The moments at the supports due to this deformation are computed from the three-moment-equation which is shown in Table 1 in the form of a determinant. The value of a determinant remains unchanged if all its coefficients are multiplied by the same factor. The coefficients in Table 1 have been multiplied by E I in order to obtain more convenient numerical values.

A continuous expression for X_n extending over all the spans r, $1 \leq r \leq m$, cannot be given. However, for each individual span r, X_n can be expressed as a function of the moments at the adjacent supports. If the end moments of span r due to the deformation δ_{nn} are $M_{(r-1)n}$ and M_{rn}, then the X_n-area in that span is in accordance with Eqs. 66, 67, and 83

TABLE 1

$M_{(n-2)n}$	$M_{(n-1)n}$	M_{nn}	$M_{(n+1)n}$	$M_{(n+2)n}$	
......	......				0
$EI\ \gamma_{n-1}$	$EI(\beta_{n-1}+\beta_n)$	$EI\ \gamma_n$			0
	$EI\ \gamma_n$	$EI(\beta_n+\beta_{n+1})$	$EI\ \gamma_{n+1}$		-1
		$EI\ \gamma_{n+1}$	$EI(\beta_{n+1}+\beta_{n+2})$	$EI\ \gamma_{n+2}$	0
			......	......	0

$$X_n = R_r^2\, \phi_r^2\, \Phi_r^L\, M_{(r-1)n} + R_r^2\, \phi_r^2\, \Phi_r^R\, M_{rn} \quad \ldots\ldots\ldots \quad (84)$$

Eq. 84 applied successively to all spans yields the complete influence area for X_n.

Influence areas other than for bending moments at the supports are derived directly from the latter ones by superposition. Only X_{r-1} and X_r contribute to a desired effect in span r. Thus, by Eq. 68 the shear at any point ρ in span r is

$$V_r = -\frac{\omega}{\phi_r} - \frac{1}{R_r\,\phi_r} X_{r-1} + \frac{1}{R_r\,\phi_r} X_r \ (\text{for } 0 \leq \omega \leq \rho) \quad \ldots \quad (85a)$$

and

$$V_r = \frac{\omega^1}{\phi_r} - \frac{1}{R_r\,\phi_r} X_{r-1} + \frac{1}{R_r\,\phi_r} X_r \quad (\text{for } \rho \leq \omega \leq \phi) \quad \ldots \quad (85b)$$

the bending moment at any point ρ in span r is

$$M_r = \frac{\sin\,\omega\,\sin\,\rho^1}{\sin\,\phi_r}\left(R_r - e\right) + \left(\cos\,\rho - \frac{\cos\,\phi_r}{\sin\,\phi_r}\,\sin\,\rho\right) X_{r-1}$$

$$+ \left(\cos\,\rho^1 - \frac{\cos\,\phi_r}{\sin\,\phi_r}\,\sin\,\rho^1\right) X_r \quad (\text{for } 0 \leq \omega \leq \rho) \quad \ldots\ldots \quad (86a)$$

and

$$M_r = \frac{\sin \omega^1 \sin \rho}{\sin \phi_r}\left(R_r - e\right) + \left(\cos \rho - \frac{\cos \phi_r}{\sin \phi_r} \sin \rho\right) X_{r-1}$$

$$+\left(\cos \rho^1 - \frac{\cos \phi_r}{\sin \phi_r} \sin \rho^1\right) X_r \quad (\text{for } \rho \leq \omega \leq \phi) \;.\;.\;.\;.\;.\;.\;. \quad (86b)$$

and the torsional moment at any point ρ in span r

$$T_r = -\frac{\sin \omega \cos \rho^1}{\sin \phi_r}\left(R_r - e\right) + \frac{\omega}{\phi_r} R_r + \left(\frac{1}{\phi_r} - \frac{\cos \rho^1}{\sin \phi_r}\right) X_{r-1}$$

$$-\left(\frac{1}{\phi_r} - \frac{\cos \rho}{\sin \phi_r}\right) X_r \quad (\text{for } 0 \leq \omega \leq \rho) \;.\;.\;.\;.\;.\;.\;.\;.\;. \quad (87a)$$

and

$$T_r = \frac{\sin \omega^1 \cos \rho}{\sin \phi_r}\left(R_r - e\right) - \frac{\omega^1}{\phi_r} R_r = \left(\frac{1}{\phi_r} - \frac{\cos \rho^1}{\sin \phi_r}\right) X_{r-1}$$

$$-\left(\frac{1}{\phi_r} - \frac{\cos \rho}{\sin \phi_r}\right) X_r \quad (\text{for } \rho \leq \omega \leq \phi) \;.\;.\;.\;.\;.\;.\;.\;. \quad (87b)$$

APPLICATIONS AND CONCLUSIONS

The Simple Span Curved Girder.—It will be of interest to compare the maximum bending moments of the simple span curved girder (Eq. 45) with the maximum bending moments of a straight girder of equivalent length $L = R\,\phi$.

On the curved girder, a concentrated load on centerline causes the maximum moment

$$M = \frac{\sin^2 \phi/2}{\sin \phi} \; R\,P \;.\;.\;.\;.\;.\;.\;.\;.\;.\;.\;.\;.\;.\;. \quad (88a)$$

at midspan. The corresponding moment for the straight girder is

$$M = \frac{P\,L}{4} = \frac{\phi}{4} \; R\,P \;.\;.\;.\;.\;.\;.\;.\;.\;.\;.\;.\;.\;.\;.\;. \quad (88b)$$

The ratio $\nu_c = \dfrac{4 \sin^2 (\phi/2)}{\phi \sin \phi}$ is plotted in Fig. 13 for varying values of ϕ.

On the curved girder, a uniformly distributed load on centerline causes the maximum moment

$$M = 2\,p \int_0^{\phi/2} \frac{\sin \omega \sin (\phi/2)}{\sin \phi} \; R^2 \, d\omega = 2\,p\,R^2 \, \frac{\sin (\phi/2)}{\sin \phi} \left[1 - \cos (\phi/2)\right] . \quad (89a)$$

The corresponding moment for the straight girder is

$$M = p \frac{L^2}{8} = p\,R^2 \, \frac{\phi^2}{8} \;.\;.\;.\;.\;.\;.\;.\;.\;.\;.\;.\;.\;.\;.\;. \quad (89b)$$

The ratio $\nu_u = \dfrac{16 \sin(\phi/2)\,[1 - \cos(\phi/2)]}{\phi^2 \sin \phi}$ is plotted in Fig. 13 for varying values of ϕ.

Fig. 13 shows the increase of maximum bending moments due to curvature to be small. Thus, it will be sufficiently accurate, for practical applications, to compute the bending moments on the equivalent straight beam and multiply the results by the factor ν_u.

The greatest torsional moments occur at the supports. In Fig. 14 the T/R-line for $\rho = \phi = 30^o$ is plotted to scale.
The solid line in Fig. 14, which has its maximum at

$$\omega = \cos^{-1}\left(1 - \frac{\phi^2}{3!} + \frac{\phi^4}{5!} - \dots\right)$$

represents the case of rigid torsional restraints.

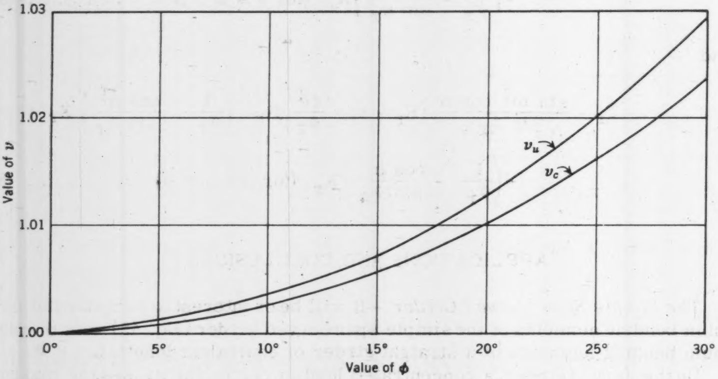

FIG. 13

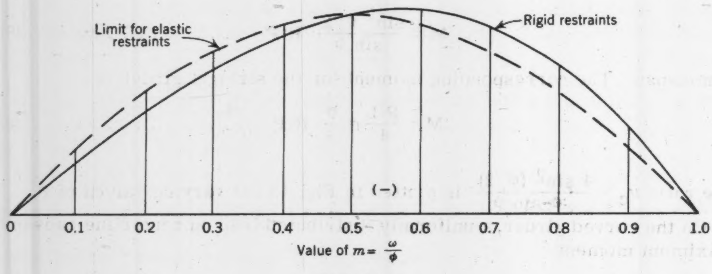

FIG. 14

In the case of elastic restraints, the term U k/(1+2 k) of Eqs. 60 to 65 appears as a correction to the influence line for rigid restraints. The dotted line in Fig. 14 shows the T/R-line for elastic restraints if k/(1+2 k) = 0.5, which obviously is the mathematical limit if the elasticity of the restraints becomes infinite. In practice this limit cannot be reached since with k = ∞ the structure would not be stable. It may be noted, however, that for k = ∞ the T/R-line becomes symmetrical. Furthermore the corrective function U is assymmetrical and hence $\int_0^{\phi} U\, d\omega = 0$. This means that for uniform loading over the full span, the elasticity of the restraints has no influence on the end torsional moments nor on any other effect. For concentrated loads, the case of rigid restraints gives only slightly higher torsional moments and it will be safe without being wasteful to neglect the elasticity of the restraints in all practical cases. It is extremely difficult to correctly assess the magnitude of this elasticity, which is partly due to the elastic yielding of the foundations.

The preceding remarks were concerned only with loads acting on centerline. The effect of eccentricity, however, can easily be seen from Eqs. 45 and 46.

If for instance transverse cross sections are taken through the influence area for the bending moment at midspan, the resulting influence branches become zero if extended to the center of curvature C (Fig. 15). Obviously the effect of e is negligibly small if the ratio R/b is sufficiently big, which is always the case for bridges. For example on a 26 ft. roadway deck with both lanes loaded, as this is the governing loading, the center of gravity of the load can come off the center line as far as $e = \pm 1.5$ ft. By equal triangles the influence ordinates then change in the transverse direction by only $\pm 150/R\,\%$.

The T/R-area for $\rho = \phi = 30^{\circ}$, that is the influence area for the torsional end moment at B is shown in a similar manner in Fig. 16. Here the influence branches if extended to the center of curvature C attain the value ω/ϕ and, as can be seen, the eccentricity of the load is of the greatest importance.

The Continuous Curved Girder.—The continuous girder has been analyzed under the assumption of rigid torsional restraints only. Judging from the results obtained for the simple span, it would appear that this assumption involves only a small error on the safe side in cases where some degree of elasticity does exist.

In order to solve the three-moment-equation for the continuous girder, the end slopes of the simple girder have to be known. For constant I and J, the end slopes have been computed and plotted as functions of ϕ in Fig. 17. In connection with this diagram, it may be noted that Eqs. 80 (a) and 80 (b) give inaccurate results for small angles ϕ because the results appear in the form of differences of large numbers. For this reason Eqs. 80(a) and 80(b) have been expanded into McLaurin's series. Thus,

$$\frac{E\,I}{R\,\phi}\,\beta = \frac{1}{\sin^2\phi}\left[\frac{2}{3!}\phi^2 - \frac{8}{5!}\phi^4 + \frac{32}{7!}\phi^6 - \dots + \mu\left(\frac{16}{6!}\phi^4 - \frac{128}{8!}\phi^6 + \dots\right)\right] \qquad (90a)$$

and

$$\frac{E\,I}{R\,\phi}\,\gamma = \frac{1}{\sin^2\phi}\left[\frac{1}{3!}\phi^2 - \frac{2}{5!}\phi^4 + \frac{3}{7!}\phi^6 - \dots + \mu\left(\frac{14}{6!}\phi^4 - \frac{96}{8!}\phi^6 + \dots\right)\right] \qquad (90b)$$

For a straight girder of equivalent length $L = R\phi$ the end slopes are

$$\frac{E\,I}{R\,\phi}\,\beta^{x} = \frac{1}{3} \qquad (91a)$$

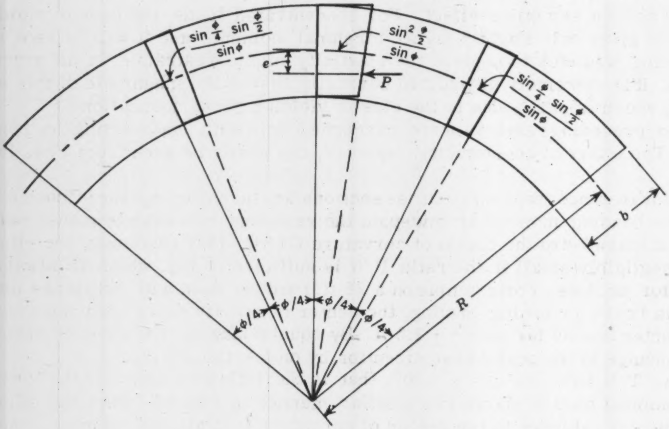
$\frac{\sin\frac{\phi}{4}\ \sin\frac{\phi}{2}}{\sin\phi}$
$\frac{\sin^2\frac{\phi}{2}}{\sin\phi}$
e
P
$\frac{\sin\frac{\phi}{4}\ \sin\frac{\phi}{2}}{\sin\phi}$
b
R
φ/4
φ/4
φ/4
φ/4

FIG. 15

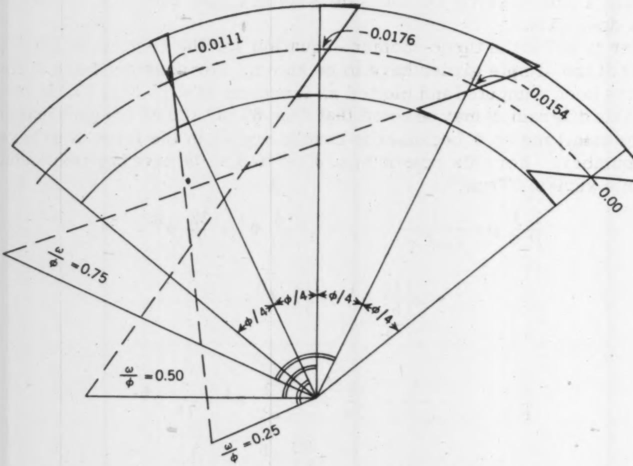
-0.0111
-0.0176
-0.0154
0.00
$\frac{\omega}{\phi}$ =0.75
$\frac{\omega}{\phi}$ =0.50
$\frac{\omega}{\phi}$ =0.25
φ/4
φ/4
φ/4
φ/4

FIG. 16

and

$$\frac{E\,I}{R\,\phi}\,\gamma^{x} = \frac{1}{6} \quad \text{. . . . . (91b)}$$

In order to clearly demonstrate the influence of the curvature on the magnitude of the end slopes, the results obtained from Eqs. 90 (a) and 90 (b) are

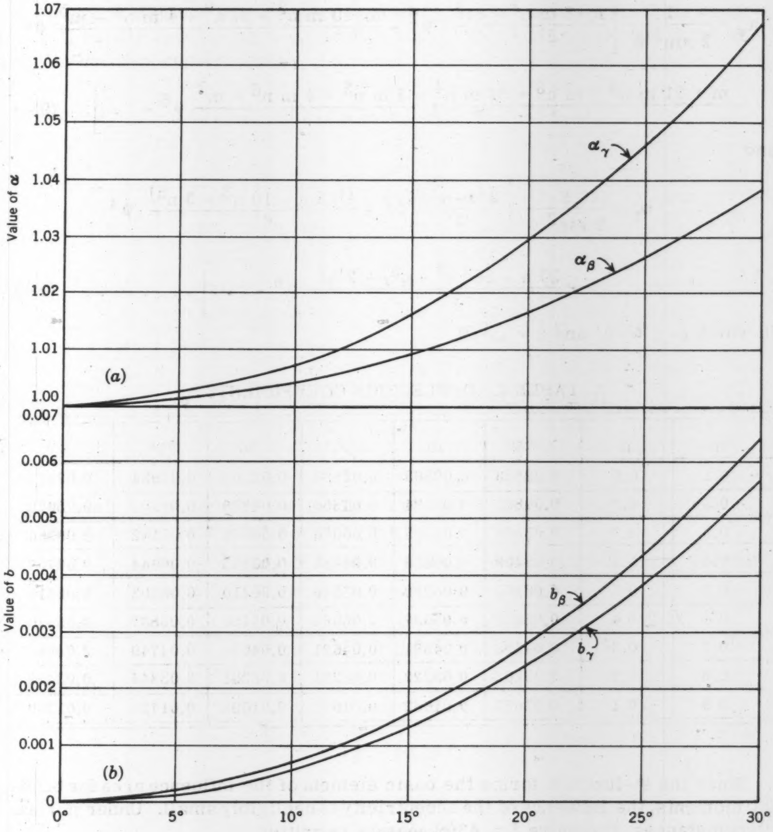

FIG. 17.—COEFFICIENTS FOR END SLOPES

represented in the following form:

$$\frac{E\,I}{R\,\phi}\,\beta = \frac{1}{3}\,a_\beta + \mu\,b_\beta \quad \text{. . . . . (92a)}$$

and

$$\frac{E\,I}{R\,\phi}\,\gamma = \frac{1}{6}\,a_\gamma + \mu\,b_\gamma \quad \ldots\ldots\ldots\ldots\ldots \quad (92b)$$

Similar to the end slopes, the Φ-function has been computed for constant I and J. The notation of Eq. 83(b) has been used and a_y and b_y have been expanded into series. Thus,

$$a_y = \frac{1}{2\sin^2\phi}\left[\frac{m+3\,m\,n^2 - m^3}{3!}\,\phi^2 - \frac{m+10\,m\,n^2 + m\,n^3 + 4\,m\,n^4 - m^5}{5!}\,\phi^4 + \frac{m + 21\,m\,n^2 + m\,n^3 + 34\,m\,n^4 + 3\,m\,n^5 + 4\,m\,n^6 - m^7}{7!}\,\phi^6 - \ldots\right] \ldots \quad (93a)$$

and

$$b_y = \frac{1}{2\sin^2\phi}\left[\frac{2\left(n-n^3\right)}{3!}\,\phi^2 - \frac{4\left(13\,n - 10\,n^3 - 3\,n^5\right)}{6!}\,\phi^4 + \frac{30\,n - 14\left(n^3 - n^5\right) - 2\,n^7}{7!}\,\phi^6 - \ldots\right] \ldots\ldots\ldots \quad (93b)$$

in which $m = \omega/\phi$ and $n = \omega^1/\phi$.

TABLE 2.—DEFLECTION COEFFICIENTS a_y

m	n	5°	10°	15°	20°	25°	30°
0.1	0.9	0.02853	0.02863	0.02880	0.02903	0.02934	0.02973
0.2	0.8	0.04805	0.04824	0.04856	0.04899	0.04957	0.05029
0.3	0.7	0.05958	0.05983	0.06026	0.06084	0.06162	0.06260
0.4	0.6	0.06409	0.06438	0.06487	0.06555	0.06644	0.06757
0.5	0.5	0.06260	0.06289	0.06340	0.06410	0.06503	0.06619
0.6	0.4	0.05609	0.05637	0.05684	0.05750	0.05837	0.05946
0.7	0.3	0.04556	0.04581	0.04621	0.04676	0.04749	0.04841
0.8	0.2	0.03205	0.03222	0.03251	0.03291	0.03344	0.03411
0.9	0.1	0.01653	0.01662	0.01677	0.01698	0.01725	0.01760

Since the Φ-function forms the basic element of the influence area for bending moments, the influence of the eccentricity is negligibly small. Under normal circumstances, therefore Eq. 83(b) may be rewritten

$$\Phi^L = a_y + \mu\left(a_y - b_y\right) = a_y + \mu\,c_y \quad \ldots\ldots\ldots\ldots \quad (94)$$

The coefficients a_y and b_y are indicated in Tables 2 and 3.

It may be noted that for $\phi = 0$ Φ^L is given by the corresponding function for

straight girders which is

$$\phi^{L} = \frac{m\,n + m\,n^2}{6} \; . . . . (95)$$

The ϕ^R - lines are obtained by exchanging m and n.

***The Simple Span Girder with Fixed Ends.*—The method of analysis used for continuous girders may also be used for simple span girders, the ends of which are rigidly restrained with respect to bending as well as torsion. This condition will hardly ever arise in connection with bridge structures, but is not unusual in building construction.**

TABLE 3.—DEFLECTION COEFFICIENTS b_y

m	n	5°	10°	15°	20°	25°	30°
0.1	0.9	0.02851	0.02857	0.02865	0.02877	0.02892	0.02911
0.2	0.8	0.04802	0.04813	0.04829	0.04851	0.04880	0.04917
0.3	0.7	0.05954	0.05967	0.05989	0.06018	0.06056	0.06105
0.4	0.6	0.06404	0.06419	0.06444	0.06478	0.06522	0.06578
0.5	0.5	0.06255	0.06270	0.06296	0.06330	0.06376	0.06434
0.6	0.4	0.05605	0.05618	0.05643	0.05675	0.05718	0.05772
0.7	0.3	0.04553	0.04566	0.04586	0.04613	0.04649	0.04694
0.8	0.2	0.03203	0.03211	0.03226	0.03245	0.03271	0.03304
0.9	0.1	0.01652	0.01656	0.01663	0.01674	0.01687	0.01704

If the influence line for the bending moment at the left support is desired, then the three-moment-equation becomes

$$M_L\, E\, I\, \beta + M_R\, E\, I\, \gamma = -1 \; . . . . (96a)$$

and

$$M_L\, E\, I\, \gamma + M_R\, E\, I\, \beta = 0 \; . . . . (96b)$$

from which

$$M_L = \frac{-1}{E\, I\, \beta - e\, I\left(\gamma^2/\beta\right)} \; . . . . (97a)$$

and

$$M_R = \frac{1}{E\, I\left(\beta^2/\gamma\right) - E\, I\, \gamma} \; . . . . (97b)$$

Further, by Eq. 84

$$X_L = R^2\, \phi^2\, \frac{-\phi^L}{E\, I\, \beta - E\, I\left(\gamma^2/\beta\right)} + R^2\, \phi^2\, \frac{\phi^R}{E\, I\left(\beta^2/\gamma\right) - E\, I\, \gamma} \; . . (98)$$

If it is required to investigate the fixed girder for one load condition, only then the complete ϕ-functions in the previous equation can be replaced by the ϕ-ordinates at the point of load application.

Girders With Variable Moments Of Inertia.—In the case of simple span curved girders, only the variations of the torsional stiffness enter the analysis. The integrals of Eqs. 34, 37, and 41 can be evaluated numerically or graphically.

In the case of continuous spans, the amount of work involved in evaluating all the integrals numerically or graphically is considerable. However, considering that the bending moments are relatively little affected by the curvature of the girder and that in the evaluation of the integrals for β, γ, and ϕ, the torsional moments and stiffnesses make only relatively small contributions, the following approximate procedure is suggested.

To compute the end slopes, Eqs. 92(a) and 92(b) may be used if the factors 1/3 and 1/6, respectively, are replaced by the end slopes of an equivalent straight girder with variable moment of inertia. These end slopes are easily computed or taken from available tables. The factors a_β, a_γ, b_β, b_γ, may be taken from Fig. 17 without any corrections.

Similarly in Eq. 94, ϕ^L may be computed or taken from available tables for straight girders, but must then be increased by the ratio $6(a_y + \mu c_y)/(m n + m n^2)$.

APPENDIX.—NOTATION

The following symbols have been adopted for use in this paper:

A, B = points of support at left and right end of simple beam, respectively. Also the vertical reactions at these points;

$a_\beta b_\beta a_\gamma b_\gamma$ = coefficients determining the end slopes β and γ;

a_y b_y = coefficients determining the bending ordinates y;

e = eccentricity of load application;

J = torsional stiffness factor (in^4);

M = bending moment;

N = shearing modulus of elasticity;

P = external load;

R = radius of curvature of girder;

T = torsional moment;

T_P = external torsional moment;

V = shearing force;

X = any redundant (statically indeterminate) force;

y = ordinate of bending line or area due to unit end moment;

β, γ = end slopes due to unit end moment;

ξ = rotation of support due to unit moment;

ρ, ρ^1 = angle to point for which an influence line is determined;

ϕ = total angle of curvature;

ω, ω^1 = angle to point of load application or to point at which displacements are computed;

Φ = unit bending function;

subscript o = indicates effects of external loading on the primary system;

subscript 1 = indicates effects of the redundant force on the primary system;

subscript r = makes reference to the rth span;

superscript a = denotes the effects of the load $P = 1$; and

superscript b = denotes the effects of the external moment $T_p = e$.

AMERICAN SOCIETY OF CIVIL ENGINEERS
Founded November 5, 1852
TRANSACTIONS

Paper No. 3155

LONG REINFORCED CONCRETE COLUMNS

A SYMPOSIUM

PAGE

ULTIMATE STRENGTH OF HINGED COLUMNS

By Bengt Broms and I. M. Viest 309

Discussion:
By G. C. Ernst 339
J. J. Hromadik 340
T. Jumikis and A. S. Hall 345
Bengt Broms and I. M. Viest 346

ULTIMATE STRENGTH ANALYSIS OF RESTRAINED COLUMNS

By Bengt Broms and I. M. Viest. 348

DESIGN

By Bengt Broms and I. M. Viest. 367

Discussion:
By J. G. MacGregor and C. P. Siess. 385
Phil M. Ferguson 391
Bengt Broms and I. M. Viest. 397

ULTIMATE STRENGTH OF HINGED COLUMNS

By Bengt Broms,[1] M. ASCE and I. M. Viest,[2] F. ASCE

Discussion by Messrs. G. C. Ernst; J. J. Hromadik; T. Jumikis and A. S. Hall; and Bengt Broms and I. M. Viest

---

SYNOPSIS

Theoretical analyses are presented for the ultimate strength of long hinged reinforced concrete columns. Both concentric and eccentric loads are considered. The treatment of concentrically loaded columns is based on Engesser's tangent modulus formula and the treatment of eccentrically loaded columns is based on the principles advanced by von Kármán. Both analyses utilize the stress-strain relationship for concrete determined by Hognestad from tests of short eccentrically loaded columns.

The analyses are compared with the test results of six experimental investigations carried out in the past. The test data, including 48 concentrically and 79 eccentrically loaded long hinged columns and the analyses are in good agreement, thus indicating that the analyses with their basic assumptions yield reliable results.

INTRODUCTION

Extensive investigations of short concentrically and eccentrically loaded columns lead in the past to the development of generally applicable analytical expressions for predicting the ultimate strength of short reinforced concrete columns. The experimental studies have shown that for short columns the effect of lateral deflections on the strength is small, and that short columns are not in danger of buckling. Accordingly, the analytical expressions disregard both deflections and buckling. On the other hand, it is known that the strength of long columns may be reduced significantly by both of these factors. The analyses presented in this paper take them into account.

Reinforced concrete columns may fail either by material failure or by buckling. Material failure occurs through the crushing of concrete in compression. Buckling occurs when the lateral deflection of the column increases without any increase of load.

Note.—Published essentially as printed here, in January, 1958, in the Journal of the Structural Division, as Proceedings Paper 1510. Positions and titles given are those in effect when the paper or discussion was approved for publication in Transactions.

[1] Assoc. Prof. of Civ. Engrg., Cornell Univ., Ithaca, N. Y.; formerly Research Asst., Dept. of Theoretical and Applied Mechanics, Univ. of Illinois, Urbana, Ill.

[2] Bridge Research Engr., ASSHO Road Test, Ottawa Ill.; formerly Research Assoc. Prof. of Theoretical and Applied Mechanics, Univ. of Illinois, Urbana, Ill.

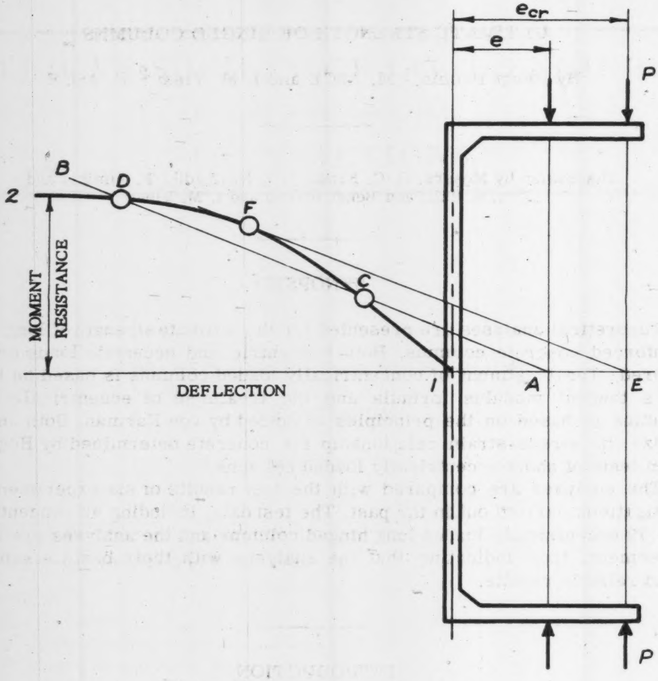
e_{cr}
e
P
B
2
D
F
C
MOMENT RESISTANCE
DEFLECTION
1
A
E
P

FIG. 1.—BUCKLING OF A HINGED COLUMN

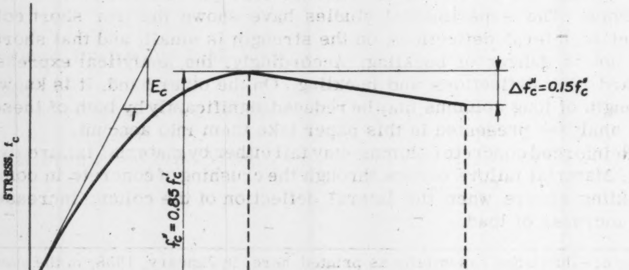

FIG. 2.—ASSUMED STRESS-STRAIN RELATIONSHIP FOR CONCRETE

Buckling of an eccentrically loaded hinged column is illustrated in Fig. 1 in which the moment resistance of a column and the external moment are shown as functions of the deflection at midheight. Fig. 1 is drawn for a constant load P applied to a particular column at varying eccentricity. The moment resistance depends, therefore, only on the deflection of the column, whereas the external moment depends on the sum of the deflection and eccentricity.

The moment resistance is shown in Fig. 1 as the curve 1-2, the external moment as the straight line A-B for eccentricity e and as the straight line E-F for eccentricity e_{cr}. These two lines are parallel because their slope depends only on the magnitude of the load P, that is constant. The straight line A-B intersects the curve 1-2 at points C and D for which the moment resistance is equal to the external moment. These two points represent two positions of equilibrium; stable equilibrium at C, and unstable equilibrium at D. When the eccentricity of the load P is increased, points C and D move closer together. At the eccentricity e_{cr} line A-B becomes line E-F, tangent to the curve 1-2. At an increase of the eccentricity beyond e_{cr} no position of equilibrium is possible. Thus, e_{cr} is the critical eccentricity corresponding to buckling of the column under the load P.

A column fails by material failure if the strength of the column material is exceeded before buckling is reached. For example, if the moment resistance curve in Fig. 1 ended at point C, the column would fail by material failure when the load P has reached eccentricity e.

Notation.—The letter symbols adopted for use in this paper are defined where they first appear and are arranged alphabetically, for convenience of reference, in Appendix II.

ULTIMATE STRENGTH ANALYSIS

Basic Assumptions.—The assumptions for the theories presented in this paper were generally chosen so as to give a lower limit for the ultimate strength of both concentrically and eccentrically loaded long reinforced concrete columns.

Stress-strain relationship for concrete.—The assumed stress-strain relationship for concrete in compression is shown in Fig. 2. It was derived by Hognestad[3] (1) from the tests of short columns subjected to combined bending and axial load. It consists of a parabola and a sloping straight line.

The initial part of the curve in Fig. 2 is a second degree parabola expressed by the equation for concrete stress, f_c,

$$f_c = f_c'' \left[\frac{2\epsilon}{\epsilon_o} - \left(\frac{\epsilon}{\epsilon_o}\right)^2 \right] \ldots\ldots\ldots\ldots\ldots (1)$$

in which ϵ and ϵ_o are the concrete strains at f_c and f_c'', respectively. The initial modulus of elasticity is taken as

$$E_c = 1{,}800{,}000 + 460\, f_c'' \ldots\ldots\ldots\ldots\ldots (2)$$

---

[3] Numerals in parentheses, thus (1), refer to corresponding items in Appendix I.

The strain at the maximum stress is $\epsilon_o = 2\, f''_c/E_c$. Between the strain ϵ_o and the ultimate strain ϵ_u, the stress-strain relationship is a descending straight line. The ultimate strain ϵ_u is taken as 0.0038.

The maximum stress f''_c is taken as 0.85 times the cylinder strength f'_c. This relationship is believed to be correct only for vertically cast columns.

It is assumed further that concrete resists no tensile stresses. Because the concrete between the cracks carries some tensile stresses, the actual column deflections should be smaller than the computed ones. Thus, the assumption that no tensile stresses exist in the concrete should give somewhat lower ultimate loads than the actual.

The deflection of the column at buckling depends on the magnitude of strains in the concrete and steel. Because the buckling load depends on the deflection and because buckling can occur at almost any value of concrete strain, it is necessary to know the strains with a reasonable accuracy at all loads. Accordingly, a simplified stress block, such as a rectangle or a trapezoid, cannot yield generally accurate results and the use of a more complicated, but also more accurate, Hognestad's stress block is necessary.

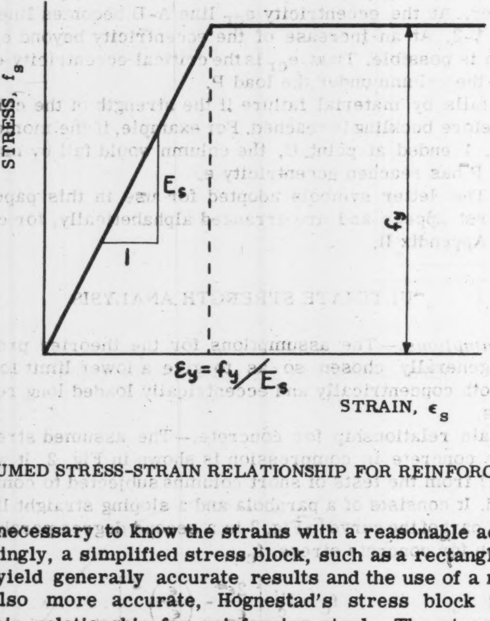

FIG. 3.—ASSUMED STRESS-STRAIN RELATIONSHIP FOR REINFORCING STEEL

Stress-strain relationship for reinforcing steel.—The stress-strain diagram for the reinforcing steel is assumed trapezoidal with the flat portion equal to the yield point stress f_y as shown in Fig. 3. The modulus of elasticity, E_s, is taken in all computations as 30,000,000 psi.

Bernoulli's hypothesis.—Linear distribution of strains across the column cross-sections is assumed at all load levels.

Shape of deflected column.—It is assumed that the deflected shape of a column is a part of a cosine wave as shown in Fig. 4. This assumption is theoretically correct only for small lateral deflections and for constant modulus of elasticity along the column. Such conditions are satisfied only in concentrically loaded columns.

For eccentrically loaded columns, the use of the cosine wave assumption implies that the modulus of elasticity is constant along the column and equal

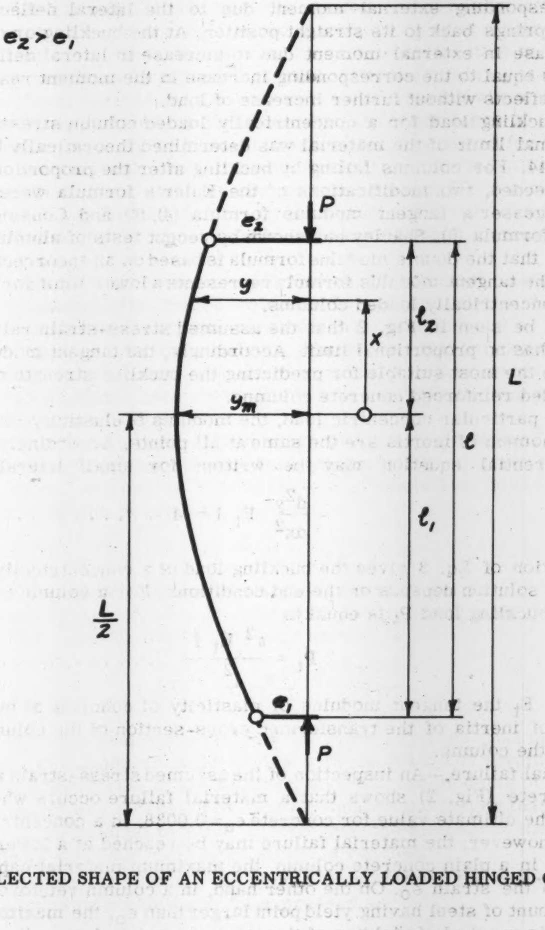

FIG. 4.—DEFLECTED SHAPE OF AN ECCENTRICALLY LOADED HINGED COLUMN

to the average modulus at the section of failure. The stiffness at the section of failure is the smallest one; therefore, the actual deflections are smaller than the computed ones, and the computed ultimate loads should be somewhat smaller than the actual.

Effect of shear on deflection.—For a solid cross-section, the effect of shear on deflections is small. It is disregarded in the theory presented herein.

Concentrically Loaded Columns.—

Buckling.—A concentrically loaded long compression member remains straight as long as the load remains below the buckling load. When a column subjected to an axial load lower than the critical is deflected slightly from its straight position of equilibrium, its moment resistance increases faster than the corresponding external moment due to the lateral deflection, and the column springs back to its straight position. At the buckling or critical load, the increase in external moment due to increase in lateral deflection of the column is equal to the corresponding increase in the moment resistance. The column deflects without further increase of load.

The buckling load for a concentrically loaded column stressed below the proportional limit of the material was determined theoretically by Euler (2), (3) in 1744. For columns failing by buckling after the proportional limit has been exceeded, two modifications of the Euler's formula were proposed in 1889: Engesser's tangent modulus formula (4), (5) and Considère's double modulus formula (6). Shanley has shown by recent tests of aluminum columns (7), (8), (9) that the double modulus formula is based on an incorrect assumption and that the tangent modulus formula represents a lower limit for the buckling load of concentrically loaded columns.

It can be seen in Fig. 2 that the assumed stress-strain relationship for concrete has no proportional limit. Accordingly, the tangent modulus formula should be the most suitable for predicting the buckling strength of concentrically loaded reinforced concrete columns.

At any particular concentric load, the modulus of elasticity of the concrete and the moment of inertia are the same at all points. Accordingly, the following differential equation may be written for small lateral deflections:

$$-\frac{d^2y}{dx^2} E_t I = M \quad \ldots\ldots\ldots\ldots\ldots\ldots \quad (3)$$

The solution of Eq. 3 gives the buckling load of a concentrically loaded column. The solution depends on the end conditions. For a column hinged at both ends the buckling load P_t is equal to

$$P_t = \frac{\pi^2 E_t I}{l^2} \quad \ldots\ldots\ldots\ldots\ldots\ldots \quad (4)$$

in which E_t the tangent modulus of elasticity of concrete at buckling, I the moment of inertia of the transformed cross-section of the column, and l the length of the column.

Material failure.—An inspection of the assumed stress-strain relationships for concrete (Fig. 2) shows that a material failure occurs when the strain reaches the ultimate value for concrete $\epsilon_u = 0.0038$. In a concentrically loaded column, however, the material failure may be reached at a lower strain. For example, in a plain concrete column, the maximum material capacity corresponds to the strain ϵ_o. On the other hand, in a column reinforced with very large amount of steel having yield point larger than ϵ_o, the maximum material capacity is reached at yielding of the steel at a strain larger than ϵ_o. Therefore, the limiting value of the strain at failure of a concentrically loaded column depends on the strength of concrete, percentage of reinforcement, and the yield point of reinforcement.

The material capacity of columns with reinforcement having a yield point lower than ϵ_o is always reached at the strain ϵ_o. For the practical range of concrete strengths, ϵ_o varies from approximately 1.2% to 2.3%. Thus, for concentrically loaded columns reinforced with structural or intermediate grade steel, ϵ_o represents the limiting strain.

The material capacity of columns with reinforcement having a yield point higher than ϵ_o may be reached either at the strain ϵ_o or at a higher strain. Up to the strain of ϵ_o, the load carried by each material (that is, steel and concrete) is increasing with increasing strain. After the strain ϵ_o is exceeded, however, the load carried by the concrete is decreasing whereas the load carried by the steel continues to increase. For low percentages of reinforcement, the loss in capacity of concrete cannot be compensated for by the increase of the load carried by the reinforcement so that material failure occurs at ϵ_o. On the other hand, for high percentages of steel, the loss in capacity of concrete is compensated for by the increase of the load carried by the reinforcement and the column is able to carry further increases of load beyond the strain ϵ_o.

It can be seen from the preceding discussion, that in most cases material capacity of concentrically loaded columns is reached at the strain ϵ_o. If present, the increase of capacity by straining the column beyond ϵ_o is usually small. It is assumed in the analysis, therefore, that for concentrically loaded columns ϵ_o represents the limiting value. In other words, if a concentrically loaded column does not buckle before reaching the unit shortening of ϵ_o, it fails by a material failure.

Evaluation of ultimate load.—The tangent modulus of elasticity E_t in Eq. 4 may be evaluated from the stress-strain diagram for concrete (Fig. 2) as $df_c/d\epsilon$. Therefore, as long as the strain ϵ at ultimate load does not exceed ϵ_o, the tangent modulus is given by

$$E_t = E_c\left(1 - \frac{\epsilon}{\epsilon_o}\right) \quad \text{. . . . . (5)}$$

in which E_c is the initial modulus of elasticity given by Eq. 2.

For rectangular symmetrically reinforced concrete columns, the moment of inertia I of the transformed section may be written as

$$I = \frac{b\,d^3}{12} + \frac{E_s\,p}{E_t}\,\frac{b\,d\left(d''\right)^2}{4} \quad \text{. . . . . (6)}$$

in which E_s/E_t is the modular ratio, b is the width and d the total depth of the cross section. The modular ratio varies with the load. For strains smaller than the yield point strain of the reinforcement ϵ_y, the modulus of elasticity E_s may be taken as 30×10^6 psi. For strains equal to and larger than the yield point strain ϵ_y, E_s is equal to zero. Accordingly, the moment of inertia I decreases suddenly when the yield point strain is reached.

For strains smaller than ϵ_o, the relationship between the concentric load and the corresponding strains may be expressed as

$$\frac{P}{f''_c\,b\,d} = \frac{f_s\,p}{f''_c} + \frac{2\,\epsilon}{\epsilon_o} - \left(\frac{\epsilon}{\epsilon_o}\right)^2 \quad \text{. . . . . (7)}$$

in which f_s is equal to $E_s\,\epsilon$ for strains smaller than ϵ_y, and equal to f_y for strains equal to or larger than ϵ_y.

Eqs. 4, 5, 6 and 7 contain four unknowns; P, E_t, I, and ϵ. Thus, the buckling load may be evaluated by simultaneous solution of all four equations. If the resulting ϵ is larger than ϵ_0, the strength of the column is governed by material failure and its capacity may be evaluated from Eq. 7 by substituting $\epsilon = \epsilon_0$. Similarly, the critical length l for a column of known cross-section and a known value of the load P may be found by a simultaneous solution of Eq. 4-7 for l, E_t, I and ϵ.

Eccentrically Loaded Columns.—

Buckling.—Under an eccentric loading, a column deflects laterally, and the lateral deflection increases with the load. If the stresses in the column remain below the proportional limit, at large deflections the load approaches the value of the buckling load for the same column loaded concentrically.

A general theory for determining the buckling load of an eccentrically loaded column in which the maximum stresses have exceeded the proportional limit of the material was proposed by von Kármán (10) in 1910. The theory is based on the stress-strain relationship of the column material and on the assumption of linear strain distribution. The deflected shape of the column is determined by numerical integration of angle changes along the column length. The validity of von Kármán's theory was proved by tests of hinged rectangular steel columns reported by Chwalla (11) in 1934.

The determination of the exact shape of the deflected column by numerical integration is very laborious. Roš and Brunner (12) simplified von Kármán's theory by assuming the deflected column shape as a half sine-wave. Westergaard and Osgood (13) proposed the use of a part of a cosine-wave as the deflected column shape. The sine-wave assumption is inconsistent with the actual conditions in that it corresponds to zero curvature, that is, an infinite stiffness, at the ends of the column. The cosine-wave assumption is theoretically correct only at small lateral deflections as long as the stresses in the column remain below the proportional limit. When the proportional limit is exceeded, the cosine-wave assumption gives results on the safe side.

The basic work on buckling of eccentrically loaded reinforced concrete columns was carried out by Baumann (14) in 1930-33. Using von Kármán's procedure in conjunction with experimentally determined properties of concrete, he found a good agreement between the tests and the theory. More recently, Ernst, Hromadik, and Riveland (15) applied von Kármán's method, as modified by Westergaard and Osgood, to reinforced concrete columns, limiting themselves to hinged columns with equal eccentricities at both column ends and using Hognestad's stress-strain relationship for concrete. The method presented herein is essentially the same as that presented by Ernst, Hromadik, and Riveland but it is applicable to hinged columns both with equal and unequal eccentricities at the column ends.

An eccentrically loaded column becomes unstable when one of the following conditions is satisfied: $\frac{de}{dy_m} = 0$, $\frac{dP}{dy_m} = 0$, or $\frac{dM}{dy_m} = 0$. If the relationship between the load P, moment M and strains is unique, as is assumed in this derivation, all three conditions give the same buckling load.

In the following, the eccentricities at the ends of the column are expressed in terms of the maximum total deflection y_m. The buckling load is then computed from the condition $de/dy_m = 0$.

A deflected hinged column is shown schematically in Fig. 4. Because it is assumed that the deflected shape of the eccentrically loaded column is a part of a cosine-wave, it follows that

$$y = y_m \cos\frac{\pi x}{L} \quad \ldots\ldots\ldots\ldots\ldots\ldots (8)$$

The eccentricities at the column ends are then expressed as

$$e_1 = y_m \cos\frac{\pi l_1}{L} \quad \ldots\ldots\ldots\ldots\ldots\ldots (9)$$

and

$$e_2 = y_m \cos\frac{\pi l_2}{L} \quad \ldots\ldots\ldots\ldots\ldots\ldots (10)$$

Observing that $l_1 + l_2 = l$, rearranging and adding of Eq. 9 and 10 gives

$$\frac{\pi}{L} = \frac{1}{l}\left(\text{arc cos}\,\frac{e_1}{y_m} + \text{arc cos}\,\frac{e_2}{y_m}\right) \quad \ldots\ldots\ldots (11)$$

The first derivative of Eq. 11 with respect to y_m includes expressions de_1/dy_m and de_2/dy_m which are equal to zero at buckling. After substituting from Eq. 9 and 10, the derivative of Eq. 11 may, therefore, be written as

$$\left.\begin{aligned} \frac{d\left(\frac{\pi}{L}\right)}{dy_m} &= \frac{1}{l\,y_m}\left(\cot\frac{\pi l_1}{L} + \cot\frac{\pi l_2}{L}\right) \\ \text{or as}\qquad \frac{y_m}{\frac{\pi}{L}}\,\frac{d\left(\frac{\pi}{L}\right)}{dy_m} &= \frac{\cot\frac{\pi l_1}{L} + \cot\frac{\pi l_2}{L}}{\frac{\pi l}{L}} \end{aligned}\right\} \quad \ldots\ldots\ldots (12)$$

Solution of Eq. 12 gives the critical slenderness l, at which a column will buckle under an assumed load, and the corresponding values l_1 and l_2. The corresponding end eccentricities may then be computed from Eq. 9 and 10.

A graphical solution of Eq. 12 is shown in Fig. 5. In Fig. 5(a), Eq. 12 is solved for several values of $\pi\, l/L$ and l_1/l. In Fig. 5(b), Eqs. 9 and 10 are solved for several values of the same two quantities. Fig. 5(a) and 5(b) are combined into Fig. 5(c) and 5(d) relating the left side of Eq. 12 to $\pi\, l/L$ and e_2/y_m, respectively, for several ratios of e_1/e_2.

The left side of Eq. 12 may be evaluated from the relationships between the curvature and the deflection of the column, and between the axial load, moment, and deflection. The curvature and the maximum total deflection are related as follows:

$$\frac{1}{\rho} = -\frac{d^2y}{dx^2} = y_m\left(\frac{\pi}{L}\right)^2 \cos\frac{\pi x}{L} \quad \ldots\ldots\ldots (13)$$

At the point of maximum moment

$$\frac{1}{\rho_m} = y_m\left(\frac{\pi}{L}\right)^2 \quad \ldots\ldots\ldots\ldots\ldots\ldots (14)$$

Because the curvature may be expressed also as

$$\frac{1}{\rho_m} = \frac{\epsilon_4 - \epsilon_1}{d}$$

Eq. 14 may be written in the following form:

$$\frac{\epsilon_4 - \epsilon_1}{d} = y_m\left(\frac{\pi}{L}\right)^2 \quad \ldots\ldots\ldots\ldots\ldots\ldots (15)$$

in which ϵ_4 and ϵ_1 are the strains at the section of maximum moment and d is the depth of the column (Fig. 6).

At the point of maximum moment, the relation between the load, moment and maximum total deflection may be expressed as

$$y_m = \frac{M_{col}}{P} \quad \ldots\ldots\ldots\ldots\ldots\ldots (16)$$

The relationship between P, M_{col} and the strains may be determined from statics, and the stress-strain relationship for the particular material as will be shown subsequently.

The critical eccentricity and the length of the column, for which an assumed load is the buckling load, may be determined from Eq. 15 and Eq. 16 with the aid of Fig. 5(c,d). For a constant value of P, several corresponding values of $(\epsilon_4 - \epsilon_1)$ are chosen, and the corresponding values of M_{col} are computed. For each value of $(\epsilon_4 - \epsilon_1)$ the deflection y_m is determined from Eq. 16, and the value of π/L is determined from Eq. 15. For each set of corresponding values of y_m and π/L, the quantity

$$\frac{y_m}{\frac{\pi}{L}} \; \frac{d\left(\frac{\pi}{L}\right)}{dy_m}$$

is computed. Finally, Fig. 5(c) and 5(d) are entered with the vertical ordinate, and the critical length l and eccentricity e_2 are evaluated from the horizontal ordinates.

If dimensionless ratios y_m/d, $\pi\, d/L$, $M_{col}/f''_c\, b\, d^2$ and $P/f''_c\, b\, d$ are used instead of y_m, π/L, M_{col} and P, respectively, the method of solution is unaffected because the right side of Eq. 12 remains unchanged. However, the results are obtained in terms of ratios l/d and e_2/d instead of l and e_2.

The equations derived above are a general solution for buckling of eccentrically loaded hinged columns. They are applicable to columns of any cross-section and of any material.

Relationships between loads, moments and strains.—The distribution of stresses in a reinforced concrete column is determined by two strains, the stress-strain relationships for concrete (Fig. 2) and steel (Fig. 3) and the cross-section of the column. The load P and moment M_{col} are expressed in terms of strains by summation of the stresses in the cross-section.

For rectangular cross-sections with symmetrical reinforcement illustrated in Fig. 6, the following equations may be derived:

$$\frac{P}{f''_c\, b\, d} = \frac{p\left(f_{s2} + f_{s3}\right)}{2\, f''_c} + \frac{A}{\epsilon_4 - \epsilon_1} \quad \ldots\ldots\ldots\ldots (17)$$

$$\frac{M_{col}}{f''_c\, b\, d^2} = \frac{p\left(f_{s3} - f_{s2}\right)}{4\, f''_c}\,\frac{d''}{d} + \frac{B}{\left(\epsilon_4 - \epsilon_1\right)^2} - \frac{\epsilon_4 + \epsilon_1}{\left(\epsilon_4 - \epsilon_1\right)^2}\,\frac{A}{2} \quad \ldots (18)$$

in which parameters A, B and steel stresses f_{s2} and f_{s3} are known functions of concrete strains ϵ_1 and ϵ_4.

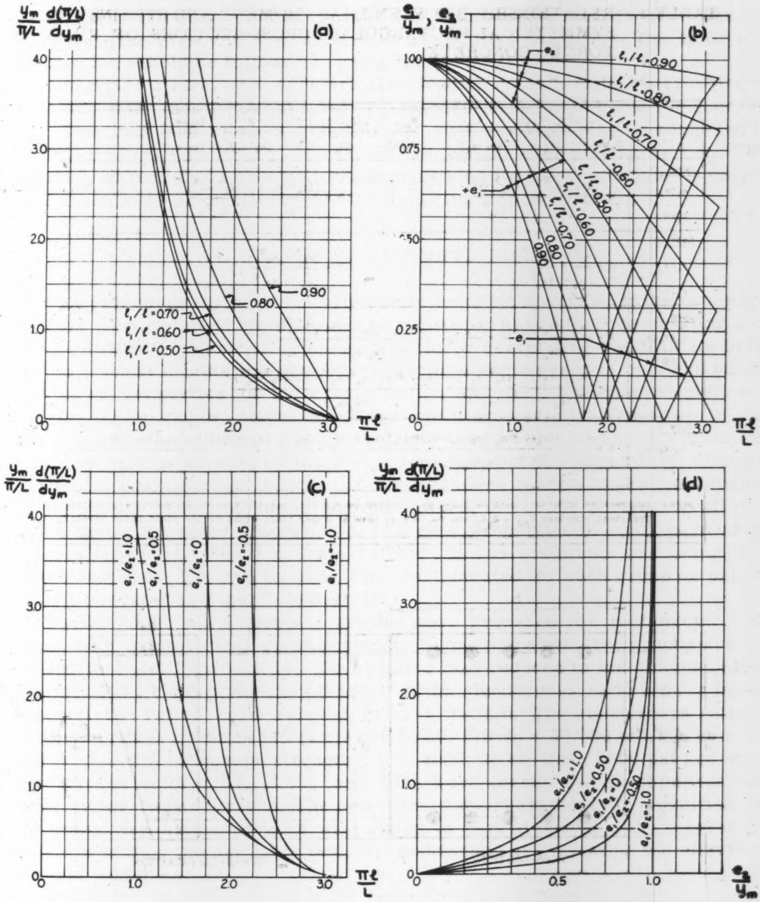

FIG. 5.—SOLUTION OF EQ. 12

Formulas for parameters A and B are shown in Table 1. Four expressions are given for each parameter. Each formula is applicable within certain limits for ϵ_4 and ϵ_1. Formulas for cases 1 and 3 refer to full cross-section

in compression, whereas formulas for cases 2 and 4 refer to a cross-section partly in compression and partly in tension.

TABLE 1.—RELATIONSHIP BETWEEN LOAD, MOMENT AND STRAINS FOR SYMMETRICAL RECTANGULAR CROSS-SECTIONS OF REINFORCED CONCRETE

	$\frac{P}{f_c'' bd} = \frac{p(f_{s2}+f_{s3})}{2f_c''} + \frac{A}{(\epsilon_4-\epsilon_1)}$ $\qquad$ $\frac{M_{col}}{f_c'' bd^2} = \frac{p(f_{s3}-f_{s2})}{4f_c''}\frac{d''}{d} + \frac{B}{(\epsilon_4-\epsilon_1)^2} - \frac{(\epsilon_4+\epsilon_1)}{(\epsilon_4-\epsilon_1)^2}\frac{A}{2}$
Case 1 $\epsilon_4<\epsilon_o$ $\epsilon_1>0$	$A = \frac{(\epsilon_4^2-\epsilon_1^2)}{\epsilon_o} - \frac{(\epsilon_4^3-\epsilon_1^3)}{3\epsilon_o^2}$ $\qquad$ $B = \frac{2(\epsilon_4^3-\epsilon_1^3)}{3\epsilon_o} - \frac{(\epsilon_4^4-\epsilon_1^4)}{4\epsilon_o^2}$
Case 2 $\epsilon_4<\epsilon_o$ $\epsilon_1<0$	$A = \frac{\epsilon_4^2}{\epsilon_o} - \frac{\epsilon_4^3}{3\epsilon_o^2}$ $\qquad$ $B = \frac{2\epsilon_4^3}{3\epsilon_o} - \frac{\epsilon_4^4}{4\epsilon_o^2}$
Case 3 $\epsilon_o<\epsilon_4<\epsilon_u$ $\epsilon_1>0$	$A = \frac{2\epsilon_o^3-3\epsilon_o\epsilon_1^2+\epsilon_1^3}{3\epsilon_o^2} + \frac{(\epsilon_u-0.85\epsilon_o)(\epsilon_4-\epsilon_o)-0.075(\epsilon_4^2-\epsilon_o^2)}{(\epsilon_u-\epsilon_o)}$ $B = \frac{2(\epsilon_o^3-\epsilon_1^3)}{3\epsilon_o} - \frac{(\epsilon_o^4-\epsilon_1^4)}{4\epsilon_o^2} + \frac{(\epsilon_u-0.85\epsilon_o)(\epsilon_4^2-\epsilon_o^2)-0.10(\epsilon_4^3-\epsilon_o^3)}{2(\epsilon_u-\epsilon_o)}$
Case 4 $\epsilon_o<\epsilon_4<\epsilon_u$ $\epsilon_1<0$	$A = \frac{2}{3}\epsilon_o + \frac{(\epsilon_u-0.85\epsilon_o)(\epsilon_4-\epsilon_o)-0.075(\epsilon_4^2-\epsilon_o^2)}{(\epsilon_u-\epsilon_o)}$; $B = \frac{5\epsilon_o^2}{12} + \frac{(\epsilon_u-0.85\epsilon_o)(\epsilon_4^2-\epsilon_o^2)-0.10(\epsilon_4^3-\epsilon_o^3)}{2(\epsilon_u-\epsilon_o)}$

Note: Compressive strains should be taken as positive quantities, tensile strains as negative quantities. The steel stresses $f_{s2} = E_s\epsilon_2$ and $f_{s3} = E_s\epsilon_3$ have an upper limit equal to the yield point stress f_y

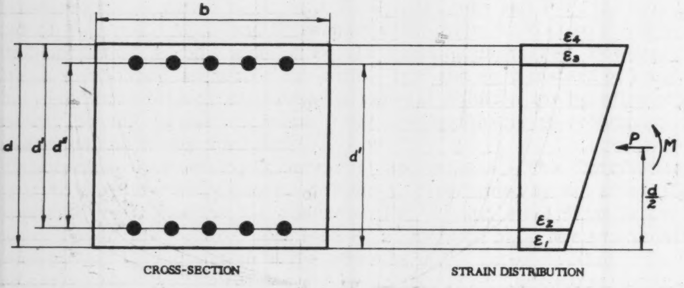

CROSS-SECTION STRAIN DISTRIBUTION

FIG. 6.—DISTRIBUTION OF STRAIN IN A COLUMN

The steel stresses are related to steel strains ϵ_2 and ϵ_3 as $f_{s2} = E_s\,\epsilon_2$ and $f_{s3} = E_s\,\epsilon_3$, and strains ϵ_2 and ϵ_3 may be expressed as

$$\epsilon_2 = \epsilon_4 - \left(\epsilon_4 - \epsilon_1\right)\frac{d'}{d} \quad \ldots\ldots\ldots\ldots\ldots(19)$$

$$\epsilon_3 = \epsilon_1 + \left(\epsilon_4 - \epsilon_1\right) \frac{d'}{d} \quad \ldots\ldots\ldots\ldots\ldots (20)$$

It should be noted from Fig. 3 that the steel stresses f_{s2} and f_{s3} have an upper limit equal to the yield point stress f_y.

In the derivation of Eqs. 17 and 18, compressive strains were taken as positive quantities and tensile strains as negative quantities. The same sign convention should be followed in using these equations.

Material failure.—An eccentrically loaded column fails by crushing of concrete when the maximum strain ϵ_4 reaches the ultimate value for concrete ϵ_u. The load and moment at failure of such a column may be computed by solution of Eq. 9, 10, 15, 16, 17, 18, 19, and 20 after placing $\epsilon_4 = \epsilon_u$. This solution differs from the well-known equations for short columns (1) only in that it accounts automatically for the deflections of the column.

GRAPHS OF ULTIMATE LOADS

The procedure for eccentrically loaded columns described in the preceding section does not lend itself easily to a direct evaluation of the buckling load for a particular column. It is more suitable for correlating the ultimate loads to the critical lengths and eccentricities for a whole group of columns having the same properties of the cross-section and the same characteristics of loading other than the magnitude of the initial eccentricity. The ultimate load for a particular column of the group may then be obtained by interpolation.

It is not necessary to make a separate set of computations for each particular column cross-section. If dimensionless quantities are used instead of the actual loads, moments and dimensions, one group pertains to all columns having the same properties of concrete, properties of steel, percentage of reinforcement, effective depth ratio d'/d, and conditions of loading. For convenient use, the results may then be tabulated for each group or plotted as is illustrated in Figs. 7 through 10.

Twenty-eight dimensionless graphs were prepared for rectangular columns with symmetrical reinforcement. Eight representative graphs are included in Figs. 7 through 10. The ultimate load reduced to the dimensionless quantity $P/f''_c\, b\, d$ is plotted as a function of the slenderness ratio l/d for initial eccentricity ratios e_2/d ranging from 0 to 1.0. The slenderness ratio is covered in each graph in the range of 0 to 60. For $f_y = 50{,}000$ psi, $e_1/e_2 = 1.0$ and $d'/d = 0.9$, concrete strengths $f'_c = 2000, 3000, 4000, 6000$ psi and steel percentages p of 1.0%, 2.0%, and 4.0% were included in all combinations, thus, giving twelve graphs. The selection of the characteristic quantities for the remaining sixteen graphs was aimed in part at checking the theoretical analysis against the available test data and in part at evaluating the effects of several variables.

Effects of Variables.—The eight representative graphs included in Figs. 7 through 10 illustrate the effects of slenderness ratio, eccentricity ratio, concrete strength, percentage of reinforcement, yield point of reinforcement, ratios of end eccentricities, and long duration of loading. An inspection of the graphs shows that the slenderness ratio l/d and the eccentricity ratio e_2/d are the most important variables. An increase of l/d from 0 to 60 or an increase of e_2/d from 0 to 1.0 may reduce the ultimate load more than 80 percent. The effects of concrete strength f'_c and of the percentage of reinforce-

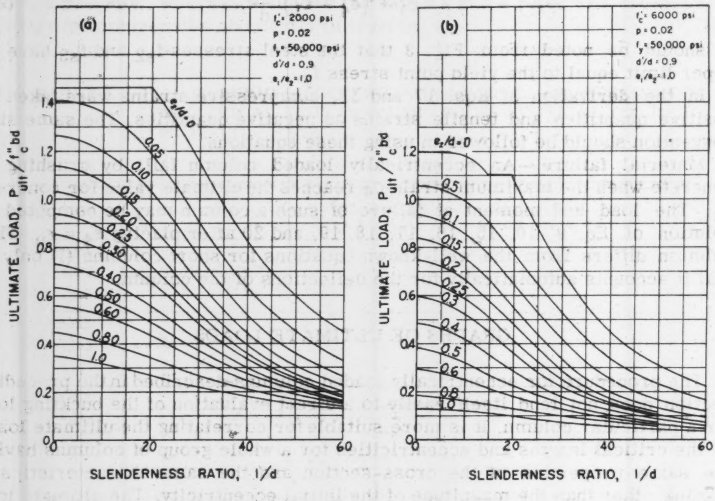

FIG. 7.—ULTIMATE LOAD GRAPHS

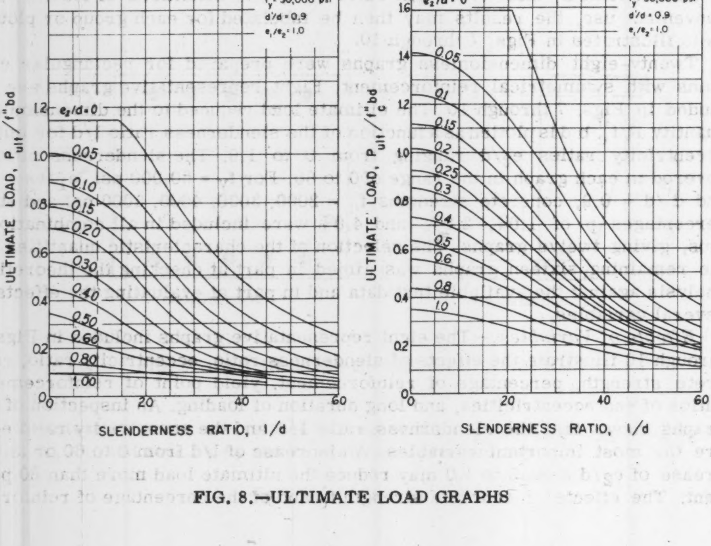

FIG. 8.—ULTIMATE LOAD GRAPHS

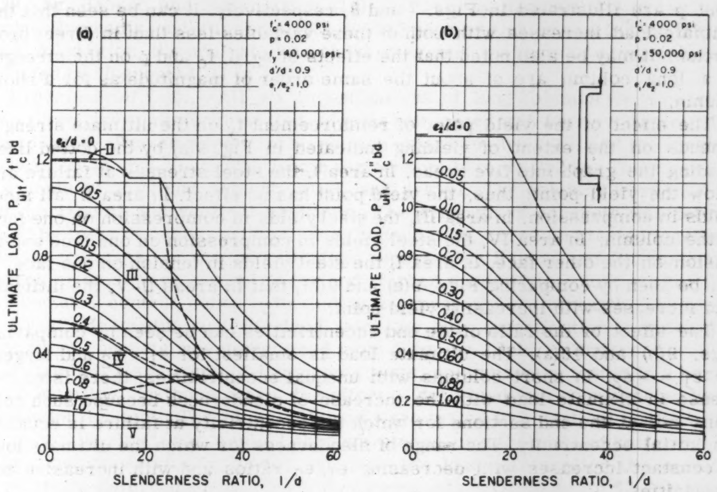

FIG. 9.—ULTIMATE LOAD GRAPHS

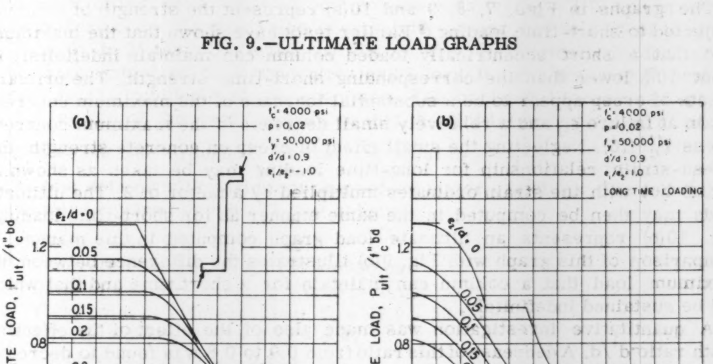

FIG. 10.—ULTIMATE LOAD GRAPHS

ment p are illustrated in Figs. 7 and 8, respectively. It can be seen that the ultimate load increases with both of these variables less than in direct proportion. It may be also noted that the effects of e_2/d, f'_c and p on the strength of a long column are of about the same order of magnitude as for a short column.

The effect of the yield point of reinforcement f_y on the ultimate strength depends on the extent of yielding indicated in Fig. 9(a) by the dotted lines dividing the graph into five areas. In area I, the steel stresses at failure are below the yield point; thus, the yield point has no effect. In area II, all steel yields in compression. In area III, the steel yields in compression on one face of the column. In area IV, the steel yields in compression on one face and in tension on the other face. In area I, the steel yields in tension on one face. It can be seen by comparing Figs. 9(a) and 9(b), that in areas II-V, the ultimate load increases with increasing yield point.

The effect of the ratio of the end eccentricities can be seen by comparing Figs. 9(b) and 10(a). The ultimate load is smallest for $e_1 = e_2$ and largest for $e_1 = -e_2$. In short columns with unequal eccentricities, there is no decrease in ultimate load with the increase of slenderness because such columns fail at the end sections for which the eccentricity at failure is equal to the initial eccentricity. The range of slenderness for which the ultimate load is constant increases with decreasing e_1/e_2 ratios and with increasing eccentricities.

The graphs in Figs. 7, 8, 9 and 10(a) represent the strength of columns subjected to short-time loading.[4] Earlier tests have shown that the maximum load that a short eccentrically loaded column can maintain indefinitely is about 10% lower than the corresponding short-time strength. The primary effects of creep appear to be a substantial increase of the maximum concrete strain at failure ϵ_u and a relatively small decrease of the maximum concrete stress f''_c (16). Neglecting the small effect of creep on concrete strength, the stress-strain relationship for long-time loading may be taken as shown in Fig. 2 but with the strain ordinates multiplied by a factor of 2. The ultimate loads may then be computed in the same manner as for short-time loading. Fig. 10(b) represents an ultimate load graph computed in this manner. A comparison of this graph with Fig. 9(b) illustrates the difference between the maximum load that a column can maintain for a short time and that which can be sustained indefinitely.

A quantitative investigation was made also of the effect of the effective depth ratio d'/d. A decrease of this ratio from 0.9 to 0.8 was found to decrease the ultimate load as much as 10%.

EXPERIMENTAL CHECK OF ANALYSES

The theoretical analyses of the strength of concentrically and eccentrically loaded long reinforced concrete columns presented in this paper are based on a set of assumptions derived from several investigations of related problems. To check the accuracy of the analyses, the theoretical ultimate loads were compared with the results of tests of 48 concentrically and 79 eccentrically loaded long hinged columns. The test data were obtained in six independent investigations reported by Baumann (14) in 1934, by Thomas (17) in

---

[4] A test to failure in a conventional testing machine carried out in a few hours.

1939, by Hanson and Rosenström (18) in 1947, by Rambøll (19) in 1951, by Ernst, Hromadik and Riveland (15) in 1953, and by Gehler and Hütter (20) in 1954. In addition, the analysis was checked against the tests of short columns reported by Hognestad (1) in 1951.

Experimental Data.—All six investigations of long columns were carried out with square or rectangular tied columns reinforced with four symmetrically placed bars. The smallest cross-section was 3-in.-by-3-in. and the largest one was 10-in.-by-10-in. The length varied from 74 in. to 252 in. The concrete was made of Portland cement, sand, and gravel. The columns were cast in both horizontal and vertical positions. The strength of concrete was determined by tests of cubes, prisms, or cylinders cast, cured and tested together with the columns. In the investigation reported by Hanson and Rosenstrom, control prisms were cut out of the undisturbed ends of the columns after the test because control cubes indicated an unexpectedly low strength. The tests by Ernst, Hromadik, and Riveland were the only investigation in which the strength of concrete was determined from 6-in.-by-12-in. cylinders.

In Rambøll's and some of Baumann's tests, columns were tested in a horizontal position, in those cases, the effect of dead load was counteracted by a suspension system. The other columns were tested in a vertical position. In all tests, the load was applied through hinges usually made of knife edges.

In most eccentrically loaded columns, the load was applied at a certain eccentricity determined by direct measurements.[5] Of these, in 52 columns, the eccentricities were equal at both column ends ($e_1/e_2 = 1.0$) and in three columns tested by Baumann the eccentricity at one end was equal to zero ($e_1/e_2 = 0$). In 24 tests by Gehler and Hütter, the "eccentrically loaded" columns were subjected to a concentric axial load P and a transverse load H applied at the middepth of the specimen. The horizontal force was kept at 1%, 2%, or 3% of the vertical load, so that the "initial eccentricity" at middepth was constant throughout the test and equal to $e = \frac{H\,l}{4\,P}$.

The test data provide a wide coverage of six major variables. The following ranges were covered by the 127 long columns:

1. Slenderness, $l/d = 11.7 - 40.7$
2. Concrete strength, $f'_c = 2130 - 6900$ psi
3. Ratio of reinforcement, $p = 0.005 - 0.050$
4. Yield point of reinforcement, $f_y = 28.9 - 53.8$ ksi
5. Effective depth, $d'/d = 0.77 - 0.91$
6. Eccentricity, $e_2 = 0 - 0.833$

Both the concentrically and eccentrically loaded columns covered, separately, almost complete ranges of variables 1 through 5. The minimum eccentricity for the eccentrically loaded columns was $e_2/d = 0.005$.

From the numerous existing tests of short columns, Series II and III of Hognestad's investigation (1) were selected for checking the equations presented in this paper. Columns in both series had a rectangular cross-section 10-in.-by-10-in. reinforced symmetrically with 2.4% and 4.8% of longitudinal bars, respectively. All columns were 75 in. long and had equal end eccentricities, that is, $e_2 = e_1$. The eccentricities varied from 0 to 12.5 in. All col-

---

[5] In Thomas' tests, the initial eccentricities were determined also from strain and deflection measurements, but the directly measured initial eccentricities were used in this study.

TABLE 2.—HOGNESTAD'S TESTS OF SHORT COLUMNS

Specimen	Concrete Strength f'_c, in psi	Eccentricity e_2/d	$\frac{P_{test}}{f''_c\, b\, d}$	$\frac{P_{calc}}{f''_c\, b\, d}$	$\frac{P_{test}}{P_{calc}}$
		Series II			
B-6a	4080	0	1.314	1.312	1.00
b	4040	0	1.224	1.315	0.93
C-6a	2020	0	1.308	1.630	0.80
b	1520	0	1.566	1.836	0.85
			Average Col. 6		0.90
A-7a	5240	0.325	0.515	0.553	0.93
b	5810	0.25	0.575	0.622	0.92
B-7a	4080	0.25	0.738	0.689	1.07
b	4040	0.25	0.723	0.692	1.04
C-7a	1970	0.25	0.844	0.881	0.96
b	1520	0.25	0.983	0.922	1.07
			Average Col. 7		1.00
A-8a	5520	0.50	0.345	0.359	0.96
b	5810	0.50	0.308	0.346	0.89
B-8a	4700	0.50	0.390	0.395	0.99
b	4260	0.50	0.403	0.414	0.97
C-8a	1820	0.50	0.639	0.612	1.04
b	1820	0.50	0.639	0.620	1.03
			Average Col. 8		0.98
A-9a	5100	0.75	0.205	0.211	0.97
b	5170	0.75	0.208	0.208	1.00
B-9a	4700	0.75	0.235	0.226	1.04
b	4370	0.75	0.241	0.238	1.01
C-9a	1880	0.75	0.456	0.446	1.02
b	1730	0.75	0.446	0.460	0.97
			Average Col. 9		1.00
A-10a	5100	1.25	0.106	0.102	1.04
b	5170	1.25	0.100	0.101	0.99
B-10a	4260	1.25	0.120	0.121	0.99
b	4370	1.25	0.119	0.119	1.00
C-10a	2300	1.25	0.227	0.222	1.02
b	1770	1.25	0.300	0.252	1.19
			Average Col. 10		1.04
			Average Series II Standard Deviation		0.989 0.073
		Series III			
B-11a	3870	0	1.520	1.636	0.93
b	4010	0	1.422	1.614	0.88
C-11b	2070	0	2.006	2.189	0.92
			Average Col. 11		0.91
A-12a	4150	0.25	0.892	0.848	1.05
b	5050	0.25	0.758	0.792	0.96
B-12a	4300	0.25	0.828	0.839	0.99
b	4010	0.25	0.833	0.856	0.97
C-12a	2300	0.25	1.286	1.147	1.12
b	2200	0.25	1.230	1.163	1.06

TABLE 2.—*CONTINUED*

			Average Col. 12		1.03
A-13a	5350	0.50	0.484	0.514	0.94
b	4850	0.50	0.510	0.541	0.94
B-13a	3580	0.50	0.592	0.639	0.93
b	4290	0.50	0.564	0.571	0.99
C-13a	2300	0.50	0.770	0.800	0.96
b	2070	0.50	0.778	0.829	0.94
			Average Col. 13		0.95
A-14a	5350	0.75	0.312	0.339	0.92
b	5100	0.75	0.353	0.353	1.00
B-14a	3580	0.75	0.457	0.462	0.99
C-14a	1950	0.75	0.696	0.655	1.06
b	2070	0.75	0.591	0.641	0.92
			Average Col. 14		0.98
A-15a	5100	1.25	0.203	0.184	1.10
b	4850	1.25	0.192	0.193	0.99
B-15a	3800	1.25	0.229	0.245	0.93
b	4630	1.25	0.214	0.201	1.06
C-15a	1950	1.25	0.437	0.426	1.03
b	2070	1.25	0.423	0.414	1.02
			Average Col. 15		1.02
			Average Series III Standard Deviation		0.985 0.061

umns were cast and tested in the same vertical position. The strength of concrete was determined by tests of 6-in.-by-12-in. control cylinders.

The slenderness and eccentricity ratios and the ultimate loads reduced to the dimensionless quantity P_{test}/f''_c b d are listed in Table 2 for short columns (l/d = 7.5), in Table 3 for long concentrically loaded columns, and in Table 4 for long eccentrically loaded columns.

Computated Ultimate Loads.— Tables 2, 3, and 4 contain, also, computed ultimate loads reduced to the dimensionless quantity P_{calc}/f''_c b d. It was assumed in computing the theoretical loads for short concentrically loaded columns that the strain at failure ϵ is equal to ϵ_o and that the steel stress at failure f_s is equal to the yield point of reinforcement f_y. The ultimate loads were then computed directly from Eq. 7. In computing the ultimate loads for the short eccentrically loaded columns, the maximum strain in concrete at

TABLE 3.—TESTS OF CONCENTRICALLY LOADED LONG COLUMNS[a]

Specimen	Concrete Strength f'_c, psi.	Cross-Section d-by-b, in.-by-in.	Slenderness l/d	$\frac{P_{test}}{f''_c\ b\ d}$	$\frac{P_{calc}}{f''_c\ b\ d}$	$\frac{P_{test}}{P_{calc}}$
Baumann 1930-1933 (14)[b]						
I	2200	3.94 x 7.87	32.1	1.026	0.947	1.08
III	2330	5.51 x 5.51	22.9	1.285	1.221	1.05
V	3830	5.47 x 6.97	23.3	1.172	1.187	0.99
Va	3830	5.51 x 7.01	23.2	1.223	1.191	1.03
VI	3610	3.86 x 7.80	32.7	0.955	0.729	1.31
VIa	3610	3.94 x 7.87	32.1	0.950	0.748	1.27
VIII	4180	7.01 x 7.17	17.5	1.345	1.158	1.16
VIIIa	4180	7.09 x 7.09	15.5	1.531	1.182	1.30
3	4870	6.30 x 9.84	40.7	0.585	0.405	1.44
15	5630	6.34 x 9.72	40.4	0.418	0.386	1.08
				Average		1.171
				Standard Deviation		0.142
Thomas, 1938 (17)						
LC1	3530	6.00 x 6.00	14.7	1.224	1.288	0.95
LC2	3840	6.00 x 6.00	20.7	1.043	1.125	0.93
				Average		0.940
Hanson and Rosentrõm, 1945-1946 (18)						
1a	5270	5.16 x 7.13	25.8	0.973	0.713	1.36
2a	5980	5.20 x 7.17	25.6	0.833	0.693	1.20
3a	7110	5.31 x 7.20	25.1	0.750	0.673	1.11
				Average		1.223
Rambøll, 1949-1950 (19)						
13	4860	5.59 x 7.13	13.0	0.790	1.064	0.74
14	4380	5.59 x 7.13	13.0	1.040	1.080	0.96
15	4220	5.79 x 7.13	12.6	0.983	1.090	0.90
16	4220	5.75 x 7.20	12.7	0.980	1.089	0.90
27	5010	5.55 x 7.17	20.6	0.768	0.897	0.86
28	4880	5.75 x 7.20	19.9	0.642	0.905	0.71
33	4700	5.63 x 7.20	30.1	0.686	0.619	1.11
				Average		0.883
				Standard Deviation		0.125

TABLE 3.–*CONTINUED*

Gehler and Hütter, 1940-1942 and 1951-1952 (20)						
Ia	3270	5.50 x 6.30	40	0.562	0.517	1.09
				0.601		1.16
Ib	3920	5.50 x 6.30	30	0.749	0.701	1.07
				0.776		1.11
Ic	3670	5.50 x 6.30	25	1.033	0.871	1.19
				1.108		1.27
Id	3560	5.50 x 6.30	20	1.042	1.027	1.01
				1.182		1.15
Ie	3560	5.50 x 6.30	15	1.276	1.076	1.19
				1.214		1.13
IIa	3520	5.50 x 6.30	40	0.703	0.672	1.05
				0.754		1.12
1	4250	5.50 x 6.30	40	0.312	0.422	0.74
				0.352		0.83
2	4430	5.50 x 6.30	40	0.376	0.524	0.72
				0.491		0.94
3	4100	5.50 x 6.30	40	0.606	0.794	0.76
				0.531		0.67
4	2690	5.50 x 6.30	30	0.744	0.816	0.91
				0.717		0.88
5	3790	5.50 x 6.30	30	0.626	0.710	0.88
				0.658		0.93
6	4980	5.50 x 6.30	30	0.621	0.640	0.97
				0.621		0.97
				Average		0.989
				Standard Deviation		0.163
Ernst, Hromadik and Riveland, 1952 (15)						
3	3430	6.00 x 6.00	15	1.046	1.179	0.89
4	3430	6.00 x 6.00	25	0.961	0.894	1.07
				Average		0.980

[a] Only specimens with l/d larger than 10 are listed in this table.

[b] Numerals in parenthesis refer to corresponding items in Bibliography.

TABLE 4.—TESTS OF ECCENTRICALLY LOADED LONG COLUMNS

Specimen	Concrete Strength f'_c, psi.	Cross-Section d-by-b, in.-by-in.	Slenderness l/d	Eccentricity Ratio e_2/d	$\frac{P_{test}}{f'_c\, b\, d}$	$\frac{P_{calc}}{f'_c\, b\, d}$	$\frac{P_{test}}{P_{calc}}$
Baumann, 1930-1933 (14)							
Ia	2290	3.94 x 7.87	32.1	0.083	0.566	0.63	0.90
IIIa	2360	5.51 x 5.51	22.9	0.083	0.869	0.89	0.98
4	4670	9.84 x 9.84	12.0	0.166	0.562	0.63	0.89
5	4640	4.92 x 9.84	25.9	0.166	0.404	0.32	1.26
6	4670	6.30 x 9.84	40.7	0.166	0.206	0.15	1.37
7	3480	9.84 x 9.84	11.7	0.166	0.662	0.68	0.97
8	3480	4.96 x 9.84	25.6	0.166	0.366	0.36	1.02
9	3460	6.38 x 9.84	40.2	0.166	0.251	0.18	1.39
10	5100	9.88 x 9.96	11.7	0.333	0.364	0.41	0.89
11	5100	4.96 x 9.92	25.6	0.333	0.207	0.15	1.38
12	5070	6.38 x 9.84	40.2	0.333	0.094	0.09	1.04
13	5600	9.88 x 9.72	11.8	0.333	0.344	0.38	0.91
14	5600	4.96 x 9.76	25.6	0.333	0.159	0.14	1.14
19*	4070	5.11 x 9.84	24.7	0.166	0.501	0.51	0.98
26*	5070	9.84 x 9.92	12.6	0.166	0.707	0.70	1.01
32*	4680	9.84 x 9.84	12.6	0.166	0.786	0.79	0.99
					Average		1.070
					Standard Deviation		0.175
Thomas, 1938 (17)							
LC3	3450	6.00 x 6.00	23.7	0.005	1.018	0.99	1.03
LC4	3440	6.00 x 6.00	26.7	0.005	0.994	0.89	1.12
LC8	3330	6.00 x 6.00	14.7	0.027	1.049	1.01	1.04
LC7	3810	6.00 x 6.00	20.7	0.037	0.894	0.88	1.02
LC6	3970	6.00 x 6.00	23.7	0.042	0.830	0.75	1.11
LC5	3640	6.00 x 6.00	26.7	0.047	0.921	0.74	1.24
LC12	3030	6.00 x 6.00	14.7	0.027	1.063	1.13	0.94
LC11	2700	6.00 x 6.00	20.7	0.037	1.139	1.01	1.13
LC10	2730	6.00 x 6.00	23.7	0.042	1.006	0.86	1.17
LC9R	2900	6.00 x 6.00	26.7	0.017	0.912	0.91	1.05
PLC1	2720	3.00 x 3.00	33.1	0.056	0.884	0.87	1.02
PLC2	2800	3.00 x 3.00	33.1	0.056	0.850	0.85	1.00
					Average		1.073
					Standard Deviation		0.080
Hanson and Rosenström, 1945-1946 (18)							
1b	5270	5.16 x 7.13	25.8	0.166	0.417	0.30	1.39
2b	5980	5.20 x 7.13	25.6	0.166	0.356	0.28	1.27
3b	7110	5.31 x 7.20	25.1	0.166	0.349	0.26	1.34
					Average		1.333
Rambøll, 1949-1950 (19)							
17	4280	5.59 x 7.09	13.0	0.083	0.902	0.76	1.19
18	4030	5.67 x 7.13	12.8	0.083	0.866	0.77	1.12
19	4120	5.59 x 7.09	13.0	0.166	0.762	0.60	1.27
20	4150	5.63 x 7.17	12.9	0.166	0.805	0.60	1.34
21	3930	5.71 x 7.20	12.7	0.333	0.481	0.38	1.27
22	3970	5.67 x 7.17	12.8	0.333	0.502	0.38	1.32
23	4000	5.67 x 7.13	12.8	0.666	0.154	0.13	1.18
24	3750	5.67 x 7.13	12.8	0.666	0.164	0.14	1.17
25	4810	5.67 x 7.17	12.8	0.833	0.093	0.08	1.16
26	4560	5.55 x 7.13	13.1	0.833	0.098	0.08	1.16

TABLE 4.–*CONTINUED*

29	5040	5.67 x 7.17	20.1	0.166	0.431	0.42	1.03
30	4630	5.63 x 7.17	20.3	0.333	0.278	0.24	1.16
31	4980	5.67 x 7.20	20.1	0.666	0.094	0.09	1.04
32	5040	5.59 x 7.20	20.4	0.833	0.074	0.07	1.06
34	5050	5.71 x 7.17	29.6	0.083	0.527	0.38	1.39
35	4540	5.67 x 7.20	29.9	0.166	0.336	0.33	1.02
36	4590	5.63 x 7.20	30.1	0.666	0.080	0.08	1.00
37	4650	5.71 x 7.17	29.6	0.333	0.164	0.15	1.09
38	5540	5.71 x 7.17	29.6	0.833	0.051	0.05	1.02
					Average		1.157
					Standard Deviation		0.115
Gehler and Hütter, 1940-1942 and 1951-1952 (20)							
7	3020	5.50 x 6.30	15	0.0376	1.196	1.11	1.08
					1.134		1.02
8	4200	5.50 x 6.30	20	0.051	0.873	0.85	1.03
					0.810		0.95
9	4110	5.50 x 6.30	30	0.075	0.597	0.56	1.07
					0.555		0.99
10	3260	5.50 x 6.30	40	0.101	0.357	0.38	0.94
					0.388		1.02
11	3210	5.50 x 6.30	15	0.075	1.029	0.96	1.07
					1.117		1.16
12	4200	5.50 x 6.30	20	0.101	0.721	0.72	1.00
					0.735		1.02
13	4390	5.50 x 6.30	30	0.150	0.411	0.42	0.98
					0.418		1.00
14	2830	5.50 x 6.30	40	0.201	0.341	0.32	1.07
					0.306		0.96
15	3210	5.50 x 6.30	15	0.113	0.957	0.87	1.10
					1.043		1.20
16	3020	5.50 x 6.30	20	0.152	0.668	0.71	0.94
					0.777		1.09
17	3710	5.50 x 6.30	30	0.225	0.403	0.38	1.06
					0.358		0.94
18	2890	5.50 x 6.30	40	0.302	0.276	0.26	1.06
					0.266		1.02
					Average		1.032
					Standard Deviation		0.066
Ernst, Hromadik and Riveland, 1952 (15)							
7	3430	6.00 x 6.00	15	0.125	0.761	0.74	1.03
8	3430	6.00 x 6.00	25	0.250	0.618	0.50	1.24
11	3430	6.00 x 6.00	15	0.250	0.554	0.52	1.07
12	3430	6.00 x 6.00	25	0.250	0.368	0.33	1.12
13	3430	6.00 x 6.00	25	0.375	0.236	0.24	0.98
					Average		1.088
					Standard Deviation		0.089

---

[a] End eccentricity $e_1 = 0$; in all other columns $e_1 = e_2$.

failure, ϵ_4, was assumed equal to $\epsilon_u = 0.0038$. Setting $e_1 = e_2 = e$ and $l_1 = l_2 = l/2$, the eccentricity of load may be expressed from Eqs. 9, 15 and 16 as

$$e = \frac{M_{col}}{P} \cos\left[\frac{l}{2\,d}\sqrt{(0.0038 - \epsilon_1)\ \frac{P\,d}{M_{col}}}\right] \quad \ldots\ldots\ldots (21)$$

For several chosen values of ϵ_1 and f'_c, the ratio M_{col}/P was computed from Eqs. 17, 18, 19, and 20. The corresponding eccentricities e causing failure were then computed from Eq. 21. The resulting values were plotted in graphs of $P_{calc}/f'_c\ b\ d$ versus e/d for each series as functions of the concrete strength f'_c. The ultimate loads for the test columns were obtained by entering the graphs with the known eccentricity and concrete strength. It should be noted that the eccentricity, e, is the eccentricity at the end of the column and, thus, not subject to change during the test.

The theoretical ultimate loads for long concentrically loaded columns were computed directly from Eqs. 4, 5, 6, and 7 for each test column.

The theoretical ultimate loads for long eccentrically loaded columns were obtained from the graphs of ultimate loads. This procedure involved several interpolations and for some columns also extrapolations; therefore, the resulting $P_{calc}/f''_c\ b\ d$ values in Table 4 are given only to two decimal places.

The computed loads are based on the dimensions and material properties of the test columns as reported in the respective test reports. Data not given in the reports were estimated. Of these, the most important were the assumption concerning the relationships between the strength of concrete in the columns, cylinders, prisms, and cubes.

The stress-strain relationship assumed in the analysis for concrete is based on the strength f''_c. In computing the ultimate loads for vertically cast columns, this quantity was assumed related to the strength of 6 x 12-in. control cylinders as $f''_c = 0.85\ f'_c$. For horizontally cast columns, the relationship $f''_c = f'_c$ was assumed as indicated by earlier tests (16). Where cylinder strengths were not given, the following relationships were assumed between the strength of cylinders, prisms and cubes: $f'_c = f'_{pr}$ and $f'_c = 0.8\ f'_{cu}$.

Analyses Versus Tests.—The ratios of the test to computed ultimate loads for short columns are listed in the last column of Table 2. For all short concentrically loaded columns, the ratio is equal to or smaller than 1.0 and, thus in agreement with Hognestad's observation of the presence of small accidental eccentricities (1). The average ratio for the short concentrically loaded columns is 0.901 and the standard deviation is 0.060. For all short eccentrically loaded columns, the ratios are close to 1.0. The over-all average is 1.000 and the standard deviation is 0.058. It should be noted, however, that a good over-all agreement between the theory and the Hognestad's test data should be expected in view of the fact that the properties of the concrete stress block shown in Fig. 2 were derived from the same investigation (1). On the other hand, the excellent agreement from group to group and for all individual columns is significant in judging the correctness of the theoretical equations and of the basic assumptions.

The analysis of the ultimate strength of long columns is compared with the test data in the last columns of Tables 3 and 4 and in Figs. 11 and 12 giving the ratio P_{test}/P_{calc} for every column. An examination of the tables and figures shows that the scatter is noticeably larger for the concentrically loaded columns; that of the 127 columns tested, six concentrically loaded columns were more than 20% weaker and none of the eccentrically loaded columns was more than 11% weaker than predicted by the theory; that the average ratio is higher for the eccentrically than for the concentrically loaded columns; and that no definite trends exist with any of the six major variables except as mentioned previously.

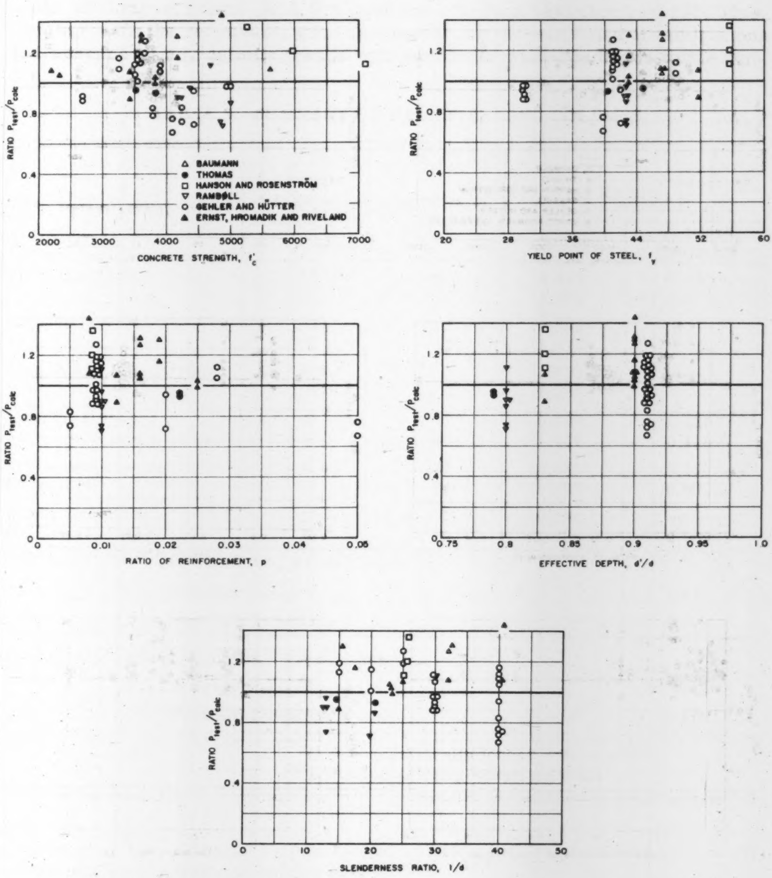

FIG. 11.—TEST RESULTS CONCENTRICALLY LOADED COLUMNS

The comparisons are summarized in Table 5. The average values for the individual investigations show that in all but one case the average is smaller for the concentric than for the eccentric loading. This result is identical with that for short columns tested by Hognestad, thus indicating that it is difficult to obtain concentric hinged loading. Furthermore, the averages for eccentrically loaded columns of every investigation exceed 1.00. This agrees with the

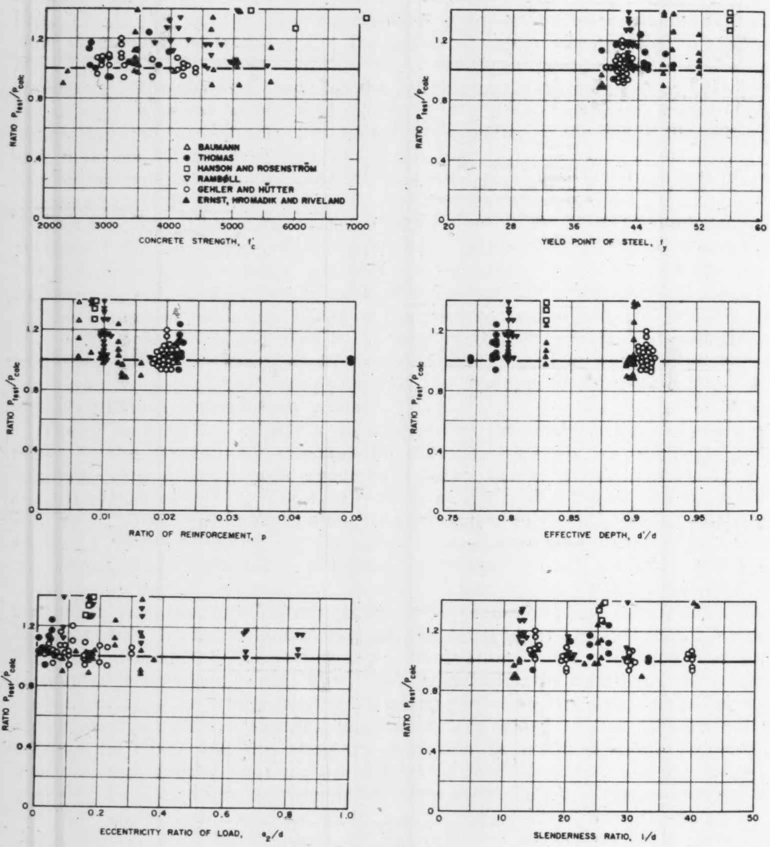

FIG. 12.—TEST RESULTS ECCENTRICALLY LOADED COLUMNS

fact that several assumptions of the theory represent a minimum condition as far as the ultimate strength is concerned. Finally, the higher over-all standard deviation for concentrically loaded columns reemphasizes the smaller spread in the P_{test}/P_{calc} ratios for eccentrically loaded columns. The poorer agreement for the concentrically loaded columns is understandable because differences and small unavoidable errors in testing techniques affect the test value of ultimate load more for a concentrically than for an eccentrically loaded column.

The over-all average value of the ratio of measured to computed ultimate loads of long columns is 1.066 and the standard deviation is 0.153. This, together with the reasonably good agreement for the individual investigations and absence of any definite trends with any major variable, leads to the conclusion that the ultimate load of hinged columns can be predicted accurately by the analyses presented in this paper.

TABLE 5.—SUMMARY OF DATA FOR LONG COLUMNS

Investigation	Type of Loading	Number of Columns	Test Results, $\frac{P_{test}}{P_{calc}}$	
			Average	Standard deviation
Baumann (14)	^{x}C	10	1.171	0.142
	^{xx}E	16	1.070	0.175
Thomas (17)	C	2	0.965	-----
	E	12	1.073	0.080
Hanson and Rosenström (18)	C	3	1.123	-----
	E	3	1.333	-----
Rambøll (19)	C	7	0.883	0.125
	E	19	1.157	0.118
Gehler and Hütter (20)	C	24	0.989	0.163
	E	24	1.032	0.066
Ernst, Hromadik and Riveland (15)	C	2	0.980	-----
	E	5	1.088	0.089
Concentrically Loaded Columns, 48 specimens				
Average P_{test}/P_{calc}				1.024
Standard Deviation				0.178
Eccentically Loaded Columns, 79 specimens				
Average P_{test}/P_{calc}				1.091
Standard Deviation				0.129

^{x}C = concentrically loaded columns
^{xx}E = eccentrically loaded columns

CONCLUSIONS

The ultimate load analyses presented herein were aimed primarily at improving the knowledge of the effect of deflections and buckling on the strength of reinforced concrete columns and to provide a tool for further studies.

The good agreement with the available test data indicates that the analyses are based on reasonable assumptions. It particularly serves as a further proof that Hognestad's stress block approximates well the actual stress-strain relationship for concrete subjected to combined axial compression and bending.

As a tool for further studies, the analyses permit the evaluation of the effects of various variables on the column strength. Such studies are indispensable in preparation of simplified design procedures.

And finally, the analyses permit construction of ultimate load tables and graphs, that can be used conveniently whenever it is necessary to evaluate accurately the ultimate loads of hinged reinforced concrete columns.

ACKNOWLEDGMENTS

The studies reported in this symposium were carried out as a part of a cooperative investigation conducted by the Engineering Experiment Station of the University of Illinois under the auspices and sponsorship of the Reinforced Concrete Research Council of the Engineering Foundation. The paper is based on the doctoral dissertation of the senior author (21).

APPENDIX.—BIBLIOGRAPHY

1. "A Study of Combined Bending and Axial Load in Reinforced Concrete Members," by E. Hognestad, Univ. of Illinois Engrg. Experiment Station Bulletin No. 399, Urbana, 1951. Also published as Bulletin No. 1 of the Reinforced Concrete Research Council of the Engrg. Foundation.

2. "De Curvis Elasticis, Additamentum I, Methodus Inveniendi Lineas Curvas Maximi Minimive Proprietate Gaudentes," by L. Euler, Lausanne and Geneva, 1744, pp. 267-268.

3. "Sur la force des colonnes," by L. Euler, Memoires de l'Academie de Berlin, Vol. 13, Berlin, 1759, pp. 252-282.

4. "Ueber die Knickfestigkeit gerader Stäbe," by F. Engesser, Zeitschrift d. Arch., U., Ing., Ver. zu Hannover, Vol. 35, Hannover, 1889, p. 455.

5. "Die Knickfestigkeit gerader Stäbe, by F. Engesser, Zentralblatt der Bauverwaltung, Berlin, December 5, 1891, p. 483.

6. "Résistance des pièces comprimées," by A. Considère, Congrès International de Procedés de Construction, Exposition Univ. Int. de 1889, Vol. 3, Paris, 1889, p. 371.

7. "The Column Paradox," by F. R. Shanley, Journal of the Aeronautical Sciences, Vol. 13, No. 12, December, 1946, p. 678.

8. "Inelastic Column Theory," by F. R. Shanley, Journal of the Aeronautical Sciences, Vol. 14, No. 5, May, 1947, pp. 261-267.

9. "Applied Column Theory," by F. R. Shanley, Transactions, A.S.C.E., Vol. 115, 1950, pp. 698-727.

10. "Untersuchungen über Knickfestigkeit," by T. v. Kármán, Mitteilungen über Forschungsarbeiten auf dem Gebiete des Ingenieurwesens, No. 81, Berlin, 1910.

11. "Theorie des aussermitting gedrückten Stabes aus Baustahl," by E. Chwalla, Der Stahlbau, Vol. 7, Berlin, 1934, No. 21, pp. 161-165, No. 22, pp. 173-176, No. 23, pp. 180-184.

12. "Die Knicksicherheit von an beiden Enden gelenkig gelagerten Stäben aus Konstruktionsstahl," by M. Roš and J. Brunner, Eidg. Material-prufüngsanstalt an der E.T.H. in Zürich, Bericht No. 13, Zürich, 1926.

13. "Strength of Steel Columns," by H. M. Westergaard and W. R. Osgood, Transactions, A.S.M.E., Vol. 50, 1928, pp. 65-80.

14. "Die Knickung der Eisenbeton-Säulen," by O. Baumann, Eidg. Material-prüfungsanstalt an der E.T.H. in Zürich, Bericht, No. 89, Zurich, 1934.

15. "Inelastic Buckling of Plain and Reinforced Concrete Columns, Plates and Shells," by G. C. Ernst, J. J. Hromadik and A. R. Riveland, Univ. of Nebraska Engrg. Experiment Station Bulletin No. 3, Lincoln, 1953.

16. "Sustained Load Strength of Eccentrically Loaded Short Reinforced Concrete Columns," by I. M. Viest, R. C. Elstner and E. Hognestad, Proceedings, A.C.I., Vol. 52, March, 1956, pp. 727-755.

17. "Studies in Reinforced Concrete. VII. The Strength of Long Reinforced Concrete Columns in Short Period Tests to Destruction," by F. G. Thomas, Dept. of Scientific and Industrial Research, Building Research Technical Paper No. 24, London, 1939.

18. "Tryckförsök med slanka betongpelare," by R. Hanson and S. Rosenström, Betong, Vol. 32, No. 3, Stockholm, 1947, pp. 247-262.

19. "Reinforced Concrete Columns," by B. J. Rambøll, Teknisk Förlag, Copenhagen, 1951.

20. "Knickversuche mit Stahlbetonsäulen," by W. Gehler and A. Hütter, Deutscher Ausschuss für Stahlbeton, No. 113, Berlin, 1954.

21. "Ultimate Strength of Long Reinforced Concrete Columns," by B. Broms, Thesis presented to Univ. of Illinois, at Urbana, Ill., in June, 1956 in partial fulfillment of the requirements for the degree of Doctor of Philosophy.

22. "Buckling Strength of Metal Structures," by F. Bleich, McGraw-Hill Book Co., Inc., New York, 1952.

23. "Flexural Strength and Elastic Properties of Pretensioned Beams," by H. J. Brettle, Thesis presented in partial fulfillment of the requirements for the degree of Doctor of Philosophy, Univ. of N.S.W., Sydney, Australia.

APPENDIX II.—NOTATION

The following symbols have been adopted for use in this paper:

A = a parameter given in Table 1;

A_s = total area of longitudinal column reinforcement;

B = a parameter given in Table 1;

b = width of cross-section (Fig. 6);

d = total depth of cross-section (Fig. 6);

d' = effective depth of reinforcement (Fig. 6);

d'' = distance between centroids of compression and tension reinforcement (Fig. 6);

E_c = modulus of elasticity of concrete;

E_s = modulus of elasticity of steel;

E_t = tangent modulus of elasticity;

e = end eccentricities of load for the case of $e_1 = e_2$ (Fig. 1);

e_1, e_2 = end eccentricities of load; e_2 is taken as the larger of the two values; e_2 is always taken as a positive quantity (Fig. 4);

e_{cr} = critical eccentricity;

f_c = concrete stress;

f'_c = compressive strength of 6-in.-by-12-in. concrete cylinders;

f''_c = compressive strength of concrete in flexure (Fig. 2);

f'_{cu} = compressive strength of 8-in. concrete cubes;

f'_{pr} = compressive strength of concrete prisms;

f_s = steel stress;

f_{s2} = steel stress corresponding to strain ϵ_2;

f_{s3} = steel stress corresponding to strain ϵ_3;

f_y = yield point of reinforcement;

I = moment of inertia;

l = length of column (Fig. 4);

l_1, l_2 = lengths defined in Fig. 4;

L = equivalent length defined in Fig. 4;

M = bending moment;

M_{col} = moment resistance of a column;

P = applied load;

P_t = critical load computed by the tangent modulus theory;

p = $\frac{A_s}{b\,d}$, ratio of reinforcement;

x = distance in the direction of column axis from the point of maximum column deflection (Fig. 4);

y = lateral deflections of column including the initial eccentricity (Fig. 4);

y_m = maximum lateral deflection including the initial eccentricity (Fig. 4);

ϵ_2, ϵ_3 = steel strains (Fig. 6);

ϵ = strain;

ϵ_1, ϵ_4 = concrete strains (Fig. 6);

ϵ_o = compressive strain corresponding to maximum concrete stress (Fig. 2);

ϵ_u = ultimate concrete strain in flexure (Fig. 2);

ϵ_y = yield point strain of reinforcement;

$\frac{1}{\rho}$ = curvature; and

$\frac{1}{\rho_m}$ = curvature at $x = 0$.

DISCUSSION

G. C. ERNST,[6] F. ASCE.—The authors have presented, with impressive completeness, a long needed theoretical analysis for the ultimate strength of long hinged reinforced concrete columns. Their confirmation of the theory by a detailed comparison with the test results of past investigations is convincing and should lead to the development and use of such charts as represented by Figs. 7 through 10 for ultimate strength design.

The evaluation of the ultimate load for concentrically loaded columns is based soundly on the stress-strain relationships of the two materials and is defensible for all column lengths. Especially clear is the discussion of the relationship between strain and buckling or material failure. Eqs. 4, 5, 6, and 7 provide a means of solution for the load corresponding to any column length or the critical length for a specific load, for a concentrically loaded hinged column of known cross-section if the stress-strain curves of the steel and concrete are known or assumed. Inasmuch as the solution for Eq. 4 depends on the end conditions, it is possible to develop the concentrically loaded column curves $\left(e_2/d = 0\right)$ for any desired end condition.

The extension of the Westergaard-Osgood modification of Kármán's method to include unequal end eccentricities, with the graphical solution of Eq. 12

---

[6] Prof. of Civ. Engrg. and Dir. of Engrg. Experiment Sta., Univ. of Nebraska, Lincoln, Neb.

in Fig. 5, is a valuable addition. Also, the discussion of the relationship between strains and buckling or material failure for eccentrically loaded long hinged reinforced concrete columns is helpful.

With regard to the effect of long-time loading, it would seem desirable to test long eccentrically loaded columns under sustained loading in order to confirm or modify the strain assumption made in developing Fig. 10(b). This is important, in that it would seem that applications requiring such columns would also frequently involve sustained loads of significant magnitude. Investigation of the effect of end conditions on long eccentrically loaded columns is needed to complete the problem.

J. J. HROMADIK.[7]—The authors are to be commended on their presentation of a most comprehensive and detailed evaluation of existing data in relation to inelastic buckling of rectangular reinforced concrete columns. Although the column problem has probably generated more theses than any other single subject, much still remains to be accomplished in the field of concrete columns. Indeed, the authors have provided excellent tools for further studies.

The United States Navy's concern regarding column action is focused on the behavior of long piles supporting waterfront structures in deep waters. These piles comprise various cross-sections of both prestressed and reinforced concrete. Knowledge of the column behavior of these sections is paramount to the economy of design. This has led to a need for generalization of the theory by this writer. As others also may desire a generalized theory applicable to various cross-sections, some suggestions are offered as a supplement to the authors' tools. Notations, other than those of the original paper, will be defined where they first appear.

Concentrically loaded columns.—The theories of the original paper can be applied readily to concentrically loaded cross-sections of prestressed concrete. In design, where the initial residual prestress is relatively low, say 400 psi or less, the prestress load will have little to negligible effect on the ultimate load. The sections can be treated as plain concrete. The general tangent modulus relation is

$$\frac{l}{d} = C\sqrt{E_t/f_c} \quad \ldots\ldots\ldots\ldots\ldots\ldots (21)$$

where the stability factor, C, is a function of the end conditions and the cross-section. Table 6 lists values of C for hinge-ended columns for the various cross-sections indicated. Corresponding buckling curves for these sections are presented in Fig. 13 for an f''_c of 6000 psi. The curve for the octagonal section with a hollow circular core is not included, as it is nearly coincidental with the solid rectangular section.

In designs in which the prestress load exceeds 400 psi, its effect on the ultimate P/A load is measurable. For an initial residual prestress of 1000 psi the ultimate load will be somewhat lower in the long column range, approximately 10% for an l/d of 40. This approximation is based on the following relation for a rectangular cross-section:

$$\frac{P}{A} + f_q - (\epsilon_s - \epsilon_q)\, E_s\, p = f_c \quad \ldots\ldots\ldots\ldots (22)$$

---

[7] Senior Proj. Engr., U. S. Civ. Engrg. Lab., Port Hueneme, Calif.

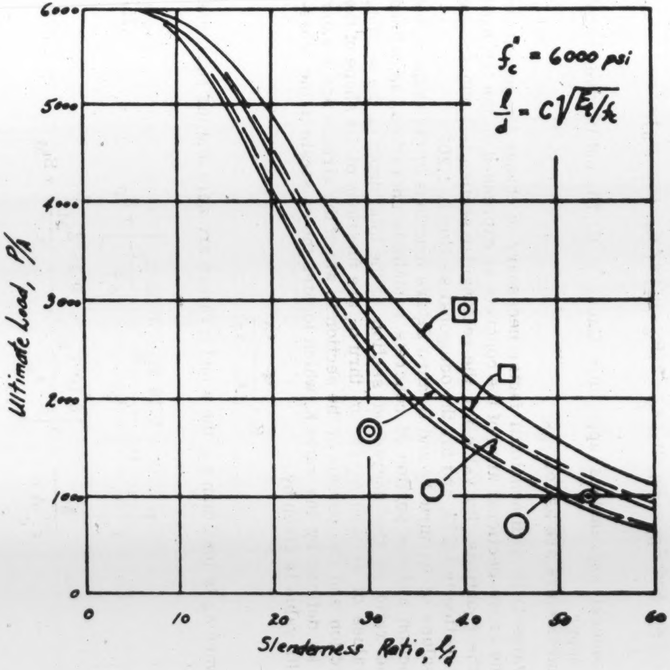

FIG. 13.—ULTIMATE LOAD VS SLENDERNESS RATIO CONCENTRIC LOAD

TABLE 6.—C-VALUES

SECTION	VALUE of C
1 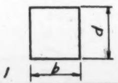	$\frac{\pi}{4}\sqrt{1.33}$
2 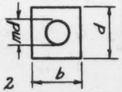	$\frac{\pi}{4}\sqrt{\frac{5.33-\pi m^4}{4-\pi m^2}}$
3 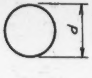	$\frac{\pi}{4}$
4 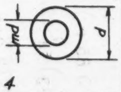	$\frac{\pi}{4}\sqrt{1+m^2}$
5 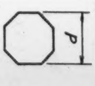	$\frac{\pi}{4}\sqrt{\frac{3+\tan^2\phi}{3}}$ n = number of sides $\phi = \frac{180°}{n}$
6 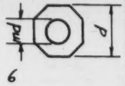	$\frac{\pi}{4}\sqrt{\frac{n\tan\phi(3+\tan^2\phi)-3\pi m^4}{3(n\tan\phi-\pi m^2)}}$

in which f_q is the initial residual prestress, ϵ_s is equal to ϵ, the concrete strain at which f_c is measured, and ϵ_q denotes initial strain under prestress load. Eq. 22 is valid only for values of $(\epsilon_s - \epsilon_q)\, E_s\, p < f_q$; where $(\epsilon_s - \epsilon_q) E_s\, p \geq f_q$, the prestress is no longer effective and the equation for plain concrete applies.

Eccentrically loaded columns.—In line with the authors' assumptions, their Eqs. 17 and 18, relationships between loads, moments, and strains, can be expressed in general form so as to be applicable to any cross section. The following general equations can be derived:

$$\frac{P}{f''_c\, A} = D\left[\frac{0.05\, W_p - 0.0075\, X_p}{\epsilon_u - \epsilon_o} + \frac{0.10\, Y_p}{\epsilon_o} - \frac{0.05\, Z_p}{\epsilon_o^2}\right] + S_p \quad . \; . \; . \; .(23)$$

in which $W_p = (a_1 + a_2)(\epsilon_u - 0.85\, \epsilon_o)$, $X_p = a_1\, \epsilon_4 + a_2\, \epsilon_1$, $Y_p = (A_1 - a_1)\epsilon_4 + (A_2 - a_2)\, \epsilon_1$, and $Z_p = (A_3 - a_3)\, \epsilon_4^2 + 2\, (A_4 - a_4)\, \epsilon_1\, \epsilon_4 + (A_5 - a_5)\, \epsilon_1^2$.

and

$$\frac{M}{f''_c\, A\, d} = D\left[\frac{0.05\, W_M - 0.0075\, X_M}{\epsilon_u - \epsilon_o} + \frac{0.10\, Y_M}{\epsilon_o} - \frac{0.05\, Z_M}{\epsilon_o^2}\right] + S_M \quad . \; . \; .(24)$$

in which $W_M = (b_1 + b_2)(\epsilon_u - 0.85\, \epsilon_o)$, $X_M = b_1\, \epsilon_4 + b_2\, \epsilon_1$, $Y_M = (B_1 - b_1)\, \epsilon_4 + (B_2 - b_2)\, \epsilon_1$, and $Z_M = (B_3 - b_3)\, \epsilon_4^2 + 2\,(B_4 - b_4)\, \epsilon_1\, \epsilon_4 + (B_5 - b_5)\, \epsilon_1^2$.

The general expressions apply for Cases I, II, III, and IV given in the original paper.

The parameters are as follows:

The value D is a dimensional factor necessary to change the quantity to that of the cross-sectional area of the concrete as expressed on the left hand side of the equations. Its value for the rectangular section is 1.000, for the circular section is 1.273, and for the octagonal section is 1.207.

The values of A_1 thru A_5 and B_1 thru B_5 are functions of the shape of the cross-section and the portion of concrete remaining uncracked, as defined by k, the ratio of the uncracked section to the total depth of the section.

The values of a_1 thru a_5 and b_1 thru b_5 are functions of the shape of the cross-section and the portion of the section in which the strains are greater than ϵ_o, as defined by the ratio K, which locates the ϵ_o strain in the cross-section. Its value is given by

$$K = \frac{\epsilon_4 - \epsilon_o}{\epsilon_4 - \epsilon_1}$$

Hence, when ϵ_4 is less than ϵ_o, the a and b values are zero and the equations reduce to

$$\frac{P}{f''_c\, A} = D\left[\frac{0.10\, Y_p}{\epsilon_o} - \frac{0.05\, Z_p}{\epsilon_o^2}\right] + S_p \quad . \; . \; . \; . \; . \; . \; . \; . \; . \; .(25)$$

$$\frac{M}{f''_c\, A\, d} = D\left[\frac{0.10\, Y_M}{\epsilon_o} - \frac{0.05\, Z_M}{\epsilon_o^2}\right] + S_M \quad . \; . \; . \; . \; . \; .(26)$$

TABLE 7.—PARAMETER VALUES FOR RECTANGULAR CROSS SECTIONS

k	A_1	A_2	A_3	A_4	A_5	B_1	B_2	B_3	B_4	B_5
K	a_1	a_2	a_3	a_4	a_5	b_1	b_2	b_3	b_4	b_5
0.05	0.975	0.025	0.951	0.024	0.001	0.463	0.012	0.452	0.012	0.000
0.10	1.900	0.100	1.806	0.094	0.006	0.856	0.044	0.816	0.041	0.002
0.15	2.775	0.225	2.572	0.203	0.022	1.184	0.091	1.103	0.082	0.008
0.20	3.600	0.400	3.252	0.348	0.052	1.452	0.148	1.324	0.129	0.018
0.25	4.375	0.625	3.853	0.522	0.103	1.666	0.210	1.489	0.177	0.032
0.30	5.100	0.900	4.379	0.721	0.179	1.829	0.271	1.607	0.222	0.049
0.35	5.775	1.225	4.834	0.941	0.284	1.947	0.328	1.687	0.260	0.067
0.40	6.400	1.600	5.225	1.175	0.425	2.025	0.375	1.736	0.289	0.085
0.45	6.975	2.025	5.556	1.419	0.606	2.068	0.407	1.761	0.307	0.099
0.50	7.500	2.500	5.831	1.669	0.831	2.081	0.419	1.768	0.313	0.105
0.55	7.975	3.025	6.057	1.918	1.107	2.069	0.406	1.762	0.307	0.098
0.60	8.400	3.600	6.238	2.162	1.438	2.037	0.363	1.748	0.289	0.073
0.65	8.775	4.225	6.378	2.397	1.828	1.990	0.285	1.730	0.260	0.024
0.70	9.100	4.900	6.484	2.616	2.284	1.933	0.167	1.712	0.222	-0.056
0.75	9.375	5.625	6.559	2.816	2.809	1.872	0.004	1.695	0.177	-0.174
0.80	9.600	6.400	6.610	2.990	3.410	1.810	-0.210	1.681	0.129	-0.339
0.85	9.775	7.225	6.641	3.134	4.091	1.753	-0.478	1.671	0.082	-0.560
0.90	9.900	8.100	6.656	3.244	4.856	1.706	-0.806	1.665	0.041	-0.847
0.95	9.975	9.025	6.662	3.313	5.712	1.674	-1.199	1.663	0.012	-1.211
1.00	10.000	10.000	6.662	3.338	6.662	1.662	-1.662	1.663	0.000	-1.663

TABLE 8.—PARAMETER VALUES FOR CIRCULAR CROSS SECTIONS

k	A_1	A_2	A_3	A_4	A_5	B_1	B_2	B_3	B_4	B_5
K	a_1	a_2	a_3	a_4	a_5	b_1	b_2	b_3	b_4	b_5
0.05	0.304	0.008	0.297	0.008	0.000	0.145	0.004	0.141	0.004	0.000
0.10	0.792	0.047	0.748	0.044	0.003	0.352	0.021	0.333	0.019	0.001
0.15	1.370	0.130	1.254	0.117	0.014	0.569	0.052	0.523	0.046	0.005
0.20	1.997	0.263	1.771	0.226	0.037	0.772	0.095	0.691	0.082	0.013
0.25	2.645	0.451	2.273	0.372	0.079	0.950	0.147	0.829	0.122	0.024
0.30	3.292	0.697	2.742	0.550	0.147	1.096	0.202	0.934	0.162	0.040
0.35	3.924	1.001	3.169	0.756	0.246	1.207	0.255	1.009	0.198	0.057
0.40	4.530	1.364	3.547	0.983	0.382	1.282	0.300	1.056	0.226	0.074
0.45	5.098	1.784	3.874	1.224	0.560	1.325	0.332	1.081	0.245	0.087
0.50	5.622	2.259	4.149	1.473	0.786	1.338	0.344	1.087	0.251	0.093
0.55	6.097	2.783	4.375	1.722	1.061	1.326	0.331	1.082	0.245	0.086
0.60	6.517	3.351	4.553	1.964	1.388	1.295	0.288	1.068	0.226	0.062
0.65	6.880	3.957	4.689	2.191	1.766	1.249	0.212	1.051	0.198	0.014
0.70	7.184	4.589	4.788	2.396	2.193	1.196	0.102	1.034	0.162	-0.060
0.75	7.430	5.236	4.856	2.574	2.662	1.141	-0.044	1.019	0.122	-0.166
0.80	7.618	5.884	4.898	2.720	3.164	1.089	-0.222	1.007	0.082	-0.304
0.85	7.751	6.511	4.921	2.830	3.681	1.046	-0.426	1.000	0.046	-0.472
0.90	7.834	7.089	4.932	2.902	4.187	1.015	-0.643	0.996	0.019	-0.662
0.95	7.873	7.577	4.935	2.939	4.638	0.998	-0.850	0.994	0.004	-0.853
1.00	7.881	7.881	4.935	2.946	4.935	0.994	-0.994	0.994	0.000	-0.994

TABLE 9.—PARAMETER VALUES FOR OCTAGONAL CROSS SECTIONS

k	A_1	A_2	A_3	A_4	A_5	B_1	B_2	B_3	B_4	B_5
K	a_1	a_2	a_3	a_4	a_5	b_1	b_2	b_3	b_4	b_5
0.05	0.453	0.012	0.441	0.011	0.000	0.215	0.006	0.210	0.005	0.000
0.10	0.974	0.054	0.924	0.050	0.004	0.437	0.024	0.415	0.022	0.001
0.15	1.556	0.137	1.432	0.123	0.014	0.655	0.055	0.605	0.049	0.005
0.20	2.186	0.271	1.953	0.233	0.037	0.860	0.098	0.774	0.085	0.013
0.25	2.856	0.465	2.472	0.384	0.081	1.044	0.152	0.917	0.126	0.025
0.30	3.554	0.730	2.978	0.576	0.154	1.201	0.211	1.031	0.170	0.041
0.35	4.229	1.055	3.434	0.795	0.260	1.319	0.268	1.111	0.208	0.060
0.40	4.854	1.430	3.824	1.030	0.400	1.397	0.315	1.160	0.237	0.077
0.45	5.429	1.855	4.155	1.274	0.581	1.440	0.347	1.184	0.256	0.091
0.50	5.954	2.330	4.430	1.524	0.806	1.453	0.359	1.191	0.262	0.096
0.55	6.429	2.855	4.656	1.773	1.082	1.441	0.346	1.186	0.256	0.090
0.60	6.854	3.430	4.837	2.017	1.413	1.409	0.303	1.172	0.237	0.065
0.65	7.229	4.055	4.977	2.252	1.803	1.362	0.225	1.155	0.208	0.016
0.70	7.554	4.730	5.083	2.471	2.259	1.305	0.107	1.136	0.170	-0.064
0.75	7.819	5.428	5.156	2.663	2.765	1.246	-0.050	1.120	0.126	-0.177
0.80	8.013	6.098	5.200	2.814	3.284	1.192	-0.234	1.108	0.085	-0.320
0.85	8.147	6.728	5.223	2.924	3.804	1.148	-0.439	1.100	0.049	-0.490
0.90	8.230	7.310	5.233	2.997	4.313	1.117	-0.657	1.096	0.022	-0.680
0.95	8.272	7.831	5.236	3.036	4.796	1.099	-0.879	1.095	0.005	-0.885
1.00	8.284	8.284	5.237	3.047	5.237	1.094	-1.094	1.095	0.000	-1.095

that is Case I and II of the original paper. For this condition of strain, the value K as given by the above relation is negative, defining the location of the ϵ_o strain as outside the cross-section.

The values of S_p and S_M are the steel contributions to the loads and moments respectively. No attempt is made to evaluate these, as their value is dictated by the number of bars and their location and requires individual consideration. S_p and S_M can be evaluated in accordance with the original paper.

Tables 7, 8, and 9 evaluate the preceding parameters for the rectangular, circular, and octagonal cross-sections, respectively, with examples of application for rectangular cross sections as follows:

1) $\epsilon_4 = 1.5 \times 10^{-3}$ $\quad K = 0 \;\therefore$ all "a" and "b" values = 0

$\epsilon_1 = -1.0 \times 10^{-3}$ $\quad k = 0.60$

$\epsilon_o = 2.0 \times 10^{-3}$

$$Y_p = 8.400\,(1.5) + 3.600\,(-1.0)$$

$$Z_p = 6.238\,(1.5)^2 + 2\,(2.162)\,(1.5)\,(-1.0) + 1.438\,(-1.0)^2$$

2) $\epsilon_4 = 3.0 \times 10^{-3}$ $\quad K = \dfrac{3.0 - 2.0}{3.0 - (-1.0)} = 0.25$

$\epsilon_1 = -1.0 \times 10^{-3}$ $\quad k = 0.75$

$\epsilon_o = 2.0 \times 10^{-3}$

$$W_M = (1.666 + 0.210)\left(\epsilon_u - 0.85 \times 2.0\right)$$

$$X_M = 1.666\,(3.0) + 0.210\,(-1.0)$$

$$Y_M = (1.872 - 1.666)\,(3.0) + (0.004 - 0.210)\,(-1.0)$$

$$Z_M = (1.695 - 1.489)\,(3.0)^2 + 2\,(0.177 - 0.177)\,(3.0)\,(-1.0) + (-0.174 - 0.032)\,(1.0)^2$$

The tabulated values, while well within the accuracy of the assumptions, show a slight deviation from exact values, due to "rounding off" quantities. Where designs include a hollow circular core, the general expressions for the circular section, in terms of the core diameter, apply as a negative quantity.

The general equations presented, together with the authors' theory, offer a means of constructing a family of buckling curves for a wider variety of cross-sections. Their application to the rectangular section is not necessarily recommended, as they tend to be more complex than the relations of the original paper. They are offered as a means of comparison. The equations are, however, recommended for investigations dealing with the circular and the octagonal sections. It is recognized that other factors, beyond the scope of this discussion, as creep, spiral reinforcement, duration of load, etc., may necessarily influence the solution. These should be treated accordingly. If the general expressions, as presented, do nothing more than prompt additional study, they will have served their purpose.

T. JUMIKIS,[8] **and A. S. HALL,**[9] **M. ASCE.**—The investigation of buckling in reinforced concrete lags far behind that of flexure, as regards both theory and experiment. The authors' paper is, therefore, very welcome. Besides making a distinct contribution to the subject, it contains a most useful bibliography and will no doubt stimulate interest and discussion.

While agreeing with much of the theory put forward, there are one or two sections that the writers would like to discuss. First, there is the question of the manner in which the columns fail. The authors divide these into buckling failures and material failures. As the definition of "buckling," they take the usual mathematical concept of instability. Presumably, it is to be divorced from the idea of material failure. Now whether or not this idealized situation could occur in other media, it is certainly very difficult to imagine a true buckling failure in reinforced concrete. Furthermore, the instability concept envisages a state of completely neutral equilibrium, whereas Bleich (22) suggests that this is, strictly speaking, the result of approximation. If in the basic differential equation the exact term is used for curvature instead of the approximate term $\frac{d^2y}{dx^2}$, the sharp discontinuity at the Euler load changes to a transition zone. In effect, there is really no load for which the deflection is indeterminate. Every load is associated with a distinct deflection shape and, consequently, with specific strains and stresses in the material. Thus, for any practical column the final collapse is still due to a material failure.

Incidentally, it would seem that the mathematical definition of buckling has very little application in the field of reinforced concrete and, indeed, in many other fields of structural engineering. Most engineers would prefer to use the term buckling for cases in which the applied bending moment is a function of the deflection. This definition has its pitfalls, and the writers would be interested to know if any satisfactory definition along these lines has been evolved.

In the work on eccentrically loaded columns, the authors neglect the tensile strength of the concrete between cracks, admitting that this will lead to the predicted ultimate loads being somewhat lower than the actual. Coupled with this is the assumption of a cosine curve of deflection as a basis for the mathematical theory. This surely implies that the effective moment of inertia is constant throughout the length of the column and, hence, that cracking takes place at close spacing over the full length. It is more likely that cracking will occur over a limited length near the mid-section gradually extending as the load increases. This expectation is supported by photographs of tests such as those reported by Hognestad (1). Work carried out at the New South Wales University of Technology by Brettle (23) suggests that the difference between the actual case and the assumption of uniformity is considerable. The effective moment of inertia of a cross-section immediately after cracking is very much smaller than its value before cracking, the reduction depending on the steel percentage and on the axial compression. Even after some simplification, the writers conceive the column as one that has a reduced section over the middle part of its length.

On this view the major part of the curvature will take place in this portion, and the deflected shape will not resemble a cosine wave, but may approximate more to a triangle with a rounded apex. Again, photographs of test specimens support this contention. It is possible that a number of test results discarded by investigators as being caused by local material faults have really been examples of the suggested behaviour. Such deviations from the cosine wave would involve more discrepancy in some ranges of slenderness than in others.

---

[8] Lecturer, School of Civ. Engrg., Univ. of N. S. W., Sydney, Australia; formerly Asst. Designing Engr., Julius Poole and Gibson, Cons. Engrs., Sydney, Australia.

[9] Assoc. Prof. of Civ. Engrg., N. S. W. Univ. of Tech., Sydney, N. S. W., Australia.

Any attempt to take account of discontinuity due to cracking leads to the necessity for some form of numerical analysis that, as the authors remark, is very laborious.

BENGT BROMS,[10] M. ASCE, and I. M. VIEST,[11] F. ASCE.—The collapse of a reinforced concrete member failing in flexure is always accompanied by crushing of concrete. Nevertheless, the crushing is not necessarily the primary cause of failure. As a matter of fact, the strength of a great majority of beams designed according to current codes is governed by the yield strength of reinforcing bars rather than by the compressive strength of concrete. Similarly, the relationship between a "buckling" and a "material" failure, as defined by the authors, is based on the primary cause of failure. In both cases collapse is accompanied by crushing of concrete as was pointed out by Messrs. Jumikis and Hall. However, whereas in the case of material failure the weakness of the material is primarily responsible for the failure, in the case of buckling the instability of the column as a whole triggers the events leading to collapse. This distinction between "material" and "buckling" failures is useful in the mathematical formulation of the problem as presented by the authors.

In discussing the deflected shape of a long column, Messrs. Jumikis and Hall suggested that a triangle with a rounded apex may resemble the deflected shape better than the cosine wave used by the authors. They stated that "it is possible that a number of test results discarded by investigators as being caused by local material faults have really been examples of the suggested behavior." The comparisons between the theory and the existing tests included all reliable data known to the authors. Excluded were only short columns $\frac{L}{d}$ smaller than 10 and columns reported in original test reports (14), (15), and (19) as failing at one end in bearing (that is, failures were attributable to faulty experimental techniques).

In the analysis presented by the authors, the assumption was made that concrete cannot resist any tension. The writers agree with Messrs. Jumikis and Hall that cracking often occurs only over a limited length near the section of maximum moment. The strength of an eccentrically loaded column is related to the magnitude of the lateral deflection. Therefore, it is relatively unimportant what the real shape of the deflected column is as long as the computed deflections approximate the actual deflections at the section of failure. The agreement between the theory and the test data indicates that the deflections computed on the basis of the cosine wave assumption are reasonable.

The original paper includes a complete solution only for columns of rectangular cross-section. Mr. Hromadik's extension to columns of other shapes should prove useful as a tool for both further research and preparation of design charts for special applications.

---

[10] Assoc. Prof. of Civ. Engrg., Cornell Univ., Ithaca, N. Y.

[11] Bridge Research Engr., AASHO Road Test, Ottawa, Ill.

Two additional experimental investigations of slender columns were suggested by Mr. Ernst. One of these concerned with sustained load strength, the other with the effects of end restraints. The theoretical investigations of both problems, one presented in the paper under discussion and the other in the second paper of this symposium, have indicated that both items may affect appreciably the ultimate strength of slender columns. However, in the absence of test data the theoretical treatments of both items must be regarded as tentative. The need for an experimental investigation of the effect of end restraints is particularly pressing.

The writers wish to thank the discussors for their contributions and to express their hopes that the discussions as well as the original paper will stimulate further studies of long reinforced concrete columns.

ULTIMATE STRENGTH ANALYSIS OF RESTRAINED COLUMNS

By Bengt Broms,[1] M. ASCE, and I. M. Viest,[2] F. ASCE

SYNOPSIS

Theoretical analyses are presented for the ultimate strength of long restrained reinforced concrete columns. The analyses are based on the same principles as the analyses of the ultimate strength of long hinged columns presented in the first paper of this symposium. The treatment of concentrically loaded columns is founded on the tangent modulus theory suggested by Engesser, the treatment of eccentrically loaded columns follows the principles advanced by Kármán, and both treatments utilize the stress-strain relationship for concrete determined by Hognestad from tests of short eccentrically loaded columns. The consideration of the end restraints requires the addition of a new assumption and necessitates new methods of solution.

The results of the analyses are presented in dimensionless graphs. The following variables are included: (1) concrete strength, (2) percentage of reinforcement, (3) yield point of reinforcement, (4) end restraint, (5) eccentricity, (6) slenderness ratio, and (7) duration of loading.

INTRODUCTION

Reinforced concrete columns are usually restrained by adjoining members. At loading of a restrained column, the moment from the load is divided between the column and the restraining members in proportion to their relative stiffnesses. An increase of the stiffness of the restraining members decreases the moment acting on the column and increases the ultimate load capacity of the column. Thus, the strength of a restrained column depends on both the properties of the column and of the restraining members.

The behavior of a restrained long column under load is illustrated in Fig. 1. The eccentricity of the load is defined as the ratio of the fixed end moment to the axial load. The fixed end moment is resisted in part by the restraining moment of the adjoining members and in part by the moment resistance of the column. The part resisted by the adjoining members is illustrated in Fig. 1 by coil springs. Deflections of the column produce a restraining moment in the spring proportional to the rotation of the end of the column and shown as line 1-3. The moment resistance of the column depends on the cross-section of the column, the stress-strain relationship of the column material, and the magnitude of stresses. The sum of the moment resistance and of the restrain-

---

Note.—Published essentially as printed here, in May, 1958, in the Journal of the Structural Division, as Proceedings Paper 1635. Positions and titles given are those in effect when the paper or discussion was approved for publication in Transactions.

[1] Assoc. Prof. of Civ. Engrg., Cornell Univ., Ithaca, N. Y.; formerly Research Asst., Dept. of Theoretical and Applied Mechanics, Univ. of Illinois, Urbana, Ill.

[2] Bridge Research Engr., ASSHO Road Test, Ottawa, Ill.; formerly Research Assoc. Prof. of Theoretical and Applied Mechanics, Univ. of Illinois, Urbana, Ill.

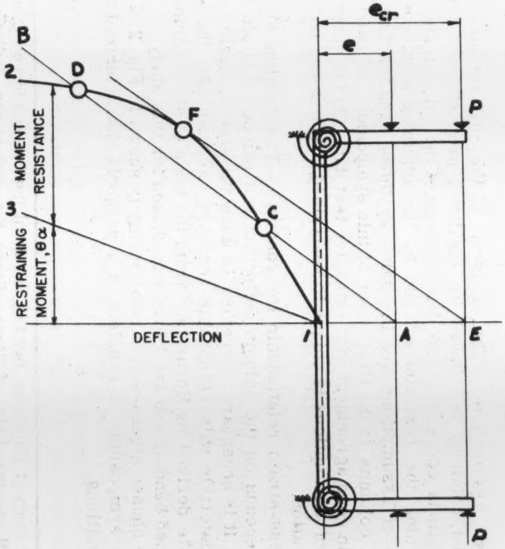
B
2
D
F
C
3
MOMENT RESISTANCE
RESTRAINING MOMENT, $\theta\alpha$
DEFLECTION
e_{cr}
e
P
P
I
A
E

FIG. 1.—BUCKLING OF A RESTRAINED COLUMN

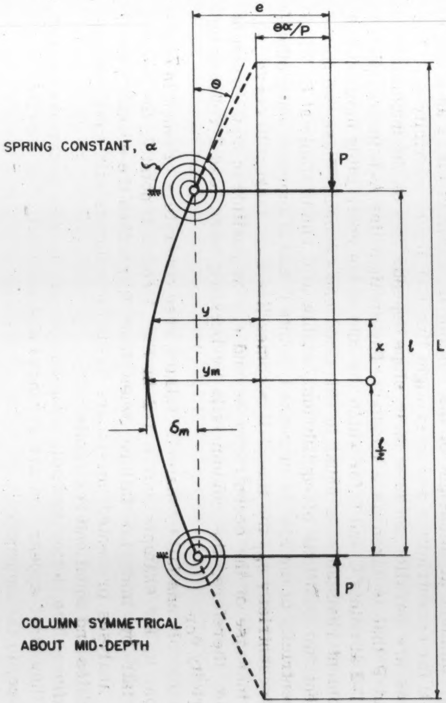
e
$\theta\alpha/P$
θ
SPRING CONSTANT, α
P
P
y
y_m
δ_m
x
l
L
$\frac{l}{2}$
COLUMN SYMMETRICAL ABOUT MID-DEPTH

FIG. 2.—DEFLECTIONS OF ECCENTRICALLY LOADED RESTRAINED COLUMNS

ing moment at midheight of the column is shown as line 1-2. This sum depends only on the column deflections.

Whereas the moment resistance depends only on the deflection, the external moment depends on the sum of the deflection and eccentricity. The external moment at midheight of the column is shown in Fig. 1 as straight line A-B for eccentricity e and as straight line E-F for eccentricity e_{cr}. The two lines are parallel because their slope depends only on the magnitude of the load P that is taken as a constant. The straight line A-B intersects the curve 1-2 at points C and D for which the sum of the restraining moment and the moment resistance is equal to the fixed end moment. These two points represent two positions of equilibrium, stable at C and unstable at D. When the eccentricity of the load is increased, points C and D approach each other. At the eccentricity e_{cr} the line A-B becomes line E-F, tangent to curve 1-2. At an increase of the eccentricity beyond e_{cr} no position of equilibrium is possible, therefore, the column fails by buckling when load P reaches the eccentricity e_{cr}.

Shorter columns fail by material failure when concrete is crushed in compression. If, for example, curve 1-2 in Fig. 1 ended at point C, the column would fail by material failure when load P reaches the eccentricity e.

The analyses presented herein are limited to columns with equal end eccentricities and equal end restraints.

Notation.—The letter symbols adopted for use in this paper are defined where they first appear and are arranged alphabetically, for convenience of reference, in the Appendix.

ULTIMATE STRENGTH ANALYSIS

Basic Assumptions.—The analyses of the ultimate strength of long restrained columns are based on idealized properties of the materials, on assumptions concerning the deformations of the column, and on assumptions concerning the restraint offered by the adjoining members. The first two groups of assumptions are the same as those used for the analyses of long hinged columns in the first paper of this symposium, of which analyses were found in good agreement with extensive test data. On the other hand, the third group of assumptions is unique to restrained columns and lacks experimental verification.

Stress-strain relationship for concrete.—The buckling load of a long column depends on the column deflection and can occur at almost any value of strain. It is necessary, therefore, to know the stress-strain relationships for both materials with reasonable accuracy. Accordingly, the stress block for concrete derived by Hognestad[3] from the tests of short columns subjected to combined bending and axial load was chosen for this study.

The chosen stress-strain relationship is shown in Fig. 2 of the first paper of this symposium. It consists of a parabola characterized by the following two equations,

---

[3] "A Study of Combined Bending and Axial Load in Reinforced Concrete Members," by E. Hognestad, Univ. of Illinois Engrg. Experiment Sta. Bulletin No. 399, Urbana, Ill., 1951. Also published as Bulletin No. 1 of the Reinforced Concrete Research Council of the Engrg. Foundation.

$$f_c = f''_c \left[\frac{2\epsilon}{\epsilon_o} - \left(\frac{\epsilon}{\epsilon_o} \right)^2 \right] \ldots\ldots\ldots\ldots\ldots \quad (1)$$

$$E_c = 1{,}800{,}000 + 460\, f''_c \ldots\ldots\ldots\ldots\ldots \quad (2)$$

and of a descending straight line between the strain ϵ_o, corresponding to the maximum stress, and the strain ϵ_u at which failure occurs. All other characteristics of the relationship are incorporated in Fig. 2[4] of the first paper of this symposium. It may be noted that for a given cylinder strength of concrete, f'_c, all properties of the idealized stress-strain relationship may be evaluated.

It is assumed further that no tensile stresses exist in concrete. Because the concrete between the cracks carries some tensile stresses, the deflections and end rotations of an actual column are smaller than assumed. The error in deflections results in a decrease, but the error in end rotations results in an increase of the ultimate load of the assumed column. Thus, the assumption that no tensile stresses exist in concrete may give either higher or lower ultimate loads than the actual, depending on the relative effects of deflections and end rotations.

Stress-strain relationship for reinforcing steel.—The assumed stress-strain diagram for steel is shown in Fig. 3 of the first paper of this symposium. It is representative of steels with a flat yield point used predominantly for reinforcing bars. The modulus of elasticity, E_s, is taken in all computations as 30,000,000 psi.

Bernoulli's hypothesis.—Linear distribution of strains across the column cross-section is assumed at all load levels.

Shape of deflected column.—It is assumed that the deflected shape of a column is a part of a cosine wave as shown in Fig. 2. This assumption is theoretically correct only for small lateral deflections and for a constant modulus of elasticity along the column. Such conditions are satisfied in concentrically loaded columns.

For eccentrically loaded columns, the use of the cosine-wave assumption implies that the modulus of elasticity is constant along the column and equal to the average modulus at the section of failure. The stiffness at the section of failure is the smallest one. Therefore, the actual deflections and end rotations are smaller than the computed ones so that the computed ultimate loads may be either lower or higher than the actual.

It is probable that the inaccuracy of the cosine-wave assumption has larger effect on the end rotations than on the maximum deflection. However, no quantitative evidence, either experimental or theoretical, is available on the effect of the cosine-wave assumption on the accuracy of the computed ultimate load for restrained columns.

End restraint.—Columns in structures are usually restrained by adjoining members. Rotation at the end of a column produces a restraining moment acting in a direction opposite to that of the rotation. It is assumed in the following analyses that the restraining moment is proportional to the end rotation of the column.

---

[4] The relationship $f''_c = 0.85\, f'_c$ is believed to be correct only for vertically cast columns. For horizontally cast columns the relationship $f''_c = f'_c$ was indicated by earlier tests. (See Ref. 16 of first paper of symposium).

$$M_{rst} = \alpha\ \theta \ldots\ldots\ldots\ldots\ldots\ldots\ldots (3)$$

in which α is the coefficient of end restraint defining the degree of fixity of the adjoining members and θ is the angle of rotation at the end of the column.[5]

The assumed relationship between the restraining moment and end rotations is shown in Fig. 3 as a solid line. This relationship approximates the actual conditions up to the yielding of tensile reinforcement in the restraining members. After the commencement of yielding, end rotations occur without any appreciable further increase of restraining moment as is indicated in Fig. 3 by the dotted horizontal line. Yielding of the restraining members is not considered in the analyses presented in this paper.

Concentrically Loaded Columns.—

Buckling.—The buckling load for a concentrically loaded column stressed below the proportional limit of the material was determined theoretically by Euler.[6] For columns stressed beyond the proportional limit, Euler's formulas were modified by Engesser through the use of the tangent modulus of elasticity.[7] Euler's and Engesser's well known solutions are limited to columns with hinged or fixed ends whereas reinforced concrete columns are usually restrained at their ends by the adjoining frame members. A summary of buckling of restrained columns has been made by Timoshenko.[8] Timoshenko's

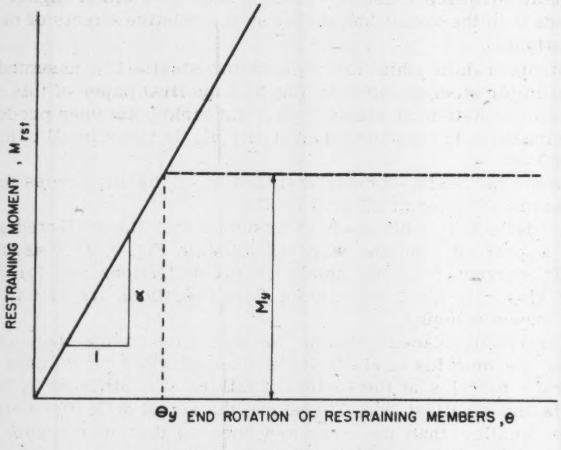

FIG. 3.—ASSUMED RELATIONSHIP BETWEEN MOMENT AND ROTATIONS FOR RESTRAINING MEMBERS

solutions are restricted to columns stressed below the proportional limit. If the stresses exceed the proportional limit, the solutions need to be modified. The modification presented herein utilizes the tangent modulus of elasticity.

---

[5] Because θ is a dimensionless quantity, α has the dimension of a moment.

[6] "De Curvis Elasticis, Additamentum I, Methodus Inveniendi Lineas Curvas Maximi Minimive Proprietate Gaudentes," by L. Euler, Lausanne and Geneva, 1744, pp. 267-268.

[7] "Ueber die Knickfestigkeit gerader Stäbe," by F. Engesser, Zeitschrift d. Arch., U. Ing., Ver. zu Hannover, Vol. 35, Hannover, 1889, p. 455.

[8] "Theory of Elastic Stability," by S. Timoshenko, McGraw-Hill Book Co. Inc., First Ed., New York and London, 1936.

The assumed stress-strain diagram for concrete (Fig. 2 of first paper of symposium) has no proportional limit. Accordingly, the following differential equation may be written for small lateral deflections of a reinforced concrete column:

$$-\frac{d^2y}{dx^2} E_t I = M \qquad (4)$$

in which E_t is the tangent modulus and I is the moment of inertia of the transformed cross-section. For a hinged column subjected to concentric load P and to moment M applied at one end, the solution of Eq. 4[9] may be written as

$$y = \frac{M}{P}\left(\frac{\sin k' x'}{\sin k' l} - \frac{x'}{l}\right)$$

in which $k' = \frac{P}{E_t I}$, x' is the distance from the end at which only load P is applied, and l refers to the length of the column. If equal moments M are applied at both ends, the following solution is obtained by considering the symmetry:

$$y = \frac{M}{P}\left[\frac{\sin k' x'}{\sin k' l} + \frac{\sin k' (l - x')}{\sin k' l} - 1\right] .$$

The corresponding end rotation may be evaluated as the first derivative of the deflection at x' = 0. Expressing P in terms of k', E_t and I, the end rotation of a column subjected to axial load and end moments M is given by the following formula:

$$\theta_M = \left[\frac{dy}{dx'}\right]_{x'=0} = \frac{M}{E_t I} \frac{1}{k'} \; t\,g\left(\frac{k' l}{2}\right) .$$

The end rotation of a restrained column may be expressed as

$$\theta = \theta_o + \theta_M$$

in which θ_o is the rotation of the corresponding hinged column and θ_M is the end rotation caused by the restraining moments M_{rst}. The restraining moments act in the direction opposite to the direction of the end rotations. Thus, $M_{rst} = -M$ and

$$\theta = \theta_o - \frac{M_{rst}}{E_t I} \frac{1}{k'} \; t\,g\left(\frac{k' l}{2}\right) .$$

Substituting from Eq. 3 for θ and rearranging gives

$$M_{rst} = \frac{k' E_t I \theta_o}{t\,g\left(\frac{k' l}{2}\right) + \frac{k' l}{2} \frac{2 E_t I}{\alpha l}}$$

At buckling the end rotations θ and, thus also, M_{rst} approach infinity. This condition is satisfied if

---

[9] The solution is identical to that presented by Timoshenko[8] except that the tangent modulus E_t has been substituted for the modulus of elasticity E.

$$t\,g\left(\frac{k'\,l}{2}\right) + \frac{k'\,l}{2}\;\frac{2\,E_t\,I}{\alpha\,l} = 0 \quad \ldots\ldots\ldots\ldots\ldots (5)$$

Eq. 5 is the general expression for the buckling load of a concentrically loaded column with equal elastic restraints at both ends. For a column with both ends fixed $\alpha = \infty$, so that

$$\frac{k'\,l}{2} = \pi$$

and

$$P = \frac{4\,\pi^2\,E_t\,I}{l^2} \quad \ldots\ldots\ldots\ldots\ldots (5a)$$

Material failure.—An inspection of the assumed stress-strain relationship for concrete shows that a material failure occurs when the strain reaches the ultimate value for concrete $\epsilon_u = 0.0038$. However, it has been pointed out in the first paper of the symposium that failure of a concentrically loaded column may occur at a lower strain and that columns made of commonly used materials usually fail at the concrete strain ϵ_o. Accordingly, it is assumed in the following analysis that a concentrically loaded column fails by material failure if the column strain reaches the value of ϵ_o.

If the steel stress at column failure is designated as f_s, the ultimate load corresponding to material failure may be evaluated from the following equation:

$$\frac{P}{f''_c\,b\,d} = \frac{f_s\,p}{f''_c} + 1 \quad \ldots\ldots\ldots\ldots\ldots (6)$$

in which $f_s = E_s\,\epsilon_o \leqq f_y$.

Evaluation of ultimate load.—The tangent modulus E_t and the moment of inertia I in Eq. 5 may be evaluated for any column of known dimensions and properties of materials. The tangent modulus E_t at any strain ϵ, (Fig. 2 of first paper of symposium) is equal to $df_c/d\epsilon$. As it is assumed that material failure occurs when ϵ reaches ϵ_o, only the portion of the stress-strain diagram for concrete given by Eq. 1 is of interest for concentrically loaded columns so that

$$E_t = E_c\left(1 - \frac{\epsilon}{\epsilon_o}\right) \quad \ldots\ldots\ldots\ldots\ldots (7)$$

in which E_c is the initial modulus of elasticity given by Eq. 2.

For rectangular symmetrically reinforced concrete columns, the moment of inertia I of the transformed section may be written as:

$$I = \frac{b\,d^3}{12} + \frac{E_s\,p}{E_t}\;\frac{b\,d\,(d'')^2}{4} \quad \ldots\ldots\ldots\ldots\ldots (8)$$

in which E_s/E_t is the modular ratio. The modular ratio varies with the load. For strains smaller than the yield point strain of the reinforcement ϵ_y, the modulus of elasticity E_s may be taken as 30×10^6 psi. For strains equal to and larger than the yield point strain ϵ_y, E_s is equal to zero. Accordingly, the moment of inertia I decreases suddenly when the yield point strain is reached.

For strains smaller than ϵ_o, the relationship between the concentric load and the corresponding strains may be expressed as

$$\frac{P}{f''_c\,b\,d} = \frac{f_s\,p}{f''_c} + \frac{2\,\epsilon}{\epsilon_o} - \left(\frac{\epsilon}{\epsilon_o}\right)^2 \quad \ldots\ldots\ldots\ldots\ldots (9)$$

in which f_s is equal to $E_s \epsilon$ for strains smaller than ϵ_y, and equal to f_y for strains equal to or larger than ϵ_y.

Eqs. 5, 7, 8 and 9 contain four unknowns: P, E_t, I and ϵ. Thus, the buckling load may be evaluated by simultaneous solution of all four equations. If the resulting ϵ is larger than ϵ_o, the strength of the column is governed by material failure. Substitution of $\epsilon = \epsilon_o$ into Eq. 9 results in Eq. 6 for the capacity of columns failing by material failure.

Comparison with test data.—No test data are available for concentrically loaded columns partially restrained at the ends. Four long columns with both ends fixed and two long columns with one end fixed and one hinged were tested by Baumann.[10] As all six columns had rectangular cross-section and were reinforced symmetrically, their failure loads may be computed by the procedure presented in this paper.[11]

The dimensions of all six columns and the properties of materials[12] are given in Table 1 including also the ultimate test and computed loads, reduced to the dimensionless quantities $P_{test}/f''_c\, b\, d$ and $P_{calc}/f''_c\, b\, d$, and the ratios P_{test}/P_{calc}. In Table 1 all columns had 1 percent of longitudinal reinforcement. In the computations of ultimate loads, the yield point of the reinforcement was assumed as 46,600 psi and the effective depth was assumed as $d' = 0.9\, d$. It can be seen that the computed values agree reasonably well with the test values, although for the columns fixed at both ends the computed values are consistently larger than those obtained from the tests.

TABLE 1.—TESTS OF CONCENTRICALLY LOADED FIX-ENDED LONG COLUMNS

Specimen	Concrete Strength f'_c,[a] psi	Cross-Section d-by-b, in.-by-in.	Slenderness l/d	$\frac{P_{test}}{f''_c\, b\, d}$	$\frac{P_{calc}}{f''_c\, b\, d}$	$\frac{P_{test}}{P_{calc}}$
Both Ends Fixed						
17	3360	3.54 x 7.87	32.4	1.065	1.142	0.93
21	5810	3.50 x 7.87	32.7	0.907	1.036	0.88
22	5810	3.50 x 7.87	32.7	1.029	1.036	0.99
23	6390	5.08 x 9.76	21.4	0.897	1.126	0.80
One End Fixed, One Hinged						
18	3360	3.58 x 7.91	34.2	0.996	0.940	1.06
20	4070	5.12 x 9.84	23.0	1.094	1.109	0.99

[a] All columns were cast horizontally; therefore, $f'_c = f'_{pr}/0.85$.

Eccentrically Loaded Columns.—

Buckling.—Von Kármán proposed[13] a general theory for buckling of eccentrically loaded columns stressed beyond the proportional limit. The theory is based on the stress-strain relationship of the column material and on the assumption of linear strain distribution. Von Kármán's theory was simplified by Westergaard and Osgood[14] who assumed that the deflected shape of the column is a part of a cosine wave. The modified von Kármán's theory was applied to hinged reinforced concrete columns in the first paper of this symposium.

---

[10] "Die Knickung der Eisenbeton-Säulen," by O. Baumann, Eidg. Materialprüfungsanstalt an der E. T. H. in Zürich, Bericht, No. 89, Zürich, 1934.

[11] It can be shown that the buckling load for columns fixed at one end and hinged at the other end is given by the equation $P = \frac{20.16\, E_t\, I}{l^2}$.

[12] Baumann determined the strength of concrete by tests of control prisms. Prism strength is comparable to the strength of cylinders.

[13] "Untersuchungen über Knickfestigkeit," by T. von Kármán, Mitteilungen über Forschungsarbeiten auf dem Gebiete des Ingenieurwesens, No. 81, Berlin, 1910.

The approach used for hinged columns is followed in this paper for restrained columns, except that a rigorous solution for determination of the critical eccentricity is replaced by a graphical procedure illustrated in Fig. 4. The procedure requires computation of several corresponding values of the eccentricity e and the maximum deflection δ_m for a particular column subjected to a chosen constant load P. The eccentricity e is increased until it has

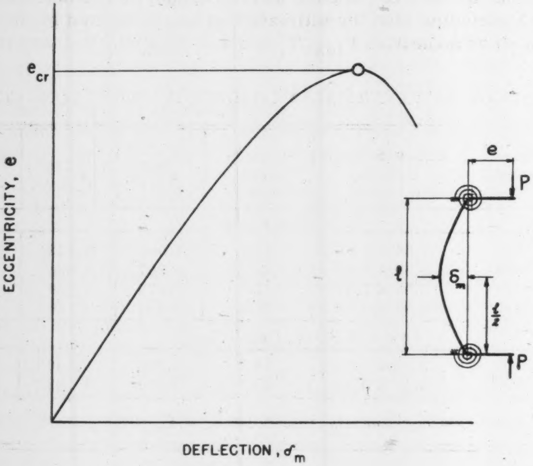

FIG. 4.—BUCKLING OF RESTRAINED COLUMN

reached e_{cr}, at which value the deflection of the column increases without any further increase in eccentricity.

A deflected restrained column is shown in Fig. 2. It is assumed that the deflected shape of the column is a part of a cosine wave. Thus

$$y = y_m \cos \frac{\pi x}{L} \quad \ldots\ldots\ldots\ldots\ldots\ldots (10)$$

The end eccentricities of a restrained column are composed of two parts as shown in Fig. 2: the deflection y at x = 1/2,

---

[14] "Strength of Steel Columns," by H. M. Westergaard and W. R. Osgood, Transactions, A.S.M.E., Vol. 50, 1928, pp. 65-80.

$$y_m \cos \frac{\pi}{2}\frac{l}{L},$$

and the eccentricity due to the end restraint, M_{rst}/P. But the restraining moment is assumed proportional to the end rotation θ that may be determined from Eq. 10 as

$$\theta = \left[-\frac{dy}{dx}\right]_{x=\frac{l}{2}} = \frac{\pi}{L}\, y_m \sin \frac{\pi}{2}\frac{l}{L}.$$

Using Eq. 3, the eccentricity due to the end restraint may be expressed as

$$\frac{\alpha}{P}\,\frac{\pi}{L}\, y_m \sin \frac{\pi}{2}\frac{l}{L}$$

so that the following relationship exists between the end eccentricity e, the deflection and the end restraint:

$$e = y_m \cos \frac{\pi}{2}\frac{l}{L} + \frac{\alpha}{P}\,\frac{\pi}{L}\, y_m \sin \frac{\pi}{2}\frac{l}{L} \quad \ldots\ldots\ldots (11)$$

It should be noted that for $\theta = 0$, the eccentricity e is equal to the deflection y at $x = l/2$:

$$e_o = y_m \cos \frac{\pi}{2}\frac{l}{L} \quad \ldots\ldots\ldots\ldots (12)$$

Eq. 12 represents the initial eccentricity before any rotation of the ends and before any redistribution of moments to the adjoining members. Because eccentricity is defined as the ratio of moment to axial force, the initial eccentricity, e_o, for a restrained column is equal to the ratio of the fixed end column moment to the axial force.

Eq. 11 gives the vertical ordinate for Fig. 4. The horizontal ordinate, that is, the corresponding maximum deflection δ_m of a restrained column may be written, with the aid of Fig. 2, as

$$\delta_m = y_m + \frac{\alpha}{P}\,\frac{\pi}{L}\, y_m \sin \frac{\pi}{2}\frac{l}{L} - e \quad \ldots\ldots\ldots\ldots (13)$$

Eq. 11 contains three unknowns: e, y_m and L. The necessary two other relationships may be determined from the column curvature and from the moment equilibrium at column mid-depth.

The curvature and the maximum total deflection are related as follows:

$$\frac{1}{\rho} = -\frac{d^2y}{dx^2} = y_m \left(\frac{\pi}{L}\right)^2 \cos \frac{\pi x}{L} \quad \ldots\ldots\ldots\ldots (14)$$

At the point of maximum moment

$$\frac{1}{\rho_m} = y_m \left(\frac{\pi}{L}\right)^2.$$

Because the curvature may also be expressed as

$$\frac{1}{\rho_m} = \frac{\epsilon_4 - \epsilon_1}{d},$$

the following relationship may be written:

$$\frac{\epsilon_4 - \epsilon_1}{d} = y_m \left(\frac{\pi}{L}\right)^2 \quad \ldots\ldots\ldots\ldots\ldots (15)$$

in which ϵ_4 and ϵ_1 are the strains at the section of maximum moment and d is the depth of the column (Fig. 6 of first paper of symposium).

At the point of maximum moment, the relation between the load, moment and maximum total deflection may be expressed as

$$y_m = \frac{M_{col}}{P} \quad \ldots\ldots\ldots\ldots\ldots\ldots (16)$$

The quantities M_{col} and P may be determined if the strains in the cross-section are known.

Having Eq. 11, 13, 15, and 16 the critical eccentricity, for which the assumed load is the buckling load, may be determined. For a constant value of P, several values of the quantity $(\epsilon_4 - \epsilon_1)$ are chosen and the corresponding values of M_{col} computed from the relationship between strains, load, and moment. For each value of $(\epsilon_4 - \epsilon_1)$ the deflection y_m is determined for Eq. 16 and the value π/L from Eq. 15. For the desired column length l and the end restraint α the values of e and δ_m are then computed from Eq. 11 and 13. The relationship between the eccentricity e and the deflection δ_m is plotted as shown in Fig. 4. The maximum value, e_{cr}, is the critical eccentricity of the load P.

The procedure derived represents a general solution for buckling of eccentrically loaded restrained columns. It is applicable to columns of any cross-section and of any material.

Relationships between loads, moments and strains.—The distribution of stresses in a reinforced concrete column is determined by two strains, the stress-strain relationships for concrete and steel (Figs. 2 and 3 of first paper of symposium), and the cross-section of the column. The load P and moment M_{col} are expressed in terms of strains by summation of the stresses in the cross-section. The relationships are independent of the end conditions and, therefore, are the same for restrained columns as for hinged columns (See first paper of this symposium).

For rectangular cross-sections with symmetrical reinforcement illustrated in Fig. 4, the following equations may be derived:

$$\frac{P}{f''_c\, b\, d} = \frac{p\left(f_{s2} + f_{s3}\right)}{2\, f''_c} + \frac{A}{\epsilon_4 - \epsilon_1} \quad \ldots\ldots\ldots\ldots (17)$$

$$\frac{M_{col}}{f''_c\, b\, d^2} = \frac{p\left(f_{s3} - f_{s2}\right)}{4\, f''_c}\,\frac{d''}{d} + \frac{B}{\left(\epsilon_4 - \epsilon_1\right)^2} - \frac{\epsilon_4 + \epsilon_1}{\left(\epsilon_4 - \epsilon_1\right)^2}\,\frac{A}{2} \quad \ldots (18)$$

in which parameters A, B, and steel stresses f_{s2} and f_{s3} are known functions of concrete strains ϵ_1 and ϵ_4.

Formulas for parameters A and B are listed in Table 1 of first paper of symposium. Four expressions are given for each parameter. Each formula is applicable within certain limits for ϵ_4 and ϵ_1. Formulas for cases 1 and 3 refer to full cross-section in compression, whereas formulas for cases 2 and 4 refer to a cross-section partly in compression and partly in tension.

The steel stresses are related to steel strains ϵ_2 and ϵ_3 as $f_{s2} = E_s\, \epsilon_2$ and $f_{s3} = E_s\, \epsilon_3$, and strains ϵ_2 and ϵ_3 may be expressed as

$$\epsilon_2 = \epsilon_4 - \left(\epsilon_4 - \epsilon_1\right) \frac{d'}{d} \quad \ldots\ldots\ldots\ldots (19)$$

$$\epsilon_3 = \epsilon_1 + (\epsilon_4 - \epsilon_1)\frac{d'}{d} \quad \ldots\ldots\ldots\ldots (20)$$

It should be noted from Fig. 3 of first paper of symposium that the steel stresses f_{s2} and f_{s3} have an upper limit equal to the yield point stress f_y.

In the derivation of Eq. 17 and 18, compressive strains were taken as positive quantities and tensile strains as negative quantities. The same sign convention should be followed in using these equations.

Material failure.—An eccentrically loaded column fails by crushing of concrete when the maximum strain ϵ_4 reaches the ultimate value for concrete ϵ_u. The load and moment at failure of such a column may be computed by solving Eq. 11, 12, 15, 16, 17, 18, 19, and 20 after placing $\epsilon_4 = \epsilon_u$.

GRAPHS OF ULTIMATE LOADS

The procedure for eccentrically loaded columns described in the preceding section does not lend itself easily to a direct evaluation of the buckling load for a particular column. It is more suitable for correlating the ultimate loads to the critical lengths and eccentricities for a whole group of columns having the same properties of the cross-section, the same coefficient of end restraint and the same characteristics of loading other than the magnitude of the initial eccentricity. The ultimate load for a particular column of the group may then be obtained by interpolation.

It is not necessary to make a separate set of computations for each particular column cross section. If dimensionless quantities are used instead of the actual loads, moments and dimensions, one group pertains to all columns having the same properties of concrete, properties of steel, percentage of reinforcement, effective depth ratio d'/d, the same coefficient of end restraint and conditions of loading. For convenient use, the results may be tabulated for each group or plotted as is illustrated in Figs. 5 through 9.

Eleven dimensionless graphs were prepared for rectangular columns with symmetrical reinforcement, equal end restraints and initial eccentricities at both ends. In each graph the quantity $P/f''_c\, b\, d$ is plotted as a function of the slenderness ratio l/d for several ratios of the initial eccentricity to the column depth, e_o/d. In all computations the effective depth was taken as $d' = 0.9\, d$.

Comments on Variables.— The ten representative graphs shown in Figs. 5 through 9 illustrate the effects of the slenderness ratio, initial eccentricity ratio, degree of end restraint, concrete strength, percentage of reinforcement, yield point of reinforcement, and long duration of loading. An inspection of the graphs reveals that the slenderness ratio l/d, the initial eccentricity ratio e_o/d and the degree of end restraint $\alpha/f''_c\, b\, d^2$ are the most important variables. It is probable that the relative magnitude of the initial end eccentricities and the relative magnitude of the end restraints at the two ends of the column may have also an important effect on the magnitude of the column load capacity. These effects were not considered in the study reported herein.

Eccentricity of load.—The graphs in Figs. 5 through 9 are plotted for the initial eccentricity ratios e_o/d. The initial eccentricity e_o is defined as M/P, in which M is the fixed end moment. As load is applied, a part of the fixed end moment is distributed to the adjoining members and the column carries only part of the moment. Thus, the eccentricity at failure of a restrained column is smaller than the initial eccentricity.

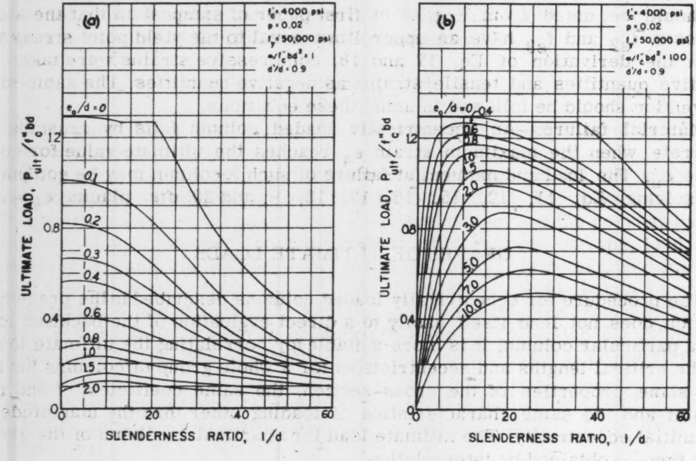

FIG. 5.—ULTIMATE LOAD GRAPHS

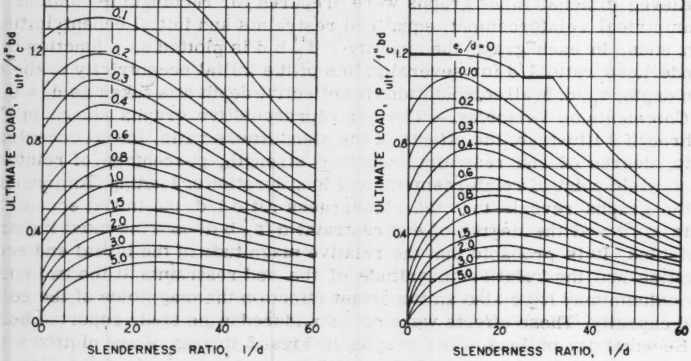

FIG. 6.—ULTIMATE LOAD GRAPHS

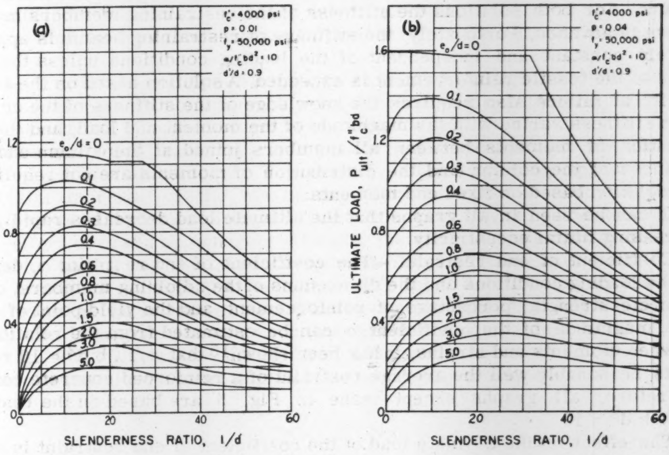

FIG. 7.—ULTIMATE LOAD GRAPHS

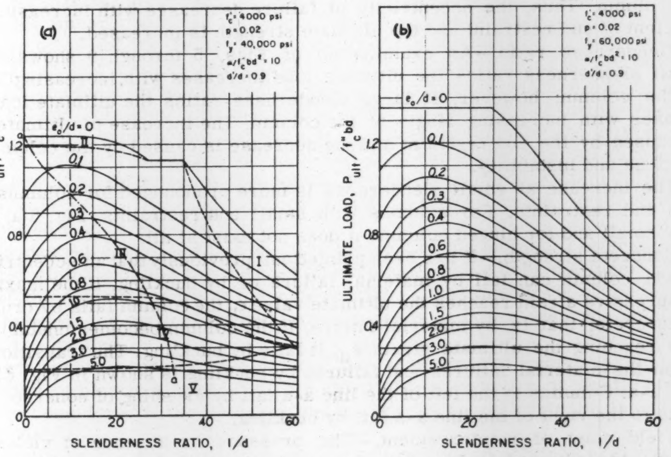

FIG. 8.—ULTIMATE LOAD GRAPHS

The initial eccentricity was chosen for this study because the solution based on such an eccentricity is simpler than that based on the eccentricity at failure. For both solutions the stiffness of the restraining members must be known in advance. Fortunately, the stiffness of restraining beams is approximately constant and independent of the loading conditions unless the yield point of the tensile reinforcement is exceeded. A solution based on the eccentricity at failure also requires the knowledge of the stiffness of the column. That stiffness varies with the magnitude of the moment and load, and the distribution of moments between all members joined at the column end. The stiffness of the column and the distribution of moments are not required in the solution based on fixed end moments.

It can be seen in all graphs that the ultimate load decreases rapidly with increasing initial eccentricity.

Coefficient of end restraint.—The coefficient of end restraint α, depends on the loading conditions and the dimensions of the adjoining members, on the concrete strength, percentage of reinforcement, and the yield point of steel. The magnitude of the coefficient α can be estimated from the relationship between moments and strains. It has been shown[15] that $\alpha/f''_c\, b\, d^2 = 10$ represents reasonably well the average restraint of a reinforced concrete column. Therefore, all graphs except those in Fig. 5 are based on the restraint $\alpha/f''_c\, b\, d^2 = 10$.

The effect on the ultimate load of the coefficient of end restraint is shown in Figs. 5(a) and 5(b). There is no effect for columns with $l/d = 0$ but the effect is large for columns with intermediate and large slenderness ratios. With increasing coefficient of end restraint, a larger part of the fixed end moments is attracted by the adjoining members and only a smaller part by the column. Thus, the eccentricity at failure decreases with increasing coefficient of end restraint and the ultimate strength is increased.

Slenderness ratio.—An examination of Figs. 5 through 9 shows that at small slenderness ratios the ultimate load increases with increasing length of the column; however, at large slenderness ratios the ultimate load decreases with increasing length of the column. The increase of ultimate load is caused by the end restraint and the decrease is caused by the column deflections and instability.

The increase at small slenderness is more pronounced for columns with high end restraints. For columns with small end restraints Fig. 5(a) it is very small and for hinged columns it does not exist at all.

Concrete strength.—It has been pointed out previously that an eccentrically loaded column can fail by material failure or by buckling. If the maximum compressive strain reaches the ultimate value ϵ_u the column fails by crushing of concrete, that is, by material failure. If the column becomes unstable before reaching the ultimate strain ϵ_u, it fails by buckling. The transition between the material failures and failures by buckling is shown in Fig. 8(a) as line a-a. Columns to the left of the line a-a fail by crushing of concrete; columns to the right of the line a-a fail by buckling.

Yield point of reinforcement.—The presence or absence of yielding at failure is indicated in Fig. 8(a). In area I the steel stresses at failure are below the yield point value, in area II all steel yields in compression, in area

---

[15] "Ultimate Strength of Long Reinforced Concrete Columns," by B. Broms. Thesis presented to Univ. of Illinois, Urbana, Ill., in June, 1956, in partial fulfilment of the requirements for the degree of Doctor of Philosophy.

III the steel yields in compression on one face only, in area IV the steel yields in compression on one face and in tension on the other, and in area V the steel yields in tension on one face only. The yield point has no effect on the ultimate load in area I and has the largest effect on the ultimate load in area IV.

Long duration of loading.—The graphs in Figs. 5 through 8 and 9(a) represent the strength of columns subjected to short-time loading.[16] Studies of short eccentrically loaded columns and of long hinged columns (see first paper of this symposium) have indicated a lower ultimate strength when failure occurs under sustained loads. The primary effects of creep appear to be a substantial increase of the maximum concrete strain at failure ϵ_u and a relatively small decrease of the maximum concrete stress f_c''. Neglecting the small effect of creep on concrete strength, the stress-strain relationship for long-time loading may be taken as shown in Fig. 2 of first paper but with the strain ordinates multiplied by a factor of 2. The ultimate loads may then be computed in the same manner as for short-time loading. Fig. 9(b) represents an ultimate load graph computed in this manner. A comparison of this graph with Fig. 9(a) illustrates the difference between the maximum load that a column can resist for a short time and that which can be sustained indefinitely.

LIMITATIONS

In the preceding analyses of the ultimate load of restrained columns, it was assumed that the end rotation of the column is smaller than the rotation that causes formation of a plastic hinge in the adjoining member. It has been assumed that the moment that resists the rotation at the ends of the column increases linearly with the rotation. However, a plastic hinge may form in the restraining members before or at the ultimate column load thus decreasing the strength of the restrained column as is illustrated in Fig. 10. The restraining moment produced by the restraining members increases linearly with the end rotations until the plastic hinge has formed, but further end rotations occur without any increase in the restraining moment (curve 1-3). The sum of the restraining moment and moment resistance is indicated by the curve 1-2. Buckling of the column occurs when the maximum deflection of the column has reached the point F and the corresponding eccentricity of the applied load is equal to e_{cr}.

The dashed curve 1-2 in Fig. 10 is the sum of the moment resistance and the restraining moment for the case when a plastic hinge does not form. Buckling of the column occurs at the eccentricity e'. The magnitude of the difference between the critical eccentricities depends on how closely the points F' and F are located.

The ultimate capacity of a column may be decreased considerably by the formation of plastic hinges. Thus the effect of the formation of plastic hinges must be considered if the increase in capacity due to end restraint is utilized in the design.

The theory for the ultimate strength of long hinged columns presented in the first paper of this symposium was verified by an extensive set of test data. On the contrary, except for a few tests of concentrically loaded columns

---

[16] A test to failure in a conventional testing machine carried out in a few hours.

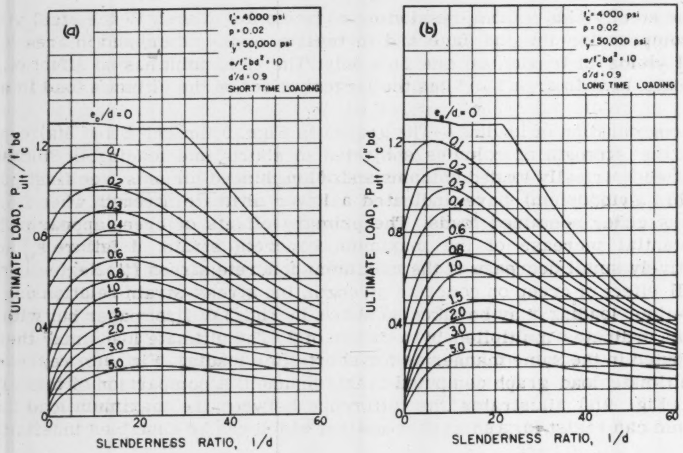

FIG. 9.—ULTIMATE LOAD GRAPHS

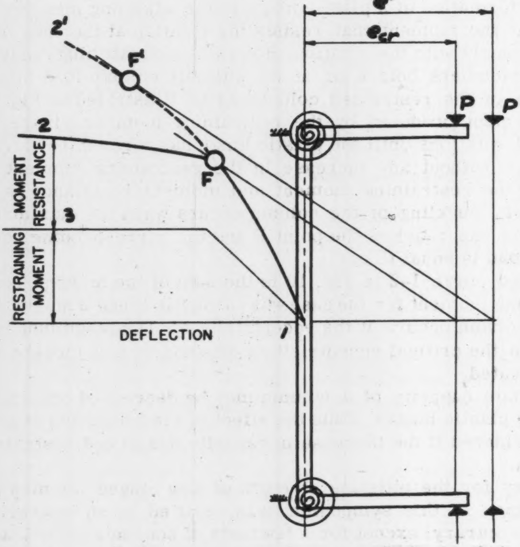
e'
e_{cr}
2'
F'
2
F
P
P
3
1
MOMENT RESISTANCE
RESTRAINING MOMENT
DEFLECTION

FIG. 10.—EFFECT OF PLASTIC HINGE

with fixed ends, no test data are available for long restrained reinforced concrete columns. The absence of test data is especially important because the theory involves two assumptions in addition to those used in the theory of hinged columns: (1) for computations of end rotations the deflected shape of the column is assumed a part of the cosine wave, and (2) the restraining moment is assumed proportional to the end rotations. No quantitative evidence is available on the effect of the cosine-wave assumption on the accuracy of the computed ultimate load of restrained long columns and on the relationship between restraining moments and end rotations. The effects of these additional assumptions on the ultimate strength of restrained columns should be investigated by experimental means.

APPENDIX.—NOTATION

The following symbols have been adopted for use in this paper:

A = a parameter given in Table 1 of first paper;

A_s = total area of longitudinal column reinforcement;

B = a parameter given in Table 2;

b = width of cross-section (Fig. 6 of first paper);

d = total depth of cross-section (Fig. 6 of first paper);

d' = effective depth of reinforcement (Fig. 6 of first paper);

d'' = distance between centroids of compression and tension reinforcement (Fig. 6 of first paper);

E_c = modulus of elasticity of concrete;

E_s = modulus of elasticity of steel;

E_t = tangent modulus of elasticity;

e = end eccentricity of load (Fig. 2);

e_{cr} = critical eccentricity (Fig. 1);

e_o = initial eccentricity of load;

f_c = concrete stress;

f'_c = compressive strength of 6 x 12-in. concrete cylinders;

f''_c = compressive strength of concrete in flexure (Fig. 2 of first paper);

f'_{pr} = compressive strength of concrete prisms;

f_s = steel stress;

f_{s2} = steel stress corresponding to strain ϵ_2;

f_{s3} = steel stress corresponding to strain ϵ_3;

f_y = yield point of reinforcement;

I = moment of inertia;

k' = $\frac{P}{E_t I}$;

L = equivalent length defined in Fig. 2;

l = length of column (Fig. 2);

M = bending moment;

M_{col} = moment resistance of a column;

M_{rst} = moment resistance of restraining members;

P = applied load;

p = $\frac{A_s}{b\,d}$, ratio of reinforcement;

x = distance in the direction of column axis from the middepth (Fig. 2);

y = lateral deflections of column including the initial eccentricity and the effect of end restraint (Fig. 2);

y_m = maximum lateral deflection including the initial eccentricity and the effect of end restraint (Fig. 2);

α = $\frac{M_{rst}}{\theta}$, coefficient of end restraint (Fig. 3);

δ_m = maximum lateral deflection (Fig. 2);

ϵ = strain;

ϵ_o = compressive strain corresponding to maximum concrete stress (Fig. 2 of first paper);

ϵ_1, ϵ_4 = concrete strains (Fig. 6 of first paper);

ϵ_2, ϵ_3 = steel strains (Fig. 6 of first paper);

ϵ_u = ultimate concrete strain in flexure (Fig. 2 of first paper);

ϵ_y = yield point strain of reinforcement;

θ = end rotation (Fig. 3);

$\frac{1}{\rho}$ = curvature; and

$\frac{1}{\rho_m}$ = curvature at $x = 0$.

DESIGN

By Bengt Broms,[1] M. ASCE, and I. M. Viest,[2] F. ASCE

With Discussion by Messrs. J. G. Mac Gregor and C. P. Siess; Phil M. Ferguson; and Bengt Broms and I. M. Viest

SYNOPSIS

The design procedure presented in this paper involves the strength of a short column, the eccentricity determined from an elastic analysis, and a reduction coefficient. Depending on the method used in computing the short column strength, the procedure may be applied at either working or ultimate load level.

The reduction coefficient is based on the results of a theoretical analysis of the strength of long columns presented in the first paper of this symposium. It is shown that the strength of a hinged column with the eccentricity obtained from an elastic analysis represents a lower limit for the strength of restrained columns. It is shown further that the ratio of the strength of a long column to that of a short column depends primarily on the slenderness ratio and on the ratio of end eccentricities. These two variables are taken into account in the reduction coefficient.

The design procedure is compared with the available test data for hinged columns.

INTRODUCTION

Since 1936, the ACI Building Code requirements[3,4,5,6,7], have prohibited the use of eccentrically loaded reinforced concrete columns with the length to depth ratio larger than 20. As most columns have some eccentricity, this provision prevents a general use of slender reinforced concrete columns. It was, therefore, considered desirable to undertake a study of long columns for the purpose of examining the current design procedures.

Note.—Published essentially as printed here, in July, 1958, in the Journal of the Structural Division, as Proceedings Paper 1694. Positions and titles given are those in effect when the paper or discussion was approved for publication in Transactions.

[1] Assoc. Prof. of Civ. Engrg., Cornell Univ., Ithaca, N. Y.; formerly Research Asst., Dept. of Theoretical and Applied Mechanics, Univ. of Illinois, Urbana, Ill.

[2] Bridge Research Engr., AASHO Road Test, Ottawa, Ill.; formerly Research Assoc. Prof. of Theoretical and Applied Mechanics, Univ. of Illinois, Urbana, Ill.

[3] "Building Regulations for Reinforced Concrete (ACI 501-36-T)," Proceedings, ACI, Vol. 32, March, April, 1936, p. 407.

[4] "Building Regulations for Reinforced Concrete (ACI 318-41)," ACI, 1941.

[5] "Building Code Requirements for Reinforced Concrete (ACI 318-47)," Proceedings, ACI, Vol. 44, September, 1947, p. 1.

[6] "Building Code Requirements for Reinforced Concrete (ACI 318-51)," Proceedings, ACI, Vol. 47, April, 1951, p. 913.

[7] "Building Code Requirements for Reinforced Concrete (ACI 318-51)," Proceedings, ACI, Vol. 52, May, 1956, p. 913.

The first step in the ensuing investigation was the development of theoretical analyses for hinged and restrained columns, taking into account the effects of increased lateral deflections due to loading and the limitation on strength imposed by buckling. These analyses are presented in the other papers of this symposium. The analyses were based on the principles advanced by Euler,[8] Engesser,[9] von Kármán,[10] and Westergaard and Osgood,[11] and on the behavior of short eccentrically loaded columns reported by Hognestad.[12] The analyses for concentrically and eccentrically loaded hinged columns were found in a reasonable agreement with the available test data. The analysis for concentrically loaded restrained columns was checked against a few tests of columns with fixed ends. No applicable test data were available for eccentrically loaded restrained columns.

The theoretical analyses for eccentrically loaded columns cannot be used directly for evaluating the ultimate strength of a particular column. They are more suitable for correlating the ultimate loads for a whole group of columns having the same properties of the cross-section and the same characteristics of loading other than the magnitude of the initial eccentricity. The results of such a correlation for one group of columns are shown in Fig. 1.

Ultimate load graphs such as those in Fig. 1 were used for evaluating the effects of several variables on the ultimate strength of long columns (see other papers of symposium) and for development of a simple design procedure. The design procedure and its development are reported herein.

Notation.—The letter symbols adopted for use in this paper are defined where they first appear and are arranged alphabetically, for convenience of reference, in the Appendix.

REDUCTION COEFFICIENT

Method of Approach.—The graphs of ultimate load of the type shown in Fig. 1 may be used for design of slender reinforced concrete columns. The principal advantage of this method is a high degree of accuracy that can lead to the best utilization of column materials. However, it requires a separate graph for each combination of the following variables; concrete strength, percentage and yield point of the reinforcement, ratio of effective depth to total depth, end restraint, ratio of end eccentricities, and ratio of end restraints. Although the method could be simplified substantially by designing all columns as hinged, a large number of graphs still would be needed. Furthermore, the computations necessary for obtaining an ultimate load graph are extremely tedious. Thus, with the exception of unusual cases in which the additional effort required for an accurate analysis is warranted, it is desirable to have a simpler method even if it is less accurate. Such a method may be devised by neglecting the effects of less important variables and by approximating the effects of the most important variables.

---

[8] "De Curvis Elasticis, Additamentum I, Methodus Inveniendi Lineas Curvas Maximi Minimive Proprietate Gaudentes," by L. Euler, Lausanne and Geneva, 1744, p. 267.

[9] "Ueber die Knickfestigkeit gerader Stabe," by F. Engesser, Zeitschrift d. Arch.-u. Ing., Ver. zu Hannover, Vol. 33, 1889, p. 455.

[10] "Untersuchungen uber Knickfestigkeit," by T. Von Karman, Mitteilungen uber Forschungsarbeiten auf dem Gabiete des Ingenieurwesens, No. 81, Berlin, 1910.

[11] "Strength of Steel Columns," by H. M. Westergaard and W. R. Osgood, Transactions, ASME, Vol. 50, 1928, p. 65.

[12] "A Study of Combined Bending and Axial Load in Reinforced Concrete Members," by E. Hognestad, Bulletin, Univ. of illinois Engrg. Sta., No. 399, Urbana, 1951. Also published as Bulletin No. 1 of the Reinforced Concrete Research Council of the Engrg. Foundation.

The curves in Fig. 1 show that the ultimate strength of a reinforced concrete column is affected substantially by the slenderness ratio l/d, the eccentricity ratio e/d, and the degree of end restraint $\alpha/f''_c\, b\, d^2$. The curves in Fig. 2 show that the strength of concrete f'_c and the percentage of reinforcement, p, also have important effects on the ultimate load. Furthermore, the first paper of this symposium has shown that the ultimate load varies significantly with the ratio of end eccentricities, and it is believed that the ratio of end restraints may also be significant (see second paper of symposium).

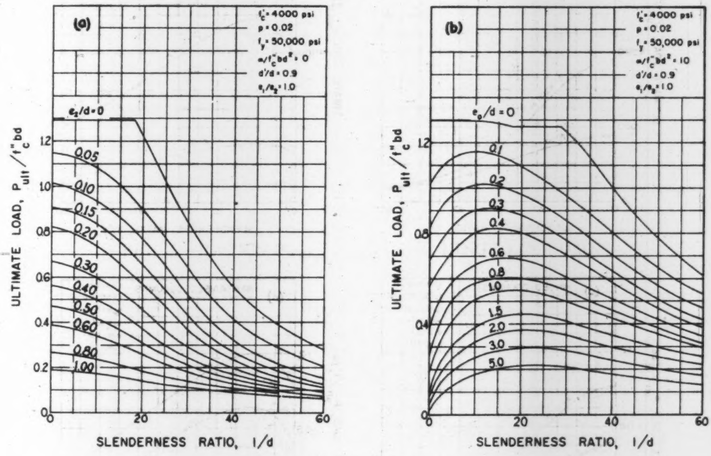

FIG. 1.—ULTIMATE LOAD GRAPHS

Accordingly, any approximate procedure for computing the ultimate load capacity of a long reinforced concrete column has to account for the effects of a large number of important variables.

A study of the ultimate loads shows that some of the significant variables have a similar effect on the strength of short and long columns. This is illustrated in Figs. 3 and 4 for hinged and restrained columns, respectively. Taking the theoretical ultimate load for l/d = 0 as the strength of a short column P_{short}, the ratios P_{long}/P_{short} in Figs. 3 and 4 show that, for the selected combinations of variables, the effects of f'_c, f_y, p and duration of loading do not vary greatly for the practical ranges of values. The variation of P_{long}/P_{short} with e/d is also small for hinged columns. Thus, if the strength of a long column is expressed as the product of the short column strength and of a reduction coefficient, the reduction coefficient has to account only for the effects of l/d, ratio of end eccentricities e_1/e_2 and end restraints. The other variables are accounted for in the expressions for the strength of short columns.

Restrained Versus Hinged Columns.—A comparison between the ultimate strength of hinged and restrained columns can be based on the eccentricities determined from the fixed end moments, from the moments at failure or from the moments determined by an elastic analysis.

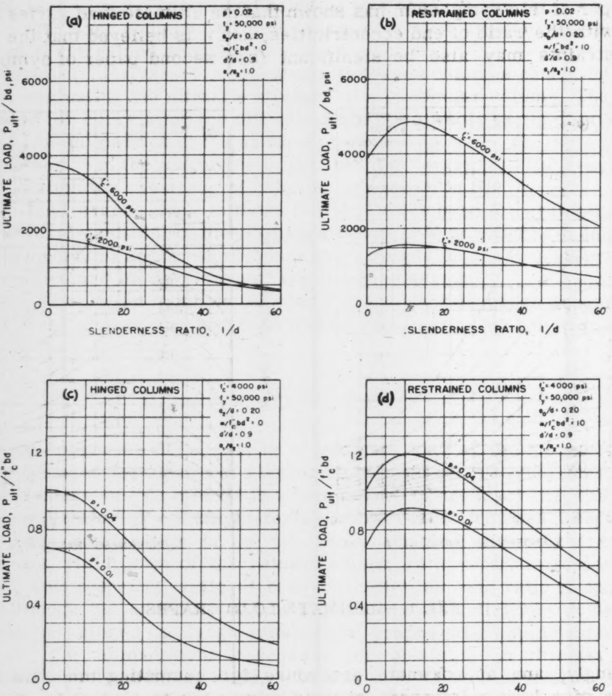

FIG. 2.—EFFECTS OF VARIABLES ON ULTIMATE LOADS

A comparison based on the eccentricity determined from the fixed end moments can be made on the basis of ultimate load graphs. A comparison based on the eccentricity at failure is impractical because such an eccentricity depends on the relative stiffness of columns and beams. The stiffness of beams is approximately constant and independent of the loading conditions, but the stiffness of the column varies with the magnitude of moment and load.

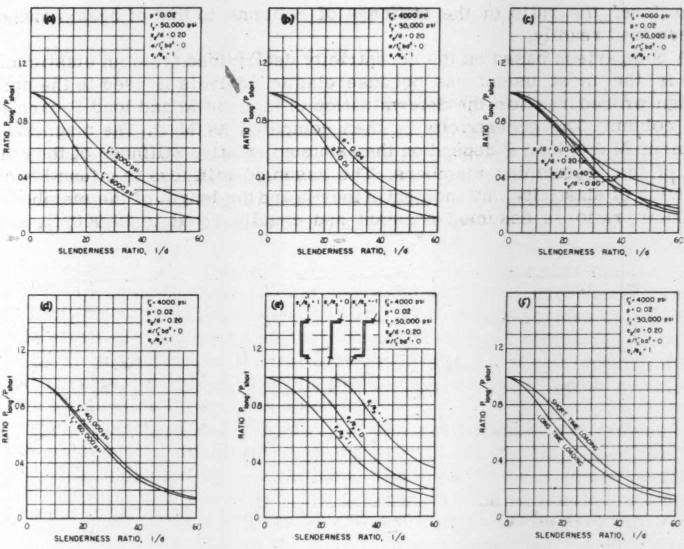

FIG. 3.—RATIOS P_{long}/P_{short} FOR HINGED COLUMNS

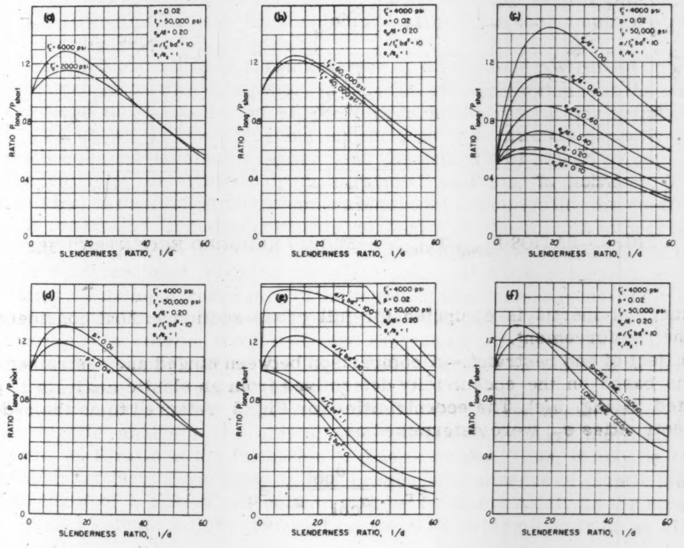

FIG. 4.—RATIOS P_{long}/P_{short} FOR RESTRAINED COLUMNS

Therefore, the ratio of the stiffness of columns to that of beams cannot be determined readily.

A comparison based on the eccentricity determined from an elastic analysis is the most useful one because elastic analysis is used in the current design procedures for the determination of moment M and load P carried by the column. The eccentricity is then computed as M/P. The magnitudes of moment M and load P depend on the assumed relative stiffness of the column and of the restraining members. The assumed stiffness is a function of the modulus of elasticity, the moment of inertia and the length of the member. The modular ratio is assumed constant and usually equal to $30{,}000/f'_c$, and the moment of inertia is computed for full cross-section without consideration of the reinforcement.

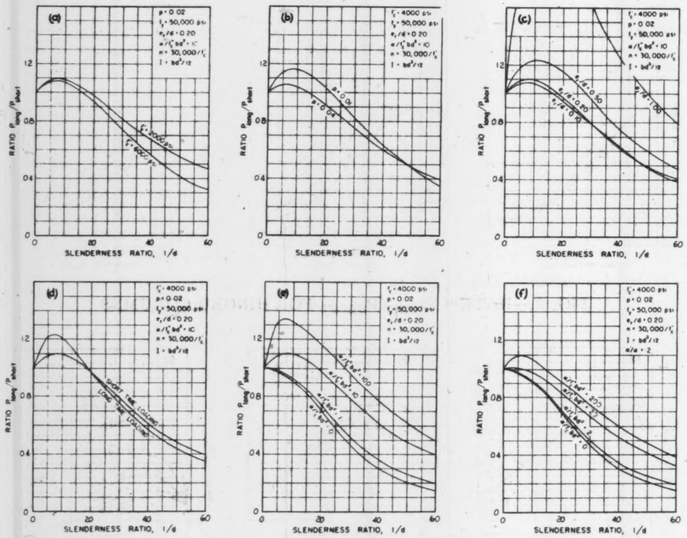

FIG. 5.—RATIOS P_{long}/P_{short} BASED ON REDUCED ECCENTRICITIES

Effect of end restraint.—A comparison between hinged and restrained columns based on the eccentricity determined from an elastic analysis is presented in Fig. 5(e). The eccentricities for Fig. 5, referred to as the reduced eccentricities e_r, were determined as

$$e_r = \frac{\alpha_{col}}{\alpha_{col} + \alpha} \; e_o \quad \text{. . . . .} \quad (1)$$

in which e_r refers to the reduced eccentricity determined by elastic analysis, e_o is the initial eccentricity based on fixed end moment $\alpha_{col} = \frac{2\ E\ I}{l} = \frac{196.2\ f''_c\ b\ d^3}{l}$, column stiffness, and α is the assumed coefficient of end restraint. (For the usual design assumptions $EI = 83.33\ f'_c\ b\ d^3$; and $f''_c = 0.85\ f'_c$.) The corresponding ultimate loads were then found in the corresponding graphs of ultimate loads for restrained columns. (See paper two of this symposium.)

It can be seen in Fig. 5(e) that the reduction of strength decreases with increasing coefficient of end restraint. Accordingly, if the chosen coefficient of end restraint is equal to the actual one existing in the structure, the ultimate strength of a restrained column is always higher than the strength of the corresponding hinged column computed with the reduced eccentricity.

In addition to the effect of end restraint, Fig. 5 also includes curves showing the effect of concrete strength, percentage of reinforcement, eccentricity ratio e_r/d, and creep on the ratio of P_{long}/P_{short}. It can be seen, that for practical ranges of values, all of these effects are small. The only exceptions are the e_r/d ratios larger than about 0.5.

Error in assumed end restraint.—If the coefficient of end restraint used in the calculations is larger than the actual one, the restrained column is weaker than indicated by calculations. The error in the assumed coefficient of end restraint may come from two sources: (1) The estimation of the stiffness of the restraining members, (2) the cosine-wave assumption with respect to the rotations at the ends of the column in an elastic analysis. The effect of an error in the assumed end restraint on the reduction coefficient is shown in Fig. 5(f). It is assumed in this figure that the estimated coefficient of end restraint is twice the actual value. It can be seen that even in this case the ultimate strength of a restrained column is higher than the computed strength of the corresponding hinged column.

Effect of plastic hinges.—The analyses of strength of restrained columns, used in connection with this paper, is based on the assumption that the column fails before the formation of plastic hinges in the restraining members. It has been shown in the preceding subsections that ultimate capacity of restrained columns is always higher than the strength of hinged columns with the eccentricity determined from an elastic analysis. If, however, plastic hinges form in the restraining members before the column fails, the coefficient of end restraint and the ultimate strength of the column is decreased.

Plastic hinges form in the restraining members when the stress in the tensile reinforcement reaches the yield point. At further increases of end rotations the moment resistance of the restraining members remains approximately constant: thus plastic hinges in the restraining members change the behavior of the column from that of a restrained column to that of a hinged column. The eccentricity of the load is equal to M/P in which M is the moment resistance of the plastic hinge.

It can be shown that in reinforced concrete structures designed according to an elastic analysis the elastic M/P ratio usually is not much different from the M/P ratio at the formation of plastic hinges. Thus, it may be stated in conclusion that, regardless of the presence or absence of plastic hinges, the strength of a restrained column may be evaluated safely as the strength of a hinged column with the reduced eccentricity determined from an elastic analysis.

Approximate Reduction of Strength Caused by Slenderness.—It has been shown in the previous section that it is safe to evaluate the strength of a restrained column as the strength of a corresponding hinged column. Neglecting the effects of end restraints permits a further simplification of the reduction coefficient; it needs to be expressed only as a function of the slenderness ratio l/d and of the ratio of end eccentricities e_1/e_2.

The reduction of the strength with increasing slenderness is shown in Fig. 3(f) for short and long time loading of columns having concrete strength of 4000 psi, the ratio of reinforcement of 0.02, the yield point of steel of 50,000 psi and the eccentricity ratio of 0.20. The parameters were chosen so as to give the largest reduction of column strength which is apt to be encountered in the design. The design reduction coefficient is based on the dashed line approximating the theoretical curve for long time loading in Fig. 3(f).

If the computations of the ultimate strength of eccentrically loaded columns are based on the initial eccentricity, the strength is reduced even for very short columns. It can be seen in Fig. 3(f) that for slenderness ratio $l/d = 5$ the ultimate strength is equal to 95% of the theoretical value for $l/d = 0$ and for slenderness ratio $l/d = 10$ the ultimate strength is decreased to 84%. If then, it is desired to design columns for slenderness ratios equal to or smaller than 10 on the basis of the initial eccentricity and the short column strength, the equations for the short column strength should be based on the theoretical strength of columns with $l/d = 10$. This is indicated in Fig. 3(f) by the horizontal dashed line at $P_{long}/P_{short} = 0.84$.

For columns with l/d larger than 10, the decrease of the ultimate strength may be accounted for as is indicated in Fig. 3(f) by the sloping dashed line. Because the value of the reduction coefficient for columns with $l/d = 0 - 10$ should be equal to 1.0, the equation of sloping dashed line is

$$\frac{P_{long}}{P_{short}} = 1.0 - 0.03a \leqq 1.0 \quad \ldots\ldots\ldots\ldots (2)$$

in which a is a dimensionless parameter accounting for the effects of slenderness ratio and the ratio of end eccentricities. The dashed line, representing the case of equal end eccentricities, corresponds to $a = (l/d) - 10$.

It can be seen in Fig. 3(e) that the case of equal end eccentricities requires the largest reduction. The P_{long}/P_{short} curves for various e_1/e_2 ratios may be approximated by parallel straight lines. The distance between the straight lines is a function of the ratio e_1/e_2 and of the ratio e_2/d. Neglecting the effect of e_2/d, the following value of the dimensionless parameter gives a safe value of the ratio P_{long}/P_{short}:

$$a = \frac{l}{a} - 15 + 5\,\frac{e_1}{e_2} \quad \ldots\ldots\ldots\ldots\ldots\ldots (3)$$

Combining Eqs. 2 and 3, the reduction coefficient for the design of eccentrically loaded slender reinforced concrete columns may be written in the following form:

$$\frac{P_{long}}{P_{short}} = 1.45 - 0.03\,\frac{l}{d} - 0.15\,\frac{e_1}{e_2} \leqq 1.0 \quad \ldots\ldots (4)$$

in which P_{long} refers to the ultimate strength of a long eccentrically loaded column, P_{short} denotes the ultimate strength of the corresponding short column, l is the length of column, d is the total depth of column, e_1 denotes numerically smaller end eccentricity, and e_2 refers to numerically larger end eccentricity.

It should be noted that for columns with equal end eccentricities, that is, $e_1/e_2 = 1.0$, the reduction coefficient given by Eq. 4 is:

$$\frac{P_{long}}{P_{short}} = 1.3 - 0.03 \frac{l}{d} \quad \ldots\ldots\ldots\ldots\ldots \quad (5)$$

that is identical with the reduction coefficient given in the current ACI Building Code.[7]

The range of short columns may be obtained from Eq. 4 by placing $P_{long}/P_{short} = 1.0$. It can be seen that this range increases with decreasing ratio of end eccentricities. For equal end eccentricities, the range is the same as given by the current ACI Building Code,[7] that is, up to $l/d = 10$ no reduction is required due to slenderness. For $e_1/e_2 = 0$, the upper limit for short columns is $l/d = 15$ and for equal and opposite eccentricities it is $l/d = 20$.

Eq. 2 may be used for concentrically loaded columns after placing $e_1/e_2 = 1.0$.

Effect of Transverse Loading.—If one or more transverse loads are applied to the column, the maximum moment is increased and the buckling strength is decreased. Comparisons of the theoretical ultimate loads with tests of columns subjected to combinations of an axial and a transverse load applied at mid-depth[1] indicated that it is sufficiently accurate to compute the strength of such columns as for eccentrically loaded equivalent columns. The equivalent column has the same dimensions as the original one but it is subjected to eccentric load equal in magnitude to the axial load and causing the same maximum moment as the transverse load.

For a single concentrated transverse load H applied at mid-depth, the equivalent eccentricities are the same at both column ends and are equal to:

$$e = \frac{H\ l}{4\ P} \quad \ldots\ldots\ldots\ldots\ldots\ldots\ldots \quad (6)$$

in which e refers to equivalent eccentricity, H is the transverse load applied at mid-depth, and P is the axial load.

DESIGN PROCEDURES

Two approximate design methods are presented in this section. One is a working load procedure and the other an ultimate load procedure. In both methods the column load is computed as the product of the short column load and the reduction coefficient given by Eq. 4 with the end eccentricities determined from an elastic analysis of the structure.

Working Load Design.—The allowable load for short reinforced concrete columns may be computed from formulas in Sections 1103, 1104, and 1109 of the current ACI Building Code.[7] The allowable load for a long column may be obtained by multiplying the allowable load for the corresponding short column by the reduction coefficient given by Eq. 4. It should be noted that for columns with equal end eccentricities, including the axially loaded columns, this procedure is identical with that in Section 1107 of the current ACI Building Code.[7] The only difference is the absence of a limit on slenderness for eccentrically loaded columns discussed in the later portion of this paper. For columns with unequal eccentricities, the procedure presented herein is less conservative than that in the current ACI Building Code.

The working load procedure is compared with the ultimate test loads for 46 concentrically and 79 eccentrically loaded hinged columns in Fig. 6 and in Tables 1 and 2. The test data are the same as those discussed and summarized in connection with the theoretical analysis of hinged columns in the first paper of this symposium.

The ratios of the test to the design load, given in Tables 1 and 2 and plotted in Fig. 6 as functions of the slenderness, represent the actual factors of safety. It can be seen that for any one value of the slenderness, the factor of safety varies considerably and is consistently higher for concentric loading. The smallest ratios P_{test}/P_{des} are 1.51, 1.85, and 1.96. All of these correspond to the e/d = 0.666. All other factors of safety exceed the value of 2.0. They increase consistently as e/d decreases. For e/d= 0.833, the only eccentricity higher than 0.666, the factor of safety varies from 2.59 to 3.58. All of these variations are caused primarily by the formulas used for computing the allowable load on the short column.

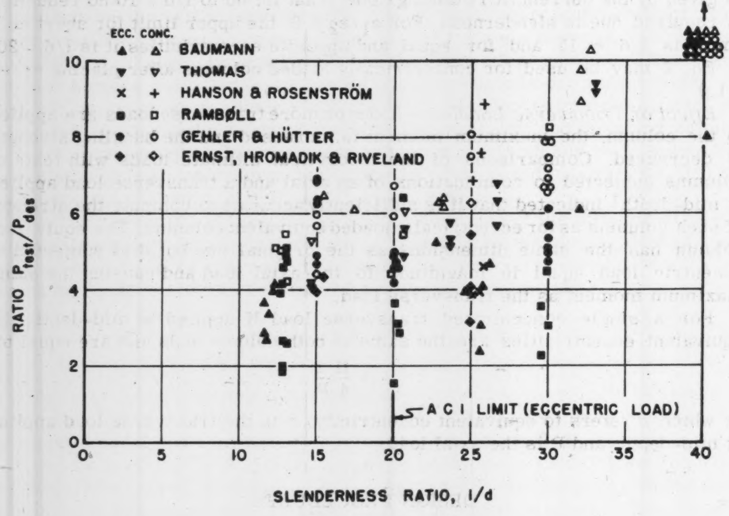

FIG. 6.—COMPARISON OF WORKING LOAD DESIGN PROCEDURE WITH TEST DATA

The effect of the slenderness on the factor of safety can be seen in Fig. 6 for the test columns and the theoretical effect is shown in Fig. 7. In the range of l/d = 10 - 25 the effect is small and beyond l/d = 30 the factors of safety increase very rapidly. This is because the reduction coefficient is a straight line equal to zero at l/d = 43.3. (For $e_1/e_2 = 1.0$ for unequal end eccentricities this value is higher.)

TABLE 1.—CONCENTRICALLY LOADED COLUMNS

Specimen	Slenderness l/d	Working Load P_{test}/P_{des}	Ultimate Load P_{test}/P_{ult}
Baumann, 1930-1933 (14)[a]			
I	32.1	8.90	2.19
III	22.9	6.28	1.54
V	23.3	6.15	1.49
Va	23.2	6.38	1.55
VI	32.7	10.27	2.44
VIa	32.1	9.73	2.30
VIII	17.5	6.08	1.43
VIIIa	15.5	6.44	1.51
3	40.7	31.06	6.81
15	40.4	19.72	4.44
Thomas, 1938 (17)			
LC1	14.7	5.28	1.28
LC2	20.7	6.03	1.44
Hanson and Rosenström, 1945-46 (18)			
1a	25.8	8.85	1.98
2a	25.6	7.57	1.70
3a	25.1	6.82	1.51
Rambøll, 1949-50 (19)			
13	13.0	4.18	0.93
14	13.0	5.42	1.22
15	12.6	5.04	1.13
16	12.7	5.03	1.13
27	20.6	5.41	1.22
28	19.9	4.40	0.98
33	30.1	8.27	1.85
Gehler and Hütter, 1940-42 & 1951-52 (20)			
Ia	40.0	21.73	5.98
		23.23	5.32
Ib	30.0	7.86	1.70
		7.86	1.76
Ic	25.0	7.50	1.69
		8.05	1.82
Id	20.0	5.91	1.34
		6.70	1.52
Ie	15.0	5.96	1.35
		5.67	1.28
IIa	40.0	19.29	4.90
		20.68	5.25
2	40.0	13.33	3.14
		17.38	4.09
3	40.0	15.15	3.99
		13.26	3.50
4	30.0	7.44	1.68
		7.16	1.62
5	30.0	6.57	1.45
		6.90	1.53
6	30.0	6.68	1.47
		6.68	1.47
Ernst, Hromadik and Riveland, 1952 (15)			
1	15.0	4.38	1.02
2	25.0	6.24	1.45

[a] Numbers in parenthesis refer to corresponding numbers in Bibliography of first paper of this symposium.

TABLE 2.—ECCENTRICALLY LOADED COLUMNS

Specimen	Slenderness l/d	Eccentricity Ratio e_2/d	Working Load P_{test}/P_{des}	Ultimate Load	P_{test}/P_{ult}
				Eq.	Eq.
Baumann, 1930-1933 (14)[a]					
Ia	32.1	0.083	6.09	1.57	1.51
IIIa	22.8	0.083	5.20	1.33	1.28
4	12.0	0.166	3.34	0.88	0.80
5	25.9	0.166	4.64	1.24	1.09
6	40.7	0.166	14.58	4.07	3.57
7	11.7	0.166	3.68	0.98	0.90
8	25.7	0.166	4.04	1.07	0.95
9	40.2	0.166	15.21	3.94	3.55
10	11.7	0.333	2.81	0.77[b]	0.69
11	25.7	0.333	3.03	0.89[b]	0.75
12	40.2	0.333	8.00	2.16[b]	1.86
13	11.8	0.333	2.68	0.75	0.66
14	25.7	0.333	2.37	0.69[b]	0.58
19	24.7	0.166	3.94	1.05	0.94
26	12.6	0.166	4.12	1.10	0.98
32	12.6	0.166	3.95	1.04	0.96
Thomas, 1938 (17)					
LC3	23.7	0.005	5.31	1.31	1.29
LC4	26.7	0.005	6.31	1.54	1.52
LC8	14.7	0.027	4.05	1.02	1.00
LC7	20.7	0.037	4.84	1.21	1.18
LC6	23.7	0.042	5.12	1.29	1.25
LC5	26.7	0.047	6.75	1.71	1.66
LC12	14.7	0.027	4.15	1.04	1.02
LC11	20.7	0.037	5.60	1.42	1.39
LC10	23.7	0.042	5.74	1.47	1.43
LC9R	26.7	0.017	5.66	1.42	1.39
PLC1	33.1	0.056	9.39	2.37	1.80
PLC2	33.1	0.056	9.15	2.30	1.76
Hanson and Rosenström, 1945-46 (18)					
1b	25.8	0.166	4.60	1.28	1.15
2b	25.6	0.166	3.94	1.12	0.98
3b	25.1	0.166	3.86	1.12	0.95
Rambøll, 1949-1950 (19)					
17	13.0	0.083	4.85	1.24	1.18
18	12.8	0.083	4.57	1.17	1.12
19	13.0	0.166	4.76	1.33	1.23
20	12.9	0.166	5.07	1.40	1.30
21	12.7	0.333	3.90	1.13*	1.07
22	12.8	0.333	4.11	1.19*	1.12
23	12.8	0.666	1.85	1.28*	1.28*
24	12.8	0.666	1.96	1.30*	1.30*
25	12.8	0.833	2.63	1.44*	1.44*
26	13.1	0.833	2.59	1.48*	1.48*
29	20.1	0.166	3.62	1.00	0.93
30	20.3	0.333	3.06	0.90*	0.83
31	20.1	0.666	1.51	1.21*	1.21*
32	20.4	0.833	2.86	1.62*	1.62*
34	20.6	0.083	6.40	1.62	1.54
35	29.9	0.166	4.47	1.23	1.15
36	30.1	0.666	3.02	0.89*	0.82

TABLE 2.—*CONTINUED*

37	29.6	0.333	2.27	1.70*	1.70*
38	29.6	0.833	3.58	1.95*	1.95*
Gehler and Hütter, 1951-1952 (20)					
7	15.0	0.0376	4.89	1.21	1.18
			4.63	1.15	1.12
8	20.0	0.051	4.91	1.21	1.16
			4.56	1.12	1.08
9	30.0	0.075	6.11	1.54	1.47
			5.69	1.43	1.37
10	40.0	0.101	20.20	3.74	3.56
			22.00	4.07	3.88
11	15.0	0.075	6.34	1.18	1.13
			6.88	1.28	1.23
12	20.0	0.101	4.51	1.15	1.08
			4.60	1.17	1.10
13	30.0	0.150	4.99	1.30	1.21
			5.07	1.32	1.23
14	40.0	0.201	16.11	4.26	4.03
			14.44	3.82	3.61
15	15.0	0.113	6.25	1.21	1.15
			6.82	1.32	1.25
16	20.0	0.152	4.18	1.10	1.04
			4.85	1.28	1.21
17	30.0	0.225	5.36	1.44	1.32
			4.75	1.27	1.17
18	40.0	0.302	15.67	4.20	3.85
			15.07	4.04	3.70
Ernst, Hromadik and Riveland, 1952 (15)					
7	15.0	0.125	4.31	1.14	1.06
8	25.0	0.125	5.41	1.43	1.34
11	15.0	0.250	3.93	1.12	1.01
12	25.0	0.250	4.01	1.15	1.04
13	25.0	0.375	3.14	0.93	0.83

[a] Numbers in parenthesis refer to corresponding numbers in bibliography of first paper of this symposium.

[b] Tension equation governs; in all other cases compression equations govern the computed load.

The factor of safety for columns may be compared with the factor of safety for beams shown in Fig. 7 as a horizontal dashed line. For steel with a yield point of 50,000 psi the allowable unit stress is 20,000 psi and the factor of safety for beams is approximately 2.5. It can be seen in Fig. 7 that the factor of safety is higher for columns than for beams as long as the eccentricity ratio e/d is smaller than 0.7. Thus, the procedure presented herein must be limited to eccentricity ratios smaller than or equal to 0.7. This limit is approximately the same as that included in the current ACI Building Code.[7]

Ultimate Load Design.—For very short columns, that is, columns with the maximum eccentricity at failure equal to the initial eccentricity, the ultimate strength may be computed from Eqs. A7 through A13 in the Appendix of the ACI Building Code.[7] If, however, the maximum eccentricity at failure is larger than the initial eccentricity, the short column strength is reduced. For

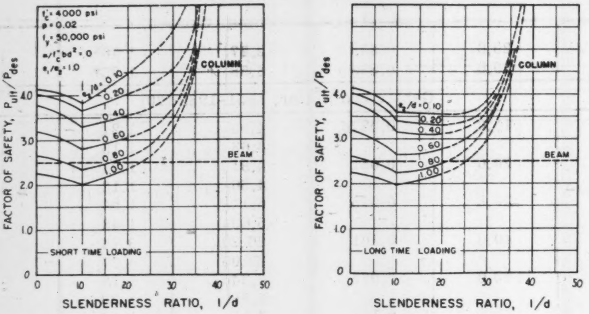

FIG. 7.—VARIATION OF FACTOR OF SAFETY FOR WORKING LOAD DESIGN

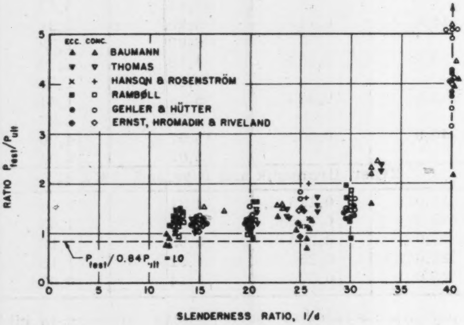

FIG. 8.—COMPARISON OF ULTIMATE LOAD DESIGN PROCEDURE WITH TEST DATA

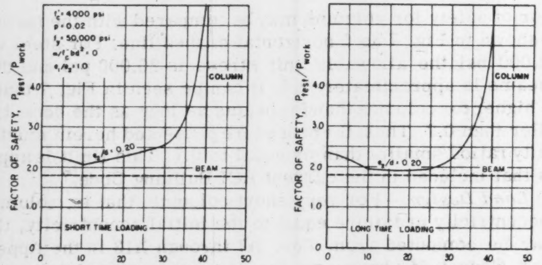

FIG. 9.—VARIATION OF FACTOR OF SAFETY FOR ULTIMATE LOAD DESIGN

slenderness ratios not exceeding $l/d = 15 - 5\left(e_1/e_2\right)$, the column strength may be computed safely as the product of the value given by the Eqs. A7 through A13 and 0.84. The ultimate strength of long columns may then be computed as the product of the value given by Eqs. A7 through A13 quoted above, of 0.84 and of the reduction coefficient given by Eq. 4 in this paper.

The numerical reduction factor 0.84 accounts for the effect of the increase of the eccentricity due to lateral deflections. Because deflections cause some decrease of the ultimate strength in most short columns, it is logical and most convenient to include the factor 0.84 into the load factor for column loads. In other words, if the design of short columns is based on the initial eccentricity, the load factor for columns should be larger than that for beams. Furthermore, a higher load factor is desirable for columns also because of the differences in modes of failure. A 10% increase is considered satisfactory for this purpose. Thus, for a design based on the initial eccentricity and the ultimate strength equations not accounting for the deflections caused by load, the load factor for columns should be approximately 30% higher than for beams.

The ultimate strength of members designed according to the provisions of the Appendix to the ACI Building Code[7] is governed by the following load factor equations: (Eqs. 7 are applicable when effects of wind and earthquake loading can be properly neglected.)

$$U = 1.2\ B + 2.4\ L \quad \dots\dots\dots\dots\dots (7a)$$

$$U = K\ (B + L) \quad \dots\dots\dots\dots\dots (7b)$$

in which U is the ultimate strength capacity of section, B refers to effect of basic load consisting of dead load plus volume change due to creep, elastic action, shrinkage, and temperature, L denotes the effect of live load plus impact, and K is the load factor equal to 2 for columns and members subjected to combined bending and axial load and equal to 1.8 for beams and girders subjected to bending only. For the loading conditions given by Eq. 7(a), the load factor is the same for columns and for beams. For the loading conditions given by Eq. 7(b), the load factor for columns is approximately 11% higher than for beams.

It has been pointed out that for a design based on initial eccentricity the load factors governing the design of columns should be 30% higher than the load factors for beams. The following load factor equations satisfy this requirement:

$$U = K\ (1.2\ B + 2.4\ L) \quad \dots\dots\dots\dots\dots (8a)$$

$$U = 1.8\ K\ (B + L) \quad \dots\dots\dots\dots\dots (8b)$$

in which K is the numerical factor equal to 1.3 for columns and members subjected to combined bending and axial load, and equal to 1.0 for beams and girders subjected to bending only.

The ultimate strength of short columns $\left[l/d = 15 - 5\left(e_1/e_2\right)\right]$ designed with the aid of the load factor Eq. 8 may be computed safely from Eqs. A7 through A13 and the initial eccentricity. The ultimate strength of long columns may then be computed as the product of the short column strength and the reduction coefficient given by Eq. 4.

Computed ultimate loads are compared with test results in Fig. 8 and in Tables 1 and 2. The computed ultimate loads were determined as the product of the short column strength and the reduction coefficient given by Eq. 4. The short column strength of concentrically loaded columns was determined from Eq. A6. The short column strength of eccentrically loaded columns was determined by both alternate procedures given in the Appendix to the ACI Building Code: (1) from Eqs. A7 through A10 and (2) from Eqs. A7 through A9 and A11. Fig. 8 is based on the first procedure.

It can be seen in Fig. 8 that for most columns with l/d ratio smaller than 30 the test values of ultimate load are between 0.84 and 1.5 times the computed value. Only three columns fall below the dotted line representing the load ratio of 0.84 and none exceeds the value of 2.0. This relatively narrow range of values is in sharp contrast with the wide scatter in a similar comparison for working load design shown in Fig. 6.

It has been pointed out in the preceding text that the ultimate strength of short columns may be computed safely with the initial eccentricity as the

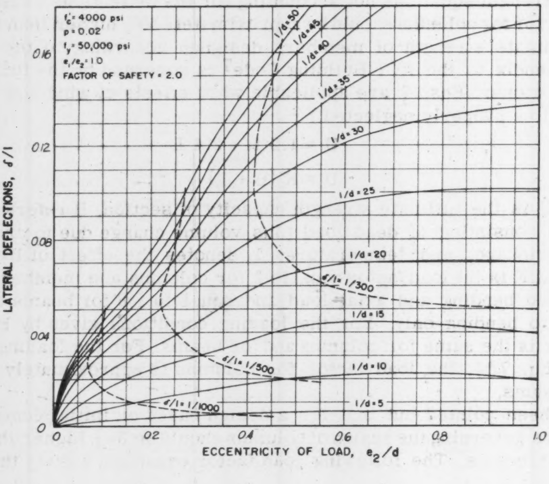

FIG. 10.—THEORETICAL DEFLECTIONS OF HINGED COLUMNS AT WORKING LOADS

product of the ultimate strength Eqs. A7 through A11 in the Appendix to the ACI Building Code[7] and 0.84. The points below the dashed line in Fig. 8 represent columns that failed at a load lower than the computed one. It can be seen in Fig. 8 that only three columns failed at a load lower than the one computed by this procedure.

If, however, the factor 0.84 is not included in the design computations, the points in Fig. 8 located below P_{test}/P_{ult} = 1.0 represent columns that failed at a load lower than the calculated one. An inspection of Fig. 8 and of the last two columns in Table 2 shows that P_{test}/P_{ult} is smaller than 1.0 fairly frequently especially if the short column strength is computed from Eqs. A7 through A9 and A11 (last column in Table 2).

Similarly as the working load design, the load ratio is almost unaffected by the slenderness in the range of 10 to 25 but increases sharply with slenderness for l/d larger than 30. Accordingly, the safety factor, computed as the ratio of the theoretical ultimate load for a hinged column to the working load (B + L), also increases rapidly beyond l/d larger than 30. (The working loads (B + L) were computed from Eq. 8(b) taking the ultimate strength capacity of the section, U, as the product of Eqs. A7 through A10, 0.84 and the reduction coefficient given by Eq. 4.) This is illustrated in Fig. 9 for one set of design conditions; only the eccentricity ratio $e_2/d = 0.20$ is shown, because the variation of the factor of safety with the eccentricity ratio e_2/d is small. Fig. 9 includes also a horizontal dashed line representing the factor of safety for beams.

Deflections.—The design procedures presented in the preceding sections are based on the consideration of the ultimate strength and are, therefore, safe from the standpoint of load capacity. However, proper functioning of a column does not depend necessarily on the strength only. Excessive deflections at working loads may also limit the usefulness of an eccentrically loaded column.

Lateral column deflections increase with the slenderness ratio and eccentricity as is shown in Fig. 10 for hinged columns subjected to short time loading. It can be seen that for the set of conditions chosen for Fig. 10, combinations of large slenderness ratios and large eccentricities may result in working load deflections in excess of the tolerable magnitude. It should be noted, however, that the curves in Fig. 10 are theoretical values for hinged columns based on a factor of safety of 2.0. Because reinforced concrete columns are always restrained at the ends and since the end restraints are certainly effective at working loads, the actual deflections are substantially smaller than those shown in Fig. 10. Furthermore, for large slenderness the factor of safety increases rapidly above the nominal value. Thus, in usual applications excessive deflections are unlikely so that no limitations are necessary on either the slenderness ratio of the column or on the eccentricity of the load.

CONCLUSIONS

(1) The simplified design procedure for long reinforced concrete columns presented in this paper was developed on the basis of theoretical analysis of the strength of hinged and restrained columns subjected to concentric and eccentric loads.

(2) The simplified design procedure involves the short column strength, the eccentricity of load computed by an elastic analysis and a reduction coefficient. It may be used both with a working load design and with an ultimate load design.

(3) The proposed reduction coefficient is based on the strength of hinged columns. It accounts for the effects of slenderness ratio and the ratio of end eccentricities. For columns with equal end eccentricities it is the same as the reduction coefficient included in the current ACI Building Code,[7] but it calls for smaller reductions in columns with unequal end eccentricities.

(4) The limit of l/d = 20 for eccentrically loaded columns included in the current ACI Building Code[7] does not appear necessary.

(5) The proposed design procedure was checked against the test data for 125 concentrically and eccentrically loaded columns and was found to give safe designs.

APPENDIX.—NOTATION

The following symbols have been adopted for use in this paper:

A_s = total area of longitudinal column reinforcement;

a = dimensionless parameter;

B = effect of basic load consisting of dead load plus volume change due to creep, elastic action, shrinkage, and temperature;

b = width of column cross-section;

d = overall depth of column cross-section;

d' = effective depth of reinforcement;

E = modulus of elasticity of concrete;

e = end eccentricity for columns with $e_1 = e_2$;

e_1, e_2 = end eccentricities of load; e_2 is the larger of the two values and is always taken as a positive quantity;

e_o = initial end eccentricity of load in a restrained column;

e_r = reduced eccentricity determined by an elastic analysis;

f'_c = compressive strength of 6 by 12-in. concrete cylinders;

f''_c = compressive strength of concrete in flexure;

f_y = yield point of reinforcement;

H = transverse load applied at mid-depth of column;

I = moment of inertia of column cross-section;

K = load factor;

L = effect of live load plus impact;

l = length of column;

M = bending moment;

n = modular ratio;

P = applied column load;

P_{des} = design column load for working load design;

P_{long} = ultimate strength of long column;

P_{short} = ultimate strength of short column;

P_{test} = ultimate strength of a column determined by test;

P_{ult} = computed ultimate strength of a column;

P_{work} = working load for a column designed by the ultimate load procedure;

p = A_s/bd; ratio of reinforcement;

U = ultimate strength capacity of the section;

α = assumed coefficient of end restraint;

α_{col} = column stiffness; and

δ = maximum lateral deflection.

DISCUSSION

J. G. MAC GREGOR,[13] A. M. ASCE and C. P. SIESS,[14] F. ASCE.—The authors are to be commended on the large amount of excellent work represented by their series of three papers on long reinforced concrete columns. The range of the variables studied shows the effect of every practical variable.

Material Failures.—If an analysis similar to that described by Clark, Sidebottom, and Shreves[15] is used to determine the long column strength, the distinction between material failures and instability failures becomes more evident. Fig. 11 shows a family of moment-load curves constructed for hinged-end columns of various l/d ratios and with $e_1/e_2 = +1$. These curves relate axial load at any stage of loading to the maximum moment occurring in the column at the same load (at the section of maximum deflection). If this curve passes through a maximum, the column under consideration will fail initially by inelastic instability that leads in turn to material failure as shown by the dashed lines. If the moment-load curve intersects the interaction curve before reaching a maximum, as it does for $l/d = 5$, the column will fail by material failures. The long column curves obtained by this method agree with those published in Fig. 3.

Column Tests.—In a report[16] published by the American Society of Civil Engineers (ASCE), ratios of test strength to computed strength are reported for 185 eccentrically loaded columns. The computed strengths are based on the actual failure eccentricity at the section of failure. The average ratio of test to computed strength using the final eccentricity for all 185 columns is 0.98. However, when the strength is computed on the basis of initial eccentricity, it is only 0.94 for the 114 columns tested by Hognestad and only 0.89 for all 185 columns reported. This emphasizes the fact that there is a reduction in the strength of columns with an l/d as small as 7.5.

---

[13] Asst. Prof. of Civ. Engrg., Univ. of Alberta, Edmonton, Alta, Canada; formerly, Research Asst., Dept. of Civ. Engrg., Univ. of Illinois, Urbana, Ill.

[14] Research Assoc., Prof. of Civ. Engrg., Univ. of Illinois, Urbana, Ill.

[15] "Inelastic Analysis of Eccentrically Loaded Columns," by M. E. Clark, M. Sidebottom, and R. W. Shreeves, Proceedings, ASCE, Vol. 83, No. EM 4, October, 1957.

[16] "Report of ASCE-ACI Joint Committee on Ultimate Strength Design," Proceedings, ASCE, Vol. 81, No. 809, October, 1955.

Design Equations for Long Columns.—By ignoring end restraints in deriving a design equation, the authors are being justifiably conservative. In addition to the reasons listed by the authors, the following points also support this stand. The restrained column analysis developed in the second paper of this symposium takes into account all reductions in column stiffness under loading but assumes that the stiffness of the restraining members remains constant throughout the life of the column. In tests of rigid frames reported by F. E. Richart,[17] the EI of a flexural member at ultimate load under short-time loadings was about 0.4 times the EI of the uncracked section at working loads. This reduction was caused by cracking, plastic action in the compression zone, and so forth. Creep from sustained loading in the restraining members would further reduce their stiffness as would yielding of the reinforcement in these members. Each reduction in the stiffness of the restraining members brings the column action closer to that of a hinged-end column.

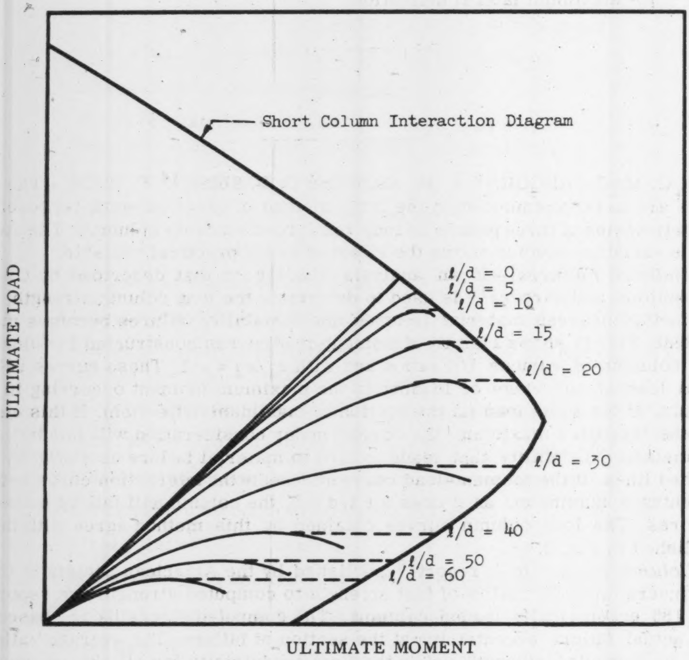

FIG. 11.—MOMENT LOAD CURVES FOR ECCENTRICALLY LOADED COLUMN OF A GIVEN INITIAL ECCENTRICITY (e/d = 0.2)

---

[17] "Tests of the Effect of Brackets in Reinforced Concrete Rigid Frames," by F. E. Richart, Journal of Research, Bur. of Standards, Vol. 1, No. 2, August, 1928, p. 189.

In developing a column design formula, the loading conditions expected in structures should be considered. Briefly, three types of column failures can be distinguished. First, the load and moment may be of short duration as is the case with wind loads. Second, and perhaps most common in practice, the column will be loaded to a certain percentage of its capacity under a sustained deadload, and then more or less rapidly loaded to failure. Third, the total applied load or moment also may be of long duration as in a warehouse.

The first loading condition corresponds to the short-time load analysis and also corresponds to the type of loading used in the column tests used to check the validity of the authors' design equations. The close check between the short-time load analysis for hinged-end columns and these column tests establishes the validity of the analysis used.

The second loading condition corresponds approximately to the assumptions made in the authors' long-time analysis. It has been assumed that sustained loadings cause the strains to double but do not affect the strength of the concrete in the column. This is the case for a column loaded with a sustained working load that is rapidly increased until the column fails, as was shown in the tests reported by Viest, R. Elstner, and E. Hognestad,[18] F. ASCE.

A design equation for long columns should apply, basically, to the case of a sustained working load rapidly increased until failure occurs but, when necessary, should be modified to take account of failure under sustained high loads. The validity of such a design formula can be checked only by comparing it to the results of tests on long columns loaded in this way. The writers know of no tests of eccentrically loaded long columns that involved sustained loading. A possible exception would be the column tests described by Viest, Elstner, and Hognestad in which the columns had an l/d of about 7.5 including the end blocks. Therefore, it is not possible to determine the accuracy of a proposed long-column design formula by comparing it to test results as has been done by the authors. Because the short-time load analysis checks closely with available test results and because the assumptions made to extend this analysis are reasonable and are based on experimental studies, the writers have accepted the long-time analysis in the authors' first paper as a valid analysis for the type of column loadings experienced in structures. Accordingly, the following reduction equation for long eccentrically loaded columns failing in compression under the usual types of loadings is proposed:

$$R = 1.20 - 0.025\left(\frac{l}{d}\right) - 0.13\,\frac{e_1}{e_2} \leqq 1 \quad \ldots\ldots\ldots\ldots \quad (9)$$

This equation was derived by fitting a line to the long-time load analysis shown in Fig. 3(f). It was also compared to an analysis made as mentioned above and based on the assumption that the ratio of total sustained-load strain to elastic strain is three. Eq. 9 and the curve from Broms and Viest's long-time load analysis are plotted in Fig. 12. For simplicity, only the curves for $e_1/e_2 = +1$ have been plotted in this figure. The close agreement between Eq. 9 and the curve from the long-time load analysis can be seen clearly.

Eq. 4, proposed by the authors, is also plotted in Fig. 12. This equation does not represent the behavior of a long column. The authors also recognized this and modified their equation by multiplying it by a factor of 0.84, representing the theoretical long-column strength reduction for l/d = 10. The resulting equation (Eq. 4 times 0.84) is:

---

[18] "Sustained Load Strength of Eccentrically Loaded Short Reinforced Concrete Columns," by I. M. Viest, R. Elstner, and E. Hognestad, Proceedings, ACI Journal, Vol. 52, March, 1956, p. 727.

$$R = 1.218 - 0.0252\left(\frac{l}{d}\right) - 0.126\,\frac{e_1}{e_2} \leqq 0.84 \quad \ldots\ldots\ldots (10)$$

Eq. 10 is also plotted in Fig. 12. For l/d greater than 10, Eq. 10 is almost identical with Eq. 9. As can be seen from Fig. 12 and Eqs. 9 and 10, the multiplying factor of 0.84 is actually an integral part of the long-column reduction formula, and as such we believe it should be included in the equation.

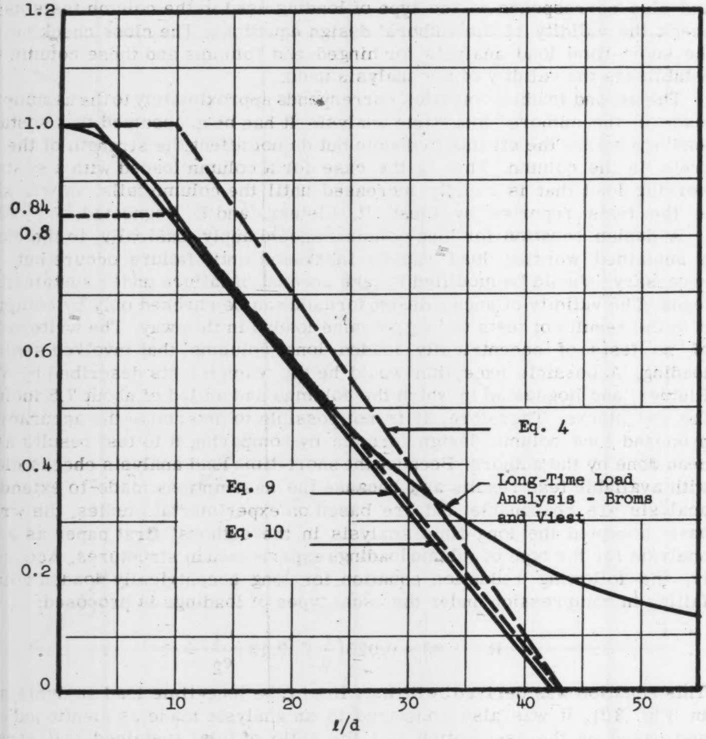

FIG. 12.—COMPARISON OF LONG-COLUMN EQUATIONS FOR $e_1/e_2 = +1$

Because the 0.84 term is actually a part of the required long-column formula, it cannot be considered as a part of the load factor. Thus, the actual load factor for columns that the authors propose for use in Eqs. 8(a) and 8(b) is K = 1.1 not 1.3 as stated in their paper. The use of Eq. 4 and the proposed load factor for columns leads one to the belief that column design is considerably more conservative than actually is the case.

The form of Eq. 10, that is, the upper limit at 0.84, tends to penalize short columns. Thus, columns of $l/d = 7$, 8 and 9 are required to have safety factors equal to 110%, 106%, 103%, respectively, of the safety factor for a column with $l/d = 20$. These factors do not reflect the relative safety of such columns or the relative possibilities of construction errors such as honeycombing. Since columns with l/d ratios less than 10 are common in modern construction, especially with the trend to higher concrete buildings, it does not seem logical to limit the strength of columns with l/d less than 10, to preserve an equation which by itself is not correct.

Modification for Sustained High Loads.—Tests by J. R. Shank,[19] F. ASCE and H. Rüsch[20] have shown that the strength of concrete cylinders and prisms subjected to sustained high loads is reduced by 10% to 30%. This strength reduction must be considered in the design of columns subjected to sustained loads to failure (the third loading condition). Thus, for this loading condition, the short-column strength can be approximated by using a reduced concrete strength equal to $0.85\ f'_c$ in the computations to allow for the reduction in concrete strength under sustained high loads. This reduction is in addition to the commonly accepted $0.85\ f'_c$ factor[16] used to correlate the strength of concrete in flexure with the strength of a standard 6-in. by 12-in. cylinder.

The term "sustained load" must also be defined. Several foreign codes specify that a load of three days duration or longer should be considered a long-time load. This appears to be a reasonable value. In the above mentioned tests by Rüsch, concrete loaded to 80% of its short-time strength failed in about four days, that loaded to 75% of its short-time strength failed in seventy days.

Tension Failures.—For eccentrically loaded columns failing in tension, the actual length reduction factor is considerably smaller than that required for compression failures [see, for example, the curve for $e_2/d = 0.8$ in Fig. 3(c)]. The limiting case is a beam loaded in pure moment with no axial load. In such a beam there is no l/d effect. For this reason, Eq. 9 should be limited to compression failures and the following reduction equation is proposed for the tension failure region:

$$M' = M_o + \left(R\ M_b - M_o\right) \frac{e_b}{e} \quad \ldots\ldots\ldots\ldots (11)$$

in which M' is the desired reduced moment for a long column, M_o is the moment capacity at $P = 0$, M_b is the moment capacity at a balanced tension-compression failure in a short column, e_b is the eccentricity corresponding to M_b for a short column, and R is the long-column reduction factor from Eq. 9. Fig. 13 compares the various proposed reduction equations and the theoretical analysis by the authors. If design is carried out using an interaction diagram, Eq. 11 could be replaced with a straight line joining $\left(R\ M_b\right)$ and M_o. This matter is not just of academic importance because the lower portions of the interaction curve apply to many situations in which large moments combine with relatively small axial forces, such as in the girders of rigid frames.

---

[19] "Plastic Flow of Concrete at High Overloads," by J. R. Shank, Proceedings, ACI Journal, Vol. 45, February, 1949, p. 443.

[20] "Investigations into the Strength of Concrete Under Sustained Load," by H. Rüsch, RILEM Colloquium, Munich, November, 1958.

Shape Effects.—The authors' analysis was derived using a square column with steel concentrated in two faces. Strictly speaking, the long-column curves obtained apply only to columns of this cross-section. From the column tests[16] quoted previously, we see that circular columns of l/d = 7.5 tested by Hognestad had a mean long-column strength ratio of 0.93 whereas the rectangular columns tested by Hognestad had a strength ratio of 0.955. The effect of various cross-sections on the buckling strength of concrete columns is also indicated in the discussion by Hromadik of the first paper of this symposium. The radius of gyration of a circular reinforced concrete column ranges from about 0.26d to 0.30d, whereas that of a rectangular reinforced concrete column ranges from about 0.29d to 0.35d. If the curves for a square column and a circular column in Hromadik's discussion are replotted in terms of l/r, they reduce almost to one curve. This suggests that the long-column reduction equation should be written in terms of l/r rather than l/d,

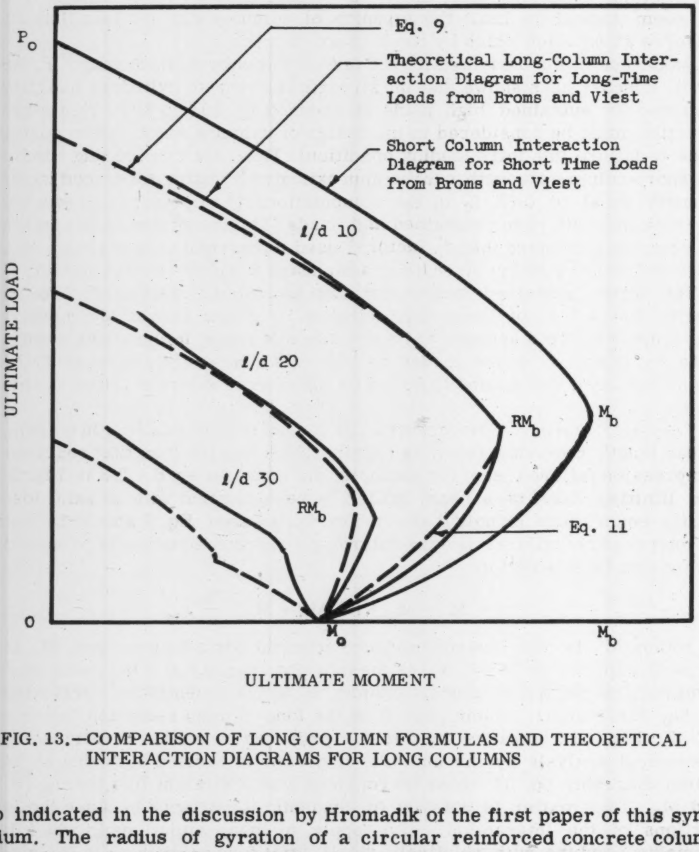

FIG. 13.—COMPARISON OF LONG COLUMN FORMULAS AND THEORETICAL INTERACTION DIAGRAMS FOR LONG COLUMNS

or alternatively, that a different reduction equation should be used for each type of cross-section. Because the l/r of a circular column is between 105% and 125% of that of a square column of the same l/d, the error involved in using d instead of r might be serious for the longer columns.

Miscellaneous.—The writers would like to have the authors state which e_1/e_2 ratio should be used in the design of long "centrically loaded" columns, along with the reasons for their choice.

Summary.—(1) The authors' short-time and long-time load analyses are valid for the column shapes considered. The decision to neglect the beneficial effects of end restraint in a long column design equation is conservative, but is well grounded.

(2) A design equation for long columns should apply basically to the case of a sustained working load rapidly increased until failure occurs, but when necessary should be modified to take account of failure under sustained high loads.

(3) The validity of a column design formula can be determined only by comparing it to tests of columns loaded under sustained loads. If comparisons are made on the basis of long-column tests now available, all of which involve only short-time loadings, the design formula under consideration will appear to have a greater factor of safety than it actually has.

(4) The following long-column design equations are proposed. These apply to eccentrically loaded columns restrained against sidesway and designed on the basis of initial eccentricity:

(a) For eccentrically loaded columns failing in compression under a sustained working load that is rapidly increased until failure occurs, the length effect should be taken into account by Eq. 9.

(b) For eccentrically loaded columns failing in compression under sustained high loads, lasting more than three days, the effect of sustained high loads should be taken into account by using a reduced concrete strength equal to 0.85 f'_c in computing the short-column strength.

(c) For case (a) or (b), with eccentrically loaded columns failing in tension, the length effect should be taken into account by Eq. 11, in which M_o, M_b, and e_b are computed for the short column using the appropriate concrete strength for the loading involved.

(d) For columns fixed at one end, other end free to rotate and translate, the length l in Eq. 9 should be taken as twice the height of the column and take $e_1 = e_2 = e_{max}$.

(e) For columns fixed at one end, other end free to translate but fixed against rotation, the length l in Eq. 9 should be taken equal to the height of the column and take $e_1 = e_2 = e_{max}$.

PHIL M. FERGUSON,[21] F. ASCE.—Much valuable information is contained in this paper and in the authors' two preceding papers (papers one and two of this symposium) on this general subject. The analysis of reinforced concrete columns as long columns, taking into account both the case of "elastic" buckling and material failures that occur under smaller lateral deflections, is a considerable accomplishment. Nothing in this discussion questions these theoretical analyses.

---

[21] Prof. of Civ. Engrg., Univ. of Texas, Austin, Tex.

However, columns as a portion of a frame are much influenced in their behavior by the action of the frame as a whole. This interaction between columns and other frame members is much more varied than can be represented by any single restraint mechanism.

The authors correctly point out that the "ultimate strength of restrained columns is always higher than the strength of hinged columns—." They then recommend the use of a reduction coefficient for all long columns and base this reduction solely on the strength of hinged columns, with no recognition given to the higher strength available with restrained columns in a frame. Because the strength differences between long hinged columns and long restrained columns are major and not minor differences, these design recommendations appear to be economically unsound for a large percentage of all column designs. It is suspected that this percentage might be from 80% to 90%.

The authors seem not to have differentiated in their analyses between columns subject to direct loads that are essentially matters of statics and those moment loads that are impressed by angle changes and hence are deformation type moments. This distinction is important and must be incorporated before a column study can lead to realistic design specifications.

For this discussion columns will be considered under several groupings:

1. Columns where sidesway effects may be ignored. (a) Interior columns with similar eccentricities at each end as in Fig. 14(a). (b) Exterior columns in reversed bending as in Fig. 14(b).
2. Columns in which sidesway is important. (a) One story rigid frames as in Fig. 14(c). (b) Buildings in which lateral wind loads produce important column shears and moments as in Fig. 14(d).
3. Columns directly loaded between joints as in Fig. 14(e).
4. Free standing, "flagpole" type columns as in Fig. 14(f).

By far the largest number of columns fall in group 1 and this discussion is primarily related to this large group. Limitations of time, amongst other commitments, have prevented an adequate study of the columns in group 2. The number of columns in groups 3 and 4 are quite small.

This discussion is directed entirely to ultimate strength design.

Interior Columns Without Sidesway.—The authors recommend that the end moments on columns be established on the basis of an elastic analysis of the frame. There is now no adequate alternate to this procedure. However, it should be emphasized that columns (without sidesway) usually receive their moment loads only from joint rotations. These moments are impressed or deformation type moments and are far from being statically determined. Any change in joint rotation causes a corresponding change in column moment and in the resulting eccentricity, e, of the load on the column.

While this situation might be more accurately analyzed by the use of differential equations, this discussion will be presented in the simpler terms ordinarily related to moment distribution and frame analysis.

The analysis of the column in Fig. 15 will first be based on elastic conditions. Assume equal and opposite moments at the two ends, that are indicated as P e in the adjacent moment diagram. This moment produces an angular deflection at the end, or joint, that is consistent with the joint rotation used in frame analysis. Because the column deflects when carrying moment, there will be an additional moment $P\ \delta_m$ at the center of column, that adds to P e. The critical column moment is thus the center moment:

$$M_c = p\ e + P\ \delta_m$$

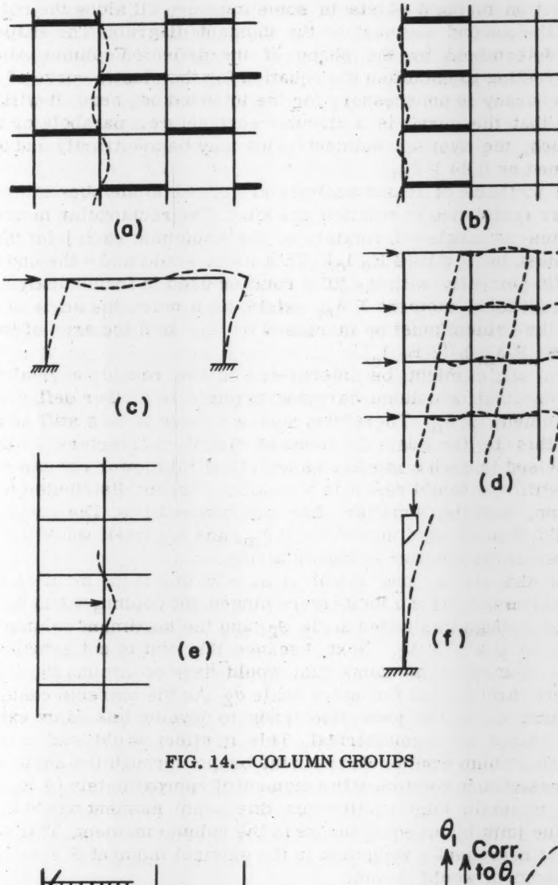

FIG. 14.—COLUMN GROUPS

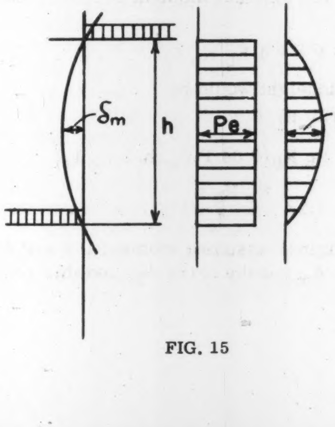
δ_m
h
Pe
$P\delta_m$

FIG. 15

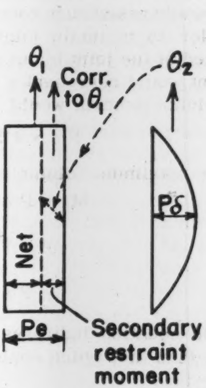
θ_1
Corr. to θ_1
θ_2
Net
Pe
$P\delta$
Secondary restraint moment

FIG. 16

This deflection moment exists in some measure all along the column, as indicated by the second segment of the moment diagram. The shape of this segment is determined by the shape of the deflected column. Although it would be interesting to establish the equation for the elastic curve of the column, such accuracy is unnecessary for the intended use here. It will be adequate to say that the curve is a circular segment or a parabola or a cosine curve. As such, the average moment value may be arbitrarily and approximately assumed as $0.64 \; P \; \delta_m$.

The usual methods of frame analysis are based on member stiffness that is the member resistance to rotation at a joint. The rectangular moment area $P \; e \; h$ indicates an angle of rotation of the column at each joint that, from symmetry, must be $P \; e \; h/(2 \; E_c \; I_c)$. This alone would make the end slope of the column fit perfectly with the joint rotation used in frame analysis. However, if an additional moment $P \; \delta_m$ exists, as it must, the angle of rotation at the end of the column must be increased by θ_2 = half the area of the M/E I diagram = $0.64 \; P \; \delta_m \; h/(2 \; E_c \; I_c)$.

This extra angle might be interpreted in two roughly equivalent ways. One might say that a column carrying moment is further deflected by the secondary moment, $P \; \delta_m$. Therefore, such a column is less stiff against end rotation. If this is the case the moment distribution factors for the joints should be revised in such a manner as to reflect this lower column stiffness. The lesser stiffness would result in a smaller moment distributed to the end of the column, that is, smaller than the original P e. The center column moment would then be less than $P \; e + P \; \delta_m$, and δ_m itself would also be reduced, because of the smaller moments acting.

Instead of the above, one might first say that if the moment P e were statically determined and the joints were hinged, the column would be entirely free to rotate through this added angle θ_2, and the maximum column moment would indeed be $P \; e + P \; \delta_m$. Next, because the joint is not actually hinged, consider the change in moments that would develop around the joint if the joint did rotate through this full extra angle θ_2. As the extreme case, assume that the column above the joint also tends to develop this same extra angle θ_2 and that beams are symmetrical. This in effect would lead to the statement that each column would pull one of the beams through the angle θ_2. Each beam would resist such rotation with a moment of approximately $(4 \; E_b \; I_b \; \theta_2/L)$. In order to maintain joint equilibrium this beam moment would have to be balanced at the joint by an equal change in the column moment. This balancing moment would represent a reduction in the original moment P e such that the end column moment would become

$$P \; e - 4 \; E_b \; I_b \; \theta_2/L = P \; e - 4 \; E_b \; K_b \; \theta_2 \; . \; . \; . \; . \; . \; . \; . \; . \; . \; . \; (12)$$

and the maximum column moment at midheight would be

$$\begin{aligned} M_c &= P \; e + P \; \delta_m - 4 \; E_b \; K_b \; \theta_2 \\ &= P \; e + P \; \delta_m - 4 \; E_b \; K_b \left(0.64 \; P \; \delta_m \; h/2 \; E_c \; I_c\right) \\ &= P \; e + P \; \delta_m \left(1 - 1.28 \; \frac{E_b \; K_b \; h}{E_c \; I_c}\right) . \; . \; . \; . \; . \; . \; . \; . \; . \; . \; . \; (13) \end{aligned}$$

This equation indicates that the original assumed moment $P \; e + P \; \delta_m$ is larger than that which could accompany δ_m and the extra θ_2, and this regardless of how small δ_m may have been assumed. It should also be noted that this smaller moment would imply a smaller θ_2, but that the smaller θ_2 would simply reduce the negative term and not change the form of the equation. It thus becomes obvious that the column design may safely be based on a moment smaller than the sum of the moment P e obtained from an elastic analysis and the moment P δ_m.

The parenthesis in the equation for M_c should also be examined as to its absolute value. If δ_m were initially assumed at its final correct value, the final angle changes could be shown diagramatically as in Fig. 16. The moment P e and the angle θ_1 would be known from frame analysis. The angle θ_2 would result from the deflection moment represented at mid-height by P δ_m. The angle θ_2 would develop the secondary restraining moment represented by the negative term in the equation for M_c. This restraining moment would in turn produce a negative angle change that might just as accurately be considered as a reduction in θ_1. With the use of the correct assumed δ_m, the equation for M_c would then be exact, within the elastic range of the materials, except for errors in the assumed shape of the deflection curve. Such errors could only have the effect of modifying the average deflection ordinate to something other than 0.64 δ_m and of modifying the constant of 1.28. Because it is difficult to imagine a column shape that would have an average deflection ordinate less than 0.5 δ_m, the 1.28 constant might range between 1.00 and 1.30.

The parenthesis in the equation for M_c becomes zero when $1.28\ E_b\ K_b\ h/E_c\ I_c = 1$. Or, if the conservative value of 1.00 is used instead of 1.28 when $E_b\ K_b = E_c\ I_c/h$. Thus, if the beam is at least as stiff as the column, the final moment on the column will not exceed P e as obtained from elastic analysis of the frame. If the beam is the stiffer member, the column design moment will be less than P e. Thus, in a frame, the longer and smaller such a column is made, the less probable it becomes that the "initial" end moment P e can influence the buckling of the column. The joint restraint can even be large enough to reverse the sign of the end moment on the column in the case of a very slender column. A design based simply on the frame moment P e will thus be a conservative way of preventing failure of such columns.

It is noted that should the column stresses approach failure and thus change the column into one that is less stiff, this effect can be represented in the formula for M_c by using a lower value of E_c. Thus, before failure, the column stiffness would be further reduced relative to that of the beam, and M_c would become still smaller, with P e replaced by a resultant end moment of opposite sign.

In the case of a very stiff column, in which column stiffness is twice that of the beam, δ_m will be numerically small and the effect of the resulting P δ_m term is reduced at least 50% by the negative term representing the frame action. If in addition the value of E_c decreases, under overstress, by as much as 50%, this reduction in the P δ moment becomes at least 75%. It is strongly suspected in this case that the proper constant in the equation for M_c should be closer to 1.28 than to 1.00. In such case these reductions become about 64% and 95%, respectively.

This discussor thus concludes that, except for columns extremely stiff with respect to the floor system, it will be amply safe in ultimate strength design to proportion for the moment P e obtained from elastic frame analysis with no addition for deflection moment or length effects. As a restriction against very long columns, the proviso might be added that such columns must not be smaller than the hinged column needed to carry the axial load with zero eccentricity. This conclusion applies only to interior columns without significant sidesway.

Exterior Columns in Reversed Bending.—A column such as that in Fig. 14(b) may be considered as loaded in moment by equal angle changes at each end. In such a case the maximum moments from frame action occur at the ends of the columns, and the maximum deflection moments are nearer the quarter or fifth points of the column. Thus, deflection moments are less likely to create total moments in excess of the end moments.

Compared to the previous analysis of the interior column, this case has only one beam to restrain the two columns (one above and one below), but the deflection effect is so very much smaller that further analysis seems unnecessary. Fig. 3(e) shows a curve for a specific column having $e_1/e_2 = -1$, that is intended to represent this case. Although this curve shows no reduction in strength until L/d is 30, it is unduly conservative because it is based on hinged ends and does not recognize the effective restraint provided by the frame.

It appears that ultimate strength design for these columns based on the P e moments computed from elastic frame analysis is quite safe, and that no recognition needs to be given to deflection problems. It might appear that a moment applied at only one end of the column might produce more of a deflection problem. However, this case could not be as serious a problem as that of the interior column already discussed. Because the reversed bending moment P e will be larger, it is the governing case.

Columns With Important Sidesway.—When sidesway is important, especially where lateral loads such as wind or earthquake forces are a significant part of the loading, an entirely different problem exists. The column shears and moments in this case are more a matter of statics than a matter of impressed moments caused by end rotations. In other words, P e moments computed for such columns remain undiminished as joints rotate; hence deflection moments are directly additive. Time has prevented this discussor from carrying out a more thorough analysis of such columns. It appears that the authors' hinged column assumption is desirable here. However, it would appear that each half of the column approximates half of a column loaded as in Fig. 14(a), that would mean that $e_1/e_2 = +1$ would be more correct for use in their equations than $e_1/e_2 = -1$.

Columns Directly Loaded Between Joints.—The authors' analysis of restrained columns appears more directly applicable to this case than to columns loaded through connecting beams. This is a loading that can be measured chiefly in terms of statics, and the authors' analysis is based on a static moment P e. For a proper understanding of the entire column problem, these predominantly static moments must be contrasted with moments impressed by angle changes. The authors' method appears poorly adapted to the latter case, as in the interior columns first discussed.

Free Standing, "Flagpole" Type Columns.—There are only a small number of cantilever type columns and these include those crane columns that are not braced across the crane bay. If these columns are actually fixed at their bases, their curvature is exactly like that in the upper half of a hinged end column that is similarly loaded at each end. Thus, as for any other material, design must be based on the use of an effective length twice the actual column length. Under this condition the hinged end column analysis is exactly correct.

The Authors' 0.84 Factor to Account for Deflection.—This discussion has in a large measure been concerned with deflection moment and the counterbalancing effect of frame restraint. For interior and exterior columns it has been shown that deflection moments are generally not important, because frame restraint reduces or cancels the apparent ill effects. here thus seems to be no need for a reduction factor of 0.84 for these cases, that constitute the majority of all columns.

If the 0.84 factor is needed for some cases, and it is not yet established clearly where this would be, it should certainly not be written into the load factor for all columns. Neither would it appear desirable to apply it to increase the design axial loads. It should be directly related to the moments involved and then only for the particular columns in which it is needed. Thus, the proposal that the factor K in the authors' suggested load factors be made 1.3 is totally unacceptable to this discussor.

Effect of Plastic Hinges.—The authors' consideration of the effects of plastic hinges in restraining members seems to provide one of the reasons they recommend that the strength of hinged columns be used for all designs. For the interior and exterior columns (without sidesway) that have been the primary reason for this discussion, it appears that the restraint moments discussed are all in the reverse sense to those that might create hinges. Thus, the restraints that this analysis has considered are available for some range even after the formation of plastic hinges.

This available resistance assumes the beam has also been designed for maximum moments based on elastic frame analysis. If such beams should (at some future date) be designed by limit design procedures, it might be necessary to consider deflection-caused moment from long columns in the beam design in order to avoid failure in the beam. However, limit design is not yet an approved design method in reinforced concrete in the United States. By the time limit design is adopted, it is hoped that much more comprehensive studies of columns will also have defined more exactly the associated problems of long slender columns.

BENGT BROMS,[22] M. ASCE and I. M. VIEST,[23] F. ASCE.—Perhaps the most important practical finding of these studies of long reinforced concrete columns was that the current (1956) design requirements[7] for eccentrically loaded long columns should be liberalized. It is gratifying that all discussors concurred with this finding particularly because two of the discussors, Ferguson and Siess, are members of the Building Code Committee of the American Concrete Institute (ACI) charged with updating the current design requirements.

Basic Assumptions.—Two of the basic assumptions, chosen by the authors in deriving the approximate design procedure, were discussed: the effects of end restraints and the effects of sustained loading. It is interesting that, in his discussion of the first paper of this symposium, Ernst singled out these two assumptions as items in need of further experimental studies.

The authors based their method on the ultimate strength of hinged columns. MacGregor and Siess state that "In ignoring end restraints . . . the authors are being justifiably conservative" while Ferguson concludes that

---

[22] Assoc. Prof. of Civ. Engrg., Cornell Univ., Ithaca, N. Y.

[23] Bridge Research Engr., AASHO Road Test, Ottawa, Ill.

"Since the strength differences between long hinged columns and long restrained columns are major and not minor differences, these design recommendations appear to be economically unsound for large percentage of all column designs." The obvious disagreement between MacGregor, Siess and the authors on one side, and Ferguson on the other side points to the fact that the question of end restraints urgently needs further studies. The authors believe that until such studies have filled the gap in the present knowledge of the effect of end restraints, their conservative approach is justified, particularly because it already represents a liberalization of the current requirements.

In the interest of future developments, the authors consider it desirable to point out that Ferguson's approximate treatment of end restraints is inapplicable to reinforced concrete columns because it is based on an elastic solution. Theories of plastic buckling, such as the one presented by the authors in the first two papers of this symposium, show that the elastic solution represents an upper limit to the actual strength and, thus, is generally unsafe.

The writers' approach to columns subjected to sustained loading was based on experimental evidence for short columns[18] as has been pointed out by MacGregor and Siess. This experimental evidence suggests that the approach is applicable not only to sustained working loads but also to sustained overloads which do not cause failure. Only columns loaded to more than 85% of their short-time strength failed under sustained loads. On the other hand, some columns loaded up to 94% of their short-time strength sustained the loads without failure; the strength of such columns, when subsequently loaded to failure with fast loading, was lower than their short-time strength but the decrease was accounted for by the permanent deflections caused by creep during the sustained load tests.

Accordingly, sustained loading may affect the column strength in two ways: (1) by increase in deflections and (2) by decrease in concrete strength. The first effect is always present and may be expected to increase with increasing slenderness of the column; therefore, it should be included in the length effects. The second effect, however, is present only if the column fails under sustained load and is independent of the column length; therefore, it should be used for computing the sustained load strength of all columns without regard to their slenderness.

Design Equations.—MacGregor and Siess proposed to base the design of long columns on the equation for short columns and a reduction coefficient. This is the same approach as that selected by the authors. However, the two approaches differ in the definition of the short column: while the authors defined the short column as one with $l/d \leqq 10$ to 20 (depending on the ratio of end eccentricities), the discussors defined it as one with $l/d \leqq 2.8$ to 13.2. In essence, the discussors suggest that for equal end eccentricities there are no short columns as in such case deflection will always cause some reduction in strength.

The available experimental evidence quoted by the discussors and the theoretical studies reported by the authors show clearly that the approach chosen by the discussors (Eq. 9) is closer to reality. The only advantage offered by the approach selected by the authors is the simplicity of the design within the selected range of short columns which encompasses the majority of practical cases.

Furthermore, the design procedure proposed by the writers includes a factor of 0.84 which represents the reduction in ultimate strength of columns with $l/d = 10$. The factor 0.84 is an integral part of the reduction coefficient so that it may be misleading to include it in the load factor as has been pointed out by all discussors.

Accordingly, it appears preferable to account for the lengths effects by the reduction factor proposed by the discussors:

$$R = 1.20 - 0.025 \frac{l}{d} - 0.13 \frac{e_1}{e_2} \leqq 1.0 \quad \ldots\ldots\ldots \quad (9)$$

For columns with large eccentricities (tension failures), MacGregor and Siess proposed an equation representing a smooth transition to the case of pure bending (Eq. 11). As the end eccentricities may differ in magnitude, the quantity e in the proposed equation should be replaced by the larger end eccentricity e_2:

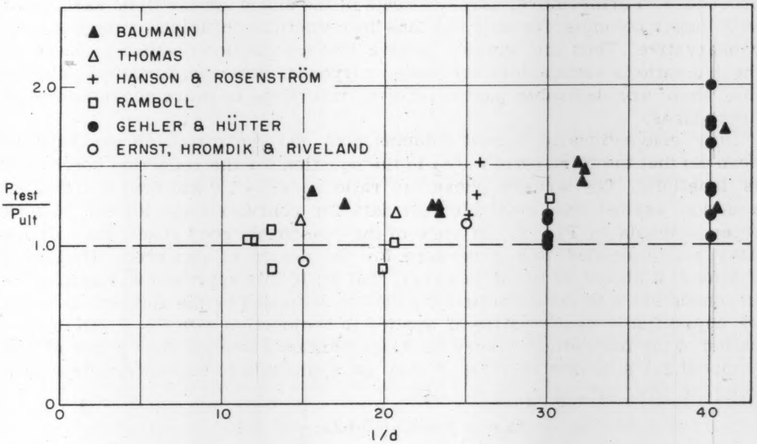

FIG. 17.—COMPARISON OF EQ. 11 WITH TEST DATA

$$M' = M_o + \left(R\, M_b - M_o\right) \frac{e_b}{e_2} \quad \ldots\ldots\ldots\ldots (11)$$

Eq. 11 is in a reasonably good agreement with the writers' theoretical values. MacGregor and Siess are to be congratulated for this ingenious extension beyond the range covered by the procedure proposed by the authors.

Miscellaneous Comments.—The design procedures proposed by the authors and by the discussors are approximate in that the more exact analysis indicates that several factors not included in the reduction coefficient R affect the strength of long columns somewhat differently from the strength of short columns (Fig. 3). It is, therefore, the opinion of the authors that the adequacy of the design equation can be best checked by direct comparisons with the test data. Such comparisons were represented in Fig. 8. The fact that the tests were conducted with fast loading rather than with sustained working loads followed by fast loading does not invalidate the comparisons as suggested by MacGregor and Siess; it only limits their direct applicability. However, this limitation is not serious since theoretical considerations indicate that the effects of sustained working loads are small [less than the difference between the two curves in Fig. 3(f)].

The largest effect of the shape of the cross-section may be expected to be associated with concentrically loaded columns. The curves presented by Hromadik in his discussion of the first paper of this symposium indicate that even for this type of loading the effect of the shape of cross-section is no greater than the differential effects of concrete strength and percentage of reinforcements which have also been neglected in the approximate design procedure. Furthermore, larger effects of the shape appear to be associated with longer columns; for such columns the reduction coefficient is particularly conservative. Thus the authors believe that a reduction coefficient based on the l/d ratio is satisfactory for design purposes. However, further studies of this item are desirable particularly in reference to more accurate design procedures.

For conventionally loaded columns both end eccentricities are equal to zero so that the third term e_1/e_2 in the equation for the reduction coefficient is indefinite. The writers chose the ratio $e_2/e_1 = 1.0$ and then checked the equation against the available test data for concentrically loaded columns (open symbols in Fig. 8). In view of the reasonably good check, the authors have recommended this procedure for the design of concentrically loaded columns. It should be noted, however, that while this approach was applicable in connection with the reduction coefficient proposed by the authors, it would be unjustifiably conservative if applied in conjunction with Eq. 9. An examination of the theoretical curves for hinged columns (see the first paper of this symposium) suggests that Eq. 9 may be applicable to concentrically loaded columns after setting $e_1/e_2 = -1.0$:

$$R_{axial} = 1.33 - 0.025 \frac{l}{d} \leqq 1.0$$

A comparison with the test data for concentrically loaded columns shown in Fig. 17 suggests that Eq. 11 fits the data even better than the reduction coefficient proposed originally by the authors.

Sidesway.—The analysis presented by the writers does not take into account the effect of sidesway which will decrease the strength of hinged and restrained columns.

In many structures, however, sidesway is prevented by shear walls and for these cases authors' reduction coefficients are applicable.

Where sidesway can take place the strengths of the vertical members are reduced considerably. For design considerations, these structures can often be replaced by equivalent structures with no sidesway.

MacGregor and Siess have proposed such substitutions to take into account the effect of sidesway in two special cases. These two cases are undoubtedly the most common ones encountered in design and therefore the proposed method of design is considered a useful extension of the original paper.

AMERICAN SOCIETY OF CIVIL ENGINEERS
Founded November 5, 1852
TRANSACTIONS

Paper No. 3163

TORSIONAL ANALYSIS OF SUSPENSION BRIDGE TOWERS

By Frank Baron,[1] F. ASCE, and Anthony G. Arioto,[2] A.M. ASCE

SYNOPSIS

An analytical procedure is presented for determining the moments, shears, and displacements of suspension bridge towers that are subjected to a torque about their longitudinal axes. Numerical examples are given to illustrate the procedure.

INTRODUCTION

The design of a large suspension bridge tower is based on many considerations besides those of torsion. Among these considerations are the influences of (1) vertical forces along the longitudinal axis of a tower, (2) horizontal forces that are parallel to the longitudinal axis of the roadway, and (3) lateral forces that are normal to the plane described by these two axes. In item 2, the horizontal forces at the top of the tower are associated with the unbalanced horizontal cable tensions and are considered to consist of two parts, namely: (a) forces that are symmetric with respect to the longitudinal axis of the roadway, and (b) forces that are anti-symmetric with respect to this axis.

The forces that are grouped in item 2b produce a torque about the longitudinal axis of the tower. These forces, or torques, can be caused by traffic loads on one side of the roadway or by aerodynamic forces which tend to twist the roadway. The magnitude of the torque on a tower is dependent on several factors. Among these factors are the dead load, live load, width between cables,

---

Note.—Published essentially as printed here, in January, 1960, in the Journal of the Structural Division, as Proceedings Paper 2354. Positions and titles given are those in effect when the paper or discussion was approved for publication in Transactions.

[1] Prof. of Civ. Engrg., Univ. of California, Berkeley, Calif.

[2] Assoc. Civ. Engr., County of Santa Clara, Calif.

sag to span ratio, and the characteristics of the towers, stiffening trusses, and side spans. The influences of these factors on the torsional deformations of suspension bridges are discussed in the reports of the several Boards of Engineers appointed to study the causes of failure in the first Tacoma Narrows Bridge. Not all these factors will be discussed herein. Particular attention will be given to the effects of a torque on a tower itself.

In studying the torsional deformations of bridges for static or dynamic loads, the torsional rigidities of the tower need be known. This holds because the net torque on a tower is dependent on the relative rigidity of the tower to a twist about its longitudinal axis and the relative "stiffnesses" of the side span and center span cables to displacements at the top of the tower. The displacements of the saddles at the top of the tower are out of phase with each other and are associated with the angle of twist about the longitudinal axis of the tower. An additional factor influencing the net torque on a tower is the horizontal length of cable that is firmly attached to a saddle as the saddle goes through the angle of twist. As a result of the change in the horizontal positions of the side span and center span cables at the top of a saddle, the cables offer an additional restraint to torsional deformations of the tower. This restraint is proportional to the angle of twist and to the ratio of the horizontal length of cable attachment to the width between cables. This latter restraint is practically negligible for most bridges. It was considered[3] in the studies of the Golden Gate Bridge towers.

For loads as in item 2b, the torsional rigidity of a tower can influence the resulting deformations of the roadway, the stiffening truss, and the bracing elements of the roadway system. This should be obvious for static loads. For example; if a roadway is subjected to torsional loads, the twist of each tower will be defined by the equilibrium position of the side span and center span cables at the top of each saddle. For a tower with no torsional rigidity, the equilibrium position is defined by the relative stiffnesses (to torsional displacements) of the side span and center span cables. In this case, no unbalanced horizontal cable tension can exist at the top of each saddle. On the other hand, if a tower is infinitely stiff to torsion, any unbalanced horizontal cable tension due to torsional loads is resisted by the tower as the tower is fixed in position. This, of course, assumes that the saddles are fixed and that the cables do not slip.

The role which a tower plays in the torsional oscillations of a suspension bridge is less obvious. This is partly because a tower can play a different role in the various modes of vibration. For example, if the towers of a bridge are infinitely stiff, the fundamental torsional mode is largely prevented by the resistance of the towers to twist around their vertical axes. A twist at the top of the tower is necessary for large out-of-phase motions of the cables in the fundamental mode and is mutually dependent on the stiffnesses of the side spans, towers, and center span. The same conclusion[4] was made by the Board consisting of O. H. Amman, T. von Karran, Hon. Members, ASCE, and G. B. Woodruff, F. ASCE. For other torsional oscillations, particularly those in the higher modes, the side spans and towers will participate with the center span to a different degree than that indicated by a study of the fundamental mode. The participation will also differ from that indicated by a study of the vertical oscillations only. The following quotation[5] is of particular interest herein:

---

[3] "The Golden Gate Bridge," report of the Chf. Engr. (Joseph B. Strauss) to the Board of Directors of the Golden Gate Bridge and Highway Dist., Calif., September, 1937, pp. 90-105.

[4] Report to John M. Carmody by Board of Engrs., Othmar H. Ammann, Theodore von Karman, Glen B. Woodruff, March 28, 1941; pp. 61, 62, 125, 133. See "The Failure of the Tacoma Narrows Bridge," a reprint of original reports, Texas Engrg. Experiment Sta., Bulletin No. 78, 1944.

> "Observations of the Tacoma Narrows Bridge and on the models indicated that under certain vertical oscillations of the center span, particularly those in the higher modes, the side spans and towers remained practically motionless or oscillated with a different frequency. In other words, they did not always contribute to the dynamic motions of the center span. This is corroborated by the calculations in Appendix VI which show that in the higher modes no more energy is required for such oscillations with the tower tops fixed than with side span participation."
>
> "It appears that the side spans have greater influence on the torsional oscillations of the center span. The towers, however, offer much greater resistance to twisting than to bending parallel to the bridge axis and contribute therefore a material resistance to torsional oscillations of the bridge."

Concerning the effect of a static torque on a tower itself, the torque can cause deformations and stresses that are associated with the bending moments, twisting moments, and shears in the legs and struts of the tower. The moments and shears can modify the proportions and placement of the struts and of details, as for example at the base of a tower and the lacing of the struts. They can also influence the placement of horizontal stiffening diaphrams in the legs of a tower. It is reported[6] that the three top struts of the Golden Gate Bridge towers were laced together in pairs and that the lacing of the web members was increased as a result of an investigation of the effects of a torsion. This same report outlines the analytical procedure that was used in determining the effects of the torque. In the procedure, the shaft was assumed to be as effective as a circular section of equal polar moment of inertia and the torsional properties of the struts were neglected. Subsequent model studies indicated that the cellular shafts were about half as effective as was thus assumed. The procedure led to the formation and solution of twelve simultaneous equations.

The damage that can occur in a tower due to the torsional oscillations of a bridge is strikingly illustrated by the towers of the first Tacoma Narrows Bridge. Concerning these towers, each Board reporting on the damage to the bridge stressed the great damage that was done to the cells, anchorages, splices, and top struts of the towers as a result of the torsional oscillations and the subsequent failure of the bridge. It is reported that the towers were near collapse when the roadway peeled off the suspenders. For a detailed description of the damage to the towers, the reader is referred elsewhere.[4,7,8]

---

[5] Ibid. p. 33.

[6] "The Golden Gate Bridge," report of the Chf. Engr. (Joseph B. Strauss) to the Board of Directors of the Golden Gate Bridge and Highway Dist., Calif., September, 1937, p. 101.

[7] Reports to Paul Carew by Board of Narrows Bridge Loss Committee; Clifford E. Paine, Chmn., Hardy Cross, Shortridge Hardesty.

[8] Kolton D. Robinson, Wilbur M. Wilson; June 2, 1941, especially pp. 42-48. Report to James A. Davis by Board of Investigation, Tacoma Narrows Bridge: L. J. Sverdrup, Chmn., Francis Donaldson, and Russell G. Cone; Part 1, February 2, 1941, March 4, 1941. Part 2, June 26, 1941. Part 3, January 26, 1941.

An inspection of the literature shows that much has been written concerning the effects of forces on towers as listed in items 1, 2a, and 3.[3,9,10] The effects of these forces are in general clearly understood. Appreciably less has been written concerning the effects of a torque on a tower and, apparently, the latter effects are less clearly understood. This paper will deal with an analytical procedure for determining the deformations, shears, and moments in a tower that is subjected to a torque. The discussion will be restricted to towers with vertical legs and horizontal struts at different elevations of the legs.

ANALYSIS FOR TORSIONAL LOADS

Statical Relationships.—The tower shown in Fig. 1 is subjected to a net torque, M_y, about the y-axis. The net torque is associated with the unbalanced horizontal cable tensions at the top of the tower and with the angle of twist, ψ_y, relative to the base of the tower. The tower is assumed to consist of two equal vertical legs, r number of closed panels, and 0 + r number of horizontal struts. It is assumed that the relationships between the bending moments and flexural deformations and the twisting moments and torsional deformations are known for each leg and strut, that is;

$$\Delta\phi_x = \frac{m_x\, ds}{E\, I_x} \qquad \text{(1a)}$$

$$\Delta\phi_y = \frac{m_y\, ds}{G\, J_y} \qquad \text{(1b)}$$

for a leg, and

$$\Delta\phi_y = \frac{m_y\, ds}{E\, I_y} \qquad \text{(2a)}$$

$$\Delta\phi_x = \frac{m_x\, ds}{G\, J_x} \qquad \text{(2b)}$$

for a strut. In Eqs. (1) and (2), the angle-changes, $\Delta\phi$, and the corresponding moments, m, are about axes designated by the subscripts. The values of E I and G J are measures of the stiffnesses of an element to unit deformations. In the succeeding analysis, the effects of shearing deformations due to transverse shears, v_z, are neglected and each leg and strut is assumed to be of constant cross-section between adjacent joints defined by the intersections of the center-line of the members.

The following notations will be used in the analysis of the tower:

b = width between center lines of legs and center lines of cables;

h_s = total height of tower;

h_{jk} = height between center lines of two adjacent struts, j and k;

h_{01} = height between center lines of the first panel at the base of the tower;

---

[9] "The Suspension Bridge Tower Cantilever Problem," by Blair Birdsall, Transactions, ASCE, Vol. 107, 1942, p. 847.

[10] "The Golden Gate Bridge," report of the Chf. Engr. (Joseph B. Strauss) to the Board of Directors of the Golden Gate Bridge and Highway Dist., Calif., September, 1937, pp. 93-100.

E = Young's modulus;

μ = Poisson's ratio;

$G = E/2(1 + \mu)$ = shearing modulus;

I_{sj}, I_{sk} = moments of inertia of struts j and k, respectively, about y axes;

$G\,J_{sj}, G\,J_{sk}$ = torsional rigidities of struts j and k, respectively, about x axes;

$I_{ij}, I_{jk}, I_{k\ell}$ = moments of inertias of legs ij, jk, and kℓ, respectively, about x axes;

$G\,J_{ij}, G\,J_{jk}, G\,J_{k\ell}$ = torsional rigidities of legs ij, jk, and kℓ, respectively, about y axes;

$G\,J_{tower} = M_y\, h_s/\psi_y$ = torsional rigidity of the entire tower;

$v_{z;sj}, v_{z;sk}$ = transverse shears in struts j and k, respectively, along the z axis;

$m_{y;sj}, m_{y;sk}$ = bending moments at the ends of struts, j and k, respectively, about y axes;

$m_{x;sj}, m_{x;sk}$ = twisting moments in struts j and k, respectively, about x axes;

$v_{z;ij}, v_{z;jk}, v_{z;k\ell}$ = transverse shears in legs ij, jk, and kℓ, respectively, along the z axis;

$m_{x;ij}, m_{x;jk}, m_{x;k\ell}$ = bending moments at ends i, j, and k of legs ij, jk, and kℓ, respectively, about x axes;

$m_{y;ij}, m_{y;jk}, m_{y;k\ell}$ = twisting moments in legs ij, jk, and kℓ, respectively, about y axes;

M_y = net torque about the longitudinal axis of the tower;

θ_{xk}, θ_{yk} = slopes with respect to the x and y axes, respectively, at joint k;

Δ_{zk} = deflection along the z axis at joint k;

$\psi_{y;sk}$ = angle of twist of a chord through joints k, k relative to the base of the tower, about the y axis

ψ_y = angle of twist of a horizontal chord at the top of the tower, relative to the base, about the y-axis;

$$a_{ij} = \frac{h_{ij}}{b};\ a_{jk} = \frac{h_{jk}}{b};\ a_{k\ell} = \frac{h_{k\ell}}{b} = \text{dimensionless ratios;}$$

$$e_{1;jk} = \frac{E\,I_{jk}}{G\,J_{jk}};\ e_{2;jk} = \frac{E\,I_{sj}}{E\,I_{jk}};\ e_{3;jk} = \frac{G\,J_{sj}}{G\,J_{jk}},\ e_{4;jk} = \frac{EI_{sk}}{E\,I_{jk}};$$

$$\text{and } e_{5;jk} = \frac{G\,J_{sk}}{G\,J_{jk}} = \text{dimensionless ratios.}$$

The sign convention that is used for the shears and moments is illustrated in Fig. 2. Positive values of the shears and moments in the legs and struts are defined in Fig. 2. The shears are represented as force vectors along the z-axis and the moments as moment vectors about the x and y-axes, respectively. The same sign convention is used for rotations and displacements except that the interchange concept[11,12,13] between statics and geometry is employed (Fig. 3). In this concept, a rotation or angle-change about an axis is treated as a force along the axis of rotation, and a displacement along an axis is treated as a moment about the axis of displacement. The concept is general, provided that the angle-changes and rotations are small. By means of this concept, computations

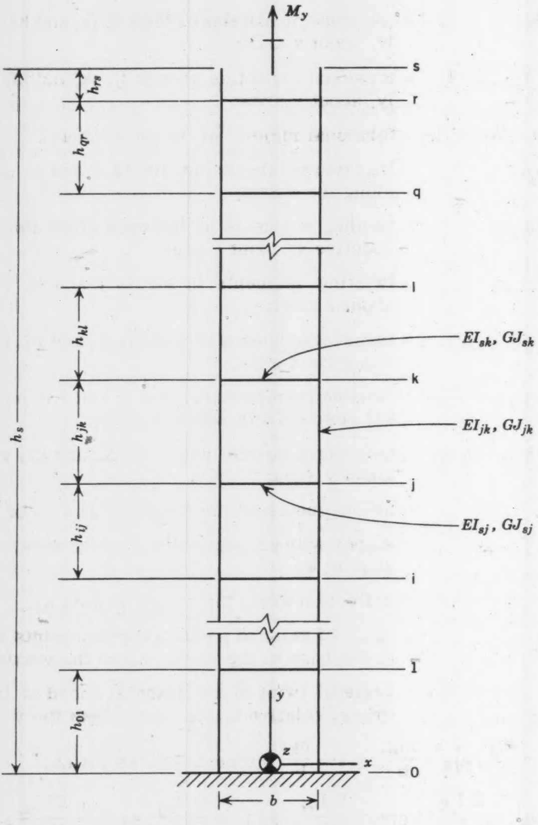

FIG. 1.—DIMENSIONS

---

[11] "Numerical Methods of Analysis in Engineering," edited by L. E. Grinter, Macmillan Co., N. Y., 1949. See Chap. 8, "Successive Corrections—A Pattern of Thought," by Frank Baron.

[12] "Laterally Loaded Plane Structures and Structures Curved in Space," by Frank Baron and James P. Michalos, Transactions, ASCE, Vol. 117, 1952, p. 279.

[13] "A Circuit Analysis of Laterally Loaded Continuous Frames," by Frank Baron, Proc. Paper No. 1147, ASCE, Vol. 83, No. ST1, January, 1957.

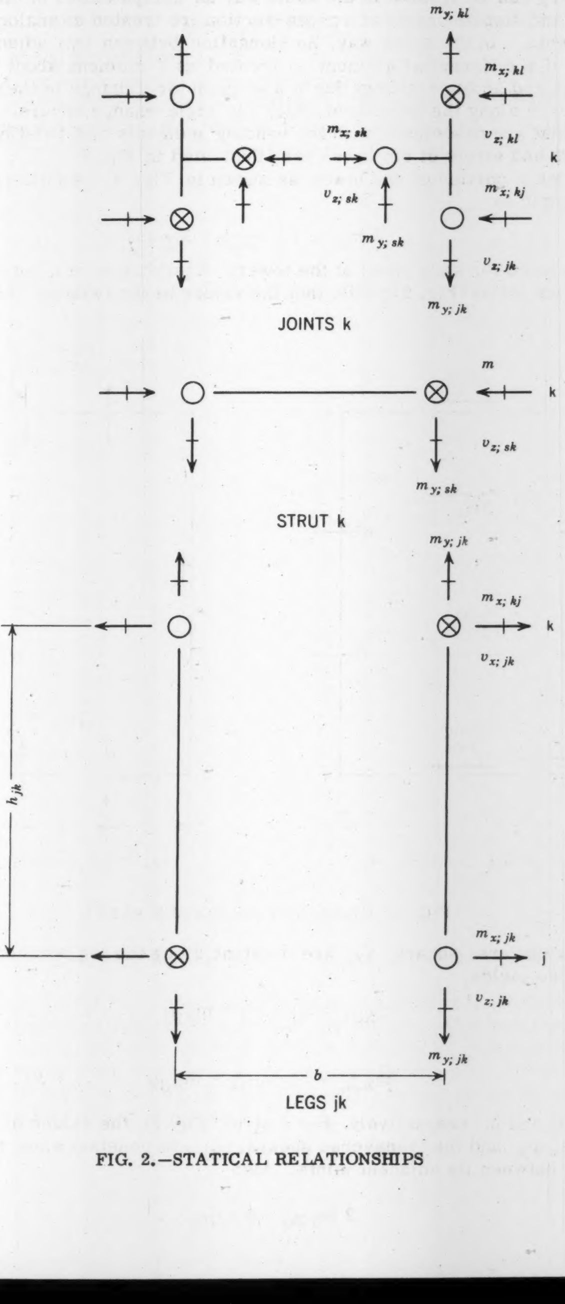
m y; kl
m x; kl
m x; sk
v z; kl
k
v z; sk
m x; kj
m y; sk
v z; jk
m y; jk
JOINTS k
m
k
v z; sk
m y; sk
STRUT k
m y; jk
m x; kj
k
v x; jk
h jk
m x; jk
j
v z; jk
m y; jk
b
LEGS jk

FIG. 2.—STATICAL RELATIONSHIPS

of geometry can be treated in the same way as computations of statics. The rotations and displacements at a cross-section are treated as analogous shears and moments. In the same way, an elongation between two adjacent cross-sections of a differential element is treated as a moment about the axis of elongation, and an angle-change due to a moment (or a change in shear) is treated as a force along the axis about which the angle-change occurs. The angle-changes that are associated with the bending moments and twisting moments in the legs and struts of the tower are illustrated in Fig. 3.

Consider a portion of the tower as shown in Fig. 4. Equilibrium of this portion requires

$$2\ m_{y;jk} + b\ v_{z;jk} = M_y \ \ldots\ldots\ldots\ldots\ldots\ldots \ (3)$$

Eq. (3) is valid for each panel of the tower. Equilibrium of a leg between any two adjacent joints (Fig. 2) yields that the values of the twisting moments, m_y,

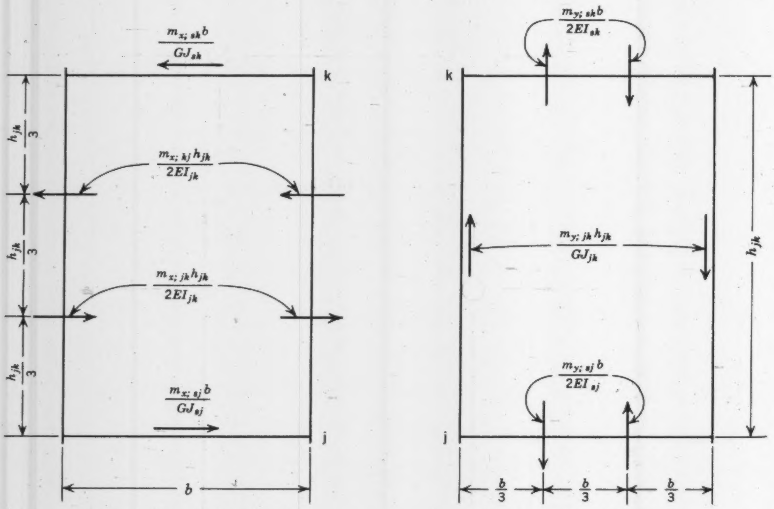
$\frac{m_{x;sk}b}{GJ_{sk}}$
k
$\frac{h_{jk}}{3}$
$\frac{m_{x;kj}h_{jk}}{2EI_{jk}}$
$\frac{h_{jk}}{3}$
$\frac{m_{x;jk}h_{jk}}{2EI_{jk}}$
$\frac{h_{jk}}{3}$
$\frac{m_{x;sj}b}{GJ_{sj}}$
j
b
$\frac{m_{y;sk}b}{2EI_{sk}}$
k
$\frac{m_{y;jk}h_{jk}}{GJ_{jk}}$
h_{jk}
$\frac{m_{y;sj}b}{2EI_{sj}}$
j
$\frac{b}{3}$
$\frac{b}{3}$
$\frac{b}{3}$

(*a*) ANGLE CHANGES, $\delta\theta_x$ (*b*) ANGLE CHANGES, $\delta\theta_y$

FIG. 3.—GEOMETRY OF CLOSED PANEL

and the transverse shears, v_z, are constant along the leg between the joints. Statics also yields,

$$m_{x;ji} = h_{ij}\ v_{z;ij} - m_{x;ij} \ \ldots\ldots\ldots\ldots\ldots\ldots \ (4a)$$

and

$$m_{x;kj} = h_{jk}\ v_{z;jk} - m_{x;jk} \ \ldots\ldots\ldots\ldots\ldots\ldots \ (4b)$$

for legs ij and jk, respectively. For a strut (Fig. 2), the values of the twisting moments, m_x, and the transverse shears, v_z, are constant along the length of the strut between its adjacent joints. Also,

$$2\ m_{y;sj} = b\ v_{z;sj} \ \ldots\ldots\ldots\ldots\ldots\ldots \ (5a)$$

and

$$2\, m_{y;sk} = b\, v_{z;sk} \quad \text{. . . . .(5b)}$$

for struts j and k, respectively.

Now consider an element of the tower as shown in Fig. 5. The element consists of an interior panel (jjkk) and portions of the legs in the adjacent panels. For the element as shown, full lengths of legs ij and only stubs of legs kℓ are considered. The reasons for selecting this element in the analysis will become apparent. Now select the moments and shears at sections ij, jk, and kℓ of the legs in the element as reference moments and shears. Observe that only the values of m_x and v_z at these sections need be selected as references because the value of m_y in a leg is related to v_z as given by Eq. (3). In terms of the reference moments m_x and v_z the following equations for moments and shears can be obtained by means of statics:

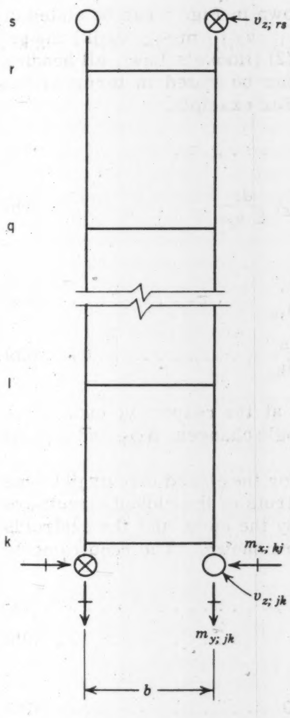

FIG. 4.—PORTION OF TOWER

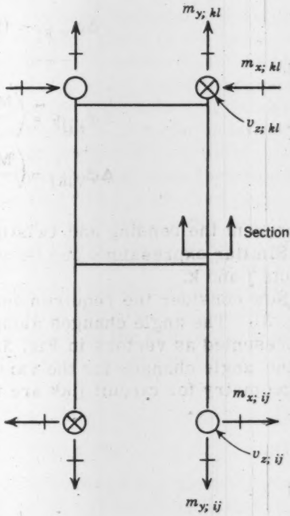

FIG. 5.—ELEMENT OF TOWER

$$m_{x;sj} = m_{x;jk} + h_{ij}\, v_{z;ij} - m_{x;ij} \quad \text{. . . . .(6a)}$$

$$m_{x;sk} = m_{x;k\ell} + h_{jk}\, v_{z;jk} - m_{x;jk} \quad \text{. . . . .(6b)}$$

$$m_{y;sj} = \frac{b}{2}(v_{z;jk} - v_{z;ij}) \quad \ldots\ldots\ldots\ldots \text{(6c)}$$

$$m_{y;sk} = \frac{b}{2}(v_{z;k\ell} - v_{z;jk}) \quad \ldots\ldots\ldots\ldots \text{(6d)}$$

$$v_{z;sj} = v_{z;jk} - v_{z;ij} \quad \ldots\ldots\ldots\ldots \text{(6e)}$$

and

$$v_{z;sk} = v_{z;k\ell} - v_{z;jk} \quad \ldots\ldots\ldots\ldots \text{(6f)}$$

Thus, all moments and shears in the element shown in Fig. 5 can be stated in terms of the reference moments and shears; $m_{x;ij}$, $v_{z;ij}$; $m_{x;jk}$, $v_{z;jk}$; $m_{x;k\ell}$; and M_y. Observe that by means of Eqs. (1) and (2) (Hooke's Law), all bending and twisting deformations of the element can also be stated in terms of the same reference moments and shears, and M_y. For example,

$$\Delta\phi_{x;jk} = m_{x;jk}\,\frac{ds}{E\,I_{jk}} \quad \ldots\ldots\ldots\ldots \text{(7a)}$$

$$\Delta\phi_{x;kj} = (h_{jk}\,v_{z;jk} - m_{x;jk})\,\frac{ds}{E\,I_{kj}} \quad \ldots\ldots\ldots\ldots \text{(7b)}$$

and

$$\Delta\phi_{y;jk} = \left(\frac{M_y - b\,v_{z;jk}}{2}\right)\frac{ds}{G\,J_{jk}} \quad \ldots\ldots\ldots\ldots \text{(8a)}$$

$$\Delta\phi_{y;kj} = \left(\frac{M_y - b\,v_{z;jk}}{2}\right)\frac{ds}{G\,J_{kj}} \quad \ldots\ldots\ldots\ldots \text{(8b)}$$

represent the bending and twisting deformations at the respective ends of leg jk. Similar expressions can be written for the angle changes, $\Delta\phi_x$ and $\Delta\phi_y$, of struts j and k.

Now consider the requirements of geometry for the closed circuit jjkk (see Fig. 3). The angle changes along the legs and struts of the closed circuit are represented as vectors in Fig. 3. In Fig. 3, only the sums and the centroids of the angle changes for the various members are shown. The requirements of geometry for circuit jjkk are fulfilled when

$$\Sigma\Delta\phi_x = 0 \quad \ldots\ldots\ldots\ldots \text{(9a)}$$

$$\Sigma\Delta\phi_y = 0 \quad \ldots\ldots\ldots\ldots \text{(9b)}$$

and

$$\Sigma y\,\Delta\phi_x + \Sigma x\,\Delta\phi_y = 0 \quad \ldots\ldots\ldots\ldots \text{(9c)}$$

Eqs. (9) hold because for any closed circuit, the sum of the angle changes about any axis must equal zero and, if the angle changes are small, the sum of the angle changes times their respective distances to any axis must equal zero. Eq. (9b) is automatically satisfied for circuit jjkk because of anti-symmetry. From Eqs. (9a) and (9c) and by rearranging terms, the following equations are obtained:

$$m_{x;k\ell} = K_{x;k\ell}'\,m_{x;ij} + K_{z;k\ell}'\,h_{ij}\,v_{z;ij} + K_{x;k\ell}\,m_{x;jk} + K_{z;k\ell}\,h_{jk}\,v_{z;jk} \cdot \quad \text{(10a)}$$

$$h_{k\ell}\, v_{z;k\ell} = C_{x;k\ell}'\, m_{x;ij} + C_{z;k\ell}'\, h_{ij}\, v_{z;ij} + C_{x;k\ell}\, m_{x;jk} + C_{z;k\ell}\, h_{jk}\, v_{z;jk} + C_{y;k\ell}\, M_y \qquad (10b)$$

in which $K_{x;k\ell}'$ through $C_{y;k\ell}$ are coefficients which are summarized in the Appendix. These coefficients are dimensionless and depend on the relative bending and torsional stiffnesses of the legs and of the struts; that is, they depend on the values of the a and e terms of the respective panels. The a and e terms are listed in the notations. For example:

$$a_{k\ell} = h_{k\ell}/b \qquad (11a)$$

$$e_{1;k\ell} = E\, I_{jk}/G\, J_{jk} \qquad (11b)$$

and

$$e_{2;k\ell} = E\, I_{sj}/\, E\, I_{jk} \qquad (11c)$$

Eqs. (10a) and (10b) relate the reference moment and shear at section $k\ell$ of the tower with the reference moments and shears at sections ij and jk, respectively. Although the equations are stated in terms of moments and shears, they are equations of geometry for panel jjkk and take into account the requirements of statics for each segment of the element, and the properties of materials. Two such equations can be written for each panel of the tower. The resulting simultaneous equations can be solved for the moments and shears in the tower in any number of possible ways. For example, the resulting equations can be solved by means of iteration or by successive elimination of unknowns. If desired, the equations can be written in matrix form and can be solved by means of an inverse matrix. The solution will be presented herein in another form and is an example of a more general method that has been developed by the senior writer. The general method will be described in another paper.

Concerning the solution herein, Eqs. (10a) and (10b) are recurrence equations; that is, the same kinds of equations recur for each panel of the tower. Consequently, all moments, shears, and displacements of the tower can be stated in terms of a reference moment and shear at a selected section of the tower and in terms of M_y. In this case, the reference moment and shear are selected to be $m_{x;01}$ and $v_{z;01}$ at the base of the tower. In terms of the reference moment and shear, and M_y, the moment and shear at section $k\ell$ are respectively written as follows:

$$m_{x;k\ell} = T_{x;k\ell}\, m_{x;01} + T_{z;k\ell}\, h_{01}\, v_{z;01} + T_{y;k\ell}\, M_y \qquad (12a)$$

$$h_{k\ell}\, v_{z;k\ell} = N_{x;k\ell}\, m_{x;01} + N_{z;k\ell}\, h_{01}\, v_{z;01} + N_{y;k\ell}\, M_y \qquad (12b)$$

in which $T_{x;k\ell}$ through $N_{y;k\ell}$ are influence coefficients and are associated with section $k\ell$. In the same way, the moments and shears at sections jk and ij are written as:

$$m_{x;jk} = T_{x;jk}\, m_{x;01} + T_{z;jk}\, h_{01}\, v_{z;01} + T_{y;jk}\, M_y \qquad (13a)$$

$$h_{jk}\, v_{z;jk} = N_{x;jk}\, m_{x;01} + N_{z;jk}\, h_{01}\, v_{z;01} + N_{y;jk}\, M_y \qquad (13b)$$

and

$$m_{x;ij} = T_{x;ij}\, m_{x;01} + T_{z;ij}\, h_{01}\, v_{z;01} + T_{y;ij}\, M_y \qquad (13c)$$

$$h_{ij}\, v_{z;ij} = N_{x;ij}\, m_{x;01} + N_{z;ij}\, h_{01}\, v_{z;01} + N_{y:ij} \cdot M_y. \qquad (13d)$$

in which $T_{x;jk}$ through $N_{y;jk}$ and $T_{x;ij}$ through $N_{y;ij}$ are associated with sections jk and ij, respectively.

Now substitute Eqs. (12a) to (13d) into Eqs. (10a) and (10b). Observe that the coefficients of $m_{x;01}$, h_{01} $v_{z;01}$, and M_y on the left side of each resulting equation must equal the coefficients of the corresponding terms on the right side of the same equation. From these Eqs., the following relationships between the T and N terms at sections ij, jk, and kℓ are obtained:

$$\left\{\begin{array}{llllll} T_{x;k\ell} = & K_{x;k\ell}'\, T_{x;ij} & + K_{z;k\ell}'\, N_{x;ij} & + K_{x;k\ell}\, T_{x;jk} & + K_{z;k\ell}\, N_{x;jk} & \ldots \text{(14a)} \\ \bullet\ = & \bullet & \bullet & \bullet & \bullet & \text{(14b)} \\ \bullet\ = & \bullet & \bullet & \bullet & \bullet & \text{(14c)} \end{array}\right.$$

and

$$\left\{\begin{array}{llllll} N_{x;k\ell} = & C_{x;k\ell}'\, T_{x;ij} & + C_{z;k\ell}'\, N_{x;ij} & + C_{x;k\ell}\, T_{x;jk} & + C_{z;k\ell}\, N_{x;jk} & \ldots \text{(15a)} \\ \bullet\ = & \bullet & \bullet & \bullet & \bullet\ +C_{y;k\ell} & \text{(15b)} \\ & \bullet & \bullet & \bullet & \bullet & \text{(15c)} \end{array}\right.$$

All of these equations are essentially of the same form, except Eq. (15b). The equations that are not specifically written above can be formed by a cyclical substitution of the y and z subscripts for the x subscripts of the T and N terms (where the dots are shown). Also, Eq. (15b) has a $C_{y;k\ell}$ term in it whereas the others do not. The $C_{y;k\ell}$ term in Eq. (15b) is a result of the same term appearing in Eq. (10b).

Eqs. (14) and (15) are recurrence equations for the interior panels of the towers. However, the values of the T and N terms at the base and at the top of the tower need be defined. An inspection of the boundary conditions at the base of the tower yields the following values of $T_{x;b0}$ through $N_{z;b0}$ and $T_{x;01}$ through $N_{z;01}$:

$$T_{x;b0} = 0; \quad T_{y;b0} = 0; \quad T_{z;b0} = 0 \quad \ldots\ldots\ldots\ldots \text{(16a)}$$

$$N_{x;b0} = 0; \quad N_{y;b0} = 0; \quad N_{z;b0} = 0 \quad \ldots\ldots\ldots\ldots \text{(16b)}$$

and

$$T_{x;01} = 1; \quad T_{y;01} = 0; \quad T_{z;01} = 0 \quad \ldots\ldots\ldots\ldots \text{(17a)}$$

$$N_{x;01} = 0; \quad N_{y;01} = 0; \quad N_{z;01} = 1 \quad \ldots\ldots\ldots\ldots \text{(17b)}$$

In Eqs. (16a) and (16b) the subscripts b0 are introduced for ease in defining the boundary conditions at the base of the tower and in obtaining the values of the T and N terms for the interior panels of the tower. The subscripts b0 are associated with an imaginary panel below panel 0011.

The values of the T and N terms which are given by Eqs. (16) and (17) are for a tower that is fixed at its base; that is, strut 0 is infinitely stiff. They can easily be adjusted for a tower that is hinged at its base. For the case being considered, the values are verified as follows: From Eq. (12) and with the above values of $T_{x;01}$ through $N_{z:01}$, we obtain

$$m_{x;01} = T_{x;01}\, m_{x;01} + T_{z;01}\, h_{01} v_{z;01} + T_{y;01}\, M_y = I\, m_{x;01} \quad \ldots\ldots \tag{18a}$$

and

$$h_{01} v_{z;01} = N_{x;01}\, m_{x;01} + N_{z;01} h_{01} v_{z;01} + N_{y;01}\, M_y = I\, h_{01} v_{z;01} \quad \ldots \tag{18b}$$

Further, from Eqs. (40a) to (41e) (see Appendix), we obtain

$$T_{x;12} = K_{x;12}; \quad T_{y;12} = 0 \quad T_{z;12} = K_{z;12} \quad \ldots\ldots \tag{19a}$$

and

$$N_{x;12} = C_{x;12}; \quad N_{y;12} = C_{y;12}; \; N_{z;12} = C_{z;12} \quad \ldots \tag{19b}$$

These relationships, when substituted into Eq. (12), yield

$$m_{x;12} = K_{x;12}\, m_{x;01} + K_{z;12}\, h_{01}\, v_{z;01} + 0 \cdot M_y \quad \ldots\ldots\ldots\ldots \tag{20a}$$

and

$$h_{12}\, v_{z;12} = C_{x;12}\, m_{x;01} + C_{z;12}\, h_{01}\, v_{z;01} + C_{y;12}\, M_y \quad \ldots\ldots\ldots \tag{20b}$$

Eqs. (20) are identical to those obtained by means of Eqs. (10). In this way, the values of $T_{x;b0}$ through $N_{z;b0}$ and $T_{x;01}$ through $N_{z;01}$ are verified.

The values of the T and N terms for each section of a tower can now be obtained by means of the boundary conditions at the base of the tower (see Eqs. (16) and (17)) and by means of the recurrence Eqs. (14) and (15). In other words, all moments and shears in the tower now are known in terms of $m_{x;01}$, $h_{01}\ v_{z;01}$, and M_y (see Eqs. (12)). The only unknowns at this stage of the analysis are the values of $m_{x;01}$ and $h_{01}\ v_{z;01}$ at the base of the tower. The boundary conditions at the base of the tower and the requirements of statics and geometry for each panel of the tower are already satisfied. It only remains to satisfy the boundary conditions at the top of the tower (Fig. 4).

The unbalanced horizontal component of the cable tension at the top of a saddle is resisted by a projecting leg of the tower as shown in Fig. 4. The shear in a projecting leg of the tower is given by

$$v_{z;rs} = M_y/b \quad \ldots\ldots\ldots\ldots\ldots\ldots \tag{21}$$

By definition of a moment and shear, the following relationships are obtained:

$$m_{x;rs} = a_{rs}\, M_y \quad \ldots\ldots\ldots\ldots\ldots \tag{22a}$$

and

$$h_{rs} v_{z;rs} = a_{rs}\, M_y \quad \ldots\ldots\ldots\ldots\ldots \tag{22b}$$

in which $a_{rs} = h_{rs}/b$. However, from Eqs. (12), we also have

$$m_{x;rs} = T_{x;rs}\, m_{x;01} + T_{z;rs}\, h_{01}\, v_{z;01} + T_{y;rs}\, M_y. \quad \ldots\ldots \tag{23a}$$

and

$$h_{rs}\, v_{z;rs} = N_{x;rs}\, m_{x;01} + N_{z;rs}\, h_{01} v_{z;01} + N_{y;rs}\, M_y. \quad \ldots \tag{23b}$$

in which the coefficients $T_{x;rs}$ through $N_{y;rs}$ are defined by the boundary conditions at the base of the tower (see Eqs. (17) and by the recurrence equations Eqs. (14) and (15). The values of $m_{x;01}$ and $h_{01}\ v_{x;01}$ are determined by means of the boundary conditions at the top of the tower (see Eqs. (22)). From these conditions and Eqs. (23), we obtain

$$m_{x;01} = X_{rs}\, M_y \quad \ldots\ldots\ldots\ldots\ldots \tag{24a}$$

$$m_{y;01} = Y_{rs} M_y \quad \text{(24b)}$$

and

$$h_{01} v_{z;01} = Z_{rs} M_y \quad \text{(24c)}$$

in which

$$X_{rs} = \frac{(a_{rs} - T_{y;rs}) N_{z;rs} - (a_{rs} - N_{y;rs}) T_{z;rs}}{T_{x;rs} N_{z;rs} - N_{x;rs} T_{z;rs}} \quad \text{(25a)}$$

$$Z_{rs} = \frac{(a_{rs} - N_{y;rs}) T_{x;rs} - (a_{rs} - T_{y;rs}) N_{x;rs}}{T_{x;rs} N_{z;rs} - N_{x;rs} T_{z;rs}} \quad \text{(25b)}$$

and

$$Y_{rs} = \frac{a_{01} - Z_{rs}}{2\, a_{01}} \quad \text{(25c)}$$

All moments and shears in the tower are now defined. For example:

$$m_{x;k\ell} = X_{k\ell} M_y \quad \text{(26a)}$$

$$h_{k\ell} v_{z;k\ell} = Z_{k\ell} M_y \quad \text{(26b)}$$

and

$$m_{y;k\ell} = Y_{k\ell} M_y \quad \text{(26c)}$$

in which

$$X_{k\ell} = T_{x;k\ell} X_{rs} + T_{z;k\ell} Z_{rs} + T_{y;k\ell} \quad \text{(27a)}$$

$$Z_{k\ell} = N_{x;k\ell} X_{rs} + N_{z;k\ell} Z_{rs} + N_{y;k\ell} \quad \text{(27b)}$$

and

$$Y_{k\ell} = \frac{a_{k\ell} - Z_{k\ell}}{2\, a_{k\ell}} \quad \text{(27c)}$$

Eqs. (26) and (27) are valid for any other section of the tower, as for example section jk. For the latter section, the above equations are rewritten by substituting jk for $k\ell$.

Geometrical Relationships.—The slopes and displacements of the joints of the tower, and the chord rotations of the struts, can be determined by means of elementary geometry. Fig. 6 shows the contributions of the angle changes in a leg jk to the slopes and displacement at a joint m. In determining the total slopes and displacement at a joint m, the contributions of the angle changes of all legs, 01 through ℓm, must be considered. Consequently, the slopes $\theta_{x;m}$ and $\theta_{y;m}$ at a joint m are given by

$$\theta_{x;m} = \int_0^m d\theta_x = M_y \sum_{k=1}^{k=m} \frac{h_{jk}}{E\, I_{jk}} \left[X_{jk} - \frac{1}{2} Z_{jk} \right] \quad \text{(28a)}$$

and

$$\theta_{y;m} = \int_0^m d\theta_y = M_y \sum_{k=1}^{k=m} \frac{h_{jk}}{G\, J_{jk}} Y_{jk} \quad \text{(28b)}$$

in which the summations are for legs 01 through ℓm. The displacement of joint m, in the direction of the z axis, is given by

$$\Delta_{z;m} = \int_0^m y_m \, d\theta_x \quad \ldots\ldots\ldots\ldots\ldots \quad (28c)$$

in which y_m is positive downward and is measured from joint m to each respective angle change, $d\theta_x$. Eq. (28c) is rewritten as follows:

$$\Delta_{z;m} = M_y \left[\begin{array}{l} \displaystyle\sum_{k=1}^{k=m} \frac{h_{jk}}{E\,I_{jk}} \left(h_m - h_k + \frac{1}{2} h_{jk}\right) X_{jk} \\ \displaystyle -\frac{1}{2} \sum_{k=1}^{k=m} \frac{h_{jk}}{E\,I_{jk}} \left(h_m - h_k + \frac{1}{3} h_{jk}\right) Z_{jk} \end{array} \right] \quad \ldots\ldots \quad (29)$$

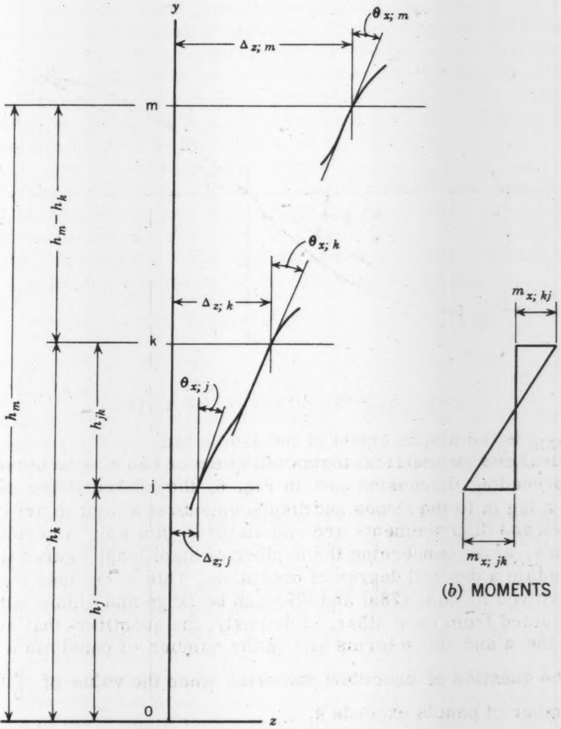

(a) DISPLACEMENTS

(b) MOMENTS

FIG. 6.—CONTRIBUTIONS TO SLOPES AND DISPLACEMENTS

in which h_m and h_k are distances measured from the base of the tower to joints m and k, respectively. The rotation about the y axis of a chord through the ends of a strut at elevation m is given by

$$\psi_{y;m} = \frac{2}{b} \Delta_{z;m} \quad \text{. . . . .} \quad (30)$$

and is shown in Fig. 7.

The slopes, displacement, and rotation at the top of the tower are given by the same equations as Eqs. (28), (29), and (30), except that s is substituted for m. If the torsional rigidity of the tower is defined by

$$(G\,J)_{tower} = \frac{M_y}{\psi_{y;s}} h_s \quad \text{. . . . .} \quad (31)$$

then

$$(G\,J)_{tower} = \frac{b\,h_s}{2\,\Delta_{z;s}} M_y \quad \text{. . . . .} \quad (32)$$

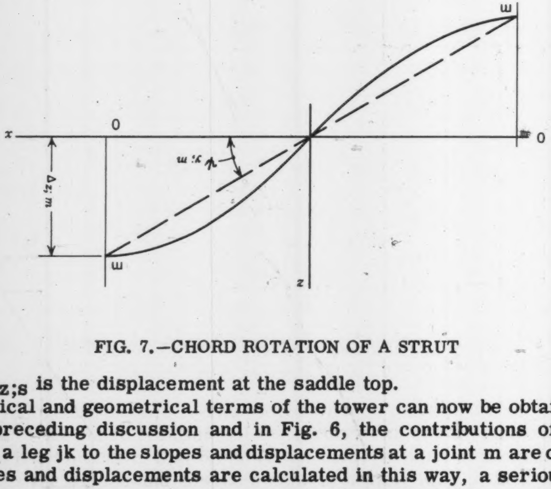

FIG. 7.—CHORD ROTATION OF A STRUT

in which $\Delta_{z;s}$ is the displacement at the saddle top.

All statical and geometrical terms of the tower can now be obtained.

In the preceding discussion and in Fig. 6, the contributions of the angle changes in a leg jk to the slopes and displacements at a joint m are considered. If the slopes and displacements are calculated in this way, a serious question can, at times, arise concerning the number of significant figures that are required to obtain a desired degree of precision. This is because the quantities that are involved in Eqs. (28a) and (29) can be large and almost alike and are being subtracted from each other. Obviously, the quantities that are involved depend on the a and the e terms and on the number of panels in a tower. In general, the question of precision can arise when the value of h/b is about 4 and the number of panels exceeds 4.

When desired, the sequence of calculations for slopes and displacements can be modified by rewriting Eqs. (28) and (29) in a form that will improve the accuracy of the computations. This can be done by calculating the changes, $\delta\theta_x$ and $\delta\Delta_z$, that occur between each pair of adjacent struts, and successively calculating the slope and displacement at each strut until the slope and displacement at strut m (or r) is obtained.

A TABULAR FORM FOR CALCULATIONS

Table 1 can be used for the systematic calculations of the moments and shears in a tower that is subjected to a torque. The calculations are for moments and shears only because the geometrical relationships of the tower can only be obtained when the moments and shears are known (see Eqs. (28a) to (32)).

Table 1 consists of several rows and columns as in a matrix. Table 1 is a matrix but will not be described as such at this time. In column A, the values of the K', K, C', and C terms as given by Eqs. (40) and (41) (see Appendix) are listed for each section from 12 through rs. No such values need be computed for sections b0 to 01. If desired, a separate table (or program) can be defined for computing the values of the K', K, C', and C terms for the various sections of the tower. These terms depend only on the relative proportions of the panels of the tower and on the relative stiffnesses to bending and torsion of the legs and the struts of the tower. Consequently, these terms can firstly be computed for each section of a given tower and can then be listed in the table as shown. It will be observed that in column A provision also has been made for writing $m_{x;k\ell}$ and $h_{k\ell}\, v_{z;k\ell}$ for each section $k\ell$; that is, for each section 01 through rs. The reason for this provision will be explained later.

Col. B, C, and D of Table 1 are headed by $m_{x;01}$, $h_{01}\, v_{z;01}$, and M_y, respectively. The calculations and terms that are listed in a column are associated with the heading of the column. In the same way, the calculations and terms that are listed in a row, such as $k\ell$, are associated with the section that is designated by the row. The calculations and terms that are listed in the table are for the T and N terms of the following equations:

$$m_{x;k\ell} = T_{x;k\ell}\, m_{x;01} + T_{z;k\ell}\, h_{01}\, v_{z;01} + T_{y;k\ell}\, M_y \; . \; . \; . \; . \; . \qquad (33a)$$

and

$$h_{k\ell}\, v_{z;k\ell} = N_{x;k\ell}\, m_{x;01} + N_{z;k\ell}\, h_{01}\, v_{z;01} + N_{y;k\ell}\, M_y \; . \; . \; . \; . \; . \qquad (33b)$$

Observe that the same equations, except for subscripts, can be read in Table 1 for each section of the tower.

To calculate the T and N terms that are associated with each section of the tower, proceed as follows:

(1) Enter in rows b0 and 01 the values of the T and N terms that are associated with the boundary conditions at the base of the tower. These values are given by Eqs. (16) and (17).

(2) Now calculate in a consecutive way the values of the T and N terms that are associated with sections 12 through rs. These values are calculated by means of Eqs. (14) and (15) and are listed in Table 1 as sums of corresponding products. Observe that the values of the T and N terms for a given section are obtained by means of the values that were obtained for the T and N terms of the two preceding sections. Also observe that for a section such as $k\ell$ the calculations of the T and N terms are listed in rows and are identical in form to each other, except for the calculations of $N_{y;k\ell}$. In the latter calculation, the value of $C_{y;k\ell}$ must be included as shown.

TABLE 1.—FORM FOR CALCULATIONS

Section	Ⓐ	Ⓑ $m_{x;01}$	Ⓒ $h_{01}V_{z;01}$	Ⓓ M_y
b0	$m_{x;b0}$	$T_{x;b0} - 0$	$T_{z;b0} = 0$	$T_{y;b0} = 0$
	$h_{b0}V_{z;b0}$	$N_{x;b0} = 0$	$N_{z;b0} = 0$	$N_{y;b0} = 0$
01	$m_{x;01}$	$T_{x;01} = 1$	$T_{z;01} = 0$	$T_{y;01} = 0$
	$h_{01}V_{z;01}$	$N_{x;01} = 0$	$N_{z;01} = 1$	$N_{y;01} = 0$
	⋮	⋮	⋮	⋮
kℓ	$K_{x;k\ell}^{1} = \surd$	$\surd\cdot T_{x;ij} = \surd\surd$	$\surd\cdot T_{z;ij} = \surd\surd$	$\surd\cdot T_{y;ij} = \surd\surd$
	$K_{z;k\ell}^{1} = \surd$	$\surd\cdot N_{x;ij} = \surd\surd$	$\surd\cdot N_{z;ij} = \surd\surd$	$\surd :N_{y;ij} = \surd\surd$
	$K_{x;k\ell} = \surd$	$\surd\cdot T_{x;jk} = \surd\surd$	$\surd\cdot T_{z;jk} = \surd\surd$	$\surd\cdot T_{y;jk} = \surd\surd$
	$K_{z;k\ell} = \surd$	$\surd\cdot N_{x;jk} = \surd\surd$	$\surd\cdot N_{z;jk} = \surd\surd$	$\surd\cdot N_{y;jk} = \surd\surd$
	$m_{x;k\ell}$	$T_{x;k\ell} = \Sigma\surd\surd$	$T_{z;k\ell} = \Sigma\surd\surd$	$T_{y;k\ell} = \Sigma\surd\surd$
	$C_{x;k\ell}^{1} = \surd$	$\surd\cdot T_{x;ij} = \surd\surd$	$\surd\cdot T_{z;ij} = \surd\surd$	$\surd\cdot T_{y;ij} = \surd\surd$
	$C_{z;k\ell}^{1} = \surd$	$\surd\cdot N_{x;ij} = \surd\surd$	$\surd\cdot N_{z;ij} = \surd\surd$	$\surd\cdot N_{y;ij} = \surd\surd$
	$C_{x;k\ell} = \surd$	$\surd\cdot T_{x;jk} = \surd\surd$	$\surd\cdot T_{z;jk} = \surd\surd$	$\surd\cdot T_{y;jk} = \surd\surd$
	$C_{z;k\ell} = \surd$	$\surd\cdot N_{x;jk} = \surd\surd$	$\surd\cdot N_{z;jk} = \surd\surd$	$\surd\cdot N_{y;jk} = \surd\surd$
	$C_{y;k\ell} = \surd$			$\surd\cdot 1 = \surd\surd$
	$h_{k\ell}V_{z;k\ell}$	$N_{x;k\ell} = \Sigma\surd\surd$	$N_{z;k\ell} = \Sigma\surd\surd$	$N_{y;k\ell} = \Sigma\surd\surd$
	⋮	⋮	⋮	⋮
rs	$K_{x;rs}^{1} = \surd$	$\surd\cdot T_{x;pq} = \surd\surd$	$\surd\cdot T_{z;pq} = \surd\surd$	$\surd\cdot T_{Y;pq} = \surd\surd$
	$K_{z;rs}^{1} = \surd$	$\surd\cdot N_{x;pq} = \surd\surd$	$\surd\cdot N_{z;pq} = \surd\surd$	$\surd\cdot N_{y;pq} = \surd\surd$
	$K_{x;}^{rs} = \surd$	$\surd\cdot T_{x;qr} = \surd\surd$	$\surd\cdot T_{z;qr} = \surd\surd$	$\surd\cdot T_{y;qr} = \surd\surd$
	$K_{z;rs} = \surd$	$\surd\cdot N_{x;qr} = \surd\surd$	$\surd\cdot N_{z;qr} = \surd\surd$	$\surd\cdot N_{y;qr} = \surd\surd$
	$m_{x;rs}$	$T_{x;rs} = \Sigma\surd\surd$	$\surd\ T_{z;rs} = \Sigma\surd\surd$	$T_{y;rs} = \Sigma\surd\surd$
	$C_{x;rs}^{1} = \surd$	$\surd\cdot T_{x;pq} = \surd\surd$	$\surd\cdot T_{z;pq} = \surd\surd$	$\surd\cdot T_{y;pq} = \surd\surd$
	$C_{z;rs}^{1} = \surd$	$\surd\cdot N_{x;pq} = \surd\surd$	$\surd\cdot N_{z;pq} = \surd\surd$	$\surd\cdot N_{y;pq} = \surd\surd$
	$C_{x;rs} = \surd$	$\surd\cdot T_{x;qr} = \surd\surd$	$\surd\cdot T_{z;qr} = \surd\surd$	$\surd\cdot T_{y;qr} = \surd\surd$
	$C_{z;rs} = \surd$	$\surd\cdot N_{x;qr} = \surd\surd$	$\surd\cdot N_{z;qr} = \surd\surd$	$\surd\cdot N_{y;qr} = \surd\surd$
	$C_{y;rs} = \surd$			$\surd\cdot 1 = \surd\surd$
	$h_{rs}V_{z;rs}$	$N_{x;rs} = .\Sigma\surd\surd$	$N_{z;rs} = \Sigma\surd\surd$	$N_{y;rs} = \Sigma\surd\surd$
	$m_{x;01}$ = Eq.34a;		$h_{01}V_{z;01}$ = Eq. 34b	

(3) From the boundary conditions at the top of the tower, calculate the values of $m_{x;01}$ and $h_{01}\ v_{z;01}$; that is, by means of

$$m_{x;01} = \frac{(a_{rs} - T_{y;rs})\, N_{z;rs} - (a_{rs} - N_{y;rs})\, T_{z;rs}}{T_{x;rs}\, N_{z;rs} - N_{x;rs}\, T_{z;rs}}\, M_y \quad . \ . \ . \ . \ (34a)$$

and

$$h_{01}\ v_{z;01} = \frac{(a_{rs} - N_{y;rs})\, T_{x;rs} - (a_{rs} - T_{y;rs})\, N_{x;rs}}{T_{x;rs}\, N_{z;rs} - N_{x;rs}\, T_{z;rs}}\, M_y \quad . \ . \ . \ (34b)$$

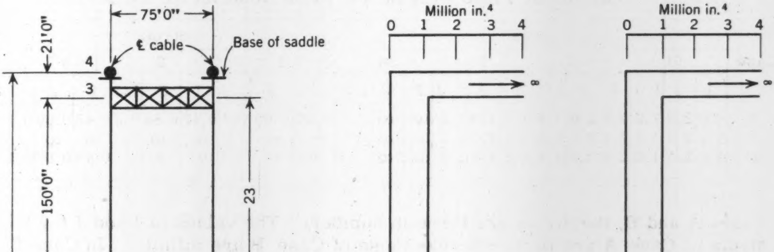

(a) DIMENSIONS (b) VALUES OF I_x (c) VALUES OF J

FIG. 8.—DIMENSIONS OF TOWER

(4) Reenter Table 1 and list the numerical values of $m_{x;01}$ and $h_{01}\ v_{z;01}$. Then calculate, by means of the T and N values that are listed in the table, the numerical values of the moments and shears at sections 12 through rs.

If desired, all other moments and shears can be determined by statics, and the geometrical relationships can be determined by means of Eqs. (28) through (32). Concerning the latter calculations, it is observed that the values of the T and N terms that are implicit in Eqs. (28) and (29) are already listed in the table. The same terms can be used when Eqs. (28a) and (29) are modified because a greater degree of precision is desired.

NUMERICAL EXAMPLES

Three numerical cases (A, B, and C) of a tower are given in this section. The over-all dimensions of the tower are the same for each case and are given in Fig. 8a. The values of I and J also are the same for the legs of each case and are listed in Table 2. Their distribution is as shown in Figs. 8b and 8c. The bending and torsional stiffnesses of the struts are different for each case and are represented by the values of I and J that are listed in Table 2. In Cases A and B, the struts are three in number. The values of I and J for the struts of Case A are finite whereas those of Case B are infinite. In Case C, the tower is braced with a single strut; namely, strut 3. The values of I and J for the latter strut are the same as those for strut 3 of Case A.

TABLE 2.—VALUES OF I AND J (IN 10^6 IN.^{4}) FOR NUMERICAL EXAMPLES

Case	Legs												Struts								
	01			12			23			34			1			2			3		
	I	J	I/J	I	J	I/J	I	J	I/J	I	J	I/J	I	J	I/J	I	J	I/J	I	J	I/J
A	4.0	2.5	1.6	2.8	2.0	1.4	1.2	1.0	1.2	∞	∞		0.36	0.09	0.4	0.42	0.84	0.5	0.48	0.96	0.5
B	4.0	2.5	1.6	2.8	2.0	1.4	1.2	1.0	1.2	∞	∞		∞	∞		∞	∞		∞	∞	
C	4.0	2.5	1.6	2.8	2.0	1.4	1.2	1.0	1.2	∞	∞		0	0		0	0		0.48	0.96	0.5

The analytical procedure is best illustrated by Case A. The values of the e terms firstly are calculated for each panel of the tower. They are summarized in Table 3. The values of the K', K, C', and C terms then are calculated (see Appendix) for sections 12, 23, and 34 of the tower. These values are listed in Table 4. In Table 4, the boundary conditions at the base of the tower are entered and are designated by the values of the T and N terms associated with sections b0 and 01. The values of the T and N terms are defined by Eqs. (14a) to (15c) and are successively calculated for sections 12, 23, and 34. The values of $m_{x;01}$ and $h_{01}\, v_{x;01}$ then are calculated by means of Eqs. (24a) and (24c), respectively, and are listed at the bottom of Table 4. These values can now be reentered in Table 4 to obtain the moments and shears at sections 12 and 23 of the tower (See Eqs. (12)). All other moments and shears in the tower can now be obtained by means of statics only. The final moments and shears at significant stations of the tower are given in Table 5.

TABLE 3.—VALUES OF e TERMS[a] FOR CASE A

	Values of				
	$e_{1;jk}$	$e_{2;jk}$	$e_{3;jk}$	$e_{4;jk}$	$e_{5;jk}$
jk = 01	4.16	∞	∞	0.09	0.36
jk = 12	3.64	0.129	0.45	0.15	0.42
jk = 23	3.12	0.35	0.84	0.40	0.96

[a] For $G = E/2\,(1 + \mu)$; $\mu = 0.3$

For Case B, the analytical procedure becomes greatly simplified as each panel can be treated separately. This is because each panel is bounded by infinite struts. Consider a panel jjkk with infinite struts at j and k. For this panel, the moments and shears in the legs of the panel are given by

$$m_{x;jk} = X_{jk}\, M_y \quad \text{. . . . . (35a)}$$

$$m_{y;jk} = Y_{jk}\, M_y \quad \text{. . . . . (35b)}$$

and

$$h_{jk}\, v_{z;jk} = Z_{jk}\, M_y \quad \text{. . . . . (35c)}$$

in which

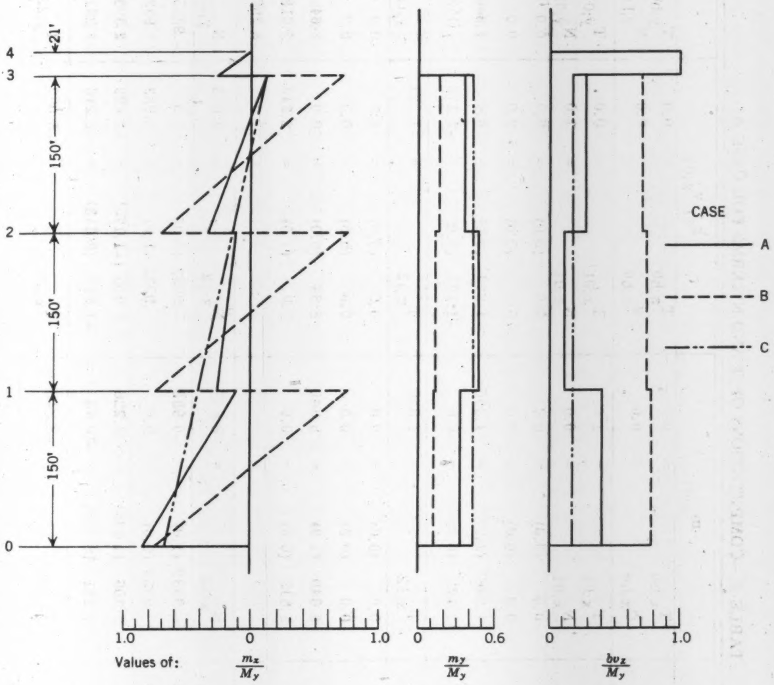

FIG. 9.—MOMENTS AND SHEARS IN TOWER

$$X_{jk} = \frac{a_{jk}\, e_{1;jk}}{2\left[\frac{1}{3}\, a_{jk}^2 + e_{1;jk}\right]} \quad \text{. . . . . (36a)}$$

$$Y_{jk} = \frac{a_{jk}^2}{6\left[\frac{1}{3}\, a_{jk}^2 + e_{1;jk}\right]} \quad \text{. . . . . (36b)}$$

and

$$Z_{jk} = 2\, X_{jk} \quad \text{. . . . . (36c)}$$

From Hooke's Law and considerations of geometry, we obtain

TABLE 4.—COMPUTATIONS OF T AND N TERMS FOR CASE A

Section		$m_{x;01}$	$h_{01}v_{z;01}$	M_y
b0	$m_{x;b0}$	$T_{x;b0}$ = 0.0	$T_{z;b0}$ = 0.0	$T_{y;b0}$ = 0.0
	$h_{b0}v_{z;b0}$	$N_{x;b0}$ = 0.0	$N_{z;b0}$ = 0.0	$N_{y;b0}$ = 0.0
01	$m_{x;01}$	$T_{x;01}$ = 1.0	$T_{z;01}$ = 0.0	$T_{y;01}$ = 0.0
	$h_{01}v_{z;01}$	$N_{x;01}$ = 0.0	$N_{z;01}$ = 1.0	$N_{y;01}$ = 0.0
12	$K_{x;12}$ = 0.0	0.0 (0.0) = 0.0	0.0 (0.0) = 0.0	0.0 (0.0) = 0.0
	$K_{z;12}$ = 0.0	0.0 (0.0) = 0.0	0.0 (0.0) = 0.0	0.0 (0.0) = 0.0
	$K_{x;12}$ = 1.346	1.346 (1.0) = 1.346	1.346 (0.0) = 0.0	1.346 (0.0) = 0.0
	$K_{z;12}$ = -1.173	-1.173 (0.0) = 0.0	-1.173 (0.0) = -1.173	-1.173 (0.0) = 0.0
	$m_{x;12}$	$T_{x;12}$ = 1.346	$T_{z;12}$ = -1.173	$T_{y;12}$ = 0.0
	$C_{x;12}$ = 0.0	0.0 (0.0) = 0.0	0.0 (0.0) = 0.0	0.0 (0.0) = 0.0
	$C_{z;12}$ = 0.0	0.0 (0.0) = 0.0	0.0 (0.0) = 0.0	0.0 (0.0) = 0.0
	$C_{x;12}$ = 8.640	8.640 (1.0) = 8.640	8.64 (0.0) = 0.0	8.64 (0.0) = 0.0
	$C_{z;12}$ = 2.613	2.613 (0.0) = 0.0	2.613 (1.0) = 2.613	2.613 (0.0) = 0.0
	$C_{y;12}$ = -8.986			-8.986 (1.0) = -8.986
	$h_{12}v_{z;12}$	$N_{x;12}$ = 8.640	$N_{z;12}$ = 2.613	$N_{y;12}$ = -8.986
23	$K_{x;23}$ = -0.9333	-.9333 (1.0) = -0.933	-.9333 (0.0) = 0.0	-.9333 (0.0) = 0.0
	$K_{z;23}$ = 0.9333	.9333 (0.0) = 0.0	.9333 (1.0) = 0.933	.9333 (0.0) = 0.0
	$K_{x;23}$ = 2.395	2.395 (1.346) = 3.226	2.395 (-1.173) = -2.809	2.395 (0.0) = 0.0
	$K_{z;23}$ = -1.231	-1.231 (8.640) = -10.63	-1.231 (2.613) = -3.216	-1.231 (-8.986) = 11.06
	$m_{x;23}$	$T_{x;23}$ = -8.343	$T_{z;23}$ = -5.092	$T_{y;23}$ = 11.06

	$C_{x;23}$	= -58.24	-58.24 (1.0) = -58.24	-58.24 (0.0) = 0.0	-58.24 (0.0) = 0.0
	$C_{z;23}$	= 57.07	57.07 (0.0) = 0.0	57.07 (1.0) = 57.07	57.07 (0.0) = 0.0
	$C_{x;23}$	= 72.64	72.64 (1.346) = 97.78	72.64 (-1.173) = -85.21	72.64 (0.0) = 0.0
	$C_{z;23}$	= 3.919	3.919 (8.640) = 33.80	3.919 (2.613) = 10.24	3.919 (-8.986) = -35.22
	$C_{y;23}$	= -13.10			-13.10 (1.0) = -13.10
	$h_{23}v_{z;23}$		$N_{x;23}$ = 73.40	$N_{z;23}$ = -17.90	$N_{y;23}$ = -48.32
34	$K_{x;34}$	= -1.143	-1.143 (1.346) = -1.538	-1.143 (=1.173) = 1.341	-1.143 (0.0) = 0.0
	$K_{z;34}$	= 1.143	1.143 (8.640) = 9.874	1.143 (2.613) = 2.986	1.143 (-8.986) = -10.27
	$K_{x;34}$	= 3.374	3.374 (-8.343) = -25.15	3.374 (-5.092) = -17.18	3.374 (11.06) = 37.29
	$K_{z;34}$	= -1.615	-1.615 (73.40) = -118.6	-1.615 (-17.90) = 28.92	-1.615 (-48.32) = 78.05
	$m_{x;34}$		$T_{x;34}$ = -138.4	$T_{z;34}$ = 16.06	$T_{y;34}$ = 105.1
	$C_{x;34}$	= -9.984	-9.984 (1.346) = -13.44	-9.984 (-1.173) = 11.71	-9.984 (0.0) = 0.0
	$C_{z;34}$	= 8.841	8.841 (8.640) = 76.39	8.841 (2.613) = 23.10	8.841 (-8.986) = -79.44
	$C_{x;34}$	= 15.36	15.36 (-8.343) = -128.2	15.36 (-5.092) = -78.21	15.36 (11.06) = 169.9
	$C_{z;34}$	= .6046	.6046 (73.40) = 44.38	.6046 (-17.90) = -10.82	.6046 (-48.32) = -29.21
	$C_{y;34}$	= -4.193			-4.193 (1.0) = -4.19
	$h_{34}v_{z;34}$		$N_{x;34}$ = -20.82	$N_{z;34}$ = -54.22	$N_{y;34}$ = 57.02

$$m_{x;01} = \frac{(0.28 - 105.1)(-54.22) - (0.28 - 57.02)(16.06)}{(-138.4)(-54.22) - (-20.82)(16.06)} M_y = 0.8412\, M_y$$

$$h_{01}\, v_{z;01} = \frac{(0.28 - 57.02)(-138.4) - (0.28 - 105.1)(-20.82)}{7838} M_y = 0.7234\, M_y$$

$$\delta\Delta_{z;kj} = \frac{h_{jk}^2}{12\ E\ I_{jk}}\ Z_{jk}\ M_y \ \ldots\ldots\ldots\ldots\ (37a)$$

and

$$\delta\psi_{y;kj} = \frac{a_{jk}\ h_{jk}}{6\ E\ I_{jk}} Z_{jk}\ M_y \ \ldots\ldots\ldots\ldots\ (37b)$$

Eqs. (35) and (36) can be verified by means of Eqs. (37) and by means of statics for panel jjkk. For example, Eqs. (36c) can be verified by means of

$$\delta\theta_{y;kj} = \frac{m_{y;jk}\ h_{jk}}{G\ J_{jk}} = \delta\psi_{y;kj} \ \ldots\ldots\ldots\ldots\ (38a)$$

and

$$2\ m_{y;jk} + b\ v_{z;jk} = M_y \ \ldots\ldots\ldots\ldots\ (38b)$$

Eqs. (35) and (36) can also be verified by means of the general equations that are listed in the Appendix. The latter equations are based on the requirements of statics and on the requirements of continuity for a closed panel. The final moments and shears for Case B were obtained by means of Eqs. (35) and (36) and are summarized in Table 5.

Case C is included for comparison with Case A and to indicate that the analytical procedure presented herein can be extended to include the effects of non-prismatic members between the joints of a closed panel. The details of this extension will not be given herein. Suffice it to state that the analytical procedure presented in the preceding section remains the same. The only change that occurs is in the values of the K', K, C', C terms that are listed in the Appendix. The latter values can be obtained by means of the shear and torsion analogy presented by the senior writer in another paper.[12] For the specific case of a tower with a single strut, the latter analogy can be applied directly. It then becomes a special case of the analytical procedure presented herein. The results for Case C are summarized in Table 5.

The final results for Cases A, B, and C are summarized in Table 5 and Fig. 9. Observe that the torsional stiffness (G J) of the tower is about the same for Case A and C and is about 3.25 times greater for Case B. However, the distributions and magnitudes of the moments and shears in the legs and struts of the tower are appreciably different for Cases A, B, and C. For example, the percentage of the total torque that is resisted by the transverse shear in the legs at Section 01 is represented by $bv_{z;01}$ and is 36.2%, 75.7%, and 13.5% for Cases A, B, and C, respectively.

No general conclusions concerning the influence of struts on the torsional behavior of suspension bridge towers are to be made from the above examples. These examples are solely intended to illustrate the analytical procedure of the preceding section. A more detailed study of the torsional characteristics of suspension bridge towers has been made and will be reported on in another paper. The latter study has been made for specific towers, such as the Golden Gate and the Tacoma Narrows Bridge Towers, and for a general class of towers in which the variables are the numbers of struts, height to width ratios of the towers, and the bending and torsional stiffnesses of the legs and struts. The study has been programmed for the use of digital computers and has been specifically coded for an IBM-701 digital computer.

The program for the analysis of a single tower has also been coded for IBM-701 and 704 digital computers.

GENERAL STATEMENTS

The procedure that is presented herein is part of a more general procedure developed by the senior writer. The general procedure will be described in a subsequent paper. It is applicable to any structure that lies in space, is subjected to loads or deformations in any direction, and has elements which lie along a closed path. The elements of the structure can consist of differential elements, curved or segmental members, or closed panels as, for example, in this instance.

TABLE 5.—RESULTS OF NUMERICAL CASES A, B, AND C

			Case A	Case B	Case C
LEGS	m_x/M_y	$m_{x;34}/M_y$	0.28	0.28	0.28
		$m_{x;23}/M_y$	0.358	0.701	0.156
		$m_{x;12}/M_y$	0.284	0.732	0.427
		$m_{x;01}/M_y$	0.841	0.757	0.697
	m_y/M_y	$m_{y;34}/M_y$	0.0	0.0	0.0
		$m_{y;23}/M_y$	0.380	0.150	0.433
		$m_{y;12}/M_y$	0.457	0.134	0.433
		$m_{y;01}/M_y$	0.319	0.121	0.433
	$b\,v_z/M_y$	$b\,v_{z;34}/M_y$	1.0	1.0	1.0
		$b\,v_{z;23}/M_y$	0.240	0.701	0.135
		$b\,v_{z;12}/M_y$	0.086	0.732	0.135
		$b\,v_{z;01}/M_y$	0.362	0.757	0.135
STRUTS	m_x/M_y	$m_{x;3}/M_y$	0.402	0.981	0.394
		$m_{x;2}/M_y$	0.246	1.43	0.0
		$m_{x;1}/M_y$	0.166	1.49	0.0
	m_y/M_y	$m_{y;3}/M_y$	0.380	0.150	0.433
		$m_{y;2}/M_y$	0.0768	-0.0157	0.0
		$m_{y;1}/M_y$	-0.138	-0.0127	0.0
GEOMETRY		$\Delta_{z;4}$* (inches)	5.34	1.68	5.70
		$\Psi_{y;4}$* (10^{-3} Radians)	11.9	3.72	12.7
		GJ_{tower} (10^{12} lb in.^{2})	42.7	137.	40.2

* Values of $\Delta_{z;4}$ and $\Psi_{y;4}$ are for M_y equal to 90 x 10^6 in.-lb

CONCLUSIONS

The specific procedure given herein minimizes the number of calculations that need to be made for the analysis of a tower subjected to a torque. The procedure lends itself to the use of a high-speed digital computer, a desk calculator. All moments, shears, and displacements of the tower are obtained by means of the procedure.

APPENDIX.—NOTATION

The requirements of continuity for a closed circuit jjkk (see Fig. 3) are fulfilled when

$$m_{x;k\ell} = K_{x;k\ell}' \, m_{x;ij} + K_{z;k\ell}' \, h_{ij} \, v_{z;ij} + K_{x;k\ell} \, m_{x;jk} + K_{z;k\ell} \, h_{jk} \, v_{z;jk} \quad (39a)$$

$$h_{k\ell} \, v_{z;k\ell} = C_{x;k\ell}' \, m_{x;ij} + C_{z;k\ell}' \, h_{ij} \, v_{z;ij} + C_{x;k\ell} \, m_{x;jk} + C_{z;k\ell} \, h_{jk} \, v_{z;jk} + C_{y;k\ell} \, M_y \quad \ldots \quad (39b)$$

in which

$$K_{x;k\ell}' = \frac{e_{5;jk}}{e_{3;jk}} \quad \ldots \quad (40a)$$

$$K_{z;k\ell}' = \frac{e_{5;jk}}{e_{3;jk}} \quad \ldots \quad (40b)$$

$$K_{x;k\ell} = (1 + 2 \, a_{jk} \frac{e_{5;jk}}{e_{1;jk}} + \frac{e_{5;jk}}{e_{3;jk}}) \quad \ldots \quad (40c)$$

$$K_{z;k\ell} = -(1 + a_{jk} \frac{e_{5;jk}}{e_{1;jk}}) \quad \ldots \quad (40d)$$

and

$$C_{x;k\ell}' = -12 \, a_{jk} \, a_{k\ell} \frac{e_{1;jk} \, e_{4;jk}}{e_{3;jk}} \quad \ldots \quad (41a)$$

$$C_{z;k\ell}' = 12 \, a_{jk} \, a_{k\ell} \frac{e_{1;jk} \, e_{4;jk}}{e_{3;jk}} - \frac{a_{k\ell}}{a_{ij}} \frac{e_{4;jk}}{e_{2;jk}} \quad \ldots \quad (41b)$$

$$C_{x;k\ell} = 12 \, a_{jk} \, a_{k\ell} \frac{e_{1;jk} \, e_{4;jk}}{e_{3;jk}} + 12 \, a_{jk}^2 \, a_{k\ell} \, e_{4;jk} \quad \ldots \quad (41c)$$

$$C_{z;k\ell} = \frac{a_{k\ell}}{a_{jk}} \quad 1 + \frac{e_{4;jk}}{e_{2;jk}} + 6 \, a_{jk} \, e_{1;jk} \, e_{4;jk} - 4 \, a_{jk}^3 \, e_{4;jk} \quad \ldots \quad (41d)$$

$$C_{y;k\ell} = -6 \, a_{jk} \, a_{k\ell} \, e_{1;jk} \, e_{4;jk} \quad \ldots \quad (41e)$$

The various a and e terms are dimensionless ratios and are listed in the Notations.

The above equations can be verified by inspecting the requirements of geometry for panel jjkk; namely,

$$\Sigma \Delta \phi_x = 0 \quad \ldots \quad (42a)$$

$$\Sigma \Delta \phi_y = 0 \quad \ldots \quad (42b)$$

and

$$\Sigma y \; \Delta\phi_x + \Sigma x \Delta\phi_y = 0 \; . \; . \; . \; . \; . \; . \; . \; . \; . \; . \; . \; . \; . \; . \; (42c)$$

An inspection of Fig. 3 shows that Eq. (42b) is automatically satisfied because the distribution of the angle changes, $\Delta\phi_y$, is anti-symmetric with respect to the vertical axis. From Fig. 3, Eq. (42a) can be rewritten as

$$\frac{b}{G\,J_{sk}}\, m_{x;sk} + \frac{h_{jk}}{E\,I_{jk}}\, m_{x;kj} - \frac{b}{G\,J_{sj}}\, m_{x;sj} = \frac{h_{jk}}{E\,I_{jk}}\, m_{x;jk} = 0 \; . \; . \; . \; . \; (43)$$

Substitution of Eqs. (6a), (6b) and (4b) into Eq. (43) yields the expressions for the $K_{x;k\ell}'$ to $K_{z;k\ell}$ terms of Eq. (39a).

The $C_{x;k\ell}'$ to $C_{y;k\ell}$ terms of Eq. (39b) can be obtained by means of Eq. (42c). From Fig. 3, we obtain

$$\Sigma y \; \Delta\phi_x = \frac{bh_{jk}}{G\,J_{sj}}\, m_{x;sj} + \frac{2}{3}\,\frac{h_{jk}^2}{E\,I_{jk}}\, m_{x;jk} - \frac{1}{3}\,\frac{h_{jk}^2}{E\,I_{jk}}\, m_{x;kj} \; . \; . \; . \; . \; . \; . \; . \; (44)$$

in which y is positive downward and is measured from a z-axis at the mid-point of strut k. From Fig. 3, we now obtain

$$\Sigma x \, \Delta\phi_y = \frac{b^2}{6\,E\,I_{sj}}\, m_{y;sj} - \frac{b^2}{6\,E\,I_{sk}}\, m_{y;sk} - \frac{b\,h_{jk}}{G\,J_{jk}}\, m_{y;jk} \; . \; . \; . \; . \; (45)$$

in which x also is measured from the z-axis at the midpoint of strut k. Substitution of Eqs. (44) and (45) into Eq. (42c), and rewriting all moments in terms of the reference moments and shears at sections ij, jk, and $k\ell$, yields the expressions for $C_{x;k\ell}'$ to $C_{y;k\ell}$.

AMERICAN SOCIETY OF CIVIL ENGINEERS

Founded November 5, 1852

TRANSACTIONS

Paper No. 3183

ENGINEERING EDUCATION AND THE CONSTRUCTION INDUSTRY

By C. H. Oglesby,[1] F. ASCE and John W. Fondahl,[2] M. ASCE

With Discussion by Messrs. Paul F. Keim; Theodore B. Appel, Jr.; Henry G. Howard; and C. H. Oglesby and John W. Fondahl

SYNOPSIS

The joint problems confronting civil engineering education and the construction industry are met herein. The point is made that construction should not be considered a business but a definite part of the civil engineering profession. A civil engineer must make the fullest use of his formal education in order to do both engineering and management work. The civil engineering profession has much to gain by strengthening its ties with the construction industry. This could be accomplished through construction-sponsored research in the colleges as well as by the bolstering of college curricula.

INTRODUCTION

The findings of the ASCE Task Committee on Professional Education[3] leave little room for complacency. Rather, they demonstrate clearly that civil engineering has lost stature when compared to other fields of engineering and science. Among the reasons given for this loss are that other fields appear to offer greater challenge and opportunity, a higher regard from the public, and larger financial rewards.

Note.—Published essentially as printed here, in February, 1959, in the Journal of the Construction Division, as Proceedings Paper 1959. Positions and titles given are those in effect when the paper or discussion was approved for publication in Transactions.

[1] Prof. of Civ. Engrg. Stanford Univ., Stanford, Calif.

[2] Assoc. Prof. of Civ. Engrg., Stanford Univ., Stanford, Calif.

[3] "Report of the Task Committee on Professional Education," Civil Engineering, February, 1958, p. 111.

The Task Committee made several recommendations for improving the status of civil engineering, among them that

> "The American Society of Civil Engineers should give greater attention to the needs of the construction industry and to the development of programs whereby the Society and the engineering colleges may better serve the industry."

Without question, this recommendation offers real possibilities. Construction, basically, is a civil engineering function. It requires the knowledge and application of such fundamental subjects as structural theory, soil mechanics, hydraulics, and engineering economy. It is true that construction combines management functions with civil engineering, but the manufacturing industry has also combined mechanical engineering with management. Construction is the nation's largest single industry, with a 1957 dollar volume of $47,000,000,000, or 11% of the gross national product. It offers an almost new area of opportunity that can help civil engineering to regain its position among the professional and scientific fields.

In the past, the prevailing attitude of civil engineers and civil engineering educators has been that construction is not a part of civil engineering. As a result of this attitude, construction has been largely ignored in civil engineering education. However, since World War II, a growing awareness of and attention to construction has been developing in a number of engineering schools.

THE PLACE OF THE CIVIL ENGINEER IN CONSTRUCTION

The Task Committee on Professional Education recommended that ASCE and colleges should better serve the construction industry. This statement by the committee recognizes the Society's policy of including qualified men from the construction industry in its membership, thereby classifying them as professional civil engineers. As a matter of fact, members with construction interests constitute the second-largest segment in the society, if registration in technical divisions can be used as a measure.[4] Of the 49,539 registrations for 1957 in the 14 technical divisions, 8,190 were in the Construction Division. Only the Structural Division, with 12,000 members, was larger. The next two most numerous listings were for the Soil Mechanics and Foundations Division with 5493 and the Highway Division with 5280.

From a somewhat different point of view, one can say that of the major industries with which civil engineers are concerned, construction predominates. A comprehensive survey[5] made in 1946 shows that 65% of all the civil engineers polled are affiliated with construction activities, as contrasted with utilities, 9.1%, personal services (including education) 7.4%, manufacturing 7.4%, and transportation 4.2%. There is, then, much evidence that construction is an area of primary importance to civil engineers. On the other hand, many civil engineers do not consider construction a legitimate part of civil engineering. For example, the Task Committee reported that "only a small percentage of the educators interviewed believe that it is the responsibility of the engineering colleges to provide training in the practical and business side of engineering." Admittedly, "practical and business" and

---

[4] Official Register, ASCE, 1958, p. 23.

[5] "The Engineering Profession in Transition," Engrs. Joint Council, 1947, p. 10.

"construction" are not synonymous terms. Yet the parallel is close enough, when verified by several year's observation, to support the contention that many civil engineering educators believe that education for the construction industry is not a proper function of engineering colleges.

In some states the boards of professional registration discount or refuse to give credit for experience that has been gained in a contractor's organization. In at least one state organizations of consulting engineers have taken militant action to make professional registration for engineers in the employ of contractors difficult, if not impossible. The model registration law sponsored by the National Society of Professional Engineers (NSPE) singles out contractor's employees, and only them, for unfavorable mention. Section 12-6, "Work as Contractor," reads as follows:

> "The mere execution, as a contractor, of work designed by a professional engineer or the supervision of the construction of such work as a foreman or superintendent shall not be deemed to be the practice of engineering."

While there is little doubt that in many cases the execution of such work is not equivalent to the practice of engineering, in other cases the "mere execution" of the work may require engineering skill and knowledge surpassing that of the professional engineer who is responsible for the design. Such a clause will probably result in construction experience being automatically rejected. There is no reason why both construction and design experience cannot be examined at face value to judge if an appropriate degree of engineering competence has been required.

This reluctance on the part of many civil engineers to admit that construction is civil engineering arises mainly through a failure to recognize the great change in construction organizations in the last decade (since 1950). In years-past construction operations were predominately managed by ambitious tradesmen who, by hard work and perserverance, became owners and superintendents. Certainly these men, able as they were, could not be classed as civil engineers. In recent years this situation has changed markedly and the change is continuing at an even faster rate. As the president of one large construction firm puts it "Construction is being taken over by professional people—engineers, accountants and lawyers." Increasingly, graduate engineers are being employed by contractors to be developed into managers and construction superintendents.

There is much evidence to demonstrate how construction personnel is changing. Replies to a questionnaire[6] circulated in 1955 by the Associated General Contractors (AGC), if expanded to cover the industry, would indicate that the contractors' needs for civil engineers would equal the output of all accredited schools in the United States. Although these conclusions may represent an unwarranted extension of limited data, because they are based on a 12% reply to the questionnaire, they indicate clearly that contractors are turning increasingly to the engineering schools for their future executives and supervisors. Engineering teachers can testify that their graduates are entering construction firms in large numbers. Statistics gathered[7] by the AGC in 1955 indicate that between 15% and 25% of the civil engineering graduates enter construction on graduation and more change to it sometime after graduation.

---

[6] The Constructor, November, 1955, p. 70.

[7] The Constructor, William A. Klinger, January, 1956, p. 73.

As a specific example, approximately one-third of all civil engineering graduates from Stanford University since World War II, are with contractors. All the signs are that within a few years, a high percentage of all construction management will be graduate engineers.

At least two forces have contributed to the shift to engineers in management personnel for contractors. One of these is the increasing size and complexity of construction projects that demands that construction supervision have greater ability to visualize, analyze, and fit the many fragments into an integrated whole. Along with this increased complexity of work has come the realization by contractors that engineers are more than "troublemakers" and "surveyors." During World War II, many contractors were forced to hire engineers or to work closely with them, and in so doing, the contractors discovered that engineers had talents that they had not previously noticed.

A second reason for the shift to engineers is that trade unionism has clogged the traditional source of construction supervision, that was the ranks of skilled tradesmen. Contractors increasingly are saying that many of today's workmen have developed such strong union loyalties and are so ingrained with union thinking that they do not make good members of the management team. Also, tightened jurisdictional lines prevent the tradesman from gaining the breadth of knowledge so important in good supervision.

Civil engineers employed by contractors are often called on to do engineering design as well as management and supervision. In many cases the problems encountered are equal in difficulty, if not more difficult than those of the design engineers who developed the original plans for the project. For example, cofferdams, caissons, falsework, and other temporary installations may present much more difficult situations than are involved in the permanent structure. Again, the design of contractor's plant often calls for skills from every area of the civil engineer's education, including structures, hydraulics, soil mechanics, highways, electrical engineering, and thermodynamics.

Why do large numbers of civil engineers find work with contractors preferable to that in the more traditional areas? No single answer applies in all cases, but some of the most common are as follows:

1. Construction offers earlier opportunity for responsibility. In most contracting organizations, engineers are quickly placed in positions of responsibility in which they are faced with technical and management decisions of considerable importance. In contrast, in many public agencies and private design offices, young engineers may serve several years in routine surveying, drafting, and other menial chores before they have this opportunity. Word of these differences travels fast on the college and post-college grapevines and soon influences both new employment and job transfers.

Many civil engineers feel strongly that college graduates need several years apprenticeship before they are given authority to make important decisions. This question could be argued at length, but is not pertinent to this paper. If the young engineer has a choice, he most certainly will choose the position that promises early responsibility.

2. Construction offers a feeling of permanence and belonging. The construction industry is becoming increasingly aware that the key to success is talented and loyal personnel. Where once contractors hired men for a single project and dropped them when it was over, many firms now offer permanence better than that in numerous engineering offices. At the same time, the contractors often have profit-sharing and bonus plans and retirement and insur-

ance schemes equal to or better than those available elsewhere, and even more important, contractors are including their engineers as members of the top management team to a far greater extent than many engineering firms do.

Contrary to popular belief, the writers' experience indicates that permanence in employment, once the trial period is over, is as good with contractors as with public agencies and most private engineering firms. In contrast, continuity of employment is least certain with the private consulting firms that have highly variable work loads. The design staffs of some engineer-contractor firms are likewise affected. Engineers with these firms often find themselves included in a pool of engineers and draftsmen that moves from company to company. Many of them have the status of temporary employees and have little chance to ever become truly a part of the firm.

3. Construction offers financial incentives to the man who is willing to work for them. As a general rule, starting salaries with contractors are about the same as with public agencies and private consulting firms. However, the engineer who does well with a contractor will find that salary increases come more rapidly and that the ceiling is higher than in other fields. In common with private practice, construction also offers the opportunity for the man to have his own business. This avenue is of course closed to the engineer who chooses public works as a career. On the other hand, construction is not for the man who wants a 40-hr week with the leisure time activities that accompany it. He must expect long hours and an intensive work pace.

4. Construction offers a wide variety of problems requiring the use of every phase of the engineer's education. Moreover it is probable that each day will present new situations. Many engineers feel that such diversification offers more challenge and stimulation than those fields that tend to invoke specialized or routine duties.

Thus, construction offers challenge, financial rewards, and variety of work equal to or better than that found in other areas of civil engineering.

THE RESPONSIBILITY OF CIVIL ENGINEERING SCHOOLS TO EDUCATE MEN FOR THE CONSTRUCTION INDUSTRY

Central to the problem of civil engineers in construction is the recommendation of the Task Committee that the engineering colleges better serve the construction industry. This recommendation implies that engineering schools have a responsibility to alter or supplement their present offerings in order to direct more attention to construction. The question is, does such a responsibility exist?

Spokesmen for the construction industry say emphatically that traditional civil engineering education should be modified to meet construction needs. 88% of the contractors who replied to the 1955 AGC survey stated that they preferred emphasis on training in general management, construction planning, and plant layout rather than in advanced engineering design. Any sampling of the opinions of engineering graduates now engaged in construction will provide strong support for this statement. Thus, if civil engineering schools wish to meet the needs of that segment of their graduates that enter construction a reexamination of present offerings is certainly in order.

The arguments of those from the industry will carry little weight with engineers and engineering teachers who believe that construction is really not civil engineering and that those who enter it are in reality leaving the profession. However, there are other considerations. Civil engineering designs are not an end in themselves; they must be converted into concrete, steel, and other materials, and this conversion is called construction. If the designer knows nothing of construction practices, procedures, and costs he cannot possibly produce really economical designs. Neither will he be able to oversee construction work properly and fairly. Thus, some minimum knowledge of construction is essential to civil engineers as designers and field engineers.

In a broader sense, civil engineering as a profession will gain far more than it loses by strengthening its ties with construction. First of all, the glamour and appeal of construction will attract many able young men into civil engineering schools as an avenue into construction. Enrollments will increase in contrast to the present decrease; that will help to regain some of the status that has been lost to other branches. Other areas of civil engineering will also gain men, as some of those who start toward construction will develop other interests instead.

In years ahead the ASCE and other professional societies will be strengthened by an increase in membership. Construction practices will themselves be improved, because, with more civil engineers in construction, there will be increased probability that the ideas and wishes of the design engineer will be closely followed because the contractor's staff will better understand the designer's intentions. Construction work will proceed more smoothly and harmoniously, because of mutual understanding between designer and field engineer on the one hand and contractor on the other. The end result will be better and more economical projects for the engineer's clients.

It is also worth while to consider the results if civil engineering education largely ignores construction. In the first place, construction is demanding and will find technically trained personnel since it offers the rewards that attract competent men. Thus, if civil engineering does not meet its requirements other branches of learning will. Already some schools of architectural engineering, architecture, and business have developed curricula specifically aimed at construction. As of 1956, at least nineteen schools offered curricula[8] and degrees in "light construction," and numerous others have proposed programs in construction engineering. Industrial engineering and management consultants also are looking toward construction as a fruitful field. The signs are plain—if civil engineering ignores construction, other schools and departments will absorb it or new departments will develop. There is, for example, the case in which mechanical engineering grew away from manufacturing and left a void that is now filled by industrial engineering.

THE CONTRIBUTION THAT CIVIL ENGINEERING SCHOOLS CAN MAKE TO CONSTRUCTION

Assuming agreement on the idea that construction is an integral part of civil engineering and that the schools have a responsibility toward it, there then is the further question of what contribution, if any, the engineering schools can make to construction.

Many engineering educators who are unacquainted with the subject think that construction courses are "trade school stuff" and not proper subjects for university study or credit. It must be admitted that construction courses can be taught at a trade-school level with principal attention devoted to routine computations, memorization, and endless details on "how to do it." However, this problem is not unique to construction courses; are not many courses in structures, hydraulics, and highways taught by "handbook" methods, with little attempt to challenge the students' creative and imaginative abilities?

---

[8] Building, U. S. Gypsum Co., Summer, 1956, pp. 7-9.

In construction courses, as in other areas, the subject matter can be presented in a way that develops technical competence and straight thinking of a high order. As one of many examples, carefully designed problems in earthmoving can offer a serious challenge to the students' knowledge of statics and dynamics. Because construction procedures are less bound by restrictions, such as building codes for structures, they offer an excellent vehicle for developing curiosity and a critical attitude about present techniques and methods.

In addition, construction courses provide a highly favorable atmosphere in which to treat subjects of importance to civil engineers as professional men and citizens. These would include among others, engineering economy, construction costs, labor problems, accident prevention, and the legal aspects of engineering. The point of this argument is that construction as a subject should not be condemned or ruled out as being unsuitable for undergraduate or graduate college work. Condemnation, if any, should be aimed at the method in which the subject is treated.

Another impression of many civil engineering instructors is that there is something second-rate and even unethical about contracting. From such a viewpoint it is logical to reason that construction is not a worthwhile topic for professional engineers. This impression arose many years ago when "gyppo" contractors were numerous and dealing with them sometimes involved risking life and limb. To illustrate, the specifications for the Hetch Hetchy Dam of the city of San Francisco, dated May, 1919, contained a clause reading "—the intimidation of any engineer or inspector by the Contractor or any of his employees shall be sufficient reason to annul the contract." Old ideas die slowly, and many civil engineers still retain this impression. Worse yet, many engineering teachers continue to present construction in this light. These men fail to recognize that construction is not only the country's largest industry but that it has "come of age." Too few engineers are aware that the day of the "gyppo" is largely passed, and that the construction industry is mainly under the management of highly qualified professional and business people.

Central to the topic of the contribution that engineering schools can make to construction is that of subject matter. This topic can best be approached in two parts. First, based on the assumption that construction is an integral part of civil engineering activity and that practically all civil engineers will have some dealings with the construction side of their profession, what subject matter should be taught to all students as a part of their required studies? Second, based on the belief that the construction industry is properly looking to the civil engineering schools for their future key personnel and that construction is a field worthy of attention at the college level, what specialized subject matter should be offered to students who wish to prepare for careers in the construction industry?

Considering the first question, it must be recognized that the four-year engineering curriculum is already crowded. At the slightest indication that the time given to any presently included subject matter might be reduced or released, there is strong competition from each field of specialization for that time. It follows that there can be little specialization and no room for the learning of mere techniques that can be acquired in later practice.

The authors feel that there are several bases on which courses can be justified as part of required undergraduate studies. These include:

1. That the subject matter have future value to the majority of students in their professional careers.
2. That the subject matter present fundamentals with which further knowledge can be acquired through graduate study or practice or both.
3. That the subject matter be such that it is either difficult to master through independent effort or that it is extremely unlikely that the majority of students will take the time to pursue it if left to their own choices.
4. That the subject matter develop the broad viewpoint rather than the restricted view of any specialized group in the profession.

The authors feel that a certain minimum knowledge of construction practices meets all of these criteria for inclusion in the four-year civil engineering curriculum. This does not mean that it is necessary or desirable to give construction topics a large segment of the very limited time that is available. However a person must have a starting point before he can, on his own, expand his knowledge of any complex subject. For example, much can be learned about the legal problems of contractor-engineer relations through the technical and daily press, but only if the man has some basic knowledge of contract law and procedures. Thus, two main aims of undergraduate construction courses should be to lay the groundwork for self-education and to stimulate interest.

What should every graduating civil engineer know about construction? He should have an idea of the problems, methods of doing business, and viewpoints of the contractor. He should be well-grounded in the obligations that he will have in the matter of contract administration. He should know that, as a professional engineer, he must act as an impartial judge in disputes between contractor and owner. He must realize his obligation to prepare specifications and contract provisions fairly rather than aimed in the single direction of protecting the owner and engineer. He must recognize that the plans and specifications that he prepares, and his actions in over-seeing the contractor must lead to safe and acceptable working conditions for those employed on the project. He must be concerned with costs because he is not a good engineer if his designs are uneconomical. This involves more than merely designing for minimum material requirements. It demands a genuine appreciation of the advantages of repetition and mass production, re-use of forms, use of standard rather than special items, and simplicity in details. It includes a knowledge of the elements that make up the cost of labor, equipment, and overhead. This in turn involves an introduction to such matters as typical union working rules, questions of labor jurisdiction, how to arrive at a realistic figure for owning and operating a piece of equipment under given conditions, and why "bid-unbalancing" may be a sound and justifiable practice under some circumstances and risky and unethical under others. Finally, he should understand the process of making an estimate and the procedure by which an intelligent contractor puts together a competitive bid. This will not only furnish him means for analyzing his own design work, but it will give him considerably more understanding in the administration of contract work as the representative of an owner.

Much of the material suggested can be presented within the framework of courses now offered in the usual curriculum as, for example, contracts and specifications and structural design. Ideally, all of this subject matter should be presented in such courses without artificial separation between design and construction. A major obstacle to such a procedure is that very few college professors have construction experience or even an understanding attitude towards the contractor's problems. If a faculty includes one or two men with such experience or understanding, then those men should offer the course in contracts and specifications, and consideration should be given to a course with some such title as "Construction Costs and Methods" to cover other topics previously mentioned.

If an engineer's education is aimed specifically at construction, he must have considerably more knowledge than that previously suggested as a minimum for all civil engineers. He must learn something of the problems of law, finance, and labor relations which face all management. He should become familiar with techniques and procedures of other disciplines, such as those of industrial engineering, which offer means for improving construction techniques. He should increase his technical competence so that he can design machines, structures, and devices that will economically and safely do their appointed tasks. All in all, the civil engineer in construction needs advanced professional training just as much as does the structural, hydraulic, or highway engineer.

Some attention to professional subjects needed by engineers in construction may be possible at the undergraduate level. However, it can be found only at the schools at which the curriculum includes elective units and at which construction courses are offered. Even at these schools, however, there will be room for, at the most, three or four construction-related courses. It follows that intensive study, if done in college, must necessarily come in the fifth year.

The report of the Education Committee of the AGC, as reported[9] in October 1956, indicates the thinking of many contractors. It states, in part

> "The group endorsed in principle, as a long-range objective, the proposal by W. A. Klinger[7] for the establishment of five-year college curriculum to educate engineers for the construction industry. The committee also recognized the immediate need of the bachelor of science degree in civil engineering that would be awarded at the end of four yr. The chief purpose of the five-year course, resulting in a master's degree in construction engineering, would be to train the student as a construction administrator."

It is pertinent at this point to raise the question, "Should the construction industry rather than the colleges provide advanced training for its engineers and future executives?" There are now a number of companies, such as the Perini Corp.,[10] who are doing so. In general, the plans place the young engineer in jobs covering the major phases of the companies' operations. Over a period of several years he works in the office on such assignments as quantity takeoff and estimating and in the field as a surveyor, cost engineer, and assistant to a superintendent. These training programs vary widely among companies. In some cases, the schedule of assignments is quite rigidly followed, whereas in others, the company's immediate needs take precedence over the training program. Some companies provide special lectures by company officials and use other means to make the program meaningful, whereas other companies place all responsibility for training on the supervisor under whom the trainee is working.

---

[9] The Constructor, October, 1956, pp. 31-32.

[10] Engineering News-Record, New York, N. Y., November 7, 1957, p. 145.

There are several reasons why the in-service training program is not a satisfactory solution to the over-all problem of education for construction.

1. In-service training programs are suitable only for large firms, because smaller companies do not have the work volume necessary to sustain a group of trainees. It follows that, because the great majority of contracting firms are relatively small in size, in-service programs will not solve the problem for most of the industry. To illustrate, the highway field is one in which the work volume of firms is considerably larger than in many other areas of construction. Yet, of the members of the Highway Division of the AGC, 92% are classed as small businesses because they do less than $5,000,000 volume per year. Few of these firms can or would sustain a training program.

2. Training programs, unless very carefully planned and controlled, will be just apprentice training. Although they will teach the trainees current practices, they will stifle curiosity and a questioning attitude, both of which are essential if the younger men are to develop greater potential than their predecessors.

3. The basic plan for most training programs makes it difficult to obtain and disseminate information on promising new developments both inside and outside the construction field. Keeping abreast of new developments is a full-time job. Then, even if the data are located, it is extremely difficult to distribute the detailed findings to the trainees at their scattered locations. Thus, to have an effective program, the company must establish a full-blown school.

It is presumptuous for educators, who have as yet made little contribution to construction, to suggest that the engineering schools can provide a better education for construction than the industry itself can. There is, however, much precedent in other fields to support this point of view. In the past, prospective lawyers "read" law in law offices, business managers started learning their functions as office boys, and accountants started as bookkeepers. Today, the colleges provide the education for professionals in these and most other fields. Certainly, as construction engineering and management become more and more professional, the colleges will take over the educational role as they have in the other areas.

Research is another area in which the colleges can make a significant contribution to the construction industry, if precedent from other disciplines can be taken as a criterion. Since, to date (1959) there is little more than a stirring in this direction, only scattered proof can be offered.

The construction industry lags far behind most others in expenditures for research. The 48-billion dollar building industry spends approximately 250-million dollars, or 1/2% of its income, for research compared with 3% for several other industries such as chemicals and electrical equipment.[11] Furthermore, 95% of the research in building construction is concerned with manufactured products and materials. Although no data are available on research expenditures on the highway and heavy construction phase of the industry, there is little evidence of formal research except in developmental work by manufacturers of machinery and equipment. Thus, it must be concluded that contractors, as such, do almost nothing in the way of formal or long-range research nor do they support research by others.

---

[11] Architectural Forum, David Allison, May, 1958, p. 132.

Three viewpoints or attitudes of construction executives largely account for their indifference and even hostility when the question of research is raised. The first is the belief that construction procedures and operations are variable and non-repetitive and therefore cannot be analyzed scientifically. This reasoning also leads to the attitude that, even if something worthwhile were learned, it would have little value because the particular job would be completed before the findings could be put to use. The second viewpoint is that improvements in construction methods or equipment come through original ideas and inventions rather than through the painstaking step-by-step analysis called for by research. There is much to justify this viewpoint, as most of the advance in methods and machinery has come in this way. The third attitude rises from the construction executive's belief that his firm already knows most of the answers and that study of its procedures will develop nothing new. Thus, the only result of a study by outsiders would be to make the company's secrets available to their competitors. Several construction executives have candidly told the writers that, for the reasons given, they had little sympathy for research efforts, particularly by the colleges. They suggested that, if research were to be carried out, it should be supported by government and not by industry.

It is the writers' belief, based on serious thought and study, that research by the colleges and universities can make a real contribution to the construction industry. First, the colleges can bring to bear on construction problems the resources of all branches of knowledge, ranging through engineering, mathematics and statistics, business and management, and even including psychology and other social sciences. Second, the colleges can, and should, take a more detached and broader view towards possible approaches and solutions to problems. Almost any contractor will admit that he does not have time nor disposition for the long look. Any idea must pay off at once to be worth the effort. Finally, the research findings of colleges can be disseminated widely through teaching and publications, in contrast to today's attitude of secrecy.

Among the areas in which ideas from other disciplines, coupled with research to adapt them to construction, indicate promise are the following:

1. Simple industrial engineering techniques such as crew-balance studies, process chart analysis, and methods standardization. A few construction companies have made great progress in this direction. Some of them have stated privately that the savings often bring a reduction in cost of as much as 20%. However, they guard their methods carefully from competitors and educators alike to maintain the competitive advantage that results. It appears then, that both the development of techniques and the wider dissemination of information about existing practices offer promise.

2. Improved techniques for planning and scheduling. These could range from rather simple procedures to solutions by statistical or computer techniques in complex situations.

3. The application of statistical methods to diverse problems. These may well range from determining proper balance in equipment groups to a statistical approach to the effects of weather and climate on construction operations.

4. The application of data processing equipment, including computers, to contractor's record-keeping and computation problems.

5. The application of ideas and equipment from other fields, such as developments in automation, to construction.

6. The adaptation to construction of ideas and practices in a number of management problems such as personnel development and training, employee relations, and accident prevention, to name a few.

This list is far from complete. However, it does indicate that many disciplines can have ideas and techniques of value to construction. The colleges and universities, as contrasted with industry, provide the best situation for this cross-fertilization.

There are, of course, many other more traditional areas for research in construction, such as the development of and proving of new materials and products and the development and improvement of machinery and equipment. Here also an expanded research program in the colleges could be of real value to the industry.

Properly directed and programmed research for construction could do much to strengthen today's modest efforts in construction education. Income from research on a continuing basis would permit the schools to expand their staffs and to include specialists on them that they cannot now afford. A combined program of research and teaching, coupled with adequate compensation, could attract able men from the industry into teaching and thus aid in solving one of the most critical problems of the colleges. Advanced or graduate students could earn their college expenses and broaden their knowledge at the same time while doing research work. At present, many of them devote this time to menial and non-learning jobs to make their way through school. In fact, money spent on suitable research works twice, once in supporting staff and students and again in the knowledge that it produces.

This statement is not an argument that colleges go all-out on research in competition with commercial testing agencies or private consultants. College research should meet the double test of strengthening the educational effect of a school and, filling a gap that cannot be closed by commercial or consulting personnel.

It seems clear, however, that properly chosen and financed research in the colleges can be of value to the construction industry in two ways. First, it can develop concepts and techniques of value to the industry. Second, it can strengthen the educational program of the schools that, in turn, will produce better-educated men for the industry.

CURRENT PRACTICES AND TRENDS IN EDUCATION FOR CONSTRUCTION

The colleges and universities have been studying the problem of education for construction for many years. Some schools such as the Massachusetts Institute of Technology (MIT) began programs slanted toward construction before 1930. Many other schools gave courses[12] pertaining to construction before World War II. Spokesmen for the industry, such as Adolph J. Ackerman, F. ASCE, pointed out[13] the special educational needs of the construction industry and suggested changes in the traditional civil engineering curriculum to meet these needs.

---

[12] "Content of Courses Pertaining to Construction," report by the Civ. Engrg. Div. of the ASEE, June, 1941, M.I. Evinger, Committee Chmn.

[13] Proceedings, ASEE, 1943 meeting, pp. 406-417.

Following World War II, construction education gained considerable impetus and the civil engineering departments of a number of schools began programs aimed specifically at construction. At some schools students could choose a "construction option" as contrasted with structures, hydraulics, or some other speciality. Other schools offered almost the same selection of courses as free electives but without the "option" label.[14] In almost all cases, the curriculum combined the conventional accredited civil engineering program of the school in question with such construction oriented subjects as estimating, equipment and methods, accounting, law, and labor relations. During this same period, several schools of architecture, architectural engineering or business offered programs[8] in "building construction." These programs are directed largely at home and commercial building.

Beginning in the early or middle 1950's, several schools expanded their offerings in construction to include a fifth year devoted mainly to developing the business, management, and construction subjects that could not be fitted into a crowded 4-yr program. As should be expected, each school has chosen a pattern suited to its own organization, traditions, and faculty strength. Three of these are as follows:

1. Texas A. and M. College.[15]—A joint program in civil engineering and business administration leading to BS degrees in both civil engineering and business administration.
2. Cornell University.[16]—A 5-yr curriculum leading to a BS degree in civil engineering. Construction and management are treated as essential elements of civil engineering at the same level as technical and cultural subjects. In general, the content of the Cornell program agrees with that proposed by William A. Klinger,[7] who is one of the spokesmen on educational matters for the AGC.
3. Stanford University.[17]—A fifth-year program leading to the degree of Master of Science in Civil Engineering-Construction. The program (See Table 1) includes a series of required graduate construction courses plus a few required courses in management and technical areas. The remainder of the year is given to elective courses in management and technical subjects, selected by the student with the advice of his adviser. The philosophy of the Stanford program is that no prescribed program can fit all the many facets of construction. It is better that each individual select a program to fit his interests than to fit all to a single pattern.

To date, then, the pattern in construction education in civil engineering schools has been the development at some schools of a few undergraduate construction and related courses within the framework of conventional civil engineering, then the development of a fifth-year program in a handful of schools in which staff strength and interest and a favorable academic climate have made this development possible. However, far too little is being done to meet the expected demands for engineers educated to fit the needs of the construction industry.

---

[14] Civil Engineering Bulletin, R. L. Peurifoy, C. H. Oglesby, and F. H. Kellogg, Civ. Engrg. Div., ASEE, February, 1951, pp. 2-9.

[15] The Constructor, S. R. Wright, February, 1957, pp. 77-78.

[16] Engineering News Record, New York, N. Y., November 7, 1957, pp. 23-25.

[17] Western Construction, January, 1956, pp. 72-74; also February, 1958, pp. 48-49.

TABLE 1.—REQUIREMENTS FOR MASTERS DEGREE IN CIVIL ENGINEERING—CONSTRUCTION AT STANFORD UNIVERSITY

Forty-five or more quarter-units total, divided as follows:

	Quarter Units
1. Required undergraduate civil engineering courses. (Fully satisfied if the candidate has an ECPD accredited B.S. degree in civil engineering.)	
2. Undergraduate construction courses (6 quarter units)	
Construction Estimates and Costs	3
Construction Equipment and Methods	3
3. Core group in construction and business (15 quarter units)	
Construction Administration	4
Advanced Construction Equipment and Methods	4
Concrete Construction	3
Advanced Engineering Economy (Equipment ownership and replacement)	2
Depreciation (Tax aspects of equipment ownership)	3
4. Electives in Business Management and Related Subjects (Minimum—14 quarter units)	
Construction Problems (special investigations)	3
Civil Engineering Economy (Economics of Public works)	2
Business Law—Contracts, quasi-contracts	3
Business Law—Sales, Negotiable Instruments	3
Business Law—Agency, Partnership, Corporations	3
Industrial Organization and Management	4
Time and Motion Study	4
Engineering Accounting	3 or 5
Business Economics	3
Management Accounting	3
Cost Accounting	3
Business Finance	3
Industrial Management	3
Psychological Aspects of Business	3
Industrial (Labor) Relations	4
Purchasing	3
5. Required and Elective Courses in Advanced Civil Engineering and Related Technical Subjects (Minimum 10 quarter units)	
REQUIRED	
Advanced Foundation Design	3
Harbor Structures	3
ELECTIVES	
Structural Geology	5
Engineering Geology	3
Principles of Mining	3
Mine Plant and Equipment	4
Introduction to Electronics	3
Advanced courses in civil engineering including those in structures, soil mechanics, hydraulic engineering, and highways (50 or more quarter units from which to choose)	
Courses in engineering mechanics.	
Courses in mechanical, electrical, and industrial engineering.	

What are the prospects for more attention to construction from the engineering schools in the years ahead? Every indication is that they are bleak.

1. There has been a failure on the part of the construction industry to make its needs known to the colleges. To date, only a small group of contractors and a handful of educators have made their voices heard.
2. There has been a failure on the part of the construction industry to support education and research in the colleges at a level even closely comparable to that supplied by other industries. In all frankness, money talks! Financial support through scholarships, fellowships, research grants and, in some cases, faculty salaries will do much to create an interest in construction on the part of college administrators.
3. The slow pace at which changes take place in the colleges has deterred advancement. Contractors will find it difficult to believe that to change the curriculum or add a course may require several years time. Often changes must wait on the retirement of a department head or a senior professor who has an intrenched interest in a large block of student time. Again, at some schools a personality clash or rivalries within the department may prevent desirable alterations. Changes favoring construction may prove particularly difficult to introduce because many college people do not consider that it is engineering or on a par with other subjects.
4. The trend away from professional education and towards science among engineering educators has held up progress in this regard. Today, whenever possible, new appointments to engineering faculties are given to men with PhD degrees. There are few if any men in construction practice or education with PhD degrees, nor will there be many in the years immediately ahead. It follows that very few in the new generation of college professors will be professional men with construction interests. Thus, the already meager interest in construction education among college faculties will fall even farther.
5. The relatively low enrollment in civil engineering as compared with other branches of engineering and science has discouraged development of the program. Under these circumstances, the colleges will be cutting down on the size of their civil engineering budgets and staffs. The pressure will be to reduce the number of courses now being given, and this will make it doubly hard to add construction subjects.

Thus, it appears clear that there are many obstacles to developing a widespread program of construction education in our colleges. Most certainly much stronger efforts must come from the construction industry than are now being exerted if much is to be accomplished in the years ahead.

CONCLUSIONS

This paper has attempted to face up squarely to the joint problems confronting civil engineering education and the construction industry. In summarizing the following points have been made.

1. A civil engineer's answer to the question of "What the construction industry should have from the engineering colleges," depends on his concept of the relationship between the construction industry and the civil engineering profession. The answer of one who considers construction as simply a business with which he must have dealings, will be entirely different from that of

one who considers construction an integral and vital part of the civil engineering function. This paper is based on the latter viewpoint.

2. Civil engineers are in demand by the construction industry, are entering it in ever increasing numbers, and are taking over much of its management. For the civil engineer who will work hard, construction offers an exciting challenge, the chance to use every part of his education, and substantial rewards for accomplishment.

3. The civil engineering profession as a whole has much to gain by strengthening its ties with construction. This can result only through the joint efforts of design engineers, contractors, and educators.

4. Education pertaining to construction merits a place at both undergraduate and graduate levels, provided it is treated professionally. It is important that all civil engineering graduates have certain minimum knowledge of construction practices and problems, whereas those who plan to make construction their life's work should receive additional specialized education.

5. Research on construction problems has a proper place in the colleges. Furthermore, it can make a substantial contribution both to the industry and to the colleges.

6. To date, the engineering schools have made little progress toward meeting the specialized educational needs of the construction industry. It is true that a number of schools provide some emphasis on construction at the undergraduate level and a few have organized fifth-year programs. So far, however, the overall effort has been small compared to the need and opportunity. Moreover, there are a number of obstacles in the way of greater activity, and there is little reason for optimism in the future unless attitudes change both on the part of industry and the colleges.

As of today (1959), the engineering colleges have a golden opportunity, through education for construction, to make a substantial contribution to the industry, and to the people that construction serves. As in any important undertaking, there are many problems; however, neither the industry nor the colleges have made a sincere attempt to overcome them. Only through real concern on the part of a substantial number of contractors, engineers, and educators, coupled with a generous application of industry interest and financial support, can the opportunity be made into a reality.

DISCUSSION

PAUL F. KEIM,[18] **F. ASCE.**—Messrs. Oglesby and Fondahl are correct in saying that in many cases the problems encountered by engineers in contractors' organizations are "equal in difficulties if not more difficult than those of the design engineers who developed the original plans for the project." I also concur with the statement "Again, the design of contractors plant often calls for skills from every area of the civil engineer's education, including structures, hydraulics, soil mechanics, highways, electrical engineering and thermodynamics."

---

[18] Foreign Service Reserve Officer, USOM-Cairo, Dept. of State, ICA, Washington 25, D.C.

If the preceding is so, then the contractors need full-fledged civil engineers for their organizations in all areas of work and responsibility. However, to expect engineering graduates to be able to accept responsible positions in any company without a period of apprenticeship there is asking too much of the men and of their colleges. I say this without any modification as to the time the graduates have been in college or to the curriculum pursued. The college can give the education in principles and in detail, if there is time, covering the construction business but, in my judgment, the best, if not the only, contribution the civil engineering departments can make to the construction industry is to educate civil engineers.

Certainly the construction industry offers a feeling of permanence and belonging; it has financial incentives, and in it there is a wide variety of problems requiring every phase of education, so why not educate the students in universities and train them in industry? Much is said about what civil engineering can do for construction; many things are suggested that construction can do for the universities and colleges. Many of the latter are important, but are only corollary to the fundamental action that industry can take, to accept as a legitimate cost of doing business the apprenticeship period or training phase (that period after graduation in which we must learn the ways of our chosen company before production commensurate with the potential is possible).

Some say that certain detail given in a fifth or sixth year can shorten this hiatus, but the writer's experience has not confirmed this, if you wish to have leaders rather than technicians. The authors state, "In a broader sense, civil engineering as a profession will gain far more than it loses by strengthening its ties with construction." This may be true, but in this day of extreme competition for men, the construction industry can lose much more than civil engineering can if it does not recognize civil engineering's intrinsic value to it.

Subject matter is important, but universities are not the place to train men specifically for a job or for an industry. This does not mean that any area will be ignored, but there is only time to paint the broad picture in principles of action and not in any single detail. At the University of California, Berkeley, California there is a chance for interested students to take many courses in business administration and economics thus giving them an idea of business and management. At the same time, all civil engineers take courses in engineering economy and in contracts and specifications. Many take a course in construction engineering beyond their requirements, that gives them a conception of selection of plant, material, and equipment as well as the principles of organizational management. If construction industries show more willingness to use our nominal 4-yr student graduates in a training program within the industry, we shall be well on our way to the integration of civil engineering and construction that we all want and need for the best mutual development.

THEODORE B. APPEL, JR.,[19].—The authors have given a splendid analysis of a situation that has come on us in a gradual fashion so that, unfortunately, many of us refuse to acknowledge its existence. The writer refers to the obligation of engineering colleges to provide means for civil engineering students desiring to equip themselves to operate intelligently and efficiently at a professional and executive level in the construction industry. The authors point out the opposition that exists to the idea of wholeheartedly including qualified construction men among civil engineers and the difficulties of enlisting support from contractors for research by the colleges in the construction field.

---

[19] Chf. Engr. The C. S. Johnson Co., Champaign, Ill.

Prior to the Civil War civil engineers were pre-eminent in the field of engineering. Since then one group after another has seen fit to dissociate themselves from ASCE and to establish new professions and societies. One cannot avoid wondering whether or not much of this has come about because some of our predecessors lacked vision. Will we witness yet another division? The engineering colleges could help prevent this were they to provide adequate construction courses, as some appear to be doing, within the framework of their departments of civil engineering, where it undoubtedly belongs.

The authors mention the reluctance of engineering educators "to provide training in the practical and business side of engineering." In the writer's opinion this is extremely regrettable. We must have instruction in the basic sciences, the humanities and in professional subjects, but that is not all. Witness the training given to dental and medical students while in college. Compare the medical school graduate as he approaches his internship with autopsies and clinical service behind him and the engineering student with little or no "hardware" or business courses when he arrives on his first construction job. Admittedly it is 7 or 8 yr of college against 4 yr. The conclusion could be that Stanford University's fifth year is a step in the right direction.

The fundamental function of colleges is to teach. It is their obligation to their alumni, to the voters, if they are tax supported, and to society as a whole to teach those things that will fit our young men and young women for the profession or occupation of their choosing. It would appear that this fundamental obligation is being overlooked. There should be no question as to whether the engineering college or the contractor should do the job. It is presumptuous for those of us who are not educators to think we can do a better job than they. Education is their speciality, their main activity, not a side line.

The writer wishes that the authors had been more specific as to the type of research that is required to sustain a proper program of instruction in the field of construction. There is much research that needs to be done but that is not suitable for engineering college staffs to undertake. The problem of securing proper research contracts is one for which there appears to be no easy solution. It is not likely that contractors will rush forward to fill the vacuum. It may be that the colleges will have to bide their time, to establish their competence to teach construction, and to educate the contractors on the benefits to all of suitable research programs. In this respect the colleges may have to "lift themselves up by their own boot straps."

Contractors could materially assist education for the construction industry were they to make provision for "sabbatical summers" for the engineering college staff members desiring construction experience.

HENRY G. HOWARD,[20] F. ASCE.—The writer heartily agrees with Messrs. Oglesby and Fondahl that research by the colleges and universities can make a real contribution to the construction industry. It is necessary for the construction industry and colleges and universities to get together in a spirit of determination in order to learn to understand each other's needs and problems and to contribute toward solving them. With this purpose in mind, it is believed that both parties could reap great benefits.

---

[20] Chf. Bridge Engr. Southern Div., Michael Baker, Jr. Inc., Jackson, Miss.

The writer cannot agree with the construction executives that if research were to be carried out, it should be supported by the government. The government is now overloaded with functions that are not related to it, with a tax load on the population that is approaching the unbearable. It is, therefore, the writer's conviction that such a program should not be added to the government load.

It also seems to the writer that the discount or refusal to give credit for experience gained in the construction field toward professional registration is taking an excessively narrow view of professional engineering. It is not the intent to give the impression that the requirements for registration as a professional engineer should be made more lenient, but it is firmly believed that construction experience should be given due consideration. The writer agrees with the authors that there is no reason not to examine both design and construction experience at face value. There have been too many serious accidents on construction projects and failures of structures in the past few years. Is it possible that some of these might have been averted if there had been registered professional engineers in the construction organization?

In these days of rapid development of new design procedures and methods of construction, with ultimate design and limit design and all the rest, it seems as though the "mere execution" of the designer's work requires the services of a professional engineer who understands the design phase as well as the construction phase. Several states now require contractors to be licensed in order to do business in their state. Perhaps it is desirable to require contractors to have in their employ registered professional engineers for the execution of certain appropriate phases of their work.

The writer sees the possibility for much improvement in relations between the construction industry, professional engineers, and our engineering schools.

C. H. OGLESBY,[21] F. ASCE and JOHN W. FONDAHL,[22] M. ASCE.—Each discusser has raised questions that deserve comment:

1. Mr. Keim indicates doubt as to the value of college education beyond the fourth year for the student interested in construction. He views further study as detail work or training directed towards shortening the period until a man can pay his own way in industry.
2. Mr. Appel points out that the fundamental function of colleges is to teach and desires a more specific discussion of the type of research that might supplement this teaching effort.
3. Mr. Howard comments further on the question of governmental vs. industry sponsorship of research activity and expresses the conviction that it should be the function of the industry.

Insofar as the 4-yr curriculum is concerned, the writers agree with Mr. Keim that students should be educated as civil engineers in a broad sense. No longer is there the opportunity to graduate a "construction engineer," a structural engineer, a sanitary engineer, or a hydraulics engineer in 4 yr. The already crowded curriculum does not permit any degree of specialization, and the mounting trend towards additional engineering-science courses makes it difficult to retain even the introductory professional engineering courses. The undergraduate, construction-related program at the University of California, Berkeley, Calif., described by Mr. Keim parallels that at Stanford Univ., Stanford, Calif., where required courses in engineering economy and contracts and specifications plus limited opportunity for elective courses in business administration or construction equipment and methods are provided.

---

[21] Prof. of Civ. Engrg., Stanford Univ., Stanford, Calif.

[22] Asst. Prof. of Civ. Engrg., Stanford Univ., Stanford, Calif.

By implication, at least, Keim indicates his belief that a year in industry is more important to the civil engineer in construction than is a graduate year in college. The Stanford civil engineering faculty and its construction industry advisors disagree entirely with him. When Stanford embarked on a fifth year, graduate-level construction program in 1955, its aim was to give construction students the same opportunity to specialize in a field of interest that is offered to men interested in structures, hydraulics, or transportation. In view of both the complexity of the industry's problems and the primary importance of construction to our national economy, this step seemed justified. There was no intention to develop "hardware" courses or to concentrate on the details of specific construction techniques. These can be learned better during the apprenticeship period following graduation. Rather it was intended that, as in other fields of civil engineering, courses could be developed that would offer basic principles and approaches to problems and would develop broader viewpoints which would be of value in the long-range development of the individual and the industry itself. Moreover, it was believed that there were many courses in civil, industrial, and other branches of engineering and in the Graduate School of Business and other university departments that could contribute to a sound education for careers in construction. The degree granted at the end of fifth year of graduate study is a Master of Science in Civil Engineering. Students, if they desire, may elect to have an added subdesignation on their diplomas indicating their field of specialization such as construction, structural engineering, and so forth. The point is that construction is recognized as a part of civil engineering in which students can puruse advanced study on a truly professional level.

Mr. Appel's comments deal with research in the colleges and universities. The writers attempted to be specific in suggestions for types of research that might be undertaken by the engineering colleges, the reasons why the colleges were in a favorable position to conduct research, and the criteria for undertaking such work. On the other hand, some of his points call for additional comment. It is certainly true that the fundamental function of a college is to teach. However, good teaching means far more than collecting together facts about existing practices and passing them on to a new generation. Teaching at its best includes a quest for new ideas and for better ways of accomplishing goals. In other words, good teachers are several years ahead of practice, not several years behind it. Thus, in this broad sense, teaching and research are inseparable. The good teacher is continually involved in research in his field of interest. Otherwise he would stagnate and would cease to inspire his better students. Most colleges recognize the connection between good teaching and research. They encourage faculty members to participate in it, but with the stipulation that it contribute to teaching and not be an end in itself.

It is true that in some instances the balance between teaching and research has been lost. There may be faculty members who are poor teachers and good researchers or who wish to devote almost all of their time to research. In the case of tax-supported institutions, funds appropriated for teaching may be diverted to research. Likewise in private institutions money designated for teaching may at times support a faculty member's research interests. Even so, the writers can testify from their own experience that modest research efforts have enhanced their effectiveness as teachers. In their opinions it would be tragic to allow a few excesses to destroy an effective educational instrument.

Research has a second important function in education that should not be overlooked. Good students, particularly at the graduate level, are drawn primarily by the reputation of the school or department and its individual faculty members. This reputation is developed in a large measure through publications that report the results of research activity. Drawing students in this manner helps to maintain the balance between research and teaching because the students drawn to a college through the reputation of its staff members rightfully expect to take courses under these men. Research, then, makes an important contribution by bringing outstanding students.

A third value of research is to justify and support a larger and more diversified faculty. If, for example, each faculty member devotes one third time to research, a two-man faculty can be increased to three, or a four-man faculty to six. This is not to suggest, however, that a separate research faculty be developed; to do so would destroy the usefulness of research to teaching.

A fourth function of research is to provide financial help for students who serve as part-time research assistants. Because any educational program needs good students to be successful, and many of them need financial assistance, this aspect of research can be highly important.

In summary, appropriate research activity has an important place in the college's function of teaching because:

1. It improves the quality of teaching;
2. It aids in obtaining better students; and
3. It makes possible needed financial support by offering something of value in return.

The measures of "appropriate research activity" in the colleges are:

1. The aim should be to add to basic knowledge or to develop techniques having broad application;
2. The activity must contribute to the faculty man's teaching competence;
3. The research activity must be in balance with teaching activity and subordinate to it;
4. There must be freedom to publish the results so that the findings are circulated as widely as possible; and
5. Student assistants should participate in the projects to the greatest possible degree.

If college research activities are to stay within the preceding outlined areas, they must avoid projects dealing with design and analysis for which the fundamental data are already available. This, in the writer's view, is consulting work, and should be treated as such. If (a) a faculty member has special knowledge or talents, and (b) he can handle a specific project and still do full justice to his obligations as a teacher, he should be free to undertake the work. If he does so, his actions should be governed by the rules of conduct for consulting engineers.

Finally there is Mr. Howard's question of government vs. industry sponsorship in research or construction. The writers are in full agreement with Mr. Howard that industry sponsorship is appropriate and more desirable, but probably as a long-range objective. Early prospects for such sponsorship seem poor, at least in the engineering construction field with which the writers have closest contact. Suitable projects for the colleges are generally long range and require publication of findings. Individual construction firms operate on a short-range basis and feel that they must protect any competitive advantage that they would gain by sponsoring a research project. There are, however, examples of industry-sponsored research activity in other highly competitive fields such as aircraft and electronics. Possibly these could serve as a precedent and a research program for construction could be patterned after them. The principal difference is that both of these industries are research conscious, while construction is not. Possibly, as Mr. Appel suggests, the colleges may have to educate contractors on the benefits to all of suitable research programs. This may take considerable time.

Regarding government sponsorship or research in construction: public officials should not overlook the fact that government finally is the principal beneficiary if construction costs of public works projects are reduced. Possibly a contractor will benefit the first time the research findings are put to use, but bids will be lower on similar work in the years to come.

AMERICAN SOCIETY OF CIVIL ENGINEERS
Founded November 5, 1852
TRANSACTIONS

Paper No. 3191

DISTRIBUTIONS OF EXTREME WINDS IN THE UNITED STATES

By H. C. S. Thom[1]

With Discussion by Messrs. J. Lieblein; and H. C. S. Thom

SYNOPSIS

Following previous work, annual extreme wind speed data for airports in the United States were corrected for anemometer type and reduced to a standard 30-ft elevation. The Fisher-Tippett Type II distribution was fitted, giving 0.50, 0.02, and 0.01 quantiles. Confidence intervals of 0.90 for the quantile isolines and a nomogram for conversion of quantiles to desired elevations are developed.

INTRODUCTION

In a previous paper[2] the best available design variable, the annual extreme-mile wind speed, was chosen on the basis of a rational consideration of the requirements for wind-speed values in structural design. The extreme-mile wind speed is defined as the 1-mile passage of wind with the highest speed for a day. This led to the basic-data series of annual extreme-fastest-mile wind speeds which were found to lack homogeneity because of changes in anemometer elevations. This difficulty was overcome by reducing the annual extreme wind speeds by Hellmann's one seventh power law, which was found to be suitable for such conversion by P. O. Huss.[3] The conversion was made to a stand-

---

Note.—Published essentially as printed here, in April, 1960, in the Journal of the Structural Division, as Proceedings Paper 2433. Positions and titles given are those in effect when the paper or discussion was approved for publication in Transactions.

[1] Chf. Climatologist, Office of Climatology, U. S. Weather Bur.

[2] "Frequency of Maximum Wind Speeds," by H. G. S. Thom, Proceedings, ASCE. Vol. 80, 1954, 11 pp.

[3] "Relation between Gusts and Average Wind Speeds," by P. O. Huss, Daniel Guggenheim Airship Inst., Akron, Ohio, Report No. 140, 1946.

ard elevation of 30 ft as suggested by the Structures Committee. This gave a data series suitable for climatological analysis.

The Fisher-Tippett extreme-value distribution theory was reviewed and their Type II distribution was chosen to fit the annual extreme wind series. A probability paper for the distribution was developed and a method of plotting was shown. The method of maximum likelihood was applied to estimate the parameters β and γ of the Type II distribution function

$$F(x) = \exp\left[-(x/\beta)^{-\gamma}\right] \qquad (1)$$

In Eq. 1 F(x) is the probability of a wind speed being less than x. The mean recurrence interval R is given by the relationship

$$R = 1/[1-F(x)] \qquad (2)$$

The differential equations for estimating β and γ were found to be

$$\frac{\partial L}{\partial \beta} = \frac{n}{\hat{\beta}} - \hat{\beta}^{\hat{\gamma}-1} \sum_{i=1}^{n} x_i^{-\hat{\gamma}} = 0 \qquad (3)$$

and

$$\frac{\partial L}{\partial \gamma} = \frac{n}{\hat{\gamma}} - \sum_{i=1}^{n} \log x_i + \frac{n_i \sum_{i=1}^{n} x^{-\gamma} \log x_i}{\sum_{i=1}^{n} x_i^{-\hat{\gamma}}} = 0 \qquad (4)$$

It was shown how to solve these equations graphically. This method is laborious and satisfactory only for fitting one or a few distributions. Large-scale fitting problems such as the one of concern here must be accomplished with the aid of electronic digital computers. The results of fitting for mixed City Office and Airport Office data at Fort Wayne, Ind. are available.[2]

DATA REDUCTION

Shortly after the 1954 paper[2] was completed, discussions with George J. Malloy[a] suggested that the wind regimes in the open country (airport stations) might be quite different than downtown locations (city stations). A study of Boston, (Mass.) city office and airport data showed that the probability of exceeding 60 mph at the airport was twice that at the city office. This surprising discovery threw doubt on the validity of previously furnished climatological series used in several studies;[4,5,6,7] however, there were no facilities available at the time to study the matter further. Recently the Bridge Division of the Bureau of Public Roads, United States Department of Commerce, (BPR) provided the support necessary to make the present study.

---

[a] Chf. Engr., Travelers Fire Insurance Co.

[4] "American Standard Building Code Requirements for Minimum Design Loads in Buildings and Other Structures," by Amer. Standards Assn., A58.1-1955, Approved September 3, 1955.

[5] "Wind Forces on Structures: Nature of Wind," by R. H. Sherlock, Proceedings, ASCE, Vol. 84, No. ST4, July, 1958.

[6] "Wind Pressures in Various Areas of the United States," by G. N. Brekke, Natl. Bur. of Standards, Bldg. Materials and Structures Report 152, 1959.

[7] "Statistics of Extremes," by E. J. Gumbel, Columbia Univ. Press, New York, 1958.

The present analysis has the advantage over previous work of an additional 8 or 9 yr of records at airport stations. These were processed separately from city office data. Corrections were made for anemometer type where necessary, and all data series were reduced to a standard 30-ft elevation by Hellman's law. The city office data were processed in a similar manner for comparison purposes. Altogether 131 airport station records and 165 city station records were processed. Ten city station records, near large bodies of water, were included with the airport records in order to adequately reflect coastal conditions. This made a total of 141 open-country stations with about 1,700 yr of record averaging about 15 yr per station. As will be seen later the isotachs of wind are more reliable than the average record length might indicate because several stations contribute to the establishment of an isotach.

The 0.02 quantiles (wind speed for which the probability of being exceeded is 0.02) for city office versus airport stations are shown in Fig. 1. Although the 0.02 quantiles at city offices exceed the airport values at a few stations, probably because of exposure or random sampling, the preponderance of airport wind speeds are considerably greater than those for city offices. In fact, the weighted average of this quantile for airports is 74.8 mph as contrasted to the city offices weighted average of 55.3 mph. Thus at high quantiles, airport speeds average about 20 mph faster than city offices. This is sufficient reason not only to strictly avoid mixing airport and city observations, but also to use the airport data as a measure of open-country conditions. Extreme wind speeds are assumed to come from any direction unless local conditions dictate otherwise. Special conditions of exposure will be cited subsequently.

CLIMATOLOGICAL ANALYSIS

A review of the literature on extreme value distributions published since 1954, showed nothing which would change our method of analysis. E. J. Gumbel pointed out[7] a fact which was not explicitly mentioned[2] by the writer, although Eq. 5, to be presented subsequently, and the logarithmic scale on the abscissa Fig. 3 of the 1954 paper[2] should have made it clear. This is that the Type II distribution may be transformed to a Type I by a logarithmic transformation. The fitting of logarithms of the wind speed was tried with J. Lieblein's estimation procedure,[8] but the results were not satisfactory because the method, at present, does not have the necessary tables to handle large subsamples. A very excellent and exhaustive discussion of extreme-value distribution theory is now available.[7]

L. E. Anapol'skaia and L. S. Gandin,[9] using the writer's 1954 paper[2] as a basis, rederived the moments of the Type II distribution which were already well known, and then applied these to fitting the distributions to Russian stations. The efficiency of the moment estimate for β is poor, and its use results, in effect, in discarding about 40% of the observations, a very undesirable practice with scarce meteorological data. Presumably they could not use the more efficient method of maximum likelihood because of a lack of electronic digital computer facilities. The Russian authors did not indicate familiarity with rather extensive work in the field of extreme-value theory of the well-known Russian mathematician B. V. Gnedenko.

---

[8] "A Method of Analyzing Extreme Value Data," Natl. Advisory Comm. for Aero., Washington, Tech. Note 3053, 1954.

[9] "Metodika Opredeleniia Raschetnykh Skorostei Vetra dlia Proektirovaniia Vetrovykh Nagruzok na Stroitel'nye Sooruzheniia," by L. E. Anapol'skaia and L. S. Gandin, Meteorologiia i Gidrologiia, No. 10, 1958, pp. 9-17.

Since near-optimum methods of fitting were already available,[2] Eqs. 3 and 4 were used in fitting Fisher-Tippett Type II frequency curves to the climatological series from the 141 open-country stations. This was accomplished using the IBM 650 electronic computer in an iteration procedure which gave the

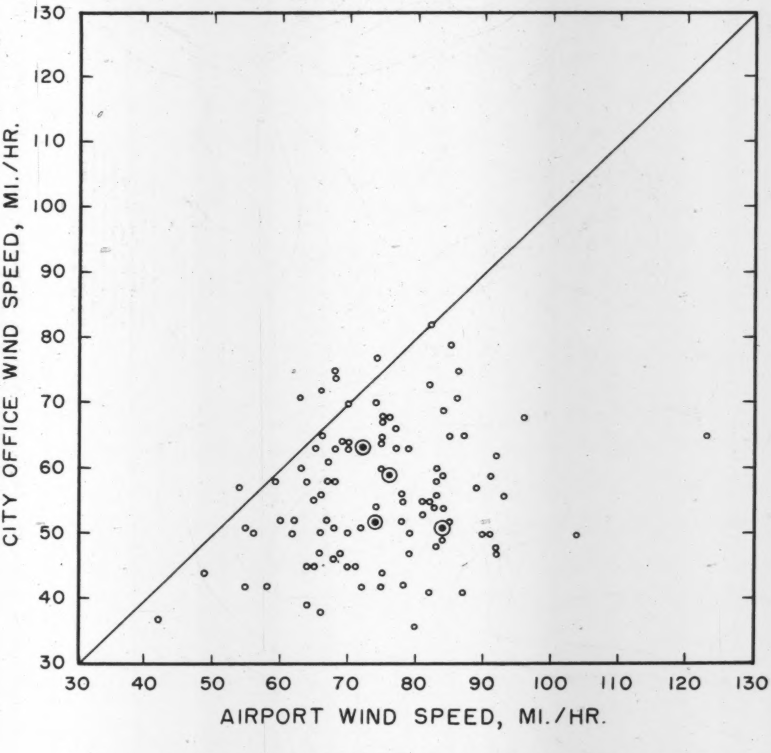

FIG. 1.—CITY OFFICE VS. AIRPORT FOR 0.02 WIND-SPEED QUANTILES

β and γ roots of Eqs. 3 and 4 to a prescribed accuracy. The computer was used on these to compute a series of quantiles among which were the 0.01 (100 yr), 0.02 (50 yr), and the 0.50 quantiles (medians) (2 yr mean recurrence interval winds). These were plotted on maps and analyzed with isolines whose intervals are suitable for conversion to pressure. These are shown in Figs. 2, 3, and 4. The particular quantiles were chosen because it was thought that the 50-yr and 100-yr values might be directly suitable for many design problems

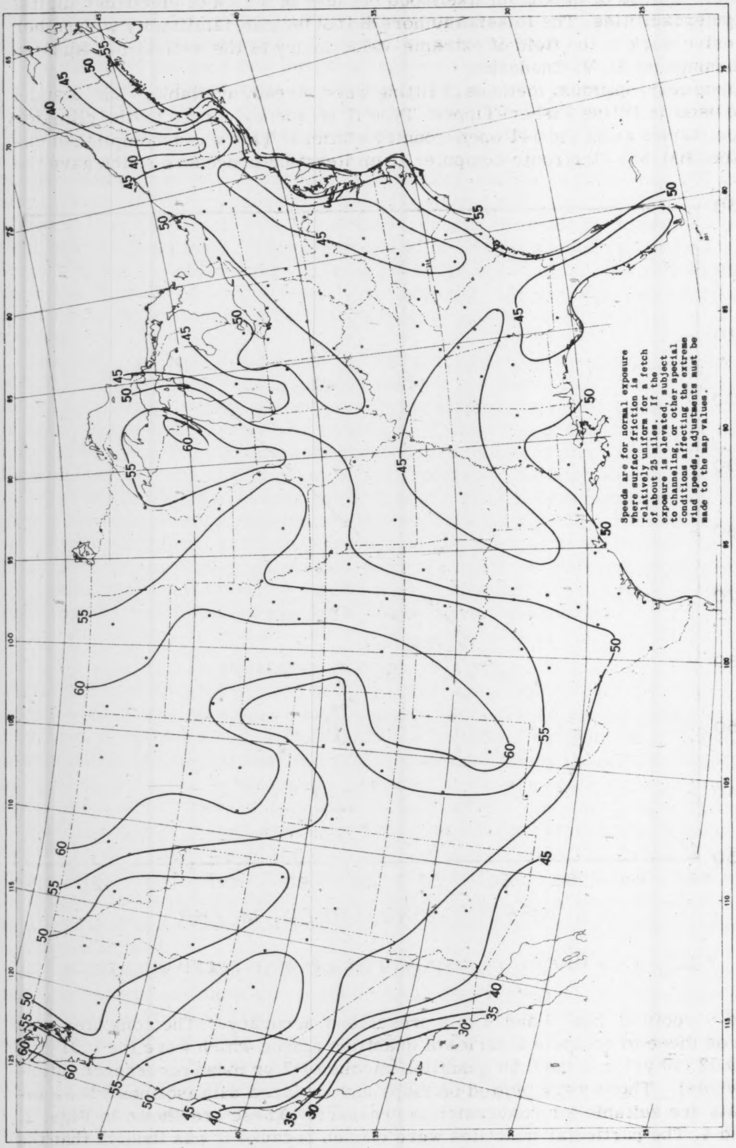

50
55
45
40
45
40
50
55
45
50
45
50
50
45
45
50
55
60
45
50
50
55
60
60
55
50
60
55
45
50
55
60
50
55
60
40
35
30
55
50
45
40
35
30

Speeds are for normal exposure where surface friction is relatively uniform for a fetch of about 25 miles. If the exposure is elevated, subject to channeling, or other special conditions affecting the extreme wind speeds, adjustments must be made to the map values.

FIG. 2.—ISOTACH 0.50 QUANTILES, IN MILES PER HOUR. ANNUAL EXTREME-MILE 30 FT ABOVE GROUND, 2-YR MEAN RECURRENCE INTERVAL.

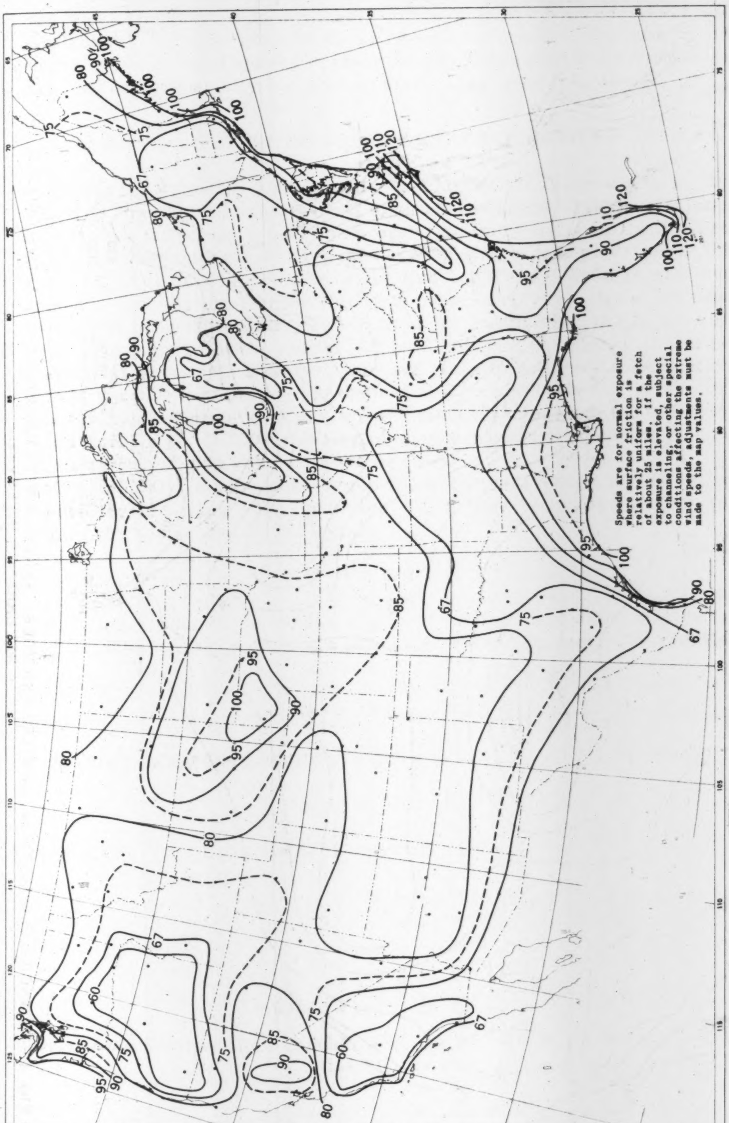

Speeds are for normal exposure where surface friction is relatively uniform for a fetch of about 25 miles. If the exposure is elevated, subject to channeling, or other special conditions affecting the extreme wind speeds, adjustments must be made to the map values.

FIG. 3.—ISOTACH 0.02 QUANTILES, IN MILES PER HOUR. ANNUAL EXTREME-MILE 30 FT ABOVE GROUND, 50-YR MEAN RECURRENCE INTERVAL.

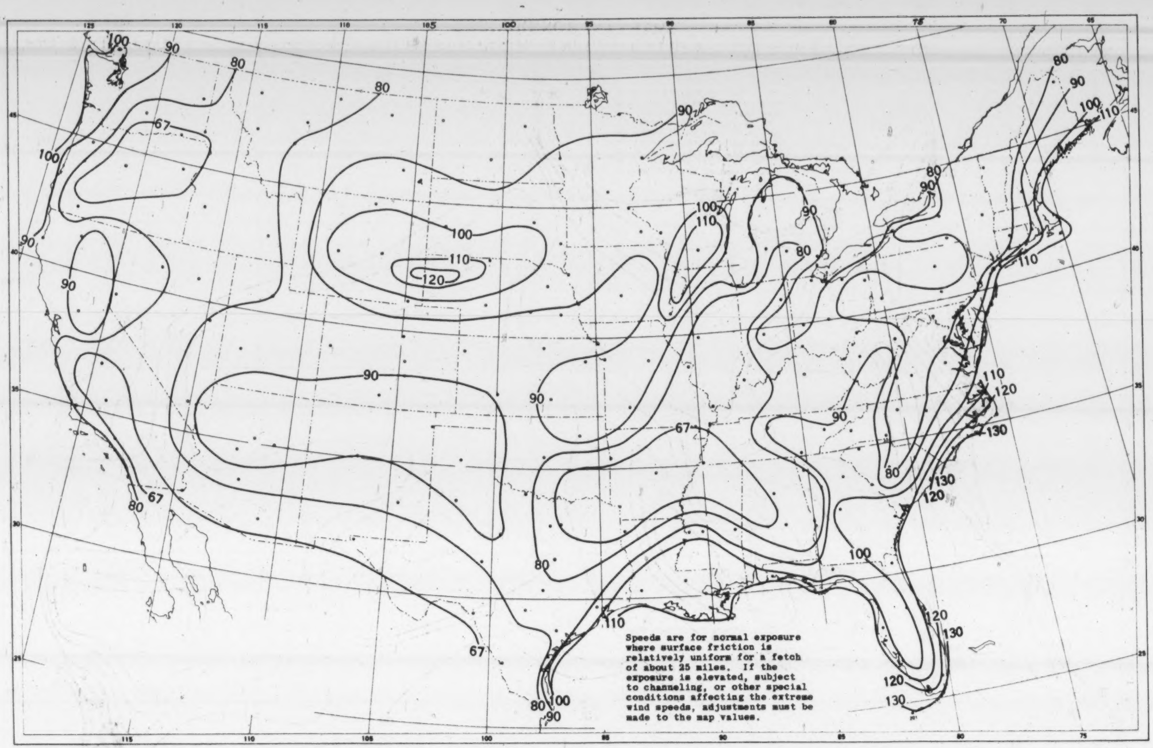
125
120
115
110
105
100
95
90
85
80
75
70
65
45
40
35
30
25
100
90
80
80
67
100
90
90
100
110
120
90
80
67
90
100
110
90
80
90
67
90
80
110
90
80
110
120
130
130
120
80
100
120
130
120
130
110
80
100
90
110
100
90
80

Speeds are for normal exposure where surface friction is relatively uniform for a fetch of about 25 miles. If the exposure is elevated, subject to channeling, or other special conditions affecting the extreme wind speeds, adjustments must be made to the map values.

FIG. 4.—ISOTACH 0.01 QUANTILES, IN MILES PER HOUR. ANNUAL EXTREME-MILE 30 FT ABOVE GROUND, 100-YR MEAN RECURRENCE INTERVAL.

while the median was added to provide the means for obtaining any desired quantile. The 50-yr map is roughly comparable in recurrence interval to the available[4,5,6] simple maps of 40-yr record extremes. The latter show considerably lower wind speeds in many areas. This reflects further the marked differences between city and open-country, high-wind conditions.

DETERMINATION OF OTHER QUANTILES

In the 1954 paper,[2] a probability paper was developed which is shown in Fig. 5. This may be readily used to obtain the entire distribution function F for any location on the maps. The process is simply to locate the desired point on the 0.50 and 0.02 maps, read off the wind speeds, and plot them at 0.50 and 1 - 0.02 = 0.98 on Fig. 5. A straight line connecting these points gives the complete distribution F from which any quantile may be read on the abscissa. Fig. 5 has been deliberately left without an example so that it may be used more conveniently by the reader. It was impossible to make all three maps absolutely consistent, however, they are close to being so. A check on estimating the 0.01 quantile by this method, at a considerable number of arbitrary latitude-longitude intersections, showed discrepancies from the 0.01 map of no more than 5 mph. If 100-yr, 50-yr or median values are needed, it is recommended that the map values always be used.

Occasionally, a procedure which holds on the average for all stations is needed for obtaining other quantiles. This may be easily found as follows: Taking the reciprocal of Eq. 1 gives

$$1/F = \exp(x/\beta)^{-\gamma} \quad \ldots\ldots\ldots\ldots\ldots\ldots \quad (5)$$

Taking logarithms twice (double logs) and solving for x which may be labelled x_{F_1} because it corresponds to a particular F_1 and, in fact, is a quantile. This yields

$$x_{F_1} = \beta/\log(1/F_1)^{1/\gamma} \quad \ldots\ldots\ldots\ldots\ldots\ldots \quad (6)$$

Repeating this for the quantile x_{F_2} gives

$$x_{F_2} = \beta/\log(1/F_2)^{1/\gamma} \quad \ldots\ldots\ldots\ldots\ldots\ldots \quad (7)$$

Dividing Eq. 7 by Eq. 6 yields the quantile ratio

$$x_{F_2}/x_{F_1} = [\log(1/F_1)/\log(1/F_2)]^{1/\gamma} \quad \ldots\ldots\ldots\ldots \quad (8)$$

This is equivalent to

$$x_{F_2}/x_{F_1} = \left[\frac{\ln F_1}{\ln F_2}\right]^{1/\gamma} \quad \ldots\ldots\ldots\ldots\ldots \quad (9)$$

because the negative signs cancel. Since $\log F \sim -(1-F)$ for F near 1, it follows that

$$x_{F_2}/x_{F_1} \sim [(1-F_1)/(1-F_2)]^{1/\gamma} \quad \ldots\ldots\ldots\ldots\ldots \quad (10)$$

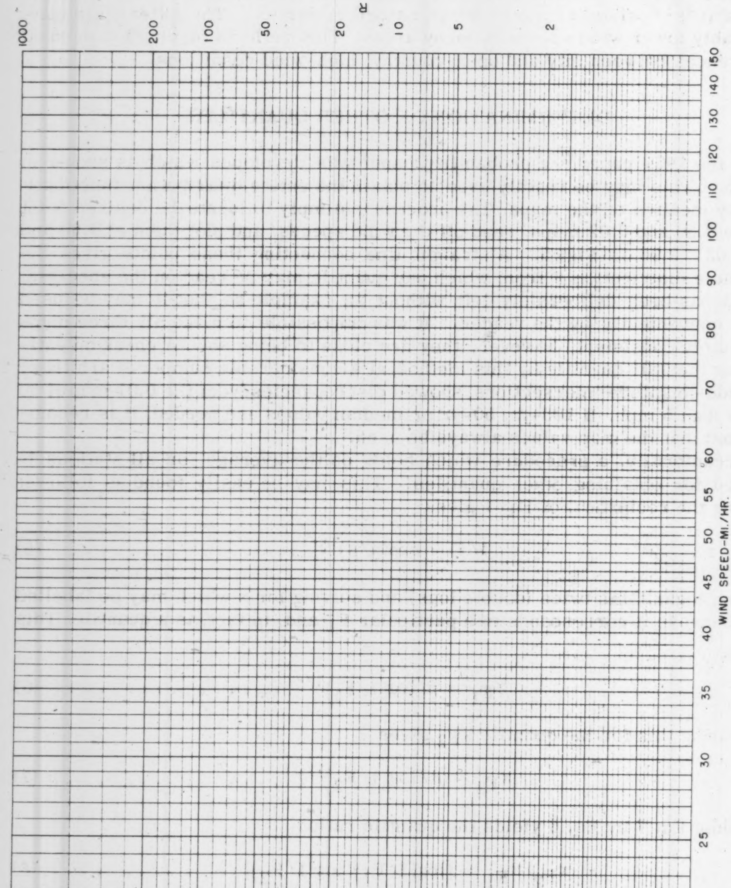

FIG. 5.—MAXIMUM-VALUE PROBABILITY PAPER, FISHER-TIPPETT TYPE II DISTRIBUTION.

The right-hand term, by Eq. 2, is seen to be the reciprocal of the mean recurrence intervals, hence

$$x_{R_2}/x_{R_1} \sim (R_2/R_1)^{1/\gamma} \quad \ldots\ldots\ldots\ldots\ldots (11)$$

Eq. 11 indicates that for large mean recurrence intervals two wind speeds are in the ratio of their corresponding mean recurrence intervals raised to the $1/\gamma$ power.

From an examination of the 141 available values of γ, the weighted average value was found to be about 9. For $R_1 = 50$ and $R_2 = 100$, the quantile ratio is easily found, by Eq. 11, to be close to 1.08. Hence the 100-yr quantile is 1.08 times the 50-yr quantile. For $R_1 = 50$ and $R_2 = 200$, the ratio is close to 1.16, and the 200-yr wind is about 1.16 times the 50-yr wind. Some indication of the variability of γ is given by the fact that it was found that 90% of the values of γ lay between 5.5 and 15.5 and 70% between 6.5 and 11.5. Thus the ratio $x_{F_{100}}/x_{F_{50}}$ will be between 1.05 and 1.13 for 90% of the samples and between 1.06 and 1.11 for 70% of the stations.

Occasionally design problems arise where it is desired to limit the risk of failure in a specific period after construction or installation. For example, if one makes an installation which will be removed or becomes obsolescent after 3 yr, the risk only occurs within this period. To determine the probability of exceeding the design value the procedure is as follows:

It was seen earlier that F is the probability of the annual extreme wind speed not exceeding some design value. (Then, of course, 1 - F will be the probability of the speed exceeding that design value). Hence, the probability that no annual extreme speed in an n-yr period will exceed the design value is F^n. Hence the probability of at least one speed exceeding the design value is

$$P_n = 1 - F^n \quad \ldots\ldots\ldots\ldots\ldots (12)$$

where P_n is the probability of exceeding the design value in the first n yr. To express in terms of mean recurrence interval R, it is only necessary to rearrange Eq. 2 to give

$$F = (R-1)/R. \quad \ldots\ldots\ldots\ldots\ldots (13)$$

Substitution into Eq. 12 yields

$$P_n = 1 - [(R-1)/R]^n \quad \ldots\ldots\ldots\ldots\ldots (14)$$

If P_n is fixed in advance then R may be found by the inversion of Eq. 14 to be

$$R = 1/[1-(1-P_n)^{1/n}] \quad \ldots\ldots\ldots\ldots\ldots (15)$$

As an example, assume an installation that is to remain $n = 3$ yr with a mean recurrence interval $R = 50$. Then $P_3 = 1 - (49/50)^3 = 1 - 0.94 = 0.06$. On the other hand, suppose it is desired to make $P_3 = 0.03$, then by Eq. 15, $R = 1/(1-0.97)^{1/3} = 1/(1-0.99) = 100$. Hence, the mean recurrence interval must be 100 yr. This form of analysis would appear to lead to very small probabilities; however, it must be remembered that P_n considers only the wind speed exceeding the design value and does not consider the probabilities of other factors in a design, which, if included, give quite different results.

Approximate 0.90 confidence intervals for the probabilities of the isotachs on Figs. 2, 3, and 4 may be obtained as follows: For a single station with average record of 15 yr, the relative frequency u/n of winds below a given quantile will be distributed in a binomial distribution

$$f(u) = \binom{15}{u} (1-F)^u \, F^{15-u} \quad \ldots\ldots\ldots\ldots\ldots (20)$$

on a scale of $u/15$. In drawing isotachs four stations were, in effect, used to define the isotach at a given point, that is, drawing proceeded by groups of four stations in order to obtain proper curvature. Hence, it is assumed that an isotach, at any point, is approximately as accurate as a four-station mean. The correlation between extreme winds in such groups of four was found to be near zero. Consequently, the four values of u are distributed independently and their mean $u/60$ has the distribution

$$f(u) = \binom{60}{u} (1-F)^u \, F^{60-u} \quad \ldots\ldots\ldots\ldots\ldots (21)$$

on a scale of $u/60$. The 0.90 confidence interval for the estimated probability F may be found by summing Eq. 21 such that

$$0.05 = \sum_{u=0}^{u=u_{0.05}} f(u) \quad \ldots\ldots\ldots\ldots\ldots\ldots (22)$$

and

$$0.95 = \sum_{u=u_{0.95}}^{u=n} f(u) \quad \ldots\ldots\ldots\ldots\ldots\ldots (23)$$

in determining the values of $u_{0.05}$ and $u_{0.95}$. This was done by graphical interpolation of the binomial distributions for $n = 60$ and $F = 0.50$, 0.98, and 0.99. This gave the general confidence value $u_F/60$, which will be somewhat too broad for the binomial gives nonparametric limits. These must be used, however, because the exact distribution of u is not known. In the above order, the confidence intervals were found to be (0.39, 0.61), (0.94, 0.995) and (0.96, 0.998). These have the following interpretation: If π is the true or population value of the probability estimated by F, the confidence interval will include π with 0.90 probability. The confidence intervals may be converted to u_{1-F} by subtracting from unity.

Conversion to confidence values for the quantiles, as read from the Figs. 2, 3, and 4, is somewhat more complicated. One of two procedures may be followed: The distribution curve F, for a particular location, may be drawn on the graph paper of Fig. 5 using the 0.50 and 0.02 values read from the maps for that location, as discussed previously. Then the probability confidence values for the desired probability may be plotted and the quantile confidence limits read off directly from the F-line in miles per hour.

The other method of obtaining confidence limits for the quantiles is to find β and γ from the quantiles $x_{0.50}$ and $x_{0.02}$ read from the maps at a chosen location. From Eq. 8 it follows immediately by taking logarithms that

$$\begin{aligned} \gamma &= \ln[\ln(1/0.50)/\ln(1/0.98)] \,/\, \ln(x_{0.98}/x_{0.50}) \\ &= 1.25276/\ln(x_{0.98}/x_{0.50}) \quad \ldots\ldots\ldots\ldots\ldots\ldots (24) \end{aligned}$$

Now for a particular quantile it follows from Eq. 7 that

$$\ln \beta = \ln x_F + (1/\gamma) \ln \ln (1/F) \qquad (25)$$

To obtain β, the median value (F = 0.50) may be always used in Eq. 25 giving

$$\ln \beta = \ln x_{0.50} + 0.69315(1/\gamma) \qquad (26)$$

Hence to obtain a chosen quantile x_F knowing β and γ from Eqs. 24 and 26, it is only necessary to solve Eq. 25 for ln x_F giving

$$\ln x_F = \ln \beta - (1/\gamma) \ln \ln (1/F) \qquad (27)$$

The quantile confidence limit is then obtained from Eq. 27 by substituting β and γ and the corresponding probability confidence limits for F.

For the average β, 45, and the average γ, 9, substitution of the F intervals into Eq. 27 gives the 0.90 confidence intervals for the 0.50, 0.02, and 0.01 quantiles (2 yr, 50 yr, and 100 yr mean recurrence intervals) as (45, 49), (61, 81), and (64, 90) respectively, all in miles per hour.

WIND CLIMATE AND ELEVATION CONVERSION

For present purposes extreme winds may be the result of three meteorological situations: extratropical cyclones, tropical cyclones, and thunderstorms. Tornadoes have not been considered in this study because there are no valid observations of their extreme speeds. Furthermore, the probability of a tornado striking a single structure is extremely small. Extratropical cyclones generally produce high winds during the winter months because they are energized by the temperature contrasts between air masses. Such contrasts tend to be larger during the colder months. Thunderstorms and tropical cyclones are both convectionally driven and hence produce high winds during the summer months. The West Coast, Great Lakes region, and mountainous areas usually have their extreme winds during the colder months due to extratropical cyclones. The Gulf Coast and Atlantic Coast, as far north as Southern Maine, have experienced most extreme winds from tropical cyclones. The effect of these storms often extends inland from 100 to 200 miles. The remainder of the United States experiences extreme winds largely from thunderstorms. This type of storm accounts for over one third of the extreme-wind situations in the United States proper.

The isotach quantiles shown on the maps of Figs. 2, 3, and 4 are for normal conditions of exposure only. Such conditions prevail where the surface friction is relatively uniform for a fetch of about 25 miles. If the exposure is elevated, subject to channeling of the wind, or other unusual or special conditions affecting wind speed, suitable adjustments to the map values must be made.

Water areas have a marked effect on extreme-wind speeds. Where a location has unobstructed access to a large body of water, extreme winds may be 30 mph or more greater than a short distance inland. The isotachs near large-water bodies in Figs. 2, 3, and 4 have been drawn to reflect, as much as possible, this effect of water. High winds in cyclones and near water tend to remain steady over longer periods than for thunderstorms. They also tend to be much more widespread in a given situation and hence cause widespread damage, although damage to individual structures may not be greater than for thunderstorm winds.

Gust factors and pressure conversion will not be discussed in detail herein since they have been very adequately treated.[6] Based on the work of Huss[3] and

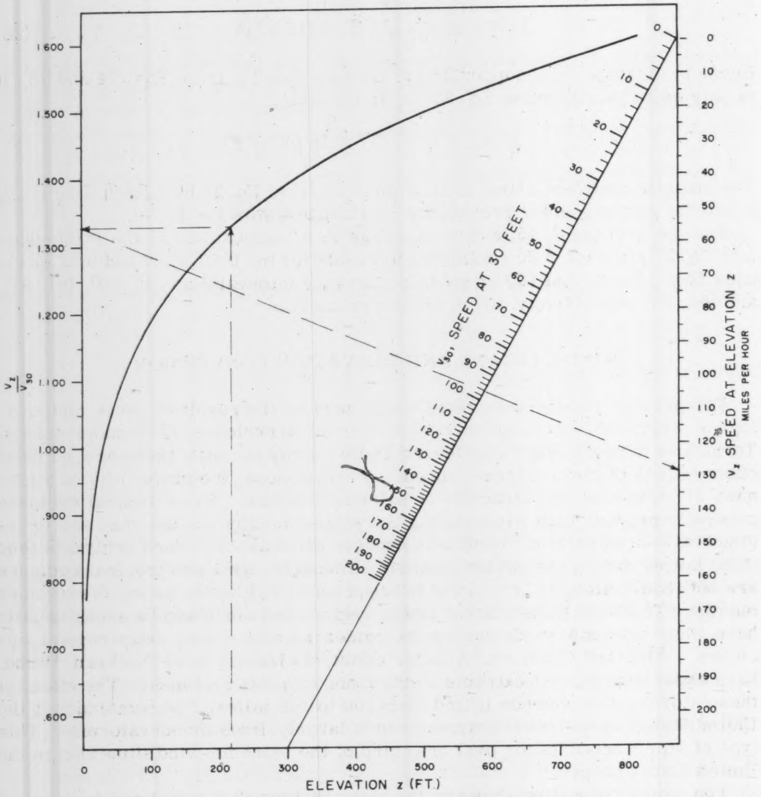

FIG. 6.—WIND SPEED-HEIGHT NOMOGRAM FOR SOLUTION OF EQ. 28.

others, a standard gust factor at 30 ft was taken as 1.3 by G. N. Brekke.[6] This or other gust factors may be multiplied by the wind speeds shown on Figs. 2, 3, and 4 to give gust speeds. When the wind speed V is in miles per hour, the velocity pressure in pounds per square foot, given by Brekke,[6] is $0.00256\ V^2$ for normal sea-level conditions. This applies over the greater part of the United States, since elevation differences are not sufficient to affect the constant greatly.

Since the increase of speed with height depends in the first 1,000 ft mainly on surface friction, the type of storm situation could make little difference. Huss[3] found that the one-seventh power law gave good approximations up to

350 ft over land for the fastest mile for all quantiles having probabilities less than 0.90. There is no evidence to indicate that it does not hold to higher levels over land so it has been assumed here that it is valid up to 850 ft. The Hellman formula, with one-seventh power, is

$$V_z = V_{30}(z/30)^{1/7} \ldots\ldots\ldots\ldots\ldots\ldots (28)$$

Where z is the desired elevation in feet, V_{30} is wind-speed quantile at 30 ft in miles per hour, and V_z is the converted speed at elevation z. This equation has been solved in the nomogram of Fig. 6. The nomogram may be easily understood by following the dotted lines from z = 215 ft to the curve, thence to the V_z/V_{30} scale, thence to V_{30} = 96 mph, and finally to the V_z scale to find the speed at 215 ft, V_{215} = 128 mph. The nomogram may also be used in reverse to convert winds at higher levels to the 30-ft elevation. If this step is followed by a forward conversion step, the nomogram gives a means of converting from a given elevation to any other elevation. The nomogram should not be used for elevations below 30 ft as the one-seventh power law is of doubtful validity below this elevation.

ACKNOWLEDGMENTS

This study was supported, in part, by the Bureau of Public Roads, United States Department of Commerce.

The writer is particularly indebted to H. N. Wilcox, of the Bridge Division, BPR, who recognized the need for and promoted this study, and who, through many technical discussions, helped guide the study into its present form. Sincere thanks must also be extended to the meteorologists of some 300 first-order Weather Bureau Stations, who took time from their busy schedules to tabulate the basic data. Gladys Crown and Maurice Kasinoff processed these data to final form. The latter also did all manual computations and worked the model distribution problem for checking the electronic computer. G. L. Barger, acting director of the National Weather Records Center at Asheville, N. C., aided immeasurably by expediting the collection of the data and performance of card punching and electronic-computer work. Especial thanks are due to R. L. Joiner and J. R. Roddy for preparing the IBM 650 program and to Grady McKay for running the computation project through under considerable pressure to get the job done. Sincere thanks are also offered to W. W. Buck, Jr., for his careful rendition of the illustrations.

DISCUSSION

J. LIEBLEIN.[10]—Thom has developed very useful methods of application of the specialized statistical theory that relates to extreme phenomena. His interest in the writer's method of fitting extremes by means of order statistics is appreciated even though the attempt to use it was not successful in the particular application. The writer has learned that another paper on very similar matters was not available to the author at the time of writing and might have had a bearing on the method of analysis used.[11] This paper describes the fitting of a large number of extreme-value distributions of Type III (or Weibull type) closely related to Type II used by Thom. The method used was that first tried by the author converting to Type I by means of lagarithms and then using order statistics for estimation. Over 200 distributions were fitted, by the aid of an electronic computer (SEAC), each, based on a set averaging 25 (extreme) observations, and the results were found to be quite satisfactory.

---

[10] Mathematical Statistician, David Taylor Model Basin, U. S. Navy Dept., Washington, D. C.

Thom suggests that the reason for difficulty with the method was because the tables did not extend to sufficiently large sub sample sizes. It may be pointed out in large samples the averaging of many subgroups of size 6 (to which the tables are as yet limited) would give estimators that would tend to approach normality, in contrast to behavior in smaller sample sizes. Such regularity gives grounds for believing that more difficulty in fitting by this method may be expected with small than with large samples. Therefore, it would be of interest to have had the results of the attempted fit of logarithms, to shed light on effects of small versus samples.

Under the heading "Climatological Analysis," Thom makes the sole mention of efficiency of an estimate, when stating that use by Russian workers of the moment estimate for β, with efficiency of about 60%, wastes 40%, of the scarce data. However, the quantities of interest in such meteorological investigations are presumably quantiles, as used by the author. The quantiles are not the parameters of the distribution, but certain functions of them. Thus, the quantile X_F (where F specifies the quantile - for example, F = 0.98 for the 0.02 quantile) is related to the parameter β and γ by Eq. 27. This suggests that efficiency of an estimator of the quantile will, in general, depend, not only on the efficiencies as regards the parameters β and γ, but also on which quantile, F, is being estimated.

Maximum likelihood estimates are generally efficient for indefinitely large samples and are, therefore, often assumed to be near optimum for samples of finite size even though there is then some shrinkage of efficiency away from perfection (except in special cases). However, when the estimate involves a variable quantity such as F, then this shrinkage due to finite samples may vary with F, for a given sample size, and be serious for some F-quantiles even though slight for others. This point would seem to warrant theoretical investigation if it is essential to have estimators with known and high efficiency in connection with analyzing costly data.

For example, work of this nature by the writer for the Type I extreme-value distribution,[8] shows the following, from Table III(b): for subgroups of size n = 6 the efficiency of a certain (non maximum-likelihood) estimator of each of the two parameters is about 96% and 77%, and for the 0.50 - quantile it is 99%, whereas for the 0.01 - quantile the efficiency is only 83%.

Also of interest are Eqs. 14 and 15 which relate (mean) recurrence intervals and various-year probabilities. Although complicated looking, they may be simplified to crude rules of thumb by taking advantage of the fact that large recurrence intervals R are usually the ones of interest, so that (1/R) is small and the approximation

---

[11] "Statistical Investigation of the Fatigue Life of Deep-Groove Ball Bearings," by J. Lieblein and M. Zelen, Journal of Research of the Natl. Bur. of Standards, Vol. 57, No. 5, November, 1956, RP 2719, pp. 273-316.

$$(R-1)/R = 1 - (1/R) \approx e^{-1/R} \quad \ldots\ldots\ldots\ldots \quad (29)$$

may be used. Then Eq. 14 gives

$$P_n = 1 - [(R-1)/R]^n \approx 1 - e^{-n/R} \quad \ldots\ldots\ldots \quad (30a)$$

$$\approx n/R \quad \ldots\ldots\ldots\ldots\ldots\ldots \quad (30b)$$

by using Eq. 29 again, in reverse. This gives, corresponding to Eq. 15

$$R \approx n/P_n \quad \ldots\ldots\ldots\ldots\ldots\ldots \quad (31)$$

For n = 3 yr, R = 50, Eq. 29 gives $P_n = 3/50 = 0.06$, and for n = 3 yr, $P_3 = 0.03$, Eq. 31 gives R = 3/0.03 = 100, agreeing perfectly with the result of the author's examples.

The fact that this type of analysis produces small probabilities is entirely reasonable, even without reference to other design factors as stated by the author. Extreme wind speeds, having recurrence intervals of something like 100 or 50 yr, are necessarily improbable (though not impossible) of happening in n = 1 yr. As one increases the period, n, under consideration beyond n = 1 yr, the probability of happening (at least once) during n yr increases according to Eq. 14 but while n is only a few years, the probability still remains small. It is not until n reaches a significant fraction n/R = perhaps 14 or more (by which time, incidentally, Eqs. 30b and 31 but not Eq. 30a break down) that the unfavorable probability P_n becomes appreciable. In fact, for n = R the probability is

$$P_n = 1 - [1 - (1/R)]^R \quad 1 - e^{-1} = 0.632 \ .$$

Thus, the design speed is, on the probability basis, about twice as likely to be exceeded within the recurrence interval as after it.

The final point to be considered here concerns Thom's examination of confidence intervals for probabilities, under the heading "Determination of Other Quantiles". It would be useful to mention the fundamental National Bureau of Standards tables on binomial probabilities,[12] even though they could not be directly used here because they go only up to n = 49 instead of 60. The Introduction to these tables lists others, one going up to n = 150. The graphs used in interpolation in the paper might be very useful to include because the only other standard graphs relative to the binomial distribution available are the classical "Clopper - Pearson charts," but these have been constructed only for 0.95 and 0.99 confidence intervals, not 0.90. Another useful reference[13] is available in connection with use of Eq. 27. One of the tables (Table 2) gives very detailed values for the function -ln (-ln F) appearing in this equation.

---

[12] Tables of the Binomial Probability Distribution, Natl. Bur. Standards Applied Math. Series No. 6, U. S. Govt. Printing Office, 1950.

[13] Probability Tables for the Analysis of Extreme-Value Data, Natl. Bur. Standards Applied Math. Series No. 22, U. S. Govt. Printing Office, 1953.

H. C. S. THOM.[14]—The discussion by Lieblein of the application of order statistics to the fitting of extreme wind distributions nicely supplements the writer's paper. Because the discussion was written, plans are being made to extend his tables to higher subsample values. The writer did not include more of such material for fear of diverging to far from the engineering aspects. Furthermore, the basic theoretical discussion of the distribution was given elsewhere.[2]

The question of efficiency is, of course, important and in fact was uppermost in adopting the method of fitting, but it did not seem appropriate to go into the details in this paper. Certainly the main interest is in the sampling errors in the quantiles; however, there is nothing to show that the quantiles obtained from the method of maximum likelihood are appreciably less efficient than those obtained from order statistics.

Lieblein's approximation to the return period is useful, and the reference to the probability of the design wind occurring during the recurrence interval is interesting.

The writer did not make reference to binomial tables as they were not used. In addition to those Lieblein mentioned, there is Romig's table[15] that covers n = 50 to 100.

---

[14] Chf. Climatologist, Office of Climatology, U. S. Weather Bur., Washington, D. C.

[15] 50-100 Binomial Tables, by Harry G. Romig, John Wiley and Sons, Inc., New York, 1947.

AMERICAN SOCIETY OF CIVIL ENGINEERS

Founded November 5, 1852

TRANSACTIONS

Paper No. 3192

CHARTS FOR DESIGN OF REINFORCED CONCRETE COLUMNS

By W. H. Gardner, Jr.,[1] M. ASCE, and Donald H. Kline,[2] A.M. ASCE

With Discussion by Messrs. George B. Begg, Jr.; James R. Krusling; and W. H. Gardner, Jr. and Donald H. Kline

SYNOPSIS

Curves are presented which enable the designer to immediately determine the necessary size and reinforcing for a given thrust and moment. The curves are based on the ultimate strength of the column section and cover six column sizes for each of three concrete strengths. The curves are directly applicable to square tied columns with eccentricities about one axis.

INTRODUCTION

Ever since the ASCE-ACI Joint Committee on Ultimate Strength Design published their report in 1955,[3] much has been written regarding the implications of the report, both from the standpoint of design philosophy and member sizes resulting from ultimate strength design.[4,5] A recent paper[6] by Alfred L. Parme, M. ASCE, discusses thoroughly the comparison between member

---

Note.—Published essentially as printed here, in May, 1960, in the Journal of the Structural Division, as Proceedings Paper 2461. Positions and titles given are those in effect when the paper or discussion was approved for publication in Transactions.

[1] Assoc. Prof. of Civ. Engrg., Duke University, and Partner, Gardner and Meir, Cons. Engrs., Durham, N. C.

[2] Partner, Gardner and Meir, Cons. Engrs., Durham, N. C.

[3] "Report, ASCE-ACI Joint Committee on Ultimate Strength Design," Proceedings, ASCE, Vol. 81, October, 1955.

[4] "Simplification of Design by Ultimate Strength Procedures," by Phil M. Ferguson, Transactions, ASCE, Vol. 123, 1958, p. 602.

[5] "Guide for Ultimate Strength Design of Reinforced Concrete," by Charles S. Whitney and Edward Cohen, Proceedings, ACI, Vol. 53, November, 1956, pp. 455-490.

[6] "Practical Aspects of Ultimate Strength Design," by Alfred L. Parme, Proceedings, ASCE, Vol. 84, No. ST5, September, 1958.

sizes as designed by the conventional "working load" method and by ultimate strength. The economy to be gained by using ultimate strength design for columns with eccentric loads is clearly demonstrated therein. The writers have noted these substantial savings in columns actually designed.

At present, the designer who wishes to take advantage of the smaller column sizes permitted by ultimate strength analysis must perform several more steps in his computations that he would perform if he were using the conventional approach to the problem.[7] Several ingenious graphical solutions for the cumbersome formulas of ACI 318 - 56 have been published, and these design aids considerably lessen the time required to choose a section.[4,8] The curves here presented (Figs. 1 through 18) are an adaptation of those devised by Charles S. Whitney.[9] Although not as general, these curves permit faster determination of reinforcing when designing, or ultimate load capacity when checking. Examples later show how easily these steps can be accomplished.

LIMITATIONS AND ASSUMPTIONS

The writers understand that column design tables, similar to those of I. E. Morris,[10] are being prepared for ultimate loads rather than working loads. The publication date of these data is still uncertain, however. The curves presented herein are an effort to make immediately available design aids that, while not covering all possible column sections, should prove useful in the design of most conventional type structures. For the sake of more immediate presentation, therefore, the curves have been drawn only for square columns eccentrically loaded about one axis and symmetrically reinforced, with the steel arranged parallel to the axis of bending and a fixed percentage of the section depth therefrom. The reinforcing has been placed at 0.2 of the depth from the tension and compressive faces; this arrangement suffices without undue loss of accuracy for the column sizes shown.

The conditions to which the curves apply are:

1. Columns are square.
2. Axial loads are eccentric about one axis by an amount up to 1.25 times the section depth.
3. Tensile and compressive reinforcement is symmetrical about the axis of bending, the centroid of the steel at each face being 0.3 of the section depth from the axis.
4. Concrete and reinforcing strengths are as shown on the charts.

Spot checking of the curves has indicated a maximum error of $1\frac{1}{2}\%$ with most errors being less than 1%.

Notation corresponds to that defined in the ACI Building Code.[11]

---

[7] Concrete Reinforcing Steel Institute Handbook-Revised, 1957 Edition, pp. 255-336.

[8] "Ultimate Strength Design Charts for Columns Controlled by Tension," by Tung Au, Proceedings, ACI, Vol. 54, December, 1957.

[9] "Application of Plastic Theory to the Design of Modern Reinforced Concrete Structures," by Charles S. Whitney, Journal, Boston Soc. of Civ. Engrg., Vol. XXXV, January, 1948, p. 29.

[10] "Allowable Loads on Eccentrically Loaded Concrete Columns," by I. E. Morris, Atlanta, Ga.

[11] "Building Code Requirements for Reinforced Concrete," ACI 318-56, Proceedings, ACI, Vol. 52, May, 1956, p. 981.

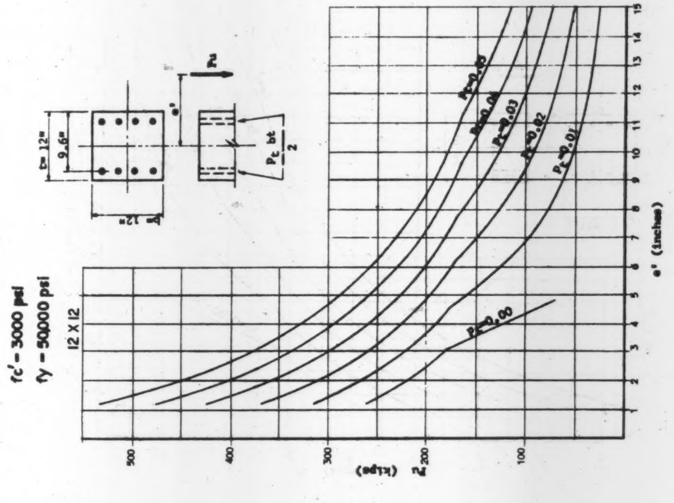
fc' - 3000 psi
fy - 50,000 psi
12 X 12
t= 12"
9.6"
b= 12"
e'
Pu
$P_t \frac{bt}{2}$
Pt=0.05
Pt=0.04
Pt=0.03
Pt=0.02
Pt=0.01
Pt=0.00
Pu (kips)
500
400
300
200
100
1
2
3
4
5
6
7
8
9
10
11
12
13
14
15
e' (inches)

FIG. 1

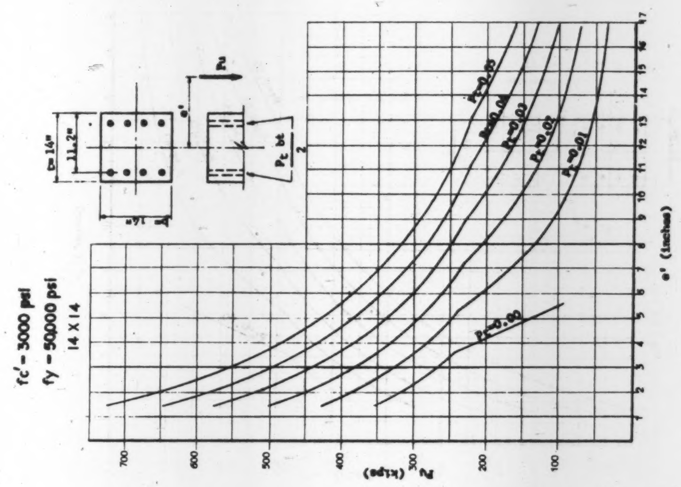
fc' - 3000 psi
fy - 50,000 psi
14 X 14
t= 14"
11.2"
b= 14"
e'
Pu
$P_t \frac{bt}{2}$
Pt=0.05
Pt=0.04
Pt=0.03
Pt=0.02
Pt=0.01
Pt=0.00
Pu (kips)
700
600
500
400
300
200
100
1
2
3
4
5
6
7
8
9
10
11
12
13
14
15
16
17
e' (inches)

FIG. 2

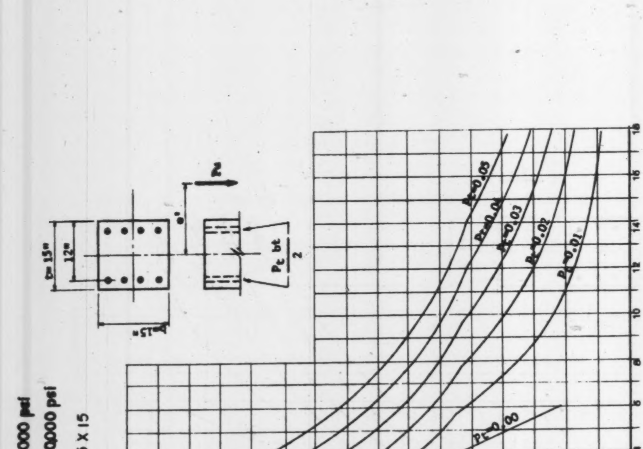
fc' - 3000 psi
fy - 50,000 psi
15 X 15
t= 15"
12"
b=15"
e'
Pu
$\frac{P_t\,bt}{2}$
Pt=0.05
Pt=0.04
Pt=0.03
Pt=0.02
Pt=0.01
Pt=0.00
800
700
600
500
400
300
200
100
Pu (kips)
2
4
6
8
10
12
14
16
18
e' (inches)

FIG. 3

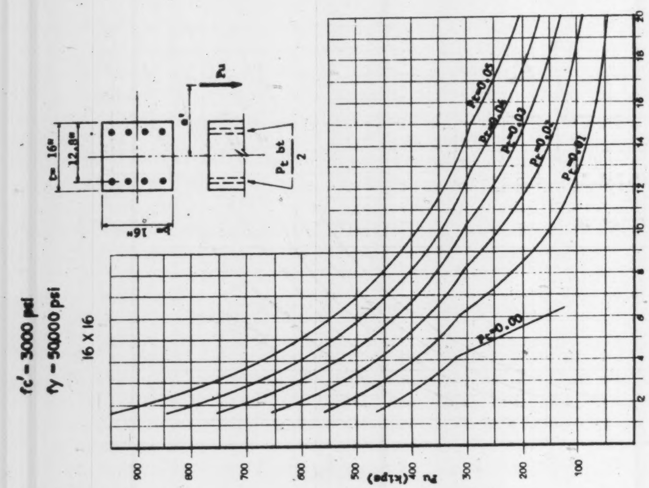
fc' - 3000 psi
fy - 50,000 psi
16 X 16
t= 16"
12.8"
b= 16"
e'
Pu
$\frac{P_t\,bt}{2}$
Pt=0.05
Pt=0.04
Pt=0.03
Pt=0.02
Pt=0.01
Pt=0.00
900
800
700
600
500
400
300
200
100
Pu (kips)
2
4
6
8
10
12
14
16
18
20
e' (inches)

FIG. 4

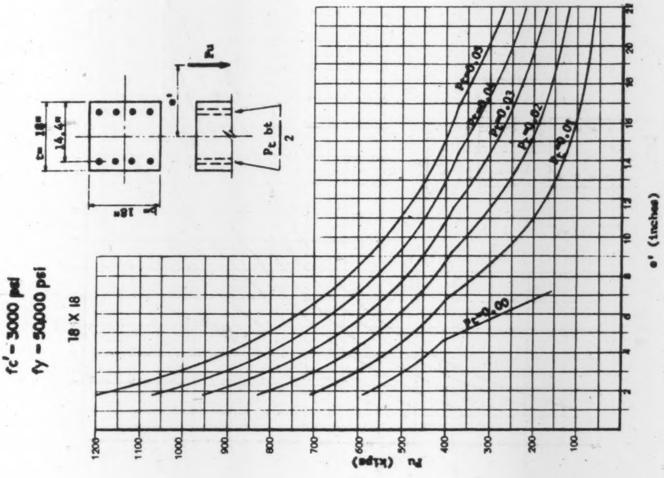
fc' - 3000 psi
fy - 50,000 psi
18 X 18
t= 18"
14.4"
b= 18"
e'
Pu
Pt bt / 2
Pt=0.08
Pt=0.04
Pt=0.03
Pt=0.02
Pt=0.01
Pt=0.00
1200
1100
1000
900
800
700
600
500
400
300
200
100
Pu (kips)
2
4
6
8
10
12
14
16
18
20
22
24
e' (inches)

FIG. 5

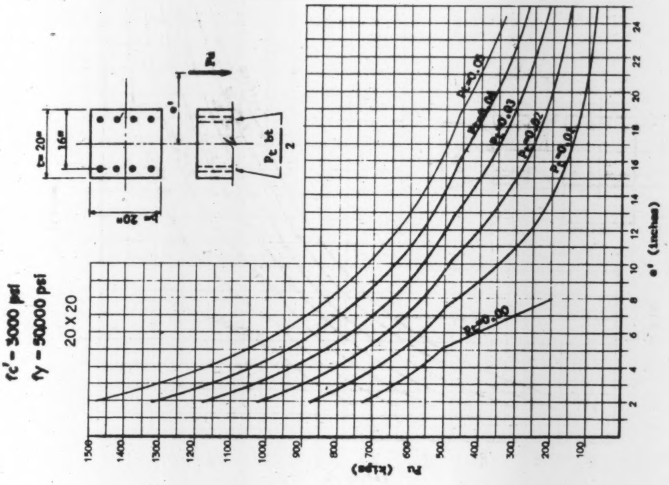
fc' - 3000 psi
fy - 50,000 psi
20 X 20
t= 20"
16"
b= 20"
e'
Pu
Pt bt / 2
Pt=0.08
Pt=0.04
Pt=0.03
Pt=0.02
Pt=0.01
Pt=0.00
1500
1400
1300
1200
1100
1000
900
800
700
600
500
400
300
200
100
Pu (kips)
2
4
6
8
10
12
14
16
18
20
22
24
e' (inches)

FIG. 6

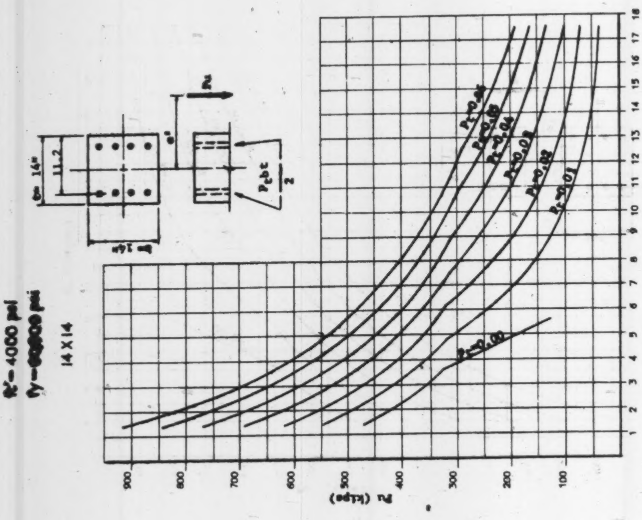
f'c = 4000 psi
fy = [illegible] psi
14 X 14
t = 14"
11.2
b = 14"
e'
N
$P_t bt / 2$
$P_t = 0.06$
$P_t = 0.05$
$P_t = 0.04$
$P_t = 0.03$
$P_t = 0.02$
$P_t = 0.01$
$P_t = 0.00$
Pu (kips)
900
800
700
600
500
400
300
200
100
e' (inches)
1 2 3 4 5 6 7 8 9 10 11 12 13 14 15 16 17 18

FIG. 8

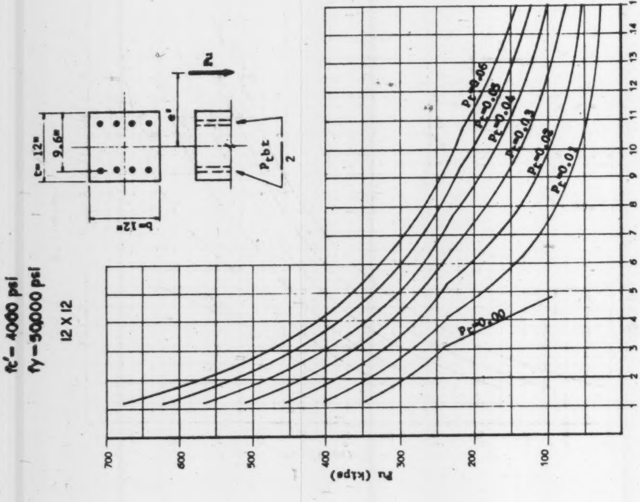
f'c = 4000 psi
fy = 50,000 psi
12 X 12
t = 12"
9.6"
b = 12"
e'
N
$P_t bt / 2$
$P_t = 0.06$
$P_t = 0.05$
$P_t = 0.04$
$P_t = 0.03$
$P_t = 0.02$
$P_t = 0.01$
$P_t = 0.00$
Pu (kips)
700
600
500
400
300
200
100
e' (inches)
1 2 3 4 5 6 7 8 9 10 11 12 13 14 15

FIG. 7

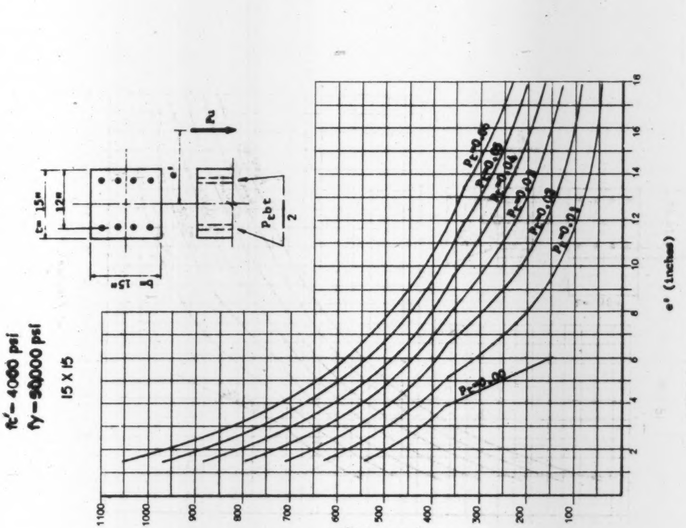
f'c – 4000 psi
fy – 90,000 psi
15 X 15
t = 15"
12"
b = 15"
e'
Pu
$\frac{P_t bt}{2}$
Pt=0.06
Pt=0.05
Pt=0.04
Pt=0.03
Pt=0.02
Pt=0.01
Pt=0.00
Pu (kips)
1100
1000
900
800
700
600
500
400
300
200
100
e' (inches)
2
4
6
8
10
12
14
16
18

FIG. 9

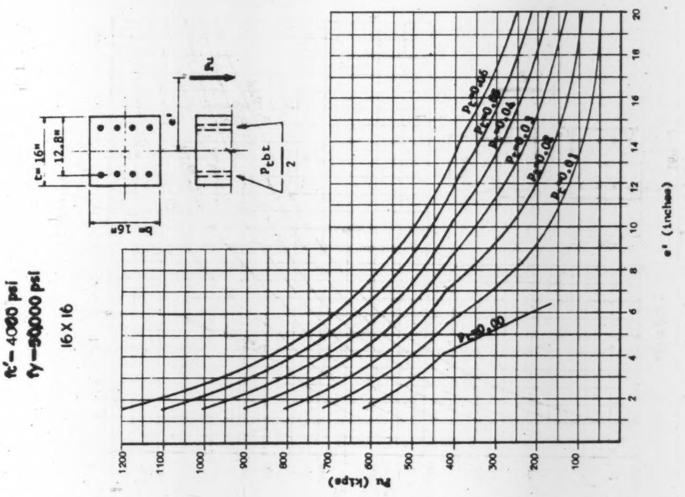
f'c – 4000 psi
fy – 90,000 psi
16 X 16
t = 16"
12.8"
b = 16"
e'
Pu
$\frac{P_t bt}{2}$
Pt=0.06
Pt=0.05
Pt=0.04
Pt=0.03
Pt=0.02
Pt=0.01
Pt=0.00
Pu (kips)
1200
1100
1000
900
800
700
600
500
400
300
200
100
e' (inches)
2
4
6
8
10
12
14
16
18
20

FIG. 10

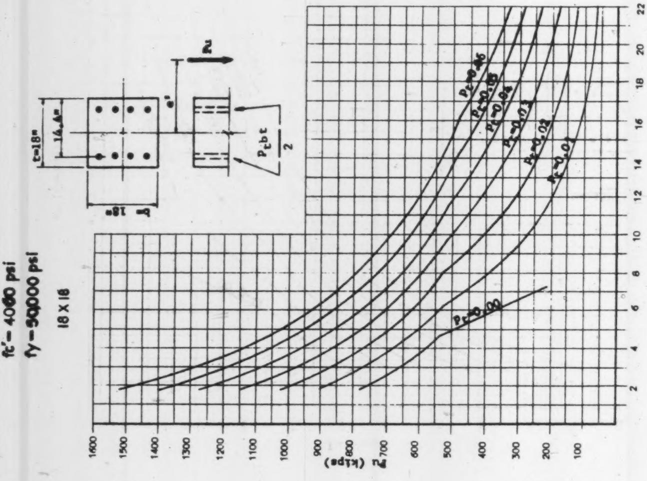
fc' = 4000 psi
fy = 50,000 psi
18 X 18
t = 18"
14.4"
b = 18"
e'
Pu
$\frac{P_t bt}{2}$
Pt = 0.06
Pt = 0.05
Pt = 0.04
Pt = 0.03
Pt = 0.02
Pt = 0.01
Pt = 0.00
Pu (kips)
1600
1500
1400
1300
1200
1100
1000
900
800
700
600
500
400
300
200
100
e' (inches)
2
4
6
8
10
12
14
16
18
20
22

FIG. 11

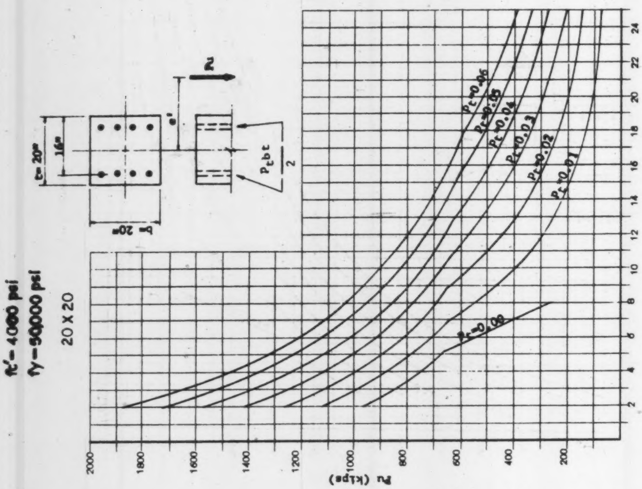
fc' = 4000 psi
fy = 50,000 psi
20 X 20
t = 20"
16"
b = 20"
e'
Pu
$\frac{P_t bt}{2}$
Pt = 0.06
Pt = 0.05
Pt = 0.04
Pt = 0.03
Pt = 0.02
Pt = 0.01
Pt = 0.00
Pu (kips)
2000
1800
1600
1400
1200
1000
800
600
400
200
e' (inches)
2
4
6
8
10
12
14
16
18
20
22
24

FIG. 12

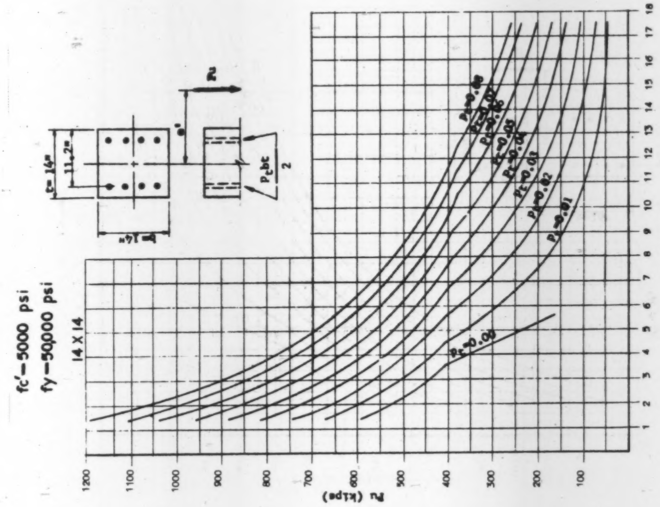
fc'–5000 psi
fy–50,000 psi
14 X 14
t= 14"
11.2"
b= 14"
e'
Pu
Pt bt/2
Pt=0.08
Pt=0.07
Pt=0.06
Pt=0.05
Pt=0.04
Pt=0.03
Pt=0.02
Pt=0.01
Pt=0.00
Pu (kips)
1200
1100
1000
900
800
700
600
500
400
300
200
100
e' (inches)
1 2 3 4 5 6 7 8 9 10 11 12 13 14 15 16 17 18

FIG. 14

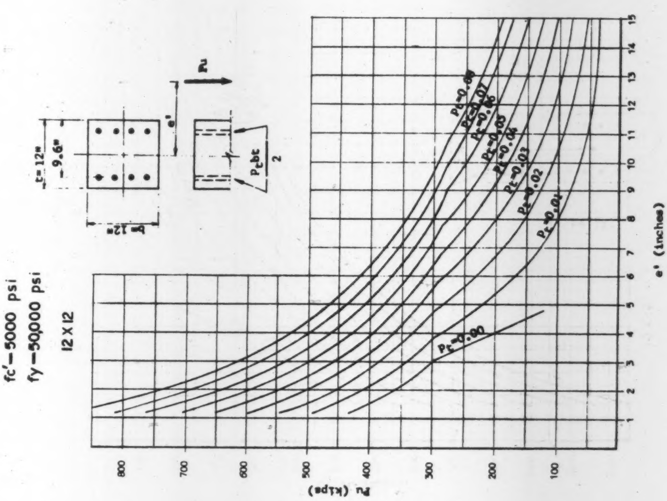
fc'–5000 psi
fy–50,000 psi
12 X 12
t= 12"
9.6"
b= 12"
e'
Pu
Pt bt/2
Pt=0.08
Pt=0.07
Pt=0.06
Pt=0.05
Pt=0.04
Pt=0.03
Pt=0.02
Pt=0.01
Pt=0.00
Pu (kips)
800
700
600
500
400
300
200
100
e' (inches)
1 2 3 4 5 6 7 8 9 10 11 12 13 14 15

FIG. 13

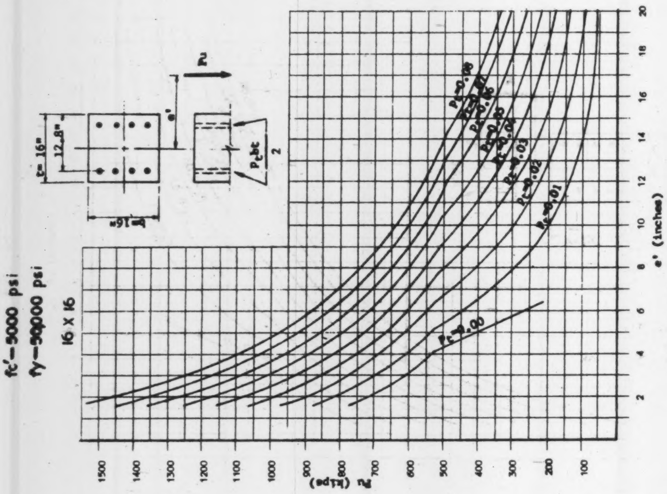
fc'–5000 psi
fy–50,000 psi
16 X 16
t= 16"
12.8"
b=16"
e'
Pu
$\frac{P_t bt}{2}$
Pt=0.08
Pt=0.07
Pt=0.06
Pt=0.05
Pt=0.04
Pt=0.03
Pt=0.02
Pt=0.01
Pt=0.00
Pu (kips)
1500
1400
1300
1200
1100
1000
900
800
700
600
500
400
300
200
100
e' (inches)
2
4
6
8
10
12
14
16
18
20

FIG. 16

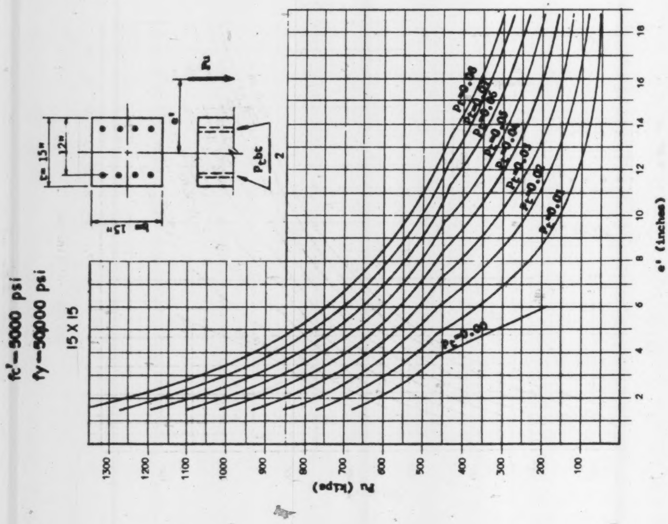
fc'–5000 psi
fy–50,000 psi
15 X 15
t= 15"
12"
b= 15"
e'
Pu
$\frac{P_t bt}{2}$
Pt=0.08
Pt=0.07
Pt=0.06
Pt=0.05
Pt=0.04
Pt=0.03
Pt=0.02
Pt=0.01
Pt=0.00
Pu (kips)
1300
1200
1100
1000
900
800
700
600
500
400
300
200
100
e' (inches)
2
4
6
8
10
12
14
16
18

FIG. 15

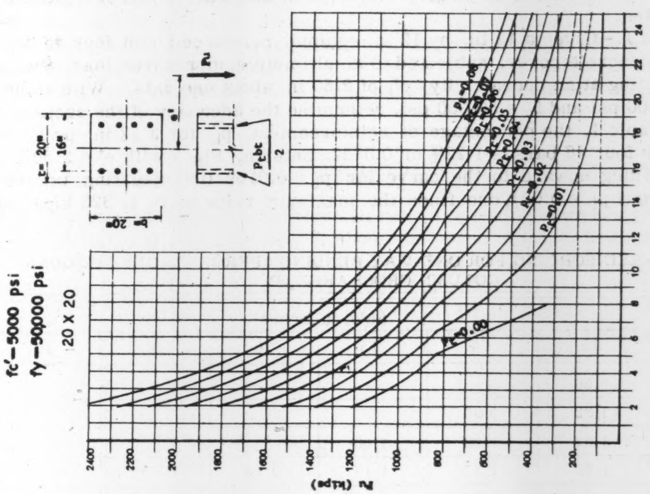
fc'—5000 psi
fy—50,000 psi
20 X 20
b= 20"
t= 20"
16"
e'
Pu
$\frac{P_c bt}{2}$
Pu (kips)
2400
2200
2000
1800
1600
1400
1200
1000
800
600
400
200
e' (inches)
2
4
6
8
10
12
14
16
18
20
22
24
Pt=0.08
Pt=0.07
Pt=0.06
Pt=0.05
Pt=0.04
Pt=0.03
Pt=0.02
Pt=0.01
Pt=0.00

FIG. 18

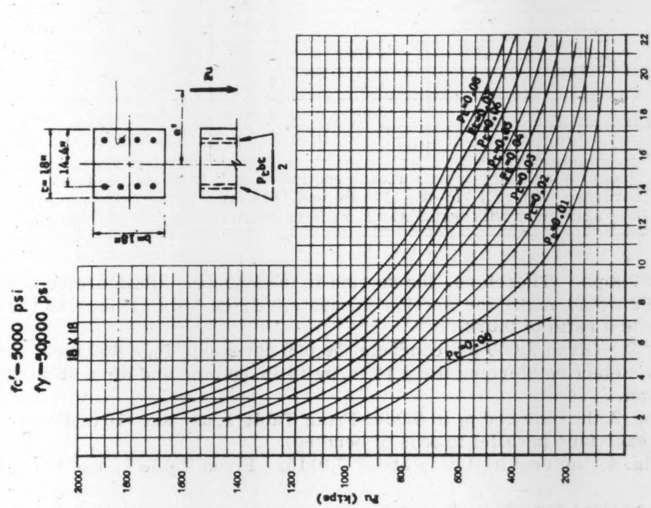
fc'—5000 psi
fy—50,000 psi
18 X 18
b=18"
t= 18"
14.4"
e'
Pu
$\frac{P_c bt}{2}$
Pu (kips)
2000
1800
1600
1400
1200
1000
800
600
400
200
e' (inches)
2
4
6
8
10
12
14
16
18
20
22
Pt=0.08
Pt=0.07
Pt=0.06
Pt=0.05
Pt=0.04
Pt=0.03
Pt=0.02
Pt=0.01
Pt=0.00

FIG. 17

USE OF CHARTS

The use of the charts is largely self-evident and will be demonstrated by two examples.

Example 1.—Given a 12 in. by 12 in. column, reinforced with four #6 bars with 2 in. concrete cover, subjected to an ultimate compressive load, Pu, of 350 kips acting at an eccentricity, e', of 2.50 in. about one axis. With values of fc' = 4,000 psi and f_y = 50,000 psi, determine the adequacy of the section.

From Table 1, the percentage of reinforcement, p_t, for a 12 in. by 12 in. column with four #6 bars is 1.22% or 0.0122. Entering Fig. 7 with e' = 2.50 in., and proceeding upward to the curve for $p_t = 0.0122$ (interpolating between $p_t = 0.01$ and $p_t = 0.02$), one finds the maximum value of P_u is 323 kips, or less than 350 kips. Therefore, the section is inadequate. (Reinforcing such that $p_t = 0.02$ would make the section adequate. From Table 1, four #8 bars would provide a ratio of 0.022).

TABLE 1.—REINFORCING FOR ONE-WAY BENDING. PERCENTAGES OF SQUARE COLUMN GROSS AREA, P_t

Reinforcement	Side, in Inches					
	12	14	15	16	18	20
Four #5	0.86					
Four #6	1.22	0.90				
Four #7	1.67	1.22	1.06			
Six #6	1.83	1.35	1.17	1.03		
Four #8	2.20	1.62	1.40	1.24	0.97	
Four #9	2.78	2.04	1.78	1.56	1.23	1.00
Four #10	3.55	2.58	2.26	1.98	1.57	1.27
Four #11	4.33	3.22	2.77	2.45	1.92	1.56
Six #10	5.29	3.90	3.39	2.97	2.35	1.90
Six #11	6.50	4.77	4.16	3.65	2.89	2.34
Eight #10			4.53	3.97	3.13	2.54
Eight #11			5.55	4.88	3.85	3.12
Ten #11						3.90

This table includes as many bars for each section as will fit along two faces of the column, in accordance with ACI 318-56, 1103 (b) and 1104 (a). Reinforcement placed in this manner is in agreement with assumptions made in constructing ultimate load charts.

Example 2.—Given 3,000 psi concrete, 50,000 psi steel, P_u = 450 kips, and e' = 3.20 in. Select reinforcing for a 14 in. by 14 in. column and for a 16 in. by 16 in. column.

From Fig. 2, the required p_t is 0.034. From Table 1, use six #10 (with three bars along each face parallel to axis of bending).

From Fig. 4, the required p_t is about 0.0115. From Table 1, use four #8 bars.

If the conditions for which the curves were drawn are not satisfied, the designer may be able to adapt them to his situation after studying the effects of varying the parameters in the ACI 318 - 56 formulas or similar expressions. One common case to which the curves can be adapted arises with the use of concrete having a compressive strength of 3,750 psi. If one multiplies the values of P_u obtained from the curves for 4,000 psi concrete by 3,750/4,000 or 0.94, one obtains a value of P_u always on the conservative side with a maximum error of 4%. For instance, if fc' were 3,750 psi instead of 4,000 psi in Example 1, the maximum value of P_u with the given reinforcement would be 0.94 x 323 = 304 kips.

CONCLUSIONS

It is hoped that these design aids will help in breaking down resistance to the use of ultimate strength design. It should be borne in mind, however, that the curves presented are merely graphical solutions of Eqs. 9 and 13 of the Joint Committee Report (Eqs. A9 and A11 in the Appendix, ACI 318 - 56) for certain types of column sections. As such, they eliminate the need to do some arithmetic, but they do not reduce the requisite understanding of the provisions of the report.

DISCUSSION

GEORGE B. BEGG, JR.,[12] M. ASCE.—Gardner and Kline have presented valuable charts for the design of reinforced concrete columns. These design aids certainly will help their avowed purpose of "breaking down resistance to the use of ultimate strength design."

However, the writer questions whether the units p_t and e' are variables that should be plotted. As the writer pointed out previously,[13] the introduction of such variables only represent intermediate steps toward a solution that can me made more directly. For example, at the end of a normal analysis of a floor system, the ultimate load and moment on a column are known. The design question becomes "What column size and reinforcement are required by this load and moment? This being the question, why not replace e' with M_u and plot actual bar arrangements instead of values of p_t?

If the charts are extended (and it is to be hoped that they will be) to different bar arrangements, column shapes and higher stresses, a set of indexes might help a more rapid convergence. A typical index would plot the upper line (pt or given bars) for each column size of a constant concrete and steel stress. The designer, knowing his design stresses, goes to the index and picks out the smallest column for his load and moment. In turn, he moves to the applicable chart and picks out the reinforcement.

---

[12] Chf., Design and Research Sect., Structural Engrg. Branch, Publ. Bldgs. Service, Genl. Services Admin., Washington, D. C.

[13] Discussion of "Design of Symmetrical Columns with Small Eccentricities in One or Two Directions," Journal, ACI, Vol. 30, No. 9, March, 1959.

JAMES R. KRUSLING,[14] **M. ASCE.**—The design of reinforced concrete structures using ultimate strength procedures is simpler and more realistic than the conventional straight line method. At present there are several shortcomings to the method, such as lack of criteria covering bond and diagonal tension and the fact that continuous structures are analyzed by elastic theories which do not give the true ultimate strength because of stress redistribution. These deficiencies will probably be overcome shortly, judging from the amount of literature on this subject that has been recently published in various technical journals.

Gardner and Kline have presented a series of curves to simplify the design of square columns for a given thrust and moment. These curves make the design or investigation of square columns unbelievably simple and as such, the authors are to be commended for their contribution to the literature on ultimate strength design.

These curves may also be utilized for the design or investigation of rectangular sections with symmetrical reinforcement, by using the slicing method.[15] Basically all that needs to be done is to multiply the ultimate load by the ratio of the depth of the column to its new width. The charts then can be used directly. The percentage of steel obtained from the curves should be multiplied by the rectangular proportions to obtain the necessary steel area.

W. H. GARDNER, JR.,[16] **M. ASCE, and DONALD H. KLINE,**[17] **A.M. ASCE.**—In his discussion, Krusling correctly and concisely explained a modified use of the charts for rectangular columns. Actually, not only the width, but also the depth, may be varied, although this latter operation is a little more involved and probably not worthwhile except when designing a number of columns of the same size.

Begg suggested several ways in which the charts could be more directly applied to design problems, principally the plotting of moment instead of eccentricity and actual bar combinations instead of percentages of reinforcing. The parameters used were chosen to permit the drawing of one set of base curves for each concrete strength. Different scales were drawn on transparencies of these base curves, resulting in the charts presented. Constructing the charts in this simplified manner would not have been possible if moments and bar combinations had been plotted.

The writers wish to note that the column design tables mentioned as being computed are available.[18] These tables are arranged and indexed substantially along the line suggested by Begg and are extremely useful.

---

[14] Principal Structural Design Engr., Div. of Engrg., City Dept. of Pub. Wks., Cincinnati, Ohio.

[15] "Basic Reinforced Concrete Design: Elastic and Creep," by G. E. Large, 2nd Ed., Ronald Press Co.

[16] Assoc. Prof. Civ. Engrg., Duke Univ. and Partner, Gardner and Meir, Cons. Engrs., Durham, N. C.

[17] Partner, Gardner and Meir, Cons. Engrs., Durham, N. C.

[18] "Reinforced Concrete Column Tables Ultimate Strength Design," by Hugh Fenlon, Atlanta, Ga.

TABLE 2.—REINFORCING FOR ONE-WAY BENDING; PERCENTAGES OF SQUARE COLUMN GROSS AREA, P_t

Reinforcement	Side, in Inches					
	12	14	15	16	18	20
Four 14^S		4.60	4.00	3.52	2.78	2.25
Four 18^S					4.94	4.00
Six 14^S		6.89	6.00	5.27	4.17	3.37
Six 18^S						6.00

Note.—This table includes as many bars for each section as will fit along two faces of the column in accordance with ACI 318 - 56, 1103 (b) and 1104 (a). Reinforcement placed in this manner is in agreement with assumption made in constructing ultimate load charts.

Table 1 presented the percentage of reinforcing for various bar combinations possible with bars #11 and smaller. Because use of 14 S and 18 S bars is becoming more widespread, Table 2 is offered as an extension of Table 1 to include these bars.

AMERICAN SOCIETY OF CIVIL ENGINEERS

Founded November 5, 1852

TRANSACTIONS

Paper No. 3198

BUCKLING OF ONE-STORY FRAMES AND BUILDINGS

By John E. Goldberg,[1] F. ASCE

SYNOPSIS

Buckling of plane frames and of complete one-story building structures is considered in this paper. The theory of buckling of plane, one-story frames is discussed and applied to the collapse of rectilinear frames using a generalization of the slope-deflection method. Both the symmetrical and anti-symmetrical or lurching modes of collapse of plane frames are considered. The relation of the buckling of the plane frames to the buckling of the complete structure is pointed out and a theory for the buckling of such space structures is presented. It is shown that the buckling analysis of the complete structure can be reduced to a sequence of computationally simple problems. Illustrative examples are included.

INTRODUCTION

The theory of buckling of plane frames is now well established, and no serious difficulties are met in the determination of the critical loads of, at least, elementary plane frames. The proper application of valid methods based upon this theory leads to a generally satisfactory, if not overly conservative, design for such frames from the standpoint of possible collapse by reason of instability or buckling.

Plane frames, however, generally do not exist singly. A building structure normally consists of a set of such frames. These are interconnected by floors

---

Note.—Published essentially as printed here, in October, 1960, in the Journal of the Structural Division, as Proceedings Paper 2629. Positions and titles given are those in effect when the paper or discussion was approved for publication in Transactions.

[1] Prof., Structural Engrg., Purdue Univ., Lafayette, Ind.

or roofs, or by structural systems designed specifically to resist or to aid in the distribution of lateral loads. Under certain circumstances, these floors, roofs or lateral systems may perform an additional function; that of providing a bracing system against a lurching or sidesway mode of buckling.

Plane frames may buckle in either a lurching or sidesway mode, involving lateral displacement of the joints, or in a mode that does not involve lateral displacement of the joints. These modes are frequently called the "anti-symmetrical" and "symmetrical" modes, respectively, although these designations are applicable strictly to the corresponding modes of symmetrical, symmetrically loaded frames.

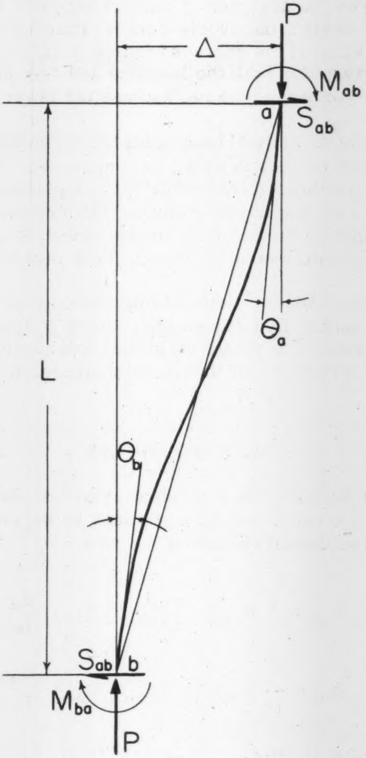

FIG. 1.—APPLIED FORCES AND DISTORTION OF A COLUMN

It is generally assumed that a plane frame will buckle in a lurching mode at a lesser loading than would be required to cause buckling in the symmetrical mode. This assumption, however, is not necessarily valid if lateral support is provided in the form of floors, roofs, or explicit lateral bracing systems. A relatively small amount of lateral support in any of these forms may be sufficient to increase the critical loading for the sidesway mode to a level at which it exceeds the critical loading for the so-called symmetrical mode. Under these circumstances and with the added condition that the frame and loading are symmetrical, the symmetrical mode of buckling takes on the greater significance.

This situation leaves the designer or analyst with two alternatives. He may accept, as a basis of design, the overly conservative critical loading for the lurching mode of buckling of the unbraced frame. Alternatively, he may determine the critical loadings for both the lurching and symmetrical modes, if the latter is possible for the braced frame, and use the lower of these as a design basis.

The determination of the critical loading for the symmetrical mode of buckling of each of a set of plane frames is easily accomplished. The determination of the critical loading for unbraced frames or for independently braced frames in the lurching mode of buckling is also simple. The critical loadings of a set of mutually braced frames in the lurching modes presents a slightly more complicated but still straightforward problem. This problem is analyzed in the present paper.

A procedure is presented for determining whether or not a complete one-story structure will buckle in a sidesway or lurching mode under a specified set of loads. The procedure is relatively simple and has the advantage that it is based upon concepts of rigid frame theory which are familiar to civil and structural engineers.

BASIC FORMULAS

If a member ab is subjected to a constant axial load as shown in Fig. 1, the bending moments at the end a and the end b may be expressed in terms of the angular and transverse displacements of its ends

$$M_{ab} = K_{ab}\left[A_{ab}\theta_a + B_{ab}\theta_b - \left(A_{ab} + B_{ab}\right)\frac{\Delta_{ab}}{L_{ab}}\right] \quad \dots\dots\dots \text{(1a)}$$

$$M_{ba} = K_{ab}\left[A_{ab}\theta_b + B_{ab}\theta_a - \left(A_{ab} + B_{ab}\right)\frac{\Delta_{ab}}{L_{ab}}\right] \quad \dots\dots\dots \text{(1b)}$$

in which $K_{ab} = E\,I/L$, E is the appropriate modulus of elasticity, I denotes the moment of inertia of the cross section, L is the length of the member, A and B are constants, θ is the angular displacement at the end designated by the subscript, and Δ refers to the relative transverse displacement of the ends.

The values of the constants A and B depend upon the sign and magnitude of the axial load and may be expressed completely[2] as functions of the ratio of the axial load to the Euler load of the member, P/P_e, due consideration being given to the use of the appropriate modulus in the Euler formula:

For compressive axial load,

---

[2] "Stiffness Charts for Gusseted Members Under Axial Load," by John E. Goldberg, Transactions, ASCE, Vol. 119, 1954, p. 43.

$$A = \frac{\sin p L - p L \cos p L}{\frac{2}{p L}(1 - \cos p L) - \sin p L} \quad \ldots\ldots\ldots\ldots\ldots (2a)$$

$$B = \frac{p L - \sin p L}{\frac{2}{p L}(1 - \cos p L) - \sin p L} \quad \ldots\ldots\ldots\ldots\ldots (2b)$$

and for tensile axial load,

$$A = \frac{p L \cosh p L - \sinh p L}{\frac{2}{p L}(1-\cosh p L) + \sinh p L} \quad \ldots\ldots\ldots\ldots\ldots (3a)$$

$$B = \frac{\sinh p L - p L}{\frac{2}{p L}(1-\cosh p L) + \sinh p L} \quad \ldots\ldots\ldots\ldots\ldots (3b)$$

In Eqs. 2 and 3

$$p L = \pi \sqrt{|\rho|} \quad \ldots\ldots\ldots\ldots\ldots\ldots\ldots (4a)$$

and

$$\rho = \frac{P}{P_e} = \frac{P}{\pi^2 E I/L^2} \quad \ldots\ldots\ldots\ldots\ldots\ldots\ldots (4b)$$

The axial load is positive when compressive. The values of the slope-deflection coefficients A and B may be taken from Table 1 or Figs. 2 and 3. A more extensive set of charts which gives the values of these coefficients for gusseted members has been presented[2] previously. It may be noted that, when the axial load is zero, the coefficients A and B take on the values 4 and 2, respectively.

Referring to Fig. 1 and taking moments about either end leads to the following formula for the transverse shear:

$$S_{ab} = \frac{-1}{L_{ab}} \left(M_{ab} + M_{ba} + P_{ab} \Delta_{ab}\right) \quad \ldots\ldots\ldots (5)$$

Substitution of Eqs. 1 into Eq. 5 yields

$$S_{ab} = \frac{-K_{ab}}{L_{ab}} \left(A_{ab} + B_{ab}\right)\left(\theta_a + \theta_b - 2\frac{\Delta_{ab}}{L_{ab}}\right) - P_{ab} \frac{\Delta_{ab}}{L_{ab}} \quad \ldots (6)$$

It is of interest to investigate the effect of various end conditions at the base of the column upon Eqs. 1 and 6. If the lower end, $\underline{a}$, is elastically restrained by a rotational spring having a spring rate Q_a, the moment at the lower end has the magnitude

$$M_{ab} = -Q_a \theta_a \quad \ldots\ldots\ldots\ldots\ldots\ldots\ldots (7)$$

By Eq. 1a, therefore,

$$K_{ab}\left[A_{ab}\theta_a + B_{ab}\theta_b - \left(A_{ab} + B_{ab}\right)\frac{\Delta_{ab}}{L_{ab}}\right] = -Q_a \theta_a \quad \ldots (8)$$

which leads to

$$\theta_a = \frac{1}{A_{ab} + \dfrac{Q_a}{K_{ab}}} \left[- B_{ab}\, \theta_b + \left(A_{ab} + B_{ab}\right) \frac{\Delta_{ab}}{L_{ab}} \right] \quad . . . . . (9)$$

TABLE 1.—SLOPE DEFLECTION COEFFICIENTS A AND B FOR VARIOUS VALUES OF LOAD RATIO ρ

ρ	A	B	ρ	A	B
3.9	-78.34	78.58	0.3	3.589	2.109
3.8	-39.05	39.54	0.2	3.730	2.070
3.7	-24.69	25.39			
3.6	-17.87	18.79	0.1	3.865	2.033
3.5	-13.73	14.86	0	4.000	2.000
3.4	-10.91	12.24			
3.3	- 8.86	10.40	-0.1	4.131	1.968
3.2	- 7.30	9.02	-0.2	4.255	1.938
3.1	- 6.05	7.96	-0.3	4.384	1.910
3.0	- 5.03	7.12	-0.4	4.502	1.883
2.8	- 3.449	5.884	-0.5	4.619	1.857
2.6	- 2.252	5.019	-0.6	4.736	1.834
2.5	- 1.749	4.678	-0.7	4.849	1.811
2.4	- 1.300	4.383	-0.8	4.959	1.789
2.2	- 0.519	3.901	-0.9	5.069	1.769
2.0	0.143	3.521	-1.0	5.175	1.749
1.8	0.717	3.224	-1.2	5.383	1.713
1.6	1.224	2.980	-1.4	5.583	1.681
1.5	1.457	2.873	-1.6	5.777	1.651
1.4	1.673	2.778	-1.8	5.964	1.623
1.2	2.090	2.610	-2.0	6.147	1.598
1.0	2.468	2.468	-2.5	6.580	1.544
0.9	2.645	2.404	-3.0	6.99	1.499
0.8	2.816	2.346	-4.0	7.75	1.43
0.7	2.981	2.291	-5.0	8.42	1.38
0.6	3.140	2.241	-7.0	9.62	1.30
0.5	3.295	2.194	-9.0	10.69	1.26
0.4	3.444	2.150			

Substitution of Eq. 9 into Eqs. 1 and 6 yields

$$M_{ba} = K_{ab} \left[\left(A_{ab} - \frac{B_{ab}^2}{A_{ab} + \dfrac{Q_a}{K_{ab}}} \right) \theta_b - \left(A_{ab} + B_{ab}\right) \left(1 - \frac{B_{ab}}{A_{ab} + \dfrac{Q_a}{K_{ab}}} \right) \frac{\Delta_{ab}}{L_{ab}} \right] \quad . . . . (10)$$

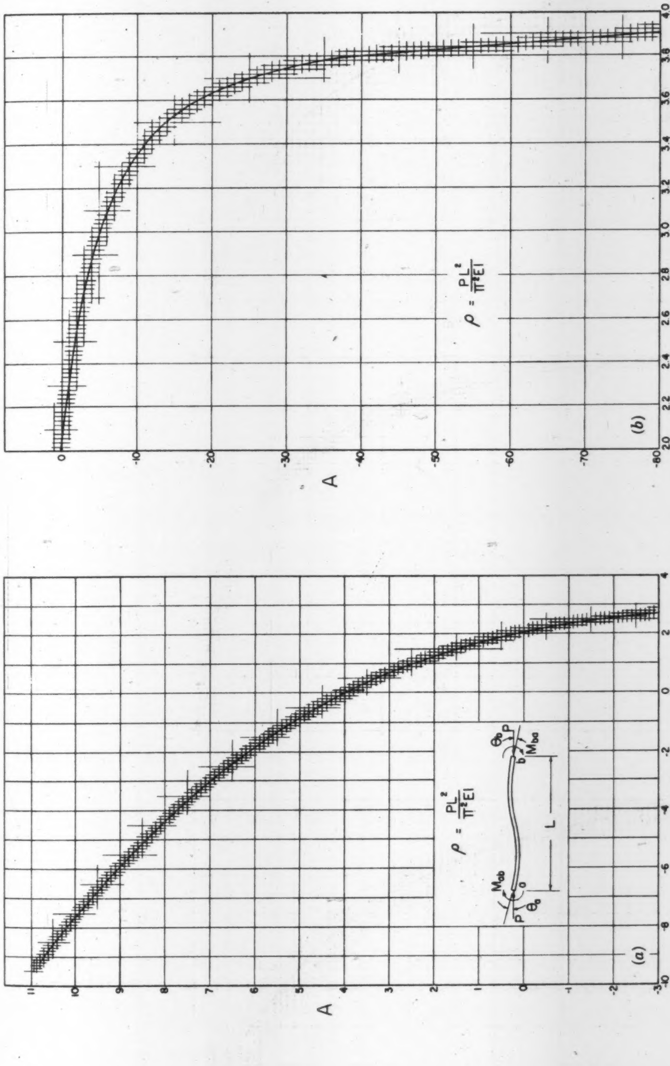

FIG. 2.—VALUES OF A

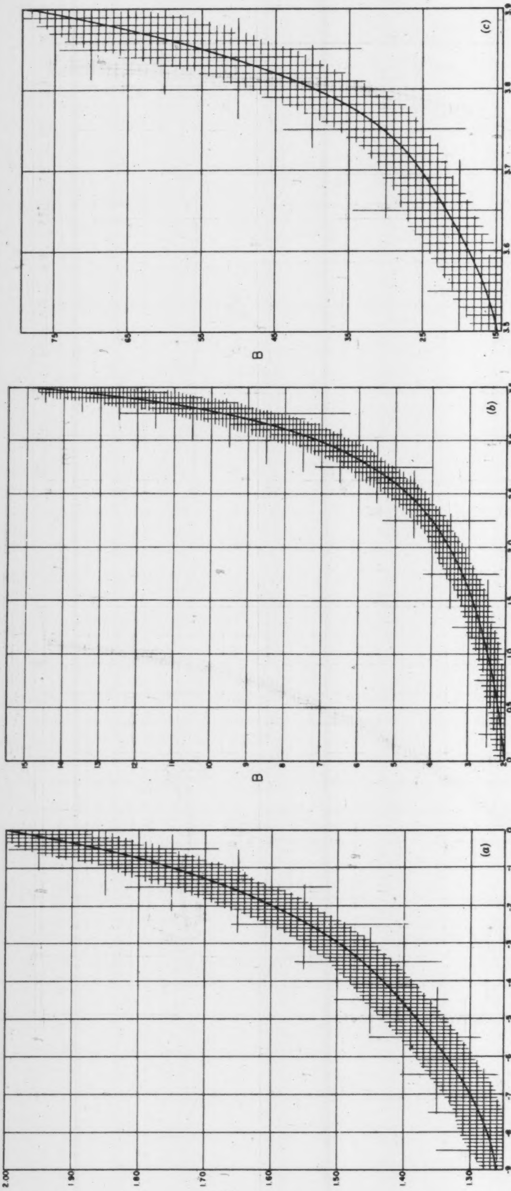

FIG. 3.—VALUES OF B

and

$$S_{ab} = -\frac{K_{ab}}{L_{ab}}\left(A_{ab} + B_{ab}\right)\left[\left(1 - \frac{B_{ab}}{A_{ab} + \frac{Q_a}{K_{ab}}}\right)\theta_b\right.$$

$$\left. - \left(2 - \frac{A_{ab} + B_{ab}}{A_{ab} + \frac{Q_a}{K_{ab}}}\right)\frac{\Delta_{ab}}{L_{ab}}\right] - P_{ab}\,\frac{\Delta_{ab}}{L_{ab}} \quad \ldots\ldots (11)$$

These may be written somewhat more compactly, if desired, with the introduction of several new and easily evaluated coefficients. Let

$$A_{ab} + B_{ab} = C_{ab} \quad \ldots\ldots\ldots\ldots\ldots (12a)$$

$$A_{ab} - \frac{B^2_{ab}}{A_{ab} + \frac{Q_a}{K_{ab}}} = A'_{ab} \quad \ldots\ldots\ldots (12b)$$

$$1 - \frac{B_{ab}}{A_{ab} + \frac{Q_a}{K_{ab}}} = c_{ab} \quad \ldots\ldots\ldots (12c)$$

and

$$2 - \frac{A_{ab} + B_{ab}}{A_{ab} + \frac{Q_a}{K_{ab}}} = c'_{ab} \quad \ldots\ldots\ldots\ldots (12d)$$

Then Eqs. 10 and 11 may be written in the form

$$M_{ba} = K_{ab}\left(A'_{ab}\,\theta_b - C_{ab}\,c_{ab}\,\frac{\Delta_{ab}}{L_{ab}}\right) \quad \ldots\ldots\ldots (13)$$

$$S_{ab} = -\frac{K_{ab}}{L_{ab}}\,C_{ab}\left(c_{ab}\,\theta_b - c'_{ab}\,\frac{\Delta_{ab}}{L_{ab}}\right) - P_{ab}\,\frac{\Delta_{ab}}{L_{ab}} \quad \ldots\ldots (14)$$

It may be noted that Eqs. 10 and 11 reduce directly to rather simple forms when Q takes on the limiting values of zero and infinity corresponding to the pinned condition and the built-in condition, respectively, at the base of the column.

Thus, for a pinned base:

$$M_{ba} = K_{ab}\,\frac{\left(A^2_{ab} - B^2_{ab}\right)}{A_{ab}}\left(\theta_b - \frac{\Delta_{ab}}{L_{ab}}\right) \quad \ldots\ldots\ldots (15a)$$

or

$$M_{ba} = K_{ab}\ \frac{C_{ab}}{A_{ab}}\ \left(A_{ab} - B_{ab}\right)\left(\theta_b - \frac{\Delta_{ab}}{L_{ab}}\right) \quad \ldots\ldots\ldots\ldots\ldots \tag{15b}$$

and

$$S_{ab} = -\ \frac{K_{ab}}{L_{ab}}\ \frac{\left(A_{ab}^2 - B_{ab}^2\right)}{A_{ab}}\left(\theta_b - \frac{\Delta_{ab}}{L_{ab}}\right) - P_{ab}\ \frac{\Delta_{ab}}{L_{ab}} \quad \ldots\ldots\ldots \tag{16a}$$

or

$$S_{ab} = -\ \frac{K_{ab}}{L_{ab}}\ \frac{C_{ab}}{A_{ab}}\ \left(A_{ab} - B_{ab}\right)\ \left(\theta_b - \frac{\Delta_{ab}}{L_{ab}}\right) - P_{ab}\ \frac{\Delta_{ab}}{L_{ab}} \quad \ldots\ldots\ldots \tag{16b}$$

Also

$$A'_{ab} = A_{ab} - \frac{B^2{}_{ab}}{A_{ab}} = \frac{A^2{}_{ab} - B^2{}_{ab}}{A_{ab}} = \frac{C_{ab}}{A_{ab}}\ \left(A_{ab} - B_{ab}\right) \quad \ldots \tag{17a}$$

$$c_{ab} = 1 - \frac{B_{ab}}{A_{ab}} = \frac{A_{ab} - B_{ab}}{A_{ab}} \quad \ldots\ldots\ldots\ldots \tag{17b}$$

and

$$c'_{ab} = 2 - \frac{A_{ab} + B_{ab}}{A_{ab}} = c_{ab} \quad \ldots\ldots\ldots\ldots\ldots \tag{17c}$$

For a built-in base:

$$M_{ba} = K_{ab}\left[A_{ab}\ \theta_b - \left(A_{ab} + B_{ab}\right)\frac{\Delta_{ab}}{L_{ab}}\right] \quad \ldots\ldots \tag{18a}$$

or

$$M_{ba} = K_{ab}\left(A_{ab}\ \theta_b - C_{ab}\ \frac{\Delta_{ab}}{L_{ab}}\right) \quad \ldots\ldots\ldots \tag{18b}$$

and

$$S_{ab} = -\ \frac{K_{ab}}{L_{ab}}\ \left(A_{ab} + B_{ab}\right)\ \left(\theta_b - 2\ \frac{\Delta_{ab}}{L_{ab}}\right) - P_{ab}\ \frac{\Delta_{ab}}{L_{ab}} \quad \ldots \tag{19a}$$

or

$$S_{ab} = -\ \frac{K_{ab}}{L_{ab}}\ C_{ab}\ \left(\theta_b - 2\ \frac{\Delta_{ab}}{L_{ab}}\right) - P_{ab}\ \frac{\Delta_{ab}}{L_{ab}} \quad \ldots \tag{19b}$$

Also

$$A'_{ab} = A_{ab} \qquad (20a)$$

$$c_{ab} = 1 \qquad (20b)$$

and

$$c'_{ab} = 2 \qquad (20c)$$

The formulas of this section are applied to buckling problems of certain rectangular frames, particularly one-story frames, in the following sections.

SYMMETRICAL BUCKLING

One-Story Single-Bay Frame.—Under certain conditions, a frame may buckle in a mode which does not involve lateral displacement of the joints. If one considers a one-story, single-bay rectangular frame under symmetrical conditions, as shown in Fig. 4, and sets

$$\left.\begin{aligned} \Delta_{ab} &= 0, \\ \text{and} \quad \theta_c &= -\ \theta_b \end{aligned}\right\} \qquad (21)$$

Eq. 13 for the column and girder become

$$\left.\begin{aligned} M_{ba} &= K_{ab}\, A'_{ab}\, \theta_b \\ M_{bc} &= K_{bc}\, \left(4\ \theta_b + 2\ \theta_c\right) = 2\ K_{bc}\, \theta_b \end{aligned}\right\} \qquad (22)$$

The sum of the moments acting about joint b must vanish, and therefore,

$$\left(K_{ab}\, A'_{ab} + 2\ K_{bc}\right) \theta_b = 0 \qquad (23)$$

Eq. 23 determines the magnitude of A'_{ab} which will maintain equilibrium in the symmetrically buckled configuration. The stability criterion therefore is

$$A'_{ab} = -\ 2\ \frac{K_{bc}}{K_{ab}} \qquad (24)$$

To determine the critical load, one first computes the required value of A'_{ab} by using Eq. 24. If the base of each column is fixed, the corresponding value of ρ may be read directly from Fig. 2 since $A'_{ab} = A_{ab}$. In other cases, the corresponding value of ρ is best obtained by trial-and-error. A value of ρ is assumed, and A'_{ab} is computed by means of Eqs. 12 or 17 using values of A and B from the charts of Figs. 2 and 3. The process is repeated until the value of ρ is determined which corresponds to the required value of A'_{ab}. Interpolation will be helpful in improving the successive trials. Normally, the proper value of ρ will be determined with satisfactory accuracy with only three or four trials. After establishing the correct value of ρ, the critical load is determined by use of Eq. 4b.

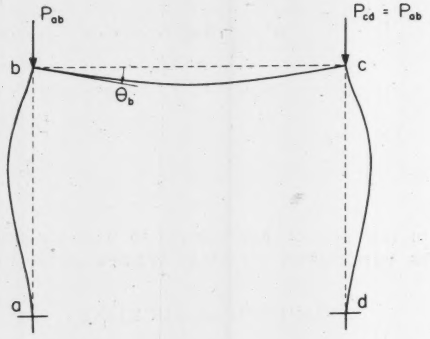
P_{ab}
$P_{cd} = P_{ab}$
b
c
θ_b
a
d

FIG. 4.—SYMMETRICAL BUCKLING OF A ONE-STORY SINGLE BAY RECTANGULAR FRAME

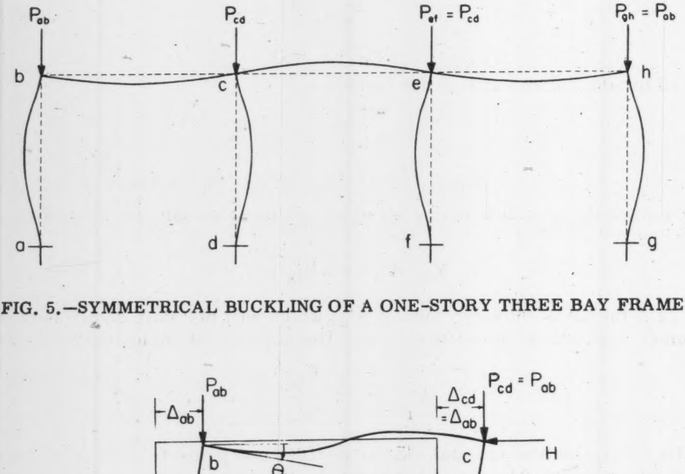
P_{ab}
P_{cd}
$P_{ef} = P_{cd}$
$P_{gh} = P_{ab}$
b
c
e
h
a
d
f
g

FIG. 5.—SYMMETRICAL BUCKLING OF A ONE-STORY THREE BAY FRAME

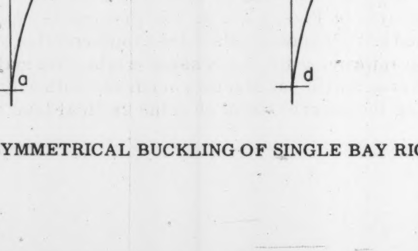
P_{ab}
Δ_{ab}
$P_{cd} = P_{ab}$
Δ_{cd}
$= \Delta_{ab}$
H
b
θ_b
c
a
d

FIG. 6.—ANTI-SYMMETRICAL BUCKLING OF SINGLE BAY RIGID FRAME

One-Story, Three-Bay Frame.—The basic equations used in the case of multi-bay frames are those which are used for single-bay frames. Because of the greater number of joint rotations, however, the procedure for determining whether or not given column loads form a critical set must differ from that employed for the single-bay frame. The single-bay frame may also be treated as a special case of the multi-bay frame. The three-bay frame, such as shown in Fig. 5, offers an opportunity to describe a general procedure for the analysis of symmetrical buckling in multi-bay frames.

The relevant moments are

$$M_{ba} = K_{ab} A'_{ab} \theta_b \quad \dots\dots\dots\dots\dots \quad (25a)$$

$$M_{bc} = K_{bc} \left(4 \theta_b + 2 \theta_c\right) \quad \dots\dots\dots\dots \quad (25b)$$

$$M_{cb} = K_{bc} \left(4 \theta_c + 2 \theta_b\right) \quad \dots\dots\dots\dots \quad (25c)$$

$$M_{cd} = K_{cd} A'_{cd} \theta_c \quad \dots\dots\dots\dots\dots \quad (25d)$$

and

$$M_{ce} = K_{ce} \left(4 \theta_c + 2 \theta_e\right) = 2 K_{ce} \theta_c \quad \dots\dots\dots \quad (25e)$$

where, in the last equation, advantage has been taken of the symmetry of the angular displacements. (The beam shears due to M_{bc}, M_{cb}, and so on, induce axial strains in columns and cause differential settlement of the beams. These effects, however, are generally small and have been neglected in this and subsequent analyses.)

The equilibrium equations,

$$M_{ba} + M_{bc} = 0 \quad \dots\dots\dots\dots\dots \quad (26a)$$

and

$$M_{cb} + M_{cd} + M_{ce} = 0 \quad \dots\dots\dots\dots \quad (26b)$$

become, upon substitution of Eqs. 25,

$$\left(K_{ab} A'_{ab} + 4 K_{bc}\right) \theta_b + 2 K_{bc} \theta_c = 0 \quad \dots\dots\dots \quad (27a)$$

and

$$2 K_{bc} \theta_b + \left(4 K_{bc} + K_{cd} A'_{cd} + 2 K_{ce}\right) \theta_c = 0 \quad \dots\dots \quad (27b)$$

These equations will be satisfied if the axial loads on the columns have their critical values.

There are several available procedures for determining whether a given set of column loads provide the values of A'_{ab} and A'_{cd} which make it possible to satisfy this pair of simultaneous equations. A trial-and-error procedure generally will be most practical.

One such procedure consists of the following steps: After selecting trial values for the column loads and computing the value of A'_{ab} and of A'_{cd}, either of the equilibrium equations may be solved for one rotation in terms of the other. For example, the second of Eqs. 27 may be solved for θ_c in terms of θ_b. This result now may be substituted into the remaining equation and it can be determined whether or not this transformed equation can be satisfied. This, it will be seen, is tantamount to the vanishing of the coefficient of θ_b in the transformed equation. If both equations can be satisfied, then the assumed loads form a critical set. If not, new values are chosen and the process is repeated.

Following this line of attack, the elimination of θ_c from the pair of equations yields

$$\left(K_{ab}\,A'_{ab} + 4\,K_{bc} - \frac{4\,K^2_{bc}}{4\,K_{bc} + K_{cd}\,A'_{cd} + 2\,K_{ce}}\right)\theta_b = 0 \quad \ldots (28)$$

which can be satisfied if the coefficient of θ_b vanishes. Thus, the stability criterion is

$$K_{ab}\,A'_{ab} + 4\,K_{bc} - \frac{4\,K^2_{bc}}{4\,K_{bc} + K_{cd}\,A'_{cd} + 2\,K_{ce}} = 0 \quad \ldots\ldots (29)$$

An alternate form may be obtained by placing the entire expression over a common denominator and setting the numerator equal to zero; in other words, multiplying through by the denominator of the fraction. This yields the stability criterion in the form,

$$\left(K_{ab}\;A'_{ab} + 4\,K_{bc}\right)\left(4\,K_{bc} + K_{cd}\,A'_{cd} + 2\,K_{ce}\right) - 4\,K^2_{bc} = 0 \,.\,.\, (30)$$

It may be noted that Eq. 30 would also be obtained if θ_b had first been eliminated from the pair of equilibrium equations. One may observe also that Eq. 30 is the expansion of the determinant formed by the coefficients of the rotations in Eqs. 27.

There are several ways to describe or define a critical set of loads. For example, the ratio between P_{ab} and P_{cd} may be specified. Thus, trial values will conform to this ratio, as will subsequent trial values, if necessary in the trial-and-error process. Alternatively, the set may be defined by specifying the actual magnitude of one of the column loads. In the associated trial-and-error process, the remaining load is adjusted until the proper value is found which permits the two equilibrium equations to be satisfied. If the critical set is to be defined in this manner, the first procedure might be found to be convenient. Suppose, for example, that the magnitude of P_{bc} is specified, and P_{ab} is subject to variation. Then the coefficients in Eq. 27 b are completely defined, and θ_c may be determined in terms of θ_b. Substitution of this result into the first equation of the pair reduces this equation to a homogeneous expression in θ_b. The proper value of A'_{ab} now may be computed in a simple manner, and the corresponding critical value of ρ for this column may be found. The analogous sequence of operations may be performed directly upon Eq. 30 and will, of course, yield the same result.

A third procedure introduces the concept of "reserve stiffness" as a stability criterion. Imagine that an external moment M_o is applied to joint b. The equilibrium equations at joints c and b, respectively, become

$$2\,K_{bc}\,\theta_b + \left(4\,K_{bc} + K_{cd}\,A'_{cd} + 2\,K_{ce}\right)\theta_c = 0 \quad \ldots\ldots\ldots (31a)$$

$$\left(K_{ab}\,A'_{ab} + 4\,K_{bc}\right)\theta_b + 2\,K_{bc}\,\theta_c = M_o \quad \ldots\ldots\ldots (31b)$$

in which the positive direction of M_o is the same as the positive direction for joint rotations. Assuming a value of unity for θ_b, the first equation is solved for θ_c. These values are now substituted into the second equation, and M_o is determined. The sign of M_o establishes whether the frame is stable or unstable under the loads corresponding to the values of A'_{ab} and A'_{cd} which have been used. If M_o is positive, that is, if M_o acts in the direction of θ_b, then the frame has "reserve stiffness," and is stable under the applied loads. Conversely, if M_o is negative, the critical loads have been exceeded, and the frame is unstable. If M_o has the value zero, the applied loads exactly constitute a critical set. Since the sign and magnitude of M_o serve as a criterion of stability, one may again use a trial-and-error procedure to determine the magnitudes of the column loads which form a critical set. The sign of the computed value of M_o indicates whether the column loads should be increased or decreased for the next trial.

By an extension of these methods, the symmetrical modes of buckling of multi-story frames may be investigated and the magnitudes of the critical loads may be established. A further generalization leads to a related procedure for treating the lurching or antisymmetrical modes of buckling of multi-story frames. While these methods already have been developed, they are beyond the scope of the present paper.

SIDESWAY BUCKLING OF FRAMES

Unbraced Single-Bay Frame.—The critical values of the column loads for the antisymmetrical or lurching mode of buckling may be determined through the use of Eqs. 1 and their particularized variations.

In the case of a single-bay rigid frame, the deformed or buckled structure appears somewhat as shown in Fig. 6. If the frame is symmetrical and symmetrically loaded, then only two equilibrium equations need be written. These state that the sum of the moments at either upper joint, say b, vanishes, and that the force H which is shown in Fig. 6 also vanishes; thus

$$M_{ba} + M_{bc} = 0 \quad \ldots\ldots\ldots\ldots\ldots\ldots \quad (32)$$

$$- S_{ab} - S_{cd} = H = 0 \quad \ldots\ldots\ldots\ldots\ldots\ldots \quad (33a)$$

By virtue of the assumed symmetry, Eq. 33a may be written simply as

$$- S_{ab} = \frac{H}{2} = 0 \quad \ldots\ldots\ldots\ldots\ldots\ldots \quad (33b)$$

Noting that Δ_{bc} is zero, these equations become, through the use of Eqs. 1, 13, and 14

$$K_{ab}\left(A'_{ab}\,\theta_b - C_{ab}\,c_{ab}\,\frac{\Delta_{ab}}{L_{ab}}\right) + 2\,K_{bc}\,\theta_b = 0 \quad \ldots\ldots \quad (34a)$$

and

$$\frac{K_{ab}}{L_{ab}}\,C_{ab}\left(c_{ab}\,\theta_b - c'_{ab}\,\frac{\Delta_{ab}}{L_{ab}}\right) + P_{ab}\,\frac{\Delta_{ab}}{L_{ab}} = \frac{H}{2} = 0 \quad \ldots\ldots \quad (34b)$$

or, upon collecting terms,

$$\left(K_{ab}\,A'_{ab} + 2\,K_{bc}\right)\,\theta_b - K_{ab}\,C_{ab}\,c_{ab}\,\frac{\Delta_{ab}}{L_{ab}} = 0 \quad \ldots\ldots \quad (35a)$$

and

$$\frac{K_{ab}}{L_{ab}} C_{ab} c_{ab} \theta_b - \left(\frac{K_{ab}}{L_{ab}} C_{ab} c'_{ab} - P_{ab}\right) \frac{\Delta_{ab}}{L_{ab}} = \frac{H}{2} = 0 \quad . \; . \; . \; . \; (35b)$$

One may again note that the constants have very simple forms when the base conditions are either fixed or hinged.

As in the previous cases, a trial-and-error procedure for the solution of Eqs. 35 and the determination of the critical load will be found to be convenient and relatively rapid. Noting that, for a frame such as shown in Fig. 6, the critical load must be less than the Euler load computed with an appropriate modulus, a trial value is selected for P_{ab} and the coefficients evaluated. Assuming Δ_{ab} to have unit magnitude, the value of θ_b is found from Eq. 35a. Substitution of this value of θ_b and the unit value of Δ_{ab} into Eq. 35b yields the value of H that would be required to hold the frame in the deflected position with the prescribed column loads. The sign of the computed value of H determines whether the axial loads are greater or less than the critical loads. If H is positive, the assumed column loads exceed the critical loads since the force H is now supporting the frame against further deflection. If H is negative, the assumed column loads are less then the critical loads, since the direction of H now implies that the frame has "reserve stiffness." If H vanishes, the assumed column loads are equal to the critical loads. In the trial-and-error procedure, if H is not zero, its sign clearly indicates whether the next trial value for the axial load should be larger or smaller.

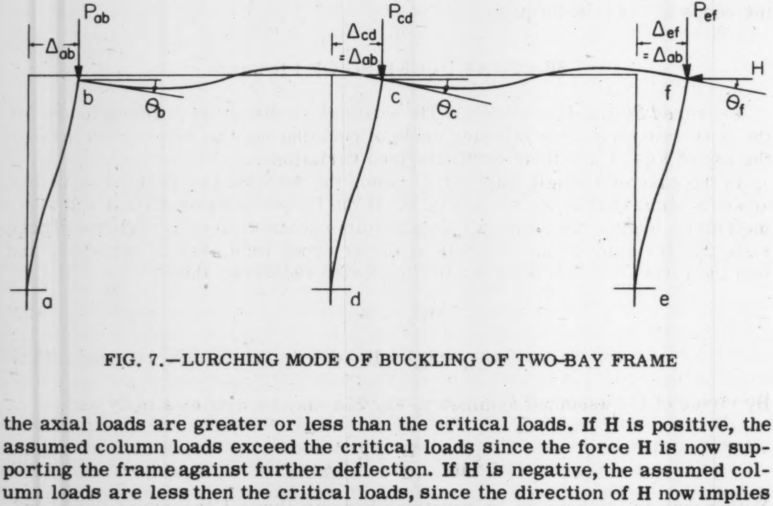

FIG. 7.—LURCHING MODE OF BUCKLING OF TWO-BAY FRAME

Multi-Bay Frames.—A two-bay frame serves to illustrate the procedure for determining the critical loads of a multi-bay frame in the lurching mode of collapse (Fig. 7).

The equilibrium equations,

$$M_{ba} + M_{bc} = 0 \quad \ldots\ldots\ldots\ldots\ldots \quad (36a)$$

$$M_{cb} + M_{cd} + M_{cf} = 0 \quad \ldots\ldots\ldots\ldots\ldots \quad (36b)$$

$$M_{fc} + M_{fe} = 0 \quad \ldots\ldots\ldots\ldots\ldots \quad (36c)$$

$$S_{ab} + S_{cd} + S_{ef} = - H = 0 \quad \ldots\ldots\ldots\ldots \quad (36d)$$

become, upon substitution of the appropriate expressions,

$$\left(K_{ab}\, A'_{ab} + 4\, K_{bc}\right) \theta_b + 2\, K_{bc}\, \theta_c - K_{ab}\, C_{ab}\, c_{ab} \frac{\Delta_{ab}}{L_{ab}} = 0 \quad \ldots \quad (37a)$$

$$2\, K_{bc}\, \theta_b + \left(K_{cd}\, A'_{cd} + 4\, K_{bc} + 4\, K_{cf}\right) \theta_c$$

$$+ 2\, K_{cf}\, \theta_f - K_{cd}\, C_{cd}\, c_{cd} \frac{\Delta_{ab}}{L_{cd}} = 0 \quad \ldots\ldots \quad (37b)$$

$$2\, K_{cf}\, \theta_c + \left(K_{ef}\, A'_{ef} + 4\, K_{cf}\right) \theta_f - K_{ef}\, C_{ef}\, c_{ef} \frac{\Delta_{ab}}{L_{ef}} = 0 \quad \ldots\ldots \quad (37c)$$

and

$$\frac{K_{ab}}{L_{ab}} C_{ab}\, c_{ab}\, \theta_b + \frac{K_{cd}}{L_{cd}} C_{cd}\, c_{cd}\, \theta_c + \frac{K_{ef}}{L_{ef}} C_{ef}\, c_{ef}\, \theta_f$$

$$- \left(\frac{K_{ab}}{L_{ab}^2} C_{ab}\, c'_{ab} + \frac{K_{cd}}{L_{cd}^2} C_{cd}\, c'_{cd} + \frac{K_{ef}}{L_{ef}^2} C_{ef}\, c'_{ef} \right.$$

$$\left. - \frac{P_{ab}}{L_{ab}} - \frac{P_{cd}}{L_{cd}} - \frac{P_{ef}}{L_{ef}} \right) \Delta_{ab} = H = 0 \quad \ldots\ldots\ldots \quad (37d)$$

As in the previous case, a trial-and-error procedure directed toward the determination of H may be employed. Trial values for the column loads are assumed, and the coefficients in the four equations are evaluated. Setting Δ_{ab} equal to unity, the three joint equilibrium equations are solved for the joint rotations. These values, together with the unit value of Δ_{ab}, are now substituted into the last equation, and the value of H determined. As in the previous case, if H is positive, the assumed column loads exceed their critical values. If, however, H is negative, the loads are less than their critical values; and if H vanishes, the loads are equal to their critical values.

If the number of joints is not large, the joint equilibrium equations may be solved easily for the joint rotations by any of the conventional algebraic methods

including Gauss' substitution and elimination procedure, Cramer's determinant method, or Crout's algorithm. If the number of joints is too large to permit the convenient use of these procedures and if a computer program is not available, the joint equations may be solved by a step-by-step procedure.

Independently Braced Frame.—Frames sometimes exist which are braced against sidesway independently of other frames by structure which may be considered to be external to the frame. This bracing may be in the form of sheathing, wall panels or diagonal tie-rods in the plane of the frame, or, say, by an eave girt that extends to solid anchorages before and behind the plane of the frame.

In certain cases, support may be provided to a critically loaded frame by adjacent frames that are lightly loaded, this support being transmitted through the bracing system. Such may be the case, for instance, in an industrial building that contains an overhead traveling crane carried by the frames of the building. Obviously, the crane can be in the plane of only one frame at any time, and thus only this frame could be critically loaded at that time. The other frames, being less than critically loaded, may be able to support the critically loaded frame against sidesway buckling.

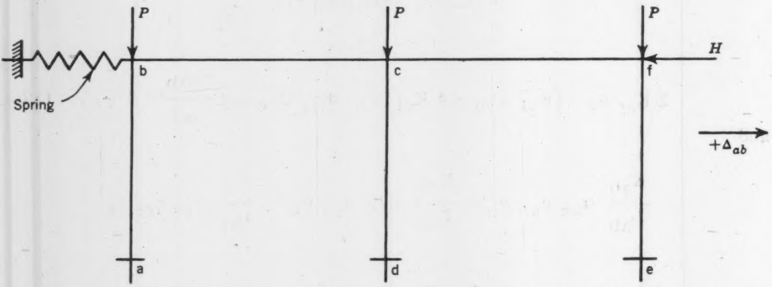

FIG. 8.—REPRESENTATION OF AN INDEPENDENTLY BRACED FRAME

Such bracing often may be represented by a linear spring as shown in Fig. 8, which also shows the fictitious supporting force, H.

For purposes of illustration, the two-bay frame of the previous section is considered with additional and external bracing represented by the spring shown at joint b.

The three joint equilibrium equations are identical with the first three of Eqs. 37. If k is the stiffness or rate of the spring, then $k\Delta_{ab}$ is the spring force. This force acts upon the frame in a direction opposite to the displacement Δ_{ab}, and, for the assumed direction of the displacement, the spring force acts in the positive direction of the fictitious force, H. Consequently, the term $k\Delta_{ab}$ must be added to the fictitious force on the right-hand side of Eq. 37d. Upon transposing this term, the shear equation for the frame becomes

$$\frac{K_{ab}}{L_{ab}} C_{ab}\, c_{ab}\, \theta_b + \frac{K_{cd}}{L_{cd}} C_{cd}\, c_{cd}\, \theta_c + \frac{K_{ef}}{L_{ef}} C_{ef}\, c_{ef}\, \theta_f$$

$$- \left(\frac{K_{ab}}{L_{ab}^2} C_{ab}\, c'_{ab} + \frac{K_{cd}}{L_{cd}^2} C_{cd}\, c'_{cd} + \frac{K_{ef}}{L_{ef}^2} C_{ef}\, c'_{ef} \right.$$

$$\left. - \frac{P_{ab}}{L_{ab}} - \frac{P_{cd}}{L_{cd}} - \frac{P_{ef}}{L_{ef}} + k \right) \Delta_{ab} = H = 0 \quad \ldots\ldots \quad (38)$$

and this equation replaces Eq. 37d. The procedure for determining the critical loads from this revised set of equations is essentially the same as that outlined in the previous section.

SIDESWAY BUCKLING OF BUILDINGS

The primary structure of certain types of one-story buildings consists of a number of parallel frames interconnected by a bracing system in the form of a truss lying in a horizontal plane at the elevation of the roof or ceiling. In some cases, the horizontal truss is omitted, and the bracing function may be performed by the roof deck. The bracing system should extend over the entire length of the building and be supported by shear walls or by braced frames at the ends of the building or at interior planes. In the absence of shear walls or braced frames, the frames which are themselves less than critically loaded so that their own independent collapse is not possible may be called upon to support the critically loaded frames.

Under these conditions, frames will not buckle individually in a sidesway or lurching mode, but rather a general collapse will occur when the loads are sufficiently large unless a symmetrical mode of buckling occurs at a lower load. A collapse involving the complete structure is called general instability.

The problem of determining whether or not a complete one-story building structure will buckle when a given set of loads is applied simultaneously to all columns includes the elements of the theory which was discussed in the preceding sections. In addition, the coupling between the frames and the coincident effect of the frames upon the bracing system must be considered.

One may, of course, arrive at an estimate or somewhat rational guess of the stiffness or spring rate provided by the bracing system to the critically loaded frame or frames. When this can be done with satisfactory accuracy, the critical loads of a spring-supported frame can be determined by application of the theory of sidesway buckling for independently braced frames as described previously. However, results obtained by treating the frames independently are not likely to be correct. While it is a simple matter to obtain a conservative approximation to the critical loads with this approach, the degree of conservatism is difficult to evaluate and may lead to an uneconomical design. A safe estimate for the upper bounds on the critical loads is also difficult to define, and consequently the designer or analyst may have a wide range from which he must extract the correct values of the critical loads.

The problem of correctly determining the critical loads for a complete one-story structure consisting of a number of parallel frames and a horizontal bracing system is amenable to solution by reasonably simple methods.

For clarity, consider the structure shown in Fig. 9. The structure is assumed to be separated, as shown in the figure, into frames and bracing system. If each frame is loaded in excess of a critical loading, the supporting force H, shown in Fig. 6 and computed by an equation having the character of Eq. 37c, will act to the left on the frame if Δ is a unit displacement to the right. The

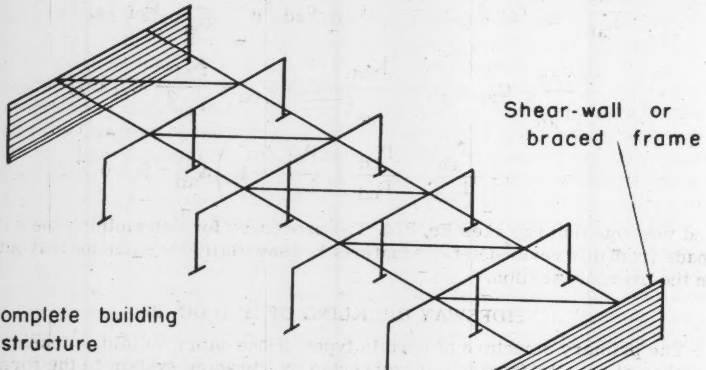
Shear-wall or braced frame

a) Complete building structure

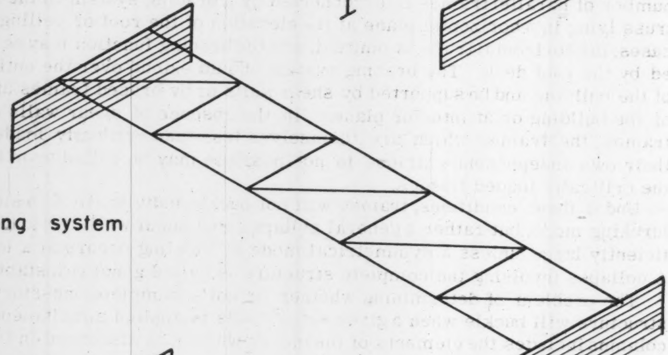

b) Bracing system

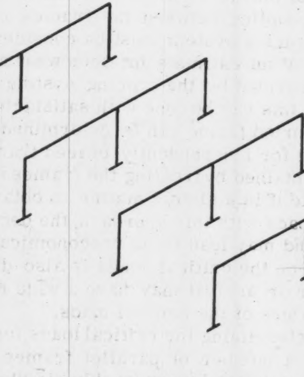

c) Frames

FIG. 9.—COMPLETE STRUCTURE AND ITS COMPONENTS

actual force will be directly proportional to the displacement, and the magnitude of H may be interpreted as a negative spring rate for the unbraced frame under the given loads.

The frames will therefore exert forces in the opposite direction upon the bracing system. Thus, if y_j is the actual lateral deflection at the top of the j-th frame and H_j is the supporting force at that frame per unit displacement, then the total force exerted upon the bracing system is

$$F_j = H_j\, y_j \quad \ldots\ldots\ldots\ldots\ldots\ldots \quad (39)$$

acting in the direction of the displacement.

The bracing system may be treated separately as an elastic structure, and influence coefficients for the several frame locations may be determined by any of the standard techniques for computing deflections. These influence coefficients are designated a_{ij} and are defined as the lateral deflection at the i-th location due to a unit load applied at the j-th location. Since each frame must be supported, each frame will exert a force upon the bracing system, and the total deflection at the i-th location will be

$$y_i = \sum_{j=1}^{r} F_j\, a_{ij} \quad (i = 1, 2, \ldots, r) \ldots\ldots\ldots\ldots \quad (40)$$

where r is the number of critically loaded frames. Substituting Eq. 39 into Eq. 40 yields the set of simultaneous equations

$$\sum_{j=1}^{r} a_{ij}\, H_j\, y_j = y_i \qquad (i = 1, 2, \ldots, r) \ldots\ldots\ldots\ldots \quad (41)$$

Since the stiffnesses, H_j, depend upon the column loads of the several frames, Eqs. 41 defines a set of column loads for which the complete structure is just stable with respect to the sidesway mode of buckling. If the column loads are not specified *a priori*, the equations form an eigenvalue problem which yields the permissible values of these loads. However, the relation between the column loads and the frame stiffnesses is so transcendental that the direct determination of the column loads by Eqs. 41 is not practical.

Fortunately, from an engineering standpoint, the problem of determining the critical loads of the structure may be replaced by the question of whether or not a specified set of loads will cause the frame to collapse. An answer to this question can be obtained with relative ease if the question is replaced by the problem of determining the stiffness of the bracing system that will prevent sidesway buckling of the complete structure under the specified loads. In particular, it is desired to determine the factor, μ, by which the stiffness of the bracing system must be multiplied to prevent buckling of the structure under the specified loads. If the stiffness is multiplied by μ, the influence coefficients for deflection are decreased by this factor and Eq. 41 becomes

$$\sum_{j=1}^{r} \frac{a_{ij}}{\mu} H_j\, y_j = y_i \quad \ldots\ldots\ldots\ldots\ldots\ldots \quad (42a)$$

or

$$\sum_{j=1}^{r} a_{ij}\, H_j\, y_j = \mu\, y_i \quad \ldots\ldots\ldots\ldots\ldots\ldots \quad (42b)$$

The relative values of the y's which satisfy Eqs. 42 can be found by an iterative procedure. After the iterative process has converged, the value of μ can be determined.

One may note that, if the frames are identical and identically loaded, H_j will be the same for all frames and may be replaced by the single value, H. Eq. 42 then may be replaced by

$$\sum_{j=1}^{r} a_{ij}\, y_j = \frac{\mu}{H}\, y_i \quad \ldots\ldots\ldots\ldots\ldots\ldots (43)$$

This equation, however, is not to be used if the frames differ or if the loadings on the frames differ.

In using the iterative procedure, one assumes a set of y's which preferably are normalized or scaled so that a selected one of the y's has a magnitude of unity. These values are substituted into the left-hand sides of Eqs. 42 or 43. This yields a new and ordinarily more correct set of numbers proportional to the deflections of the bracing system at each frame location. With both the initial set and computed set normalized to unity at the same point, the deflections of the two sets are compared point by point. If the agreement is satisfactory, the magnitude of μ may be computed. If the agreement is not satisfactory, the process should be repeated.

When convergence has been obtained, any of the final set of y's may be used to compute μ. In particular, if $y_i^{(n)}$ represents the values substituted into the left-hand side of Eq. 42, and $y_i^{(n+1)}$ is the value of the right-hand side before normalizing, then

$$\mu = \frac{y_i^{(n+1)}}{y_i^{(n)}} \quad \ldots\ldots\ldots\ldots\ldots\ldots (44)$$

in which, of course, the same frame location, i, is used in both numerator and denominator. The term μ may be recognized as the "normalizing factor," the quantity by which the output must be divided in order to normalize these quantities.

If the frames are identical and identically loaded so that Eq. 43 may be used in place of Eqs. 42, then Eq. 44 may be replaced by

$$\frac{\mu}{H} = \frac{y_i^{(n+1)}}{y_i^{(n)}} \quad \ldots\ldots\ldots\ldots\ldots\ldots (45)$$

Frequently, one wishes to determine the critical loads, under the condition of identical frames and identical loads on all frames, that a given system will support without sidesway collapse. For a given system under these conditions, μ must be taken as unity in Eq. 45, and the criterion for stability becomes

$$H \leq \frac{y_i^{(n)}}{y_i^{(n+1)}} \quad \ldots\ldots\ldots\ldots\ldots\ldots (46)$$

This equation, however, is to be used only under the conditions stated previously.

The magnitude of μ is the amount by which the stiffness of the bracing system must be multiplied to provide precisely the support that is necessary to prevent sidesway buckling of the complete structure under the imposed loads. Consequently, the computed value of μ serves as a criterion of stability since

$$\text{for stability} \quad \mu \leqq 1 \quad \ldots\ldots (47)$$

$$\text{and for instability} \quad \mu > 1 \quad \ldots\ldots (48)$$

Several examples will serve to illustrate the methods that have been presented. The reader will recognize that certain simplifications are possible. For example, when the entire structure is composed of the same material and is operating in the elastic range throughout, it may be convenient to divide all constants by the modulus and perhaps by certain dimensional factors. When portions of the structure are operating at different stress levels so that the modulus is different for different members, a reference modulus may be divided out, for example, the elastic modulus. In the interest of clarity, these simplifications are not made in the following examples.

ILLUSTRATIVE EXAMPLES

Symmetrical Buckling of Two-Bay Frame.—In this example the following data are given: The girders are 8 WF 31, the area is 9.12 sq in., $I = 109.7$ in.^{4}: The columns are 8 H 34.3, the area is 10.00 sq in., $I = 35.1$ in.^{4}, $Q = 10^8$ in.-lb per radian.

For each column

$$P_e = \frac{\pi^2 E I}{L^2} = 125{,}303 \text{ lb}$$

The stiffness factors are

$$K_{ab} = \frac{30 \times 10^6 \times 35.1}{24 \times 12} = 3.656 \times 10^6 \text{ in.-lb}$$

$$K_{bc} = \frac{30 \times 10^6 \times 109.7}{30 \times 12} = 9.142 \times 10^6 \text{ in.-lb}$$

and

$$\frac{Q}{K_{ab}} = \frac{10^8}{3.656 \times 10^6} = 27.35$$

In the symmetrical mode of buckling, $\Delta = 0$, $\theta_c = 0$. Therefore,

$$M_{bc} = K_{bc} \, (4) \, \theta_b \quad \ldots\ldots (49a)$$

$$M_{ba} = K_{ab} \, A'_{ab} \, \theta_b \quad \ldots\ldots (49b)$$

Since

$$M_{ba} + M_{bc} = 0 \quad \ldots\ldots (49c)$$

it follows that

$$\left(K_{ab} \, A'_{ab} + 4K_{bc}\right) \theta_b = 0 \quad \ldots\ldots (50)$$

Hence, the stability criterion becomes

$$A'_{ab} = -4 \frac{K_{bc}}{K_{ab}} = -4 \, \frac{9.142}{3.656} = -10.00 \quad \ldots\ldots (51)$$

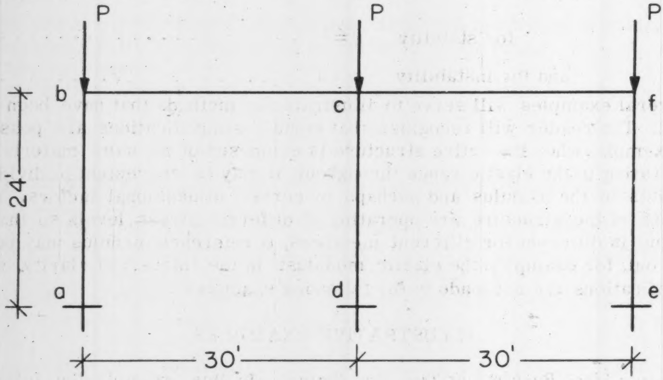
P
P
P
b
c
f
24'
a
d
e
30'
30'

FIG. 10.—ILLUSTRATIVE EXAMPLE—TWO BAY FRAMES

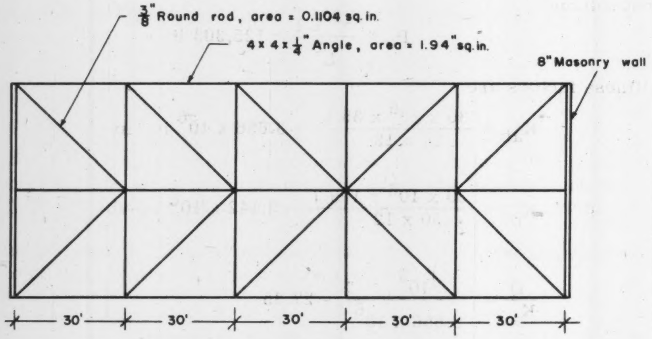
3/8" Round rod, area = 0.1104 sq. in.
4 x 4 x 1/4" Angle, area = 1.94" sq. in.
8" Masonry wall
30'
30'
30'
30'
30'

PLAN OF BRACING SYSTEM

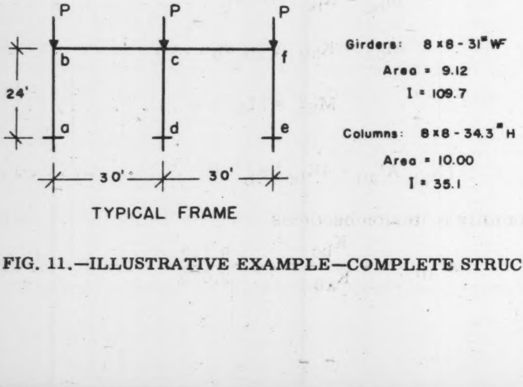
P
P
P
b
c
f
24'
a
d
e
30'
30'
Girders: 8 x 8 - 31# WF
Area = 9.12
I = 109.7
Columns: 8 x 8 - 34.3# H
Area = 10.00
I = 35.1

TYPICAL FRAME

FIG. 11.—ILLUSTRATIVE EXAMPLE—COMPLETE STRUCTURE

For trial 1, taking $\rho = 3.0$, $A = -5.03$ and $B = 7.12$ from Table 1, therefore,

$$A' = -5.03 - \frac{(7.12)^2}{-5.03 + 27.35} = -5.03 - 2.27 = -7.30$$

which is too small negatively. For trial 2, taking $\rho = 3.1$, $A = -6.05$ and $B = 7.96$, therefore,

$$A' = -6.05 - \frac{(7.96)^2}{-6.05 + 27.35} = -6.05 - 2.98 = -9.03$$

which is too small. For trial 3, taking $\rho = 3.2$, $A = -7.30$ and $B = 9.02$, therefore,

$$A' = -7.30 - \frac{(9.02)^2}{-7.30 + 27.35} = -7.30 - 4.06 = -11.36$$

By interpolation, for the critical load

$$\rho = 3.142$$

and

$$P_{cr} = 3.142\ P_e = 3.142\ (125{,}303) = 393{,}700 \text{ lbs}$$

Sidesway Buckling of Two-Bay Frame.—The same frame is used as in the previous example. All columns have equal loads. The mode of buckling is antisymmetrical; $\theta_f = \theta_b$; and $\Delta = 0$ for the girders. Therefore (see Eq. 13),

$$M_{ba} = M_{fe} = 3.656 \times 10^6 \left(A'_{ab}\,\theta_b - C_{ab}\,c_{ab}\frac{\Delta_{ab}}{L_{ab}}\right) \quad . . (52a)$$

$$M_{cd} = 3.656 \times 10^6 \left(A'_{cd}\,\theta_c - C_{cd}\,c_{cd}\frac{\Delta_{ab}}{L_{cd}}\right) \quad . . (52b)$$

$$M_{bc} = 9.142 \times 10^6 \left(4\,\theta_b + 2\,\theta_c\right) \ldots\ldots\ldots\ldots (52c)$$

$$M_{cb} = M_{cf} = 9.142 \times 10^6 \left(4\,\theta_c + 2\,\theta_b\right) \ldots\ldots (52d)$$

Also, (see Eq. 14)

$$S_{ab} = -\frac{3.656 \times 10^6}{24 \times 12}\ C_{ab}\left(c_{ab}\,\theta_b - c'_{ab}\frac{\Delta_{ab}}{L_{ab}}\right) - P_{ab}\frac{\Delta}{L_{ab}} \quad . . (53a)$$

and

$$S_{cd} = -\frac{3.656 \times 10^6}{24 \times 12}\ C_{cd}\left(c_{cd}\,\theta_c - c'_{cd}\frac{\Delta_{ab}}{L_{cd}}\right) - P_{cd}\frac{\Delta}{L_{ab}} \quad . . (53b)$$

Since the columns are identical and equally loaded, their coefficients are the same. Also, Δ may be taken equal to unity in the final calculation.

The joint equilibrium equations are

$$M_{ba} + M_{bc} = 0 \quad \ldots\ldots \quad (54a)$$

$$M_{cd} + 2M_{cb} = 0 \quad \ldots\ldots \quad (54b)$$

Also

$$S_{ab} + S_{cd} + S_{ef} = -H \quad \ldots\ldots \quad (55a)$$

or

$$2S_{ab} + S_{cd} = - H = 0 \quad \ldots\ldots \quad (55b)$$

Trial 1: $\rho = 0.9$; $P = 0.9\ (125{,}303) = 112{,}773$ lb; $A = 2.645$; $B = 2.404$. By Eqs. 12

$$A'_{ab} = 2.645 - \frac{(2.404)^2}{2.645 + 27.35} = 2.645 - 0.193 = 2.838$$

$$C_{ab} = 2.645 + 2.404 = 5.049$$

$$c_{ab} = 1 - \frac{2.404}{2.645 + 27.35} = 1 - 0.080 = 0.920$$

and

$$c'_{ab} = 2 - \frac{2.645 + 2.404}{2.645 + 27.35} = 2 - 0.168 = 1.832$$

The joint equilibrium equations become

$$3.656 \times 10^6 \left(2.838\ \theta_b - 5.049 \times .920\ \frac{\Delta}{L_{ab}}\right)$$

$$+ 9.142 \times 10^6 \left(4\ \theta_b + 2\ \theta_c\right) = 0 \quad \ldots\ldots \quad (56a)$$

and

$$3.656 \times 10^6 \left(2.838\ \theta_c - 5.049 \times .920\ \frac{\Delta}{L_{ab}}\right)$$

$$+ 2 \times 9.142 \times 10^6 \left(4\ \theta_c + 2\ \theta_b\right) = 0 \quad \ldots\ldots \quad (57a)$$

Eqs. 56a and 57a reduce to

$$46.944\ \theta_b + 18.284\ \theta_c = 16.9824\ \frac{\Delta}{L_{ab}} \quad \ldots\ldots \quad (56b)$$

and

$$36.568\ \theta_b + 83.512\ \theta_c = 16.9824\ \frac{\Delta}{L_{ab}} \quad \ldots\ldots \quad (57b)$$

which have the solution

$$\theta_b = 0.34065 \frac{\Delta}{L_{ab}} \quad \ldots\ldots\ldots\ldots\ldots \text{(58a)}$$

and

$$\theta_c = 0.05419 \frac{\Delta}{L_{ab}} \quad \ldots\ldots\ldots\ldots\ldots \text{(58b)}$$

Substituting these values into Eq. 14 yields

$$S_{ab} = \frac{-3.656 \times 10^6}{288} 5.049 \ (0.920 \times .34065 - 1.832) \frac{\Delta}{L_{ab}}$$

$$-112{,}773 \frac{\Delta}{L_{ab}} = -15{,}414 \frac{\Delta}{L_{ab}} \quad \ldots\ldots\ldots\ldots\ldots \text{(59a)}$$

and

$$S_{cd} = \frac{-3.656 \times 10^6}{288} 5.049 \ (0.920 \times 0.05419 - 1.832) \frac{\Delta}{L_{ab}}$$

$$-112{,}773 \frac{\Delta}{L_{ab}} = 1{,}443 \frac{\Delta}{L_{ab}} \quad \ldots\ldots\ldots\ldots\ldots \text{(59b)}$$

and, consequently,

$$H = (15{,}414 - 1{,}443 + 15{,}414) \frac{\Delta}{L_{ab}} = 29{,}385 \frac{\Delta}{L_{ab}} \quad \ldots\ldots\ldots \text{(60)}$$

Since H is positive for positive values of Δ, the frame is unstable under the assumed loads.

Trial 2: $\rho = 0.8$; P = 0.8 (125,303) = 100,243 lb; A = 2.816; B = 2.346; and the constants, are

$$A'_{ab} = 2.816 - \frac{(2.346)^2}{2.816 + 27.35} = 2.634$$

$$C_{ab} = 2.816 + 2.346 = 5.162$$

$$c_{ab} = 1 - \frac{2.346}{2.816 + 27.35} = 1 - 0.078 = 0.922$$

and

$$c'_{ab} = 2 - \frac{2.816 + 2.346}{2.816 + 27.35} = 2 - 0.171 = 1.829$$

The joint equilibrium equations,

$$M_{ba} + M_{bc} = 0 \tag{61a}$$

$$M_{cd} + 2\ M_{cb} = 0 \tag{61b}$$

become

$$3.656 \times 10^6 \left(2.634\ \theta_b - 5.162 \times 0.922\ \frac{\Delta}{L_{ab}}\right) + 9.142 \times 10^6 \left(4\ \theta_b + 2\ \theta_c\right) = 0 \tag{62a}$$

and

$$\begin{aligned} &3.656 \times 10^6 \left(2.634\ \theta_c - 5.162 \times 0.922\ \frac{\Delta}{L_{ab}}\right) \\ &\quad + 2 \times 9.142 \times 10^6 \left(4\ \theta_c + 2\ \theta_b\right) = 0 \end{aligned} \tag{63a}$$

and reduce to

$$46.198\ \theta_b + 18.284\ \theta_c = 17.4002\ \frac{\Delta}{L_{ab}} \tag{62b}$$

and

$$36.568\ \theta_b + 82.766\ \theta_c = 17.4002\ \frac{\Delta}{L_{ab}} \tag{63b}$$

These have the solution

$$\theta_b = 0.35562\ \frac{\Delta}{L_{ab}} \tag{64a}$$

and

$$\theta_c = 0.05311\ \frac{\Delta}{L_{ab}} \tag{64b}$$

The shears become

$$S_{ab} = \frac{-\ 3.656 \times 10^6}{288}\ 5.162\ (0.922 \times 0.35562 - 1.829)\ \frac{\Delta}{L_{ab}} - 100{,}243\ \frac{\Delta}{L_{ab}} \tag{65a}$$

and

$$S_{cd} = \frac{-\ 3.656 \times 10^6}{288}\ 5.162\ (0.922 \times 0.05311 - 1.829)\ \frac{\Delta}{L_{ab}} - 100{,}243\ \frac{\Delta}{L_{ab}} \tag{66a}$$

or

$$S_{ab} = (98{,}359 - 100{,}243)\ \frac{\Delta}{L_{ab}} = -\ 1{,}884\ \frac{\Delta}{L_{ab}} \tag{65b}$$

and

$$S_{cd} = (116{,}641 - 100{,}243)\frac{\Delta}{L_{ab}} = 16{,}398\frac{\Delta}{L_{ab}} \quad \text{. . . . . (66b)}$$

Consequently,

$$H = -(-\,1{,}884 + 16{,}398 - 1{,}884)\frac{\Delta}{L_{ab}} = -\,12{,}630\frac{\Delta}{L_{ab}} \quad \text{. . . . (67)}$$

The sign of H shows that the frame is stable under the assumed loads. Comparison with the previous trial indicates that the critical loads lie between the magnitudes assumed for the two trials. By interpolating between these two cases, the critical loads may be found to correspond to $\rho = 0.83$ or $P_{cr} = 0.83 \times 125{,}303 = 104{,}000$ lbs on each column.

It should be noted that the axial loads on the three columns need not be equal. A similar method of analysis would apply as long as the axial loads on the two outer columns are equal and the frame is symmetrical. If the axial load on the center column differs from that on each of the outer columns, or if the properties of the center column differ, the coefficients and constants will, of course, be different for this column. However, only two joint equilibrium equations will still suffice. If the loadings of all three columns differ or if the frame is not symmetrical, it will be required to write and solve simultaneously three joint equilibrium equations in the three rotations.

TABLE 2.—INFLUENCE[a] COEFFICIENTS, a_{ij}

Location of Deflection, i	Location of Unit Load, j			
	Frame 1	Frame 2	Frame 3	Frame 4
Frame 1	127.266	98.200	67.279	46.180
Frame 2	98.200	194.440	135.584	67.279
Frame 3	67.279	135.584	197.415	117.885
Frame 4	46.180	67.279	117.885	127.885

[a] The influence coefficients are in units of 10^{-6} in. per lb.

Sidesway Buckling of Complete Frame.—In this example, a complete structure, comprising four parallel frames and a bracing system as shown in Fig. 11, is considered. The frames are identical with those used in the previous examples, and the columns are assumed to be restrained elastically as in the previous examples. The bracing system is supported at its ends by masonry walls.

By conventional techniques for computing deflections such as the Maxwell-Mohr method, the deflections of the bracing system due to unit loads applied at each frame location have been determined and are listed in Table 2.

Substituting the numerical values of the a_{ij} into Eq. 42 gives for the displacements of the bracing system at each of the frame locations:

$$\left.\begin{aligned}
127.266\,H_1y_1 + 98.200\,H_2y_2 + 67.279\,H_3y_3 + 46.180\,H_4y_4 &= 10^6\,\mu\,y_1\\
98.200\,H_1y_1 + 194.440\,H_2y_2 + 135.584\,H_3y_3 + 67.279\,H_4y_4 &= 10^6\,\mu\,y_2\\
67.279\,H_1y_1 + 135.584\,H_2y_2 + 197.415\,H_3y_3 + 117.885\,H_4y_4 &= 10^6\,\mu\,y_3\\
46.180\,H_1y_1 + 67.279\,H_2y_2 + 117.885\,H_3y_3 + 127.885\,H_4y_4 &= 10^6\,\mu\,y_4
\end{aligned}\right\} \text{. . (68)}$$

To determine whether a given set of loads will or will not cause the structure to buckle in the sidesway mode, one first computes H for each frame by the method previously described in connection with the discussion of sidesway or anti-symmetrical buckling of independent frames, as illustrated in the previous example. These numerical values are then substituted into Eqs. 68 and iterations are performed upon these equations to obtain the mode shape of the buckled structure. Finally, the value of μ is found by use of Eq. 44, andInequalities 47 and 48 are applied to determine whether the frame is stable or unstable.

TABLE 3.—ITERATED VALUE OF DEFLECTIONS

	y_1	y_2	y_3	y_4
Second Cycle Normalized	271.5 0.606	428.6 0.956	448.1 1.000	296.3 0.661
Third Cycle Normalized	268.8 0.603	425.4 0.954	445.7 1.000	294.7 0.661
Fourth Cycle Normalized	268.2 0.602	424.8 0.954	445.3 1.000	294.4 0.662
Fifth Cycle Normalized	268.1 0.602	424.7 0.954	445.3 1.000	294.5 0.661
$y^{(5)}/y^{(4)}$	445.3	445.2	445.3	445.5

The case of identical loads on all frames is considered first. Each of the previous set of equations is divided through by the common factor H and the equations become

$$127.266\,y_1 + 98.200\,y_2 + 67.279\,y_3 + 46.180\,y_4 = 10^6\,\frac{\mu}{H}\,y_1 \;.\;.\;.\;. \quad (69a)$$

$$98.200\,y_1 + 194.440\,y_2 + 135.584\,y_3 + 67.279\,y_4 = 10^6\,\frac{\mu}{H}\,y_2 \;.\;.\;. \quad (69b)$$

$$67.279\,y_1 + 135.584\,y_2 + 197.415\,y_3 + 117.885\,y_4 = 10^6\,\frac{\mu}{H}\,y_3 \;.\;. \quad (69c)$$

$$46.180\,y_1 + 67.279\,y_2 + 117.885\,y_3 + 127.885\,y_4 = 10^6\,\frac{\mu}{H}\,y_4 \;.\;.\;. \quad (69d)$$

Relative values of the y's are found by iteration starting with arbitary initial values. Suppose that initial values 0.700, 1.000, 1.000, and 0.700 are used. Upon substituting into the left-hand side of Eq. 69a, the following is obtained:

$$127.266\,(0.700) + 98.200\,(1.000) + 67.279\,(1.000) + 46.180\,(0.700) = 286.9$$

Substituting the initial values into the remaining three equations yields values of 445.9, 462.6, and 307.0, respectively. It is convenient to normalize these numbers by dividing by the magnitude of one of the quantities, usually the largest. On this basis, the normalized results become 0.620, 0.964, 1.000, 0.664. Evidently, these values do not agree with the initially assumed values and must be used as the basis for a second cycle of computations. This process is repeated until convergence is obtained, which requires about five cycles in the present example.

Although the iterations were carried through the fifth cycle, it is evident that the results of the third cycle have sufficient accuracy for practical purposes. However, using the final results for y_3 and Eq. 46, and recalling that the right-hand sides of the deflection equations were $10^6\, y_i\, \mu/H$,

$$10^{-6}H = \frac{1}{445.3}$$

in which μ has been taken as unity to indicate that no additional stiffening is contemplated. This yields

$$H = 2246 \text{ lb}$$

Comparing the results of the third cycle before normalizing with the normalized values of the second cycle, which may be interpreted as input for the third cycle, yields the ratios 443.5, 445.0, 445.7, and 445.8 at the four locations. It can be shown by rigorous mathematical process, that the correct value of $10^6\ \mu/H$ lies at, or between, the limiting values of this range that is

$$443.5 \leq 10^6\ \mu/H \leq 445.8$$

or, with μ taken equal to unity

$$2243 \leq H \leq 2255 \text{ lb}$$

The range, and therefore the maximum possible error, is about 0.5 % so that it is likely that the results of the third cycle would have been sufficiently accurate for practical purposes.

It is now necessary to find the magnitudes of the column loads which, when applied to the frame, will produce an H of this magnitude.

The columns of each frame are taken, by the conditions of the problem, to be equally loaded. For a first trial, a value of $\rho = 2.2$ is assumed for each column. The trial value of the load is

$$P = 2.2\ P_e = 2.2\ (125{,}303) = 275{,}667 \text{ lb}$$

From Table 1, for $\rho = 2.2$, $A_{ab} = -\ 0.519$, and $B_{ab} = 3.901$. Also,

$$C_{ab} = 3.382$$

$$A'_{ab} = -\ 0.519 - \frac{(3.901)^2}{-\ 0.519 + 27.35} = -\ 1.086$$

$$c_{ab} = 1 - \frac{3.901}{-\ 0.519 + 27.35} = 0.8546$$

$$c'_{ab} = 2 - \frac{3.382}{-\ 0.519 + 27.35} = 1.8739$$

and

$$C_{ab}\, c_{ab} = 2.8903$$

The formulas for the relevant moments are, by Eqs. 1 and 13,

$$M_{ba} = 3.656 \times 10^6 \left(- 1.086\ \theta_b - 2.8903\ \frac{\Delta}{L}\right) \quad \text{(70a)}$$

$$M_{bc} = 9.152 \times 10^6 (4\ \theta_b + 2\ \theta_c);\ M_{cb} = 9.152 \times 10^6 (4\ \theta_c + 2\ \theta_b) \quad \text{(70b)}$$

$$M_{cd} = 3.656 \times 10^6 \left(- 1.086\ \theta_c - 2.8903\ \frac{\Delta}{L}\right) = M_{cf} \quad \text{(70c)}$$

The joint equilibrium equations,

$$M_{ba} + M_{bc} = 0 \quad \text{(71a)}$$

$$M_{cb} + M_{cd} + M_{cf} = 0 \quad \text{(71b)}$$

become, upon reduction,

$$8.916\ \theta_b + 5.001\ \theta_c = 2.8903\ \frac{\Delta}{L} \quad \text{(72a)}$$

$$10.002\ \theta_b + 18.918\ \theta_c = 2.8903\ \frac{\Delta}{L} \quad \text{(72b)}$$

and their solution is

$$\theta_b = 0.3390\ \frac{\Delta}{L} \quad \text{(73a)}$$

$$\theta_c = - 0.0265\ \frac{\Delta}{L} \quad \text{(73b)}$$

The column shears are obtained by use of Eq. 14:

$$S_{ab} = S_{ef} = \frac{- 3.656 \times 10^6 \times 3.382}{288} \left(.8546 \times .3390\ \frac{\Delta}{L} - 1.8739\ \frac{\Delta}{L}\right)$$

$$- 275,667\ \frac{\Delta}{L} = - 207,653\ \frac{\Delta}{L} \quad \text{(74)}$$

and

$$S_{cd} = \frac{- 3.656 \times 10^6 \times 3.382}{288} \left(- .8546 \times .0265\ \frac{\Delta}{L} - 1.8739\ \frac{\Delta}{L}\right)$$

$$- 275,667\ \frac{\Delta}{L} = - 194,245\ \frac{\Delta}{L} \quad \text{(75)}$$

With $\Delta = 1$ and $L = 288$

$$H = - S_{ab} - S_{cd} - S_{ef} = 2{,}116 \text{ lb} \quad \ldots\ldots \quad (76)$$

This value is slightly below the value of 2246 lbs that was found to define the limit of stability. Therefore, the assumed trial value of the column loads is too low. A slightly greater load should be chosen for a second trial, if the critical load is to be established.

Following the above procedure, and with an assumed load corresponding to $\rho = 2.4$, or $P = 2.4\ (125{,}303) = 300{,}727$ lb, it may be determined that $H = 2351$ lbs. By interpolation it is found that, for $H = 2246$ lb, $\rho = 2.311$, which determines the critical load to be $P_{cr} = 2.311\ (125{,}303) = 289{,}575$ lb.

Sidesway Buckling with Unequally Loaded Frames.— The theory and general procedure are applicable to cases in which the frames are not identical or not identically loaded. As an example, the frame of the previous problem is checked for stability for loads equal to 2.4 ρ on the third frame and 2.2 ρ on the remaining frames.

Since the bracing system is unchanged from the previous problem, the table of influence coefficients is also unchanged. Eqs. 42 become

$$127.266 \times 2116\, y_1 + 98.200 \times 2116\, y_2 + 67.279 \times 2351\, y_3$$

$$+ 46.180 \times 2116\, y_4 = 10^6 \mu y_1 \quad \ldots\ldots\ldots \quad (77a)$$

$$98.200 \times 2116\, y_1 + 194.440 \times 2116\, y_2 + 135.584 \times 2351\, y_3$$

$$+ 67.279 \times 2116\, y_4 = 10^6 \mu y_2 \quad \ldots\ldots\ldots \quad (77b)$$

$$67.279 \times 2116\, y_1 + 135.584 \times 2116\, y_2 + 197.415 \times 2351\, y_3$$

$$+ 117.885 \times 2116\, y_4 = 10^6 \mu y_3 \quad \ldots\ldots\ldots \quad (77c)$$

and

$$46.180 \times 2116\, y_1 + 67.279 \times 2116\, y_2 + 117.885 \times 2351\, y_3$$

$$+ 127.885 \times 2116\, y_4 = 10^6 \mu y_4 \quad \ldots\ldots\ldots \quad (77d)$$

These reduce to

$$0.26929\, y_1 + 0.20779\, y_2 + 0.15817\, y_3 + 0.09772\, y_4 = \mu y_1 \quad \ldots \quad (78a)$$

$$0.20779\, y_1 + 0.41144\, y_2 + 0.31876\, y_3 + 0.14236\, y_4 = \mu y_2 \quad \ldots \quad (78b)$$

$$0.14236\, y_1 + 0.28690\, y_2 + 0.46412\, y_3 + 0.24944\, y_4 = \mu y_3 \quad \ldots \quad (78c)$$

and

$$0.09772\, y_1 + 0.14236\, y_2 + 0.27715\, y_3 + 0.27060\, y_4 = \mu y_4 \quad \ldots \quad (78d)$$

For starting the iterative process, initial relative deflections are selected arbitrarily and substituted into the left-hand sides of the preceding equations.

The computed values of μy_i are then normalized and again substituted into the above equations. The process, repeated until convergence is obtained, is recorded in Table 4.

Evidently, the third cycle has converged and can serve as an accurate basis for determining the stiffness factor. By Eq. 44, using the values for y_3,

$$\mu = \frac{0.981}{1.000} = 0.981$$

Since this quantity is less than unity, the structure is stable under the assumed loads. In fact, the loads may be increased somewhat before the structure would buckle in the sidesway mode. It may be noted that the same result would be obtained by using the values at any of the other frames. It is also worthy of mention that the lower and upper limits based upon the results of the second cycle are

$$0.977 \leq \mu \leq 0.984$$

Thus, if the process were stopped at this point and the average value of μ were used, it would be known to be correct to within ± 0.3%.

TABLE 4.—ITERATED VALUES OF DEFLECTIONS

	y_1	y_2	y_3	y_4
Initial	0.600	0.900	1.000	0.650
First Cycle	0.570	0.906	0.970	0.640
Normalized	0.588	0.934	1.000	0.659
Second Cycle	0.575	0.919	0.980	0.646
Normalized	0.587	0.938	1.000	0.659
Third Cycle	0.576	0.920	0.981	0.646
Normalized	0.587	0.938	1.000	0.659

In order to establish the magnitudes of the critical loads, the stability of the structure under a second set of assumed heavier loads may be investigated. If, however, it is only desired to obtain a fairly dependable estimate of the critical load on the third frame when the loads on the columns of the remaining frames are 2.2 times the Euler loads, such an estimate may be obtained by an extrapolation based upon the present and the previous example.

To implement this approach, one may note from the previous problem that, under identical loads on all frames, it was established that

$$10^6 \frac{\mu}{H} = 445.3$$

and also that H = 2116 lb when $\rho = 2.2$. Consequently, at this loading

$$\mu = 445.3 \times 2116 \times 10^{-6} = 0.942$$

Extrapolation based upon $\mu = 0.942$ when $\rho_3 = 2.2$, and $\mu = 0.981$ when $\rho_3 = 2.4$, yields $\mu = 1.000$ when $\rho_3 = 2.497$. Hence, when the axial loads on the columns of frames 1, 2, and 4 are 275,677 lb per column, the axial loads on the columns of frame 3 are 2.497 x 125,303 = 312,882 lb.

APPENDIX.—NOTATION

A = defined constant;
A' = defined constant;
aij = influence coefficient;
B, C, c, c^1 = defined constants;
E = modulus of elasticity or appropriate modulus in inelastic case;
F_j = force exerted on bracing system by jth frame;
H = external restraining force;
H_j = supporting force per unit displacement at jth frame;
I = moment of inertia of cross section;
i = index number;
j = index number;
K = stiffness coefficient of member $(= EI/L)$;
k = linear spring rate;
L = length of member;
M = bending moment in member;
M_o = external moment;
P = axial load on member, positive when compressive;
P_{cr} = axial load at which buckling is imminent;
P_e = Euler load $\left(= \pi^2\ EI/L^2\right)$;
p = constant $(= \pi \sqrt{1}\ \rho\ l/L)$;
Q = rotational spring rate;
r = number of critically loaded frames;
S = transverse shear in member;
y_i, y_j = lateral displacements of ith and jth frames at braced points;
$y_i^{(n)}$ = nth iterated value of y_i;
Δ = relative transverse displacement of ends of member;
ρ = ratio of axial load to Euler load $\left(= P/P_e\right)$;
θ = angular displacement of tangent to end of member, angular displacement of joint; and
μ = stiffness multiplication factor and normalizing factor.

AMERICAN SOCIETY OF CIVIL ENGINEERS
Founded November 5, 1852
TRANSACTIONS

Paper No. 3202

CONSTRUCTION OF ROCKY REACH HYDROELECTRIC PROJECT

By W. N. Evans,[1] F. ASCE and J. H. Boyd,[2] M. ASCE

SYNOPSIS

Rocky Reach Dam was built in four steps in areas protected by berms and circular sheetpile cells, as much as 75 ft high, installed to rock through boulders. The million cubic yards of concrete was made from locally available gravel by four 2-cu yd tilting mixers; it was transported in 4-cu yd buckets on semi-trailers to big whirler cranes on 100-ft high gantries for placing in heavily built panel forms. Rock bolts were used to tie down a section of the dam in which fault planes were encountered. Final river diversion was effected by connecting two big rocks by cable and dropping one rock upstream as an anchor and the other into 35-fps river flow.

INTRODUCTION

The Rocky Reach Hydroelectric Power Project is located on the Columbia River about 7 miles above the City of Wenatchee in North Central Washington. There, the Columbia River flows in a tremendous canyon nearly a mile wide and 2,000 ft deep. The site chosen for the dam is one at which the river is a relatively shallow, fast flowing stream near the base of the west wall of the canyon and at which exploration had determined that bedrock in the stream reached its highest level. The general arrangement, as shown in Fig. 1, was chosen in order to provide space for a powerhouse that would accommodate the number of units proposed and for a spillway that would pass maximum floods.

Note.—Published essentially as printed here, in November, 1960, in the Journal of the Construction Division, as Proceedings Paper 2662. Positions and titles given are those in effect when the paper or discussion was approved for publication in Transactions.

[1] Vice Pres., L. E. Dixon Co., and Resident Mgr., Rocky Reach Contractors, Wenatchee, Wash.

[2] Proj. Mgr., Stone and Webster Engrg. Corp., Wenatchee, Wash.

Beginning at the west bank, a 450-ft long non-overflow forebay wall of concrete gravity section closes the gap between the powerhouse and the rock bluff. The 1,100 ft long powerhouse includes a service bay at the south end and space for the installation of eleven hydraulic turbine driven generators, seven of which are being installed. These seven will have a total peak generating capacity of 775,000 kw when operating under a 93-ft gross head. Total peak generating capacity, when all units have been installed, will be 1,215,000 kw. Adjoining the powerhouse at its north end, and connecting it to the spillway section, is an L-shaped non-overflow concrete gravity arch section 375 ft in length, called the center dam. The spillway section, that extends 750 ft across the river, provides 12 bays, each having a 50 x 58 ft clear opening, and is capable of passing river flows of up to 1,100,000 cfs. This is approximately 1½ times the 718,000 cfs maximum flood of record that was experienced at

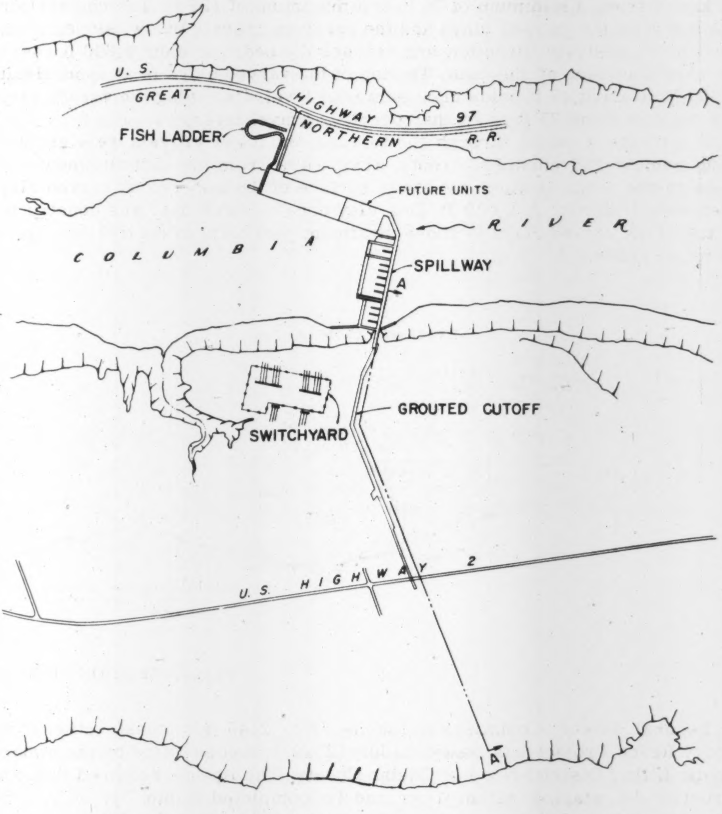
U. S.
HIGHWAY 97
GREAT
NORTHERN R.R.
FISH LADDER
FUTURE UNITS
RIVER
COLUMBIA
SPILLWAY
A
GROUTED CUTOFF
SWITCHYARD
U. S. HIGHWAY 2
A

FIG. 1.—ROCKY REACH HYDROELECTRIC POWER PROJECT

the site in 1894. The east abutment, 120 ft in length, is also a concrete gravity section and completes the concrete portion of the dam.

East of the concrete structure, the floor of the canyon is a broad terrace that extends more than 3,500 ft from the abutment to the canyon wall. Elevation of this terrace is generally about 750 ft above sea level or about 40 ft above maximum pool elevation of 710 ft. As shown in Fig. 2, the terrace consists of a deposit of pervious gravels, of varying thickness up to 125 ft, overlying bedrock. Above this gravel deposit are varved clays again varying in thickness from a minimum of 70 ft to a maximum of 125 ft. The contact surface between the varved clays and the pervious gravels below, slopes downward in an easterly direction and reaches the bedrock about 1,800 ft east of the east abutment of the dam. The top of the varved clays is at approximate el 665 ft or about 45 ft below maximum pool level. Overlying the varved clays to a depth of about 75 ft is another pervious gravel layer.

To provide a cutoff through the terrace, the lower gravels were grouted, using cement and chemical grouts, along a line from the east abutment concrete to the point at which the lower surface of the impervious varved clays intersects bedrock. A 2,000 ft long clay core earthfill dam was constructed on top of the varved clays to above maximum pool level to control seepage in the upper gravels.[3]

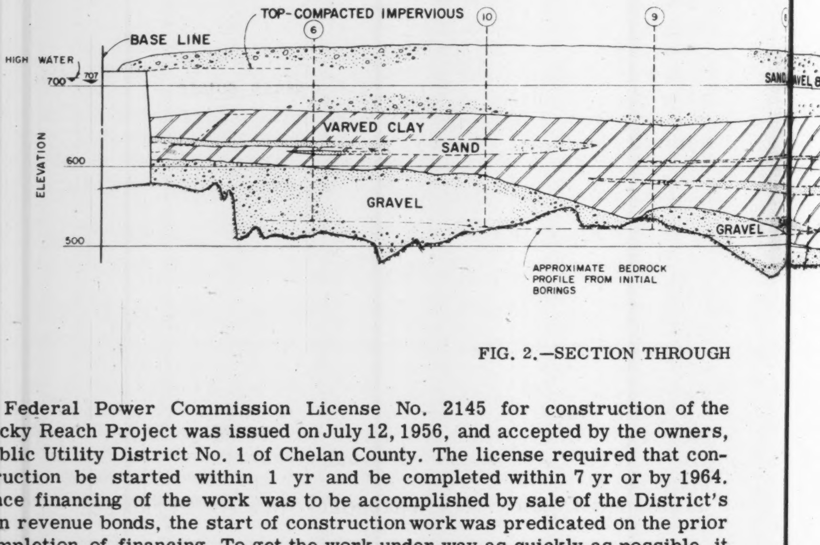

FIG. 2.—SECTION THROUGH

Federal Power Commission License No. 2145 for construction of the Rocky Reach Project was issued on July 12, 1956, and accepted by the owners, Public Utility District No. 1 of Chelan County. The license required that construction be started within 1 yr and be completed within 7 yr or by 1964. Since financing of the work was to be accomplished by sale of the District's own revenue bonds, the start of construction work was predicated on the prior completion of financing. To get the work under way as quickly as possible, it was decided to obtain financing and construct the project in two stages.

A contract for performance of stage I work was awarded on September 19, 1956. Stage I work included concrete construction for 9 of the 12 spillway bays and the east abutment, grouting work and construction of the impervious cutoff in the east bank terrace, and protection of the river bank upstream and downstream of the dam. Most of the work under the contract, except for the work on the east bank terrace, was completed by December, 1957.

---

[3] "Construction of Rocky Reach Grouted Cutoff," by W. F. Swiger, Proceedings, ASCE, Vol. 87, No. SM2, April, 1961.

Second, or final, stage work included construction of the three remaining spillway bays, center dam, powerhouse and forebay wall, and installation of all mechanical and electrical work. Included also was remaining concrete work required to raise the ogee sections of the Stage I spillways, that had been left 40 ft below final elevation for river diversion during performance of final stage work. Two final stage contracts, one a general contract and the other for electrical work, were signed in November, 1957. Although work being done under these two contracts is still in progress, it is now anticipated that the first unit will go on the line in July, 1961 with other units following in succession until the seventh is completed in February, 1962.

RIVER DIVERSION

Perhaps the major problem that confronts engineers and contractors involved in the construction of a dam on the Columbia River is diversion of the river. The cofferdam design must satisfactorily control the river to permit the maintenance of the schedule set up for performance of the work.

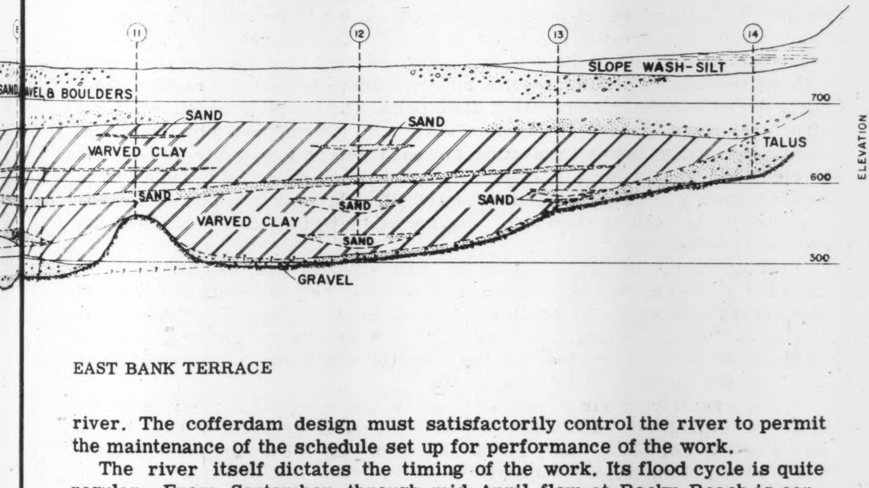

EAST BANK TERRACE

The river itself dictates the timing of the work. Its flood cycle is quite regular. From September through mid-April flow at Rocky Reach is controlled by dams upstream that regulate the flow to 100,000 cfs or below, if possible, with a minimum of about 60,000 cfs being usual. Beginning in late April, the river starts to rise and reaches its peak flow usually in late May or early June. Peak flow exceeds 500,000 cfs at Rocky Reach about once in 6 years on the average. The maximum flood of record is 718,000 cfs, and the maximum flow experienced during the construction period to date was 423,000 cfs, in 1959.

Cofferdam work affecting the main flow of the Columbia River must be accomplished within the low water period of about seven months and must be undertaken with the full realization that, if not completed in that time, the entire project may be delayed a full year. This was the basis on which the schedule of work for the Rocky Reach Project was established.

In the bidding documents for both stages of work, the engineers had included a proposed method of diverting the river. Final plans adopted for construction of all diversion structures and the design on which the plans were based were, however, made the responsibility of the contractor.

For Stage I, the contractor used a cofferdam that diverted river flow toward the right bank. Circular steel cells were used in the cofferdam to leave maximum river cross section for passage of flood waters. Rock groins on the outside and gravel groins on the inside were used to give additional stability to the cofferdam that, at some locations, was 75 ft high. Twenty-four $60\frac{1}{2}$-ft diam cells, spaced 64 ft on centers, were required to complete the cofferdam. Cells were made up of MP 101 or equivalent steel sheet piling and were joined together with small radius connectors also made up of steel sheets. End cells on the upstream and downstream legs were set into the river bank.

Fig. 3 shows the cofferdam for Stage I construction nearing completion. The rock groin along the upstream arm of the cofferdam provided slack water during construction. The cells were erected in the slack water.

Whereas overburden in the stream was shallow, it contained numerous boulders that would interfere with driving of piling. Therefore excavation to rock was considered necessary at each cell to assure proper seating of the sheets. The height and diameter of the cells and the lack of the usual support from overburden created problems in stability during erection. These were overcome through use of the self-supporting internal ring-type template. Fig. 4 shows the self supporting internal ring type template used for racking sheet piling during construction of $60\frac{1}{2}$ ft diam cells. The template consisted of two structural rings, spaced 18 ft apart vertically, and supported by five 16-in. diam pipe spuds. After excavating for each cell, the template was set and leveled. The sheets for a complete cell were racked around it and all were lightly driven to seat them. A bottom seal of silty clay was then placed immediately over the rock by clam shell, and the balance of the cell was filled with sand and gravel.

Because of the critical stability of cells without fill, it was necessary to exercise extreme care while placing fill in any cell to assure that the cell was always uniformly loaded. This was done by placing the fill always at the center of the cell using a clamshell bucket or a chute. The cells became stable when about 2/3 filled and the template was then removed. The same care was exercised in completing the fill.

Work was started simultaneously on the upstream and downstream arms of the cofferdam, and each cell was completed before erection of the next cell was started. Completed cells provided a work base for equipment during the construction of the succeeding cell.

The stage I cofferdam was designed for 500,000 cfs flows and successfully withstood the peak flow of 415,000 cfs experienced during the 1957 high water season with only normal leakage.

Because of some delay in financing, the contract for performance of final stage work was not signed until November, 1957. With 2 months of the low water season already past, it became imperative to utilize every moment of available time to make a river diversion that could be ready for the 1958 high water season. The joint venture of contractors, who were then completing the Stage I work, together with one additional participant, were the low bidders and were awarded the general contract for the Final Stage. They already had

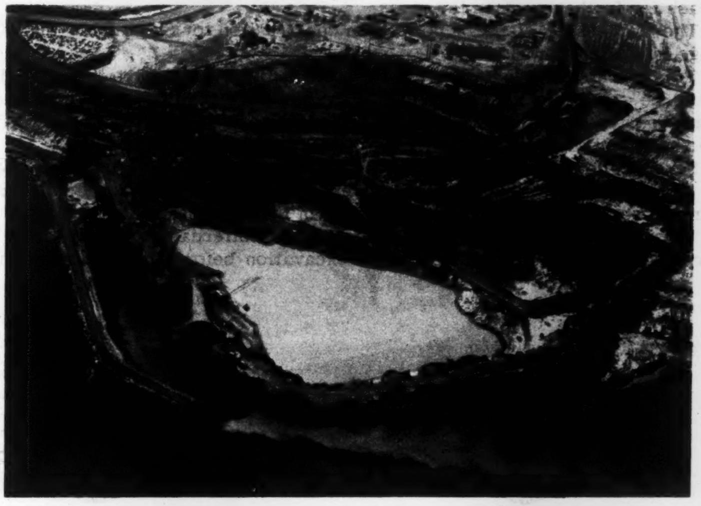

FIG. 3.—COFFERDAM FOR STAGE 1 CONSTRUCTION NEARING COMPLETION

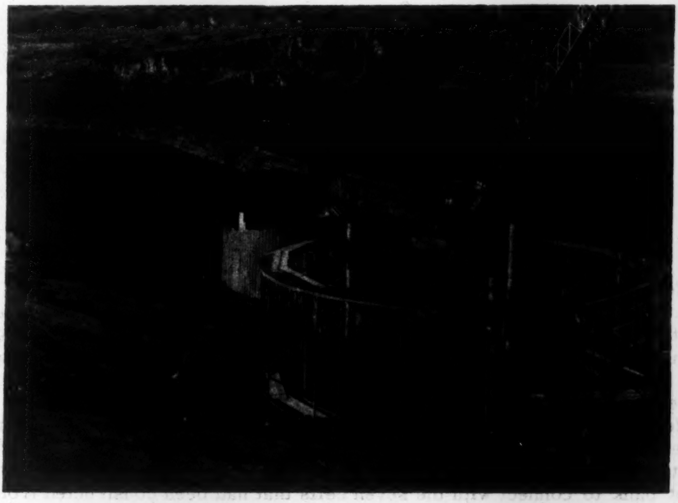

FIG. 4.—SELF SUPPORTING INTERNAL RING TYPE TEMPLATE

men and equipment at the site, and an existing Stage I cofferdam that provided a base for further work in the river.

The successive steps of cofferdam construction for Stage II, or the Final Stage, are shown in Fig. 5.

Twenty-one circular cells were used in the river where the cofferdam would be subject to high velocity flow. These were of the same diameter and were constructed in the same manner as for Stage I. They were connected to the shore by two dikes.

Seven cells were erected first in the main channel of the river, working in the shelter of a rock groin extending out from the Stage I cofferdam. Dumped rock dikes for shore connections of the main cofferdam were started on the west bank, and removal of the Stage I cofferdam was then begun. To permit starting with the powerhouse excavation before completing the main cofferdam, the contractor subdivided the work area with a temporary rock fill inner cofferdam with an impervious core. The inner cofferdam allowed a portion of the powerhouse area to be unwatered early. Fig. 6 shows the cofferdam for final stage work under construction. Primary closure was made at the gap in the right background. The temporary dike near the center of the photograph permitted the contractor to begin excavation before the main cofferdam was completed. Fig. 6 also shows construction of the upstream dike of the main cofferdam. This dike was more than 900 ft long and in some sections 75 ft high. It was constructed by dumping a rock groin out from the west bank to connect with the seven cells that had been constructed from the Stage I cofferdam. This groin made the primary closure of the cofferdam and diverted the Columbia River through the Stage I spillway sections for the first time. Velocities of up to 35 fps were encountered at the closure. To overcome

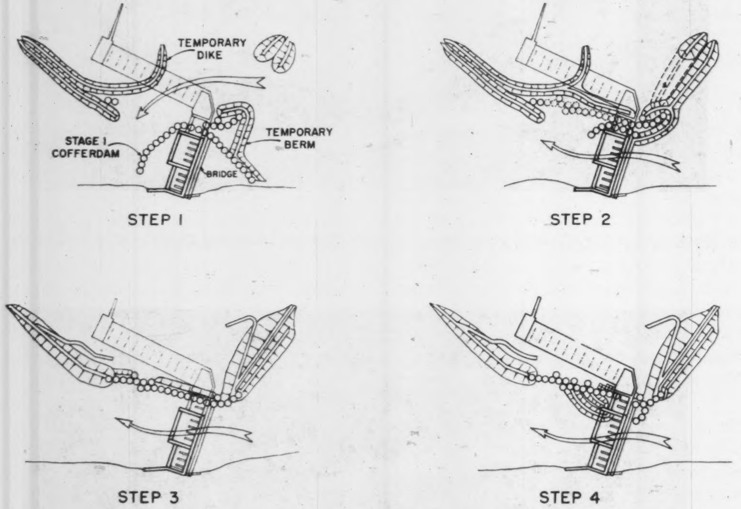

STEP 1

STEP 2

STEP 3

STEP 4

FIG. 5.—COFFERDAM CONSTRUCTION

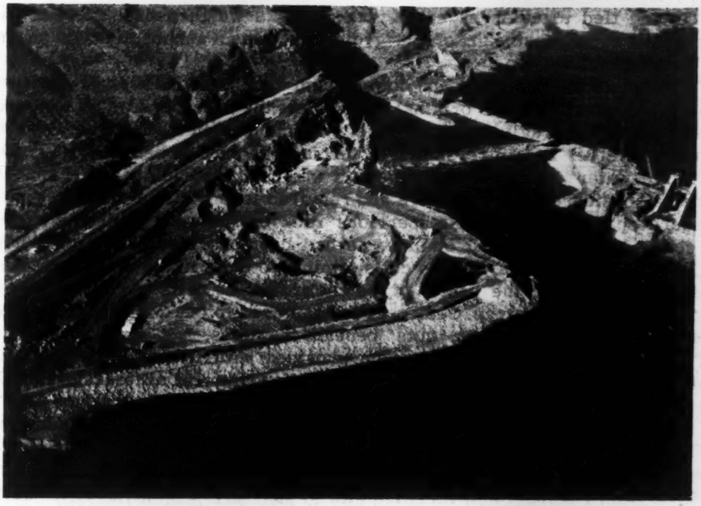

FIG. 6.—COFFERDAM FOR FINAL STAGE WORK UNDER CONSTRUCTION

FIG. 7.—COFFERDAM FOR STAGE 1 CONSTRUCTION AFTER UNWATERING

such velocities, the contractor used pairs of large pieces of quarried rock drilled and tied together by cable. These rocks weighed up to 25 tons. One rock was dumped upstream of the groin to act as an anchor, and the second was dumped into the gap.

To complete the upstream and downstream dikes, second rock groins were constructed parallel to the original groins, and the area between was cleaned to bedrock with draglines. Sand was then dumped in the area between the groins, and steel Z-piling was driven through the sand to bedrock to provide a positive water cutoff. The piling cutoff was used instead of impervious fill as it was considered more positive and required less width of dike.

Where space was available, pervious rock berms were placed as backup for cells, both inside and outside, as had been provided in Stage I. Where space was not available, backup cells similar to cells in the main cofferdam were provided. Near the center of the cofferdam the cells were so arranged as to provide for a fish trap. Cement grout was used to cut down leakage under cells and through known rock "guts" beneath the dikes.

Two main pumping stations, each provided with five 20-in. 15,000 gpm turbine pumps, were installed within the cofferdam, and all leakage into the dam was directed to these. Following initial dewatering, only a minor part of this installation was ever required to maintain dry working conditions.

The cofferdam was completed in time to take care of the 1958 high water season when flows reached a maximum of 390,000 cfs. Observations during the successful passage of this flow, and a subsequent maximum flow of 423,000 cfs in 1959, indicated that flows of 500,000 cfs for which the cofferdam had been designed could have been passed safely. A more detailed description of the river diversion is contained elsewhere.[4]

Construction of the final three spillway bays that adjoin the Stage I work was scheduled for the 1958-59 low water period. Circular cells were extended from the main cofferdam to the end of spillway block 4. Placing of the concrete for these bays was completed, and the temporary cells were removed so that water flowed through the bays during the 1959 flood season.

Following the 1960 flood season, the final stage cofferdam will be breached and the river will be permitted to flow through the intakes and draft tube spaces for the four future units. This will permit completion of concrete work on the spillway ogee sections that purposely had been left low for river diversion. In the spring of 1961, when all spillway concrete has been placed and the tainter gates have been installed, the future unit intakes will be closed off with concrete stop logs, and water will be permitted to flow over the spillway.

During design of the Project, an arrangement was made with the R. L. Albrook Hydraulic Laboratory at Washington State University at Pullman, Washington, to perform model studies of various hydraulic features. A comprehensive model of the project at 1:75 scale was built for use in these studies. The model was also used for investigation of all diversion schemes before they were constructed. Excellent agreement was obtained between model and prototype velocities and water elevations.

DEWATERING EAST BANK

The major problem encountered in the construction of Stage I was the control of seepage from the east bank into the cofferdam. The lower gravel strata proved to be considerably more pervious than had been anticipated. The depth and nature of the gravel strata and the overlying varved clays between the arms of the cofferdam made it impractical to use a sheet pile cutoff wall to control the water. It was decided, therefore, to install a line of 19 wells on the east bank, back from the area to be excavated, between the upstream and downstream arms of the cofferdam with the idea of lowering ground water levels and thereby reducing seepage into the work area. To assist in controlling ground water, and as a part of the permanent protection of the left bank, a sheet steel cutoff wall was constructed from the upstream arm of the cofferdam, a distance of 700 ft upstream and parallel to the river bank. A temporary sheet pile wall was constructed downstream from the downstream arm, a distance of 300 ft. The 19 wells had a total pumping capacity of about 30,000 gpm. It was found necessary, however, to construct, in addition, a deep sump within the cofferdam. Eighteen pumps with total pumping capacity of 160,000 gpm were installed in this sump. Fig. 7 shows this cofferdam dewatered. The main sump is also shown as is the header for the seepage wells. The line of wells at the top of the excavation and the bank of pumps in the sump maintained dry working conditions.

---

[4] "Pushing the Columbia River Around," by L. E. Dixon, Western Construction, November, 1959, p. 45.

STAGE II EXCAVATION

A total of 750,000 cu yd of material were excavated for the powerhouse and center dam structure. The bulk of this material was located within the banks of the original river and could not be reached until cofferdams had been constructed. Thus, only minor quantities from the structure excavation could be used in cofferdam construction, and the bulk was deposited downstream of the site at which it was used for construction facilities and will form a permanent useful level area.

Conventional equipment consisting of crawler type self-propelled wagon drills and jack hammers were used for drilling. Twenty-two ton end dump units that were loaded by $2\frac{1}{2}$ and $3\frac{1}{2}$ yd shovels removed excavated material to the disposal area.

Rock at the site is a biotite gneiss and includes numerous fractures along cleavage planes. The majority of these fractures are tight, but some show past slippage with gouge zones varying from a few inches to several feet wide. These shear planes posed several problems.

Originally, the center dam had been conceived and designed as a gravity section dam. However, when rock excavation had progressed to the area of the center dam it was noted that several tight fault planes in the rock dipped at an angle of approximately 54° below horizontal toward the powerhouse or generally in the direction of greatest horizontal hydrostatic thrust from the reservoir. Immediately below the toe of the center dam it was necessary to excavate for draft tube No. 11, one of the future units.

Additional rock was removed to form a stepped terrace beneath the center dam and more than 100 rock bolts, 30 ft long, were grouted into holes drilled into the rock at right angles to the bedding planes to provide additional stability at this location. The center dam was also re-designed to act as a modified gravity arch section to reduce the shear load transferred from the center dam into the rock beneath it. Thrusts developed by the arch are delivered to gravity abutments formed by the spillway sections on one end and the base of the unit intakes at the other. To assure arch action, grout stops and shear keys were provided in all contraction joints between Unit 10 of the powerhouse and block S3 of the spillway, and the arch contributing lower portion of these joints will be cement grouted under pressure prior to raising the lake.

In excavating the draft tubes of future units 8 and 9, an area was found in which two nearly parallel faults intersected, resulting in a zone of severly sheared and broken rock (see Fig. 8).

This fault zone dipped about 45° to the west with a strike making an angle of about 59° with the axis of the powerhouse. Gouge and sheared rock was as much as 12 ft thick in places. This unstable material extended under the sound rock on which the heavily loaded main powerhouse piers and intermediate draft tube piers were to be built. The fault zone was followed down from its surface exposure in the excavation to depths within reach of conventional excavation equipment. To reach greater depths a series of 3 calyx holes, 36 in. in diameter, were drilled through the rock into the zone. The gouge was then mined out under the piers and replaced with concrete. Grout pipes were installed and all shrinkage cracks were filled with grout under pressure.

CONCRETE

Gravel deposits suitable for concrete aggregate are abundant through the Columbia River Valley. After testing materials from various potential borrow areas, it was decided that material from the east bank terrace immediately adjacent to the left abutment of the dam could be processed to provide aggregate of the proper quality. The test program had revealed that material at the site was generally sound and, with the addition of a blend sand available from a pit about one mile south of the site, the required gradation could be obtained. A substantial proportion of the aggregate from a thin zone at a depth of about 10 ft had surface coatings of calcium carbonate with some opal and, as such, were potentially alkali reactive. To remove the coatings and any soft materials that might be included, all aggregate was processed through a rotating drum scrubber. Also, Type II Low Alkali cement was specified for all concrete.

The Stage I contractor elected to erect his aggregate processing plant and his concrete batching plant immediately adjacent to the aggregate source. Fig. 9 shows the layout of the aggregate processing plant and batching plant. Conveyors moved processed aggregate from a reclaim tunnel beneath stockpiles to the batching plant.

At the processing plant pit run, aggregate was run through a jaw crusher and sized by primary and secondary screening units to provide graded coarse aggregate ranging from No. 4 minimum to 6 in. maximum size. The graded coarse aggregate was then stockpiled for later selection and use in four ranges of gradation, No. 4 to 3/4 in., 3/4 in. to $1\frac{1}{2}$ in., $1\frac{1}{2}$ in. to 3 in., and 3 in. to 6 in. Fine aggregate was produced by further crushing and washing of materials selected from the secondary screening units and adding the blend sand hauled from off site. The scrubber, that also served as a classifier, was located between the primary crusher and the primary screening unit. It consisted of a 5-ft by 22-ft revolving cylinder with an interior concentric plate screen sized to reject plus 6 in. material for further crushing. Angle bars mounted on the interior perimeter of the cylinder, parallel to its longitudinal axis, tumbled the aggregate to abrade and loosen surface coatings that were then washed from the unit using water jets. Periodic tests on processed aggregate indicated that the scrubber unit has satisfactorily removed the surface coatings to provide a sound non-reactive aggregate.

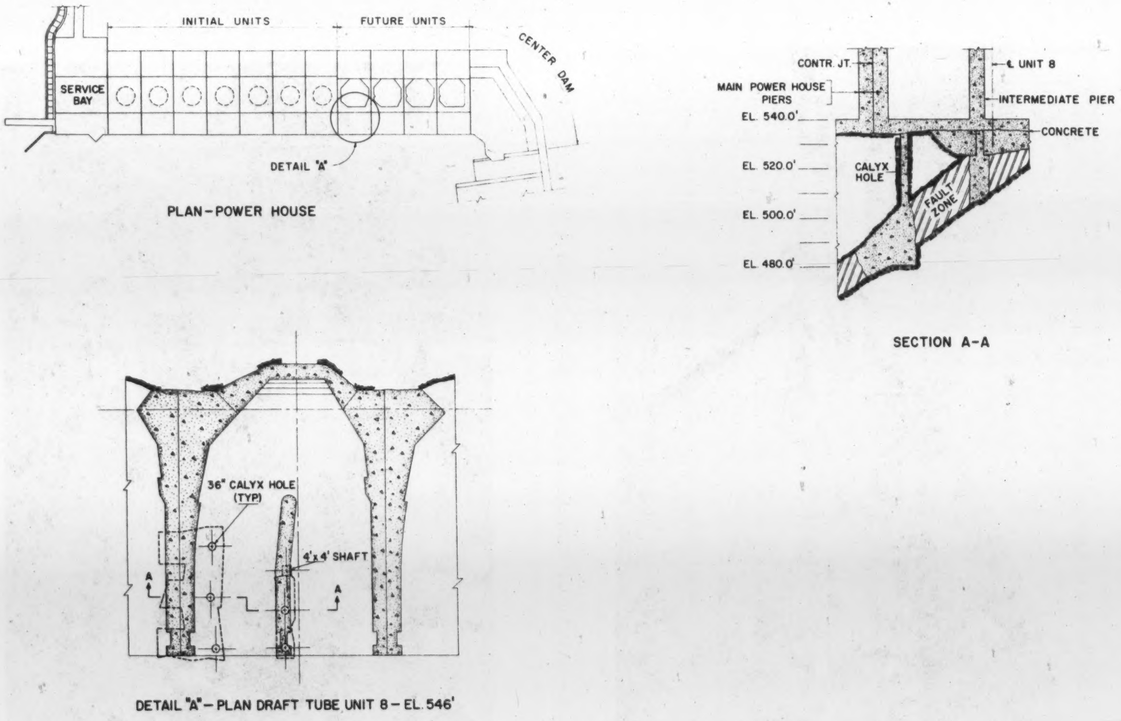
INITIAL UNITS
FUTURE UNITS
CENTER DAM
SERVICE BAY
DETAIL "A"
PLAN-POWER HOUSE
CONTR. JT.
MAIN POWER HOUSE PIERS
EL. 540.0'
EL. 520.0'
EL. 500.0'
EL. 480.0'
℄ UNIT 8
INTERMEDIATE PIER
CONCRETE
CALYX HOLE
FAULT ZONE
SECTION A-A
36" CALYX HOLE (TYP)
4'x4' SHAFT
A
A
DETAIL "A"-PLAN DRAFT TUBE UNIT 8-EL. 546'

FIG. 8.—FAULT ZONE AT FUTURE UNIT NO. 8

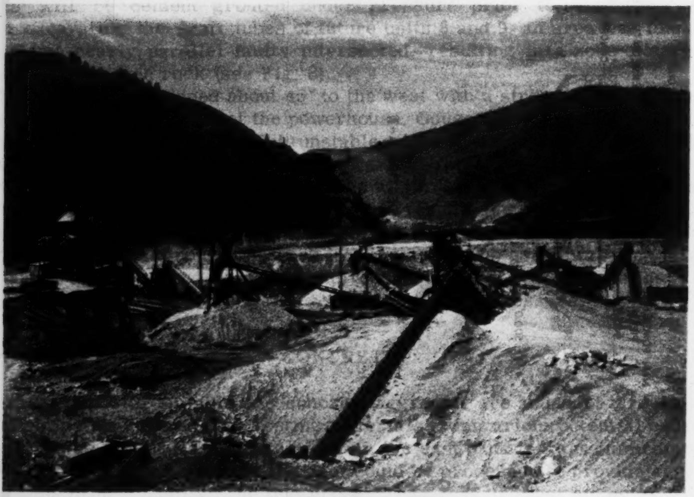

FIG. 9.—LAYOUT OF AGGREGATE PROCESSING PLANT AND BATCHING PLANT

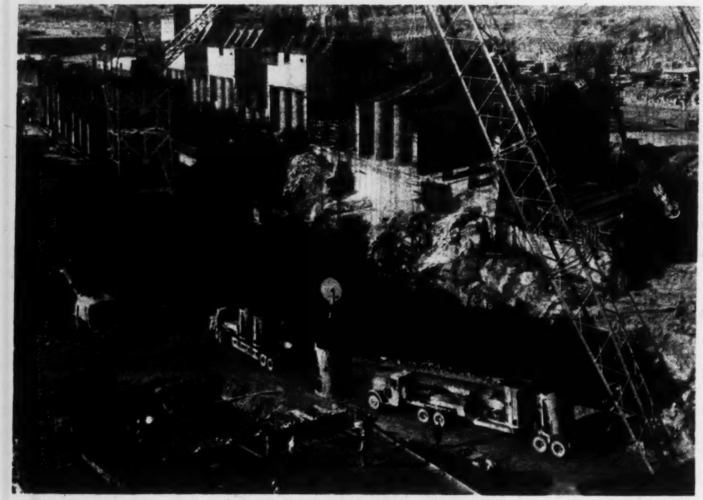

FIG. 10.—PLACING CONCRETE DURING FINAL STAGE CONSTRUCTION

Processed aggregate was selected as required from a reclaim tunnel beneath the stockpiles and conveyed by belt through a rewash unit to the concrete batching plant. The batching plant used during Stage I construction consisted of three 2-yd tilting mixers controlled for automatic and simultaneous batching of any of 12 predetermined mixes. The same plant, with the addition of a fourth 2-yd mixer, was used for final stage work. Capacity of the plant with the fourth mixer in operation was about 200 cu yd per hr. This capacity provided ample reserve as maximum yardage placed in any one day was 3,410 cu yd. Silo storage for about 7,000 barrels of cement was provided at the batch plant. All cement was transported in bulk to the site by truck.

During Stage I construction, concrete was transported from the batch plant to the placing site by a fleet of highway tractors pulling semi-trailers each carrying two 4-yd buckets. The trailers provided space for three buckets so that when any truck arrived at the placing site the handling crane could place a recently emptied bucket on the vacant space on the truck and grab a full one. This allowed for continuous operation of the unloading crane when trucks were moving into and out of unloading position and reduced the round trip time of each truck. Buckets were lifted by crawler cranes with 140-ft booms. To further reduce unloading time and complicated hose or rope connections, the contractor devised automatic grab and release hooks operated by either air or hydraulic cylinders mounted above the hook. Rotation of sheaves above the hook charged the cylinders in normal operation and opening or closing of the hook was controlled by pressure on a lever mounted on the upper inside of the hook. Every other operation of the lever opened the hook and every other operation of the lever closed the hook. With little practice, crane operators could open and close the hooks without hesitation or lost motion. Fig. 10 shows a typical concrete placing operation during performance of final stage work.

Although the final stage work was located mainly on the right bank and contained approximately 800,000 cu yd of the 1,025,000 cu yd of concrete required for the entire project, the Contractor, when awarded the final stage work, decided to maintain the batching plant he had used during construction of Stage I and again transport concrete by truck, this time across the river via a temporary bridge. The cost of hauling concrete this greater distance was easily offset by the savings made in eliminating the need of relocating the batch plant to the right bank and the need of transporting aggregate to such a plant. The bridge also provided communications across the river and made available the more spacious working and storage areas on the left bank. The bridge, consisting of a wood deck supported on 70-ft steel plate girders on concrete piers, was constructed in the dry behind the Stage I cofferdam and was located immediately upstream of the dam as shown in Fig. 11. It provided good service until the night of June 4, 1958, when, with the flow in the Columbia near its 1958 peak of 390,000 cfs, three piers of the bridge near its east end were lost (Fig. 12).

Each pier in the spillway section of the dam is stepped upstream at El 640 to provide seats for a permanent gate maintenance caisson and space for guides for the temporary stop logs used during placement of concrete in spillway ogees. To repair the bridge, the contractor supported structural steel brackets off these pier noses, with tension ties back to the spillway piers, as shown in Fig. 13. The permanent spillway bridge beams that had already been delivered to the site were erected on these brackets and the bridge was returned to service in 28 days. While the bridge was out of service, concrete operations were carried out on a limited basis by hauling the

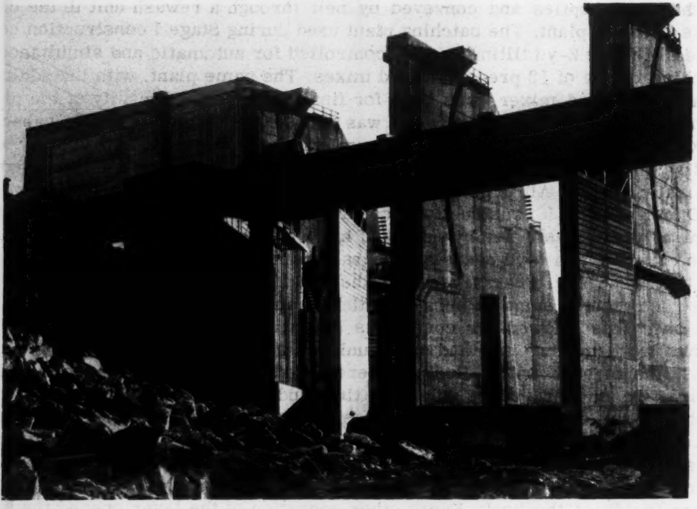

FIG. 11.—CONSTRUCTION BRIDGE

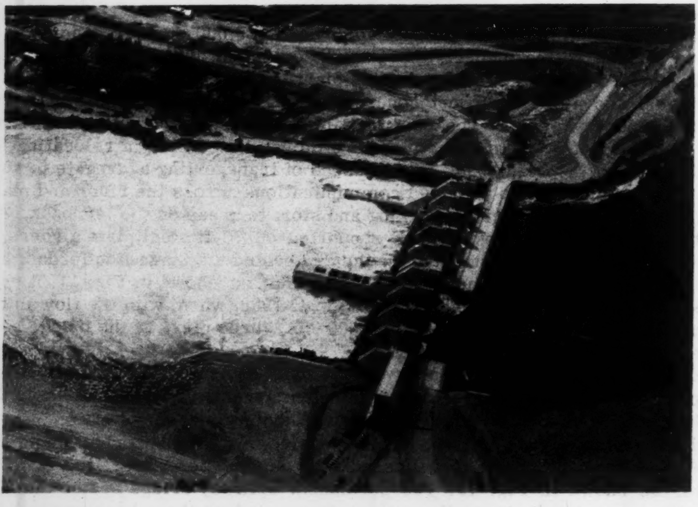

FIG. 12.—LOSS OF THREE PIERS OF THE CONSTRUCTION BRIDGE

concrete from the batch plant to the placing site across the river through Wenatchee, a total of 21 miles.

The flexibility of truck haul over rail or conveyor haul of concrete was well demonstrated in this instance. Concrete delivered to its site after this long haul suffered only slight losses in slump and entrained air and no noticeable segregation or loss in compressive strength.

For placement of final stage concrete, the contractor provided four whirler cranes, rail mounted, with structural steel gantries. Fig. 14 shows the whirlers along the upstream and downstream sides of the powerhouse provided crane coverage of the powerhouse and center dam for placing of concrete. Study indicated that gantry type whirlers with a maximum gantry height of 100 ft could reach all parts of the structure without requiring a trestle for the track system. On the intake side of the powerhouse, the track was laid as close to the intake structure as was practical with the low side of the track being on a fill supported by a 12 in. by 12 in. timber crib to prevent the fill from sloping into the concrete area. The opposite rail, in most cases, was built on solid ground. The intake track paralled the powerhouse and followed the upstream face of the center dam, first on a curve with a 220-ft centerline radius and then tangent to the spillway, and ended at approximately the west end of the spillway. The whirler type gantry cranes used on the intake side of the powerhouse were equipped with 100-ft gantries and 157-ft booms and had a capacity of 11 tons at 145-ft radius.

Whirler tracks on the draft tube, or downstream, side of the powerhouse, were built substantially the same as those on the intake side with the exception that concrete retaining walls were used in lieu of cribs. The retaining walls were built to the alignment of the centerline of the rails, so that the rails were placed directly on top of the concrete, and no ties were needed. This track accommodated two whirler type gantry cranes with 80-ft gantry heights and 140-ft booms. Both machines were of the same capacity as those used on the intake side.

The four whirlers were augmented by crawler cranes of similar capacity as the whirlers. These proved especially useful in the lower levels of the powerhouse. They also placed all of the concrete in the forebay wall and fish ladder structure, as both were out of reach of the powerhouse gantry cranes. As concrete reached greater heights in the powerhouse, use of the crawler type machines was discontinued because they couldn't reach desired heights.

When no longer required at the powerhouse, the two whirlers from the upstream side were dismantled and re-erected on temporary steel girders spanning the spillway bay openings. There they will be used in placing concrete for the spillway ogees and in installing the tainter gates.

All forms were designed for the use of heavy hardware (ties) spaced at the maximum possible distance apart. This, of course, produced quite heavy form sections, and required the use of power equipment for stripping and raising. Steel framing was used in forms in some cases, but all contact surfaces were sheathed with either tongue and groove lumber or plywood. Concrete lifts in the powerhouse varied from 5 ft to 15 ft, so standard panels were built varying in height within these limits.

Generally, forms were designed to match concrete placing rates. That is, if a 14-ft lift of concrete in a wall, for example, was congested with steel, that would affect the rate of concrete placing, forms were designed to accommodate this situation rather than to carry the full plastic load. With the exception of those for the draft tubes, intake and scroll case soffits, forebay

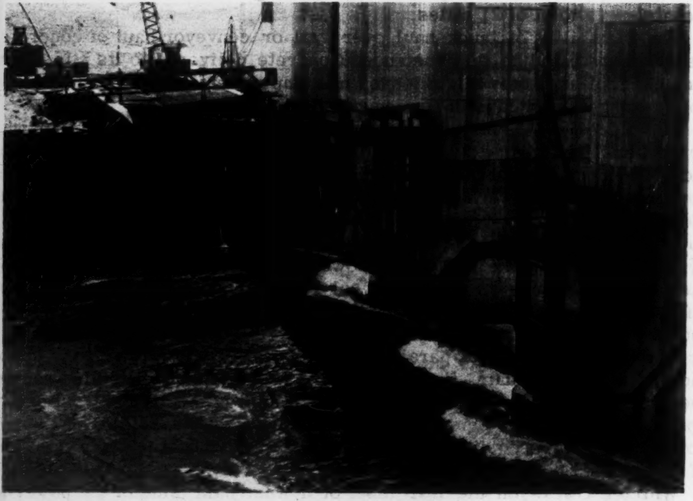

FIG. 13.—STRUCTURAL STEEL BRACKETS AND THE TIE BACKS AROUND THE SPILLWAY PIERS

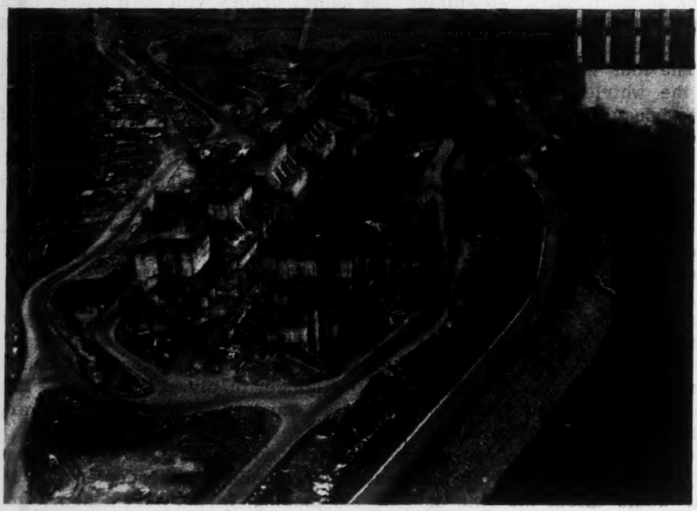

FIG. 14.—WHIRLERS ALONG THE UPSTREAM AND DOWNSTREAM SIDES OF THE POWERHOUSE

and center dams, all forms were made of wood. Wherever possible, standard panels were designed in order to provide as many re-uses as possible.

At the time of purchase, the Rocky Reach turbines were second only to the units at Grand Coulee in horsepower rating and were among the largest in North America in physical size. Fig. 15 shows an interior view of the concrete scroll case for one of the units. The section of concrete scroll case shown here is over 30 ft high. The men in the foreground give an impression of the size of the units.

As the powerhouse units were similar, and the construction schedule allowed adequate time, only a single set of specially designed draft tube, scroll case and intake soffit forms were used. All of these were constructed of steel and sheathed with plywood. Sections were made the maximum size possible complete with attached steel shoring. They were cycled from one unit to another on a systematic schedule. Fig. 16 shows a section of the shoring and forming for the scroll case roof of one of the units. Shoring and forms were designed for re-use in successive units. Such shoring and forming proved to be economical as well as expeditious. Its use eliminated the need of reforming of intricately warped surfaces and the usual forest of temporary shoring, customarily provided for each of the powerhouse units. As other formed surfaces, such as walls of the typical units, required considerably more time, it was generally found that two complete sets of forms for these areas were required to match the time cycle of the single set of draft tube, scroll case and intake soffit forms mentioned previously.

Gravity sections of the structure, such as the center dam and forebay wall were formed with standard type 5-ft steel cantilever panels sheathed with wood. The special forms for the intake soffits, draft tubes and scroll cases were fabricated off site. Wood forms were prefabricated in the job form shop. Thus, practically all built-in-place form work was eliminated from the job.

No major problems arose during the placing of the final stage concrete. The contractor's plant and equipment were adequate to produce and place concrete as quickly as space limitations would permit form work to be prepared to receive it. During the 9 month period from February 1, 1959 to November 1, 1959, a total of 400,000 cu yd were placed. Deducting from this period a three-week shut down because of labor trouble, concrete was placed at an average rate of over 11,000 cu yd per week.

FISH HANDLING FACILITIES

As is required at most hydroelectric projects constructed on west coast streams, it was necessary to provide facilities for passage of fish moving upstream to spawn. Permanent facilities were made an integral part of the concrete structures. Entrances to a fish ladder for upstream migrants are provided at the spillway and along the entire length of the powerhouse. From the entrances, fish will pass to the forebay by means of channels and a fish ladder adjacent to the west bank. Location of the fish ladder is shown in Fig. 1. A fish counting station is located at the exit to the forebay and will provide photographic record of number and species. Attraction water for the fishway passages is provided by three hydraulic turbine driven pumps pumping a total of 3,525 cfs from the tailrace. Downstream migrants will be collected at the intake to the turbine pumps and conducted to the tailrace through large diameter conduits and over free falling wiers.

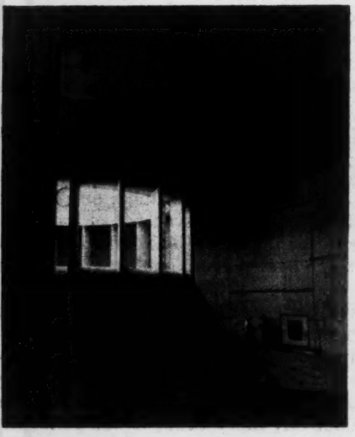

FIG. 15.—HYDRAULIC TURBINES

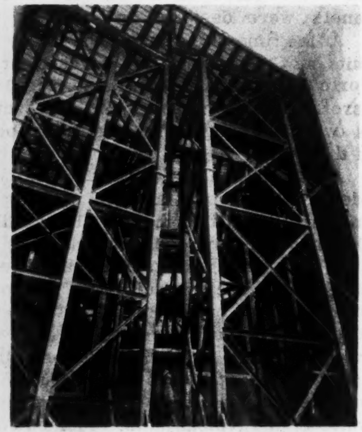

FIG. 16.—STRUCTURAL STEEL SHORING AND WOOD SHEATHED STEEL RIB FORMS

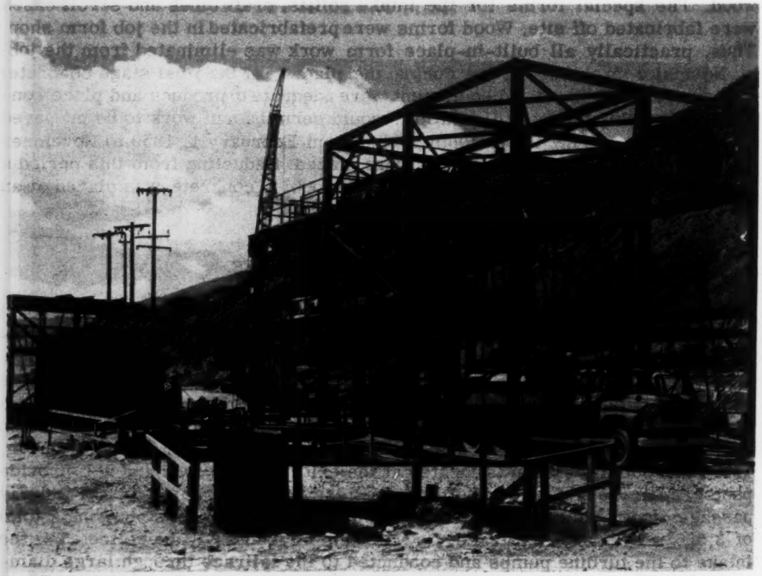

FIG. 17.—TRUCK MOUNTED FISH TRANSPORT TANK

Temporary fish-handling facilities had to be provided during the full construction period. These were required to accommodate each year the estimated 90,000 fish that would be passing upstream through the site. Also, the construction schedule itself had to be arranged so that once the fish began to move upstream their passage through the site would be uninterrupted. Since the river at no time was completely blocked off, the passage of downstream migrants was no problem. Various schemes were used, however, to accommodate the upstream migrants. During the 1957 spawning season, with the Stage I cofferdam in place, upstream migrating fish had to traverse the water passage between the cofferdam and the west bank. To reduce velocities in this section, that would otherwise be prohibitive, quarry rock was dumped along the outside of the cofferdam to form an uneven surface on the stabilizing rock groin. Velocities immediately adjacent to the groin were significantly reduced thereby, and fish were able to pass upstream.

Model tests showed that in the 1958 through 1960 seasons, while the final stage cofferdam was in place, velocities of water flowing through the uncompleted spillways would be an insurmountable obstacle to upstream migrants. A temporary fish ladder was constructed in the spillway bay nearest the east bank for fish moving upstream on that side of the river. The ladder was of the vertical baffle type and of a height sufficient to accommodate all stages of river flow.

For the west bank, a trap was constructed in the final stage cofferdam, the cells being so arranged as to support the necessary equipment and tanks. Holding ponds, and brailing and elevating equipment were arranged in a 45-ft diam steel tank in the cofferdam, and a fish passage was provided from the river through the cofferdam to the tank. A sheet piling deflector was erected extending into the river from the cofferdam cell immediately upstream of the fish passageway to provide a velocity barrier that would intercept fish passing upstream along the cofferdam and direct them into the trap. Attraction water was provided by pumps. As fish were trapped, they were lifted in hopper bottom tanks and unloaded into specially designed fish tank trucks for transportation upstream of the dam where they were returned to the river.

No record has been maintained of the number of fish using the temporary fish ladder near the east bank. During 1959, however, a total of nearly 17,000 fish were trapped and transported by truck. The arrangement of the trap in the cofferdam is shown in Fig. 14, and a closer view of the hoisting equipment for the trap is shown in Fig. 17.

RESERVOIR

All of the work involved in the construction of a hydroelectric project is not confined to the site of the dam and powerhouse. At Rocky Reach, 35 miles of State Highway and 24 miles of railway had to be relocated while traffic on each was maintained. In addition, 20 miles of existing railway embankment had to be protected or improved to withstand the higher water levels of the new reservoir itself will have a surface area of about 10,000 acres and will inundate close to 6,000 acres of farm, orchard and range lands, and a substantial part of the town of Entiat, Washington. The extent of this relocation

work and the work of clearing of the reservoir was a major construction operation in its own right and is not included herein.

MAJOR QUANTITIES INVOLVED IN CONSTRUCTION

Excavation for structures, common	**370,800**	**cu yd**
Excavation for structures, rock	**573,700**	**cu yd**
Foundation Cleanup for Concrete	**67,900**	**sq yd**
Excavation for east bank & cutoff dam, common	**2,534,100**	**cu yd**
Excavation for east bank & cutoff dam, rock	**26,100**	**cu yd**
Excavation for fills, filter zones, riprap etc.	**1,475,400**	**cu yd**
Concrete	**1,025,000**	**cu yd**
Portland Cement	**991,800**	**bbl**
Forms	**4,341,500**	**sq ft**
Reinforcing Steel	**35,100**	**ton**
Estimated Cost of Project	**$273,100,000**	

ACKNOWLEDGMENTS

The Rocky Reach Hydroelectric Power Project is being constructed for Public Utility District No. 1 of Chelan County, Washington. District Commissioners are L. J. Richardson, President, Ivan J. Compton, Secretary, and Robert O. Keiser, member. Kirby Billingsley is Manager of the District, and E. C. Metcalf is Chief Engineer. Design of the Project and supervision of its construction is being done by Stone & Webster Engineering Corp., of Boston with D. N. McCord, F. ASCE, Vice President as Construction Manager, J. H. Boyd, M. ASCE, Project Manager at the site, O. L. Hooper; F. ASCE, Chief Hydraulic Engineer, and C. W. Hubbard, Project Engineer. A joint venture consisting of L. E. Dixon Co., Hunkin Conkey, Arundel Corp., and American Pipe and Construction Co., operating under the name of Rocky Reach Dam Builders, performed Stage I Contract work. The Final Stage General Contract is held by Rocky Reach Contractors, consisting of the same four companies plus the Guy F. Atkinson Co. W. N. Evans, of the L. E. Dixon firm, is Resident Manager for the Contractors. Tullar Power Co., is contractor for electrical work, and the Selby Drilling Co. performed grouting work to provide the grout curtain cutoff in the East Bank Terrace.

AMERICAN SOCIETY OF CIVIL ENGINEERS

Founded November 5, 1852

TRANSACTIONS

Paper No. 3204

SIMPLY SUPPORTED CORNER PLATE

By Mario G. Salvadori,[1] F. ASCE and H. C. Reggini[2]

SYNOPSIS

A corner plate, simply supported on two parallel boundaries each of which is composed of two semi-infinite straight lines meeting at right angles, is uniformly loaded. Bending and twisting moments and shears and boundary reactions in the plate are determined by finite-difference integration of the corresponding boundary value problem. The penetration into the side strips of the disturbance represented by the corner is shown to be practically negligible at a distance from the inner corner of the order of the width of the side strips.

INTRODUCTION

In modern reinforced concrete design, flat slabs are often used as floors in buildings leaving an inner rectangular core with sides parallel to the outer boundaries of the building. The floor slabs may be either simply supported by or elastically built-in into the core and the outer walls, thus becoming a "corner plate" of widths a and b. (Fig. 1).

When the sides l and l' of the core are much larger than the widths a and b of the strips, the stresses away from the corner approach asymptotically, the values for infinite strips of widths a and b, respectively. It will be shown that the stresses due to a uniform load in the corner region of the plate considered simply supported are rather insensitive to the lengths l and l', so that they may be computed as l and l' were infinite as soon as $l \geq 2a$, $l' \geq 2b$.

Note.—Published essentially as printed here, in November, 1960, in the Journal of the Structural Division, as Proceedings Paper 2654. Positions and titles given are those in effect when the paper or discussion was approved for publication in Transactions.

[1] Prof. of Civ. Engrg., Columbia Univ., New York, N. Y., and Assoc., Paul Weidlinger, Cons. Engrs., New York, N. Y.

[2] Assoc. Prof., Buenos Aires Univ., Buenos, Aires, Argentina, and Assoc., H. Fernantezlong, Cons. Engr., Buenos Aires, Argentina.

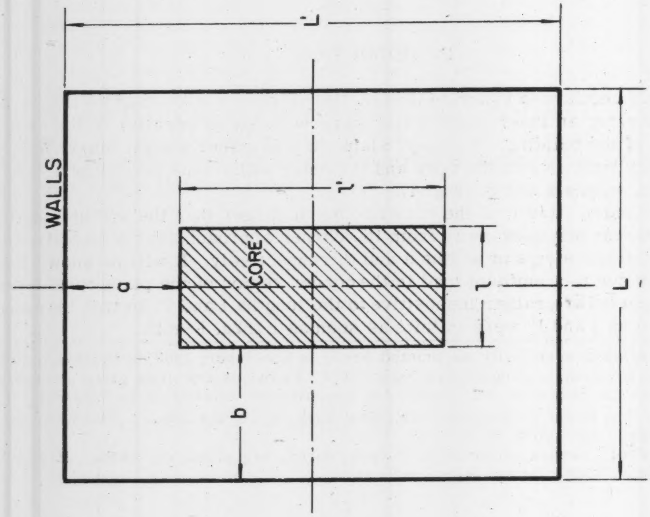
WALLS
CORE
a
b
l
l'
L
L'

FIG. 1.—FLOOR SLAB

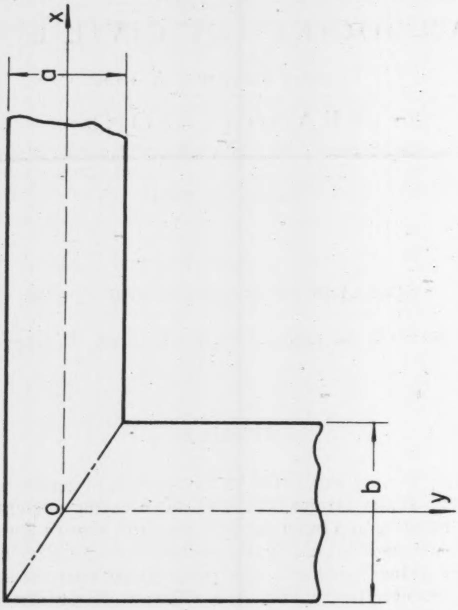

FIG. 2.—CORNER PLATE

The reentrant corner of the plate introduces a singular point in the solution of the plate equation, so that shears are infinite there. In practice, these theoretically infinite stresses do not arise, because they are relieved by plastic deformations due to diagonal tension.

The evaluation of stresses and displacements for the corner plate was obtained by numerical methods, using first-order central-difference operators and solving the corresponding equations in an electronic computer.

CORNER PLATE PROBLEM

The indefinite corner plate of Fig. 2 is simply supported on its boundary and loaded with a uniform load q. The plate deflections w are determined[3] by the following boundary value problem:

$$\nabla^2 M = q \quad \ldots\ldots\ldots\ldots \text{(1a)}$$

$$\nabla^2 w = M/D \quad \ldots\ldots\ldots\ldots \text{(1b)}$$

$$M = 0,\ w = 0 \text{ on the boundaries} \quad \ldots\ldots\ldots\ldots \text{(2)}$$

$$\lim_{x \to \infty} \frac{\partial w}{\partial x} = \lim_{y \to \infty} \frac{\partial w}{\partial y} = 0 \quad \ldots\ldots\ldots\ldots \text{(3)}$$

$$\lim_{x \to \infty} \frac{\partial M}{\partial x} = \lim_{y \to \infty} \frac{\partial M}{\partial y} = 0 \quad \ldots\ldots\ldots\ldots \text{(4)}$$

in which

$$\nabla^2 = \frac{\partial^2}{\partial x^2} + \frac{\partial^2}{\partial y^2} \quad \ldots\ldots\ldots\ldots \text{(5a)}$$

and

$$M = \frac{M_x + M_y}{1 + \nu} \quad \ldots\ldots\ldots\ldots \text{(5b)}$$

Conditions 3 and 4 are equivalent to the conditions:

$$\lim_{x \to \infty} w = \frac{q\,a^4}{384\,D}\left[5-24\left(\frac{y}{a}\right)^2 + 16\left(\frac{y}{a}\right)^4\right] \quad \ldots\ldots\ldots \text{(6a)}$$

$$\lim_{y \to \infty} w = \frac{q\,b^4}{384\,D}\left[5-24\left(\frac{x}{b}\right)^2 + 16\left(\frac{x}{b}\right)^4\right] \quad \ldots\ldots\ldots \text{(6b)}$$

$$\lim_{x \to \infty} M = \frac{q}{2}\left(\frac{a^2}{4} - y^2\right) \ldots\ldots\ldots\ldots \text{(7a)}$$

$$\lim_{y \to \infty} M = \frac{q}{2}\left(\frac{b^2}{4} - x^2\right) \ldots\ldots\ldots\ldots \text{(7b)}$$

expressing the fact that the plate is bent into cylindrical surfaces away from the corner.

---

[3] "Theory of Plates and Shells," by S. Timoshenko and Voshorsky-Krager, McGraw Hill Book Co., Inc., New York, 1959.

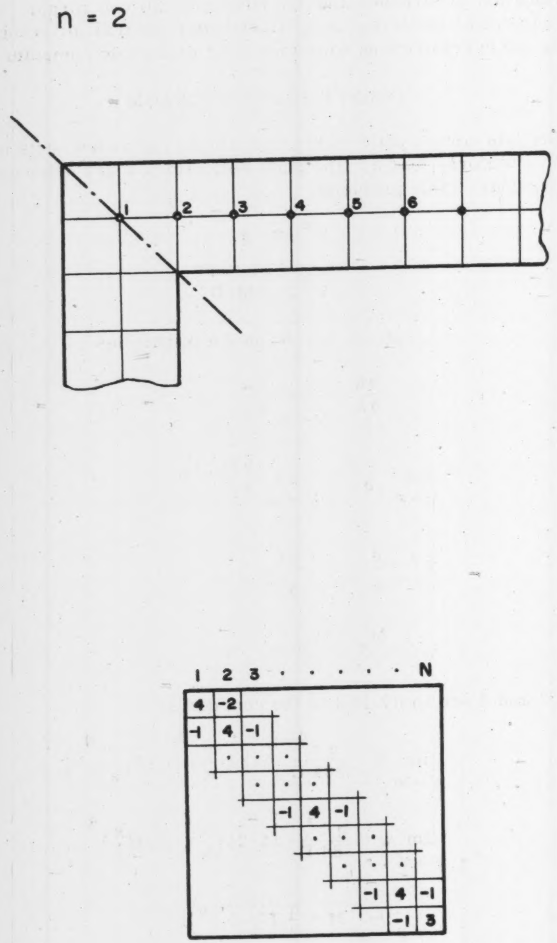
n = 2
1
2
3
4
5
6
1 2 3 . . . . . . N
4 -2
-1 4 -1
. . .
. . .
-1 4 -1
. . .
. . .
-1 4 -1
-1 3

FIG. 3(a)

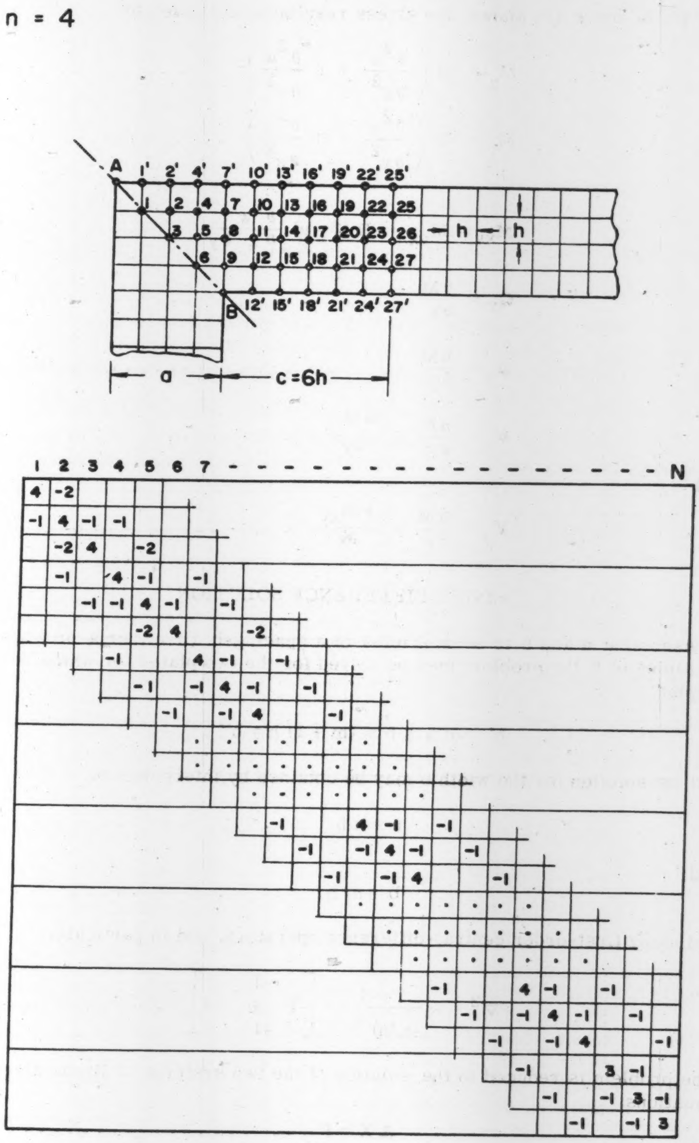
n = 4
A
1' 2' 4' 7' 10' 13' 16' 19' 22' 25'
1 2 4 7 10 13 16 19 22 25
3 5 8 11 14 17 20 23 26
6 9 12 15 18 21 24 27
B
12' 15' 18' 21' 24' 27'
h
h
a
c = 6h
1 2 3 4 5 6 7 - - - N
4 -2
-1 4 -1 -1
-2 4 -2
-1 4 -1 -1
-1 -1 4 -1 -1
-2 4 -2
-1 4 -1 -1
-1 -1 4 -1 -1
-1 -1 4 -1
-1 4 -1 -1
-1 -1 4 -1 -1
-1 -1 4 -1
-1 4 -1 -1
-1 -1 4 -1 -1
-1 -1 4 -1
-1 3 -1
-1 -1 3 -1
-1 -1 3

FIG. 3(b)

Once M and w are known, the stress resultants are given by:

$$M_x = -D \left(\frac{\partial^2 w}{\partial x^2} + \nu \frac{\partial^2 w}{\partial y^2} \right) \tag{8a}$$

$$M_y = -D \left(\frac{\partial^2 w}{\partial y^2} + \nu \frac{\partial^2 w}{\partial x^2} \right) \tag{8b}$$

$$M_{xy} = M_{yx} = -D\,(1 - \nu)\, \frac{\partial^2 w}{\partial x \;\partial y} \tag{8c}$$

$$Q_x = \frac{\partial M}{\partial x} \tag{8d}$$

$$Q_y = \frac{\partial M}{\partial y} \tag{8e}$$

$$V_x = \frac{\partial M}{\partial x} + \frac{\partial M_{xy}}{\partial y} \tag{8f}$$

and

$$V_y = \frac{\partial M}{\partial y} + \frac{\partial M_{xy}}{\partial x} \tag{8g}$$

FINITE DIFFERENCE SOLUTION

Assuming a and b to be multiples of a spacing h, (if either a or b are not multiples of h, the problem may be solved for the two plates for which, for example:

$$b' = m\ n \leq b \leq (m + 1)\ h = b''$$

and the solution for the width b may be obtained by interpolation):

$$a = n\ h \tag{9a}$$

and

$$b = m\ h \tag{9b}$$

and using first-order central-difference operators, and in particular:

$$\nabla^2 = -\frac{1}{(a/n)^2} \begin{bmatrix} & -1 & \\ -1 & 4 & -1 \\ & -1 & \end{bmatrix} \tag{10}$$

The problem is reduced to the solution of the two systems of linear algebraic equations:

$$A\ X = I \tag{11a}$$

and

$$A\,Y = X \quad \ldots\ldots\ldots\ldots\ldots\ldots \quad (11b)$$

in which A is the matrix of the coefficients, I a unit column, and X and Y are related to M and w by

$$M = \frac{q\,a^2}{n^2}\,X \quad \ldots\ldots\ldots\ldots\ldots\ldots \quad (12a)$$

and

$$w = \frac{q\,a^4}{n^4\,D}\,Y \quad \ldots\ldots\ldots\ldots\ldots\ldots \quad (12b)$$

The matrices corresponding to n = 2, 4 together with the numbering of the corresponding pivotal points are given in Fig. 3, for the case a = b, when boundary conditions 3 and 4 are used.

TABLE 1

c/h	N	Point								
		1	2	3	4	5	6	7	8	9
		X								
2	12	0.95186	1.40372	2.09458	1.56844	2.28584	2.28238	1.58451	2.19638	1.77931
3	15	0.94965	1.39930	2.08621	1.56133	2.27312	2.26779	1.57291	2.17717	1.76245
4	18	0.94916	1.39831	2.08438	1.55972	2.27044	2.26474	1.57010	2.17292	1.75905
5	21	0.94905	1.39809	2.08397	1.55935	2.26984	2.26408	1.56948	2.17197	1.75831
6	24	0.94902	1.39804	2.08387	1.55927	2.26971	2.26393	1.56934	2.17176	1.75815
		Y								
2	12	1.44089	2.40585	3.95271	2.82609	4.45228	4.49235	2.87770	4.25253	3.39123
3	15	1.42590	2.37698	3.89970	2.78303	4.37931	4.40957	2.81450	4.15181	3.30594
4	18	1.42201	2.36944	3.88595	2.77148	4.36027	4.38852	2.79650	4.12469	3.28440
5	21	1.42100	2.36748	3.88239	2.76845	4.35531	4.38307	2.79164	4.11750	3.27880
6	24	1.42075	2.36698	3.88148	2.76767	4.35404	4.38168	2.79037	4.11563	3.27735

TABLE 2

	X				Y			
	Value of c/h							
Point	2	4	6	∞	2	4	6	∞
Upper	1.57358 (5%)	1.52017 (1%)	1.51381 (1%)	1.50000	2.84794 (14%)	2.61348 (5%)	2.57619 (3%)	2.50000
Middle	2.13645 (7%)	2.03129 (1%)	2.02169 (1%)	2.00000	4.09245 (17%)	3.67044 (5%)	3.61539 (3%)	3.50000
Lower	1.63849 (7%)	1.52478 (2%)	1.51745 (1%)	1.50000	3.04072 (22%)	2.62966 (5%)	2.58873 (4%)	2.50000

Table 1 gives the values of X and of Y at points 1 to 9 in the corner region of Fig. 3 (b) ($h = a/4$), when boundary conditions 3 and 4 are applied at a distance $c = 2$ h, 3 h, 4 h, 5 h, and 6 h from the reentrant corner. It is seen that for $c/h \geq 2$ the maximum difference between any X is less than 1.2%, and between any Y value less than 3.4%. For $c/h \geq 4$, these differences reduce to 0.5% and 2.1%. It is thus seen that as soon as $1 \geq 2$ a the deflections and stress resultants may be considered practically independent of l and equal to those for $l = \infty$.

TABLE 3

n	At the origin (c/h = 6)		At the middle of infinite strip	
	X	Y	X	Y
2	0.12500 (5%)	0.01562 (4%)	0.12500 (0%)	0.01562 (17%)
4	0.13024 (1%)	0.01516 (1%)	0.12500 (0%)	0.01365 (5%)
h^2-extrapolation n=2; n=4	0.13199	0.01501	0.12500 (0%)	0.01299 (0,2%)
∞	. . .	. . .	0.12500	0.01302

Table 2 gives the values of X and Y at the pivotal points farthest from the reentrant corner for various values of c/h and for $c/h = \infty$ (cylindrical deflection), together with the percentage difference from the values for $c/h = \infty$. It is seen that the corner disturbance is less than 2% in the moment M and less than 5% in the displacement as soon as $c/h \geq 4$.

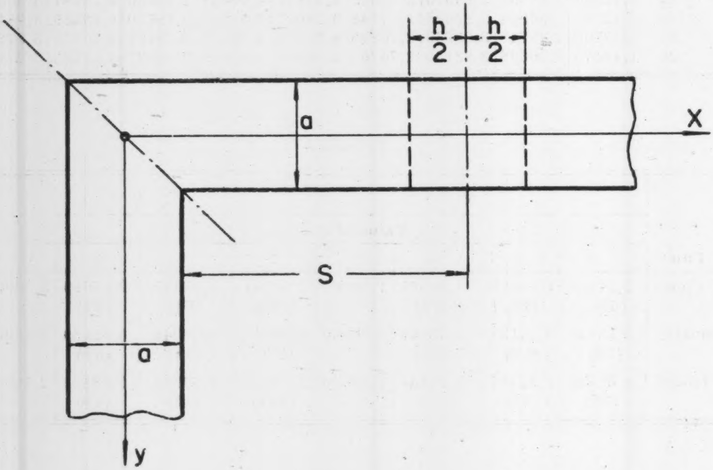

FIG. 4

In order to evaluate the influence of the spacing h on the numerical solution, the values of X and Y at the origin (center of corner) and at the point farthest from the corner at the middle of the strip were evaluated for $c/h = 6$, taking $n = 2$ and $n = 4$. Table 3 shows the results of this computation and the values obtained by h^2 extrapolations,[4] together with the percentage of error in comparison with the extrapolated values (the values for the cylindrical deflection are $X = 0.12500$, $Y = 0.01302$ and should be compared with the extrapolated values 0.12500 and 0.01299). It is seen that the values at the origin obtained with $n = 4$ are in error by 1% and that the values at the middle of the strip are in error by 5%. The extrapolated values may be considered practically correct.

FINITE CORNER PLATES

Boundary conditions 3 used in solving the case of the indefinite corner plate state the symmetry of the deflection about a line parallel to y at S (Fig. 4), since they make

$$X_{S-h/2} = X_{S+h/2} \quad \dots\dots\dots\dots\dots \quad (13a)$$

and

$$Y_{S-h/2} = Y_{S+h/2} \quad \dots\dots\dots\dots\dots \quad (13b)$$

Hence, the solutions thus obtained are also valid for symmetrical plates with $l = l' = 2\,S$. Fig. 5 gives the dimensions of these plates (for $n = 4$).

STRESS RESULTANTS

The stress resultants of Eqs. 8 are easily evaluated by means of the pivotal values of M and w using first order central difference operators.[5] The bending and twisting moments become, (assuming, for simplicity, Poisson's ratio equal to zero):

$$M_x = p\,a^2 \frac{1}{n^2}\,[-1, 2, -1]\,Y \quad \dots\dots\dots\dots\dots \quad (14a)$$

$$M_y = p\,a^2 \frac{1}{n^2} \begin{bmatrix} -1 \\ 2 \\ -1 \end{bmatrix} Y \quad \dots\dots\dots\dots\dots\dots\dots \quad (14b)$$

and

$$M_{xy} = p\,a^2 \frac{1}{4\,h^2} \begin{bmatrix} -1 & 1 \\ 1 & -1 \end{bmatrix} Y \quad \dots\dots\dots\dots\dots \quad (14c)$$

The principal moments along the diagonal of the corner (Fig. 6) are given by:

$$M_{1,2} = \frac{1}{2}\left(M_x + M_y\right) \pm M_{xy} = \frac{p\,a^2}{4\,n^2} \begin{bmatrix} \mp 1 & -4 & \pm 1 \\ -4 & 16 & -4 \\ \pm 1 & -4 & \mp 1 \end{bmatrix} Y \quad \dots\dots\dots \quad (15)$$

---

[4] "Numerical Methods in Engineering," by M. G. Salvadori and M. L. Baron, Prentice-Hall, New York, 1955, p. 75.

[5] Ibid., p. 63.

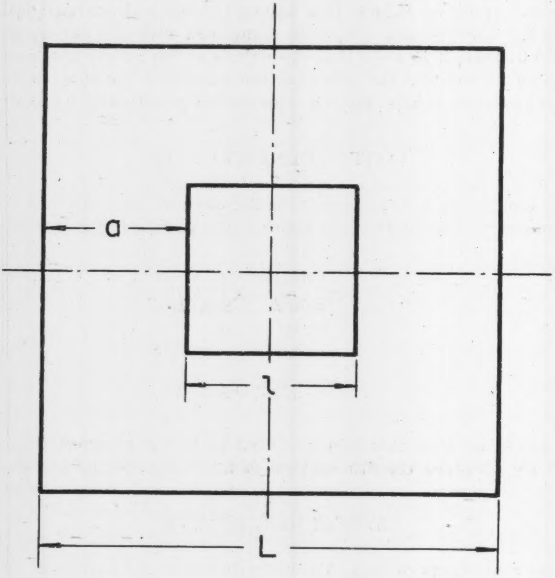

$\frac{C}{h} = 2 \qquad \frac{L}{l} = \frac{11}{3}$

$\frac{C}{h} = 3 \qquad \frac{L}{l} = \frac{13}{5}$

$\frac{C}{h} = 4 \qquad \frac{L}{l} = \frac{15}{7}$

$\frac{C}{h} = 5 \qquad \frac{L}{l} = \frac{17}{9}$

$\frac{C}{h} = 6 \qquad \frac{L}{l} = \frac{19}{11}$

FIG. 5.—SQUARE PLATES

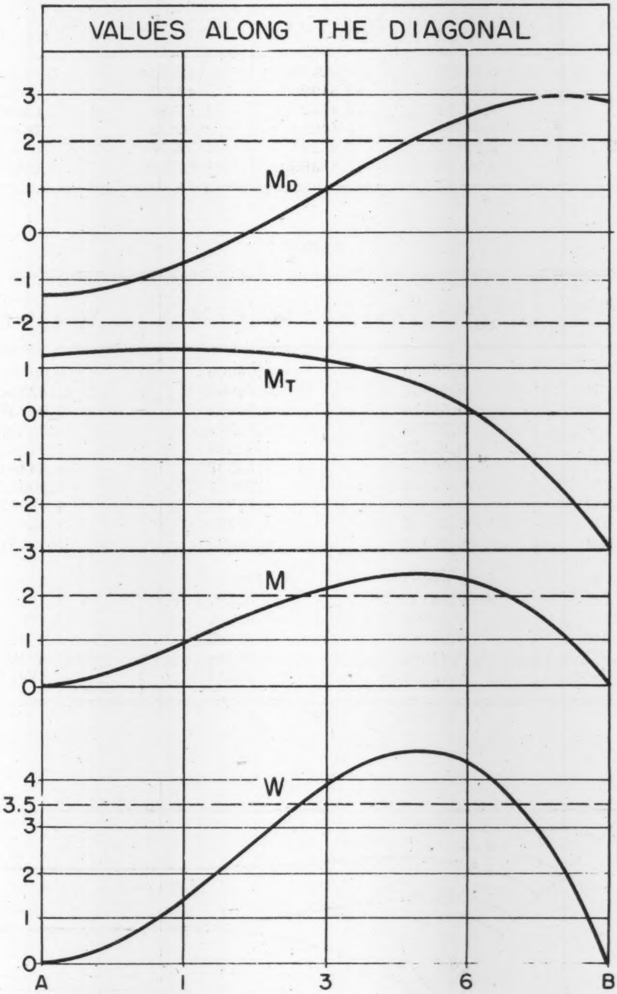
VALUES ALONG THE DIAGONAL
M_D
M_T
M
W
3
2
1
0
-1
-2
1
0
-1
-2
-3
2
1
0
4
3.5
3
2
1
0
A
1
3
6
B

FIG. 6

TABLE 4

Point	$w/\left(\frac{1}{256} \frac{p a^4}{D}\right)$	$M_D/\left(\frac{1}{16} p a^2\right)$	$M_T/\left(\frac{1}{16} p a^2\right)$	$M/\left(\frac{1}{16} p a^2\right)$
A	0,00000	(-1.42075)	(1.42075)	0,00000
1	1,42075	-0.51999	1.42075	0,94902
3	3,88148	0.98027	1.11381	2,08387
6	4,38168	2.44094	0,26605	2,26393
6-B	2,93035	2.95805	-1,38800	1,57006
B	0,00000	(2.85395)	(-2.85395)	0,00000

TABLE 5

Point	$\frac{\partial M_{xy}}{\partial x} / \left(\frac{1}{4} a p\right)$	$Q_y/\left(\frac{1}{4} a p\right)$	$V_y/\left(\frac{1}{4} a p\right)$
A	0.00000	0.00000	0.00000
1'	0.47452	0.94902	1.42354
2'	0.54554	1.39804	1.94358
4'	0.37799	1.55927	1.93726
7'	0.10421	1.56934	1.67355
10'	-0.00238	1.54632	1.54394
13'	-0.02560	1.52612	1.50052
16'	-0.02318	1.51381	1.49063
19'	-0.01702	1.50745	1.49043
22'	-0.01333	1.50484	1.49151
B	0.68093	-1.75815	-1.07722
12'	0.24197	-1.59691	-1.35494
15'	0.09764	-1.53967	-1.44203
18'	0.04463	-1.51745	-1.47282
21'	0.02346	-1.50844	-1.48498
24'	0.01570	-1.50517	-1.48947

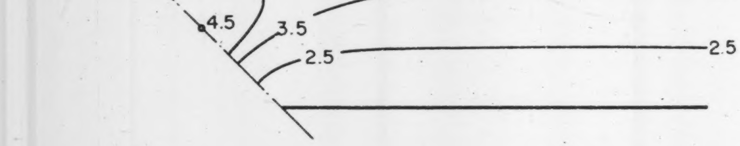

FIG. 7.—DEFLECTION

Table 4 gives the value of the displacements and of the bending moments at the pivotal points of the network for n = 4, c/h = 6.

Similarly, the reaction and shear along the outer and inner boundary are given in Table 5. They were computed by means of the following operators:

$$Q_y = \frac{\partial M}{\partial y} = p\,h\,\frac{1}{2}\begin{bmatrix}-1\\0\\1\end{bmatrix} X \quad \ldots\ldots\ldots\ldots\ldots\ldots \tag{16}$$

assuming $M_{\text{outside}} = -M_{\text{inside}}$ at the boundary,

$$Q_y = p\,h\begin{bmatrix}0\\-1\end{bmatrix} X \ \text{ at the outer edge} \quad \ldots\ldots\ldots\ldots \tag{17}$$

$$Q_y = p\,h\begin{bmatrix}1\\0\end{bmatrix} X \ \text{ at the inner edge} \quad \ldots\ldots\ldots\ldots \tag{18}$$

$$M_{xy} = p\,h\,\frac{1}{2}\begin{bmatrix}1 & -2 & 1\\0 & 0 & 0\\-1 & 2 & -1\end{bmatrix} Y \quad \ldots\ldots\ldots\ldots\ldots\ldots \tag{19}$$

assuming $W_{\text{outside}} = -W_{\text{inside}}$ at the boundary,

$$M_{xy} = p\,h\begin{bmatrix}0 & 0 & 0\\-1 & 2 & -1\end{bmatrix} Y \ \text{ at the outer edge} \ldots\ldots \tag{20}$$

$$M_{xy} = p\,h\begin{bmatrix}1 & -2 & 1\\0 & 0 & 0\end{bmatrix} Y \ \text{ at the inner edge} \ldots\ldots \tag{21}$$

The concentrated forces required to keep the corners at A and B down are:

$$S_A = 2.84\,p\,h^2 \text{ (down)}$$

and

$$S_B = -5.71\,p\,h^2 \text{ (up)}$$

The total load on the plate is 22.5 $p\,h^2$, the resultant of all the boundary forces is 23.7 $p\,h^2$.

Fig. 6 gives the values of w, M, M_1, and M_2 along the diagonal of the corner. Fig. 7 gives the contour lines of the plate deflections.

ACKNOWLEDGMENTS

The computations of this research were performed on the 650 IBM computer of The Watson Scientific Computing Laboratory at Columbia University. The writers are indebted to W. Eckart, Director of the laboratory, for permission to use the computer and to Kenneth M. King and Joyce Alsop, members of the laboratory staff, for advice and help in the programming and in the actual computation.

AMERICAN SOCIETY OF CIVIL ENGINEERS
Founded November 5, 1852
TRANSACTIONS

Paper No. 3207

TEST OF A RIVETED PLATE GIRDER WITH A THIN WEB

By Desi D. Vasarhelyi,[1] M. ASCE, Jim C. Taylor,[2]
Naresh C. Vasishth,[3] A. M. ASCE, and Chia-Yao Yuan[4]

SYNOPSIS

A detailed record of the experimental results obtained from tests on a full-size riveted plate girder with a web plate thinner than that required under the present design specifications is reported herein.

Both the web-buckling phenomenon and the diagonal-tension phenomenon of the web plate under load were carefully observed. Comparison was then made between the computed buckling loads and the values determined from experimental data. Particular emphasis was laid on the behavior of the web after being loaded beyond the conventionally termed "buckling load", with a view to evaluating the importance of the buckling of the web with respect to practical design. Study was also made on the change in the shear-carrying behavior of the web after buckling occurred and on the ability of the web to withstand loads in excess of the buckling value.

Note.—Published essentially as printed here, in October, 1960, in the Journal of the Structural Division, as Proceedings Paper 2621. Positions and titles given are those in effect when the paper or discussion was approved for publication in Transactions.

[1] Prof. of Civ. Engrg., Univ. of Washington, Seattle, Wash.

[2] Engr., Dominion Bridge Co., Vancouver, B. C., Canada.

[3] Design Engr., Moffatt, Nichl, and Taylor, Portland, Ore.

[4] Engr., Arctic Research Labs., Barrow, Alaska.

The behavior of the flanges of this girder was also carefully observed and the results are reported herein. Particular emphasis has been given to the stress distribution in the region of the cover plate cutoffs.

INTRODUCTION

Object and Scope.—This test was conducted primarily to investigate the effect of a thin web on the load-carrying capaicty of a plate girder. A reasonable amount of information was also obtained concerning the behavior of the built-up flanges.

The test specimen, with the exception of the thin web, was typical of many of the riveted plate girders in common use. Much of the testing procedure was governed by the behavior of the web. At the conclusion of the test, selected sections of the flange were cut from the girder and examined. Saw cuts were made through the rivets at various sections of the flange. Inspection of these exposed rivets helped to interpret some of the information gathered during the testing procedure[5].

Buckling of the Web Plate.—As shown in some earlier research, (10), (11), (43), and in observations made in this experiment, the web plate of a plate girder does not behave exactly in the same manner as a theoretical, flat rectangular plate of the same material and dimensions, when being loaded to the critical buckling stress.

The theoretical buckling stress of a flat plate is defined as the stress at which an exchange of stable equilibrium configurations occurs between the straight and the slight bent form. It marks the region in which continued application of load results in an accelerated growth of deflections perpendicular to the plane of the plate. Its importance lies in the fact that buckling initiates the physical processes that lead to the eventual failure of the plate (3).

In comparison with the theoretical, flat rectangular plate previously mentioned, the web plate of a plate girder behaves quite differently when the girder is under load. Because it is impossible, under ordinary fabrication conditions, to keep the web plate absolutely flat, the presence of small initial curvature will cause the web to deflect laterally as soon as the load is applied. The rate of deflection increases as the load increases until a point is reached at which the rate of deflection begins to decrease. Physically, this point marks the transition from a shear resistant web to a diagonal tension web.

If we assume, for the purpose of approximation, that the web plate is free from initial imperfection, then the web plate must be approaching a state of instability when this occurs; otherwise, the change in the shear resisting behavior in the web would not have resulted. We can, therefore, say that the load at this point is synonymous to the buckling load of the web.

Accordingly, in describing the significance of the buckling load of the web plate of a plate girder, we can say that it represents the point of transition in the shear-carrying action of the web from a state of pure shear resistance to a state of incomplete diagonal tension.

Method of Estimation of the Buckling Load by Using the Theoretical Formulas.—Due to the indeterminate nature of the edge restraint on the web plate that is developed in the riveted connection between the flange angles and the web plate, and between the vertical stiffeners and the web, and because of the complexities of the bending and shearing stress distribution along the four edges of the web plate, there does not seem to be an exact analytical method for computing the buckling load of the web plate of a plate girder.

---

[5] Numbers in parentheses refer to corresponding items in the Appendix.

According to Timoshenko, (1),(9), the web-plate buckling can be analyzed by considering the following three cases of loading:

a. Near the supports, the shearing force is the most important factor; the part of the web between the two stiffeners can be considered as a rectangular plate subjected to the action of uniform shear;

b. At the middle of the span of the plate girder, the shearing stresses can be neglected in comparison with the normal stress; then the part of the web between two stiffeners is in a condition of pure bending;

c. In the intermediate cross sections, there is a combination of normal and shearing forces.

As to the supporting conditions at the boundary, we can tell by intuition that it must be an intermediate case between simply-supported edges and clamped edges. Timoshenko suggested that for design purposes all four edges of the web plate could be considered as freely supported, because this boundary condition would yield a more conservative result and hence insure that the design was safe.

The assumption that the bending stress is constant between two stiffeners at the edges of the plate is a further simplification, since these stresses vary along the girder with the bending moment. However, to permit a solution of the buckling problem without undue complication of the analysis, the simplification of the loading condition is the first step necessary in dealing with the stability of the web plates in a plate girder.

General Formulae for the Buckling Stress.—This discussion will be confined to the critical stresses for elastic buckling. The general expression for theoretical buckling stresses of a flat rectangular plate under various types of loadings and different boundary conditions can be given as

$$\sigma_{cr}\ (\text{or}\ \tau_{cr}) = K\,\frac{\pi^2\,E}{12\left(1-\mu^2\right)}\left(\frac{t}{b}\right)^2 \quad \ldots\ldots\ldots\ldots (1)$$

in which σ_{cr} is the critical bending stress, τ_{cr} refers to the critical shearing stress, t denotes the thickness of the plate, b is the width of the plate, and K denotes the elastic buckling coefficient. The value of the elastic buckling coefficient, (K), is dependent upon the aspect ratio, the type of loading, and the condition of restraint along the edges. Numerical values of the elastic buckling coefficients, (K), for various loading and boundary conditions were computed, and tables giving values of K corresponding to certain ranges of the aspect ratios of the plate are available. However, due to the large variety of cases of loading and boundary conditions, the information is by no means complete. Values of K, covering various cases of loading and boundary conditions, are given by Bleich (2). For plates subjected to uniform shearing stress on four edges only, Paul Kuhn, (4), gives an empirical formula.

The Post-Buckling Phenomenon.—The post-buckling behavior of the web plate of a plate girder was explained by Paul Kuhn and others in the theory of incomplete diagonal tension in a series of papers published by the National Advisory Council on Aeronautics (NACA), (4), (5), (6), (7), (8), (39).

As the applied load increases and buckling occurs, the principal tensile stresses increase rapidly and undertake to carry most of the additional shear in truss action, while the principal compressive stresses increase at a much slower rate. This state of stress in the web plate is called incomplete diagonal tension, because a part of the additional shearing force is still carried by the shear action due to the continued increase in the principal compressive force; however, most of the additional shear is carried by the truss action.

The main physical characteristic of the diagonal tension action that can be observed in the web plate is the formation of diagonal buckles. The process of buckle formation is accompanied by the appearance and development of axial stresses in the stiffeners. This is due to the fact that the truss action in the web plate produces vertical and horizontal components of compressive stresses in the direction of the stiffeners as well as the flanges. The vertical compression is assumed to be resisted by the stiffener together with a certain effective width of the web. This accounts for the appearance of axial compressive stresses in the stiffeners at the buckling of the web plate. In the same manner, the diagonal tension may produce some secondary compressive stresses in the flanges.

Determination of Flange Stresses.—The analysis of flange stresses in a riveted plate girder is complicated by the fact that the girder is not a solid beam, but is composed of components that are connected by an elastic medium, namely, the rivet. Both the elastic properties of the rivet, and the rivet hole itself, affect the distribution of stresses in the beam in a somewhat uncertain manner. The solution of the problem in the past has been to treat the girder as a solid beam, and to adopt one of the standard procedures for determining the flange stresses. The rate at which stress builds up in the ends of the cover plates does not seem to be fully understood, as a result of which there are several opinions as to how far cover plates should extend past their theoretical cutoff points.

DESCRIPTION OF SPECIMEN AND TEST

Design of Specimen.—The design, workmanship, and material of this girder was in compliance with current American Assn. of State Highway Officials (AASHO) specifications, with several exceptions. For one half of the girder a 1/4-in. web was used, while on the other half, the web thickness was 5/16-in. The spacing of the vertical stiffeners has been so determined that buckling will occur sequentially during the test, rather than maintaining a spacing to comply with the specifications. Based on the expected buckling loads for the web, the flanges were designed for a total two-point load of 350 kips at basic design stresses. In computing the resisting moment of the section, the net section was used with rivet holes in both flanges deducted. Since the top flange was to be fully supported, the compression stress in the top flange did not govern the design. At the end of the girder, with 1/4-in. thick web, the cover plates were extended 12 in. past their theoretical cutoff points. At the other end, with 5/16-in. thick web, they were extended far enough to accommodate a sufficient number of rivets to develop the computed initial force that the plate had to support at the theoretical cutoff point. The general dimensions and properties of the girder cross section are shown in Table 1.

Description of Test.—The girder was tested in the 2,400,000-lb hydraulic testing machine at the University of Washington, Seattle, Wash. The general arrangement of the test is illustrated in Fig. 2. The top flange of the girder was supported by bracing frames at seven points along its length, while the bottom flange was supported at the ends and at the center line.

The location of all strain gages is shown in Fig. 1. Seventy type A-11 SR4 gages were used. Strain gages on the stiffeners were placed at mid-height on the edge of the outstanding leg of the stiffener angles. These gages were placed at symmetrical positions so that by averaging the readings in the two gages, any possible bending effect present in the stiffeners could be eliminated, thus leaving only the axial strains.

TABLE 1.—GENERAL PROPERTIES OF THE GIRDER

Specification	AASHO
Material	ASTM A-7 Steel (Rivets—ASTM A-141)
Length	56 ft - 0 in. c. to c. end brgs. (56 ft - 7 in. overall)
Depth	6 ft - 2 1/2 in. b. to b. of angles
Flange	2-L^s 6 in. x 6 in. x 3/4 in., 3 cover plates : 14 in. x 1/2 in.
Length of cover plates	1. 38 ft - 8 1/4 in. 2. 31 ft - 5 in. 3. 23 ft - 10 1/4 in.
Web	1/4 in. x 74 in. and 5/16 in. x 74 in.
Intermediate stiffeners	2-L^s — 3 1/2 in. x 5 in. x 3/8 in.
Yield stress	Web 41.4 ksi Angles 36.9 ksi Cover Plates 39.4 ksi [a]
Dead weight	Approx. 20^k
Working load	350^k total for two-point loading @ 14 ft - 0 c. to c. load
Moment of inertia (in^4)	111,677 90,930 70,717 51,029 Gross 95,700 77,547 59,860 42,634 Net
Rivets	3/4 in ϕ: holes subpunched 11/16 in. ϕ, Reamed 13/16 in ϕ

[a] From coupon tests.

Vertical deflection gages were placed along the bottom of the girder, at mid-span, at stiffener points and at each end of the girder. The gages used were 1/1000-in. dial gages; the general arrangement is shown in Fig. 1. The two deflection gages at each end of the girder served to indicate any settlement of the supports.

For the measurement of lateral deflections of the web, a special fixture was used to hold the dial gages against the web. Both 1/10,000-in. and 1/1000-in. dial gages were used.

At three selected points, 0.0001-in. dial gages were mounted directly to the flange to measure the "slip" or relative motion at the ends of a cover plate.

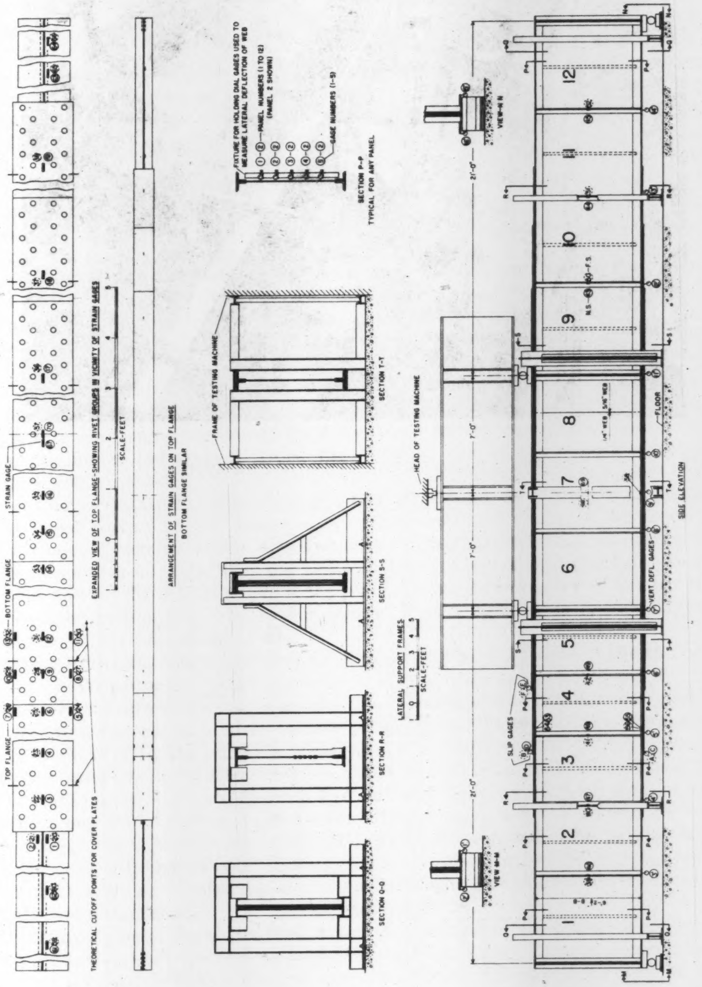
THEORETICAL CUTOFF POINTS FOR COVER PLATES
TOP FLANGE
BOTTOM FLANGE
STRAIN GAGE
EXPANDED VIEW OF TOP FLANGE-SHOWING RIVET GROUPS IN VICINITY OF STRAIN GAGES
SCALE-FEET
ARRANGEMENT OF STRAIN GAGES ON TOP FLANGE
BOTTOM FLANGE SIMILAR
FIXTURE FOR HOLDING DIAL GAGES USED TO MEASURE LATERAL DEFLECTION OF WEB
PANEL NUMBERS (1 TO 12) (PANEL 2 SHOWN)
GAGE NUMBERS (1-5)
SECTION P-P
TYPICAL FOR ANY PANEL
FRAME OF TESTING MACHINE
SECTION T-T
SECTION S-S
LATERAL SUPPORT FRAMES
SCALE-FEET
SECTION R-R
SECTION Q-Q
HEAD OF TESTING MACHINE
VIEW M-M
VIEW N-N
21'-0"
7'-0"
7'-0"
21'-0"
SLIP GAGES
VERT DEFL GAGES
FLOOR
1/4" WEB
5/16" WEB
SIDE ELEVATION
1
2
3
4
5
6
7
8
9
10
11
12

FIG. 1.—GENERAL SETUP OF THE TESTS

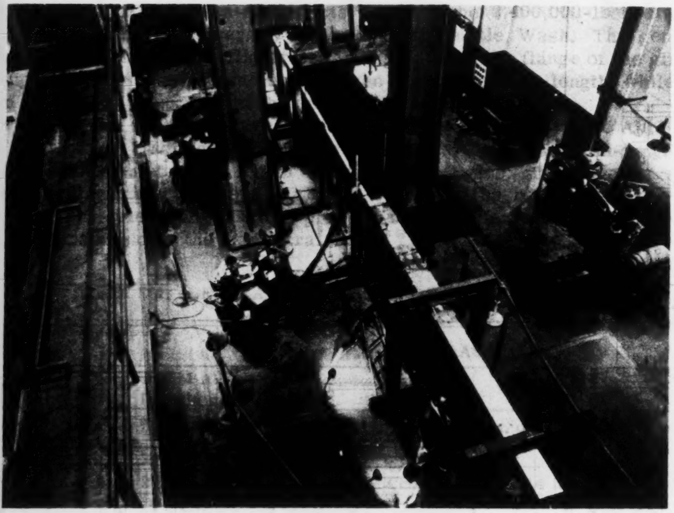

FIG. 2.—GENERAL SETUP OF THE TEST

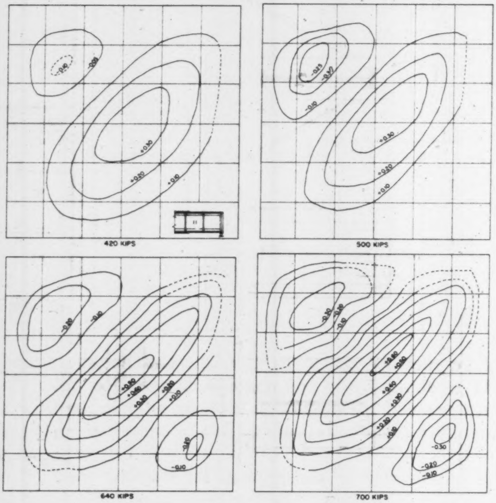

FIG. 3.—CONTOUR PLOTS SHOWING DEFLECTED SHAPES OF THE WEB IN PANEL 11 UNDER VARIOUS APPLIED LOADS

These gages were mounted in pairs, one gage on each side of the cover plate. The top flange and one side of the girder was sprayed with a coat of "whitewash", so that yielding at any point could readily be detected.

To obtain the contour plot of the deflected shape of the web, a photographic method was used (42). Samples of contour plots thus obtained are shown in Fig. 3.

Test Procedure.—In general, load was applied to the beam in 20-kip increments, and all gages were read immediately after each increment was added. The maximum load applied was increased by 60 kips each day a test was run, except when certain panels of the web buckled to the extent that yielding was indicated and had to be stiffened before more load could be added. Loading was continued in this manner until a maximum load of 740 kips was applied. At this load, it became apparent that the capacity of the web was reached, and since yielding was also observed at many places along the flange, no further load was added. The girder was, however, tested in the working range (0-350 kips) after being subjected to the maximum load.

Observation of web deflection was concentrated first on the end panels and the rest of the 1/4-in. web panels. In order to measure very small deflections at small loads, the 1/10,000-in. dial gages were used first; when the deflection became larger, 1/1000-in. dial gages were substituted. Occasionally the loading was removed in order to check for any residual deflection in the plate.

In order to make sure that the point of maximum deflection of the web panel had been detected, the measuring fixture with five dial gages was used first. The five dial gages measured the deflections at five equidistant points (including the one at the center) along the vertical line at the middle of the panel. When plotting the deflections along the vertical center line of the panel to scale, it would be apparent where the point of maximum deflection was located. It was found that this point was usually very close to the center of the panel. When the diagonal tension action appears in the web plate, the point of maximum deflection shifts slightly from the center position. In order to catch the maximum point, two or three dial gages were placed around the center of the panel at an estimated distance of 2 in. to 3 in. apart. This method usually took care of the shifting of the maximum point.

Due to the different thicknesses of the web plates, failure of the thinner web would most probably cause the failure of the beam as a whole, and thus, there would be no opportunity to observe the yielding of the thicker web plates. In order to avoid such an early failure of the girder, failure of the weaker panels was prevented by the addition of bolted stiffeners in the panels concerned. The angles used for the stiffeners were of the same cross sections as the intermediate stiffeners (5 in. x $3\frac{1}{2}$ in. x 3/8 in.) and were 62 in. long, so that they fit in between the top edge of the bottom flange angle and the bottom edge of the top flange angle, with a clearance of 1/4-in. on each end. One pair of stiffener angles was attached to each side of the web plate with 3/4-in. high tension bolts which had the same spacing as the rivets on the intermediate stiffeners. The bolts were tightened by the one-half turn method.

At the completion of the test, selected portions of the flange were cut from the girder and saw cuts were made through the rivets. The clearance between the rivets and the holes was measured and some rivets were removed for inspection. The clamping force exerted by the rivets was also measured by placing a strain gage on the rivet before removing it from the flange (43).

Correlation of Stress and Strain.—The measurement of strain in a structure is very easily and exactly accomplished through the use of the SR-4 strain gage; however, relating this strain to stress often is not so straightforward. In the case of a riveted structure, biaxial and triaxial stress conditions are known to exist in the region of the rivet holes, although at points away from the rivets a uniaxial stress field is approached. However, even if the gages were located far enough from the rivets to be in a field of uniaxial stress, there would be some doubt as to what gages located on the net section, through a row of rivets, measured in terms of the average stress or strain on that section. There would also be some doubt as to how far from a rivet the stress disturbances extended.

To establish a correlation between the measured strain and the average stress on a section, a specimen having the same dimensions and hole pattern as a typical section from the girder cover plates was tested under axial tension. By locating gages on this test specimen at the same relative position as on the girder cover plates, a relation between the average stress in the plate and the measured strain was obtained.

All graphs and curves presented herein are plotted on the basis of strain. In general, however, the equivalent stress, in kips per square inch across the gross section, can be obtained approximately by taking 3% of the strain in micro inches per inch. Where theoretical lines or curves have been shown for comparison with the experimental results, a modulus of 30,000 ksi has been assumed.

The dead load of the girder has been taken into account by converting it to an equivalent applied load and adding it to the load applied through the testing machine. Where the term "total load" is given herein the previous conversion has been included.

TEST RESULTS

Behavior of Web Plates Under Loadings Below their Buckling Loads.—It was noticed from the beginning of the tests that the web plates of the plate girder started to deflect as soon as the load was applied. This might be due to the presence of initial curvature in the web plates, which could hardly be avoided during the manufacturing procedure. Table 2 shows the values of these initial deflections as measured prior to the application of any load to the girder. However, the direction of the lateral deflection of the web plate did not necessarily follow the direction of the initial curvature.

Behavior of Web at Buckling Load.—As explained earlier, the so-called buckling load of the web plate of the plate girder can be regarded as the transition load under which there appears a change in the manner in which the shear in the panel is carried, that is the change from a shear resisting web to a diagonal tension web. For this reason, a characteristic change in the deflected surface of web began to take place at the buckling load. The web deflected in a dish-like surface at smaller loads. When the load was increased, and approached the buckling load of the panel, diagonal buckles were formed. The inclination of the buckle, which depended on the proportion of the panel, generally made a 45° to 50° angle with the longitudinal axis of the girder.

The magnitude of the lateral deflection of the web at the buckling load depended on the aspect ratio and the position of the panel. The measured deflections ranged from 45% to 85% of the thickness of the plate. A list of the buckling loads and the corresponding web deflections is shown in Table 3. (See also Figs. 4(a) and 4(b)). Residual deflections in web plates after unloading (Table

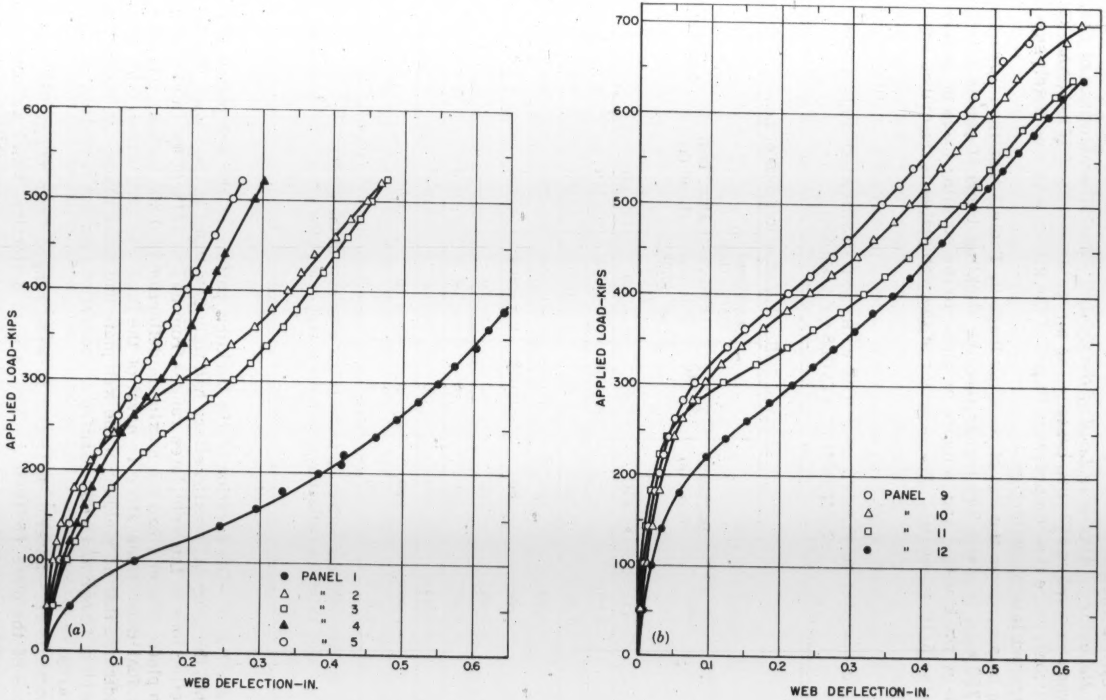

FIG. 4.—TOTAL APPLIED LOAD ON GIRDER VERSUS LATERAL DEFLECTION OF WEB

2) were generally under one hundredth of an inch and were therefore less than the initial deflections.

Web Behavior at Allowable Load of the Girder.—The allowable load of the girder was computed as 350 kips, based on the allowable stress of 18 ksi (AASHO specification), since the compression flange of the girder was completely supported against lateral deflection.

It can be seen from the list of buckling loads in Table 3 that the allowable load of 350 kips is about 25% higher than the buckling loads of panels 1 to 5 (the 1/4-in. thick webs) and is above or close to the buckling loads of panels 9 to 12 (the 5/16-in. webs). The behavior of the web plates is described separately.

TABLE 2.—INITIAL DEFLECTIONS IN THE WEBS AND RESIDUAL DEFLECTIONS AT DIFFERENT STAGES OF LOADING

Panel No.	Initial Deflection in.	Residual Deflection after Removal of Load				
		Buckling Load (k)	δ (in.)	Residual Deflection at allowable load of 350^k (in.)	Max. Test Load (k)	δ (in.)
(1)	(2)	(3)	(4)	(5)	(6)	(7)
1	-0.095	130	+0.006	+0.008	450	+0.044
2	-0.045	260	0	-0.002	480	+0.022
3	+0.040	260	+0.002	+0.006	500	+0.028
4	+0.066	280	+0.002	+0.004	490	+0.004
5	+0.062	280	0	0	520	+0.030
9	+0.073	360	0	0	640	-0.007
10	+0.048	350	0	0	640	-0.012
11	-0.069	320	0	0	620	-0.033
12	-0.072	260	0	0	620	-0.085

Notes: + sign indicates deflection towards the west side of the girder.
- sign indicates deflection towards the east side of the girder (the whitewashed side).

Panels 1 to 5.—Observation of the buckling pattern of the web plates indicated that the diagonal tension effect had fully developed in the webs. The lateral deflections in the web plates ranges from 64% to 121% of the thickness of the web plate. Panel 1 had the maximum deflection of 0.303 inches. However, the residual deflections after removal of the load was still within 0.01 inch. This indicated that no yielding of the web plate had taken place. An inspection of the web of flange and web to stiffener connections did not reveal any damage in this area.

Panels 9 to 12.—Lateral deflection in webs ranged from 43% to 91% of the thickness of the plate (5/16-in.). The largest deflection, which amounted to 0.285 in., was in the end panel (panel 12). Web plates were still found to be elastic upon removal of the load.

As a whole, it can be concluded that, the girder performed satisfactorily under the allowable load. Although the deflections at the end panels were close to or above 100% of the web thickness, the magnitude of the actual deflections seemed to be still tolerable. A list of the web deflections at the allowable load is given in Table 4.

Post-Buckling Behavior of the Webs.—As the applied load was increased beyond the buckling load of a panel, it was observed that the effect of diagonal tension became more and more pronounced. There are two points that are worth noticing.

Contrary to the general concept of buckling, the rate of increase of the lateral deflection of the web became slower, instead of faster, when passing the buckling load. This can be seen in the load-lateral deflection plot (Fig. 4 and 5) in that the slope of the part of the deflection curve above the buckling load became steeper than that immediately under the buckling load.

TABLE 3.—COMPARISON OF WEB DEFLECTIONS UNDER BUCKLING LOADS AND YIELDING LOADS

Panel No. (1)	Aspect Ratio (2)	Buckling Load			Maximum Test Load		
		Load (k) (3)	Deflection (in.) (4)	Percentage of web Thickness (6)	Load (k) (6)	Deflection (in.) (7)	Percentage of web Thickness (8)
1	0.935	130	0.213	85.2	450	0.712	284
2	0.744	260	0.150	60.0	480	0.423	169
3	0.744	260	0.200	80.0	500	0.454	182
4	0.632	280	0.138	55.2	490	0.283	113
5	0.640	280	0.112	44.8	520	0.270	108
9	0.944	360	0.150	48.1	640	0.492	157
10	0.935	350	0.160	51.3	640	0.531	171
11	0.935	320	0.165	52.9	620	0.587	188
12	0.935	260	0.152	48.7	620	0.595	191

Notes:
1. Loads shown are total applied loads on girder.
2. The buckling loads are determined from the load-deflection curves of the webs.
3. Aspect ratio $= \dfrac{\text{clear width of the web}}{\text{clear depth of the web}}$.

Another point is the gradual reorientation of the direction of the inclined buckle due to diagonal tension. As mentioned previously, the plate deflected in a dished surface when the load was relatively small. As the effect of diagonal tension gradually set in, the contour of the deflected surface was seen to elongate towards the direction of the corners, and a main buckle thus formed. This buckle first made an angle of approximately 45° with the longitudinal axis of the girder. As the load was increased the inclination of the buckle was seen to alter, and the angle that the buckle made with the longitudinal axis kept increasing, until finally, at maximum test load, there appeared one large dominate wave running diagonally from corner to corner of the panel.

UNIVERSITY OF MICHIGAN LIBRARY

Illustrations of the elongation of the web deflection contours in the direction of the diagonal can be seen in Fig. 3, for panel 11. It is very apparent that, at the final stage of loading, the main buckles always extend from one corner to the opposite corner of the plate.

The Web Plates at Maximum Test Load.—

The 1/4-in. web.—Due to the thin web and large aspect ratio, panel 1 was the first to show signs of yielding. During the process of loading, there had been no sign of any gradual damage or excessive increment of lateral deflection in the web up to 440 kips. However, when the load was increased from 440 to 460 kips, paint cracks, which represented Lueders' lines in the plate, showed that localized yielding was beginning at the corner. The Lueders' lines appeared at a distance of approximately $\frac{1}{2}$ ft from the upper outside corner of the panel extending from the upper edge of the plate toward the diagonal buckle. They ran perpendicular to the edge of the plate and vanished close to the middle of the buckle. Thus, they formed approximately 45° angles with the diagonal. Since the Lueders' lines appeared in between the loading from 440 to 460 kips, the maximum test load was estimated at 450 kips. The maximum lateral deflection of the web was measured to be 0.712 in. An inspection was made of the rest of the panels, and no other sign of yielding was detected. Stiffener angles were then bolted in the first panel to restrain the buckling.

TABLE 4.—LATERAL DEFLECTION OF WEB PLATES AT ALLOWABLE LOAD OF GIRDER—350^k

Panel No. (1)	Plate thickness t (in.) (2)	Lateral Deflection (in.) (3)	Percentage t (4)
1	1/4	0.303	121
2	1/4	0.292	117
3	1/4	0.317	127
4	1/4	0.194	77.6
5	1/4	0.159	63.7
9	5/16	0.134	42.9
10	5/16	0.156	50.0
11	5/16	0.222	71.2
12	5/16	0.285	91.3

Tests on panels 2, 3, 4, and 5 were carried out in the same manner. The loading was continued until localized yielding was observed in a panel. Stiffeners were then bolted in the panel and the same loading process was carried on again. Lueders' lines were noticed in the web plates of panels 2 and 3 during the same test run; therefore, these two panels were stiffened at the same time. Panels 4 and 5 showed localized yielding during separate tests and were reinforced with stiffeners. A list of the maximum test loads and the maximum deflections in the plates is given in Table 3.

During the loading, it is interesting to note the following: (a) Localized yielding in the web plates started at the same corresponding positions in each

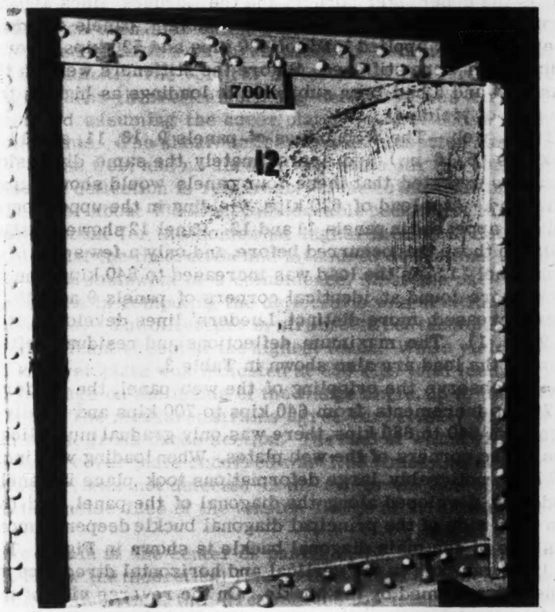

FIG. 5.—THE DIAGONAL BUCKLE AND THE LUEDERS' LINES DEVELOPED IN PANEL 12, AS VIEWED FROM THE EAST SIDE OF THE GIRDER

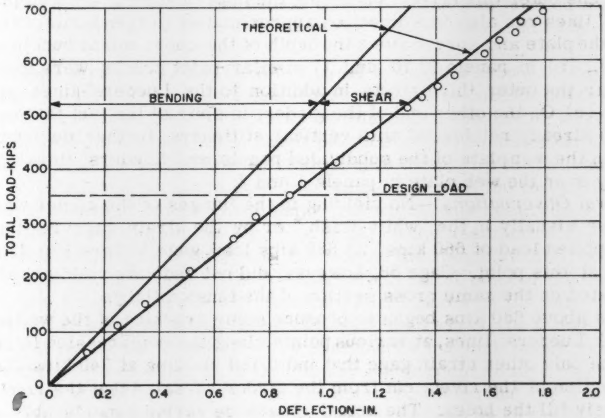

FIG. 6.—VERTICLE DEFLECTION AT MID-LENGTH

UNIVERSITY OF MICHIGAN LIBRARY

panel (that is the upper outer corner) and the Lueders' lines appeared in similar pattern as in panel 1. (b) As shown in Table 3, panels 4 and 5 showed localized yielding under applied loads of 490 kips and 520 kips, after all the panels preceding them were stiffened. Before the stiffeners were in the preceding panels, panels 4 and 5 had been subjected to loadings as high as the above and showed no sign of yielding.

The 5/16-in. web.—The web plates of panels 9, 10, 11, and 12 were of the same thickness (5/16-in.) and approximately the same dimensions. Therefore, it could be expected that these four panels would show signs of yielding at the same load. At a load of 620 kips, yielding in the upper, outer corner of the web, plates appeared in panels 11 and 12. Panel 12 showed distinct Lueders' lines similar to those that occurred before, and only a few spots of paint cracks appeared in panel 11. As the load was increased to 640 kips, the same kind of paint cracks were found at identical corners of panels 9 and 10. As the load was further increased, more distinct Lueders' lines developed at the corners of panels 9, 10, 11. The maximum deflections and residual deflections after the removal of the load are also shown in Table 3.

In order to observe the crippling of the web panel, the girder was further loaded in 20-kip increments from 640 kips to 700 kips and finally to 740 kips. At loadings from 640 to 680 kips, there was only gradual multiplication of Lueders' lines at the corners of the web plates. When loading was increased from 680 to 700 kips, noticeably large deformations took place in panel 12. A deep buckle suddenly developed along the diagonal of the panel, and the two minor buckles on each side of the principal diagonal buckle deepened more appreciably. The shape of the main diagonal buckle is shown in Fig. 5. It can be seen that yield lines ran both in the vertical and horizontal directions along the two sides of the ridge formed by the buckle. On the reverse side of the plate horizontal and vertical Lueders' lines were distributed along the low points of the diagonal buckle.

Finally the load was increased to 740 kips. Observations were made as follows: (a) In panel 12, besides the spread of the yielding zone along the diagonal line, Lueders' lines were also noticed on the plate starting from the position of the outer third rivet connecting the upper flange to the web plate. The Lueders' lines ran also in a direction approximately perpendicular to the upper edge of the plate and spread along the depth of the upper minor buckle mentioned above. (b) In panels 9, 10, and 11 similar paint cracks were found in the plate near the outer third rivets in addition to the Lueders' lines previously formed. (c) On the other end of the girder, in spite of the fact that these panels were already reinforced with vertical stiffeners, further deformation occurred in the web plate of the subdivided panels, and Lueders' lines spread extensively over the web plate in panels 1 and 2.

General Observations.—No yielding in the flanges of the girder was detected, either visually in the "white-wash," or by the strain-gage readings, up to a total applied load of 660 kips. At 680 kips load, gage 57 (see Fig. 1) indicated yielding at this point. Gage 58, however, did not indicate yielding, although it was located on the same cross section of the tension flange.

Loads above 680 kips began to produce some cracking of the white-wash along with Lueders' lines, at various points along the compression flange. Gage 1 was the only other strain gage that indicated yielding at 740 kips load.

Inspection of the rivets cut from the girder revealed that the rivets did not completely fill the holes. The actual clearance varied considerably along the length of the rivet but was generally less near the shop-formed head. The average clearance on each side of the rivet was approximately 0.010 in.; however, it was found to be two or three times this value in several instances.

Vertical Deflection.—The vertical deflection of the girder at center line is shown in Fig. 6. The theoretical bending deflection was computed using the gross section and assuming the cover plates were effective from their theoretical cutoff points. The shear deflection was computed assuming all shear was carried by the web, and no account was made for the buckling of the web.

The measured deflection is remarkably close to the total theoretical deflection. At loads over about 400 kips, considerable buckling of the web took place, and this may account for the somewhat higher measured deflections at these loads. The fact that the theoretical and measured deflections are in such close agreement may be somewhat of a coincidence, since the use of the theoretical cover-plate lengths in computing the deflections was arbitrary.

Flange Stresses.—The difference in strain between the top and bottom flanges is almost insignificant except at the highest loads. While yielding at the center of the outside cover plate was indicated at 680 kips total load, no yielding was indicated at the gage on the inside of the flange angle, up to the maximum total load of 740 kips. The measured strains agree very closely with the theoretical values based on the gross cross section. The load at which yielding in the center of the outside cover plate occurred was 1.93 times the AASHO design load. Yielding, however, was not detected in the center section of the compression flange or on the inside face of the tension flange at 2.13 times the AASHO design load.

The flange strain at the center of panels 9, 10, and 12 is shown in Fig. 7. Both flanges follow the theoretical line up to the load at which the web buckled. For loads higher than this, the stress in the top flange increases at a much faster rate than the theoretical, while the stress in the tension flange increases much slower. In panel 12, over loads of 650 kips, no increase in the tension flange strain was observed, but the strain in the compression flange increased at a much greater rate than previously. Buckling of the web became very severe over 650 kips load, and it is likely that high secondary stresses were induced in the flanges. Below the load at which yielding was noticed on the buckles of the web (620 kips) the behavior of the flanges appeared to be completely elastic.

The flange strain near the center of panel 10 is also shown in Fig. 7. These gages were located at the theoretical cutoff point of the middle cover plate. As mentioned previously, the cover plates on this end of the girder were extended far enough past their theoretical cutoff points so as to accommodate sufficient rivets to develop the initial forces coming into them. Up to the load at which the web buckled, the strain in both flanges agreed with the theoretical. Over this load, the strains followed the same pattern as was observed in panel 12. The theoretical line shown on Fig. 7 is based on the assumption that the outer cover plate is acting integrally with the rest of the flange at this point.

The flange strain in panel 9, at the theoretical cutoff point of the outer cover plate in both flanges, agrees with the theoretical based on the assumption that the outer cover plate is acting integrally with the rest of the flange. The web of this panel buckled at about 370-kips load, but no marked change in the flange strain could be noted. Only at much higher loads could some reduction in the tension flange strain be observed. It was noted, however, that the load at which the web of this panel buckled was not so clearly defined as in the other panels, and the lateral deflection was less than for panels 10, 11, and 12.

UNIVERSITY OF MICHIGAN LIBRARY

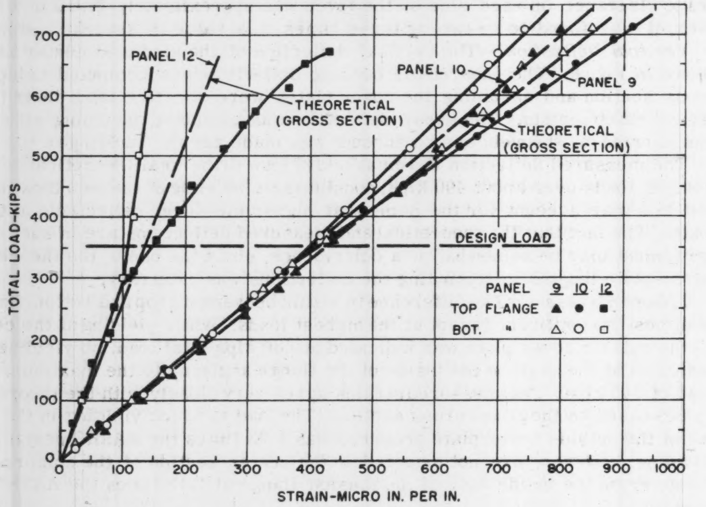

FIG. 7.—FLANGE STRAIN AT CENTER OF PANELS 9, 10, 12

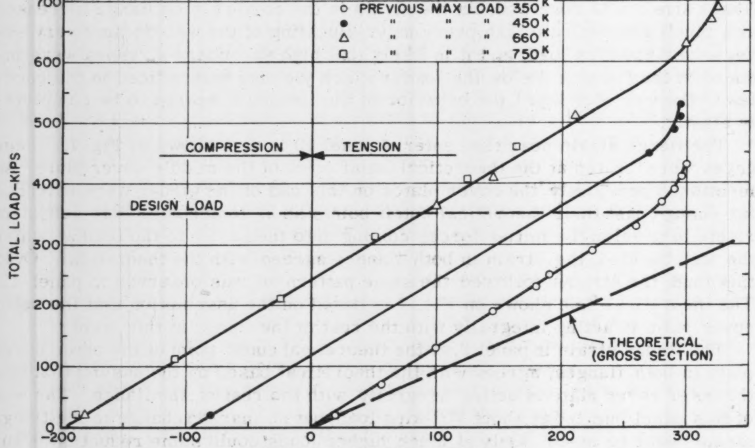

FIG. 8.—STRAIN IN MIDDLE COVER PLATE 8 INCHES FROM THE END—BOTTOM FLANGE

In general, this change in the flange strain at the buckling load of the web was only noticed in the three exterior panels at each end of the girder. The effect was more pronounced near the center of the panel and could hardly be detected over the stiffeners.

Fig. 8 shows the strain-load relationship for a point 8 in. in from the end of the middle cover plate. The cover plates on this end of the girder were extended 1 ft past their theoretical cutoff points to comply with the AASHO specification.

Up to about the working load of the girder, the strain in the cover plate increased directly with the load, although in general it was found to be between 20% and 30% less than the theoretical value. As can be seen from Fig. 8, loads higher than 400 kips did not cause any increase in the strain at this point on the cover plate. Application and subsequent removal of loads higher than 400 kips caused a residual stress to be set up in the cover plate, which was opposite in sign to that induced under loading.

The maximum load carried by the cover plate at this point was approximately 60 kips. Since there are only six rivets in the 8 in. of cover plate beyond this point, the corresponding average shear stress in the rivets should have been about 22 ksi. The maximum residual load induced in the cover plate was about 40 kips, and corresponds to an average shear stress in the rivets of about 13 ksi. These computed shear stresses are equivalent stresses, and may include the effect of frictional resistance as well as shear stresses in the rivets.

The five other points, 8 in. in from the end of the cover plates, at which the strain was measured, behaved similarly to the point just described, except that the apparent maximum shear stress in the rivets varied considerably. The lowest value observed was about 19 ksi, while the highest was about 31 ksi. The observations made at all points seemed to have only random variance, and no particular trend could be noticed either by comparing the results of one flange against the other or by comparing the areas of the flange at each particular point.

Fig. 9 shows the strain-load relationship for a point 16 in. in from the end of the middle cover plate. (The theoretical cutoff point is 12 in. in from the end). The same general phenomenon was observed at this point as was just described for the point 8 in. in from the end of the cover plate. The maximum strain induced in the plate at this point, however, was not so clearly defined as in the previous case. The residual strain in the plate did not reach a maximum or limiting value as was observed in the previous case.

The strain at this point agreed with the theoretical value (assuming that the outer plate and flange are acting integrally) up to about 450 kips. The point at which the strain first began to fall off corresponds to an average shear stress, in the 12 rivets connecting the first 16 in. of cover plate, of about 17.7 ksi. The maximum strain in the cover plate corresponds to an average rivet shear of about 22.6 ksi.

The five other points, 16 in. from the end of the cover plate, at which the strain was measured, behaved almost the same as the point described. The strain readings indicated that the outer cover plate was acting integrally with the rest of the flange until the average shear stress in the rivets connecting the last 16 in. of cover plate reached about 17 ksi. The strain in the cover plate then increased in a somewhat erratic manner to a maximum value. The maximum-value varied and corresponded to an average maximum shear stress of between 20 ksi and 31 ksi. As before, the variation seemed to be only random.

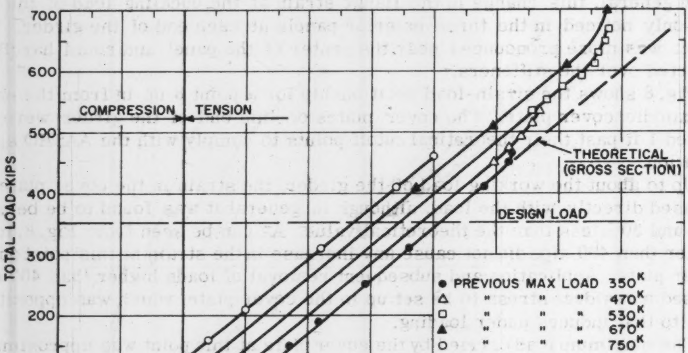

FIG. 9.—STRAIN IN MIDDLE COVER PLATE, 16 INCHES FROM THE END—BOTTOM FLANGE

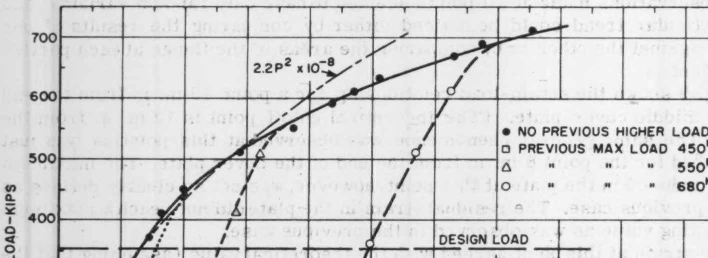

FIG. 10.—SLIP AT THE END OF THE MIDDLE COVER PLATE—BOTTOM FLANGE

In the second cover plate, at the point where the third cover plate terminates, the strain in both flanges was about 16% higher than the theoretical and happens to agree with the theoretical strain based on the net area of the flanges. The four other corresponding points at which the strain was measured also showed strains higher than the theoretical.

Cover Plate Slip.—Fig. 10 shows the slip measured at the end of the middle cover plate. Slip was measured at even the lowest loads, and there is no particular load at which a sudden "jump" was observed. As can be seen from Fig. 10, the load-slip is not reversible. The total slip at the end of the cover plate will depend upon the maximum load that has been previously applied to the girder. The solid curve in Fig. 10 connects the points corresponding to the first application of that particular load. The dashed curves connect points that were obtained while reloading the girder after a previous maximum load, as noted.

The slip measured at the two other points on the top flange followed the same general pattern as for the point just described.

Neutral Axis.—The strain at mid-depth of the girder on a cross section through a row of rivets has been measured. At loads over about 200 kips, tensile strain was measured at mid-depth of the girder, indicating an upward shift of the neutral axis. The magnitude of this shift has been calculated from the strains measured at the flanges and at mid-depth. The shift upwards is nearly constant for all loads above the design load.

ANALYSIS OF TEST RESULTS

The Determination of Buckling Load.—

From load vs. lateral deflection curves.—In this experiment, the buckling load of the web was determined by taking the corresponding load at the point of inflection of the load-lateral deflection curve of the web panel (Fig. 4 and 5). The reason for doing so was based on the assumption that the buckling load corresponds to the load at the transition point from a pure shear action to an incomplete diagonal tension action in the web. The values of the buckling loads thus determined for various panels of the girder are shown in Table 3.

From axial stresses in stiffeners.—This method is based on the assumption that the truss action in the web plate will cause the stiffeners on the two sides of the panel to take compressive stresses, while these stiffeners should be free from axial stresses before the buckling load is reached. Since the total stiffener load up to the point where truss action takes place is very small, this method could not give a result as accurate as that obtained from a graph of web deflection against applied load. In the present case, the cross section of the stiffeners used has been rather heavy, and the axial compressive stresses therefore comparatively small. The load versus stiffener-stress curves are shown in Fig. 11. Instead of indicating any specific point on the curve as the buckling load, the ranges of the applied loads within which the buckling must have occurred have been given. A list of such load ranges is to be found in Table 5.

From flange stresses.—Another phenomenon observed as a result of the buckling of the web plate was the change of the rate of increase in stress in the flanges. As revealed by the strain versus applied load plots on strain gages placed on the flanges at mid-point between two stiffeners, there was a sharp change of slope in the curve at a load corresponding to the buckling load of the panel. Since the strain versus load curves are straight lines, the breaking point

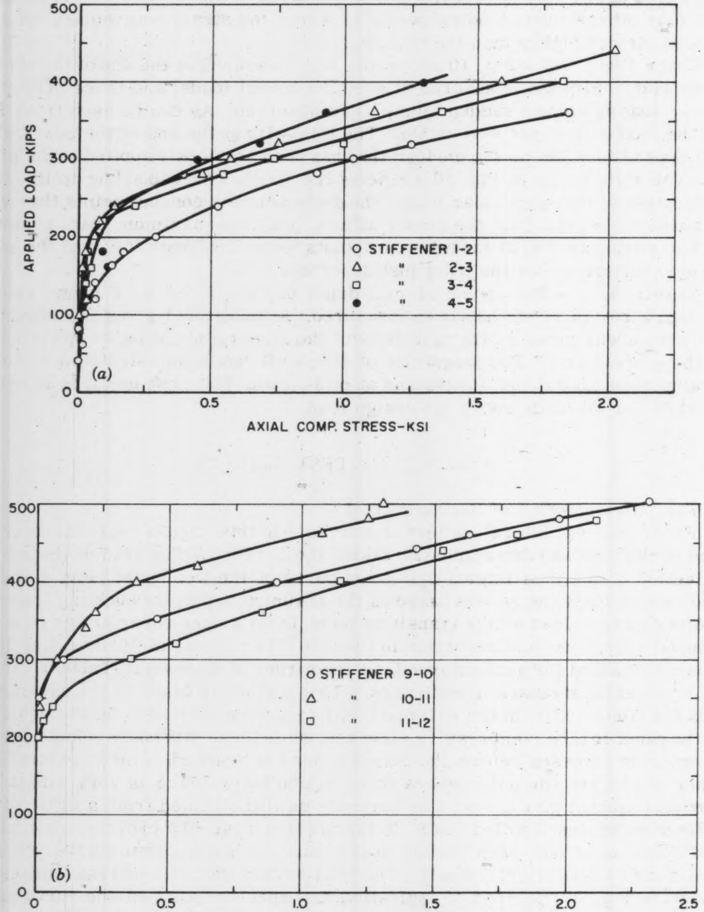

FIG. 11.—TOTAL APPLIED LOAD ON GIRDER VERSUS AXIAL COMPRESSIVE STRESSES IN STIFFENERS

is very apparent, and the buckling load can easily be located. The buckling load, indicated by the strain-gage plots, appeared to be about 5% higher than that determined from the load-deflection curve. One shortcoming of this method was that this abrupt break in the flange strain curves was only apparent in the cases of the three outer panels at each end. The flange strain against applied load plots for panels 9, 10, and 12 are shown in Fig. 7.

By plate-buckling formulae.—As pointed out earlier, the plate-buckling formula was not derived for the buckling of the web of a plate girder, but has been used for the purpose of approximation only. Nevertheless, it is interesting to note from the values in Table 5, that in certain instances the approximation is fairly close. This table was computed for the cases: (a) assuming all four edges of the web plate as freely supported and consider shearing stresses on edges only, (b) assuming the edges along the flanges as clamped, and the other two edges freely supported and consider shearing stresses only, and (c) assuming all four edges as clamped, and considering both bending and shearing stresses.

TABLE 5.—BUCKLING LOADS

Panel No.	Web Thickness (in.)	FROM EXPERIMENT		THEORETICALLY COMPUTED		
		From deflection (kips)	From stiffener stress (kips)	Freely supported edges (kips)	Two long edges clamped (kips)	Four edges clamped (kips)
(1)	(2)	(3)	(4)	(5)	(6)	(7)
1	1/4	130	100 - 140	119.6	169.2	249.4
2	1/4	260	200 - 250	171.4	265.2	300.0
3	1/4	260	200 - 240	174.4	268.2	282.2
4	1/4	280	200 - 250	228.0	362.2	335.2
5	1/4	280	200 - 250	228.6	354.4	335.2
9	5/16	360	250 - 320	257.0	353.0	420.0
10	5/16	350	350 - 320	258.4	355.8	440.0
11	5/16	320	250 - 320	254.6	352.0	430.0
12	5/16	260	200 - 250	250.8	348.2	480.0

Notes:
1. All values shown in the table are total applied loads on girder at which elastic buckling occurred in the various panels.
2. Values in column 3 are determined from the points of inflection of the load vs. web deflection curves.
3. Column 4 shows the approximate range of machine loads within which diagonal tension appeared in the web by observing the presence of axial compression in the stiffners.
4. Columns 5, 6 and 7 are computed by the formula $\tau_{cr} = k \frac{\pi^2 E}{12\left(1-\mu^2\right)} \left(\frac{t}{b}\right)^2$.

The k value used in case (b) was taken from Iguchi (2a) and the computation for case (c) has been made by using the interaction curve and computing the critical shear and bending stress under the boundary conditions of case (c).

UNIVERSITY OF MICHIGAN LIBRARY

In comparing the experimental result with the computed values, it may be observed that computation based on case (a) gave a closer approximation for the two end panels, case (b) was in good agreement with the results of panels 2, 3, 9, 10, and 11, and case (c) yielded closer values for panels 4 and 5.

Comparison of the Buckling Load and the Maximum Test Load.—It is of interest now to compare the buckling loads with the loads that caused failure. The load which caused signs of yielding in the web plate has been considered as the maximum test load of the panel. The relations, if any, that exist between the buckling load and the maximum test load of a panel are of interest. In order to show better the interrelation between the buckling loads, the maximum test loads, and the respective web deflections, the two sets of figures are tabulated under Tables 6 and 3, together with the necessary ratios for comparison.

TABLE 6.—COMPARISON BETWEEN BUCKLING LOADS AND MAXIMUM TEST LOADS OF WEB PANELS

Panel No. (1)	Aspect Ratio (2)	Buckling Loads (P_{cr}) kips (3)	Maximum Test Loads (P_{yp}) kips (4)	$\frac{P_{cr}}{P_{yp}}$, in percentage (5)	Reserve strength after buckling, in percentage (6)
1	0.935	130	450	28.9	71.1
2	0.744	260	480	54.2	45.8
3	0.744	260	500	52.0	48.0
4	0.632	280	490	57.2	42.8
5	0.640	280	520	53.8	46.2
9	0.944	360	640	56.2	43.8
10	0.935	350	640	54.7	45.2
11	0.935	320	620	51.7	48.3
12	0.935	260	620	42.0	58.0

Notes: 1. Loads shown are total applied load on girder.
2. The buckling loads are determined from the load-deflection curves of the webs.
3. Aspect ratio = $\frac{\text{clear width of the web}}{\text{clear depth of the web}}$.

1. The buckling loads vary as the $\frac{d}{t}$ ratio (clear depth to thickness) the aspect ratio and the location of the panel in the girder (that is end or inner panels). Dividing the panels into two groups according to the plate, it may be observed that the difference between the largest value for the buckling load (280 k) and the smallest value (130 k) in the first group (1/4-in. web) is 53.5%, and the difference in the second group (5/16-in. web) is 27.8%.

2. The maximum test loads vary mainly with the plate thickness and to a certain extent with the aspect ratio. Comparing the highest and the lowest maximum test loads in the same manner as in 1, a difference of 13.5% for the first

group, and 3.1% for the second group is revealed. The difference in the maximum test load apparently is very small when the plate thicknesses and aspect ratios of the panels are the same.

3. Due to the redistribution of stresses in the web plate as a result of adding the stiffeners in the adjacent panel, the maximum test loads of the panels in the first group might not represent the true picture. Therefore, no comparisons between the buckling loads and the maximum test loads were made on the basis of the results in the first group. Taking the second group for comparison, it was found that while the plate thicknesses and aspect ratios were the same for the four panels, the maximum test loads were almost the same but the buckling loads differed by as much as 27.8%.

4. Comparing the buckling loads with the maximum test loads revealed that for panel 1, the ratio of the buckling load to the maximum test load was 28.9%; that is, the plate still had a reserved strength of 72.1% after it buckled, and for panel 12, the ratio was 42%, or the reserve strength was 58%, and for all other panels the reserve strengths after buckling were approximately 50%. This shows that buckling of a web panel does not mean immediate failure. If the design were to be based on the requirement that buckling of the web plate should not take place under the working load, and a certain factor of safety were added, at least 50% of the reserve strength of the plate would be wasted.

5. As shown in the preceding analysis, the buckling load only serves to indicate that the load-carrying behavior of the web is changing from one pattern to another. It is doubtful whether the buckling load may be used as a measure of the load-carrying capacity of a panel. It has been shown that extensive yielding of the web does not take place either at the buckling load or immediately afterwards.

Flange Stresses.—The flange strains measured during the testing of this girder showed good agreement with the theoretical values based on the gross moment of inertia, except in the vicinity of the ends of the cover plates. It should not be concluded, however, that the gross moment of inertia should be used to compute the design stresses for a riveted plate girder, since the average stress across the net section of the flange will be higher than that measured by the strain gages. Yielding across the net section of the tension flange begins before the design load is ever reached, and spreads across the flange as the load increases. Noting, from Table 1, that the yield stress of the cover plates was 39.4 ksi, the AASHO design procedure implies that yielding across the net section of the tension flange should have occurred at $\frac{39.4}{18} = 2.19$ times the design load, whereas yielding was detected at the center of the outside cover plate at 1.93 times the design load. However, yielding did not occur across the net section of the outstanding leg of the flange angles at 2.13 times the design load (maximum test load).

No particular change in the location of the neutral axis or in the behavior of the compression flange was apparent after yielding across the outside cover plate of the tension flange was observed. Yielding, as indicated by cracking of the "white-wash," was observed near the rivets in the center section of the compression flange at about the same load as yielding was measured across the tension flange.

The examination of the rivets in this girder revealed that the clearance between the rivet and the hole varied considerably, but only in rare cases could it be said that there was no clearance between the rivet and the hole. In view of these observations, it is evident that before a rivet could be loaded in direct shear and bearing (as is generally assumed) some slipping of the adjoining parts must take place. Before the adjoining surfaces slip far enough to take up the clearance in the holes, the frictional resistance between the surfaces must be overcome and the rivet must undergo considerable bending distortion. (Bending of the rivet must take place since the rivet is apparently tight in the hole, just under the head) (43).

The transfer of stress by the rivets in a plate girder is similar to the transfer of stress in a very long riveted joint, inasmuch as slipping between the connected parts results only through a difference in strain between the adjoining surfaces. If there is no difference in strain between adjoining surfaces then the stresses in a built-up girder should be no different from those in a solid beam. Furthermore, if there is no relative sliding between the connected parts of a plate girder, and load transferred by the rivets must be by means of friction alone. The strains measured during the testing of this girder agreed very well with those computed by the flexure formula, and it will be shown that the relative slip measured at the ends of the cover plates can be attributed to the difference in strain in the first few feet at the end of the cover plate. Because the deflections also agreed with those computed for a solid beam, it can be concluded that the action of this riveted plate girder is not different from a solid beam, except locally at the ends of the cover plates. It also follows that the load transferred by the rivets is mainly through friction between the connected surfaces only, except at the ends of the cover plates.

At the ends of the cover plates the stresses are not so simply distributed as in the remainder of this girder. Before any cover plate may act integrally with the rest of the flange, the strain in it must reach the value of the strain in the rest of the flange. The strain in the outer cover plate builds from zero to some steady state value, while the strain in the balance of the flange decreases to some new steady state value. This difference in strain between the connected surfaces results in a relative slipping of the surfaces, which accumulates at the end of the cover plate. It is this co-called slip that was measured during the testing of the girder and is shown in Fig. 10. When this slip is small, the stress transferred to the outer cover plate will be a result of friction between the sliding surfaces, but when the slip is large enough to absorb the clearance between the rivets and the rivet holes, the load will be transferred by the rivets acting in shear and bearing. The load on the rivets will depend on the clearance in the holes, but those rivets closest to the end of the cover plates will suffer the greatest distortions. Extending the cover plates any reasonable distance beyond their theoretical cutoff points will not avoid overstressing of these end rivets. The load on the end rivets will be reduced most effectively by decreasing the spacing of the rivets at the ends of the cover plates.

Cover Plate Slip.—The distribution of strain in a highly idealized manner may be assumed in the outer cover plate to build up linearly at a rate proportional to the shear resistance that can be developed between the cover plate and the adjoining flange. If the transfer of load to the outer cover plate was only through the medium of friction, the strain distribution would be very similar to that ideal one. Assuming such a distribution exists, and using the equivalent average rivet shear stress at first determined by the strain gage readings, an expression for the slip may be evaluated at the point that corresponds with Fig. 10. The expression for this girder reduces to

$$\Delta = P^2 \times 2.2 \times 10^{-8}\text{in.}$$

in which Δ is the slip at the end of cover plate, and P denotes the load on girder in kips. This result has been plotted on Fig. 10. The theoretical slip is of the same magnitude as that measured, and follows the same general shape of curve.

The slip measured can therefore be attributed to the strain distribution at the ends of the cover plate, and it can be concluded that, in this immediate vicinity only, relative sliding between the component parts of the girder takes place.

Effect of the Thin Web on Flange Stresses.—The results of this test clearly indicate that the flange stresses in the buckled web framework cannot accurately be computed by the flexure formula. Fig. 7 seems to suggest that the load-strain relationship is still linear after buckling. This same observation was made in four other panels of the girder. The apparent additional increase in total flange load after buckling is also shown, and seems to be about 40% of the shear increment. It has been assumed that the surface strains measured on the top of the flange are representative of the average strain in the flange, but of course this assumption could be in error if the buckled web induces secondary bending stresses in the flange.

This redistribution of flange stress at the buckling load of the web follows the same pattern as was predicted and observed in connection with the investigation of the bending of thin-walled box beams (28).

CONCLUSIONS

Any conclusions drawn from this experiment must, of course, be made with certain reservations since it is not possible to assess all the variables involved on the basis of a single experiment.

1. The buckling behavior of the web of a plate girder is different from the theoretical behavior of a flat plate in the following ways: (a). Due to unavoidable initial curvature in the plate, the web starts to deflect laterally as soon as it is loaded; (b). The laterial deflection of the web does not become disproportionately large when it is loaded beyond its theoretical buckling load; (c). In the range of slenderness tested the web remains elastic and acquires no residual deflection under loads higher than the theoretical buckling load, unless the maximum test load is approached.
2. When using the theoretical buckling formula for an initially straight plate, in order to approximate the load at which diagonal tension action develops in the web, reasonably close results can be obtained if appropriate assumptions are made for the supporting and loading conditions.
3. The web of a plate girder is capable of carrying loads far in excess of its theoretical buckling load. In this experiment, the maximum test loads that caused local yielding in the web panels were from 1.75 to 3.45 times their respective buckling loads.
4. Local yielding in both the 1/4-in. web and the 5/16-in. web of this plate girder started as the maximum test load was approached, and occurred in advance of the localized yielding of the flanges.
5. After considering the theoretical buckling loads and the maximum test loads of the various panels of the plate girder, it is evident that the slenderness of the web is not a good criterion for the design of the web thickness.

6. The vertical deflection of a riveted plate girder could be accurately computed using the gross moment of inertia.

7. The neutral axis of a riveted plate girder remained very close to the center of gravity of the gross cross section for all loads.

8. Except locally, at the ends of the cover plates and across sections containing rivets, the flange stresses in a riveted plate girder can be accurately computed by the flexure formula by using the gross moment of inertia.

9. The transfer of horizontal shear stresses in this riveted plate girder was mainly accomplished through frictional resistance between the adjoining surfaces.

10. Extending the cover plates far enough past their theoretical cutoff point to develop the initial forces coming into them will insure that for all static loads the outer cover plate acts integrally with the rest of the flange at the theoretical cutoff point.

ACKNOWLEDGMENTS

This project was financed partially with Highway Planning Survey funds, the State Highway Department of Washington and The Engineering Experiment Station, University of Washington, in the Structural Engineering Laboratory of the Department of Civil Engineering, University of Washington.

APPENDIX.—BIBLIOGRAPHY

1. "Theory of Elastic Stability," by S. Timoshenko, McGraw Hill Book Co., Inc., New York, 1936.
2. "Buckling Strength of Metal Structures," by F. Bleich, McGraw Hill Book Co., Inc., New York, 1952, (a) p. 396.
3. "Handbook of Structural Stability," by G. Gerard and H. Becker, CNAC TN 3781-3784, July, 1957.
4. "A Summary of Diagonal Tension," by P. Kuhn, J. P. Peterson, and L. R. Levin, Part I, Methods of Analysis, CNAC TN 2661, May, 1952.
5. "A Summary of Diagonal Tension," by P. Kuhn, J. P. Peterson, and L. R. Levin, Part II, Experimental Evidence, CNAC TN 2662, May, 1952.
6. "Strength Analysis of Stiffened Beam Webs," by P. Kuhn and J. P. Peterson, NACA TN 1364, 1947.
7. "Investigations on the Incompletely Developed Plane Diagonal Tension Field," by P. Kuhn, NACA Rep. 697, 1940.
8. "The Strength of Plane Web Systems in Incomplete Diagonal Tension," by P. Kuhn and P. T. Chiarito, NACA ARR, August, 1942.
9. "Stability of the Webs of Plate Girders," by S. Timoshenko, Engineering, Vol. 138, 1935, p. 207.

10. "Investigation of the Behavior of Riveted Plate Girder," by S. Mackey and D. M. Brotton, Structural Engineer, Vol. 30, No. 4, April, 1952, p. 73.

11. "Discussion on Investigation of Behavior of Riveted Plate Girder," by S. Mackey and D. M. Brotton, Structural Engineer, Vol. 30, No., 11, November, 1952, p. 273.

12. "An Investigation of the Stress Distribution in a Welded Plate Girder for the Margam Plant," by S. Mackey and D. M. Brotton, Structural Engineer, Vol. 28, No. 2, February, 1950.

13. Discussion of "An Investigation of the Stress Distribution in a Welded Plate Girder for the Margam Plant," by S. Mackey and D. M. Brotton, Structural Engineer, Vol. 29, No. 2, February, 1951.

14. "Stability Problems Associated with the Design of Plate Girder Webs," by K. C. Rockey, Civil Engineering and Public Works Review, Vol. 47, Nos. 556-8 and Vol. 48, No. 559, London, 1953.

15. "Plate Girder Design: Flange Stiffness and Web Plate Behavior," by K. C. Rockey, Engineering, Vol. 184, 1957, p. 788.

16. "The Behavior of Web Plates of Plate Girders Subjected to Pure Bending," by K. C. Rockey and F. Jenkins, Structural Engineer, Vol. 35, No. 5, May, 1957.

17. "The Strength of I-Beams in Flexure," by H. Moore, Bulletin 68, Engrg. Experiment Sta., Univ. of Illinois, Urbana, Ill., 1913.

18. "The Strength of I-Beams and Girders," by H. Moore and W. M. Wilson, Bul. 86, Engrg. Experiment Sta., Univ. of Illinois, Urbana, Ill., 1916.

19. "The Basis for Design of Beams and Plate Girders," by O. A., Kerensky, A. R. Flint, and W. C. Brown, Revised British Standard 153, Structural Paper No. 48, Proceedings, I.C.E., 1956.

20. "Experimental Verification of the Strength of Plate Girders Designed in Accordance with the Revised British Standard 153: Tests on Full Size and on Model Plate Girders," by E. Longbottom and J. Heyman, Structural Paper, Proceedings, I.C.E., 1956.

21. "On the Analysis of Experimental Observations in Problems of Elastic Stability," by R. V. Southwell, Proceedings, Royal Soc. of London, Series A-135, 1932.

22. "Notes on the Southwell Method for Estimating Critical Load," by H. L. Cox, Aeronautical Research Council, R. and M., No. 2696, February, 1947.

23. "Buckling Stresses of Clamped Rectangular Flat Plates in Shear," by Budiansky and Connor, NACA TN 1559, May, 1948.

24. "Investigation of Web Buckling in Steel Beams," by Lyse Inge and H. J. Godfrey, Transactions, ASCE, Vol. 100, 1935, p. 675.

25. "Buckling Experiments on Girder with Stiffened Web," by C. Massonnet, Internatl. Assn. for Bridge and Structural Engrg., Vol. 14, 1954.

26. "Standard Specification for Highway Bridges," Amer. Assn. of State Highway Officials, Sixth Edition, 1953.

27. "Specifications for Steel Railway Bridges for Spans not Exceeding 400 Feet in Length,"Amer. Railway Engrg. Assn., 1956.

28. "Thin Walled Box Beams Under Pure Bending," by D. D. Vasarhelyi and R. O. Knudson, Internatl. Assn. for Bridge and Structural Engrg., Vol. 15, 1955.

29. "Neutral Axis and Centre of Gravity Do Not Coincide," by E. K. Timbey, Civil Engineering, Vol. 8, p. 270, April, 1938.

30. "Effective Moment of Inertia of a Riveted Plate Girder," by S. B. Lilly and S. T. Carpenter, Proceedings, ASCE, Vol. 65, October, 1939, pp. 1407-21.

31. "An Investigation of Plate Girder Web Splices," by J. M. Garrelts and I. E. Madsen, Transactions, ASCE, Vol. 107, p. 1303, 1942.

32. "Behavior of Riveted Connections in Truss-Type Members," by E. Chesson and W. H. Munse, Univ. of Illinois Structural Research Series No. 115, January, 1956.

33. Design of Plate Girders, by L. E. Moore, McGraw-Hill Book Co., Inc., New York, 1913.

34. Design of Steel Structures, by E. H. Gaylord and C. N. Gaylord, McGraw-Hill Book Co., Inc., New York, 1957.

35. "Frictional Resistance of Riveted Joints," by R. Fleming, Engineering News-Record, Vol. 84, June 3, 1920, pp. 1104-1107.

36. "Work of Rivets in Riveted Joints," by A. Hrennikoff, Transactions, ASCE, Vol. 99, 1934, p. 437.

37. "Riveted Joints," by A. E. Richard deJonge, ASME, Research Publication, 1945.

38. "Observations on the Behavior of Aluminum Alloy Test Girders," by R. L. Moore, Transactions, ASCE, Vol. 112, 1947, p. 901.

39. "An Investigation of Stiffeners on Shear-Resistant Plate-Girder Webs," by R. L. Moore, NACA Tech. Note 862, September, 1942.

40. "Buckling of Webs in Deep Steel I Girders," by G. A. Bergman and G. Westlund, Inst. of Structural Engrg. and Bridge Bldg., Royal Inst. of Tech., Stockholm, January, 1947.

41. "Behavior of Buckled Rectangular Plates under the Action of Shearing Forces," by G. A. Bergman, Royal Inst. of Tech., Stockholm, January, 1948.

42. "A Photographic Method for Determining the Deflected Shapes of Buckled Plates," by Ch. Y. Yuan and D. D. Vasarhelyi, The Trend, Vol. 12, January, 1960, p. 13.

43. "A Study of the Behavior of Rivets," by N. C. Vasishth, The Trend, Vol. 12, October, 1960, p. 11.

AMERICAN SOCIETY OF CIVIL ENGINEERS
Founded November 5, 1852
TRANSACTIONS

Paper No. 3209

MATRIX FORMULATION OF FOLDED PLATE EQUATIONS

By A. C. Scordelis,[1] M. ASCE

SYNOPSIS

An analytical procedure, utilizing matrix algebra, is developed for determining longitudinal stresses, transverse moments, and vertical deflections in folded plate structures. The procedure provides an efficient and systematic method for analyzing structures of this type. The sequence of matrix operations can be readily programmed for a digital computer having available matrix subroutines. A sequence which has been programmed for the IBM 704 digital computer is described.

INTRODUCTION

Folded plate structures have gained increasing use and popularity in the United States during the past decade. They have proved to be especially economical in the construction of long span roof systems. These roofs have generally been made of reinforced concrete, but in some cases timber combined with plywood sheathing has been used. Folded plates have also been used for bins, silos, staircases, and floor systems. A description of a number of applications of folded plates in this country together with information on the economics of this type of construction has been given by Whitney, Anderson, and Birnbaum.[2]

Methods for analyzing folded plate structures were first developed in Germany in 1930 by Ehlers[3] and Craemer.[4] Since that time there have been

---

Note.—Published essentially as printed here, in October, 1960, in the Journal of the Structural Division, as Proceeding Paper 2617. Positions and titles given are those in effect when the paper or discussion was approved for publication in Transactions.

[1] Assoc. Prof., Civ. Engrg., Univ. of California, Berkeley, Calif.

[2] "Reinforced Concrete Folded Plate Construction," by C. S. Whitney, B. G. Anderson, and H. Birnbaum, Proceedings, ASCE, Vol. 85, No. ST8, October, 1959, p. 15.

[3] "Ein neues Konstruktionsprinzip," by G. Ehlers, Der Bauingenieur, Vol. 9, 1930, p. 125.

[4] "Theorie der Faltwerke," by H. Craemer, Beton und Eisen, Vol. 29, 1930, p. 276.

numerous papers written on the subject, but no attempt will be made to review them here. This has been done to some extent by Gaafar[5] and Traum.[6] Perhaps the most extensive treatment of the subject to date is contained in a recently published book by Yitzhaki.[7] The general approach followed in this paper will be similar to his.

In contrast to the numerous papers on the analysis of folded plates structures very little information has been published on the experimental verification of the theories being used. However, Gaafar[5] has reported results on an experimental study of an aluminum folded plate that indicated fair correlation with theory.

The determination of longitudinal stresses, transverse moments, and vertical deflections is of primary interest in the analysis of a folded plate structure. These quantities may be obtained through the development and solution of a series of linear algebraic equations which are conveniently expressed in matrix form. Since the amount of computational effort is relatively large for even a simple case, the analysis can be most effectively carried out with the aid of a digital computer for which the matrix formulation is especially suited.

Notation.—The letter symbols adopted for use in this paper are defined where they first appear, in the illustrations or in the text, and are arranged alphabetically, for convenience or reference, in Appendix II.

METHOD OF ANALYSIS

A prismatic folded plate structure (Fig. 1) consists of a series of mutually supporting plates that frame into supporting diaphragms. A load applied to the structure is first carried by transverse slab action to the longitudinal joints. The reactions at the joints then resolve into forces parallel to the plates and are carried by longitudinal plate action to the diaphragms, each plate acting as a longitudinal beam spanning between supports.

The analysis is based on the following simplifying assumptions:

1. The material is elastic, isotropic, and homogeneous.
2. The structure is completely monolithic.
3. Slab action is defined by the behavior of transverse one way slabs spanning between longitudinal joints.
4. Longitudinal stresses developed in each plate due to longitudinal plate action may be calculated by the elementary beam theory; therefore, the longitudinal stresses vary linearly over the depth of each plate.
5. Supporting diaphragms are infinitely stiff parallel to their own plane, but perfectly flexible normal to their own plane.

For purposes of discussion the folded plate structure may be thought to consist of two systems intimately connected, Fig. 2. The slab system consists of a series of one way slab strips spanning between longitudinal joints. These strips are capable of transmitting shears and moments in a transverse direction only. The slab system is supported elastically by the plate system, which

---

[5] "Hipped Plate Analysis Considering Joint Displacement," by I. Gaafar, Transactions, ASCE, Vol. 119, 1954, p. 743.

[6] "The Design of Folded Plates," by E. Traum, Proceedings, ASCE, Vol. 85, No. ST8, October, 1959, p. 103.

[7] "Prismatic and Cylindrical Shell Roofs," by D. Yitzhaki, Haifa Science Publishers, Haifa, Israel, 1958.

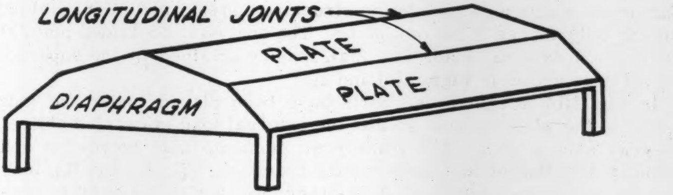
LONGITUDINAL JOINTS
PLATE
PLATE
DIAPHRAGM

FIG. 1.—FOLDED PLATE STRUCTURE

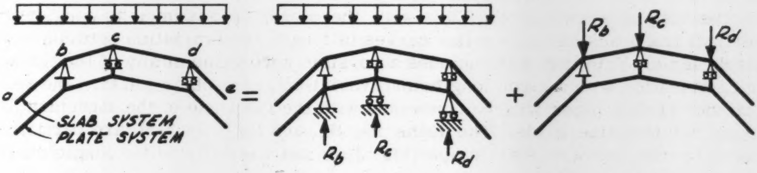
a
b
c
d
e
SLAB SYSTEM
PLATE SYSTEM
=
R_b
R_c
R_d
+
R_b
R_c
R_d

(a) (b) (c)

FIG. 2.—CONCEPT OF FOLDED PLATE STRUCTURE

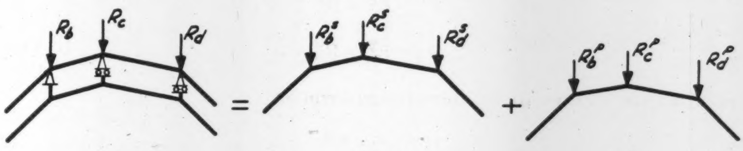
R_b
R_c
R_d
=
R_b^s
R_c^s
R_d^s
+
R_b^p
R_c^p
R_d^p

(a) (b) (c)

FIG. 3

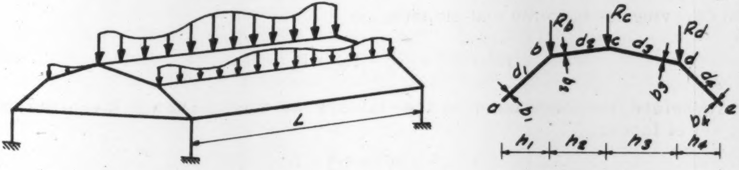
L
R_b
R_c
R_d
a
b
c
d
e
d_1
d_2
d_3
d_4
b_1
b_2
b_3
b_4
h_1
h_2
h_3
h_4

(a) (b)

FIG. 4

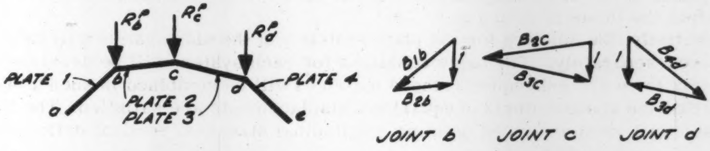
R_b^p
R_c^p
R_d^p
PLATE 1
PLATE 2
PLATE 3
PLATE 4
a
b
c
d
e
B_{1b}
B_{2b}
1
B_{2c}
B_{3c}
1
1
B_{4d}
B_{3d}
JOINT b
JOINT c
JOINT d

(a) (b)

FIG. 5

consists of a series of plates spanning longitudinally between diaphragms. The plate system acts as a membrane structure and each plate is capable of transmitting only forces in its own plane. The analysis of a folded plate structure for a given external load, Fig. 2(a), may be obtained by the superposition of the loadings shown in Figs. 2(b) and 2(c).

In Fig. 2(b) imaginary supports have been placed under the longitudinal joints of the plate system so that the external load is carried entirely by the one-way slab system. The transverse moments may be readily obtained by moment distribution and the resulting reactions, R_b, R_c, and R_d, may then be found by equations of statics. This procedure may be followed in cases where the distributed external loads in each transverse span, shown in Fig. 2(b), have similar curves of longitudinal variation between end diaphragms. Where this is not true each transverse span loading must be treated independently.

The loading shown in Fig. 2(c) will, therefore, be assumed to consist of vertical line loads having similar curves of longitudinal variation between end diaphragms. Note that this includes a possible zero value at any of the joints in combination with a given longitudinal variation at the other joints. The remainder of this paper will be concerned with the response of the structure to these vertical line loads. The loads R_b, R_c, and R_d (Fig. 3(a)) are partially taken by the one-way slab strips (Fig. 3(b)) and partially by the longitudinal plate system (Fig. 3(c)), such that

$$R_b = R_b^s + R_b^p \quad \text{(1a)}$$

$$R_c = R_c^s + R_c^p \quad \text{(1b)}$$

$$R_d = R_d^s + R_d^p \quad \text{(1c)}$$

Eqs. 1 may be written, in an abbreviated form as

$$\underline{R} = \underline{R^s} + \underline{R^p} \quad \text{(2)}$$

in which the underlining indicates that the symbol represents a matrix.

The sum of the loads taken by the plate system must equal the sum of the loads applied to the combined system, since the plate system is the only system carrying loads to the end diaphragms.

$$R_b^p + R_c^p + R_d^p = R_b + R_c + R_d \quad \text{(3)}$$

Therefore, the loads taken by the slab system must form a self equilibrating set of forces.

$$R_b^s + R_c^s + R_d^s = 0 \quad \text{(4)}$$

The division of the total load between slab and plate system must be such as to produce the same displacement in the slab system and the plate system at each of the joints b, c, and d.

Initially, the solution for the plate system and the slab system will each be treated separately. The basic equations for each system will be developed in matrix form and subsequently these matrices will be combined in such a manner that the above criteria of equal joint displacements are satisfied. The final result will yield matrices defining longitudinal stresses, vertical deflections, and transverse moments due to any combination of vertical line loads applied to the combined system.

As a typical case the structure shown in Fig. 4, which has a simple span L, will be considered. The structure has four plates, each of different thicknesses b, depths d, and horizontal transverse spans h. Edges a and e are free and the interior joints b, c, and d are subjected to vertical loads having different intensities R_b, R_c, and R_d at a given distance from one of the end diaphragms. All three loads have similar curves of longitudinal variation. The vertical joint loads R and the vertical joint deflections δ will be considered positive when they are in a downward direction.

PLATE SYSTEM

If the plates shown in Fig. 4 are assumed to have zero flexural stiffness normal to their own planes, the entire load will be carried by membrane action. The load intensities, R^p, at a given distance from the support, which are carried in this manner are shown in Fig. 5(a).

Longitudinal Stresses.—In this section a matrix will be developed defining the longitudinal stress σ at each plate edge produced by a given set of R^p loads. This matrix will be designated as the stress matrix $\underline{S_p}$ for the plate system.

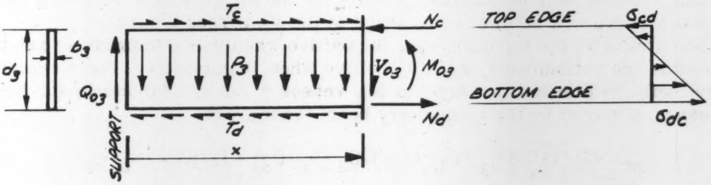

FIG. 6.—FREE BODY DIAGRAM OF A TYPICAL PLATE

The R^p loads can be resolved into plate loads P, which are loads parallel to each plate. This may be done with the aid of force triangles for unit vertical loads such as shown in Fig. 5(b). A force transformation matrix $\underline{B}$ may then be written defining the plate loads in terms of the vertical joint loads. Detailed makeup of this matrix, as well as others developed subsequently, is given in the example in the appendix.

$$\underline{p} = \underline{B}\,\underline{R^p} \quad \dots\dots\dots\dots\dots\dots\dots \quad (5)$$

Plate loads in the direction a - b - c - d - e are considered positive, and the sign of each element in the $\underline{B}$ matrix should be taken accordingly.

A free body diagram of a portion of a typical plate (plate 3 in this case) is shown in Fig. 6 with all quantities indicated acting in a positive direction. Top and bottom edges of each plate are established by going successively in the direction a - b - c - d - e.

T_c and T_d are longitudinal shears per unit length on the top and bottom edges. N_c and N_d are forces normal to the cut section that are defined by

$$N_c = \int_o^x T_c \, dx \quad \ldots\ldots\ldots\ldots\ldots\ldots (6a)$$

$$N_d = \int_o^x T_d \, dx \quad \ldots\ldots\ldots\ldots\ldots\ldots (6b)$$

Q_{o3}, V_{o3}, and M_{o3} are the end reaction, shear, and bending moment assuming the plate spanning between diaphragms is subjected to the plate load P_3 alone. The term P_3 has the same longitudinal variation as R^p and the bending moment may be expressed as

$$M_{o3} = C_S \; P_3$$

in which C_S is a constant that is a function of span and load distribution. For M_{o3} at midspan of a simple span this constant has the following values: $C_S = L^2/8$ for a uniform load; $C_S = L^2/\pi^2$ for a first harmonic sine loading in which P_3 is the maximum load intensity; and $C_S = L/4$ if P_3 is a concentrated load at midspan.

For the given case of similar longitudinal variation of P in all plates the N versus x curve will be similar in shape to the M_o versus x curve and the T versus x curve will be similar in shape to the V_o versus x curve.

The stress at the top edge, σ_{cd}, is positive when it is compressive and the stress at the bottom edge, σ_{dc}, is positive when it is tensile. The σ versus x curve will be similar in shape to M_o versus x curve. Formulas for these stresses, obtained by the elementary beam theory, are

$$\sigma_{cd} = C_S \left[\left(6/bd^2\right)_3 \left(P_3\right) + (4/bd)_3 \left(N_c/C_S\right) + (2/bd)_3 \left(N_d/C_S\right) \right] \quad \ldots (8a)$$

$$\sigma_{dc} = C_S \left[\left(6/bd^2\right)_3 \left(P_3\right) + (2/bd)_3 \left(N_c/C_S\right) + (4/bd)_3 \left(N_d/C_S\right) \right] \quad \ldots (8b)$$

A similar set of equations may be written for each plate so that

$$\sigma = C_S \left[\underline{\sigma_o} + \underline{\sigma_N} \right] \quad \ldots\ldots\ldots\ldots\ldots\ldots (9a)$$

$$\sigma = C_S \left[\underline{S_o} \; \underline{P} + \underline{S_N} \; \underline{\left(N/C_S\right)} \right] \quad \ldots\ldots\ldots\ldots (9b)$$

in which $\underline{S_o}$ and $\underline{S_N}$ are matrices that are functions of the width b and depth d of each plate. Using the relationship established in Eq. 5 between the plate loads and the vertical joint loads, Eq. 9 may be written as

$$\sigma = C_S \left[\underline{S_o} \; \underline{B} \; \underline{\left(R^p\right)} + \underline{S_N} \; \underline{\left(N/C_S\right)} \right] \quad \ldots\ldots\ldots\ldots (10)$$

The only unknown quantities on the right hand side of this expression are the $\left(N/C_S\right)$ values at each interior joint of the plate system. These may be found by noting that the algebraic sum of the stresses at each interior joint must equal zero to satisfy the condition of compatibility of longitudinal strains

$$\underline{\Sigma\sigma} = \underline{D_o} \; \underline{R^p} + \underline{D_N} \; \underline{\left(N/C_S\right)} = 0 \quad \ldots\ldots\ldots\ldots (11)$$

in which $\underline{D_o}$ and $\underline{D_N}$ are obtained by adding the proper rows of the $\underline{S_N}$ and $\underline{S_o\ B}$ matrices in Eq. 10 or by pre-multiplying the latter matrices by a matrix designated as an ADRO matrix. For example for the case shown in Fig. 5(a) there are four plates and three interior joints so that

$$\underline{\text{ADRO}} = \begin{bmatrix} 0 & 1 & 1 & 0 & 0 & 0 & 0 & 0 \\ 0 & 0 & 0 & 1 & 1 & 0 & 0 & 0 \\ 0 & 0 & 0 & 0 & 0 & 1 & 1 & 0 \end{bmatrix} \quad \ldots\ldots (12)$$

Eq. 11 may be solved for $\underline{N/C_S}$ and the result substituted back into Eq. 10 to obtain a final relationship between longitudinal stresses at the plate edges and external vertical joint loads.

$$\underline{N/C_S} = -\,\underline{D_N^{-1}}\ \underline{D_o}\ \underline{R^p} \quad \ldots\ldots\ldots\ldots\ldots (13a)$$

$$\underline{\sigma} = C_S\left[\underline{S_o}\ \underline{B} - \underline{S_N}\ \underline{D_N^{-1}}\ \underline{D_o}\right]\underline{R^p} \quad \ldots\ldots\ldots\ldots (13b)$$

or letting

$$\underline{S_p} = \left[\underline{S_o}\ \underline{B} - \underline{S_N}\ \underline{D_N^{-1}}\ \underline{D_o}\right] \quad \ldots\ldots\ldots\ldots\ldots (14)$$

$$\boxed{\underline{\sigma} = C_S\ \underline{S_p}\ \underline{R^p}} \quad \ldots\ldots\ldots\ldots\ldots\ldots (15)$$

$\underline{S_p}$ is the stress matrix for the plate system and is a function of only the dimensions and geometry of the folded plate structure cross-section.

Vertical Joint Deflections.—In this section a matrix will be developed defining the vertical deflection δ at each interior joint produced by a given set of R^p loads. This matrix will be designated as the flexibility matrix, F_p, for the plate system. The inverse of this matrix will be designated as the stiffness matrix $\underline{K_p}$ for the plate system. $\underline{K_p}$ defines the vertical load R^p at each interior joint produced by a given set of vertical joint deflections δ.

The vertical deflection δ at any interior joint can be expressed in terms of the plate displacements v of the two plates adjoining the joint. The latter displacements are parallel to the plates and will be considered positive when in the direction a - b - c - d - e. Using a Williot diagram, Fig. 7(a) depicts the real displacement, cc', at a typical joint that results from plate displacements v_2 and v_3. Fig. 7(b) indicates a free body diagram of joint c subjected to a virtual force system in which B_{2c} and B_{3c} are forces parallel to plates 2 and 3 respectively and are equal to similarly designated quantities in the force transformation matrix $\underline{B}$ of Eq. 5. All quantities shown in Fig. 7(a) and 7(b) are acting in a positive direction.

Applying the real displacements in Fig. 7(a) to the virtual forces on joint c in Fig. 7(b) the total virtual work must equal zero.

$$1 \times \delta_c - B_{2c}\,v_2 - B_{3c}\,v_3 = 0 \quad \ldots\ldots\ldots\ldots (16a)$$

$$\delta_c = B_{2c}\,v_2 + B_{3c}\,v_3 \quad \ldots\ldots\ldots\ldots\ldots (16b)$$

A similar expression may be written for each interior joint so that

$$\underline{\delta} = \underline{G}\ \underline{v} = \underline{B}^{T}\ \underline{v} \quad \ldots\ldots\ldots\ldots\ldots\ldots (17)$$

in which the displacement transformation matrix $\underline{G}$ is equal to the transpose of the force transformation matrix $\underline{B}$ of Eq. 5. Neglecting shear deformations a typical plate displacement v_3 (Fig. 8) at a given distance x from the support can be expressed as

$$v_3 = C_V \frac{M_p}{E\, I_p} \quad \ldots\ldots\ldots\ldots\ldots\ldots (18)$$

in which C_V is a constant that depends on the span and the distribution of angle

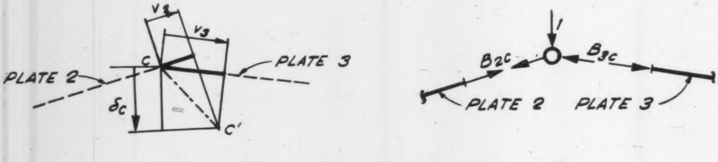
v2
v3
c
PLATE 3
PLATE 2
δc
c'
1
B2c
B3c
PLATE 2
PLATE 3

(a) (b)

FIG. 7

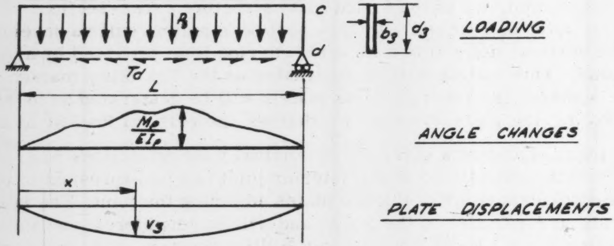
Tc
P3
c
d
Td
b3
d3
LOADING
L
Mp/EIp
ANGLE CHANGES
x
v3
PLATE DISPLACEMENTS

FIG. 8.—PLATE DISPLACEMENTS

changes and $M_p/E\, I_p$ is a specified angle change ordinate, usually the maximum ordinate.

From Fig. 6

$$M_p = M_{o3} + N_c \frac{d_3}{2} + N_d \frac{d_3}{2} \quad \ldots\ldots\ldots\ldots (19a)$$

$$M_p = C_S\, P_3 + N_c \frac{d_3}{2} + N_d \frac{d_3}{2} \quad \ldots\ldots\ldots\ldots (19b)$$

and

$$I_p = \frac{b_3\, d_3^3}{12} \quad \ldots\ldots\ldots\ldots\ldots\ldots (19c)$$

Substituting these values into Eq. 18

$$v_3 = C_D\left[(12/b\,d^3\,E)_3\,(P_3) + (6/b\,d^2\,E)_3\,(N_c/C_S) + (6/b\,d^2\,E)_3\,(N_c/C_S)\right] \ldots (20)$$

in which $C_D = C_V \cdot C_S$ is a deflection constant. For v_3 at midspan of a simple span: $C_D = 5\,L^4/384$ for a uniform load; $C_D = L^4/\pi^4$ for a first harmonic sine loading with P_3 being a midspan value; $C_D = L^3/48$ if P_3 is a concentrated load at midspan. An equation similar to Eq. 20 may be written for each plate so that

$$\underline{v} = C_D\left[\underline{v_o} + \underline{v_N}\right] \ldots\ldots\ldots\ldots (20a)$$

$$\underline{v} = C_D\left[\underline{F_o}\;\underline{P} + \underline{F_N}\;\;\underline{N/C_S}\right] \ldots\ldots\ldots (20b)$$

in which $\underline{F_o}$ and $\underline{F_N}$ are matrices that are functions of the width b, depth d, and modulus of elasticity E of each plate. Since $\underline{P}$ and $\underline{N/C_S}$ have already been expressed in terms of $\underline{R^p}$ by Eqs. 5 and 13 respectively, these substitutions may be made in Eq. 20 to yield

$$\underline{v} = C_D\left[\underline{F_o}\;\underline{B} - \underline{F_N}\;\underline{D_N^{-1}}\;\underline{D_o}\right]\underline{R^p} \;\ldots\ldots\ldots (21)$$

A final relationship between vertical joint deflections and loads taken by the plate system may now be written;

$$\underline{\delta} = \underline{G}\;\underline{v} = \underline{B^T}\;\underline{v} \text{ from (3.1)} \ldots\ldots\ldots (22a)$$

$$= C_D\;\underline{B^T}\left[\underline{F_o}\;\underline{B} - \underline{F_N}\;\underline{D_N^{-1}}\;\underline{D_o}\right]\underline{R^p} \ldots\ldots (22b)$$

or, letting

$$\underline{F_p} = \underline{B^T}\left[\underline{F_o}\;\underline{B} - \underline{F_N}\;\underline{D_N^{-1}}\;\underline{D_o}\right] \ldots\ldots\ldots (23)$$

$$\boxed{\underline{\delta} = C_D\;\underline{F_p}\;\underline{R^p}} \ldots\ldots\ldots\ldots (24a)$$

$$\boxed{\underline{R^p} = \underline{C_D^{-1}}\;\underline{K_p}\;\underline{\delta}} \ldots\ldots\ldots\ldots (24b)$$

in which $\underline{K_p} = \underline{F_p^{-1}}$. $\underline{F_p}$ and $\underline{K_p}$ are, respectively, the flexibility and stiffness matrices for the plate system and both are functions only of the dimensions and geometry of the folded plate structure cross section and the modulus of elasticity.

By substituting the value of $\underline{R^p}$ from Eq. 24 into Eq. 15 the longitudinal stresses at the plate edges σ may be expressed directly in terms of the vertical joint deflections δ.

$$\sigma = C_S\;C_D^{-1}\left[\underline{S_p}\;\underline{K_p}\right]\underline{\delta} \ldots\ldots\ldots\ldots (25)$$

SLAB SYSTEM

Fig. 9(a) shows a typical slab strip of unit width that has been taken from the slab system at a given distance from an end diaphragm. The slab strip is subjected to vertical joint loads, R^s, that form a self equilibrating system of forces. A given set of R^s loads and transverse moments m are associated with a given set of vertical joint deflections δ.

Transverse Moments.—In this section a matrix will be developed defining the transverse moment, m, at each plate edge produced by a given set of vertical joint deflections δ. This matrix will be designated as the moment matrix $\underline{S_s}$ for the slab system.

Fig. 9(b) shows a free body diagram of a typical span of the slab strip (span 3 in this case) with all quantities shown acting in a positive direction. The moment at each end of span 3 can be expressed by the slope-deflection equations as

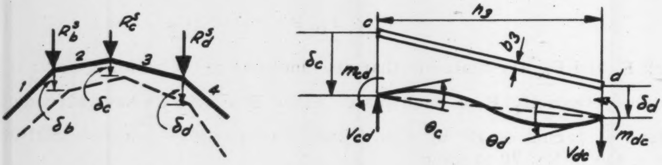

(a) (b)

FIG. 9

$$m_{cd} = 2\,E\,I_s/d\left[2\,\theta_c + \theta_d - 3\,\psi_{cd}\right]$$

$$= \left(b^3\,E/3\,d\right)_3\,\theta_c + \left(b^3\,E/6\,d\right)_3\,\theta_d$$

$$- \left(b^3\,E/2\,d\,h\right)_3\,\delta_c + \left(b^3\,E/2\,d\,h\right)_3\,\delta_d \;\ldots\ldots\; (26a)$$

$$m_{dc} = 2\,E\,I_s/d\left[\theta_c + 2\,\theta_d - 3\,\psi_{cd}\right]$$

$$= \left(b^3\,E/6\,d\right)_3\,\theta_c + \left(b^3\,E/3\,d\right)_3\,\theta_d$$

$$- \left(b^3\,E/2\,d\,h\right)_3\,\delta_c + \left(b^3\,E/2\,d\,h\right)_3\,\delta_d \;\ldots\ldots\; (26b)$$

in which $I_s = (1)\,b_3^3/12$, is the moment of inertia of a unit width of slab and $\psi_{cd} = \left(\delta_c - \delta_d\right)/h_3$, is the chord rotation. A pair of equations similar to Eqs. 26 may be written for each span so that

$$\underline{m} = \underline{m_\theta} + \underline{m_\delta} \;\ldots\ldots\ldots\ldots\ldots\ldots\; (27a)$$

$$m = \underline{K_\theta}\;\underline{\theta} + \underline{K_\delta}\;\underline{\delta} \;\ldots\ldots\ldots\ldots\ldots\; (27b)$$

The joint rotations θ may be found in terms of vertical joint deflections δ by noting that the algebraic sum of the moments at each interior joint must equal zero to satisfy equilibrium.

$$\underline{\Sigma m} = \underline{D_\theta}\;\underline{\theta} + \underline{D_\delta}\;\underline{\delta} = 0 \;\ldots\ldots\ldots\ldots\ldots\ldots\; (28)$$

in which D_θ and D_δ are obtained by adding the proper rows of the K_θ and K_δ matrices in Eq. 27, or by multiplying the latter matrices by the $\underline{ADRO}$ matrix of Eq. 12. Eq. 28 may be solved for θ and the result substituted back into Eq. 27 to obtain a final relationship between transverse moments at the plate edges and vertical joint deflections.

$$\underline{\theta} = - \underline{D_\theta^{-1}} \; \underline{D_\delta} \; \underline{\delta} \tag{29a}$$

$$\underline{m} = \left[\underline{K_\delta} - \underline{K_\theta} \; \underline{D_\theta^{-1}} \; \underline{D_\delta}\right] \underline{\delta} \tag{29b}$$

or, letting

$$S_s = \left[\underline{K_\delta} - \underline{K_\theta} \; \underline{D_\theta^{-1}} \; \underline{D_\delta}\right] \tag{30}$$

$$\boxed{\underline{m} = \underline{S_s} \; \underline{\delta}} \tag{31}$$

$\underline{S_s}$ is the moment matrix for the slab system and it is a function only of the geometry and dimensions of the folded plate structure cross section and the modulus of elasticity.

Vertical Joint Loads Taken by Slab System.—The vertical joint load R^s at each joint can be computed in terms of transverse slab moments, m, at each plate edge using equations of statics. For example, in Fig. 9(a)

$$R_c^s = \left(\frac{m_{bc} + m_{cb}}{h_2}\right) - \left(\frac{m_{cd} + m_{dc}}{h_3}\right) \tag{32}$$

One equation, similar to Eq. 32 may be written for each interior joint so that

$$\underline{R^s} = \underline{H} \; \underline{m} \tag{33}$$

The $\underline{H}$ matrix is a function of the horizontal spans h of the transverse slab system. Substituting the value of $\underline{m}$ in Eq. 31 into Eq. 33 a final relationship between vertical joint deflections and loads taken by the slab system may be obtained.

$$\underline{R^s} = \underline{H} \; \underline{S_s} \; \underline{\delta} \tag{34}$$

or letting

$$\underline{K_s} = \underline{H} \; \underline{S_s} \tag{35}$$

$$\boxed{\underline{R^s} = \underline{K_s} \; \underline{\delta}} \tag{36}$$

$\underline{K_s}$ is the stiffness matrix for the slab system. While a single vertical joint deflection will produce a set of R^s loads in equilibrium, a set of vertical joint deflections cannot exist for a single R^s joint load since the slab strip would not be in equilibrium. Thus the $\underline{K_s}$ matrix cannot be inverted.

COMBINED PLATE AND SLAB SYSTEM; HARMONIC LOADING

One approach to the analysis of the combined plate and slab system, represented in Fig. 4, is to replace the given longitudinal distribution of the vertical joint loads, R, by the superposition of harmonic loadings obtained from a

Fourier series representation of the actual loading. A harmonic loading has the property that it produces R versus x, R^p versus x, v versus x, σ versus x, R^s versus x, m versus x, and δ versus x curves of the same shape. For example, the first harmonic is a single sine wave. Each harmonic is analyzed in a similar manner, and, therefore, only the first harmonic will be considered in the following discussion.

Recalling Eq. 2 and the requirement that the plate system and the slab system must have the same vertical joint deflections, the following relationship may be written for the combined system. From Eq. 2

$$\underline{R} = \left[\underline{K_s} + C_D^{-1}\ \underline{K_p}\right] \underline{\delta} \ \ldots\ldots\ldots\ldots\ldots\ldots \tag{37}$$

in which values for R^s and R^p are obtained from Eqs. 36 and 24b, respectively.

Letting

$$\underline{K} = \left[\underline{K_s} + C_D^{-1}\ \underline{K_p}\right] \ \ldots\ldots\ldots\ldots\ldots\ldots \tag{38}$$

$$\boxed{\begin{array}{c} \underline{R} = \underline{K}\ \underline{\delta} \quad \ldots\ldots\ldots\ldots\ldots\ldots (39) \\ \\ \underline{\delta} = \underline{F}\ \underline{R} \quad \ldots\ldots\ldots\ldots\ldots\ldots (40) \end{array}}$$

in which $\underline{F} = \underline{K^{-1}}$. $\underline{K}$ and $\underline{F}$ are, respectively, the stiffness and flexibility matrices for the combined system under a harmonic loading. For a first harmonic $C_D^{-1} = \pi^4/L^4$ and R and δ are the maximum ordinates of sine curves.

Thus, to analyze the folded plate structure in Fig. 4 for any set of harmonic vertical joint loads $\underline{R}$, Eq. 40 is used to compute the vertical joint deflections $\underline{\delta}$ and then Eqs. 25 and 31 are used to compute longitudinal plate stresses, $\underline{\sigma}$, and transverse slab moments, $\underline{m}$. The quantities found are maximum ordinates of the particular harmonic curve.

Sequence of Matrix Operations for Harmonic Loading.—The entire sequence of matrix operations can be readily programmed for a digital computer. In a general case a folded plate structure will have n plates, j interior joints, and will be subjected to q different combinations of vertical joint loads. To recapitulate, the steps required for a first harmonic loading on a simple span are listed below with appropriate remarks. Detailed makeup of the input matrices is illustrated in the example given in Appendix I.

Step	Matrix Description	Matrix Size	Remarks
1	$[B]$	nxj	Input
2	$[S_N]$	2nxj	Input
3	$[S_o]$	2nxn	Input
4	$[ADRO]$	jx2n	Input
5	$[F_N]$	nxj	Input
6	$[F_o]$	nxn	Input
7	$[K_\theta]$	2nxj	Input

8	$\left[K_\delta\right]$	2nxj	Input
9	$[H]$	jx2n	Input
10	C_{SH}	Constant	Input = L^2/π^2 for first harmonic
11	C_{DH}	Constant	Input = L^4/π^4 for first harmonic
12	$[R]$	jxq	End of input = joint loading
13	$\left[S_oB\right] = \left[S_o\right]\,[B]$	2nxj	
14	$\left[D_N\right] = [ADRO]\left[S_N\right]$	jxj	
15	$\left[D_o\right] = [ADRO]\left[S_oB\right]$	jxj	
16	$\left[D_N^{-1}\right] = \left[D_N\right]^{-1}$	jxj	
17	$\left[D_N^{-1}D_o\right] = \left[D_N^{-1}\right]\left[D_o\right]$	jxj	
18	$\left[S_ND_N^{-1}\,D_o\right] = \left[S_N\right]\left[D_N^{-1}\,D_o\right]$	2nxj	
19	$\left[S_p\right] = \left[S_oB\right] - \left[S_ND_N^{-1}\,D_o\right]$	2nxj	Output - stress matrix, plate system
20	$\left[F_oB\right] = \left[F_o\right]\,[B]$	nxj	
21	$\left[F_ND_N^{-1}\,D_o\right] = \left[F_N\right]\left[D_N^{-1}\,D_o\right]$	nxj	
22	$\left[F_oB - F_ND_N^{-1}\,D_o\right] = \left[F_oB\right] - \left[F_ND_N^{-1}\,D_o\right]$	nxj	
23	$[G] = [B]^T$	jxn	G = transpose of B
24	$\left[F_p\right] = [G]\left[F_oB - F_ND_N^{-1}\,D_o\right]$	jxj	Output - flexibility matrix, plate system
25	$\left[K_p\right] = \left[F_p\right]^{-1}$	jxj	Output - stiffness matrix, plate system
26	$\left[D_\theta\right] = [ADRO]\left[K_\theta\right]$	jxj	
27	$\left[D_\delta\right] = [ADRO]\left[K_\delta\right]$	jxj	
28	$\left[D_\theta^{-1}\right] = \left[D_\theta\right]^{-1}$	jxj	
29	$\left[D_\theta^{-1}\,D_\delta\right] = \left[D_\theta^{-1}\right]\left[D_\delta\right]$	jxj	
30	$\left[K_\theta D_\theta^{-1} D_\delta\right] = \left[K_\theta \quad \left[D_\theta^{-1}\,D_\delta\right]\right.$	2nxj	
31	$\left[S_s\right] = \left[K_\delta\right] - \left[K_\theta D_\theta^{-1}\,D_\delta\right]$	2nxj	Output - moment matrix, slab system

32	$\left[K_s\right] = [H]\left[S_s\right]$	jxj	Output - stiffness matrix, slab system
33	$\left[C_{DH}^{-1} K_p\right] = C_{DH}^{-1}\left[K_p\right]$	jxj	
34	$[K] = \left[C_{DH}^{-1}K_p\right] + \left[K_s\right]$	jxj	Output - stiffness matrix, combined system
35	$[F] = [K]^{-1}$	jxj	Output - flexibility matrix, combined system
36	$[\delta] = [F][R]$	jxq	Output - midspan joint deflections
37	$[m] = \left[S_s\right][\delta]$	2nxq	Output - midspan transverse moments
38	$\left[C_{SH}S_p\right] = C_{SH}\left[S_p\right]$	2nxj	
39	$\left[C_{SH}S_pC_{DH}^{-1} K_p\right] = \left[C_{SH}S_p\right]\left[C_{DH}^{-1} K_p\right]$	2nxj	
40	$[\sigma] = \left[C_{SH}S_p C_{DH}^{-1} K_p\right][\delta]$	2nxq	Output - midspan longitudinal stresses

To obtain results for second, third, and so on numbers of harmonic loadings only steps 33 to 40 have to be repeated using new values of C_S, C_D, and R corresponding to the particular harmonic. Input matrices in steps 1 to 9 and matrices computed in steps 13 to 32 are functions of only the dimensions and geometry of the folded plate cross section and the modulus of elasticity.

COMBINED PLATE AND SLAB SYSTEM; NON-HARMONIC LOADING

While the method described in the preceding section is generally applicable to any loading, the number of harmonics necessary to represent a given loading may be excessive in certain cases. An alternate procedure suggested by Yitzhaki,[7] offers definite advantages in these cases.

For simplicity of discussion let the beam of Fig. 10(a) represent, symbolically, an entire folded plate structure consisting of the combined plate and slab system.

1. The loading shown in Fig. 10(a), in this case a set of concentrated vertical joint loads R at midspan, is obtained by the superposition of those shown in Figs. 10(b), 10(c), and 10(d).
2. In Fig. 10(b) the entire load R is assumed to be taken by the plate system alone acting as a membrane structure. Longitudinal stresses σ_1 and vertical joint deflections σ_1 are computed.
3. The deflection curve in Fig. 10(b) can be closely approximated by a first harmonic sine wave. Thus, in Fig. 10(c), the harmonic load R_1 and the transverse slab moments m_1, both resulting from this deflection curve being applied to the slab system alone, are computed.
4. In Fig. 10(d), the harmonic load R_1 is applied to the combined plate and slab system and σ_2, m_2, and δ_2 are computed by the method developed in the preceding section on harmonic loadings.

5. Thus, final values for the loading in Fig. 10(a) are obtained by superposition.

$$\underline{R} = \underline{R} + \underline{R_1} - \underline{R_1} \quad \ldots\ldots\ldots\ldots\ldots\ldots (41)$$

$$\underline{\sigma} = \underline{\sigma_1} - \underline{\sigma_2} \quad \ldots\ldots\ldots\ldots\ldots\ldots (42)$$

$$\underline{m} = \underline{m_1} - \underline{m_2} \quad \ldots\ldots\ldots\ldots\ldots\ldots (43)$$

and

$$\underline{\delta} = \underline{\delta_1} - \underline{\delta_2} \quad \ldots\ldots\ldots\ldots\ldots\ldots (44)$$

The advantage of the above procedure is that only the deflection curve of the given loading rather than the loading itself need be represented by a harmonic series.

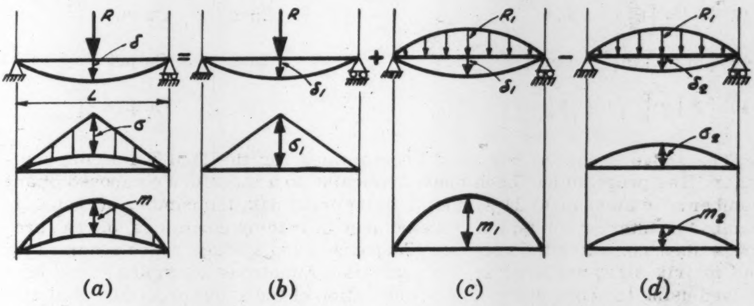

FIG. 10

Sequence of Matrix Operations for Non-Harmonic Loading.—Steps 1 to 35 are exactly the same for this sequence as for the harmonic loading with the exception that in steps 9 and 10 two constants are input rather than one.

9. $C_{SH} = L^2/\pi^2$; C_{SW} is the stress constant for given loading; such as $L/4$ for concentrated load at midspan; $L^2/8$ for a uniformly distributed load.

10. $C_{DH} = L^4/\pi^4$; C_{DW} is the deflection constant for given loading; e.g. $L^3/48$ for concentrated load at midspan; $5L^4/384$ for a uniformly distributed load.

Beyond step 35 the following sequence should be used.

Step	Matrix Description	Matrix Size	Remarks
36	$\left[C_{SW}S_p\right] = C_{SW}\left[S_p\right]$	2nxj	
37	$\left[\sigma_1\right] = \left[C_{SW}S_p\right][R]$	2nxq	Output
38	$\left[C_{DW}\,F_p\right] = C_{DW}\left[F_p\right]$	jxj	
39	$\left[\delta_1\right] = \left[C_{DW}F_p\right][R]$	jxq	Output

40	$\left[R_1\right] = \left[K_s\right]\left[\delta_1\right]$	jxq	
41	$\left[m_1\right] = \left[S_s\right]\left[\delta_1\right]$	2nxq	Output
42	$\left[\delta_2\right] = [F]\left[R_1\right]$	jxq	
43	$\left[m_2\right] = \left[S_s\right]\left[\delta_2\right]$	2nxq	
44	$\left[C_{SH}S_p\right] = C_{SH}\left[S_p\right]$	2nxq	
45	$\left[C_{SH}S_p\, C_{DH}^{-1}\, K_p\right] = \left[C_{SH}S_p\right]\left[C_{DH}^{-1}\, K_p\right]$	2nxj	
46	$\left[\sigma_2\right] = \left[C_{SH}\, S_p\, C_{DH}^{-1}\, K_p\right]\left[\delta_2\right]$	2nxq	
47	$[\sigma] = \left[\sigma_1\right] - \left[\sigma_2\right]$	2nxq	Output
48	$[m] = \left[m_1\right] - \left[m_2\right]$	2nxq	Output
49	$[\delta] = \left[\delta_1\right] - \left[\delta_2\right]$	jxq	Output

The above sequence has been programmed for the IBM 704 digital computer. The program has been made applicable to a structure composed of any number of plates up to 24 by adding to the input data the number of plates, n, number of interior joints, j, and the number of loading conditions, q. The program then computes the necessary addresses and storage space required for the matrix sizes involved in the analysis. Numerous examples have been solved using the computer. As an illustration of the above procedure a simple example is given in Appendix I in which numerical values are given only for the input matrices and the final answers for $\underline{\sigma_1}$, $\underline{m_1}$, $\underline{\delta_1}$, $\underline{\sigma}$, $\underline{m}$, and $\underline{\delta}$.

CONCLUSIONS

A matrix procedure has been developed for the determination of longitudinal stresses, transverse moments, and vertical deflections in the typical case of a simple span folded plate structure with free longitudinal edges. However, the method can be applied, with proper modifications, to cases involving other boundary conditions. Certain modifications are also necessary when the structure contains interior vertical plates. Advantage may also be taken of symmetry or antisymmetry, in cases where they exist, to decrease the amount of computation. Some of the advantages of the matrix procedure developed are as follows:

1. It can be readily programmed for a digital computer.
2. The basic matrices are functions only of the geometry and dimensions of the folded plate structure cross section and the modulus of elasticity. Thus they need not be recomputed for each different loading condition.
3. The analysis of the plate system and the slab system are separated so that the effect of changes in slab thickness or in span length for a particular cross section can be studied.

The folded plate equations, which were developed in matrix form in this paper, are based on the simplifying assumptions regarding slab and longitudinal plate behavior generally used in this type of analysis. A more precise analysis based on the theory of elasticity can also be developed in matrix form.

ACKNOWLEDGMENTS

The author wishes to express his sincere appreciation to his colleagues Frank Baron and Ray Clough for their critical review of the paper.

APPENDIX I.

The following example illustrates the analysis of a folded plate roof subjected to vertical joint loads that have a uniform distribution in the longitudinal direction. The procedure used is that described in the section on "Combined Plate and Slab System; Non-Harmonic Loading." Numerical values are only given for input and final answer matrices and kip and feet units are used throughout. In this example there are four plates (n = 4), three interior joints (j = 3), and one loading condition (q = 1).

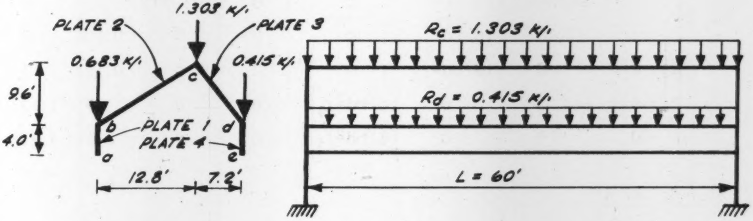

FIG. 11.—DIMENSIONS AND LOADING OF FOLDED PLATE ROOF

Dimensions and Loading.—simple span L = 60 ft, plate thickness b = 4 in. = 1/3 ft for all plates, modulus of elasticity E = 432 x 10^3 ksf.

Input Matrices:—

Step 1: $\underline{B}$ in Eq. 5 $\underline{P} = \underline{B}\ \underline{R}^p$

$$\left[B\right] = \begin{bmatrix} B_{1b} & 0 & 0 \\ B_{2b} & B_{2c} & 0 \\ 0 & B_{3c} & B_{3d} \\ 0 & 0 & B_{4d} \end{bmatrix} = \begin{bmatrix} -1.00 & 0 & 0 \\ 0 & -0.60 & 0 \\ 0 & +0.80 & 0 \\ 0 & 0 & +1.00 \end{bmatrix}$$

Steps 2 and 3: $\underline{S_N}$ and $\underline{S_O}$ in Eq. 9 $\underline{\sigma} = C_s\left[\underline{S_o}\ \underline{P} + \underline{S_N}\ \underline{\left(N/C_S\right)}\right]$

$$\left[S_N\right] = \begin{bmatrix} (2/bd)_1 & 0 & 0 \\ (4/bd)_1 & 0 & 0 \\ (4/bd)_2 & (2/bd)_2 & 0 \\ (2/bd)_2 & (4/bd)_2 & 0 \\ 0 & (4/bd)_3 & (2/bd)_3 \\ 0 & (2/bd)_3 & (4/bd)_3 \\ 0 & 0 & (4/bd)_4 \\ 0 & 0 & (2/bd)_4 \end{bmatrix} = \begin{bmatrix} 1.500 & 0 & 0 \\ 3.000 & 0 & 0 \\ 0.750 & 0.375 & 0 \\ 0.375 & 0.750 & 0 \\ 0 & 1.000 & 0.500 \\ 0 & 0.500 & 1.000 \\ 0 & 0 & 3.000 \\ 0 & 0 & 1.500 \end{bmatrix}$$

$$\left[S_o\right] = \begin{bmatrix} \left(6/bd^2\right)_1 & 0 & 0 & 0 \\ \left(6/bd^2\right)_1 & 0 & 0 & 0 \\ 0 & \left(6/bd^2\right)_2 & 0 & 0 \\ 0 & \left(6/bd^2\right)_2 & 0 & 0 \\ 0 & 0 & \left(6/bd^2\right)_3 & 0 \\ 0 & 0 & \left(6/bd^2\right)_3 & 0 \\ 0 & 0 & 0 & \left(6/bd^2\right)_4 \\ 0 & 0 & 0 & \left(6/bd^2\right)_4 \end{bmatrix} = \begin{bmatrix} 1.125 & 0 & 0 & 0 \\ 1.125 & 0 & 0 & 0 \\ 0 & 0.070312 & 0 & 0 \\ 0 & 0.070312 & 0 & 0 \\ 0 & 0 & 0.125 & 0 \\ 0 & 0 & 0.125 & 0 \\ 0 & 0 & 0 & 1.125 \\ 0 & 0 & 0 & 1.125 \end{bmatrix}$$

Step 4: ADRO

$$\left[\text{ADRO}\right] = \begin{bmatrix} 0 & 1 & 1 & 0 & 0 & 0 & 0 & 0 \\ 0 & 0 & 0 & 1 & 1 & 0 & 0 & 0 \\ 0 & 0 & 0 & 0 & 0 & 1 & 1 & 0 \end{bmatrix}$$

Steps 5 and 6: $\underline{F_N}$ and $\underline{F_O}$ in Eq. 20 $\underline{v} = C_D\left[\underline{F_o}\ \underline{P} + \underline{F_N}\ \underline{\left(N/C_S\right)}\right]$

$$\left[F_N\right] = \begin{bmatrix} \left(6/bd^2E\right)_1 & 0 & 0 \\ \left(6/bd^2E\right)_2 & \left(6/bd^2E\right)_2 & 0 \\ 0 & \left(6/bd^2E\right)_3 & \left(6/bd^2E\right)_3 \\ 0 & 0 & \left(6/bd^2E\right)_4 \end{bmatrix} = \begin{bmatrix} 2.604166 & 0 & 0 \\ 0.162759 & 0.162759 & 0 \\ 0 & 0.289352 & 0.289352 \\ 0 & 0 & 2.604166 \end{bmatrix} \times 10^{-6}$$

$$\left[F_o\right] = \begin{bmatrix} (12/bd^3E)_1 & 0 & 0 & 0 \\ 0 & (12/bd^3E)_2 & 0 & 0 \\ 0 & 0 & (12/bd^3E)_3 & 0 \\ 0 & 0 & 0 & (12/bd^3E)_4 \end{bmatrix}$$

$$= \begin{bmatrix} 1.302083 & 0 & 0 & 0 \\ 0 & 0.020345 & 0 & 0 \\ 0 & 0 & 0.048225 & 0 \\ 0 & 0 & 0 & 1.302083 \end{bmatrix} \times 10^{-6}$$

Steps 7 and 8: $\underline{K_\theta}$ and $\underline{K_\delta}$ in Eq. 27 $\underline{m} = \underline{K_\theta}\ \underline{\theta} + \underline{K_\delta}\ \underline{\delta}$

$$\left[K_\theta\right] = \begin{bmatrix} (b^3E/6d)_1^* & 0 & 0 \\ (b^3E/3d)_1^* & 0 & 0 \\ (b^3E/3d)_2 & (b^3E/6d)_2 & 0 \\ (b^3E/6d)_2 & (b^3E/3d)_2 & 0 \\ 0 & (b^3E/3d)_3 & (b^3E/6d)_3 \\ 0 & (b^3E/6d)_3 & (b^3E/3d)_3 \\ 0 & 0 & (b^3E/3d)_4^* \\ 0 & 0 & (b^3E/6d)_4^* \end{bmatrix} = \begin{bmatrix} 0 & 0 & 0 \\ 0 & 0 & 0 \\ 333.333 & 166.666 & 0 \\ 166.666 & 333.333 & 0 \\ 0 & 444.444 & 222.222 \\ 0 & 222.222 & 444.444 \\ 0 & 0 & 0 \\ 0 & 0 & 0 \end{bmatrix}$$

$$\left[K_\delta\right] = \begin{bmatrix} (b^3E/2dh)_1^* & 0 & 0 \\ (b^3E/2dh)_1^* & 0 & 0 \\ -(b^3E/2dh)_2 & (b^3E/2dh)_2 & 0 \\ -(b^3E/2dh)_2 & (b^3E/2dh)_2 & 0 \\ 0 & -(b^3E/2dh)_3 & (b^3E/2dh)_3 \\ 0 & -(b^3E/2dh)_3 & (b^3E/2dh)_3 \\ 0 & 0 & -(b^3E/2dh)_4^* \\ 0 & 0 & -(b^3E/2dh)_4^* \end{bmatrix} = \begin{bmatrix} 0 & 0 & 0 \\ 0 & 0 & 0 \\ -39.0625 & 39.0625 & 0 \\ -39.0625 & 39.0625 & 0 \\ 0 & -9.25926 & 9.25926 \\ 0 & -9.25926 & 9.25926 \\ 0 & 0 & 0 \\ 0 & 0 & 0 \end{bmatrix}$$

The values marked with an asterik are zero for a cantilever span.

Step 9: $\underline{H}$ in Eq. 33 $\underline{R}^{s} = \underline{H}\ \underline{m}$

$$\left[H\right] = \begin{bmatrix} 1/h_1^* & 1/h_1^* & -1/h_2 & -1/h_2 & 0 & 0 & 0 & 0 \\ 0 & 0 & 1/h_2 & 1/h_2 & -1/h_3 & -1/h_3 & 0 & 0 \\ 0 & 0 & 0 & 0 & 1/h_3 & 1/h_3 & -1/h_4^* & -1/h_4^* \end{bmatrix}$$

$$= \begin{bmatrix} 0 & 0 & -0.078125 & -0.078125 & 0 & 0 & 0 & 0 \\ 0 & 0 & 0.078125 & 0.078125 & -0.138889 & -0.138889 & 0 & 0 \\ 0 & 0 & 0 & 0 & 0.138889 & 0.138889 & 0 & 0 \end{bmatrix}$$

Step 10: $C_{SH} = L^2/\pi^2 = 364.756$

$C_{SW} = L^2/8 = 450.000$

Step 11: $C_{DH} = L^4/\pi^4 = 133047$

$C_{DW} = 5L^4/384 = 168750$

Step 12: $\underline{R}$ = load matrix

$$\begin{bmatrix} R_b \\ R_c \\ R_d \end{bmatrix} = \begin{bmatrix} 0.683 \\ 1.303 \\ 0.415 \end{bmatrix}$$

C. Final answers.

Steps 37 and 47: Longitudinal Stresses

$$\begin{bmatrix} \sigma_{1ab} \\ \sigma_{1ba} \\ \sigma_{1bc} \\ \sigma_{1cb} \\ \sigma_{1cd} \\ \sigma_{1dc} \\ \sigma_{1de} \\ \sigma_{1ed} \end{bmatrix} = \begin{bmatrix} -194.17 \\ -42.57 \\ 42.57 \\ -3.81 \\ 3.81 \\ -17.04 \\ 17.04 \\ 113.57 \end{bmatrix} \qquad \begin{bmatrix} \sigma_{ab} \\ \sigma_{ba} \\ \sigma_{bc} \\ \sigma_{cb} \\ \sigma_{cd} \\ \sigma_{dc} \\ \sigma_{de} \\ \sigma_{ed} \end{bmatrix} = \begin{bmatrix} -175.66 \\ -33.43 \\ 33.43 \\ -12.16 \\ 12.16 \\ -1.04 \\ 1.04 \\ 80.79 \end{bmatrix}$$

Steps 41 and 48: Transverse moments

$$\begin{bmatrix} m_{1ab} \\ m_{1ba} \\ m_{1bc} \\ m_{1cb} \\ m_{1cd} \\ m_{1dc} \\ m_{1de} \\ m_{1ed} \end{bmatrix} = \begin{bmatrix} 0 \\ 0 \\ 0 \\ -1.199 \\ 1.199 \\ 0 \\ 0 \\ 0 \end{bmatrix} \qquad \begin{bmatrix} m_{ab} \\ m_{ba} \\ m_{bc} \\ m_{cb} \\ m_{cd} \\ m_{dc} \\ m_{de} \\ m_{ed} \end{bmatrix} = \begin{bmatrix} 0 \\ 0 \\ 0 \\ -0.869 \\ 0.869 \\ 0 \\ 0 \\ 0 \end{bmatrix}$$

Steps 39 and 49: Vertical joint deflections

$$\begin{bmatrix} \delta_{1b} \\ \delta_{1c} \\ \delta_{1d} \end{bmatrix} = \begin{bmatrix} 0.05138 \\ -0.00303 \\ 0.02834 \end{bmatrix} \qquad \begin{bmatrix} \delta_{b} \\ \delta_{c} \\ \delta_{d} \end{bmatrix} = \begin{bmatrix} 0.04554 \\ -0.00010 \\ 0.01805 \end{bmatrix}$$

APPENDIX II.—NOTATION

An underlined symbol represents a matrix.

The following symbols have been adopted for use in this paper:

b = plate thickness;

C_D = deflection constant;

C_S = stress constant;

d = plate depth between longitudinal edges;

E = modulus of elasticity;

h = horizontal projection of plate depth d;

I_p = moment of inertia of a plate = $bd^3/12$;

I_s = moment of inertia of a unit width of slab = $b^3/12$;

j = number of interior joints;

L = longitudinal span;

M_o = plate moment due to P along;

M_p = total plate moment;

m = transverse slab moment at a plate edge;

N = summation of plate longitudinal edge shear T;

n = number of plates;

P = plate load (parallel to a plate);

Q_o = plate end reaction due to P alone;

q = number of loading conditions;

R = vertical joint load taken by combined plate and slab system;

R^p = vertical joint load taken by plate system;

R^s = vertical joint load taken by slab system;

T = longitudinal shear per unit length along plate edge;

V_o = plate shear force due to P alone;

v = plate displacement (parallel to a plate);

x = distance from a support along length of plate;

δ = vertical joint deflection;

θ = joint rotation in transverse slab system; and

σ = longitudinal stress at the plate edge.

AMERICAN SOCIETY OF CIVIL ENGINEERS

Founded November 5, 1852

TRANSACTIONS

Paper No. 3210

STATISTICAL AND ECONOMIC ANALYSIS OF A BIDDING TREND

By Marvin Gates,[1] M. ASCE

SYNOPSIS

Almost four hundred results of bids for heavy construction contracts are analyzed for correlation between the size of the contract and the difference between the low and second bids.

The results of this analysis are applied to four diversified areas of competitive bidding. Namely, another criteria for ascertaining the probable existence of a gross mistake in a bid is offered; a suggested maximum amount of bid guarantee is treated; the practice of using "going" prices is investigated; and three methods for increasing profits, based on probability factors, are described.

INTRODUCTION

Recently, a contractor bid 30 million dollars to do a heavy construction job. The second bidder asked 40 million dollars to do the same work. At about the same time, on another job, two other contractors submitted identical bids of $1,400,000. Much comment and speculation continues concerning both incidents. One question remaining unanswered is the odds against such occurrences. Quite understandably, if the answer to this question can be found then it may be possible to control the amount of money "left on the table." This latter term is synonymous with the term "spread." Both expressions are interchangably used throughout this paper to mean the difference between the low and second bids.

Note.—Published essentially as printed here, in November, 1960, in the Journal of the Construction Division, as Proceedings Paper 2651. Positions and titles given are those in effect when the paper or discussion was approved for publication in Transactions.

[1] Chf. Engr., Macari Bros. Constr. Co., Windsor, Conn.

The ability to predict the probable spread gives the engineer and contractor a new and important tool. Equally as important, is the continuing emergence of bidding practice as a scientific method.

Notation.—The letter symbols adopted for use in this paper are defined where they first appear, in the illustrations or in the text, and are arranged alphabetically, for convenience of reference, in the Appendix.

ACCUMULATION AND SELECTION OF DATA

The results of competitive bids in the construction industry are usually published by the trade and engineering periodicals serving the geographical location of the project. In the New England States, the weekly publication, NERBA, published by the New England Road Builders Association, carries the complete results of highway projects bid in that area. In addition, many states mimeograph and circulate the results of each bid letting to all interested parties; including all contractors prequalified to bid in the state, equipment dealers, material vendors, and engineers. Fig. 1 is a typical release by the Connecticut State Highway Department. It is their practice to publish the complete bid of each of the three lowest bidders; some states publish the complete bid of all bidders.

For the purpose at hand, the writer has drawn from his file of such publications of the bid results published by the State of Connecticut from 1957 to 1959, and the states of New Hampshire and Vermont from 1958 to 1959. Although it is probable that these files are not complete, they do reflect the bidding pattern for these New England States.

From the accumulation of data, certain contracts were rejected as not being representative of the usual highway construction projects encountered. The rejected material included:

1. Specialty contracts such as highway illumination, joint resealing, landscaping, demolition, dredging, and mechanical work.
2. Alternate bids to the base bid.
3. Contracts having less than ten unit items of work. These too were arbitrarily considered to be of a specialty contract nature; albeit the specialty work was of a heavy construction nature.

The remaining data included bids received for the construction of highways, bridges, and drainage. Where specialty work, such as fencing, was an incidental part of these contracts, they were included. The 381 bids used in this analysis represent about $200,000,000 worth of construction contracts.

TABULATION OF DATA

The range of the dollar values of the contracts under discussion varied from a low of $1,700 to a high of $8,025,000. For ease of handling the 381 observations in this great range, it was desirable to divide the data into about ten groups. Arbitrarily the progression $1000(2^n)$ was used as the basis for forming these groups. Table 1 shows the division of the groups.

The low bid, expressed as a percentage of the second bid, was computed and then rounded to the nearest whole percentage point for each of the contracts,

Number of Bidders: 11
Date of Letting:
February 8, 1960

TOWN OF WESTPORT
Roads in Sherwood Island State Park
Bituminous Concrete
Length 2,830.00 Feet, Width Varies, Depth 2½ Inches

State Park & Forest Commission
and State Agency Funds
Proj. No. S-3119

			D'Addario Services		The DeFonce Const. Co., Inc.		De Leo Bros. Inc.	
Items	Unit	Quantity	Price	Amount	Price	Amount	Price	Amount
Earth Excavation	C.Y.	3,981	.50	1,990.50	.60	2,388.60	.40	1,592.40
Removal of Existing Masonry	C.Y.	1	10.00	10.00	15.00	15.00	20.00	20.00
Trench Excavation 0'-6' Deep	C.Y.	890	1.50	1,335.00	2.00	1,780.00	1.50	1,335.00
Trench Excavation 0'-10' Deep	C.Y.	705	2.00	1,410.00	3.50	2,467.50	1.50	1,057.50
Ditch Excavation	C.Y.	520	2.00	1,040.00	2.00	1,040.00	.60	312.00
Borrow	C.Y.	9,160	1.00	9,160.00	.95	8,702.00	1.25	11,450.00
15" Reinforced Concrete Pipe	L.F.	248	3.50	868.00	4.00	992.00	4.00	992.00
18" Reinforced Concrete Pipe	L.F.	28	4.00	112.00	4.50	126.00	6.00	168.00
15" A.C.C.M. Pipe	L.F.	144	4.25	612.00	5.00	720.00	6.00	864.00
15" A.C.C.M. Pipe (Asbestos Bonded)	L.F.	356	4.75	1,691.00	6.00	2,136.00	6.00	2,136.00
18" A.C.C.M. Pipe (Asbestos Bonded)	L.F.	934	6.25	5,837.50	6.75	6,304.50	6.00	5,604.00
24" A.C.C.M. Pipe (Asbestos Bonded)	L.F.	100	8.00	800.00	8.50	850.00	9.00	900.00
Underdrain with 6" Perforated A.C.C.M. Pipe	L.F.	950	2.75	2,612.50	3.00	2,850.00	3.00	2,850.00
Type "C-L" Catch Basin	Each	10	210.00	2,100.00	225.00	2,250.00	225.00	2,250.00
Class "A" Concrete	C.Y.	10	65.00	650.00	60.00	600.00	65.00	650.00
Subbase	C.Y.	4,850	2.00	9,700.00	1.50	7,275.00	2.00	9,700.00
Formation of Subgrade	S.Y.	17,426	.15	2,613.90	.20	3,485.20	.10	1,742.60
Rolled Gravel Base	C.Y.	2,960	2.40	7,104.00	1.50	4,440.00	2.25	6,660.00
Bituminous Concrete Binder Course	Ton	1,253	9.50	11,903.50	8.75	10,963.75	9.00	11,277.00
Hot Asphalt Concrete	Ton	1,281	9.50	12,169.50	8.75	11,208.75	9.00	11,529.00
Concrete Park Curbing	L.F.	1,960	2.50	4,900.00	2.25	4,410.00	2.00	3,920.00
Two-Cable Guide Railing	L.F.	370	1.65	610.50	1.75	647.50	1.75	647.50
Compensating Type Anchorage	Each	2	40.00	80.00	40.00	80.00	40.00	80.00
Single Post	Each	18	7.50	135.00	7.00	126.00	8.00	144.00
Slope Paving	S.Y.	4	15.00	60.00	15.00	60.00	20.00	80.00
Furnishing and Placing Loam	S.Y.	41,680	.35	14,588.00	.60	25,008.00	.65	27,092.00
Placing Loam	S.Y.	7,920	.25	1,980.00	.20	1,584.00	.30	2,376.00
				$96,072.90		$102,509.80		$107,429.00

Low Bidder - D'Addario Services - $96,072.90

FIG. 1.—OFFICIAL RELEASE OF THE RESULTS OF A BID LETTING BY THE CONNECTICUT STATE HIGHWAY DEPARTMENT

according to the following formula:

$$P = \frac{\text{low bid}}{\text{second bid}} \times 100\% \ldots\ldots\ldots\ldots\ldots\ldots (1)$$

The results were tabulated in cells according to the value of P and the size of the contract (Table 2). Values of P less than 80% were grouped together. In the analysis, they are regarded as being equal to 80%. Actually, only three items fell into this group, and none were as low as 75%.

TABLE 1.—GROUP DIVISION

n (1)	1,000 (2^n) (2)	Contract group, in dollars (3)		
0 1 2	1,000 2,000 4,000	1,000	—	5,000
		5,000	—	10,000
3	8,000			
		10,000	—	15,000
4	16,000			
		15,000	—	25,000
5	32,000			
		25,000	—	50,000
6	64,000			
		50,000	—	125,000
7	128,000			
		125,000	—	250,000
8	256,000			
		250,000	—	500,000
9	512,000			
		500,000	—	1,000,000
10	1,024,000			
		1,000,000	—	2,000,000
11	2,045,000			
		2,000,000	—	4,000,000
12	4,098,000			
		4,000,000	—	8,000,000
13	8,192,000			

No distinction between the data obtained from the various states was made. Approximately 30% of the data was contributed by New Hampshire, 20% by Vermont and the remaining 50% by Connecticut.

ANALYSIS OF DATA

From Table 2, it can be seen that there is a relatively small amount of data in the first three and the last two groups. For ease of handling as well as maintaining a representative number of samples within each group, the five aforementioned groups were consolidated into two, namely:

\$1,000 - \$15,000; \$2,000,000 - \$8,000,000

TABLE 2.—DISTRIBUTION OF CONTRACTS BY SIZE AND PERCENTAGE OF SPREAD FOR CONNECTICUT, VERMONT, AND NEW HAMPSHIRE, 1957-1959[a]

Low bid, in	P = (Low bid ÷ Second bid) x 100%																						
$1,000,000	100	99	98	97	96	95	94	93	92	91	90	89	88	87	86	85	84	83	82	81	80	<80	TOTALS
1 - 5	0	0	0	0	0	1	1	0	0	0	1	0	0	0	0	0	0	0	0	0	0	0	3
5 - 10	0	0	0	0	1	0	0	1	0	0	0	0	0	0	0	0	0	0	0	0	0	0	2
10 - 15	0	0	3	1	0	2	1	1	3	1	0	1	0	0	0	1	1	0	2	0	0	0	17
15 - 25	0	4	2	1	3	3	3	2	4	4	0	0	1	1	1	2	0	0	1	1	0	1	34
25 - 50	0	9	3	7	5	4	2	1	3	0	0	0	1	3	2	0	0	0	1	0	1	1	43
50 - 125	7	6	9	7	6	6	4	6	5	3	3	2	1	0	1	0	1	0	0	0	1	1	69
125 - 250	8	7	10	9	10	5	2	1	2	0	4	1	1	1	1	0	1	0	0	0	0	0	63
250 - 500	8	12	10	9	3	8	2	0	2	2	1	1	0	0	0	0	0	0	0	0	0	0	58
500 - 1,000	6	8	10	5	4	2	2	0	2	1	0	0	0	0	0	0	0	0	0	0	0	0	40
1,000 - 2,000	4	10	4	7	2	2	2	2	1	0	0	0	0	0	0	0	0	0	0	0	0	0	34
2,000 - 4,000	0	3	3	2	1	1	0	1	0	0	1	0	0	0	0	0	0	0	0	0	0	0	12
4,000 - 8,000	2	0	0	3	0	0	1	0	0	0	0	0	0	0	0	0	0	0	0	0	0	0	6
TOTALS	35	59	54	51	35	34	20	15	22	11	10	5	4	5	5	3	3	0	4	1	2	3	381

[a] Official releases from the highway departments of Conn. (1957-1959), Vt. (1958-1959) and N. H. (1958-1959).

The midpoint, C, that represents the average worth of the contracts within the respective group was taken as the geometric mean of the limits of the group. The geometric mean, G_m, is defined as:

$$G_m = \sqrt[n]{a_1 \times a_2 \times a_3 \dots a_n} \quad \dots\dots\dots\dots \quad (2)$$

in which a is a single observation and n is the total number of observations.

The midpoints of the two consolidated groups were taken as the weighted geometric mean of the limits of the original groups comprising them.

The several values of P were similarly averaged so as to yield the geometric mean, $\overline{P}$, for each of the nine groups. The geometric rather than the arithmetic mean was used because of the more typical values obtained when the data are related logarithmically.

However, it will be remembered that P and $\overline{P}$ are the ratios of the low bid to the second bid. For the purpose at hand, it was expedient to express the percentage spread as the ratio of the difference between the second and low bid, ΔB, to the low bid, or:

$$P' = \frac{\Delta B}{\text{low bid}} \times 100\% \quad \dots\dots\dots\dots \quad (3)$$

Eq. 3 was equated to Eq. 1, thereby eliminating the term, ΔB. Similarly:

$$\overline{P}' = 100 \left(\frac{100}{\overline{P}} - 1 \right) \quad \dots\dots\dots\dots \quad (4)$$

in which $\overline{P}'$ is the average (geometric mean) spread expressed in terms of percent of the low bid.

The values of $\overline{P}'$ for each of the nine groups are shown as plotted points in Fig. 2. The points lie on a reasonably straight line indicating that a fully logarithmic correlation between $\overline{P}'$ and C exists. By the Method of Least Squares, the best fitting curve, straight line on log-log paper, was found. Table 3 shows the computations used to determine

$$p = 108\ C^{-0.266} \quad \dots\dots\dots\dots \quad (5)$$

in which C is the low bid and p is the computed percentage spread.

Expressed in dollars, the average spread, ΔB_{av}, may be stated by multiplying Eq. 5 by C to yield

$$\Delta B_{av} = 1.08\ C^{0.734} \quad \dots\dots\dots\dots \quad (6)$$

Eqs. 5 and 6 are plotted in Fig. 2.

The computed percent spread, p, is compared with $\overline{P}'$ in Table 4.

It appears that the value of $\overline{P}'$ for the group, 2 million to 8 million, is not consistent with the other values (see Fig. 2). Hence, this value was not included in the computations used to determine Eqs. 5 and 6. However, it can be logically deduced that these equations cannot be extrapolated to near infinite values of C. For example, extrapolation of the other plotted points will yield a value of $\overline{P}'$ equal to almost zero as C approaches infinity. Then, for every large value of ΔB, there must exist a corresponding value approximately equal to $-\Delta B$ in order to produce an average value of near zero. But a negative value of ΔB means that the second bidder is low. This, of course, is absurd. Therefore, lacking further data, it is logical to assume that the extrapolated values will, at some point, tend to be asymptotic to the abscissa. By inspection, from Fig. 2, it may be assumed that for values of C greater than 1.5 million dollars

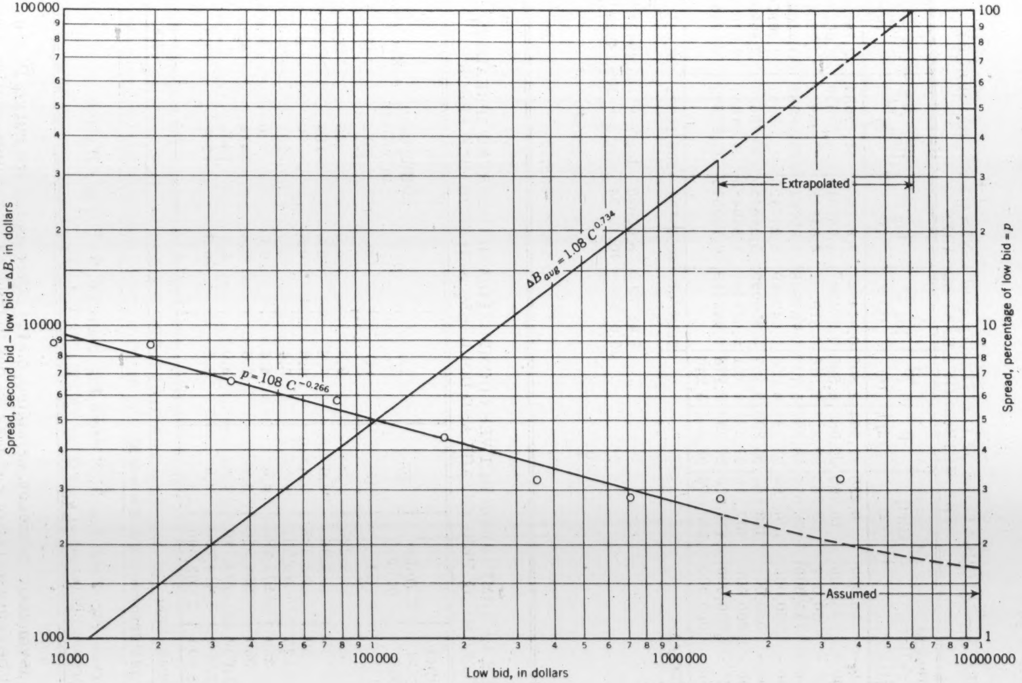

FIG. 2.—LINES OF REGRESSION FOR PERCENTAGE AND EQUIVALENT DOLLAR SPREAD OF CONTRACTS LET BY CONNECTICUT, VERMONT AND NEW HAMPSHIRE, 1957-1959

there is a reduction in the rate of change of $\overline{P'}$. Eqs. 5 and 6, therefore, are true for $10^4 \leqq C \leqq 1.5 \times 10^6$. However, it can be shown that the application of extrapolated values from Eq. 6 will yield conservative results when C exceeds 1.5×10^6.

TABLE 3.—CALCULATIONS OF CONSTANTS FOR LINES OF REGRESSION BY THE METHOD OF LEAST SQUARES

Contract group, in dollars (1)	C (mid-point) (2)	$\overline{P}$ (3)	$\overline{P'}$ (4)	$\log \overline{P'}$ (5)	log C (6)	$(\log C)^2$ (7)	$\log \overline{P'}$ log C (8)
1,000 – 15,000	9,239	91.904	8.809	0.944927	3.965645	15.72634	3.747245
15,000 - 25,000	19,365	92.083	8.598	0.934397	4.287015	18.37850	4.005740
25,000 - 50,000	35,355	93.812	6.596	0.819281	4.548455	20.68844	3.726463
50,000 - 125,000	79,057	94.588	5.722	0.757548	4.897940	23.98982	3.710425
125,000 - 250,000	176,780	95.798	4.386	0.642069	5.247425	27.53547	3.369209
250,000 - 500,000	353,550	96.893	3.207	0.506099	5.548455	30.78535	2.808068
500,000 - 1,000,000	707,110	97.323	2.751	0.439491	5.849485	34.21647	2.570796
1,000,000 - 2,000,000	1,414,200	97.299	2.776	0.443419	6.150515	37.82883	2.727255
2,000,000 - 8,000,000	3,563,600	96.856	3.246	. . .	. . .	. . .	. . .
TOTALS				5.48723	40.49494	209.14922	26.66520

$$5.48723 = 8.00000 \log a + 40.49494\, b$$
$$26.66520 = 40.49494 \log a + 209.14922\, b$$

$$b = -\ 0.26634$$
$$a = 108.16$$

TABLE 4.—COMPARISON BETWEEN COMPUTED AND OBSERVED SPREADS IN TERMS OF PERCENTAGE AND DOLLARS: AND PROBABLE ERROR[a]

Contract group in \$1,000 (1)	C (mid-point) (2)	$\overline{P'}$ (3)	p^b (4)	$p-\overline{P'}$ (5)	Difference,[c] in dollars (6)	Error[d] (7)
1 - 15	9,239	8.8	9.3	0.5	46	3.8
15 - 25	19,365	8.6	7.8	-0.8	-154	-7.3
25 - 50	35,355	6.6	6.6	0.0	0	0
50 - 125	79,057	5.7	5.4	-0.3	-237	-4.0
125 - 250	176,780	4.4	4.4	0.0	0	0
250 - 500	353,550	3.2	3.6	0.4	1414	8.3
500 - 1,000	707,110	2.8	3.0	0.2	1414	5.0
1,000 - 2,000	1,414,200	2.8	2.5	-0.3	-4242	-8.6
2,000 - 8,000	3,563,600	3.2	. . .	. . .	. . .	. . .
Algebraic total						-2.8

Probable error = - 2.8/8 = - 0.35

[a] Source: Fig. 2 and Fig. 3. [b] From Fig. 2 and Eq. 5. [c] $C\,(p - P')/100$.
[d] Expressed in terms of percentile rating (see Fig. 3).

The asymptotic tendency exhibited on the other end of the curve, $\overline{P'} = 8.8$. may not be representative and may be due to the lack of a representative cross section of results in the first three groups (Table 2).

The possibility that the plotted points tend to a Gompertz, or other higher relationship, does not appear to deserve consideration in view of the limited quantity of data in the extreme groups on both ends of Table 2.

Although Eq. 6 gives the average spread, it is also important to know the probability of deviating from this value by some predetermined amount. Ordinary elementary statistical practice could not be successfully applied here because of the skewness of the data as evidenced by the asymetrical distribution (see Table 2).

All of the bid results were plotted on a logarithmic scale, ΔB versus C, (scatter diagram). Then Eq. 6 was plotted, as well as other members of the same curve family, namely, $\Delta B = 1.08\ a\ C^{0.734}$, in which a is a dimensionless parameter ranging in value from 0.02 to 7.0. The cumulative number of results (plotted points), lying under each of the curves was tallied (an ogive). Only the results from C = \$10,000 to C = \$1,500,000 were used in this portion of the analysis.

The result of the tally is shown in Table 5. The cumulative total of 368 includes 20 additional results that became available at the time the ogive was being constructed. They are not included in the preceding portions of this analysis.

TABLE 5.—OGIVE OF ΔB LESS THAN $1.08\ a\ C^{0.734}$

a (1)	No. of contracts (2)	Cumulative total (3)	Cumulative total divided by 368 (4)	1.08 a (5)	Col. 5 ÷ Col. 4 (6)
0.02	2	2	0.005	0.022	4.40
0.033	6	8	0.022	0.036	1.64
0.05	6	14	0.038	0.054	1.42
0.10	10	24	0.065	0.108	1.66
0.20	29	53	0.144	0.216	1.50
0.25	14	67	0.182	0.270	1.48
0.33	32	99	0.269	0.356	1.32
0.50	35	134	0.364	0.540	1.48
0.67	30	164	0.446	0.724	1.62
1	81	245	0.666	1.08	1.62
1.5	50	295	0.802	1.62	2.02
2	29	324	0.880	2.16	2.45
3	32	356	0.967	3.24	3.35
4	8	364	0.989	4.32	4.37
5	0	364	0.989	5.40	5.46
6	3	367	0.997	6.48	6.50
7	1	368	1.000	7.56	7.56

It can be seen that when $a \leqq 1$, the coefficient, 1.08 a, is equal to an average of 1.6 times the ratio of results (bids) that will be equal to or less than ΔB. Therefore, the equation of the median trend line is, approximately,

$$\Delta B_{median} = 0.80\ C^{0.734} \ \ldots\ldots\ldots\ldots\ldots \quad (7)$$

In other words, for a group of contracts, each bid at C dollars, half of the time the spread will be less than ΔB from Eq. 7 and half of the time greater.

Consequently, Eq. 6 may be expanded and transposed to yield the following general relationships between the bid price, C, and any given spread, ΔB:

$$\frac{67\ \Delta B}{1.08\ C^{0.734}} = \text{constant} \ \ldots\ldots\ldots\ldots\ldots\ldots \quad (8)$$

in which the constant is equal to the number of chances out of 100 of a spread equal to or less than ΔB occurring when ΔB is not greater than $1.08\ C^{0.734}$.

Fig. 3 graphically illustrates the solution to the average spread as well as the percentage of results equal to or less than a given spread that may be expected. The probable error of these results is shown in Table 4 as about -0.35. That is to say that the mean is not exactly at the 67 percentile but rather at about the 66.65 percentile. This error is proportional to the percentile rating, and, consequently, is negligible in our study.

Eqs. 6 and 7 are shown as the sixty-seventh and fiftieth percentiles in Fig. 3.

Before concluding this analysis, a word of explanation regarding the term probable error. This value is based on the theorem that the algebraic total of the deviations about the mean is equal to zero. It is not the statistical measure known as the standard error of estimate that is the root-mean-square. This latter measure is not applicable when the data deviates greatly from the normal (Gaussian) distribution. In the case at hand, this measure indicates that almost 100% (99.7%) of the values of ΔB will fall between the 50 and 83 percentiles. This conclusion, however, contradicts the facts. There is also some question as to the use of this measure when the data are related logarithmically, because the logarithm of zero is minus infinity.

Expressing the error in terms of percentile rating at the mean (67) level rather than in terms of percentage or dollars gives a truer picture of the deviations. Expressed in terms of percentage, the error is exaggerated for large values of C. While expressed in terms of dollars, the error is exaggerated for small values of C.

The odds against an occurrence at or greater than the one hundreth percentile level is more than 368 to 1. This is comparable to a deviation from the arithmetic mean of a normal distribution greater than three standard errors. Hence, this area of Fig. 3 is termed statistically impossible.

Fig. 3 then, graphically illustrates the deviations about the mean expressed in percentile form as well as laying the foundation for the next portion of this paper, the practical applications of this analysis.

OTHER CONSIDERATIONS

Every contractor's economic status is unique. Many times the control of available raw materials, such as borrow, will set one contractor distinctly apart from his competitors, when bidding for work. Then again, one contractor may have recently completed a similar project and has at his disposal detailed cost records. Another contractor may be determined to be low bidder at any cost, in order to keep his organization intact. And yet another may have discovered an error in the bid plans and has unbalanced his bid. The list of factors both tangible and intangible, objective and subjective, affecting the final bid price is endless. How then, can the methods described be generally applied?

It has long been recognized that there is a stability of mass data, although the mass is comprised of erratic individual cases. This foundamental precept underlies the basis of actuarial science and is the foundation of the insurance industry. The reader is referred to any standard text on statistics for a detailed discussion of this and other statistical topics.[2]

---

[2] "Elementary Statistical Methods," by William A. Neiswanger, The Macmillan Co., New York, 1953.

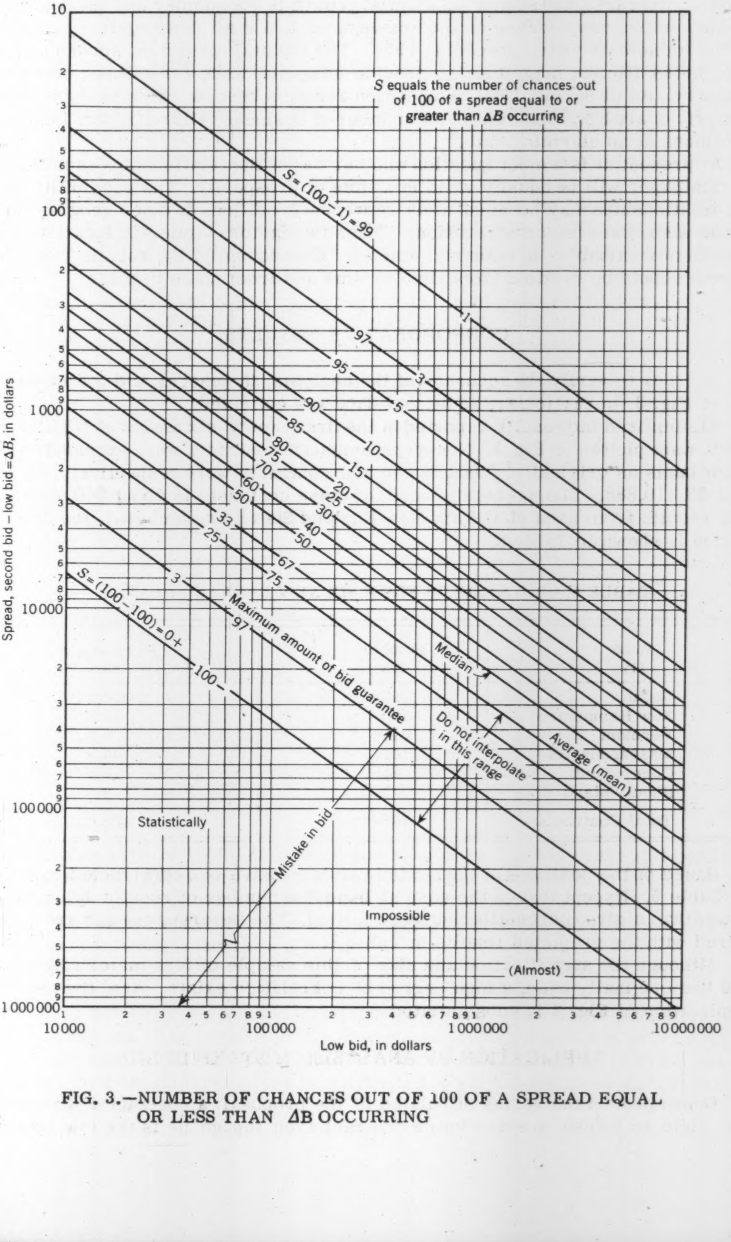

FIG. 3.—NUMBER OF CHANCES OUT OF 100 OF A SPREAD EQUAL OR LESS THAN ΔB OCCURRING

It is important to note again that the data on which this paper is based originated in three New England States from the year 1957 to 1959. This period was one of generally declining prices in the heavy construction industry. The geographical area had seen a substantial growth in the number and the potential of the contractors because of the accelerated toll road construction program in the immediate years preceding 1957. The highway program, subsequently, was of insufficient magnitude to provide adequate work for an over extended industry. As of Spring, 1960, competition remains keen, work remains scarce, and prices are low. Meanwhile, the number of business failures in this industry continues at an alarming rate.

At present, it is a moot question whether or not the relationships established in this paper will be equally valid in a time of prosperity. The possibility that the relationships may not accurately represent conditions in other geographical areas also deserves consideration. These two factors, time and location, are also major variables in actuarial science. Consequently, the results reported herein should be verified from time to time and from place to place.

CORROBORATIVE RESULTS

In order to verify the accuracy of the analysis, in general, and the reliability of Fig. 3, in particular, additional data was collected.

All itemized bid results reported in the first twenty-six issues of NERBA, in 1960, were plotted on Fig. 3. Non-representative contracts were excluded on the same basis as originally. The low and high contracts were respectively, $3,230 and $3,870,888. The aggregate worth of these contracts is about $60,000,000. Bid results from each of the six New England States are included; the distribution is shown in Table 6.

TABLE 6.—BID RESULTS FROM SIX NEW ENGLAND STATES

State (1)	Number (2)	Percentage (3)
Maine	17	12.3
New Hampshire	25	18.1
Vermont	11	8.0
Massachusetts	61	44.2
Connecticut	21	15.2
Rhode Island	3	2.2
Total Contracts	138	100.0

Based on the positions of the plotted points an ogive was constructed, similar to Table 5. Except that in the case at hand the number of results lying on or lower than a given percentile line were tallied. The observed results are compared with the predicted results in Table 7.

Although the stratification and size of this sample differs materially from the one originally used, a high degree of correlation exists. And, the general application of Fig. 3 is substantiated.

APPLICATION OF ANALYSIS: MISTAKE IN BID

Depending on the terms stipulated in the proposal, a contractor may have the right to refuse to enter into a contract even though he is the low bidder, provided he can prove a mistake in his bid. In certain situations, the contractor may have the right to withdraw his bid without penalty, that is, no forfeiture of the bid guarantee. The theory at law is that when a mistake is so large as to be obvious to the offeree, then the offeree knows that the bid is not the intended offer; however, neither does he know what the intended offer is. Therefore, no meeting of the minds ever occurred, and there is no basis for a contract.

Even though it is apparent that a bid is in error, by comparison with the other bids and the engineers' estimate, there is very often no other tangible evidence of the presence of a mistake. When this is the case, the contractor or his surety may be held bound to the forfeiture provisions in the proposal.

As a result of the analysis it is possible, statistically speaking, to ascertain at least one criteria for establishing the strongest probability that a mistake is manifest in a bid. Statistically speaking, if the chances of an event occurring are less than 3 out of 100, then it is an improbability that the event will occur. Therefore, if the difference between the low and second bids, ΔB, exceeds the 97 percentile, the low bid may be viewed as a rare item or a freak.

TABLE 7.—COMPARISON BETWEEN PREDICTED AND OBSERVED SPREADS IN TERMS OF PERCENTILE GROUPS AND AN EQUAL TO OR LESS THAN OGIVE[a]

Percentile group (1)	Individual group		Cumulative group	
	Predicted (2)	Observed (3)	Predicted (4)	Observed (5)
Less than 1	1	3	1	3
1 - 3	3	4	4	7
3 - 5	3	2	7	9
5 - 10	7	5	14	14
10 - 15	7	11	21	25
15 - 20	7	5	28	30
20 - 25	7	8	35	38
25 - 30	7	8	41	46
30 - 40	14	11	55	57
40 - 50	14	8	69	65
50 - 67	23	22	92	87
67 - 75	11	11	104	98
75 - 97	30	34	134	132
97 - 100	4	6	138	138
More than 100	0	0	138	138

[a] "NERBA," January 2, 1960 to June 25, 1960, inclusive and Fig. 3.

It is, therefore, suggested that it be considered prima facie evidence of the existence of a gross mistake in a bid if

$$\Delta B \geqq 3.24\, C^{0.734} \quad \ldots\ldots\ldots\ldots\ldots\ (9)$$

And the low bidder, if he requests, and if permitted by statute, be permitted to withdraw his bid without penalty. Eq. 9 is shown on Fig. 3 as the 97 percentile. This concession admits to 3% of the low bids as probably being in error, although some of these errors may be attributed to such intangibles as inexperience and ignorance.

A recent article[3] reports that the Corps of Engineers will include, in their future contracts, the following clause relating to bid mistakes:

> "Mistakes in Bids. The bidder hereby waives that portion of any alleged mistake or mistakes in his bid which falls within the following amounts:
>
> If bid is $250,000 or less - 5% of the bid;
>
> If bid is more than $250,000 and less than $500,000 - $12,500 plus 4% of the bid over $250,000;
>
> If bid is $500,000 or more, and less than $1,000,000 - $22,500 plus 3% of the bid over $500,000;
>
> If bid is $1,000,000 or more - $37,500 plus 2% of bid over $1,000,000.
>
> In cases where the allegation of mistakes exceeds the above waived amounts and the request for correction is allowed, such amount will be excluded from the contract price; however, the amount waived as provided herein will not be deducted for the purpose of evaluating bids to determine the low bidder.
>
> The above waiver does not apply to any clerical mistake which is obvious or apparent on the face of the bid including but not limited to (1) mistake in the extension of a unit price or prices; (2) a mistake in totaling the sums of various bid items; (3) obviously misplaced decimal point; or (4) failure to insert the unit price where amount intended can be determined from face of bid.
>
> This clause is not applicable to allegations of mistakes, which if allowed, would result in a reduction in the bid price."

It is interesting to note that the preceding schedule, if plotted on Fig. 3, would fall between the fortieth and seventy-fifth percentiles. In other words, the amount that must be waived is approximately equal to the average spread from Eq. 6. Furthermore, it recognizes the existance of two limits of p, one at p = 5%, and the other, an asymptote at p = 2% (Fig. 2). It is probable, however, that the aforementioned schedule was developed for ease of application with some sacrifice of theoretical precision, if we are to assume that the amount to be waived is intended to be related to the mean spread.

Nevertheless, mistakes in bidding are made for reasons other than mathematical or because of oversight. Specifications may be misinterpreted, anticipated sources of materials purported to be acceptable may have been misrepresented, out-of-town contractors may not have been informed of peculiar pertinant local ordinances, and the nature of payment for one or more items of work may be misconstrued (one state classifies as earth excavation the removal of a soil that requires drilling and blasting). It is not possible for a contractor to prove these allegations objectively. Neither can these factors be reduced to monetary terms without inviting skeptical replies. And yet, an unusually large sum of money left on the table is almost universally held as being indicative of an error in the bid.

In cases of extreme difference between the low and second bids, the low bidder should be permitted to withdraw his bid without penalty, since it can now be immediately ascertained if the low bid was conceived in error. On the other hand, if the low bidder has found an unusually economical method of doing a portion of the work, and he has reflected this potential economy in his estimate, then he will not ask to have his bid voided. However, this possibility should not be misconstrued and used as justification for taking advantage of an obviously erroneous proposal.

---

[3] Roads and Streets, March, 1960, p. 108.

BID SECURITY

As a guarantee that the lowest qualified bidder will enter into a contract with the owner, at the prices bid and under the terms of the proposal, all bidders are required to submit with the bid some form of bid security. As a rule, the bid securities of all but the lowest three bidders are returned immediately after the bids have been checked. After the contract is signed, the remaining securities are returned.

The bid guarantee may be in the form of a certified check, bid bond, or negotiable securities. Some states will accept the bid security in any of these three forms. Other states will not accept a bond. Still others require that the bid security must be in the form of a bond. The form of the bid security is not standard and may even vary between agencies of the same state.

The amount of the bid security varies even more widely than the form. It is customary to specify the amount of the bid security in one of three ways:

1. A percentage of the bid. This usually varies from 5% to 33 1/3%, depending on the policy of the agency.
2. A fixed dollar value. This amount is determined by the agency and is usually predicated on the engineer's estimate of the cost of construction. Many agencies employing this method set a ceiling on the amount of the security. One state uses a sliding scale for jobs costing up to $500,000. For all contracts above this value the bid security is $10,000.
3. A percentage of the bid and a minimum fixed dollar value.

It is not the purpose of the writer to compare the merits of each of the three forms and types of bid securities. Rather, it is intended to apply the previously reported statistical analysis to this aspect of competitive bidding with the aim of determining the maximum justifiable amount of bid security.

If the low bidder is awarded, but refuses to sign the contract, he must forfeit his bid guarantee. If the agency elects to award the contract to the second bidder, the cost of owning the work is increased by an amount equal to the difference between the low and second bids. Since the bid security is not a penalty for refusing to sign the contract, but rather a form of insurance against the loss of the financial advantage of the low bid, the amount of the bid security should be equal to the amount of loss that can be reasonably anticipated. Or, should the agency reject all the bids and readvertise the job, rather than award it to the second low bidder, the probability is that the amount of loss of financial advantage in this instance will not exceed that of the first alternate. That is to say, the low bid of the readvertised proposal will hardly ever exceed the second low bid of the original proposal.

To be protected 97% of the time for the loss of financial advantage, if the low bidder refuses to enter into a contract, the amount of bid security should be equal to the maximum amount that will be left on the table 97% of the time. This amount is shown as the 97th percentile in Fig. 3, and as Eq. 9. This limit is suggested as the maximum limit because it is the boundary of the realm of probability. The rare cases wherein the spread exceeds this limit have been discussed under the heading "Mistake In Bid."

A certain New England State Highway Department requires bid security in the form of a bond in the amount of one third of the bid price. If the low bidder for a job in this state bids \$150,000 and leaves \$50,000 on the table, that is, second bid is \$200,000, he must either enter into a contract and possibly lose \$50,000, or he may forfeit his bid bond, that, too, is for \$50,000. From Fig. 3 it can be seen that this amount of security protects this state for an occurrence not likely in one time out of four hundred. Moreover, this policy gives the contractor little choice of whether of not to proceed with the work or of forfeiting his bid guarantee. However, according to Fig. 3, the 97th percentile indicates a bid security of from \$20,000 to \$25,000 as being sufficient insurance for all cases within the realm of probability for contracts of this size. Nevertheless, again referring to Fig. 3, a bid security of one third is justified for contracts less than \$10,000.

The amount of the bid guarantee is often a decisive factor in the economic life of a construction company. This singular factor is too often arbitrarily chosen, sometimes to the disadvantage of the owner and also to the disadvantage of the contractor. Logically, the amount of bid security should be based on the intended purpose of this requirement, namely, to reflect the possible loss of advantage of the low bid. But this potential loss is a measurable quantity. Hence the maximum amount of bid security should be a standardized requirement consistent with the facts introduced herein.

It appears that the most equitable arrangement is to require that bid bonds insure the owner for an amount equal to the actual difference between the low and second bids. But, in addition, provide an upper forfeiture limit not in excess of $3\ \Delta B_{av}$. (Note that $3\ \Delta B_{av}$ equals $3.24\ C^{0.734}$ and is also equal to ΔB from Eq. 9). When the bid security is in a form other than a bond, the amount to be posted should not exceed $3\ \Delta B_{av}$. In the event that the low bidder elects not to contract for the work, his guarantee, less the difference between his bid and the second bid, should be refunded to him.

USE OF AVERAGE BID PRICES

The items of work enumerated in a unit price proposal may be classified according to the following categories:

1. Minor
2. Subcontract
3. Major

These divisions are not mutually exclusive, since portions of the work required under a single item may fall into all three categories. For example, a contractor bidding for a job requiring structural concrete may find that the cost of placing the concrete is minor, whereas the expense of forming and stripping is major. Any finishing, such as rubbing and painting, the contractor will "sub out."

In the case of the unique contract representative of the 381 contracts used in this example, the average of each of the unit bid prices may yield a total bid that is in line with the other bids. There is, however, no such contract. The writer does, however, recall a singular job on which he was the low bidder. On this occasion, none of the unit bid prices he submitted were the lowest tendered. This is not a rare situation. But it does emphasize the justification of the use of going prices; in certain situations at least.

From Fig. 3, 67% of all the contracts had a spread equal to or less than the mean spread. If we assume that all the unit items of a proposal are equal in dollar value, then two thirds of the items will probably be bid with a spread at or lower than the average, while the remaining one third of the items will be bid with a spread at or higher than the average. And if we assume that the magnitude of the spread is indicative of the precision of the estimating, then it may be concluded that one third of the items may be bid by employing average prices. Since the probability is that further refinement will not reduce the probable spread. Therefore, the minor items may be considered as the maximum number of different items with an aggregate worth equal to about one third of the total contract price.

The assumptions underlying this conclusion are not always true. For example, it is possible that the low and second bids were both carelessly bid, yet the spread may be very small. Obviously, there is no corrolation between spread and precision in this instance. Also, there is no such contract wherein all the items are equal in aggregate value. Nevertheless, the suggested approach is expedient.

For some small jobs, every item may appear to be insignificant in itself. And, it may be most difficult to cull out minor items. In the case of certain large jobs, one third of the total contract price may include some items that should be estimated in detail. Great care and experience are requisite to using average prices. One of the items on a job bid by this writer was for "Trench Excavation - 0 ft To Over 15 ft Deep." Seven bidders used the going price of eight to ten dollars a cubic yard. Investigation showed that in this particular case the item would have been overpriced at eighty cents a cubic yard.

It is this writer's practice to use a 10% to 20% factor instead of the one third previously mentioned. And then only after determining that the average prices are applied only to items of work under average conditions.

Minor items of work when considered together constitute about one third of the total dollar value of a project. Should every minor item be poorly bid, the total error by comparison will be a small part of the total bid. Because of this and the fact that the use of minor items is often contingent on field circumstances that are difficult to predict, these items may be bid by using the average or going unit price. If there are a large number of such items, about thirty, the probability is that compensating errors, or the law of averages, will act on the total worth of these items to yield a price comparable to the average value of the minor items, all bids considered.

Items of work that entail soliciting a price, complete from others, and to which is added only the loading (allowance for overhead and profit), are nominally termed subcontract items and are included in this category. Unlike the other two categories, there are no computations required to find the cost for doing these items of work. Consequently, the question of average prices does not arise in these cases; rather, it is supplanted by the ability to trade.

All items of work not counted as either minor or subcontract are termed major. Also, all lump sum items that are not subcontracted must be included here because the going price cannot be readily ascertained. These items should always be bid on the basis of a careful cost study. And, in the case of lump sum items, on the basis of an accurate quantity take-off as well.

Properly applied, average unit bid prices may substantially reduce the time (and cost) of preparing a bid, with no appreciable sacrifice of precision. In certain cases, the use of average unit bid prices may also reduce the amount of money otherwise left on the table. Imprudent use of this tool, however, may result in irreparable harm.

METHOD OF CONSTANT WORK

Through the years, most contractors have come to estimate their chances of success at bidding. A contractor knows that he will be successful say, one time out of ten. And, after about nine unsuccessful bids will feel that "the next one is mine." If a contractor is successful, on an average of p% of the time, and his company needs n number of jobs a year to maintain an optimum work load, then the minumim number of jobs that must be bid, N, is

$$N = \frac{100\,n}{p} \quad \ldots\ldots\ldots\ldots\ldots\ldots\ldots \quad (10)$$

From Fig. 3 it is a simple matter to find the probability of leaving a given amount on the table. Conversely, if a given amount is added to the completed bid, the probability of losing the job may also be readily evaluated. For example, a contractor has prepared a completed bid, amounting to $100,000. It has not yet been submitted and unbeknown to him, his bid is the low bid. According to Table 4, the chances are 30 out of 100 that $2,000 or less will be left on the table. If, at the last minute, the contractor decides to add $2,000 to his bid, he eliminates these 30 out of 100 chances of being low bidder. In other words, while a bid of $100,000 is 100% certain of being the low bid, a bid of $102,000 is 100-30 or 70% certain. If this contractor's past record is p = 10% (from Eq. 10), then by adding the $2,000, p is now equal to 70% of 10%, or 7%.

As p decreases, the number of jobs that must be bid in order to maintain the optimum number of contracts, n, increases. Or,

$$N = \frac{100\,n}{p\,S} \quad \ldots\ldots\ldots\ldots\ldots\ldots\ldots \quad (11)$$

in which S is the success factor and is expressed as the number of chances out of 100 of leaving more than a specified amount on the table. This specified amount is the amount added to the bid in each case. An example will illustrate the application of this method.

The optimum number of jobs a year for a certain contractor is five, $400,000 contracts. In the past years, he has had to bid an average of 50 jobs a year in order to maintain this optimum condition, or $p = \left(\frac{5}{50}\right) \times 100\% = 10\%$. The contractor, in an effort to reduce the amount of money he leaves on the table, decides to arbitrarily add $4,000 to each bid in the future. How many jobs must he now bid in order to be successful the optimum number of times, five. From Fig. 3, the probability of leaving $4,000 or less on the table when bidding $400,000 is 20 chances out of 100. Then the success factor, S, is 100 - 20 or 80%. Substituting in Eq. 11:

$$N = \frac{100\ (5)}{(10)\ 80\%} = 62.5$$

The required number of jobs to be bid is 62.5. If the contractor can reasonably expect this number of jobs to be advertised then he is safe in increasing his bids by $4,000. By so doing, his volume of work will remain constant while increasing his annual profits by 5 x $4,000 or $20,000, at the expense of bidding an additional twelve to thirteen jobs a year.

METHOD OF MAXIMUM INCOME

Every dollar added to a completed bid increases the anticipated net profit by a like amount. However, any such increase also reduces the chances of being the low bidder. The optimum condition exists when the probable gain minus the probable loss is a maximum value. The probable gain is equal to the success factor, S, multiplied by the corresponding value of the bid increase, Δb. The probable loss is equal to 100 minus S multiplied by the anticipated profits, p_a, or:

$$(S\,\Delta b) - p_a(100 - S) = \text{maximum} \quad \ldots\ldots\ldots\ldots \quad (12)$$

This expression may also be stated as:

$$S(\Delta b + p_a) - 100\,p_a = \text{maximum} \quad \ldots\ldots\ldots\ldots \quad (13)$$

But, as previously pointed out, Δb is directly proportional to $(100 - S)$ when $(100 - S)$ is equal to or less than 67. Then if $\Delta B_{(1)}$ represents the spread when $(100 - S)$ equals unity, a direct proportion may be set up from which:

$$\Delta b = (100 - S)\,\Delta B_{(1)} \quad \ldots\ldots\ldots\ldots\ldots \quad (14)$$

Now express p_a in terms of $\Delta B_{(1)}$, or:

$$p_a = j\,\Delta B_{(1)} \quad \ldots\ldots\ldots\ldots\ldots\ldots \quad (15)$$

Substituting Eqs. 14 and 15 in Eq. 13, factoring and simplifying yields:

$$S(100 - S) + j\,(S - 100) = \text{maximum} \quad \ldots\ldots\ldots\ldots \quad (16)$$

By differentiation, the maximum value is obtained when:

$$S = \frac{1}{2}\,(100 + j) \quad \ldots\ldots\ldots\ldots\ldots\ldots \quad (17)$$

in which j is equal to $p_a/\Delta B_{(1)}$. Values of S greater than 100 are meaningless and should be considered equal to 100.

An extension of the example cited under the heading Method of Constant Work will illustrate the application of this, the Method of Maximum Income.

A contractor has prepared a bid for $400,000. If he is the successful bidder he anticipates a net profit, in the bank, of $10,000. How much, if anything, should he add to his bid for maximum income? Then:

$$p_a = \$10{,}000$$

and from Fig. 3:

$$\Delta B_{(1)} = \$200$$

so that:

$$j = 10{,}000/200 = 50$$

Now substituting in Eq. 17:

$$S = \frac{1}{2}\,(100 + 50) = 75$$

and again from Fig. 3:

$$\Delta b = \$5{,}000$$

Therefore, the optimum amount this contractor should add to his bid is \$5,000. By doing this, he increases his anticipated profits by (\$5,000/\$10,000) x 100% or 50%. However, this is done at some relatively small risk. Because, if his original bid of \$400,000 was the low bid, now his chances are reduced to 75 out of 100 that his bid of \$405,000 will still be low.

The contractor should now apply the previously described Method of Constant Work to determine the effect of increasing his bid and corresponding reduction in his probability of being successful on the number of jobs he must bid in order to maintain the optimum work load for his company. In fine, the value of S should be evaluated in terms of both methods discussed.

Table 8 illustrates the probable financial advantages resulting from the application of this method. The example used in the text is also used as the basis for making the comparisons. In the table, two types of revised bids are considered. In the first instance, the number of jobs bid, N, is kept constant with respect to the original case. In the second instance, the number of successful (low) bids, n, is the constant. In either case, the probable financial advantage is significant.

Eqs. 14 and 17 may be combined to yield the general expression for finding the optimum amount to be added to the completed bid, directly:

$$\Delta b = \Delta B_{\text{median}} - \frac{p_a}{2} \qquad (18)$$

If Eq. 18 is used, the success factor, S, is found directly from Fig. 3.

In solving the illustrative examples, the longer, step-by-step method is used rather than Eq. 18. This is done only to better acquaint the reader with the mechanics of the solutions.

METHOD OF MAXIMUM PROFIT

This method is but a modification of and corrolary to the Method of Maximum Income. It has the advantage of giving the amount of profit to be added to the raw cost of the bid by a one step computation. However, it lacks the prime facility of determining a value for S. Nevertheless, if work is plentiful and past experience indicates that it is not practical to attempt to estimate the net profit from a bid, then this method will prove to be expedient. In this discussion, the symbol p_a is equal to and is used in place of the symbol Δb, since Δb is herein equal to the amount to be added to the raw cost.

From the Method of Maximum Income, when S equals 100, nothing is added to the bid. In other words, p_a is a maximum value. But when S equals 100, j must equal 100. Then,

$$\frac{p_a}{\Delta B_{(1)}} = 100$$

but,

$$\Delta B_{(1)} = \frac{\Delta B_{av}}{67} \qquad (19)$$

UNIVERSITY OF MICHIGAN LIBRARY

in which $\Delta B_{(1)}$ is the spreadat the first (1st) percentile previously discussed. Substituting in Eq. 17 and simplifying:

$$S = 50 + \frac{33\frac{1}{3}\, p_a}{\Delta B_{av}} \qquad \text{(20)}$$

Then for S to equal 100,

$$p_a \geqq 1.5\, \Delta B_{av} \qquad \text{(21)}$$

This is the allowance for profit to be added to the raw cost.

A more conservative approach is to add to the raw cost of the bid the average spread, ΔB_{av}, since this value is the average spread that will occur with contracts containing an allowance for profit. The success factor in this case is, from Eq. 17,

TABLE 8.—COMPARISON BETWEEN EARNINGS

Item (1)	Original (2)	Revised; S = 75%	
		Constant N (3)	Constant n (4)
Number of jobs bid, N	50	50	66.67
Number of successful bids, n	5	3.75	5
Percentage of time successful, p	10	7.5	7.5
Amount of bid, intended, C	$ 400,000	$ 400,000	$ 400,000
Amount added to bid, Δb	0	$ 5,000	$ 5,000
Amount of bid, submitted, $C + \Delta b$	$ 400,000	$ 405,000	$ 405,000
Anticipated profit originally, p_a	$ 10,000	$ 10,000	$ 10,000
Anticipated profit revised, $p_a + \Delta b$	$ 10,000	$ 15,000	$ 15,000
Gross income, $n\,(C + \Delta b)$	$2,000,000	$1,518,750	$2,025,000
Net income, $n\,(p_a + \Delta b)$	$ 50,000	$ 56,250	$ 75,000

$$S = \frac{1}{2}\left(100 + \frac{\Delta B_{av}}{\Delta B_{(1)}}\right) \qquad \text{(22)}$$

but $\Delta B_{av}/\Delta B_{(1)}$ equals 67. Therefore, S equals 83.5. Now, if the bid in the form of the raw cost, plus an allowance for profit equal to ΔB_{av} is 100 percent certain of being the low bid, then by adding an additional 16.5 $\Delta B_{(1)}$ to the bid it becomes 83.5 certain of being low. The total allowance for profit to be added to the raw cost is

$$p_a = 1.25\, \Delta B_{av} \qquad \text{(23)}$$

A still more conservative approach is to say that the contractor is prepared to bid the job at cost. Then from Eq. 17, S equals 50, or,

$$p_a = 0.75\, \Delta B_{av} \qquad \text{(24)}$$

Eq. 24 is the fiftieth percentile in Fig. 3.

There are, of course, an infinite number of values for p_a. The three outlined previously are presented only to facilitate a choice.

CONCLUSIONS

It is evident that a rational approach exists where intuition and hunches now prevail. It has been the primary aim of this writer to illustrate the fact that a logical and mathematical solution exists to problems of competitive bidding[4] just as it does for other problems in construction engineering. The specific techniques and suggested applications must be subordinated to this proposition.

The conclusions as such are manifested in the latter portions of the paper under the heading "Applications of Results." In summary, they are:

1. The difference between the low and second bids is related to the amount of the low bid in terms of probabilities.
2. However, additional investigation, using more advanced statistical methods, should be applied. This should be done not only to refine, but also to advance the analysis. For example, the log-probability law may better relate the variables in Table 5 as well as establish a standard error of estimate.
3. Similar provisions, relating to mistakes in bids, as used by the Corps of Engineers are justified and should be incorporated in State contracts as well. In addition, some provision should be made in the contract documents to allow an obviously erroneous bid to be withdrawn without penalty. The following clause is suggested:

> "Withdrawal of Erroneous Bid. The bidder may withdraw his bid after bids have been opened, if his bid is low and if the difference between his bid and the second low bid exceeds the following amounts:
>
> If the low bid is \$10,000 or less - \$3,000; if the bid is more than \$10,000 but not more than \$50,000 - 30% of the bid; if the bid is more than \$50,000 but less than \$1,000,000 - \$15,000 plus 10% of the bid over \$50,000; if the bid is \$1,000,000 or more - \$110,000 plus 5% of the bid over \$1,000,000.
>
> Withdrawal of the bid shall be without prejudice or penalty."

4. The amount of the bid security should not exceed the amounts listed in the preceding schedule. The forfeiture clause should also provide for reimbursement of the difference between the spread and the amount of bid security posted.
5. Generally speaking, average unit bid prices may be used to price up to one third of the dollar value of the bid without sacrificing precision.
6. The optimum profit to include in a bid is a unique value. This value depends on the probable spread that, in turn, is a function of the amount of the contract.

The application of engineering disciplines to even so subjective a topic as competitive bidding is logically and mathematically justified. The techniques, though simple, may prove to be a useful tool; for the contractor as a means of

---

[4] "Aspects of Competitive Bidding: Unbalanced Bidding and A Rational Method for Calculating Bid Prices," *75th Annual Report*, Conn. Soc. of Civ. Engrs.

UNIVERSITY OF MICHIGAN LIBRARY

increasing profits, as well as an aid to the owner-engineer to assist him in equating that is reasonable with cautiousness.

ACKNOWLEDGMENT

Valuable, constructive criticisms were made by several of this writer's associates who are in the construction and engineering professions.

APPENDIX.—NOTATION

The following symbols are adopted for use in this paper.

a = constant;
a = value of a sample;
a = dimensionless parameter;
b = constant;
C = amount of the low bid;
C = geometric mean of the limits of a contract group;
G_m = geometric mean;
j = ratio of the anticipated profit to $\Delta B_{(1)}$;
n = total number of samples;
n = dimensionless parameter;
n = number of successful bids in a given time;
N = number of bids required to yield n low bids;
p = percentage of N equal to n;
p = spread expressed as a percentage of the low bid, calculated;
p_a = anticipated profit;
P = low bid expressed a percentage of the second bid;
$\overline{P}$ = geometric average of P;
P' = spread expressed as a percentage of the low bid, observed;
$\overline{P}'$ = geometric average of P';
S = percentage of time a spread equal to or greater than ΔB will occur;
Δb = amount added to the completed bid;
ΔB = difference between the low and second bids;
ΔB_{av} = average amount left on the table;
ΔB_{median} = maximum spread occurring 50% of the time; and
$\Delta B(1)$ = maximum spread occurring 1% of the time.

AMERICAN SOCIETY OF CIVIL ENGINEERS

Founded November 5, 1852

TRANSACTIONS

Paper No. 3211

LOAD DISTRIBUTION OF DIAPHRAGMS IN I-BEAM BRIDGES

By Benjamin C. F. Wei,[1] M. ASCE

SYNOPSIS

This paper presents an analytical study of the effects of diaphragms in I-beam bridges. The structures considered in the analyses are simple-span right bridges, consisting of a continuous slab supported by five uniformly-spaced parallel beams of equal stiffness, with the beams running in the direction of traffic. The diaphragms, which may be in the form of a channel, a WF-beam, or a built-up section, are transverse framings in the structure. Several variables are studied including (1) relative stiffness of diaphragm to that of each beam, (2) the position of diaphragms in the structure, (3) relative stiffness of beams to that of slab, (4) relative dimensions of bridge, and (5) the type and position of loading. The influence of the diaphragms on the behavior of the edge beam is also included.

From the results of the analyses, studies and comparisons are made to investigate the effects of different variables on the action of diaphragms in distributing the load on the bridge. The criteria of comparison is in general the maximum moment in beams produced by unit load or 4-wheel loading, with particular emphasis on the latter to simulate the actual loading condition. For one specific case, the analytical results are compared to those given for a full-size field test. Conclusions and design recommendations with regard to the effective use of diaphragms in I-beam bridges are also presented.

INTRODUCTION

Object and Scope of Investigation.—The studies presented were undertaken to obtain a better understanding of the action of diaphragms in I-beam bridges. The I-beam bridge, consisting of a concrete roadway slab continuous over steel stringers, has found wide-spread application for highway bridges because of

---

Note.—Published essentially as printed here, in May, 1959, in the Journal of the Structural Division, as Proceedings Paper 2036. Positions and titles given are those in effect when the paper or discussion was approved for publication in Transactions.

[1] Proj. Engr., Curtiss-Wright Corp., Wright Aero. Div., Wood-Ridge, N. J.

UNIVERSITY OF MICHIGAN LIBRARY

its simplicity of design and ease of construction. The diaphragms, in the form of channels, WF-beams, or built-up angle frames, are transverse framing devices, which are added to the structure with the following purposes: (1) to improve the distribution of load in the structure to the supporting beams, (2) to facilitate erection of the span, and (3) to stiffen, in general, the bridge so that it may act more efficiently as one integral unit under load. The lateral load-distribution characteristics of diaphragms are investigated in order to obtain a rational basis for the design of diaphragms in the most common type of highway bridges.

The data contained herein apply to simple-span right bridges consisting of a continuous slab supported by five uniformly-spaced parallel beams of equal stiffness, with diaphragms framed transversely in different positions between the beams.

The problem of the I-beam bridge with a concrete slab roadway supported on beams which are interlaced with diaphragms is statically indeterminate to a high order. The exact solution to the problem is complicated and is not suitable for practical use. A numerical distribution procedure for the analysis of slabs continuous over flexible beams by N. M. Newmark, F. ASCE, furnishes[2] a convenient tool for analyzing the structure which is followed in this investigation. With this basic procedure and a technique developed for superposing the action of diaphragms to the flexible beams, a large number of analyses were performed to investigate the effects of the following variables on the action of diaphragms in the structure: (1) relative stiffness of diaphragm to that of each beam, (2) the position of diaphragms in the structure, (3) relative stiffness of beams to that of slab, (4) relative dimensions of the bridge, and (5) the type and position of loading. For one case the analytical results were compared with those derived from a field test of a full-size bridge.

The bridges considered herein have beams in the direction of traffic and a ratio of beam spacing to span equal to 0.1. The flexibility of the beams is included in the analyses. In general, the maximum moments in the beams are determined for different positions of a concentrated load on the structure.

Diaphragms of various stiffnesses framed at midspan, each third-point, each quarter-point, and midspan plus quarter-points are used. Influence coefficients for moment are obtained for a group of these structures with various proportions and relative stiffnesses of beams and slab. From the influence values, moments in the beams are determined for standard highway truck loads with spacings of beams between the limits of 5 ft to 8 ft. Based on moments under unit and truck loadings, studies are made to determine the influence of the variables in affecting the load-distributing behavior of the diaphragms in the structure. Special attentions have been directed to explore questions often raised by designing engineers such as, How effective is a relatively flexible diaphragm? Is the effectiveness of a diaphragm proportional to its stiffness? What is the best position of a diaphragm? and Are closed-spaced diaphragms necessarily more effective than a single one? The effect of diaphragms on the behavior of the edge beam is also studied.

---

[2] "A Distribution Procedure for the Analysis of Slabs Continuous over Flexible Beams," by N. M. Newmark, Engrg. Experiment Sta. Bulletin 304, Univ. of Illinois, Urbana, Ill., 1938.

Basic Assumptions.—The distribution procedure used in the analysis is based on the ordinary theory of flexure for plates. The following assumptions are involved in the solution of the problem:

1. The material in the slab is homogeneous, elastic, isotropic, and of constant thickness.
2. The resultant of the normal stresses acting on any cross-section of the slab is a pure couple.
3. Flexural strains vary linearly through the depth of the slab.
4. The beams exert only vertical forces on the slab; there is no shear between the top flange of the beams and the bottom of the slab.
5. The reaction of the beam acts on the slab along a line and is not distributed over a finite width. The torsional restraint offered by the I-beams is not included in the analysis.
6. A beam and the slab directly over it deflect the same amounts and in the same shape; that is, there is no separation between the slab and the beam.
7. The connections of the diaphragms to the beams are fully effective. In other words, the right angle relationship between the web of the beam and a line through the mid-height of the diaphragm will be kept after deformation. This condition will permit rotation of beams as shown in Fig. 1.
8. The top of the diaphragm does not touch the bottom of the slab under any loading condition.
9. Both the slab and the beams are simply supported at the ends of the span.

In addition, the value of Poisson's ratio for concrete is assumed to be zero in all the computations.

Notation.—The letter symbols adopted for use in this paper are defined where they first appear, in the illustrations or in the text, and are listed for convenience of reference, in the Appendix. The longitudinal direction is always taken as the direction of the beam.

METHOD OF ANALYSIS

Fundamental Concepts of Load Distribution in I-beam Bridges.—Fig. 2 shows a typical plan and section of the bridge analyzed. The diaphragms are located at one of the following positions, namely, midspan, each third-point, each quarter-point, and midspan plus quarter-points. To avoid confusion, the designation "each quarter-point" means only those two positions at one-quarter of the span from the simply supported ends, not including the center point. The three-point case is designated as the "midspan plus quarter-points."

Consider first an I-beam bridge without diaphragms. When a load is applied to the bridge, it is distributed by the slab to the beams and ultimately by the beams to the abutments. Obviously, the beams act as principal load-carrying elements in an I-beam bridge. Since the loads are distributed to the beams through the slab, the proportion of load each beam carries depends to a great extent on the stiffness of slab. The relation between the stiffness of beam and slab is expressed by a dimensionless coefficient

$$H = \frac{E_b I_b}{a N} \quad \text{.....................} \quad (1)$$

in which E_b is the modulus of elasticity of the material in a beam, I_b denotes

UNIVERSITY OF MICHIGAN LIBRARY

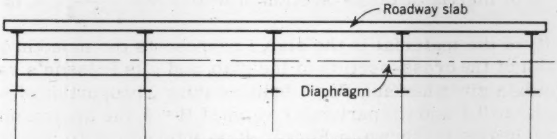
Roadway slab
Diaphragm

(*a*) BEFORE DEFORMATION

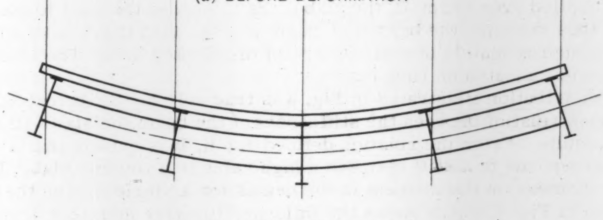

(*b*) AFTER DEFORMATION

FIG. 1.—ROTATION OF BEAMS AFTER DEFORMATION

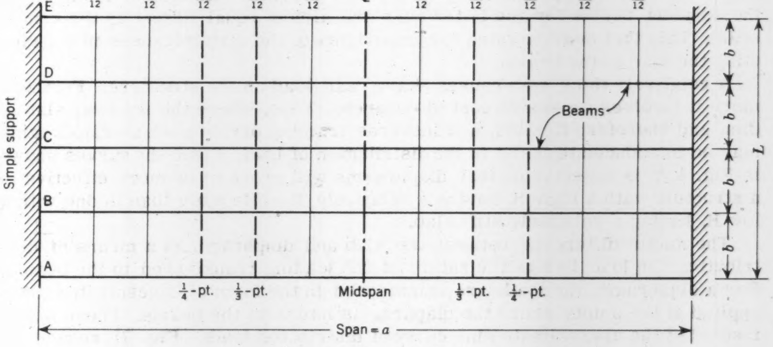
$\frac{1}{12}$
$\frac{2}{12}$
$\frac{3}{12}$
$\frac{4}{12}$
$\frac{5}{12}$
℄
$\frac{7}{12}$
$\frac{8}{12}$
$\frac{9}{12}$
$\frac{10}{12}$
$\frac{11}{12}$
E
D
C
B
A
Simple support
Beams
b
b
b
b
L
$\frac{1}{4}$-pt.
$\frac{1}{3}$-pt.
Midspan
$\frac{1}{3}$-pt.
$\frac{1}{4}$-pt.
Span = a

(*a*) PLAN OF BRIDGE

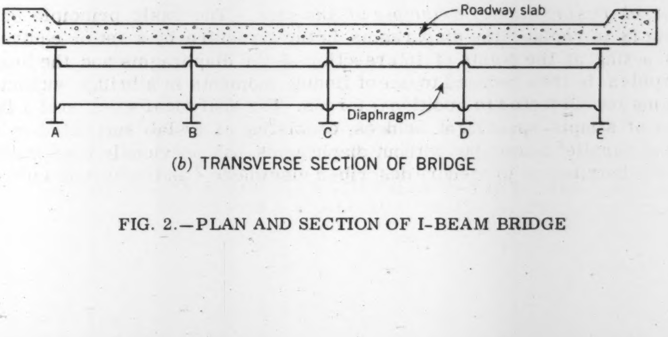
Roadway slab
Diaphragm
A
B
C
D
E

(*b*) TRANSVERSE SECTION OF BRIDGE

FIG. 2.—PLAN AND SECTION OF I-BEAM BRIDGE

the moment of inertia of cross-section of beam, $N = \frac{E\,I}{1 - \mu^2}$, E is the modulus of elasticity of the material in the slab, I represents the moment of inertia per unit of width of the cross-section of the slab, and μ is Poisson's ratio, taken as zero in the data given herein. For a bridge having a proportion of beam spacing to span equal to 0.1 and the particular value of H = 5, the approximate load distribution on beams is shown in Fig. 3. It is interesting to note that when the load is applied over beam B, the slab tends to spread the load to the adjacent beams, thus reducing the burden of beam B. The load thus transferred takes the form approximately of a sine curve of distributed load. The total distributed load is indicated on each curve.

The distribution illustrated in Fig. 3 is true only for the bridge with H = 5. A different relation between the stiffnesses of the beam and slab will yield different results. From the relation defined for H, it is evident that a low value of H corresponds to a stiff slab and a high value to a flexible slab. The effect of slab stiffness on the moment in the beams for a single load on the bridge is indicated in Fig. 4, which shows the influence lines for moments at midspan of beam C, the center beam in a 5-beam bridge with b/a = 0.1. For the curve $H = \infty$ corresponding to a slab of zero stiffness, the static moment due to a load at C is carried entirely by beam C and is equal to 0.25 P a, the other beams all having zero moment. On the other hand, if H is reduced to 0.5, corresponding to a relatively stiff slab, the moment in beam C for the same load at C becomes 0.064 P a, approximately 25% of the previous value. The moments in the adjacent beams for the latter case are almost equal to that in the center beam. This fact demonstrates the importance of the slab thickness in distributing the load to the beams.

A relatively thick slab causes heavy dead load on the structure. Furthermore it involves excessive cost of concrete. Thus, where the roadway slab is thin, and therefore flexible, a transverse framing device such as diaphragms may be introduced to assist in the distribution of load. From the curves shown in Fig. 4, it is conceivable that diaphragms will prove to be more effective in a structure with a high H, having a relatively flexible slab, than in one with a low H, having a relatively stiff slab.

The major difference between the slab and diaphragm as a means of distributing the load lies in the nature of the loading transferred to the beams. For a diaphragm, the loads are transferred in the form of concentrated loads applied at the points where the diaphragms intersect the beams. These loads, instead of the approximate sine curve of distributed loads (Fig. 3), reduce the burden of the loaded beam. All the bridges treated herein have a roadway slab. The addition of diaphragms to these structures will cause a combination of the action of the approximate sine curve of distributed loads and the concentrated loads.

General Description of Principle of Analysis.—The basic principle of the problem is to replace the diaphragms in the structure by a set of equivalent forces acting at the points of intersection of the diaphragms and the beams. The problem is then reduced to one of finding moments in a bridge without diaphragms but subjected to additional forces. The analytical solution of a large number of simple-span right bridges, consisting of a slab supported by five identical parallel beams but without diaphragms, has previously been made by using the distribution procedure described elsewhere,[2] and numerous influence

UNIVERSITY OF MICHIGAN LIBRARY

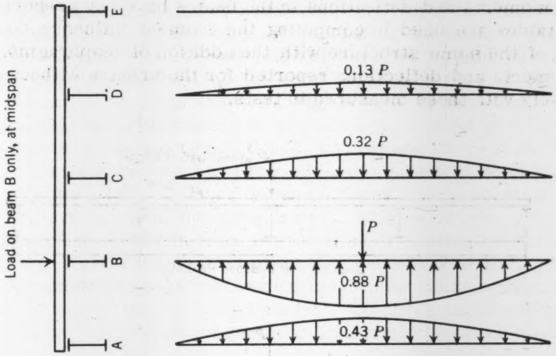
Load on beam B only, at midspan
A
B
C
D
E
0.13 P
0.32 P
P
0.88 P
0.43 P

FIG. 3.—ACTION OF SLAB IN DISTRIBUTING CONCENTRATED LOAD

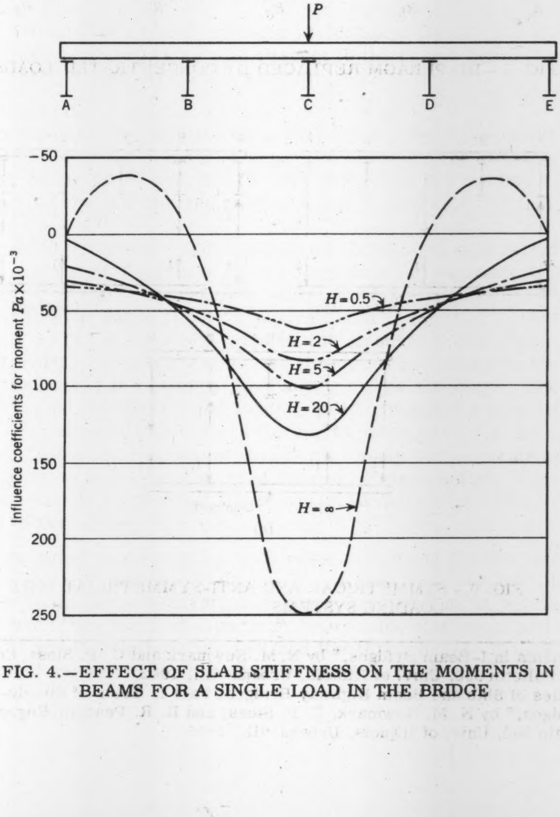

FIG. 4.—EFFECT OF SLAB STIFFNESS ON THE MOMENTS IN BEAMS FOR A SINGLE LOAD IN THE BRIDGE

tables for moments and deflections in the beams have been reported.[3] These influence tables are used in computing the moment influence coefficients in the beams of the same structure with the addition of diaphragms. The theoretical moments and deflections reported for the bridges without diaphragms agree closely with those measured in tests.[4]

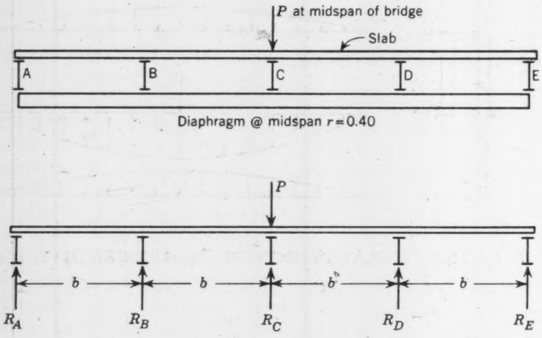
P at midspan of bridge
Slab
A
B
C
D
E
Diaphragm @ midspan r = 0.40
P
b
b
b
b
R_A
R_B
R_C
R_D
R_E

FIG. 5.—DIAPHRAGM REPLACED BY CONCENTRATED LOADS

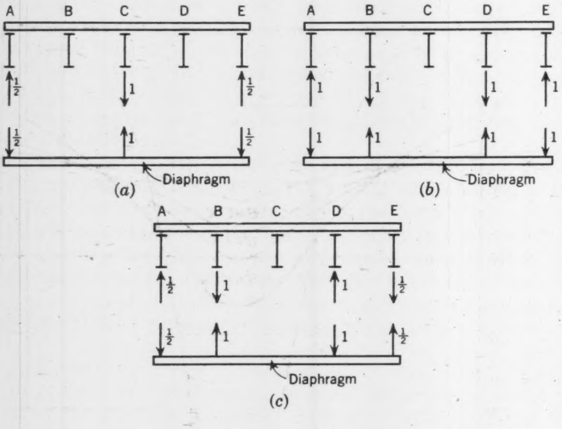
A
B
C
D
E
½
1
½
½
1
½
Diaphragm
(a)
A
B
C
D
E
1
1
1
1
1
1
1
1
Diaphragm
(b)
A
B
C
D
E
½
1
1
½
½
1
1
½
Diaphragm
(c)

FIG. 6.—SYMMETRICAL AND ANTI-SYMMETRICAL UNIT LOADING SYSTEMS

---

[3] "Moments in I-Beam Bridges," by N. M. Newmark and C. P. Siess, Engrg. Experiment Sta. Bulletin 336, Univ. of Illinois, Urbana, Ill., 1942.

[4] "Studies of Slab and Beam Highway Bridges; Part I. Tests of Simple-Span Right I-Beam Bridges," by N. M. Newmark, C. P. Siess, and R. R. Penman, Engrg. Experiment Sta. Bulletin 363, Univ. of Illinois, Urbana, Ill., 1946.

Consider a bridge consisting of a slab supported by five identical I-beams with diaphragms framed transversely at midspan of the bridge. By assuming that the connections between the individual diaphragms and the beams are fully effective, one can virtually replace the four separate pieces of diaphragm by one continuous cross beam as shown in Fig. 5. The bridge may now be analyzed by removing the diaphragm and replacing it by a set of unknown reactions at the points of intersection of the diaphragm and the beams. This set of unknown reactions can be found by the method of consistent deformation.

In order to solve a large number of cases, it was found expedient to resolve the load into its symmetrical and antisymmetrical components. The advantage of the resolution lies chiefly in reducing the number of simultaneous equations in each solution. Furthermore, this procedure was adapted to treat different relative diaphragm stiffnesses and loading conditions in one operation of computation. An outline of the method of analysis for three cases differing in the arrangement of diaphragms is presented to illustrate the procedure:

Case 1. Bridge with one diaphragm at midspan only.

Case 2. Bridge with two diaphragms at symmetrical positions with respect to midspan.

Case 3. Bridge with three diaphragms, one at midspan and two at symmetrical positions with respect to midspan.

Case 1. Bridge With One Diaphragm at Midspan Only.—The symmetrical and antisymmetrical conditions with respect to the center beam (beam C, Fig. 2) are separately considered and then combined.

(A) Symmetrical condition with respect to beam C.

(a) Using the two symmetrical unit loading systems as shown in Fig. 6(a) and (b), find the amount of separation between the diaphragm and the beams at points B, C, and D. The net deflection for the two free bodies should be used so that the end points, A and E, are kept together with zero separation.

(b) Find, from the relation obtained in (a), two sets of forces $P_{B,D}$ and P_C; one set of $P_{B,D}$ and P_C is to produce unit separation at C but no separation at B and D whereas the other set of $P_{B,D}$ and P_C is to produce unit separation at B and D but no separation at C.

(c) Find the separations between the diaphragm and the beams at B, C, and D, relative to a horizontal line through A and E, due to the symmetrical component of the external load acting on the structure. The antisymmetrical component of external loading will be included in step (c) of (B).

(d) From the coefficients in (b) and the separations found in (c), find the forces that must be present in order to make the separations equal to zero. Forces will also be present at the end points to satisfy statics. These forces or reactions represent the restraint to deflection offered by the diaphragm to the bridge.

(B) Antisymmetrical condition with respect to beam C.—The treatment of this part is similar to that in (A) except that in this case, because of antisymmetry, there would be no separation at point C as well as at points A and E.

(a) Find the amount of separation between the diaphragm and the beams at points B and D, relative to an inclined line through A-C-E, under an antisymmetrical system of loading as shown in Fig. 6(c).

(b) From the relation found in (a), find the force $P_{B,D}$ which will produce unit separation at B and D. The force P_C is not necessary since the relative separation at point C due to antisymmetrical component of the external load is equal to zero.

(c) Find the separations between the diaphragm and the beams at B and D, relative to an inclined line through A-C-E, due to the antisymmetrical component of the external load acting on the structure.

(d) Find, as in step (d) of (A), using the relation from (b) and (c), the forces that must be present to make the separations equal to zero.

(C) Combine the reactions obtained in (d) for both the symmetrical and antisymmetrical conditions. The bridge may then be analyzed as one without diaphragms but with additional forces acting along the diaphragm line on beams A, B, C, D, and E.

Case 2. Bridge With Two Diaphragms at Symmetrical Positions With Respect to Midspan.—The method used to analyze this case is similar to the one outlined in detail for Case 1. Since there are now two diaphragms in the structure, one must, in steps (A) - (a) and (B) - (a) previously mentioned, find the separations between the diaphragms and beams due to the loading systems on both diaphragms at the same time. Furthermore, if the external load is not acting at midspan of the bridge, the symmetrical and antisymmetrical loading with respect to beam C must further be resolved into symmetrical and antisymmetrical loadings with respect to midspan. This resolution is shown graphically in Fig. 7.

The combination as described in Case 1 (C) should then be composed of four loading conditions as shown in Fig. 7. However, if the load is applied at midspan, the further resolution is not necessary.

Case 3. Bridge With Three Diaphragms, One at Midspan and Two at Symmetrical Positions with Respect to Midspan.—This case can be analyzed as a combination of Cases 1 and 2 by using the method of superposition. Consider first a structure with two diaphragms at symmetrical positions with respect to midspan as the basic structure. Use the influence coefficients for moment and deflection found for this basic structure and analyze the original structure as if there is only one diaphragm at midspan. A similar procedure may be followed for a bridge with more than three diaphragms.

RESULTS OF ANALYSES

Description of Bridges Analyzed.—Eighty-five structures varying in ratios of beam spacing to span, in relative stiffnesses of beams and slab, and in stiffnesses and locations of diaphragms were analyzed. Complete results of the analyses have been reported elsewhere.[5]

One important preliminary consideration in selecting a bridge to be analyzed is the ratio of beam spacing to the span of bridge (b/a). The selection of the beam spacing has not been treated extensively in the literature of structural design. The economic phase of the study is complicated and involves several variables. In general closer spacing will call for more rockers, rollers and

---

[5] "Effects of Diaphragms in I-Beam Bridges," by B. C. F. Wei, thesis presented to the Univ. of Illinois, at Urbana, Ill., in 1951, in partial fulfillment of the requirements for the degree of Doctor of Philosophy.

UNIVERSITY OF MICHIGAN LIBRARY

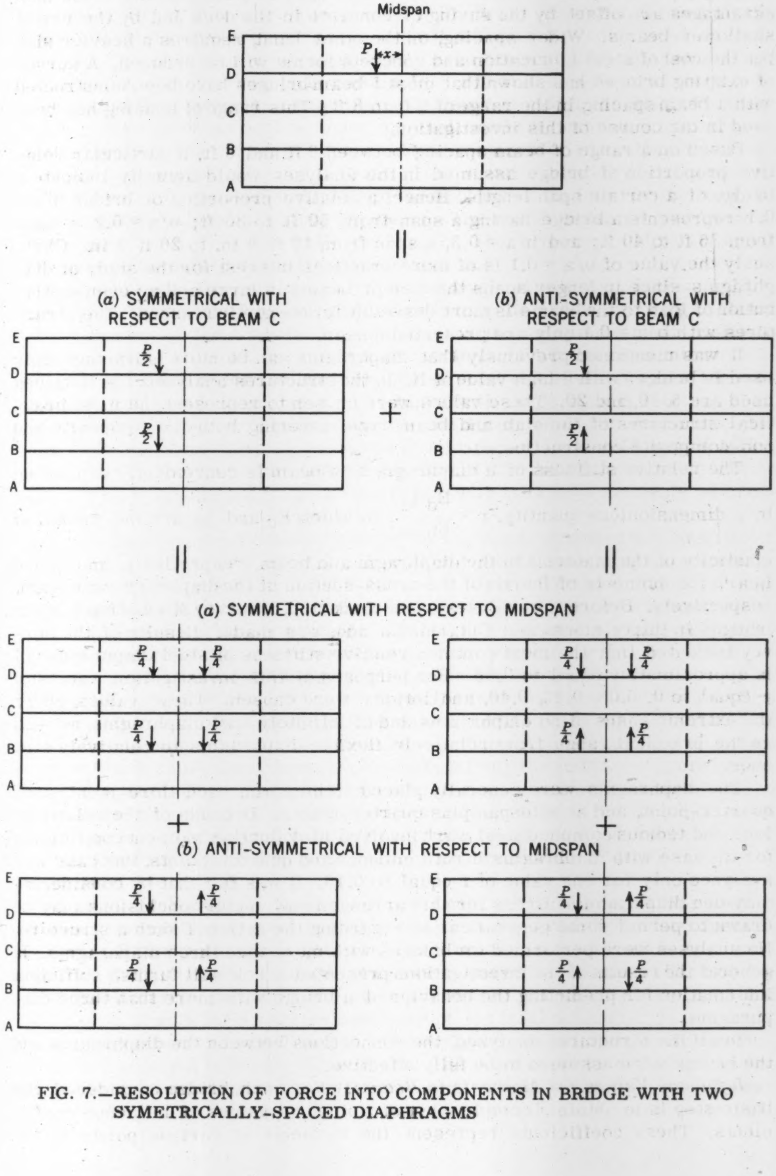
Midspan
E
D
C
B
A
P
x
(a) SYMMETRICAL WITH RESPECT TO BEAM C
(b) ANTI-SYMMETRICAL WITH RESPECT TO BEAM C
P/2
P/2
P/2
P/2
(a) SYMMETRICAL WITH RESPECT TO MIDSPAN
(b) ANTI-SYMMETRICAL WITH RESPECT TO MIDSPAN
P/4

FIG. 7.—RESOLUTION OF FORCE INTO COMPONENTS IN BRIDGE WITH TWO SYMETRICALLY-SPACED DIAPHRAGMS

bearing plates, and more steel for the diaphragm connections, but these disadvantages are offset by the saving of concrete in the deck and by the use of shallower beams. Wider spacing, on the other hand, requires a heavier slab but the cost of steel fabrication and concrete forms will be reduced. A survey of existing bridges has shown that most I-beam bridges have been constructed with a beam spacing in the range of 5 ft to 8 ft. This range of spacing has been used in the course of this investigation.

Based on a range of beam spacing between 5 ft and 8 ft, a particular relative proportion of bridge assumed in the analyses would actually indicate a bridge of a certain span length. Hence, a relative proportion of bridge $b/a = 0.1$ represents a bridge having a span from 50 ft to 80 ft; $b/a = 0.2$, a span from 25 ft to 40 ft; and $b/a = 0.3$, a span from 16 ft 8 in. to 26 ft 8 in. Obviously the value of $b/a = 0.1$ is of more practical interest for the study of diaphragms since in longer spans the size of beams is large and an even distribution of load to the beams is more desirable for economic reasons. The structures with $b/a = 0.1$ only are presented herein.

It was mentioned previously that diaphragms can be more advantageously used in bridges with a high value of H. In the structures analyzed, the H values used are 5, 10, and 20. These values were chosen to represent the most practical structures of the slab and beam type, covering both the composite and non-composite construction.

The relative stiffness of a diaphragm to a beam is conveniently expressed by a dimensionless quantity, $r = \frac{E_d I_d}{E_b I_b}$, in which E_d and E_b are the moduli of elasticity of the material in the diaphragm and beam, respectively, and I_d and I_b are the moments of inertia of the cross-section of the diaphragm and beam, respectively. Before the analyses were conducted, a survey of existing I-beam bridges in thirty states and Ontario, Canada, was made. Results of the survey indicated that the most common relative stiffness of steel diaphragm (r) is approximately equal to 0.05. For purposes of this investigation, values of r equal to 0. 0.05, 0.15, 0.40, and infinity were chosen. These values cover the extreme cases of no diaphragms and of infinitely stiff diaphragms, as well as the practical range from relatively flexible diaphragms to relatively stiff ones.

The diaphragms were generally placed at midspan, each third-point, each quarter-point, and at midspan plus quarter-points. Because of the relatively long and tedious computational work involved in evaluating moment coefficients for the case with diaphragms at both midspan and quarter-points, this case was analyzed only for one value of r equal to 0.15. It was felt that by considering only one diaphragm stiffness for this arrangement, useful conclusions may be drawn to permit some generalization regarding the action of such a structure. No analyses were performed for bridges with more than three diaphragms. In general the results of the investigations presented herein will furnish sufficient information for predicting the behavior of a bridge with more than three diaphragms.

In all the structures analyzed, the connections between the diaphragms and the beams were assumed to be fully effective.

Influence Values for Moments in Beams.—For each bridge considered, the basic step is to obtain a complete set of numerical values of influence coefficients. These coefficients represent the moments at various points in the beams for a unit load moving transversely on the bridge. Initially it was planned to find directly the maximum moment in the beam. However, the complexity of the action of structure under load made it difficult to predict at which location longitudinally the maximum moment in the beam would occur for a single load moving along the beam. For example, if a load is applied away from midspan, would the maximum moment be at midspan or under the load? Furthermore, if the maximum occurs under the load, would it occur at midspan, or at some other point on the beam? A considerable amount of computation time can be saved once a generalization is found. Thus, a large number of computations were made for moment at midspan and moment under the load for the load applied at different locations along the beam. The result indicated that the moment under the load is generally the larger. These moments directly under the load are therefore used in the investigation.

Longitudinally, the load is applied successively at midspan, 5/12 a, 4/12 a, and 3/12 a, these positions being measured from the end of the bridge. Based on the results of the analysis for diaphragms at two symmetrical positions with respect to midspan, the maximum moments in all beams occur at midspan of the bridge under the load. For these positions of diaphragms, the moments at midspan only are used. For cases with diaphragm at midspan only, and at both midspan and quarter-points, the locations of the maximum moment vary and, consequently, moments at midspan, 5/12 a, 4/12 a, and 3/12 a are derived. The magnitude and the location of the maximum moment can be obtained by interpolating from curves drawn with the known moments as ordinates and their locations as abscissas.

Fig. 8 shows a set of influence lines for the edge, intermediate and center beams for a bridge with $b/a = 0.1$, $H = 10$ and diaphragms at quarter-points. The values of r are 0, 0.05, 0.15, 0.40, and infinity. With only five points defined for each curve, it is somewhat difficult to draw the curves accurately, particularly with a large horizontal scale. However, the plotting is greatly facilitated by following the general shape of the curve for $r = 0$, for which the values of moment at points between the beams are known.[3]

From the shape of the influence curves for moment in the edge-beam (Fig. 8), the addition of more beams on the far side of the slab would cause little change in the moment carried by this beam. The influence line for an intermediate beam would also be changed only slightly by the addition of more beams on the far side. The addition of more beams on either or both sides of the bridge might bring about some change in the influence lines for moments in the center beam, but in general it is felt that the results obtained for five beams may be used for structures having either four beams or a larger number of beams than five.

Moments in Beams for Standard Truck Loads.—The standard truck loading for which moments are given is that specified in the AASHO Standard Specification for Highway Bridges. The standard H truck has the wheels of each axle spaced 6 ft apart, with front and rear axles spaced 14 ft apart. Each of the rear wheels carries a weight of four-tenths of the total weight of the truck and each of the front wheels carries one-tenth of the total weight of the truck, or one-fourth of the rear wheel weight. The weight of the truck in tons is designated by a numeral following H, as H-20. The rear wheel load P, in terms of which the maximum moment coefficients are stated, is the weight on a rear wheel increased by the impact factor. The front wheel is always taken as P/4.

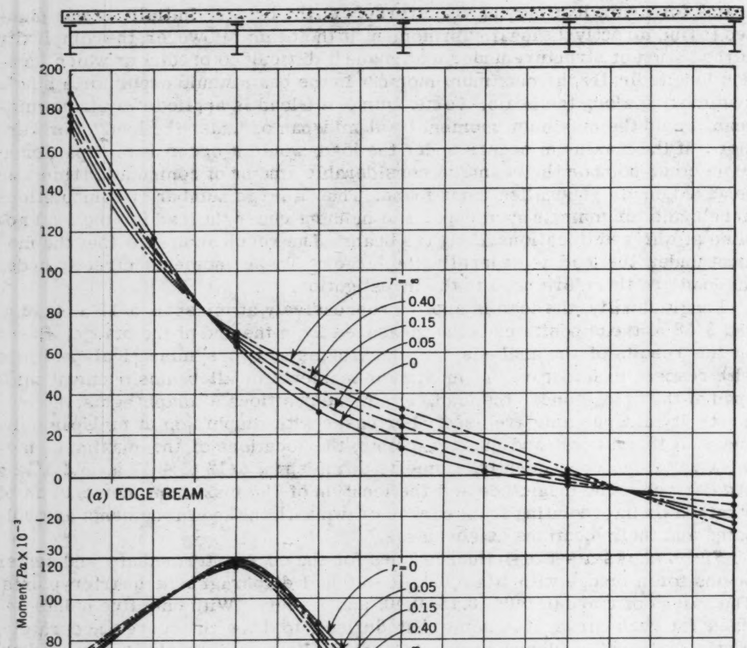

FIG. 8.—INFLUENCE LINES FOR MOMENTS IN BEAMS AT MIDSPAN FOR LOAD MOVING ACROSS THE BRIDGE AT MIDSPAN

Each truck is considered to occupy the central part of a 10-ft traffic lane. Therefore, the minimum distance between the center of a wheel and the face of a curb is taken as 2 ft, and the minimum distance between the centers of wheels of trucks in adjacent lanes is taken as 4 ft.

Beam spacings of 5 ft, 6 ft, 7 ft, and 8 ft are considered. These spacings cover the range of dimensions of most I-beam bridges. For the purpose of spacing the loads on the bridge, the face of the curb has been assumed to lie directly over the centerline of the edge beam. The loads are then applied a minimum of 2 ft from the edge beam and the maximum moment for each beam is obtained by placing the wheel loads at the highest ordinates of the respective influence lines. Results for this type of loading are given for beam spacings of 6 ft, 7 ft, and 8 ft. Unless noted otherwise this loading condition is used in plotting all graphs. For narrow beam spacings of 5 ft and 6 ft, results are given for the additional case of the outer wheel coming directly over the edge beam to produce a maximum value. This condition of loading will actually occur when the face of the curb is located at 2 ft outside the edge beam. This position of the loads designated as "edge loading" still satisfies the AASHO Specification.

For the proportion of bridges considered herein, two lanes of loading generally produce the maximum moments in the beams. This condition of loading occurs when one truck passes another in the adjacent lane. For purpose of simplification, only one truck in each lane and only the rear wheel loads of that truck are considered.

As previously mentioned, the shape of the influence line is approximated in the regions between the beams. The data for the truck loading, which are the results of computation based on the influence curves, are therefore not exact. In general, the moments computed from the influence lines are plotted against the relative diaphragm stiffnesses. A smooth curve joining the computed points assures consistent values for different relative diaphragm stiffnesses.

Comparison of Analytical and Test Results.—A recent publication[6] describes a test of a full size I-beam bridge. Part of the test program was to study the effectiveness of the diaphragms in the lateral distribution of loads in such a bridge. The bridge, representing one typical structure in the city of Houston Memorial Drive Project, is a 3-span continuous I-beam structure with the span lengths of 72-108-72 ft. The side and the center spans consist partly of a constant 33WF141 of 45 ft and 54 ft, respectively, joined over the intermediate pier by a 54 ft haunched section made of two ST16WF70.5 with a filler plate. The diaphragm studied is of a trussed type placed at midspan of the 54 ft section. Each half of the bridge consists of five longitudinal beams, running in the direction of traffic and spaced at 7 ft 6 in. apart. The concrete slab has an average thickness of 6 $\frac{1}{4}$ in.

When the positive moment section of the center span of the test bridge is considered as the simple span length, the span corresponds roughly to an analytical bridge with $b/a = 0.1$, $H = 5$ and a relative stiffness of diaphragm $r = 0.40$. Here, for conservative purposes, the value of H is computed on the basis of a non-composite section. A complete comparison of the behavior of the diaphragms in the theoretical and the test bridges was given elsewhere.[7] Fig.

---

[6] "Lateral Load Distribution Test on I-Beam Bridge," by A. White and W. B. Purnell, Proceedings, ASCE, Vol. 83, No. ST 3, May, 1957.

[7] Discussion by Benjamin C. F. Wei of "Lateral Load Distribution Test on I-Beam Bridge," by A. White and W. B. Purnell, Proceedings, ASCE, Vol. 83, No. ST 6, November, 1957.

9 showing a comparison of the percentage distribution of total moment to the five beams in the bridge is reproduced herein. Three curves are indicated; the first one given by the test, the second one from the theoretical analysis and the third one for the same bridge with the diaphragms removed. The third curve was shown to serve as a limiting case where the load distribution is entirely due to concrete slab. As predicted by theory, the total reduction of moment in the center beam under loading II due to the diaphragms is much larger

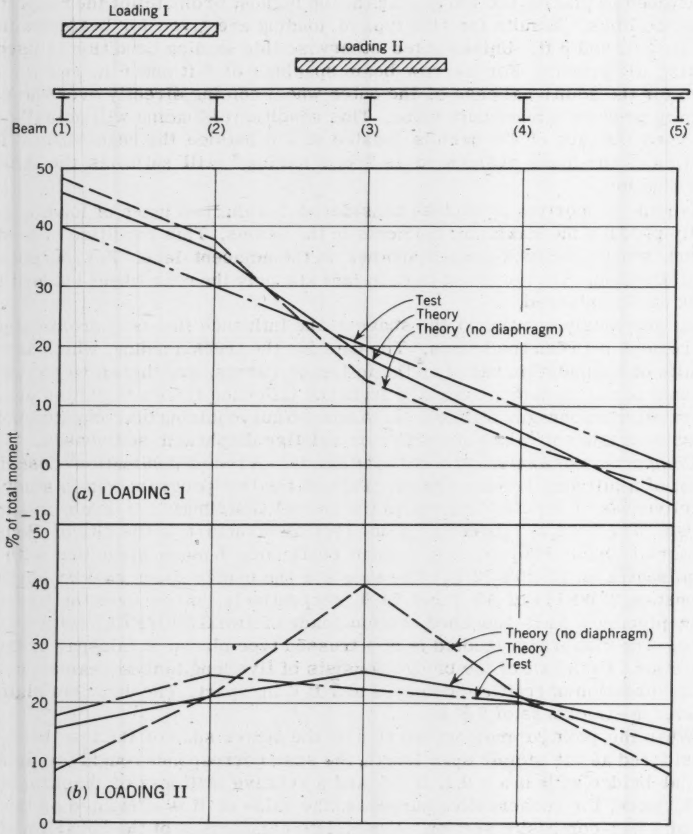

FIG. 9.—THEORETICAL AND TEST RESULTS OF DISTRIBUTION OF TOTAL MOMENT TO BEAMS

than that in the edge beam under loading I. In general, the comparison indicates good agreement between the test and the theoretical results.

ANALYSIS OF RESULTS

Relative Stiffness of Diaphragm to Beams.—One of the problems that confronts most highway bridge engineers in connection with the design of diaphragms is how stiff a diaphragm should be used in an I-beam bridge. Would the diaphragms always be effective, or would the effectiveness be directly proportional to their stiffness? Would the diaphragm behave in a similar manner under unit load as under truck loading? How much reduction of moment can be achieved by introducing a relatively flexible diaphragm in an I-beam bridge with a span from 50 ft to 80 ft? It is one of the purposes of this investigation to find answers to these questions. As previously mentioned, the study has included a range of stiffness of diaphragm, corresponding to relatively flexible to relatively stiff ones as built in actual practice. Furthermore diaphragms of infinite stiffness are introduced in each case to serve as a limiting condition for the effect of extremely stiff diaphragms.

Under unit load, the effect of increasing the stiffness of a diaphragm can be seen from the influence curves in Fig. 8. In general, the peak moments in all beams decrease as the diaphragms are made stiffer. Two facts are observed in Fig. 8: (1) Beyond $r = 0.40$ the decrease in moment becomes much less pronounced as more stiffness of the diaphragm is added. On the basis of the influence curves, the decrease in the peak moments in the beams is approximately of the same magnitude as r is increased one value higher in the pattern 0, 0.05, 0.15, 0.40, and infinity. (2) The moment for the intermediate beam is comparatively less susceptible to changes due to the addition of diaphragms than those for the edge and center beams. These two phenomena are found to be significant when the structure is subjected to standard truck loads.

Fig. 10 shows the moments in beams for the same structure under 4-wheel loading. The beam spacings are from 5 ft to 8 ft and the loads are applied transversely on the bridge at midspan. For the 5-ft beam spacing, the outer wheel is assumed to be applied over the edge beam if such loading produces a maximum, whereas for the 6 ft, 7 ft, and 8 ft spacings, the outer wheel is located at least 2 ft from the edge beam. The curves reveal that as the beam spacing and the relative diaphragm stiffness vary, the beam having the largest moment also varies. Two trends of the behavior of beams under 4-wheel loads may be observed from Fig. 10: (1) As the beam spacing increases, the increment of moment in the intermediate beam (beam B) is always larger than those in the other beams. Thus this beam has the tendency to become the significant beam in the structure. In Fig. 10 for $b = 7$ ft and 8 ft, beam B does have the largest moment; and for $b = 6$ ft, beam B becomes significant when the relative stiffness of diaphragm exceeds a certain value: (2) For beam spacings of 6 ft, 7 ft, and 8 ft, beam A has the lesser or least moment among the beams.

An understanding of how the various beams become significant for different conditions is helpful in predicting the beneficial effects of diaphragms. The curves for beams B and C in Fig. 10 are both sloping downward to the right, with beam C having generally a steeper slope. When these beams become significant, maximum moments are reduced as the diaphragms are added, the re-

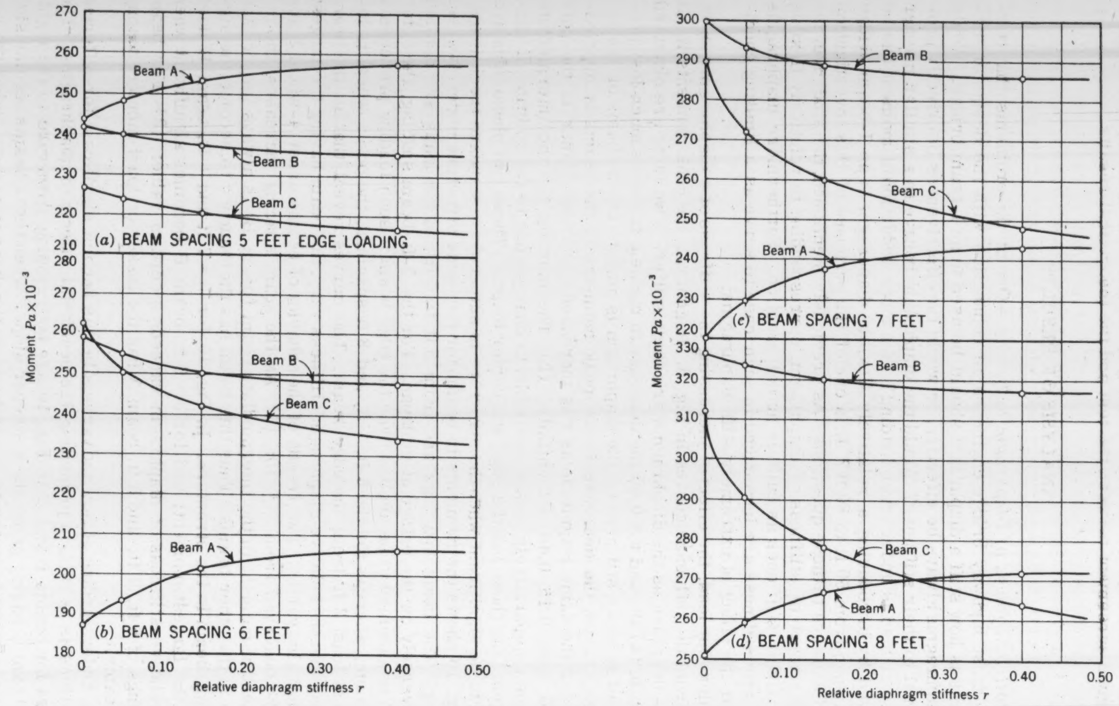

FIG. 10.—RELATION BETWEEN RELATIVE DIAPHRAGM STIFFNESS AND MAXIMUM MOMENT DUE TO 4-WHEEL LOADING

duction being larger for the case when beam C is controlling. As previously mentioned the influence line for moment in the intermediate beam is relatively irresponsive to changes in diaphragm stiffness. Thus, when this beam becomes significant, the curve expressing the relation between the moment and the diaphragm stiffness is usually flat. In other words the reduction of moment is slight even with the addition of a stiff diaphragm. However, the characteristics of the curve for beam A are such that the moment increases as the diaphragm stiffness is increased. This unusual phenomenon for edge beam will be fully studied subsequently under the heading Behavior of Edge Beams.

Consider again the curves in Fig. 10. One consistent phenomenon may be observed for all beam spacings, that is, the curves for all the beams flatten out almost to a horizontal line when it passes the value of r = 0.40. This indicates that only a negligible change of moment is obtained by using a diaphragm stiffer than 0.40. Due chiefly to the proximity of the influence lines for r = 0.40 and infinity, this characteristic was found to be present in all b/a = 0.1 structures analyzed with diaphragms at midspan, at each quarter-point, and at each third-point. It will be shown subsequently that the same characteristic also exists for different stiffnesses of beams and slab.

Therefore in an I-beam bridge having b/a = 0.1 and H in the range from 5 to 20, a diaphragm with E I of 40% that of each beam is almost as effective as an infinitely stiff one in reducing the maximum moment in the bridge. With due considerations given to the relatively greater reduction in moment and the impracticability of using stiff diaphragms in actual construction, a flexible diaphragm with a relative stiffness in the range of 5% to 10% of that of the beam is recommended for use in design. It will be shown subsequently that the lower limit (5%) is favored for bridge with a high H corresponding to composite construction.

Comparison Study for Different Positions of Diaphragms.—It has been previously mentioned that the redistribution of load to the beams through the diaphragms takes the form of concentrated loads at the points of intersection of the diaphragms and the beams. Obviously an effective position for the diaphragms should be at or near the section where the load is applied. The study in this section was to investigate the most effective positions of the diaphragms. The criterion of comparison is the maximum moment produced under a specified loading condition. Relative stiffnesses of diaphragm to beam in the range of r = 0 to infinity are included. The data from the analyses for diaphragms at midspan, each third-point, and each quarter-point are used.

Since the stiffness of a diaphragm is not proportional to its weight, comparison of structures with a total amount of diaphragm stiffness distributed at various positions such as midspan or third-points would not provide a criterion in the practical sense. An equal amount of diaphragm stiffness in each location is therefore used. For example, if the structure is provided with two diaphragms at the third-points, each with a relative stiffness of 0.10, it is compared to a structure with a single diaphragm at midspan with a relative stiffness of 0.10. The cost of diaphragms in the structure with one diaphragm at midspan would therefore be only half of that with diaphragms at each third- or quarter-point. In the figures that follow, the values r shown on the curves denote the relative stiffness of the single center diaphragm, or the stiffness of each diaphragm at third or quarter point.

Fig. 11 shows the relation between the position of the diaphragms and the maximum moment in the loaded beam due to unit load moving across the bridge (b/a = 0.1 and H = 10). When there is no diaphragm, the maximum moment in the structure is constant as represented by a horizontal line. Each curve is determined by three points, representing diaphragms at midspan, each third-point, and each quarter-point. For diaphragms at each third- or quarter-point, the plotted maximum moments were obtained from the moments at midspan, whereas for diaphragm at midspan they were obtained by interpolating between computed moments at midspan, and at 5/12, 4/12, and 3/12 of the span length of the bridge. In Fig. 11, all the curves with diaphragms are found below the straight line, r = 0. Therefore under unit load, the moments in all three beams including the edge beam are reduced with the addition of diaphragms.

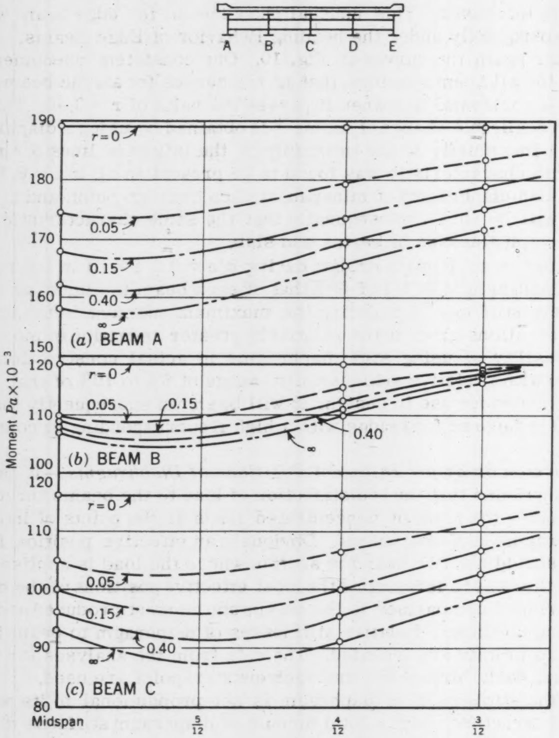

FIG. 11.—RELATION BETWEEN POSITION OF DIAPHRAGM AND MAXIMUM MOMENT IN LOADED BEAM DUE TO UNIT LOAD

In Fig. 11, an interesting relationship exists between the position of maximum moments in the beam and the location of the diaphragms. When the load

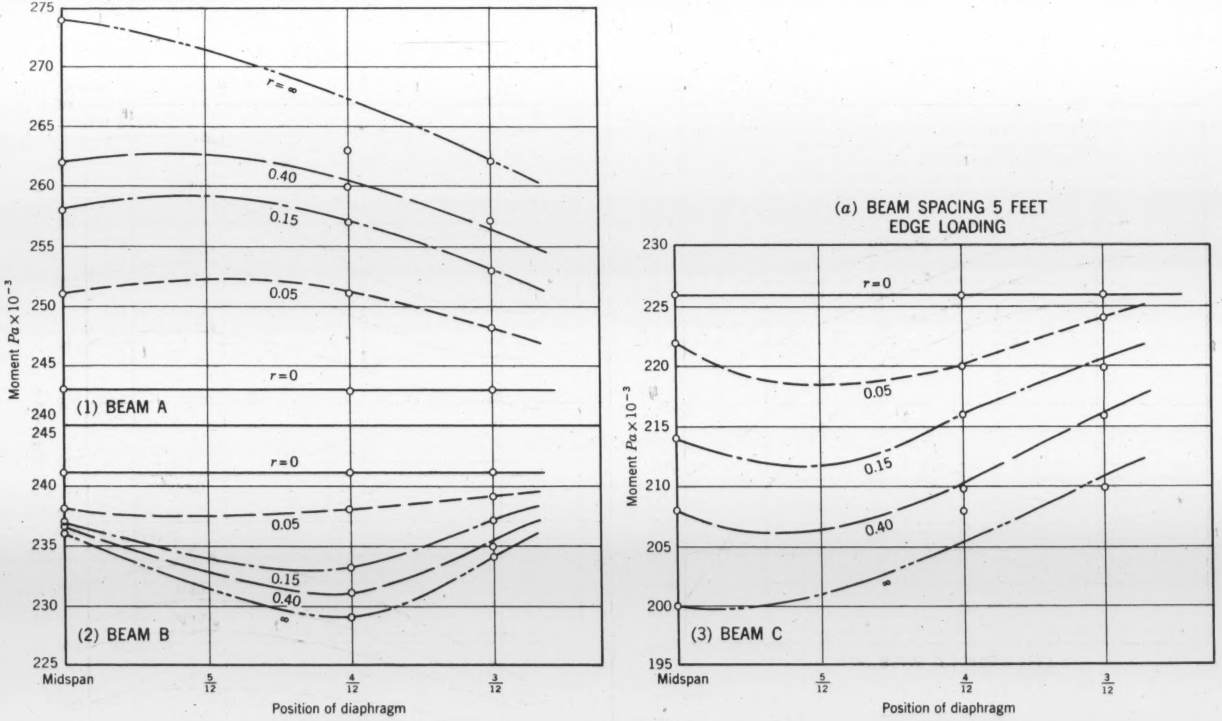

FIG. 12.—RELATION BETWEEN POSITION OF DIAPHRAGM AND MOMENT IN BEAMS DUE TO 4-WHEEL LOADING

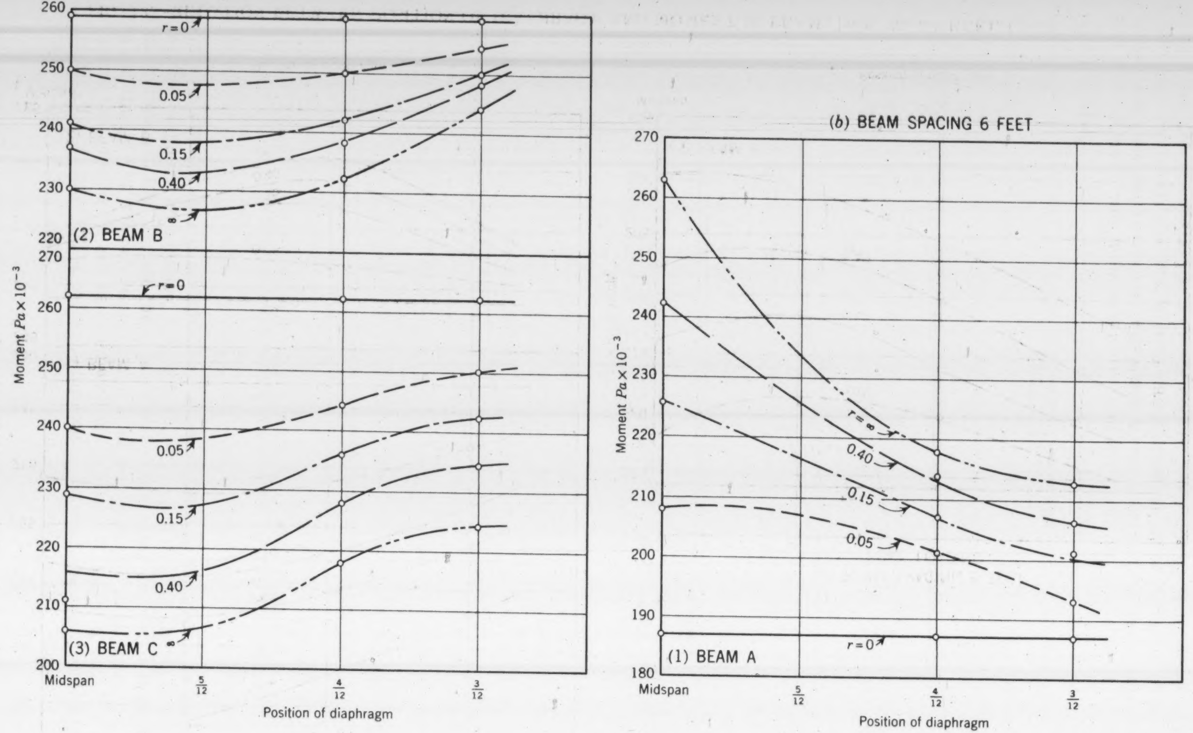
(b) BEAM SPACING 6 FEET

FIG. 12. –*CONTINUED*

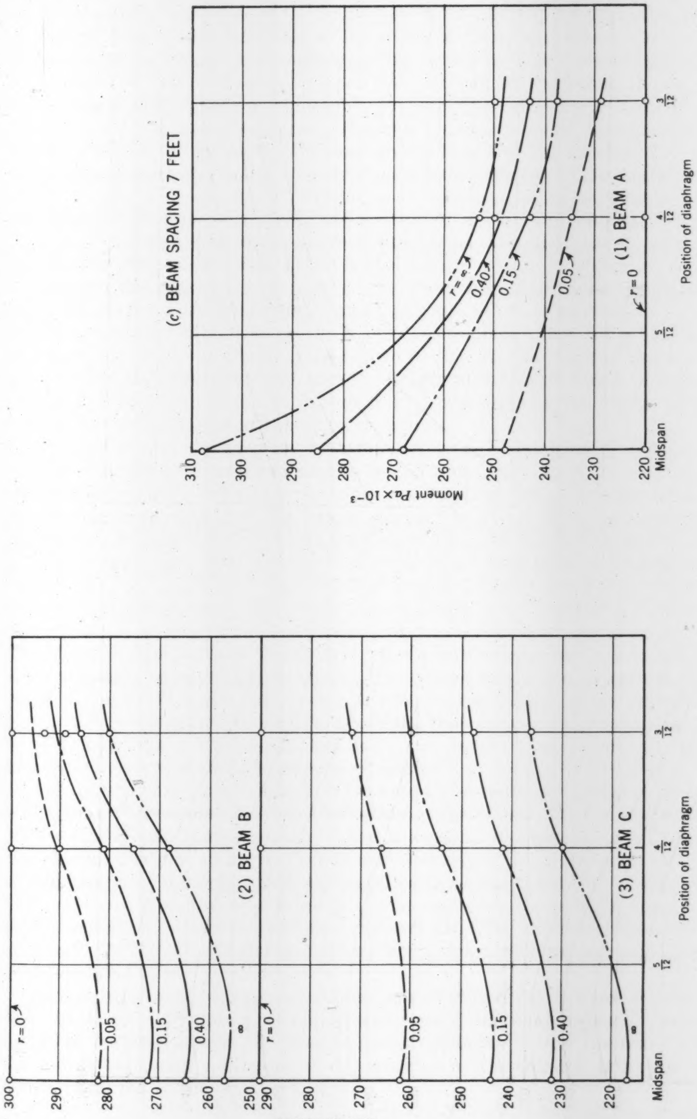

FIG. 12. —*CONTINUED*

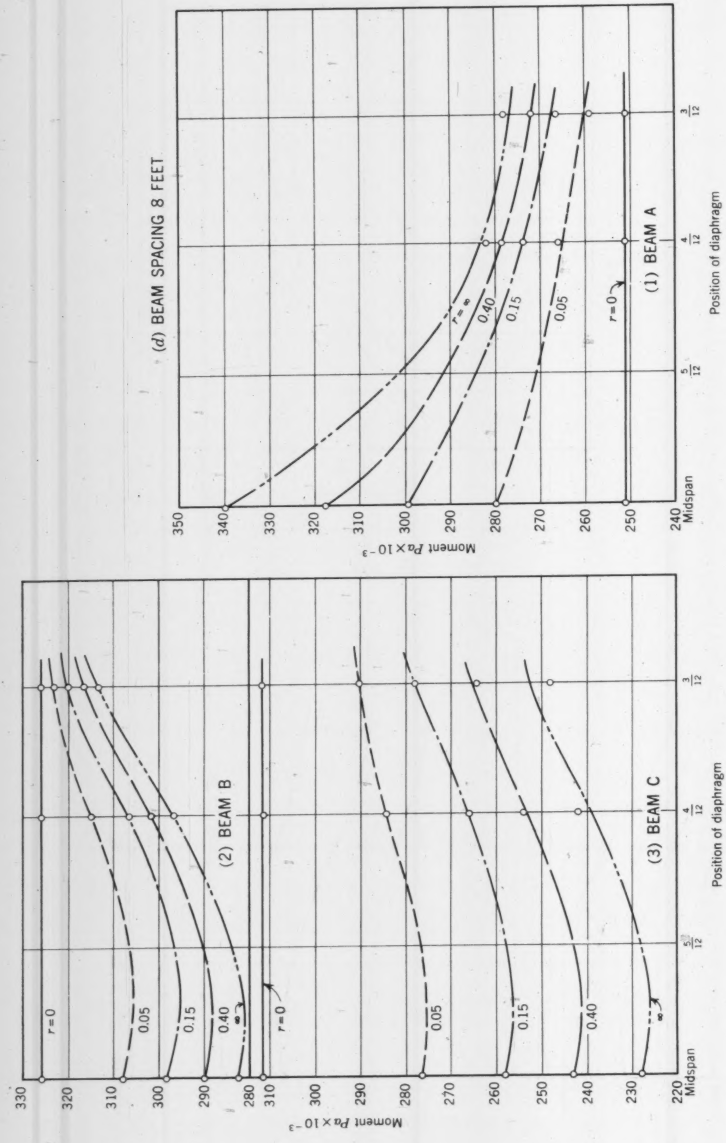

(d) BEAM SPACING 8 FEET

FIG. 12.—*CONTINUED*

is acting over the edge beam, the maximum moment in the beam is found to occur always at midspan of the bridge or in the vicinity of midspan, depending on the position of the diaphragm. Naturally a diaphragm framed at the section nearest the section of maximum moment, which in this case is the load position, transfers the load more effectively. It can be expected, therefore, that under this condition the center diaphragm acts more effectively than diaphragms at the third- or quarter-points. However, when the unit load is acting over beams B or C, the position of maximum moment for the structure with a center diaphragm shifts away from midspan considerably. This position may be as far as the third- or quarter-point of the bridge. As a result the center diaphragm is some distance from the section of maximum moment, or the load position, and thus can not be more effective than the diaphragms at the third- or quarter-points. In Fig. 11(c) it can be seen that for beam C and a stiff diaphragm, the maximum moment for the case with diaphragms at third-points becomes slightly less than that with diaphragm at the midspan.

Except for the slight deviation, it may be concluded that, for all three beams and three positions of diaphragms shown in Fig. 11, the trend of the curves indicates that the structure with the diaphragm at midspan yields the least moment. The moment becomes larger for diaphragms at the third-points, and largest for diaphragms at the quarter-points.

Similar curves showing the relation between the position of the diaphragm and the moment in the beams under 4-wheel loading are given in Fig. 12. Under truck loading, it is necessary to assume a spacing of the beams in the bridge before the moments can be computed. Consideration is given to beam spacings of 5 ft, 6 ft, 7 ft, and 8 ft. The variations of moment in the beams for different relative diaphragm stiffnesses with these beam spacings are shown in Figs. 12(a), (b), (c), and (d). The value of r indicated on each curve represents the relative stiffness of the single center diaphragm or the relative stiffness of each of the diaphragms at the third- or quarter-points. As previously mentioned, the computation of moment for 4-wheel loading generally involves some approximation because the influence lines from which the moments are computed are approximated in the regions between the beams. This approximation may cause some points to deviate from the true curve. In general, the curves were smoothed and cross-checked for consistency in all cases studied. The trend of the curves was found to be consistent.

Fig. 12 shows an interesting fact; whereas, for the intermediate and the center beams, the curves showing the relationship between the moments and the position of diaphragms indicate a trend similar to that for unit loading, the edge beam exhibits an entirely different behavior. Not only does the position of diaphragm at midspan yield the maximum moment, but the addition of diaphragm increases the moments in the beam under the truck loading. These deviations bring out the major importance of studying the structure under truck loading. The peculiar behavior of the edge beam will be more fully studied subsequently.

Except for the edge beam, the same conclusion for unit loading may be applied in the comparison of the three positions of diaphragms under truck loading. The structure with the diaphragm at midspan yields the least moment, the moments become larger for diaphragms at the third-points, and largest for diaphragms at the quarter-points.

Diaphragms at Both Midspan and Quarter-Points.—So far, the analysis of the positions of the diaphragm has been limited to those of midspan, each third-point, and each quarter-point. In the analyses for b/a = 0.1, the case with diaphragms at both midspan and quarter-points has been treated for H = 5, 10, and 20. Owing to the laborious computation involved, only one value of relative diaphragm stiffness, r = 0.15, was analyzed. Results computed for all three values of H indicated that the structures consistently displayed the same characteristics. It appeared possible then, with the limited information at hand, to interpret the general behavior of the bridge with three diaphragms.

Table 1 compares the moments in the loaded beam for a unit load moving across the bridge. Column 3 indicates the moment values for the bridge with three diaphragms, one at midspan and one each at quarter-points, each with a relative stiffness equal to 0.15. Column 4 indicates moments for bridge with one center diaphragm having a stiffness equal to that of the central one in the bridge with three diaphragms. It is surprising to note that the maximum controlling moments in beam A check closely for these two cases for all three values of H. This indicates that in a bridge which already has a diaphragm at midspan, the addition of diaphragms at the quarter-points will not reduce significantly the maximum moment. However, the moments in beams B and C are reduced slightly with the addition of extra diaphragms.

TABLE 1.—COMPARISON OF MAXIMUM MOMENTS IN BEAMS DUE TO UNIT LOAD[a,b]

Relative Stiffness of Beams, H (1)	Beam (2)	0.15 0.15 0.15 Diaphragms at Midspan and 1/4 - points (3)	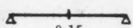 0.15 Diaphragm at Midspan (4)
5	A B C	0.159 0.101 0.089	0.159 0.101 0.092
10	A B C	0.167 0.105 0.093	0.168 0.109 0.100
20	A B C	0.172 0.108 0.096	0.174 0.116 0.109

[a] Relative proportions of bridge b/a = 0.1
[b] Values of moments to be multiplied by Pa

Similar comparisons for moments under 4-wheel loading are given in Table 2 for beam spacings of 6 ft, 7 ft, and 8 ft. Again, the values of moment are surprisingly close for the two cases, as they were under unit load.

Under both unit load and standard truck loads, the effect on the moment of beams in a bridge with three diaphragms, one at midspan and two at the quarter-points, can be approximated by the assumption that the structure has only one diaphragm at midspan with those at quarter-points omitted. In other words, as far as the maximum moment is concerned, the addition of diaphragms at each quarter-point of a bridge which already has a midspan diaphragm will not alter appreciably the behavior of the bridge.

It follows from this conclusion that when diaphragms other than the one at the midspan are required for construction of long span I-beam bridges, they

TABLE 2.—COMPARISON OF MAXIMUM MOMENTS IN BEAMS DUE TO 4-WHEEL LOADING[a,b]

Relative Stiffness of Beams, H (1)	Beams (2)	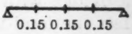 Diaphragm at Midspan and 1/4 - points (3)	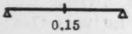 Diaphragm at Midspan (4)
(a) Beam spacing = 6 feet			
5	A	0.229	0.223
	B	0.243	0.240
	C	0.226	0.230
10	A	0.225	0.226
	B	0.242	0.240
	C	0.236	0.229
20	A	0.228	0.231
	B	0.245	0.252
	C	0.239	0.242
(b) Beam spacing = 7 feet			
5	A	0.264	0.262
	B	0.270	0.271
	C	0.238	0.244
10	A	0.264	0.268
	B	0.271	0.272
	C	0.256	0.244
20	A	0.270	0.276
	B	0.273	0.279
	C	0.257	0.264
(c) Beam spacing = 8 feet			
5	A	0.295	0.291
	B	0.292	0.294
	C	0.246	0.257
10	A	0.299	0.300
	B	0.304	0.298
	C	0.269	0.258
20	A	0.304	0.307
	B	0.300	0.298
	C	0.268	0.280

[a] Relative proportions of bridge b/a = 0.1
[b] Values of moments to be multiplied by Pa

may be made of nominal size and spaced at not more than 25 ft apart as specified by AASHO.

Relative Stiffness of Beams to Slab.—The relative stiffness of beams to slab, defined by the expression $H = \frac{E_b I_b}{a N}$, is one of the important factors affecting the behavior of an I-beam bridge. The effect of different values of H on the moments in beams of a bridge without diaphragms has been presented earlier under the heading Fundamental Concepts of Load Distribution in I-Beam Bridges. It is obvious that, for a bridge with a high H corresponding to a structure with a relatively flexible slab, the load will not be distributed effectively to the supporting beams. Since a thick roadway slab serves as an effective means of distributing the load that comes on it, the advantage of framing diaphragms in the bridge can best be realized when the slab of the bridge is relatively thin. Herein it was intended to analyze bridges having values of H larger than the nominal amount.

Newmark stated in his paper[8] on design of I-beam bridges that in general the value of H for representative designs of a 60-ft span may range from 3 to 8 for non-composite beams, from 5 to 15 for composite I-beams, and from 15 to 30 for concrete T-beams. For other span lengths, the values of H are roughly proportional to the span, increasing slightly less rapidly than the span increases. For a 60-ft span bridge with beam spacing of 6 ft ($b/a = 0.1$), the values of H considered herein are 5, 10, and 20. These values correspond roughly to the three types of construction stated by Newmark.

From the formula by which H is expressed, the computation of H is subject to considerable uncertainty since both the modulus of elasticity and moment of inertia of the concrete slab are involved. Neither of these quantities can be determined accurately. The modulus of elasticity of concrete depends on several factors, such as the aging of the concrete, the type of aggregate, the plastic flow of concrete, and others. The moment of inertia of the concrete depends on the state of the slab under load. When the slab cracks from moments in the transverse direction, the relative flexural stiffness of slab is reduced at the section where cracking occurs. However, the average transverse stiffness is only slightly reduced by cracking since there are usually fairly large sections of slab that still remain whole. For this reason and to simplify the computation, the value of I used in determining H has been computed for a plain concrete slab of full depth h, without cracks. The increase in stiffness resulting from the presence of transverse steel may offset to some extent the decrease caused by cracking. This choice of I for the slab in determining H has been justified by tests.

Fig. 13(a) and (b) show the percentage change of maximum moment under standard truck loads for bridges having $b/a = 0.1$ and various H and diaphragm stiffnesses. Since the effect on edge beam will be treated separately under the heading Behavior of Edge Beam, the maximum moments shown in Fig. 13(a) and (b) were obtained for either the intermediate or the central beam in which the maximum occurs, and the change in moment was computed with respect to the same bridge, but without diaphragms. Diaphragms at midspan and at each third-point in bridges with beam spacings ranging from 5 ft to 8 ft are considered.

As an illustration to show how much the reduction would be in a 60-ft span bridge with a beam spacing of 6 ft, consider the bridge with diaphragms at each

---

[8] "Design of I-Beam Bridges," by N. M. Newmark, Transactions, ASCE, Vol. 114, 1949, p. 997.

third-point, each having a stiffness 10% that of a beam. The maximum moments are reduced approximately 4%, 6%, and 16% from those in the same bridge without diaphragm, for H = 5, 10, and 20, respectively. If for the same bridge the same diaphragm is placed at midspan, the reduction would be approximately 4%, 7%, and 13%, for H = 5, 10, and 20, respectively. This illustration indicates that the reduction in live load moment in the interior beams of a composite structure could be of an appreciable amount even with the addition of a relatively flexible diaphragm. This advantageous effect of diaphragms shall be utilized in the design of these beams.

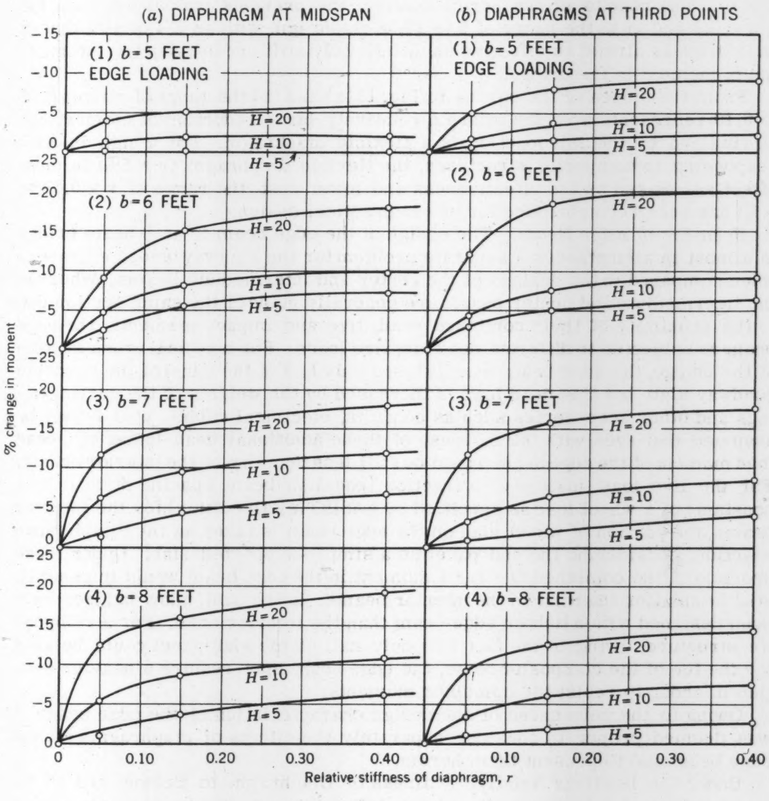

FIG. 13.—REDUCTION OF MOMENT IN INTERIOR BEAMS

In Fig. 13(a) and (b) where the reduction of moments is pronounced in the cases with the beam spacings from 6 ft to 8 ft, the effect of diaphragms becomes less significant even in the bridge with a high value of H for beam spacing of 5 ft and under edge loading.

For all three values of H in Fig. 13(a) and (b), the reduction of moment remains almost constant when the relative diaphragm stiffness (r) exceeds 0.40. This phenomenon has been previously studied for the particular value of H = 10. The results shown herein confirm the previous conclusion that, for b/a = 0.1 and H in the range of 5 to 20, a diaphragm with an E I of 40% that of each beam is almost as effective as an infinitely stiff one in reducing the maximum moment in the bridge.

From the slopes of the curves in Fig. 13(a) and (b) the range of r from 0.05 to 0.10 represents a region where a relatively large reduction of moment can be obtained by the introduction of a flexible diaphragm. For a high H, corresponding to composite structures, the flexible diaphragm (r = 5%) is most effective. Based on the effectiveness and lower cost, the range of r = 0.05 to 0.10 has been recommended for use in practical design.

Behavior of Edge Beam.—The design of the edge beam in an I-beam bridge is almost in all instances a separate problem for the highway bridge engineers when compared to the designs of the center and intermediate beams. Whereas the intermediate and center beams are generally made of the same section due to the proximity of their combined dead, live and impact moments, the edge beam is subjected to different dead and live loads. For a typical cross section of the bridge, the edge beam usually takes only half of the panel of the concrete roadway slab, but this dead load is increased by the weights of the curb, railings and other accessories such as conduits, electrical cables, etc. It may be assumed that even with the increase of these additional dead loads, the dead load moment of the edge beam would be still less than that of the interior beams. For the live load, instead of a fraction (equal to beam spacing divided by a constant) of a wheel load as specified by AASHO (sixth edition) for the interior beams, the portion of wheel load on the edge beam is taken as the simple span reaction, considering the end panel as a simply-supported slab. Under these provisions, the combined D + L + I moment in the edge beam would in general, still be smaller than that in the interior beams. In the past, many bridges have been designed with a lighter edge beam than the interior ones. For a composite structure, owing to the fact that only half of the slab panel could be used for the tee of the composite beam, the edge beam may require a heavier section in order to resist the combined moments.

Owing to the uniqueness of the design characteristics of the edge beam, it was deemed proper to consider separately the effects of diaphragms on the edge beam and to present them herein.

Under the headings Relative Stiffness of Diaphragm to Beams, and Comparison Study for Different Positions of Diaphragms, it was emphasized that while the interior beams showed a reduction of moments due to the addition of diaphragms under 4-wheel loading, the moment in the edge beam is increased. From Figs. 10 and 12, the following factors affecting the edge beam are noted: (1) as the stiffness of diaphragms increases, the moments become greater; (2) the increase in moments is more pronounced in the range of relatively flexible diaphragm stiffness; and (3) the increase is more significant when the diaphragm is framed at midspan and, as the diaphragms are spaced farther from the midspan of the bridge, the increase becomes less.

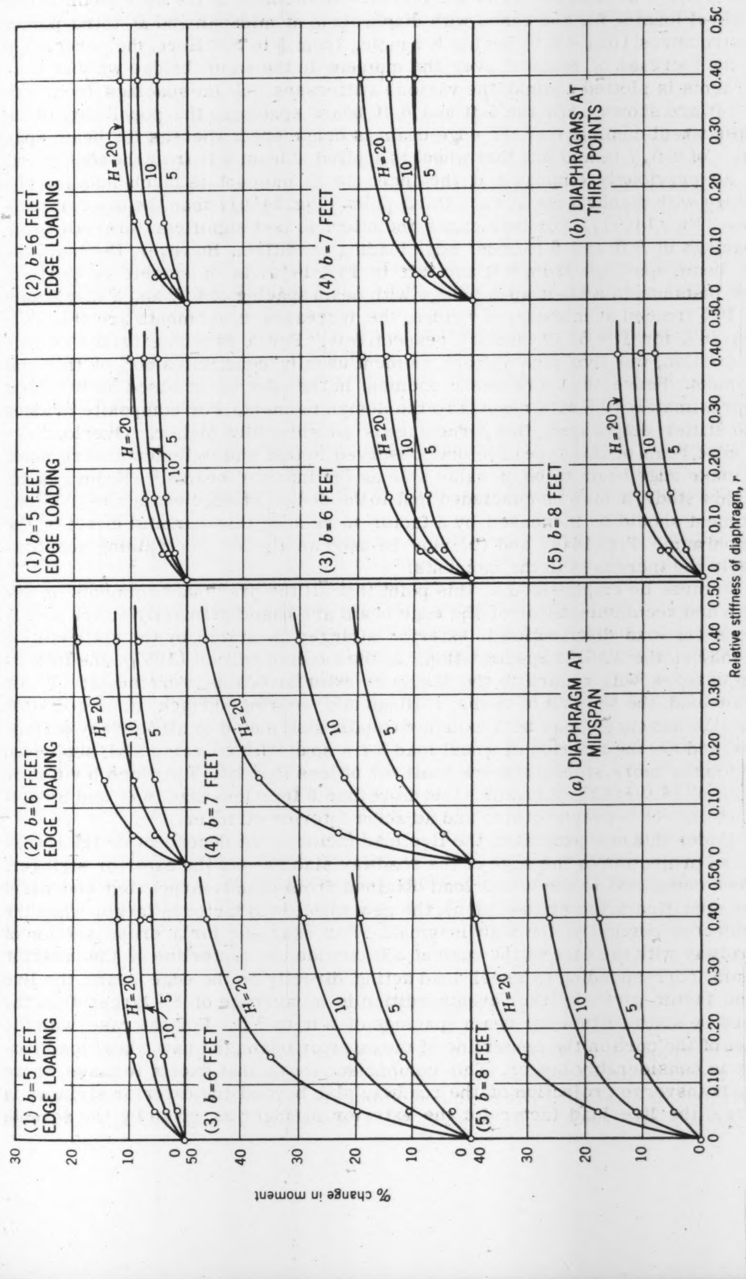

FIG. 14.—INCREASE OF MOMENT IN EDGE BEAM

Figs. 14 (a) and (b) show the increase of moment in the edge beam under 4-wheel loading for the cases with diaphragms at midspan and at third-points of structures (b/a = 0.1) having H ranging from 5 to 20. Here, the percentage of the increase of moment over the moment in the same bridge without diaphragms is plotted against the various stiffnesses. Beam spacings from 5 ft to 8 ft are shown. For the 5-ft and 6-ft beam spacings, the possibility of an outer wheel coming over the edge beam is considered, whereas for beam spacings of 6 ft, 7 ft, and 8 ft that wheel is applied at least 2 ft from the edge beam.

As previously emphasized, the increase in moment is much less for the bridge with diaphragms at each third-point (Fig. 14(b)) than the one for midspan (Fig. 14(a)). For both cases, the effect is less significant in small beam spacings of 5 ft and 6 ft under edge loading condition. However, the increase for beam spacings from 6 ft and 8 ft in Fig. 14(a) is of sizable proportion. For instance, in a 60-ft span bridge with beam spacing of 6 ft and a diaphragm of 10% framed at midspan of bridge, the increases in moments are 9%, 17%, and 28%, for H = 5, 10, and 20, respectively. For a two-lane bridge of this proportion, the live plus impact moment usually constitutes 60% of the total moment. Hence, the increases in moment in the edge beam based on H = 10 is approximately 10% with respect to the design moment. For composite bridges and stiffer diaphragm, this percentage is considerably higher. Overloadings of edge beam of this type have been observed in test and statements were made to make edge beam to be of same size as the interior beams.[6] From results of this study, it may be concluded that in the design of edge beam, the live load moment should be increased by a factor to remedy this harmful effect of the diaphragm. Fig. 14(a) and (b) may be used as a guide in obtaining quantitatively the increases in the moments.

It must be emphasized at this point that all the previous comments on design and recommendation of the edge beam are based primarily on the provisions for load distribution in exterior stringer as stated by the sixth edition (1953) of the AASHO Specification. In the seventh edition (1957), the following changes with regard to the design of exterior beams were made; (1) for dead load, the weights of curbs, railings and wearing surface, if placed after the slab has cured, may be considered equally distributed to all roadway stringers, and (2) the fraction of wheel load for a span with concrete slab supported by four or more steel stringers shall not be less than b/5.5 in which b = 6 ft or less; b/(4.0 + 0.25 b) in which b is more than 6 ft or less than 14 ft, and b = distance in feet between outside and adjacent interior stringer.

Under this new provision, the live load factor is not dependent on the transverse projection of the edge of the roadway slab beyond the exterior stringer. When compared to the wheel load obtained from simply-supported end panel (as specified in the sixth edition), the new wheel load factor is larger when the projected portion of the slab is small. For example, for a cross-section of roadway with the face of the curb at 2 ft outside the centerline of the exterior beam, corresponding to wheel load acting directly on the edge beam, the live load factor given by the seventh edition is an average of 8% larger than the ones by sixth edition for beam spacings of 6 ft to 8 ft. For the case with the face of the curb on the centerline of the exterior beam, the new wheel load factor is considerably larger. This comparison shows that except in cases where the transverse projection of the roadway slab beyond the exterior stringer is large, the live load factor for the exterior stringer as given by the seventh edition of the AASHO Specification has already been made greater than that derived by the conventional computation of using simply-supported end panel.

CONCLUSIONS

Throughout the presentation of the paper, emphases have been given to I-beam bridges with a relative proportion of $b/a = 0.1$ and H in the range of 5 to 20. As shown under the heading Description of Bridges Analyzed, these proportions were chosen to represent a practical range of longer span I-beam bridges covering both the composite and non-composite construction. The following conclusions may be drawn from the results of this analytical study:

1. A diaphragm with a relative stiffness of 40% of that of each beam is almost as effective as an infinitely stiff one in reducing the maximum moment in the bridge. For practical considerations, a flexible diaphragm with a relative stiffness in the range of 5% to 10% of that of the beam is recommended for use in design. The lower limit (5%) being favored for bridges with a high H. corresponds to composite construction and the higher limit (10%), to non-composite structures.
2. Under both unit and standard truck loads, the addition of diaphragm reduces the maximum moments in the interior beams. In general, the reduction in moment is largest in the structure with the diaphragm at midspan. It becomes less for diaphragms at the third-points, and least for diaphragms at the quarter-points.
3. Although under unit load the moment in the edge beam is reduced, under 4-wheel truck loads the addition of diaphragm causes an increase in the moment. The increase is more significant for the case with diaphragm framed at midspan and becomes less as they are spaced farther from the midspan. Percentages of increase in moments in the edge beam of various bridges have been shown in Fig. 14(a) and (b). Live load moments in edge beams computed on the assumption of simply-supported end panel, should be increased in design by a factor based on Fig. 14(a) and (b) to account for this harmful effect of the diaphragms.
4. The effect of diaphragms on the moment of beams in a bridge with three diaphragms, one at midspan and one each at the quarter-points can be approximated by the assumption that the structure has only one diaphragm at midspan with those at the quarter-points omitted. In other words, as far as the maximum moment is concerned, the addition of diaphragms at each quarter-point of a bridge which already has a midspan diaphragm will not alter appreciably the behavior of the bridge. From this conclusion it follows that, when diaphragms other than the one at midspan are required for long-span bridges, they may be constructed of nominal size and spaced at not more than 25 ft apart as specified by AASHO.

ACKNOWLEDGMENTS

The major part of the study presented herein is based on a report[5] which formed a part of an investigation of the reinforced concrete slab as conducted by the Engineering Experiment Station of the University of Illinois in cooperation with the Division of Highways of the State of Illinois and the Bureau of

Public Roads of the United States Department of Commerce. The writer is sincerely thankful to Newmark and C. P. Siess, F. ASCE, for their guidance, encouragement, and many valuable suggestions during the performance of the work.

APPENDIX.—NOTATION

The following symbols are adopted for use in the paper. The longitudinal direction is always taken as the direction of the beams.

a = span of bridge, center to center of supports;

b = transverse spacing of beams;

E = modulus of elasticity of the material in the slab;

E_b = modulus of elasticity of the material in a beam;

E_d = modulus of elasticity of the material in a diaphragm;

H = $\frac{E_b I_b}{a N}$ = dimensionless coefficient which is a measure of the stiffness of a beam relative to that of the slab;

h = total depth of slab;

I = moment of inertia per unit of width of the cross-section of the slab, for a homogeneous material, $I = h^3/12$;

I_b = moment of inertia of the cross-section of a beam (or transformed moment of inertia of a T-beam);

I_d = moment of inertia of the cross-section of a diaphragm;

L = length of the diaphragm when it is considered as one cross beam, equal to 4b for the bridges analyzed;

M = bending moment in a beam or in a T-beam, positive when producing compression in the top fibers;

N = $\frac{E I}{1 - \mu^2}$ = measure of stiffness of an element of the slab;

P = concentrated load applied to the slab;

R = reactions offered by the diaphragms to the beams in the bridge;

r = $\frac{E_d I_d}{E_b I_b}$ = dimensionless coefficient which is a measure of the stiffness of a diaphragm relative to that of a beam.

Δ = vertical deflection of beams, positive downward;

δ = vertical deflection of diaphragms, positive downward; and

μ = Poisson's ratio for the material in the slab.

AMERICAN SOCIETY OF CIVIL ENGINEERS
Founded November 5, 1852
TRANSACTIONS

Paper No. 3235

VENTILATED BUILDING FOUNDATIONS IN GREENLAND[a]

By Roger H. Williams,[1] F. ASCE

With Discussion by Messrs. John A. Pihlainen; and Roger H. Williams

SYNOPSIS

The ventilated foundation systems used in certain permafrost areas in Greenland are described. Presented herein are those factors of heat transfer, moisture content, ground water conditions, and structural details which affected the designs as well as the siting, orientation, and maintenance problems involved.

Ventilated foundations are used in permafrost areas where materials, if thawed, lose their ability adequately to support the proposed structures. It is obvious if such a system is used, it must provide for the removal of heat from the soil in such a manner that no underlying soils which would lose their strength are thawed. Fig. 1 depicts a typical ventilated foundation construction.

In areas of borderline or discontinuous permafrost, extreme caution in the use of this type structure must be exercised to prevent retrogression of the permafrost level into unsatisfactory materials. In these areas it is necessary to determine whether ventilated foundations are practicable or whether some other treatment is necessary.

At times it may be feasible to excavate some unsatisfactory material and replace it with non-frost-susceptible fill. This is a question of economics in which the cost of excavation and backfilling is compared with the additional

---

Note.—Published essentially as printed here, in September, 1959, in the Journal of the Construction Division, as Proceedings Paper 2142. Positions and titles presented are those given when the paper was approved for publication in Transactions.

[a] Presented at the June 1957 ASCE Convention, in Buffalo, N. Y.

[1] Proj. Mgr., Metcalf & Eddy, Boston, Mass.

cost of a ventilated system. This occurs when rock is relatively near the surface and it must be determined whether to excavate all the way to rock, thus eliminating the need for ventilation or to excavate part way and provide ventilation.

The purpose of ventilated foundations for heated structures is to permit cold air to be circulated beneath the heated floor with the object of removing heat transmitted through the floor thus preventing it from entering the ground, and also during cold weather to remove heat from the ground thus maintaining satisfactory ground temperatures to preserve the permafrost.

Since all of our ventilated foundations are constructed on gravel pads, it might be well to consider at this point construction and purpose of this pad. The gravel pad is as its name connotes constructed of non-cohesive material which is non-frost-susceptible. The area of the pad is usually such that it will extend from 10 ft to 15 ft outside of the exterior foot line on all sides of the structure. It is constructed with extreme care to insure that the desired compaction is obtained to support the proposed structure without settlement that would jeopardize the structural integrity or the usefulness of the structure.

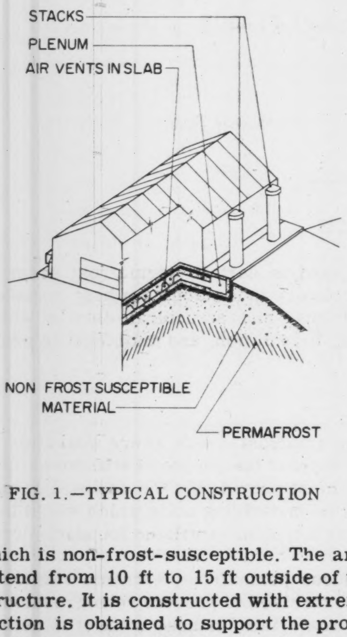

FIG. 1.—TYPICAL CONSTRUCTION

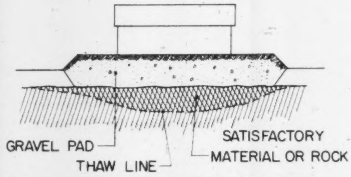

(a) CASE-I. THAW BELOW PAD

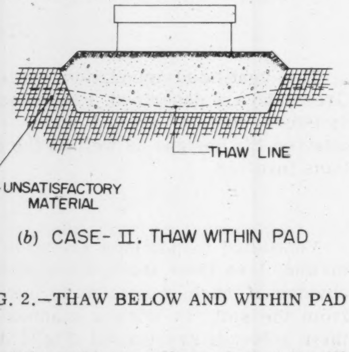

(b) CASE-II. THAW WITHIN PAD

FIG. 2.—THAW BELOW AND WITHIN PAD

The thickness or depth of the gravel pad is designed to prevent thawing of any underlying material which, if thawed, would cause unacceptable foundation settlements. This does not mean that the pad is always thick enough to prevent thawing below its bottom surface since it is possible to have strata at considerable depth which have satisfactory load bearing qualities, but these in turn may be underlain by unsatisfactory materials (Fig. 2).

It is obvious then that the thickness of the pad is dependent on the temperature to be maintained in the heated structure, the air-moving characteristics of the ventilated floor system, the freezing and thawing indexes, the heat absorption and transmission properties of the floor materials and the gravel pad materials, including their water contents.

An ideal gravel pad would be one completely saturated with water since the high specific heat of water would inhibit thaw penetration, hence requiring less thickness of pad to protect underlying materials. If such were possible, provisions would, of course, have to be made to prevent this water from entering the ventilating system where it might freeze and reduce the effectiveness of or entirely eliminate air movement. While a saturated pad as previously described is highly desirable, usually it is not easily obtained using normal arctic construction methods. To insure continuous saturation, it would be necessary to dike around the pad with some impervious material or to use some waterproof membrane to contain the water. The cost of such a system and the construction time involved would be such that it is considered more practical to use added depths of fill and consider only that moisture content that can be reasonably estimated to be held in the granular material by capillary action. It is evident from this analysis that fine granular material having high water retention characteristics is desirable for pad construction provided, of course, it is non-frost-susceptible.

In certain respects moisture is advantageous in the design of pads for ventilated foundations. There are two ways in which the presence of water may be disadvantageous. The first of these concerns the layer of melt water which exists, in some cases, at the thaw line in the active zone as the thaw progresses downward from spring through summer. Since the materials in glacial deposits usually are far from uniform, there may be a large variation in the depths of thaw below the surface in a given watershed. This is usually quite true in many relatively flat areas that are naturally picked for development and here even small variations may be important.

The variation in depth of thaw results in a water surface on top of the frozen material that may be quite dissimilar from the surface contours. This dissimilarity is usually increased by the raising in some places and the lowering in others of the frost line by the construction of gravel pads and the excavation of unsuitable materials and replacement with soils of different thermal characteristics. Such artificial changes in the surface topography result in the creation of subsurface frozen dikes and troughs that may have a substantial effect on the distribution and run-off of the subsurface water. The heat inherent in this water may have serious effects on subsurface materials if its flow is concentrated. Where such conditions might exist, provisions must be made to insure that flowing water is diverted from any area where thawing of the ground through which it flows would be detrimental to any foundation. The problems that this water, or water from any source, creates if permitted into the ventilating system ducts will be presented subsequently under maintenance matters.

The second way that water can cause a problem is in the case of subpermafrost or intra-permafrost aquifers. In areas of shallow or discontinuous permafrost or permafrost in badly fissured rock, it is possible that the thaw below a ventilated foundation may intercept an aquifer that is under pressure due to the back freeze of its course downstream from the site of thaw. Such a condition might exist since it is possible that the back freeze downstream where the aquifer might be nearer the surface and thus exposed (that is, not under a heated building) would occur before back freeze under the structure

where the maximum thaw could be deeper due to the heat of the building. If in this situation the aquifer upstream is also below the freeze line, water could flow upward and into the ventilating system and by freezing there cause trouble. These water courses are hard to locate and, unless extensive subsurface data is available, it is difficult to predict their behavoir. It is believed that this condition has not been encountered under any ventilated foundations in Greenland. It has, however, occurred in two non-ventilated slat-on-grade structures.

In summation, the purpose of the pad is to support the structure above unsatisfactory materials that must be kept frozen, and that by its ability to absorb heat in the summer and release heat in the winter, it is an important part of any ventilated foundation system.

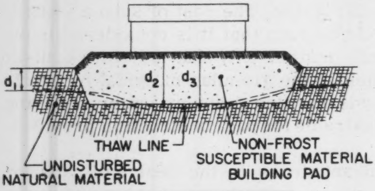
d1
d2
d3
THAW LINE
NON-FROST SUSCEPTIBLE MATERIAL BUILDING PAD
UNDISTURBED NATURAL MATERIAL

CASE I

AIR THAWING INDEX	1960 DEGREE DAYS
AIR FREEZING INDEX	4920 DEGREE DAYS
SURFACE THAWING INDEX	1175 DEGREE DAYS
FOR EACH LAYER OF UNDISTURBED NATURAL MATERIAL:	
SOIL CLASSIFICATION	SM
THICKNESS	1 FT
DRY UNIT WEIGHT	97.6 LBS/CU FT
MOISTURE CONTENT	21.8 PERCENT
TOTAL DEPTH OF THAW (d_1)	6 FT

FIG. 3.—TYPICAL BUILDING FOUNDATION, CASE I

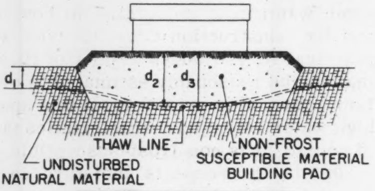
d1
d2
d3
THAW LINE
NON-FROST SUSCEPTIBLE MATERIAL BUILDING PAD
UNDISTURBED NATURAL MATERIAL

CASE	II	III
BUILDING TEMPERATURE	65°F	85°F
THAWING INDEX BELOW FLOOR SLAB	1585 DEGREE DAYS	2500 DEGREE DAYS
FOR BUILDING PAD		
SOIL CLASSIFICATION	SP	SP
THICKNESS	8 FT	8 FT
DRY UNIT WEIGHT	140 LBS/CU FT	140 LBS/CU FT
MOISTURE CONTENT	4 %	4 %
FOR UNDISTURBED NATURAL MATERIAL: SAME DATA AS CASE I		
TOTAL DEPTH OF THAW	(d_2) 9.3 FT	(d_3) 10.4 FT

FIG. 4.—TYPICAL BUILDING FOUNDATION, CASES I AND II

Extensive studies by the Corps of Engineers, U. S. Army, at the Arctic Construction and Frost Effects Laboratory (including the analysis of data obtained at Thule relative to subsurface temperatures during the years 1951-1953) have resulted in the establishment of standard procedures to determine the proper thickness of building pad knowing the other factors involved. These procedures are set forth elsewhere.[2]

---

[2] "Arctic and Subarctic Construction, Calculation Method for the Determination of Depths of Freeze and Thaw in Soils," Corps of Engrs., Engrg. Manual, Chapter 6, Part 15.

Figs. 3 and 4 show a typical building foundation and indicate the factors that must be considered in determining the depth of pad. They also show the effect of raising the building temperature.

Excessive depth of thaw at least may result in undesirable settlements and at most failures that may jeopardize the utility of the structure or cause its destruction.

Three types of ventilated floor systems have been used in Greenland. The first (Fig. 5) and simplest has been utilized in small buildings not generally requiring motor vehicle or aircraft access. This system consists of a timber crib work placed on a gravel pad of sufficient thickness, with the building placed on a crib approximately 3 ft above the surface of the gravel. This system provides ample space for air to circulate. One disadvantage is that it also permits warm air to circulate in the warm seasons.

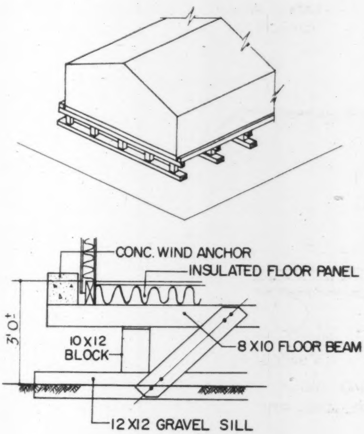

FIG. 5.—CRIB TYPE FOUNDATION

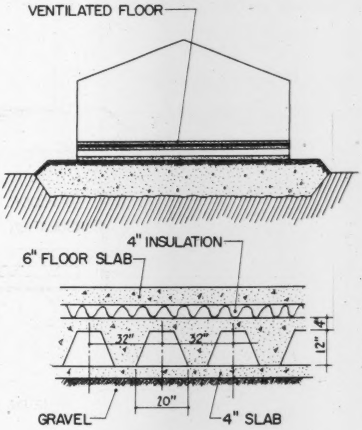

FIG. 6.—PAN TYPE FOUNDATION

However, because this system provides efficient ventilation, it is effective and, of course, relatively inexpensive. It is extremely satisfactory for light buildings in areas with a high freezing index and a low thawing index as long as snow is not permitted to accumulate in the crib space during the freezing season. Since the areas in which construction has taken place have relatively light snowfall and practically unidirectional winds during the freezing period, snow accumulation has not been a problem. By proper spacing and orientation of buildings, snow deposits can be controlled to accumulate only in areas where they will not substantially impair ventilated foundations of this type.

Structures placed on this type foundation generally have been prefabricated panel type single story structures with either load bearing walls or wood or light steel frames. These structures are designed to be capable of experiencing some differential settlement without incurring any structural damage or impairing their utility. Structures placed on this foundation in general have been limited to one-story buildings, 30 ft to 40 ft wide. Because the winds are unidirectional, the length of this structure is not limited by foundation ventilation considerations. By placing the long axis of the building parallel to the direction of wind, snow accumulation is limited to a deposit at the lee end of the building. Structures more than 200 ft long have been built. One two-story concrete Officers' Quarters has been built with the first floor elevated and supported on concrete columns. In general, buildings larger than those previously mentioned, particularly those with loads heavier than are experienced in housing facilities, are more suitably supported on ventilated foundations of the second or third types, which now will be described.

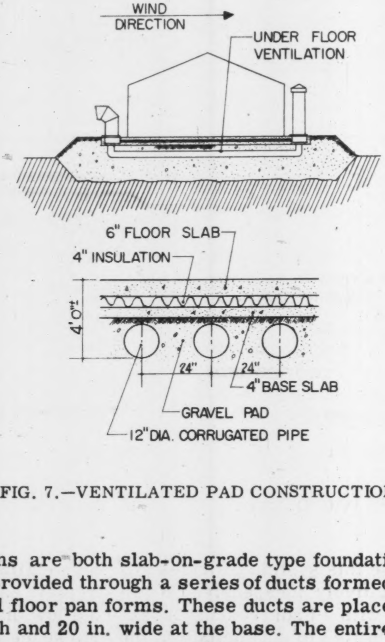

FIG. 7.—VENTILATED PAD CONSTRUCTION

The two systems are both slab-on-grade type foundations. In one (Fig. 6) the ventilation is provided through a series of ducts formed in a concrete slab by the use of metal floor pan forms. These ducts are placed 32 in. on centers and are 12 in. high and 20 in. wide at the base. The entire slab on the gravel pads consists of 4 in. of concrete on which the pans are placed and concrete poured to a depth of 4 in. above top of pans. Over this, 4 in. of cellular glas insulation is placed and finally the floor slab of concrete, usually 6 in. thick and reinforced with wire mesh, is constructed. Individual footings for columns extend below this slab into the gravel pad. In some cases the ventilation ducts are carried down below the normal level under thick slabs such as those used for generator foundations and truck lift piston enclosures.

In the second type of slab on grade ventilated foundation system (Fig. 7) (which is the third type used in Greenland and the final one described herein), the ventilation is provided through corrugated metal pipes placed in the gravel pad. An insulated floor is constructed on top of the pad. These pipes are usually 12 in. in diameter and placed 24 in. on centers with invert 48 in. below top of floor slab. The pipes are manifolded at both ends and by a plenum and stacks are extended up the sides of the buildings as may be required.

The pan type ventilating system may be used with or without a plenum and stack system. For relatively small isolated buildings located in areas of little snow fall and where the building pad can be elevated a few feet above the surrounding level, no stacks or plenums may be necessary. In larger (Fig. 8) structures where several structures of varying shapes and heights may be located in close proximity to each other, turbulence is possible resulting in irregular snow drifting patterns. In these cases where there is any possibility that the ducts might be clogged with snow, means of assuring air circulation in the winter, by the installation of plenums and stacks, are necessary.

Plenums or stacks are also required in large buildings to increase air flow by utilizing the stack effect. This effect is obtained by making stacks on the windward side just tall enough to eliminate the entrance of snow and those on the lee side higher, usually up to the eave height, and always above leeward accumulations. Another advantage (Fig. 9) is gained by orienting large buildings with air ducts parallel to the wind. Since these buildings are usually for use as warehouses, shops, and hangars, it permits the entrances to be placed on the sides parallel to the direction of the wind. Thus, these sides are swept clear of snow, minimizing snow removal operations.

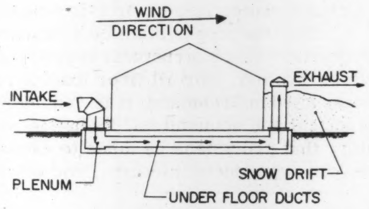

FIG. 8.—TYPICAL UNDERFLOOR COOLING SYSTEM

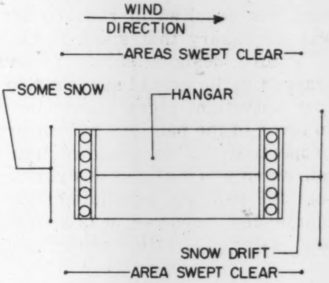

FIG. 9.—ORIENTATION

Plenums running continuously for the length of the side of buildings have been used as have metal stacks set on top of manifolds from the underfloor ducts. Some of these metal stacks have 90° elbows on top similar to a ship's topside vent cowls. Thus, if for some reason the building cannot be oriented directly with the wind, the ventilator can be adjusted for maximum air flow. Both underfloor systems have dampers which are closed during the warm weather to minimize thawing in the subgrade and opened in the cold weather to permit back freeze.

Little maintenance of the ventilating structures has been necessary on the elevated floor or the pan type slab on grade construction. Care must be exercised in the disposal of liquid wastes that leakage or spillage is not permitted to permeate the gravel pad, since the heat in such liquid may cause detrimental thawing and the moisture may enter the ventilating ducts, manifolds, or plenums. Since the ducts are kept as cold as possible, provision should be made so that no water, water vapor, or snow will get into them. This includes seepage of subsurface water through the joints in the corrugated iron pipe (which is the nestable type) since this pipe is not watertight. Annual inspection at the end of the summer season, the removal of any obstructions to the full flow of air, and the removal of subsurface water in the thawed area beneath the building which might enter the ducts, are essential. During the past winter season a considerable amount of hoar frost has been observed to have collected in the ducts under buildings using the corrugated metal pipe ducts. In some cases this has completely blocked the flow of air in several ducts under one building. It appears that the hoar frost is formed by the flow of cold dry air into the duct where heat from the building, and moisture from subsurface water, is absorbed into the air. As the air approaches the exhaust end of the duct it is cooled again, becomes super-saturated, and the water thus released is deposited on the cold metal surfaces. The reduction in cross-section area of the duct has resulted in reduced air flow which has retarded the back freeze. It was necessary that steps be taken immediately to reopen the effected ducts.

Future designs should provide for removal of water that may become trapped in the gravel surrounding the corrugated metal pipes, or it is possible that watertight pipes should be used, or that the pipe system be eliminated in favor of the pan type system provided the necessary structural and thermal properties can be designed into the floor system. For all floor loading requirements of the types of structures constructed in Greenland, it is considered that the pan-type ventilated floor is practical and economical. Its use is recommended, however, it is still mandatory that provisions be made to exclude any water or water vapor from the pan-type ducts, plenums, and stacks.

CONCLUSIONS

Satisfactory foundations for heated buildings can be adequately designed and constructed in permafrost regions. It is most important that the soil properties, the heat transfer phenomenon, the subsurface water flow, the snow drift patterns, and the movement of air for ventilation be properly evaluated if the methods described are to be successful.

DISCUSSION

JOHN A. PIHLAINEN.[3]—This description of ventilated building foundations in Greenland is a valuable contribution in a field in which little published experience is available. Although a fundamental principle of construction in permafrost areas, that of minimal thermal disturbance, has long been realized, it is only relatively recently that calculated designs based on this principle have been attempted. Although the ventilation of foundations to minimize thawing can be used on many types of foundations, it is readily adaptable to the gravel-pad type of construction.

---

[3] Northern Bldg. Sect., Div. of Bldg. Research, Natl. Research Council, Ottawa, Canada.

In assessing the performance of any foundation in permafrost areas, the soil and ice conditions must be known. The information in Fig. 3 of the paper by Mr. Williams indicates the natural subsoil to be a silty sand with a moisture content of 21.8%. Comparable moisture contents or, more correctly, ice contents, observed in Canada range from 20% to 200%.[4] Normally, the thawing of silty fine sands with low ice contents, such as 20%, does not cause unacceptable foundation settlements unless the relatively small ice contents occur in segregated form. Unfortunately, Mr. Williams has not shown that unacceptable foundation settlements would have occurred on thawing; the successful performance of the gravel pad may therefore be questioned on this aspect. If objectionable settlements will not occur on thawing, then the design of the gravel pad is based more on combating frost action than on the thaw of permafrost. From the information presented, it is not clear which has been the deciding factor.

Mr. Williams has indicated that caution must be exercised in the use of this foundation type in areas of sporadic permafrost and that in such areas the system may not be practical, presumably from an economic point of view. This restriction is accepted but it is further suggested that these limiting factors apply in some areas of continuous permafrost as well.

In the tundra of Greenland and the Canadian Arctic Islands, the thawing index (an approximation of the energy available for thawing) is considerably less than in the forested regions of continuous permafrost further south. Thus even though the insulating properties of gravel are poor, relatively small amounts of granular material are required in such areas in order to prevent disturbance of permafrost under buildings with ventilated foundations. This, combined with the fact that in Canada granular materials are generally more common in the tundra than in forested regions, suggests the gravel-pad type of foundation to be economic in these areas of the Far North.

It is interesting to note that surface air temperature observations from 1946 to 1949 at Thule[5] show the thawing index to be approximately 555 degree days and not 1960 degree days as shown in Fig. 3. The difference in these values is of sufficient magnitude to affect many aspects of the design and performance of the structures described.

In contrast, the thawing index may vary from 2000 to 3000 degree days in the forested regions of continuous permafrost; this necessitates much thicker gravel pads under buildings if disturbance of permafrost is to be avoided. The greater difficulty of locating and utilizing gravel further complicates the use of the gravel-pad type of foundation and may well result in its being uneconomical in these areas. There is a danger in the design of foundations for this forested region of overlooking the increased energy of seasonal thaw over the tundra region since observed seasonal depths of thaw are often similar in both areas. This may be attributed to the exceptional insulating qualities of the mantle of living vegetation and peat, commonly known as "muskeg," that covers most of the forested regions of continuous permafrost. Because of its extremely high thermal resistance, greatly assisted by its ability to retain large quantities of water, variations in the energy of seasonal thaw are not reflected in a varying depth of thaw; in many cases the depth of thaw is confined to the vegetative cover.

---

[4] "Permafrost Investigations at Aklavik, 1953 (Drilling and Sampling)," by J. A. Pihlianen and G. H. Johnston, Natl. Research Council, Div. of Bldg. Research, NRC 3393, Ottawa, Canada, January, 1954.

[5] "Climatological Summary, Thule, Greenland," U. S. Dept. of Commerce, Weather Bur., Washington, D. C., 1950.

During construction, it is difficult to preserve this natural form of insulation and the result is a substantial increase in the depth of thaw. For example, at Inuvik, N.W.T., an area under natural conditions maintained a 2-ft depth of thaw but after the stripping of 12 in. to 18 in. of living vegetation and peat, the depth of thaw in the underlying granular material increased during the following summer to 8 ft. The introduction of a gravel-pad type of foundation in such an area would therefore require as much caution as in areas of sporadic permafrost.

Mr. Williams has suggested that, from thermal and frost action considerations, an ideal pad would be one saturated with water but that the cost of construction involved makes this impractical. Before accepting this suggested improvement to the gravel pad type of foundation, it may be useful to review briefly the function of a gravel pad.

Where thawing of the perennially frozen ground produces little or no volume change, the function of a gravel pad supporting any type of structure would be to arch over small-scale settlements due to minor material changes. Where the thawing of subsurface material will probably produce significant settlements, however, the function of the gravel pad is to insulate so that the resultant thaw produces only settlements that can be accommodated by the arching action of the granular pad. The introduction of a structure introduces additional heat loads which must be dissipated by ventilation and/or balanced by the insulation of additional gravel fill.

It is suggested that an approach to achieving an approximation to an ideal pad having high thermal resistance, an arching property, and yet one nonsusceptible to frost action might be to introduce into the gravel above the ground surface layers of peat (or any material with good water retention properties). Since these potentially frost-susceptible materials are in a closed system, they could substantially improve the poor thermal properties of gravel without the danger of frost action. Such a method has been used extensively in Norwegian railroad construction although in a reverse situation to decrease depth of frost penetration into the rail bed.[6] If this type of pad was successful, it would reduce the amount of gravel that is necessary; then perhaps the pad type of construction might become economically feasible in the forested areas of continuous permafrost.

ROGER H. WILLIAMS,[7] F. ASCE.—The comments of Mr. Pihlainen are indeed timely in that he stresses the economics of any type of foundation design when applied to a specific area and set of circumstances. The description of the foundations given in the paper were those of actual types used at some military air bases in Greenland, including but not limited to the Thule area. In these cases, large deposits of relatively good granular materials were available as were large amounts of heavy construction equipment required for the construction of large airfield facilities in short periods of time. These factors led to the almost universal use of the foundation described in which permafrost was encountered. Structures constructed in other areas such as forest areas and areas of heavy peat require proper analysis and probably a different approach.

---

[6] "Protection Against Frost Heaving on the Norwegian Railways," by Sv. Skaven-Haug, Géotechnique, Vol. IX, No. 3, September, 1959, p. 87.

[7] Proj. Engr., Metcalf & Eddy, Boston, Mass.

The use of 21.8% moisture content in the natural subsoil was arbitrarily picked to illustrate the depth of thaw penetration and it was not intended to indicate that this material, as such, would be unacceptable. The example shows how to determine the expected depth of thaw. The materials below this point then must be scrutinized to determine their ice content and their acceptability. When this is done, it can be determined whether or not any unacceptable material has been protected sufficiently. It should be remembered, however, that even though the water or ice content is only 21.8% when the pad is constructed, that this may change due to infiltration through the pad. This infiltration and cycling of freezing and thawing may result in unacceptable conditions in the future.

The thawing index used in Fig. 3 of 1960 degree days was not intended to represent conditions of Thule but was used solely as an example (it has been encountered at other bases in Greenland). While the 1946 to 1949 observations at Thule show a thawing index of approximately 555 degree days, one would be quite remiss in using this figure for design because it is based on such a short observation period. High indices (1196 degree days in 1957, 704 degree days in 1959, and 906 degree days in 1960) have been observed.

AMERICAN SOCIETY OF CIVIL ENGINEERS

Founded November 5, 1852

TRANSACTIONS

Paper No. 3239

LESSONS OF COLLAPSE OF VANCOUVER 2ND NARROWS BRIDGE

By A. Hrennikoff,[1] F. ASCE

With Discussion by Messrs. Kuang-Han Chu; Robert Dannemann; and A. Hrennikoff

SYNOPSIS

Some conclusions are presented from a study of the collapse of the Second Narrows Bridge in Vancouver, B. C., in the summer of 1958. In this tragic occurrence is seen not only a mere consequence of an error in design but also a manifestation of the effects of some factors not yet fully appreciated. Realization of their true significance may be one positive aspect of the disaster.

GENERAL

The collapse of the Second Narrows Bridge in Vancouver, B. C., has been described[2] by F. M. Masters, F. ASCE, and J. R. Giese, of Madjeski and Masters, Harrisburg, Pa., who, together with J. R. H. Otter of Rendel, Palmer, and Tritton, and Ralph Freeman, F. ASCE, of Freeman, Fox, and Partners,

---

Note.—Published essentially as printed here, in December, 1959, in the Journal of the Structural Division, as Proceedings Paper 2305. Positions and titles given are those in effect when the paper or discussion was approved for publication in Transactions.

[1] Prof., Civ. Engrg., Univ. of British Columbia, Vancouver, B. C., Canada.

[2] "Findings on Second Narrows Bridge Collapse at Vancouver," by F. M. Masters and J. R. Giese, Civil Engineering, February, 1959.

both of London, England, and A. B. Sanderson of Victoria, B. C., were the principal engineering advisers to the Royal Commission under Sherwood Lett, appointed by the Government of British Columbia to investigate the disaster. The writer was engaged by the Royal Commission for the study of one particular part of the bridge, the grillage of the falsework bent supporting the bridge during the erection. This grillage proved to be the cause of the collapse. The lessons that the writer discerns in the catastrophe are as follows:

1. The inapplicability of the usual column formulas for the design of the webs of the grillage beams in buckling.
2. The weakening effect of the plywood pads interposed in the grillage.
3. The general inadequacy of the column formula given by the Canadian Specifications CSA, 1952.

Prior to the examination of these matters it is necessary to describe the construction of the grillage and its status with regard to the buckling failure.

CONSTRUCTION OF THE GRILLAGE

The falsework bent supported by the grillage, that caused the failure, is shown in Fig. 1. This photograph was taken shortly before the collapse. The grillage itself is presented in Fig. 2. The two columns of the bent, with the base plates 5-3/4 in. thick underneath them, were supported by two tiers of beams which rested on piles. The upper tier of four beams or stringers, 36 W-160, extended transversely to the bridge from one column to the other and was supported under each column by a group of four built-up, welded, grillage beams. These beams rested on open-end pipe piles filled with concrete. Plywood pads, 3/4 in. thick, were interposed between the column base and the stringers, and also between the latter and the grillage beams. The weakness of the grillage was due to the lack of diaphragms or adequate stiffners in the upper tier stringers, which, in the opinion of the Royal Commission, led to the buckling of the webs of the stringers, precipitating the collapse of the falsework bent and with it the bridge itself. (It may be mentioned that the Royal Commission discovered also some computation errors in the design of the stringers, consistent with the conclusion attributing failure to the buckling of the stringer webs.) The bottom tier grillage beams were provided with proper diaphragms and were fully adequate. The piles underneath them were also amply strong and rigid.

BUCKLING OF WEBS OF GRILLAGE STRINGERS

As may be seen in Fig. 2, the four stringers were held together by four packs of wooden blocking, two of which were located just outside the falsework columns and the two others at the third points of the distance between the column centers. The ends of the two outer stringers were also connected by vertical angle brackets to the diaphragms on the grillage beams.

The buckling of the webs of the stringers occurred underneath the column bases in the manner of Fig. 3. The bottom flanges of the stringers were held in place by the friction on the grillage beams, while their top flanges moved sideways parallel to themselves together with the column base, as the column rocked about the hinge at its top end, underneath the truss. With the top flanges

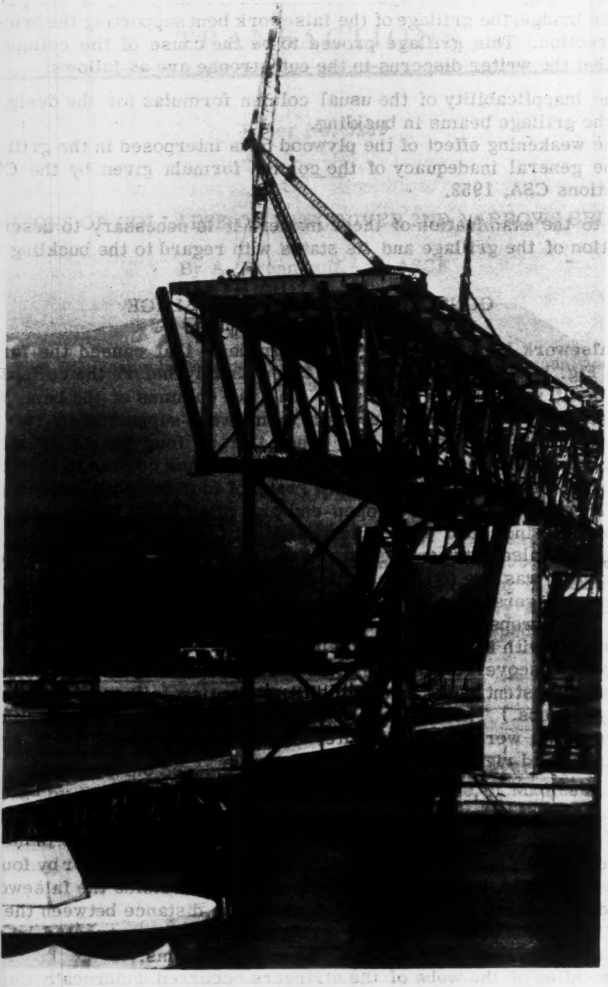

FIG. 1.—FALSEWORK BENT SUPPORTED BY GRILLAGE SHORTLY BEFORE FAILURE

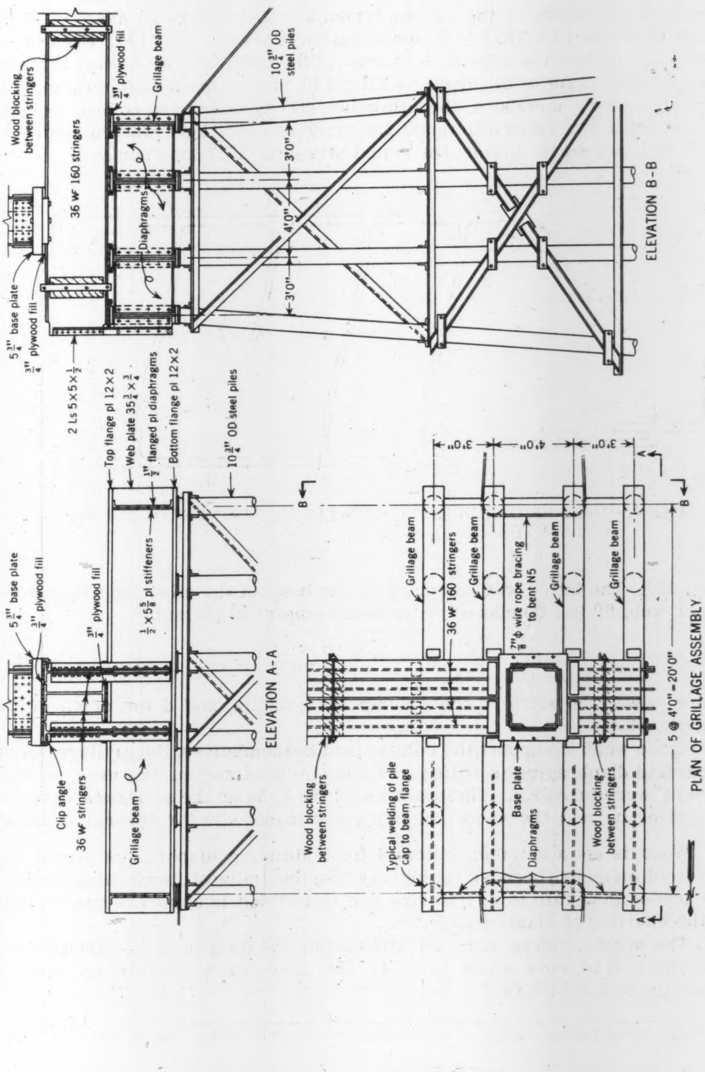
Wood blocking between stringers
3/4" plywood fill
Grillage beam
36 W 160 stringers
Diaphragms
5 3/4" base plate
3/4" plywood fill
2 Ls 5×5×1/2
10 3/4" OD steel piles
3'0"
4'0"
3'0"
ELEVATION B-B
Top flange pl 12×2
Web plate 35 3/4 × 3/4
1/2" flanged pl diaphragms
Bottom flange pl 12×2
10 3/4" OD steel piles
B
1/2 × 5 5/8 pl stiffeners
5 3/4" base plate
3/4" plywood fill
3/4" plywood fill
Clip angle
36 W stringers
Grillage beam
ELEVATION A-A
Grillage beam
36 W 160 stringers
Grillage beam
7/8" φ wire rope bracing to bent N5
Grillage beam
Grillage beam
Typical welding of pile cap to beam flange
Wood blocking between stringers
Diaphragms
Base plate
Wood blocking between stringers
3'0"
4'0"
3'0"
A
A
B
B
5 @ 4'0" = 20'0"
PLAN OF GRILLAGE ASSEMBLY

FIG. 2.—GRILLAGE

fixed in direction but free to move sideways, the structural action of the stringer webs in the course of buckling was equivalent to a pin-ended column (Fig. 4) of the length L = 32-1/4 in. equal to the distance between the flange fillets. In this action the stringers were grossly underdesigned. Their slenderness ratio was 171 against the allowable 120 for main members and 140 for the secondary ones according to the column formula of the American Assn. of State Highway Officials (AASHO) 1955 specification (Curve 1, Fig. 13). Even using a much more lenient Canadian Specification, CSA 1952, (Curve 2, Fig. 13) with the permissible limit of slenderness ratio 140 for the main members and 200 for the secondary members, the allowable stress, using the normal column formula with a 33% extra allowance for erection conditions, was computed to be 11.2 kips per sq in. against the actual stress of 17.2 kips per sq in. (point X, Fig. 13). The latter was computed on the basis of the effective width of the stringer web, 60 in., computed by the usual empirical formula[3]

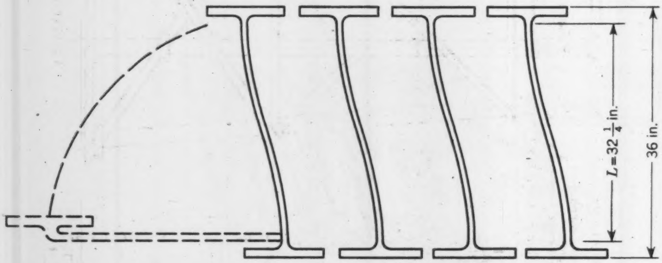

FIG. 3.—MANNER OF BUCKLING OF WEBS OR STRINGERS BENEATH COLUMN BASES

$$w = b + \frac{d}{2} \qquad (1)$$

in which b was the width of the column base, 42 in., and d the depth of the stringers, 36 in.

Being too weak to support the column load by themselves, the grillage beams needed rigid diaphragms or stiffeners for their stabilization. However, no such members were provided. The brackets on the ends of the stringers were totally ineffective and the wooden blocking was inadequate for several reasons:

1. Wood is not a suitable material for stabilizing diaphragms placed between steel members because the highest possible value of its modulus of elasticity across the grain is only 40 kips per sq in.; that is some 750 times lower than the modulus of elasticity of steel.
2. The wooden blocks were not fitted under the flanges of the stringers.
3. The blocks were made loose by shrinkage caused by the dry spell of weather preceding failure.

---

[3] "Structural Design in Steel," by Thomas Shedd, John Wiley and Sons, 1934, p. 87.

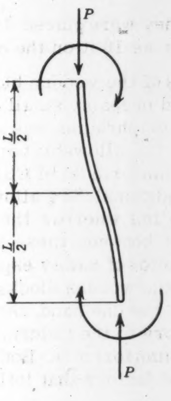
P
$\frac{L}{2}$
$\frac{L}{2}$
P

FIG. 4.—EQUIVALENT STRUCTURAL ACTION OF STRINGER WEBS IN THE COURSE OF BUCKLING

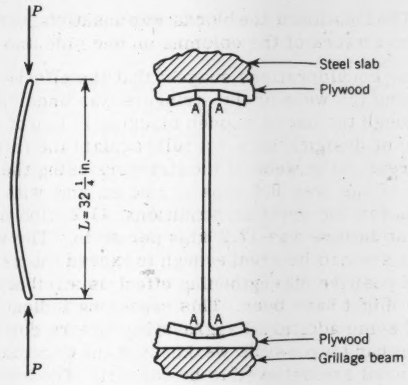
P
$L = 32\frac{1}{4}$ in.
P
A A
A A
Steel slab
Plywood
Plywood
Grillage beam

FIG. 5.—BENDING OF FLANGES

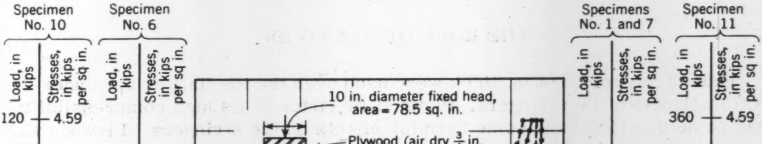

FIG. 6.—COMPRESSIBILITY TESTS OF THE PLYWOOD PADS

4. The location of the blocks was unsatisfactory. They were placed 3 ft 6 in. from the centers of the columns on one side and as far as 16 ft on the other.

These considerations suggest that the effectiveness of the wooden blocks in stabilizing the webs of the stringers was uncertain and probably small.

Although the use of wooden blocking in lieu of rigid diaphragms was a grave mistake of design it does not fully explain the failure. The allowable compression stress in the webs of the stringers using the column formula of CSA, 1952 specifications was 8.4 kips per sq in. and with an additional 33% allowance, common for the erection conditions, 11.2 kips per sq in., whereas the actual stress at failure was 17.2 kips per sq in. The spread between these figures does not seem to be great enough to exceed the usual factor of safety especially if some positive strengthening effect is attributed to the wooden blocks, weak as they might have been. This reasoning indicates, on the one hand, the presence of some additional aggravating factors contributory to the failure, and on the other hand a possible weakness of the Canadian column formula. Both these conjectures are believed to be correct. The additional factors that influenced the failure were as follows:

1. The action of the plywood packing at the top and bottom flanges of the stringers.
2. The imperfections of the shape of the stringers.
3. The difference of the stringers in depth.

THE ROLE OF PLYWOOD

Pads of plywood 3/4 in. thick were used over the top flanges and under the bottom flanges of the stringers. Plywood, by virtue of its high compressibility, had some beneficial and some harmful effects on the stringers. Plywood was beneficial because it levelled off the local irregularities of contacts. Thus, if one of the four stringers were smaller in depth than the others, the compressibility of the plywood would still allow it to carry an appreciable part of the load. Without soft packing of this kind the undersize stringer would be completely free of load. For the same reason the load carried by the stringers was distributed nearly equally between the grillage beams underneath them, whereas without the plywood, the grillage beams near the center of the footing would have carried most of the load.

However, the high compressibility of plywood had also some harmful effect induced by the comparatively low bending strength of the stringer flanges about the longitudinal axis. The flanges bent, as indicated in Fig. 5, with formation of plastic hinges at the sections A on the sides of the web, reducing the restraints at the top and bottom of the web from fixed to something approaching pinned and thereby decreasing its resistance to buckling. The computations leading to the conclusion presented here are based on the compressibility tests of the plywood pads, the results of some of which are shown in the graphs of Fig. 6.

Plywood Tests.—The plywood used in the tests was of the same kind as on the bridge. It was 3/4 in. thick and was made of 7 plies of Douglas Fir. At the time of testing it was air-dry with 7% moisture content. In all cases the plywood was compressed between the table of the testing machine and the fixed upper head that was in the form of a circle 10 in. in diameter. Some of the specimens were squares 12-in.-by-12-in., others were circles 10 in. in diameter and still others, smaller circles, 5.78 in. in diameter having an area exactly one-third of the area of the bigger circles. The specimens were loaded to a unit stress somewhat higher than the estimated stress of from 2 kips per sq in. to 2-1/4 kips per sq in. experienced in the grillage; they were kept under the full load for a period of time and were then unloaded.

The stress-strain curves of the plywood were characterized by the following features:

1. Plotted to the same scale of unit stress, all curves were practically the same thus proving that the unit stress versus unit strain relations did not depend on the areas loaded.

2. In the region up to a stress of 0.6 kips per sq in. to 0.7 kips per sq in., the curves were comparatively steep and straight with the corresponding modulus of elasticity of approximately 40 kips per sq in. Between the stresses of approximately 0.7 kips per sq in. and 1.5 kips per sq in., the curves were flat with the modulus of elasticity reduced to as little as 4 kips per sq in. Beyond the flat region the slope of the curves increased gradually to a modulus as great as 30 kips per sq in.

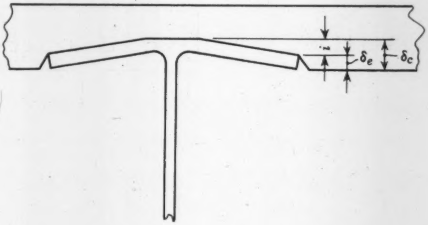

FIG. 7.—DEFORMATIONS OF STRINGER FLANGE AND PLYWOOD PAD IN TRANSMITTING LOAD FROM COLUMN BASE TO STRINGERS

3. The curves of unloading were very steep. There was virtually no rebound of deformation on removal of 85% to 90% of the load. A small rebound occurred on removal of the final remains of the load. This peculiarity of the stress-strain relation of plywood had an important bearing on the resistance of the web of the stringer to buckling, as will be subsequently explained.

4. When the load was kept constant the deformation continued to increase with time. In other words, the plywood was subject to creep, the rate of which, as is usual in creep tests, decreased quickly with time. Additional tests indicated that the amount of creep at different loads varied inversely with the slope of the stress-strain curve, that is, the creep effects were greater on the flatter parts of the curve.

The stress-strain graphs described here made it possible to perform computations pertaining to the load distribution on the stringers.

Formation of Plastic Hinges in Flanges of Stringers.—Fig. 7 shows the deformations of the stringer flange and the plywood pad in transmitting the load

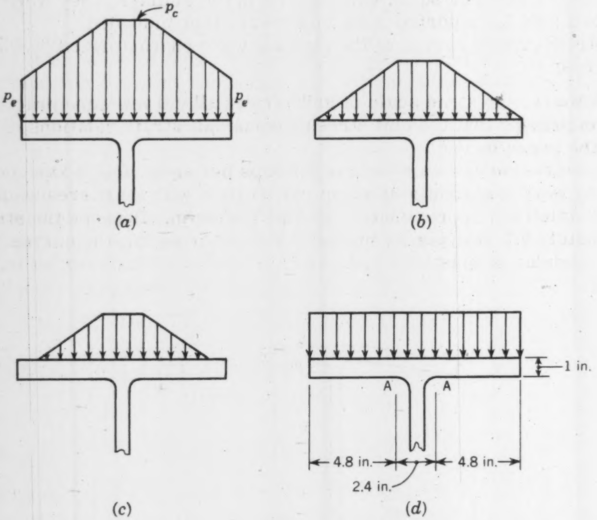
p_c
p_e
p_e
(a)
(b)
1 in.
A
A
4.8 in.
4.8 in.
2.4 in.
(c)
(d)

FIG. 8.—DISTRIBUTION OF UNIT PRESSURES

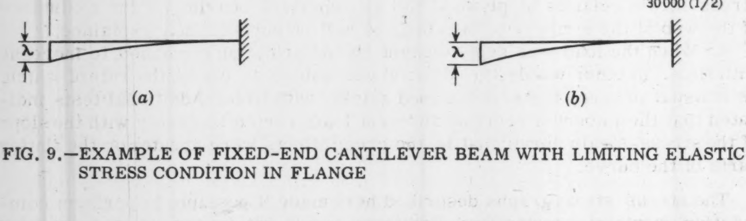
4.8 in.
Load
Parabola
$\frac{33}{30000\,(1/2)}$
$\frac{M}{EI} = \frac{f}{Ey}$
λ
(a)
4.8 in.
Load
Cubic parabola
$\frac{M}{EI} = \frac{f}{Ey}$
$\frac{33}{30000\,(1/2)}$
λ
(b)

FIG. 9.—EXAMPLE OF FIXED-END CANTILEVER BEAM WITH LIMITING ELASTIC STRESS CONDITION IN FLANGE

from the column base to the stringers. The edges of the flange deflect an amount λ in relation to the center, and the plywood pad compresses the amounts

δ_e at the edges and δ_c at the center, because the heavy steel slab resting on the plywood pad virtually cannot bend.

Evidently,

$$\lambda = \delta_c - \delta_e \qquad (2)$$

The distribution of unit pressure between the plywood and the flange is likely to be of the type shown in Fig. 8(a) with the edge pressure p_e being smaller than the center pressure p_c due to a smaller compression of plywood at the edges compared to the center. In an extreme case the pressure at the edge may be zero as shown in Figs. 8(b) and 8(c).

That a uniform distribution of pressure in the grillage in accordance with Fig. 8(d) was impossible, becomes clear from the following computation:

Column load per stringer at the time of failure = 675 kips; Length of base slab along the stringer = 42 in.; Load per inch of length of one stringer = 675/42 = 16.0 kips per in. Referring to Fig. 8(d), the load per square inch:

$$p = \frac{16.0}{12} = 1.32 \text{ kips per sq in.}$$

Considering 1 in. of the length of the flange, the bending moment at the beginning of fillet, point A, is

$$M_A = \frac{1}{2}\,(1.32)(4.8)^2 = 15.2 \text{ kip-in. per in.}$$

With

$$I/C = \frac{1}{6}\,(1)\ (1)^2 = \frac{1}{6} \text{ cu in. per in.}$$

the maximum bending stress

$$f = 15.2\ (6) = 91.2 \text{ kips per sq in.}$$

This stress is so great that it calls for development of plastic hinges at A.

Using the plastic section modulus

$$I/C = 1.5\left(\frac{1}{6}\right) = \frac{1}{4} \text{ cu in. per in.}$$

instead of the elastic section modulus, in the formula for the bending stress, the latter comes to 15.2(4) = 60.8 kips per sq in., which is again much greater than the yield stress. This computation demonstrates the impossibility of a uniform distribution of pressure over the flange in accordance with Fig. 8(d). The pressure then must be distributed in the manner of one of Figs. 8(a), 8(b), or 8(c).

With the stresses at the edges of the flanges thus reduced, the moment at the points A must decrease and an additional computation is needed in order to demonstrate that the plastic condition in the flanges is unavoidable.

Assume tentatively, by way of demonstration ad absurdum the existence of the limiting elastic stress condition in the flange, with the extreme bending stress equal to the yield stress 33 kips per sq in., and find the deflection λ of the edge of the flange in relation to the center, as in a fixed-ended cantilever beam of 4.8 in. length (Fig. 9).

Using a uniform pressure distribution [Fig. 9(a)], by the moment-area theorem and remembering that

$$\frac{M}{E\,I} = \frac{f}{E\,y} \quad \ldots\ldots\ldots\ldots\ldots\ldots\ldots \quad (3)$$

$$\lambda = \frac{1}{3}\,(4.8)\,\frac{33}{(30{,}000)\,(0.5)}\,\left(\frac{3}{4}\right)(4.8) = 0.0127 \text{ in.}$$

Using a triangular pressure distribution [Fig. 9(b)]

$$\lambda_1 = \frac{1}{4}(4.8)\,\frac{33}{(30{,}000)\,(0.5)}\,(4/5)\,(4.8) = 0.0102 \text{ in.}$$

Thus no matter how the load may be distributed over the flange an elastic deflection of the edge of the flange may only be of the order of 0.01 in.

Remembering that the mean pressure between the plywood and the stringer flange is 1.32 kips per sq in., the mean compression of the plywood is found by

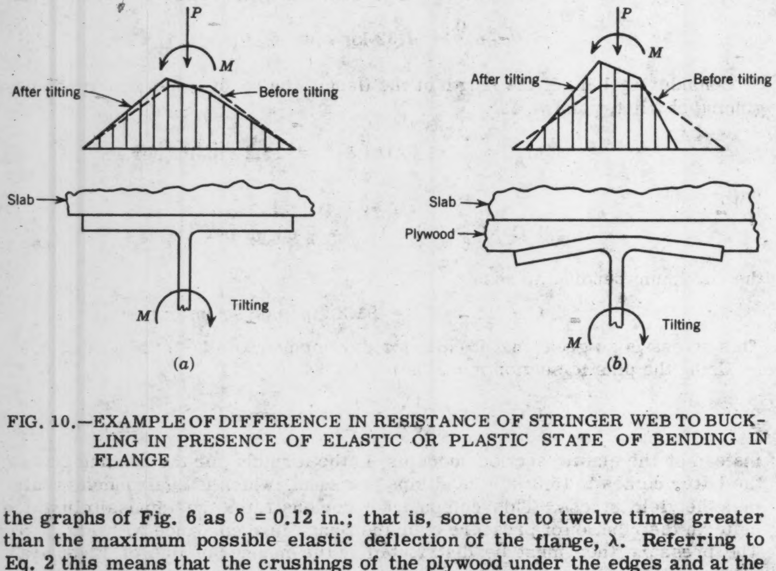

FIG. 10.—EXAMPLE OF DIFFERENCE IN RESISTANCE OF STRINGER WEB TO BUCKLING IN PRESENCE OF ELASTIC OR PLASTIC STATE OF BENDING IN FLANGE

the graphs of Fig. 6 as δ = 0.12 in.; that is, some ten to twelve times greater than the maximum possible elastic deflection of the flange, λ. Referring to Eq. 2 this means that the crushings of the plywood under the edges and at the center must nearly be equal, but with the equal crushings the pressure between the plywood and the stringer flange must be uniform. This deduction, however, has been disproved. Then the assumption of the elastic stress condition in flanges must be false too, and the flange must deform plastically.

The gist of this reasoning may be stated in the following. The combination of high compressibility of plywood and of a very small maximum possible elastic deflection in the flange would make the pressure on the flange under the elastic conditions nearly uniform; that, however, is impossible in view of the low bending strength of the flange. The conclusion, then, is that the flanges bend inelastically forming plastic hinges (sharp bends) at the sections A, thus decreasing the compression of plywood at the edges and producing the pressure distribution in the manner of Figs. 8(a), 8(b), or 8(c).

It may be pointed out also that in the absence of the plywood pads, (with the column base resting directly on the flanges) the pressure distribution would still be of the types of Figs. 8(b) or 8(c), but the bending of the flange would be elastic.

The presence of the elastic or plastic state of bending in the flange makes a great difference in the resistance of the stringer web to buckling, as is illustrated in Figs. 10(a) and 10(b). When the steel slab rests directly on the stringer and bending is elastic, a slight clockwise tilting of the stringer, as a stage preliminary to buckling, brings into play a resisting counter clockwise moment through a tighter contact and a greater pressure between the slab and the beam on the left side of the flange and a looser contact on the right side bringing with it an elastic reduction of the pressure. When, however, plywood is interposed between the slab and the beam [Fig. 10(b)], whose flanges are bent inelastically, the resistance to a similar clockwise tilting is greatly reduced because a tighter contact on the left side brings no more pressure as the left side of the flange rotates about the plastic hinge, whereas a looser contact on the right side of the flange tends to remove nearly all pressure due to a virtual absence of an elastic rebound in the plywood, already referred to in the course of the description of the plywood tests. In order to continue to develop the normal load P and at the same time to offer a due moment resistance the flange must crush the plywood deeply and must turn much more in the direction of tilting than when the plywood is absent. This behavior signifies a greatly reduced resistance to buckling in the presence of plywood.

It should be pointed out that the high compressibility of plywood can produce the undesirable effects examined here only when combined with a low bending strength of the flange. A greater thickness of the flange would preclude the possibility of formation of plastic hinges and the reduction of buckling resistance. Again, the presence of effective diaphragms between the stringers would stabilize them and prevent their buckling even in spite of the formation of the plastic hinges in their flanges.

IMPERFECT SHAPE OF STRINGERS

Rolled sections are never geometrically perfect and definite small tolerances are permitted in mill practice with regard to their deviations from the theoretical dimensions and shapes. Normally the effect of these imperfections on strength is minor and need not be specially provided for in design, but occasionally these irregularities give rise to dangerous situations, that must be recognized by proper provisions in the specifications. Buckling of the webs of the grillage stringers is one of these cases. The danger of this condition arises from the fact that specifications, such as those of AASHO, give only one column formula for the design of compression members and the imperfections visualized in this formula are relatively much smaller than the ones encountered in compression of the webs of the beams.

The use of an ordinary column formula in checking the buckling of the webs of stringers in grillages is apparently a recognized practice judging by the examples presented by Shedd[3] who uses for this purpose the normal American Railway Engineers Assn. (AREA) and American Institute of Steel Construction (AISC) column formulas. This practice, in the opinion of the writer, is unsafe.

In order to study the buckling strength of the beam web experimentally, the writer tested two pieces of 36W160, 12 in. long, cut from crops left from fabrication of the grillage stringers involved in the failure of the bridge. The two specimens were nearly identical having been made from adjacent parts of the same length. The tests were performed in the universal testing machine with the upper head fixed, so that both the top and the bottom flanges of the beam behaved as fixed in direction and position. This was not the same condition of end restraints as in the bridge grillage, but it was more convenient to reproduce in the laboratory and it served its purpose. The arrangement of the tests is shown in Figs. 11(a) and 11(b). The two tests differed only in the presence of the plywood pads interposed between the loading plates and the beam flanges in the set-up of Fig. 11(b). No such pads were present in the other test.

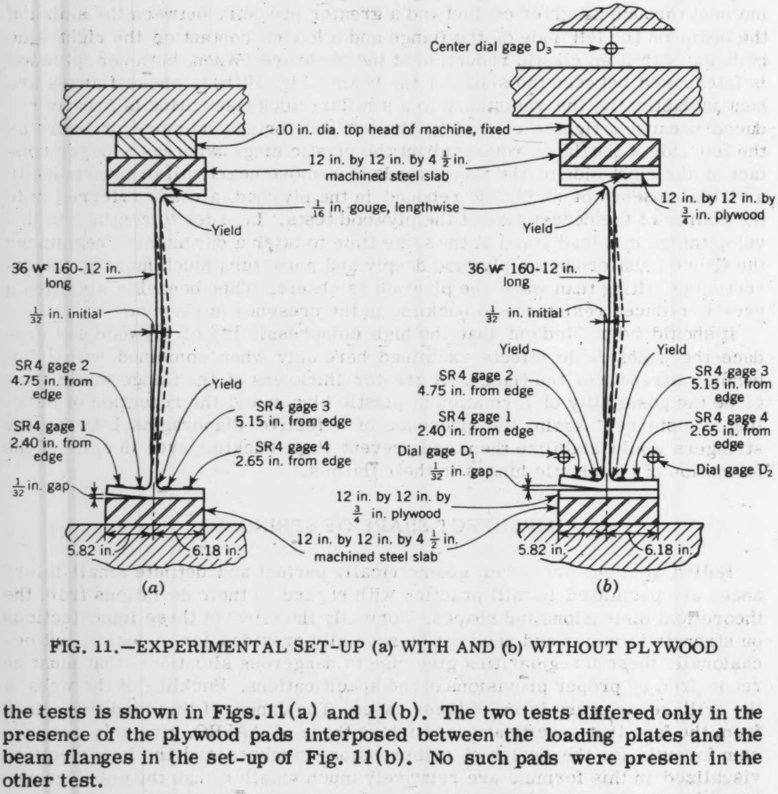
Center dial gage D_3
10 in. dia. top head of machine, fixed
12 in. by 12 in. by 4 ½ in. machined steel slab
$\frac{1}{16}$ in. gouge, lengthwise
12 in. by 12 in. by ¾ in. plywood
Yield
Yield
36 W 160-12 in. long
36 W 160-12 in. long
$\frac{1}{32}$ in. initial
$\frac{1}{32}$ in. initial
Yield
Yield
SR4 gage 2 4.75 in. from edge
Yield
SR4 gage 2 4.75 in. from edge
SR4 gage 3 5.15 in. from edge
SR4 gage 3 5.15 in. from edge
SR4 gage 1 2.40 in. from edge
SR4 gage 1 2.40 in. from edge
SR4 gage 4 2.65 in. from edge
SR4 gage 4 2.65 in. from edge
Dial gage D_1
Dial gage D_2
$\frac{1}{32}$ in. gap
$\frac{1}{32}$ in. gap
12 in. by 12 in. by ¾ in. plywood
12 in. by 12 in. by 4 ½ in. machined steel slab
5.82 in.
6.18 in.
5.82 in.
6.18 in.
(a)
(b)

FIG. 11.—EXPERIMENTAL SET-UP (a) WITH AND (b) WITHOUT PLYWOOD

A significant feature of the test specimens was the presence of numerous imperfections.

1. The web of the beam was 3/16 in. off center making the widths of the two halves of both flanges different by 3/8 in.

2. The shape of the cross section was not truly rectangular so that although the top flange of the specimen, after being placed in the testing machine, was fully covered by the bearing plate the bottom flange had a gap under one half of it as great as 1/32 in. at the edge.

3. The top flange had a narrow depression or a gouge 1/16 in. deep, running lengthwise and located just off center.

4. The web had a curvature whose center rise was approximately 1/32 in.

The imperfections (1) and (2) were within the tolerances permitted by the usual practice.[4] The permissible limits of the curvature of the web and of the depression in the flange are not known to the writer but the fact that the stringers passed the bridge inspection leads him to believe that all irregularities were within the allowable limits.

The following values of the maximum loads and the corresponding unit stresses were observed:

Specimen with Plywood.—Maximum load 139 kips; unit stress, assuming uniform compression, 139/12(0.653) = 17.73 kips per sq in.

Specimen without Plywood.—Maximum load 143 kips; unit stress assuming uniform compression, 143/12(0.653) = 18.23 kips per sq in.

As has already been stated, the actual stress in the stringer web of the grillage at failure, with flanges less firmly restrained than in the test, was found to be 17.2 kips per sq in.

Considering the test as a pure compression of a fixed-ended column of the length L = 32$\frac{1}{4}$ in., the failure load may be found by Euler's formula

$$P_{cr} = \frac{\pi^2 E I}{l^2} \quad \ldots\ldots\ldots\ldots\ldots\ldots\ldots \quad (4)$$

using for l the^3 length $\frac{1}{2}(32\frac{1}{4}) = 16\frac{1}{8}$ in., and for I the value $I = 12(0.653)^3/12 = 0.2787$ in.^{4} This gives

$$P_{cr} = \frac{\pi^2 (30{,}000)(0.2787)}{\left(16\frac{1}{8}\right)^2} = 317 \text{ kips}$$

and

$$f_{cr} = \frac{317}{(12)(0.653)} = 40.5 \text{ kips per sq in.}$$

Because Euler's formula is applicable only within the elastic range, and the value of the critical stress computed by this formula exceeds the lower yield stress found by experiment to be $f_y = 33.9$ kips per sq in., it follows that, theoretically, the critical stress should be close to 33 kips per sq in. and the critical load close to 258 kips.

The reason that the true buckling loads were found to be only half as great as computed must be sought in imperfections of the rolled sections and particularly in the initial curvature of the web. This conclusion was strongly suggested by the test in which the plywood was not used. As may be seen in Fig. 11(a), the bottom flange of the specimen had a small gap under it on the left side and was therefore supported at the commencement of testing under its right side only. The moment created by the one-sided support of the bottom flange might have been expected to cause the bending of the web to the left. This, however, had never happened in view of the initial curvature of the web directed to the right. The influence of the curvature was greater than the influence of the moment at the bottom flange and so the web deflected in the direction of the original curvature until the specimen finally failed. The gap underneath the left side of the beam had never closed.

---

[4] "Steel Construction Manual," Amer. Inst. of Steel Constr., New York, 1948, p. 64.

Similar behavior was observed in the test involving the plywood pads [Fig. 11(b)] except that the empty space under the bottom flange soon disappeared as the plywood compressed.

Electrical resistance SR4 strain gages were used on the inside of the bottom flanges. In the test with plywood the gages registered high stresses indicating formation of plastic hinges next to the web as predicted by the theoretical considerations. Peeling of the shop paint also indicated formation of plastic hinges at the two extremities of the web [see Fig. 11(b)] when the latter began to buckle. In the test without the plywood, peeling of the paint was also noticed at the approach of buckling failure at two locations, namely, at the bottom of the web and on the right hand side of the top flange [see Fig. 11(a)] where the latter was weakened by a deep depression.

These results proved definitely the weakening effect of the beam imperfections, although these imperfections were probably not unusual. The tests also confirmed the influence of the compression of plywood on formation of plastic hinges in flanges, but they were non-conclusive in demonstrating the weakening effect of plywood on the buckling of the webs of the stringers, because the two observed values of the buckling load, 139 kips with plywood and 143 kips without it, were not sufficiently far apart. Apparently the effect of the imperfections on the buckling load was so great as to nearly conceal the unfavorable influence of the compressibility of the plywood.

DIFFERENCE OF DEPTHS OF STRINGERS

Evidence was found suggesting a difference in depth of the four stringers forming the grillage, with the extreme northerly stringer being 1/4 in. undersize. Although the plywood pads were beneficial in this connection they could not equalize the loads perfectly and the second northerly stringer must have carried an excess load estimated at 10%. Under the conditions resulting in failure, overstress of this magnitude probably did have some significance, however, it normally should be covered by the usual factor of safety inherent in the allowable stresses.

COLUMN FORMULAS

The results of the compression tests of the beam sections showed the important effect on their strength of the imperfections of the shape, that might at first glance seem trivial. In the light of these findings it appears incorrect to design grillage beams in buckling by the same column formulas as are used for the compression members in general. The usual column formulas are intended primarily for the members of trusses and steel frames and although they provide for the presence of some imperfections and defects in shape, these imperfections are apparently less significant than the ones encountered in the beam sections subjected to buckling of the web. This may be demonstrated by applying the column formula to the tests just discussed:

Using[3]

$$l = \frac{1}{2}\left(32\frac{1}{4}\right) = 16\frac{1}{8}$$

and

$$r = \frac{0.653}{\sqrt{12}} = 0.191, \frac{l}{r} = 85.5$$

Then the allowable stress by AASHO, 1955 specification, with an addition of 33% allowance for erection conditions, comes to 16.8 kips per sq in. This value is much too close to the failure stresses 17.73 and 18.23 kips per sq in., observed in the tests. These results show that a new and more conservative column formula must be devised for the design of grillage webs in buckling in the absence of web stiffeners.

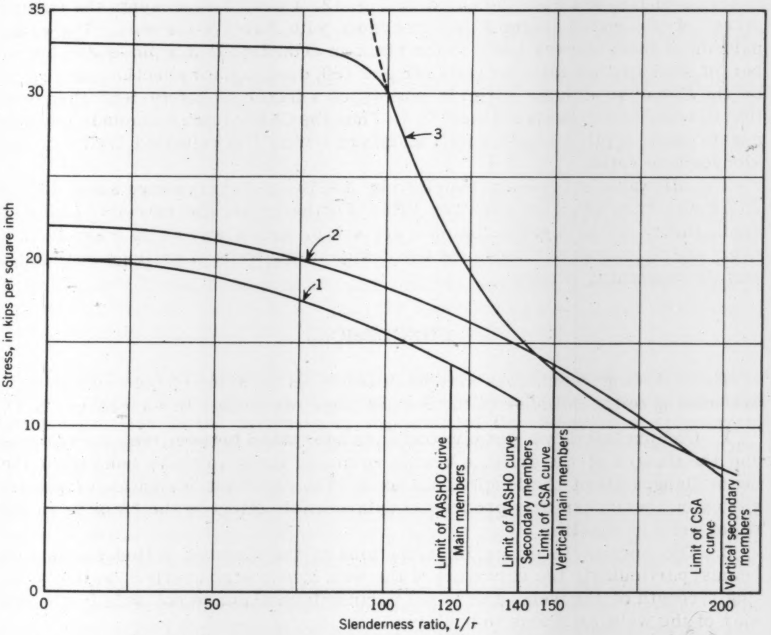

FIG. 12.—COMPRESSION STRESSES AS A FUNCTION OF SLENDERNESS RATIO

Attention must be drawn also to the inadequacy of the column formula of CSA, 1952 specifications, not only for the design of grillages but for general design purposes. In the statement of this formula the length l is defined as the unsupported length without specifying the conditions of restraint on the ends. Although the end conditions in compression members are often somewhat indeterminate, this is not always so, and there are situations in which the ends are pinned, as is recognized in the AASHO column formula and as is the case with webs of grillage beams subjected to buckling. Because the CSA column formula does not disqualify such members it should be safe in application to them, but actually it is not.

This statement may be best demonstrated by the three curves (Fig. 12) representing the compression stress as a function of the slenderness ratio l/r. The curves 1 and 3 show the allowable stresses, with an additional 33% allowance for erection, corresponding respectively to the column formulas of AASHO, 1955 and CSA, 1952 specifications. The limits of applicability of these formulas, in terms of l/r, are also indicated in Fig. 12. Curve 3 represents the failure stress of pin-ended columns in accordance with Euler's formula. The comparison of these curves leads to the striking deduction that a pin-ended member, of slenderness ratio between 145 and 190, designed for erection conditions by the Canadian column formula possesses a factor of safety less than one, that the member so designed must fail. Thus the CSA column formula is grossly unsafe when applied to pin-ended members within the indicated limits of the slenderness ratio.

The allowable stresses prescribed by AASHO are everywhere some 10% to 25% lower than the ones given by CSA. Furthermore, the extreme limits of applicability of the AASHO formula are set in such a way as to make it safe everywhere, except of course for the design of the webs of grillage beams, as was demonstrated earlier.

CONCLUSIONS

The following conclusions may be drawn from the study of the grillage failure leading to the collapse of the Second Narrows Bridge in Vancouver, B. C.

1. Compressibility of the plywood pads interposed between the column bases and the flanges of the grillage beams normally leads to sharp bending of the beam flanges about the longitudinal axis. The resultant formation of plastic hinges on the flanges may produce an unfavourable effect on the stability of the beam webs in buckling.

2. The seemingly minor imperfections in the shape of rolled sections of beams, particularly the curvature of the web, have a strong effect on the buckling strength of the web. The usual column formulas are not safe in the design of the webs of beams in buckling.

3. The column formula given by the Canadian specification CSA 1952 is unsafe for design of pin-ended members within certain limits of the slenderness ratio.

DISCUSSION

KUANG-HAN CHU,[5] **F. ASCE.**—Hrennikoff has made a valuable contribution in his study of the causes of the collapse of the Vancouver Narrows Bridge, Vancouver, B. C. The writer, however, cannot agree with Hrennikoff in the use of American Assn. of State Highway Officials formula for pin-end columns, $f = 15000 - \frac{1}{3}\left(\frac{l}{r}\right)^2$ in evaluating the buckling strength of the web of 36 in. WF section. The above formula was based on the Final Report of ASCE Committee of Steel Column Research.[6]

In the derivation of this formula, a reduced length of 85% of the full length was assumed. Therefore, for an ideally simply supported column, the formula should be $f = 15000 - \frac{1}{3}\left(\frac{l}{0.85r}\right)^2$. Applying this to the example shown in the paper, with $l/r = 85.5$, the allowable stress with 33% increase should be 15.5 ksi instead of 16.8 ksi. This value of 15.5 ksi corresponds to factors of safety of 1.14 and 1.17, respectively, with respect to the test values of 17.73 ksi and 18.23 ksi. These factors of safety are for erection stresses. For normal loading, they correspond to factors of safety of 1.52 and 1.56, respectively. These values, although about 15% lower than the specified value of 1.76 (referring to steel with minimum yield of 33,000 psi), seem to be adequate.

ROBERT DANNEMANN.[7]—Every important structural accident has, besides all the tragic consequences it may carry, the virtue of stimulating research and imagination in the direction of the truth of the behavior of structures, with the result of sometimes discovering traditional or important errors.

In the writer's opinion, the origin of the collapse lays principally in the inappropriate combination of structural elements, and was not caused solely by the local buckling of the elements that failed. Looking at Fig. 13 it becomes obvious that the whole supporting system has a weak point in the upper tier stringers of the base. These elements have an appreciable vertical stiffness, but a very low lateral one. Every deviation from theoretical ideal conditions in the support system may produce moments and shear forces that act on the rigid base of the bent. The results could be elastic or thermal elongations of the bridge, rotation of the upper support of the bent produced by cantilever construction, eccentricities in the application of forces in the stringers due to shape irregularities and so forth. But in any of these cases the tendency of the base to translate could not be resisted by the webs of the stringers. For this reason the assimilation of the actual buckling case to a column with hinged ends does not seem to be correct, because we are in the presence of a forced translation of the upper part of the stringers. In this case the local buckling is greatly influenced by the magnitude of that disturbing lateral force.

---

[5] Prof., Civ. Engrg. Dept., Illinois Inst. of Tech., Chicago, Ill.

[6] "Steel Column Research," Final Report of Special Committee, Transactions, ASCE, Vol. 98, 1933, pp. 1457, 1458.

[7] Civ. Engr., Santiago de Chile.

To demonstrate this fact it is interesting to analyze the effects of a local eccentricity in load application in the flange of one of the four stringers. Accepting a local eccentricity of 1 in. produced by flange irregularities, as those described by Hrennikoff, the moment in the head of that stringer, considering a width of 1 in., will be (Fig. 14): $M = 16.0 . 1 = 16$ in.-kips; $Q = \frac{(1 + 0.5) . 16}{36} = 0.668$ kips.

This shearing force must be distributed in equal parts to the four stringers: $Q_1 = \frac{0.668 \text{ kips}}{4} = 0.167$ kips. The maximal moment in the web is as follows: $M_1 = 0.167 \times 16.125 = 2.7$ in-K; $S = 1\ 0.653^{2/6} = 0.0715$ cu in.; $f = 2.7/0.0715 = 37.7$ kips per sq in.

This stress will produce a lateral flexure failure similar to that actually observed in the four stringers. The example demonstrates how sensible the system is to any irregularity, and that the local buckling problem for ideal conditions loses importance when compared with the other disturbing factors mentioned, resulting in a combined stability problem.

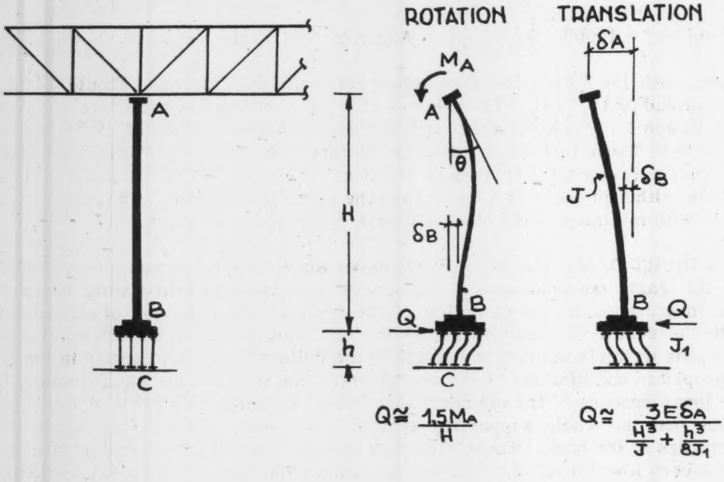
ROTATION
TRANSLATION
A
B
C
H
h
M_A
A
θ
δ_B
Q
B
C
δ_A
J
δ_B
B
Q
J_1
$Q \cong \frac{1.5 M_A}{H}$
$Q \cong \frac{3E\delta_A}{\frac{H^3}{J} + \frac{h^3}{8J_1}}$

FIG. 13

Referring now to the other conclusions of the committee, the writer observed that the initial imperfections in the shape of the stringers (about 1/32 in.) give a very low eccentricity, because it means only the 1/1150 part of the height of the web. S. Timoshenko considers[8] eccentricities reaching from 1/1000 up to

---

[8] "Strength of Materials," by S. Timoshenko, 3rd Ed., Von Nostrand, New York, 1955-1956.

L/400 as normal irregularities. Also european codes[9] fixes an eccentricity of r/20 + L/500, which represents more than twice that observed in this case.

The Royal Commission's judgment about the CSA formulas seems to prove that, for slender columns, it is probably better not to forget that the Euler value is the upper limit of buckling resistance. As this value is easy to obtain, it seems to be convenient, to prevent dangerous extrapolations from empirical curves, to relate the permissible buckling load for slender columns directly to the Euler value, using a convenient load factor.

The study about the plywood influence upon the compression strength contains some very interesting considerations, but the tests prove that this influence, in this case, is not important. Both tests, with and without plywood, differ by only 2.8%, proving this fact.

At the same time, this result demonstrates that the degree of fixation of the web, considered as a partially restrained beam, does not change very much. Using the Hickerson method, and making some simplifying assumptions about load distribution, plastic hinges, and compression modulus of plywood, the writer made an approximate computation of the degree of fixation that results with 3/4 in. plywood, obtaining a degree of 0.90. Comparing this value with unity (fully restrained) that results in the case of direct support on steel, it is comprehensible that the inflection point in the elastic deformation of the column (web) will suffer only a little variation, justifying a reduced change in the actual buckling length.

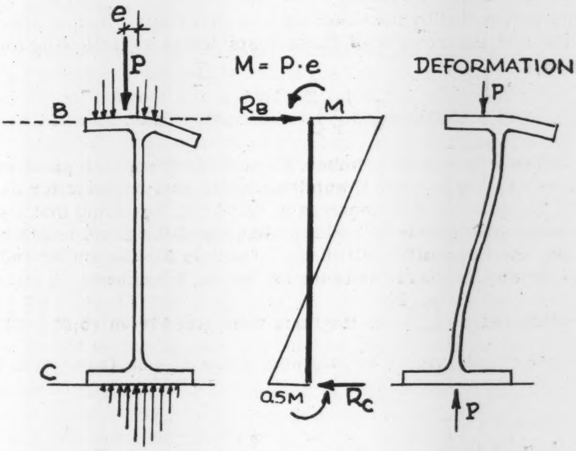

FIG. 14

The writer found the degree of fixation a function of the compression modulus of the plywood, the thickness of the layer, and the total compression force.

---

[9] German Steel Structure Stability Specifications DIN 4114.

Therefore, it is possible that in other cases, with a thicker layer of plywood, less modulus and load, the degree of fixation in the head of the web will decrease more than in this case and a considerable reduction of buckling strength may take place.

A. HRENNIKOFF,[10] **F. ASCE.**—The discussion by Kuang-Han Chu questions the writer's interpretation of the column formulas. Chu attaches a different significance than the writer to the term l in the formula for the pin-ended members of the Standard Specifications of the American Assn. of State Highway Officials (AASHO):

$$f = 15{,}000 - \frac{1}{3}\left(\frac{l}{r}\right)^2 \text{ psi} \quad \ldots\ldots\ldots\ldots\ldots\ldots (5)$$

The specification clearly states that in this formula, l signifies the length of the pin-ended member, as the author has used it, whereas according to Chu, l should be taken as the length of the member divided by 0.85. For justification of his interpretation, Chu refers to the Final Report of the Special Committee on Steel Column Research.[6]

The tests performed by the Committee involved only columns provided with riveted ends and the results of these tests led to the following formula for such members:

$$f = 15{,}000 - \frac{1}{4}\left(\frac{l}{r}\right)^2 \text{ psi} \quad \ldots\ldots\ldots\ldots\ldots\ldots (6)$$

in which l is the length of the member. Because no tests with pin-ended members had been carried out, the Committee had to use judgment for devising an appropriate formula for the members of this kind. Realizing that a pin-ended column is more susceptable to buckling than one of the same length but having riveted ends, the Committee felt that the formula for the pinned ends may be of the same type as for the riveted ends but having a somewhat greater numerical coefficient before $\left(\frac{l}{r}\right)^2$ in the term subtracted from 15,000. This higher coefficient was found, largely by judgment, using $\frac{l}{0.85}$ instead of l in Eq. 6, that is,

$$\frac{1}{4}\left[\frac{\left(\frac{l}{0.85}\right)}{r}\right]^2 = \frac{1}{2.89}\left(\frac{l}{r}\right)^2 \sim \frac{1}{3}\left(\frac{l}{r}\right)^2 \quad \ldots\ldots\ldots (7)$$

In other words, the Committee felt that a pin-ended column of the length l was as strong as a column with riveted ends of the length $\frac{l}{0.85}$. This reasoning of the Committee, consistent with the writer's interpretation, was apparently misconstrued by the discusser.

Dannemann attributes the failure of the grillage stringers to their lack of lateral rigidity. The writer has no quarrel with this conclusion because to him the lack of lateral rigidity in a strongly compressed member means much the same thing as the longitudinal instability, but he disagrees with the reviewer's diagram and computations.

---

[10] Prof., Civ. Engrg., Univ. of British Columbia, Vancouver, B. C., Canada.

Dannemann's sketch of the falsework column in Fig. 13, under the title "Rotation," shows moment M_A at its top end. The writer does not see how this moment could have been developed in the presence of a hinge connection between the column and the truss. The hinge involved two cylindrical surfaces of 2 ft-6 in. and 2ft-8 in. radii on which the column rocked in relation to the truss. A key prevented relative linear displacement of the two members. Under these conditions the reaction of the truss on the column was forced to act centrally at all times in relation to the top end of the column.

Dannemann's picture of the deformation of the column and grillage in the same figure under the title "Translation" violates statics. The only force which he shows in this figure is the horizontal force Q. Because this is an internal force between the column base and the grillage, its direction as shown must be judged, in view of the indicated manner of deformation of the grillage stringers, as that of the force acting on the grillage, which is opposite to the one acting on the column. With these considerations in mind, the free-body diagram of forces acting on the column, implied in this figure, would be as shown in Fig. 15, which is manifestly impossible in view of all moments acting in the same direction.

With a small horizontal displacement of the top of the column caused by temperature and indicated in a grossly exaggerated manner in Fig. 16, the thrust in the column must follow one of the lines AB, AB_1 or AB_2. Which of these three is the correct one and how great is the eccentricity e, is determined, as in all statically indeterminate conditions, by the deformations involved, which in this case consist of the flexural deformation of the column, the compression of the two plywood pads, and the flexure of the webs and flanges of the stringers. The structure below the plywood may be considered absolutely rigid.

The thrust cannot take the line AB, because the absence of eccentricity at the bottom would result in a central compression of all members involved and thus would not allow for a tilt of the column base. Nor could the thrust follow the line AB_2 because the inclinations of the column base as determined by the flexure of the column on the one hand, and by the compression of the plywood, on the other, would be incompatible. Consequently, the thrust line must follow the direction AB_1, and the amount of eccentricity, e, must be such as to make the angular deformations of the column and of the plywood packing compatible, as shown pictorially in Fig. 17. (The compression of the bottom plywood pad is left out in this figure for simplicity of presentation.)

It is not wrong to use the vertical and horizontal components N and Q in place of the thrust P, but the fact that these components keep a certain ratio between them, implied in the magnitude of the eccentricity e must not be forgotten. By the way, the direction of Q under these conditions comes out opposite to the one indicated by the discusser.

The fact that there is an eccentricity, e, at the bottom of the column and in the supporting structure does not mean that each stringer receives a thrust with the same eccentricity e, but it means that the thrust is divided unequally between the stringers, the extreme stringer one the side of the eccentricity receiving the greatest share of the load and through that compressing the plywood the most.

Ignoring any differences and imperfections in stringers and considering the top and the bottom plywood pads identical, one can realize that the upper and the lower halves of the stringers must bend in a similar manner in order to keep the work of their deformation at a minimum. The stringer thrusts then must be parallel to the column thrust P and must pass through the centers of their deformed webs (see Fig. 17) while their magnitudes P_1, P_2 and so forth adjust in a proper relation to e.

Erroneous results naturally follow if the conditions of statics are used without realizing the true structural action of the column and its support.

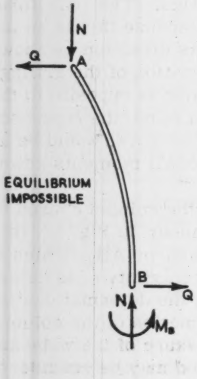

FIG. 15

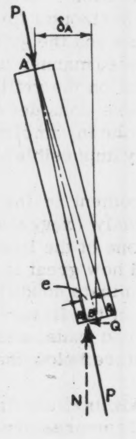

FIG. 16

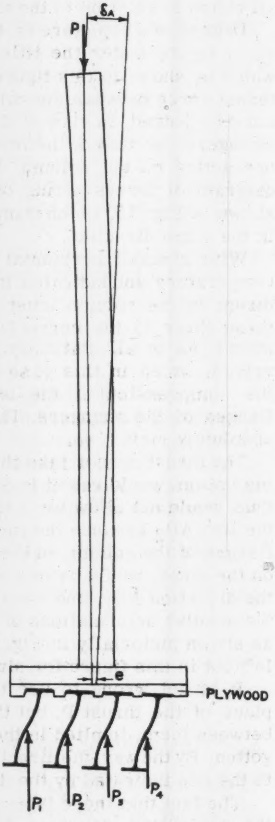

FIG. 17

Dannemann assumes an arbitrary eccentricity of the thrust at the top of the stringer and only half as great an eccentricity at its bottom. In the first place, in the conditions assumed by the discusser the beam flanges would cease to be parallel and this would immediately require compensating deformations on the part of the plywood pads which would shift the eccentricity towards the equality of the top and bottom moments. Furthermore, the assumed eccentricity results in a plastic stress at the top of the web. (It seems as though the discusser has forgotten to add on the direct compression stress.) From this, Dannemann concludes that the stringer is over-stressed. Actually, however, the conclusion should be that the discusser's assumption of the amount of eccentricity is unrealistic because a tendency of the web to bend in the direction of assumed eccentricity, that is, in a counterclockwise direction, in Fig. 14, would immediately lead to a shift of the load P in the direction of a reduced eccentricity.

Dannemann discusses also the two principal points brought up in the paper: the imperfections of the shape of rolled sections and the role of plywood. He is inclined to attach no special significance to the observed imperfections of the stringers, in general, and to the initial curvature of their webs, in particular, citing some figures in support of his opinion. Actually the amount of initial curvature in a column cannot be judged too large or too small without regard to the column formula used for the design of the member. If the column formula is very conservative then even a large curvature is not excessive. The author wrote his conclusions having in mind the column formulas used on this continent and more particularly the ASSHO and CSA formulas. His experiment with compression of fixed ended 36 WF 160 beams described in the paper resulted in the following values:

Theoretical failure stress by Euler's formula = f_y =	33 kips/sq in.
Actual failure stress from experiment	18.23 kips/sq in.
Allowable stress by AASHO, without extra erection allowance, and using l = 16 1/8 in.	12.58 kips/sq in.

The comparison of the first two figures indicates that the imperfections reduce the strength of the beam nearly in half, and the ratio of the last two figures shows that the factor of safety in using the AASHO formula for the design of the beam web in question is reduced to as little as 1.45. From this the writer concludes that in the conditions of the test the effect of irregularities in the beam shape is very substantial and that the AASHO formula is not suitable for the design of the beam. This puts a question mark on the use of AASHO column formula for the design of beam webs in buckling in general, that is, outside of the conditions of the test, but, of course, does not prove definitely its unsuitability in those regions. A different and stricter compression formula appears to be needed for the design of beam webs at least within certain limits of l/r and the German formula, referred to by the reviewer, may possibly meet the requirements.

Dannemann also does not think that the plywood pads had any substantial effect on instability of the stringers, basing his belief on a theoretical derivation which, unfortunately, was omitted from his discussion. The writer himself had followed the same line of theoretical approach, but the results were inconclusive, and knowing the complexity of the matter he is unwilling to accept, without proof, the discusser's statement.

It should be noted that the opinions expressed by the author in his original paper are his own and not the ones of the Royal Commission, for which he is not authorized to speak. His views, however, in no way contradict the findings of the Royal Commission.

The writer wishes to add that in his recently conducted new tests involving buckling of webs of 36 WF 160 beams there has been found some corroboration of the thoughts expressed by him in the paper under discussion. However, detailed description of these tests will have to wait until the results are fully worked out.

The writer is grateful to the discussers for their contributions to the subject of the paper. He regrets, however, the absence of comments on his criticism of the column formula of the Canadian Standards Association within certain limits of the slenderness ratio.

AMERICAN SOCIETY OF CIVIL ENGINEERS
Founded November 5, 1852
TRANSACTIONS

Paper No. 3241

RIVETS AND HIGH-STRENGTH BOLTS

A SYMPOSIUM

PAGE

COUNCIL RESEARCH

By E. J. Ruble 694

STRENGTH IN TENSION

By William H. Munse, Kenneth S. Petersen, and Eugene Chesson, Jr. 700
Discussion:
By Richard T. Douty 719
W. R. Penman and Ethan F. Ball 726
William H. Munse, Kenneth S. Petersen, and Eugene Chesson, Jr. 727

BEHAVIOR OF BEAM-TO-COLUMN CONNECTIONS

By William H. Munse, Wyatt G. Bell, and Eugene Chesson, Jr. 729

FATIGUE TEST OF JOINTS OF HIGH-STRENGTH STEEL

By Norman G. Hansen 750

EFFECTS OF FABRICATION TECHNIQUES

By Desi D. Vasarhelyi, Said Y. Beano, Ronald B. Madison, Zung-An Lu, and Umseh C. Vasishth 764

INSTALLATION AND TIGHTENING OF BOLTS

By Ethan F. Ball and J. J. Higgins 797
Discussion:
By Alfred Zweig 807
M. Zar 808
William H. Munse 808
Raymond Archibald 809
Ethan F. Ball and J. J. Higgins 809

HIGH-STRENGTH BOLTS ON MACKINAC BRIDGE

By John W. Kinney 811

COUNCIL RESEARCH

By E. J. Ruble,[1] F. ASCE

SYNOPSIS

The aims of the Rivet and Bolt Council and its methods of planning and conducting research are presented. The various organizations and universities sponsoring the Council are listed. The investigations that have recently been completed or those nearing completion are summarized and a complete bibliography of all published reports sponsored by the Council is included (as of 1961).

ORGANIZATION

The Research Council on Riveted and Bolted Structural Joints was formed in 1947 by representatives of interested groups to plan and conduct extensive research leading to safer and more economical design and construction of metal structures. The principal advantage of such a council is that it brings together for discussion and planning a diversified group of design engineers, steel fabricators, rivet and bolt manufacturers, erection engineers, college professors, metallurgists, research engineers, and many other scientists.

The Council depends entirely for membership on organizations interested in the behavior of riveted and bolted structural joints. The Council conducts its research on a budget of approximately $60,000 per yr and the following organizations are its principal financial sponsors:

1. American Institute of Steel Construction
2. American Iron and Steel Institute
3. Association of American Railroads
4. Bureau of Public Roads
5. Canadian Institute of Steel Construction
6. Industrial Fasteners Institute
7. The Engineering Foundation

Note.—Published essentially as printed here, in March, 1959, in the Journal of the Structural Division, as Proceedings Paper 1969. Positions and titles given are those in effect when the paper or discussion was approved for publication in Transactions.

[1] Research Engrg. Structures, Research Center, Assoc. of Amer. R. R., Chicago, Ill.

8. Illinois Division of Highways
9. Washington State Council for Highway Research
10. Pennsylvania Department of Highways

In addition to the direct financial sponsorship, the various universities where the research is being conducted, such as the University of Illinois, Urbana, Northwestern University, Evanston, Ill., University of Washington, Seattle, Wash., and Lehigh University, Bethlehem, Pa., contribute the time of the professors, testing equipment, and other services, that are considered valuable and sizeable contributions.

The Council meets once a year, usually for three interesting and informative days in February, and is usually attended by approximately fifty members and visitors. The Council meetings are interesting as all groups enter into an open and frank discussion of the results of the research.

RESEARCH PROJECTS

The Council has several investigations underway (as of 1961) and the accompanying papers cover part of its work on the study of bolted joints and high strength steels. In addition to these papers, the Council has completed the following investigations:

1. The Effect of Bearing Pressure on the Static Strength of Riveted Joints.—This research was conducted at the University of Illinois and it was determined that the ratio of allowable unit tension stress to unit bearing stress of 1 to 1.50 could be increased to 1 to 2.25 without any decreases in the static strength of the joint.

2. The Effect of Rivet Pattern on the Static Strength of Structural Joints.—This investigation on structural plate joints was conducted at the University of Illinois with an aim of developing a rivet pattern that would result in the greatest strength or efficiency of the riveted joint. No definite conclusions regarding the superiority of one particular rivet pattern was reached. However, it was concluded that no rivet pattern can be expected to develop a greater efficiency than 75% to 85% and that the well-known equation of s^2 (4 g) is sufficiently accurate for all practical purposes.

3. The Strength of Rivets in Combined Shear and Tension.—This research was conducted at the University of Illinois and resulted in definite data on the strength of single rivets when subjected to various combinations of concurrent tension and shear loading.

4. The Effect of Grip on the Fatigue Strength of Riveted and Bolted Joints.—This research was conducted at Northwestern Technological Institute and clearly indicated that the increased clamping action resulting from the cooling of the longer rivets increased the fatigue strength.

5. The Effect of Rivet Pattern on the Fatigue Strength of Riveted Joints.—This investigation was conducted at Northwestern Technological Institute to determine if the fatigue strength of a riveted joint could be increased by a change in the rivet pattern.

At the present time (1961) the Council has several other investigations that are either nearing completion or are underway. These investigations are:

1. Fatigue Tests on Cumulative Damage in Structural Joints.—The Council has often questioned whether the data obtained from laboratory fatigue tests of

structural joints are indicative of what may be expected in an actual structure. In the laboratory the maximum and minimum stresses are usually maintained constant during an entire test, whereas, in an actual structure, the maximum stresses may vary considerably from cycle to cycle. For this reason the Council authorized an investigation at the University of Illinois to secure data on riveted joints subjected to a sinusoidal variation of maximum cyclic stress with a constant minimum cyclic stress; this stress pattern was based on actual stresses in railroad bridges as determined by the research staff of the Association of American Railroads.

2. Effect of Bearing Pressure on the Fatigue Strength of Riveted Joints.— The Council realized that while the ratio of allowable unit tension stress to unit bearing stress of 1 to 1.50 could be increased for static loading conditions, it should not be increased for joints subjected to repeated loading until more data were available on the subject. For this reason, the Council has authorized an extensive investigation at the University of Illinois on this subject.

3. The Effect of Pattern on the Static Strength of Truss-Type Structural Joints.—This investigation, that is being conducted at the University of Illinois, is a continuation of the work done on structural plate joints. However, the joints now being studied are fabricated from plates and angles and are similar to those found in actual trusses. The load is applied to the members through gusset plates with either rivets or bolts connecting the plates to the members.

4. Static and Fatigue Strength of Bolted Structural Joints.—The assembly of structural joints using high-strength bolts is a fairly new method to the structural engineering profession, and results directly from the large amount of reasearch on fabricated joints that has been conducted by the Council within recent years. The Council has realized the importance of this subject and has sponsored a large number of investigations at various universities and while the investigations on this subject have not been completed, the Council has released many progress reports on the subject in addition to the published reports shown in the bibliography. A few of the interesting projects now underway on this study are:

a. The Study of Nuts.—Some trouble has been encountered with the stripping of nuts, especially where the strength of the bolt is considerably higher than the minimum requirement and the strength of the nut is close to the minimum requirement. A project has been started at the University of Illinois to make detailed study of nuts having different hardness, including both heavy duty and regular nuts.

b. The Study of Washers.—Northwestern Technological Institute is studying the basic principles of washer design to determine if the strength of bolted joints can be increased by a change in the shape of the washer.

c. The Study of Large Bolted Splices.—The availability of the 5,000,000 lb testing machine at Lehigh University has made it possible to study large joints, typical of those that might be used in extremely large bridge chord splices. This investigation also includes a study to determine if the unit shear values can be increased for bolted joints.

APPENDIX.—BIBLIOGRAPHY OF PUBLISHED COUNCIL REPORTS

General.

1. "Progress Report of Research Council on Riveted and Bolted Structural Joints," Proceedings, AREA, Vol. 51, 1950.
2. "New Concepts in Structural Joint Design," Research Council on Riveted and Bolted Structural Joints, Engrg. Foundation, December, 1953.

Project I.

1. "Effect of Bearing Ratio on Static Strength of Riveted Joints," by Jonathan Jones, Proceedings, ASCE, Vol. 82, No. ST6, November, 1956.
2. "The Effect of Bearing Pressure on the Static Strength of Riveted Connections," by W. H. Munse, Univ. of Illinois Experiment Sta. Bulletin.

Project II.—Effect of Rivet Pattern on the Static Strength of Structural Joints.

1. "A Study of the Practical Efficiency under Static Loading of Riveted Joints Connecting Plates," by W. M. Wilson, W. H. Munse, and M. A. Cayei, Univ. of Illinois, Engrg. Experiment Sta. Bulletin 402, 1952.
2. "Effective Net Section of Riveted Joints," by F. W. Schutz, Proceedings, 2nd Ill. Structural Engrg. Conf., November, 1952.
3. "Here's a Better Way to Design Splices," Engineering News-Record, Vol. 150, Part I, January 8, 1953, p. 41.
4. "Behavior of Riveted Connections in Truss-Type Members," by E. Chesson and W. H. Munse, Proceedings, ASCE, Vol. 83, No. ST1, January, 1957.

Project III.—Strength of Rivets in Combined Shear and Tension.

1. "How Much Combined Stress Can a Rivet Take?" by T. R. Higgins and W. H. Munse, Engineering News-Record, New York, Vol. 149, December 4, 1952, p. 40.
2. "The Static Strength of Rivets Subjected to Combined Tension and Shear," by W. H. Munse and H. L. Cox, Univ. of Illinois, Engrg. Experiment Sta. Bulletin 437, December, 1958.

Project IV.—Static and Fatigue Strength of Bolted Structural Joints.

1. "Specifications for Assembly of Structural Joints Using High Tensile Steel Bolts," January, 1951.
2. "Specifications for Assembly of Structural Joints Using High Strength Steel Bolts," February, 1954.

3. "Conditions Affecting the Slip of Structural Steel Bolted Joints," by R. A. Hechtman, Trend in Engineering, October, 1949.
4. "High Strength Bolts as a Means of Fabricating Steel Structures," by W. M. Wilson, Proceedings, Highway Research Bd., December, 1950.
5. "Slip of Structural Steel Double-Lap Joints Assembled with High-Strength Bolts, Part I," by D. R. Young and R. A. Hechtman, Trend in Engineering, April, 1951.
6. "Slip of Structural Steel Double-Lap Joints Assembled with High-Strength Bolts, Part II," by D. R. Young and R. A. Hechtman, Trend in Engineering, July, 1951.
7. "Laboratory Tests—High Tensile Bolted Structural Joints," by W. H. Munse, D. T. Wright, and N. M. Newmark, Proceedings, ASCE, Vol. 80, Separate No. 441, May, 1954.
8. Discussion by A. J. Francis, of "Laboratory Tests-High Tensile Bolted Structural Joints," by W. H. Munse, D. T. Wright, and N. M. Newmark, Proceedings, ASCE, Vol. 80, Separate No. 563, December, 1954.
9. "Slip of Joints under Static Loads," by R. A. Hechtman, D. R. Young, A. G. Chin, and E. R. Savikko, Proceedings, ASCE, Vol. 80, Separate No. 484, September, 1954.
10. Closure by W. H. Munse, D. T. Wright, and N. M. Newmark of "Laboratory Tests-High Tensile Bolted Structural Joints," by W. H. Munse, et al., Proceedings, ASCE, Vol. 81, Separate No. 664, April, 1955.
11. "Laboratory Tests of Bolted Joints," by W. H. Munse, D. T. Wright, and N. M. Newmark, Transactions, ASCE, Vol. 120, 1955.
12. "Bolted Connections—Research," by W. H. Munse, Proceedings, ASCE, Vol. 81, Separate No. 650, March, 1955.
13. "A Study of the Behavior of Large I-Section Connections," by J. R. Fuller, T. F. Leahey, and W. H. Munse, Proceedings, ASCE, Vol. 81, Separate No. 659, April, 1955.
14. "Research on Bolted Connections," by W. H. Munse, Transactions, ASCE, Vol. 121, 1956.

Project V.—Effect of Grip on the Fatigue Strength of Riveted and Bolted Joints.

1. "Effect of Grip on the Fatigue Strength of Riveted and Bolted Joints," by F. Baron and E. W. Larson, Jr., Proceedings, AREA, Vol. 54, 1953.
2. "Comparative Behavior of Bolted and Riveted Joints," by F. Baron and E. W. Larson, Jr., Proceedings, ASCE, Vol. 80, Separate No. 470, August, 1954.

Project VI.—Fatigue Strength of High-Strength Steel Riveted Joints.

1. "Static and Fatigue Properties of Carbon, Silicon and High-Strength Low-Alloy Steel Plates Having a Hole," by F. Baron and E. W. Larson, Jr., Proceedings, ASTM, Vol. 53, 1953.

2. "Properties and Behavior of a High Strength Rivet Steel," by F. Baron and E. W. Larson, Jr., Proceedings, ASTM, Vol. 53, 1953.

Project VII.—Effect of Rivet Pattern on the Fatigue Strength of Structural Joints.

1. "The Effect of Certain Rivet Patterns on the Fatigue and Static Strengths of Joints," by F. Baron and E. W. Larson, Jr., Research Council on Rivets and Bolted Structural Joints, Engrg. Foundation, February, 1955.

Project VIII.—Fatigue Tests on Cumulative Damage in Structural Joints.

1. "Cumulative Damage in Structural Joints," by W. H. Munse, James R. Fuller, and Kenneth S. Peterson, AREA Bulletin, Vol. 60, No. 544, June, July, 1958.

STRENGTH IN TENSION

By William H. Munse,[1] M. ASCE, Kenneth S. Peterson,[2] A. M. ASCE,
and Eugene Chesson, Jr.,[3] M. ASCE

With Discussions by Messrs. Richard T. Douty; W. R. Penman and Ethan F. Ball; and William H. Munse, Kenneth S. Petersen, and Eugene Chesson, Jr.

SYNOPSIS

A study was made to determine the fastener behavior in a tension-type structural connection assembled with either ASTM A-325 high strength bolts or rivets of A-141 rivet material. In this study such factors as the flexibility of the connected members, the magnitude of the initial clamping force in the fasteners, the number of lines of fasteners, and the grip of the fasteners have been considered.

INTRODUCTION

Whether rivets and bolts should be permitted to carry loads in direct tension has been studied by engineers[4] for many years and, on occasion, some have strongly objected to their use in this manner. Even now (1961), a few design specifications prohibit or discourage the use of structural connections which are subjected to direct tensile loads. And yet, from time to time, experimental studies have been conducted which demonstrate the ability of rivets and bolts to carry such loads effectively.

In an earlier study reported by T. F. Leahey and Munse,[5] a number of tests were conducted to determine the behavior of rivets and high-strength bolts loaded in direct tension by means of a structural T-connection, such as may be found in some heavy wind-bracing connections, crane hangars, etc. Leahey studied the behavior, under static and fatigue loads, of this T-type connection

---

Note.—Published essentially as printed here, in March, 1959, in the Journal of the Structural Division, as Proceedings Paper 1970. Positions and titles given are those in effect when the paper or discussion was approved for publication in Transactions.

[1] Prof. of Civ. Engrg., Univ. of Illinois, Urbana, Ill.

[2] Asst. Chief Engr., Atlantic Steel Co., Atlanta, Ga.; formerly Research Asst. in Civ. Engrg., Univ. of Illinois, Urbana, Ill.

[3] Asst. Prof. in Civ. Engrg., Univ. of Illinois, Urbana, Ill.

[4] "Riveted Joints, a Critical Review of the Litterature Covering their Development, with Bibliography and Abstracts of the Most Important Articles," by Richard A. E. de Jonge, ASME, Research Publication, 1945.

[5] "Static and Fatigue Tests of Rivets and High-Strength Bolts in Direct Tension," by T. F. Leahey and W. H. Munse, (unpublished Progress Report, Structural Research Series No. 80, Univ. of Illinois, 1954). "Research on Bolted Convections," by W. H. Munse, Transactions, ASCE, Vol. 121, p. 1255.

when assembled with two lines of fasteners, that is, one line on each side of the web of the T. His study included such variables as the initial tension in the bolts, the spacing of the bolts, and the use of inclined bearing surfaces under the heads of the bolts.

Although Leahey's tests answered a number of questions concerning the behavior of connections with high-strength bolts when loaded in tension, many other problems still required study. Attention has been given to some of these factors in the tests reported herein. The flexibility of the members, the grip of the fasteners, and the effectiveness of the fasteners in members fabricated from wide-flange sections and assembled with two or four lines of fasteners have been examined.

LABORATORY TESTS

Specimens.—Whereas the previous specimens had been cut from a 24 I 100, the members for this current series of tests were fabricated from several wide-flange sections. In the previous tests it was noted that the prying action at the toes of the relatively thin flanges apparently reduced the capacity of the bolted connections to a value below the total tensile strength of the fasteners (as determined by tensile tests of the individual bolts). In order to consider this matter further, flanges of several thicknesses and widths were included in the present program.

In actual tension connections (connections of members such as the T-sections of this study) the total thickness or grip may vary considerably, even though the stiffness of the connected sections is not changed. Since this variation in grip might affect the prying action, because of the greater deformation and elongation possible in longer bolts, a pilot test was made using a 2-in. fill plate between the flanges of a specimen (24 I 100). The test data indicated an increase in ultimate strength of more than 14% with the increased grip. In order to investigate this matter further, many of the new test specimens were fabricated with a fill plate.

Four major variables have been included in the present tests: (a) the number of lines of fasteners, (b) the flange width, (c) the flange thickness, and (d) the type of connector. A summary of the specimens and a listing of the test sections are included in Fig. 1. The twenty-eight tests provided one riveted and one bolted specimen with a fill plate and similar specimens without fill plates for all specimen types plus two additional specimens, CB9 and EB9, which were added for a further study of the effect of flange stiffness. (Specimens were marked with the following code: The first letter designates the specimen type and size of the T-section (Fig. 1); the second indicates whether the specimen was bolted (B) or riveted (R); if a P is included in the mark, the specimen was tested with a 2-in. fill plate between the flanges; V indicates variable prestress in the bolts; and the 9 refers to the 9-in. flange width used in the final two tests. Thus, riveted specimens AR, ARP, BR, . . . were identical in geometry to bolted specimens AB, ABP, BB, . . . respectively.)

The T-sections for the test specimens were of ASTM A-7 structural steel and the fasteners consisted of bolts meeting ASTM designation A-325 or rivets from material meeting ASTM designation A-141.

Tests of full-size bolts and of standard 0.505-in. round coupons cut from the bolts were conducted to obtain information on their properties. From the

0.505-in. coupons, it was found that the N-bolts had strengths of 120,000 psi to 138,200 psi and averaged 126,600 psi. (The fasteners of each specimen were marked according to the orientation of the specimen in the testing machine. All of the N (north) bolts were from one manufacturer, and all of the S (south) bolts were from another. Nuts and flat hardened washers were also provided by both manufacturers; Beveled washers were not required for the wide-flange shapes.) Coupons of S-bolts gave strengths of 126,000 psi to 146,300 psi with an average of 136,000 psi. Five full-size bolts of each length and manufacturer were also tested in tension. The average strength of the four bolts tested to failure with a 10° wedge under their heads and the strength of the other bolt tested to failure without the wedge are presented in Table 1. All of the bolts and nuts used in this series of tests passed the minimum requirements of ASTM A-325-55T specifications; however, eleven of the thirty S-bolts stripped the nut threads.

In the tests of the connections, bolts from both manufacturers produced stripping failures of the nuts. These stripping failures probably resulted because of the relatively high strength of some of the bolts, particularly the S-bolts, and the difference or variation in strength of the nut materials provided with those bolts. Hardness tests on the nuts of the S-bolts gave readings of 69 to 85 Rockwell B with an average value of 79 (approximately 143 Brinell), Similar hardness tests on the nuts with the N-bolts produced a range of 90 to 98 Rockwell B with an average value of 95 (approximately 209 Brinell).

TABLE 1.—TENSILE STRENGTH OF FULL-SIZE BOLTS

Bolt length, in inches (1)	Ultimate Tensile Strength, in Pounds			
	N - Bolts		S - Bolts	
	Wedged[a] (2)	Not Wedged (3)	Wedged[a] (4)	Not Wedged (5)
3	45,500	45,800	44,550	46,700
4	45,300[b]	45,500	42,550	42,400
4.75	47,350	47,100	48,520	48,300
5	44,150	43,800	45,890	43,800
6	46,820	46,000	45,700	44,600
7	44,720	44,800	49,220	49,600

[a] 10° wedge, average of four tests unless otherwise noted. [b] 10° wedge, average of two tests.

For the various rivets used, coupons of 0.252-in. diameter and 1-in. gage length were turned from driven, but unfractured, rivets which had been removed from the specimens after testing. The ultimate strength of these coupons are shown in Col. 4 of Table 2. These coupons reflected better the strength of the rivets after driving than would coupons prepared from undriven rivets.

Assembly.—The bolts for the connection tests were individually calibrated. In these calibrations the elongations and the torques required for the desired bolt loads were measured. As would be expected, the shorter bolts required somewhat less total elongation than did the longer bolts to attain 0.9 of the elastic proof load (EPL) required by the 1954 Research Council Specifications. There was some variation between individual bolts of the same length and manufacturer, and between one manufacturer and the other, however, these variations were not great. The torque required to load the bolts to 0.9 EPL was found to be reasonably constant for all lengths, and equal to approximately 320 lb-ft (which is the approximate equivalent torque for the minimum bolt tension recommended by the Research Council on Riveted and Bolted Structural Joints in its 1954 specification). The prescribed minimum tension was obtained at one-half to three-fourths of a turn of the nut from an initial finger-tight position.

Three electric resistance strain gages, 120° apart, were applied to the shanks of all eight bolts on the first specimen to be tested. In view of the uniformity of the average strains observed in each of the eight bolts of that test, it was decided to use strain gages on only two bolts in each of the subsequent tests with the exception of specimens designated EB9 and CB9; no strain gages were used on the bolts of the latter members. For a bolt with strain gages, the average strain found necessary in the calibrations to obtain the desired bolt tension was used to set the prestress in that bolt during assembly. For all of the other bolts (those without strain gages) the tension was set on the basis of the elongations obtained in the calibration tests.

All holes were match-drilled and carefully alined before the specimens were assembled. For the bolts with strain gages it was necessary to drill 15/16-in. holes, however, the other bolt holes and all the rivet holes were drilled 13/16-in. diameter.

During the assembly of the riveted members by a large structural steel fabricator, the inside rows of rivets were driven first, the fit-up bolts were then removed, and the outer rivets were driven. The bolted specimens were alined carefully also, fit-up bolts were installed and then the test bolts were tightened in a predetermined sequence. On checking, the first bolts tightened in a specimen were sometimes found to be below the desired prestress and therefore had to be retightened, however, adjustments were made until all of the bolts had a minimum prestress of 0.9 EPL (except for specimens BBV and BBVP in which only 0.1 EPL was used for the inside fasteners).

Test-Procedures.—Most of the specimens were tested in a universal testing machine of 300,000-lb capacity. The load was applied in steps of 10,000 lb or 20,000 lb and the readings or measurements were taken after all load increments. Each specimen was loaded until the maximum load was reached and the first fastener failure occurred in one or more inside fasteners. The loading was then continued until all of the inside fasteners failed, or until one of the outside fasteners failed. As soon as an outside fastener failed the test was discontinued.

During the tests the following readings were taken: Strains in selected bolts, elongation of all fasteners, and flange separations in one quadrant of all specimens. Small gage point holes (less than 1/16 in. deep) were drilled in both ends of the fasteners and in the flanges to receive the points of the extensometers that were used to measure bolt elongations and flange separations. The 3/8-in. by 5/8-in. grid of points for the flange separation measurements is shown in Fig. 1.

TABLE 2.—RESULTS OF TESTS OF

Specimen (1)	Equivalent Rivet Size[a] (2)	Ultimate Load, in Kips (3)	Ultimate Strength of Rivets, in psi (4)	Predicted Load[c] Based on Rivet Strength, in Kips (5)	Efficiency, in % (6)
Specimens with Two					
AR	3H	141.3	83,600[b]	173.4	81.5
ARP	5H	104.4	67,350	139.7	74.7
Specimens with Four					
BR	3C	164.4	89,600	371.7	44.2
BRP	5C	161.3	81,500	338.1	47.7
CR	4C	210.0	76,500	317.3	66.2
CRP	6C	202.4	65,450	271.5	74.5
DR	4H	211.5	73,950	306.7	69.0
DRP	6C	199.3	65,300	270.9	73.6
ER	4.75C	254.6	82,700	343.0	74.2
ERP	7C	276.4	86,600	359.2	76.9
FR	4.75H	212.0	67,050	278.1	76.2
FRP	7C	270.0	86,600	359.2	75.2

[a] H indicates rivets which were hot formed; C identifies cold formed rivets; all rivets based on two coupon tests. [c] Based on coupon tests of driven rivets and actual hole

Riveted specimen ER is shown in Fig. 2 on completion of its test. In Fig. 3 the residual flange deformations remaining in several bolted specimens of identical flange width but varying thicknesses are shown.

TEST RESULTS

Before studying the test results it should be noted that in the analysis of the data, a number of factors must be considered. Because of the widely varying

RIVETS AND RIVETED CONNECTIONS

Efficiency With Plate ÷ Efficiency Without Plate (7)	Type and Location of Failure (8)	Distribution of Total Strain to Fasteners,[d] in %				Rivet Most Highly Strained (13)
		North (9)	South (10)	East (11)	West (12)	
Lines of Fasteners						
0.92	Shank 3S	53	47	41	59	2N
	Shank 3S	49	51	59	41	3S
Lines of Fasteners						
1.08	Head 2N	49	51	51	49	3N
	Shank 2S	54	46	44	56	2N
1.13	Shank 3N	48	52	49	51	2N
	Shank 2S	50	50	59	41	3N
1.07	Shank 2S	48	52	41	59	2S
	Shank 2S	48	52	51	49	3S
1.04	Shank 1S, 2S, 1N, 2N, 3N	51	49	53	47	3N
	Shank 1S, 2S, 1N, 2N	53	47	45	55	2S
0.99	Head 3S and 4N	50	50	48	52	2N
	Head 2N	49	51	47	53	2S
1.04[e]						

---

were driven hot. [b] Based on one coupon test; all other ultimate rivet strengths are diameters. [d] At maximum load for which records were obtained. [e] Average.

grips for specimens with and without fill plates and cut from different wide-flange sections, the ductility and strength of the fasteners must be kept in mind when comparisons are made of the results from the various tests. The differences in grip may affect the deformations which are produced by a given load. The longer bolts will probably deform more than the shorter bolts since two bolts of identical material but of two different lengths will not have the same elongation at a given load. Unequal loading of the bolts, because of eccentricities or warping in the specimens, also will have an effect on the behavior of

TABLE 3.—RESULTS OF TESTS

Spec. (1)	Bolt Length, in inches (2)	Ultimate Load, in Kips (3)	Ultimate Load for Bolt ÷ Ultimate Load for Rivet (4)	Predicted Load Based on Bolt Strength, in Kips (5)	Efficiency, in % (6)	Efficiency with Plate ÷ Efficiency without Plate (7)
(a) Specimens with Two						
AB	3	134.0	0.948	180.1	74.4	1.02
ABP	5	136.8	1.310	180.1	76.0	
CB9	4	175.0		175.7	99.6	
EB9	4.75	169.0		191.8	88.1	
(b) Specimens with Four						
BB	3	175.6	1.068	360.2	48.8	1.03
BBP	5	181.6	1.126	360.2	50.4	
BBV	3	183.4		360.2	50.9	1.00
BBVP	5	184.3		360.2	51.1	
CB	4	229.2	1.091	351.4	65.2	1.02
CBP	6	245.7	1.214	370.1	66.4	
DB	4	219.6	1.038	351.4	62.5	1.11
DBP	6	256.0	1.284	370.1	69.2	
EB	4.75	300.0	1.178	383.5	78.2	1.03
EBP	7	302.7	1.095	375.8	80.5	
FB	4.75	274.1	1.293	383.5	71.5	1.07
FBP	7	286.7	1.062	375.8	76.3	
		Average	1.142		Average	1.04

[a] At maximum load that records were obtainable. [b] All fasteners failed simultane-

the members. The webs of specimen EB9, for example, before testing were found to be bowed almost 1 in. because of the out of squareness of the flanges.

The question of nut-stripping failures must also be considered. Failure by thread stripping is not sudden and considerable load may be carried even after stripping has started. However, it is obvious that higher loads can be sustained by bolts for which the nuts strip, if the bolts are assembled with nuts strong enough to cause failure by bolt fracture. This point must be kept in mind when comparing the test results since many of the failures were initially by stripping. Finally, it should be remembered that the cross-sectional area of a driven 3/4 in. diameter rivet is approximately 0.518 sq in. whereas the stress area of a 3/4 in. diameter bolt is 0.334 sq in. Thus, the lower-strength rivets may, in some cases, develop a load-carrying capacity approaching that of comparable size high-strength bolts. The results of the tests are given in Tables 2 and 3.

OF BOLTED CONNECTIONS

Type and Location of Failure	Distribution^a of Total Strain to Fasteners, in %				Most Highly Strained Bolt	Efficiency of Bolt ÷ Efficiency of Rivet
	North	South	East	West		
(8)	(9)	(10)	(11)	(12)	(13)	(14)
Lines of Fasteners						
Nut 2S	56	44	25	75	2N	0.913
Nut 3S	57	43	43	57	2N	1.018
Nut 2N, Bolt 2S	34	66	51	49	3S	-
Nut 3S	61	39	73	27	3N	-
Lines of Fasteners						
Nut 3S	71	29	62	38	2N	1.107
Bolt 3N	55	45	56	44	3N	1.059
Bolts 2N and 3N	57	43	58	42	3N	-
Bolts 2N, 3N and 2S	54	46	55	45	3N	-
Nuts 2N and 3N	36	64	57	43	3S	0.984
Bolt 2N	53	47	57	43	3N	0.892
Nuts 2N and 3N	31	69	61	39	3S	0.906
Bolt 3N	53	47	54	46	3S	0.939
. . .[b]	77	23	50	50	3N	1.056
Bolts 1N, 2N and 1S Nuts 2N and 2S	66	34	51	49	3N	1.047
Nuts 2S and 3S	74	36	41	59	2N	0.938
Nuts 2S and 3S	58	42	50	50	2N	1.016
					Average	0.990

ously in the bolt except 2S and 3S which failed in the nut.

Members With Two Lines of Fasteners.—Two riveted and four bolted specimens with two lines of fasteners were tested. The type A specimens, AR, ARP, AB, and ABP, were fabricated from a 24WF130 section (the same rolled shape as that used for the type B specimens), specimen CB9 was fabricated from a 30WF210 section (the same section as the type C and D specimens) and specimen EB9 was fabricated from a 36WF300 section (the section used for the type E and F specimens). However, in each instance the flanges of the members had been cut to a width of 9 in.

In order to study the behavior of the bolts during the tests, the elongations of the bolts were determined with SR-4 strain gages or by means of a mechanical extensometer. These measurements indicated that the load was not always distributed uniformly to the bolts, a condition that might affect the ultimate load-carrying capacity of the members. However, the most heavily strain-

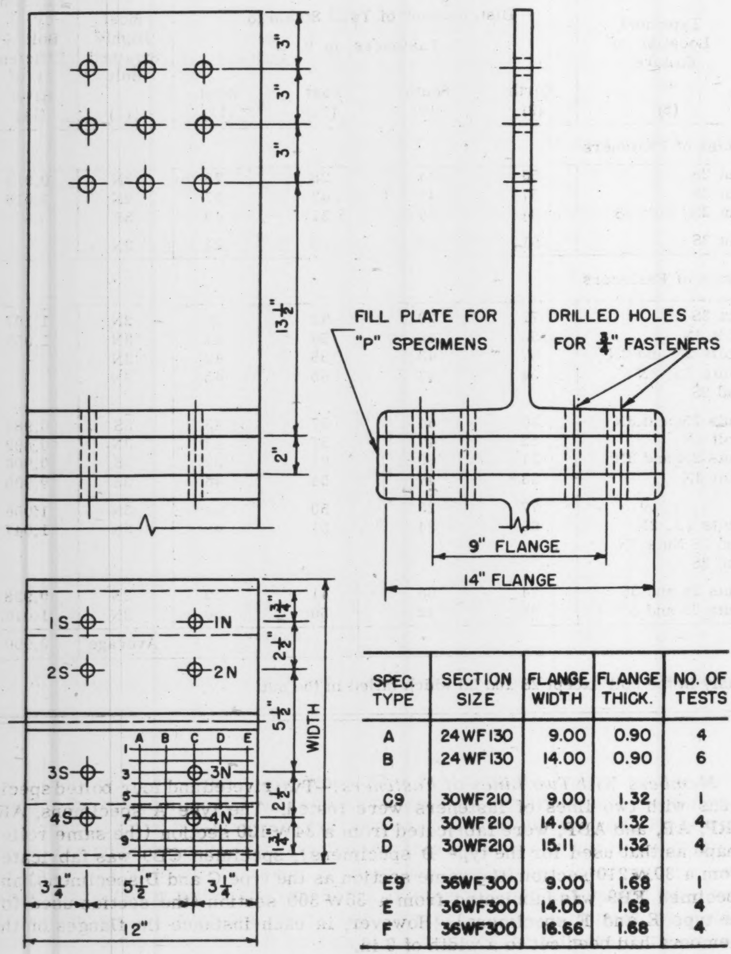
3"
3"
3"
13½"
2"
FILL PLATE FOR "P" SPECIMENS
DRILLED HOLES FOR ¾" FASTENERS
9" FLANGE
14" FLANGE
1S
1N
2S
2N
3S
3N
4S
4N
A B C D E
1 3 5 7 9
1¾"
2½"
5½"
2½"
1¾"
WIDTH
3¼"
5½"
3¼"
12"

SPEC. TYPE	SECTION SIZE	FLANGE WIDTH	FLANGE THICK.	NO. OF TESTS
A	24WF130	9.00	0.90	4
B	24WF130	14.00	0.90	6
C9	30WF210	9.00	1.32	1
C	30WF210	14.00	1.32	4
D	30WF210	15.11	1.32	4
E9	36WF300	9.00	1.68	1
E	36WF300	14.00	1.68	4
F	36WF300	16.66	1.68	4

TOTAL TESTS: 28

FIG. 1.—DETAILS OF TEST SPECIMENS

ed bolts did not always fail, particularly in the cases where failure was by thread stripping.

The more sensitive SR-4 strain gage measurements indicated small changes in bolt tension or bolt strain starting at a load of 4,000 lb to 5,000 lb per bolt. However, elongation measurements made with the mechanical extensometers did not reflect noticeable changes in bolt load until the loads on the bolts averaged as much as 10,000 lb to 20,000 lb per bolt. Cols. 9 through 13 of Tables 2 and 3 indicate the manner in which the load was distributed to the rivets and bolts during the latter stages of testing. However, when compared with the information in Cols. 8 the locations of the failures, it is found that in only several instances did the most highly strained bolt or rivet provide the point of failure. Thus, the unequal distribution of load to the fasteners is certainly not the only factor affecting the strength or efficiency of the connections.

Stripping of the nuts or shearing of the rivet heads causes a decrease in the elongation of the affected fasteners and, at the same time, provides a weakened location at which failure can initiate. When this type of shearing takes place in the fasteners, the applied load will be redistributed and produce increased strain in the other bolts or rivets. Such behavior also seems to be reflected in the data of Tables 2 and 3.

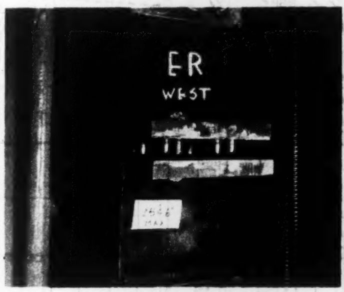

FIG. 2.—SPECIMEN ER AFTER FAILURE

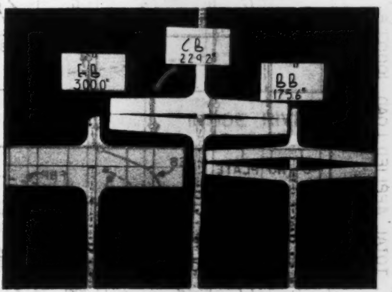

FIG. 3.—PERMANENT DEFORMATION OF BOLTED MEMBERS AFTER TESTS

Study of the bolt-elongation plots for specimens AB, CB9, and EB9 in Fig. 4 (right-hand edge of upper diagram) indicates that the bolts in CB9 and EB9 deformed less for a given load than did the bolts in AB. The stiffer flanges probably reduced the effect of prying action considerably, thereby allowing more of the load capacity of the bolts to be utilized in carrying the applied load. In addition, the bolt elongation in specimens CB9 and EB9 were further reduced at any given load because the bolts in these specimens had a yield strength approximately 10% greater than that of the bolts in specimen AB. Further confirmation of the reduced prying action with the stiffer flanges is obtained from the fact that specimens CB9 and EB9 developed almost the full capacity of the individual bolts, although unequal distribution of the load to the bolts and nut stripping failures no doubt reduced the efficiencies of these specimens.

Members With Four Lines of Fasteners.—The B specimen may be considered as the basic member. Then, all others vary from this basic type by thickness or width of flanges and, of course, by the fasteners used.

The strain in the inner bolts of specimen BB began increasing at a total load of 10,000 lb and continued to do so until failure occurred (Fig. 4). However, the strain in the outer bolts decreased slightly as the member was loaded to 160,000 lb, and then began to increase. Thus, in the early stages of loading the entire load is carried by the inner bolts.

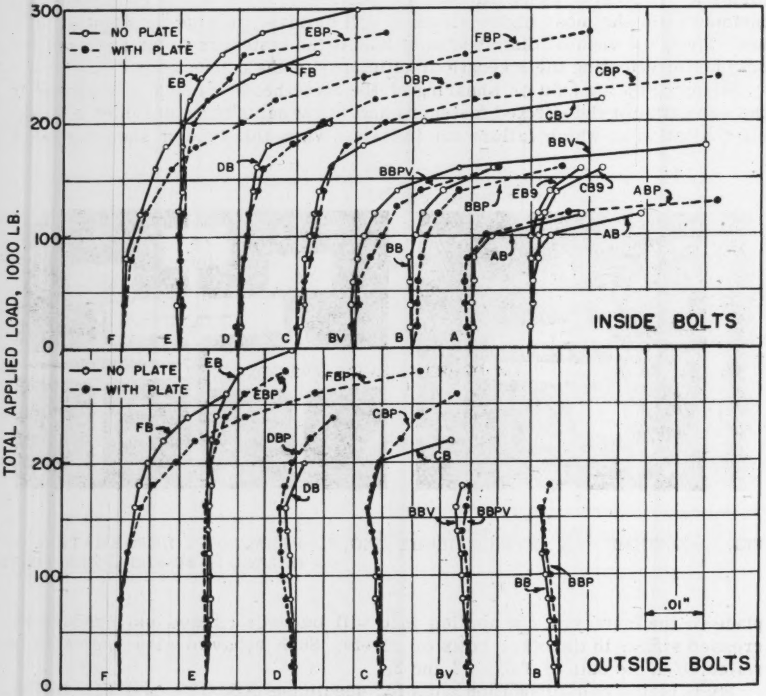

FIG. 4.—LOAD VERSUS BOLT ELONGATION FOR MEMBERS WITH TWO LINES OF FASTENERS

An additional indication of the behavior of the members may be obtained from the flange separation measurements. It is interesting to note in Fig. 6 that point E7 (the outer bolt line) of specimen BB did not exhibit a flange separation until the load reached 160,000 lb, further indicating the unequal distribution of bolt load in the inner and outer bolt lines. The flange separation at the web was large, but the edges of the flanges remained in contact at most points throughout the entire test. Failure occurred in Nut 3S, one of the nuts on the inner bolt lines, at a load comparable to 48.8% of the total strength of the eight fasteners. Therefore, even if the outer bolts had carried none of the applied load at failure, the inner bolts were less than 100% effective.

Specimen BBP, identical to BB except for a fill plate, behaved in a manner similar to that previously described; but failure occurred at an efficiency which was 3% greater than that of specimen BB. This higher efficiency of BBP may have resulted from the more uniform loading, shown in Table 3, or from the longer bolt lengths.

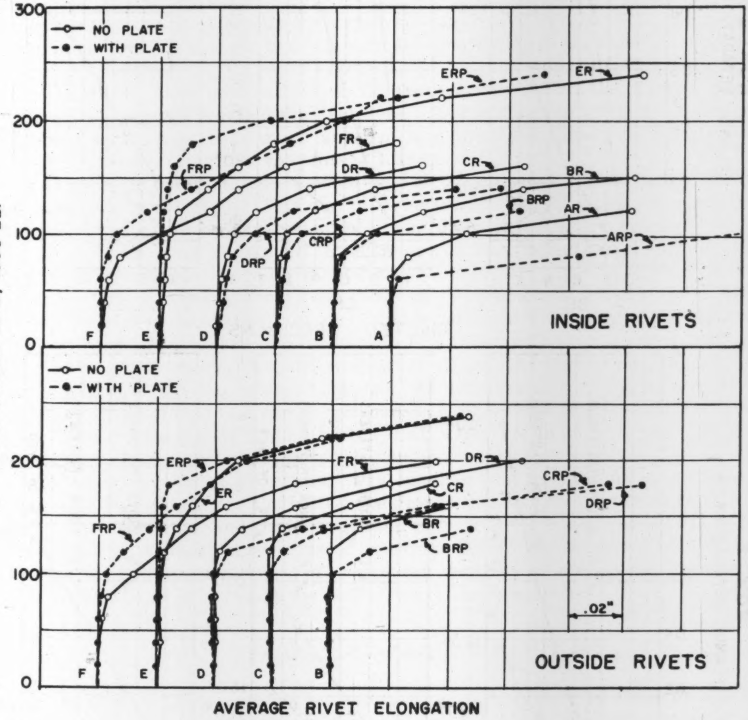

FIG. 5.—LOAD VERSUS BOLT ELONGATION FOR MEMBERS WITH FOUR LINES OF FASTENERS

The inner rivets of specimen BR showed a change in elongation after approximately 80,000 lb had been applied, the outer fasteners began to show a change when the load on the specimen reached 120,000 lb and at a load of 164,000 lb failure occurred in one of the rivets as the shank was pulled out of

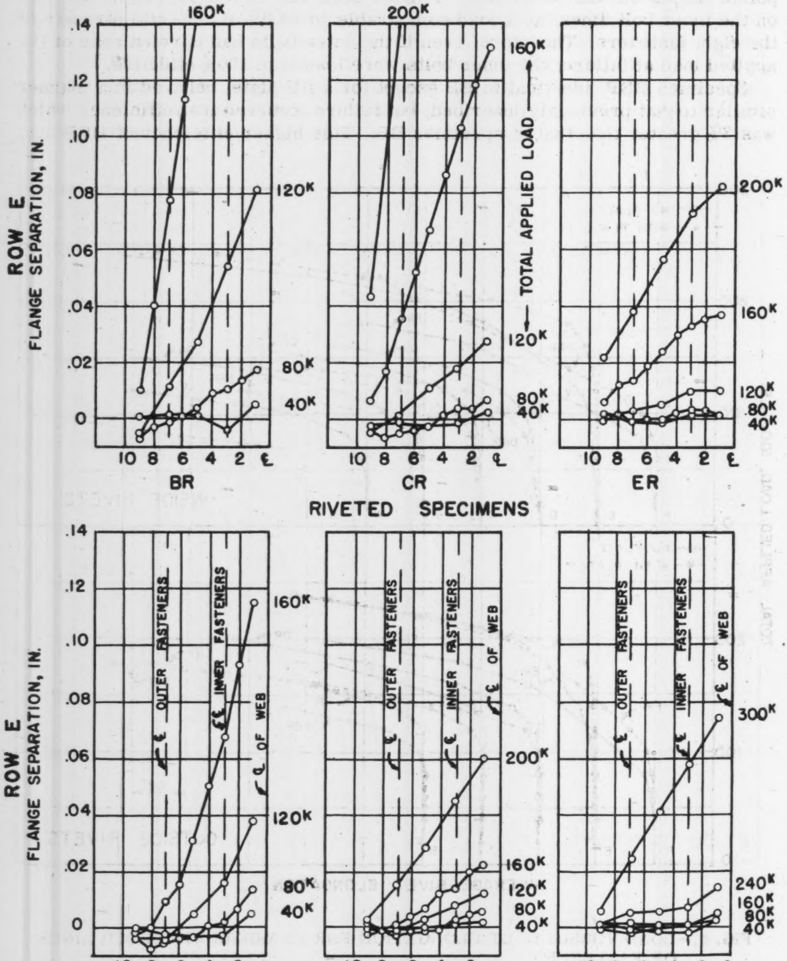

FIG. 6.—FLANGE SEPARATION OF RIVETED AND BOLTED MEMBERS WITH FOUR LINES OF FASTENERS

the driven head which had been formed off center. The ultimate load-carrying capacity of the member undoubtedly was reduced by this type of failure, particularly since the specimen seemed to be rather uniformly loaded.

The rivets of specimen BRP exhibited deformation characteristics similar to those of BR. However, near failure, the longer fasteners of specimen BRP deformed somewhat more than those of specimen BR (Fig. 5). In addition, the inclusion of a fill plate and better-formed rivet heads in specimen BRP, despite more unequal loading, gave an efficiency 3.5% greater than that for specimen BR.

During the loading of the B-type specimens with four lines of fasteners, the flanges separated at the webs but rarely at the toes of the flanges. Such deformations require that the inner fasteners elongate more than the outer fasteners. As the load was increased further, the inner fasteners failed while the outer fasteners were generally still far from failure. Had the flanges been stiffer, their bending would have been less, the distribution of the load to the fasteners would have been more uniform, and the outer fasteners would have reached a greater strain at the time of failure.

Although the outer fasteners contribute to the ultimate load capacity, their effectiveness is not great. This can be demonstrated readily by a comparison of the loads carried by various specimens. Specimen AB, for example, with two lines of fasteners developed an efficiency of 74.4% whereas specimen BB with four lines of fasteners developed an efficiency of only 48.8%. However, specimen BB carried approximately 30% more load than did specimen AB. Similar comparisons of the other specimens show that although the specimens with two lines of fasteners are more efficient, those with four lines of fasteners always carry more load, the magnitude of the increase depending on the flange stiffness and the mode of failure. As the stiffness of the flanges was increased, it was found that the effectiveness of the outer bolts increased somewhat. Nevertheless, they did not become fully effective in carrying the applied load because of the deformation in the flanges.

The amount of flange separation was considerably greater for the riveted specimens than it was for the bolted specimens because the rivets were more ductile than the bolts and could withstand a greater total elongation. This is evident in Fig. 6 where three riveted specimens may be compared with three comparable bolted specimens. The greater ductility of the rivets, however, did not seem to affect greatly the efficiency of the members.

FAILURE OF FASTENERS

Of the twelve riveted members tested, three had rivet-head failures which occurred when the shanks withdrew from the heads which had been driven off-center. In two cases, the heads were so badly off center that they were only 1/32 in. thick at one point along the head-shank junction. This condition and the resulting failures can be expected to reduce the efficiencies of the members. In contrast, well-formed rivets which were subjected to large bending rarely showed any signs of initiation of failure in the heads. Occasionally a hairline crack could be seen on the more heavily strained side of a bent rivet although failure occurred in the shank.

Failure by stripping of the nuts developed in eleven of the sixteen bolted members. In those eleven members, three failures were in nuts from N-bolts, seven were in nuts from S-bolts, and one involved nuts from both manufacturers. However, even after stripping began, the members, in most cases, continued to carry a large percentage of the maximum load. Care must be taken in comparing specimens having only bolt failures with specimens having nut failures or a combination of failure types since the latter failures may have been premature and thus the ultimate loads and efficiencies lower than would have been the case if only the bolts had failed.

Col. 14 of Table 3 compares the test efficiencies of identical bolted and riveted specimens. The average efficiency of the riveted specimens was 1% greater than that of the bolted members, however, this difference is not significant. Although the efficiencies of the riveted and bolted connections are approximately the same, it is apparent from Col. 4 of Table 3 that, in all but one instance, the bolted members were actually stronger (average of 14%) than their riveted counterparts.

EFFECT OF FLANGE STIFFNESS

The AB, CB9, and EB9 specimens had identical flange widths and bolt pattern but had different flange thicknesses and therefore different bolts and bolt lengths. A comparison of the deformation of the several flanges is graphically portrayed in Fig. 7. The flange separation at a given load was largest for specimen AB, CB9 had less bending, and EB9 showed almost no bending and only slight separation. The flange separation plots were similar for Row A and Row E (Fig. 1 shows the location of the rows) of these three specimens and for all the other members tested, indicating fairly uniform bending along the length of the flanges.

The type E and the wider type F specimens were the stiffest considered in the study. The importance of this stiffness is evident from an examination of the fastener deformations in Figs. 4 and 5. The outer fasteners of both specimen EB and EBP showed an increase in strain at almost the same time as did the inner fasteners. In addition, the bending of the flanges was small by comparison with the more flexible specimens. Both specimens EB and EBP failed by rupturing several fasteners simultaneously. However, the inner fasteners had strained somewhat more than had the outer bolts, and undoubtedly failed first. The impact created by their failure probably caused the outer fasteners to fail and gave the appearance of a simultaneous failure of the inner and outer bolts.

The outer fasteners of the riveted type E specimens also began to elongate almost at the same time as did the inner fasteners, and the flanges of both specimens separated completely before failure. Thus, the stiffness of the flanges, whether riveted or bolted, affected the fastener elongation and flange deformation markedly.

A comparison of the efficiencies shown in Tables 2 and 3 demonstrates that as the stiffness of the flanges increased, the efficiencies also increased. It is apparent also that increasing the thickness of the flanges increased the ultimate load-carrying capacity of the specimens. This fact is shown in Fig. 8 where the efficiencies of the specimens are plotted against a measure of the flange stiffness. A curve has been drawn through the average values for the specimens with four lines of fasteners and shows the increase in efficiency with an increase in flange thickness. There are insufficient data to draw a

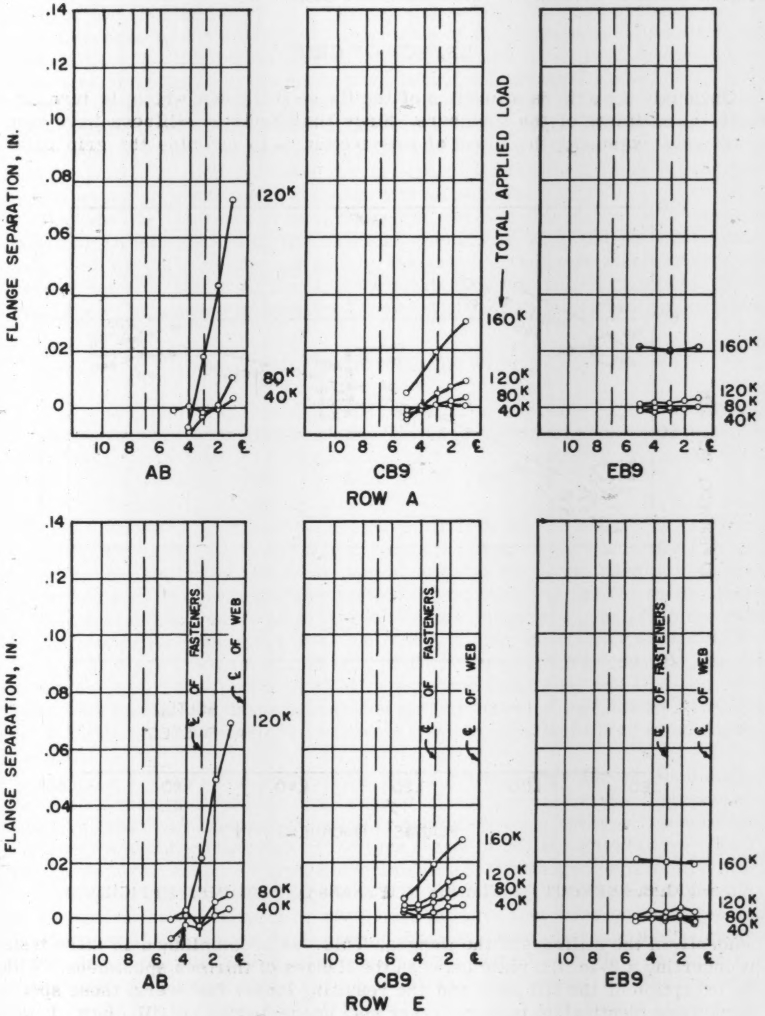

FIG. 7.—FLANGE SEPARATION FOR MEMBERS OF VARIOUS FLANGE THICKNESS

comparable curve for the specimens having two lines of fasteners although a similar trend is evident for these members also.

EFFECT OF GRIP

Obviously the grip is a function of the flange thickness which, in turn, affects the stiffness of the members. Since the effects of stiffness have been previously examined, the intent of this section is to examine the grip independently of the stiffness of the flanges. This was accomplished in these tests by inserting a 2-in. fill plate between the flanges of thirteen specimens. With the exception of the fill plate and the resulting longer fasteners, these specimens were identical to thirteen other specimens having no fill plate. It was thought that because of such a fill plate, the longer fasteners would have greater elongations, the prying action of the flanges would be reduced, and the connection efficiencies might be increased.

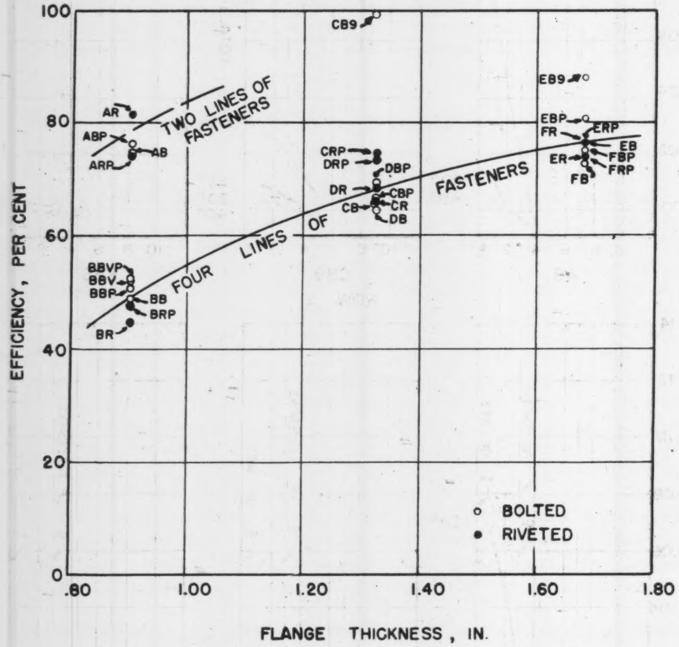

FIG. 8.—EFFECT OF FLANGE STIFFNESS ON SPECIMEN EFFICIENCY

Figs. 4 and 5 show that with few exceptions the elongations of the fasteners in specimens with a fill plate were greater at any given load than the elongations of the shorter fasteners. The several exceptions were probably caused by differences in the mechanical properties of the fasteners. In addition, the inequalities in distribution of load to the fasteners of a given specimen also may have contributed to the unexpected behavior in several cases.

When flange-separation plots similar to Figs. 6 and 7 were prepared for the specimens with a fill plate, at any given load, greater flange separations were found for the specimens with a fill plate than for those specimens without the plate. In addition, there did appear, in some cases, to be a reduction in the prying action of the specimens with a fill plate.

Perhaps the best way of examining the effect of the plates is to examine the relative efficiencies of the identical specimens with and without a plate. Cols. 7 of Tables 2 and 3 show that, on the average, the plate increased the efficiency approximately 4% for both the riveted and the bolted members. However, such an increase in efficiency does not appear to be of great importance.

EFFECT OF FLANGE WIDTH

The type D and F specimens were identical to the type C and E specimens in every respect except flange width. The D and F specimens were tested as rolled with flange widths of 15.1 in. and 16.7 in., respectively, while the C and E specimens were cut down to a 14-in. flange width.

The deformation characteristics of specimen DR (15.11-in. flange) were similar to those of specimen CR (14.00-in. flange) but the efficiency of specimen DR, shown in Col. 6 of Table 2, was somewhat higher than that of specimen CR. A detailed study of the data shows that the rivets used in specimen DR were the most ductile of those tested, and this may account for the tendency of that specimen to reduce its prying action more than was possible in the case of specimen CR. Specimens DRP and CRP, having identical type rivets, deformed in much the same manner, but DRP carried 1.6% less load than did specimen CRP. Thus for the 30 W 210 specimens with 14 in. and 15.1-in. wide flanges no signigicant difference exists in their behavior, and, the small change in edge distance for these comparatively flexible specimens was of no consequence.

The type F specimens, connections with a greater edge distance and stiffer flange than the type D specimens, because of this increased edge distance, exhibited a behavior somewhat different from that shown by the type D specimens. The inner and outer fasteners of the type F specimens elongated more rapidly than those of the narrower type E specimens, and the flanges separated faster, too. However, the ultimate loads of the F specimens were reduced, possibly as a result of the nut failures or rivet head failures that were encountered and also because of the greater prying action possible. A comparison of efficiencies and loads for the 36 W 300 specimen with 14 in. and 16.7-in. flanges is not entirely valid because the E type specimens all failed in the shank of the fasteners while the F type specimens failed in the rivet head or nut. Such a comparison shows, however, that the effect of the wider flange is to reduce the efficiency approximately 3½%, although this value may be a little high since all the specimens having other than shank failures were the wider members.

EFFECT OF INITIAL TENSION

Specimens BBV and BBVP were included in the test program to determine whether a lower prestress (0.1 of elastic proof load) in the inner bolts might permit a greater transfer of load to the outer bolts. The inner fasteners did pick up strain faster for specimens BBV and BBVP than they did in the comparable but fully torqued specimens, BB and BBP. However, the outer fasteners behaved in a similar manner for all four specimens. In the early stages of loading, the flanges of the members with the lower prestress in the inner bolts opened up more at the web than did the members with uniform prestress but, when the load reached 160,000 lb, there was little difference in the bending of the flanges. The ultimate loads were somewhat higher with the lower prestress, but the difference was slight (average of approximately 3%) and might have been less had there been no nut failure in specimen BB.

CONCLUSIONS

1. The efficiency of a tensile joint of the type tested in this investigation is the same whether assembled with bolts furnished to ASTM A-325 specifications or rivets purchased to ASTM A-141 specifications. However, the bolted members carried, on the average, approximately 14% more load.
2. Members with eight fasteners in four lines are generally less efficient but are stronger than similar members with four fasteners in two lines.
3. The stiffness of the flanges affected the efficiency of the members (a range in efficiency of 30% was obtained for the specimens tested). In one case it was found that an increase in flange thickness from 0.90 in. to 1.32 in. provided as great an increase in strength as did the addition of two outer lines of bolts.
4. Inclusion of a fill plate between the flanges of this type of connection will have only a slight effect on the efficiency (approximately 4% increase for these tests).
5. Small changes in flange width were of little consequence in these tests.
6. Prestress as low as 0.1 EPL in the bolts in the inner two lines of a specimen with four lines of fasteners will have almost no effect on the strength or efficiency of the member.

ACKNOWLEDGMENTS

The tests described herein were a part of an investigation on riveted and bolted connections being performed in the Civil Engineering Department, under a cooperative agreement between the Engineering Experiment Station of the University of Illinois, the Illinois Division of Highways, the Department of Commerce--Bureau of Public Roads, and the Research Council on Riveted and Bolted Structural Joints. The tests were planned in cooperation with the Project IV Committee of the Research Council on Riveted and Bolted Structural Joints.

DISCUSSION

RICHARD T. DOUTY,[6] **A. M. ASCE.**—It is unfortunate that stripping of the nut initiated failure in some cases, since nut requirements might, therefore be tightened in order to achieve the full potential of high-strength bolts.

In 1957 the writer conducted[7] a series of tests similar to these reported by the authors. It was one of the purposes of this limited research project to investigate whether in plastically designed structures high-strength bolted connections could be used instead of welded connections. The testing arrangement was similar to that used by the authors (Fig. 9). Portions of wide-flange shapes were used as structural tees. These tees were fastened to a relatively inflexible base with high-strength bolts and the load applied at the web so that the bolts were in tension; hardened washers were used. The purpose of these tests was to study the action of fasteners in tension when subjected to prying forces. These forces occur when the rigidity of the flange is such that excessive separation at the web of the tee contributes to failure of the fasteners. It was hoped that with the evidence developed, a bolted connection could be designed to provide enough rotation capacity so that it could be used in plastically designed structures. The tests were similar to the authors' except that only high-strength bolts were used and just one line of these on either side of the web of the tee. Edge distance, flange thickness, bolt size, and initial pretension were the variables studied.

A theoretical investigation of the tension in the bolts was made throughout the elastic, plastic, and strain-hardening range of the flange. The tests were used to substantiate the theoretical analysis.

Theoretical Analysis.—It is assumed for simplicity that under yield conditions plastic hinges form at (1) the line of fasteners and (2) the juncture of web to flange. The effect of the fillet is disregarded.

In Fig. 9, k is the ratio of net area at the line of fasteners to the total cross-sectional area of the flange (the fillet is disregarded); P' denotes the prying force and exists as a compressive contact force at the extremity of the edge distance; M_p represents the full plastic moment of the flange cross section = $\sigma_y\, b\, t^2/4$; and P is the tensile load on the web of the tee. The load at which plastic deformation of the flange begins to occur is denoted by P_{pl}. This is the deformation which provides plastic rotation characteristics of a connection using such a flexible structural tee. Such a connection can take the form of a tee-stub moment connection (Fig. 10) or a standard connection which, for purposes of analysis, is considered to be an assembly of tees (Fig. 11). In addition, ΣT is the sum of the tensile forces existing in the various fasteners.

From statics (Fig. 9):

$$P_{pl} = \frac{2\,M_p}{d}\,(1+k) = \frac{b\,t^2}{2\,d}\,(1+k)\,\sigma_y \quad \ldots\ldots\ldots\ldots (1)$$

---

[6] Graduate Asst., Cornell Univ., Ithaca, N. Y.; formerly, Graduate Asst., Georgia Inst. of Tech., Atlanta, Ga.

[7] "Characteristics of Flexible Flange Connections and Fasteners," by R. T. Douty, thesis presented to the Georgia Inst. of Tech., at Atlanta, Ga., in June, 1957, in partial fulfilment of the requirements for the degree of Master of Science.

from which

$$t = \sqrt{\frac{2\ P_{pl}\ d}{b(1 + k)\ \sigma_y}} \ldots\ldots\ldots\ldots\ldots\ldots\ldots (2)$$

which is the flange thickness necessary for providing plastic rotation capacity at a given P_{pl} (Fig. 13). Then,

$$P'_{pl} = \frac{k\ M_p}{e} = \frac{k\ d\ P_{pl}}{2\ e(1 + k)} \ldots\ldots\ldots\ldots (3)$$

and

$$\sum T_{pl} = 2\ P'_{pl} + P_{pl} = P_{pl}\left(\frac{k\ d}{e(1 + k)} + 1\right) \ldots\ldots\ldots (4)$$

Since Eqs. 3 and 4 are valid into the strain-hardening range, by substituting the strain-hardening moment M_{st} for M_p, the total force in the fasteners at any load greater than P_{pl} is found to be

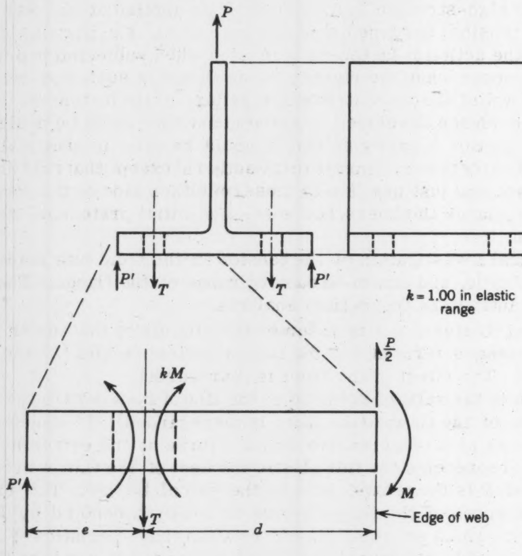

FIG. 9.—FORCES ACTING ON TEE FLANGE

$$\sum T_{st} = P_{st}\left[\frac{k\ d}{e(1 + k)} + 1\right] \ldots\ldots\ldots\ldots\ldots (5)$$

Similar equations are available for the elastic range if a force P'_{el} at the extreme edge is assumed to resist the moment at the bolt line and this moment, in turn, equals the negative moment at the fillet. Neglecting the web width, and since equilibrium requires

$$M_{web} = M_{bolts} = k\,S\,\sigma = \frac{k\,b\,t^2\,\sigma}{6} \; \ldots\ldots\ldots\ldots \; (6)$$

$$P_{el} = \frac{2}{3}\,k\,\frac{b\,t^2}{d}\,\sigma \; \ldots\ldots\ldots\ldots \; (7)$$

$$P'_{el} = \frac{P_{el}\,d}{4\,e} \; \ldots\ldots\ldots\ldots \; (8)$$

and

$$\sum T_{el} = P_{el} + 2\,P'_{el} = P_{el}\left(\frac{d}{2\,e} + 1\right) \ldots\ldots\ldots\ldots \; (9)$$

Test Results.—The results of four of the tests of the tees in tension are given in Fig. 12; the test data are in Table 4. From Eqs. 4, 5, and 9 a plot of bolt tension versus tensile load on the tee can be constructed. This plot, which is the dashed line in Fig. 12 is constructed in four segments. Eq. 9 is valid throughout the elastic range and linear from zero to first yielding of the flange. The value of P_{el} at first yielding is given by Eq. 7. The second segment is constructed from Eq. 4 which gives the bolt tension when the flange has become fully plastic. Eq. 5 gives the segment in the strain-hardening range if any tensile load on the web in excess of P_{pl} is used for P_{st}. The upper limit of the curve is determined by the yield strength of the bolt. The theoretical bolt-tension curve is completed by erecting a vertical line at the bolt pretension load to intersect the curve given by Eqs. 4, 5, and 9. The theoretical curve at bolt-tension values less than this pretension load is then ignored. The tension in the bolts is not the tensile load on the web divided by the number of bolts. The prying force P' contributes to the amount of tension in the bolts.

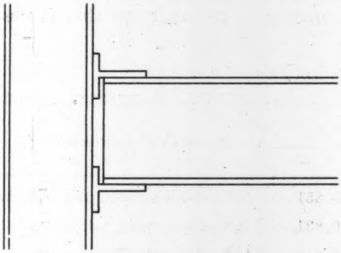

FIG. 10.—A MOMENT CONNECTION FOR DEVELOPING THE PLASTIC MOMENT OF A BEAM

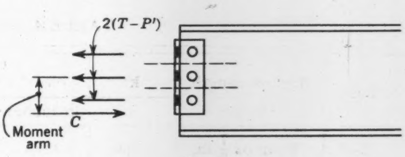

FIG. 11.—STANDARD A3 CONNECTION CONSIDERED AS AN ASSEMBLY OF THREE TEES

Except for test T-3 the bolts were pretensioned considerably in excess of the required minimum for high strength bolts.[8] From Fig. 12(d) there is evidence that such an initial overstress may produce slightly harmful effects in that the curve of measured tension breaks from the pretension load at the computed plastic load instead of continuing upward to the predicted curve, as might be expected under the assumptions of the analysis. Since the curve of measured tension after break-off follows practically the same slope as the computed curve, it is possible that this one test is not indicative of such a conclusion. At most there is approximately 15% difference between the computed tension and measured tension in Fig. 12(d).

---

[8] "Specifications for Assembly of Structural Joints Using High Strength Bolts," Amer. Inst. of Steel Construction, New York, 1954.

In Fig. 13 the separation of the flange of the tee used in test T-4 measured at the web is plotted against the tensile load on the web. Fig. 13 shows that the computed value of P_{pl} gives a reasonable web-tension value at which the flexibility of the flange will begin to contribute to plastic rotation capacity of a connection using such a flexible flange.

Test of a Moment Bracket.—Following the tee tests a moment bracket, shown in Fig. 14, was fabricated and tested. The theoretical analysis of the bracket involved a consideration of the bracket flange and web as a vertical stack of tees. The analysis of the bracket is not given herein, but is similar to that of the tees used for Fig. 12. The plastic moment capacity of such a bracket consists of the contribution of the P_{pl} of each tee of the stack about the centroid of the compressive bearing area. According to the analysis this is the moment at which the moment-rotation curve becomes non-linear. The load computed from the analysis given in this discussion at which rotation becomes non-linear is shown on Fig. 14. This is the plastic moment of the connection.

TABLE 4.—TEST DATA

Test	High-Strength Bolts	k	e	t	Bolts Pretensioned to
		In inches			
T-3	Four of $\frac{7}{8}$ in.	0.786	1.75	0.851	40% of the elastic proof load
T-4	Four of $\frac{7}{8}$ in.	0.786	1.125	0.831	122% of required minimum
T-5	Six of $\frac{5}{8}$ in.	0.765	1.75	0.849	117% of required minimum
T-6	Four of $\frac{7}{8}$ in.	0.786	1.75	0.909	130% of required minimum

It seems reasonable that the upper portion of the bracket flange will strain-harden before the load is redistributed by yielding of the flange, such that yielding occurs in the lower portion. The latter portion is adjacent to the area that is in compressive bearing. This lower portion contributes so little to the moment capacity of the bracket however that it is probably insignificant. Fig. 14 indicates that the theoretical approach is valid.

Design Example of Tee-Stub Moment Connection to Develop the Plastic Moment of a Beam.—The tentative theoretical approach developed in this discussion, if verified by more extensive investigation, would apply to a tee-stub moment connection shown in Fig. 10. The bolts maintain their resistance to slip from friction throughout the plastic range of the flexible flange and thus could be counted on to resist the reaction at the end of the beam.

Example.—The floor beams in a certain structural system are designed plastically for an ultimate load of 400 psf. This corresponds to a working load of 200 psf with a safety factor of 2. The beam spacing is 8 ft on centers; col-

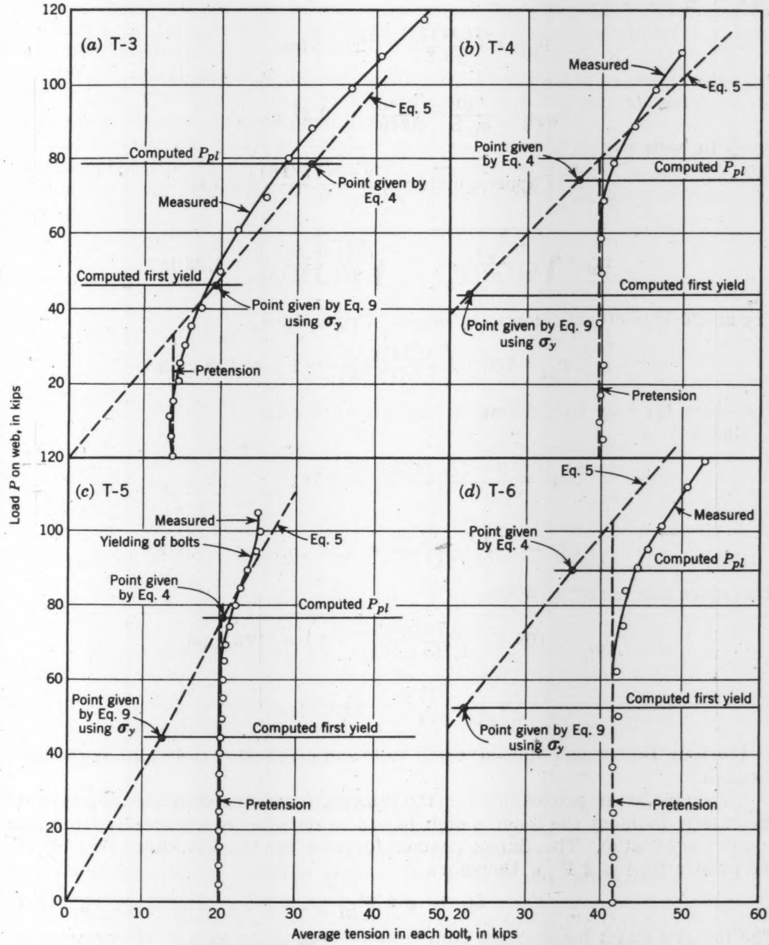

FIG. 12.—ACTUAL BOLT TENSION COMPARED WITH COMPUTED TENSION

umns are 29 ft apart. The beam required is an 18WF50. The plastic moment is 169 kip-ft; the shear at the connection is 47 kips. The design for the tee-stubs proceeds as follows:

Given that the flange width of the tee is 9 in., e will be 1.75 in. assuming a gage of 5½ in. Then

$$P_{pl} = \frac{169(12)}{18.5} = 109.5 \text{ kips}$$

$$t_{web} = \frac{P_{pl}}{\sigma_y\, b} = \frac{109.5}{33(9)} = 0.37 \text{ in.}$$

Use ½ in. web

$$\text{k is approximately} = \frac{9 - 2(15/16)}{9} = 0.791$$

$$t_{pl} = \sqrt{\frac{2\, P_{pl}\, d}{b(1+k)\, \sigma_y}} = \sqrt{\frac{2(109.5)2.5}{9(1.791)33}} = 1.02 \text{ in.}$$

Try an ST 18WF80 with flame cut edges. From Eq. 4,

$$\sum T_{pl} = 109.5\left(\frac{0.791\text{x}2.5}{1.75(1.791)} + 1\right) = 179 \text{ kips}$$

Therefore try four 1 in. diameter high-strength bolts.

Check

$$k = \frac{9 - 2(1.0625)}{9} = 0.761$$

$$t_{pl} = \frac{2(109.5)2.43}{9(1.761)33} = 1.01 \text{ in.} \qquad \text{(OK)}$$

Therefore use the ST 18WF80

$$\sum T_{pl} = 109.5\left(\frac{0.761\text{x}2.43}{1.75(1.761)} + 1\right) = 175 \text{ kips}$$

$$T_{pl} = \frac{175}{4} = 43.8 \text{ kips}$$

Use four 1-in. round high-strength bolts and pretension to 49 kips as recommended.[8]

To arrive at an expression for the friction force resisting the reaction at the plastic moment the tension stub has to be considered separately from the compression stub. The flange contact force of the tension stub (Fig. 10) at the plastic load is 2 P'_{pl}; therefore

$$Q_1 = \mu\, 2\, P'_{pl} \quad \ldots\ldots\ldots\ldots\ldots\ldots \quad (10)$$

The flange contact force of the compression stub is the sum of the pretension forces (T_i) plus the external forces, or

$$Q_2 = \mu\left(\sum T_i + P_{pl}\right) \quad \ldots\ldots\ldots\ldots\ldots \quad (11)$$

Therefore the total friction force resisting slip is

$$Q = Q_1 + Q_2 = \mu\left(2\,P'_{pl} + P_{pl} + \sum T_i\right) \ldots\ldots\ldots \quad (12)$$

From Eq. 4 it is shown that the frictional force resisting slip throughout the loading range will not drop below the frictional force provided by the pretension load. In fact, as strain-hardening occurs with rotation the force resisting slip increases.

The force resisting slip as computed by Eq. 12 and using a conservative coefficient of friction of 0.25 is 93 kips. This is almost twice as much as the shear encountered in this typical situation.

Results and Implications.—These tests show that it is possible to use a bolted connection to develop the plastic moment capacity of a section. The flexibility of the connection flange provides the necessary plastic rotation capacity.

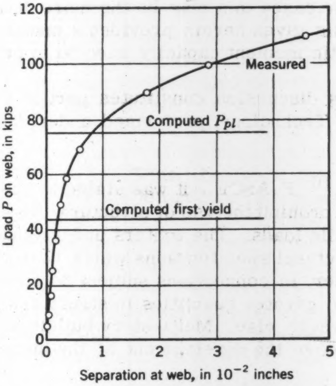

FIG. 13.—MAXIMUM SEPARATION OF TEE FLANGE FOR TEST T-4

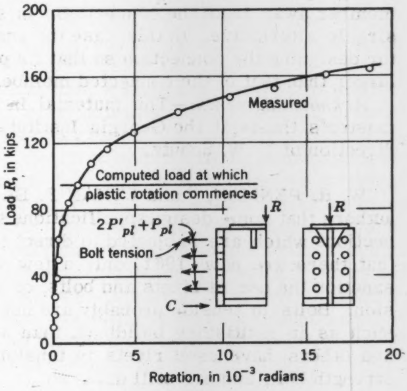

FIG. 14.—ROTATION OF BRACKET

It is possible to predict the tension that will exist in the fasteners at the plastic moment of the connection. Fasteners of adequate strength can then be provided. This bolt tension is a function of flange rigidity, edge distance, and reduced section due to fastener holes. The amount of pretensioning is not a factor.

The plastic moment of a given connection can be computed without fear that failure will occur in the fasteners if adequate fasteners are provided to resist the computed tension.

A bolted connection designed to rotate at a given moment can take several forms: (1) a tee-stub moment connection (design example in this discussion), (2) a moment bracket (rotation capacity of such a bracket as tested is given in Fig. 14), and (3) a standard connection of framing angles (not considered herein, but which should fit the approach given in this discussion).

Up to the present time (1961) it has been assumed that a welded connection is more desirable for providing continuity in plastically designed structures. However, all that is needed is a connection that will provide the necessary rotation capacity at a given moment. A bolted connection using a flexible flange fits this requirement well. The prying forces contribute to the tension in the bolts but designs can be created to handle these forces.

Bolted connections have many advantages over welded connections. Discontinuity of material at the connection reduces the possibility of total collapse from the formation of brittle fracture or fatigue cracks. Bolts, due to the large pretension forces placed on them, are inherently capable of standing up under fatigue conditions. Field erection procedures are simplified. Less skilled labor is needed for assembling a bolted connection than a welded connection. Shop and field tolerances can be less rigid. Finally, bolted structures enjoy certain dismantling advantages.

It is true that a bolted connection could be used in plastically designed structures if purposely overdesigned to force the hinge to occur in the connected member away from the connection. In some cases this may be the more desirable alternative. In this case the analysis given herein provides a means for designing the connection so that its plastic moment capacity is equal to or larger than that of the connected member.

Acknowledgments.—The material in this discussion constitutes part of a master's thesis at the Georgia Institute of Technology, performed under the direction of F. W. Schutz.

W. R. PENMAN,[9] and ETHAN F. BALL,[10] F. ASCE.—It was stated by the authors that some design specifications still prohibit the use of structural connections which are subjected to direct tensile loads. The writers understand that there are now (1961) only a few structural specifications which do not sanction the use of rivets and bolts, or either, in connections subject to tension. Bolts in tension probably are used in greater quantities in structures, such as in multistory buildings, than anywhere else. Multi-story buildings, and others, have used rivets in tension before the development of the high-strength bolt, and are still doing so.

There are many applications of bolts which are used in tension; for example the flange bolts or studs in high-pressure and high-temperature piping systems and cylinder-head studs in engines.

It was stated that the cross-sectional area of a driven $\frac{3}{4}$ in. diameter rivet is approximately 0.518 sq in. compared to the stress area of a $\frac{3}{4}$ in. bolt being 0.334 sq in., and that lower-strength rivets may develop a load-carrying capacity approaching that of high-strength bolts. This rivet area is based on a $\frac{3}{4}$ in. rivet completely filling a $\frac{13}{16}$ in. hole when hot driven. This condition is only true in cases of short grip lengths, and even then it is dependent on the human element in driving any particular rivet. Design would require the use of the area of the nominal diameter of the rivet, that is, 0.442 sq in. for a $\frac{3}{4}$ in. rivet.

Nut-stripping failure occurred in some of the tests and it should be emphasized that the ASTM took steps in 1957 to increase the nut proof load and that ASTM Specification A325-58T requires the minimum nut-stripping values to be approximately 25% higher than those of the minimum bolt-strength values.

---

[9] Gen. Mgr., Lebanon Plant, Bethlehem Steel Co., Bethlehem, Pa.

[10] Chf. Engr. Fabricated Steel Constr. Div. of Bethlehem Steel Co., Bethlehem, Pa.

WILLIAM H. MUNSE,[11] **M. ASCE, KENNETH S. PETERSON,**[12] **A. M. ASCE, and EUGENE CHESSON, JR.,**[13] **M. ASCE.**—Both discussions correctly suggest that stripping failures of the nuts are less likely now that the proof loads for heavy hexagon series nuts have been increased in ASTM Specification A325-58T. This increase was requested by the Research Council on Riveted and Bolted Structural Joints because the results of various laboratory studies, including the writers' investigation, and field experience had indicated that nut stripping was a possibility under the specification in use at the time the tests were conducted. The writers' paper was based on a study reported to the Research Council on Riveted and Bolted Structural Joints in November 1956.

Penman and Ball suggest that only a few structural specifications do not sanction the use of rivets or bolts in connections subject to tension. The AASHO specification states[14] "Rivets in direct tension should, in general, not be used." The section then goes on to give an allowable stress formula for rivets under combined tension and shear. The AREA specification[15] does not refer to the use of rivets or bolts in tension nor does it provide allowable working stresses for fasteners so loaded. The other major specification[16] widely used in the United States provides an allowable tensile stress on the nominal diameter of the fasteners equal to that permitted for A-7 steel in tension.

Penman and Ball also correctly indicate that a rivet only rarely fills a rivet hole. Nevertheless, the area of a $\frac{13}{16}$ in. rivet hole is 0.518 sq in. and, if a rivet in such a hole has a clearance of 0.007 in. (a reasonable value for a rivet with a grip of several inches), the area of the rivet shank will be approximately 0.500 sq in. Thus, the use of the nominal hole size to determine the strength of a rivet would produce only a small error (4%) in any evaluation of its tensile capacity based on the material properties. In addition, the statement which the discussers questioned, "lower strength rivets may develop a load carrying capacity approaching that of comparable size high-strength bolts," refers to the load in pounds, not to stress in pounds per square inch. That certain riveted specimens sustained almost as much load as similar bolted specimens may be seen readily in Table 3. However, in all fairness to the A-325 specifications, the bolted connections having load capacity no more than or only slightly better than the riveted joints failed by nut stripping. Had the nuts been of the strengths as now (1961) specified, one would expect the bolted joints to develop somewhat greater loads than were shown in the paper. In addition, unless the toes of the flanges of connections of the type considered separate completely, thereby removing the prying action in the joint, we cannot expect the bolts (or rivets) to reach their full tensile capacity. This point was illustrated in Fig. 8.

Douty's test results and analysis are a welcome addition to the paper. These are for members with two lines of fasteners and, as such, should be comparable to the results of several of the tests reported by the writers. A more effective comparison and evaluation, however, would be possible had the ultimate strengths and specimen details of Douty's tests been reported.

---

[11] Prof. of Civ. Engrg., Univ. of Illinois, Urbana, Ill.

[12] Asst. Chief Engr., Atlantic Steel Co., Atlanta, Ga.; formerly Research Asst. in Civ. Engrg., Univ. of Illinois, Urbana, Ill.

[13] Asst. Prof. of Civ. Engrg., Univ. of Illinois, Urbana, Ill.

[14] "Standard Specifications for Highway Bridges," Amer. Assn. of State Highway Officials, 7th Edition, 1957.

[15] "Specifications for Steel Railway Bridges for Fixed Spans not Exceeding 400 Feet in Length," Amer. Ry. Engrg. Assn., 1958.

[16] "Specification for the Design, Fabrication and Erection of Structural Steel for Buildings," Amer. Inst. of Steel Construction, 1956.

The analysis presented by Douty provides an approximate extension of an analysis long used for the design of tension brackets. The amplification of this analysis to include the development of plastic deformation in the flanges provides another step in the analysis of the behavior of such a member. However, this does not provide an indication of the ultimate strength of such members nor does it provide an indication of the behavior of the members with four lines of fasteners. The analysis of this later type of member can be expected to be much more complex.

In the analysis presented by Douty a number of simplifying assumptions have been made. Consequently, the computed relationship can only be considered as approximate. For example, it would be more realistic for the prying force shown in Fig. 9 to be applied at a point someplace between the bolt line and the toe of the flange. From measurements in the writers' tests such has been observed to be the case. Also, it is shown that the ductility of the fasteners has an effect on the prying action in the members and to total ultimate strength of the fasteners. These factors, as well as a number of others, should be given further consideration before this analysis is used in design.[17]

In his discussion, Douty has suggested that an overstress in the bolts may produce harmful effects on the behavior of tension brackets. It is difficult to see how such an evaluation can be justified in light of the results of many tests wherein high-strength bolts have been torqued to a condition approaching failure but still retain their full tensile strength. Other tests reported by the writers[5] have shown that similar strengths are obtained when various levels of initial tension are placed in such bolts. Consequently, it would seem unwise to draw a conclusion concerning the effect of a high tension on the basis of a single test.

---

[17] "Strength of Moment Connections Using High Tensile Strength Bolts," by F. W. Schultz, Jr., Proceedings, AISC Natl. Engrg. Conf., 1959, p. 98.

BEHAVIOR OF BEAM-TO-COLUMN CONNECTIONS

By William H. Munse,[1] M. ASCE, Wyatt G. Bell,[2] A. M. ASCE,
and Eugene Chesson, Jr.,[3] M. ASCE

SYNOPSIS

The tests reported herein were performed as the first phase of an extensive program designed to study the general behavior of beam-to-column connections assembled with rivets or bolts; they included four standard flexible connections. Three of the test specimens were assembled with rivets and high-strength bolts and were tested at different moment-to-shear ratios. The fourth specimen was assembled entirely with rivets so as to provide a study of the effect of fastener on the behavior of the connections.

A study is made of the moment-rotation characteristics, the moment-resisting capacity, the position of the center of rotation, the slip and shear deformation of the connections, the deformation of the fasteners, and the separation of the column flanges.

The tests reveal that the connections, although assumed for design purposes to behave as simple supports, actually provide some end restraint and that the restraint provided by the connections was increased slightly by the use of high-strenght bolts in lieu of rivets to fasten the connection angles to the column flanges.

INTRODUCTION

The ASTM A-325 high-strength bolt[4] has become widely accepted as a fastener for the assembly of structural joints.[5] Most specifications for the design of steel structures now (1958) permit the use of high-strength bolts in lieu of rivets of the same diameters. [More recently (1960) a substitution of two bolts for three rivets is permitted in certain connections.]

One of the most important features of the heat-treated high-strength bolt is the high clamping force developed in the bolt when it is properly tightened. This high tension, generally about twice the maximum developed by rivets as

---

Note.—Published essentially as printed here, in March, 1959, in the Journal of the Structural Division, as Proceedings Paper 1971. Positions and titles given are those in effect when the paper or discussion was approved for publication in Transactions.

[1] Prof. of Civ. Engrg., Univ. of Illinois, Urbana, Ill.

[2] Structural Engr., J. N. Pease and Co., Charlotte, N. C.; formerly Research Asst., Univ. of Illinois, Urbana, Ill.

[3] Asst. Prof. in Civ. Engrg., Univ. of Illinois, Urbana, Ill.

[4] "Tentative Specifications for Quenched and Tempered Steel Bolts and Studs with Suitable Nuts and Plain Washers," ASTM A325-55T, 1955.

[5] "Specification for Assembly of Structural Joints Using High Strength Steel Bolts," Research Council on Riveted and Bolted Structural Joints, Engrg. Foundation, 1954 and 1955.

a result of shrinkage during cooling, assures the permanent tightness and soundness of bolted structural joints. In addition, since the clamping force of the bolts does not depend on shrinkage, it is possible to consistently develop the same clamping force with any length of bolt.

High-strength bolts are well adapted to the field assembly of structural connections for a number of reasons, some of which are as follows:

1. The installation of the bolts requires no heating equipment and thus fire hazards are eliminated.
2. Bolting crews can be trained quickly since the equipment required to install the bolts is simple to operate.
3. The bolts are especially economical where it becomes necessary to replace a small number of loose rivets.
4. Bolts may be installed with either power or hand-operated tools.
5. Field erection costs are often lower when A-325 bolts are used in lieu of field rivets.

Consequently, bolts have become competitive with rivets and often replace them for the field assembly of structural connections.

The use of high-strength bolts for the field erection of structures may result in the assembly of many beam-to-column connections with a combination of rivets and bolts. Although data on the behavior of all-riveted beam-to-column connections are available,[6,7,8,9,10] few tests have been performed on connections containing both rivets and bolts. Three of the four specimens tested and reported herein were assembled with a combination of rivets and bolts to provide data on the behavior of such connections. A fourth specimen was assembled entirely with rivets to provide a direct comparison of the moment-rotation characteristics and the general behavior of connections using the two methods of assembly. All of the test specimens were similar to an all-riveted specimen previously tested by R. A. Hechtman, F. ASCE, and B. G. Johnston, F. ASCE.[9]

The flexible beam-to-column connection, which is designed to resist only vertical loads, is probably the one most frequently used in building construction. To facilitate design, many of these connections have been standardized. These standard connections and the corresponding beam reactions for which they may be used are available.[11] Although assumed to be simple, these connections do provide some restraint at the ends of the beam and, under normal loading conditions, are subjected to both shear and moment.

---

[6] "Tests to Determine the Rigidity of Riveted Joints of Steel Structures," by W. M. Wilson and H. F. Moore, Univ. of Illinois Experiment Sta., Bulletin 104, December, 1917.

[7] "Elastic Properties of Riveted Connections," by J. C. Rathbun, Transactions, ASCE, Vol. 101, 1936, p. 524.

[8] "Investigations on Beam and Stanchion Connections," by C. Batho, Report, Steel Structures Research Committee, Dept. of Scientific and Industrial Research, Great Britian, Vols. 1-2, 1931-34.

[9] "Riveted Semi-Rigid Beam-to-Column Building Connections," by R. A. Hechtman and B. G. Johnston, Progress Report 1, Steel Structures Research Committee, Amer. Inst. of Steel Construction, 1947.

[10] "Riveted Joints, a Critical Review of the Literature Covering their Development, with Bibliography and Abstracts of the Most Important Articles," by A. E. R. de Jonge, ASME, Research Pub., 1945.

[11] "Steel Constructions," Amer. Inst. of Steel Construction, Fifth Ed., 1955.

The tests described herein provide information on the effect of several ratios of moment-to-shear on the general behavior of one type and size of flexible beam-to-column connection. The studies include an evaluation of the moment-rotation characteristics, the moment-resisting capacity, the type and location of failure, the slip and shear deformation, the position of the center of rotation of the connections, the deformation of the column flanges, and the deformation of the fasteners.

DESCRIPTION OF SPECIMENS AND TESTS

Description of Specimens.—Each of the test specimens was designed to provide data on the behavior of two identical beam-to-column connections and consisted of two 18 WF 50 beam stubs 4 ft long fastened to the flanges of a 12 WF 65 column stub 3.5 ft long. The beam stubs were fastened to the column flanges with standard AISC type K-4 connections,[11] each composed of two 6 in. by 4 in. by 3/8 in. by $11\frac{1}{2}$ in. angles (Fig. 1).

Three of the test specimens, FK-4A, FK-4B, and FK-4C, were identical in detail except that specimen FK-4C had web stiffeners at the beam supports (3/8 in. thick bar stiffeners were welded to the beam webs and flanges and were located on both sides of the beam webs). The connection angles for these specimens were fastened to the beam webs with rivets of ASTM A-141 material[12] and to the column flanges with ASTM A-325 high-strength bolts. The details for specimen FK-4R were identical to those for the bolted specimens except that the connection angles were riveted to the column flanges as well as the beam webs.

Preparation of Specimens.—All of the material for the specimens was furnished by the fabricator from ASTM Designation A-7 stock;[13] the angle material was sheared from one length of material in order that its properties would be uniform from one member to the next.

The rivets in the test specimens and for coupons were furnished by the fabricator from ASTM Designation A-141 stock. It was specified that all rivets, except those fastening the angles to the column flanges of specimen FK-4R, be machine-driven. Since the connection of the angles to the column flanges would normally be made in the field, the rivets for this part of the connection were hand-driven to simulate field conditions.

All of the $2\frac{1}{2}$ in. long high-strength bolts, the nuts, and the washers conformed to the requirements of ASTM Designation A-325-55T. The grip of the bolts was 15/16 in., the combined thickness of the column flange and the connection angle.

The cutting, milling, punching, and riveting of the test specimens were done in a structural fabricating shop using standard fabrication techniques. However, the final assembly of specimens FK-4A, FK-4B, and FK-4C with high-strength bolts through the connection angles and column flanges was completed in the laboratory.

---

[12] "Tentative Specification for Structural Rivet Steel," Amer. Soc. for Testing Materials, ASTM A141-52T, 1952.

[13] "Tentative Specification for Steel for Bridges and Buildings," Amer. Soc. for Testing Materials, ASTM A7-55T, 1955.

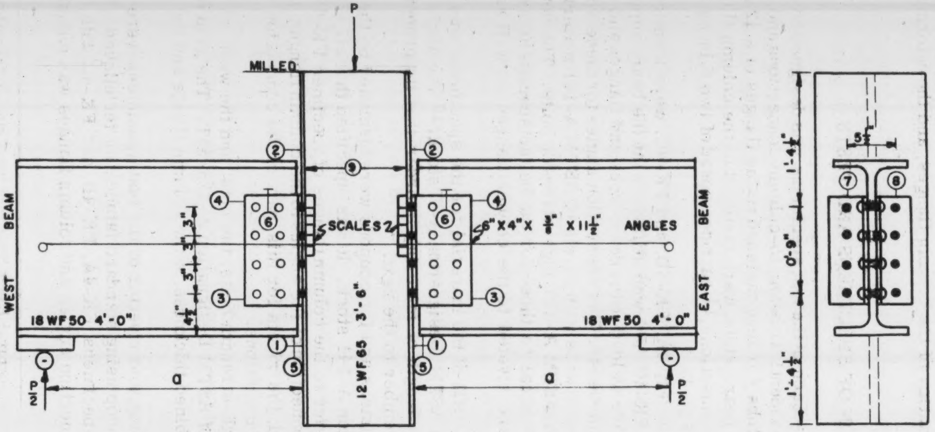
P
MILLED
WEST BEAM
EAST BEAM
18 WF 50 4'-0"
18 WF 50 4'-0"
12 WF 65 3'-6"
SCALES
6" X 4" X 3/8" X 11 1/2" ANGLES
3"
3"
3"
4 1/2"
a
a
P/2
P/2
1
2
3
4
5
6
7
8
9
1'-4 1/2"
0'-9"
1'-4 1/2"
5 1/2"

SPEC. NO.	TYPE OF FASTENER		a
	BEAM WEB	COL. FLG.	
FK-4A	RIVETS	BOLTS	40"
FK-4B	RIVETS	BOLTS	20"
FK-4C	RIVETS	BOLTS	10"
FK-4R	RIVETS	RIVETS	40"

NOTE: ALL FASTENERS 3/4"; ALL HOLES PUNCHED 13/16"

(NO) SLIP, DEFORMATION AND ROTATION DIALS

○⌄○ DEFLECTION WIRE

STIFFENERS FOR FK-4C LOCATED AT THE SUPPORTS

FIG. 1.—GENERAL DETAILS OF SPECIMENS AND INSTRUMENTATION

To simulate field conditions for shop-painted members, the contact surfaces between the connection angles and column flanges were painted with one coat of red oxide paint. However, before painting, the contact surfaces between the connection angles and column flanges were wire-brushed by hand to remove loose mill scale or rust. Any grease or foreign material found on the contact surfaces was removed with a solvent. The paint was then applied with a brush and allowed to dry for approximately 1 week prior to the assembly of the connections. The contact surfaces between the connection angles and beam webs were not painted since this part of the connection is normally made in the shop prior to painting.

The high-strength bolts, which were used in the laboratory to complete the final assembly of the bolted test specimens, were all calibrated in the laboratory to obtain the nut rotations, torques, and bolt elongations at a bolt tension of 25,600 lb (the minimum required by the specifications[5]). The elongation readings were then used to obtain the minimum required tension in the bolts during the assembly of the test specimens.

The bolts were tightened with a manual torque wrench to an elongation corresponding to only the minimum required bolt tension so that the test connections would have the minimum rigidity of bolts which are installed in accordance with the specifications[5] for bolting. For the forty-eight bolts used, the average elongation at the required minimum bolt tension was 0.0046 in., the average torque was 300 lb-ft., and the average nut rotation was 6/10 of a turn. The rotation of the nut was measured from a finger tight position, achieved by turning the nut as far as possible with the fingers while the material to be joined was properly fitted-up with adjacent fitting-up bolts.

For the bolting of the test specimens the position of the column was reversed from that to be used in the testing machine so that the weight of the beams would produce bearing against the bolts in the same direction as would the beam reactions during the tests. This procedure produced bearing at some, if not all, of the bolts and simulated field conditions whereby the weight of the beam causes it to bear on the bolts before they are tightened.

Properties of Materials.—One coupon was taken from each leg of the 6 in. by 4 in. by 3/8 in. angle and tested in the as-rolled condition. The mechanical properties of the angle material, as determined from these coupon tests, are listed in Table 1. It can be seen that the angle material satisfied the requirements[13] of ASTM Designation A7-55T, but that the material from the 6-in. angle leg had a slightly higher yield point and ultimate strength than the coupon material from the 4-in. angle leg.

Coupons were machined from the bolts and the undriven rivets to dimensions proportional to the Standard "0.505-in. Coupon" as provided[14] by ASTM Designation E8-54T. These coupons had a diameter of 0.250 in. and a 1.00 in. gage length. The mechanical properties of the undriven rivets and the bolts are listed in Table 2.

Full-size bolts were tested in the as-received condition to determine the proof load and the ultimate strength of the bolts (the proof load is that load,

---

[14] "Standard Methods of Tension Testing of Metallic Materials," ASTM Standard E8-54T, 1954.

as required[4] by ASTM Designation A325-55T, to which a bolt must be subjected without experiencing any permanent set; tolerance of $\pm$0.0005 in. is allowed as the difference between the measurements made before and after the loading).

TABLE 1.—MECHANICAL PORPERTIES OF ANGLE MATERIAL[a]

Origin of coupon[b]	Elongation in 8 in., in %	Reduction in area, in %	Yield Strength,[c] in kips per square inch		Ultimate strength, in kips per square inch
			Upper	Lower	
4 in. leg	28.1	53.9	39.3	37.7	62.5
6 in. leg	31.3	51.0	41.3	38.4	65.4
Average	29.7	52.5	40.3	38.1	64.5

[a] Standard 8-in. gage length.
[b] All angles were 6 in. by 4 in. by 3/8 in. by 11 $\frac{1}{2}$ in.
[c] Determined by "drop of beam."

TABLE 2.—MECHANICAL PROPERTIES[a]

	Elongation in 1 in., in %	Reduction in area, in%	Yield strength,[c] in kips per square inch	Ultimate strength, in kips per square inch
		Rivet Material[b]		
	35.5	65.0	35.6	62.2
	35.0	62.0	37.3	64.1
Average	35.3	63.5	36.5	63.2
		High-Strength Bolt Material[b]		
	18.0	53.5	87.9	125.7
	15.0	53.3	. . .	147.4
Average	16.5	53.4	87.9	136.6

[a] Standard 0.252 in. coupons. [b] All fasteners nominally 3/4 in. diam. by 2 1/4 in. long. [c] Determined by "drop of beam" fornvets, by 0.2% offset for bolts.

The bolts were first loaded to the required proof load, 28,400 lb for 3/4 in. diameter bolts, and then unloaded to check for permanent set. The bolts were next tested to failure either in direct tension with parallel surfaces or in ten-

sion with a 10° wedge under the head of the bolt. The average ultimate strength of the bolts was 46,700 lb; thus they met the requirements[4] of ASTM Designation A325-55T.

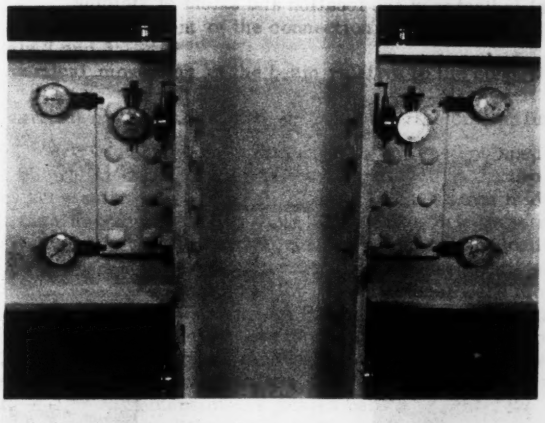

FIG. 2.—INSTRUMENTATION FOR ROTATION AND SLIP MEASUREMENTS

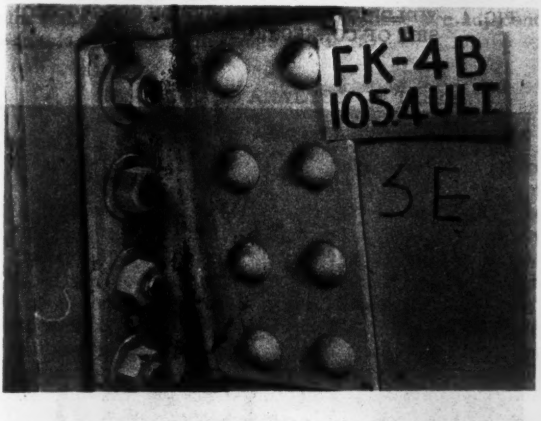

FIG. 3.—YIELDING AND TEARING OF CONNECTION ANGLE OF SPECIMEN FK-4B

Instrumentation and Equipment.—All of the test specimens had similar instrumentation, however some minor changes were made as the tests progressed. This instrumentation included mechanical dials, SR-4 electric resistance strain gages, scales for the determination of deflections, extensometers, and a qualitative visual indicator of the location and extent of yielding.

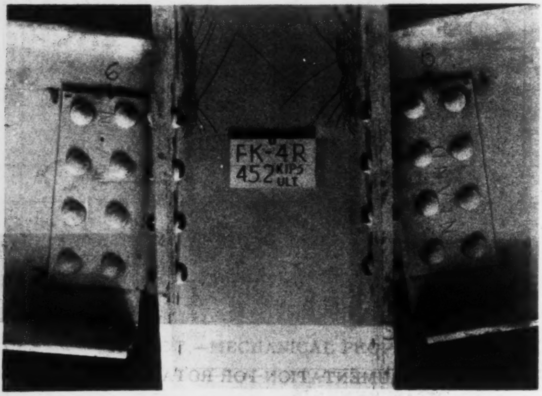

FIG. 4.—YIELDING OF COLUMN WEB ON COMPRESSION SIDE OF CONNECTIONS

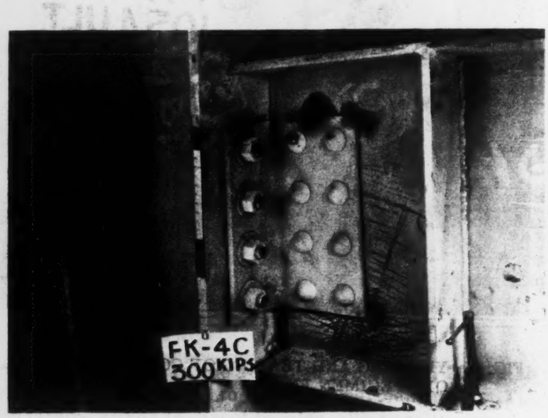

FIG. 5.—YIELDING OF ANGLES AND BEAMS OF SPECIMEN FK-4C

Mechanical dials were used to obtain rotations and movements in the tests (Figs. 1 and 2). These dials were used to measure:

1. The rotation of the end of the beam relative to the column—dials 1 and 2;
2. The angular movement of the beam relative to the connection angles—dials 3 and 4;
3. The vertical movement of the connection angles relative to the column flanges—dials 7 and 8;
4. The vertical movement of the beam relative to the connection angles—dial No. 6;
5. The vertical movement of the beam relative to the column flange—dial 5.

The SR-4 electric resistance strain gages were used on specimen FK-4A to indicate the relative distribution of the column load to the two beam reactions. The gages were mounted on the flanges of each beam midway between the column face and the beam support. Since the strain-gage readings for specimen FK-4A indicated an equal distribution of the column load to the beam reactions, the use of the gages was discontinued in subsequent tests.

The deflection scales, graduated in 0.05 in. divisions, were mounted on the edges of the column flanges as shown in Fig. 1. These scales were read with reference to a fine wire stretched between two rods which were mounted over the supports at the mid-depth of the beams. As the column was loaded, the scales moved downward relative to the wire which remained in a horizontal position. Thus, the movement of the scales relative to the wire represented the deflection of the center of the beams at the supports relative to the column.

Two types of extensometers were used in the tests, one to determine the deformation of the fasteners through the connection angles and the column flanges and the other to measure the separation of the column flanges. (The points at which the flange separation was measured are adjacent to the numbers on the inside of the column flange in Fig. 5).

RESULTS AND ANALYSIS OF TESTS

Description of Tests.—Three of the test specimens, FK-4A, FK-4B, and FK-4R, were tested to maximum load-carrying capacity, however, the fourth specimen, FK-4C, could be loaded only to 300,000 lb, the maximum capacity of the testing machine. In the tests, the specimens were subjected to a number of load increments. After each increment of loading measurements were taken and a visual inspection of the various components was made.

The distance from the column faces to the beam supports, shown as a in Fig. 1, was maintained constant during each test. However, the bearing plates which were fastened to the beam flanges moved outward relative to the supports. This movement can best be understood by visualizing a line connecting the bearing plate with the center of rotation of the connection (assumed to be located at approximately mid-depth of the beam). Then, as the column deflects downward, this line rotates about the center of rotation of the connection and the horizontal distance between the bearing plate and the column face increases. Since it was considered desirable to maintain a constant distance between the column faces and the beam supports during the tests, the bearing plates moved outward by slipping and introduced, between the bearing plates and the supports, a friction force which must be considered in determining the actual moment on the connections.

The beam reaction which acted normal to the beam flange and the friction force which acted parallel to the beam flange were included in the determination of the connection moments. However, the magnitude of the effect of the friction force on the connection moment depended largely on the span length. Specimen FK-4C, a short-span member, required a greater beam reaction to produce a given connection moment than did the other members and, as a result, received the greatest moment correction for the frictional force.

The total connection moments, including the effect of the beam reactions and the friction force, have been noted in the figures herein as adjusted connection moments to differentiate them from the moments based only on the vertical beam reactions. All references in the text to connection moment, unless otherwise identified, pertain to the adjusted connection moment as defined herewith. With the exception of the data of Fig. 7 (to be presented subsequently), all of the test data have been analyzed and are studied in terms of the adjusted connection moment.

Test Results.—Because all the connections were identical in detail except for the use of rivets in lieu of bolts through the angles and column flanges of specimen FK-4R, it was found that the general behavior of all of the specimens was quite similar. Only the behavior of specimen FK-4A is presented herein; a comparison of the test results for all of the other specimens is made subsequently.

Specimen FK-4A was the first specimen tested and, in order to assure the determination of all important characteristics of its behavior, more observations and instrumentation readings were taken than in subsequent tests. However, the principal measurements in the tests were the rotation measurements and these were obtained in each instance to provide the desired moment-rotation relationships. The average moment-rotation curve for specimen FK-4A, as well as the other specimens, is presented in Fig. 6.

At a connection moment of 260 in.-kips, the heels of the connection angles on the tension side of FK-4A began to separate from the column flanges. However, since the fasteners on the tension side of the connection has experienced no change in elongation at this moment, the separation or deformation of the angles occurred only between the two lines of fasteners connecting the angles to the column flanges; the toes of the angles remained in contact with the column.

At a moment of 225 in-kips, yield lines began to appear at the fillet of the angles on the compression side of the connections and was indicative of the high bearing pressure of the heels of the angles against the column flanges. At a moment of 285 in.-kips similar yield lines began to appear at the fillets of the column web opposite the heels of the connection angles, further indicating the presence of high bearing pressures. Yield lines of this type, at a later stage of the test of specimen FK-4R, are visible in Fig. 4.

The connection angles of FK-4A were found to have separated from the column flanges a distance of 0.50 in. at a moment of 362 in.-kips and to have started yielding at the fillets on the tension side at a moment of 450 in.-kips. Then, as the beams continued to rotate relative to the column faces, the beam flanges

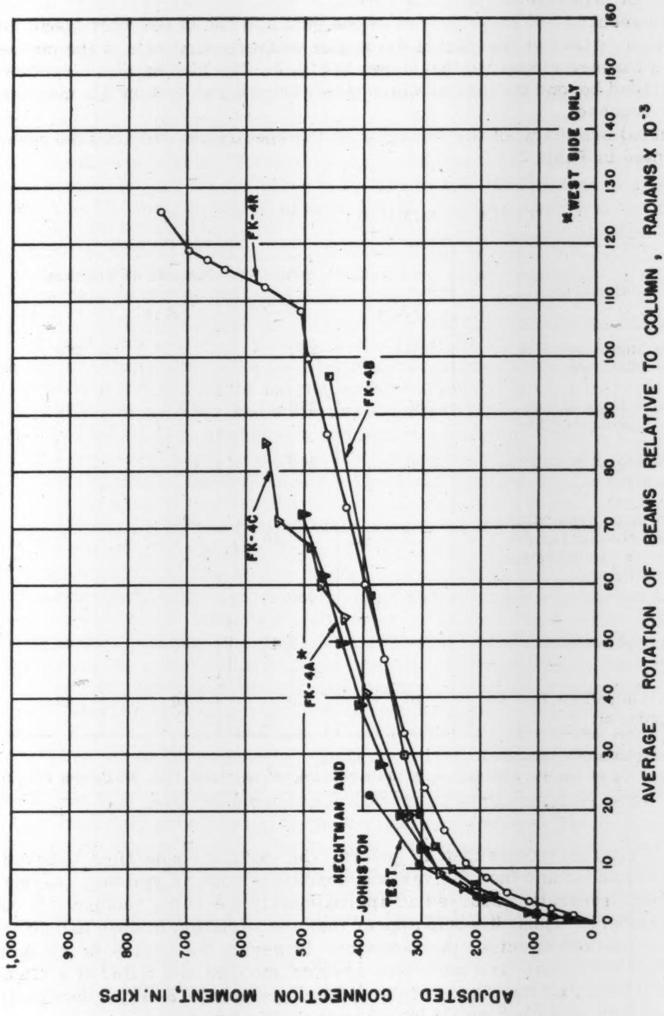

FIG. 6.—COMPARISON OF MOMENT-ROTATION CURVES FOR RIVETED AND BOLTED CONNECTIONS

in compression came into bearing against the column flanges. Shortly after the beam flanges had made contact with the column flanges, yield lines appeared at the fillets of the column opposite the points of contact and indicated the concentration of pressure in the column web.

At a moment of 585 in.-kips, one of the east and one of the west connection angles began to tear at the fillet of the angles on the tension side of the connections, in a manner similar to that shown in Fig. 3. The loading of the specimen was continued beyond the load at which this tearing began and until a maximum load was reached.

A general summary of the behavior of the specimens and the test results is presented in Table 3.

TABLE 3.—SUMMARY OF TEST RESULTS

Condition	Adjusted Connection Moment, in inch-kips			
	FK-4A	FK-4B	FK-4C	FK-4R
Yielding of angles at fillet on compression side	225	230	. . .[a]	235
Yielding of column at web fillet on compression side	285	270	270	290
Yielding of angles at fillet on tension side	450	360	490	360
Moment at large separation of angles from column flanges and magnitude of separation	362 0.50 in.	380 0.60 in.	390 0.45 in.	395 0.60 in.
Tearing of angles	585	450	. . .[b]	450
Maximum load resisted by specimens, kips	46.86	105.4	300 +	45.2
Distance from column face to beam support, in.	40	20	10	40

[a] Observation not recorded.

[b] No tearing of angles although maximum capacity of machine, 300,000 lb was reached.

It is of interest to note that, in general, the various connections behaved in a similar manner and that the various conditions such as yielding, tearing of angles, etc., generally occurred at approximately the same moments in each of the members. Thus, it would appear that the variation in span had no consistent or marked effect on the behavior. However, the angles of the bolted specimen FK-4A tore at a somewhat greater moment and failed at a slightly greater load than did the angles of the riveted specimen FK-4R, indicating that the bolts might provide a small increase in strength to failure.

During all of the tests, the separation of the connection angles from the column flanges caused the angle legs which were fastened to the column flanges to pull in toward the beam webs. As a result, the legs of the angles were soon bearing against the fasteners and causing deformations of the bolt holes and bending of the fasteners. As the bolted connection angles continued to separate from the column flanges, the flat heat-treated washers between the nuts and angles began to bend in the same direction as the deformed angles but, although these washers experienced severe bending, only one washer cracked.

With the exception of specimen FK-4C, which was loaded to the maximum capacity of the testing machine without failure, all of the connections experienced a tearing of the angles on the tension side of the connections. Although the connections were subjected to both moment and shear, the tearing of the angles resulted primarily from the bending moment. This can be seen readily from a comparison of the behavior of specimen FK-4C with that of specimens FK-4A, FK-4B, and FK-4R. Specimen FK-4C resisted a vertical beam reaction of 150,000 lb, almost three times the allowable beam reaction for this type of connection, without experiencing a tearing of the angles. However, the angle of specimens FK-4A, FK-4B, and FK-4R tore at beam reactions of 16,000 lb, 29,500 lb, and 12,900 lb, respectively.

It is interesting that all of the angles which experienced tearing had a slight depression approximately 1 in. long in the fillet, as shown in Fig. 3 (arrow.) These depressions, a result of the shearing operations, evidently weakened the angles sufficiently to initiate tearing under the tensile loading reported. The angles which did not tear had a similar depression, however, because of the manner in which the two angles of a connection are assembled, the depressions in the untorn angles were located on the compression side of the connections.

Moment-Rotation Characteristics.—The term rotation, as used herein, refers to the rotation of the end of a beam relative to the column. This rotation was measured with two mechanical dials mounted at the end of the beam flanges and bearing against the center of the column flange.

The deformation in the angles at the tension side of the connection angles was found to provide the largest component in the rotation at the ends of the beams. Nevertheless, there were a number of other factors which also contributed to the rotation, including: The extension of the fasteners which connected the angles to the column flange, the deformation of the column flanges, and the angular movement between the beam web and the connection angles.

Two moment-rotation curves were obtained for each test specimen except specimen FK-4A. From these data it was evident that there was little difference between the moment-rotation characteristics of the two connections for a given specimen and that all of the curves were of the same general shape (Fig. 6). At low loads (moments up to 200 in.-kips) the rotation of the beams was approximately proportional to the connection moment. Then, as the connection angles began to yield, the rotation increased in a non-linear manner with respect to the applied moment, however, as the moment was increased still further, the rotation assumed a new linear variation with moment and continued this behavior up to the maximum moment for which the rotation readings were taken.

The average moment-rotation curves for the various specimens and a similar all-riveted specimen tested at Lehigh University[9] (Bethlehem, Pa.) are shown in Fig. 6 and clearly demonstrate that the behavior of the various members was quite similar. A comparison of the moment-rotation curves of specimens FK-4A (bolted) and FK-4R (riveted), members fabricated of the same angles, beams, and column materials, indicates a slightly greater resistance

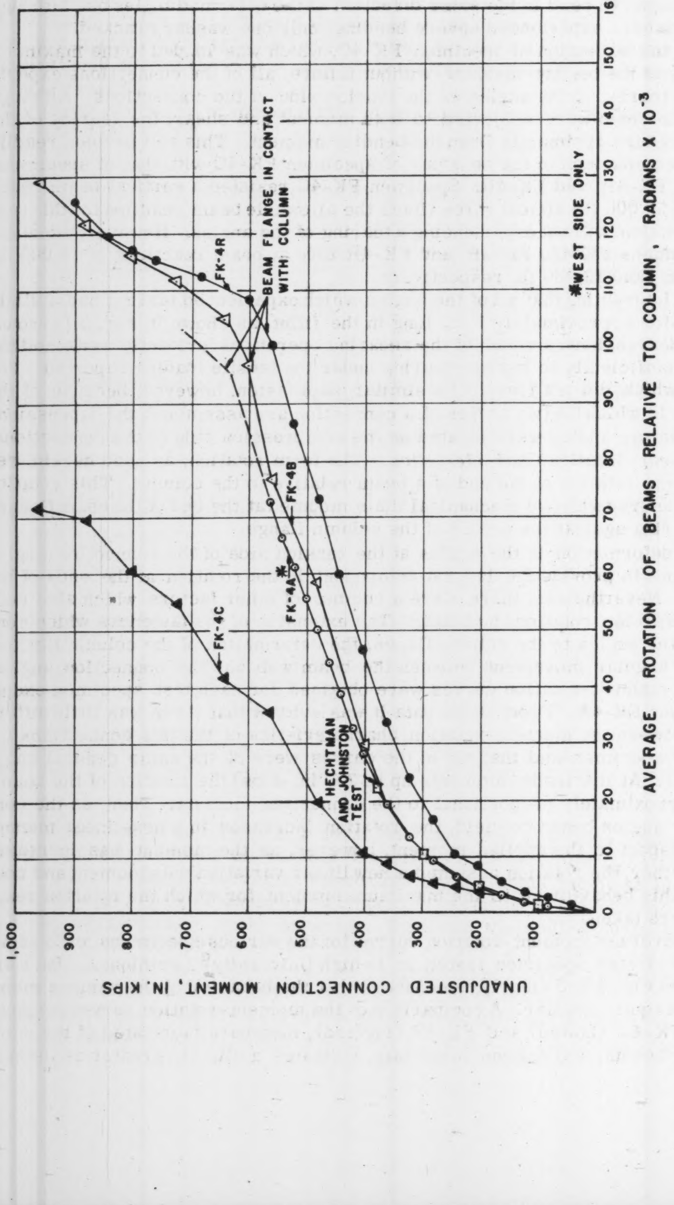

FIG. 7.—UNADJUSTED MOMENT-ROTATION CURVES

to rotation for specimen FK-4A. This slight increase in resistance to rotation may have resulted from the stiffening effect of the heat treated washers and from the greater resistance of the bolts to bending and elongation.

A comparison of the moment-rotation curves for the two riveted specimens, FK-4R and the Lehigh specimen, indicates a greater resistance to rotation for the Lehigh specimen. However, the rotation,[9] produced by a given moment, may vary by as much as 20% to 50% for identical specimens supplied by several fabricators. The difference of the moment-rotation data for these two specimens may also be due, in part, to the use of different rotation instrumentation in the two tests. The rotation of the beams of the Lehigh specimen was measured with level bars,[9] whereas mechanical dials were used for specimen FK-4R.

The relationship between the rotation of the ends of the beams at the column and the moment of the vertical beam reaction (unadjusted connection moment) is shown in Fig. 7. A comparison of the unadjusted moment-rotation curves in Fig. 7 with the adjusted moment-rotation curves in Fig. 6 shows the marked effect of the friction force and the horizontal component of the beam reaction on the connection moment.

TABLE 4.—MOMENT-RESISTING CAPACITY

Specimen	Actual end moment M, in inch kips	Reduction in mid-span stress,[a] in kips per square inch	Percentage Rigidity, $\frac{M}{M_F} \times 100$
FK-4A	150	1.7	12.6
FK-4B	136	1.5	11.5
FK-4C	125	1.4	10.5
FK-4R	90	1.0	7.6

[a] Based on allowable mid-span stress of 20.0 kips per square inch.

Moment-Resisting Capacity.—Standard flexible beam-to-column connections are generally assumed to behave as simple supports and the supported beam is designed for the simple-beam moment. However, these connections do offer some resistance to rotation at the ends of the beam.

With the moment-rotation curves from the test connections (Fig. 6) and a graphical construction developed[8] by C. Batho, it is possible to evaluate the end restraint which the test connections would provide for a particular beam size, span, and loading. The beam size chosen for the analysis was the same as that used for the test specimens (18 W 40). A laterally supported span of 11.2 ft was chosen for which a uniform load of 9,400 lb per ft would produce beam reactions equal to the maximum allowed[11] by AISC Specifications for the K4 connection and a maximum stress of 20 kips per sq in. at the center of the span. The results of the analysis, in which the columns were assumed fixed against rotation, are given in Table 4.

The data in Table 4 indicate that the K4 standard beam-to-column connection provides partial restraint at the end of the beam (approximately 11.5% of

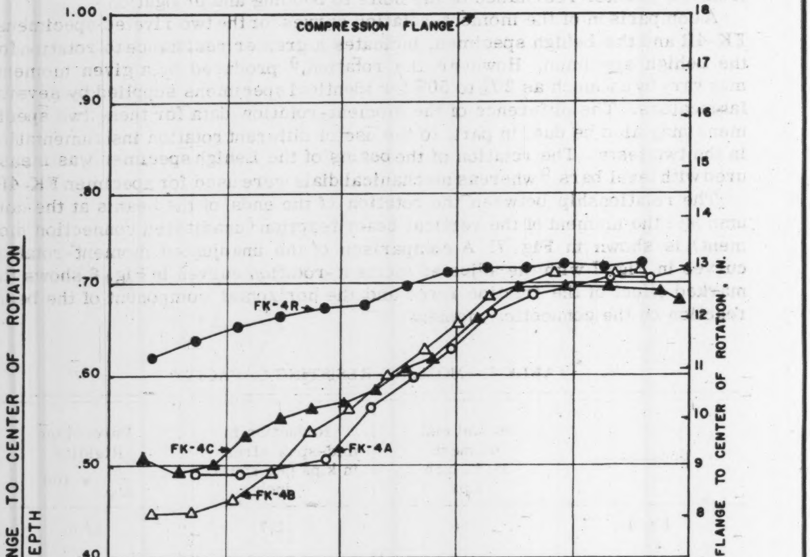

FIG. 8.—POSITION OF EFFECTIVE CENTER OF ROTATION DURING TESTS

the fixed-end moment for bolted connections). In addition, the data indicate that the restraint is somewhat greater when high-strength bolts rather than rivets are used to fasten the connection angles to the column flanges.

Effective Center of Rotation.—The readings from the rotation dials (dials 1 and 2, Fig. 1) were used to determine the locus of the points about which the connections seemed to rotate during the tests. The location of these points, the distance from the tension flange of the beams to the center of rotation of the connections, was studied and is plotted in Fig. 8 for the connection moments.

During the first few increments of loading the center of rotation of the bolted connections was near the mid-depth of the beams. However, as the moment increased, the center of rotation moved toward the compression flange. When the compression flange of the beams came into contact with the column flange, the effective center of rotation was found to have reached a point approximately 70% of the beam depth from the tension flange of the beams.

The effective center of rotation of the riveted connections was approximately 62% of the beam depth from the tension flange of the beams for the first loading. However, the position of the effective center of rotation had moved to approximately the same location as that for the bolted connections when the beam and column flanges came into contact.

Deformation of Fasteners.—The deformation (elongation) of the fasteners which connected the angles to the column flanges was measured during the tests with an extensometer. Although the deformation presented herein refers to the change in length of the fastener, it may include also the effects of bending of the fasteners, which results from the bending of the angles and the pulling-in of the angle legs. Nevertheless, the data gives a general indication of the deformation in the various fasteners.

The elongations of the bolts which were used to fasten the connection angles to the column flanges of specimens FK-4A, FK-4B, FK-4C indicated that a slight decrease in length occurred, and hence a decrease in load, in all of the fasteners during the initial stages of loading. However, the decrease in the length of the top fasteners, those most highly loaded in tension, probably resulted from a bending of the bolts and the angles rather than a reduction in bolt load.

As the connection moments were increased to the maximum values, the extensometer readings indicated an increase in the length of the top tension bolts. However, there is some question as to whether the increase in length resulted entirely from an increase in bolt load above the initial prestress, the bending of the bolts, or a combination of the two. The other three bolts did not experience any noticeable change in length.

A comparison of the deformation characteristics of the rivets of specimen FK-4R and the bolts of specimen FK-4A is presented in Fig. 9. These curves reveal one of the most important differences between the behavior of the connections with rivets and those with bolts: The rivets exhibited a much greater elongation than did the bolts at moments greater than 200 in.-kips. Since the initial prestress in the bolts was approximately twice that in the rivets, a much greater external load was required to produce additional deformation in the bolts. This, no doubt, accounts, at least in part, for the greater rotation noted for the riveted connections.

In the latter stages of testing of specimen FK-4R the tearing of the angles weakened them and caused a slightly greater portion of the load to be resisted

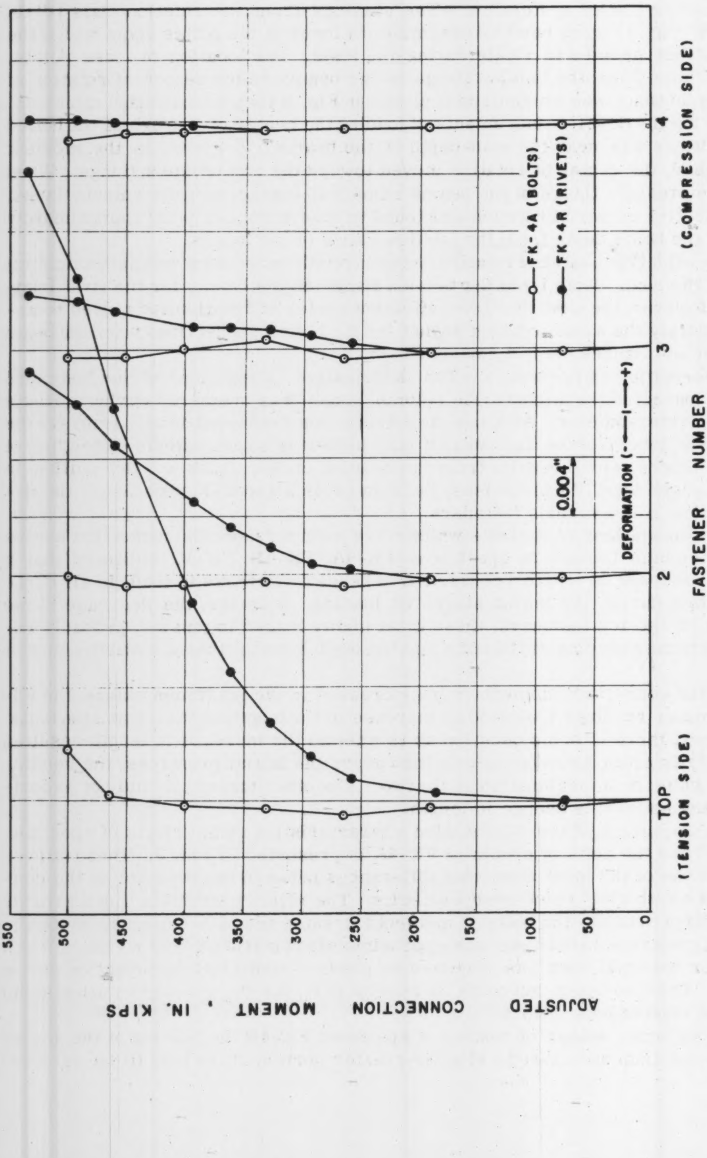

FIG. 9.—AVERAGE DEFORMATION OF RIVETS AND BOLTS (SPECIMENS FK-4R AND FK-4A)

by the top rivet of the untorn angle. Then, as tearing progressed, a greater portion of the tensile force in the torn angle was resisted by the No. 2 rivet, as indicated by an increase in its deformation. The deformation characteristics of the No. 3 and 4 rivets for both the torn and untorn angles were similar. However, after the beam and column flanges came into contact, all of the fasteners began to resist (in tension) the external load.

Separation of Column Flanges.—The separation of the column flanges was measured with an extensometer (dial No. 9, Fig. 1) at points spaced at 3-in. intervals along the center line of the fasteners through the column flanges. The flange-separation measurements on the two sides of the web, were averaged and the results plotted from the column center line in the manner shown in Fig. 10 for specimens FK-4C and FK-4R.

All of the column flanges deformed in a similar fashion. That is, the maximum separation occurred near the gage points between the top and the No. 2 fasteners, and the direction of the movement of the flanges reversed at a point near the No. 4 fasteners. However, the contribution of this separation of the column flanges to the rotation of the ends of the beams was relatively small.

Slip and Deformation.—In addition to the instrumentation previously examined, the test specimens were provided with instrumentation to measure slip and deformation in the connections. The slip and deformation dials are numbered 5, 6, 7, and 8 in Fig. 1.

The dials numbered 7 and 8 were selected to obtain the slip of the connection angles relative to the column flanges. But, the data from these dials were difficult to interpret because of the error introduced by the angular movement or rotation of the outstanding legs of the connection angles in a plane parallel to the column flanges. This angular movement of the legs resulted principally from the pulling-in of the legs at the tension side of the connections and affects the movement or slip of the outstanding legs of the angles relative to the column flanges.

No sudden changes or irregularities were noted in the slip readings of any of the bolted specimens, even though the shear on one of the members, FK-4C, reached 100,000 lb (28,400 psi shear on the bolts) before the slip dials were removed. Thus, the deformations were primarily the result of elastic and plastic deformations of the connections rather than slip, although the holes provided the normal 1/16 in. clearance for the bolts. Major slip was absent because the bolted specimens were fabricated with at least a part of the bolts initially in bearing, just as would normally be the case in the field.

The No. 6 dials (Fig. 1) were used to obtain a measure of the vertical movement of the beam webs relative to the connection angles. But, again, no major slip was observed because the beam reactions were not large enough to overcome the friction between the connection angles and the beam webs, and the short rivets probably filled the holes, allowing little or no clearance for slipping.

The vertical movements of the beams relative to the column flanges were obtained with the No. 5 dials (Fig. 1). These movements, when corrected for the effect of the rotation of the ends of the beams, provided relationships of the same general type as those obtained from dials 7 and 8, the slip of the connection angles relative to the column. However, this should be expected since

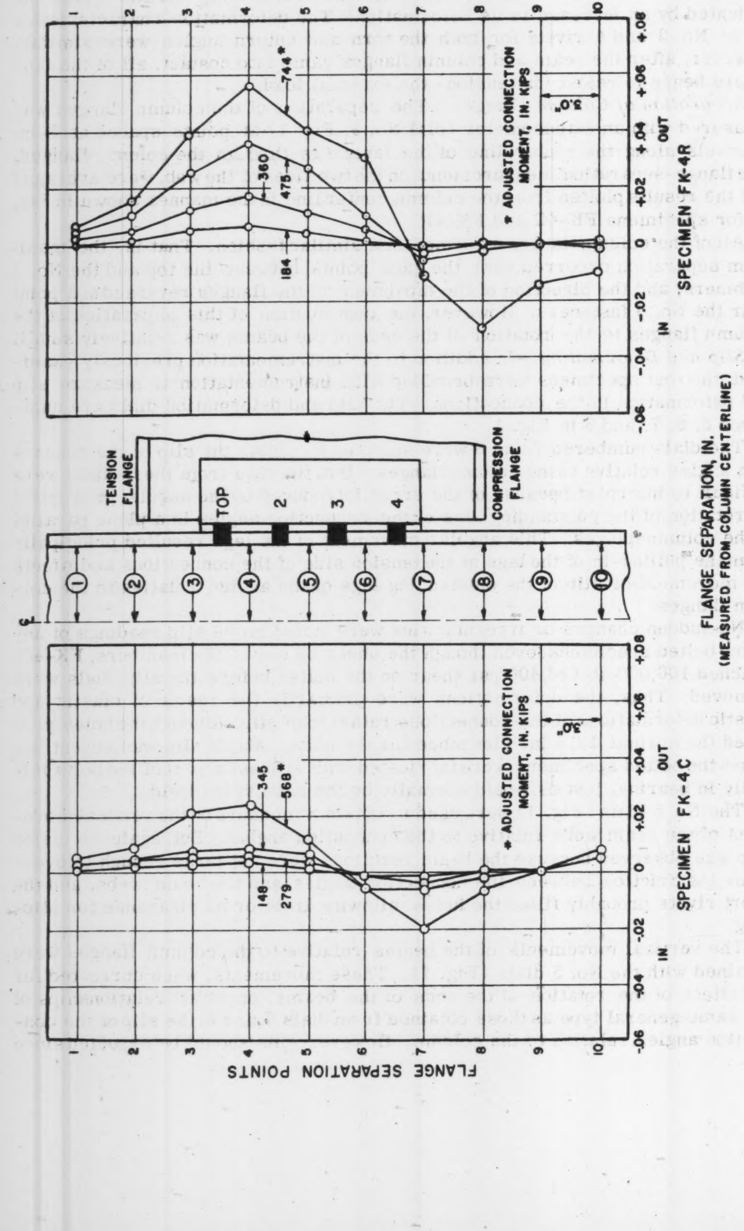

FIG. 10.—AVERAGE SEPARATION OF COLUMN FLANGES

no slipping was evident between the angles and column flanges or between the beam webs and angles.

CONCLUSIONS

The results of the tests reported herein may be summarized briefly as follows:

1. The standard (flexible) K-4 connection, which is assumed for design purposes to behave as a simple connection, provides some restraint against rotation (approximately 10% fixity with an 18 W 50 at working stresses).
2. The moment-rotation characteristics of the riveted and the bolted connections were similar. The three bolted connections, although subjected to loads producing different moment-shear ratios, all gave the same general relationship between moment and rotation.
3. The rotation of the connections resulted primarily from the deformation of the angles. The elongation of the fasteners, the deformation of the column and the slip between the connected parts had only a negligible effect on the rotation.
4. The use of high-strength bolts in lieu of rivets to fasten the connection angles to the column flanges increased slightly the restraint provided by the test connections.
5. The point about which the connections seemed to rotate during the tests moved from an initial position near the mid-depth of the beam toward the compression side of the connections.
6. The test connections were subjected to bending moment and shear. However, the deformation and subsequent tearing failure of the connection angles resulted primarily from the bending moment; the effects of shear deformation were small.
7. The test connections failed by tearing of the angles without rupture of the fasteners, even though, in one case, the applied load reached a value nearly three times as great as the allowable design load for the connections. This tearing initiated at depressions which had been created during the shearing operations.
8. The rivets, which fastened the connection angles to the column flanges, experienced permanent elongation at a lower connection moment than did the hgih-strength bolts.

ACKNOWLEDGMENTS

The tests described herein are a part of an investigation on riveted and bolted joints being carried on in the Civil Engineering Department of the Engineering Experiment Station at the University of Illinois in cooperation with the Illinois Division of Highways, the Department of Commerce-Bureau of Public Roads, and the Research Council on Riveted and Bolted Structural Joints. The tests were planned in cooperation with the Project IV Committee of the Research Council.

FATIGUE TESTS OF JOINTS OF HIGH-STRENGTH STEEL

By Norman G. Hansen,[1] F. ASCE

SYNOPSIS

A program of fatigue testing, in direct tension, of joints made from structural steels having various properties is presented herein. Rivets and high-strength (A325) bolts were used as fasteners, but the middle plate of the double-lap specimens was always the critical element in fatigue. The clamping force was the most important variable governing the fatigue strength of the joints tested. In the riveted joints, the variations of clamping force subordinated whatever superiority one steel had over another. Joints having high clamping force have high fatigue strength; the joints connected with high-strength bolts show much higher fatigue strength than those connected with rivets, even approaching the yield points of some of the steels.

PURPOSE OF TESTS

From the outset, the leading objective of the program has been to determine how much increase in load is allowable when steels of higher nominal strength than the usual ASTM-A7 steel are used in structures (or parts thereof) in which fatigue strength is the limit of usefulness. The many tests with static loading, and those using the weldable structural steel A373 and the A7 steels were made for comparative purposes. Initially the test program used as fasteners only rivets, of either carbon steel, A141, or manganese steel, A195. Somewhat later, tests were begun using A325 high-strength bolts. The purpose in varying the fasteners was to discover what effects this variation would have on the fatigue behavior of the plate material. As the second, or supporting purpose of the entire program, it was hoped to elucidate the effects on fatigue life of several variables, including joint arrangement, properties of the main plate materials and of the fasteners, and intensity of stress.

DESCRIPTION OF TEST PROGRAMS

Two test programs have been conducted, of which the second is of principal concern in this paper. For background and comparison some data will be in-

---

Note.—Published essentially as printed here, in March, 1959, in the Journal of the Structural Division, as Proceedings Paper 1972. Positions and titles given are those in effect when the paper or discussion was approved for publication in Transactions.

[1] Genl. Engr., Engrg. Div., Military Constr., Office, Chf. of Engrs., U. S. Army, Washington, D. C.

cluded from the first program. In both, the test method has been to subject specimens prepared from rolled plates to a cycle of direct tensile stress, varying in each cycle from zero to a preset maximum; this maximum stress is a principal variable. All specimens of each steel were taken from a single plate throughout both programs. Steel A, for example, designates steel from only one plate. Different steels to the same specification were obtained from different mills. Table 1 gives the physical properties of the steels tested; mill scale was left on. In the first program, sixteen different steels were tested in the form of a plate with a hole, and the effect of the stress concentration due to the hole was assessed by comparison with results on similar plate specimens without the hole. A few more than one hundred tests of plates with a hole were made.

TABLE 1.—PHYSICAL PROPERTIES OF THE MAIN PLATE MATERIALS

Material (1)	Kind of Steel (2)	Yield strength for 0.2% offset, in psi (3)	Ultimate strength, in psi (4)	Elongation, in %		Reduction in Area, in % (7)	Hardness, Rockwell "B" (8)
				8-in. gage length (5)	2-in. gage length (6)		
A	High-strength	51,600	77,800	26.4		62.1	83.1
G	Low-alloy (ASTM A242-50T	53,600	75,200	26.7		60.4	80.4
I	Carbon (ASTM-A7)	38,600	70,250	26.5		54.2	80
K	Carbon (ASTM-A7)	34,100	57,600	33.6		63.0	80
L	Silicon (ASTM-A94)	45,800	81,900	20.0		56.2	87
M	Silicon (ASTM-A94)	56,600	92,900	20.9		45.9	88.2
N	Silicon (ASTM-A94)	48,800	84,500	20.2		54.1	87
P[a]	High strength steel	56,450	89,250		24.0	59.6	
Q[a]	Weldable structural steel (ASTM-A373)	37,500	60,720	31.5			
T	High strength steel	66,600	89,400	23.2	47.5	63.3	86.4

[a] Data furnished by manufacturer.

In the second program, the test specimens were double lap joints, with the thicknesses of the outer and middle plates chosen to make the middle plate always critical. The fasteners, whether rivets or bolts, were not intended to fail in fatigue, and they did not. There were three patterns of joints, as shown in Fig. 1; Pattern A with two fasteners in a line, Pattern B with four in a line, and Pattern C with four in a rectangle. Pattern C is a doubling in width of Pattern A; the ratio of net to gross area, 74.5%, and the ratio of gage to diameter of fastener (g/d ratio), 4.25, are the same for these two patterns. The ratios

for Pattern B are higher; net to gross area, 85% and g/d = 7.33. Seven steels from the first program, plus three others, were tested, although not all of them with all combinations of pattern and fastener. A total of two hundred and ten specimens were tested in fatigue under the second program; and static-load tests were made of each kind of specimen tested in fatigue.

All of the fatigue tests were performed on the direct-tension machine of the Northwestern Technological Institute, Evanston, Ill. This is a dual machine of Wilson Type, and contains two independent testing units mounted in a single frame. In each unit, a fixed and a movable pull head are so mounted that the load can be maintained concentric with the axis of the specimen. A walking beam transmits the motion from a gear train and an eccentric to the movable head. Load capacity is 250,000 lb and the operating speed is approximately 170 cycles per min. Load measurement is by means of a proving ring.

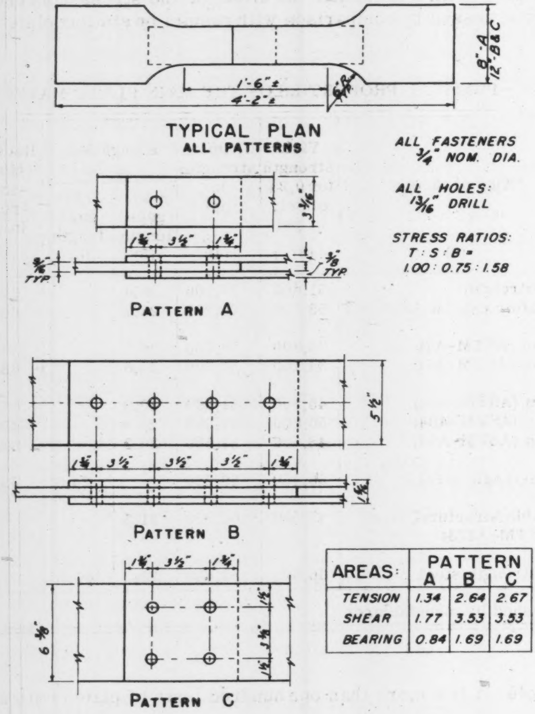
1'-6"±
4'-2"±
6"R
8"-A
12"-B&C
TYPICAL PLAN
ALL PATTERNS
ALL FASTENERS
3/4" NOM. DIA.
ALL HOLES:
13/16" DRILL
STRESS RATIOS:
T : S : B =
1.00 : 0.75 : 1.58
1 3/4"
3 1/2"
1 3/4"
TYP
TYP
PATTERN A
5 1/2"
PATTERN B
6 7/8"
PATTERN C

AREAS:	PATTERN A	PATTERN B	PATTERN C
TENSION	1.34	2.64	2.67
SHEAR	1.77	3.53	3.53
BEARING	0.84	1.69	1.69

FIG. 1.—SPECIMENS FOR STATIC AND FATIGUE TESTS OF JOINTS

Holes in all specimens were drilled, or sub-drilled and reamed, in the laboratory. The rivets were driven in a large commercial shop in accordance with good practice. The high tensile bolts were tightened in the laboratory to reach the minimum tension of 25,600 lb specified at that time for the $\frac{3}{4}$ in. diameter bolt.

STATIC TEST RESULTS

Some of the rivets were removed after driving, and tested for shear strength. Based on driven rivet areas, the carbon steel rivets were found to have an ultimate shear strength of 47,000 psi and the manganese steel rivets 54,500 psi, or 15% higher. A study of clamping force in 128 of the carbon steel rivets was made by Y. Yoshimi, A. M. ASCE, using the relaxation method. The study revealed that after the fatigue failure of the joints, the clamping force of the individual rivets in them varied from 1,000 lb to nearly 20,000 lb - 30% had less than 5,000 lb; 20% had more than 11,000 lb; the other half fell between these values.

The results of 26 static load, tension tests of riveted joints of seven steels are presented in Table 2. In many cases, initial failure occurred by double shear of the rivets, with the manganese steel rivets showing definitely higher strength, approaching and in six cases exceeding the strength of the main plate. When the rivets failed, they were removed, replaced by high-strength bolts, and the specimen retested. (It had been shown in other research that this procedure had little effect on main-plate strength.) So in all cases the main plate, which in fatigue proved critical, was tested to failure. The results showed close correlation of actual plate strength with strength predicted from the coupon properties of the main plate materials and the geometry of the joints. Three different rules for predicting joint efficiencies were applied, and the degree of correlation varies somewhat among them, but all three predict higher efficiency for Pattern B joints than for Patterns A or C. Actually, in Pattern B, the joints developed 80% to 88% efficiency, averaging 84.6%; while in Patterns A and C the joints developed 76% to 82% efficiency, averaging approximately 79%. Patterns A and C differed approximately 1% in efficiency. In general, then, static tests showed that plates in the riveted joints had ultimate static strengths closely related to the coupon properties of the main plate materials.

FATIGUE TEST RESULTS

For reasons both of brevity and of clarity, not all the results of the fatigue test programs are presented. From the first program, only those steels are considered which were subsequently tested in the form of riveted or bolted joints. From the second program all of the tests of joints of Pattern B have been omitted. These joints had a higher predicted and actual efficiency in static tests than did those of Patterns A and C, however, in fatigue tests no clear superiority was evident for this pattern. Direct comparison would be confusing, but the results would not alter the conclusions.

Fatigue test results are given in Tables 3 through 5 and are presented graphically in Figs. 2 through 7. The tabulated maximum tensile stress in each cycle

TABLE 2.—RESULTS OF THE STATIC TENSION TESTS OF THE RIVETED JOINTS

Steel	ASTM Specification	Fastener		Edge Conditions[b]	Ultimate Load for Failure, in pounds		Ultimate Stress for Failure, in psi		Type of Plate Fracture	Plate Efficiency, in %
		Pattern	Type[a]		Rivets	Plate	Rivets[c]	Plate[d]		
(1)	(2)	(3)	(4)	(5)	(6)	(7)	(8)	(9)	(10)	(11)
I	A7	A	C	(a)		95,000		71,000	Brittle	75.5
L	A94	A	C	(a)	96,000	118,000	54,300	88,900	Ductile	79.2
L	A94	A	C	(a)	98,500	116,000	55,700	86,900	Brittle	77.9
N	A94	A	C	(b)	103,000	115,400	58,300	86,500	Brittle	77.5
N	A94	A	C	(b)	100,500	121,000	56,900	90,600	Brittle	81.3
L	A94	A	M	(a)	110,000	119,400	62,200	89,500	Ductile	80.2
L	A94	A	M	(a)	111,000	116,000	62,800	86,900	Ductile	77.9
I	A7	B	C	(a)		180,000		68,200	Ductile	83.0
I	A7	B	C	(a)		174,600		66,100	Brittle	80.5
L	A94	B	C	(a)	190,000	223,000	53,800	84,500	Ductile	86.8
L	A94	B	C	(a)	186,000	211,000	52,700	80,000	Ductile	82.1
N	A94	B	C	(b)	188,000	226,000	53,300	85,600	Ductile	88.0
N	A94	B	C	(b)	193,000	218,000	54,700	82,600	Ductile	84.8
L	A94	B	M	(a)		225,000		85,300	Ductile	87.5
L	A94	B	M	(a)		219,000		83,000	Ductile	85.2
I	A7	C	C	(a)	189,000	198,000	53,500	74,100	Ductile	78.6
L	A94	C	C	(a)	186,000	238,000	52,700	89,100	Ductile	79.9
L	A94	C	C	(a)	184,000	228,000	52,1000	85,500	Ductile	76.5
N	A94	C	C	(b)	190,000	230,000	53,800	86,100	Ductile	77.2
N	A94	C	C	(b)	188,000	231,000	53,300	86,600	Ductile	77.5
L	A94	C	M	(a)	230,000	241,000	65,100	90,400	Ductile	80.8
L	A94	C	M	(a)	229,000	236,000	64,900	88,500	Ductile	79.2
K	A7	C	M	(a)		169,000		63,300	Ductile	82.0
G	A242	C	M	(a)		221,000		82,800	Ductile	82.1
A	A242	C	M	(a)		225,000		84,300	Ductile	81.0
M	A94	C	M	(a)		266,000		99,600	Ductile	80.1

[a] C = Carbon steel, M = Manganese steel. [b] (a) = Milled, (b) = Machine flame cut and post-heated. [c] Based on nominal diameter of rivets. [d] Based on net section of main plate.

was obtained by dividing the load applied by the testing machine, by the net section of the main plate material. In Figs. 2 through 7, this value is plotted to linear scale as the ordinate. For the abscissa, which represents the number of stress cycles to failure, a non-linear scale has been selected. This scale is proportional to the square root of the number of cycles. Other scales, linear and non-linear, were considered. The choice was based not on any rational theory, but on visual clarity plus the implication that, with increasing life, equal numerical differences become less significant.

TABLE 3.—FATIGUE TESTS OF PLATES WITH A HOLE

Steel (1)	Stress Range, in ksi (2)	Life, in Thousands of Cycles (3)	Steel (1)	Stress Range, in ksi (2)	Life, in Thousands of Cycles (3)	Steel (1)	Stress Range, in ksi (2)	Life, in Thousands of Cycles (3)
A	0-31.5	398	K	0-31.5	167	N	0-37.5	234
(A242)		398	(A7)		190	(A94)		341
				0-30	382			
	0-27	530		0-27	730		0-35	493
		601			935			503
		793						
				0-25	835		0-33	733
	0-25	2,030			1,156			775
		2,080						
				0-23	1,428		0-31.5	2,137[a]
								3,160[a]
G	0.40	159	L	0-35	209			
(A242)		192	(A94)		446			
						T	0-42.5	381
	0-37.5	293		0-31.5	852			386
		304			2,509[a]			
							0-40	648
	0-35	657		0-27	1,916			785
		1,803			2,012[a]			
	0-31.5	2,013[a]					0-37.5	3,000[a]
								3,000[a]
I	0-31.5	216	M	0-35	281			
(A7)		312	(A94)		318			
	0-27	492		0-31.5	368			
		561			688			
		901		0-30	437			
				0-27	981			
	0-25	2,000[a]			2,137[a]			

[a] Specimen did not fail.

Of the fifteen steels tested in the form of a plate with a hole, results are given in Table 3 and shown in Fig. 2 for those eight steels subsequently tested in joints. The plates were 5/8-in. thick; the test section of the plate, 4-in. wide by 16-in. long, had a hole reamed to 1-1/16-in. diameter in its center.

Comparison with the data in Table 1 shows a fairly good correlation between the static and fatigue test results; the steels with higher physical properties also had, in general, higher fatigue strength. The seven steels not shown gave similar results. One steel of those shown, Steel T, was originally made to a

TABLE 4.—FATIGUE TESTS OF BOLTED JOINTS

Steel/ Pattern (1)	Stress Range, in ksi (2)	Life, in Thousands of Cycles (3)	Steel/ Pattern (1)	Stress Range, in ksi (2)	Life, in Thousands of Cycles (3)	Steel/ Pattern (1)	Stress Range, in ksi (2)	Life, in Thousands of Cycles (3)
A/A	0-40	1,552	G/C	0-42.5	889	M/A	0-42.5	1,567
		948			821			1,410
					542			1,057
	0-38	1,671		0-40.5	1,627		0-40	1,760
					1,609			1,205
	0-37	3,000[a]			977			1,008
	0-33	3,000[a]		0-30	3,000[a]	M/C	0-40.5	1,810
								1,473
				0-27	3,000[a]			1,145
A/C	0-40.5	1,507	K/A	0-36	237		0-39	1,695
		985			195			1,490
					112			1,459
	0-39	1,825		0-33	3,000[a]	T/A	0-42.5	3,000[a]
					2,905			1,283
								614
	0-37.5	3,000[a]		0-30	3,000[a]			
		1,452					0-40	2,343
								899
G/A	0-40	3,000[a]	K/C	0-37.5	382			874
		2,054			312			
		942			225	T/C	0-47	522
								499
	0-36	1,737		0-35	1,337			
		1,720			1,244		0-42.5	2,254
								1,254
	0-30	3,000[a]		0-30	3,000[a]			822
							0-40.5	2,398[b]
								1,141[b]

[a] Specimen did not fail. [b] Failed in grip.

United States Navy specification (it later became commercially available). It is definitely higher in both static and fatigue properties, as shown in Fig. 2, so that a separate curve has been drawn for it. The A7 steels fall well below the high-strength steels, as their static properties would lead one to expect. The remaining five high-strength steels are represented by a third curve, in-

termediate between the other two. At 1,000,000 cycles, the difference in fatigue strength between the A7 steels and the five high-strength steels is about 5 ksi.

TABLE 5.—FATIGUE TESTS OF RIVETED JOINTS

Steel/Pattern (1)	Stress Range, in ksi (2)	Life, in Thousands of Cycles (3)	Steel/Pattern (1)	Stress Range, in ksi (2)	Life, in Thousands of Cycles (3)	Steel/Pattern (1)	Stress Range, in ksi (2)	Life, in Thousands of Cycles (3)
A/C	0-30	368	L/A	0-30	1,320	N/C	0-27	311
		294	(M)		750			309
		275			194			267
		253						
		230		0-27	1,346		0-25	1,120
		221			980			966
		218			966			621
		161						
						P/C	0-30	814
G/C	0-30	572	L/C	0-30	1,151			501
		279	(M)		1,022			483
		241			767			323
		209						227
		200		0-27	1,255			211
		166			914			211
		160			528			185
		110						174
			L/A	0-30	1,584			173
I/A	0-30	775			922			
		612			496	Q/C	0-30	5,000[b]
								3,000[b]
	0-27	1,282		0-27	2,924			2,300
		1,082			1,579			1,790
		681			992			1,490
I/C	0-30	1,557	L/C	0-27	576	T/C	0-30	336
		1,015			384			257
					168			216
	0-27	1,820						204
		781		0-25	3,000[b]			200
					1,570			173
K/C	0-30	319			535			149
		232						147
		182	N/A	0-30	760			
		181			754			
		179			579			
		153						
		153		0-27	3,000[b]			
		149			2,090			
					1,524			

[a] (M) = Manganese steel rivets, all other joints fastened with carbon steel rivets.
[b] Specimen did not fail.

A direct comparison of manganese steel rivets with carbon steel rivets, with no other variable than the fastener, was made in the case of one steel only.

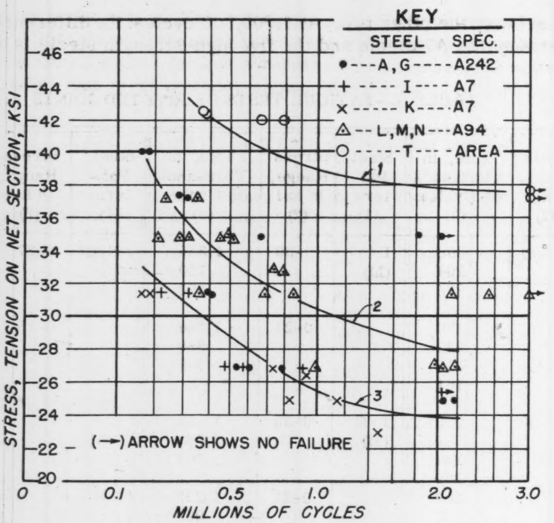

FIG. 2.—PLATES WITH A HOLE

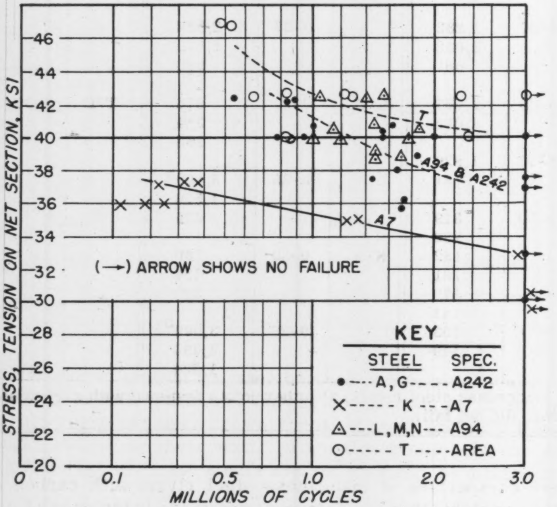

FIG. 3.—BOLTED JOINTS

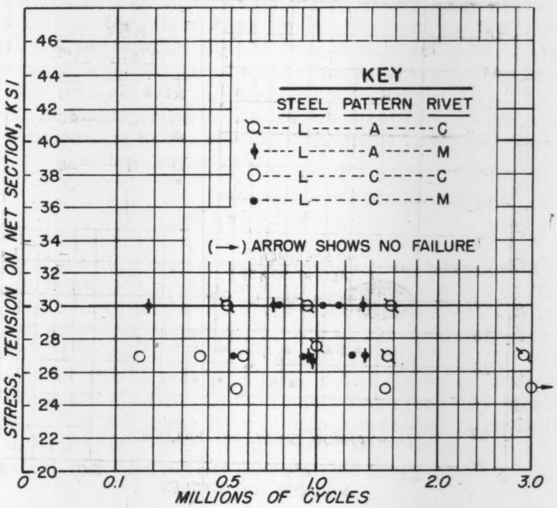

FIG. 4.—RIVETED JOINTS WITH CARBON AND MANGANESE STEEL RIVETS

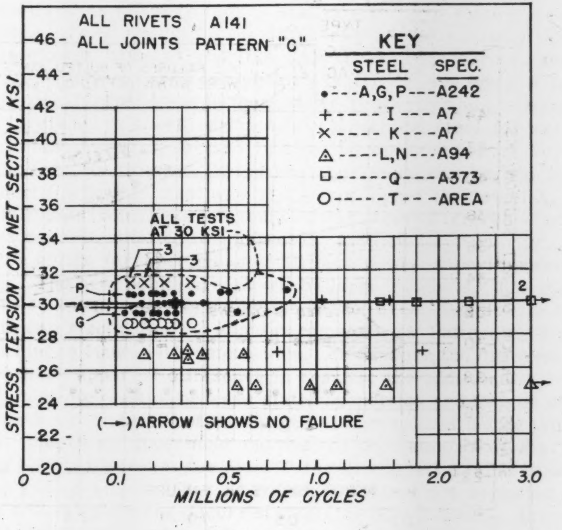

FIG. 5.—RIVETED JOINTS, PATTERN C

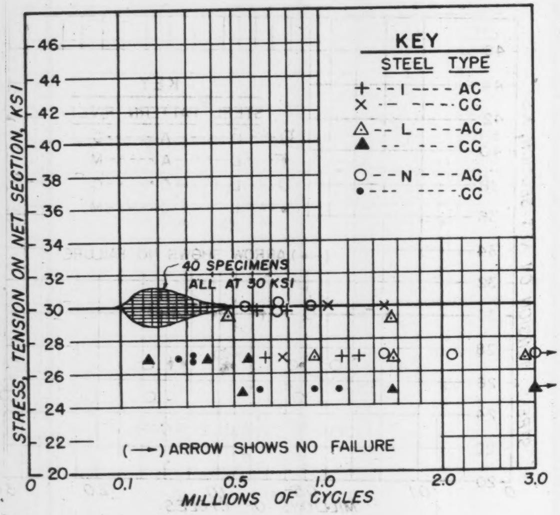

FIG. 6.—RIVETED JOINTS, PATTERNS A AND C

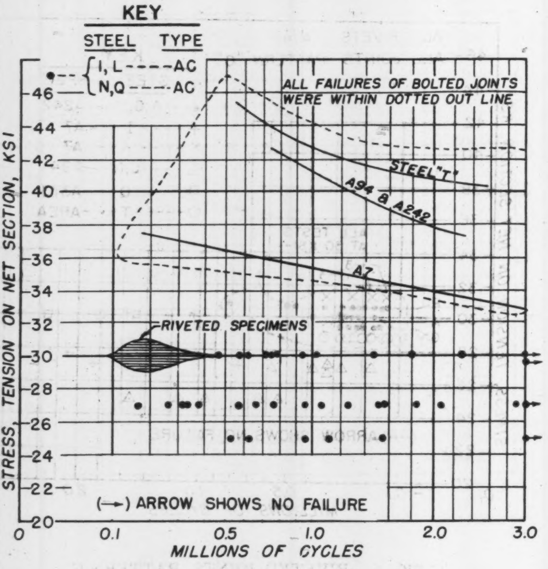

FIG. 7.—COMPARISON OF RIVETED AND BOLTED JOINTS

The results, shown in Fig. 4, do not show that either rivet produced a joint clearly stronger than the other under the conditions of the tests. If there is any advantage, it appears to be with the manganese steel rivet. Large scatter in results occurred in the groups of specimens not presented, as well as those shown. The short grip, 1-5/16 in., may have affected the present comparison of rivet steels. At longer grips, the manganese steel rivets might consistently develop a higher clamping force. Results using these rivets have been excluded from the remaining tables and figures.

BOLTED JOINTS

Five steels (of the eight tested as plates with a hole) were tested in fatigue, with high tensile bolts as fasteners, in joints of Patterns A and C. The results are shown in Fig. 3 and Table 4. As in the tests of plates with a hole, the high yield-point steel shows above the others, with an indicated fatigue strength, at 1,000,000 cycles, of almost 43 ksi. This compares with 39 psi for this steel in Fig. 2. The one A7 steel (Steel K) showed definitely lower average fatigue strength. There is more scatter in the results from the other steels, nevertheless fatigue strengths in these bolted joints correspond fairly well in relative position with static strengths. Silicon steel M, with lower yield but higher ultimate than steel T showed almost equal fatigue life.

RIVETED JOINTS

In Figs. 4 and 5, the scatter which characterized all the tests of riveted joints is evident. All specimens in Fig. 5 were Pattern C. In the outlined area appear the results of an effort to reduce scatter effects by testing more specimens at a single stress; except for the different plate materials, all the specimens were as closely alike as possible. All these tests were at zero to 30 ksi. The contrast between the near equality of the fatigue lives of these six steels, with the great differences in their static properties, may be observed.

One steel, furnished to specification A373 (structural steel for welding), a late addition to the program, seemed to show exceptionally long fatigue life under the same test conditions. Two of the specimens ran beyond 3,000,000 cycles. The ductility of this steel was 31.5%, not higher than steel K. No explanation of the result from these few tests on this steel is offered. Later tests under different conditions failed to confirm the indicated superiority.

In Fig. 6, 16 points for specimens of Pattern A are superimposed on the previous chart. The new points are shown by large symbols. The cluster of tests at zero to 30 ksi is represented by the shaded area. Despite the fact that Pattern A, with two rivets, has the same parameters as Pattern C, it appears that somewhat higher fatigue life is obtained. As between the different steels, however, there is no apparent difference in results; the additional points confirm the absence of correlation between static properties and fatigue strength.

Fig. 7 presents a comparison of the fatigue-test results of bolted joints with riveted joints. The three uppermost curves are the same as in Fig. 3, representing respectively the trends for Steel T, the silicon and A242 high-strength steels, and the carbon steels. The individual points are not replotted, but all the failures of bolted specimens occurred within the dotted outline. In the cases of riveted joints (with the one possible exception, the A373 steel), the different steels were not distinguishable from one another in fatigue strength, so a single symbol is used for all of them. The highest maximum cyclic stress at which riveted joints were tested was 30 ksi, at which stress most of the riveted joints failed at roughly 200,000 cycles. The few specimens of bolted joints tested at this same maximum stress did not fail even after 3,000,000 cycles. Only one bolted specimen failed at 33 ksi; this was the carbon steel of lowest yield point. The effect of the high clamping power of the high strength bolts in increasing the resistance of joints to repeated load is apparent.

REVIEW OF RESULTS

Before considering conclusions, some qualifying considerations are stated as follows:

1. In all the tests, the stress cycle used was from zero to maximum tension; and this tension was set rather high with a view toward producing failures within a reasonable period of testing machine operation. These test conditions do not correspond to common service conditions in buildings or bridges.
2. The rivets were comparatively short. Longer rivets have been shown to develop higher clamping power by virtue of greater shrinkage on cooling. Hence the comparison made herein of carbon and manganese steel rivets and high tensile bolts may not be equally applicable to joints of greater thickness.
3. There was a wide variation observed in the surface condition of the plates of the various steels. Some were quite smooth; others rough or pitted in varying degree. Examination of the results does not show the roughest plates to be the weakest in fatigue, but there was some indication of such an effect. Since all specimens of any one steel were taken from a single plate, this factor may have influenced the results.
4. The symmetry of clamping forces, as well as the average clamping force, of the fasteners within a joint, probably influenced the fatigue life. This factor of possible or probable asymmetry of clamping force with resulting variations in stress concentration, may well be of dominant importance in at least some of the results.

CONCLUSIONS

From the test results and analysis, the following conclusions are drawn:

1. In the bolted joints, the fatigue strength is related to the static-test properties of the plate material.
2. Joints fastened with rivets of manganese steel, A195, were not clearly superior to similar joints using ordinary carbon steel rivets, A141, in fatigue strength.
3. As tested in fatigue in riveted joints, no plate steel showed superiority over A7 steel to correlate with higher static strength. One possible exception, the A373 steel needs further testing before a conclusion relating to it can be stated.
4. The joints connected with high-strength bolts show much higher fatigue strength than those connected with rivets, even approaching the yield points of some of the steels.
5. The most important variable governing the fatigue strength of a joint is clamping force. In riveted joints, as tested, the variations, and the distribution

within a joint of those variations, of clamping force, subordinates whatever superiority one steel has over another. Joints having uniformly high clamping force, such as the bolted joints, have high fatigue strength.

It is proposed, in future programs, to pursue further the evaluation of high-strength steels in fatigue, by more careful isolation or measurement of the variables and by increasing the number of like specimens tested. In view of the importance assigned to the factor of stress concentration at the edges of the hole due to bearing, tests have been initiated to establish a lower limit under a control condition of full bearing, no clamping. Tests using less severe stress cycles than zero to maximum tension, such as 1/2 S to S, which occur more commonly in bridges, are also planned.

ACKNOWLEDGMENTS

This paper has been prepared on behalf of the engineers who performed the research and also on behalf of Project Committee VI, of which the writer was (1956-1960) chairman, of the Research Council on Riveted and Bolted Structural Joints. The Council sponsored, and the Committee in general guided the research, which was conducted at Northwestern University during 1952-1957. The responsible research men include: Frank Baron, F. ASCE, B. J. Covington, M. ASCE, K. J. Kenworthy, E. W. Larson, M. ASCE, L. B. McCammon, Jr., F. ASCE, C. W. Muhlenbruch, Jr., M. ASCE, T. M. Ridley, A. M. ASCE, L. T. Wyly, F. ASCE, and Yoshimi. The writer wishes to express his appreciation for suggestions and criticism during the preparation of the paper to members of the Project Committee and to the research men who helped by consultation or correspondence.

EFFECTS OF FABRICATION TECHNIQUES

By Desi D. Vasarhelyi,[1] M. ASCE, Said Y. Beano,[2] Ronald B. Madison,[3] A. M. ASCE, Zung-An Lu,[4] and Umesh C. Vasishth,[5] A. M. ASCE

SYNOPSIS

A considerable amount of earlier investigation of the characteristics of structural joints assembled with high tensile bolts were focused on the possibility of slip in the range of currently used design stresses. Other tests clarified the behavior of such joints under fatigue loads.

Some questions about the possible effects of various fabricating processes still were open; some others arose as new techniques and ideas developed both in methods of tightening the fasteners and in design principles. The question of the efficiency of joints being influenced by such factors as punching of the holes, misalignments, and the paint on the faying surfaces has been left for the present investigations.

The high practical value found in the one-turn-of-the-nut method drew the attention to its possible effects on the behavior of joints. This was especially so in the case of large and long joints, in which the gradual development of slip required more insight into the behavior of such joints.

A certain tendency toward considering the coefficient of friction in the design of the joint made a more thorough study of this factor necessary. Thus the three-fold scope of the later investigations conducted on high tensile bolted joints.

Tests on joints with drilled and with misaligned punched holes, both with mill scale and with painted faying surfaces showed that, as expected, the punching of the holes does and the misalignment and the paint do not affect significantly the efficiency of the joint. The effect of punching of the holes proved to be the same for bolted joints as for riveted ones. As a matter of fact, the efficiency of the bolted joints in view of these effects, can be sufficiently predicted by formulas used to estimate the efficiency of riveted joints. The con-

---

Note.—Published essentially as printed here, in March, 1959, in the Journal of the Structural Division, as Proceedings Paper 1973. Positions and titles given are those in effect when the paper or discussion was approved for publication in Transactions.

[1] Assoc. Prof. of Civ. Engrg., Univ. of Washington, Seattle, Wash.

[2] Graduate Student, Univ. of Washington, Seattle, Wash.

[3] Engr., Bethlehem Pacific Steel, San Francisco, Calif.

[4] Engr., Washington Toll Bridge Authority, Seattle, Wash.

[5] Engr., former Graduate Student, Univ. of Washington, Seattle, Wash.

dition of the faying surfaces, whether painted or unpainted, apparently does not affect the efficiency.

A sufficient number of small (4 bolt) joint tests and a series of tests on large joints proved that the one-turn-of-the-nut method acts the way it would be predicted from the presence of the higher clamping force.

Systematic analysis of all available data on slip tests throws more light on the behavior of the coefficient of friction in the joints. It shows that the major factor determining its value is the treatment of the faying surfaces. Such factors as clamping force, tension: shear ratio, etc., have well defined but only minor influence on the value of the coefficient of friction.

These results and others should be of great value in the drafting of specifications for joints assembled with high tensile bolts.

EFFECT OF PUNCHED HOLES, MISALIGNMENT, AND PAINTED FAYING SURFACES

Fifteen tests of double-lap joints assembled with 12 high tensile bolts of 3/4-in. diameter and four tests of double-lap joints with only one row of 4 high tensile bolts of 7/8-in. diameter have been conducted. Some of the tests were conducted at -24°F, others at room (between 66°F and 76°F) temperature. The slip and the elongation of the joints were measured. The first major slip load, ultimate strength, energy absorption and efficiency of the joints were studied (1)(2).[6]

Specimens.

Description.—Fifteen 12-bolt specimens, designated Type U and Type X (Fig. 1), were tested. They were made of 3/4-in. and 3/8-in. plates of ASTM A 7-51T semi-killed steel, and joined by twelve 3/4-in. high tensile steel bolts (ASTM A 325) in 13/16-in. diameter drilled or punched holes. The holes were misaligned as shown in Fig. 1. All bolts were tightened to a torque of 320 ft-lb, the recommended approximate equivalent torque for required minimum tension (3) in 3/4-in. bolts. This torque corresponds to an average tension in the bolts of 26,000 lb.

Two types of specimens were tested: Type U with a tension:shear ratio of 1.00:0.75 and Type X with a tension:shear ratio of 1.00:1.00. Specimens of each type were tested under the following conditions: (1) drilled holes, mill-scale faying surfaces, room temperature; (2) drilled holes, red-lead faying surfaces, room temperature; (3) punched holes, red-lead faying surfaces, -24°F. Two specimens of each type were tested except for condition (2).

To this series of 12-bolt specimens four 4-bolt specimens made of 1/2-in. and 1/4-in. plates of ASTM A 7-51T semi-killed steel have been added, joined by 7/8-in. high tensile bolts in 15/16-in. drilled holes in one row. These are also shown in Fig. 1 and designated Type ZU and ZX, the first having a tension: shear ratio of 1:0.75, the second one of 1:1. Two of each type were tested, both with painted faying surfaces, and one in each set of two having one outside hole misaligned as shown in Fig. 1.

Preparation.—The specimens were cut, shaped, and drilled in the structural shop of the laboratory, the punching was done in the structural-steel plant.

---

[6] Numerals in parentheses refer to corresponding items in Appendix I.

The specimens with red-lead faying surfaces were painted (on the faying surfaces only) with Type 1 red lead (TT-P-86) at least 7 days prior to assembly.

While assembling the specimens, the tightening of the bolts was gradual in six separate stages (three on the laboratory floor and three in the testing machine) assuring that all bolts were brought to the same final torque. After the bolts had been properly torqued, the slip gages, thermocouples (for low-temperature tests only), and slide-wire elongation gages were mounted. If a low-temperature test was to be run, the entire specimen from clevis to clevis was enclosed in the cooling bag.

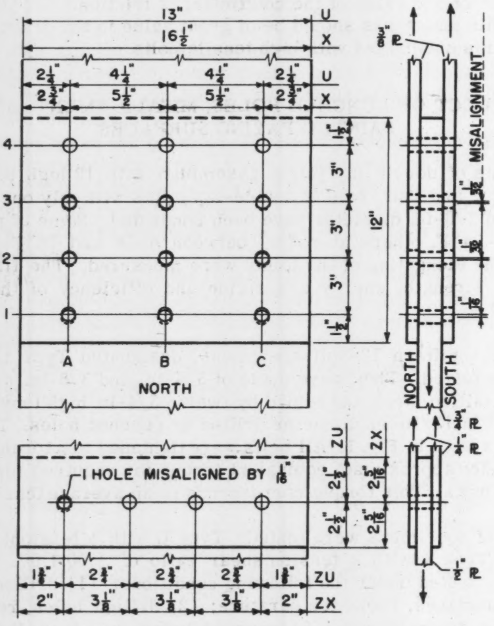
13"
U
16½"
X
2¼"
4¼"
4¼"
2¼"
U
2¾"
5½"
5½"
2¾"
X
4
3
2
1
A
B
C
NORTH
1½"
3"
3"
3"
1½"
12"
¾" PL
MISALIGNMENT
1/32"
1/32"
1/16"
NORTH
SOUTH
¾" PL
¼" PL
I HOLE MISALIGNED BY 1/16"
ZU
ZX
2½"
2½"
2 5/16"
2 5/16"
½" PL
1⅛"
2¼"
2¼"
2¼"
1⅛"
ZU
2"
3⅛"
3⅛"
3⅛"
2"
ZX

FIG. 1.—SPECIMEN TYPES U AND X (TOP) AND ZU AND ZX (BOTTOM)

***Description of Tests*.—All specimens were loaded in the 2,400,000-lb hydraulic testing machine to failure.**

Measurements were taken of the temperature of the specimen, of the slip at the center of each side of the joint, and of the elongation along three lines on each face of the joint.

***Results*.**

Slip in the Joint.—The slip behavior of specimens U and X is summarized in Figs. 2 and 3, and in Table 1.

The specimens with mill-scale faying surfaces showed no signs of appreciable slip until the average shear on the gross area of the bolts had become greater than 15,000 psi. For a design tension: shear ratio of 1.00:0.75, the value 15,000 psi is equivalent to the working load. The specimens which were tested at -24°F with painted faying surfaces behaved in the same manner. However, the specimens tested at room temperature with painted faying surfaces began slipping at an average shear of only 5,000 psi (1/3 the working load for a ratio of 1.00:0.75.

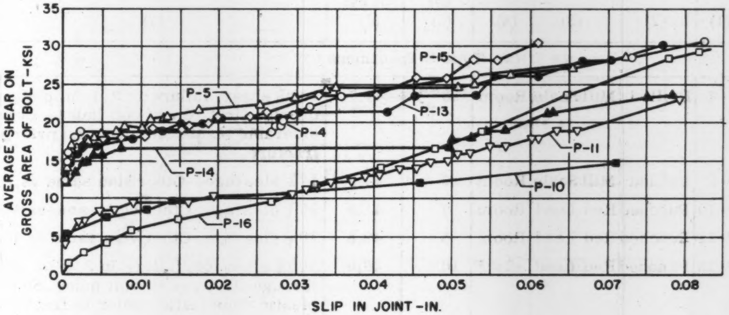

FIG. 2.—RELATIONSHIP BETWEEN SHEAR AND SLIP FOR TYPE U JOINTS

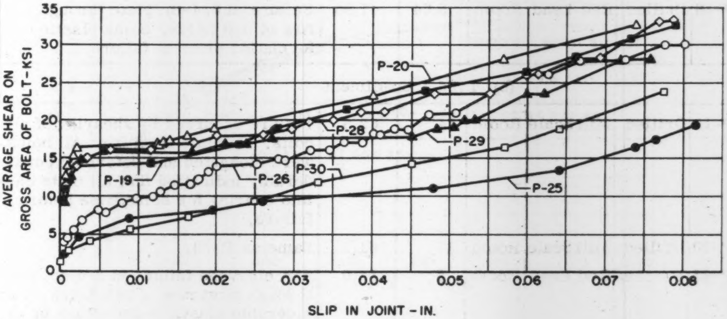

FIG. 3.—RELATIONSHIP BETWEEN SHEAR AND SLIP FOR TYPE X JOINTS

Ultimate Strength and Elongation of the Joint.—The elongation behavior of specimens U and X is summarized in Figs. 4 and 5. A comparison of the computed and observed ultimate loads is given in Table 2. The apparent elongation of the joint due to slip was not subtracted from the total elongation in preparing

TABLE 1.—DESCRIPTION OF PLATE FAILURE

Specimen Number (1)	Holes (2)	Faying Surface (3)	Test Temperature (4)	Average Shear at First Major Slip, in ksi (5)	Average Shear at Ultimate Load, in ksi (6)	Short Description of the Fracture, % Cleavage in the Fracture (7)
			(a) Type U Specimens			
P-4	Drilled	Mill Scale	Room	18	47.7	100% shear, failure in 3/4-in. plate through first row of bolt holes. Considerable plastic deformation prior to fracture.
P-5	Drilled	Mill Scale	Room	18	47.9	17% cleavage. Otherwise same as P-4.
P-10	Punched	Red Lead	Room	6	41.6	80% cleavage. Otherwise same as P-4.
P-11	Punched	Red Lead	Room	5	42.8	10% cleavage. Otherwise same as P-4.
P-13	Punched	Red Lead	-24° F	16	46.0	100% cleavage, failure in 3/4-in. plate through first row of bolt holes. Some plastic deformation prior to fracture.
P-14	Punched	Red Lead	-25° F	17	30.6	100% cleavage. Practically no plastic deformation prior to fracture. Otherwise same as P-13.
P-15	Punched	Red Lead	-29° F	17	32.0	Same as P-14.
P-16	Drilled	Red Lead	Room	5.64	47.85	Failure in 3/4-in. plate through first row of bolt holes. Some plastic deformation prior to failure.
			(b) Type X Specimens			
P-19	Drilled	Mill Scale	Room	14	62.5	Failure occurred by shearing of all bolts. No plate fracture. All holes were elongated and deformed considerably indicating that all bolts came into bearing for some time before failure.
P-20	Drilled	Mill Scale	Room	17	61.1	Same as P-19.
P-25	Punched	Red Lead	Room	5	56.0	45% cleavage failure in 3/4-in. plate through first row of bolt holes. Considerable plastic deformation prior to fracture.
P-26	Punched	Red Lead	Room	5	55.6	6% cleavage. Otherwise same as P-25.
P-28	Punched	Red Lead	-24° F	15	40.0	100% cleavage failure in 3/4-in. plate through first row of bolt holes. Practically no plastic deformation prior to fracture.
P-29	Punched	Red Lead	-25° F	16	44.6	Same as P-28.
P-30	Drilled	Red Lead	Room	5.64	60.2	Same as P-19.

Figs. 4 and 5 and is responsible for the "kink" which can be seen on some of the curves just prior to the inset of the yielding.

The specimens with drilled holes had the greatest strength and elongation. Those with punched holes had approximately 90% as much strength and only approximately 60% as much elongation as the ones with drilled holes. Those which were tested at -24°F had approximately 75% as much strength and only approximately 20% as much elongation as the drilled specimens tested at room temperature.

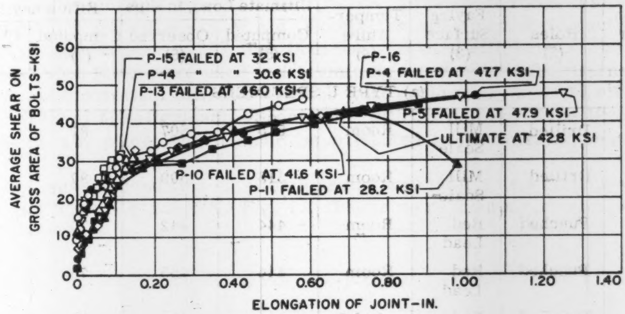

FIG. 4.—RELATIONSHIP BETWEEN SHEAR AND ELONGATION FOR TYPE U JOINTS

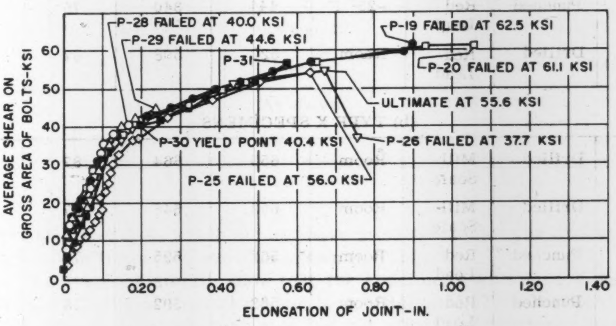

FIG. 5.—RELATIONSHIP BETWEEN SHEAR AND ELONGATION FOR TYPE X JOINTS

Type of Fracture.—A short description of the plate fracture, including the percentage of cleavage present, is given in Table 1.

All specimens U and X tested at room temperature underwent considerable plastic deformation prior to failure. Except for specimen P-13, all specimens tested at -24°F underwent little plastic deformation.

Specimens P-19, P-20, and P-30 (tension: shear ratio 1.00:1.00, drilled holes) failed by shearing of the bolts; all other specimens failed by fracture in the 3/4-in. plate through the first row of holes. All the holes in specimens P-19, P-20, and P-30 were found to be considerably elongated and deformed. This indicates that all the bolts had come into bearing long before the specimen finally failed.

TABLE 2.—COMPARISON OF COMPUTED AND OBSERVED EFFICIENCY

Specimen Number (1)	Holes (2)	Faying Surface (3)	Temperature (4)	Ultimate Load, in Kips: Computed (5)	Ultimate Load, in Kips: Observed (6)	Efficiency, in %: Computed (7)	Efficiency, in %: Observed (8)
(a) TYPE U SPECIMENS							
P-4	Drilled	Mill Scale	Room	515	507	87	85.6
P-5	Drilled	Mill Scale	Room	515	509	87	86.0
P-10	Punched	Red Lead	Room	444	442	75	74.6
P-11	Punched	Red Lead	Room	444	455	75	76.9
P-13	Punched	Red Lead	-24° F	444	487	75	82.4
P-14	Punched	Red Lead	-25° F	444	325	75	55.0
P-15	Punched	Red Lead	-25° F	444	340	75	57.5
P-16	Drilled	Red Lead	Room	522	508	87	84.7
(b) TYPE X SPECIMENS							
P-19	Drilled	Mill Scale	Room	653	664	87	88.4
P-20	Drilled	Mill Scale	Room	653	648	87	86.4
P-25	Punched	Red Lead	Room	562	595	75	79.4
P-26	Punched	Red Lead	Room	562	592	75	78.8
P-28	Punched	Red Lead	-24° F	562	425	75	56.6
P-29	Punched	Red Lead	-25° F	562	475	75	63.3
P-30	Drilled	Red Lead	Room	661	640	87	84.2

Except for specimen P-10, all fractures which occurred at room temperature were primarily shear fractures; all specimens tested at -24°F failed with nearly 100% cleavage fracture. The type of fracture present in the broken specimen was identified by visual observation.

Joint Efficiency.—To compute joint efficiency the relative gage method was used (4). The efficiencies of the joints tested, both computed and acutal, are summarized in Table 2. One should note the close agreement between the computed and actual efficiencies for the specimens tested at room temperature. The specimens tested at -24°F had (except for specimen P-13) actual efficiencies of approximately 25% less than the computed efficiency. The results of actual coupon tests were used in determining the theoretical efficiency of the joint and the theoretical ultimate load the joint could carry at 100% efficiency.

The Effect of Misalignment.—Specimens with 12 bolts of Type U and X did not indicate any effect which could be attributed to the misalignment of the holes.

A more severe condition of misalignment was built in specimens Q-1 and Q-3, of the Type ZU and ZX (Fig. 1). These were compared with identical specimens Q-2 and Q-4, which did not have misalignment. The observed ultimate loads and efficiencies were as shown in Table 3.

TABLE 3.—EFFECT OF MISALIGNMENT

Specimen Number (1)	Tension: shear ratio (2)	Misalignment (3)	Ultimate Load, in kips (4)	Efficiency, in % (5)
Q-1	1:0.75	As shown	225	71.8
Q-2	1:0.75	None	235	74.9
Q-3	1:1	As shown	275	72.0
Q-4	1:1	None	302	89.1

These results consistently show that the specimens with severe misalignment support a lower ultimate load and lose efficiency. This leaves the problem of just how much misalignment would not affect the efficiency open. The question needs further study.

EFFECT OF BOLT-TIGHTENING METHOD ON SLIP AND EFFICIENCY

The general effect of the one-turn-of-the-nut method in large joints was studied in two specimens of 80 bolts. One of the latter was a rather long joint. Twenty-six 4-bolt specimens were tested in addition to these (6).

Test and Test Method.

Slip Test of Eighty-Bolt Joints 153-M and 155-N.

Preparation of Specimens.—The properties of Joints 153-M and 155-N are shown in Table 4. The specimens are shown in Figs. 6, 7, 8, and 9. The properties of the steel are listed in Table 5. The bolts were of 1-in. diameter high tensile type meeting the ASTM specification A-325, and marked P, in 17/16-in. diameter holes. Before assembling the joints all faying surfaces were properly cleaned from rust and grease. The bolts were tightened by a complete turn of the nut, starting from the finger-tight condition.

Tightening Bolts by One Turn of Nut.—Punch marks were made on the nuts and on the ends of the bolt shanks so that the marks for the bolt lay on a radial line through the center of the bolt end. Thus when the mark on the nut traveled 360° and came back onto the same radial line, a complete turn of the nut was indicated. An impact wrench driven by compressed air was used which torqued approximately 90% of the bolts of Specimen 155-N. The rest of the bolts were torqued by a hand wrench with self-locking socket and the hoist mounted on the testing machine. With that particular procedure the torquing of a bolt from finger-tight position to a complete turn of the nut took from 12 sec to 20 sec.

Measurement of Slip and Strain.—When all bolts had been tightened, dials and strain gages were fitted on the specimen. For specimen 155-N, fourteen dials were used to measure slips and twelve SR-4 Type A-11 gages were cemented to the lap plates to measure strains. For specimen 153-M, sixteen dials and twenty-four gages (sixteen on lap plates, eight on edges of the butt plate) were used (Figs. 8 and 9). A Baldwin strain indicator and a Young indicator with switch boxes were used for taking strain readings.

TABLE 4.—PROPERTIES OF SPECIMENS

Spec. No.	Surface Condition	Net Ten. Area Sq in.	Nominal Double Shear Area Sq in.	Tension: Shear Ratio	Faying Area Per Bolt	Approx. Bolt Tension kips
153-M	Mill Scale	92	125.6	1.00:0.73	57.6	70
153-M	Mill Scale	98	125.6	1.00:0.78	36.3	72.5
153-X	Mill Scale	33.94	42.4	1.00:0.80	55.8	69
155-Y	Mill Scale	33.25	47.1	1.00:0.71	30.6	72.5

Test Procedure.—Loads were applied in increments of 200,000 lb until the full capacity of the machine was reached. Each loading took approximately 1 min and was maintained while readings of dials and gages were taken; this took approximately 6 min on the average. The higher loads (more than 2,000,000 lb) were maintained at each step for an additional 10 min so that any significant change in slip or strain which occurred within the short period of time after loading might be discovered. The load was released in steps of 400,000 lb.

Test to Fracture of Twenty-seven-Bolt and Thirty-Bolt Joints 153-X and 155-Y.

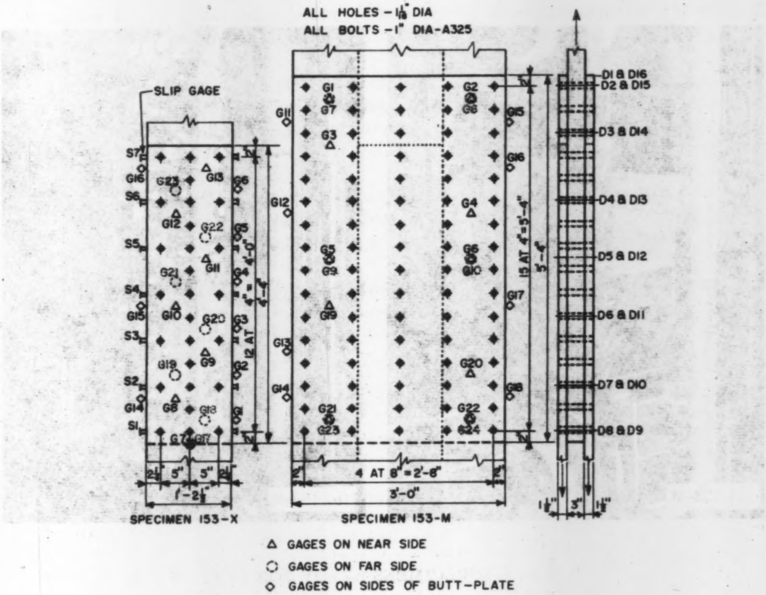
ALL HOLES - 1 1/16" DIA
ALL BOLTS - 1" DIA-A325
SLIP GAGE
S1 S2 S3 S4 S5 S6 S7
G1 G2 G3 G4 G5 G6 G7 G8 G9 G10 G11 G12 G13 G14 G15 G16 G17 G18 G19 G20 G21 G22 G23 G24
12 AT 4" = 4'-0"
2 1/2" 5" 5" 2 1/2"
1'-2 1/2"
SPECIMEN 153-X
4 AT 8" = 2'-8"
2" 2"
3'-0"
15 AT 4" = 5'-4"
5'-8"
SPECIMEN 153-M
D1 & D16
D2 & D15
D3 & D14
D4 & D13
D5 & D12
D6 & D11
D7 & D10
D8 & D9
1 1/2" 3" 1 1/2"
△ GAGES ON NEAR SIDE
◌ GAGES ON FAR SIDE
◇ GAGES ON SIDES OF BUTT-PLATE

FIG. 6.—SPECIMENS 153-M AND 153-X

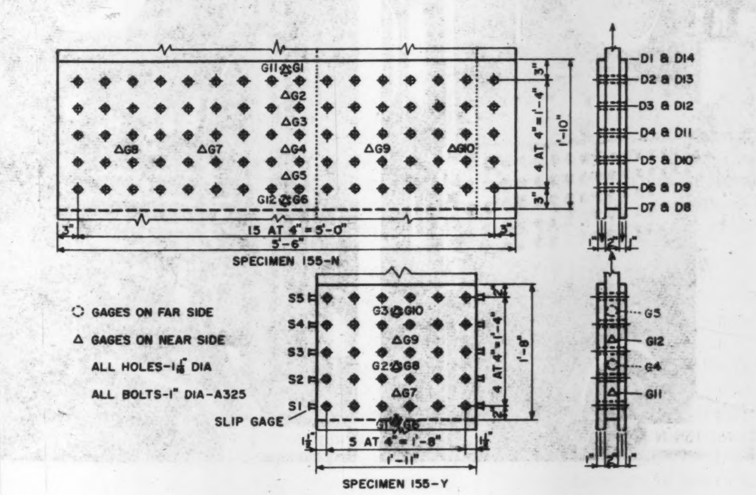
G11 G1 G2 G3 G4 G5 G6 G7 G8 G9 G10 G12
3" 4 AT 4" = 1'-4" 3"
1'-10"
3" 15 AT 4" = 5'-0" 3"
5'-6"
SPECIMEN 155-N
D1 & D14
D2 & D13
D3 & D12
D4 & D11
D5 & D10
D6 & D9
D7 & D8
1" 2" 1"
◌ GAGES ON FAR SIDE
△ GAGES ON NEAR SIDE
ALL HOLES-1 1/16" DIA
ALL BOLTS-1" DIA-A325
S1 S2 S3 S4 S5
SLIP GAGE
G3 G10 G9 G2 G8 G7 G1 G6
2" 4 AT 4" = 1'-4" 2"
1'-8"
1 1/2" 5 AT 4" = 1'-8" 1 1/2"
1'-11"
SPECIMEN 155-Y
G5 G12 G4 G11
1" 2" 1"

FIG. 7.—SPECIMENS 155-N AND 155-Y

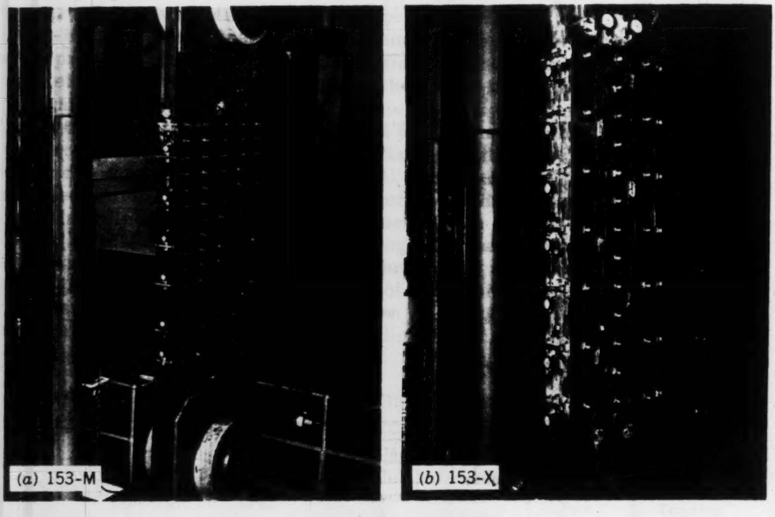

(*a*) 153-M

(*b*) 153-X

FIG. 8.—SPECIMENS READY FOR TEST

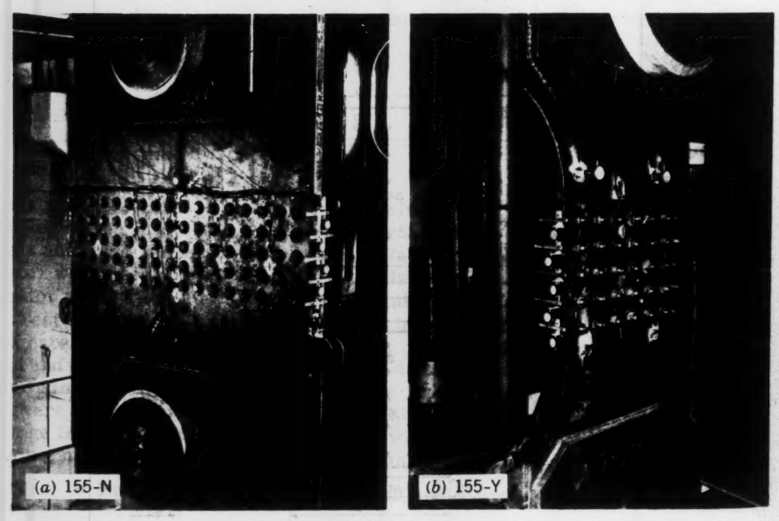

(*a*) 155-N

(*b*) 155-Y

FIG. 9.—SPECIMENS READY FOR TEST

Preparation of Specimens.—The joints tested were specimens 153-X and 155-Y which are shown in Figs. 6, 7, 8, and 9. The properties of the two specimens are listed in Table 4.

Specimen 153-X was cut from specimen 153-M, and specimen 155-Y was cut from specimen 155-N. The 1-in. diameter bolts were of ASTM type A-325, marked C for specimen 153-X and marked P for specimen 155-Y. The specimens 153-X and 155-Y were designed so that they could be broken in the 2,400,000-lb testing machine.

The procedure used to prepare, clean, and to fit the specimens in the testing machine was identical with the procedure used in the previous slip test.

Tightening Bolts.—The tightening procedure was essentially the same as previously described.

Measurement of Strain, Slip and Elongation.—Dial gages were used for measuring the slip at various rows and the over-all elongation of the specimens. Strains at various points on the plates were measured by SR-4 Type A-11 gages. A Baldwin strain indicator and Young indicator with switch boxes were used for taking strain readings.

TABLE 5.—AVERAGE PROPERTIES OF THE STEEL

Spec. No.	Plate Thickness	Upper Yield ksi	Lower Point ksi	Ult. Strength ksi	Elong. in 2 in. %	Red. of Area %
153	1.5	33.5	32.0	64.3	35.1	57.7
153	3	30.1	30.4	64.9	35.9	57.6
155	1	31.2	29.5	56.8	40.6	68.3
155	2	33.6	34.4	65.0	34.6	52.6

For specimen 155-Y, twelve SR-4 gages were used. In this specimen, which had 5 rows of bolts, the slip was measured at each row by dial gages fixed at either end. Over-all elongation of the specimen was measured by four dial gages, two on each side. These dial gages were attached to the butt plate at the top end of the joint. They had a wire attachment extending to the other end of the joint and firmly clamped there to the lap plates. The arrangement of all gages can be seen in Fig. 9.

Specimen 153-X had twenty three SR-4 gages. The slip was measured for each alternate row with fourteen dial gages. For overall elongation a similar arrangement was used as in specimen 155-Y. The arrangement of these gages can be seen in Fig. 8.

Test Procedure.—Loads were applied in increments of 100,000 lb. All dial and strain readings were taken at each increment of load up to the yield point. Each loading took approximately 1 min and the reading of gages took from 6 min to 8 min. Whenever a major slip occurred the loading was stopped and readings taken. Reading of SR-4 gages were discontinued when the specimen started to yield. Slip readings were taken until all the bolts were in bearing.

Dials for slip readings were removed before breaking the joint. Overall elongation was measured for the entire duration of the test.

Calibration of Bolts.

The Calibration of the Bolts.—In order to find the clamping force produced by one turn of the nut, load-elongation curves were drawn for each kind of bolt. Two bolts of each kind were tested and the load-elongation curves for the bolts used in these specimens are given in Fig. 10.

The Determination of the Clamping Force.—To compare slip characteristics for different types of joints tightened by the one-turn-of-the-nut method does not appear to be a scientifically rigorous approach. Different grip lengths give different clamping forces when the nut is given one complete turn. The clamping force also differs with different batches of bolts. One may only expect a certain average clamping force by this method as all the bolts yield with elongation resulting from one full turn of the nut.

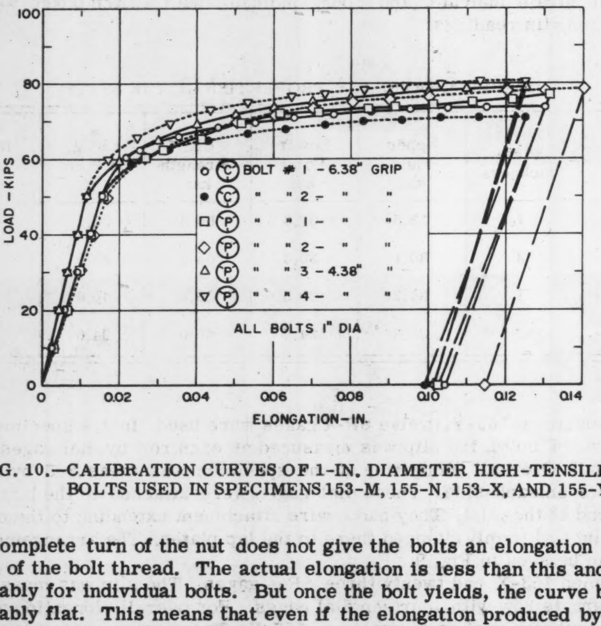

FIG. 10.—CALIBRATION CURVES OF 1-IN. DIAMETER HIGH-TENSILE BOLTS USED IN SPECIMENS 153-M, 155-N, 153-X, AND 155-Y

One complete turn of the nut does not give the bolts an elongation equal to the pitch of the bolt thread. The actual elongation is less than this and differs considerably for individual bolts. But once the bolt yields, the curve becomes considerably flat. This means that even if the elongation produced by turning the nut varies within 50% or more in this range, the clamping force varies by approximately 12.5% of the 0.2% yield value depending on the shape of the curve. In other words, once yielding occurred, variations in the angle of rotation of the nut would not influence significantly the clamping force.

Thus the average clamping forces are 72,500 lb for P bolts of 4.38-in. grip which were used for specimens 155-N and 155-Y; 70,000 lb for P bolts of 6.38-in. grip which were used for specimen 153-M, and 69,000 lb for C bolts of 6.38-in. grip which were used for specimen 153-X. The adoption of these average values seems to be consistent with the precision obtainable in the one-turn-of-the-nut method.

Data and Result of the Slip Test of the 80-Bolt Joints.—The two specimens had been previously tested by torquing the bolts to the required minimum bolt tension (3) and the results analyzed (7). The present second investigation was done in the same general manner except the bolts were tightened by the one-turn-of-the-nut method (6).

Slip Characteristics.

The General Development of Slip.—The joints slipped in the same general manner as when the bolts were tightened to the required minimum bolt tension (7), but apparently the higher clamping force reduced the slippage considerably for a given load. Figs. 11 and 12 show the averages of two slip gages on each gage line for specimen 153-M and specimen 155-N, respectively, at different loads. It was found (7) that the specimens 153 and 155 under required minimum bolt tension had their major slips at approximately 2,000 hips and 1500 kips, corresponding to nominal bolt shears of 15.91 ksi and 11.92 ksi, and coefficients of friction of 0.30 and 0.22. By the one-turn-of-the-nut method, specimen 153-M had its first major slip at a 2406-kip load, corresponding to a nominal bolt shear of 19.51 ksi, and a coefficient of friction of 0.215 whereas specimen 155-N showed no major slip at all within the capacity of the machine. The coefficient of friction for the first major slip of specimen 155-N is therefore greater than 0.207, at a nominal shear greater than 19.10 ksi.

Distribution of Slip Among Rows.—The rows of holes nearest the applied loads, as in the previous tests (7), began to slip earliest and also have maximum amounts of slip at any load (Figs. 11 and 12). This means that the applied load is picked up only by the two end rows of bolts at low loads, but is shared gradually by interior rows as the load increases. Based on the assumption that the fraction of load taken up by each row is proportional to the slip of that row, it is found that for specimen 153-M the distribution of load in rows is symmetrical with respect to the middle section at higher loads, while for specimen 155-N the distribution has never been symmetrical. No definite trend can be emphasized as the test covered only two specimens.

Major Slip.—At the first and only major slip that occurred in specimen 153-M, all rows of holes slipped about the same amount, on the order of 1/64 in. or one quarter of the clearance. Strain readings showed little change at the major slip. It is certain that the bolts were not yet in bearing at this stage. Previous tests of the same specimens (7) showed that the slip might have gone as far as 0.10 in. before all the bolts actually came into bearing.

Load Partition.

Load Partition in Individual Plates.—Comparison with the results of previous tests (7) show that the first row of bolts took up a greater percentage of load in the present test than in the previous ones.

The load partition computed from strain readings seems to be somewhat erratic and the partition based on uniform friction conforms better to that computed from slips. But for specimen 153-M the load partition based on strain is close to that computed on the assumption of uniform friction. Whether it is true that the longer the joint, the more uniform is the friction between plates, has yet to be ascertained by further tests. However, it should not be concluded that computation of load partition by slip is more reliable than computation of load partition by strain.

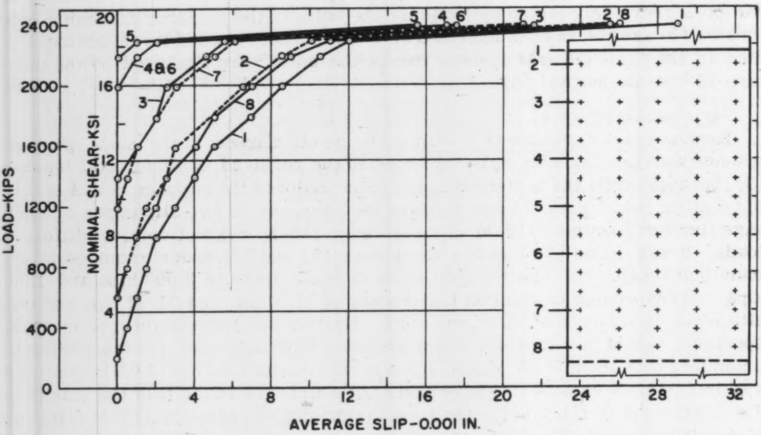

FIG. 11.—SLIP IN SPECIMEN 153-M

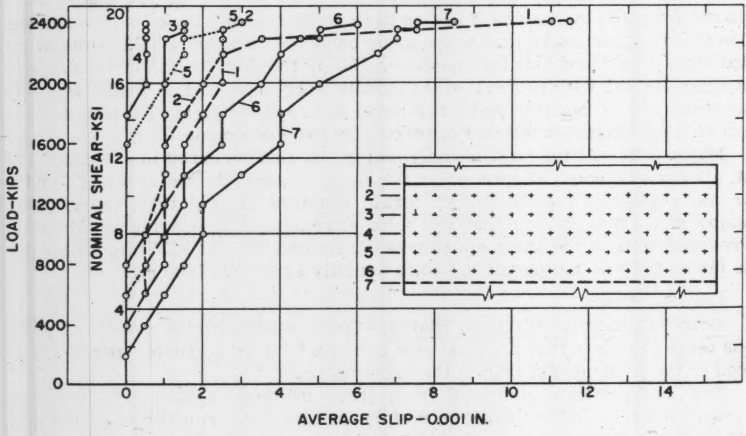

FIG. 12.—SLIP IN SPECIMEN 155-N

Distribution of Load in Two Lap Plates.—Slip and strain data show that the distribution of the applied load between the two lap plates may not be exactly equal. For specimen 153-M, the rear plate slipped slightly more than the front plate and consequently took less load than the front plate. Strain readings show this consistently. For specimen 155-N, the front plate slipped far less than the rear plate but jumped up at approximately 2,300-kip load. This was accompanied by a slight reduction of strains in most gages.

Slip and Strain on Unloading.—When the load was reduced from maximum to zero, the slips of most of the rows recovered somewhat, and the strain readings did not return to the original values. This means that the measured slip consists of not only a permanent slide between the plates but also an elastic deformation of the plate due to the applied load. Investigation of the slip and strain curves of specimen 153-M discloses a clear relation between the behavior of slip and strain on releasing the load. The apparent slips of the end rows evidently have a greater fraction resulting from elastic deformation than those of the middle rows have. The readings for end sections depart more from the original values on reducing the load than those for the middle sections do, the departure being positive for sections near one end of the plate and negative for sections near the other end.

Data and Results of Fracture Test of 27-Bolt and 30-Bolt Joints 153-X and 155-Y.

Slip Characteristics

The General Development of Slip.—The joint slipped in the same general manner as in the previous test. Figs. 13 and 14 show the averages of two slip gages on each gage line in the joints at different loads. The first major slip was noticed in specimens 153-X and 155-Y at loads of 999 kips and 742 kips, which correspond to a nominal shear of 23.6 ksi and 15.73 ksi and a nominal coefficient of friction of 0.268 and 0.170. Before the first major slip was obtained specimen 155-Y slipped a small amount at a load of 640 kips corresponding to a nominal bolt shear of 13.6 ksi and a nominal coefficient of friction of 0.146.

Distribution of Slip Among Rows.—In accordance with expectations, the rows at the ends (that is, rows nearest to the applied load) start slipping first and show the maximum slip at any stage. This can be seen in Figs. 13 and 14 for specimens 153-X and 155-Y. In specimen 155-Y, row 2 shows less slip than the middle row for a great length of time, and seems to be taking a minimum share of the load. Whereas in specimen 153-X the middle row shows no slip until there is a major slip in the whole specimen. It also shows minimum slip all the time. Specimen 153-X shows some symmetry in the distribution of load with respect to the middle row.

Strain Variations.—The strain under different loadings in the lap plates and in the center plate of specimen 153-X as measured by SR-4 gages can be seen in Fig. 15. Similarly, Fig. 16 gives strains in the lap plates and in the center plate of specimen 155-Y. These strain values can be interpreted as the average strains in the particular sections of the plates at the different loads. All strain gages that lie within the joint show consistently greater values of strains in sections that lie nearer to the applied loads. The gages which lie outside the first row of bolts however show a much smaller value of strain.

Load Partition.

Load Partition in Individual Plates.—The percentage of applied load present at different sections of the plates and the load transferred at each row of bolts

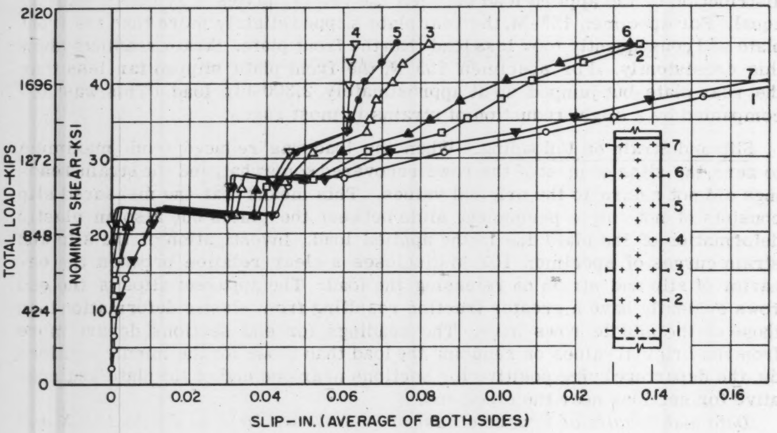

FIG. 13.—SLIP IN SPECIMEN 153-X

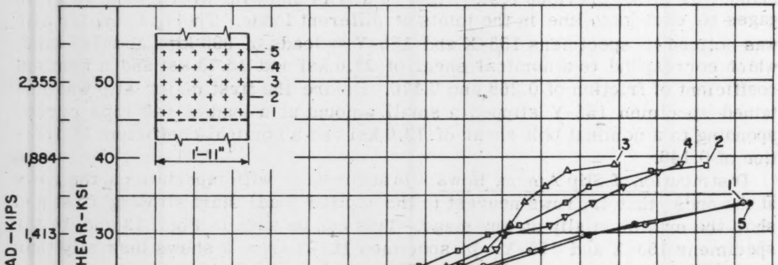

FIG. 14.—SLIP IN SPECIMEN 155-Y

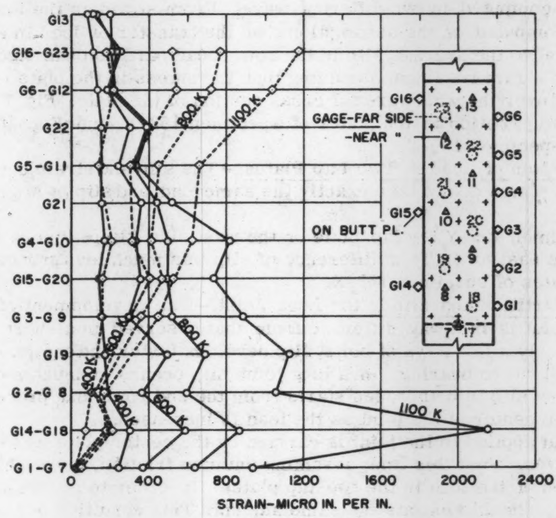

FIG. 15.—STRAINS IN PLATES OF SPECIMEN 153-X

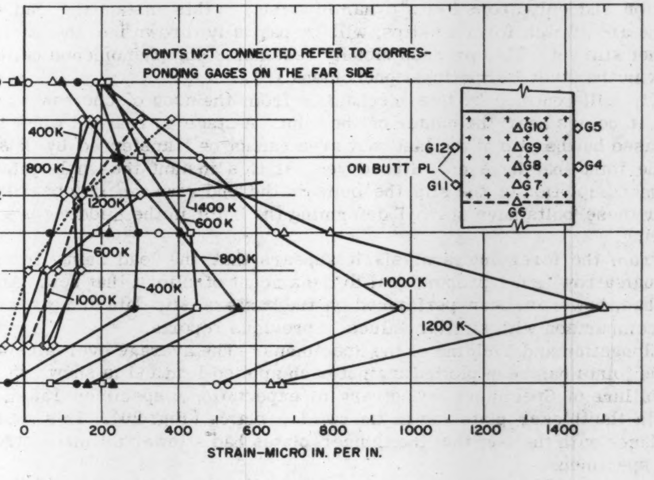

FIG. 16.—STRAINS IN PLATES OF SPECIMEN 155-Y

have been computed in two different ways. From slip data the load partition has been computed on the assumption that the transfer of load in each row is proportional to the average slip in the row. Load partition has also been computed from strain readings, assuming that the stress in the plate is uniformly distributed over the whole area of cross section of the plate. Fig. 17 shows the typical load partition in the plates of specimen 153-X, and Fig. 18 shows the same for specimen 155-Y.

Distribution of Load in Two Lap Plates.—The slip and strain data show that the two lap plates do not take exactly the same load, and slip by slightly varying amounts.

In specimen 155-Y the lap plate on the west side slipped more than the lap plate on the east side. This difference of slip was much less pronounced in the two lap plates of specimen 153-X.

Load Partition and Slip in the Long Joint.—The development of the slip in the long joint is in a way different from that observed in a short joint. In a joint with only a few rows of bolts, slip develops faster and one jerk may bring the bolts close to bearing. In a long joint slip occurs in much more distinct stages. The slip in both cases starts from the end rows and proceeds inward towards the center of the joint as the load is increased.

The load applied to the joint is carried by the center plate up to the edge of the lap plates. Past this line, assuming uniform friction, there should begin a distribution of the load to the two lap plates. In order to accomplish this the three plates should elongate the same amount. This condition obviously cannot prevail near the end of the lap plates because there the center plate carries full load while the lap plates carry only small load. Consequently slip between the plates is forcibly started as a result of the difference of strain between the center and the lap plates. This creates an area over which the coefficient of friction suddenly drops to its dynamic value. In this instant the load carried by the area which forcibly slips, will be partially thrown into the parts which did not slip yet. This process closely resembles the phenomenon called slip-stick in the study of frictional phenomena (8).

Slip will continue by this mechanism from the area of one row to another until it comes near the center of the joint. A stage is reached when the load released by the slip of the last part area cannot be transferred by those parts of the joint that have not slipped yet. At this instant the whole joint slips.

On completion of the slip the bolts in the end rows go into bearing first. After these bolts have started deforming the bolts in the middle rows go into bearing.

From the foregoing analysis it appears that the load being transferred through a row is not proportional to the amount of slip at that row. An analysis has, however, been performed on the basis of slip data and given here in for comparison with similar values in previous reports.

Elongation and Yielding of the Specimens.—The average over-all elongation of the joints has been plotted against each applied load and is shown on Fig. 19.

Failure of Specimens.—Contrary to expectations, specimen 155-Y did not fail in the thicker plate but in the two lap plates (Fig. 20). This was in accordance with the fact that the thinner plates had a lower ultimate strength in this specimen.

Specimen 153-X failed by shearing bear the bolts. At a load of 2,260 kips one end bolt in the bottom row sheared off. The load was dropped to observe

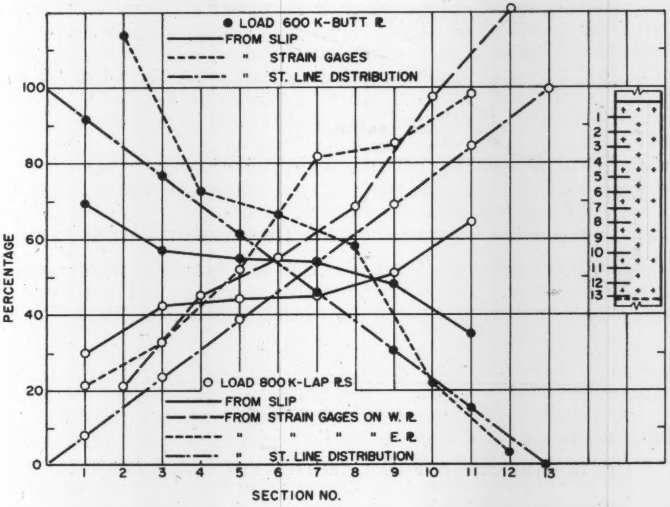

FIG. 17.—LOAD PARTITIONS IN 153-X COMPUTED ON VARIOUS ASSUMPTIONS

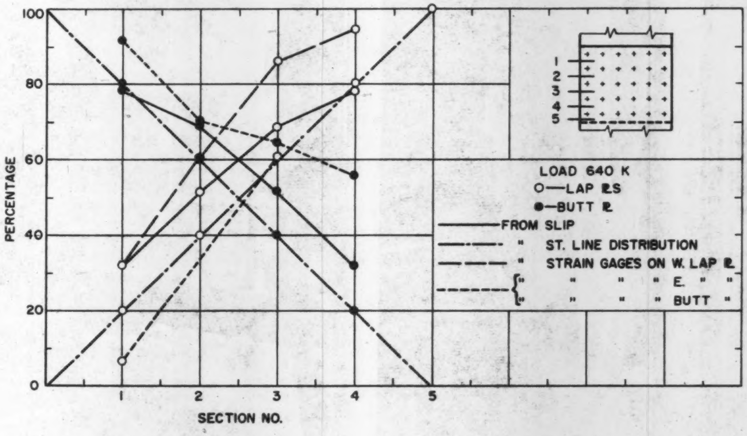

FIG. 18.—LOAD PARTITIONS IN 155-Y COMPUTED ON VARIOUS ASSUMPTIONS

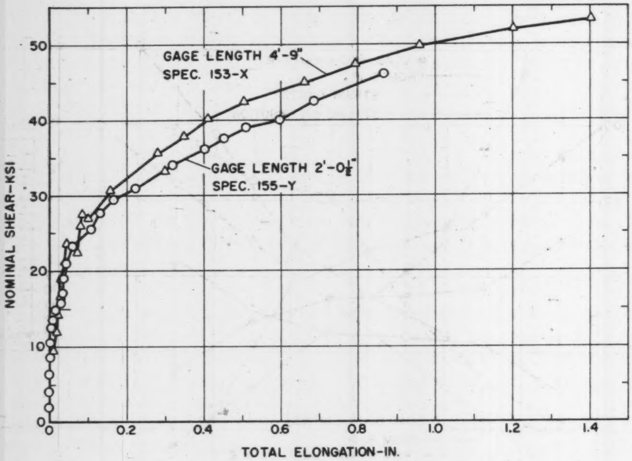

FIG. 19.—AVERAGE OVERALL ELONGATION OF SPECIMENS 153-X AND 155-Y

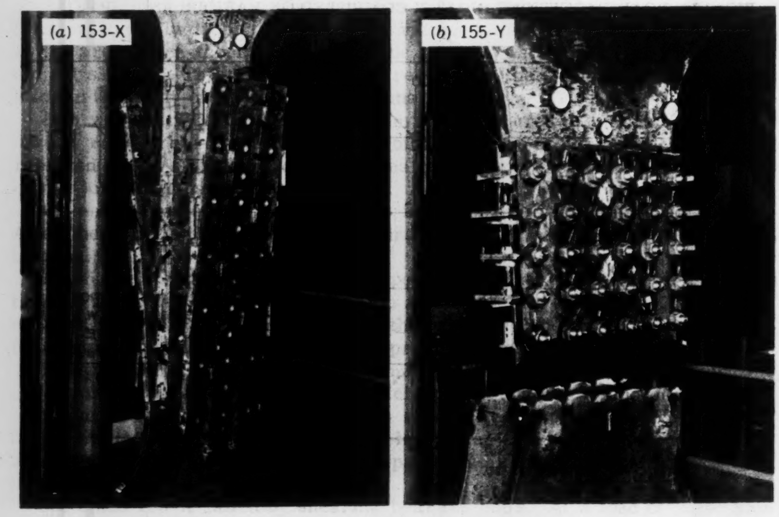

FIG. 20.—SPECIMENS AFTER TEST

what had happened. On increasing the load to 2,259 kips the two other bolts in the bottom row sheared off. The load was again dropped and on reloading after the observations two bolts in the top row and the one bolt in the second row from the bottom dropped off at a load of 2,248 kips. On reloading again the last bolt in the top row and the one bolt in the second row from the top sheared off at a load of 2,276 kips. After this all the remaining bolts sheared off at once.

Efficiency of Joint.—The efficiency of the joints 153-X and 155-Y has been computed in this report by the relative gage method (4). This method gives the efficiency of the joint when failure occurs in the plate. Specimen 153-X failed by shearing of bolts, therefore the efficiency computed herein does not check closely with its observed value. In specimen 155-Y failure occurred in the plates and the observed efficiency checks closely with the computed efficiency. The results of this analysis are the following:

Specimen 153-X had 2,276 kips observed and 2,401 computed ultimate load, 81% observed and 87% computed efficiency. Specimen 155-Y had 2,164 kips observed and 2,080 computed ultimate load, 83% observed and 79.6% computed efficiency.

Probability Test of C_6 Type Four-Bolt Joints.—In order to discover any effects of the one-turn-of-the-nut method of tightening the bolts on the nominal coefficient of friction, a special set of tests were run on four-bolt joints.

Preparation of Specimens.—The C_6 type specimens were made of ASTM A 7-51T steel plates, 1/2-in. and 1-in. thick. Thirteen double assemblies were made which provided specimens for twenty-six tests.

Tightening Bolts.—The bolts used for these small joints were 1-in. in diameter and 4-in. long, and were marked BIS on the head. The holes were of 17/16-in. diameter. One-half turn has been used since previous tests showed that the nuts will strip at approximately 3/4 turn, the grip being only 2 in. Calibration tests of the bolts showed that the full clamping capacity of the bolt is developed by one-half turn.

Test Procedure.—The ends of the assembled specimen were bolted to two prefabricated connecting pieces. The whole assembly was lifted to and fixed in the 300,000-lb testing machine. Two dials were used, one on each edge of the specimen to measure slip. Load was applied in 10-kip increments and the corresponding slip values taken until the evidence of bearing was noticed. The sudden drop of load indicated the occurrence of a major slip.

Test Data and Results.

General Development of Slip.—The joints slipped in the same general manner as when the bolts were tightened to the required minimum bolt tension (3) (9), but apparently the higher clamping force reduced the slippage considerably for a given load.

Fig. 21 shows the load-slip curves of all the twenty six C_6 type specimens. The average value of nominal bolt shear at which major slip occurred is 21.67 ksi, corresponding to an applied load of 136.2 kips and coefficient of friction of 0.284 when the bolt tension is 60 kips. Previous test results (3)(9) showed that under the minimum required bolt tension of 42.5 kips, major slip occurred in similar C_6 type joints at average nominal bolt shears of 13.8 ksi and 15.3 ksi corresponding to coefficients of friction 0.25 and 0.29; and under 52.5 kips bolt tension, major slip occurred at an average nominal bolt shear of 21.8 ksi corresponding to coefficient of friction 0.33. The value 21.8 ksi for 52.5-kip bolt tension seems to upset the general trend that major slip occurs at higher nominal shear value when bolts have higher tension. But this should certainly be attributed to the fact that only three specimens were tested under 52.5-kip bolt tension (9).

In the test of the four-bolt specimens, four different ways of slipping were noticed:

1. Slip started gradually, jumped suddenly at a certain load value forming a so-called major slip which was indicated by a sudden drop of load with or without an accompanying load report. Then slip increased gradually again as the load increased.
2. Slip progressed gradually all the way, no drop of load occurred within the load range.
3. Slip appeared in the same general way as described in item 1. Load dropped twice indicating two major slips.
4. Same as items 1 and 3, except load dropped three times indicating three major slips.

Three C_6 type specimens (No. 2, 9, and 10) were assembled with the center lines of the lap and butt plates inclined at a small angle of approximately $1\frac{1}{2}°$.

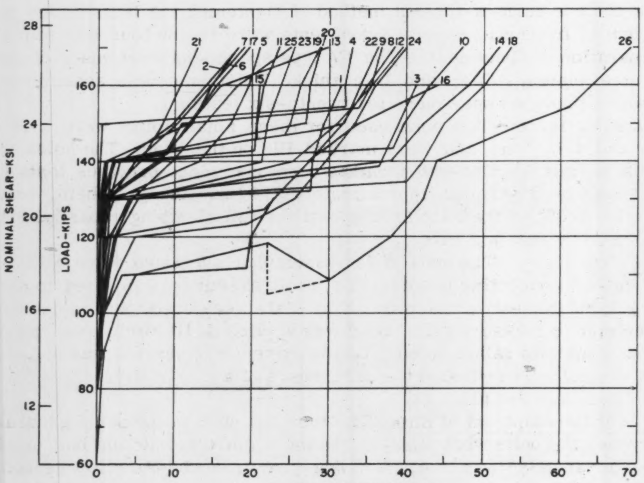

FIG. 21.—SLIP IN C_6 TYPE SPECIMEN S

No particular behavior in slipping can be attributed to the misalignment of the specimen so far as these few tests are concerned.

Amount of Slip.—The amount of major slips in the four-bolt joints varied from 1/10 to 1/2 the clearance, but the majority was around 1/64-in., or 1/4 the clearance. The maximum amount of slip (average the readings of two dials) at 170-kip load was 0.069-in. (Fig. 21), greater than the nominal clearance of the hole. Actually many joints had been in at least partial bearing after major slips occurred, but the reading on the slip dials continued to increase probably because the contacting parts of the metal were deformed.

Probability of Slip.—In all types of similar joints, there is always a certain range of load value within which slip will most probably occur. The probability analysis of slip for the C_6 type joints indicates that major slip is most likely to occur when the nominal bolt shear is between 22 ksi and 23 ksi.

STUDY OF NOMINAL COEFFICIENT OF FRICTION IN JOINTS

Sixteen reports from the universities of Illinois, Northwestern and Washington have been searched for data. An exhaustive study showed that the most important factor in determining the nominal coefficient of friction is the treatment of the faying surface. Twelve other factors have been considered, some of which proved to have no effect, some others have only minor effects on the coefficient of friction. In certain cases these effects are well definable. A statistical analysis has been applied where sufficient number of data could be found (10).

Apparent Coefficient of Friction in Joints Fastened by High Tensile Steel Bolts.

Object and Scope of Investigation.—The slip characteristics of the joints tested in various structural laboratories have been analyzed. This has been done with a view to investigating the factors which may have some influence on the value of the nominal coefficient of friction and if possible find the extent of such influence. Only the values of nominal or apparent coefficient of friction for the first major slip were analyzed. Joints tested under static loading have only been considered.

An effort has also been made to find by a statistical approach the lack of control in the estimation of the coefficient of friction in order to enable one to determine its safe value. In many cases the number of joints of a particular type tested is so small that a statistical approach cannot be used successfully.

Definition of Terms.—The term coefficient of friction of spliced materials as used herein is the nominal value found by dividing the total load on the joint at the first major slip by the total clamping force of all the bolts multiplied by the number of slipping planes in the joint. For example, a double lap joint would have two slipping planes while a single lap joint would have only one slipping plane. This definition is based on the most conventional concept of friction and it is understood that it does not perfectly describe the complex phenomena resulting in measurable slip in a joint. This measured slip results, in part, from deformations of the joined plates and in part from their actual relative motion. The two types of slip are interrelated and their selection would neither be practicable nor practical. Observations made on large joints (6)(7) indicate that the first slip measured during the test of a joint is mainly the result of combined causes and only the so-called first major slip is unequivocally a slip in which the whole of the joined plates take part in the motion.

The term first major slip refers to the first such relative motion of the joined plates, in which one whole plate unmistakably takes part. This is represented on graphical presentations of slip-force curves as a definite horizontal portion. On larger joints gages in all positions simultaneously indicate such slips. This first major slip might be the one which brings all or part of the connectors into bearing. Defining the nominal coefficient of friction in connection with this first major slip seems to provide it with more definite technical meaning.

Method of Analysis.—A list was prepared of all the specimen joints that were relevant to this report and the properties of these joints and their slip characteristics were recorded. This led to such an accumulation of data which cannot be presented herein, but which is available elsewhere (10).

The conclusions of each progress report were also studied. This was done in order to enable the selection of the factors influencing the coefficient of friction of a joint from the factors that did not definitely influence it.

The significance of each factor affecting the value of the nominal coefficient of friction was then studied. These factors were then chosen as variables and a tabulation was made of all the joints similar in respect to all variables but one.

The statistical analysis followed the practice of using frequency charts and control diagrams to study the lack of control in the values of the coefficient of friction. The available tests were used in three different groups for this approach. This was done in order to arrive at a probable value that can be recommended for the coefficient of friction.

Factors Affecting Friction.—Any factor affecting the first major slip in a joint necessarily reflects in the value of the nominal coefficient of friction. Some factors seem to have a more definite effect than others, thus it is in order to group them as follows:

Factors that Seem to Affect Significantly the Coefficient of Friction

Condition of Faying Surface.—From the laws of friction it directly follows that the coefficient of friction depends on the roughness of the surface. Consequently the condition of faying surface makes all the difference in the value of the nominal coefficient of friction. It is the most important factor (9)(11)(12)(13)(14)(15).

Bolt Tension.—It has been stated (11) that the nominal coefficient of friction is independent of the clamping force of the bolts. This seems in line with the generally known laws of friction. It has also been stated (16): "The coefficient of friction was independent of the clamping force of the fasteners, provided the tensile stress on the net cross-section area did not exceed approximately one-half of the upper yield point stress of the plates in the joint." Which means that beyond a particular value of bolt tension the design is governed by the net area in tension. Due to stress concentration the plate near the bolt holes yields at a stress in the net section corresponding to half the value of the upper yield point.

In view of this consideration the nominal coefficient of friction in a joint made by high tensile bolts can be affected by bolt tension (12)(13).

Tension: Shear Ratio.—The tension: shear ratio seems to have an effect on the nominal coefficient of friction. This is probably due to the fact that a greater stress in the net section reduces the clamping force in the bolts due to Poisson's ratio effect and also causes the plate to yield earlier near the bolt holes (12)(13).

Type and Size of Joint.—The results of the tests (6)(7)(9)(13) seem to show that the type and size of joint have some influence on the nominal coefficient of friction. In the lap plate joint probably slight bending occurs and friction is called on only to take a component of the total load (13). In the case of joints with several rows, the end rows slip first.

Duration of Load.—A tentative conclusion (13) shows that duration of load has an effect on the value of the nominal coefficient of friction. This can also be seen from results of tests. Sustained load probably creates some creep along the surfaces in contact making them smoother (12).

Misalignment of Holes.—Misalignment of holes can affect the nominal value of the coefficient of friction because some bolts may be in bearing (fully or partly) to start with. Unless the plate or the bolt deforms at that place, slip will not occur.

Temperature in the Case of Painted Surfaces.—The paints harden at low temperatures and show greater resistance to slip. But this seems to be of no practical importance as the strength is again lost as temperatures rise (2).

Factors that Seem to Have no Significant Effect on the Coefficient of Friction.

Size of Faying Area.—The area of surfaces in contact has no effect on the value of the nominal coefficient of friction. This result also seems to be in line with the laws of friction (11)(12).

Thickness of Lap Plates.—The thickness of lap plates seems to have no effect on the value of the nominal coefficient of friction as long as the average stress in the lap plate does not exceed 60% of the tensile yield point of steel. The effect of this variable is probably negligible because the reduction of bolt tension due to diminishing of the thickness of the plate on account of Poisson's ratio effect is negligible. But it possibly becomes more effective when the portion of the plate near the bolt hole yields (12).

Clearance in Bolt Holes.—There appears to be no effect due to the clearance in the bolt holds on the nominal coefficient of friction as long as the bolts are not in bearing to start with (12).

Type of Loading (Tension or Compression).—It has been noted (16) that there seems to be some effect of the type of loading on the value of the nominal coefficient of friction; but this has been contradicted elsewhere (12). Probably the effect, if any, is due to the Poisson's ratio effect in the plate.

Bolt Grip.—It has been stated (9) that the length of the grip does not seem to have any influence on the coefficient of friction. In other conclusions (17), no mention has been made of any influence of the bolt grip, nor do the results show any great effect of this factor.

Effect of Various Factors on Nominal Coefficient of Friction

Condition of Faying Surface.—Many groups of joints have been tested which were similar in all respects except in the condition of their faying surface. A list of all the specimens which fall in this group can be found (10).

In general it is evident that any kind of paint tends to act as a lubricant and reduces the coefficient of friction. The value of the nominal coefficient of friction seems to be rather small in the case of surfaces painted with red lead and varnish. The values of the nominal coefficient of friction in the case of lacquered surfaces show a particular behavior. In one of the series of tests a specimen with lacquered surface showed greater coefficient of friction than similar specimens with mill scale surfaces. Sand blasting seems to make the surfaces rough and increases the coefficient of friction.

In general, mill scale surfaces from which loose scales have been removed seem to show a reasonable roughness of the surface and a greater nominal coefficient of friction. This means that if the surfaces cannot be made rough then at least no kind of paint should be used on their faying surfaces.

The faying surface treatments are listed as follows in the order of decreasing coefficient of friction using average values:

1. Rusted and wire brushed (0.51).
2. Rusted (0.48).
3. Sand blasted (0.47).
4. Mill scale (0.30).
5. Lacquered (0.28).
6. Galvanized (0.26).
7. Aluminum suspension paint (0.17).
8. Varnished (0.14).
9. Rust prevention paint (0.11).
10. Black graphite paint (0.09).
11. Red lead (0.065).

To these the following can be added from more recent tests:

a. Mill scale, flame cleaned and wire brushed (0.43).
b. Read lead, sand blasted (0.42).
c. Red lead, plates assembled wet (0.31).
d. Red lead, flame cleaned (0.22).
e. Second coat of red lead on a dry one, assembled wet (0.10).

Because only two specimens of each kind were tested, the results should not be attributed the same weight as attributed to the first enumerated ones.

Bolt Tension.—The data which have been used to study the effect of bolt tension on the coefficient of friction fall into two groups, one with tension: shear ratio of 1:0.94 and the other with tension: shear ratio of 1:0.75. They indicate that the value of the nominal coefficient of friction is fairly constant up to a certain range of bolt tension. When the bolt tension is increased beyond a particular value the value of the nominal coefficient of friction decreases as indicated.

It may be reasonable to infer from this that the value of the nominal coefficient of friction decreases at higher values of bolt tension. This decrease is of the order of approximately 0.07 which is not of such magnitude as to call for the limiting of the value of bolt tension.

Tension: Shear Ratio.—Five groups of tests have been used to find the effect of the tension: shear ratio.

Only test groups which consist of several tests were included in the plots. It is noticeable that as the tension: shear ratio increases the increase in the nominal coefficient of friction is somewhat steeper at first and tends to level off. The increase is of the order of approximately 0.06.

Type and Size of Joints.

Joints with Two or Three Bolts.—A survey of the slip characteristics of lap and butt joints fastened by two or three bolts having an average bolt tension of 35 kips showed that the values of nominal coefficient of friction vary from 0.18 to 0.60 which seems to be a rather large variation. These variations may be due to the fact that the number of bolts and size of joints is too small to average out any variations in the condition of surface, the actual tension achieved in the bolt, or any other possible reason. This also seems to be a reason to be more conservative in estimating the coefficient of friction in the smaller joints.

Joints with Four or Six Bolts.—The ninety-two joints tested with four or six bolts show an average coefficient of friction of about 0.31 ranging from a minimum of 0.18 to a maximum of 0.45. In this case, though the average value is lower than in the smaller joints, there is not a great variation.

If one considers the fifty-one joints with four to eight bolts having an average bolt tension of 42.5 kips one finds the average value of nominal coefficient of friction as 0.337 with a minimum of 0.22 and a maximum of 0.45, which is an even lesser variation.

Twenty-six joints tested with four bolts each and having an average bolt tension of 60 kips show an average value of nominal coefficient of friction of 0.284, a minimum of 0.233 and a maximum of 0.322, this is a still smaller variation.

Joints with Twenty Bolts or More.—Six joints assembled with twenty to thirty bolts show an average value of nominal coefficient of friction of 0.22, a minimum of 0.17, and a maximum of 0.30.

Five joints assembled with eighty bolts show an average value of nominal coefficient of friction of 0.23, a minimum of 0.21, and a maximum of 0.30.

Summing the approximate values of average coefficient of friction in connection with the number of bolts in the joint:

Two or three bolts, average 0.45 (0.18 to 0.60)
Four to six bolts, average 0.31 (0.18 to 0.45)
Twenty and more bolts, average 0.22 (0.17 to 0.30)
Eighty bolts, average 0.23 (0.21 to 0.30)

Effect of Size.—The number of joints tested having less than four bolts or more than four bolts is small to draw any definite conclusions. The average value of the nominal coefficient of friction seems to decrease with the size of joints as does the range between the minimum and maximum values of the nominal coefficient of friction. If one studies the joints with four to six bolts it is found that there is less lack of control of the value of nominal coefficient of friction in joints having higher bolt tension. All the large joints tested have an average bolt tension of 42.5 kips or greater. All the joints tested with two or three bolts have a bolt tension of 35 kips.

Effect of Shape of Joint.—Joints in which the number of rows is more than four times the number of bolts in each row seem to have a small value of nominal coefficient of friction. Three joints (9) having ten rows of bolts with two bolts in each row show an average value of nominal coefficient of friction of 0.22, a minimum of 0.21, and a maximum of 0.23. One joint with thirteen rows of bolts having alternate rows of one and three bolts showed a coefficient of friction of 0.17.

Duration of Load.—The data on the effect of sustained loading indicate that there is a 20% decrease in the value of the nominal coefficient of friction when tested under such conditions. The observation is based only on a single specimen. However, this would mean that the value of the coefficient of friction should be estimated with care when used in connection with sustained loading.

Statistical Analysis

Selection of Joints.—It was found that the most important factor affecting friction is the type of faying surface. The variation in the value of coefficient of friction becomes so great with the change of faying surface that it does not seem reasonable to group joints with different types of faying surfaces for statistical treatment. The generally accepted practice is to make joints with members having mill scale surfaces. Joints with mill scale faying surfaces give us the most reasonable average values of coefficient of friction. The available data seem to justify a statistical treatment of these joints only.

Analysis of All Joints Having Mill Scale Surfaces.—An analysis was made of all the 127 joints tested under short time static loading in tension having mill scale surfaces. The cumulative frequency distribution curve for the coefficient of friction as observed in these joints show a considerable variation in the value of coefficient of friction. The value that occurs most frequently, or the mode, is 0.31 as can be found on a frequency hystogram. The central value (or arithmetic mean) of the coefficient of friction is 0.3128.

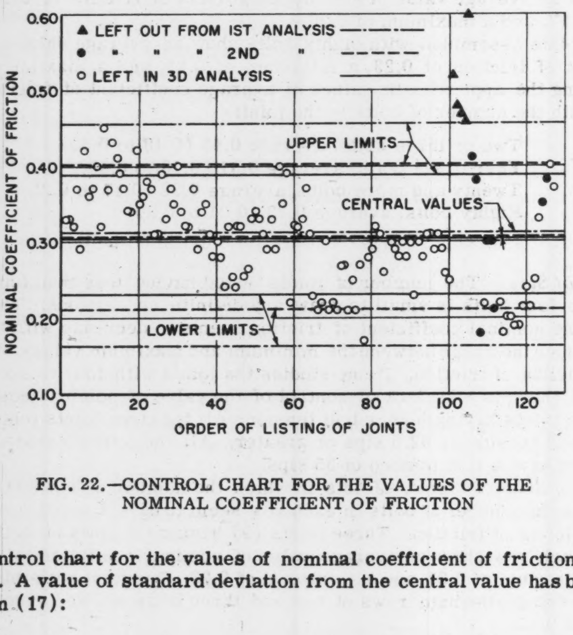

FIG. 22.—CONTROL CHART FOR THE VALUES OF THE NOMINAL COEFFICIENT OF FRICTION

The control chart for the values of nominal coefficient of friction is shown in Fig. 22. A value of standard deviation from the central value has been computed from (17):

$$\sigma = \frac{\sum_{i=1}^{n} X_i^2}{n} \quad \ldots\ldots\ldots\ldots\ldots\ldots \quad (1)$$

in which σ is the standard deviation, X denotes the central value, X_i is the value for joint i, and n presents the number of joints.

The value of σ was found to be 0.05. If one draws a line parallel to the line representing the central value at a distance of 3 σ in Fig. 22 one gets 0.1628 as the lower limit for the value of coefficient of friction. According to probability analysis this means that there is one chance in approximately 374 that there can occur a value lower than 0.1628 for the coefficient of friction.

Analysis of All Joints with Mill Scale Surfaces Omitting Four Joints.—In order to arrive at a more reasonable value, a second analysis was made omitting four joints with two or three bolts having the value of coefficient of friction greater than 0.45. These values were considered too high to deserve the weight given to them by this method of analysis. Moreover one is more concerned with low values than with high ones.

The central value of coefficient of friction for the rest of the 123 joints was 0.3062. The standard deviation was found to be 0.0316 which gave 0.2114 as the value for the lower limit for the coefficient of friction (Fig. 22).

CONCLUSIONS

The results of the three facets of the presented investigation allow the formulation of several conclusions.

Effect of Misaligned Holes.—The tests of specimens in which the misalignment extended over two rows of bolts did not reveal any significant effect on the ultimate strength or efficiency. The ultimate strength and efficiency of joints of a single row of bolts, in which only one outside hole was misaligned, showed slight decrease of both ultimate load and of efficiency.

Effect of Punched Holes.—The ultimate strength, efficiency, elongation, and strain-energy absorption of the joints with punched holes at room temperature were definitely less than those with drilled holes. Ultimate strength and efficiency were decreased approximately 10%; elongation and strain-energy absorption, 40%.

Effect of Painted Faying Surfaces.—Red lead paint on the faying surfaces was found to have definite effect on the friction developed between the faying surfaces at room temperature. The specimens with painted faying surfaces began slipping at approximately one-third the working load (working load was taken to be that load which produced an average shear on the gross area of the bolts of 15,000 psi). The specimens with unpainted mill scale faying surfaces did not slip until after the working load had been reached. At -24°F, however, the red lead painted faying surfaces developed practically the same friction as the unpainted mill scale. However this does not seem to have any noticeable effect on the efficiency of the joint.

Effect of Low Temperature.—At -24°F the joints failed with a brittle fracture. At this temperature the fractures were 100% cleavage with almost negligible plastic deformation. Although the ultimate strength and the efficiency of the joints were decreased only 25%, the elongation and the strain-energy absorbed were decreased approximately 80%.

Low temperatures did have one beneficial effect on the specimens: Even though the faying surfaces were painted with red lead, the joints did not slip until the working load had been reached.

One-Turn-of-the-Nut Method

1. The one-turn-of-the-nut method of tightening the bolts reduces the slip in bolted joints appreciably by providing higher clamping forces to the plates.
2. For joints tightened by the one-turn-of-the-nut method, the length of grip of the bolts plays an important part in the slip characteristics of the joints.

3. The nominal coefficient of friction for first major slip seems to be lower in joints tightened by the one-turn-of-the-nut method than in joints tightened by the required minimum bolt tension. Nevertheless, due to the higher clamping force, the load which will produce slip is also higher.

4. The partition of the load in joints tightened by the one-turn-of-the-nut method is similar to that tightened by the required minimum bolt tension.

5. The efficiency computed by a proposed formula (4) agreed closely with the experimental value in specimens with bolts tightened by the one-turn-of-the-nut method, even though the formula would not strictly apply to the one in which the bolts sheared.

Coefficient of Friction.

1. The most important factor in determining the value of the coefficient of friction in a bolted joint is the condition of the faying surfaces.

2. Factors reducing the coefficient of friction are: Increasing bolt tension, decreasing tension: shear ratio, increasing size of the joint, increasing number of bolts in the joint, and sustained loading.

3. In statistical terms, the lack of control increases with decreasing size of joint and decreasing number of bolts.

APPENDIX.—REFERENCES

1. "Slip of Joints under Static Loads," by R. A. Hechtman, A. G. Young, J. M. Chin, and J. M. Savikko, Proceedings, ASCE, Vol. 80, No. 484, September, 1954.

2. Sixth Progress Report on the Behavior of Bolted Joints with Misaligned Punched Holes and Painted Faying Surfaces at Room and at Subzero Temperature," by R. B. Madison and D. D. Vasarhelyi, Research Council on Riveted and Bolted Structural Joints, Univ. of Washington, Seattle, June, 1956.

3. "Specifications for Assembly of Structural Joints Using High Strength Steel Bolts," Amer. Inst. of Steel Construction, Ind. Fasteners Inst., February, 1954.

4. "The Efficiency of Riveted Structural Joints," by F. W. Schutz and N. M. Newmark E.E.S. Structural Research Series No. 30, Univ. of Illinois, Urbana, September, 1952.

5. "Ninth Progress Report Research Council on Riveted and Bolted Structural Joints," by S. Y. Beano, and D. D. Vasarhelyi, Univ. of Washington, Seattle, January, 1958.

6. "Seventh Progress Report on the Tests of Large Bolted Joints Tightened by the One-Turn-of-the-Nut Method," by Z. A. Lu, D. D. Vasarhelyi, and U. C. Vasishth, Research Council on Riveted and Bolted Structural Joints, Univ. of Washington, Seattle, January, 1957.

7. "Fifth Progress Report on Slip of Structural Steel Double Lap Joints Assembled with High Strength Steel Bolts," by R. A. Hechtman, T. R. Flint, and P. L. Koepsell, Research Council on Riveted and Bolted Structural Joints, Univ. of Washington, Seattle, February, 1954.

8. "Frictional Phenomena," by A. Gemant, Chemical Pub. Co., Inc., Brooklyn, N. Y., 1950.

9. "Fourth Progress Report on Slip of Structural Steel Double Lap Joints Assembled with High Strength Bolts," by P. L. Koepsell, H. L. Payne, and R. A. Hechtman, Research Council on Riveted and Bolted Structural Joints, Univ. of Washington, Seattle, February, 1954.

10. "Eighth Progress Report on a Study of the Nominal Coefficient of Friction in Structural Steel Joints Fastened by High Tensile Bolts," by U. C. Vasisth and Z. A. Lu, Research Council on Riveted and Bolted Structural Joints, Univ. of Washington, Seattle, June, 1957.

11. "First Progress Report on Slip of Structural Steel Double Lap Joints Assembled with High Strength Bolts," by D. R. Young, R. A. Hechyman, Research Council on Riveted and Bolted Structural Joints, Univ. of Washington, Seattle, January, 1951.

12. "Third Progress Report on Slip of Structural Steel Double Lap Joints Assembled with High Strength Bolts," Research Council on Riveted and Bolted Structural Joints, Univ. of Washington, Seattle, January, 1953.

13. "Static Tests of Bolted and Riveted Joints," by D. T. Wright, Univ. of Illinois, Urbana, January, 1952.

14. "Laboratory Tests of Structural Joints with Over-Stressed Steel Bolts," by J. R. Fller and W. H. Munse, Progress Report, Univ. of Illinois, Urbana, January, 1953.

15. "Static Tests of Riveted and Bolted Lap Joints," by M. A. Cayci, W. H. Munse, and W. M. Wilson, Progress Report, Univ. of Illinois, Urbana, December, 1949.

16. "Second Progress Report on Slip of Structural Steel Double Lap Joints Assembled with High Strength Bolts," by A. G. Chin, and R. A. Hechtman, Research Council on Riveted and Bolted Structural Joints, Univ. of Washington, Seattle, January, 1952.

17. "Results of Static and Fatigue Tests of Riveted and Bolted Joints Having Different Lengths of Grip," by F. Baron and E. W. Larson, Jr., Progress Report, Northwestern Univ., Evanston, Ill., January 2, 1952.

18. "Comparative Tests of Structural Joint Connected with High Strength Bolts and a Structural Joint Connected with Rivets and High Strength Bolts," by J. W. Carter, J. C. McCalley, and L. T. Wyly, Amer. Ry. Engrg. Assn., Bulletin 517, September-October, 1954.

19. "Laboratory Tests-High Tensile Bolted Structural Joints," by W. H. Munse, D. T. Wright, and N. M. Newmark, presented at the Centennial Convocation at Chicago, Univ. of Illinois, September, 1952.

20. "Effect of Grip upon Fatigue Strength of Riveted and Bolted Joints," by Frank Baron and E. W. Larson, Jr., Second Progress Report to Committee Members, Project No. 5, Research Council of Riveted and Bolted Structural Joints, Northwestern Univ., Evanston, Ill., January, 1951.

21. "Effect of Repeated Loadings in Structural Connections with High Strength Bolts," by W. S. Beam and W. H. Munse, Progress Report, Univ. of Illinois, Urbana, January, 1955.

22. "The Testing and Inspection of Engineering Materials," by H. E. Davis, G. E. Troxell, C. T. Wiskocil, McGraw-Hill Book Co., Inc., New York, 1955.

INSTALLATION AND TIGHTENING OF BOLTS

By Ethan F. Ball,[1] F. ASCE, and J. J. Higgins[2]

With Discussion by Messrs. Alfred Zweig; M. Zar; William H. Munse; Raymond Archibald; and E. F. Ball and J. J. Higgins

SYNOPSIS

This paper describes the procedures which have been used to be certain that high-strength bolts are installed and tightened to produce the minimum bolt tension required by specifications. It outlines the studies and tests that have been made to develop a safe, practical, and economical method of bolt tightening. Details of procedures are described and illustrated.

INTRODUCTION

The use of high-strength steel bolts as permanent fasteners for structural steel joints has become general only since the formation of the Research Council on Riveted and Bolted Structural Joints in 1947, and the publication of specifications approved by the Council in 1951. However, the use of heat-treated carbon bolts, torqued to a high tension, is not new. Many contractors used such bolts for temporary erection purposes in the 1930's, and have continued to use them in erecting all structures of any magnitude since the building of the Golden Gate Bridge in San Francisco, Calif.

The determination of the number of heat-treated bolts required in a stress-carrying joint was based on shear values approximately 50% greater than those permitted for rivets of the same diameter. It is also of interest to note that washers of ordinary carbon steel, not heat-treated, were utilized in the operations, and the nuts used were standard size, not heavy and not heat-treated.

Fig. 1 shows a bridge joint fitted up not only for riveting, but also for carrying erection loads; this is a joint in the New Orleans Bridge across the Mississippi River. The one side of the diagonal member connection shown has 149 holes for fasteners and there are 50 pins and an equal number of bolts to hold the joint which, in this case, is sufficient for fitting-up purposes and for

---

Note.—Published essentially as printed here, in March, 1959, in the Journal of the Structural Division, as Proceedings Paper 1974. Positions and titles given are those in effect when the paper or discussion was approved for publication in Transactions.

[1] Chf. Engr., Fabricated Steel Constr., Bethlehem Steel Co., Bethlehem, Pa.

[2] Supervisor of Erection Tool Houses and Safety, Fabricated Steel Constr., Bethlehem Steel Co., Bethlehem, Pa.

carrying load encountered during erection. While this joint was eventually riveted, it is similar to one using A-325 bolts as permanent fasteners. The temporary bolts shown are high-strength with regular pattern nuts and mild steel washers.

TIGHTENING

In the period before the founding of the Research Council, no attempt was made to attain any precise amount of minimum tension or clamping force in the bolts. The bolts were tightened with impact wrenches and operators were instructed only to make certain that they were really tight, with the joint material in contact.

With the development of the specifications for using bolts in permanent connections, engineers became interested in more precise methods of obtaining the required tension in the bolts. The specifications state the minimum tension necessary to obtain clamping power, but do not require any specific method to be used to attain the tension. Some erectors have used hand-torque wrenches alone for tightening. Others tightened with impact wrenches and checked with hand-torque wrenches. It was soon recognized by various experimenters that the approximate torque values given in the specifications are not reliable measures of the tension in the bolts. The torque required varies with the lubrication used on the bolts, and with small differences in the threads of bolts and nuts. Hand-torque wrenches have to be calibrated for each lot of bolts at each application to determine the correct torque-tension ratios for that application.

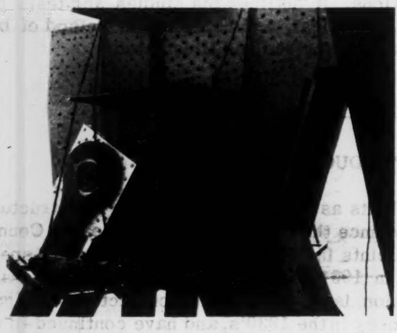

FIG. 1.—BRIDGE JOINT FITTED UP FOR RIVETING

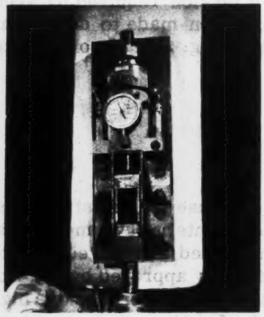

FIG. 2.—HOLLOW-RAM CALIBRATING DEVICE

It soon became apparent that bolts must be tightened with impact wrenches for reasons of economy and practicability. After tightening to a degree governed by the intuition of the skilled operator, a certain percentage of the bolts were checked with calibrated torque wrenches. Bolts were re-torqued or replaced when checks proved unsatisfactory. This method worked, but it placed a premium on the use of skilled operators who were accustomed to the "feel" of bolts when they had attained proper tension.

The next method developed was the use of calibrated impact wrenches. This method required the maintenance of a constant air pressure, adjusted to stall the wrench when proper tension was reached. The correct air pressure was determined by testing wrenches periodically on the job with a calibrating device. The calibrating device in Fig. 2 consists of a hollow ram hydraulic jack of 60-ton capacity. The yoke which pulls against the ram is guided by a substantial frame which bears against the cylinder, and by torquing a bolt held between the yoke and bottom face plate, the jack is energized by the stress in the bolt. A hydraulic gauge, reading total load, indicated the bolt tension directly. A similar device is shown in Figs. 3 and 4.

The calibrated-wrench method was used to tighten several million high-strength bolts throughout the United States and was successful because fewer skilled men were required to do the work. It proved to be economical and practical when the bolts on a job were primarily of the same diameter and approximately the same length, thus requiring the same air pressure. However, it became quite impractical for joints requiring different size bolts which meant additional wrenches, with different air pressures. One joint in a modern multistoried building may demand four or even five sizes of bolts, from 3/4 in. diameter to 1¼ in. diameter. Each size of bolt would need a separate impact wrench calibrated to stall at some determined air pressure. The complexity of using so many wrenches with so many air pressures at a single joint is increased by the need of having still more air hoses carrying air at the higher pressure necessary to ream out holes, cut out shop rivets, chipping, etc. Manifestly some other method of tightening had to be developed.

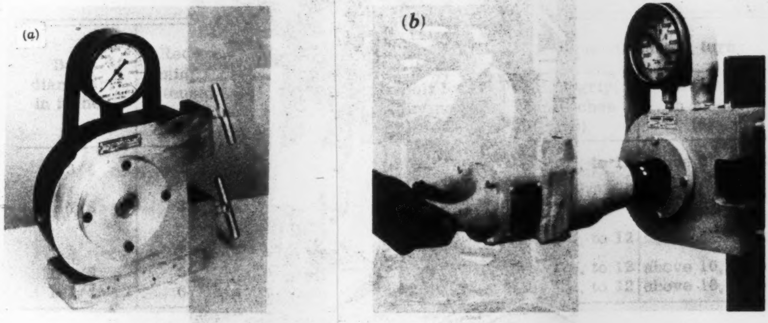

FIG. 3.—CALIBRATING DEVICE

It was realized, even when the method of calibrating impact wrenches and doing a satisfactory job, that something had to be done to reduce the amount of equipment needed. It was felt that one of the most promising developments would be a method of torque control which would permit operation at any air pressure, preferably 100 psi or more, to eliminate the need for a separate air line for other operations. An adjustable friction clutch device was developed that could be applied to the impact wrench between wrench and socket. The clutch could be adjusted to slip at prescribed torques and would hold its adjustment fairly well. However, it added weight to the power tool and its size prevented use in close quarters, both of which made it undesirable.

The air-tool manufacturers also studied the problem and finally developed a built-in torque control which would shut off the air pressure at specified torques. The adjustment or settings still had to be made experimentally and checked daily with a calibrating device. This tool worked fairly well, but in no way helped with the growing and larger problem of joints having several sizes of bolts, or with another problem which presented itself when bolt heads had to be tightened instead of nuts. Since these torque-control tools measure torque, and it requires far more torque to properly tighten a bolt from the head than it does from the nut end, it was clear that torque did not provide the measure of tension needed.

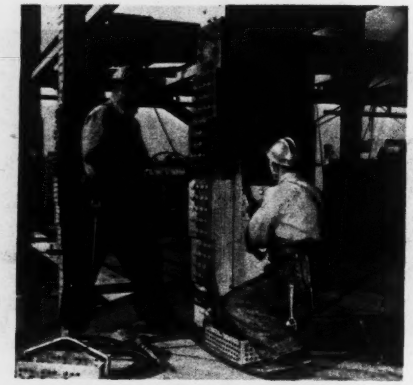

FIG. 4.—ADJUSTABLE FRICTION CLUTCH

It was obvious that a measure of tension other than torque was needed to do a good job, and that there must be developed a more foolproof, as well as more practical, method of bolting.

While contractors were searching for a more practicable method of tightening, the American Association of Railroads (A.A.R.) was trying to find a reliable way to tighten bolts at remote locations, without power tools, and using unskilled labor. In 1954, E. J. Ruble, F. ASCE, conducted a large number of tests to determine if the number of turns of the nut could be used as the criterion for bolt tension.[3,4]

---

[3] Amer. Ry. Engrg. Assn. Bulletin, Vol. 56, No. 520, January, 1955.

[4] "Tightening High-Strength Bolts," by F. P. Drew, Proc. Paper No. 786, ASCE, Vol. 81, 1955.

Ruble's tests covered bolts ranging from 5/8 in. to 1-1/8 in. in diameter using laminated material drawn up tight with A-325 bolts used as fitting-up bolts. He found, for all diameters, that one-half turn from a finger tight position produced the minimum bolt tension required by specifications. He also found that two to three turns were required to break the bolt or strip the threads. He recommended that bolts be given one full turn of the nut from finger tightness in order to be above the minimum tension required. In 1955, the Research Council, in Appendix B to the specifications, approved one turn of the nut from hand-tight position as a satisfactory method of tension control. In all of the foregoing the turns are measured from the finger or hand-tight position after the steel surfaces have been drawn together with fitting-up bolts.

This one-turn method was tried but it was soon found to be impractical to use finger or hand tightness as a reliable starting point for measuring the amount of turn. Because of the effect of dents and dirt accumulating in threads, experience proved it was difficult and time consuming to determine the hand-tight position. Furthermore, steel erectors objected to tightening bolts by hand when they had impact wrenches available to do the work. The need for establishing a better starting point for final stressing was clearly indicated. It was also evident that all tightening should be done with impact wrenches for practical reasons.

TABLE 1.—REQUIRED NUT TURN

Bolt diameter, in inches (1)	Required minimum tension, in pounds[a] (2)	Torque at least $\frac{1}{2}$ turn		Torque at least $\frac{3}{4}$ turn	
		Bolt grip, in inches (3)	Bolt length, in inches (4)	Bolt grip, in inches (5)	Bolt length, in inches (6)
3/4	25,600	to 5	to $6\frac{1}{2}$	above 5, to 10	above $6\frac{1}{2}$, to 12
7/8	32,400	to 5	to $6\frac{1}{2}$	above 5, to 10	above $6\frac{1}{2}$, to 12
1	42,500	to 8	to $9\frac{1}{2}$	above 8, to 12	above $9\frac{1}{2}$, to 14
1-1/8	50,800	to 8	to 10	above 8, to 12	above 10, to 16
1-1/4	64,500	to 8	to 19	above 8, to 12	above 10, to 16

[a] Equal to 90% of the minimum proof load.

After numerous experiments, a turn-of-nut method was developed which has proved to be safe, practical, and economical. From experience with riveting it was known that drawing the component material together properly, commonly called fitting-up, must precede any routine procedure for final bolting. Therefore, fitting-up was established as the first operation to be performed.

Next a reasonably uniform starting point from which to measure nut turn had to be determined. This was found by adapting a procedure workmen normally use in power bolting; they install the bolts with the nuts started on a thread or two by hand, then spin the nut down tight, using the impact wrench as a nut runner, to a snug condition. The most reliable starting point, for measuring the amount of turn, was found to be this snug condition. This condition is obtained by spinning the nut until the wrench starts to impact, which occurs when the turning of the nut is resisted by friction between the face of the nut and the surface of the steel. This snug position is naturally tighter than the hand-tight position and, therefore, less additional turning is required to bring the bolt to its proper tension. Numerous trial runs have shown that the amount of turn required from the snug position varies from one-half to three-quarters turn depending on the bolt diameter and grip. Table 1 gives the nut turn required for bolts of the most common diameters and lengths.

Table 1 was determined by trying various amounts of nut turn and measuring the tension obtained in the bolts. Bolts tightened in accordance with Table 1 will have no less than the minimum tension specified by the Research Council.

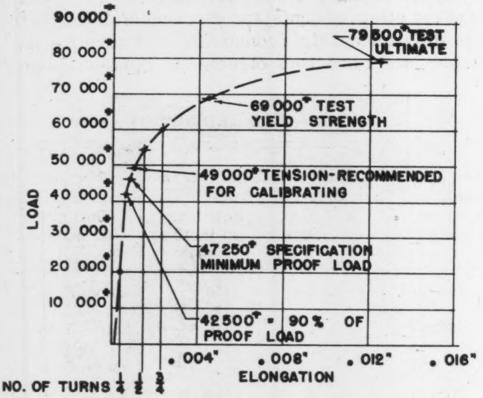

FIG. 5.—STRESS-STRAIN CURVE FOR 1-IN. DIAMETER BY 4-IN. LONG BOLT

It may be of interest to examine Fig. 5, on which there is plotted an actual stress-strain curve for a 1-in. diameter by 4-in. long bolt. On this curve there is shown the tension corresponding to one-quarter, one-half, and three-quarters turn of the nut for a similar bolt from the trial runs. This curve shows how the bolting procedure agrees with the specification requirements.

INSTRUCTIONS

ERECTORS:

1. Fair-up holes with enough pins to maintain dimensions and plumbness of the structure. Pins are not to be removed until bolts in balance of holes have been tightened.
2. Install bolts in the remaining holes.
3. Tighten a pattern of bolts as for riveting, being sure that the connected parts are properly fitted. (This instruction deserves comment: It should be

emphasized that the steel must be fitted-up so that faying surfaces are in contact before the tightening of the bolts is started. Some of the permanent bolts already placed in the holes are used for fitting-up purposes, and they are tightened by means of impact wrenches, without regard to the amount of nut-turn. The essential feature in this operation is to make certain that the piles of steel are tightly fit together. The typical truss joint shown in Fig. 6 illustrates the number of pins and the number of fitting-up bolts used in an actual field joint for riveting. Fig. 7 shows another joint being fitted-up.)

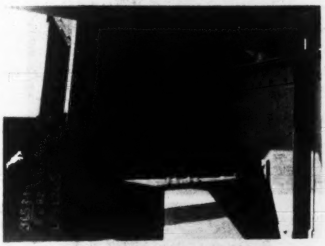

FIG. 6.—PINS AND FITTING-UP BOLTS FOR FIELD RIVETING

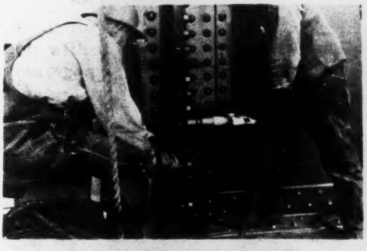

FIG. 7.—FITTING-UP BOLTS FOR BOLTED JOINT

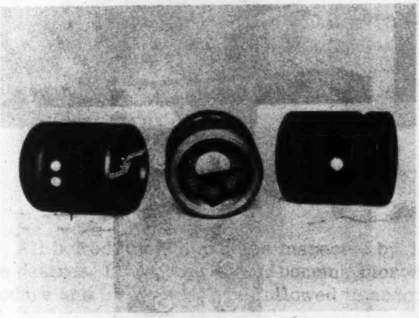

FIG. 8.—MARKING SOCKET

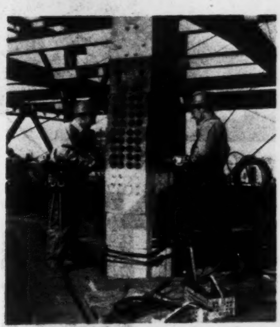

FIG. 9.—COMPLETED JOINT

4. Using an impact wrench, with a marking socket, spin the nut of each bolt used to fit-up, to a snug condition, then continue to tighten it to the number of turns specified in Table 1. (This instruction also requires comment: The marking socket shown in Fig. 8 marks the outside face of the nut or head during the operation, so that workmen or inspectors can see at a glance whether

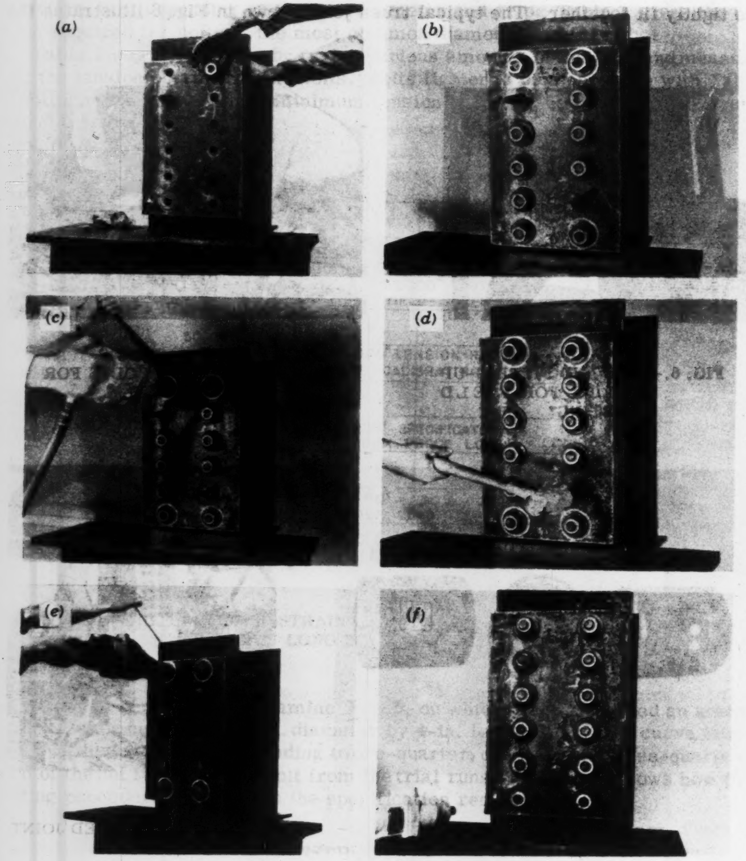

FIG. 10.—INSTRUCTION STEPS

or not the bolt has been tightened. In some cases, for clearance reasons, the head of the bolt must be turned instead of the nut. The same procedure should be followed, with the same amount of turn. Turning the head normally requires a little longer time than turning the nut. The amount of air pressure used for the wrenches need not be constant; it usually varies from 80 psi to 120 psi, depending on type of wrench, diameter of bolt, type of joints, and conditions at the site. Legible marks should be placed on the outside walls of the wrench sockets, 180° apart, for visual determination of nut-turn. Marks must be differentiated either by color or by number of marks.)

5. Replace pins with bolts and tighten as in step 4.
6. Check the tightness of each fit-up bolt with an impact wrench. Usually no further torquing is required, but some may require one-quarter turn.
7. The tightening crew should mark a completed joint with an identifying symbol. Fig. 9 shows a typical completed joint before painting.

Fig. 10 shows the steps in this job.

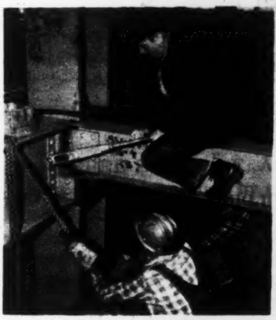

FIG. 11.—INSPECTION OF BOLTS

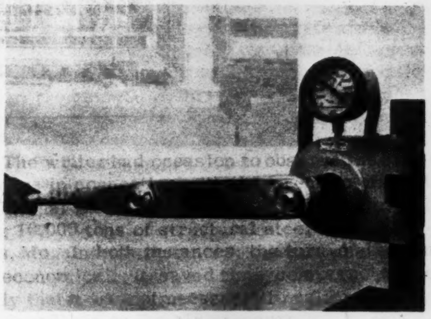

FIG. 12.—CALIBRATION OF WRENCH

All bolted joints should be inspected by the contractor, and by the owner if he desires. Inspectors should become thoroughly familiar with the bolting procedure and insist that it be followed in accordance with the instructions.

As joints are completed, the inspector should note that they bear identification symbols. He should also see that all nuts have a mark on the outside face, made by the wrench sockets during the tightening. He should also check a number of the bolts mechanically, as shown in Fig. 11, to see that they have been torqued to at least the specified minimum tension. This check can be made with a hand-torque wrench, with a dial gauge calibrated on the job to determine the torque-tension ratio. Fig. 12 shows a hand-torque wrench being calibrated by means of a hydraulic calibrating device.

EXAMPLES

A heavy mill-type building is shown in Fig. 13. The building shown is the secondary crusher unit for Erie Mining Company at Aurora, Minn. It contains

4,000 tons of steel and 70,000 A-325 fasteners. It is a tall structure which required cranes with 140 ft booms plus 30 ft jibs to erect it.

A typical highway bridge structure is shown in Fig. 14. In Fig. 14 are shown two adjacent water crossings on the northeast extension of the Pennsylvania Turnpike. The continuous girders span the Lehigh River and the deck trusses are over a creek. There were 75,000 A-325 bolts used to fasten 4,200 tons of material.

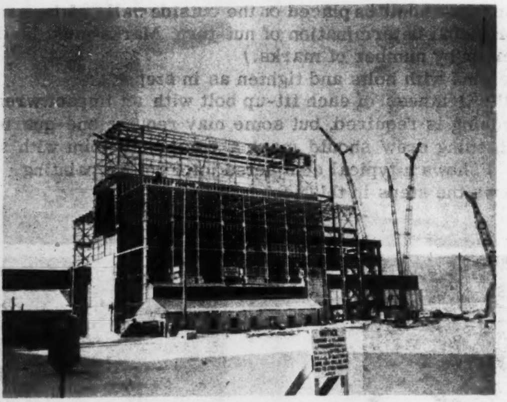

FIG. 13.—HEAVY MILL-TYPE BUILDING

FIG. 14.—HIGHWAY BRIDGE

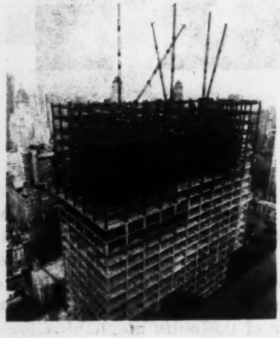

FIG. 15.—38-STORY BUILDING

A 38-story New York, N.Y., building is shown in Fig. 15. This building is more than 500 ft high, requiring 13,000 tons of structural steel, and 240,000 A-325 bolts.

Figs. 13 through 15 are representative of the type of structures which are now being bolted. They were selected from many examples of comparable size and importance. All of these structures utilized high-strength bolts for field connections, and all bolts were tightened in accordance with the procedures previously described.

CONCLUSIONS

Since 1951 the writers' company has installed and tightened over 15,000,000 high-strength bolts, by various methods, with no record of failure. The described method has proved to be reliable, practical, and economical. However, improvements are still being sought. Equipment manufacturers are always improving their impact wrenches and accessory equipment and trying to develop new and better types. It is, therefore, quite possible that the method of tightening described herein, even though it is satisfactory, may be superseded by some better method in the future.

DISCUSSION

ALFRED ZWEIG,[5] F. ASCE.—The writer had occasion to observe the erection method described by the authors in connection with the erection of 6,000 tons of structural steel for the National Bank Building in Detroit, Mich. The same method was used in erecting 10,000 tons of structural steel for the Plymouth Assembly Plant in St. Louis, Mo. In both instances, the turn-of-the-nut method proved satisfactory and economical. It saved time compared to the previously used methods, especially that it was not necessary to calibrate daily the impact wrenches and to check regularly on the air pressure.

The original doubt that insufficient air pressure might result in insufficiently tightened bolts was dispelled by a demonstration which was conducted prior to the start of the erection of the National Bank Building. Even with air pressures 20% to 30% below the previously specified minimum, the bolts turned in accordance with the procedure described by E. F. Ball, F. ASCE, and J. J. Higgins reached the specified tension, the only difference being that it took longer to obtain the required half or three-quarter turn.

There is, however, one point which in the writer's opinion needs refinement. Item 3 of the instructions reads: "Tighten a pattern of bolts for riveting, being sure that the connected parts are properly fitted." In the comment on this item they state: "Bolts. . . used for fitting-up purposes. . . are tightened by means of impact wrenches without regard to the amount of nut turn."

Item 6 of the instructions then states: "Check the tightness of each fitted-up bolt with an impact wrench. Usually no further torquing is required, but some may require one-quarter turn."

---

[5] Senior Structural Engr. and Assoc., Albert Kahn Associated Archts. and Engrs., Inc., Detroit, Mich.

It must be noted that while the tightening process of all bolts, except the fitting-up bolts, is designed to be as fool-proof as possible, leaving no guesswork of feel to the erector, this is not the case with the fitting-up bolts. There, the instruction states that they should be tightened without regard to the amount of nut turn and, then, they should be checked. The check again is up to the feel of the operator. If the bolt feels sufficiently tight, no torquing is required, but some may require a quarter turn. Who is to decide and on what basis?

From the foregoing, it is apparent that the tightening of the fitting-up bolts is not as rigidly and rationally controlled as that of the other bolts. It would strengthen the procedure if a simple method could be devised to alleviate this shortcoming.

M. ZAR,[6] F. ASCE.—Most of the problems requiring clarification revolve around the fact that bolt tension is determined by measuring torque. This is not as reliable as most engineers would like, but it is the only known method for inspection.

In general, it has been conclusively shown that when the steel is drawn up tight and the nuts have been tightened one half turn from a snug position, the bolts will always be above minimum tension. It is important to recognize, however, that many experienced bolters rely on instinct and judgment, instead of following the half-turn procedure, and this is the prime reason for requiring a thorough inspection ritual. On some jobs, for example, where the turn-of-the-nut method was supposedly used, there were no marks on the wrench chuck to indicate the amount of revolution. There is some vagueness associated with Instruction No. 6. which reads "Check the tightness of each fit-up bolt with impact wrench." There is some doubt as to what is meant by "check." The ability to tighten the nut on the fit-up bolt is a function of the available air pressure. It is possible for these original fit-up bolts to lose some tension as the remainder of the joint is tightened. Of course, where fit-up bolts are not high-strength bolts, this problem does not exist, since the fit-up bolts would be replaced with high-tension bolts as described in instruction 4.

WILLIAM H. MUNSE, JR.,[7] M. ASCE.—A variety of methods have been used to tighten high-strength structural bolts. Initially torque was used to develop and also measure the clamping force in the bolts, however, it was soon found that the clamping force provided in a high-tensile bolt on the basis of torque varied considerably and was affected by a number of different factors. Consequently, some better means was required to produce the tension or clamping force in the bolts.

On the basis of laboratory studies it has been suggested that the turn-of-the-nut might be used as an effective means of tightening high-strength bolts.[4] Initially it was suggested that one full turn of the nut from the finger-tight position be used to provide the high desired clamping force. However, the finger-tight position is rather difficult to establish and does not provide a consistent starting point on which to base the number of turns. In addition, the number of turns to failure from the finger-tight position has been found to vary somewhat. In some instances failures have occurred at 1 1/2 turns and in others at 2 1/2 to 3 turns, depending on the rigidity of the abutments, and the strength and ductility of the nuts and bolts, as well as the tightness of the joint at the time torquing was initiated. Consequently, one full turn may, in some instances, dissipate a greater percentage of the available bolt ductility than is desirable.

---

[6] Assoc., Sargent and Lundy, Engrs., Chicago 3, Ill.

[7] Prof. of Civ. Engrg., Dept. of Civ. Engrg., Univ. of Illinois, Urbana, Ill.

What is needed is a procedure that will provide, in all cases, a clamping force which exceeds slightly the initial yield elongation of the bolt material but not by an excessive amount. This will provide the high clamping force desired for the most effective use of high strength bolts and still retain as much as possible of the bolt and nut ductility. It appears that the procedure described by the authors comes close to providing such a condition. The initial snugging up provides approximately 5,000 lb clamping force in a 3/4-in. bolt and the added one half turn then provides a clamping that is at least equal to the yield strength material. Even with this high tightening, the bolt, as provided under current specifications, will still retain a great deal of its deformation capacity.

The half-turn method also appears to be a simple procedure to use in the field—another important advantage. However, since this procedure does, in fact, carry the clamping in the high-tensile bolts beyond the initial yield strength of the material, the availability of additional ductility of deformation capacity may be questioned for those instances when the bolts must be retightened several times. It would appear that a repeated application of one half turn of the nut might, with a small number of repetitions, produce failure in the bolt assembly. Information concerning this problem would be of interest.

RAYMOND ARCHIBALD,[8] F. ASCE.—This paper provides instructions that may result in a universal method of tightening high-strength bolts. There is, however, one section of these instructions with which the writer is not in full agreement. Instruction 6 seems to diverge from a well-established method to a pure guessing game. No record is kept of the fitting-up bolts, as to turns of the nuts but depends entirely on the feel or instinct of the erector.

Since the actual clamping force of the bolts is of such major importance, as little as possible should be left to chance. The writer believes that after the joint has been completed, the fitting-up bolts should be loosened and put through the same process as the other bolts to make sure 1/2 or 3/4 turns on the nuts have been obtained.

E. F. BALL,[9] F. ASCE AND J. J. HIGGINS,[10].—It was noted by Zweig, Zar, and Archibald, that the turn-of-nut method does not seem to control the tightening of the fitting-up bolts as rigidly as that of the other bolts. It has been found, however, in field testing completed joints with calibrated torque wrenches, that the tension in the bolts used for fitting up is not different from the tension in the other bolts. This was also found to be the case in laboratory test made at Lehigh University, Bethlehem, Pa.[11]

Experience in high-strength bolting since July 1959, has demonstrated that better results can be obtained by using a large percentage of the bolts in a joint for fitting-up purposes, even up to 100%. In most cases, proper fit-up can be obtained without tensioning the bolts beyond the snugging-up condition. Final tightening is then accomplished by giving all of the bolts one-half or three-quarters of a turn, working progressively away from the fixed or rigid ends to the free edges.

---

[8] Assoc., J. E. Greiner Co., Phoenix, Ariz., Chf. Bridge Engr., Alaska Div. of Highways, Juneau, Alaska.

[9] Chf. Engr., Fabricated Steel Constr., Bethlehem Steel Co., Bethlehem, Pa.

[10] Supervisor of Erection Tool Houses and Safety, Fabricated Steel Constr., Bethlehem Steel Co., Bethlehem, Pa.

[11] "Static Tension Tests of Compact Bolted Joints," by Robert T. Foreman and John L. Rumpf, Proceedings, ASCE, Vol. 86, No. ST6, June, 1960.

Zar emphasizes the desirability of a thorough inspection. The writers agree with him on this and also agree that the calibrated-torque-wrench method of checking tension in the bolts is the only practical known method for field inspection.

Munse asks if the writers have any records regarding the capacity of bolts after retightening several times. Tests have been made[12] from which it was concluded that bolts, properly installed, could be re-used as often as five times without reaching ultimate, and still have a factor of safety against rupture of approximately 2. In practice, bolts are usually tightened only once, but in rare cases they might be tightened two or possibly three times.

---

[12] "Calibration and Installation of High Strength Bolts," by Robert A. Bendigo and John L. Rumpf, Fritz Engrg. Lab. Report No. 271.7, September, 1959.

HIGH-STRENGTH BOLTS ON MACKINAC BRIDGE

By John W. Kinney[1]

SYNOPSIS

A brief description of the Mackinac Bridge project is given and details are described as to the particular application of bolted connections. The procedure for bolting and inspection as developed on the project is outlined. Some of the more common troubles are described and illustrated. Conclusions resulting from experiences are drawn.

The use of more than 1,000,000 high-strength bolts in the Mackinac Bridge, Michigan was an important factor in keeping steel erection on schedule and allowing opening of the bridge to traffic on the scheduled date, November 1, 1957.

A brief description of the Mackinac Bridge will include many outstanding features. Its cost, $100,000,000, including administration, engineering, and interest during construction, makes it the most costly bridge project yet undertaken (as of 1960). Its length, over the often rough waters of the Straits of Mackinac, of 17,917 ft, or over 3 miles, rates the bridge as a major structure. The center suspended span of 3,800 ft ranks second only to the Golden Gate's center span of 4,200 ft (as of 1961). The two side spans of 1,800 ft each, two unloaded backstay spans of 472 ft each, and the two anchorages of 135 ft each, make the total length of the suspended span structure 8,614 ft from back to back of anchorages, the longest single suspension bridge presently built.

In order to make financing possible, it was essential that the bridge be completed to the point of opening to traffic in four construction seasons from the time of financing. Winter conditions at the Straits of Mackinac make marine operation impossible during the winter months. The construction season is short, usually from the middle of April to the middle of December for marine work. Interruptions of the work during the construction season were caused at intervals by storms, or by winds and rough seas of less than storm intensity.

The contract for the superstructure steel was a unit-price contract for $44,532,000, the largest bridge contract awarded to date (1960).

The 1954 season was devoted to foundation work on the main bridge piers, and the start of steel fabrication on the main towers.

Steel erection was started on July 2, 1955 on the main towers. The towers were topped out to their height of 552 ft on December 6. The backstay spans were floated out in November and December. This schedule allowed the start

---

Note.—Published essentially as printed here, in March, 1959, in the Journal of the Structural Division, as Proceedings Paper 1975. Positions and titles given are those in effect when the paper or discussion was approved for publication in Transactions.

[1] Resident Engr. for D. B. Steinman, Cons., Engr., New York, N. Y.

of cable work early the following season and its completion in 1956. Riveting of the towers and backstay spans proceeded during their erection and assembly. It proved difficult to maintain scheduled progress on riveting, because of a lack of qualified men. Consequently, the towers went through their first winter with the riveting approximately 60% complete from the bottom up. The upper unriveted splices were bolted and pinned in a 40-60 ratio. Similarly, the backstay spans were not completely riveted, and some of the chord splices and other connections went through the winter bolted and pinned.

The difficulty of maintaining the riveting schedule led the contractor to propose the use of high-strength bolts for all of the approach truss spans scheduled for 1956, and the suspended spans scheduled for 1957. This proposal was accepted by the consulting engineer; somewhat more than 1,000,000 high-strength bolts were required for this work.

All of the steel to be bolted had been designed for 7/8 in. and 1 in. rivets. All of the truss chords, both in the approach spans and in the stiffening trusses for the suspended spans, were assembled and reamed before erection.

The truss approaches, totaling 9,303 ft long, consist of seven continuous span units of four spans, the longest unit being 480-560-560-480 ft in length. The depth of the trusses in these long spans is 45 ft at the center of the span and 53 ft over the intermediate piers. Construction is of the deck-truss type, with the floor beams, 54 ft long, being framed through the trusses which are on 34 ft centers. Silicon steel, ASTM A94, was used for highly stressed truss chords and diagonals, and structural carbon steel, ASTM A7, in the balance. The maximum grip of bolts used in the connections was $4\frac{1}{8}$ in., and the number of plies connected was up to six. Stringers were spliced to develop continuity over several floor beams. Erection of all members except the floor system was done from the water by the cantilever method, by the means of anchoring adjacent trusses, and the use of falsework of which there was usually one bent in each span, and full cantilever erection in the fourth span of each unit.

The suspended spans are of the deck-truss type, with stiffening trusses 3,766 ft long in the center span, and 1,775 ft long in each side span. The depth of the trusses is 38 ft, and the panel lengths approximately 39 ft. Trusses are 68 ft on centers, and are provided with a top and bottom lateral bracing system as well as sway bracing. Floor beams, 68 ft long, are of truss construction, and were shop-assembled and riveted. Silicon steel was used in the stringers, stiffening truss chords and other highly stressed members. The maximum grip in the bolted connections is 5 in., and the maximum number of plies connected is six. Units of two panel lengths were assembled and bolted with high-strength bolts in an assembly yard on shore.

The assembled units consisted of both trusses, the connecting floor beams, and top and bottom lateral bracing. The units weighed from 100 tons to 150 tons, and were shipped from the assembly yard to the site on barges, two units per barge. The units were raised by means of lifting struts which were rolled on top of the main cables. The two lifting struts used for each lift were each provided with two 9-part falls, which were attached to the floor trusses of the unit. When the units were lifted into place, the four suspender ropes, already installed, were connected to their brackets on the trusses by means of socketed connections on the suspenders. Balanced erection both ways from each tower was followed. A feature of stiffening-truss erection is the fact that the final shape of the truss is not developed until all dead load is applied. This makes it impossible to make up the chord and diagonal connections between the units as erection proceeds. As the stage is reached where the joints make up and the holes are fair, which may be a temporary condition, the connections must be bolted and pinned in the case of riveted connections. A big advantage in the use of high-strength bolts in these connections is that bolting can be permanently made at scattered points as soon as they are fair and ready, without the necessity of temporary bolting and pinning. Final bolting of the chords and diagonals was kept well ahead of second-pass erection.

The erection of the floor system followed as a second pass. All of the stringers, cross beams, steel grid flooring, and railing were hoisted at the towers and erected in a balanced sequence from the towers. Stringers and cross beams were bolted as erected. This was immediately followed by the placing of the floor grid, which was then welded sufficiently to carry the erecting crane and straddle buggy. All material for the second pass was moved from the towers to the point of erection over the grating by straddle buggies; likewise the truck crane shuttled between erection points on opposite sides of each tower. The use of high-strength bolts speeded up the placing of the grating and the use of the floor system.

Some examples of bolted connections are shown in Figs. 1, 2, and 3.

Before the start of bolting, the Specifications for Assembly of Structural Joints Using High-Strength Steel Bolts, approved by the Research Council on Riveted and Bolted Structural Joints of the Engineering Foundation of February, 1954, were agreed on.

Before the use of high-strength bolts was agreed on, early in 1956, some of the approach steel had already been shipped to the job. The specifications (for riveted joints) called for a coat of lacquer on the contact surfaces, one coat of red lead and oil paint on the balance. The lacquer coat as well as the red lead coated surface under the washers of the bolts was removed by sandblasting.

One of the first questions to come up in the field checking of bolts was the possibility that the bolts could be overtightened, as well as undertightened. As the truss-chord connections, and others, are subject to reversal of load, and because of the importance of the bolted joints, it was agreed that everything possible would be done to assure against possible damage due to overtightening, as well as the possibility of undertightening.

Test runs were made on a number of bolts in a calibrator. The 7/8-in. bolts used in this series were tightened to the required tension. Air pressure was adjusted by means of air-line pressure regulators so that the required bolt tension was reached in 10 sec. Torque readings were then made on each bolt for comparison with the tabular value. A set of new impact wrenches was procured by the contractor for use on high-strength bolts to assure uniformity of equipment. A number of tests on new 7/8-in. bolts showed torque readings close to 400 ft-lb at the recommended bolt tension for calibrating of 37,000 lb. Similar tests on new 1-in. bolts showed torque readings close to 700 ft-lb at a bolt tension of 49,000 lb. Tabular values are 480 ft-lb and 710 ft-lb for nonlubricated bolts and nuts. The observed difference in torque was considered due to the light oil film present on the nuts as furnished.

With a stress area of 0.4612 sq in. on 7/8-in. bolts, and 0.6051 sq in. on 1-in. bolts, the tension of 37,000 lb on 7/8-in. bolts is equal to a stress of 80,225 psi and the tension of 49,000 lb on 1-in. bolts is equal to a stress of 80,978 psi.

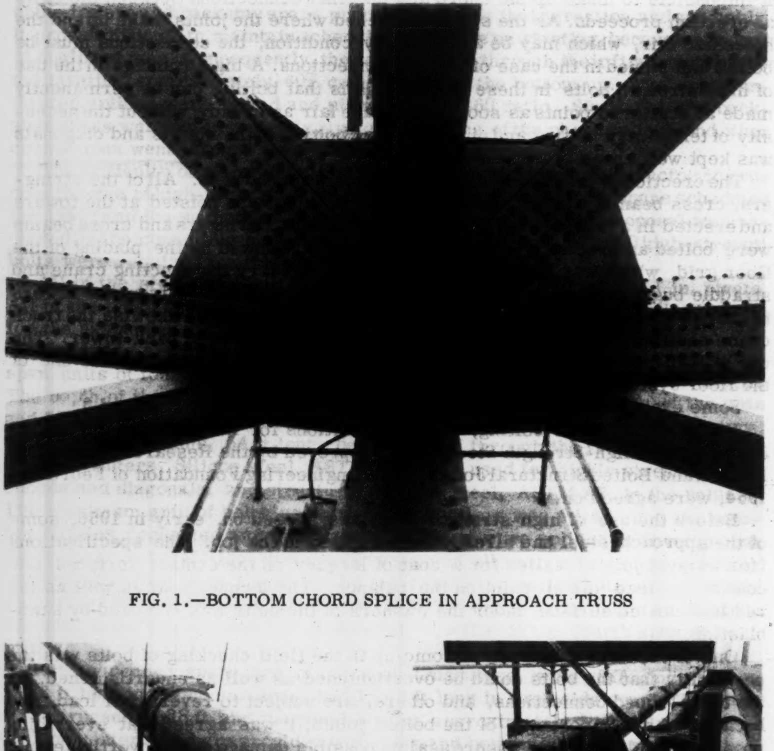

FIG. 1.—BOTTOM CHORD SPLICE IN APPROACH TRUSS

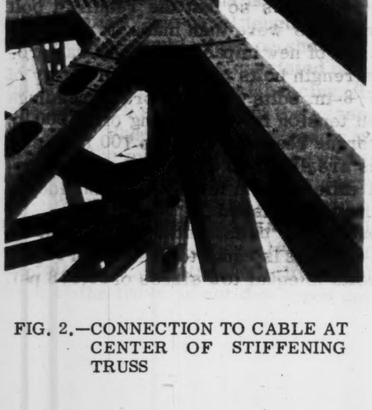

FIG. 2.—CONNECTION TO CABLE AT CENTER OF STIFFENING TRUSS

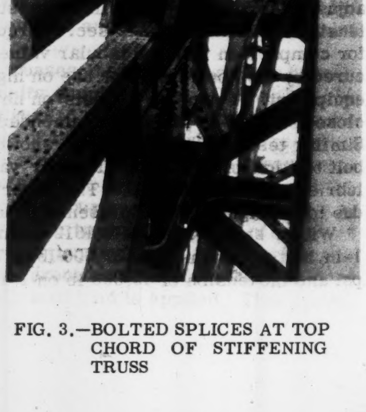

FIG. 3.—BOLTED SPLICES AT TOP CHORD OF STIFFENING TRUSS

It was found in the early stages of bolting that more than 10% of the bolts in the connections torqued more than 600 ft-lb in the case of 7/8-in. bolts. If the torque in the calibrator at 37,000 lb tension was correct at 400 ft-lb, a torque of 600 ft-lb would indicate that the bolt was stressed to approximately 120,000 psi or over the minimum ultimate strength of 115,000 psi. It is probable that the lubrication failed, giving higher torque readings, before such stress was reached.

A number of tests by tightening to failure with an impact wrench showed that the nuts would eventually strip. In no case did failure occur by breaking the bolts, or by stripping the bolt threads.

In order to observe the condition of the overtorqued bolts, a number of 7/8-in. bolts were removed, with torques ranging up to 600 ft-lb. The bolts were checked with a thread gauge for stretch or buttressing of threads and the nuts were checked for excessive looseness; no apparent damage was observed. A second series of eighteen 7/8-in. bolts torquing more than 600 ft-lb was removed for examination. This group appeared representative of bolts more than 600 ft-lb (Table 1). Torques ranged from 640 ft-lb to 780 ft-lb. At 640 ft-lb some galling, and some polishing of the bolt threads was noted on some of the bolts. Some binding of either a new or an old nut was noted. At 680 ft-lb slight damage to the crest of the bolt thread was noted on one bolt. In most cases there was some restraint in running a new or the original nut on the bolt. At 720 ft-lb slightly increased damage to the crests of bolt threads was noted, and generally more difficulty in running on a new or original nut was encountered. At 740 ft-lb one bolt showed slight damage to crests of threads and difficulty in running on a new nut. At 780 ft-lb one bolt showed no apparent damage and no trouble in running on a new or the original nut.

It appeared from the foregoing that 600 ft-lb torque was as high as could consistently be allowed without probability of damaging a 7/8-in. bolt

Since the ultimate failure by tightening appeared to be caused by stripping the nut, the contractor proposed to salvage any 7/8-in. bolts which torqued more than 600 ft-lb as long as there was no visible damage, and a new nut could be run on the bolt without restraint.

Several objections to this procedure are apparent. Even though there is no visible damage, there is a possibility (1) that the bolt threads may be slightly buttressed, causing loss of contact area and excessive contact pressure on the threads of nut and bolt, (2) if the bolt has been stretched beyond its elastic limit, the thread pitch is changed, resulting in excessive thread pressures and cumulative failure, (3) polishing, or the opposite action of galling the bolt threads, will throw the torque-tension relation completely off, or (4) the character of the bolt steel may have been changed by work hardening of the threads, with possible embrittlement, which might lead to failure.

In an effort to get more information on the overtorqued bolts, it was decided to break some of the samples at the Michigan College of Mining and Technology, Sault Ste. Marie, the results are shown in Table 1.

Two new 7/8-in. bolts were picked as a control. There was a considerable variation in the ultimate load, but both bolts broke in a normal manner through the thread (Fig. 4, bolts A and B). The maximum stresses were 104,900 psi and 130,500 psi.

Six bolts on which the torque reading was from 640 ft-lb to 780 ft-lb and on which a new nut could be run without restraint, were selected for testing with new nuts. All of these bolts failed through stripping of the nut thread. The ul-

TABLE 1. –TESTS[a] ON HIGH-STRENGTH BOLTS[b]

Bolt	Torque, in foot-pounds[c]	Old nut run up[d]	New nut run up[d]	Description	Ultimate load, in pounds	Ultimate stress, in pounds per square inch[e]	Bolt Hardness		Nut Hardness	
							Rockwell	Brinnell	Rockwell	Brinnell
Overtorqued 7/8-in. high-strength bolts removed from truss connections[f]										
1[g]	720	No	No	Old nut has slight bind						
2	670	No	Yes	No visible damage						
3[h]	720	Yes	No	No visible damage	60,750	131,800			B74	135
4[h]	640	Yes	Yes	No visible damage	59,650	129,000	C22	237	B76	139
5[h]	780	Yes	Yes	No visible damage	61,740	134,000			B75	137
6[g]	680	Yes	No	No visible damage	32,980	71,500	C24	247		
7	680	No	No	1st thread hit, damaged						
8[g]	680	Yes	No	No visible damage	38,350	83,000				
9	680	No	No	Crest of threads damaged						
10	720	No	No	Crest of threads damaged						
11	740	No	Yes	Crest of threads damaged						
12	720	No	No	Crest of threads damaged						
13	720	No	Yes	No visible damage						
14	720	No	No	1st thread hit, damaged						
15[h]	680	Yes	Yes	No visible damage	64,170	139,000	C24	247		
16	640	No	No	Top of threads polished						
17	640	No	No	1/3 of 1st thread galled						
18	640	No	Yes	No visible damage						
New bolts[j]										
A[g]					48,370	104,900	C25	253		
B[h]					60,150	130,500				

[a] At Sault Branch of Michigan College of Mining and Technology on May 22, 1956. [b] Specifications for 7/8-in. bolts: Ultimate load = 53,000 lb, ultimate stress = 115,000 psi, stress area = 0.4612 sq in. [c] Accepted torque = 400 ft-lb to 600 ft-lb. [d] Refers to whether or not the old nut, or a new nut, can be run onto the overtorqued bolt by hand. [e] Based on area of 0.4612 sq in. [f] Failure of overtorqued bolts, with new nuts, was by stripping of nut. [g] Loading rate: crosshead, no load, 1 in. per min. [h] Loading rate: crosshead, no load, 1/10 in. per min. [j] New bolts failed by breaking through thread.

timate stress was quite variable, as expected, and in some cases was surprisingly high, 139,000 psi; the lowest stress causing failure was 71,500 psi.

The engineers concluded that all 7/8-in. bolts which torqued more than 600 ft-lb should be removed and rejected, and that torque exceeding 1,050 ft-lb be cause for rejection of 1-in. bolts. In both cases, the value is 150% of the torque producing the recommended tension for calibrating.

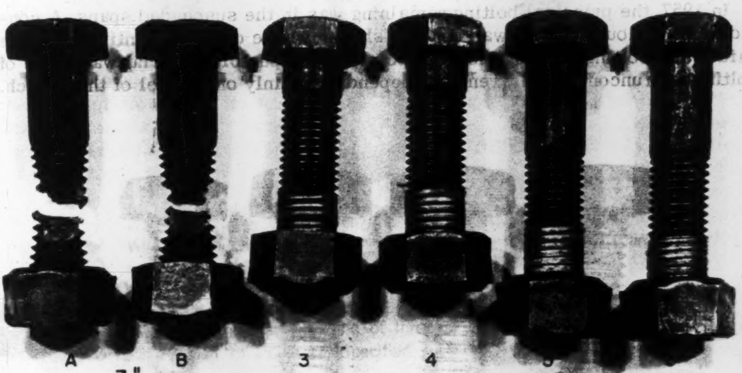

7/8" Bolts Tested to Failure in Tension
A and B New bolts and nuts Normal failure
3,4,5,6 Torqued at 640-780, Removed from structure
New nut installed and tested All bolts stripped the nuts in testing Ultimate strengths varied from 71,500 psi to 139,000 psi New bolts ultimate 104,900 psi to 130,500 psi

FIG. 4.—TENSION FAILURE OF 7/8-IN. BOLTS

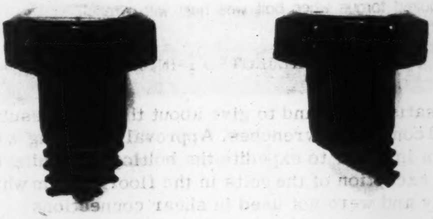

FIG. 5.—FAILURE OF 1-IN. BOLTS

The procedure was set up to torque all bolts. Any bolts torquing below 400 ft-lb for 7/8-in. bolts, and 700 ft-lb for 1-in. bolts were tightened further by a partial turn of the nut with the torque wrench at the time of torquing. In some cases, it was found that the torque would not come up on tightening, indicating that failure had started, and such bolts were rejected. The nuts were not backed off before reading the torque, as non-reversible torque wrenches were used.

The tightening procedure outlined was followed during 1956. Rejections came down to an estimated 3% to 4%.

The turn-of-the-nut method of tightening was tried, but consistent results were not obtained, possibly due to the large variation in number of plies, thickness of metal, stiffness of parts, and fit of the connections.

In 1957, the principal bolting remaining was in the suspended spans. A considerable amount of this was done on shore, where closer attention could be paid to the bolting, both by the contractor and inspectors. A trial was made of bolting with uncontrolled wrenches, depending mainly on the feel of the wrench.

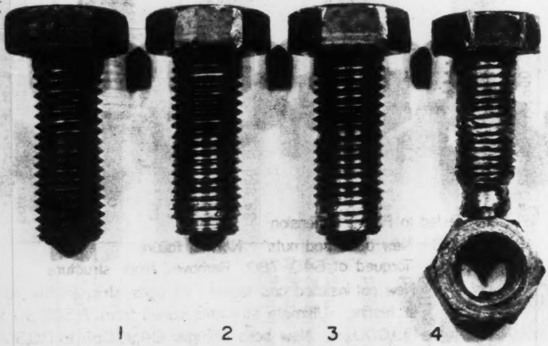

1 Torqued @ 650 Torque did not increase with 1/2 turn additional. Bolt found stretched.

2-3 Bolts found overtorqued badly buttressed threads.

4 Bolt was sucked through a misaligned hole by drawing up on the nut. Bolt turned during torquing but would not develop required torque when bolt was held with wrench.

FIG. 6.—REJECTED 1-IN. BOLTS

This proved to be satisfactory and to give about the same results as tightening with calibrated and controlled wrenches. Approval of bolting with uncontrolled wrenches was given in order to expedite the bolting. Torquing of all bolts was continued, with the exception of the bolts in the floor system which, in general, were fasteners only and were not used in shear connections.

It was hoped that torquing could be considerably reduced in line with reported experience on other jobs. While the percentage of cut-outs was low, the occurrence was not uniform. Torquing was continued, both to detect overtorqued bolts and to make the final tightening on undertorqued bolts.

A few other difficulties, for the most part rarely occurring, will be described. Fig. 5 shows two 1-in. bolts in which a fissure developed in the bolt head in cold forming. These bolts broke normally in a tension machine, and apparently the

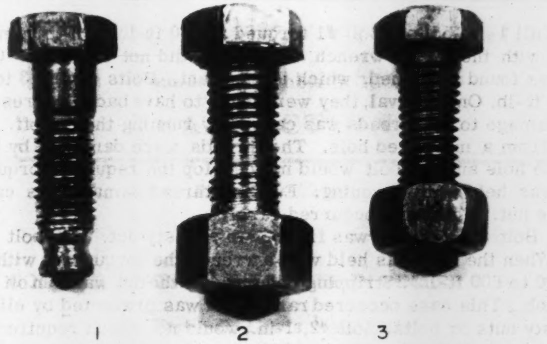

1 A rusty nut was used on this bolt. Bolt turned when torqued. When the head was held with a wrench the torque was within allowable limits. Stripping occurred as the nut was run off.

2 Would not reach required torque with torque wrench, probably overstressed on original tightening. Impact wrench was reapplied, completing stripping of threads.

3 Bolt torqued at 800 Specified limit 400-600 Note stretch

FIG. 7.—REJECTED BOLTS

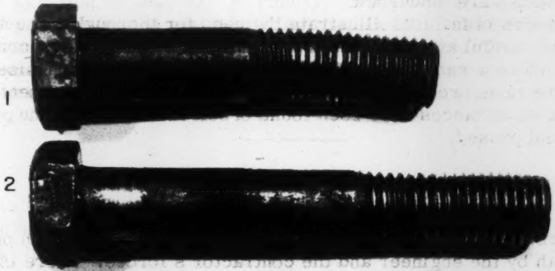

1 Hillside washer under head turned while tightening, causing bend

2 Soft Bolt Included with shipment of H. S. Bolts Note stretch Discovered when the bolt would not reach required torque

FIG. 8.—REJECTED 1-IN. BOLTS

fissures did not affect the strength of the bolt; such bolts were subsequently accepted.

Fig. 6, all 1-in. bolts: Bolt #1 torqued at 650 ft-lb. On tightening 1/2 turn additional with the torque wrench, the torque did not increase. On removal, the bolt was found stretched, which is apparent. Bolts #2 and 3 torqued more than 1,050 ft-lb. On removal, they were found to have badly buttressed threads. Further damage to the threads was caused by running the nut off. Bolt #4 was removed from a misalined hole. The threads were damaged by being pulled through the hole and the bolt would not develop the required torque even when the head was held while torquing. Further thread damage was caused by removing the nut. This case occurred rarely.

Fig. 7, Bolt #1, 7/8 in., was fitted with a rusty nut. The bolt turned when torqued. When the head was held with a wrench the torque was within allowable limits (400 to 600 ft-lb). Stripping occurred as the nut was run off with the impact wrench. This case occurred rarely and was prevented by eliminating the use of rusty nuts or bolts. Bolt #2, 1 in., would not reach required torque with a torque wrench, indicating that the bolt was already overstressed. An impact wrench was re-applied completing the stripping of threads. Bolt #3, 7/8 in., torqued at 800 ft-lb and was removed. Stretch and increased pitch can be noted.

Fig. 8, both 1-in. bolts: Bolt #1 extended through a structural channel requiring a bevel washer. The bevel washer turned under the nut during tightening, causing the bolt to bend. This effect can be found by observation of the bolt in the connection. Bolt #2 was a soft bolt, included with a shipment of high-strength bolts. This is thought to be the result of an error in the warehouse. No high-strength markings were found on the bolt head. This bolt would probably have passed, except that torquing disclosed that the bolt would not develop the required torque. A further check of the bolt stock disclosed a keg of soft bolts which were discarded.

The instances of failures illustrate the need for thorough inspection by the engineer and careful attention to workmanship on the part of the contractor in order to produce a satisfactory bolted job. It should be emphasized that rejections were rare, probably much less than with a carefully inspected riveted job, and that no instances have been found of bolt failures after the points were corrected and passed.

CONCLUSIONS

Considerably more time must be spent on bolt inspection than on rivet inspection both by the engineer and the contractor's forces. There is a definite need for setting an upper limit on allowable torque as well as a lower limit. It has been established that there is a definite possibility of damaging bolts by overtorquing. The trend toward bolting will continue in view of the excellent overall results, and the better production possible with bolts, also tools and methods will be improved so that inspection time can be reduced.

There is reason for confidence that continued inspection of the Mackinac Bridge will prove that high-strength bolting is completely satisfactory, as well as an expetitious method of making connections on heavy truss work including the stiffening trusses of suspension bridges. (A discussion, in 1961, with the operators of the Mackinac Bridge, revealed that no trouble with high-strength bolts has developed in the more than 3 yr that the bridge has been in use.)

AMERICAN SOCIETY OF CIVIL ENGINEERS

Founded November 5, 1852

TRANSACTIONS

Paper No. 3248

DESIGN CONSIDERATIONS FOR FATIGUE IN TIMBER STRUCTURES

By Wayne C. Lewis,[1] M. ASCE

With Discussion by Messrs. Paul G. Fluck; Floyd E. Schneider; and Wayne C. Lewis

SYNOPSIS

Working stresses for timber are developed from average test values for clear wood by applying factors for normal variability, indeterminacy of stress analysis, natural strength-reducing characteristics present in structural timbers, and duration of loading. Normally, no allowance is made for fatigue—that is, to provide for the possibility that failure may result from an accumulation of cyclic stressing during the life of the structure. This paper summarizes information now available on fatigue of wood and investigates the adequacy of design based on present-day working stresses with respect to fatigue.

INTRODUCTION

Fatigue has been termed the "forgotten member of the design family." T. M. Barlow, in 1929, stated[2] that

> "Fokker's reasons for retaining wood-wing construction for monoplanes are summed up in the word 'fatigue.' Claims of new materials to lightness must be reviewed in association with their fatigue limits. Fatigue in properly seasoned wood is unknown."

Note.—Published essentially as printed here, in May, 1960, in the Journal of the Structural Division, as Proceedings Paper 2470. Positions and titles given are those in effect when the paper or discussion was approved for publication in Transactions.

[1] Engr., Forest Products Lab. Forest Service, U. S. Dept. of Agric., Madison, Wisc.

[2] "The Weight of Aircraft," by T. M. Barlow, Aircraft Engineering, Vol. 1, 1929, p. 29. (Abstracted in "Abstracts of Articles on the Fatigue of Metals under Repeated Stress Appearing in the Technical Press from July 1, 1928, to June 30, 1929," prepared by ASTM Research Committee on Fatigue of Metals.)

It is more likely that, with the approximate methods of design used in that day, actual stresses which were repeated in aircraft were so low that fatigue failures did not develop during the life of the aircraft. A more nearly accurate analysis of the aspects of fatigue failures in timber is contained in the report of the subcommittee on duration of load and fatigue, of the Committee on Timber Structures.[3] Pointing out that wood is subject to fatigue failures in the same way as other materials, the report states:

> "The fatigue strength of large numbers of repetitions of stress of fibrous materials, such as wood, is a higher proportion of the static strength than of crystalline materials like metals. As a consequence, actual stresses in a wood structure are usually lower than the repeated stresses that will produce failure during the normal service life of a structure."

Though there have been but few fully authenticated examples of fatigue failures in actual service, laboratory studies have clearly demonstrated that if a wood structural member or part is subjected to a sufficient number of repetitions of stress of sufficient magnitude, it will fail. Fatigue failures in wood have the same appearance as static failures. This points out the possibility that some service failures in fatigue have been classified as static structural failures.

In metals such as steel, where the ordinary static failure is accompanied by ductile flow, there is a noticeable difference between that kind of failure and failure from fatigue, which is characterized by its brittle appearance. Fatigue failures in steel show the crystalline character of the metal, and, in the vernacular, it is said that the component having the failure has "crystallized."

Much more is known about fatigue of metal, riveted joints, and the cold working and stress relieving of metal parts and structural components than is known of wood. This is largely because the science of fatigue behavior is an empirical one, and machine parts are more often stressed a sufficient number of times so that fatigue failures develop; although some moving parts of machines, such as Pitman arms, continue to be made from wood because of their superior fatigue resistance and their high strength-weight ratio.

As refinements are made in design methods, and with the growth of the glued laminating industry, more and more will there be a need to consider the possibility of failure from fatigue in engineered structures of wood. It is the purpose of this paper to assemble what information is available on the fatigue resistance of wood stressed in different ways and, on the basis of results of experimental programs completed to date (1960), to analyze existing data in light of the working stresses usually used in the design of civil engineering structures.

FATIGUE TERMS AND RESULTS DESCRIBED AND DEFINED

Before any good understanding of fatigue is possible, it is necessary to define and describe just what fatigue is. Fatigue in engineering materials is defined as the progressive damage and failure that occur when a structure or part is subjected to repeated loads of a magnitude smaller than the indicated static strength. "Static strength," as used in the definition, means the one-time load strength and is the strength of a member as measured by a static-stress test of 5 min to 10 min duration.

---

[3] "Duration of Load and Fatigue in Wood Structures," Proceedings, by Committee on Timber, ASCE, Vol. 83, No. ST 5, 1957.

Stresses in engineering members are of various types. If they come into the member slowly and stay for a length of time, they are said to be a static stress. If they come on quickly and stay for a short period, they are classified as an impact or shock loading. Actual stressing in any member may be a combination of static and dynamic loading, and in design the cumulative effects should be considered in two ways. One, that of duration of load, is handled by the factor for normal or long-time loading discussed[4] by L. W. Wood where a factor of 5/8 is applied to the average static-strength property for accumulations of about 10 yr in developing a working stress.

In fatigue, if the repetitions of design stress or near-design stress probable or possible during the normal life of the structure are more than 100,000 cycles, some such consideration for fatigue should be made. In design considerations, either duration or repetition of load will usually be a governing factor; and if repetition of load governs, then the design stress used should be less than that which would produce a fatigue failure under the number of repetitions possible or probable during the life of the structure.

How is fatigue resistance measured? In test, specimens are loaded repetitively to a predetermined level of stress and the number of cycles that produces failure is determined. For a number of different specimens loaded to different maximum stresses, several values of stress and numbers of cycles to failure will be obtained. When these values are plotted with the maximum repeated stresses as ordinates and the corresponding numbers of cycles of stress to failure (usually on a logarithmic scale) as abscissas, it is possible to connect the points into a curve of descending order. As the magnitude of repeated stress decreases, the number of cycles to failure increases. The curve is called the S-N diagram. Fig. 1 shows a typical S-N diagram for wood in shear.

In tests of steel and some other materials, the S-N diagram levels out on the lower portion, and it is possible to draw a horizontal line below which repeated stresses will not produce fatigue failure in an infinite number of cycles. The level of stress for the horizontal portion is called the endurance limit, and is defined as the maximum stress which can be repeated an infinite number of times without inducing failure. In wood, many metals other than steel, and plastics, the S-N curve continues to decrease even beyond 10,000,000 cycles, a common end point in test, so fatigue strength becomes the important term. Since fatigue strength is the maximum stress than can be repeated for a given number of cycles without causing failure, any value for fatigue strength must include the number of cycles—thus, "fatigue strength for 10 million cycles" or "fatigue strength for 100,000 cycles." For practical purposes, fatigue strenght for 10,000,000 cycles can be used for wood in civil engineering in the same way that the endurance limit is used for steel, because there is only a remote possibility that so many repetitions of stress will be encountered in actual use.

The fatigue behavior of materials is influenced by the amplitude of the stress cycle as well as by the amount of the maximum stress. The greater the difference between the minimum and the maximum stresses for each cycle, the

---

[4] "Safety Factor in Design of Timber Structures," by L. W. Wood, Proceedings, ASCE, Vol. 84, ST 7, 1958.

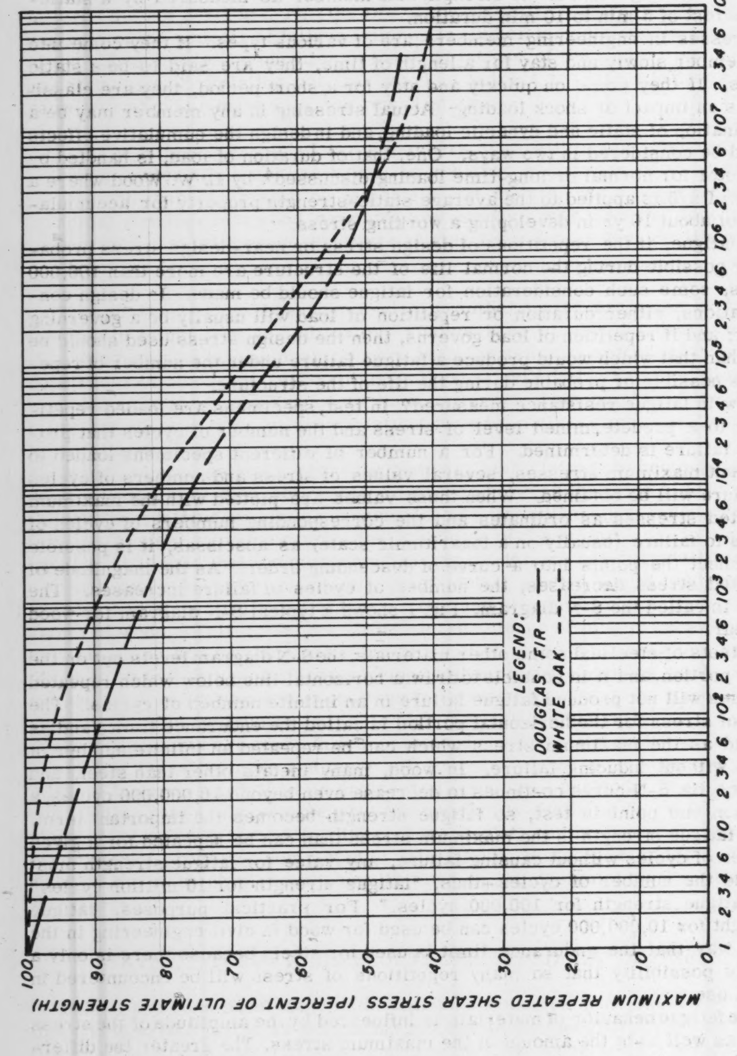

FIG. 1. S-N CURVES FOR GLUE SHEAR IN LAMINATED DOUGLAS FIR AND WHITE OAK. RATIO OF MINIMUM REPEATED SHEAR STRESS TO MAXIMUM REPEATED SHEAR STRESS FOR EACH CYCLE WAS 0.10.

smaller will be the number of cycles before failure. The ratio of minimum to maximum repeated stress is called the stress ratio, R. It and other terms are defined by ASTM in its manual on fatigue testing.[5]

If groups of tests are made on the same material with the same kind of specimen at different stress ratios, the result will be a family of S-N curves, of which the curves with the greatest stress amplitude (lowest stress ratio) will be in the lowest position, relatively. This means that the fatigue life (number of cycles to failure) will be less at a given maximum stress when the minimum repeated stress is 10% of the maximum stress per cycle (stress ratio 0.10) than if it is 30% (stress ratio 0.30).

Stresses in a structure may be repeated, as from zero to some value, or from some value to another higher one in the same direction, or they may be partially or completely reversed. Partially reversed loading occurs where repeated stresses are not the same in either direction; fully reversed stresses are of equal magnitude, as in compression and tension or as in positive and negative shear. Fully reversed stressing is the most severe loading condition and will give S-N diagrams in the lowest position. Partially reversed stressing gives S-N diagrams higher in position than does fully reversed stressing, but lower in position than does repeated stressing. The stress ratio is expressed as -1 for fully reversed loading and as a negative deciman for partially reversed loading.

Nearly all fatigue tests on wood and wood construction have been made under repeated loading conditions, because this is the most common loading in such structures as timber-bridge stringers, other beams subjected to repeated loads, and components of arches and trusses. Because some dead load always remains on the members, and for practical reasons in testing, a stress ratio of 0.10 has been selected for most of the tests. In the following sections of this paper, the available information on fatigue-test results pertinent to timber and glued wood constructions is summarized.

FATIGUE OF WOOD IN BENDING

Much of the timber put into structures where repeated loading may be a factor is used for beams, such as stringers in bridges and girders in buildings, where vibratory stresses from heavy machines are transmitted through the floor system. A report has been made[6] on an investigation of the fatigue resistance of quarter-scale bridge stringers of green and dry southern pine. This research was jointly financed by the Association of American Railroads (AAR) and the U. S. Forest Products Laboratory.

Beams are subjected to a combination of forces, tension, and compression in opposite faces in areas of greatest bending moment and shear in areas of greatest total force as near supports. The span-depth ratio and location of loads determine the relative importance of the bending and shear stresses. In the study of quarter-scale stringers, specimens were loaded at the third points, and in the green and dry specimens with either straight of 1:12 sloping grain, failure in bending was critical under either static or fatigue (repeated) loading. In some of the dry specimens, artificial checks were cut in the shear portion to simulate the maximum checks that could occur from drying. In those specimens, shear was critical, and all of the fatigue specimens and most of the static specimens failed in shear.

---

[5] "Manual on Fatigue Testing," by Committee E-9 on Fatigue, ASTM, Special Tech. Publication No. 91, 1949.

[6] "Fatigue Resistance of Quarter-Scale Bridge Stringers of Green and Dry Southern Pine," by W. C. Lewis, AREA Bulletin, No. 538, 1957, p. 363.

The fatigue tests on green material indicated that, if the repeated maximum stresses were low enough so that compression failures did not develop, the specimen withstood 10,000,000 repetitions for a stress ratio of 0.10 without any failure. The fatigue strength for no failure at 10,000,000 cycles was indicated to be 50% of the static strength for straight-grained material, and 60% of the static strength for 1:12 slope of grain. The fatigue strength of the green material tested was indicated to be about 3,000 psi for both the straight-grained specimens and those with 1:12 slope of grain.

The fatigue tests of the dry specimens without the artificial checks indicated that the fatigue failures in the straight-grained specimens were in compression followed by tension and that, for a stress ratio of 0.10, the fatigue strength at 10,000,000 cycles was about 50% of the static strength, or about 7,000 psi for the material tested. Those with the 1:12 slope of grain usually failed in corss-grain tension with no visible compression, and the indicated fatigue strength for 10,000,000 cycles was about 45% of the static strength, or 4,500 psi for the material tested.

The air-dry specimens with the artificial checks, which reduced the width of the area in shear by one-half, indicated that fatigue strength for 10,000,000 cycles was 35% of the static strength for both the straight-grained specimens and those with a 1:12 slope. This amounted to 300 psi computed on the gross section for straight-grained material and 250 psi for material with a 1:12 slope.

FATIGUE OF WOOD IN COMPRESSION OR TENSION

Until a few years ago, the phenomenon of fatigue failure was associated only with tensile stressing. All fatigue failures observed in service were associated with a tension crack or failure. In most structures, members are sufficiently large so that nearly pure stresses occur in critical areas where fatigue failures could develop. The information already presented on compression introduced by bending is useful in appraising the possibility of fatigue failures in compression. If, as is borne out by those tests, stresses in compression are high enough so that failures can develop in green material after a very few cycles and those stresses are 50% or more of the modulus of rupture, there is little possibility of fatigue failure. In terms of compressive strength, there is little question about the resistance to fatigue. Compressive strength of green wood is 1/2 to 2/3 of the modulus of rupture, so the fatigue strength for 10,000,000 cycles in compression parallel to grain would be at least 75% of the static strength for green material.

The static compressive strength of air-dry wood ranges from about 45% to 60% of the modulus of rupture. The fatigue bending tests of air-dry wood with straight grain indicated that the fatigue strength for 10,000,000 cycles (stress ratio 0.10) was about 50% of the modulus of rupture. On that basis, the fatigue strength in compression can be estimated to be at least 80% of the compressive strength parallel to the grain. These analyses can be considered conservative, since, in members so stressed, the ability of the member to carry compressive loads is not lost entirely when compression failures develop in the fibers. Members with compression failures will be strong enough to carry practically the same loads as those that produced the failure.

This is not so in tension parallel to the grain. When a tension failure develops, either in service or during test, the breakage of fiber that results means that the portion that failed is incapable of carrying further load. If the failure is complete, it means the member can carry no load. It has been reported[7] that fatigue strength in tension parallel to grain for Douglas fir and white oak for 10,000,000 repetitions of stress (stress ratio 0.10) was 50% or more of the static strength. Static tensile strength values of the Douglas fir ranged from 9,000 psi to 20,900 psi for a range in specific gravity of 0.40 to 0.55, with an average of 14,370 psi for a specific gravity of 0.47 (based on weight and volume of ovendry wood). Corresponding values for white oak ranged from 9,000 psi to 24,300 psi for a range in specific gravity from 0.54 to 0.83, with an average of 16,620 psi for a specific gravity of 0.66.

FATIGUE OF BOLTED JOINTS

The Central Research Laboratory of the AAR has been engaged in a fatigue study of bolted joints corresponding to the joints used in trestles where sway bracing is bolted to piling. While quantitative values of fatigue strength are not available because the study has not been completed, important qualitative information on the mode of failure has been obtained. The failures in fatigue in the wood members of a bolted joint are indefinite, in that the end point in test is an arbitrary one based on an enlargement of the hole in which the bolt is fitted. Repetitions of load, by increasing the size of hole, produce a joint that has more slippage than can be tolerated. As a result, it becomes necessary to repair the joint. The fatigue damage requires a maintenance expenditure but does not cause a loss in strength, and the type of failure does not endanger the structure itself.

FATIGUE OF GLUED JOINTS USED IN LAMINATED MEMBERS

Because more glued-laminated members are now used in structures than formerly, the question of the fatigue resistance of the glue and the glued joints in wood is an important consideration for repetitions of loading. A series of tests was conducted[7] that involved (1) tension parallel to grain of Douglas fir and white oak specimens, with and without glued scarf joints; (2) tension perpendicular to the grain in specimens of Douglas fir; and (3) glue shear (corresponding to stresses that can be introduced in glue lines between lamina) in laminated Douglas fir and white oak. It was concluded that, as long as proper considerations are made for any reduction in static strength, there is no greater likelihood that fatigue failures will develop in the well-made glued joints than in the wood.

In the glued-laminated shear specimens, failures occurred both under static loading and from fatigue in the wood itself, rather than in the glue line, so values obtained are significant from the standpoint of fatigue of wood in shear. Fatigue strength at 10,000,000 cycles of stress (stress ratio 0.10) was about 45% of the static strength for both species. Static strength averaged about 750 psi for the Douglas fir and 1,300 psi for the white oak. On that basis, for material of the quality included in those tests, the fatigue strength for 10,000,000 repetitions of stress would be about 340 psi for Douglas fir and 580 psi for white oak.

---

[7] "Fatigue of Wood and Glued Joints Used in Laminated Construction," by W. C. Lewis, Proceedings, Forest Products Research Soc., Vol. 5, 1951, p. 221.

THE RELATION OF FATIGUE STRENGTH TO WORKING STRESSES

While the data on fatigue of wood are admittedly incomplete, there is sufficient information available for some comparisons based on working stresses currently recommended. In any structure subjected to a large number of repetitions of stress, the engineer is interested in determining whether or not the design stresses he uses are below those that will cause either failure or excessive maintenance from fatigue produced by repetitions of stress. Wood points out[4] that, in arriving at working stresses for normal loading, factors for (1) variability, (2) duration of load, (3) a combination of other factors, and (4) the strength ratio based on the maximum defect allowed in a certain stress grade are applied to the strength of clear wood in arriving at a working stress. A working stress developed in this way gives a near minimum factor of safety of 1-1/4 to 1-1/2, with an average more nearly equal to 2 to 2-1/2.

If factor (2) and the near minimum of safety are combined, the minimum combined factor is 5/8 times 4/5, or 0.50, for normal loading; the 0.50 is equal to or less than the indicated fatigue strength for 10,000,000 cycles of stress in the following instances:

1. Bending of green, straight-grained material
2. Bending of green, 1:12 slope-of-grain material
3. Bending of air-dry, straight-grained material
4. Compression parallel to surface, green material
5. Compression parallel to surface, air-dry material
6. Tension parallel to grain, air-dry material

The values were less than the 0.5 obtained by combining the factor for duration of load and a near minimum factor of safety only in (1) bending of air-dry specimens with a 1:12 slope of grain, where the fatigue strength was indicated to be 45% of the modulus of rupture; (2) shear of artificially checked specimens with either straight grain or 1:12 slope with an indicated fatigue strength for 10,000,000 cycles of 35% of static strength; and (3) the laminated shear specimens of Douglas fir and white oak with an indicated fatigue strength for 10,000,000 cycles of 45%.

The question naturally arises: "Why was near minimum factor of safety used in the combination of factors?" Repeated loadings do not reduce the margin of safety from static loading. Tests at the Forest Products Laboratory, involving specimens loaded repeadedly in bending up to 1,000,000 times to 50% of static strength, have shown no measurable reduction in static strength. This finding is supported by tests of metal and other materials. Until actual fatigue failure starts, the strength of a material is not impaired.

All analyses in this paper are based on the fatigue strength for 10,000,000 cycles, and the results presented are based on tests wherein the minimum stress for each cycle was 10% of the maximum for that cycle. Indications are that in most civil engineering structures the number of repetitions probable in service is much less than that. Committee 7, Wood Bridges and Trestles of the American Railway Engineering Association, which cooperates with the staff of the Central Research Laboratory of the AAR, estimates that the stringers in a short-span railroad bridge will have no more than 2,000,000 repetitions of stress during the normal life of the structure. At fewer cycles of stress than 10,000,000, the fatigue strength would be a higher percentage of the static strength. Because of this, it appears reasonable to assume that fatigue resistance of timber in most applications is adequate with present design allowables. Only in the case of more severe loading, such as fully or partially reversed loading, is there doubt.

The limited amount of data available on the phenomenon of fatigue of wood, and a corresponding lack of information on the number and nature of repetitions imposed in service, suggest further research.

DISCUSSION

PAUL G. FLUCK.[8]—The concise and readable paper by Mr. Lewis is a very worthwhile contribution to the literature on fatigue. Because of the lack of an elementary textbook covering the fatigue properties of the many common engineering materials, engineering educators find papers of this type very useful.

Mr. Lewis defines fatigue as ". . .the progressive damage and failure that occur when a structure or part is subjected to repeated loads. . . ." Certainly this definition is correct but the "progressive" nature of this phenomenon often causes confusion. Before rupture begins, the effect of repeated loading is not "progressive" in the usual sense of wearing out or getting weaker or rusting or decaying. Mr. Lewis has pointed out that, "Until actual fatigue failure starts, the strength of a material is not impaired." The early stages of repeated loading must involve a "progressive" effect but it is not readily detected.

FLOYD E. SCHNEIDER.[9]—The author has written an excellent paper presenting much factual data. However, all the data that he has presented is based on tests of small clear wood specimens while the results obtained on a few full size timbers tested have been quite different.

The largest variance in fatigue testing between the small clear specimens and the full size timbers have been the results obtained in horizontal shear. The paper leaves the impression that the present design stresses for timber are satisfactory for static and repeated loading. The writer would like to point out that this is not necessarily so, especially in horizontal shear.

The S-N curve, Fig. 1, would give the impression that high shear values can be attained under repeated loading. The author also states that the fatigue strength at 10,000,000 repetitions of load for glued-laminated douglas fir is about 340 psi. A few full size glued-laminated stringers were recently tested at the AAR Laboratory and their results indicated that if the shear stresses exceed 150 psi, failure could be expected in less than 2,000,000 cycles. This is considerably less than the 340 psi indicated.

---

[8] Prof. of Mech., Univ. of Wisconsin, Madison, Wis.

[9] Structural Engr. of the A. T. & S. F. Ry., Chicago, Ill.

Due to the fact that the shear strength in wood may not be as high as commonly thought, AREA Committee #7 is requesting a research project to check shear and bending failures on both full-size sawn and laminated timbers under repeated loading. The investigation is to be conducted at the AAR Research Center with the cooperation of the National Lumber Manufacturers Association and the Wood Preservers Association.

Another aspect in the paper that should be corrected is that dealing with the "Fatigue of Bolted Joints." Mr. Lewis says quantitatave values of fatigue are not available because the report has not been completed; the preliminary study is[10] complete, however.

The author comments that slippage of a joint causes a maintenance expenditure and not a loss in strength. A joint that is slipping is certainly not as strong as one that is tight and whether it will endanger the structure depends on the location of the joint. A slipping joint in some cases might be acceptable but usually would assume that slipping joints would create a dangerous condition, and should be considered as failed in that they are usually unserviceable.

WAYNE C. LEWIS,[11] M. ASCE.—It should be noted that the study of fatigue is, at best, an empirical science and the more information that can be contributed the better will be the understanding of it.

As to Schneider's comments relative to possible low fatigue resistance in shear of large members of Douglas fir—the presence of a weak bond between occasional annual growth rings of that species has been observed in both large and small specimens to affect adversely the static and fatigue shear strength. It may be that some downward adjustment of working stress will be required to provide a margin of safety for both static and repeated stresses.

Such a reduction in working stress may well eliminate the danger of fatigue failure for there have been service failures in shear similar to those mentioned by Schneider, in which the repetitions could not have been contributory. The weak bond was indicated from both the character of the failure and the low stress imposed.

Unfortunately, because of the variability of a natural material like wood, it is difficult to predict strength properties of a single specimen accurately, and in a fatigue test, unless a control static test specimen is available as a means of estimating the strength of the fatigue specimen, it is not possible to determine whether an abnormally few or many cycles of stress before failure was due to fatigue resistance or a low or high static strength. Because in tests of large specimens it is difficult or not impossible to have an accurately matched control specimen, tests of both kinds (large and small) are necessary, one type corollary to the other.

The Forest Products Laboratory is (1961) evaluating the static strength of glued-laminated Douglas fir (with the rings oriented parallel to planes of shear) after as many as 9×10^6 cycles of 45% of the static strength. Applied stresses have ranged from 380 psi to 420 psi in shear and, to date, there have been no failures during the repetitions of load. These specimens are $1\frac{3}{4}$ in. by $3\frac{3}{4}$ in. by 43 in. and are loaded at third points of a 39-in. span. This material is air dry. Future work in the same study will evaluate other material at other moisture contents and after other exposures.

---

[10] "Static and Repeated - Load Strength of Bolted Timber Joints," AREA, Bulletin 551, June, July, 1959.

[11] Engr., Forest Service, Forest Products Lab., Madison, Wis.

The paper summarizing the fatigue tests of bolted joints[10] is a welcome addition to the information on strength of timber assemblies. It was published between the preparation and publication of the writer's paper.

AMERICAN SOCIETY OF CIVIL ENGINEERS
Founded November 5, 1852

TRANSACTIONS

Paper No. 3250

IMPACT OF COMPUTERS ON ENGINEERING EDUCATION

By Gordon P. Fisher,[1] F. ASCE

With Discussion by Messrs. William A. Boe; Francis E. Swain; Warner Lansing; and Gordon P. Fisher

SYNOPSIS

The modern electronic computer is having a significant effect on the engineering profession. This effect, naturally, is also felt in the engineering schools. In this paper there is examined the influence of the computer on (a) curriculum, (b) research, and (c) relations with engineering practice.

INTRODUCTION

The interest and attention of engineers in recent years have been caught by the startling prospect of a machine which not only will perform designs automatically and permit more accurate analysis, but do these things with great speed and with nearly complete relief from tedious and repetitive calculations. It is little wonder then that this machine, the modern electronic computer, is having a great influence on the engineering profession. This paper covers but a single and particular aspect of this influence—the impact of the electronic computer on engineering education. While the influence of computers on engineering practice has been quite significant and substantial, it is

---

Note.—Published essentially as printed here, in April, 1960, in the Journal of the Structural Division, as Proceedings Paper 2428. Positions and titles given are those in effect when the paper or discussion was approved for publication in Transactions.

[1] Assoc. Prof. of Civ. Engrg., Cornell Univ., Ithaca, N. Y.

only now that it is beginning to be felt broadly in educational circles. Thus, this appraisal is not so much a matter of recording known progress to date as it is one of speculation on the future. It is an attempt, limited by one's flair for philosophy and prophecy, to define some of the more apparent emerging problems and, where possible, to consider how to meet them with at least a skeletal policy of procedure. The University has played a uniquely important role in the invention and development of the electronic computer. Today the University finds itself in the position of being forced to respond to the profound effects of this machine, and it is rightly concerned that its response be geared to the demands of the future.

The University's own needs in research and its obligations to supply talent for this new skill and industry it has spawned require an adjustment of traditional operations. Both of these motives are reflected in practically every University function. The various facets of this general challenge will be grouped arbitrarily into five areas of concern:

1. Curriculum;
2. Research;
3. Relations with engineering practice;
4. Effects on and from other areas within the University; and
5. The computer center.

It will be readily apparent that some of the things to be discussed will fall equally well under several of these subdivisions. The present discussion is restricted to digital computers, or properly speaking, electronic automatic stored-program digital computers, which is to be understood whenever the term "computer" is used. While most of the examples to be cited are drawn from structural engineering, it is hoped that the viewpoints so limited will apply or at least afford extrapolation to engineering broadly.

CURRICULUM

Because of the many philosophical dilemmas which arise, curricular problems will require the largest share of attention. The overriding question concerning curricular policy would seem to be a decision as to whether major emphasis shall be placed on educating users of computing equipment or designers of computing equipment. Since the number of users is certain to surpass enormously the number of designers, the direction is clearly in favor of the former. What is required is more fundamental education for imaginative use of computers and less attention to detailed design of actual computer hardware. The computer is essentially a tool, and the teaching of the use of tools most remain subordinated to the teaching of principles. This fact alone sets a limit on how much can and should be done in teaching computer techniques.

It is not the duty of the University to produce finished specialists in computer design, although a few institutions with the specialized facilities and faculty may find this to be a stimulating side-interest. Rather, those undergraduate students interested in design and manufacture of computers should be provided with a general fundamental program in electronics, solid-state physics, high-speed circuitry and switching theory, mathematical logic and number theory, and other subjects necessary to technical competence. But such a program should be vested with the idea that proficiency in design can be acquired by those who wish it by later experience in the computer industry. In addition, the student should be given two things:

(1) the means for a broad appreciation of those new and promising scientific devices or principles which may form the basis for future developments in design of computers, and
(2) an opportunity to become acquainted with users and users' problems.

There is no reason to add any new technical course to the curriculum. A reorientation of subject matter within the present framework of formal technical courses should be sufficient, and in fact, much of what is required is already available. What is suggested here is a judicious pruning of course material to make room for new concepts and for firming up of fundamental ideas underlying computer design. Furthermore, whatever is taught that is especially useful to computer designers should be, at the same time, sufficiently general for wide applicability to other allied interests.

In this sense, the needs of the computer user are not really contrary to those of the designer. To be sure, the potential designer must have much more specific technical information than the user, but for both, the general principle holds true: a healthy breadth of scientific understanding fitting to the particular field of study, with computer aspects incorporated as sidelights within the regular academic program. The major change in the educational program for the user should be a shift in the attitudes of the teaching staff. As many professors as possible should inform themselves of the potentialities of computers, and this knowledge cannot help but have a natural and beneficial effect on the material taught and the manner in which it is presented. This viewpoint has been ably stated by A. S. Householder,[2] as follows:

> "---the important and lasting effect ---, the effect which it seems to me we should emphasize and encourage, is not to be measured in terms of the numbers of courses dealing directly with computers nor with the number of graduates who have had such courses. It is rather to be measured in terms of organization and accents exhibited in the standard courses. More important than the number of your graduates who can draw a flow chart is the number of your instructors who have had direct computational experience, even if only a little."

It follows readily that a formal course devoted soley to programming, coding, and other operational techniques is essentially vocational or job-training in nature, and is not academic nor particularly professional. It is therefore not desirable, although auxiliary short courses, seminars, and colloquies outside the regular program can be beneficial. On the other hand, in spite of an already crowded curriculum, serious consideration should be given to the addition on the undergraduate level of a thorough and demanding course devoted to numerical analysis, and this course should include, for maximum effectiveness, actual machine computation. Beyond this, the natural inquisitiveness of good students stimulated by the encouragement and example of a faculty knowledgeable in computer use and by the opportunity for close personal contact with computers, should be all that is necessary.

---

[2] "The Effect of Computers on the Training of Applied Mathematicians and Scientists," by A. S. Householder, Proc. of the First Conference on Training Personnel for the Computing Machine Field, Wayne Univ., Detroit, by A. W. Jacobson, Wayne University Press, 1955.

The unifying element linking the computer applications of many diverse fields of engineering is the universality of mathematics. Many educators foresee an unprecedented mathematization of engineering in coming years and are beginning to urge that undergraduate training in mathematics go well beyond the usual terminus of differential equations. Such an improvement in general mathematical scope and ability, a trend which is developing quite independently of the demands of computer usage, will be of great benefit. However, much can be done with those courses already in the curriculum. It is inconceivable, for example, that an adequate course in differential equations can be limited to solution of a few types of equations in closed form and ignore a systematic examination of numerical methods of solution for other types, those types that eventually may prove to be of the greatest interest and applicability for engineers. Certainly any increased mathematical instruction should give considerably more attention than at present is accorded to matrix algebra beyond the simple aspects of determinants taught in Freshman mathematics courses. Likewise, some attention must be given to iteration or relaxation methods, not only applications but especially the underlying mathematical principles.

The advantages of matrix analysis and iteration in the solution of simultaneous equations, especially with computers, make it a rather natural response to give preference or at least equal emphasis in technical courses to those theories or methods which lead to simultaneous equations. This response is particularly natural when the effort involved in writing the equations is small. In fact, this begins to be the case. For example, it has been a fashion until recently in teaching structural theory to de-emphasize, almost to exclusion, the method of slope deflection in favor of moment distribution for rigid frame analysis. This relative dominance was assigned for the very practical reason that moment distribution usually allows great time-savings in manual computation by avoiding the burden of solving simultaneous equations. But now, the advent of machine computation has seen the slope-deflection method dusted off and ranked in importance on a par with moment-distribution. And there is an extra dividend: a thorough treatment of slope deflection reveals its essential kinship with the classical analysis method known as consistent deformation, the practical difference being largely whether one selects the loads or the deformations as the unknowns. A shift in accents similar to that described, often with increased depth of understanding, seems possible in most areas of engineering.

Even the principles underlying some of our classical theories will require some re-examination in the light of secondary problems that arise in computer solutions. A case in point is the recent increase of concern with ill-conditioned simultaneous equations, whose solution may go wildly erratic or divergent. At best, the solution may be so much in error as to render the solution either worthless for practical use or hardly worth the effort of programming it for the computer. Special attention has been given to detecting such situations and predicting in advance of programming the magnitude of the error to be expected.[3] But beyond these purely mathematical consequences of ill-condition, it is natural to seek for deeper reasons within the theoretical physical approach itself that may have given rise to such equations in the first place. Again falling back on structural theory for example, a previous observation may be recalled that in framework analysis either the forces or the deformations may be selected as the unknowns. It has been suggested by Southwell[4] and others that Castigliano's Method of Least Work may often result in ill-conditioned equations and yield answers whose unreliability is not readily deduced.

---

[3] "Ill-Conditioned Equations and Matrices," by R. B. McCalley, Jr., presented at ASCE Conference on Electronic Computation, Kansas City, Mo., November, 1958.

The least-work method is a strain energy method which employs as unknowns the forces in arbitrarily selected members and employs as coefficients the corresponding displacements. One might test for ill-condition by making small changes in the displacements and observing the resulting changes in the forces, but deciding whether the changes are acceptable from a design viewpoint is always subject to considerable uncertainty. On the other hand, if definite external forces are selected as the constant coefficients and the displacements as the wanted quantities, as in applying Rayleigh's Principle of Minimum Potential Energy, it is extremely unlikely that ill-conditioned equations will result for a competently designed framework. For any unsuitable framework, ill-condition would be indicated by large changes in the displacements as a result of slight changes in the external loads. But in this case, it is much easier to judge that the displacements are unacceptable for design. Thus, the latter method seems preferable.

The example cited is quite typical in that the re-examination of fundamental aspects as described really does not involve the computer at all. Rather, the problem has become an object of general concern largely through a wider experience with complex systems, systems of a type seldom attacked before computers were available. This example is but one illustration of the sort of revision of basic ideas that may be prompted by use of computers and of an influence which certainly will be reflected in teaching the related subject matter.

The examples developed here are intended to be indicative rather than exhaustive, but should serve to affirm the significant influence of the digital computer on engineering curricula. The key proposition expressed is that changes in curricula necessary to meet the needs of both designers and users of computers should be largely shifts of accent rather than addition of courses directly concerned with computers. This reorientation will depend for maximum effectiveness and vitality on two things:

1. Emphasis on increased mathematical ability, particularly in the direction of numerical analysis, and
2. Wider personal participation of teaching staff in machine computation.

It is not the intention here to discourage the addition of fundamental courses where necessary. That this need is rapidly becoming more urgent has been apparent for some time, and the digital computer is yet another pressure in the same direction. From this viewpoint, reorientation of subject matter within the present curricular framework is only a minimum answer rather than the optimum. We ask for increased mathematical ability, we ask for increased sophistication in basic sciences, and yet we wish to retain equally desirable technical and humanities courses. All this in four years! The net result is a dilemma for the engineering curriculum planner. It is high time that engineering educators give serious consideration to extending the period of undergraduate education. Engineering is the only profession attempting to educate in four years. The others—law, medicine, the ministry—

---

[4] "Current Trends in Structural Research," by R. V. Southwell, Research, Engrg. Structures Supplement, Colston Papers, Vol. II London, 1949, p. 1.

require six to eight, exclusive of graduate study and internship. At Cornell University, where there is a five-year undergraduate program, some ten years' happy experience has revealed that its adoption was a wise and far-sighted decision.

RESEARCH

The second aspect of computer influence to be discussed is university research. The teaching program of a university has natural ties to its research efforts and indeed, depends upon the research activities of professors for much of its enrichment. The computer is proving to be a versatile tool which is expanding tremendously the potential scope of research. Many examples come to mind. Complex and repetitive calculations formerly prohibitive in terms of computation time are now handled with ease and rapidity. This new ability has helped to bolster the quality and scope of graduate work, particularly research theses which often suffer in the student's attempt to meet a June deadline. There is no longer any reason for graduate students to eliminate interesting problems as thesis topics solely because of the prospect of too much computation. Large amounts of data may be quickly reduced to averages and meaningful answers. Fewer assumptions and simplifications need be made; analysis may be more complex and design more refined with the same or less work than ever before. Difficult theoretical problems may be approximated by simple mathematical models and so lead step by step to a deep and detailed understanding. Experiments may be enlarged in scope and based on more complete and comprehensive data.

Indeed, the computer is especially beneficial in experimentation. It may be used to simulate processes or equipment, predicting their performance without ever building the prototype. Many devices, such as jet engines and nuclear reactors, may be designed gradually through several preliminary phases without costly prototype experiments. Machinery and structures may be optimized to find the best combination of possibly dozens of design variables in terms of final performance and cost. Optimizing by digital computer has been a boon in highly empirical situations where trial and error solution is mandatory, where previously the limited number of trials economical in manual computation gave low confidence levels in design.

One might go on citing example upon example, but these few are sufficient to show that the possibilities in research are limited only by the versatility of the human mind. It is clear that a high premium is placed on intuition and physical understanding. The computer cannot formulate problems but only follow detailed logical instructions. The computer is no substitute for intelligence. It is unlikely, for example, that Gauss could have reached his conclusions on normal distribution simply by feeding large amounts of data to a computer and waiting for something to appear. Competent, fundamentally-trained persons are, as always, uniquely necessary to important research, but their efforts can be advanced immeasurably by the modern computer. They need not be computer experts, but should have more than passing awareness of computer capabilities and should seek opportunities for personally applying their problems to the computer. One danger must be mentioned: As J. C. Hetrick has noted,[5] "a common reaction when computers are available is to assume that all problems, and even all sections of all problems, must be solved electronically." In our present passion for computers, there is an undesirable tendency for persons skilled in machine computation to look down upon their colleagues who have no such experience. This is an unfortunate attitude. It must be remembered that there will always be those persons who can make significant contributions irrespective of current fashions in scientific tools.

---

[5] "Panel Discussion on Manpower Needs and Educational Programs," by J. C. Hetrick, Wayne Univ. Conference, as noted Ref. 1, p. 32.

With the potentialities of the machine, and with the imagination and discrimination of the fundamentally-educated engineer, there is little doubt that the computer can be a tremendous stimulant to both research and its allied teaching program.

RELATIONS WITH ENGINEERING PRACTICE

The University, in addition to adjusting its curricular and research programs, must look beyond these bounds to its relationship with engineering practice. The University should stand ready to help solve those computer problems for which consulting practice and industry are not equipped, although it is not explicitly clear what form this help will take. Certainly service courses, clinics, and seminars sponsored by the University can be of major benefit to both industry and the University itself, especially as they allow interchange of ideas. There should be a strong spirit of geniality on the part of both, and on the University's part a readiness to communicate new ideas, with suggestions for their practical application.

However, the relationship between the University and engineering practice is not entirely one-sided. Industry, in its search for employees, is already beginning to place unwarranted emphasis on proficiency of graduates in computer design and use. It would be unwise for the University to give way to this clamor for increased quality and quantity of users and designers by instituting formal vocational courses in computer programming, coding, operation, and hardware building. It should insist that industry assume its fair share of training of computer personnel, especially in those areas which may be regarded as job-training, and for which industry is best equipped to give.

There is another point at which the University must stand guard. While most of the basic research leading to changes in design specifications originates within the University, practicing engineers have, and rightly so, a stronger voice in the final adoption of specifications. Practicing engineers have a large monetary investment in computer programs for design procedures based on current specifications. There are well-founded fears that they may be exceedingly reluctant to see any changes that would devalue or eliminate those programs and require extensive revisions, the more so as their competitive position is reduced. There is already enough inertia in translating research results into good design practice, and engineers in both the University and everyday practice must cooperate to avoid this possible deterrent to progress. Many traditional methods of analysis and design based on overly-simplified approximations will be gradually discarded in spite of a natural hesitancy to give up familiar procedures. In the words of Nathan Newmark,[6] F. ASCE,

---

[6] "A Revolution in Design Practice," by N. M. Newmark, Civil Engineering, May, 1958.

> "We tend [now] to use computers, because of the gain in speed or productivity, along with methods that are outmoded or at least inaccurate and undependable. . . . The next step is the development and use of more accurate analytical procedures. But we must look forward eventually to the development of more fully automated design techniques. This implies more sophisticated design criteria and more rationally based design specifications. When that time comes it will certainly be the end of the handbook engineer."

Overly-simplified methods have grown out of a desire to reduce the demands on the time and ability of the designer, but this is no longer a tenable reason for retaining them in view of the speed and refinement possible with computers. In fact, the increased computational ability with modern computers provides the University with considerable incentive to teach advanced analytical methods. The receptiveness of the profession to such refined and better methods will be hastened largely by the efforts of the University in providing fundamental technical education and in producing, thereby, competent and imaginative engineers spontaneously receptive to new ideas.

OTHER UNIVERSITY AREAS

Other areas within the University also have felt the influence of the computer. While it is not the purpose of this paper to discuss the influence of computers on fields other than engineering, brief recognition must be given to the support and nourishment which engineering stands to receive from this source. Engineers cannot afford to overlook or fail to encourage the recent advances and prospects in machine translation of languages, and in automated search and retrieval of library documents, both of which will spur research by easing particularly troublesome tasks. Of major importance is the recent stimulation of applied mathematics, and especially numerical analysis. It was not so long ago that the very term "numerical analysis" was a profanity in mathematical circles, but now it is quite an acceptable endeavor for a mathematician. Important basic research in applied mathematics is under way. Much attention has already been given to developing the laws which govern numerical analysis, since the use of discrete numbers throws out the traditional rules of algebra. Problems such as ill-condition, the distribution and propagation of errors, choice of numerical method, and choice of interval are now recognized by mathematicians as legitimate and intellectually satisfying areas for investigation. There has grown up a healthy ebb and flow of ideas between engineering and applied mathematics, and in a sense, this recent mathematical activity is a return blessing, since many of the problems first appeared in engineers' efforts at computer solution. In short, engineering education stands to gain many benefits from this interchange of computer ideas and experiences with other areas of the University.

COMPUTER CENTER

One of the really effective media within the University for exchange of ideas and abilities among the staff is the computer center, which serves to bring together people of a wide range of interests. It is therefore pertinent to examine its role in supporting the University's general educational efforts.

It is widely agreed that a single moderately large computing facility accessible to all is preferable to several small facilities duplicated and maintained by autonomous departments within the University. The computer should be easily available to personnel from all University departments, not only to professors and graduate students in carrying out their researches, but also to undergraduates as their interest and ability allows and to neighboring industries which need help in computing problems. The University computer center should be strictly educational in nature, helping users and providing consultation where necessary, but accepting no fundamental responsibility for solving problems without direct participation of the user. It is the user, in most instances, who knows most clearly the physical aspects of his problem and is the best judge of its progress and satisfaction in solution. Full participation by the user may not be expeditious for large-scale research programs or when demands on machine time approach capacity, but the computer center should never be like a soft-drink machine where the consumer puts in his dime and takes out a bottle. Such a purely accommodating service operation is not education nor will it stimulate new ideas. The delivery of computing service must be secondary to academic objectives and, consistent with this concept, the University computing center should never encourage contracts for outside computing jobs. Likewise, it is unfair and inconsistent for a University administration to insist that the computing center be self-supporting, any more than the library should be, since there will always be a consequent inclination to schedule the paid work to the detriment of the equally important unpaid. The staffing and operation of a computer center and periodic acquisition of improved machines raise serious financial problems beyond the scope of this paper. No university can treat with indifference an initial expenditure of a half-million dollars and an annual budget of $50,000. Nevertheless, any financial arrangement must be consistent with the center's function as a laboratory to support the formal curriculum and the research necessary to invigorate the teaching staff. It is most important that a dominant educational role of the computer center always be fostered.

CONCLUSIONS

It has been interesting to speculate on the influence which digital computers are having and will have on engineering education. Even these remarks serve to show that it is one of the most generally significant revolutions ever faced by engineers. In spite of the problems, financial, operational, and philosophical, there emerges a pattern of invigoration, of enthusiasm, of willingness to revise traditional thinking, of increased research potential, of deep and renewed appreciation of fundamentals. Whether or not the suppositions expressed herein stand the test of time, few persons would deny that engineering education is being impelled into an era of genuine enrichment.

DISCUSSION

WILLIAM A. BOE,[7] **M. ASCE.**—The paper by Mr. Fisher is well worth reading. Digital computers have had and will have a great effect on civil engineering. Problems that took days to solve, such as the stresses in suspension bridges due to suspender deflections, can be solved in a matter of minutes by computers. In the architectural and civil engineering offices, we find today that many engineering designs are being pulled out of graphs and tables that were tabulated by the digital computer. There will be even more of this in the future. What will become of the design engineer? Is he merely to be a "handbook" engineer? If he is, it would be more economical to hire one with no engineering training.

This writer firmly believes that there is a need for the design engineer and that he must be able to fulfill the following requirements:

1. He must be able to apply his theoretical knowledge to problems that have not been set up in the computers. The digital computer is expensive to operate and many problems can be worked more economically on hand computers. A problem that has not been programmed for the computer can usually be worked out faster by ordinary methods.

2. He must be able to use his imagination and come up with practical solutions to problems. He must be able to visualize new techniques in building, new materials with which to make his design, and to use theories that fit his design. Not all beams are supported on knife edges and all loads are not uniform or pin pointed. The theories are only as good as the assumptions, no matter how they are computed. The one comment heard most by this writer is that engineers have no imagination. Colleges and universities must assume much of this responsibility. Many professors "spoon-feed" the student instead of allowing him to work out the solutions by himself. The student's imagination must be kindled.

3. He must be able to supervise the drawing of plans and to write specifications so that the structure can be built. If the structure cannot be built, the design solution is worthless, no matter how it has been computed. A partner of a large engineering firm told this writer that he can always find a structural analyst, but that it is difficult to find an engineer who can turn out a good set of plans.

Colleges and universities should take a long look at what they want their civil engineering graduates to accomplish through their education. Very few graduates will have direct contact with programming-design calculations, while many will be called upon to draw up plans, write specifications, supervise construction, and make design computations that require no digital computers.

It was pleasing to this writer to find that Mr. Fisher did not believe that the college curriculum had to be changed to include computer design, but that an awarness of its use should be included and encouraged. All engineering graduates should have a good fundamental knowledge of the mathematics involved in computer computations.

---

[7] Structural Engr., Green Engrg. Co., Middleton, Wis.

FRANCIS E. SWAIN,[8] **M. ASCE.**—The author has presented an excellent paper which points out the resounding influence which the engineer's new tool, the electronic digital computer, is having upon the engineering profession in general and upon engineering education in particular.

Electronic computers have had a pronounced effect in many areas of the engineering profession, as the author notes. Many organizations, both public and private, have used such equipment for investigative, design, and research studies for 8 years or more. The impact upon engineering educational institutions, other than on those which have been concerned with graduate studies in the research and development of computers for some time, has been felt more recently. Some engineering schools, even now, have not installed or do not have access to electronic computing equipment, while others only recently have acquired such machines. One reason for this delay undoubtedly has been the limited funds available to many schools for the rental or purchase of a computer. Other institutions may have put off the inclusion of computing work in their curricula until definite trends and requirements in what is needed are established. As the author points out, however, the university now finds itself in the position of being forced to respond to the profound effects of the electronic computer. This pressure may, in many instances, be more than slightly discomforting. The manner in which the university responds is of utmost importance if the true functions of the institution are to be carried out in this field.

The author states that the overriding question concerning curricular policy would seem to be a decision as to whether major emphasis shall be placed on educating users of computing equipment or designers of computing equipment. The writer wonders if the paramount question concerning curricula is not so much whether designers or users should be produced, but rather how best can all engineering students be educated in the fundamental overall capabilities and potentialities of computers, regardless of whether they may go on into the development of new machines or use them to solve engineering problems. Many students, such as those taking architectural, chemical, civil, and mechanical engineering, probably would have little interest in the design of computing equipment. Such interest would lie primarily with students of electrical engineering and mathematics, depending upon whether they were interested in the design of computer hardware or the development of the logic for the machine.

The writer concurs, in the main, that no new technical courses dealing exclusively with computers need be added to the curriculum to educate either potential designers or users. There is no more reason to provide special courses for future computer designers than there is need to have such courses for potential designers of radio, radar, telemetering, or television equipment. A thorough fundamental knowledge in electronics, solid state physics, circuits, and mathematical logic should, as the author notes, suffice for all.

Engineering students can be better fitted for potential users by providing them with a good foundation in fundamentals, particularly in basic sciences and mathematics, including numerical analysis. A progressive faculty interested in and with some knowledge of machine computation is indispensable as the author points out. One important responsibility of all engineering faculties is to impress firmly upon the students that to sit before a desk-type calculator and do hundreds or thousands of computations is not to do professional engineering work. Doctors have medical technicians to run their laboratory tests and lawyers have stenographers and typists to perform the mechanical operations in the preparation of their briefs. Too many engineers have considered too long that depressing key-board buttons and reading calculator dials constituted professional engineering services. When pressed for a reason for so doing, the answer most always is, "This is the way we always have done it." Engineers must be made to know that their profession is going to acquire additional stature and prestige only through the professional use of their technical talents and training. The application of electronic computing equipment as a tool to do routine and repetitive calculations is a big step toward achieving this goal. In some instances this may not be an easy task to perform. Perhaps by constant impressions and suggestions over the longer 5-year undergraduate programs, time-worn traditions and the "way we have always done it" attitude may be changed.

---

[8] Chf., Automatic Data Processing Branch, Office of Asst. Commr. and Chf. Engr., U. S. Bur. of Reclam., Denver, Colo.

The author presents two important points in his discussion under "Research;" namely, that the computer is no substitute for intelligence, and that the computer cannot formulate problems but only follow detailed logical instructions. Due undoubtedly to catchy phrases and misinformation appearing in the popular press during the early history of computers, many engineers look upon the devices as "magic brains" or "machines that think." They were led to believe that electronic calculators were all powerful in solving all problems, and that to use such machines one had to be a member of that exclusive society which includes Einstein and von Neumann. Engineers in school and those in practice must be made to know the capabilities and the limitations of computers if they are to use the machines intelligently as powerful tools. These engineers must also be made aware that computers are most impartial; they will process nonsense as well as good information.

The writer would like to place emphasis on the author's statement that the university must look beyond the bounds of curriculum adjustment and research programs to its relationship with engineering practice. It has been the writer's experience that many practicing engineers in the field or in small design offices are not making use of computers in any manner because of their complete unfamiliarity with the machines. Remarks are often made in some such form as, "I don't know whether I have any problems that can be solved on a computer because I don't know what such machines can do." The university can fill the need for supplying such information by furnishing or sponsoring short courses, seminars, clinics, and adult education courses in appropriate areas. A true university should be of service to its complete family, not only to those still in attendance within its hallowed halls. Where such instruction can be given by industry, the university should not be called upon to serve, as the author notes. Company-sponsored classes may not be possible in many instances, however, because of the lack of trained personnel within a given organization.

The author concludes his thought provoking discourse with two important statements; namely, that the influence which digital computers are having and will have on engineering education is one of the most generally significant revolutions ever faced by engineers, and that few persons will deny that engineering education is being impelled into an era of genuine enrichment. The writer believes also that through the intelligent application of the electronic computer, the engineer himself is entering into an era which will be full of both personal and professional enrichment. High-speed computing devices give the engineer a new tool which will permit him to drop the role of numerical technician and to assume the mantle of a truly professional person.

WARNER LANSING.[9]—It is most important that engineering institutions have a clear understanding of their new responsibilities pertaining to computers. Mr. Fisher's excellent paper has "hit the mark" very well in treating this complicated topic.

It is easy to agree with Mr. Fisher when he says, in effect, that changes in curricula should be primarily a shifting of accents within courses, rather than the introduction of courses devoted to computers per se. To put it a little differently, very few engineers, proportionately, become engaged in the actual programming of analyses with which they are concerned. On the other hand, many are required to specify the particular physical problems on which they are working in such a way that they can be programmed by specialists. In a closely related situation, an engineer may be required to state his problem in such a way that it will conform to the pattern of a completely general program that is already available. In either event, this requires a somewhat more analytical approach than was developed in the usual undergraduate curriculum of the 1940's and 1950's; Mr. Fisher indicates that this situation is now (1960) in the process of change.

New emphasis must be placed on certain mathematical techniques, specifically the numerical solution of differential equations, and matrix methods. But again, the analytical approach necessary to formulate the physical problem in terms of these techniques, rather than dwelling excessively on the techniques themselves, should be the primary aim.

Based on the writer's experience one should not overly emphasize the iteration techniques in use for obtaining solutions to simultaneous linear algebraic equations and eigenvalue problems. Granted, they are essential steps in many digital computer programs, but once the engineer has mastered the fundamental concepts, the details can be best left to the professional programmer.

Mr. Fisher mentions ill-conditioned equations and the related question of whether a displacement method or a force method is more suitable for use in large scale redundant structure analyses. It is interesting to note that both methods are used extensively within the aircraft industry, and in some cases, even within the same company.

The writer has seen the force method used on many aircraft-structures analysis and can't recall ever encountering an ill-conditioned equations situation. One sets an automatic check on this in most cases, when the design is optimized. After a redundant solution is first obtained, stringer areas, skin gages, bending sections, and so forth, are modified, and additional runs are made. If the load distribution were to change drastically, and in an incomprehensible manner, one would assume an ill-conditioned set of equations to be the cause; however, the writer has never seen this happen (except as the result of ordinary mistakes).

In the case of aircraft structures, there doesn't seem to be any clear-cut advantage of the force method over the deflection method, or vice versa. A tendency has been noted, however, for stress analysts, who are primarily interested in stress distributions, to favor one of the force methods. On the other hand, the dynamic analysts, whose structural interests are confined primarily to influence coefficients, usually prefer one of the displacement methods. The writer personally believes that this is due to the fact that stress analysts are accustomed to thinking mostly in terms of forces and equilibrium, while the dynamic analysts are trained to think more along displacement lines. It goes without saying that both stress distributions and influence coefficients may be obtained in a routine fashion by either method.

---

[9] Structural Methods Group Leader, Grumman Aircraft Engrg. Corp., Bethpage, N. Y.

In actual practice one of the big problems associated with any moderately complex computer analysis is establishing confidence in the result. After all, many things can go wrong—faulty basic equations, faulty program, faulty input data. In general, an examination of limiting cases is the most convincing approach available. Obviously, each situation must be examined on its own merits, but it does seem that it is not too soon to acquaint the engineer with his responsibilities along these lines while he is still in school.

GORDON P. FISHER,[10] F. ASCE.—As the views of persons not directly associated with academic matters, the contributions of the discussers are especially welcomed in providing a broader base for considering the role of digital computers in engineering education. It is, of course, satisfying to the writer that no essential conflict of opinion has been voiced. In fact, a remarkable response to the paper has been the scores of letters, uniformly endorsing the writer's views, from persons without time to prepare formal discussion but yet interested enough to write from various parts of the United States, Latin America, and Western Europe. On the other hand, a trace of disappointment must be expressed over the lack of some opposing views with which to generate interesting arguments.

Opinions change with the passage of time and the accumulation of experience, yet in the time since the inception of the paper the writer finds himself still substantially in accord with his original notions. The only real change of attitude that has occurred is that the writer has overcome, to a large extent, his reluctance to permit computer programming, per se, as part of regular engineering instruction. He believes that it is desirable and efficient to give a formal connected treatment of digital computing and computer programming in order to have students gain as quickly as possible some computing facility, and to transmit in a deliberate way some of the philosophy of the use and capabilities of digital computers. It seems reasonable at this point of time that some exposure to the methods and discipline of digital computing as an engineering tool should be given, and indeed required, in much the same manner as elementary instruction in engineering drawing, engineering measurement, and other semi-professional skills normally associated with engineering. Such required computer instruction for all engineers should be limited, insofar as possible, and need not consume more than about one-third of a regular semester course. It has been found that a substantial start in preparing students to use digital computers may be made with about 20 hr of formal instruction in ALGOL language, and that this may be done as early as one likes in the curriculum, even in the freshman year. Within so short a time, the student can be given very little in the way of console experience, but this is no longer either desirable or necessary for ALGOL and similar languages which do not have a one-for-one command relationship to the basic machine language, making it impossible, practically speaking, for a student to sit at the console of the machine and to half-step his way through his program while de-bugging. Swain rightly points out that merely pressing key board buttons and reading registers does not constitute professional engineering. It is true that access to the console provides some incentive for a student to do digital computing, perhaps because engineers just enjoy playing with gadgets as a form of recreation, and some self-satisfaction in having a complex machine under his control. However, it has been the writer's experience that students can learn to program quite intelligently in a language such as ALGOL and understand both the machine capabilities and the logical structure of computation without ever having had console experience. Instruction with ALGOL and similar languages which are problem-oriented, rather than machine-oriented, allows the instructor to put emphasis where it belongs: on the problem, on mathematical techniques for its solution, and on the logical structuring of the solution. Beyond this, it is necessary to point out to the student that digital computation, even in a very refined and sophisticated analysis, is not an end in itself but merely a very powerful and important aid to engineering judgment and intuition. Boe has pointed out that much engineering is necessary beyond analysis and computation before a structure can be built.

---

[10] Prof. of Civ. Engrg., School of Civ. Engrg., Cornell Univ., Ithaca, N.Y.

The writer concurs in Boe's opinion that use of a digital computer is not always appropriate and that the efficacies of the sliderule and desk computer should not be overlooked. It is the duty of the instructor to point out to students those situations in which digital computation by high-speed machine is inappropriate in relation not only to the size and character of the computation, but also to the refinement of the analysis. There is still an unfortunate predilection on the part of many engineers to use computers for outmoded and approximate analyses, thereby gaining only speed and automation without increased understanding, saving money but hardly improving the structure. The new generation of engineers should know better.

Lansing has questioned the writer's opinion on the relative merits of the displacement method and the force method in handling large-scale redundant structural analyses; any bias expressed in the paper was unintentional. The method to be used depends largely on whether the displacements or the forces are most definitely known, and how the problem can be most easily formulated. And Lansing is quite correct in his opinion that there doesn't seem to be any clear-cut advantage of the force method over the deflection method, or vice versa. On the other hand, this argument has become somewhat academic due to the work of S. O. Asplund, F. ASCE on the identical formulation of the force and deflection equations, a single set of equations and associated matrix manipulations that will handle either forces or deflections, with the dividend of being able to handle mixed methods in which some of the deflections and some of the loads are known in advance. This is especially useful for statically indeterminate structures in which external loads are known but redundant forces are not, and deformations corresponding to the redundants are known (commonly zero) but other deformations are not.

The writer further agrees with Lansing's opinion that iteration techniques should not be overemphasized for obtaining solutions to simultaneous linear algebraic equations and eigenvalue problems. On the other hand, iteration techniques are mandatory for non-linear problems, such as analysis of structures in the plastic domain.

There are still many difficulties in coupling computer instruction into the broad aspects of engineering education, and still many divergences of opinion on the best way to do so, but few engineers question any longer the usefulness of computers or the wisdom of teaching their use. This is a measure of the impact that computers have had on engineering education.

AMERICAN SOCIETY OF CIVIL ENGINEERS

Founded November 5, 1852

TRANSACTIONS

Paper No. 3252

DYNAMIC EFFECTS OF EARTHQUAKES

By Ray W. Clough,[1] F. ASCE

With Discussion by Messrs. Clarence J. Derrick; George W. Housner; A. A. Eremin, John A. Blume; and Ray W. Clough

SYNOPSIS

The principal factors controlling the dynamic response of structures to earthquakes are summarized and are related to the lateral force provisions recommended for inclusion in the Uniform Building Code by the Structural Engineers Association of California (SEAOC). These provisions are seen to conform very well with the concepts of dynamic theory.

INTRODUCTION

Experience with recent earthquakes in Tehachapi, Calif. and Mexico City, Mex. has shown that it is possible to build economical, attractive structures which are highly resistant to earthquake affects. But at the same time, these earthquakes demonstrated that where the dynamic effects of earthquakes are not fully understood or properly accounted for, the results can be disastrous.

The purpose of this paper is to summarize the principal factors controlling the dynamic response of structures to earthquakes, and to relate these factors to current trends in the development of the earthquake provisions in building codes. It will be seen that the lateral force requirements recently recommended by the SEAOC take cognizance of the major factors affecting the dynamic response of structures and, thus, provide a rational basis for the design of earthquake-resistant structures.

Note.—Published essentially as printed here, in April, 1960, in the Journal of the Structural Division, as Proceedings Paper 2437. Positions and titles given are those in effect when the paper or discussion was approved for publication in Transactions.

[1] Prof. of Civ. Engrg., Univ. of California, Berkeley, California.

Before going into the details of the dynamic response theory, it will be useful to emphasize a few pertinent facts regarding the nature of earthquakes. An earthquake is, of course, simply a ground-vibration phenomenon. Since the earth is elastic in its gross characteristics, and possesses mass, it will vibrate when subjected to a shock loading just as will any other mechanical system. Thus, when a slippage occurs suddenly at a fault zone, shock waves are propagated through the earth in all directions, and when the surface manifestations of these waves pass any given point on the earth, it (and any structure located on it) will be caused to vibrate. Motions induced by the ground vibrations may have both vertical and horizontal components, but since buildings normally have considerable excess strength in the vertical direction it is customary to consider only the effects of the horizontal motions in earthquake-resistant design. It should be emphasized that the forces developed during an earthquake are not applied directly to the structure, but rather are inertia forces resulting from the motions of the structure.

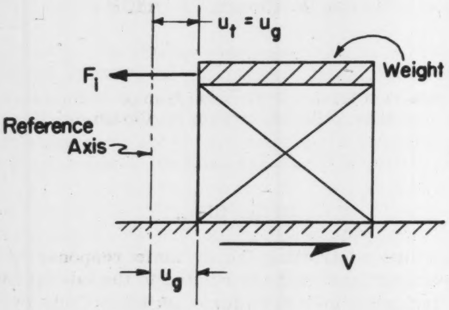

FIG. 1.—EARTHQUAKE FORCES, RIDGID STRUCTURE

EARTHQUAKE EFFECTS ON A RIGID STRUCTURE

In order to provide a suitable background for this study of the dynamic-response problem, it will be useful to consider first the effect of an earthquake on a rigid structure. Such a structure is shown in Fig. 1. It is assumed that both the building and its foundations are rigid so that the earthquake motions of the ground, u_g, are transmitted directly to the building. In this case, it is clear that an effective earthquake force, F_i, will be developed in the structure equal to the product of the ground acceleration and the mass of the structure,

$$F_i = \ddot{u}_g \frac{W}{g} \quad \ldots\ldots\ldots\ldots\ldots\ldots\ldots \quad (1)$$

in which $\ddot{u}_g$ is the ground acceleration, W denotes the weight of the structure, and g is the acceleration of gravity. For convenience, Eq. 1 is usually rearranged so that the force is given as the product of the weight of the structure and a seismic coefficient, C, which represents the ratio of the ground acceleration to the acceleration of gravity:

$$F_i = \frac{\ddot{u}_g}{g} W = C\,W \quad (2)$$

in which

$$C = \frac{\ddot{u}_g}{g} \quad (3)$$

For design purposes, it is common practice to express the earthquake force in terms of the shearing force developed at the base of the structure. In this case, simple statics show that the base shear, V, is equal to the force F_i, and is given by

$$V = C\,W \quad (4)$$

Eq. 4 demonstrates that the dynamic analysis of a rigid structure is very simple. All that is required is an estimate of the maximum ground acceleration which will occur during the earthquake. This acceleration, expressed as a ratio to the acceleration of gravity is the seismic coefficient C in the formula.

The rigid-structure concept provided the basis for the lateral-force provisions of some of the earliest earthquake codes, which specified that a structure should be designed for a certain percentage of gravity (say 10% or 12%), regardless of the characteristics of the structure. Unfortunately, the dynamic-response characteristics of actual structures are not so simple. Their flexibility and mass impart to them vibration characteristics which directly affect the magnitude of the seismic forces to which they will be subjected during an earthquake.

DYNAMIC RESPONSE OF A FLEXIBLE STRUCTURE

The effect of a structure's flexibility on its response may be discussed most easily by reference to a simple, one-story structure, as shown in Fig. 2. The weight of the structure, W, is assumed to be concentrated at the roof level. Such a structure is said to have a single degree of freedom (considering plane motion only) because only one type of deformation is possible, represented here by the displacement, u. The significant dynamic properties of this structure, in addition to its weight, are the stiffness of the columns, k, which represents the force developed per unit displacement, and the damping, c, which represents the force per unit velocity. In the explanation which follows, damping will be omitted for simplicity, but the effect of damping will be included with the final results.

In the absence of damping, the base shear in this structure may be expressed as the product of the displacement and the column stiffness,

$$V = k\,u \quad (5)$$

Dynamic equilibrium conditions (using d'Alembert's principle) show that the base shear must balance the inertia force of the mass, that is,

$$\frac{W}{g}\ddot{u}_t + k\,u = 0 \quad \text{. . . . .} \quad (6)$$

(noting the sign convention assumed in Fig. 2). It will be noted that the inertia force here depends on the total motion of the mass, rather than the ground motion, as was the case only in Fig. 1. It is convenient to express the total acceleration as the sum of the ground acceleration and the relative acceleration of the mass with respect to the ground, thus

$$\ddot{u}_t = \ddot{u}_g + \ddot{u} \quad \text{. . . . .} \quad (7)$$

Then Eq. 6 may be rewritten as

$$\frac{W}{g}\ddot{u} + k\,u = -\frac{W}{g}\ddot{u}_g = F_e \quad \text{. . . . .} \quad (8)$$

Eq. 8 is identical with that which would apply to a stationary structure subjected to an effective force, F_e, equal to the product of the mass of the structure and the ground acceleration. Thus the dynamic effects of earthquakes may be studied by considering the structure to be stationary and applying to it an effective earthquake force, F_e.

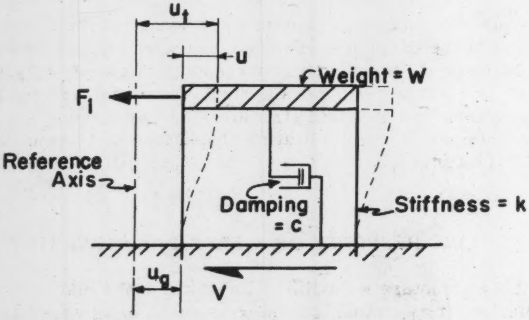

FIG. 2.—EARTHQUAKES FORCES, FLEXIBLE STRUCTURE

Now it is clear that this effective force is not directly resisted by shears in the columns; the mass must first be accelerated, and, thus, the inertia of the structure modified the dynamic effect of the applied load. The base shear, V, in this case, depends on the nature of the applied force F_e (that is, the time history of the ground acceleration) and also on the vibration characteristics of the structure. If the ground displacements were a simple harmonic motion of period T_p, as shown in Fig. 3, the effective earthquake force could be expressed

$$F_e = F_o \sin p\,t = -\ddot{u}_{go}\frac{W}{g}\sin p\,t \quad \text{. . . . .} \quad (9)$$

in which

$$p = \frac{2\pi}{T_p} \quad \ldots\ldots\ldots\ldots\ldots\ldots\ldots\ldots \quad (10)$$

In this case, the maximum (steady state) base-shear force is given by

$$V_{max} = u_{max}\, k = F_o \left[\frac{1}{1 - \left(\frac{T}{T_p}\right)^2}\right] = W \frac{\ddot{u}_{go}}{g} \left[\frac{1}{1 - \left(\frac{T}{T_p}\right)^2}\right] \quad \ldots \quad (11)$$

in which

$$T = 2\,\pi \sqrt{\frac{W}{g\,k}} \quad \ldots\ldots\ldots\ldots\ldots\ldots \quad (12)$$

is the period of vibration of the structure. From Eq. 11 it is clear that the response of the structure depends, in a very direct fashion, on the natural period of vibration of the structure, which depends, in turn, on its stiffness and weight. The base shear may be either less than or greater than that of a rigid structure, depending on how close to resonance this system is, that is, how near its natural period of vibration is to the period of the applied ground motion.

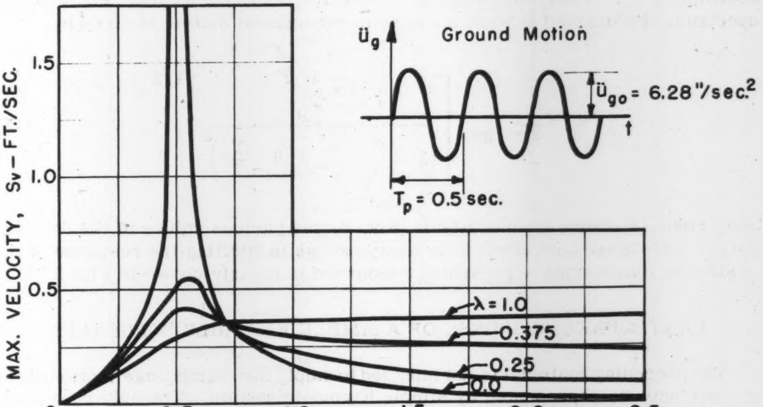

FIG. 3.—RESPONSE TO HARMONIC MOTION

It is sometimes convenient to express the response of a structure to a specific ground motion in terms of a velocity coefficient, S_v, as follows:

$$V_{max} = \frac{W}{g}\,\frac{2\,\pi}{T}\,S_v \quad \ldots\ldots\ldots\ldots\ldots\ldots \quad (13)$$

where S_v represents the maximum velocity produced in the structure by the particular motion. The velocity coefficient for simple harmonic ground motion, therefore, is given by

$$S_v = \frac{T}{2\pi} \ddot{u}_{go} \left[\frac{1}{1 - \left(\frac{T}{T_p}\right)^2} \right] \ldots\ldots\ldots\ldots\ldots (14)$$

A graph representing the variation of the velocity coefficient, S_v, with the period of vibration of the structure for a harmonic ground motion of a particular amplitude and period, is shown in Fig. 3. Such a graph is called the velocity spectrum of the ground motion because it shows the maximum velocity developed by this motion for a complete spectrum of periods of vibration of the structure.

It will be recalled that the preceding remarks refer to the response of an undamped structure. If the structure is damped, that is, if it has some form of resistance which depends on the velocity of motion, as represented by the viscous damper shown in Fig. 2, the magnitude of this damping force will also affect the response of the structure. The magnitude of the viscous damping of a system, c, is usually expressed as a ratio to a critical or reference damping coefficient, c_c. Thus, the damping ratio λ, is given by $\lambda = c/c_c$. The velocity spectrum of a damped system for a harmonic-ground motion is given by

$$S_v = \frac{T}{2\pi} \ddot{u}_{go} \left[\frac{1 + \left(2\lambda \frac{T}{T_p}\right)^2}{\left[1 - \left(\frac{T}{T_p}\right)^2\right]^2 + \left(2\lambda \frac{T}{T_p}\right)^2} \right]^{1/2} \ldots\ldots\ldots (15)$$

and, also, is shown graphically in Fig. 3, for various values of the damping ratio. The important effect that damping has in limiting the response of the system at frequencies approaching resonance is clearly shown in Fig. 3.

EARTHQUAKE RESPONSE OF A SIMPLE FLEXIBLE STRUCTURE

The preceding material is not intended to imply that earthquake motion of the ground may be represented by simple harmonic motion. The only reason for including this explanation is to emphasize, with a familiar example, the important influence of the period of vibration of the structure on its response to a given ground motion. That an earthquake is far from a simple harmonic motion is clearly shown by Fig. 4, which presents the ground acceleration measured at Taft, Calif., from the Tehachapi earthquake of July 21, 1952. The motion may be characterized best as a series of erratic, almost random, acceleration pulses. Thus, the concept of resonance which was applied to harmonic motions has no place in the treatment of earthquake response.

On the other hand, the response to an earthquake motion can be expressed in terms of a velocity spectrum, just as was described previously, if the velocity spectrum is determined properly; and, again, the response will be found to depend on the period of vibration of the structure. For a completely arbitrary ground motion, such as is represented by an earthquake, the velocity

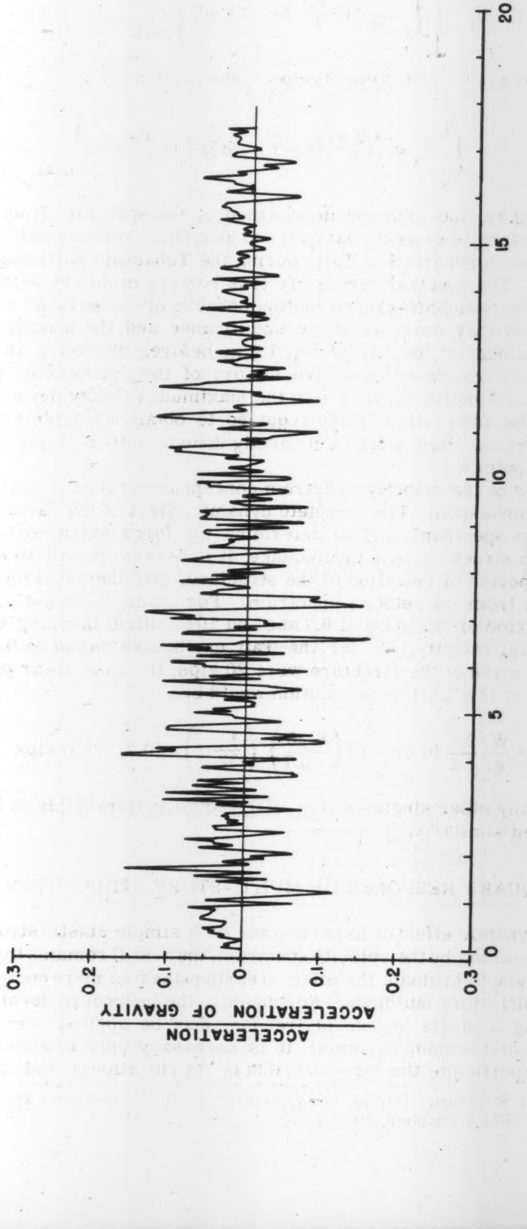

FIG. 4.—ACCELEROGRAM RECORDED AT TAFT, CALIFORNIA JULY 21, 1952 (COMPONENT N21E)

spectrum of an undamped system may be evaluated from

$$S_v = \left[\int_0^t \ddot{u}_g \sin \frac{2\pi}{T}(t - \tau)\, d\tau\right]_{max} \quad \text{. . . . .} \quad (16)$$

while for a damped system, the velocity spectrum is given by

$$S_v = \left[\int_0^t \ddot{u}_g\, e^{-\lambda\left(\frac{2\pi}{T}\right)(t - \tau)} \sin \frac{2\pi}{T}(t - \tau)\, d\tau\right]_{max} \quad \text{. . . .} \quad (17)$$

In both Eqs. 16 and 17, the primary dependence of the spectral values on the period of the structure is evident. Damped and undamped velocity spectra calculated for the motion recorded at Taft, during the Tehachapi earthquake, are shown[2] in Fig. 5. The spectral curves are less regular in this case than they were for the simple harmonic-ground motion because of the erratic nature of the earthquake, but they have the same significance and the maximum base shear can be obtained by the use of Eq. 13, as before. Since Eq. 16 (or 17) must be evaluated throughout the entire history of the earthquake, for any given period of vibration, in order to find the maximum velocity developed for that one period, the calculation effort required to obtain a complete velocity spectrum is enormous. Such work is generally done by either analog or automatic digital computers.

The importance of the velocity-spectrum concept in earthquake engineering cannot be over-emphasized. The complete dynamic effect of the earthquake is represented by the spectrum, and to determine the force which would be developed in a given structure, by a given quake, it is necessary only to evaluate the damping and period of vibration of the structure, and then find the appropriate value of S_V from the velocity spectrum. For example, if the structure of Fig. 2 had a period of vibration of 0.7 sec and 10% critical damping, the corresponding spectral velocity, S_V, for the Taft earthquake would be 0.9 ft per sec. Then, if the mass of the structure were 20 kips, the base shear produced in this structure by this earthquake motion would be

$$V = \frac{W}{g}\,\frac{2\pi}{T}(0.9) = 20\left(\frac{6.28}{0.7}\right)\left(\frac{1}{32.2}\right)(0.9) = 5.0 \text{ kips}$$

The response of any other single-degree-of-freedom system to this earthquake could be evaluated similarly.

EARTHQUAKE RESPONSE OF MULTI-STORY STRUCTURES

Although the dynamic effect of an earthquake on a simple elastic structure is completely represented by the velocity spectrum, there still remains the important question of how to evaluate the effect of earthquakes on more complex systems such as multi-story buildings. Fortunately, the procedure developed for structures having a single degree of freedom may be applied similarly to multiple-degree-of-freedom systems. It is necessary only to evaluate first the vibration properties of the structure, that is, its vibration periods and mode

---

[2] "Behaviour of Structures During Earthquakes," by G. W. Housner, Proceedings, ASCE, Vol. 85, No. EM 4, October, 1959, p. 109.

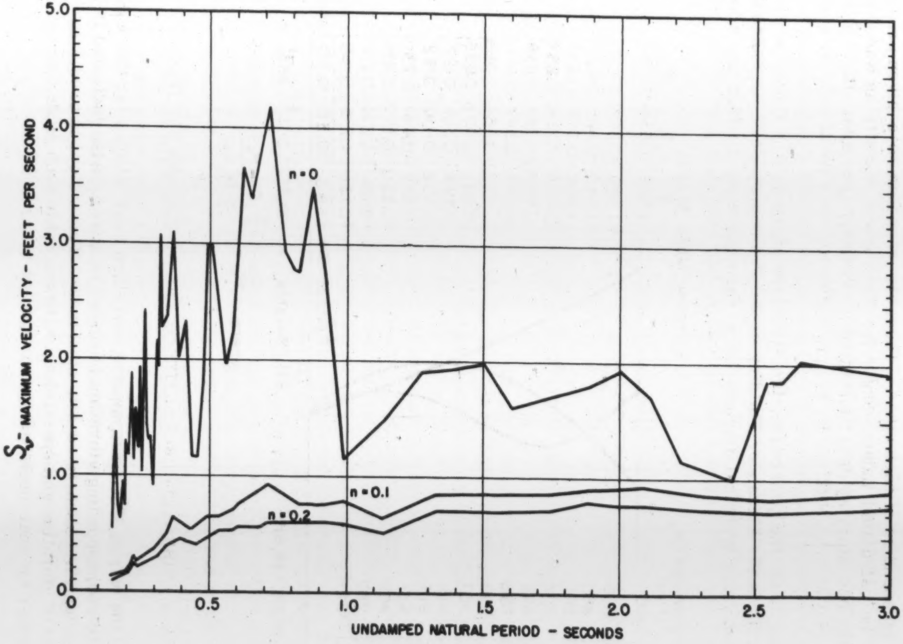

FIG. 5.—VELOCITY SPECTRUM FOR TAFT EARTHQUAKE, JULY 21, 1952

shapes. A structure may vibrate with as many different mode shapes and periods as it has degrees of freedom, and a multi-story building will have one degree of freedom for each story (considering plane motion only) if the weight is assumed to be concentrated at the floor levels. Thus a 10-story building will have ten vibration mode shapes and periods.

Now the important characteristic of these vibration modes is that they are completely independent of each other. Thus, the response to a given ground motion can be calculated independently for each mode, exactly as was described for the one-story system illustrated previously. The total effect of the earthquake may then be obtained by simply adding together the individual mode effects.

To demonstrate the procedure, the structure shown in Fig. 6 will be considered. This is the Alexander Building in San Francisco, Calif. undoubtedly the subject of more technical discussions on earthquake effects than any other

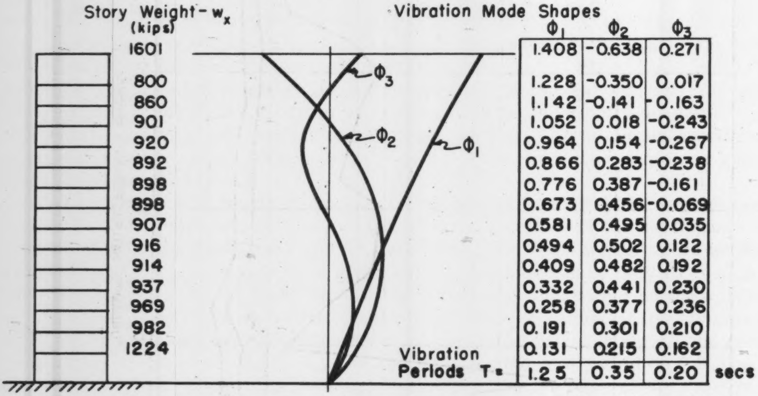

Story Weight - w_x (kips)	Φ_1	Φ_2	Φ_3
1601	1.408	-0.638	0.271
800	1.228	-0.350	0.017
860	1.142	-0.141	-0.163
901	1.052	0.018	-0.243
920	0.964	0.154	-0.267
892	0.866	0.283	-0.238
898	0.776	0.387	-0.161
898	0.673	0.456	-0.069
907	0.581	0.495	0.035
916	0.494	0.502	0.122
914	0.409	0.482	0.192
937	0.332	0.441	0.230
969	0.258	0.377	0.236
982	0.191	0.301	0.210
1224	0.131	0.215	0.162
Vibration Periods T =	1.25	0.35	0.20 secs

Total Weight = $14{,}619^k$; Eff. Weights = $10{,}377^k$ 2431^k 595^k = W_n

where $W_n = \dfrac{\left(\sum_x \Phi_{xn} w_x\right)^2}{\sum_x \Phi_{xn}^2 w_x}$

FIG. 6.—VIBRATION PROPERTIES OF THE ALEXANDER BUILDING

building in the world. The first, second, and third mode shapes for this building, and the corresponding vibration periods are shown. Also indicated is the effective weight, W_n, associated with each mode. This weight is used, together with period of vibration and spectral velocity value for each mode, to calculate the base shear for that mode, using the equation

$$V_n = \frac{W_n}{g} \frac{2\pi}{T_n} S_{v_n} \quad \dots\dots\dots\dots\dots\dots (18)$$

which is the same as Eq. 13 except that the subscript n has been added to indicate that values appropriate to the nth mode of vibration are to be used. The effective-weight for the n^{th} mode is obtained from the relationship

$$W_n = \frac{\left(\sum_x \phi_{xn} w_x\right)^2}{\sum \phi_{xn}^2 w_x} \quad \ldots\ldots\ldots\ldots\ldots \quad (19)$$

in which ϕ_{xn} represents the displacement at the x^{th} floor level in the n^{th} mode of vibration, and w_x represents the weight of the x^{th} floor. The base shear calculated for each of the three modes of vibration, using the velocity spectrum of the Taft earthquake record and assuming 10% damping, is shown in Fig. 7.

In addition to the base shear for the multi-story structure, of course, the manner in which the forces are distributed through the height of the structure is also required. In general, the force in the n^{th} mode at height x, F_{xn}, is given by the base shear for that mode multiplied by a distribution coefficient, as follows:

$$F_{xn} = V_n \left[\frac{\phi_{xn} w_x}{\sum_x \phi_{xn} w_x}\right] \quad \ldots\ldots\ldots\ldots\ldots \quad (20)$$

The distribution of forces for the three modes considered in this analysis is also shown in Fig. 6.

As was mentioned previously, the total response of the structure to the earthquake motion may be obtained by superposition of the responses calculated for each mode. Thus, if we had the time-history of the base-shear variation for each mode, the time-history of the total base shear could be determined by merely adding the individual response terms at each instant of time. However, it should be recognized that the total maximum base shear developed by the Taft earthquake cannot be obtained by merely adding the base shears shown in Fig. 6, even though each value represents the maximum force developed in that particular mode. This is because the maximum velocities represented by the velocity-spectrum values for the different periods of vibration would occur at different times during the history of the quake, and thus they do not represent simultaneous affects. Accordingly, the value obtained by direct superposition of the maximum modal forces will always exceed the true maximum forces. For example, a complete analysis of the response of the Alexander Building to the El Centro earthquake of 1940, showed[3] that the superposed modal maxima gave a base shear force which exceeded the true maximum base shear by about 28%.

Since it is possible to obtain only an approximation to the maximum response by direct superposition of the modal maxima, it is equally rational and considerably simpler to calculate only the fundamental mode response, and to increase it by a factor to account for higher mode effects. Referring again to the analysis of the response of the Alexander Building to the El Centro quake, it was found that the true maximum base shear was about 19% greater than that given by the first mode spectral-response value. This increase applies only to this particular building and earthquake, of course, but it may be considered representative of the order of magnitude of higher mode effects in tall buildings. (However, it may be noted here that increasing the fundamental mode

---

[3] "On the Importance of Higher Modes of Vibration on the Earthquake Response of a Tall Building," by R. W. Clough, Bulletin, Seismological Soc. of Amer., Vol. 45, No. 4, October, 1955, p. 289.

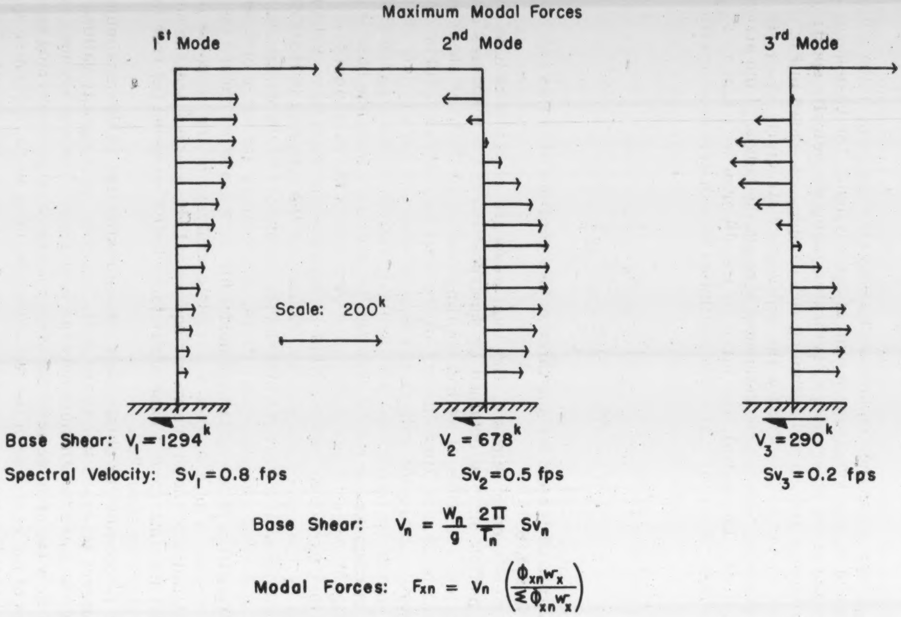
Maximum Modal Forces
1st Mode
2nd Mode
3rd Mode
Scale: 200k
Base Shear: $V_1 = 1294^k$
$V_2 = 678^k$
$V_3 = 290^k$
Spectral Velocity: $Sv_1 = 0.8$ fps
$Sv_2 = 0.5$ fps
$Sv_3 = 0.2$ fps
Base Shear: $V_n = \frac{W_n}{g} \frac{2\pi}{T_n} Sv_n$
Modal Forces: $F_{xn} = V_n \left(\frac{\Phi_{xn} w_x}{\Sigma \Phi_{xn} w_x}\right)$

FIG. 7.—RESPONSE OF ALEXANDER BLDG. TO TAFT QUAKE

response by a constant factor to account for higher mode effects is not entirely rational, because the higher modes provide different effects at different heights. A better procedure would be to add a specified fraction, say 50%, of the second and third mode maxima to the first mode maximum to obtain an estimate of the total forces developed throughout the height.)

INELASTIC RESPONSE TO EARTHQUAKES

The procedure described previously makes possible the analysis of earthquake forces in any type of structure, and would apparently provide a complete picture of the dynamic effects of earthquakes. However, when the forces due to a moderately severe quake are calculated by this procedure, it is found that they exceed, by a significant amount, the design forces which would be specified by building codes. For example, in the previously mentioned study of the response of the Alexander Building to the El Centro earthquake of 1940, it was found that the base shear was about 20% of the weight of the building. Even the relatively moderate Taft earthquake would have produced a base shear of about 10% of the buildings' weight. On the other hand, building codes would specify a value of about 3% to 5% for the base-shear coefficient for this structure. This would appear to indicate that the lateral-force provisions of building codes are quite unconservative in providing resistance to a severe quake.

At the same time, however, it must be recognized that buildings having considerably less strength than is required by modern codes have withstood rather severe quakes with only moderate damage. This apparent discrepancy may be attributed, in part, to the fact that buildings possess considerable strength in excess of the design values due to use of conservative design stresses and to the participation of non-structural elements in resisting lateral deformations. Nevertheless, this factor does not fully explain the relatively slight damage exhibited by many ordinary buildings which have gone through heavy quakes. Even more important in many cases, is the fact that, as the response of the building builds up, cracking and yielding begin to take place, and these inelastic deformations absorb a large part of the vibrational energy of the structure. As a result, the continued build-up of energy which is required to develop the maximum velocities indicated by the spectral response curves is prevented.

On this basis, it is clear that inelastic deformations of the structure are a predominate factor in limiting the forces developed in a structure by a strong earthquake. Moreover, it is evident that earthquake codes have empirically taken account of this effect, since the code provisions provide strengths which are not sufficient to resist the earthquake forces elastically. To account for this effect rationally requires that inelastic action be incorporated into the analysis, and this may be accomplished effectively only through the use of automatic digital or analog computers. A study of this type was performed[4] by J. Penzien in which he evaluated the inelastic response of a single-story system to the El Centro earthquake of 1940. A part of the results of this study is presented in Fig. 8, in a form somewhat similar to the velocity-spectrum curves discussed previously (except that maximum displacement rather than velocity is the quantity presented.) The dashed curve in Fig. 8 represents the

---

[4] "Elasto-Plastic Response of a Single Mass System Subjected to a Strong-Motion Earthquake," by J. Penzien, presented at the February, 1959 meeting of the ASCE at Los Angeles, Calif.

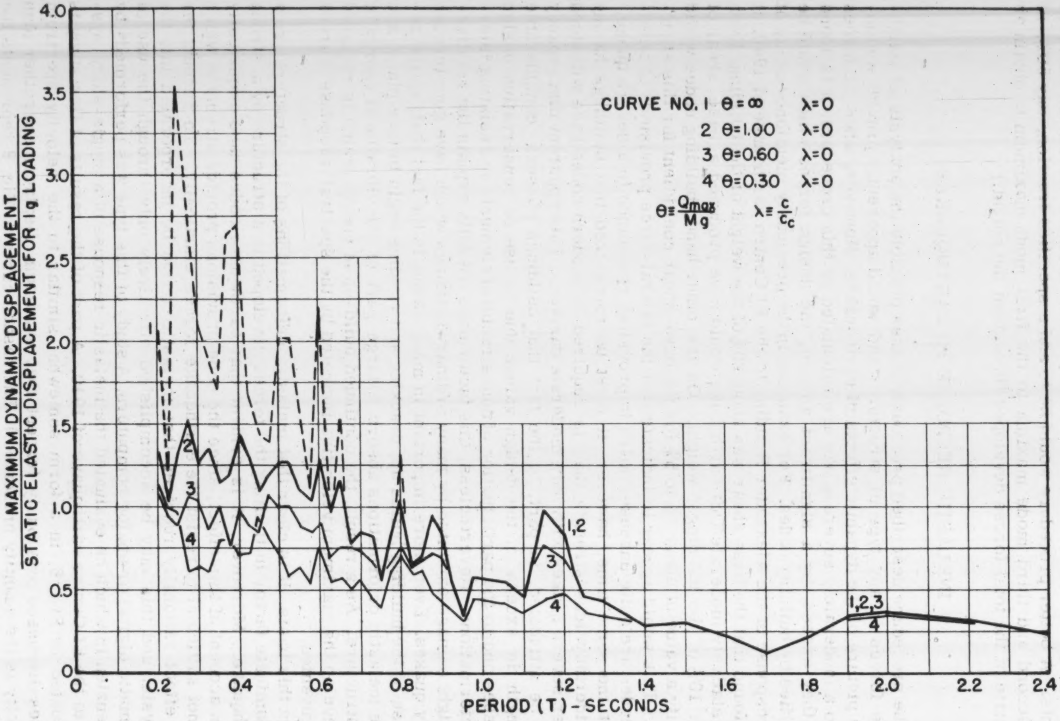

FIG. 8.—MAXIMUM DYNAMIC RESPONSE FOR EL CENTRO, CALIF. EARTHQUAKE OF MAY 18, 1940 E-W COMPONENT (FROM REFERENCE 3)

maximum elastic response of the structure for varying values of period of vibration, while the solid lines indicate the inelastic response for several values of plastic limit. This limit is represented by the parameter θ, which is the ratio of the lateral force which would initiate yielding to the weight of the structure. Thus, decreasing values of θ indicate decreasing elastic strength. The important effect that inelastic deformations have in limiting displacements is evident in this figure, since the weaker structures are seen to undergo smaller displacements.

DYNAMIC CHARACTERISTICS OF THE EARTHQUAKE

One other aspect of the earthquake-response problem should be considered herein—the dynamic characteristics of the earthquake itself. As was noted previously, the velocity spectrum depends on the nature of the earthquake motion and may be quite different for different quakes. Thus, the difficulties of establishing a standard spectrum for use in earthquake codes is obvious. However, enough earthquake records have now been obtained to establish certain general characteristics of the velocity spectra. These average characteristics were evaluated by G. W. Housner and are presented[2] in Fig. 9. Two basic points may be recognized from the curves of Fig. 9. First, comparison of curves A and B shows that propagation of the quake through the ground for a long distance not only reduces the general intensity of the motion (as might be

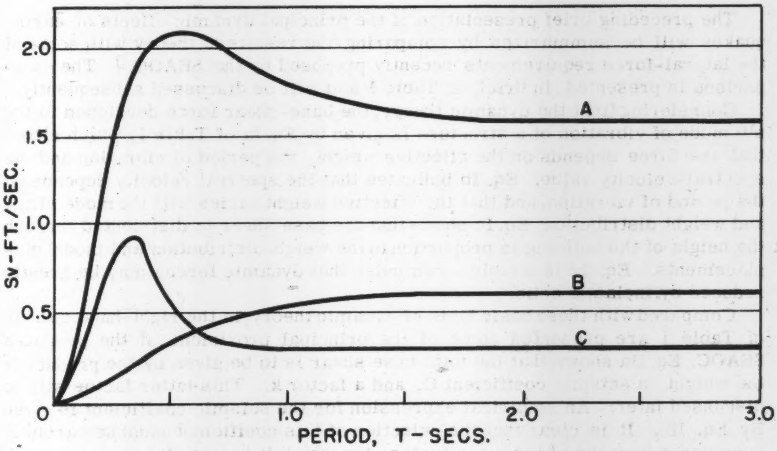

A. ± 25 Miles from center of large earthquake

B. ± 70 Miles from center of large earthquake

C. ± 10 Miles from center of small earthquake

FIG. 9.—UNDAMPED VELOCITY SPECTRUM CURVES (FROM REFERENCE 1)

expected), but of equal importance, it tends to filter out the short-period components of the motion more effectively than the long-period components. Thus, while a nearby earthquake will tend to cause the most severe damage to stiff, short-period structures, a quake at a greater distance will not affect such structures appreciably and will concentrate its effects instead on the flexible, long-period buildings.

The second basic principle is demonstrated by curve C, which shows that small, nearby quakes still further emphasize the short-period components of the motion, and thus may be expected even more exclusively to limit their damaging effects to the short-period, stiff structures. Flexible, tall buildings will show very slight effects from such local quakes.

SUMMARY

The preceding brief presentation of the principal dynamic effects of earthquakes will be summarized by comparing the results of theory with some of the lateral-force requirements recently proposed by the SEAOC.[5] The comparison is presented, in brief, in Table 1 and will be discussed subsequently.

Considering first the dynamic theory, the base-shear force developed in the n^{th} mode of vibration of a structure is given by Eq. Ia of Table 1, which shows that the force depends on the effective weight, the period of vibration and the spectral-velocity value. Eq. Ib indicates that the spectral velocity depends on the period of vibration, and that the effective weight varies with the mode shape and weight distribution. Eq. Ic shows that the base shear is distributed through the height of the building in proportion to the weight distribution and modal displacements. Eq. Id is simply a reminder that dynamic forces may be greatly reduced by inelastic action.

Compared with these basic facts of dynamic theory, in the right-hand column of Table 1 are presented some of the principal provisions of the proposed SEAOC. Eq. IIa shows that the total base shear is to be given by the product of the weight, a seismic coefficient C, and a factor k. This latter factor will be discussed later. An empirical expression for the seismic coefficient is given By Eq. IIb. It is clear that the selection of this coefficient must be carefully considered because of the many factors for which it is intended to account. A primary factor, of course, is the quantity $\frac{2\pi}{T} S_v$ (frequency times spectral velocity) and the variation of this quantity is represented in Eq. IIb by the negative cube root of the period. This, however, is only a part of the task assigned to the expression of Eq. IIb. Other factors which must be represented by the equation are the difference between the effective first mode weight, W_1 and the total weight and the influence of higher modes of vibration (because only a single mode is considered in Eq. Ia). Finally, but still of great importance, the factor C, in Eq. IIa, must take account of the energy-absorption effects of inelastic action which greatly alter the maximum response values. Accounting for all of these factors places a heavy burden on the expression of Eq. IIb, but it would appear to do the job as well as any possible choice on the basis of current knowledge.

Eq. IIc provides for distribution of the calculated base shear through the height of the building. Comparison with Eq. Ic shows that the two are identical if the vibration displacements increase linearly with height. It will be noted in Fig. 6 that the first mode for the Alexander Building is essentially of this shape. Other buildings may tend to emphasize either the shear or the flexural distortion to a greater extent but this appears to be a reasonable assumption for a typical building of tall, slender proportions.

---

[5] "Recommended Lateral Force Requirements," Seismology Committee, SEAOC, presented at the October 2, 1958 meeting of the SEAOC at Yosemite, Calif.

Finally as shown in Eq. IId, the factor k is assigned a value between limits of 2/3 and 4/3. The purpose of this factor is to account for the varying plastic-deformation capacities of different types of construction. It is evident that considerable amounts of energy must be absorbed in plastic deformations if the response of a structure is to be reduced materially below the amplitude of motion which would be developed elastically. Consequently, it is important that the structure possess adequate capacity for plastic deformation. The "k" value of 2/3 is intended to be applied to structural types which may undergo sizeable amounts of plastic deformation without suffering major damage, while the factor of 4/3 would be applied to structures which can undergo only minor amounts of plastic deformation.

TABLE 1.—COMPARISON OF DYNAMIC THEORY WITH PROPOSED SEAOC CODE

I.—Dynamic Theory	II.—Proposed SEAOC Code
a. $V_n = \frac{W_n}{g} \frac{2\pi}{T} S_v$	a. $V = k\ C\ W$
b. $S_v = f(T)$	b. $C = \frac{0.05}{3\sqrt{T}}$
$W_n = \left(\frac{\Sigma \phi_{xn}\ w_x}{\Sigma \phi_{xn}^2\ w_x} \right)^2$	accounts for: velocity spectrum effective weight higher modes inelastic action
c. $F_{xn} = V_n \frac{\Sigma \phi_{xn}\ w_x}{\Sigma \phi_{xn}\ w_x}$	c. $F_x = V \frac{w_x\ h_x}{w_x\ h_x}$
d. Inelastic action greatly affects magnitudes of dynamic forces	d. $k = 0.67$ to 1.33 accounts for varying yield capacity of different types of construction

It is apparent from the preceding remarks that current concepts regarding the lateral-force provisions of building codes have advanced considerably beyond the original rigid-structure treatment. The seismology committee which promulgated the lateral-force provisions proposed by the SEAOC has done a remarkable job of relating the practical requirements of a building code to the essential features of dynamic theory. There is still a need for extensive research on the inelastic response of structures, and further studies of the characteristics of earthquakes will be needed to define a standard earthquake. However, it is encouraging to find a proposed building code which so nearly represents the current state of the art in this rapidly developing field.

DISCUSSION

CLARENCE J. DERRICK,[6] F. ASCE.—The author's brief justification of the SEAOC proposal,[7] on the ground of consonance with the essentials of dynamic theory leaves a number of unanswered questions.

One of these is how the extremely simple expression for the basic seismic factor, "C" = $\frac{0.05}{\sqrt[3]{T}}$, which employs a single criterion, can express, simultaneously: (a) S_v which varies principally with "damping" (the variation with T being directly with the first power), (b) W_n which is a function of the distribution of mass and elasticity along the height of the structure, and not of T, (c) The "influence" of higher mode response," which, as Clough showed,[8] varies more with "damping" than with the pattern of the spectrum; and (d) "Inelastic action," which Jacobsen concluded,[9] may be represented, for "amplitudes of earthquake interest" by the results of elastic analysis, employing the concept of "equivalent viscous damping."

The simplicity of C is more perplexing when it is considered that the SEAOC proposal ignores "damping," distribution of elasticity along the height of the structure, and the influence of foundation conditions.

The author's comparison of V_n, the base shear deduced from dynamic theory with V, the base shear prescribed by the SEAOC proposal, seems to imply direct proportionality, if not approximate identity. It is evident, from the constitution of the two expressions that such implication is unreasonable. The dynamic expression is influenced by both damping and distribution of elasticity along the height of the structure. These two variables, however, are not recognized by the SEAOC proposal.

This non-recognition of damping, by the SEAOC proposal, makes difficult the rationalization of V. If some reasonable value of damping, such as 20% of "critical" is selected, the ratio of V_n/V may be established, for a given spectrum, at various periods. This ratio is not constant, being higher at shorter periods than at longer periods, the variation being from as high as 6.0 to as low as 2.0, depending upon the spectrum employed. At given periods, the ratio may be made to vary by substituting a spectrum deduced from records made on soft ground for those computed from recordings on hard ground. Since the SEAOC proposal does not recognize the influence of variations in foundation conditions, such comparisons are inconclusive.

The author places considerable emphasis upon the presumed beneficial effect of "inelastic action" without offering any adequate explanation. At present, the effect of "inelastic action" in complex multi-story buildings has not been explored, either analytically or experimentally. That such action occurs seems probable but as Jacobsen concludes, the contribution seems capable of anticipation by conventional elastic analysis, using the concept of equivalent viscous damping. The author's use of this factor as a basis for justification appears speculative. Since the SEAOC proposal contains no quantitative criteria for either "damping" or "inelastic action," such justification is not reasonable.

---

[6] Cons. Structural Engr., Los Angeles, Calif.

[7] "Recommended Lateral Force Requirements," Structural Engrs. Assn. of Calif., July, 1959.

[8] "On the Importance of Higher Modes of Vibration in the Earthquake Response of a Tall Building," by R. W. Clough, Bulletin, Seismological Soc. of Amer., Vol. 45, No. 4, October, 1955.

[9] "Frictional Effects in Composite Structures Subjected to Earthquake Vibrations," by L. S. Jacobsen, Dept. of Mech. Engrg., Stanford Univ., March 9, 1959, p. 1.

This adverse criticism applies particularly to the factor K, which the Seismology Committee of SEAOC, describes as a "bonus consideration for certain types of construction." From the explanation given in the "Introduction" to the published "Recommendations," the values of K appear to have been derived empirically. There is no suggestion of any quantitative use of "inelastic action," particularly since the values are not affected by either the nature of materials used or the manner of their interconnection.

The value of V, in the SEAOC proposal, is prescribed by the actual weight and a "seismic factor," the product, K C. Since K is established by the general type of construction, empirically, if not arbitrarily, much depends upon the precision with which C is evaluated.

The sole criterion of C is the reciprocal of the cube root of T, which is described as the fundamental free period of the structure. The precise evaluation of this sole criterion is critical. The author's statement that the SEAOC proposals "provide a rational basis for design of earthquake-resistant structures" implies satisfaction with the prescriptions for establishing the value of T.

Except for one specific type of construction, the proposal permits the designer to submit "properly substantiated technical data for establishing the period T." In lieu of such submission, the value of T may be "determined" by use of a formula,

$$T = \frac{0.05\ H}{\sqrt{D}} \qquad \ldots\ldots\ldots\ldots\ldots\ldots (21)$$

in which H is the height and D the breadth of the building, at the base, in the direction considered.

This formula does not contain, either expressly or by implication, the basic criterion for free period, the "mass/elasticity" ratio. Hence, it is not rational. Moreover, the criterial ratio, $H/\sqrt{D}$, is associated with free period in "flexure", the influence of "shear" deflection disregarded. For a specific type of structure—for example, with a "moment-resisting space frame" which, acting without interference from more rigid elements is capable of resisting 100% of the required lateral forces (defined by K and C)—the designer is required to assume that $T = 0.10\ N$, where N is the number of stories. This formula derives its dubious validity from consideration of "shear" deflection alone, the "flexural" deflection being disregarded.

This leads to some curious conclusions. For such a structure, the free period is presumed to be the same in both principal directions, regardless of the orientation of columns or direction of principal floor members. Moreover, since this type of construction, regardless of materials used or the manner of their interconnection, enjoys the lowest value of K, the value of V, identical in both principal directions, is $V = \frac{0.072}{\sqrt[3]{N}}\ W$. This indicates that the base shear is solely a function of total weight and number of stories.

Since a competent structural engineer can evaluate T, with design accuracy, from the physical peculiarities of the proposed structure and he is obliged, by Sub-section (e) to perform the most difficult of such evaluation for another purpose, there appears to be only one reason for use of a formula to "determine" the fundamental free period. It must be inferred that, in the SEAOC proposal, T is a device for controlling C and other prescriptions, within limits deemed proper. This is not unjustifiable but it is empirical and may be opinionative. It is not consonant with dynamic theory.

From the standpoint of practical design, there is some justification for establishing V, the design base shear, as a fraction of V_n, the actual maximum dynamic base shear. This was explained by Housner,[10] and is a doctrine generally accepted by structural engineers in Southern California, including the writer. This doctrine is simple, merely that the designer should consider two levels of protection rather than one. The first is minimization, if not elimination, of all damage, "non-structural" as well as structural, likely to be produced by earthquakes of "moderate" local intensity. The second is absolute protection against collapse, even at the cost of some structural failure, during an earthquake of maximum local violence, or, as Housner puts it, "extremely strong ground motion."

The "spectra" provide a simple solution. Except for variations along the distribution of T due to response of different types of foundation columns, "moderate" earthquakes have about half the damage potential of "extremely strong" earthquakes. The ratio of $\frac{V_n}{V}$ becomes 2.0.

This conclusion appears to have been reached, intuitively and empirically by code-makers, in so far as structural steel construction is concerned. By coincidence, the elastic limit of steel is about half the ultimate strength and, by keeping the "allowable working stress" below the elastic limit, there is provided a "factor-of-safety" at the "near-collapse stress" level. Hence, a steel frame building that, as Housner puts it, will "ensure that no damage result(ed) from moderate elastic vibrations" will probably possess "an adequate factor of safety against collapse in event of extremely strong ground motion", for example, by taking advantage of "inelastic action" and permitting some minor structural damage. This empirical solution does nto apply, necessarily, to all materials of construction.

In practice, the adequacy of such design depends upon the ratio, $\frac{V_n}{V}$.

If this ratio exceeds 2.0, the "factor-of-safety" against collapse is reduced. If it exceeds 2.5, for example $\frac{60,000}{24,000}$, there is no "factor-of-safety" in a structural steel frame except that provided by the still unproven contribution by "inelastic action." For ratios above 3.0, the "equivalent viscous damping ratio" used to represent "inelastic action" would have to reach values not consonant with present information. Some of the ratios indicated by comparing values of V with spectra indicate that the framers of the SEAOC proposal anticipated damping approaching the "over-damped" or "dead-beat" condition.

This has a direct bearing upon another of the author's parallels—the comparison of F_x, the "distributed base shear" of the SEAOC proposal, with F_{xn}, the dynamic counterpart. These are shown as functions of V and V_n, respectively. Hence, their ratio, $\frac{F_{xn}}{F_x} = \frac{V_n}{V}$.

---

[10] "Behavior of Structures During Earthquakes," by G. W. Housner, Proceedings, ASCE, Vol. 85, No. EM 4, October, 1959, p. 128.

Two practical problems are involved. One of these is the use of F_x as a criterion of probable story distortion, during "moderate" earthquakes, to control "non-structural" damage. It is evident that, if the ratio, $\frac{V_n}{V}$, is greater than 2.0, the computed distortion will be less than the probable maximum and "non-structural" damage may result. The ratios deduced from the SEAOC proposal indicate that extensive "non-structural" damage should be developed by a "moderate" earthquake and, that, following "extremely strong ground motion," practically nothing but a frame-work, probably severely distorted, will survive.

The other problem is more serious, in one type of building.

In the SEAOC proposal, the reduced values F_x are used to compute M, the "overturning" moment. The true value of M is the sum of the moments of the actual "equivalent inertia forces" capable of producing the maximum dynamic distortion, as maximum response. The resultants of both F_x and F_{xn} act at approximately 2/3 of the height of the structure and, from the ratio, $\frac{V_n}{V}$, the $\sum F_x h_x$ is $\frac{V_{xn}}{V}\left(\sum F_{xn} h_x\right)$. Hence, to evaluate the maximum "overturning" moment from F_x, there should be a correction factor, increasing the $\sum F_x h_x$ by $\frac{V_n}{V}$. The SEAOC proposal provides a correction factor, but it decreases the summation by $J = \frac{0.5}{\sqrt[3]{T^2}}$ with limits 1.0 to 0.33.

The factor J, in effect, lowers the position of the resultant of the reduced lateral loading, $\sum F_x$, from the position established by the assumption of "triangular distribution," for example, approximately 2/3 of the height, to as low as 2/9 H. No adequate explanation has yet been offered for this procedure.

It is the actual "equivalent inertia force" that must be considered in designing at "near-collapse stress" levels. At maximum distortion, both the normal dead and live load and the axial "overturning" load are applied eccentrically to the wall columns. In the critical first story, this eccentricity is a function of V_n, the actual maximum base shear, and not of V, the reduced quantity reflecting design for "moderate" ground motion. Moreover, this eccentric loading is applied to columns under substantial bending strain produced by the actual maximum base shear, V_n.

This combination of strain is particularly critical in tall, narrow-based buildings. It is not unlikely that, in such structures, complying with the SEAOC proposal, the response action of first story columns might terminate, abruptly and decisively, before any considerable relief could be developed by "inelastic action" in upper stores.

The aim of the Seismology Committee appears to have been production of a set of simple rules and formulas, equally applicable in all situations, and to all materials and methods of construction. In its present development, the art of aseismic design does not appear to have reached the point of such accomplishment. The author's justification of the SEAOC proposal, on the ground of consonance with dynamic theory, does not seem to warrant the strong, general approval which he expresses.

GEORGE W. HOUSNER.[11]—The author has given a very clear explanation of the dynamic effects of earthquake ground motion and of the manner in which the proposed SEAOC code provisions are related to the dynamic analysis of structures. In view of the fact that the SEAOC provisions will likely supersede those now in use, the writer would like to place on record some historical remarks about the development of earthquake codes, particularly with respect to the original Los Angeles (LA) code provisions that were adopted in 1940.

The Los Angeles provisions applied only to structures not exceeding 150 ft in height. The base shear of a structure was specified to be

$$V = \frac{0.6}{n + 3.5} W \qquad (21)$$

in which n is the number of stories of the structure and W is the total weight of the structure. This expression for V can be compared with that of the SEAOC code if use is made of the empirical formula for the fundamental period of vibration, $T = 0.1\,n$, to express n in terms of T. Table 2 compares the expressions for V and corresponding expressions for the velocity spectrum S_V, with $K = 1$. The two curves of S_V are shown in the accompanying diagram where they are drawn on a graph of the average velocity spectra.[12] The LA curve is coincident with the 40% of critical damping curve. It is seen that the SEAOC and the LA curves are similar with the SEAOC giving smaller values below $T = 0.9$ sec.

TABLE 2.—COMPARISON OF BASE SHEARS OF LOS ANGELES AND SEAOC CODES

Los Angeles	SEAOC
$V = \frac{0.06}{T + 0.35} W$	$V = \frac{0.05}{(T)^{1/3}} W$
$V = \frac{2\pi}{T} \frac{W}{g} S_V$	$V = \frac{2\pi}{T} \frac{W}{g} S_V$
$S_V = 0.31 \frac{T}{T + 0.35}$	$S_V = 0.26\ (T)^{2/3}$

It is seen that the LA code incorporates the spectrum concept but with the period not appearing explicitly. It was explained to the writer by R. R. Martel that it was felt, at the time the LA code was formulated, that expressions involving T explicitly might tend to mislead the designer into overestimating the accuracy and logic of his computations.

The distribution of shear over the height of a building was specified in the LA code to be

$$V_i = \frac{0.6}{N + 4.5} W_i \ (N \lesssim 12) \qquad (22)$$

---

[11] Prof. of Engrg., California Inst. of Tech., Pasadena, Calif.

[12] "Behavior of Structures During Earthquakes," by G. W. Housner, Proceedings, ASCE, Vol. 85, EM 4, October, 1959.

in which V_i is the shear in the i-th story from the top, W_i is the total weight above the midheight of the i-th story, and N is the number of stories above the story under consideration. The SEAOC code states that $V_i = \sum F_x$ where $F_x = V \frac{W_x h_x}{\sum wh}$ as explained by the author. The LA code was limited to buildings of thirteen stores or less. A comparison of the provisions of the SEAOC and LA codes, indicating the distribution of shears for a uniform ten-story building, with each floor and roof of equal mass, is shown in Fig. 10, with the base shear the same in both cases. It is seen that the distributions are very similar with the SEAOC curve giving somewhat smaller shears in the upper parts of the structure.

It is, thus, seen that over the range of applicability of the LA code, the provisions of the SEAOC code are essentially the same, the chief difference being that the SEAOC code gives somewhat smaller values for base shears and for the shears over the height. The SEAOC code extends the provisions to structures exceeding 150 ft in height and expresses the provisions in different language.

A new feature of the code is the prescription of different seismic factors for buildings of different types. This is an attempt to take into account the different capabilities of structures to absorb vibrational energy by plastic deformation. The writer would like to emphasize the author's statement concerning the desirability of additional study and research on this point. As illustration of this need, it can be pointed out that for a building that can absorb energy plastically, and for ground motion whose velocity spectrum is essentially constant, there is evidence that the seismic design forces should be independent of the period of vibration, if the safety factor is based on collapse. On the other hand, if the safety factor is based on some maximum stress or strain, the seismic forces should be dependent upon the period of vibration.

Since the velocity response spectrum[12,13] is now playing a large role in earthquake and explosive-induced ground shock problems, it is perhaps in order to set down for the record a brief history of its development. The first case of an attempt to determine a spectrum was in 1857, when Robert Mallet constructed a falling-pin seismometer.[14] This instrument consisted of a set of cylindrical rods of different lengths standing on end. When the earthquake strikes, the pins oscillate and some of them may fall over, thus giving an indication of the character of the ground motion. Since the oscillating pin is a non-linear, inverted pendulum, the falling-pin seismometer is actually a type of spectrum instrument which, however, suffers from the difficulty of assigning a meaning to the results.

After the great Tokyo earthquake in 1923, K. Suyehiro[15] constructed an instrument consisting of thirteen ordinary, lightly damped pendulums of different periods whose maximum amplitudes of vibration during an earthquake were recorded. This instrument was thus the forerunner of the reed-gage, and the thirteen data points given by it determine the displacement-response-spectrum. A similar instrument was later constructed by the United States Coast and Geodetic Survey, (USC&GS) Dept. of Commerce in San Francisco,

---

[13] "The Response Spectrum Technique," by D. E. Hudson, Proceedings of the 1956 World Conf. on Earthquake Engrg., Earthquake Engrg. Research Inst., San Francisco, Calif., 1956.

[14] "The Great Neapolitan Earthquake of 1857," by R. Mallet, London, 1862.

[15] "Engineering Seismology," by K. Suyehiro, Proceedings, ASCE, Vol. 58, No. 4, May, 1932.

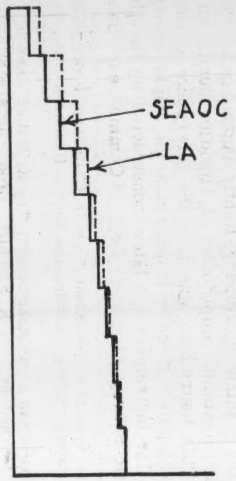

FIG. 10.—SEISMIC SHEARS TEN STORY BUILDING

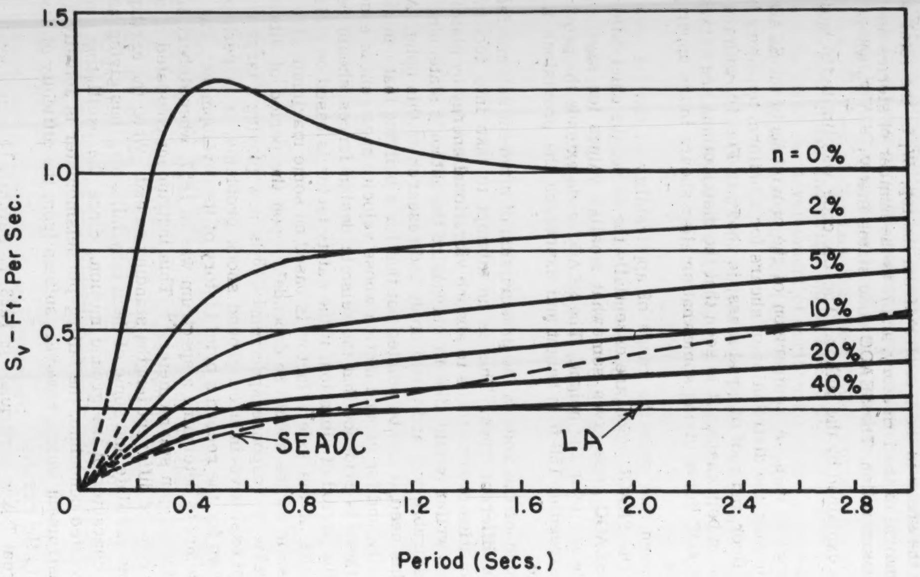

FIG. 11.—AVERAGE VELOCITY SPECTRA

and more recently similar instruments have been used in the Soviet Union by A. G. Nazarov.[16] So far as is known, no ground motion of destructive intensity has been recorded on any of these instruments.

M. A. Biot, in his Ph.D. thesis at the California Institute of Technology, (CIT) (1932) treated the dynamics of vibrating structures and later computed the undamped spectrum for one component of the Helena, 1935 earthquake. This was the first earthquake spectrum curve. It was published[17] later with some additional spectra of small earthquakes. Undamped spectrum curves were computed at the CIT for both components of the following earthquakes: El Centro, 1934; El Centro, 1940; Helena, 1935; Vernon, 10 March 1933; Sub Terminal, 10 March 1933. These are described in a paper by the writer.[18] The logical procedure would have been to compute a set of damped spectrum curves for each earthquake but the difficulties in computation forestalled this until suitable computing machines were developed. After the war, this project was undertaken on the analog computer at the CIT under sponsorship by the Office of Naval Research and spectrum curves for various amounts of damping were computed for a large number of earthquake ground motions.[19,20]

Since 1950, the availability of computing machines has made possible the ready computation of spectra and numerous spectra have been computed by various workers in this field. The USC & GS now has a special spectrum analyzer, developed by T. K. Caughey of the CIT, with which it is planned to compute the spectra of all future strong ground motions. Through collaboration between D. E. Hudson at the CIT, the USC & GS, and the National Science Foundation there have been developed and installed one hundred so-called 'seismoscopes' that will record during an earthquake the 0.75 sec period-10% critical damping point on the spectrum curves for both components of motion.[21,22] These should provide valuable information during the next destructive earthquake in the Los Angeles or San Francisco areas.

A. A. EREMIN,[23] M. ASCE.—Mr. Clough has shown an interesting analysis of the Building codes for seismic forces and forces computed from the dynamic equations for vibrated structures. The similarity of the seismic force expressions was correctly shown.

The theory of vibration of structures has a wide range of application. Therefore, applying the dynamic equations from the theory of vibration to the seismic force, the design of buildings may be considerably improved.

---

[16] "Analytical Methods of Engineering Seismology," by A. G. Nazarov, Academy of Science of Armenian SSR, 1959.

[17] "Analytical and Experimental Methods in Engineering Seismology," by M. A. Biot, Transactions, ASCE, Vol. 108, 1943.

[18] "Characteristics of Strong-Motion Earthquakes," by G. W. Housner, Bulletin Seismological Soc. of Amer., Vol. 37, No. 1, January, 1947.

[19] "Spectrum Analysis of Strong-Motion Earthquakes," by J. L. Alford, G. W. Housner, and R. R. Martel, ONR Report NR-081-095, California Inst. of Tech., 1951.

[20] "Spectrum Analysis of Strong-Motion Earthquakes," by G. W. Housner, R. R. Martel, and J. L. Alford, Bulletin, Seismological Soc. of Amer., Vol. 43, No. 2, April, 1953.

[21] "The Wilmot-Survey Type of Strong-Motion Earthquake Record," by D. E. Hudson, California Inst. of Tech., 1958.

[22] "Analysis of Strong-Motion Accelerometer Data from the San Francisco Earthquake of March 22, 1957," by D. E. Hudson and G. W. Housner, Bulletin, Seismological Soc. of Amer., Vol. 48, No. 2, July, 1958.

[23] Assoc. Bridge Engr., Calif. State Highway Dept., Sacramento, Calif.

Generally, in computing critical seismic force, the maximum magnitude of seismic shock is considered. With dynamic equations, greater precision in seismic stresses may result by considering the maximum intensity of seismic shock.

It is well known that the intensity of seismic shock varies not only with the magnitude of the nearest fault line and distance of the fault line to the structure, but also with the geologic properties of the ground at the fault line.

In Fig. 3 the graphs for spectral velocity may be changed by inclusion of the factor $\frac{2\pi}{T}$ in the expression for spectral velocity S_v. More direct graphs for seismic force will result.

The author made a valuable contribution by introducing the dynamic equations for seismic force analysis.

JOHN A. BLUME,[24] F. ASCE.—A useful summary of basic dynamic principles as applied to the earthquake response of idealized single-mass elastic systems has been presented. Mr. Clough has also considered the modal response of elastic multi-story buildings and, with the aid of the work of Penzien in inelastic response,[25] has drawn interesting comparisons to the SEAOC code.[5]

It is gratifying to the writer, as a member of the committee which drafted this code, to find the author in general agreement with the document and its various simplified approaches to the complex earthquake problem. Some word of caution might be indicated, however, to prevent those not familiar with all aspects of engineering seismology from interpreting the paper to mean that the SEAOC code might be a substitute for dynamic analysis of special or unusual structures such as high slender buildings, or buildings of marked asymmetry in plan or in elevation.

The SEAOC code is "intended to provide minimum standards as design criteria toward making buildings and other structures earthquake-resistive."[5] This carefully worded quotation from Section 2312(a) should not be overlooked. Moreover, in the introduction to the code document, the committee reports: "like any progressive building code, this is an interim code. The committee realizes there is much work to be done as the results of research and further study become available."

The SEAOC code is an advanced document which, although containing some approximations and compromise values is modern, is based on a great deal of study and structural-dynamic considerations, and is in terms and procedures which introduce new and significant parameters to earthquake codes. The main committee consisted of 16 engineers. Many others participated in sub-committees, study groups, and as code consultants. Six members of the main committee had previously served as members of the joint committee of the San Francisco Section, ASCE and the Structural Engineers Association of Northern California which proposed[26] several concepts that are now incorporated in the SEAOC Code. Thus it can be said that committee efforts leading to this present document were expended intermittently over 10 yr with thousands of man hours of volunteer time. In addition, independent but related research and analysis of the energy absorbtion value of buildings has been conducted.[27] It is perhaps no coincidence that the author finds some similarity to his dynamic considerations in view of the amount of effort, earthquake experience, and judgment applied to the CEAC Code.

---

[24] Pres., John A. Blume & Associates, Engrs., San Francisco, Calif.

[25] "Dynamic Response of Elasto-Plastic Frames," by Joseph Penzien, Proceedings, ASCE, Vol. 86, No. ST 7, July, 1960.

[26] "Lateral Forces of Earthquake and Wind," by Anderson, Blume, Degenkolb, Hammill, Knapik, Marehand, Powers, Rinne, Sedgwick, and Sjoberg, Transactions, ASCE, Vol. 117, 1952.

The data on the Alexander Building studies to which the author refers, as well as the structure's properties, are available.[28] In this connection, it must be noted that the weights and periods of the building, as shown in Fig. 6, are not in complete agreement with those determined for the prototype. The weights in kips, starting at the top level, were found to be:[28]

1.550, 0.749, 0.809, 0.850, 0.869, 0.841, 0.841, 0.847, 0.856, 0.865, 0.863, 0.886, 0.918, 0.931, and 1.173.

The periods in seconds are as follows:

Mode:	1st	2nd	3rd	4th
Parallel to Montgomery Street	1.25	0.41	0.24	0.17
Parallel to Bush Street	1.33	0.45	0.26	0.19

Although the differences are not great, they should be explained in view of the importance of this structure as a "guinea pig." Perhaps the writer has treated the building as a "shear" building rather than one that has flexural and ground rotation participation as well as shear deformation. Additional references to the structure would also be of interest since they consider, among other items, the actual response of the building to an earthquake.[27,29]

Other approaches[2,27,30,31,32] to inelastic behavior and design lead to results similar to those reported by Mr. Clough, although conditions can vary widely between buildings and between types of buildings. A big step toward obtaining agreement in the SEAOC Committee came when the concept of various types of buildings having different energy capacities and ductility values (even though designed for the same lateral forces) was introduced. This led to the variable "K" values in the code and introduced the parameters of energy absorbtion and reserve frame ductility in a new manner.

It would be possible, of course, to question certain expressions in the code from an academic viewpoint. A completely rigorous approach to some of the parameters might, and did, result in somewhat different terms. Such matters were fully recognized by the SEAOC Committee but in view of the general problem, the need for simplicity, limits to the amount of acceptable change from existing documents, and compromise measures, the terms and values were developed as shown.[5] It has been said that the camel is a horse designed by a committee. However, the camel is a very practical animal in his natural environment.

---

[27] "Structural Dynamics in Earthquake-Resistant Design," by John A. Blume, Proceedings, ASCE, Vol. 84, No. ST 4, July, 1958.

[28] "Period Determinations and Other Earthquake Studies of a Fifteen-Story Building," by John A. Blume, Proceedings, World Conf. on Earthquake Engrg., San Francisco, Calif., Chapter 11, June, 1956.

[29] "A Comparison of Theoretical and Experimental Determinations of Building Response to Earthquakes," by D. E. Hudson, Proceedings, 2nd World Conf. on Earthquake Engrg., Tokyo, Japan, July, 1960.

[30] "Effect of Inelastic Behavior on the Response of Simple Systems to Earthquake Motions," by A. S. Veletsos, and N. M. Newmark, Proceedings, 2nd World Conf. on Earthquake Engrg., Tokyo, Japan, July, 1960.

[31] "A Reserve Energy Technique for the Design and Rating of Structures in the Inelastic Range," by John A. Blume, Proceedings, 2nd World Conf. on Earthquake Engrg., Tokyo, Japan, July, 1960.

[32] "Energy Consumption by Structures, in Strong-Motion Earthquakes," by G. V. Berg and S. S. Thomaides, Univ. of Michigan Report 2881-2-P, March, 1960.

It should be noted that (1) codes must be simple to be accepted and to be used; (2) earthquake codes cannot wait for precise or scientific methods; (3) codes should not be considered as a complete answer to the design of all structures, especially these of a special or unique nature; (4) a group of dedicated men has produced a workable document with at least general consideration of structural-dynamic behavior; and (5) the SEAOC code, now adopted by the International Building Officials Conference as well as the City and the County of Los Angeles, represents, in the opinion of a great many engineers, a logical and practical minimum earthquake design procedure for typical structures. However, the need for sound engineering judgement for the effective use of this or any other code should not be overlooked.

RAY W. CLOUGH,[33] F. ASCE.—Most of the discussion of this paper was concerned with the comparison made by the writer relating the proposed SEAOC Code provisions with respect to lateral forces to the principles of dynamic theory. This is not surprising in view of the fact that the theory is long established and well accepted.

Housner's comments demonstrating the relationship between the proposed SEAOC Code and the Los Angeles code of 1940 are very illuminating, in that they demonstrate the fact that the men responsible for framing that earlier code also were cognizant of the basic requirements of dynamic theory, whether consciously or by intuition. The present proposal clearly is a product of a long process of evolution, and its creators are happy to acknowledge their debt to previous codes.[34]

The summary of the development of the response spectrum technique as applied to earthquake engineering is a valuable addition by Housner. He has, however, deemphasized his own part in this development. There is no doubt in the mind of the writer that the computation of the spectral response curves for all available strong-motion earthquake records by Housner and his colleagues[19,20] and his subsequent work in evaluating them and establishing average spectra[3] constitute one of the great steps forward in earthquake engineering, and the profession is greatly indebted to him for this fine work.

Eremin has pointed out that the spectral velocity graphs can be modified by multiplying by $2\pi/T$ to make them more directly representative of the seismic force developed in a structure. This is quite true; the resulting graph is called the acceleration spectrum, and is essentially a plot of the base shear coefficient as a function of period. However, the velocity spectrum, though less closely related to the seismic forces, seems to be a more fundamental property of the earthquake, both because it tends to be somewhat independent of the period of the structure (at least for the longer periods) and also because it bears a similar relationship to both the displacement and the acceleration spectra. For this reason, it tends to be preferred in scientific discussions of the earthquake behaviour of structures.

---

[33] Prof. of Civ. Engrg., Univ. of California, Berkeley, Calif.

[34] "Building Code Provisions for Aseismic Design," by R. W. Binder and W. T. Wheeler, Proceedings, 2nd World Conf. on Earthquake Engrg., Tokyo, Japan, July, 1960.

Blume has made many valuable comments regarding the relationship between dynamic theory and the proposed SEAOC code. As a member of the Committee that developed this proposal as well as of the Joint Committee that framed one of its most significant[26] predecessors, he is well qualified to make this contribution. His caution that the code, although based on structural-dynamics considerations, is not intended as a substitute for dynamic analysis (at least of special and unusual structures) should be emphasized again. Also, the five points listed in the final paragraph of his discussion are wholeheartedly endorsed by the author.

In reply to Blume's question with regard to the vibration properties of the Alexander Building that were used in the example analysis presented in the paper, these data were originally evaluated by E. C. Robison and J. E. Rinne, F. ASCE, in an unpublished study on the Alexander Building. Subsequently, while Robison was working with the writer, the same data were used as the basis for an investigation on the effects of higher modes of vibration on the response of tall buildings.[8] Although they differ slightly from the data presented by Blume, due to slight differences in the assumed elastic properties of the building, and although Blume's data (that were published at a later data[28]) are undoubtedly more exact, the Robison data seemed adequate to serve as the basis for an example in the present paper. In effect, the example concerns a building slightly different from the Alexander Building, but the method of analysis is correct as presented.

The discussion by Derrick seems to be intended primarily as a criticism of the proposed SEAOC code and seems to go somewhat beyond the scope of the paper, that was limited to a comparison of the basic provisions of the code with the requirements of dynamic theory. Blume's comments, referred to previously, serve to answer many of Derrick's complaints in general terms. One specific point raised by Derrick that seems to justify further discussion is his contention that the effects of inelastic action can be predicted by an elastic analysis and a suitable viscous damping coefficient. As Derrick himself points out later in his discussion, such analyses would require damping values approaching the "overdamped" condition to obtain agreement between theory and observation. Furthermore, it clearly is incorrect to say that the effect of inelastic action has not been explored in view of the many recent papers on the subject.[30,31,32,35] It would be foolish to assume that the problem is completely solved, but sufficient evidence is available now to convince the writer that inelastic action is an extremely important aspect of the earthquake response problem, and one that cannot be treated adequately by assumption of any viscous damping coefficient.

Another point in Derrick's discussion that deserves comment is the question as to the validity of the formula for computing the period of vibration of the structure. The writer certainly does not wish to claim that this formula can be expected to give accurate predictions of the period for all possible structural configurations, and he doubts that the members of the Committee that proposed the code would make excessive claims for it. However, it does seem important to relate the seismic coefficient to the period of vibration, regard-

---

[35] "Elasto-Plastic Response of Idealized Multi-story Structures Subjected to a Strong-motion Earthquake," by J. Penzien, Proceedings, 2nd World Conf. on Earthquake Engrg., Tokyo, Japan, July, 1960.

less of how difficult it is to express the period in a form suitable for code purposes, rather than merely to list a number of empirical base shear coefficients for different forms of structures. As was stated by R. W. Binder, F. ASCE, and W. T. Wheeler,[34] F. ASCE, "it was felt that if the Code were based on a period concept, new and better methods of determining periods of a structure could and would be developed." Obviously, no seismic code can take account completely of all the requirements of dynamic theory, but the writer believes that the Seismology Committee of the Structural Engineers Association has done an admirable job of relating theories to practice.

AMERICAN SOCIETY OF CIVIL ENGINEERS
Founded November 5, 1852
TRANSACTIONS

Paper No. 3253

LONG SPAN PRESTRESSED CONCRETE FOLDED PLATE ROOFS

By John C. Brough, Jr.,[1] M. ASCE, and B. H. Stephens, Jr.,[2] A. M. ASCE

With Discussion by Messrs. A. A. Eremin; and John C. Brough, Jr., and B. H. Stephens, Jr.

SYNOPSIS

The design and construction of long span prestressed concrete folded plate structures are presented herein. The economics of such design is indicated by including actual construction costs of four roof structures. A simplified design procedure is outlined and a typical case presented. Field experience with construction methods utilized and recommendations for field inspections are included based on the authors' observations.

INTRODUCTION

The design and construction methods utilized for creating low cost, long span, fire resistant roof structures are presented. It is generally agreed that building costs must be reduced to the minimum, yet the continuing demand for longer spans usually results in pushing cost ever upward.

It has also been recognized that in order to obtain longer span construction, the shape of the structure becomes a dominant factor. The proper utilization of shape for economical usage of material can and does result in enhancing the esthetic value. The full utilization of the structural shape eliminates the addition of superfluous embellishment that can become quite expensive.

Note.—Published essentially as printed here, in October, 1960, in the Journal of the Structural Division, as Proceedings Paper 2630. Positions and titles given are those in effect when the paper or discussion was approved for publication in Transactions.

[1] Cons. Engr., Memphis, Tenn.

[2] Assoc., John C. Brough, Jr., Cons. Engrs. Struct., Memphis, Tenn.

The folded plate shape of roof structure has come into wide usage because of its low cost of construction for long span, high load carrying capacity, rigidity, and because it furnishes esthetic interest. Selection of concrete for the shell material furnishes a high degree of fire resistivity, ease of molding to the desired alinement and profile, a great degree of permanence, and low construction and maintenance costs.

The decision for utilizing concrete narrows is the remaining problem to that of obtaining the most economical usage of materials that will provide the required loading capacity. The profile of the folded plate roof has an important bearing on the economy of the structure. This corrugated configuration can, however, have many variations to accomplish the requirements of the construction. Each must meet the needs of its span conditions, that is simple span or multiple span with varying conditions of continuity.

Let us consider, for example, a simple span of $62\frac{1}{2}$ ft in which we shall arbitrarily assume a column spacing along the ends of this longer span of, say, 23 ft. The slope of each plate will be assumed to be $3\frac{1}{2}$-on-12, vertical to horizontal (Fig. 1). A trial analysis will indicate this corrugated configuration to be unsuitable for conventionally reinforced concrete due to the very small area of concrete available at the ridge, causing high compressive stresses and a very high percentage of steel reinforcement necessary. This can primarily be attributed to the shallow ratio of depth from ridge to valley for the long span of $62\frac{1}{2}$ ft and the absence of sufficient concrete area in the ridge.

Several remedies for this condition become readily apparent. These could be (1) to steepen the slope of the plate and add a third plate horizontally at the ridge to provide sufficient concrete area to reduce the high compressive stresses, (2) to steepen the slope of the plates in order to provide a deeper section from ridge to valley, (3) to provide a combination of each of those stated in (1) and (2), or (4) prestress the structure to utilize all of the concrete area as a homogeneous section.

This paper shall advance a method of analysis for the design of post-tensioned prestressed concrete folded plate structures. The entire cross-sectional area of concrete of each plate will thus be utilized for flexure as a homogeneous section.

The design of the structure is more easily understood with the assumption of one individual leaf isolated from the others (Fig. 2). Consider the plate oriented in its working position and compute its section properties about the horizontal axis extending through its center of gravity.

Notation.—The letter symbols adopted for use in this paper are defined where they first appear, in the illustrations or in the text, and are arranged alphabetically, for convenience of reference in the Appendix.

DERIVATION OF FORMULA UTILIZED

Fig. 2 indicates the terms used in the following presentation. The formulas used in the design will be derived. The moment of inertia of an inclined plate on a horizontal axis taken thru c. g. of section is derived as follows:

$$d_A = t\ d_x \qquad \text{(1a)}$$

$$d_Y = \frac{a}{12}\ d_x \qquad \text{(1b)}$$

$$d_x = 12/a\ d_y \qquad \text{(1c)}$$

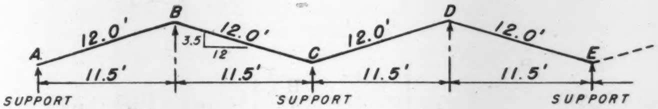
A
B
C
D
E
12.0'
12.0'
12.0'
12.0'
3.5
12
11.5'
11.5'
11.5'
11.5'
SUPPORT
SUPPORT
SUPPORT

FIG. 1.—TYPICAL CROSS SECTION THROUGH MULTIPLE FOLDS

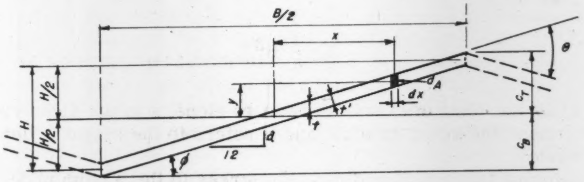
B/2
x
θ
H
H/2
H/2
y
d_A
dx
t'
t
d
12
φ
c_T
c_B

FIG. 2.—SECTION PROPERTIES OF ONE FOLDED PLATE

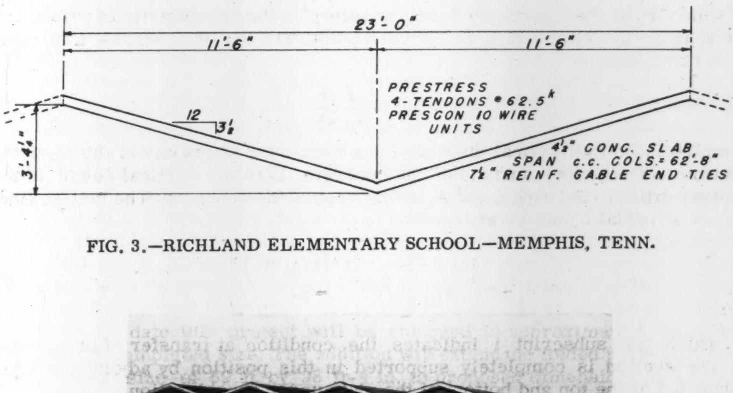
23'-0"
11'-6"
11'-6"
PRESTRESS
4-TENDONS @ 62.5^k
PRESCON 10 WIRE
UNITS
12
3½
3'-4¼"
4½" CONC. SLAB
SPAN c.c. COLS.= 62'-8"
7½" REINF. GABLE END TIES

FIG. 3.—RICHLAND ELEMENTARY SCHOOL—MEMPHIS, TENN.

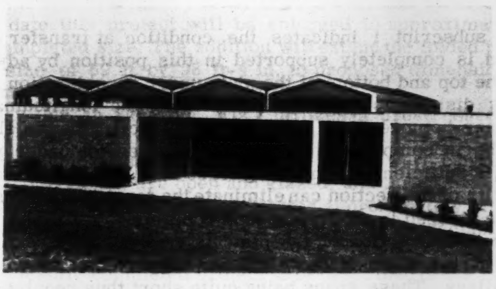

FIG. 4.—FRONT ELEVATION OF RICHLAND ELEMENTARY SCHOOL

$$I = \int_{-H/2}^{+H/2} y^2\, t\, dx = \int_{-H/2}^{+H/2} y^2 \left(t\, \frac{12}{a}\right) dy = \frac{12\, t}{a} \int_{-H/2}^{+H/2} y^2\, dy \quad . . . . (2a)$$

and

$$I = \frac{12t}{a} \left[\frac{y^3}{3}\right]_{-H/2}^{+H/2} = \frac{12\, t}{a}\left[\frac{\left(\frac{H}{2}\right)^3}{3} + \frac{\left(\frac{H}{2}\right)^3}{3}\right] = \frac{12\, t}{a}\left[\frac{H^3}{24} + \frac{H^3}{24}\right] \quad . . . . (2b)$$

from which we obtain

$$I = \frac{t}{a} H^3 \quad . . . . (3)$$

in which t' is the slab thickness normal to slope, a is the slope rise on 12, t is the vertical thickness of slab, and H refers to the height valley to ridge center to center.

The tensioning force required for zero stress in the bottom under working load, midspan is[3]

$$F = \frac{M_{tl}}{e + k_t} \quad . . . . (4)$$

in which F is the prestress force, e refers to the eccentricity of prestress force from the c. g. and k_t is the kern point. The top fiber stress, mid-span at working load is

$$f_{ct} = \frac{F\, H}{A_c\, C_b} \quad . . . . (5)$$

in which C_b is the vertical distance from the center of gravity of the concrete section to the bottom surface of the concrete, H is the vertical height of the section valley to the ridge, and A_c is the area of the concrete. The bottom fiber stress at initial condition at transfer

$$f_{cb} = \frac{F_i}{A_c}\left[1 + \frac{e - \left(M_{dl}/F_i\right)}{k_t}\right] \quad . . . . (6)$$

in which the subscript i indicates the condition at transfer of prestress.

The section is completely supported in this position by adjoining leaves connected at the top and bottom of the plate under consideration.

The stress distribution acting axially along the longitudinal axis is the same as for any homogeneous beam, that is, rectangular in shape. The top surface will be in compression, the bottom in tension under gravity loads. Application of a sufficient prestressing force at a suitable distance below the center of gravity of the section can eliminate the tension stresses. This is the same principle utilized in all prestressed concrete.

The transverse direction of the plate is analyzed as a continuous slab of length equal to the width of the plate and supported at the fold lines of the ridges and valleys. These spans being quite short thus require only nominal steel reinforcing as dictated by slab thickness and bending moment. Distribution bars are provided in the longitudinal direction in an amount ordinarily utilized for temperature steel.

---

[3] "Design of Prestressed Concrete Structures," by T. Y. Lin.

The prestressing tendons extending in the longitudinal direction of the plate are draped parabolically to locate the center of force at or above the lower kern point at the ends of the span. This will prevent the occurrence of top tension in the concrete at the ends of the span.

The eccentric force application by the prestressing-steel chambers the section along its longitudinal axis, offsetting the deflection normally present in conventionally reinforced concrete. The resulting camber supports the plate in its geometrical position, thus eliminating critical secondary stresses caused by rotation of the ends at the supports that would be inevitable with deflections encountered in conventionally reinforced concrete. Reductions of the plate action deflections along the ridges and valleys permit analysis of the transverse slab by moment distribution with a reasonable degree of accuracy.

The ends of the plates behind the anchorage are thickened to provide for distribution of the concentrated force applied by the tendons. Additional reinforcing in the form of transverse and tie steel is provided in the area immediately behind the tendon anchorages to resist the bursting of the concrete created by the prestress force.

The end leaves of a transverse section through the structure must be provided with tension ties to resist the horizontal force component. This may be accomplished by providing a tie beam, gable wall or other means, at or near the supports, that is adequate for resistance of the horizontal reaction.

Construction methods utilized for forming, steel placement, concrete placement, curing and protection, tendon tensioning, and grouting follow the normal construction techniques.

The authors have four projects completed to date (1960), utilizing post-tensioned, prestressed, cast-in-place concrete folded plate designs. The earliest was a roof structure for the Richland Elementary School for the Memphis, Tenn., Board of Education (Fig. 3). This building was designed in 1956, and constructed in 1957. A photograph of the complete building is shown in Fig. 4. An addition, including additional folds to the prestressed concrete folded plate roof over the cafetorium is under construction (1960).

The Memphis Art Academy also utilized the methods described in this presentation (Figs. 5 and 6). The prestressed folded plate roof covers the third floor and is located approximately 50 ft above the first floor. Shoring had to be provided for the entire height in order to construct this structure in place. At some future date this project will be enlarged to approximately four times its present completed size. The addition will extend the folded plate roof from its present size of 69 ft by 98 ft-4 in. to proposed dimensions of 320 ft by 98 ft-4 in. and cover an entire fine arts center.

The Holiday Inn in Sarasota, Fla., utilizes a prestressed folded plate roof over the one story private club facilities (Fig. 7). A different exterior appearance was achieved as the ends of the roof folds were cantilevered beyond the end walls, the gables are open and glazed, and thrust being taken by tension ties between supporting columns located approximately 3 ft below the low point of the valleys. The valley frequency of 15 ft is appreciably shorter than the other projects being described.

The most recently completed project to be described is the Richland Junior High School (Figs. 8-10) for the Memphis Board of Education. This project provides the largest area covered (to 1960) by means of the methods described

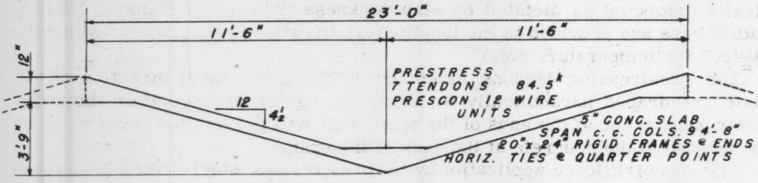
23'-0"
11'-6"
11'-6"
12"
3'-9"
12
4½
PRESTRESS
7 TENDONS 84.5k
PRESCON 12 WIRE
UNITS
5" CONC. SLAB
SPAN c.c. COLS. 94'-8"
20"x24" RIGID FRAMES @ ENDS
HORIZ. TIES @ QUARTER POINTS

FIG. 5.—MEMPHIS ACADEMY OF ARTS—MEMPHIS, TENN.

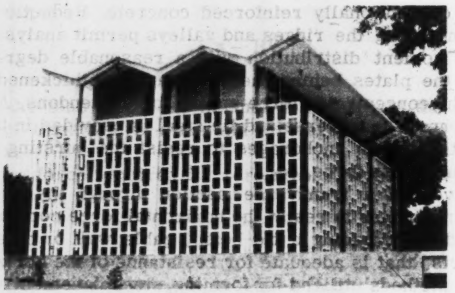

FIG. 6.—MEMPHIS ART ACADEMY

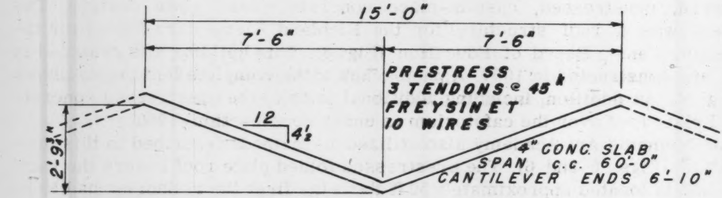
15'-0"
7'-6"
7'-6"
2'-9¾"
12
4½
PRESTRESS
3 TENDONS @ 45k
FREYSINET
10 WIRES
4" CONC. SLAB
SPAN c.c. 60'-0"
CANTILEVER ENDS 6'-10"

FIG. 7.—HOLIDAY INN, SARASOTA, FLORIDA

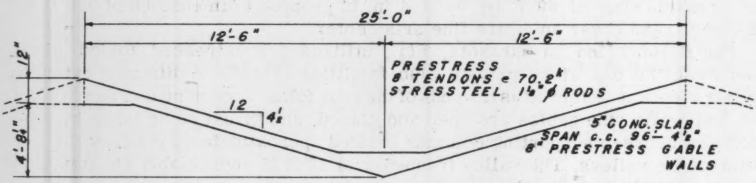
25'-0"
12'-6"
12'-6"
12"
4'-8¼"
12
4½
PRESTRESS
8 TENDONS @ 70.2k
STRESSTEEL 1⅛" ø RODS
5" CONC. SLAB
SPAN c.c. 96'-4½"
8" PRESTRESS GABLE
WALLS

FIG. 8.—RICHLAND JUNIOR HIGH SCHOOL—MEMPHIS, TENNESSEE

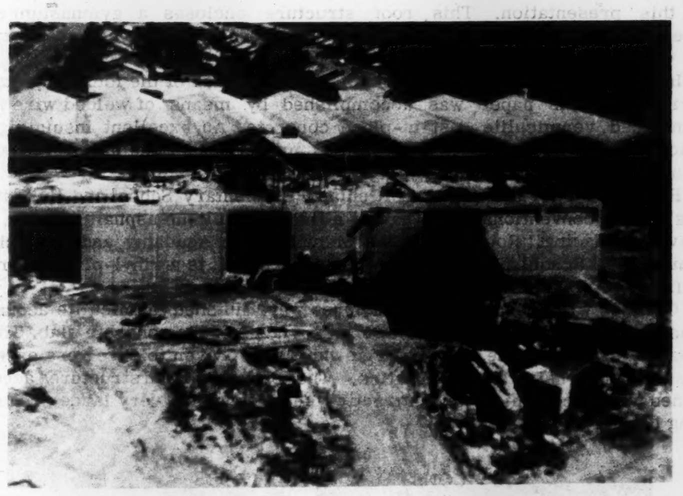

FIG. 9.—EXTERIOR VIEW OF FOLDED PLATE ROOF UPON COMPLETION OF CONCRETE PLACING. RICHLAND JUNIOR HIGH SCHOOL

FIG. 10.—INTERIOR VIEW OF UNDERSIDE OF FOLDED PLATE ROOF IMMEDIATELY AFTER FORM REMOVAL. RICHLAND JUNIOR HIGH SCHOOL

in this presentation. This roof structure encloses a gymnasium and a cafetorium. The span is $96\frac{1}{2}$ ft and slab thickness of 5 in. was necessary for the valley frequency of 25 ft.

Insulation of the folded plate roof slabs on each of the four projects described in this paper was accomplished by means of welded wire mesh reinforced vermiculite cast-in-place concrete. An excellent insulating coefficient was obtained by using a mix proportion of one part portland cement to six parts of vermiculite aggregate.

Roofing materials for the Richland Elementary School and Holiday Inn was of the conventional type having a five-ply built-up asphalt and felt, with gravel surfacing. Roofing for the Memphis Art Academy and the Richland Junior High School projects was "Cocoon," which is a vinyl-plastic sprayed on finish. Color selected was white.

Ceilings within each of the structures were finished vermiculite acoustical plastic applied directly to the bottom surfaces of the concrete slab. Thus, a pleasing esthetic value was achieved which was proven to have very excellent acoustic absorbsion characteristics. The total completed structures accomplished very economical and attractive enclosures for very large areas with long clear spans.

CONSTRUCTION METHODS

Forming was accomplished by utilizing steel scaffolding of the demountable type. For shoring to the ground, wood trussed rafters were placed on top of this scaffolding (Fig. 11). The trussed rafters simplified the erection of the straight gable shape of each bay. The deck was placed, using $\frac{3}{4}$ in. plywood applied directly to the top of the wood trussed rafters. The design considerations for dimensioning the structure to use full size sheets of plywood realized maximum economy in forming.

Reinforcement placing was handled in the conventional manner with variation in placing sequence. Bottom layer reinforcement was the longitudinal distribution steel, supported on slab bolsters extending from valley to ridge. The slab's positive moment reinforcement, extending transversely, was placed on top of the distribution steel. The prestressing tendons were placed directly on top of the bottom steel and tied to the bottom mat at the correct location in the leaf. Tendons were draped in parabolic curves (Fig. 12) spaced 3 in. on center at the center of the long span and raised to locate the center of prestress force at the bottom kern point at the ends. The bottom tendon extended straight through at the valley. After all tendons were placed, the end bearing plates were substantially anchored to the end form. All cable sheaths were carefully examined to repair any separation or indentation that could permit leakage of cement mortar and hamper elongation of the prestress reinforcement. The reinforcing bars for slab negative moments at the valleys and ridges, stirrup ties and grids for resistance of bursting of concrete at the end anchorages were placed last. Fig. 13 shows the placement of prestress tendons, anchorage plates, and conventional reinforced steel at a valley support location.

Prestressing tendon couplers that were necessary for the long cables were arranged in a staggered pattern as shown in Fig. 14. Concrete placing was accomplished with concrete slumps ranging from 2 in. to 3 in. Vibration was

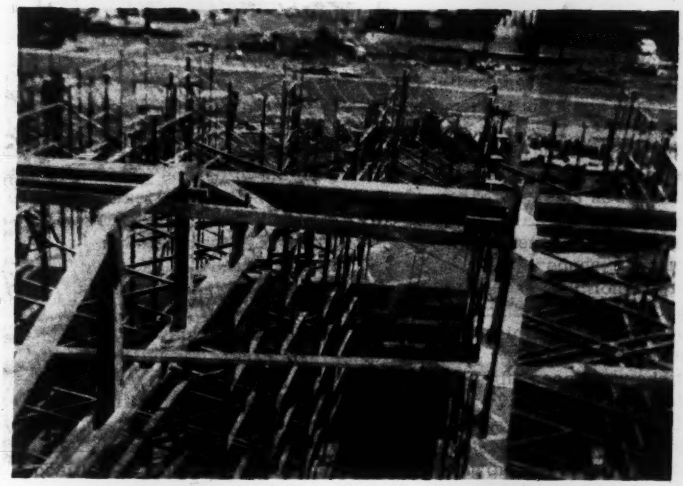

FIG. 11.—SCAFFOLD SUPPORT OF FORMING FOR RICHLAND JUNIOR HIGH SCHOOL

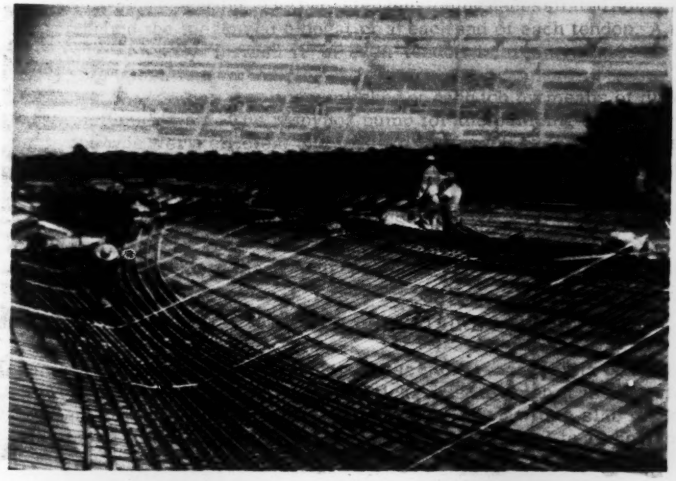

FIG. 12.—PRESTRESS TENDONS AND REINFORCING FOR FOLDED PLATE ROOF OF RICHLAND JUNIOR HIGH SCHOOL

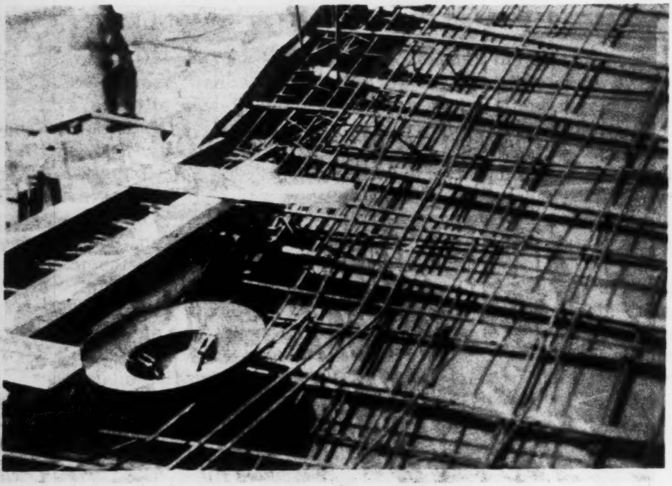

FIG. 13.—VALLEY OF FOLDED PLATE ROOF AT SUPPORTING COLUMN SHOWING ROOF DRAIN IN COLUMN—RICHLAND JUNIOR HIGH SCHOOL

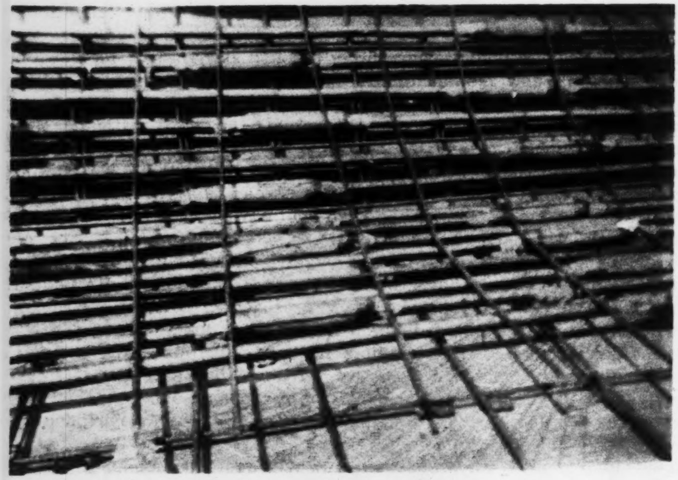

FIG. 14.—VALLEY OF FOLDED PLATE ROOF NEAR CENTER OF 97 FT SPAN SHOWING STRESS-STEEL TENDON COUPLERS IN PLACE—RICHLAND JUNIOR HIGH SCHOOL

handled carefully and no difficulty was experienced in consolidating the material. Finishing requires more labor than the conventional level surfaces and particular care must be exercised in screed placement to yield the desired straight lines to the ridges and valleys. Concrete placement in the vicinity of the prestress tendon anchorages and bearing plates must be performed most carefully as the high bearing stresses will not permit any poor concrete or honeycomb.

The tensioning of prestress reinforcement was deferred until the field cylinders verified the specified minimum strength concrete. A sequence of tensioning cables was selected to keep the center of prestress forces as near to the center of gravity of the final prestress force as possible. Each leaf had identical tendons tensioned prior to starting the next cable sequence. Tensioning was performed by jacking from both ends simultaneously to reduce, as much as possible, the differential stress along the tendon created by friction within the conduits. Experience has demonstrated that most formulas for estimating the amount of over-tensioning necessary to overcome friction are inadequate.

Selection of a friction coefficient of approximately twice that recommended by the manufacturer seems to come closer to indicating the necessary additional force. Very little difference in frictional resistance could be observed between tendons having large drape and angle change as compared with the straightest tendon. It is concluded that the wobble of the conduit along its placed position is much more responsible for creating the frictional resistance than is the angular change of the parabolic drape of the tendon. The delay created by the time required for the frictional slippage of each tendon to take place within the flexible metal conduit was reduced by tensioning each cable to the maximum initial force permissible to keep the end bearing stresses within the maximum allowable. All cables were then retensioned to obtain the total required elongation. The two-step tensioning necessitated some bookkeeping to record the measured elongation at each end of each tendon. A check of final force actually furnished in each tendon is also available as a by-product of this operation.

Grouting of the tendons was accomplished on each job by means of different types of grout equipment. The "Moyno" pump for the pumping of the portland cement grout was very efficient and positive in its action (Fig. 15), whereas other types of pumps became inoperative when speed was most necessary.

ECONOMICS

Contractors costs for these four projects are summarized in Table 1.

DESIGN PROCEDURE

Assume a slab thickness and compute the moment of inertia of the cross section for the inclined position to the vertical axis in which it is to perform. This moment of inertia of one plate is derived by Eq. 3 with a slab thickness of $4\frac{1}{2}$ in. normal to the slope, and a slope of plate 3.5 vertical to 12 horizontal.

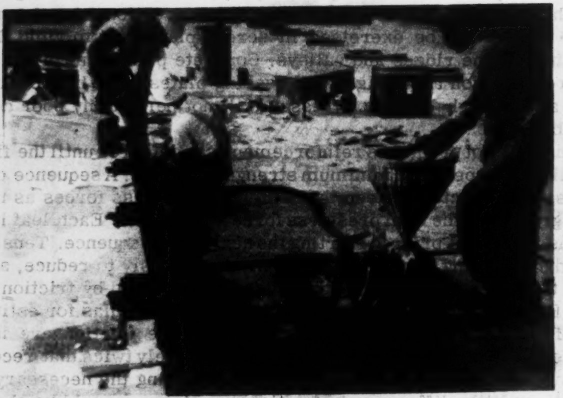

FIG. 15.—GROUTING OF POST-TENSIONED CABLES

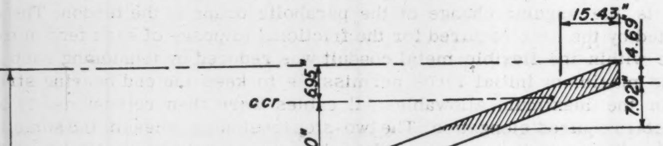
15.43"
4.69"
7.02"
6.95"
ccr
44.94"
32.0"
cgs
6"

FIG. 16.—ULTIMATE MOMENT STRESS CONDITION

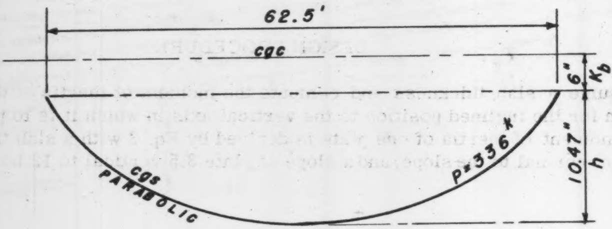
62.5'
cgc
6"
K_b
P=336 k
10.47"
h
CGS
PARABOLIC

FIG. 17.—LOCATION OF PRESTRESS FORCE ARRANGED IN PARABOLIC CURVE

Thus,

$$t = \frac{t'}{\cos\phi} = \frac{4.5}{0.96} = 4.6875 \text{ in.}$$

$$I = \frac{4.6875}{3.5} (40.25)^3 = 87{,}300 \text{ in.}^4$$

$$\text{Area} = 4.6875\ (11.5\text{-by-}12) = 647 \text{ in.}^2 \text{ (cross section of one plate)}$$

$$r^2 = \frac{87{,}300}{647} = 135\text{:}\ c_t = c_b = \frac{H+t}{2} = \frac{44.94}{2} = 22.47 \text{ in.}$$

and

$$k_t = k_b = \frac{r^2}{c} = \frac{135}{22.47} = 6.0 \text{ in.}$$

in which k is the kern point and r is the radius of gyration.

Assume center of gravity of tendons as being e′ above bottom of section at midspan. Prestress force eccentric arm is therefore:

$$e = c - e' = 16.47 \text{ in. max. (Assume } e' = 6.0 \text{ in.)}$$

Compute the longitudinal bending moments acting on the section for the dead load of the slab, the applied dead loads such as the roofing, insulation and ceiling, and the live load for which the structure shall be designed. The following values shall be used as an illustrative example.

The dead load for a $4\frac{1}{2}$ in. slab is

$$\frac{4.5}{12} = \frac{w'}{144} = 54 \text{ psf}/\cos\phi = \frac{54}{0.96} = 56.25\text{-by-}11.5 = 646 \text{ plf}$$

The additional applied dead load consists of the built up roofing (5.5), the applied 2 in. vermiculite concrete insulation (6.5), and the $\frac{1}{2}$ in. acoustical plaster (1.7), producing a total additional applied dead load of 13.7 psf. The live load was 25 psf.

$$13.7 \text{ psf}/\cos\phi = 14.25 \text{ psf}$$
$$14.25\ (11.5) = 164 \text{ plf}$$

and

$$25.0\ (11.5) = 287.5 \text{ plf}$$

The total load then (95.5 psf 11.5 ft) equals 1.1 kip per ft.

$$M_{dl} \text{ Slab} = 0.646 \left(\frac{62.5^2}{8}\right) = 315.5 \text{ ft-kip}$$

$$M_{dl} \text{ Applied} = 0.164 \left(\frac{62.5^2}{8}\right) = 80.1 \text{ ft-kip}$$

$$M_{ll} = .2875 \text{ by} \left(\frac{62.5^2}{8}\right) = 140.4 \text{ ft-kip}$$

$$M_{tl} = 1.0975 \left(\frac{62.5^2}{8}\right) = 536.0 \text{ ft-kip}$$

TABLE 1.—CONSTRUCTION COSTS

RICHLAND ELEMENTARY SCHOOL[a]
MEMPHIS, TENNESSEE

ITEM	QUANTITY	UNIT COSTS		COST		TOTAL
		LABOR	MATERIAL	LABOR	MATERIAL	
3750 psi Concrete	90 cu yd	4.72	12.12	$ 425.70	$ 1,091.70	$ 1,517.40
Concrete Finishing	6112 sq ft	0.03	—	188.38	—	188.38
Curing & Protection	6112 sq ft	0.01	0.01	61.12	61.12	122.24
Concrete Forms & Shoring	6232 sq ft	0.40	0.20	2,492.80	1,246.40	3,739.20
Intermediate Grade Reinforcing Steel	19129 lbs	0.02	0.09	382.58	1,721.61	2,104.19
Prestress Reinforcing	2050 linear ft	0.294	1.24	602.57	2,550.00	3,152.57
Sub-totals				$ 4,153.15	$ 6,670.90	$10,824.05
Sales Tax 3% Material						124.59
F.O.A.B., SS & Insurance 10% Labor						667.07
Net Cost						$11,615.73

Area Covered = 63.63 ft by 93.0 ft Horiz. Proj. = 5,917.6 sq ft
Cost per square foot = $1.963

RICHLAND JUNIOR HIGH SCHOOL[b]
MEMPHIS, TENNESSEE

ITEM	QUANTITY	UNIT COSTS		COST		TOTAL
		LABOR	MATERIAL	LABOR	MATERIAL	
3750 psi Concrete	393 cu yd	3.00	$15.30	$ 1,179.00	$ 6,012.90	$ 7,191.90
Concrete Finishing	20,371 sq ft	0.03	—	611.13	—	611.13
Concrete Curing & Protection	20,371 sq ft	0.01	0.01	203.71	203.71	407.42
Concrete Forms & Shoring	24,007 sq ft	0.371	0.20	8,906.60	4,801.40	13,708.00
Intermediate Grade Reinforced Steel	57,077 lbs	0.02	0.085	1,141.54	4,851.55	5,993.09
Prestress Reinforced Stress Steel	11,746 linear ft	0.153	0.60	1,802.94	7,061.52	8,864.46
Sub-totals				$13,844.92	$22,931.08	$36,776.00
Sales Tax 3% Material						687.93
F.O.A.B.; SS & Insur. 11% Labor						1,522.94
Net Cost						$38,986.87

Horizontal Projection
Area Covered = 97.71 ft by 175.6 ft = 17,193 sq ft.
Average Net Cost per square foot = $2.27

MEMPHIS ART ACADEMY[c]
MEMPHIS, TENNESSEE

ITEM	QUANTITY	UNIT COSTS		COST		TOTAL
		LABOR	MATERIAL	LABOR	MATERIAL	
Slab 3750 psi Concrete	153 cu yd	3.00	15.50	$ 459.00	$ 2,372.00	$ 2,831.00
Columns 3000 psi Concrete	8 cu yd	5.00	14.00	40.00	112.00	152.00

TABLE 1.—CONTINUED

ITEM	QUANTITY	UNIT COSTS		COST		TOTAL
		LABOR	MATERIAL	LABOR	MATERIAL	
Concrete Finishing	6,687 sq ft	0.03	—	$ 201.00	$ —	$ 201.00
Concrete Rubbed Finish	3,688 sq ft	0.15	—	553.00	—	553.00
Columns & Beam Forms	2,485 sq ft	0.75	0.35	1,864.00	870.00	2,734.00
Slab Forms and Shoring	6,000 sq ft	0.45	0.25	2,700.00	1,500.00	4,200.00
Intermediate Grade Reinforced Steel	29,610 lbs	0.02	0.0885	592.20	2,619.50	3,211.70
Post-tensioned tendons	4,250 linear ft	0.13	1.46	553.00	6,248.00	6,801.00
				$ 6,962.20	$13,721.50	$20,683.70
Sales Tax						225.50
Labor, Tax & Insurance						836.00
Job Equipment & Supervision						1,084.00
Net Cost						$22,829.20

Horiz. Projection Covered = 98.33 ft by 69.0 ft = 6,785 sq ft = $3.36 per square foot

HOLIDAY INN[d]
SARASOTA, FLORIDA

ITEM	QUANTITY	UNIT COSTS		COST		TOTAL
		LABOR	MATERIAL	LABOR	MATERIAL	
3750 psi Concrete	92 cu yd	4.25	16.00	$ 391.00	$ 1,472.00	$ 1,863.00
Concrete Finishing	6,660 sq ft	0.10	—	666.00	—	666.00
Concrete Protection and Cure	6,660 sq ft	0.01	0.005	66.00	33.00	99.00
Forms, Shoring and Removal	7,214 sq ft	0.415	0.18	2,993.81	1,298.52	4,292.33
Intermediate Grade Reinforcing Steel	16,650 lbs	0.25	0.07	416.25	1,165.50	1,581.75
Post-Tensioned Tendons	1,765 linear ft	0.184	1.15	324.00	2,027.04	2,351.04
Sub-totals				$ 4,857.06	$ 5,996.06	$10,853.12
Hoisting Crame Rental						408.00
Sales Tax 3.25% Material						192.10
Insurance, SS, F.O.A.B., Etc.						1,087.98
Net Cost						$11,997.23

Horiz. Area Covered = 73.17 ft by 84 ft = 6150 sq ft = $1.95 per square foot

---

[a] Roof over cafetorium spanning 62 ft-8 in., slab thickness 4 1/2 in., valley frequency 23 ft o. c.; slope 3 1/2-on-12; 7 1/2 in. thick reinforcing gable end wall ties included. Post-tensioning tendons 4 per leaf @ 62.5^k ea.; "Prescon" 10G2 Cables.

[b] Roof over gymnasium and cafetorium, span 96 ft-4 1/2 in., slab thickness 5 in., valley frequency 25 ft o. c.; slope 4 1/2-on-12; 8 in. thick reinforcing and prestressed concrete gable walls included. Post-tensioning cables 8 per leaf @ 70.2^k ea. Stressteel Corp. 1 1/8 Rod Tendons; Cable ties 7/8 in. Rod Tendons.

[c] Roof over third floor of art school spanning 94 ft-8 in., slab thickness 5 in., valley frequency 23 ft o. c.; slope 4 1/2-on-12. Thrust of end leaves resisted by tensors across ridges located at quarter points and by 20 in-by-24 in. concrete rigid frame supports at ends of span. Post-tensioning tendons 7 per leaf @ 84.5^k Prescon 12G2 Cables.

[d] Roof over club; span 60 ft; slab thickness 4 in., valley frequency 15 ft o. c.; slope 4 1/2-on-12; 8 in.-by-16 in. tensor ties @ 3 ft below valley. Post-tensioned cables 3 per leaf @ 45 kips each Prescon 6G2 Cables.

Having established the section properties and the load moments, use the conventional methods for computing the required prestressing force to furnish zero stress in the bottom at midspan with total load moment.

$$F = \frac{M_{tl}}{e + k_t} = \frac{536. \times 12{,}000}{16.47 + 6.0} = 286 \text{ kip;}$$

$$F = \frac{286}{.85} = 336 \text{ kip (initial force assuming 15\% losses)}$$

Using, say, four cables requires F = 71.5 kip per tendon; F_i = 82 kip per tendon. The initial tensioning force required for each cable should be increased adequately for overcoming tendon friction and wobble of conduit.

Solving for the several stresses occurring in the section due to moment, prestress force, and eccentric arm we have the following:

Under total load; unit stresses at midspan will be

$$F_{top} = \frac{F\ H}{A_c\ c_b} = \frac{286\ (44.94)}{647\ (22.47)} = 884 \text{ psi top compression}$$

$$0 \text{ psi bottom compression}$$

in which H is the vertical height of the section, valley to ridge, and c_b is the vertical distance from the c. g. of concrete section to the bottom surface.

Under slab load only, the unit stresses at the time of transfer or prestress force will be;

$$F_{bot} = \frac{F_i}{A_c}\left[1 + \frac{e - \frac{M_{dl}}{F_i}}{k_t}\right] = \frac{336}{647}\left[1 + \frac{16.47 - \frac{315.5}{336}}{6.0}\right]$$

$$\frac{336}{647}\ (1.866) = 968 \text{ psi compression}$$

Using the allowable steel and concrete stress[4]

Prestressing Steel f'_s = 240,000 psi f'_{sy} = 210,000 psi

temporary $f'_s = .70\ f'_s$ = 168,000 psi

at design loads = $.60\ f'_s$ = 144,000 psi

Concrete f_c = 3,750 psi

temporary compression $f_c = 0.55\ f'_c$ = 2,060 psi

temporary tension w/reinf. $f_c = 6\sqrt{f'_c}$ = 367 psi

compression (at design TL) $f_c = 0.45\ f'_c$ = 1,688 psi

tension (at design TL) $f_c = 3\sqrt{f'_c}$ = 183 psi

anchorage bearing $f_{cp} = 0.6\ f'_c\ \sqrt[3]{A_c/A_b}$ $\quad f_c = 3\sqrt{f'_c}$

The position of the prestressing steel can be varied throughout the length by draping the tendons in either a parabolic, circular or tangential pattern and reducing the eccentricity at the ends of the span. Locating the center of the prestressing force at the kern point at the ends will prevent tensile stress in the top at the end supports.

---

[4] Joint Committee 323 ACI - ASCE for Prestressed Concrete for Tensioned Members.

The ends of the span require additional thickness in order to have sufficient bearing area for transfer of the concentrated forces exerted by the end-bearing plates of the prestressing tendons. The stresses occurring at the bearing plate are usually the most critical concrete stresses that will be encountered in the folded plate section and particular attention should be given this area. The jacking forces required to stress the tendons to initial stress will need to be increased to overcome friction and wobble effect. Most manufacturers' standard end bearings are designed for use with 5,000 psi concrete in lieu of the 3,750 psi concrete sufficient for all other requirements of the section. Additional thickness is easily obtained by tapering the end-4 ft uniformly in the form of a symmetrical haunch above and below the slab to the additional thickness required.

The prestress force is assumed to be furnished by four tendons of 71.5^k each (84^k initial before losses) spaced approximately $4\frac{1}{2}''$ o. c. starting from the bottom, common to slope, at the center of the span. The tendons will be arranged in a parabolic curve to have the center of prestress force passing thru the lower kern point at the ends of the span.

The cgs of the prestressing force is eccentric and provides an upward reaction. This eccentricity equals:

$$h = c_b - 6'' - K_b$$

The cgs at mid-span is 6" above the bottom of the concrete, thus it is determined that h = 10.47" or 0.87' (see Figure - 17).

An analysis of the shear conditions assuming the leaf supported by a gable beam at each end of the span. The properties of the section have previously been determined. The vertical reaction at each end is calculated as being:

$$V = 1.1^k \times \frac{62.5'}{2} = 34.4^k$$

The upward force resultant V_s at each support, due to the parabolic alignment of the cgs of the prestressing tendons, may be computed: (see Fig. 17).

$$V_s = 4\,\frac{Fh}{L} = \frac{4 \times 286^k \times 0.87'}{64'} = 15.5^k$$

in which h is the eccentricity of the cgs of the prestressing tendons and L the horizontal length of tendon out to out. The prestressing resultant thus reduces the shear which must be carried out by the concrete.

$$V_c = V - V_s = 34.4^k - 15.5^k = 18.9^k$$

A check of the shearing unit stresses is computed by the formula:

$$v_c = \frac{V_c Q}{I\ b} = \frac{18.9^k \times 3278}{87{,}300 \times 16.07''} = 46.3 \text{ psi}$$

Q is the statical moment of the area outside of the section about the axis under consideration and b the width of the section on the same axis.

The principal tensile stress can then be calculated by the formula:

$$S_t = \sqrt{v^2 + \left(\frac{f_c}{2}\right)^2} - \frac{f_c}{2}$$

The term f_c used in this instance is the average compressive unit stress of the entire cross section thus

$$f_c = \frac{F}{A_c} = \frac{286^k}{647 \text{ in}^2} = 442 \text{ psi}$$

hence

$$S_T = \sqrt{46.3^2 + \left(\frac{442}{2}\right)^2} - \frac{442}{2} = 4.6 \text{ psi}$$

$$(\text{allowable} = .03\ f'_c = 112 \text{ psi})$$

and the allowable principal tensile stress for ultimate load will be

$$v'_c = .08\ f'_c = .08 \times 3750 \text{ psi} = 300 \text{ psi}$$

The section should be checked for shear created by an ultimate load capacity of at least twice the total design load;

$$V_{ult} = 2 \times V_{tl} = 2 \times 34.4 = 68.8^k$$

V_s is recomputed for the ultimate strength of the prestressing steel to furnish $V_s = 26.0^k$

$$V_c = 68.8^k - 26.0^k = \qquad 42.8^k$$

$$v = \frac{42.8^k \times 3278}{87{,}300 \times 16.07} = \qquad 115.0 \text{ psi}$$

$$S'_t = \sqrt{(115)^2 + \left(\frac{442}{2}\right)^2} - \frac{442}{2} = 28.0 \text{ psi}$$

The section is analyzed for cracking moment, assuming the modulus of rupture of the concrete equals

$$7.5\sqrt{f'_c} = 7.5\sqrt{3750} = 460 \text{ psi}$$

hence the moment capacity of the concrete and of the steel are each computed and added:

$$M_s = F\left(e + k_t\right) = 286^k\ (16.47'' + 6.0'') = 536'^k$$

$$M_c = \frac{f_c I}{c_b} = \frac{460 \times 87{,}300}{22.47'' \times 12} = \qquad \underline{149'^k}$$

$$\text{Cracking } M = M_s + M_c = \qquad 685'^k$$

The safety factor of cracking moment is therefore $\frac{685'^{k}}{536'^{k}} = 1.28 \times TL$ also considering no increase in dead load is occasioned, the factor of live load to cause cracking is:

$$\frac{\text{Cracking } M\text{-}M_{dl}}{M_{LL}} = \frac{685'^{k} - 395.6'^{k}}{140.4'^{k}} = 2.06 \times LL$$

The analysis of factor against cracking indicates a lower prestressing force could be used to furnish an adequate structure with no probability of cracking throughout the design loading conditions.

The section is then checked for ultimate load moment and the factor of safety established. The prestress tendons will furnish a tensile force of:

$$f'_s = \frac{286^k}{0.6} = 480^k$$

This force will be resisted by the ultimate strength of concrete assuming a pressure block at the top of the concrete section. The ultimate unit stress in the concrete is computed as:

$$0.85\ f'_c = 0.85 \times 3750 \text{ psi} = 3190 \text{ psi}$$

The total compressive force must equal the tensile force furnished by the steel, hence the area of concrete necessary to furnish this force is:

$$A_c = \frac{480^k}{3.19k/\square''} = 150.5 \text{ sq. in. required}$$

The center of compressive resistance, ccr, for ultimate loading is established as follows:

Compute equivalent width of section as:

$$b = \frac{T}{\sin\phi} = \frac{4.5''}{.28} = 16.07''$$

Compute area funished by top triangle:

$$\frac{4.69''}{2} \times 16.07'' = 37.7 \text{ sq. in.}$$

Additional area of stem required:

$$150.5 - 37.7 = 112.8 \text{ sq. in.}$$

Additional vert. depth needed:

$$\frac{112.8}{16.07} = 7.02 \text{ in.}$$

$$ccr = \frac{37.7 \; \frac{2 \times 4.69''}{3} + 112.8 \; \frac{7.02}{2} + 4.69}{150.5} = 6.95 \text{ in.}$$

below top surface

Lever arm for ultimate moment =

$$44.94'' - (6.0'' + 6.95'') = 32.0 \text{ in.}$$

Ultimate load moment:

$$M_{ult} = 480^{k} \; \frac{32.0''}{12''} = 1280 \text{ ft kips}$$

The total load factor of safety is therefore:

$$\frac{1280'^{k}}{536'^{k}} = 2.38 \times \text{T. L.}$$

and the factor of safety for LL =

$$\frac{1280'^{k} - 395.6'^{k}}{140.4'^{k}.} = 6.28 \times \text{LL plus DL}$$

The transverse bending in successive plates is analyzed by the conventional moment distribution methods utilized for continuous structures. The span length is the slope length from valley to ridge. The valley and ridge serve as support for the slab. This being a short span, 11 ft -6 in. in the example, moments will be no greater than would be encountered in a level slab with supports at the same frequency (Fig. 1).

For example, assume fixed and negative moments at the valley and ridge of $\frac{w\ l^2}{12}$ and midspan positive moments of one half this value. Compute stiffness and distribution factors in the usual manner and compute the maximum and minimum moments for each span. End leaves deserve special consideration and need provision for support by means of columns, edge beams, upturned leaf or wing or thickened to provide stiffness to the cantilever beyond the last valley or ridge.

Analysis of a 1-ft wide strip transverse to the main span is derived by the following means (Fig. 1):

$W_{dl} = (4.5/12)\ 144 = 54$ lbs $W_{ll} = 25\ (\cos \phi) = 24.5$ lb

$W_{dl} = \qquad 14$

$W_{dl} = \qquad \overline{68}$ psf $W^{tl} = 68 + 24.5 = 92.5$ lb

$$\mathrm{FEM}_{dl} = 68 \times \frac{(12)}{12}\ 2 = .816 \text{ ft - kip } \mathrm{FEM}^{tl} = 92.5 \times \frac{(12)^2}{12} = 1.11 \text{ ft - kip}$$

$$I = 91.2 \text{ in.}^4$$

$$K = I/L = \frac{91.2}{12} = 7.6$$

Distribution factors = 1.0; 0.43; 0.56; 0.50; 0.50

	A		B			C			D			E		E
D.F	1.0		.43	.57		.50	.50		.50	.50		.50	.50	.50
FEM$_{dl}$	-.816		-.816	-.816		-.816	-.816		-.816	-.816		-.816	-.816	
FEM$_{tl}$	-1.11	+0.56	-1.11	-1.11	+.56	-1.11	-1.11	+.56	-1.11	-1.11		-1.11	-1.11	
Dist.	-0.13	+0.13	-0.56	-0.15	+.12	-0.17	-0.15	+.11	-0.15	-0.15		-0.15	-0.15	
Add	-1.24	+0.40	-1.67	-1.26	+.13	-1.28	-1.26	+.11	-1.26	-1.26		-1.26	-1.26	
C.O.	+1.24		+0.18	-0.23										
Dist. M.	0	+1.09	-1.49		+0.81	-1.27		+.78	-1.26		+.78	-1.26		
Min. A_s		+0.216	-.296		+0.161	-.252		+.155	-.250		+.155	-.25		

No. 3 @ 6 in. oc No. 3 @ 4½ in. oc No. 3 @ 8 in. oc No. 3 @ 5 in. oc No. 3 @ 8¾ in. oc No. 3 @ 5 in. oc.

Distribution Steel Longitudinal = (0.0025) (4.5) (12) = No. 3@10 in. o.c.
Average Steel per square foot = 0.337 sq in = 1.15 psf

The end leaf is unopposed. Therefore, a tie must be provided to resist the horizontal component. Thus, the vertical Load of end leaf = 1.11 (31.25) = 34.7 kip, and the horizontal component = 34.7 x 12/3.5 = 119 kip. This can be resisted by a prestress force of this amount or reinforcing steel = $\frac{119}{20}$ = 5.95 in. 2, say, 6 - No. 9 Bars.

Analysis of stress distribution and variation may be computed in the manner described by H. Simpson.[5]

DEFLECTION

The moment due to prestress (Fig. 17) is computed as

M due to prestress = p e = 336 x 6/12 = 168 ft uniform

plus 336 x $\frac{10.47}{12}$ = 293 ft kip parabolic

M_{dl} Slab = 315.5 ft -kip

M_{dl} Applied = 80.1 ft -kip

M_{ll} = 140.4 ft -kip

Instantaneous upward deflection due to prestress is

$$\left(\frac{168 \text{ ft. kip}}{8} + \frac{5 \times 293}{48}\right) \frac{62.5^2 \times 12^2 \times 12{,}000}{3{,}500{,}000 \times 87{,}300} = 1.14 \text{ in. initial;}$$

$$0.85 \times 1.14 = .965 \text{ in. after losses}$$

Downward deflection due to M Slab:

$$\left(\frac{5 \times 315.5}{48}\right) \frac{62.5^2 \times 12 \times 12{,}000}{3{,}500{,}000 \times 87{,}300} = 0.73 \text{ in. } (1.27 \text{ in. assuming } 2.0 \times 10^6 E)$$

---

[5] "Design of Folded Plate Roofs," by Howard Simpson, Proceedings, ASCE, Vol. 84, No. ST 1, January, 1958.

Hence, immediate upward deflection at transfer = 1.14 - 0.73 = 0.41 in.

$$\text{Added DL deflection} = \frac{80.1}{315.5} \times 0.73 = 0.19 \text{ in.}$$

$$= (.965 - .73 - .19)\, 2 = .09 \text{ in.}$$

after loss of initial prestress and effect of creep.

Instantaneous downward deflection due to live load moment is

$$\frac{140.4}{315.5} \times .73 = 0.325 \text{ in.}$$

ACKNOWLEDGMENTS

The Richland Elementary and Junior High Schools in Memphis, Tenn., and the Memphis Art Academy were designed by Mann and Harrover, Architects of Memphis. The Holiday Inn of Sarasota, Fla., was designed by William Bond, Architect of Memphis. The schools were built by the S&W Construction Co., Inc., of Memphis. The Art Academy was built by the Whitsitt Construction Co. of Memphis, while the Holiday Inn was build by Allen Brothers and O'Hara, Inc.

APPENDIX.—NOTATION

The following symbols have been adopted for use in this paper:

A_c = area of concrete;

A_s = area of steel;

a = slope rise on 12;

B = spacing of valleys;

b = horizontal projection of plate width;

c = vertical distance from c.g. of section to top or bottom surface;

c.g. = center of gravity;

DL = dead load;

e = eccentricity of prestress force from the c.g.;

e' = distance from surface to center of prestress force;

F- = prestress force after losses;

F_i = prestress force at time of transfer;

f_c = allowable concrete unit stress;

f'_c = design concrete strength;

f_s = allowable steel unit stress;

f'_s = ultimate strength of steel:

H = vertical height of section valley to ridge;
h = vertical distance above or below c.g. of concrete section;
I = moment of inertia of section;
i = subscript indicating condition at transfer of prestress;
K = stiffness factor;
k = kern point;
L = length of span center to center of supports principle span;
LL = live load;
M = bending moment;
Q = moment of area;
r = radius of gyration;
S = principle tensile stress;
S' = principle tensile stress for ultimate;
T = thickness of slab normal to section;
T' = thickness of slab vertically;
TL = total load;
ult. = ultimate;
V = shear;
v = unit shear;
W = total load on section for span considered;
w = unit load per sq ft;
x = distance from support to point under consideration;
ω = width of plate along the surface; and
ϕ = angle of intersection of plate slope with the horizontal.

DISCUSSION

A. A. EREMIN,[6] M. ASCE.—As noted by the authors, a deficiency in the compressive zone of long span folded concrete roof slabs is often found. In addition to the methods of overcoming this deficiency cited by Brough and Stephens, one may add the increasing of the compressive zone area by gradually increasing the thickness of the slab toward the top of the folds. In so doing, the aesthetic effect of the folds is not destroyed.

---

[6] Cons. Structural Engr., Berkeley, Calif.

As is well known, an expensive element of cost in the construction of this type of structure is the required falsework. In precast and prestressed folded slabs this cost can be reduced by precasting the slab on the ground in units of one or two folds. The completed units may then be lifted and installed in place in the same manner as for bridge girders.

In constructing folded roof slabs, great care must be used to determine the sequence of placing the concrete. It would be of interest to know what placing sequence was used in the illustrative example.

JOHN C. BROUGH, JR.,[7] M. ASCE, and B. H. STEPHENS, JR.,[8] A.M. ASCE.—It is quite true, as stated by Eremin, that if it is necessary to provide additional area in the concrete compressive zone (especially as would probably be required in conventionally reinforced sections), the tapered section of the plate leaf is an excellent method of furnishing the required area. The writers have contemplated this method on some projects, but in satisfying asethetic desires other solutions were utilized.

The cost of construction of the four projects listed in the paper include the cost of falsework required. These costs have been included in the forming costs.

The placing sequences of concrete on the four projects were as follows:

Richland Elementary School.—Entire roof placed in one operation. Concrete time required approximately 5 hr for the 90 cu yd in the plate leaves and gable end walls. Runways were located along ridges and placing operation proceeded across the 63.6-ft span, achieving a monolithic structure.

Richland Junior High School.—Concrete was placed in two operations with 4 days intervening between the two operations. A construction joint was located on the ridge intersection half way along the 175-ft dimension. Each placing required approximately 8 hr to 9 hr. Runways were located on the ridges and concrete placed, proceeding in the span direction. Two monolithic sections resulted with a properly tied construction joint. A concrete retarder would have been advantageous on this building especially due to the high ambient temperatures occurring at the time of placing concrete (August). Considerable crazing occurred on the first pour and a lesser amount on the second due to remedial procedures instituted. It is interesting to note the prestress force closed the majority of the crazing cracks.

Memphis Art Center and Holiday Inn.—The buildings were monolithic operations without construction joints. Concrete placement was accomplished two leaves at a time on the Art Center and some difficulty was encountered to preserve fresh edge surfaces due to equipment breakdown mid-way in the operation.

---

[7] Cons. Engr., Harry B. Hunter and Assoc., Memphis, Tenn.

[8] Harry B. Hunter and Assoc., Memphis, Tenn.

AMERICAN SOCIETY OF CIVIL ENGINEERS

Founded November 5, 1852

TRANSACTIONS

Paper No. 3255

DESIGN OF PRESTRESSED CONCRETE BEAMS BY COMPUTER

By Joseph J. Bonasia,[1] A.M. ASCE

With Discussion by Messrs. Richard J. Newson; and
Joseph J. Bonasia

SYNOPSIS

The economical design of prestressed concrete beams is of special interest to engineers concerned with the development of the present highway program. Several groups, such as the Bureau of Public Roads, the American Association of State Highway Officials, and the Prestressed Concrete Institute recognized the advantages of prestressed concrete and developed standard I-type sections for use as stringers on simple-span highway bridges.

This paper illustrates how an electronic digital computer is advantageously used to select and design standard posttensioned prestressed concrete beams. Two charts are presented which provide information for the rapid selection of satisfactory beams used as interior stringers in simple span, composite beam highway bridges with AASHO H20-S16-44 live load. A description of the method of obtaining the required prestressing force and its location for the results obtained is also presented.

INTRODUCTION

In 1956 the Bureau of Public Roads (BPR)adopted twenty-two cross sections recommended for use as prestressed concrete beams for highway bridges with cast-in-place deck slabs. Eleven of these sections are considered in this paper. Similarly in 1957 the Joint Committee of the American Association of State Highway Officials (AASHO) and the Prestressed Concrete Institute (PCI)

Note.—Published essentially as printed here, in April, 1960, in the Journal of the Structural Division, as Proceedings Paper 2446. Positions and titles given are those in effect when the paper or discussion was approved for publication in Transactions.

[1] Civ. Engr., Lockwood, Kessler & Bartlett, Inc., Cons. Engrs., Syosset, N. Y.

presented four cross sections for use as standard beams which are also considered in this paper. The dimensions of these beams are listed in Table 1.

Having decided to use either set of recommended standard beams, the problem becomes one of selecting the appropriate sizes for the various spans and loading conditions. The graphical charts developed herein facilitate the selection of the beam sizes. Curves representing slab thicknesses of 6, 7, and 8 in. are drawn for each beam. Using these curves, the selection of the proper size beam and maximum beam spacing for any given span length without a prior knowledge of the magnitude and location of the prestressing force is possible.

TABLE 1.—STANDARD SECTIONS[a]

Beam No.	A_c	H	B_t	T_t	T'_t	B_b	T_b	T'_b	B'
				(a) AASHO-PCI					
1	276	28	12	4.000	3.000	16	5.0	5.0	6
2	369	36	12	6.000	3.000	18	6.0	6.0	6
3	560	45	16	7.000	4.500	22	7.0	7.5	7
4	789	54	20	8.000	6.000	26	8.0	9.0	8
				(b) BPR					
1	296	28	15	4.375	1.125	18	4.0	6.0	6
2	320	32	15	3.375	1.125	18	4.0	6.0	6
3	349	36	16	4.250	1.250	18	4.0	6.0	6
4	377	40	17	4.125	1.375	18	4.0	6.0	6
5	405	44	18	4.000	1.500	18	4.0	6.0	6
6	448	44	15	4.375	1.125	20	6.5	7.0	6
7	481	48	17	4.125	1.375	20	6.5	7.0	6
8	525	54	19	3.875	1.625	20	6.5	7.0	6
9	592	60	22	5.000	1.500	20	6.5	7.0	6
10	724	68	25	4.750	1.750	22	6.0	7.5	7
11	804	78	27	4.625	1.875	22	6.0	7.5	7

[a] Areas are in square inches. Dimensions are in inches.

Also described is a program which may be used to design interior and exterior posttensioned prestressed concrete beams for simple-span highway bridges. It is applicable for use with various methods of prestressing. The program will determine the following for both the interior and exterior beam:

1. Required area of prestressing steel and its eccentricity at midspan.
2. Prestressing force required at the jacks.
3. Initial and final flexure stresses at top and bottom fibers of the beams.
4. Ultimate strength of the beam.
5. Required area and spacing of web reinforcement.
6. Camber and dead-load deflection.

Throughout the paper, appropriate sections of the AASHO "Standard Specifications for Highway Bridges;" the BPR "Criteria for Prestressed Concrete

Bridges;" and the Joint ASCE-ACI Report on Prestressed Concrete prepared by Committee 323 are followed. Further assumptions, specifications, and terminology for the various materials are stated.

The two programs are coded for the Bendix G-15D General Purpose Digital Computer. The programming method used is the Intercom interpretive and compiling system, with input and output in floating point. The term "program," used throughout this paper, specifies the complete set of coded instructions required to solve a particular problem and is permanently recorded on paper tape punched by the computer. The accuracy of the input and output is limited to five significant figures.

TERMINOLOGY

a. Bridge and Beam Dimensions:

A = gross area of concrete beam;

A_i = area of interior beam;

A_f = area of fascia (exterior) beam;

A_s = area of prestressing steel;

A_s' = area of a prestressing steel unit;

A_v = area of web reinforcement;

B = effective width of top flange of composite section;

B' = width of beam web;

D = distance from center of exterior beam to edge of sidewalk;

d = distance from extreme compression fiber to centroid of prestressing force;

e = distance from centroid of prestressing reinforcement to centroid beam;

h = total depth of beam;

I = moment of inertia about centroid of cross section;

I_c = moment of inertia about centroid of composite section;

j = ratio of distance between centroid of compression and centroid of tension to the depth d;

L = length of span, center to center bearing;

S = stringer (beam) spacing;

s = longitudinal spacing of web reinforcement;

T = thickness of cast-in-place slab;

W = total width of sidewalk;

Y_t, Y_b = distance top, bottom fiber to centroid of beam;

Z_t, Z_b = section modulus top, bottom, of beam; and

Z_t^c, Z_b^c = section modulus top, bottom of composite section.

b. Loads:

DL = effect of dead load;

F = effective prestressing force after deduction of all losses;

F_j' = prestressing force required at jacks for prestressing unit, A_s';

F_o = prestressing force at transfer;

I_L = impact fraction;

M_G = bending moment due to dead load beam;

M_L = bending moment resisted by composite section;

M_S = bending moment due to dead load of cast-in-place slab, wearing surface and diaphragms;

m_u = required ultimate bending moment;

M_u = ultimate resisting moment;
V_c = shear taken by concrete;
V_D = shear due to dead load;
V_F = shear resisted by prestressing tendons;
V_L = shear due to live load; and
V_u = shear due to specified ultimate load and effect of prestressing.

c. Stresses and Strains;
E_c = flexural modulus of elasticity of concrete;
E_{ci} = flexural modulus of elasticity of concrete at transfer;
E_S = flexural modulus of elasticity of prestressing steel;
f'_c = compressive strength of concrete at 28 days;
f'_{ci} = compressive strength of concrete at time of initial prestressing;
f_{cs} = concrete stress at the centroid of the prestressing steel;
f'_s = ultimate strength of prestressing steel;
f_{se} = effective steel prestress after losses;
f_{sy} = nominal yield point stress of prestressing steel;
f'_y = yield point stress of conventional reinforcing steel;
Δ_1 = deflection at time of prestressing; and
Δ_2 = deflection due to dead load of slab.

d. Friction:
e_n = base of Naperian logarithms;
K = friction wobble coefficient;
T_o = steel stress at jacking end;
T_x = steel stress at any point x;
μ = friction curvature coefficient; and
α = total angular change of prestressing steel profile in radians from jacking end to point x.

SPECIFICATIONS

a. Allowable Concrete Stresses:
Beam concrete f'_c = 5000 psi
Slab concrete f'_{cs} = 3000 psi
Concrete strength at time of prestressing f'_{ci} = 4000 psi
Initial compressive stress $0.55\ f'_{ci}$ = 2200 psi
Initial tensile stress $3\sqrt{f'_{ci}}$ = 190 psi
Final compressive stress $0.40\ f'_c$ = 2000 psi
Final tensile stress = 0

b. Allowable Steel Stress:
Ultimate stress f'_s = 240,000 psi
Nominal yield point stress f_{sy} = 215,000 psi
Nominal yield point stress, conventional reinforcement f'_y = 33,000 psi

c. Sign Convention:
Compression (+)
Tension (-)

FORMULAS FOR BEAM SELECTION

The design procedures for prestressed concrete are well known and assumed familiar to the structural engineer; therefore, only certain principles are stated herein. For composite construction, no temporary intermediate supports are assumed used during the placing of the beam and pouring of the concrete deck slab. Therefore, the beam alone carries the dead load while the composite section carries the live load and any dead load applied after the deck slab has set.

The stresses in concrete produced by the application of external loads and prestressing are computed by the elastic theory. The stress on any fiber due to an eccentrically located prestressing force equals the some of a uniform stress and a bending stress. Additional stresses are produced by external loads, namely, the dead load of the beam, the cast-in-place deck slab, and the live load. The combined stress acting on any fiber a distance y from the neutral axis of the beam and a distance y_1 from the neutral axis of the composite section is expressed as

$$f = \frac{F}{A} \mp \frac{F\,e\,y}{I} \pm \frac{M_G\,y}{I} \pm \frac{M_S y}{I} \pm \frac{M_L y_1}{I_c} \quad \ldots\ldots\ldots\ldots (1)$$

where e is the distance from the neutral axis of the beam to the prestressing force.

Consider the stress on the bottom fiber of the beam at the time of prestressing. From Fig. 1

$$f = \frac{F_o}{A} + \frac{F_o e}{Z_b} - \frac{M_G}{Z_b} \quad \ldots\ldots\ldots\ldots\ldots\ldots (2)$$

The allowable concrete stress, f, before losses equals 2200 psi. Under working loads and for the cases where f'_c = 5000 psi and f'_{ci} = 4000 psi, the losses due to shrinkage, creep, and elastic shortening are about 15%. Under these conditions the stress does not exceed 0.36 f'_c, that is

$$\frac{F}{A} + \frac{F\,e}{Z_b} - \frac{M_G}{Z_b} = 1{,}800 \quad \ldots\ldots\ldots\ldots\ldots\ldots (3)$$

The final stress on the bottom fiber of the beam due to the design working load is

$$f = \frac{F}{A} + \frac{F\,e}{Z_b} - \frac{M_G}{Z_b} - \frac{M_S}{Z_b} - \frac{M_L}{Z_b^c} \quad \ldots\ldots\ldots\ldots (4)$$

Let the final stress f equal zero. Substituting Eq. 3 into Eq. 4 yields

$$\frac{M_S}{Z_b} + \frac{M_L}{Z_b^c} = 1{,}800 \quad \ldots\ldots\ldots\ldots\ldots\ldots (5)$$

Eq. 5 is written in a convenient form since it contains terms independent of any prestressing force and its location. Given a span, slab thickness, stringer spacing, and any size beam, it is evident that the proper substitution of values

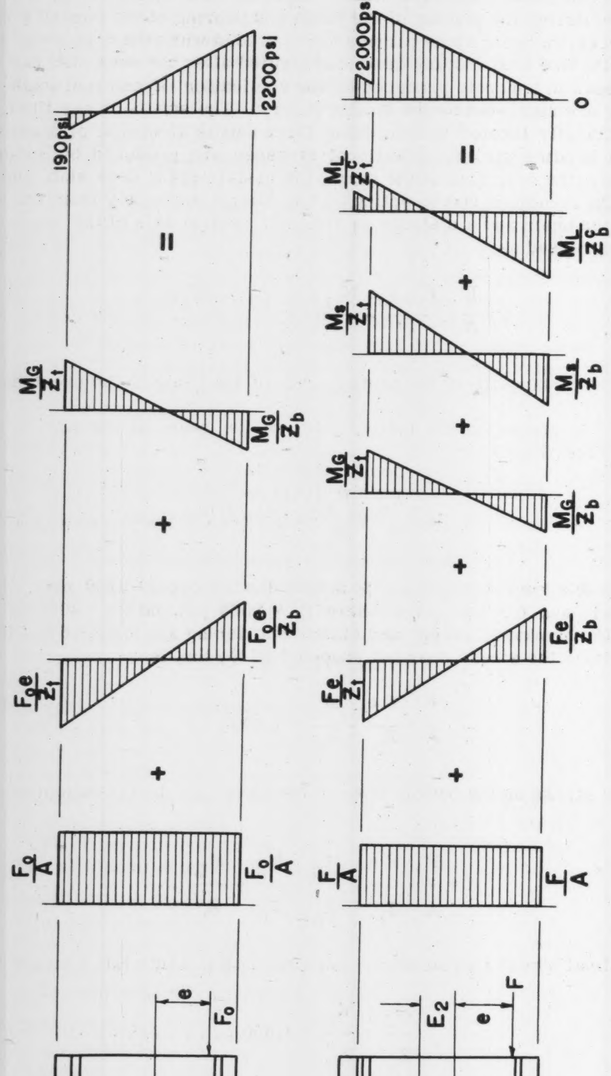
Y_t
Y_b
e
F_o
F_o/A
F_o/A
+
F_oe/Z_t
F_oe/Z_b
+
M_G/Z_t
M_G/Z_b
=
190psi
2200psi
E_2
e
F
F/A
F/A
+
Fe/Z_t
Fe/Z_b
+
M_G/Z_t
M_G/Z_b
+
M_s/Z_t
M_s/Z_b
+
M_L/Z_t^c
M_L/Z_b^c
=
2000psi
0

FIG. 1

in Eq. 5 determines the adequacy of that beam in flexure. Negative results indicate that the stresses on the selected beam are within the allowable specified limits; positive results indicate that the selected beam is overstressed.

The terms M_S and M_L in Eq. 5 are readily computed as follows:

Dead Load Moment.—Adding 15% for the dead load of the diaphragms and wearing surface, the maximum bending moment due to the dead load of the slab is

$$M_S = \frac{1.15\ w\ L^2}{8} \quad \ldots\ldots\ldots\ldots\ldots\ldots\ldots (6)$$

Live Load Moment.—The maximum live load moment is determined by placing on the span either the standard AASHO H20-S16-44 truck or the lane loading (Fig. 2). By applying to the beam the fraction of a wheel load and the impact fraction in accordance with the AASHO specifications, the design live load moment becomes

$$M_L = \left[\frac{18}{L}(L - 4.67)^2 - 112\right]\left(1 + I_L\right)\frac{S}{10} \quad \ldots\ldots\ldots\ldots (7a)$$

or

$$M_L = \left[L\ (0.08L + 4.5)\right]\left(1 + I_L\right)\frac{S}{10} \quad \ldots\ldots\ldots\ldots (7b)$$

whichever is greater. It is noted that the term L in Eq. 7a must be equal to or greater than 34 ft.

COMPUTER SOLUTION

Eqs. 5, 6, and 7 are readily adaptable for solution by the electronic computer. These equations are utilized to compute for each AASHO and BPR beam the limiting span to the nearest 1/2 ft. The stringer spacings vary from 4 ft 6 in. to 9 ft 0 in. in increments of 6 in. and the slab thickness vary from 6 in. to 8 in. in 1-in. increments. This data allowed the preparation of charts for rapid selection of satisfactory beams.

The method used is essentially a trial-and-error method for which the high-speed electronic computer is well suited. Beams are tested for successively increasing spans until the limiting values for each beam are found. A flow chart which traces the various steps followed in the design procedure is shown in Fig. 3. For purposes of this discussion, assume it is desired to obtain the limiting spans for the BPR standard sections using a 6-in. slab.

The program tape contains the necessary physical properties for all the AASHO-PCI and the BPR standard beams. By starting computations at either one of two predetermined locations, the computer will automatically use the chosen set of standard beams (Figs. 3 and 4). Initially, the slab thickness and the stringer spacing are typed by the computer.

The ability of the computer to make decisions which are based on positive or negative values, is best illustrated by the use of a simple example. AASHO

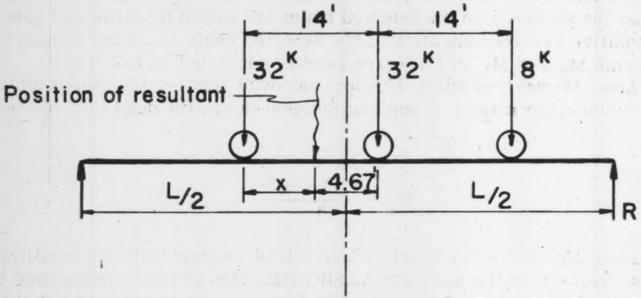
14'
14'
32K
32K
8K
Position of resultant
x
4.67
L/2
L/2
R

(*a*) Position of Standard Truck for Maximum Moment

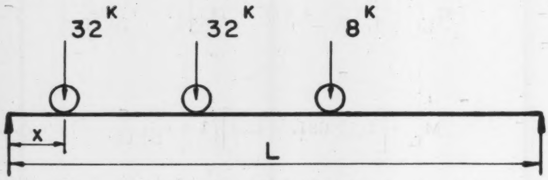
32K
32K
8K
x
L

(*b*) Position of Standard Truck for Maximum Shear

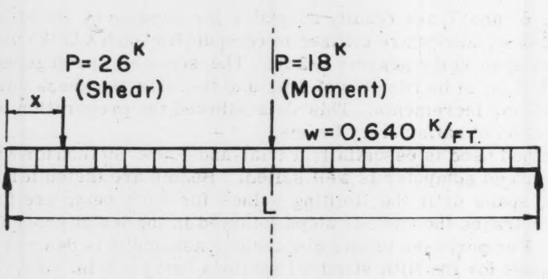
P=26K
(Shear)
P=18K
(Moment)
x
w=0.640 K/FT.
L

(*c*) Lane Loading for Maximum Moment and Shear

FIG. 2

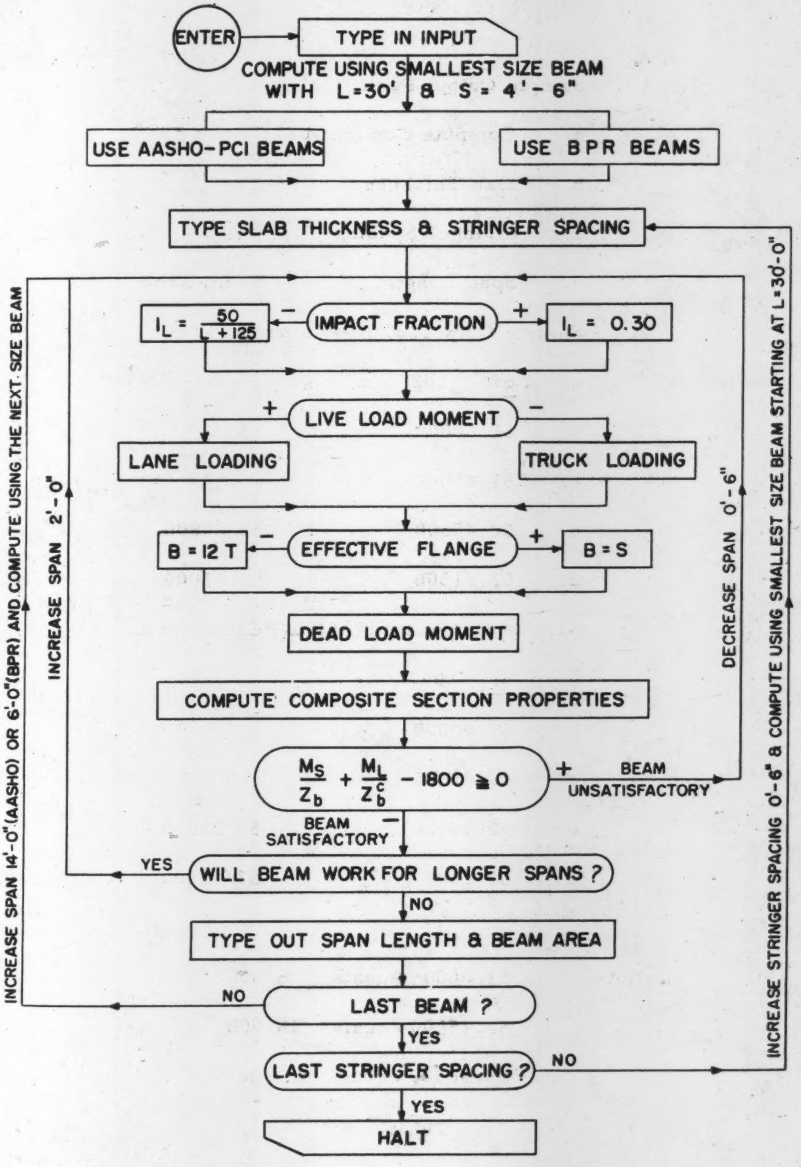
ENTER
TYPE IN INPUT
COMPUTE USING SMALLEST SIZE BEAM WITH L=30' & S = 4'-6"
USE AASHO-PCI BEAMS
USE BPR BEAMS
TYPE SLAB THICKNESS & STRINGER SPACING
IMPACT FRACTION
$I_L = \frac{50}{L+125}$
$I_L = 0.30$
LIVE LOAD MOMENT
LANE LOADING
TRUCK LOADING
EFFECTIVE FLANGE
B = 12 T
B = S
DEAD LOAD MOMENT
COMPUTE COMPOSITE SECTION PROPERTIES
$\frac{M_S}{Z_b} + \frac{M_L}{Z_b^c} - 1800 \geqq 0$
BEAM UNSATISFACTORY
BEAM SATISFACTORY
WILL BEAM WORK FOR LONGER SPANS ?
YES
NO
TYPE OUT SPAN LENGTH & BEAM AREA
LAST BEAM ?
LAST STRINGER SPACING ?
HALT
INCREASE SPAN 14'-0" (AASHO) OR 6'-0" (BPR) AND COMPUTE USING THE NEXT SIZE BEAM
INCREASE SPAN 2'-0"
DECREASE SPAN 0'-6"
INCREASE STRINGER SPACING 0'-6" & COMPUTE USING SMALLEST SIZE BEAM STARTING AT L=30'-0"
+
−

FIG. 3.—FLOW CHART

1. Sample Output Format
   - a. Compute Command
   - b. Slab Thickness
   - c. Stringer Spacing
   - d. Span Length   Beam Area
2. Sample Output for BPR Beams
   - a. qf 102 z s
   - b. 51.6000
   - c. 51.45000
   - d. 52.45500   53.29600
   - d. 52.51500   53.32000
3. Sample Output for AASHO-PCI Beams
   - a. qf 097 z s
   - b. 51.60000
   - c. 51.45000
   - d. 52.44000   53.27600
   - d. 52.6000   53.36900

Note:
51.6000 equals 6.000
52.45500 equals 45.500
53.36900 equals 369.000

FIG. 4

specifies the impact fraction which has a maximum value of 30%. Accordingly the impact equation is written in the following manner:

$$I_L = \frac{50}{L + 125} - 0.30 \geqq 0 \quad \ldots\ldots\ldots\ldots\ldots\ldots (8)$$

When the results of Eq. 8 are zero or positive, I_L equals 0.30 and when the results are negative I_L equals the computed value of the impact fraction. Using the same principle, the result of the equation

$$M = \left[L\,(0.08L + 4.5)\right] - \left[\frac{18}{L}\,(L - 4.67)^2 - 112\right] \geqq 0 \quad \ldots\ldots\ldots (9)$$

is investigated. Positive or negative results indicate whether the lane or truck loading produces the greater bending moment. The determination of the effective flange width follows the same procedure and needs no further explanation.

The moment due to the cast-in-place slab and the moment of inertia of the composite beam are computed. It is now possible to determine the adequacy of the beam using Eq. 5. A negative value indicates the stresses are within the allowable limits. At thispoint the computer assumes that the beam is suitable for a longer span and will continue to do so until otherwise instructed, as shown on the flow chart (Fig. 3). The span is increased 2 ft at a time and all computations are repeated until a positive result from Eq. 5 shows the beam is overstressed for this and longer spans. In order to attain the desired accuracy, the span length is repeatedly decreased 1/2 ft until a negative solution indicates the computer has reached the limiting span length for that beam.

Summarizing, the computer found BPR Beam No. 1 to be adequate until it reached a 46-ft span. By decreasing the span to 45 ft 6 in., a negative result is obtained from Eq. 5 which indicates the limiting span for that beam. According to previous instructions the computer now types out the span length and, for identification purposes, the beam area (Fig. 4).

If there are additional beams to investigate, the span is increased a specified amount and the next size beam is introduced. Based on preliminary studies, the spans are increased 6 ft for the BPR beams and 14 ft for the AASHO beams, thereby eliminating unnecessary computing. Upon completion of all size beams, the stringer spacing is incremented 6 in. and the entire computation cycle is repeated. At the completion of the computations for all the stringer spacings, the computer will halt.

USE OF THE CHARTS

The charts shown in Figs. 5 and 6 show curves relating span length, stringer spacing, slab thickness, and beam size. The charts are used to determine the beam size for any given span, stringer spacing, and slab thickness. They are also used to determine the maximum stringer spacing and slab thickness for any beam given the span length.

A point falling immediately to the left of a given curve indicates that that beam and any larger beam is satisfactory for the given span, stringer spacing, and slab thickness. For example, consider the AASHO beams shown in Fig. 5. A point lying to the left of the 6-in. slab curve for beam No. 3 and to the right

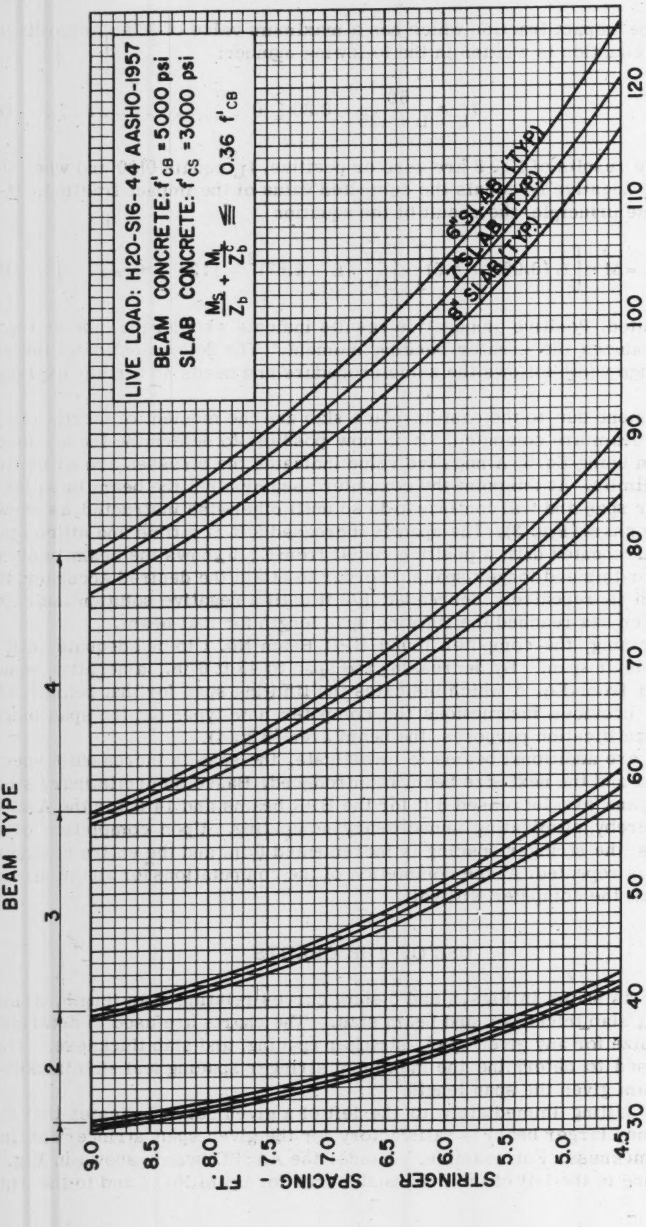

FIG. 5.—PRESTRESSED CONCRETE BRIDGE BEAMS, AASHO-PCI STANDARD SECTIONS, POST-TENSIONED

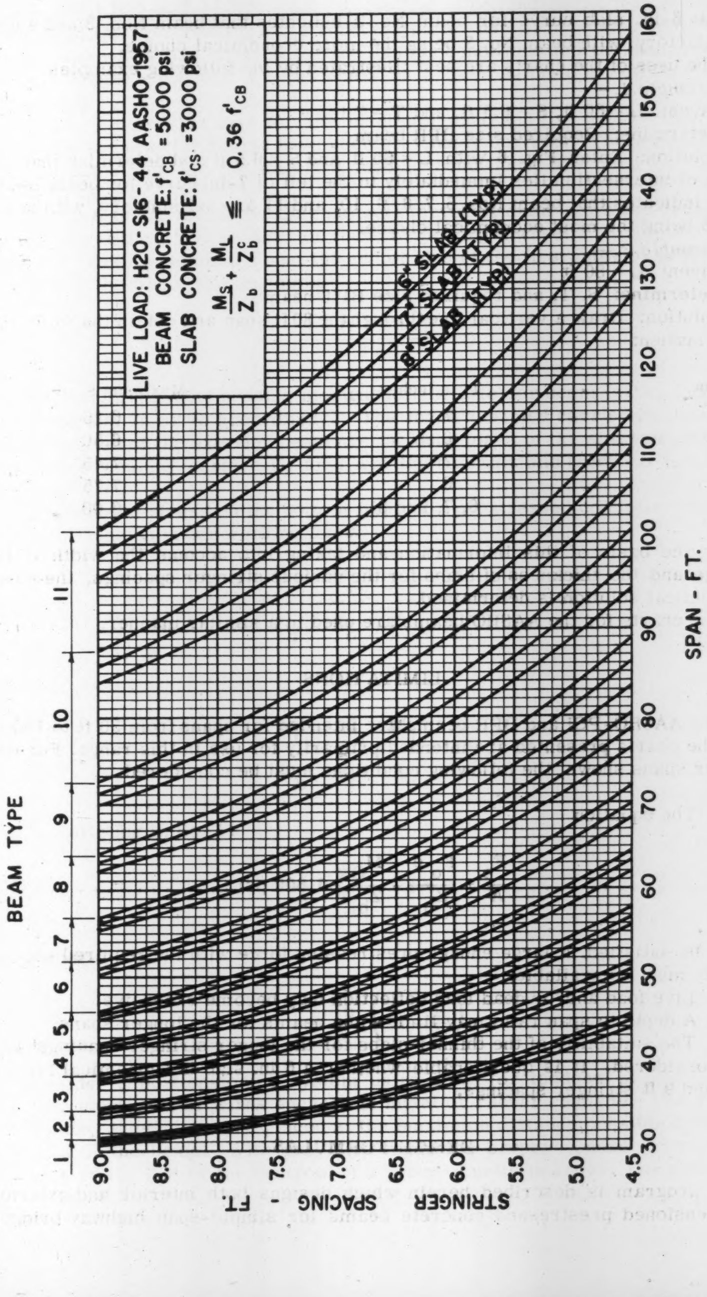

FIG. 6.—PRESTRESSED CONCRETE BRIDGE BEAMS, BPR STANDARD SECTIONS, POST-TENSIONED

of the 6-in. slab curve for beam No. 2 indicates that beam Nos. 3 and 4 are satisfactory, with beam No. 3 being the more economical choice.

The uses of the charts are best illustrated by the following examples:

Example 1.—

Given: L = 60 ft, S = 6.5 ft, and T = 7 in.

Determine: Required size BPR beam

Solution: Enter Fig. 6 with L = 60 ft and S = 6.5 ft and determine that the point of intersection lies immediately to the left of 7-in. curve for beam No. 6. This indicates that beam Nos. 6, 7, 8, 9, 10, and 11 are satisfactory, with beam No. 6 being the most economical choice.

Example 2.—

Given: L = 80 ft

Determine: S, T, and required size BPT beam

Solution: Draw a vertical line through the 80 ft span and obtain the following information:

Beam	T, in inches	Maximum S, in feet
8	7	6.25
8	6	6.50
9	7	7.45
9	6	7.75
10	6, 7, and 8	9.00

On the basis of this information and taking into account the width of the bridge and the thickness of slabs for the various stringer spacings, the most economical solution is determined.

The charts for the AASHO beams are used in a similar manner.

LIMITATIONS

The AASHO-PCI and BPR beams are intended for spans from 30 ft to 100 ft and the charts presented are intended primarily for use in this range. For the longer spans shown, the following conditions must be considered:

1. The equation

$$\frac{F_o}{A} + \frac{F_o e}{Z_b} - \frac{M_G}{Z_b} = 1{,}800 \text{ psi} \quad \ldots\ldots\ldots\ldots (10)$$

must be satisfied. A large enough prestressing force with the required eccentricity must be available.

2. Live load and/or dead load deflection may become excessive.

3. A depth to span ratio may limit some beams for the longer spans.

4. The suitability of the thinner slabs for the longer stringer spacings was not considered. It is questionable whether a 6 in. slab is economical for the 8 ft and 9 ft stringer spacings.

DESIGN FORMULAS

A program is described herein which designs both interior and exterior posttensioned prestressed concrete beams for simple-span highway bridges with AASHO H20-S16-44 live load. A method of computing the magnitude and location of the prestressing force is developed for use with the electronic computer. Equations are derived for the loading conditions and the design of the beams. These equations are presented in a form suitable for efficient programming.

Flexure.—The equations for the maximum dead and live load bending moments for the interior beams have been previously derived. These equations, with modifications for the different loading conditions, are used for the exterior beam.

The maximum live load bending moment for the exterior beam is determined by applying to the beam the reaction found by placing a wheel 2 ft from the curb (Fig. 7). Taking moments about the center line of the first interior beam, the fraction of the wheel load becomes

$$\frac{S + D - W - 2.0}{2\,S}$$

The maximum live load bending moment for the exterior beam is then found by modifying Eq. 7a or 7b accordingly. The loads assumed carried by the composite section of the exterior beam are the dead loads of the sidewalk, railing, and future wearing surface (if any) and the sidewalk and truck (or lane) live loading.

Consider the stress on the bottom fiber of a prestressed concrete beam allowing no tension under working loads

$$\frac{F}{A} + \frac{F\,e}{Z_b} - \frac{M_G}{Z_b} - \frac{M_S}{Z_b} - \frac{M_L}{Z_b^c} + 0 \quad \ldots\ldots\ldots\ldots\ldots (11)$$

Letting

$$\frac{M_G}{Z_b} + \frac{M_S}{Z_b} + \frac{M_L}{Z_b^c} = \Sigma f \quad \ldots\ldots\ldots\ldots\ldots\ldots (12)$$

and substituting in Eq. 11

$$\frac{F}{A} + \frac{F\,e}{Z_b} - \Sigma f = 0 \quad \ldots\ldots\ldots\ldots\ldots\ldots (13)$$

Solving for e,

$$e = \frac{Z_b}{F}\left(\Sigma f - \frac{F}{A}\right) \ldots\ldots\ldots\ldots\ldots\ldots (14)$$

Consider a posttensioning system using units (or tendons) of high tensile strength steel bars or wires encased in metal or rubber conduits. For greater economy these units are placed at the maximum distance possible from the centroid of the beam. With provision made for proper concrete cover, the distance to any unit or the centroid of a group of units is known. For example,

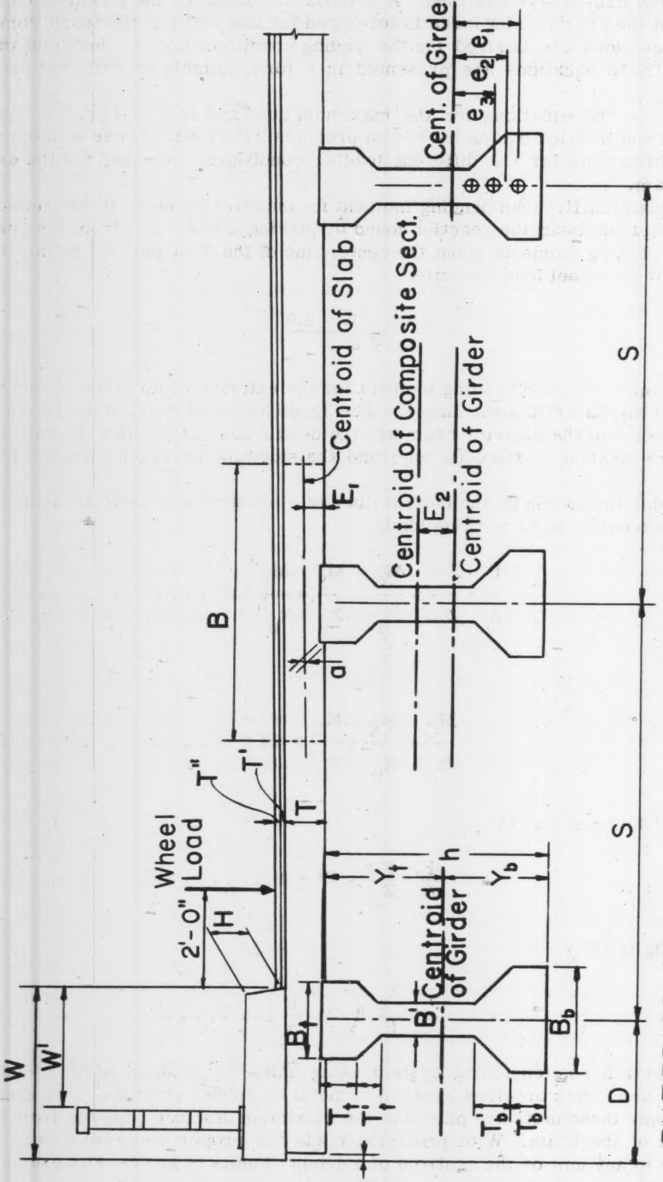
W
W'
c
T_t
T'_t
T_b
T'_b
B_t
B'
B_b
Centroid of Girder
D
EXTERIOR BEAM
2'-0"
H
Wheel Load
T"
T'
T
Y_t
h
Y_b
S
B
a
E_1
Centroid of Slab
E_2
Centroid of Composite Sect.
Centroid of Girder
INTERIOR BEAM
S
Cent. of Girder
e_3
e_2
e_1

FIG. 7

in Fig. 7, e_1 is the maximum eccentricity (distance) for unit #1; e_2 is the maximum eccentricity for units #1 and #2, etc.

Assume the concrete stresses on the bottom fiber of the beam due to the external loads are known. The effective steel prestress or the allowable design stress is 0.60 f_{sy} or 0.80 f'_s, whichever is smaller. The prestressing force for a unit or group of units having an area A_s, is therefore:

$$F = A_s f_{se} \quad \ldots\ldots\ldots\ldots\ldots\ldots\ldots (15)$$

Consider first a unit or group of units having an area A_s and located a distance e from the centroid of the beam. The prestressing force F_1, and e_1, are substituted in Eq. 13, giving

$$\frac{F_1}{A} + \frac{F_1 e_1}{Z_b} - \Sigma f \geqq 0 \quad \ldots\ldots\ldots\ldots\ldots\ldots (16)$$

Negative results indicate there is tension on the bottom fiber of the beam. For this condition, successively increasing magnitudes of the prestressing force, F, with the corresponding maximum eccentricity values, e, are substituted until positive results, indicating compression on the bottom fiber of the beam, are obtained. The prestressing force thus obtained is substituted in Eq. 14 and the computed eccentricity is for a zero stress condition.

Losses in Prestress.—The loss in steel prestress is due to creep, shrinkage, and elastic shortening of concrete, creep in steel, and friction.

Elastic Shortening of Concrete.—Since the tendons in a posttensioned member are stressed in succession, the loss in prestress for each tendon will differ. However, for practical purposes, it is sufficiently accurate to assume the same loss for each tendon.

Creep in Concrete.—This loss in prestress is taken as 2.25 times the elastic shortening.

Shrinkage of Concrete.—Recognizing that some shrinkage has taken place prior to prestressing, an average shrinkage strain of 0.0002 is used.

Creep in Steel.—The loss in prestress due to creep in steel is taken as 4% of the stress in the steel immediately after prestressing.

The total loss in steel prestress resulting from creep, shrinkage, and elastic shortening in concrete, and creep in steel is

$$\Delta f_s = 1.0400\, E_s \left(0.0002 + 3.25 \frac{f_{cs}}{E_{ci}}\right) + 0.0400\, f_{se} \quad \ldots\ldots (17)$$

where the flexural modulus of elasticity of concrete at time of prestressing is given as

$$1.8 \times 10^6 + 500\, f'_{ci}$$

The major friction losses in posttensioned members are due to the curvature of the tendons and the friction between the contact materials. The stress at the prestressing jack is

$$T_o = T_x e_n^{(K\ L\ +\ \mu \alpha)} \quad \ldots\ldots\ldots\ldots\ldots\ldots (18)$$

and the prestressing force for a tendon having an area A'_s becomes

$$F'_j = A'_s \left(f_{se} + \Delta f_s \right) e_n^{(K\ L\ +\ \mu\ \alpha)} \quad \ldots\ldots\ldots\ldots (19)$$

The total angular change α (Fig. 8(a)) is

$$\tan\ \alpha = \frac{2e}{L/2} = \frac{e}{3\ L} \quad \ldots\ldots\ldots\ldots\ldots\ldots (20)$$

where L is in feet and e is in inches.

Finally, the prestressing force at the jack is

$$F'_j = A'_s \left(f_{se} + \Delta f_s \right) e_n^{(KL\ +\ \mu e/3L)} \quad \ldots\ldots\ldots\ldots (21)$$

Ultimate Strength.—As an approximation, the ultimate resisting moment of the beam is assumed supplied by a couple T_u j d or C_u j d, where T_u is the ultimate tensile force, C_u is the compressive force supplied by the concrete, and j d is the distance between the two forces (Fig. 9). It is assumed that failure in bond and shear is prevented and that the proper keys and/or shear connectors are provided.

By specifications the ultimate strength capacity of the beam must exceed

$$m_u = DL + 3(LL + I) \quad \ldots\ldots\ldots\ldots\ldots\ldots (22a)$$

or

$$m_u = 2\ (DL + LL + I) \quad \ldots\ldots\ldots\ldots\ldots\ldots (22b)$$

whichever is greater.

Shear.—It is assumed that shear failure will not occur before ultimate flexural strength is developed and therefore the principal tensile stress at design loads is not considered. The critical section for shear is taken a distance from the support equal to one and a half times the depth of the member. The difference between the centroid of the beam at midspan and at the supports is small and therefore neglected. The trajectory of the center of gravity of the prestressing steel is assumed parabolic (Fig. 8(b)).

The tangent of the angle β is

$$\tan\ \beta = \frac{2\ e \left(\frac{L}{2} - x \right)^2}{\left(\frac{L}{2} \right)^2} \quad \ldots\ldots\ldots\ldots\ldots\ldots (23)$$

The shear carried by the tendons becomes

$$V_F = A_s\ f'_s \tan\ \beta \ldots\ldots\ldots\ldots\ldots\ldots (24)$$

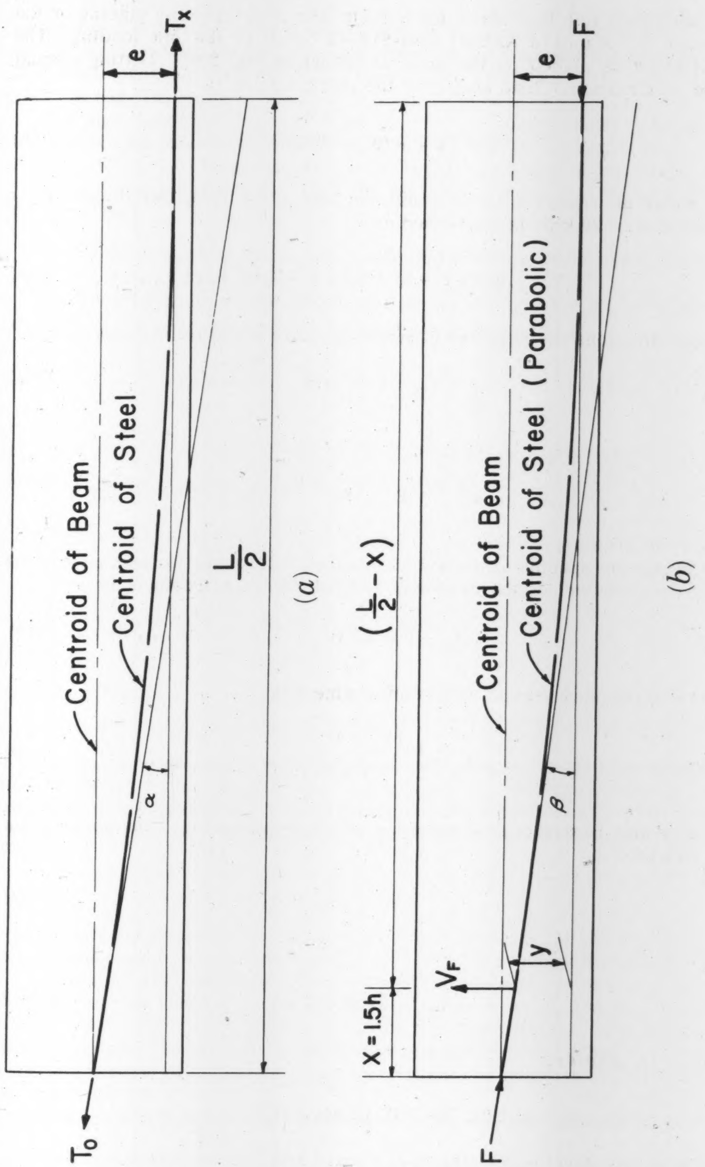
Centroid of Beam
Centroid of Steel
T_o
T_x
e
α
$\frac{L}{2}$
(a)
$X = 1.5h$
$\left(\frac{L}{2} - X\right)$
Centroid of Beam
Centroid of Steel (Parabolic)
F
F
V_F
y
e
β
(b)

FIG. 8

The maximum live load shear for a 10-ft lane is obtained by placing on the span either the standard AASHO H20-S16-44 truck or the lane loading. The standard truck is placed on the span as shown in Fig. 2(b). Letting x equal 1.5 h the maximum live load shear for the truck loading is

$$V = 72 - \frac{1}{L}(9\ h + 672) \qquad (25)$$

The shear at a point x due to a uniform load of 0.640 kip per ft and a concentrated load of 26 kips is expressed as

$$V = 0.08\ (4\ L - h) + 3.25\ \left(\frac{8\ L - h}{L}\right) \qquad (26)$$

By specifications the required ultimate capacity of the beam must exceed

$$V_u = V_D + 3\ V_L - V_F \qquad (27a)$$

or

$$V_u = 2\left(V_D + V_L\right) - V_F \qquad (27b)$$

whichever is greater.

The maximum spacing of the web reinforcement equals three-quarters the depth of the member and the minimum area of web reinforcement is

$$A_v = 0.0025\ B'_s \qquad (28)$$

The recommended area of web reinforcement is

$$A_v = \frac{1}{2}\ \frac{\left(V_u - V_c\right)}{f'_y\ j\ d}\ s \qquad (29)$$

where s is the maximum spacing of the web reinforcement. The shear taken by the concrete is

$$V_c = 0.06\ f'_c\ B'\ j\ d \qquad (30a)$$

or

$$V_c = 180\ B'\ j\ d \qquad (30b)$$

whichever is smaller.

USE OF THE COMPUTER

The program developed consists of a main program recorded on a primary tape and input data listed on secondary or supplementary tapes. The prestressed concrete beams are designed using the main program which is independent of the prestressing system used. The secondary tapes are dependent on the prestressing system and supply the required data for the system chosen. The main program is divided into four parts, as shown in the simplified flow chart in Fig. 10.

The input tapes list for each beam the various combinations of prestressing steel area and maximum eccentricity for a given prestressing system. The AASHO-PCI and BPR beams are listed together in order of increasing areas.

The information necessary for the solution of a given problem consists of the following:

1. The area of the interior beam selected from the charts (Figs. 5 and 6).
2. The area of the exterior beam.
3. The dimensions of the structure such as the span length, stringer spacing, slab thickness, and size and number of diaphragms.

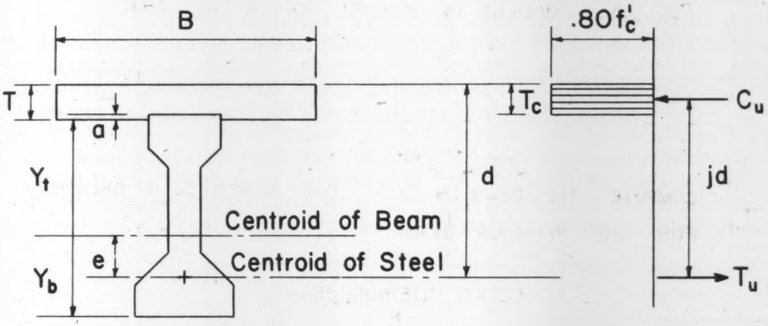

FIG. 9

The combinations of the prestressing steel area and maximum eccentricity for the selected interior beam must be placed in predetermined locations for later use in the program. The computer obtains from the supplementary tape the input for each succeeding beam (Fig. 11(a)) and solves the equation

$$A = A_i \geq 0 \quad \ldots\ldots\ldots\ldots\ldots\ldots \quad (31)$$

Negative results direct the computer to obtain the input for the next beam and zero results indicate the computer has obtained the input for the exterior beam.

Continuing, the computer obtains the flexural modulus of elasticity of the concrete at the time of prestressing and under working loads. The impact fraction, the effective steel prestress, and the maximum live load moment and shear (including impact) for a 10-ft lane are determined. They are computed using the method of decisions based on positive and negative results previously developed.

The weight of the beam and the weight of the concrete slab it supports are computed and are used to determine the design dead load moment and shear for the interior beam. The fraction of a wheel load is applied to the beam to

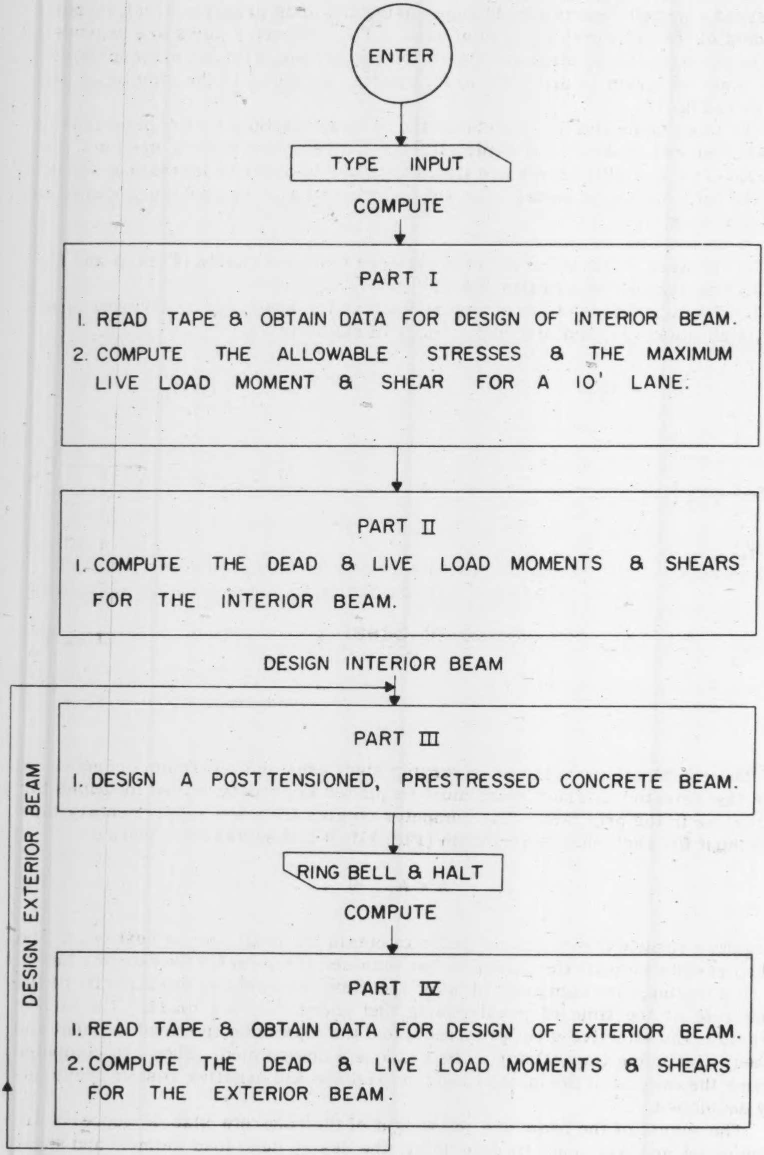
ENTER
TYPE INPUT
COMPUTE
PART I
1. READ TAPE & OBTAIN DATA FOR DESIGN OF INTERIOR BEAM.
2. COMPUTE THE ALLOWABLE STRESSES & THE MAXIMUM LIVE LOAD MOMENT & SHEAR FOR A 10' LANE.
PART II
1. COMPUTE THE DEAD & LIVE LOAD MOMENTS & SHEARS FOR THE INTERIOR BEAM.
DESIGN INTERIOR BEAM
DESIGN EXTERIOR BEAM
PART III
1. DESIGN A POST TENSIONED, PRESTRESSED CONCRETE BEAM.
RING BELL & HALT
COMPUTE
PART IV
1. READ TAPE & OBTAIN DATA FOR DESIGN OF EXTERIOR BEAM.
2. COMPUTE THE DEAD & LIVE LOAD MOMENTS & SHEARS FOR THE EXTERIOR BEAM.

FIG. 10.—FLOW CHART

determine the design live load bending moment and shear. The computer is now ready to design the interior beam.

The effective flange, the composite section properties and the stresses on the top and bottom fibers of the beam due to external loads are computed. An initial prestressing steel area is selected from the previously obtained input and the prestressing force is then computed using Eq. 15. The substitution of the prestressing force, F, and its corresponding maximum eccentricity, e, in Eq. 13 as previously explained, will indicate the state of stress on the bottom fiber of the beam. The computer will select successive areas of steel until the desired positive results are obtained. If all possible combinations of steel area and maximum eccentricity fail to provide satisfactory results, the computer will halt. The required eccentricity for zero stress condition is computed using Eq. 14.

The area of the beam, the area of the prestressing steel and the required eccentricity are then typed by the computer (Fig. 12). The losses in prestress are determined in order to compute the initial prestressing force; the prestressing force required at the jacks for the separate tendons and the initial stresses on the top and bottom fibers of the beam. The prestressing force at the jacks and the resultant initial and final concrete stresses are then typed. The ultimate strength of the beam, the shear and the deflections are computed and typed as indicated on the flow chart (Fig. 11(b)).

The halt is provided so that the critical stresses and the ultimate strength of the beam can be checked. It is possible to compute again using the next area of steel if the results found are unsatisfactory. The computer then obtains the input data for the exterior beam using the process previously described for the interior beam, and by returning to Part III, the computer designs the exterior beam.

CONCLUSIONS

The programs described herein select and design the standard AASHO-PCI and BPR posttensioned prestressed concrete beams with AASHO H20-S16-44 loading. The flexibility of the programs provide for the selection and design of any shape beam using any AASHO live loading and strength of concrete and steel.

The programs presented are applicable to building construction if they are modified as follows. First, the live load is different since it usually consists of a uniformly distributed load instead of the standard AASHO loadings. Second, although the shapes of the beams differ from the heavy bridge beams this consideration is of minor importance since only the physical properties of the beam are required in the programs. The third consideration is the effect of concentrated loads on the profile of the prestressing tendons. A parabolic curve is still possible since the envelope of the moment diagram of a unit load moving across the span is a parabola. Using the AASHO loadings, it is the experience of the writer that because of the parabolic shape of the cables and the moment envelope, the stresses at points other than midspan are not critical and therefore they are not considered.

The AASHO Specifications limit the live load deflection to 1/800 of the span for steel beams and girders. If this criteria is allowed to govern for prestressed concrete beams it then becomes unnecessary to calculate live load deflections for two reasons:

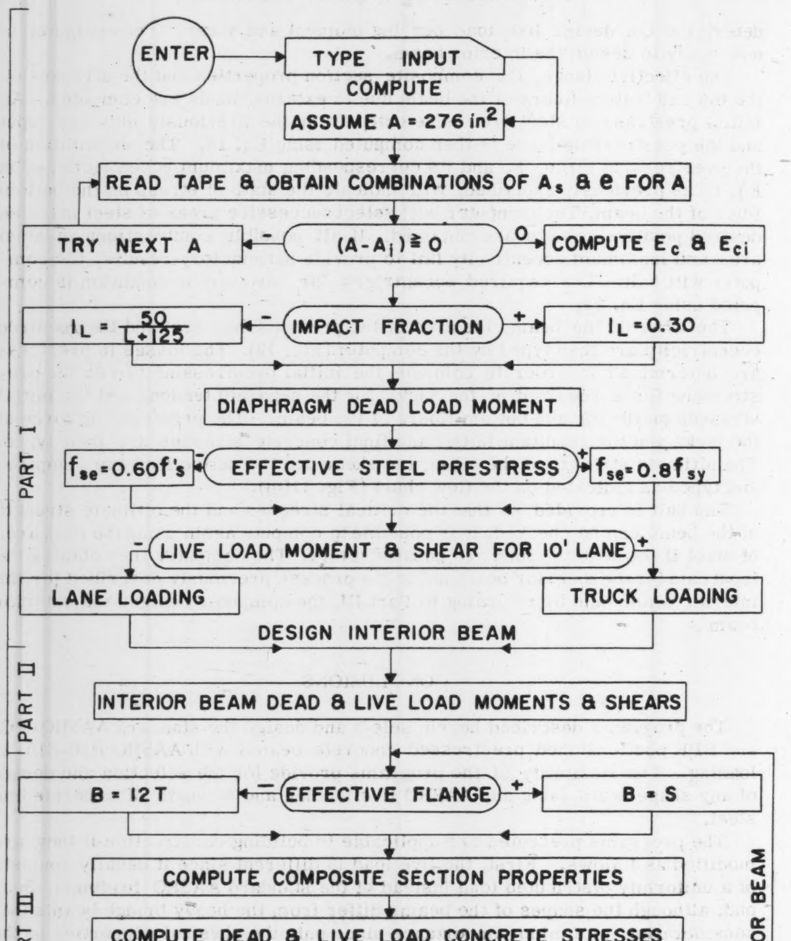
ENTER
TYPE INPUT
COMPUTE
ASSUME A = 276 in^2
READ TAPE & OBTAIN COMBINATIONS OF A_s & e FOR A
TRY NEXT A
$(A - A_i) \geq 0$
COMPUTE E_c & E_{ci}
$I_L = \frac{50}{L+125}$
IMPACT FRACTION
$I_L = 0.30$
DIAPHRAGM DEAD LOAD MOMENT
$f_{se} = 0.60 f'_s$
EFFECTIVE STEEL PRESTRESS
$f_{se} = 0.8 f_{sy}$
LIVE LOAD MOMENT & SHEAR FOR 10' LANE
LANE LOADING
TRUCK LOADING
DESIGN INTERIOR BEAM
INTERIOR BEAM DEAD & LIVE LOAD MOMENTS & SHEARS
B = 12T
EFFECTIVE FLANGE
B = S
COMPUTE COMPOSITE SECTION PROPERTIES
COMPUTE DEAD & LIVE LOAD CONCRETE STRESSES
$F = A_s f_{se}$
NO
LAST A_s & e?
YES
$\frac{F}{A} + \frac{Fe}{Z_b} - \sum f \geq 0$
RING BELL & HALT
PART I
PART II
PART III
DESIGN EXTERIOR BEAM
0
+
-

FIG. 11a.—FLOW CHART

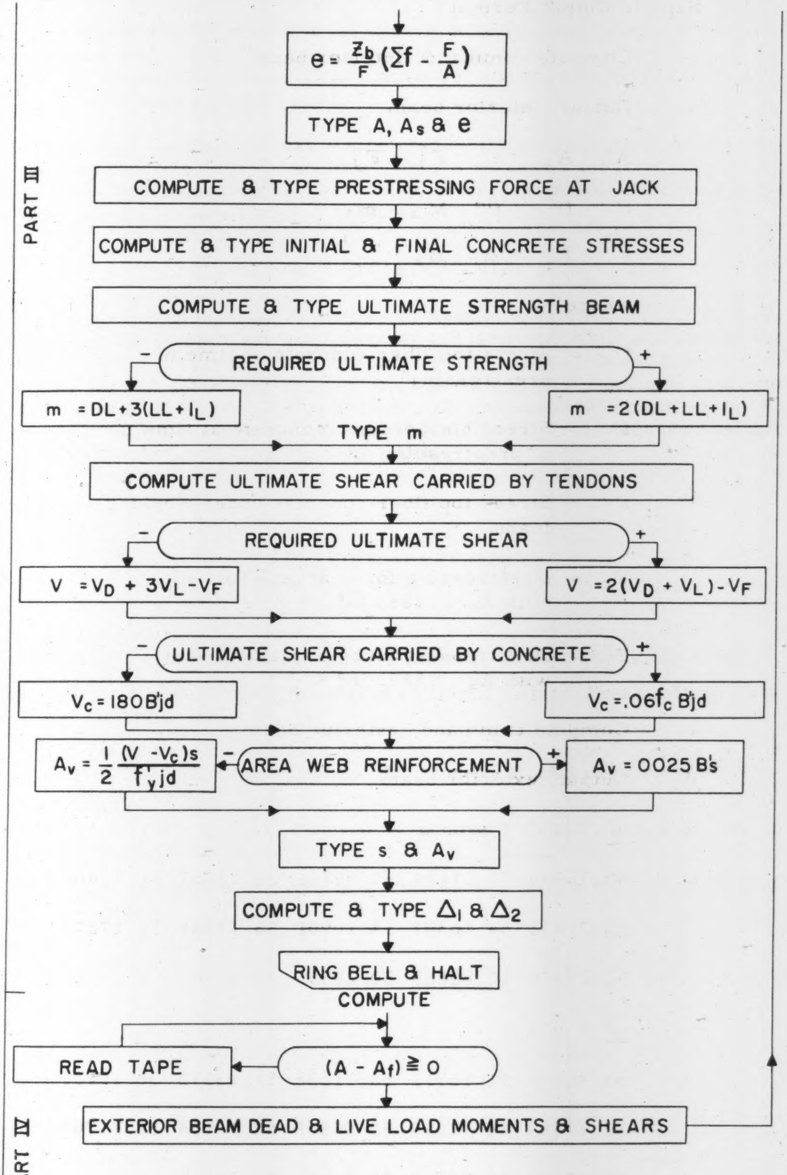
$e = \frac{Z_b}{F}(\Sigma f - \frac{F}{A})$
TYPE A, A_s & e
PART III
COMPUTE & TYPE PRESTRESSING FORCE AT JACK
COMPUTE & TYPE INITIAL & FINAL CONCRETE STRESSES
COMPUTE & TYPE ULTIMATE STRENGTH BEAM
−
REQUIRED ULTIMATE STRENGTH
+
$m = DL + 3(LL + I_L)$
$m = 2(DL + LL + I_L)$
TYPE m
COMPUTE ULTIMATE SHEAR CARRIED BY TENDONS
−
REQUIRED ULTIMATE SHEAR
+
$V = V_D + 3V_L - V_F$
$V = 2(V_D + V_L) - V_F$
−
ULTIMATE SHEAR CARRIED BY CONCRETE
+
$V_c = 180B'jd$
$V_c = .06f_c B'jd$
$A_v = \frac{1}{2}\frac{(V - V_c)s}{f'_y jd}$
−
AREA WEB REINFORCEMENT
+
$A_v = 0025 B's$
TYPE s & A_v
COMPUTE & TYPE Δ_1 & Δ_2
RING BELL & HALT
COMPUTE
READ TAPE
$(A - A_f) \geqq 0$
EXTERIOR BEAM DEAD & LIVE LOAD MOMENTS & SHEARS
PART IV

FIG. 11b.—FLOW CHART

1. Sample Output Format

   a. Compute command, interior beam

   b. Output, interior beam

      $A \quad A_s \quad e \quad F_j' \quad F_j''$

      $f' \quad f'' \quad f''' \quad M_u \quad m_u$

      $s \quad A_V \quad \Delta_1 \quad \Delta_2$

      where

      f' = Stress top fiber concrete at time of prestressing

      f'' = Stress bottom fiber concrete at time of prestressing

      f''' = Stress top fiber concrete under working loads

      F_j' = Prestressing force at jack for unit with $A_s' = .7856$ in^2

      F_j'' = Prestressing force at jack for unit with $A_s' = .5892$ in^2

   c. Compute command, exterior beam

   d. Output, exterior beam

2. a.

```
qf     000     z     s
```

   b.

```
 53.36900  51.21604  51.90766  56.13867  56.10400

 52.79632  54.16397  54.10901  58.17585  58.17278

 52.27000  50.88865  50.28555  50.17101
```

   c.

```
qf     610     z     s
```

   d.

```
 53.36900  51.15712  52.11228  56.13575  56.10181

-52.42389  54.12399  53.80865  58.13654  58.11707

 52.27000  50.40500  50.23685  50.14581
```

FIG. 12

1. There usually results a net upward deflection due to the effect of prestressing and dead load.

2. The moment of inertia of the standard beams are quite large in comparison to steel beams of equal depth.

The programs presented can also be used for the design of pretensioned prestressed concrete beams. Modifications are necessary for bond, straight or deviated (with hold-down devices) cables, concrete stresses at the ends of the beam, and the greater losses in prestress.

ACKNOWLEDGMENTS

The writer is indebted to Lockwood, Kessler & Bartlett, Inc., of Syosset, N.Y. for use of the electronic computer and the responsibility of developing the described programs. The writer gratefully thanks Edward J. Squire, F. ASCE, for his assistance and advice in preparing this paper and wishes to thank Joseph M. Dawson, Ennio M. Gherardi, and Robert O'Connell, M. ASCE, for their valuable comments and suggestions. The paper has been used as part of the writer's thesis for a Master's degree.

APPENDIX.—REFERENCES

1. "Criteria for Prestressed Concrete Bridges," Bur. of Pub. Rds., 1954.
2. "Standard Specifications for Highway Bridges," Amer. Assn. of State Highway Officials, 1957.
3. "Tentative Recommendations for Prestressed Concrete," Report on the Joint ACI-ASCE Committee on Prestressed Reinforced Concrete, Proceedings, January, 1958.
4. "Design of Prestressed Concrete Structures," by T. Y. Lin, John Wiley & Sons, Inc., New York, 1955.
5. "Design of Highway Bridges in Prestressed Concrete," Portland Cement Assn., 1958.

DISCUSSION

RICHARD J. NEWSON,[2] A. M. ASCE.—Bonasia has presented an interesting paper on a subject which is current and has especial significance for the younger engineer because it is fairly easy to understand; and, if called upon to do so, the younger engineer should have no trouble solving the kind of problem with which the paper is concerned.

Bonasia assumes that proper keys and shear or both connectors are provided to prevent failure in shear. It is thought that Mr. Bonasia could have used the Bendix G-15D to advantage by programming a check on shear flow, V Q/I, between the slab and the stem. The machine will give the spacing of the connectors if so programmed.

JOSEPH J. BONASIA,[3] A.M. ASCE.—The ACI-ASCE "Tentative Recommendations for Prestressed Concrete" states that "shear failure should not occur before ultimate flexural strength is developed." The program so provides by adequately reinforcing the web in accordance with said specifications. The program can be utilized to check the shear flow between the slab and beam if desired.

---

[2] Design Engr., Indiana State Highway Dept., Indianapolis, Ind.
[3] Civ. Engr., Ozone Pk., N.Y.

AMERICAN SOCIETY OF CIVIL ENGINEERS
Founded November 5, 1852
TRANSACTIONS

Paper No. 3256

INFLUENCE OF PARTIAL BASE FIXITY ON FRAME STABILITY

By Theodore V. Galambos,[1] A.M. ASCE

With Discussion by Messrs. Eugene Guillard; Joseph W. Appeltauer and Thomas A. Barta; and Theodore V. Galambos

SYNOPSIS

The buckling strength of a pinned-base rigid frame is considerably lower than that of an identical fixed-base frame. In current design practice in the United States, however, pinned column bases are specified for most structures because the construction of suitable foundations for fixed bases usually increases the over-all cost. It is shown that the rotational restraint offered by commonly used "pinned" column bases is sufficient to increase the buckling strength of these frames to almost that of identical fixed-base rigid frames.

INTRODUCTION

The buckling load of a pinned-base rigid frame is considerably below that of an identical fixed-base frame. This may be shown by any one of the many "exact" and approximate methods that are available for determining the buck-

---

Note.—Published essentially as printed here, in May, 1960, in the Journal of the Structural Division, as Proceedings Paper 2480. Positions and titles given are those in effect when the paper or discussion was approved for publication in Transactions.

[1] Research Asst. Prof., Fritz Engrg. Lab., Lehigh Univ., Bethlehem, Pa.

ling strength of rigid frames. Many of these methods are available elsewhere.[2,3,4,5,6]

The single-story, single-bay rectangular rigid frame will be examined as an illustration. For simplicity it will be assumed that the axial force acting on each column is equal and that the frame is symmetric. The two frames which will be compared are shown in Figs. 1(a) and (b). Fig. 1(a) shows the pinned-base frame and Fig. 1(b) shows the fixed-base frame.

The frame shown in Figs. 1(a) and (b) may buckle in one of two modes:

1. It may fail by a sidesway buckling mode.
2. It may fail in a symmetric mode if sidesway is prevented at the top of the columns.

Of these two, the sidesway type buckling is the more critical. Therefore this mode of buckling will be considered here. The solid lines in Figs. 1(a) and (b) represent the stable, undeflected shape of the frame. The dashed lines show the unstable, sideswayed frame.

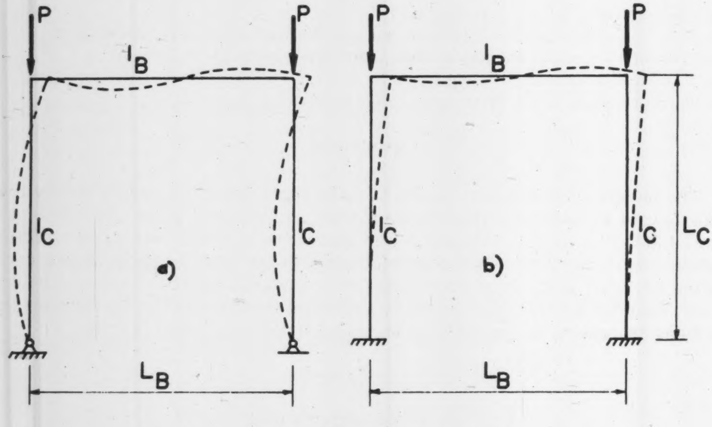

Solid Lines: Stable deflection configuration
Dashed Lines: Unstable deflection configuration

FIG. 1.—DEFLECTION CONFIGURATION OF PINNED BASE AND FIXED BASE RIGID FRAMES.

---

[2] "Buckling Strength of Metal Structures," by F. Bleich, McGraw-Hill Book Co., Inc., New York, 1952, Chapters VI and VII.

[3] "Theory of Elastic Stability," by S. Timoshenko, McGraw-Hill Book Co., Inc., New York, 1936, Chapter II.

[4] "Rational Simplifications for the Buckling Length of Columns," by T. C. Kavanagh, Column Research Council, Proceedings of the Seventh Tech. Session, May, 1958.

[5] "Guide to Design Criteria for Metal Compression Members," Column Research Council (to be published.)

[6] "Din 4114 Knickung, Kippung, Beulung," "German Buckling Specification," English translation by T. V. Galambos and J. Jones, Column Research Council, June, 1957.

The problem of the pinned-base, single-story, single-bay rigid frame has been solved[7] as has the corresponding fixed-base frame.[8] The critical buckling load of either frame is

$$P_{cr} = \frac{\pi^2 E_t I_C}{\left(k L_C\right)^2} \quad \ldots\ldots\ldots\ldots\ldots\ldots \quad (1)$$

in which P_{cr} is the load causing frame buckling, E_t denotes the tangent modulus, I_C is the moment of inertia of the columns in the plane of bending, L_C represents the length of the columns, and k is a coefficient indicating the "effective" length of the column.

The critical buckling condition of the pinned-base frame is expressed by the following buckling equation:

$$\frac{\cot \phi}{\phi} - \frac{\gamma}{6} = 0 \quad \ldots\ldots\ldots\ldots\ldots\ldots \quad (2)$$

The corresponding equation for the fixed-base frame is

$$\phi \sin \phi \cos \phi \left[\frac{\cot \phi}{\phi} - \frac{\gamma}{6}\right] = 1 \quad \ldots\ldots\ldots\ldots \quad (3)$$

In Eqs. 2 and 3, γ is a non-dimensional ratio defined as

$$\gamma = \frac{I_C L_B \tau}{I_B L_C} \quad \ldots\ldots\ldots\ldots\ldots\ldots \quad (4)$$

in which I_B is the moment of inertia of the beam in the plane of bending, L_B denotes the length of the beam, and τ is the ratio of tangent modulus to modulus of elasticity, E_t/E. The term ϕ in Eqs. 2 and 3 is equal to

$$\phi = L_C \sqrt{\frac{P_{cr}}{E_t I_C}} \quad \ldots\ldots\ldots\ldots\ldots\ldots \quad (5)$$

The relationship between the coefficients k in Eq. 1 and ϕ in Eqs. 2 and 3 is established as follows: From Eq. 5,

$$P_{cr} = \frac{\phi^2 E_t I_C}{L_C^2} \quad \ldots\ldots\ldots\ldots\ldots\ldots \quad (6)$$

If this value of P_{cr} is equated to P_{cr} of Eq. 1, the relationship between k and ϕ is

$$k = \frac{\pi}{\phi} \quad \ldots\ldots\ldots\ldots\ldots\ldots\ldots \quad (7)$$

The curves relating the effective length factor k and the non-dimensional ratio γ, as computed by Eqs. 2 and 3, are given in Fig. 2 for the two column-base conditions. The coefficient k varies from $k = 1.0$ at $\gamma = 0$ to $k = 2.0$ at $\gamma = \infty$ for the fixed-base frame. The corresponding variation of k for the pinned-base frame is from $k = 2.0$ to $k = \infty$. It must be noted that k enters into the denominator of Eq. 1 as a squared term, and thus, the reduction in strength due to a pinned-column base is quite considerable according to this theory. Taking for example the case in which $\gamma = 1.0$, $k = 1.16$ for the fixed-base frame and $k = 2.33$ for the pinned-end condition. Substitution of these values of k into

---

[7] "Buckling Strength of Metal Structures," by F. Bleich, McGraw-Hill Book Co., Inc., New York, 1952, Sect. 73

[8] Ibid., Sect. 74.

Eq. 1 shows that the fixed-base frame may carry 4.07 times as much load as the pinned-base frame. As γ increases, the difference tends to become larger. At γ = 5.0 the ratio of the two buckling strengths is 5.07.

STATEMENT OF THE PROBLEM

The foregoing discussion shows that by fixing the column bases, the buckling strength of a rigid frame can be increased by a factor of 4 or even 5. In European practice, use is made of this fact by usually specifying fixed-base structures, sometimes at no small expense to the builder. In American practice, on the other hand, the assumption of a pinned-base structure is the general rule.

It is, however, impossible to attain either a fully pinned end or a fully fixed-end condition in construction. The column bases are in a stage intermediate between the two extremes. The actual restraint depends on the details used in the construction of the bases.

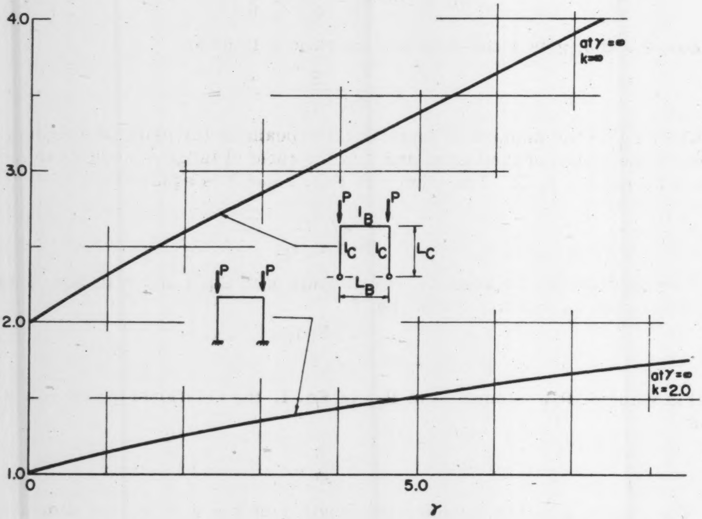

FIG. 2.—EFFECTIVE LENGTH FOR PINNED BASE AND FIXED BASE RIGID FRAMES

The purpose of this paper is to investigate the extent of the influence of partial end restraint on the buckling strength of rigid frames. The relationships between base restraint and frame stability will be established to find out how the critical load varies as the restraint changes from full fixity to a fully pinned-end condition. The problem will be solved for two frames by the slope-deflection method described by F. Bleich.[9] These frames are:

1. Single-story, single-bay rigid frame.
2. Two-story, single-bay rigid frame.

---

[9] Ibid., Sect. 60.

Base restraint is simulated in the following analysis by inserting a restraining beam between the two column bases as shown in Fig. 3(a). This beam restrains the column ends in the same way as would be done by an actual base consisting of base plates, anchor bolts, the footing, and the soil. Base restraints could also be represented by a set of springs that deform in proportion to the end rotation as shown in Fig. 3(b); $M = \beta_\theta$, in which M is the end moment, θ is the rotation, and β is the spring constant. In the subsequent derivations the frame in Fig. 3(a) will be analyzed; the approach for the system of springs (Fig. 3(b)) would be similar.

METHOD OF SOLUTION

Bleich has given[9] the moments at the ends of a member AB (Fig. 4) by the following equations:

$$M_A = \frac{E_t I}{L} \left[C\,\theta_A + S\,\theta_B - \rho\,(C + S) \right] \quad \ldots\ldots\ldots (8a)$$

and

$$M_B = \frac{E_t I}{L} \left[S\,\theta_A + C\,\theta_B - \rho\,(C + S) \right] \quad \ldots\ldots\ldots (8b)$$

in which θ_A and θ_B are end rotations of member AB, and ρ is the rotation of member AB with respect to the unloaded position. It is assumed here that the member has a uniform stiffness along its whole length. The coefficients C and S are defined as

$$C = \frac{c}{c^2 - s^2} \quad \ldots\ldots\ldots\ldots\ldots\ldots (9a)$$

and

$$S = \frac{s}{c^2 - s^2} \quad \ldots\ldots\ldots\ldots\ldots\ldots (9b)$$

in which

$$c = \frac{1}{\phi^2}(1 - \phi \cot \phi) \quad \ldots\ldots\ldots\ldots\ldots (10a)$$

and

$$s = \frac{1}{\phi^2}\left(\frac{1}{\sin \phi} - 1\right) \quad \ldots\ldots\ldots\ldots\ldots (10b)$$

Values of C and S corresponding to practical variations of ϕ are listed in Table 1. Table 1 shows various other coefficients that will be defined later.

The sign convention of Eq. 8 is the following: Joint rotations θ and bar rotations ρ are positive when the rotation takes place in a clockwise sense. For example, all joint and bar rotations of the frame in Fig. 3(a) are clockwise and therefore positive.

A critical buckling equation is obtained by writing an expression for the moment at the ends of each member, using Eq. 8. Equilibrium is maintained at each joint by setting the sum of the moments at the joint equal to zero. Additional necessary equations are obtained from statical conditions. For the frame of Fig. 3(a) for example, an additional equation is obtained by summing

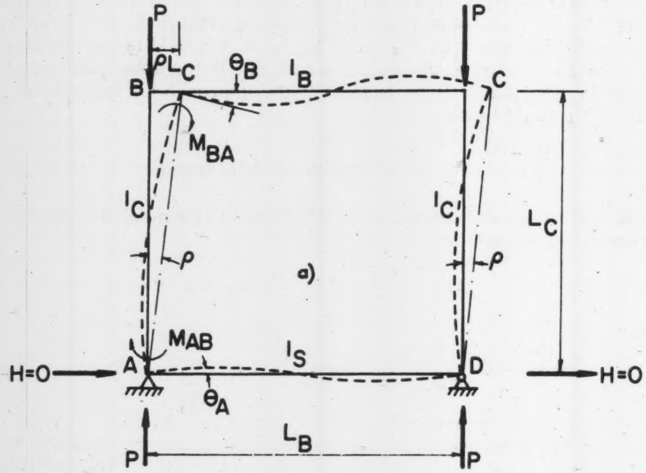
P
P
ρL_C
θ_B
I_B
B
C
M_BA
I_C
I_C
L_C
ρ
ρ
a)
M_AB
I_S
H=O
A
D
H=O
θ_A
L_B
P
P

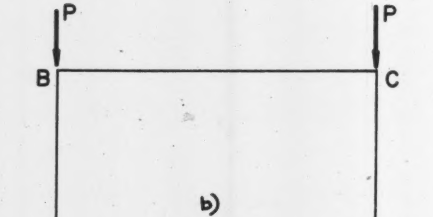
P
P
B
C
b)
A
D
M_AB = βθ_A

FIG. 3.—SINGLE-STORY SINGLE-BAY RECTANGULAR FRAME WITH BASE RESTRAINT

the horizontal reactions and equating their sum to zero. As many independent equations are necessary as the number of unknown joint rotations θ and bar rotations ρ. Stability is satisfied when the determinant of the coefficients of the unknowns is equal to zero.

BUCKLING STRENGTH OF A SINGLE-STORY, SINGLE-BAY RIGID FRAME

The frame that is to be analyzed is shown in Fig. 3(a). Because the loading and the dimensions are symmetrical, only one half of the frame need be considered, because by symmetry $\theta_C = \theta_B$, $\theta_D = \theta_A$ and $\rho_{CD} = \rho_{AB}$. The unknown joint rotations then are θ_A, θ_B, and the unknown bar rotation is $\rho_{AB} = \rho$. For these three unknowns, three independent equations must be found. Joint and bar rotations are clockwise and, therefore, positive. The moments at the ends of bar AB are, according to Eq. 8, the following:

TABLE 1

ϕ	k	S	C	K	Q	R
0		2.000	4.000	3.000	1.000	-1.000
0.1	31.416	2.000	3.999	3.002	0.997	-1.002
0.2	15.708	2.001	3.995	3.008	0.987	-1.007
0.3	10.472	2.003	3.988	3.018	0.970	-1.015
0.4	7.854	2.005	3.979	3.033	0.946	-1.028
0.6	5.236	2.012	3.952	3.075	0.877	-1.063
0.8	3.927	2.022	3.914	3.137	0.777	-1.115
1.0	3.142	2.034	3.865	3.225	0.640	-1.191
1.2	2.618	2.050	3.804	3.337	0.467	-1.287
1.4	2.244	2.070	3.732	3.491	0.241	-1.421
1.6	1.965	2.093	3.647	3.694	-0.047	-1.601
1.8	1.745	2.120	3.548	3.968	-0.420	-1.848
2.0	1.572	2.152	3.436	4.351	-0.915	-2.199
2.2	1.430	2.189	3.309	4.910	-1.601	-2.721
2.4	1.310	2.233	3.166	5.786	-2.620	-3.553
2.6	1.210	2.283	3.005	7.328	-4.323	-5.045
2.8	1.122	2.343	2.825	10.700	-7.875	-8.457
3.0	1.048	2.412	2.624	23.658	-21.034	-21.246

$$M_{AB} = \frac{E_t I_C}{L_C} \left[C_{AB}\,\theta_A + S_{AB}\,\theta_B - \rho\,\left(C_{AB} + S_{AB}\right)\right] \quad . . . . (11a)$$

and

$$M_{BA} = \frac{E_t I_C}{LC} \left[S_{AB}\,\theta_A + C_{AB}\,\theta_B - \rho\,\left(C_{AB} + S_{AB}\right)\right] \quad . . . . (11b)$$

The direction of the moments in Eq. 11 is clockwise as shown in Fig. 4. Noting that $\rho_{AD} = \rho_{BC} = 0$, the bending moments of the end B of bar BC and the end A of bar AC are

$$M_{BC} = \frac{E_t I_B}{L_B} \left[C_{BC}\,\theta_B + S_{BC}\,\theta_B\right] \tag{12a}$$

and

$$M_{AD} = \frac{E_t I_s}{L_B} \left[C_{AD}\,\theta_A + S_{AD}\,\theta_A\right] \tag{12b}$$

There is no axial force present in bars AD and BC. Since therefore $\phi = 0$, the values of the coefficients C and S are obtained from Eq. 9 as

$$C_{AD} = C_{BC} = 2 \tag{13a}$$

and

$$S_{AD} = S_{BC} = 4 \tag{13b}$$

If these values of C and S are substituted into Eq. 12, and if the subscripts of C and S are dropped in Eq. 11, the equations for the four bending moments are

$$M_{AB} = \frac{E_t I_C}{L_C} \left[C\,\theta_A + S\,\theta_B - \rho\,(C + S)\right] \tag{14a}$$

$$M_{BA} = \frac{E_t I_C}{L_C} \left[S\,\theta_A + C\theta_B - \rho\,(C + S)\right] \tag{14b}$$

$$M_{BC} = \frac{6\,E_t\,I_B\,\bar{\theta}_B}{L_B} \tag{14c}$$

and

$$M_{AD} = \frac{6\,E_t\,I_S\,\bar{\theta}_A}{L_B} \tag{14d}$$

Next, the equations of equilibrium will be written at the two joints.
(1) Joint A:

$$M_{AB} + M_{AD} = 0 \tag{15}$$

Substituting M_{AB} and M_{AD} from Eq. 14

$$\frac{E_t I_C}{L_C} \left[C\,\theta_A + S\,\theta_B - \rho\,(C + S)\right] + \frac{6\,E_t\,I_S}{L_B}\,\theta_A = 0 \tag{16}$$

In general E_t of the column will not equal E_t in the beam. Since no forces exist in the beam prior to buckling, all of the beam will remain elastic, and hence $E_t = E$ in this member. The equilibrium equation can now be rearranged as follows:

$$C\,\theta_A + S\,\theta_B - \rho\,(C + S) + \frac{6\,I_S\,L_C\,\theta_A}{I_C\,L_B\,\tau} = 0 \tag{17}$$

If the abbreviation

$$\lambda = \frac{I_S\, L_C}{I_C \cdot L_B\, \tau} \quad \ldots\ldots\ldots\ldots\ldots\ldots\ldots (18)$$

is used, Eq. 17 can be written as:

$$\theta_A\ [C + 6\lambda] + \theta_B\ [S] - \rho\ [C + S] = 0 \quad \ldots\ldots (19)$$

(2) Joint B:

$$M_{BA} + M_{BC} = 0 \quad \ldots\ldots\ldots\ldots\ldots\ldots (20)$$

Performing the same operation as for joint A, the corresponding equilibrium equation will be

$$\theta_A\ [S] + \theta_B \left[C + \frac{6}{\gamma}\right] - \rho\ [C + S] = 0 \quad \ldots\ldots\ldots (21)$$

Eqs. 19 and 21 are two equations in the three unknowns θ_A, θ_B, and ρ. One additional expression is necessary for a solution. This additional equation is obtained from the statical condition that the sum of the horizontal reactions at the bases must equal zero. Because the end moments of column AB are equal in sense to the end moments of column CD, the horizontal base reaction must act to the right for each column. But, because the moments are also equal in magnitude, this can only be possible if the horizontal reaction of each column is zero.

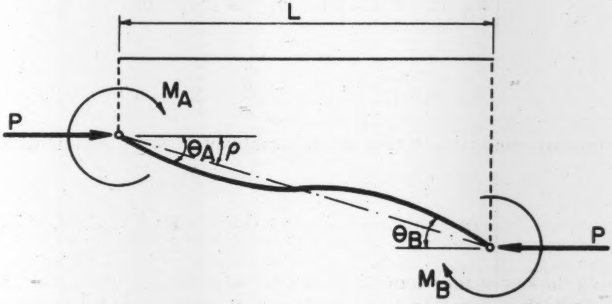

$$M_{AB} = \frac{E_t I}{L}\left[C\theta_A + S\theta_B - \rho\,(C + S)\right]$$

$$M_{BA} = \frac{E_t I}{L}\left[S\theta_A + C\theta_B - \rho\,(C + S)\right]$$

FIG. 4.—SLOPE DEFLECTION EQUATIONS

The additional equation is derived by summing moments about point B (Fig. 3(a)).

$$M_{BA} + M_{AB} + P\,L_C\,\rho = 0 \quad \ldots\ldots\ldots\ldots\ldots \text{(22)}$$

If the values of M_{BA} and M_{AB} from Eq. 14 are substituted into Eq. 22, the following equation results:

$$\theta_A\,[C+S] + \theta_B\,[C+S] - 2\,\rho\,(C+S) + \frac{P\,L_C^2\,\rho}{E_t\,I_C} = 0 \quad \ldots\ldots \text{(23)}$$

Because $\frac{P L_C^2}{E_t\,I_C} = \phi^2$ (Eq. 5), the value of ρ is

$$\rho = \left[\frac{C+S}{2\,(C+S) - \phi^2}\right] \left(\theta_A + \theta_B\right) \quad \ldots\ldots\ldots\ldots \text{(24)}$$

Substitution of ρ from Eq. 24 into Eq. 19 and 21 reduces the unknowns to θ_A and θ_B. With the abbreviation

$$K = \frac{(C+S)^2}{2\,(C+S) - \phi^2} \quad \ldots\ldots\ldots\ldots\ldots\ldots \text{(25)}$$

these equations reduce to the following:

$$\theta_A\,[C + 6\,\lambda - K] + \theta_B\,[S - K] = 0 \quad \ldots\ldots\ldots\ldots \text{(26a)}$$

and

$$\theta_A\,[S - K] + \theta_B\left[C + \frac{6}{\gamma} - K\right] = 0 \quad \ldots\ldots\ldots\ldots \text{(26b)}$$

The stability condition is that the determinant of the coefficients must be zero.

$$\begin{vmatrix} (C + 6\,\lambda - K) & (S - K) \\ (S - K) & \left(C + \frac{6}{\gamma} - K\right) \end{vmatrix} = 0 \quad \ldots\ldots\ldots \text{(27)}$$

Performing the operations indicated by this determinant, the equation for the buckling strength of a rectangular single-story, single-bay frame is

$$(Q + 6\,\lambda)\left(Q + \frac{6}{\gamma}\right) - R^2 = 0 \quad \ldots\ldots\ldots\ldots\ldots \text{(28)}$$

in which

$$Q = C - K \quad \ldots\ldots\ldots\ldots\ldots\ldots\ldots\ldots \text{(29a)}$$

and

$$R = S - K \quad \ldots\ldots\ldots\ldots\ldots\ldots\ldots\ldots \text{(29b)}$$

It can be shown that Eq. 28 reduces to the buckling condition for the pinned-base frame (Eq. 2) when $\lambda = 0$ and the buckling condition for the fixed-base frame (Eq. 3) when $\lambda = \infty$.

The relationship between the effective length factor k and the varying degrees of base fixity expressed in terms of λ is shown in Fig. 5 for several constant values of the ratio γ. The left end of the curves in Fig. 5 corresponds to the values of k for a pinned-end frame ($\lambda = 0$), and the right end of the curves approaches the k-values for a fixed-end frame ($\lambda \rightarrow \infty$) as an asymptote. The curves show that the effective length is rapidly reduced from its value for the case of a pinned-base frame as soon as a small amount of base restraint is present. For example, if this restraint is equal to the stiffness of the top beam ($I_S = I_B$, or $\lambda = 1.0$ when $L_C = L_B$) the values of k are almost equal to those for a fixed-base frame. This indicates that although the base is still relatively flexible, the small restraint offered by it produces almost the same effect as that of a fully rigid column base.

The effect of partial base fixity on the critical load is shown in Fig. 6. Here the base restraint coefficient λ is plotted versus the critical load P_{cr} (nondimensionalized by the factor $\frac{L_C^2}{\pi^2 E_t I_C}$). It can again be observed that a small of restraint at the column ends can increase the critical load considerably.

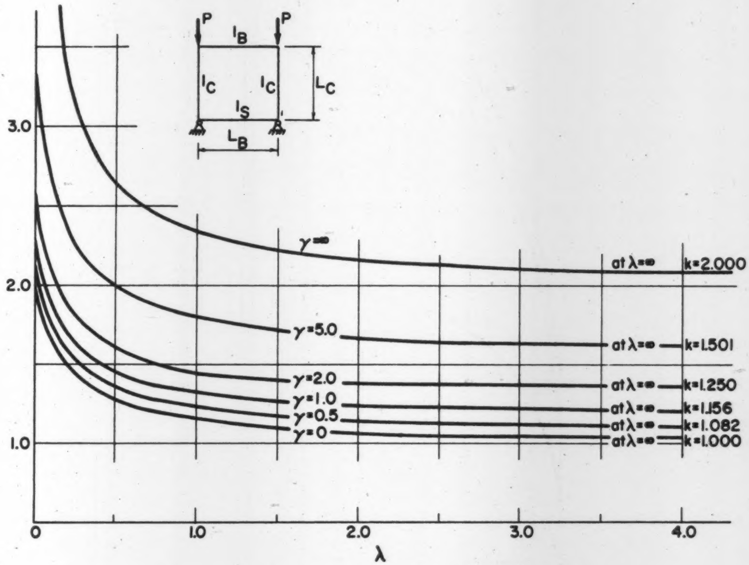

FIG. 5.—EFFECTIVE LENGTH OF COLUMNS IN A SINGLE-STORY SINGLE-BAY FRAME

In a rigid frame of usual proportions the critical load on the columns may be higher than that load which would cause partial yielding. In this case $E_t < E$ or $\tau < 1.0$. The value of k may be found approximately by assuming $\tau = 1.0$, computing λ and γ and finding k from Eq. 28 or Fig. 5. The corresponding critical load is then computed from Eq. 1. If the stress due to P_{cr} is above the proportional limit of the material, E_t and thus τ can be obtained from a stub column stress-strain diagram.[10] A new value of λ, γ, and, therefore, k and P_{cr} can now be found for this value of τ. The value of the stress will be changed, and yet another τ can be computed. This process can be repeated until sufficient accuracy is obtained.

---

[10] "Basic Column Strength," by L. S. Beedle and L. Tall, Fritz Engrg. Lab. Report 220A.34, Lehigh Univ., Bethlehem, Pa., 1959.

The additional work necessitated by the procedure outlined above will not be required, unless a very high degree of accuracy is desired. The value of λ (Eq. 18) will increase and the value of γ (Eq. 4) will decrease if τ is changed from 1.0 to its inelastic value of $\tau < 1.0$. It can be seen in Fig. 5 that if this occurs, k computed for $\tau < 1.0$ will always be smaller than k computed for $\tau = 1.0$. Thus, the error will be on the safe side if τ is taken as 1.0. This error will in general not be large, because τ is usually not much less than 1.00 and fairly large changes in λ and γ will not change k appreciably if $\gamma \leq 2.0$ and $\lambda \geq 0.5$ (Fig. 5).

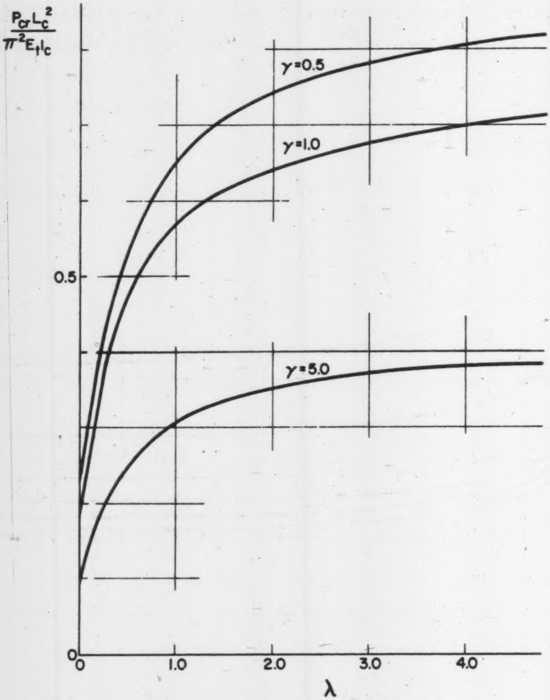

FIG. 6.—VARIATION OF CRITICAL LOAD WITH BASE RESTRAINT FOR A SINGLE-STORY SINGLE-BAY FRAME

BUCKLING STRENGTH OF A TWO-STORY, SINGLE-BAY FRAME

In order to show that a situation similar to that described above exists for other frames, the buckling strength of another structure will be computed. This is the two-story, single-bay, rectangular rigid frame shown in Fig. 7. The span of this frame is L_B, and the story heights are the same for each story (story height = L_C). The moment of inertia is equal to I_C for the columns and I_B for the beams. Base restraint is simulated by a beam which has a moment of inertia I_S.

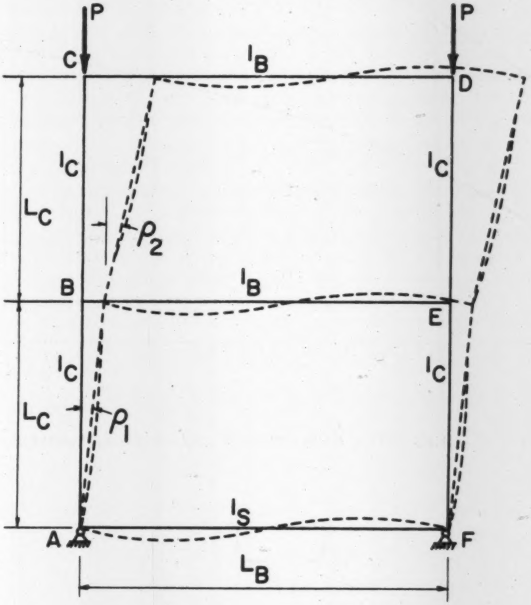

FIG. 7.—TWO-STORY SINGLE-BAY RIGID FRAME

The buckling strength of the frame shown in Fig. 7 is expressed by

$$(Q + 6\ \lambda)\left(2\ Q + \frac{6}{\gamma}\right)\ -\ R^2\left(2\ Q + 6\ \lambda + \frac{6}{\gamma}\right)\ = 0 \quad \ldots\ldots\ldots (30)$$

The derivation of this equation is given in Appendix A. Eq. 30 reduces to

$$\frac{6}{\gamma} = \frac{R^2 - Q^2}{Q} \quad \ldots\ldots\ldots\ldots\ldots\ldots (31)$$

for a pinned-base frame ($\lambda = 0$) and to

$$\left(2\ Q + \frac{6}{\gamma}\right)\left(Q + \frac{6}{\gamma}\right) - R^2 = 0 \quad \ldots\ldots\ldots\ldots\ldots (32)$$

for a fixed-base frame ($\lambda = \infty$).

The plots of γ versus k for the pinned-base case and for the fixed-base case are shown in Fig. 8, and the relationship between k and λ for several constant

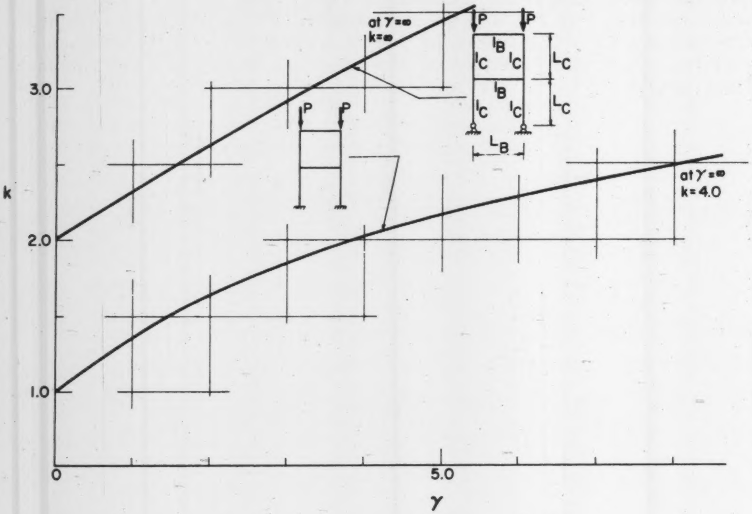

FIG. 8.—EFFECTIVE LENGTH FOR TWO-STORY FRAMES

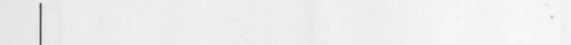

FIG. 9.—EFFECTIVE LENGTH OF COLUMNS IN ONE- AND TWO-STORY RIGID FRAMES

values of γ is shown in Fig. 9. A rapid decrease of k (and, thus, an increase of P_{cr}) for a small amount of base fixity can again be observed. The curves for the single-story frame are also shown in Fig. 9 for comparison.

APPLICATIONS OF THE THEORY

In the preceding discussion equations were developed for the buckling strength of two symmetrically loaded symmetrical rigid frames. It was shown that a small amount of base restraint, as simulated by an elastic beam between the column bases, reduces the effective length of the columns and thus increases the strength of the frame. The curves in Figs. 5, 6, and 9 indicate that if the ratio $(I_S/L_B)(L_C/I_C)$ is greater than one, the buckling strength of the frame is nearly that of a fixed-base frame.

The problem that remains to be discussed is the determination of the restraint actually offered by column bases that were designed as "pinned." This must be known in order to evaluate the stiffness I_S/L_B of the base beam. The relationship between the column base restraint and the stiffness of the fictitious base beam can be obtained in the following manner: the moment at the end of the base beam is (from Eq. 14),

$$M = \frac{6\,E\,I_S\,\theta}{L_B} \quad \ldots\ldots\ldots\ldots\ldots\ldots (33)$$

If Eq. 33 is solved for I_S/L_B,

$$\left(\frac{I_S}{L_B}\right) = \left(\frac{M}{\theta}\right)\left(\frac{1}{6\,E}\right) \quad \ldots\ldots\ldots\ldots\ldots (34)$$

If the frame is manufactured from steel, ($E = 30 \times 10^6$ psi) the stiffness is equal to

$$\left(\frac{I_S}{L_B}\right) = \left(\frac{M}{\theta}\right)\left(\frac{1}{180 \times 10^6}\right) \quad \ldots\ldots\ldots\ldots\ldots (35)$$

In Eq. 35 the value of M/θ is unknown. This ratio is the initial slope of a curve showing the relationship between a moment and the corresponding rotation for a column base.

Column bases for so-called pinned-base structures consist, in general, of plates welded to the bottom of the columns. These plates are bolted by anchor bolts to the concrete of the footing. Rotation may take place between the column base and the footing, and the whole footing may rotate in the surrounding soil.

Before any conclusions can be drawn from the theory, it is necessary to know whether this ordinary pinned-base arrangement offers sufficient restraint to base rotation to decrease the effective column length towards that of a fixed-base frame.

There are few experimental and analytical studies available that show the moment-rotation characteristics of the footing in the surrounding soil. K. H. Roscoe and A. N. Schofield made measurements[11] of the rotation of eight column footings embedded in sandy soil. (This research was part of the full scale collapse tests of rigid north-light portal frames at Cambridge University.) The footings were designed to furnish full fixity to the column bases, and the experimental moment-rotation curves show that this was indeed the case for most of the columns.

---

[11] "The Stability of Short Pier Foundations in Sand," by K. H. Roscoe and A. N. Schofield, The British Welding Journal, Symposium on the Plastic Theory of Structures, Cambridge, England, September, 1956.

An estimate of the stiffness of the foundation in the soil can be made by the following approximation: before buckling the foundation is subjected to only a compressive force. At the inception of frame buckling an additional bending moment of indeterminate magnitude is present. Because M/θ, the ratio of this moment with respect to the corresponding rotation, is required only at the start of buckling, it can be assumed that the response of the soil to the moment is purely elastic. If it is assumed also that the foundation is rigid in comparison with the soil, the rotation can be represented by a set of elastic springs (Fig. 10). The reaction of the soil at any elementary area g dx (where

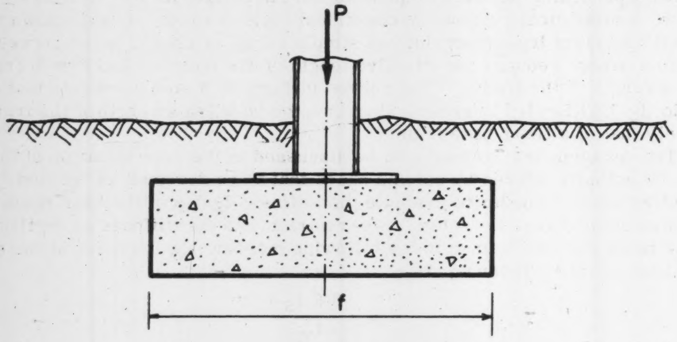

FOUNDATION BEFORE BUCKLING

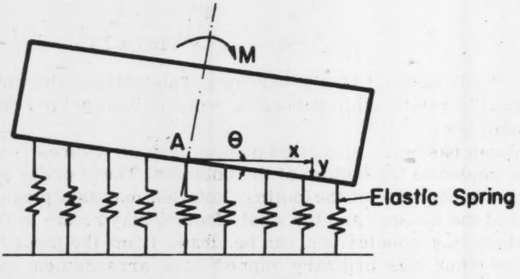

IDEALIZED SITUATION AT BUCKLING

FIG. 10.—SCHEMATIC REPRESENTATION OF RESTRAINT OFFERED BY FOUNDATIONS

g is the width of the foundation) is K y dx (where K is the force, per linear inch, that is necessary to compress the soil 1 in., and y is the deflection). Taking moments about point A in Fig. 10, it is found that $M_x = x\ Ky\ dx$. Integrating over the length f of the foundation, noting that $y = \theta\ x$,

$$M = 2 \int_0^{f/2} \theta\ K\ x^2\ dx = \frac{K\ f^3\ \theta}{12} \qquad \text{. . . . . (36)}$$

The modulus K can be correlated[12] with the "modulus of subgrade reaction," q, which is given in pounds per square inch per inch of deflection, by setting K = g q. The value of the base stiffness is then

$$\frac{M}{\theta} = \frac{g\ q\ f^3}{12} \qquad \text{. . . . . (37)}$$

Values of q must be determined by experiment or the designer can estimate them in accordance with his knowledge of the soil conditions. Magnitudes of q listed by J. H. Bateman[12] vary from 50 lb per cu in. to 400 lb per cu in.

Substitution of M/θ from Eq. 37 into Eq. 35 yields the following expression for the stiffness of the fictitious restraint beam due to the rotation of the foundation in the soil:

$$\frac{I_S}{L_B} = \frac{q\ g\ f^3}{2160 \times 10^6} \qquad \text{. . . . . (38)}$$

It must be realized that Eq. 38 is only an approximation. For a more accurate evaluation of the stiffness of foundations in soils further extensive analytical and experimental research is necessary. Eq. 38 gives only a conservative estimate for M/θ in case that no more precise information is available.

Analytical approximations have been developed for the case in which the footing does not rotate in the soil.[13] Rotation takes place between the column ends and the footing due to the deformation of the base plate, the anchor bolts, and the concrete. Results of this investigation show that the slope of the moment rotation curve is

$$\frac{M}{\theta} = \frac{b\ d^2\ E_C}{12} \qquad \text{. . . . . (39)}$$

in which b is the width of the base plate, d denotes the length of the base plate, and E_C is the modulus of elasticity of the concrete. If Eq. 39 is substituted into Eq. 35, the stiffness of the ficticious restraining beam due to a moment between the column base and the foundation is

$$\frac{I_S}{L_B} = \frac{b\ d^2}{72\ h} \qquad \text{. . . . . (40)}$$

in which n is the modular ratio $E_{steel}/E_{concrete}$.

Whichever of the two stiffnesses I_S/L_B (Eq. 38 or Eq. 40) yields the least stiffness would be used to determine the coefficient λ and thus the buckling strength of the frame.

To show the extent by which partial base fixity influences the buckling strength of a particular frame, an example is computed in Appendix II.

---

[12] "Introduction to Highway Engineering," by J. H. Bateman, John Wiley and Sons, New York, 1948.

[13] "Moment Rotation Characteristics of Column Anchorages," by C. G. Salmon, L. Schlenker and B. G. Johnston, Proceedings, ASCE, Vol. 81, No. ST 3, April, 1955.

The critical load of a rectangular rigid frame of the type and loading shown in Fig. 1 is computed. First, the critical load is determined by assuming pinned bases; next the influence of partial base fixity is included in the computation.

The following may be concluded from this example:

1. Even for as stocky a member as was used in this example (8WF31 column, 13 ft long, bent about the strong axis) it is seen that it is not worth while to compute the influence of $\tau \neq 1.0$, because the column strength is underestimated by only about 2% if $\tau = 1.0$ is used in the computations.
2. The critical load, assuming pinned bases is 217 kips including the variation of τ). If the influence of base restraint is also considered (assuming a relatively poor soil, $q = 150$ lbs./in.^{3}) it is seen that $P_{cr} = 281$ kips. Thus the increase is about 30% of the critical load for pinned bases in this problem.

CONCLUSIONS

The following conclusions may be drawn about the effects of partial base restraint from this analysis:

1. Partial base fixity has a beneficial effect on the buckling strength of rigid frames.
2. The curves in Figs. 5 and 9 show that for single-bay, single and two story rectangular rigid frames, a small amount of base restraint reduces the effective length considerably from that of the pinned-base condition.
3. Further research on the moment-rotation characteristics of common column foundations is necessary before a more accurate estimate of the base restraint can be made. Available information indicates that presently used "pinned" column bases give enough restraint to increase the buckling strength of the frame considerably, especially if the footing is large.
4. The results of this investigation indicate that the restraint offered by the base details of one and two story frames analyzed as pin-based is in many cases adequate to prevent failure by frame instability. This fact is especially important for plastically designed structures, because the buckling strength computed on the basis of pinned-ends would otherwise often limit the full realization of the mechanism.

The method permits the computation of the critical buckling load of any pinned-base frame, as long as an estimate of the base restraint can be made. For plastic design the method of analysis for determining an approximate conservative buckling load is the following: The plastic hinges of the incomplete mechanism are replaced by real hinges, and a stability analysis is made of this structure. If the critical loads of the structure for which all but the last hinge has formed is higher than or equal to the plastic collapse load, the frame will not fail by frame instability.

In Fig. 11 the curve for $\gamma = 1.0$ for a single story, single-bay frame is shown when a real hinge is placed at one of the knees. It is again seen that partial base fixity reduces the effective length rapidly, even if only a small amount of base restraint is present. Also shown in Fig. 11 is the equation representing the buckling strength, base restraint, and dimensional relationship for this structure.

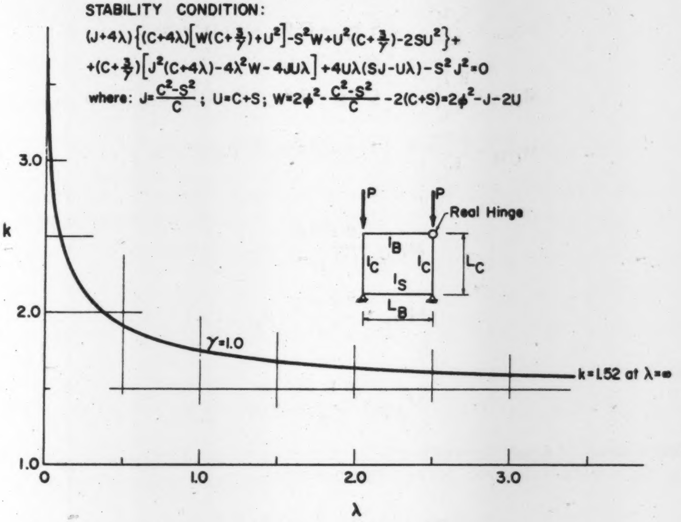

FIG. 11.—EFFECTIVE LENGTH OF COLUMNS IN A FRAME CONTAINING A HINGE

ACKNOWLEDGMENTS

This study is part of the general investigation "Welded Continuous Frames and Their Components" being carried out at Fritz Engineering Laboratory, Lehigh University, Bethlehem, Pa., under the direction of Lynn S. Beedle, F. ASCE. This investigation is sponsored jointly by the Welding Research Council and the United States Department of the Navy with funds furnished by the American Iron and Steel Institute, American Institute of Steel Construction, Office of Naval Research, Bureau of Ships, and Bureau of Yards and Docks.

William J. Eney, F. ASCE, is Director of Fritz Engineering Laboratory and Head of the Department of Civil Engineering.

The critical reviews by Jonathan Jones, F. ASCE, Le-Wu Lu, A.M. ASCE, Robert Ketter, A. M. ASCE, T. R. Higgins, and Bruno Thurlimann, M. ASCE, are gratefully acknowledged.

APPENDIX I

Derivation of the Critical Equation for a Two Story, One-Bay Frame.—The frame and its dimensions are shown in Fig. 7. Because the frame is symmetrical, only one half of the frame need be analyzed. All rotations are clockwise; thus the equations of the moments from Eq. 8 are:

$$M_{AB} = \frac{E\,I_C}{L_C} \left[C\,\theta_A + S\,\theta_B - \rho_1\,(C+S)\right] \quad \ldots\ldots\ldots \text{(41a)}$$

$$M_{BA} = \frac{E\,I_C}{L_C}\left[S\,\theta_A + C\,\theta_B - \rho_1 (C+S)\right] \quad \ldots\ldots\ldots (41b)$$

$$M_{BC} = \frac{E\,I_C}{L_C}\left[C\,\theta_B + S\,\theta_C - \rho_2 (C+S)\right] \quad \ldots\ldots\ldots (41c)$$

$$M_{CB} = \frac{E\,I_C}{L_C}\left[C\,\theta_C + S\,\theta_B - \rho_2 (C+S)\right] \quad \ldots\ldots\ldots (41d)$$

$$M_{CD} = \frac{6\,E\,I_B}{L_B}\,\theta_C \quad \ldots\ldots\ldots (41e)$$

$$M_{BE} = \frac{6\,E\,I_B}{L_B}\,\theta_B \quad \ldots\ldots\ldots (41f)$$

and

$$M_{AF} = \frac{6\,E\,I_S}{L_B}\,\theta_A \quad \ldots\ldots\ldots (41g)$$

Conditions of Equilibrium.—

1. No horizontal shear forces are present:

$$M_{BA} + M_{AB} + P\,L_C\,\rho_1 = 0 \quad \ldots\ldots\ldots (42a)$$

and

$$M_{BC} + M_{CB} + P\,L_C\,\rho_2 = 0 \quad \ldots\ldots\ldots (42b)$$

Substitution of the moments yields the following equation for ρ_1 and ρ_2:

$$\rho_1 = \frac{(C+S)\,(\theta_A + \theta_B)}{2(C+S) - \phi^2} \quad \ldots\ldots\ldots (43a)$$

and

$$\rho_2 = \frac{(C+S)\,(\theta_B + \theta_C)}{2(C+S) - \phi^2} \quad \ldots\ldots\ldots (43b)$$

2. Equilibrium at joint A:

$$M_{AB} + M_{AF} = 0 \quad \ldots\ldots\ldots (44)$$

If the values of the moments and ρ_1 and ρ_2 and the abbreviation K (Eq. 25) are substituted, the following equation results:

$$\theta_A\,[C - K + 6\,\lambda] + \theta_B\,[S - K] = 0 \quad \ldots\ldots\ldots (45)$$

3. Equilibrium at joint B:

$$M_{BA} + M_{BC} + M_{BE} = 0 \quad \ldots\ldots\ldots (46)$$

Substitution leads to:

$$\theta_A\,[S\text{-}K] + \theta_B\left[2\,C\text{-}2\,K + \frac{6}{\gamma}\right] + \theta_C\,[S\text{-}K] = 0 \quad \ldots\ldots (47)$$

4. Equilibrium at joint C:

$$M_{CB} + M_{CD} = 0 \quad \ldots\ldots\ldots\ldots\ldots\ldots (48)$$

Substitution leads to:

$$\theta_B\ [S - K] + \theta_C\ \left[C - K + \frac{6}{\gamma}\right] = 0 \quad \ldots\ldots\ldots\ldots (49)$$

Introducing the further simplifications of Q and R (Eq. 29), the three simultaneous equations are:

$$\theta_A\ [Q + 6\,\lambda] + \theta_B\ [R] = 0 \quad \ldots\ldots\ldots\ldots (50a)$$

$$\theta_A\ [R] + \theta_B\ \left[2\,Q + \frac{6}{\gamma}\right] + \theta_C\ [R] = 0 \quad \ldots\ldots\ldots (50b)$$

and

$$\theta_B\ [R] + \theta_C\ \left[Q + \frac{6}{\gamma}\right] = 0 \quad \ldots\ldots\ldots\ldots (50c)$$

Equating the determinant of the coefficients to zero, the following equation results as the buckling equation:

$$(Q + 6\,\lambda)\left(2\,Q + \frac{6}{\gamma}\right)\left(Q + \frac{6}{\gamma}\right) - R^2\left(2\,Q + 6\,\lambda + \frac{6}{\gamma}\right) = 0 \quad \ldots (51)$$

APPENDIX II

It is desired to determine the critical load on an industrial frame of the type shown in Fig. 1. The top cross beam is a 10WF33 member, and the columns are 8WF31 members, arranged in such a manner that the web is in the plane of the frame. Weak-axis buckling out of the plane of the frame is assumed to be prevented by bracing. The span length is 20 ft 0 in. and the column height is 13 ft 0 in.

1. Assuming Pinned Column Bases

Column Size: 8WF31	Beam Size: 10WF33
I_C = 109.7 in.^{4}	I_B = 170.9 in.^{4}
L_C = 156 in.	L_B = 240 in.

Assume $\tau = 1.00$

$$\gamma = \frac{I_C}{L_C} = \frac{L_B}{I_B} = 0.987$$

From Fig. 2, k = 2.33

$$\frac{k\,L_C}{r_x} = \frac{2.33 \times 156}{3.47} = 105$$

The critical stress has been given[14] (as an approximate expression) as

---

[14] "Basic Column Strength," by L. S. Beedle and L. Tall, Fritz Engrg. Lab. Report 220A.34, Lehigh Univ., Bethlehem, Pa., 1959, Eq. 11.

$$\sigma_{cr} = 33.0 - \frac{8.80 \times \left(k\ L/r_x\right)^2}{10{,}000} = 23.4 \text{ ksi}$$

or

$$P_{cr} = \sigma_{cr}\ A = 214 \text{ kips}$$

An approximation for τ is obtained as follows:

$$\tau = \frac{E_t}{E} = \frac{\dfrac{\pi^2\ E_t}{k\ L/r^2}}{\dfrac{\pi^2\ E}{k\ L/r^2}} = \frac{\sigma_{cr}}{\sigma_E} \quad \ldots\ldots\ldots\ldots\ldots (52)$$

For this problem,

$$\sigma_E = \frac{\pi^2\ E}{k\ L/r^2} = \frac{\pi^2 \times 30{,}000}{(105)^2} = 27.1 \text{ ksi}$$

and

$$\tau = \frac{\sigma_{cr}}{\sigma_E} = \frac{23.4}{27.1} = 0.864$$

Adjusting γ for $\tau < 1.00$:

$$(\gamma)_A = 0.987 \times 0.864 = 0.852$$

The corresponding value of k from Fig. 2 is 2.28. Computing the new σ_{cr}, σ_E and another value of τ, it is found that the values of k and σ_{cr} after two cycles are equal to $k = 2.27$, $\sigma_{cr} = 23.8$ ksi, and $P_{cr} = 217$ kips.

2. Including the Influence of Base Restraint

Base plate size: 12 in. by 12 in.

Modular ratio $E_S/E_C = n - 10$

From Eq. 40, $I_S/L_B = \dfrac{b\ d^2}{72\ n} = \dfrac{(12)^3}{720} = 2.40$

Footing size: 6 ft 0 in. by 6 ft 0 in.

Assume q = 150 lb per cu in.

Then, from Eq. 38,

$$I_S\ L_B = \frac{q\ g\ f^3}{2160 \times 10^6} = \frac{150\ (72)^4}{2160 \times 10^6} = 1.86$$

Because this stiffness is smaller than the stiffness of the base-plate anchorage bolt detail (Eq. 38), it will be used in subsequent computations:

$$\lambda = \frac{I_S}{L_B} \times \frac{L_C}{I_C} = \frac{1.86 \times 156}{109.7} = 2.67$$

if τ is assumed equal to 1.0 and γ = 0.987.

From Fig. 5, the corresponding value of k is 1.22, and σ_{cr} according to L. S. Beedle[14] is equal to 30.4 ksi, or P_{cr} = 277 kips. Proceeding as before to include the influence of $\tau < 1.0$, it is found that after two cycles k = 1.10, σ_{cr} = 30.8 ksi, and P_{cr} = 282 kips.

APPENDIX III.—NOMENCLATURE

The following symbols have been adopted for use in this paper:

b = width of base plate;

C = nondimensional coefficient, defined by Eq. 9;

c = nondimensional coefficient defined by Eq. 10;

d = length of base plate;

E = modulus of elasticity;

E_t = tangent modulus;

E_C = modulus of elasticity of concrete;

f = length of foundation;

g = width of foundation;

I_B = moment of inertia of beam;

I_C = moment of inertia of column;

I_S = moment of inertia of ficticious base restraint beam;

K = spring constant of soil;

K = nondimensional coefficient defined by Eq. 25;

k = effective length coefficient;

L_B = span length;

L_C = length of column;

M = bending moment;

M_{AB} = moment at the end A of member AB;

n = modular ratio;

P = axial load in column;

P_{cr} = critical load;

Q = nondimensional coefficient defined by Eq. 29;

q = modulus of subgrade reaction;

R = nondimensional coefficient defined by Eq. 29;

S = nondimensional coefficient defined by Eq. 9;

s = nondimensional coefficient defined by Eq. 10;

x = coordinate of distance;

y = coordinate of deflection;

β = spring constant;

γ = nondimensional coefficient defined by Eq. 4;

λ = nondimensional coefficient defined by Eq. 18;

ϕ = nondimensional coefficient defined by Eq. 5;

θ = joint rotation;

ρ = bar rotation; and

τ = E_t/E.

DISCUSSION

EUGENE GUILLARD,[15] F. ASCE.—Galambos shows for a symmetrically loaded frame, in which he chooses to ignore the primary bending moments normally associated with this type of frame, that as the column base restraint is increased the effective length of the column is reduced, thus increasing the buckling strength of the frame. He also shows that small amounts of restraint result in relatively large reductions in the effective length of the columns. This is interesting, but of little practical value to the designer, confronted with a real structure subjected to a normal loading configuration, until the effect of primary bending moments in the frame can also be evaluated.

The theoretical problem presented by the author has been adequately treated by F. Bleich[2] who cautions that the primary bending moments have not been considered, and further states that, "At present no suitable method is available for determining the critical load of rectangular rigid frames which takes account of the influence of these bending moments on the stability of the structure." A paper by E. Chwalla investigating the problem of lateral stability of a rigid frame subjected to transverse loads has also been reviewed.[2] The paper treats a specific problem and the analytical results indicate that the distortion of the framework prior to buckling, caused by the transverse loading of the horizontal member, reduces the buckling strength of the system only to a rather limited extent. It remains to be proved, however, that this is generally true.

In view of the preceding, the critical load computed in the illustrative problem is subject to some doubt. It, at best, can only be an upper bound to the buckling load of the frame.

In the section on the "Application of the Theory" and the illustrative example in Appendix II there are several assumptions which may be misleading and which tend to credit the normal pinned base with a fixity coefficient which is too large. For example, in the expression for the moment-rotation characteristics of the base plate connection (Eq. 39) it its assumed that there are compressive strains under the entire base plate throughout the range of interest. It is of interest to know if this is true. Also, what value of modulus of elasticity (E_c) should be used? Because, in concrete, strain increases faster than stress and permanent deformation occurs under low stress would it not be more realistic to use a lower value for E_c than that normally associated with the modular ratio? Does not the preceding reasoning also apply with regard to the stress-strain relationship of the soil under the footing?

---

[15] Res. Engr., Armour Research Foundation of Illinois Inst. of Tech., Chicago, Ill.

Considering the stiffness of the base plate connection and the stiffness of the footing in the soil, the statement is made, "Whichever of the two stiffnesses yields the least stiffness would be used to determine the coefficient λ and thus the buckling strength of the frame." Would it not be more correct to consider that the two stiffnesses are in series? The end restraint of the column would thus be less and tend more toward the pinned base.

With regard to the illustrative problem if it is assumed that the top cross beam of the frame supports a uniform load, the maximum total load that may be applied to the frame whether the column bases are pinned or fixed, is approximately 40 kips using AISC specifications. Under these conditions the footing assumed in the example appears to be much too large for the pinned base assumption.

As a final plea for conservatism in the evaluation of end restraint of columns the writer makes reference to a paper[16] by F. R. Shanley and quotes therefrom:

> In theory, end restraint has a very simple effect: It merely changes the effective column length. In practice, however, the accurate determination of the effect of end restraint for any column except a pin-ended column is a difficult problem. . . . . It is important to realize that efficiently designed structures cannot be made proportionately stronger by increasing the amount of end restraint. This fact, too, was pointed out by Mr. von Karman when he declared, in effect, that end restraint causes a marked increase in buckling strength only for long slender columns, not for shorter ones.

J. W. APPELTAUER,[17] and TH. A. BARTA.[18]—As Galambos points out in his paper, partial base fixity may be studied either by inserting a restraining beam between the column bases, a method used also by other authors (for example, Kornouhov,[19] Goder[20]), or by considering directly the end rotations.

In their research on framework stability, the results of which are due to be published in the Bulletin of the Building Research Institute (Bucharest), the authors resolved, among others, the problem of partial base fixity for different current frameworks by using the "degree of restraint (degree of fixity) ϵ."

---

[16] "Applied Column Theory," by F. R. Shanley, Transactions, ASCE, Vol. 115, 1950, p. 698.

[17] Civ. Engr., Timisoara, Rumania.

[18] Civ. Engr., Timisoara, Rumania.

[19] "Protchnost i ustoichivost starshnavyi system," by N. V. Kornouhov, Stroyisdat, Moscow, 1948.

[20] "Beitrag zur praktischen Berechnung von Rahmentragwerken nach der Stabilitätsvorschrift DIN 4114," by W. Goder, Stahlbau, Vol. 28, No. 10, October, 1959, p. 265.

The degree of restraint is the ratio of the partial-base-restraint moment versus the corresponding fixed-base moment, under the action of a unit moment, acting on the opposite end of the columns. The extreme values of the degree of restraint are $\epsilon = 0$, for a pinned base, and $\epsilon = 1$, for a fixed base. With

$$\delta = \frac{E_t\, I_c}{L_c}\ \phi \quad \ldots\ldots\ldots\ldots\ldots\ldots \quad (53)$$

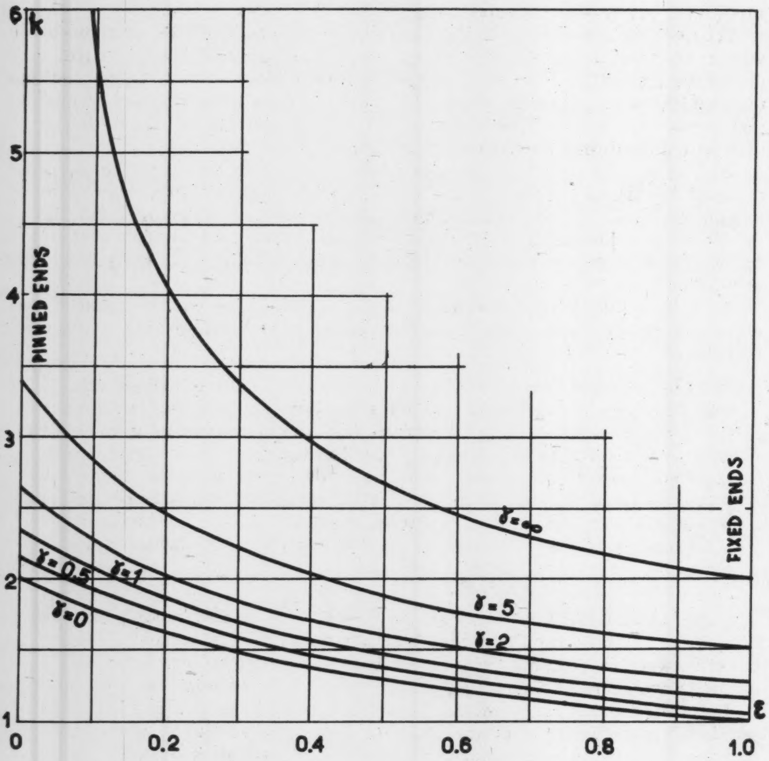

FIG. 12.—EFFECTIVE LENGTH OF COLUMNS IN A SINGLE-STORY SINGLE-BAY FRAME

in which ϕ is the rotation of the foundation under the action of a unit moment there results

$$\epsilon = \frac{1}{1 + 3\,\delta} \quad \ldots\ldots\ldots\ldots\ldots\ldots \quad (54)$$

The rotation ϕ may be determined by

$$\phi = \frac{12}{g\,q\,f^3} \quad \text{. . . . .} \quad (55)$$

that represents the reciprocal of Mr. Galambos' Eq. 37.

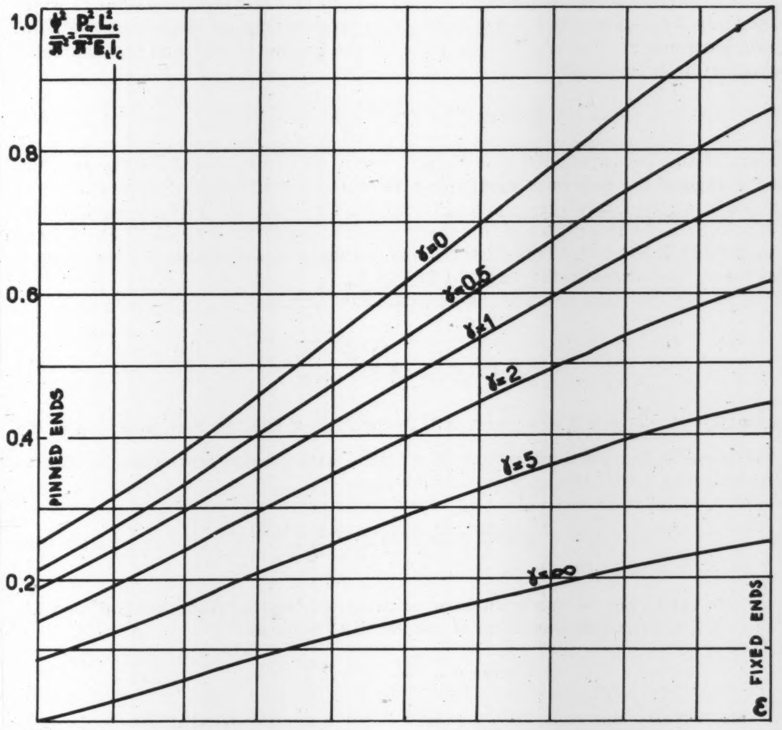

FIG. 13.—VARIATION OF CRITICAL LOAD WITH BASE RESTRAINT FOR A SINGLE-STORY SINGLE-BAY FRAME

Further data on the degree of restraint ϵ, respectively the coefficient q, is available.[21,22,23] The rotation of the base due to the deformation of the anchor-

---

[21] "The Problem of Partial Restraint in Elastic Soil," (in Rumanian) by C. N. Avram, Institutul Politehnic Timisoara, Buletinul Comunicarilor Stiintifice si Tehnice Vol. 1, 1956.

[22] "Mehanika gruntov," by N. A. Tsytovitch, Stroyisdat, Moscow, 1951. (Rumanian translation -ESAC, Bucharest, 1955).

[23] "Über den Einepanngrad einer Stütze im Fundament," by K. Opladen, Beton- u. Stahlbetonbau, Vol. 55, No. 2, February, 1960, p. 35.

bolts and the concrete, has been treated also by P. Sahmel,[24] and contrary to Galambos' statement should be added to the rotation of the foundation.

It is interesting to mention that in European practice, columns like these described by Galambos are considered, for simplicity, as having fixed ends, so that partial base fixity reduces the rigidity of the base. Moreover, this hypothesis is confirmed by Galambos' numerical example.

The Single-Story, Single-Bay Frame.—It is interesting and useful to write the stability equation and to represent its results using the degree of restraint as a parameter. The stability equation for the geometrically and mechanically symmetric frame is:

$$(1-\epsilon)\left(1-\frac{\gamma}{6}\,\phi\tan\phi\right)+3\,\epsilon\left(\frac{\tan\phi}{\phi}+\frac{\gamma}{6}\right)=0 \qquad (56)$$

Figs. 12 and 13 correspond with Figs. 5 and 6. In comparing these figures, the advantage of the degree of restraint ϵ versus the coefficient of restraint λ can be seen, as the latter very much shortens the first half ($0\leq\epsilon\leq0.5$ respectively, $0\leq\lambda\leq0.5$) of the interval, and lengthens unnecessarily the second ($0.5\leq\epsilon\leq1$ respectively $0.5\leq\lambda\leq\infty$). This distortion of the scale explains also the pronounced slope of the curves in the interval $0\leq\lambda\leq0.5$.

For $0\leq\gamma\leq10$ may be used the approximate formula

$$k=\sqrt{\frac{1+m}{2}}\;\sqrt{\frac{4(2+\gamma')-2\,\epsilon}{2+\epsilon\,(4+\gamma')}} \qquad (57)$$

in which $\gamma'=\frac{\pi^2}{12}\gamma\sim0.822\,\gamma$ and $m\leq1$ is the ratio of the two forces acting in the columns. In the particular case of a frame with a beam connected by pins to the columns ($\gamma=\infty$) the approximate formula

$$k=\frac{2}{3}\;\frac{1+2\,\epsilon}{\epsilon}\left[1-\frac{2}{3}\left(\frac{1-\epsilon}{1+2\,\epsilon}\right)^3\right] \qquad (58)$$

may be used. Eq. 57 has been derived using the "equilibrium-method" and Eq. 58 by the approximate solution of the stability equation

$$\phi\tan\phi-\frac{3\,\epsilon}{1-\epsilon}=0 \qquad (59)$$

Multi-Story and Multi-Bay Frames.—For a symmetrical single-bay, multistory frame, with n stories (Fig. 14) the following approximative formula may be used

$$k_n^{\,2}=\frac{\bar{f}_1\left[2^{n-1}\,\xi'^2\,\frac{L'_{c_1}}{L_{c_n}}\sum_1^n p-2^{n-2}\,\frac{L'_{c_2}}{L_{c_n}}\sum_2^n p\right]+\sum_2^n\bar{f}_i\left[2^{n-i}\,\frac{L'_{c_i}}{L_{c_n}}\sum_i^n p-2^{n-(i+1)}\,\frac{L'_{c_{i+1}}}{L_{c_n}}\sum_{i+1}^n p\right]}{2^{n-1}\,n\,\xi'^2\,\frac{L_{c_1}}{L_{c_n}}\,\frac{L'_{c_1}}{L_{c_n}}+\sum_2^n 2^{n-i}(n-i+1)\,\frac{L_{c_i}}{L_{c_n}}\,\frac{L'_{c_i}}{L_{c_n}}} \qquad (60)$$

---

[24] "Näherungsweise Berechnung der Knicklängen von Stockwerkrahmen," by P. Sahmel, Stahlbau, Vol. 24, No. 4, April, 1955, p. 89.

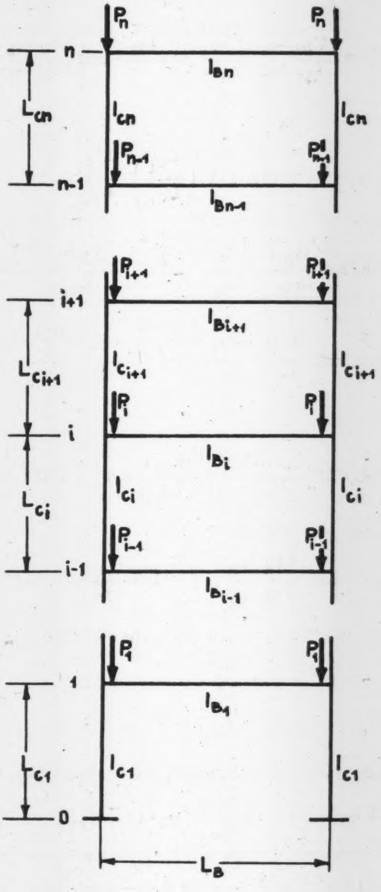
P_n
P_n
n
I_Bn
L_cn
I_cn
I_cn
P_n-1
P'_n-1
n-1
I_Bn-1
P_i+1
P'_i+1
i+1
I_Bi+1
L_ci+1
I_ci+1
I_ci+1
P_i
P_i
i
I_Bi
L_ci
I_ci
I_ci
P_i-1
P'_i-1
i-1
I_Bi-1
P_1
P_1
1
I_B1
L_c1
I_c1
I_c1
0
L_B

FIG. 14.—MULTI-STORY FRAME

with the notations

$$L'_{c_i} = L_{c_i}\,\frac{E_{t_n}\,I_{c_n}}{E_{t_i}\,I_{c_i}}\;;\;\xi' = \frac{2+\epsilon}{2(1+2\epsilon)}\;;\;p_i = \frac{P_i}{P_n}$$

The reduced deflections $\overline{f}_i$ of Eq. 60 result from the recurrence formulas:

$$\overline{f}_1 = 4n\left(3\xi^2-3\xi+1\right)\left(\frac{L_{c_1}}{L_{c_n}}\right)^2\frac{L'_{c_1}}{L_{c_n}} + 1.644\,\xi'\,\frac{L'_{B_1}}{L_{c_n}}\,\frac{L_{c_1}}{L_{c_n}}\,\frac{n\xi'\,L_{c_1} + \frac{n-1}{2}\,L_{c_2}}{L_{c_n}} + 4n\,\frac{1-\epsilon}{\epsilon}\,\xi^2\left(\frac{L_{c_1}}{L_{c_n}}\right)^2\frac{L'_{c_1}}{L_{c_n}} \; . \; . \quad (61)$$

$$\overline{f}_2=\overline{f}_1+(n-1)\left(\frac{L_{c_2}}{L_{c_n}}\right)^2\frac{L'_{c_2}}{L_{c_n}}+0.822\,\frac{L'_{B_1}}{L_{c_n}}\,\frac{L_{c_2}}{L_{c_n}}\,\frac{n\,\xi'\,L_{c_1}+\frac{n-1}{2}\,L_{c_2}}{L_{c_n}}+0.822\,\frac{L'_{B_2}}{L_{c_n}}\,\frac{L_{c_2}}{L_{c_n}}\,\frac{\frac{n-3}{2}\,L_{c_2}+\frac{n-2}{2}\,L_{c_3}}{L_{c_n}} \quad \ldots \quad (62)$$

$$\overline{f}_i=\overline{f}_{i-1}+(n-i+1)\left(\frac{L_{c_i}}{L_{c_n}}\right)^2\frac{L'_{c_i}}{L_{c_n}}$$

$$+\,0.822\,\frac{L'_{B_{i-1}}}{L_{c_n}}\,\frac{L_{c_i}}{L_{c_n}}\,\frac{\frac{n-i+2}{2}\,L_{c_{i-1}}+\frac{n-i+1}{2}\,L_{c_i}}{L_{c_n}}$$

$$+\,0.822\,\frac{L'_{B_i}}{L_{c_n}}\,\frac{L_{c_i}}{L_{c_n}}\,\frac{\frac{n-i+1}{2}\,L_{c_i}+\frac{n-i}{2}\,L_{c_{i+1}}}{L_{c_n}} \quad \ldots\ldots\ldots \quad (63)$$

$$\overline{f}_n=\overline{f}_{n-1}+1+0.411\,\frac{L'_{B_{n-1}}}{L_{c_n}}\left(2\,\frac{L_{c_{n-1}}}{L_{c_n}}+1\right)+0.411\,\frac{L'_{B_n}}{L_{c_n}} \quad \ldots\ldots\ldots \quad (64)$$

with the supplementary notations

$$L'_{B_i}=L_{B_i}\,\frac{E_{t_n}\,I_{c_n}}{E_{B_i}\,I_{B_i}}\,;\quad \xi=1{,}5\,\frac{\epsilon}{1+2\,\epsilon}=1-\xi'$$

The effective-length coefficients for the other columns may be computed from

$$k_i^{\,2}=\frac{k_n^{\,2}}{\frac{L_{c_i}}{L_{c_n}}\,\frac{L'_{c_i}}{L_{c_n}}\,\sum_i^n p} \quad \ldots\ldots\ldots\ldots\ldots\ldots\ldots\ldots \quad (65)$$

For the particular case of a three-story frame, Eqs. 60 through 65 yield

$$k_3^{\,2}=\frac{\overline{f}_1\left[4\xi'^{\,2}\,\frac{L'_{c_1}}{L_{c_3}}\left(p_1+p_2+1\right)-2\,\frac{L'_{c_2}}{L_{c_3}}\left(p_2+1\right)\right]+\overline{f}_2\left[2\,\frac{L'_{c_2}}{L_{c_3}}\left(p_2+1\right)-1\right]+\overline{f}_3}{12\,\xi'^{\,2}\,\frac{L_{c_1}}{L_{c_3}}\,\frac{L'_{c_1}}{L_{c_3}}+4\,\frac{L_{c_2}}{L_{c_3}}\,\frac{L'_{c_2}}{L_{c_3}}+1} \quad \ldots \quad (66)$$

$$k_2^{\,2}=\frac{k_3^{\,2}}{\frac{L_{c_2}}{L_{c_3}}\,\frac{L'_{c_2}}{L_{c_3}}\left(p_2+1\right)} \quad \ldots\ldots\ldots\ldots\ldots\ldots\ldots\ldots \quad (67)$$

$$k_1^{\,2}=\frac{k_3^{\,2}}{\frac{L_{c_1}}{L_{c_3}}\,\frac{L'_{c_1}}{L_{c_3}}\left(p_1+p_2+1\right)} \quad \ldots\ldots\ldots\ldots\ldots\ldots\ldots\ldots \quad (68)$$

$$\overline{f}_1 = 12\left(3\xi^2 - 3\xi + 1\right)\left(\frac{L_{c_1}}{L_{c_3}}\right)^2 \frac{L'_{c_1}}{L_{c_3}} + 1.644\xi' \frac{L'_{B_1}}{L_{c_3}} \frac{L_{c_1}}{L_{c_3}} \frac{3\xi' L_{c_1} + L_{c_2}}{L_{c_3}}$$

$$+ 12\frac{1-\epsilon}{\epsilon}\xi^2\left(\frac{L_{c_1}}{L_{c_3}}\right)^2 \frac{L'_{c_1}}{L_{c_3}} \quad \ldots\ldots\ldots\ldots\ldots (69)$$

$$\overline{f}_2 = \overline{f}_1 + 2\left(\frac{L_{c_2}}{L_{c_3}}\right)^2 \frac{L'_{c_2}}{L_{c_3}} + 0.822 \frac{L'_{B_1}}{L_{c_3}} \frac{L_{c_2}}{L_{c_3}} \frac{3\xi' L_{c_1} + L_{c_2}}{L_{c_3}}$$

$$+ 0.411 \frac{L'_{B_2}}{L_{c_3}} \frac{L_{c_2}}{L_{c_3}} \left(2\frac{L_{c_2}}{L_{c_3}} + 1\right) \quad \ldots\ldots\ldots\ldots (70)$$

$$\overline{f}_3 = \overline{f}_2 + 1 + 0.411 \frac{L'_{B_2}}{L_{c_3}} \left(2\frac{L_{c_2}}{L_{c_3}} + 1\right) + 0.411 \frac{L'_{B_3}}{L_{c_3}} \quad \ldots\ldots\ldots\ldots (71)$$

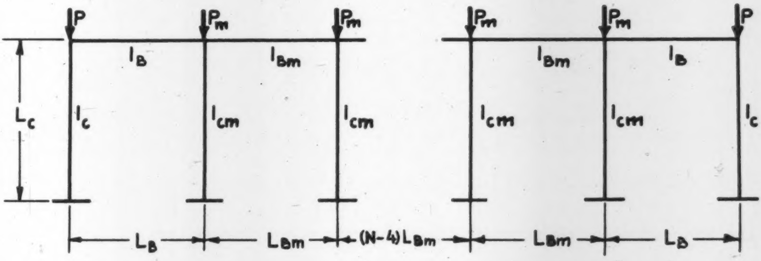

FIG. 15.—MULTI-BAY FRAME

For a symmetrical single-story, multi-bay frame, with N bays (Fig. 15) the approximate formula for the effective length of the marginal column, may be used:

$$k^2 = \overline{f} \; \frac{m\xi'^2 + (N-1)p_m \xi'^2_m}{m\xi'^2 + 2(N-1)\,\xi'^2_m} \quad \ldots\ldots\ldots\ldots\ldots\ldots\ldots (72)$$

The reduced deflection is

$$\bar{f} = \frac{4}{N}\left[\left(3\xi^2 - 3\xi + 1\right) + \frac{2(N-1)}{m}\left(3\xi_m^2 - 3\xi_m + 1\right) + 0.822\,\frac{L'_B}{L_c}\left(\xi'^2 - \xi'\,\xi'_m + \xi'^2_m\right)\right.$$

$$\left. + 0.411\,(N-2)\,\frac{L'_{B_m}}{L_c}\,\xi'^2_m + \frac{1-\epsilon}{\epsilon}\,\xi^2 + \frac{2(N-1)}{m}\,\frac{1-\epsilon_m}{\epsilon_m}\,\xi_m^2\right] \qquad (73)$$

with the new notations

$$m = \frac{E_{t_m}\,I_{c_m}}{E_t\,I_c}\;;\quad \xi_m = 1.5\,\frac{\epsilon_m}{1+2\,\epsilon_m}\;;\quad \xi'_m = 1 - \xi_m\;;\quad p_m = \frac{P_m}{P}$$

The effective-length coefficient for an intermediate column is

$$k_m^2 = k^2\,\frac{m}{p_m} \qquad (74)$$

For a symmetrical multi-story, multi-bay frame, with N bays and n stories may be used the approximate formula

$$N^* = \bar{f}_1\left\{2^{n-1}\xi'^2\,\frac{L'_{c_1}}{L_{c_n}}\sum_1^n p - 2^{n-2}\,\frac{L'_{c_2}}{L_{c_n}}\sum_2^n p + (N-1)\left[2^{n-1}\xi'^2_m\,\frac{L'_{c_{m_1}}}{L_{c_n}}\sum_1^n p_m - 2^{n-2}\,\frac{L'_{c_{m_2}}}{L_{c_n}}\sum_2^n p_m\right]\right\}$$

$$+ \sum_2^n \bar{f}_i\left\{2^{n-i}\,\frac{L'_{c_i}}{L_{c_n}}\sum_i^n p - 2^{n(i+1)}\,\frac{L'_{c_{i+1}}}{L_{c_n}}\sum_{i+1}^n p + (N-1)\left[2^{n-i}\,\frac{L'_{c_{m_i}}}{L_{c_n}}\sum_i^n p_m - 2^{n-(i+1)}\,\frac{L'_{c_{m_{i+1}}}}{L_{c_n}}\sum_{i+1}^n p_m\right]\right\} \qquad (75a)$$

$$n^* = 2^{n-1} n\,\xi'^2\,\frac{L_{c_1}}{L_{c_n}}\,\frac{L'_{c_1}}{L_{c_n}} + 2^n n(N-1)\,\xi'^2_m\,\frac{L_{c_{m_1}}}{L_{c_n}}\,\frac{L'_{c_{m_1}}}{L_{c_n}} + \sum_2^n\left[2^{n-i}(n-i+1)\,\frac{L_{c_i}}{L_{c_n}}\,\frac{L'_{c_i}}{L_{c_n}}\right.$$

$$\left. + 2^{n-i+1}(n-i+1)(N-1)\,\frac{L_{c_{m_i}}}{L_{c_n}}\,\frac{L'_{c_{m_i}}}{L_{c_n}}\right]\Bigg) \qquad (75b)$$

$$k_n^2 = N^*/n^* \qquad (75c)$$

The reduced deflections result from the recurrence formulas:

$$\bar{f}_1 = \frac{1}{N}\left\{4n\left(\frac{L_{c_1}}{L_{c_n}}\right)^2\left[\left(3\xi^2 - 3\xi + 1\right)\frac{L'_{c_1}}{L_{c_n}} + 2(N-1)\left(3\xi_m^2 - 3\xi_m + 1\right)\frac{L'_{c_{m_1}}}{L_{c_n}}\right]\right.$$

$$+ 1.644\,\frac{L'_{B_1}}{L_{c_n}}\,\frac{L_{c_1}}{L_{c_n}}\left[2n\left(\xi'^2 - \xi'\,\xi'_m + \xi'^2_m\right)\frac{L_{c_1}}{L_{c_n}} + \frac{n-1}{2}\left(\xi' + \xi'_m\right)\frac{L_{c_2}}{L_{c_n}}\right] +$$

$$+ 1.644\,(N-2)\,\frac{L'_{B_{m_1}}}{L_{c_n}}\,\frac{L_{c_1}}{L_{c_n}}\left(n\xi'^2_m\,\frac{L_{c_1}}{L_{c_n}} + \frac{n-1}{2}\,\xi'_m\,\frac{L_{c_2}}{L_{c_n}}\right)$$

$$\left. + 4n\left(\frac{L_{c_1}}{L_{c_n}}\right)^2\left[\frac{1-\epsilon}{\epsilon}\,\xi^2\,\frac{L'_{c_1}}{L_{c_n}} + 2(N-1)\,\frac{1-\epsilon_m}{\epsilon_m}\,\xi_m^2\,\frac{L'_{c_{m_1}}}{L_{c_n}}\right]\right\} \qquad (76)$$

$$\overline{f}_2 = \overline{f}_1 + \frac{1}{N}\Biggl\{(n-1)\left(\frac{L_{c_2}}{L_{c_n}}\right)^2\left[\frac{L'_{c_2}}{L_{c_n}} + 2(N-1)\,\frac{L'_{c_{m_2}}}{L_{c_n}}\right]$$

$$+0.822\,\frac{L_{c_2}}{L_{c_n}}\left[\frac{n\ \xi' + \xi'_m\ L_{c_s} + (n-1)\,L_{c_2}}{L_{c_n}}\,\frac{L'_{B_1}}{L_{c_n}} + (N-2)\,\frac{n\xi'_m L_{c_1} + \frac{n-1}{2}\,L_{c_2}}{L_{c_n}}\,\frac{L'_{B_{m_1}}}{L_{c_n}}\right]$$

$$+0.822\,\frac{L_{c_2}}{L_{c_n}}\ \frac{(n-1)\,L_{c_2} + (n-2)\,L_{c_3}}{L_{c_n}}\left(\frac{L'_{B_2}}{L_{c_n}} + \frac{N-2}{2}\,\frac{L'_{B_{m_2}}}{L_{c_n}}\right)\Biggr\} \quad \ldots\ldots\ldots \quad (77)$$

. . .

$$\overline{f}_i = \overline{f}_{i-1} + \frac{1}{N}\Biggl\{(n-i+1)\left(\frac{L_{c_i}}{L_{c_n}}\right)^2\left[\frac{L'_{c_i}}{L_{c_n}} + 2(N-1)\frac{L'_{c_{m_i}}}{L_{c_n}}\right]$$

$$+0.822\,\frac{L_{c_i}}{L_{c_n}}\left[\frac{(n-i+2)\,L_{c_{i-1}} + (n-i+1)\,L_{c_i}}{L_{c_n}}\quad\frac{L'_{B_{i-1}}}{L_{c_n}}\right.$$

$$\left. +(N-2)\quad\frac{\frac{n-i+2}{2}\ L_{c_{i-1}} + \frac{n-i+1}{2}\ L_{c_i}}{L_{c_n}}\quad\frac{L'\,B_{m_{i-1}}}{L_{c_n}}\right]$$

$$+0.822\,\frac{L_{c_i}}{L_{c_n}}\ \frac{(n-i+1)\,L_{c_i} + (n-i)\,L_{c_{i+1}}}{L_{c_n}}\left(\frac{L'_{B_i}}{L_{c_n}} + \frac{N-2}{2}\ \frac{L'_{B_{m_i}}}{L_{c_n}}\right)\Biggr\} \quad \ldots\ldots \quad (78)$$

. . .

$$\overline{f}_n = \overline{f}_{n-1} + \frac{1}{N}\Biggl\{1 + \frac{2(N-1)}{m_n} + 0{,}822\left(2\,\frac{L_{c_{n-1}}}{L_{c_n}} + 1\right)\left(\frac{L'_{B_{n-1}}}{L_{c_n}} + \frac{N-2}{2}\,\frac{L'_{B_{m_{n-1}}}}{L_{c_n}}\right)$$

$$+\ 0.822\left(\frac{L'_{B_n}}{L_{c_n}} + \frac{N-2}{2}\ \frac{L'_{B_{m_n}}}{L_{c_n}}\right)\Biggr\} \quad \ldots\ldots\ldots\ldots \quad (79)$$

Eqs. 67 and 68 may be used to compute the effective-length coefficients of the other columns.

Eqs. 60 through 79 have been obtained by an energetic method and contain all the principal parameters of the equilibrium-bifurcation problem. For the analysis of a pin-based frame it is sufficient to analyze its ground floor. For the fixed-base frame, similar formulas to these given previously, have been derived.

Portal-Frame with Crane-Loads.—The stability equation of the symmetrical frame (Fig. 16) is

$$(1-\epsilon)\,\frac{\phi 1}{n\lambda}\left(a\,\frac{6\,\lambda}{\gamma} - b\,\phi_1\right) + 3\epsilon\left(c\,\frac{6\,\lambda}{\gamma} + d\,\phi_1\right) = 0 \quad \ldots\ldots\ldots \quad (80)$$

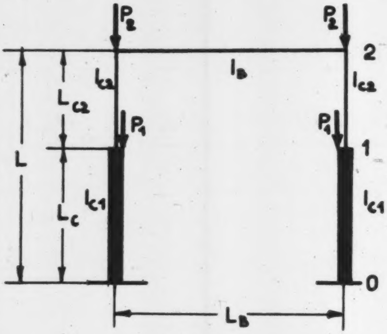

FIG. 16.—PORTAL FRAME WITH CRANE-LOADS

in which:

$$a = 1 - \frac{1}{\sqrt{n(1-p)}} \tan\phi_1 \tan\phi_2 \quad ; \qquad b = \tan\phi_1 + \sqrt{n(1-p)} \tan\phi_2 \quad ;$$

$$c = \tan\phi_1 + \frac{1}{\sqrt{n(1-p)}} \tan\phi_2 \quad ; \qquad d = 1 - \sqrt{n(1-p)} \tan\phi_1 \tan\phi_2 \, ,$$

with the notations

$$\lambda = \frac{L_{c_1}}{L_c} \; ; \; \lambda' = \frac{L_{c_2}}{L_c} = 1 - \lambda \; ; \; n = \frac{E_{t_2} I_{c_2}}{E_{t_1} I_{c_1}} \; ; \; \gamma = \frac{E_{t_1} I_{c_1} L_B}{E_B I_B L_c} \; ; \; p = \frac{P_1}{P_1 + P_2}$$

The approximate formulas

$$k_1 = \frac{R}{\lambda} \quad \text{.....................} \quad (81)$$

$$k_2 = \frac{R}{\lambda'} \sqrt{\frac{n}{1-p}} \quad \text{.................} \quad (82)$$

and

$$R = \sqrt{2 \mu \bar{f}_2 \frac{1 - p\left[1 - \frac{1}{\mu\lambda}\left(\frac{\bar{f}_1}{\bar{f}_2}\right)^2\right]}{1 - p\left(1 - \frac{\bar{f}_1}{\bar{f}_2}\right)}} \quad \text{..............} \quad (83)$$

may be used, with the reduced deflections

$$\bar{f}_1 = \lambda \left\{ \lambda \,(2\lambda - 3\,\bar{m}_o) + 3\frac{\lambda'}{n}\left[2 - \lambda'(1+p) - 2\bar{m}_o\right] + \gamma'(1 - p\lambda' - \bar{m}_o) \right\} \text{......} \quad (84)$$

and

$$\bar{f}_2 = \lambda^2 (2\lambda - 3\,\bar{m}_o) + \frac{\lambda'}{n}\left[2(1+\lambda+\lambda^2) - p\lambda'(2+\lambda) - 3\,\bar{m}_o(1+\lambda)\right] + \gamma'(1 - p\lambda' - \bar{m}_o) \;\; .. \quad (85)$$

with

$$\overline{m}_{\circ} = \frac{3}{2}\,\epsilon\,\frac{\lambda'\,[2-\lambda'\,(1+p)]+\lambda^2 n+(1-p\lambda')\,\frac{n\gamma'}{3}}{n\,\lambda + 3\,\epsilon\left(\lambda' + \frac{2}{3}\,n\,\lambda + \frac{n\gamma'}{6}\right)} \qquad (86)$$

The coefficient μ is obtained for

$$\xi \geq \lambda \text{ from } \mu = \frac{2}{n}\;\frac{(1-\xi)^2}{\overline{f}_{E_2}} \qquad (87)$$

$$\xi < \lambda \text{ from } \mu \doteq \frac{1}{1+\lambda-2\xi}\left(1+\frac{\overline{f}_{E_1}}{\overline{f}_{E_2}} - 2\,\frac{\overline{f}_{E_\xi}}{\overline{f}_{E_2}}\right) \qquad (88)$$

with

$$\xi = \frac{3}{2}\;\epsilon\,\frac{1-\lambda^2(1-n)}{n\lambda+\epsilon\,(3\lambda'+2n\lambda)}\;;\quad \overline{f}_{E_2} = \lambda^2(2\lambda-3\xi)+\frac{\lambda'}{n}\left[2(1+\lambda+\lambda^2)-3(1+\lambda)\,\xi\right]\;;$$

$$\overline{f}_{E_1} = \lambda\left[\lambda\,(2\lambda-3\xi)+\frac{3\lambda'}{n}\,(1+\lambda-2\xi)\right]\;;\;\overline{f}_{E_\xi} = \xi\left[2\xi^2-6\lambda\xi+3\lambda^2+\frac{3\lambda'}{n}\,(1+\lambda-2\xi)\right]\;.$$

Eqs. 81 through 88 resulted from an energetic analysis and may be particularized for pinned and fixed bases. Similar formulas have also been derived for frames with pinned connections between beam and columns, respectively for multi-bay frames, taking account of the non-symmetric loading. These computations also include (approximately) the spatial effect of the crane loading, in order to avoid an underestimation of the stability of the building.

The use of formulas of the type given previously, is only apparently more complicated than that of the known diagrams and charts, as these oversimplify the problem by elimination of some important parameters. The formulas could be compared to the well-known Kleinlogel formulas for the static-strength computation of frames, and to not assume special knowledge of the theory of stability on the designers part.

THEODORE V. GALAMBOS,[25] A.M. ASCE.—Mr. Guillard is correct in stating that in the presence of primary bending moments the critical load will be smaller than the critical load obtained for the same frame if the forces are all assumed to be concentrated on the column tops. The computations of the buckling load for frames in which the columns are subjected to axial force as well as bending moment is quite complicated;[2] however, and therefore, the usual procedure has been to concentrate all loads at the column tops and to perform a stability check for this simplified loading. The question here is whether this simplification can lead to dangerous situations, or whether the difference between the two buckling loads is small enough to justify the simpler method.

E. Chwalla[26] has shown that for one particular frame and loading the reduction in buckling load is very small. More recently E. F. Masur, F. ASCE,

---

[25] Research Asst. Prof., Fritz Engrg. Lab., Lehigh Univ., Bethlehem, Pa.

[26] "Die Stabilitat Lotrecht Belasteter Rechteckrahmen," by E. Chwalla, Der Bauingenieur, Vol. 19, 1938, p. 69.

L. H. Donnell, and I. C. Chang, M. ASCE,[27] and L. W. Lu, A.M. ASCE,[28] have presented systematic methods for the solution of the problem of elastic buckling of frames subjected to primary bending moments; it is hoped that with the now available improved techniques it will be possible in the near future to single out those cases of frame geometry and loading for which the simplified solution is not satisfactory. Lu[28] has computed the critical buckling loads for the following rectangular frames: concentrated load at the center of a single-story, single bay frame (Case I in Table 2), concentrated loads at the third points (Case II), uniformly distributed load (Case III), and uniformly distributed load plus concentrated loads at the column tops (Case IV). The computations were performed for pinned-base frames ($I_s = 0$), and the re-

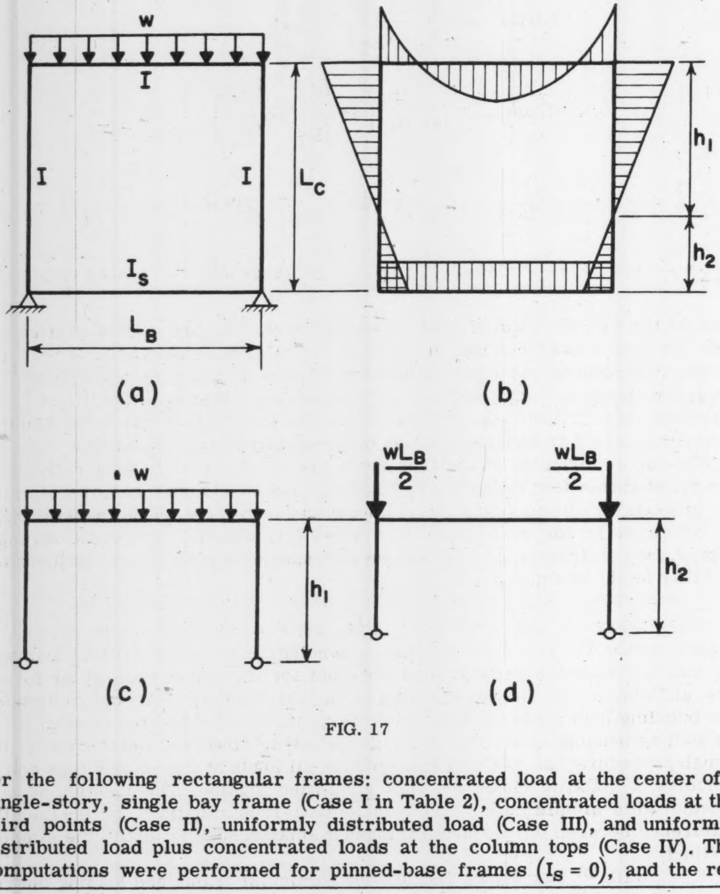

FIG. 17

---

[27] "Stability of Frames in the Presence of Primary Bending Moments," by E. F. Masur, L. H. Donnell, and I. C. Chang. Presented at the May, 1960 meeting of the Engrg. Mechanics Div. of the ASCE at Purdue Univ., in Lafayette, Ind.

[28] "The Stability of Elastic and Partially Plastic Frames," by L. W. Lu, thesis presented to Lehigh Univ. at Bethlehem, Pa. in partial fulfillment of the requirements for the degree of Doctor of Philosophy.

sults are shown in Table 2 under $I_s/I = 0$. Two column heights $\left(L_C = L_B\right.$ and $\left.L_C = L_B/3\right)$ were used, and the beam and column sizes were assumed equal $\left(I_C = I_B = I\right)$. In Table 2, P_{cr} refers to the frame subjected to primary bending moment (case a in the sketches in Table 2) and $\overline{P}_{cr}$ is the buckling load of the frame for which all loads are concentrated at the column tops (case b). The largest difference between the critical loads obtained by the two methods is 12% (Case I). It can also be observed that the simplified method seems somewhat more inaccurate for flat frames $\left(L_C = L_B/3\right)$.

Computations of the critical loads for frames with partial base fixity $\left(I_S/I = 0.5,\ 1.0 \text{ and } 1.5 \text{ in Table } 2\right)$ were made by a procedure suggested by M. G. Puwein[29] and Lu,[28] in which the frame with base restraint (Fig. 17(a)) is separated into two pinned base frames (Figs. 17(c) and 17(d)) failing under the same critical load. The fictitious pin is located at the point at which the moment in the column is zero. This is indicated in the moment diagram of Fig. 17(b). The results of the computations show (Table 2) that for the same critical load the column lengths are increased due to the presence of the restraining beam. The approximate solutions (sketches b in Table 2) were obtained with the aid of the curves in Fig. 5 for the indicated increased column heights. Comparison between the two methods of computation point to the following conclusions:

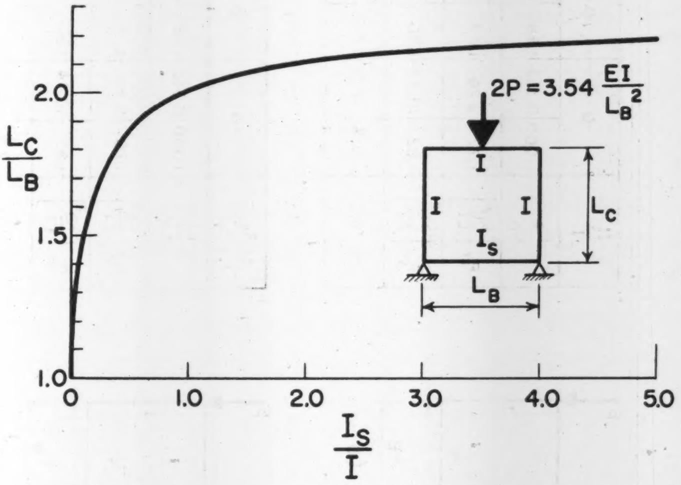

FIG. 18

1. The trend indicated in Fig. 18, in which critical length is plotted against the ratio I_S/I for the frame and loading of Case I in Table 2, proves

---

[29] "Die Knickfestigkeit des Rechteckrahmens," by M. G. Puwein, Die Bautechnik, Vol. 18, 1940, p. 32.

TABLE 2

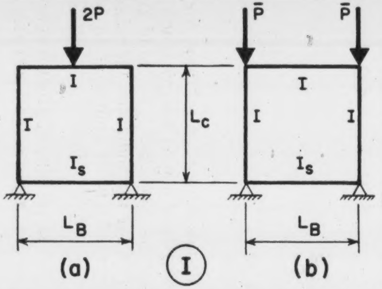
2P
$\bar{P}$
$\bar{P}$
I
I
I
I_s
I
I
I
I_s
L_c
L_B
L_B
(a)
I
(b)

$\frac{I_s}{I}$	0		0.5		1.0		1.5	
$\frac{L_c}{L_B}$	1.000	0.333	1.885	0.583	2.020	0.703	2.075	0.250
$P_{cr}\left[\frac{L_B^2}{EI}\right]$	1.77	9.29	1.77	9.29	1.77	9.27	1.77	9.29
$\bar{P}_{cr}\left[\frac{L_B^2}{EI}\right]$	1.82	10.44	1.80	10.05	1.83	9.76	1.80	9.61
% Diff.	3 %	12 %	2 %	8 %	3 %	5 %	2 %	3 %

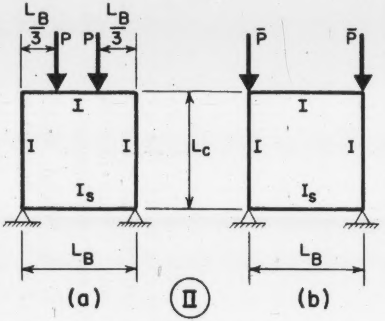
$\frac{L_B}{3}$
P
P
$\frac{L_B}{3}$
$\bar{P}$
$\bar{P}$
I
I
I
I_s
I
I
I
I_s
L_c
L_B
L_B
(a)
II
(b)

$\frac{I_s}{I}$	0		0.5		1.0		1.5	
$\frac{L_c}{L_B}$	1.000	0.333	1.885	0.575	2.020	0.697	2.075	0.741
$P_{cr}\left[\frac{L_B^2}{EI}\right]$	1.78	9.52	1.78	9.52	1.78	9.52	1.73	9.52
$\bar{P}_{cr}\left[\frac{L_B^2}{EI}\right]$	1.82	10.44	1.80	10.31	1.83	9.92	1.80	9.87
% Diff.	2 %	10 %	1 %	8 %	3 %	4 %	1 %	4%

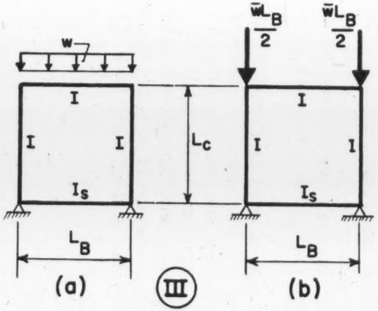
w
I
I
I
I_s
L_B
(a)
III
L_c
$\frac{\bar{w}L_B}{2}$
$\frac{\bar{w}L_B}{2}$
I
I
I
I_s
L_B
(b)

$\frac{I_s}{I}$	0		0.5		1.0		1.5	
$\frac{L_c}{L_B}$	1.000	0.333	1.885	0.564	2.020	0.689	2.075	0.730
$w\left[\frac{L_B^3}{EI}\right]$	3.57	19.48	3.57	19.48	3.57	19.48	3.57	19.48
$\bar{w}\left[\frac{L_B^3}{EI}\right]$	3.64	20.88	3.60	21.50	3.66	20.38	3.60	20.36
% Diff.	2 %	7 %	1 %	5 %	3 %	5 %	1 %	5 %

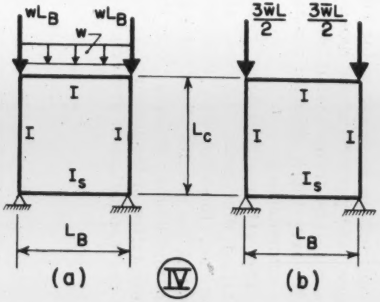
wL_B
wL_B
w
I
I
I
I_s
L_B
(a)
IV
L_c
$\frac{3\bar{w}L}{2}$
$\frac{3\bar{w}L}{2}$
I
I
I
I_s
L_B
(b)

$\frac{I_s}{I}$	0		0.5		1.0		1.5	
$\frac{L_c}{L_B}$	1.000	0.333	1.885	0.551	2.020	0.680	2.075	0.722
$w\left[\frac{L_B^3}{EI}\right]$	1.21	6.77	1.21	6.77	1.21	6.77	1.21	6.77
$\bar{w}\left[\frac{L_B^3}{EI}\right]$	1.21	6.96	1.21	7.29	1.22	6.91	1.21	6.94
% Diff.	0 %	3 %	0 %	8 %	1 %	2%	0 %	2 %

that for the exact solution, as was shown previously for the approximate solution, a small amount of base restraint has a great effect on the total resistance of the frame against buckling.

2. The increase in the stiffness of the base-beam reduces the difference between the two solutions.
3. No great error (at most 8%) results from using the simpler method.
4. The approximate method is less accurate for flat frames.

Whereas these conclusions apply in the strictest sense only to the frames and loadings shown in Table 2, there is good reason to assume that they are also generally valid. For more complicated multi-story frames the ratio of axial load to bending moment in the column becomes larger and thus, the discrepancies between the two solutions will become smaller. Even though the solutions of this report are upper bounds to the true critical load of the frame, these approximate solutions can be applied with confidence.

The foregoing discussion has been limited to frame instability in the elastic range. Lu[28] has succeeded in solving the inelastic buckling problem for simple rectangular frames subjected to primary bending moments. An experimental program is now underway at Lehigh University to verify the theoretical work. A complete report on the results of the experiments is not yet available (as of 1961); however preliminary test results have been reported by Lu[28] and L. S. Beedle, F. ASCE.[30] Fig. 23 in Ref. 30 gives test data for seven model test frames. Five of these frames were pinned at their bases, and two provided with elastic restraints at the bottom of the columns. The restrained frames showed a remarkable increase of carrying capacity, again proving the significance of partial base-fixity on the buckling strength.

The questions posed by Guillard concerning the section "Application of the Theory" and the illustrative example are justified, because no conclusive answer has been given as to how the restraint offered by usual "pinned" column bases can be evaluated. In the writer's opinion these questions cannot be fully answered now (1961) without additional experimental and theoretical research on the moment-rotation behavior of column bases. It is hoped that such research will assess the true stiffness of "pinned" column bases, thus permitting an increase in the critical load for frames buckling in the elastic range, and permitting the extension of plastic design methods to frames that would fail by frame instability for really pinned column bases, but that might well carry their ultimate plastic load if partial base restraint is included in the computations.

The writer wishes to express his thanks to Appeltauer and Barta for their detailed discussion. Of special value are the additional references in the German, Russian, and Romanian language, the more improved method of plotting the results of the computations, and the numerous additional equations for multi-story frames. The writer agrees with Appeltauer and Barta that the rotation of the anchor bolts and the concrete should be added to the rotation of the foundation in arriving at the stiffness of the column base. In this case the revised formula for the stiffness is equal to

---

[30] "On the Application of Plastic Design," by L. S. Beedle, Proceedings, Second Symposium of Naval Structural Mechanics, Brown Univ., Providence, R. I., April, 1960.

$$\frac{I_S}{L_B} = \frac{1}{\dfrac{72\ E}{g\ q\ f^3} + \dfrac{72\ E}{b\ d^2\ E_c}} \qquad \text{. . . . .(89)}$$

For the example in Appendix II the new stiffness values are $I_S/L_B = 1.05$, and $\lambda = 1.50$. The resulting value of k is then 1.27 instead 1.22, causing only a very slight change in the buckling load of the frame.

AMERICAN SOCIETY OF CIVIL ENGINEERS

Founded November 5, 1852

TRANSACTIONS

Paper No. 3257

DISCONTINUITY STRESSES IN BEAMS ON ELASTIC FOUNDATIONS

By Joseph Penzien,[1] M. ASCE

With Discussion by Messrs. R. S. Alwar; and Joseph Penzien

SYNOPSIS

A method of analysis is presented for obtaining discontinuity stresses in beams on elastic foundation and cylindrical shells subjected to axisymmetrical loading. Also presented are the solutions of numerous basic cases which provide the necessary numerical constants required in the proposed method of analysis. Several examples are included.

INTRODUCTION

The deflection of a beam on an elastic foundation and the radial displacement of a longitudinal strip along a cylinder subjected to axisymmetrical loading are given by[2]

$$E\,I\,\frac{d^4w}{dx^4} + k_f\,w = p(x) \quad \dots\dots\dots\dots\dots \text{(1a)}$$

Note.—Published essentially as printed here, in April, 1960, in the Journal of the Structural Division, as Proceedings Paper 2441. Positions and titles given are those in effect when the paper or discussion was approved for publication in Transactions.

[1] Assoc. Prof. of Civ. Engrg., Univ. of California, Berkeley, Calif.

[2] "Strength of Materials," by S. Timoshenko, Part II, D. Van Nostrand Co., New York, 1956.

and

$$D \frac{d^4w}{dx^4} + \frac{E\ h}{r^2}\ w = p(x) \quad \ldots\ldots\ldots\ldots\ldots\ldots \quad (1b)$$

Using the notation

$$\beta\ (\text{beam}) = \sqrt[4]{\frac{k_f}{4\ E\ I}} \quad \ldots\ldots\ldots\ldots\ldots \quad (2a)$$

and

$$\beta\ (\text{cylinder}) = \sqrt[4]{\frac{3(1-\mu^2)}{r^2\ h^2}} \quad \ldots\ldots\ldots\ldots\ldots \quad (2b)$$

the solution of Eqs. 1 for any segment of beam or cylinder having a constant section is given by

$$\begin{aligned} w(x) &= e^{\beta x}(A \cos \beta x + B \sin \beta x) \\ &+ e^{-\beta x}(F \cos \beta x + G \sin \beta x) + w_p(x) \quad \ldots\ldots\ldots\ldots (3) \end{aligned}$$

where $w_p(x)$ is the particular solution to the non-homogeneous equation which results from the loading p(x). By successive differentiation of Eq. 3, the slope, moment, and shear relationships for the case of a beam are expressed as

$$\begin{aligned} \theta(x) &= \beta e^{\beta x}[(B + A) \cos \beta x + (B - A) \sin \beta x] \\ &+ \beta e^{-\beta x}[(G - F) \cos \beta x + (-G - F) \sin \beta x] + w_p'(x) \quad \ldots (4) \end{aligned}$$

$$\begin{aligned} M(x) &= E\ I\ \beta^2\ e^{\beta x}[2\ B \cos \beta x - 2\ A \sin \beta x] \\ &+ E\ I\ \beta^2\ e^{-\beta x}[-2\ G \cos \beta x + 2\ F \sin \beta x] + E\ I\ w_p''(x) \ldots (5) \end{aligned}$$

and

$$\begin{aligned} V(x) &= E\ I\ \beta^3\ e^{\beta x}[(2\ B - 2\ A) \cos \beta x + (-2\ A - 2\ B) \sin \beta x] \\ &+ E\ I\ \beta^3\ e^{-\beta x}[(2\ F + 2\ G) \cos \beta x + (2\ G - 2\ F) \sin \beta x] \\ &+ E\ I\ w_p'''(x) \quad \ldots\ldots\ldots\ldots\ldots\ldots\ldots \quad (6) \end{aligned}$$

For the case of a cylinder, Eqs. 4, 5, and 6 are identical except that E I is replaced by D. The constants of integration A, B, F, and G can be adjusted to satisfy any set of boundary conditions.

If one is concerned only with a single segment of beam or a uniform cylinder having continuous loading, the four constants of integration are obtained by solving four simultaneous equations which satisfy the prescribed boundary conditions. However, if discontinuities which divide the structure into n segments, exist in either the loading or the flexural rigidity (E I, D), it becomes necessary to write a separate expression for the radial displacements in each segment between points of discontinuity. This results in 4 n unknown constants of integration which requires writing 4 n equations to satisfy continuity between segments and the prescribed boundary conditions of the system. Considerable work is involved in setting up and solving such equations; therefore, it is the purpose of this paper to present the complete solution to numerous basic cases involving a uniform beam on an elastic foundation having continuous loadings, along with a method of analysis which makes use of these data in solving the more general discontinuous case described above.

METHOD OF ANALYSIS

The method of analysis described herein, for obtaining discontinuity stresses in beams or cylinders, makes use of an iterative procedure, similar to that introduced by H. Cross, for continuous beams and frames.[3] This iterative procedure, commonly known as moment distribution, consists of first obtaining fixed-end moments in each element resulting from the application of applied loads or resulting from some prescribed joint displacement. While the resulting deformations are compatible, the joints are not in static-moment equilibrium; therefore, it is necessary to allow the joints to rotate one by one until each joint in the structure is in static equilibrium. While the rate of convergence of this procedure is not within the scope of this investigation, the examples included in this paper would indicate that, generally, a more rapid rate of convergence is obtained when applying the method to beams on elastic foundation and to cylinders, than when applying it to continuous beams and frames.

To define the changes in the end moments during this iteration, one must predetermine the following quantities: (1) stiffness factor, K, of each element defined as that moment required at the end of an element to produce a unit rotation of that end, (2) carry-over factor, C, for each element defined as the moment produced at one end of an element resulting from placing a unit moment at the opposite end, and (3) distribution factors, DF, at each joint defined as the fractional parts of an externally applied joint moment carried by each element entering the joint.

The general method of analysis presented herein for determining discontinuity stresses makes use of the above iterative procedure along with the use of the principle of superposition. This general method is outlined in the subsequent steps.

Step No. 1.—

(a) The beam or cylinder is considered as externally restrained against radial displacements and rotations at all points of discontinuity except at the free ends. Locations of concentrated loadings, such as those produced by stiffening rings around a cylinder, are considered as discontinuity points and are, therefore, restrained in the manner described above.

---

[3] "Analysis of Continuous Frames by Distributing Fixed-End Moments," by H. Cross, Transactions, ASCE, Vol. 96, 1932, p. 1.

Distributed loadings which, in the case of cylinders, may be due to temperature changes or internal pressures are placed on the beam or cylinder and the fixed-end shears and moments are determined.

(b) The external-moment restraint at each discontinuity point is now removed by the iterative procedure described previously which results in a balanced set of end moments at each discontinuity point.

(c) Knowing the end moments found in Step 1(b), one must now determine the end shears for each segment. This step is best illustrated by considering a single beam or cylinder segment A B as shown in Fig. 1. For the case of a cylinder, this segment is considered as a flat plate on an elastic foundation where the foundation stiffness is equivalent to the hoop stiffness provided by the cylinder. With the end moments $M_{A\,o}$ and $M_{B\,o}$ for segment A B in Fig. 1(a) known, the unknown end shears $V_{A\,o}$ and $V_{B\,o}$ are determined by separating the total loading on the segment into three separate, but equivalent, loadings as shown in Figs. 1(b), 1(c), and 1(d). This separation is necessary due to the fact the elastic foundation forces on the segment in Fig. 1(a) are unknown.

The fixed-end moments and shears for the segment in Fig. 1(b) are those obtained in Step 1(a).

The moments M_A'' and M_B'' in Figs. 1(b) and 1(c), respectively, are now determined to satisfy the conditions that

$$M_A'' = M_{A\,o} + FEM_A$$

and

$$M_B''' = M_{B\,o} + FEM_B \quad \ldots\ldots\ldots\ldots\ldots (7)$$

The corresponding end shears are determined next for these cases; thus, the total end shears (Fig. 1(a)) can be determined by superposition as follows:

$$V_{A\,o} = V_A' - V_A'' + V_A'''$$

$$V_{B\,o} = V_B' - V_B'' + V_B''' \quad \ldots\ldots\ldots\ldots\ldots (8)$$

(d) Force equilibrium considerations at the restrained discontinuity points will now yield the reaction forces necessary, at these points, to prevent the normal displacements.

Step No. 2.—A complete set of stiffness-influence coefficients are now obtained as follows:

(a) Restrain all discontinuity points as in Step 1(a) and produce a unit normal displacement at one of the discontinuity points without allowing any joint rotations.

(b) Remove the external moment restraints for each discontinuity by iteration in the same manner as in Step 1(b). This results in known end moments for each segment of the beam or cylinder, for example, $M_{A\,A}$ and $M_{B\,A}$ in Fig. 2.

(c) The end shears are determined, for this case, in a manner similar to that in Step 1(c), as illustrated in Fig. 2. Using superposition, the algebraic

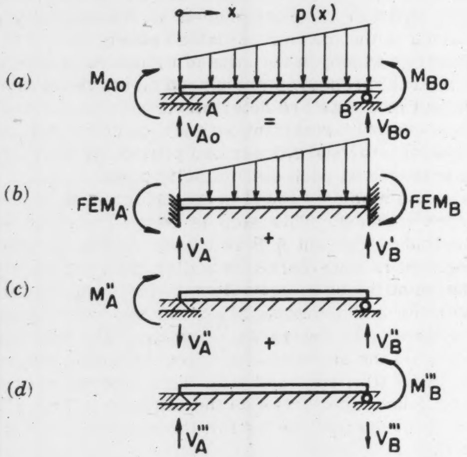
x
p(x)
(a)
MAo
A
B
MBo
VAo
=
VBo
(b)
FEMA
FEMB
V'A
+
V'B
(c)
M''A
V''A
+
V''B
(d)
M'''B
V'''A
V'''B

FIG. 1

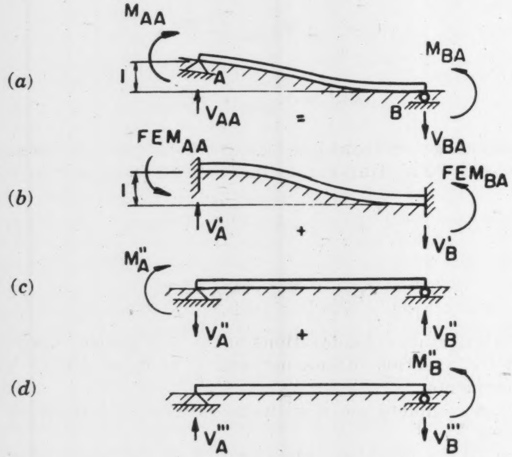
MAA
(a)
1
A
MBA
VAA
=
B
VBA
FEMAA
(b)
1
FEMBA
V'A
+
V'B
M''A
(c)
V''A
+
V''B
M''B
(d)
V'''A
V'''B

FIG. 2

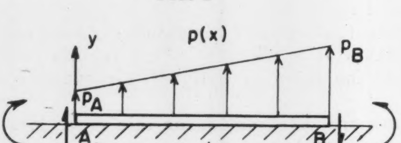
y
p(x)
pB
pA
A
B
L
MA
VA
VB
MB
x

FIG. 3

sum of the moments and shears in Figs. 2(b), (c), and (d) must equal the moments and shears, respectively, in Fig. 2(a). For those segments not adjacent to the point of unit displacement, the fixed-end moments (FEM) will be zero.

(d) The normal forces required at all discontinuity points are now calculated from the known end shears in a manner similar to that in Step 1(d). These forces are the stiffness-influence coefficients.

(e) Steps 2(a) through 2(d) must be repeated for a unit displacement at each of the remaining discontinuities, in order that the complete set of influence coefficients be known. These coefficients, when written in matrix form, produce a symmetrical matrix about the diagonal due to Maxwell's law of reciprocal deflections.

Step No. 3.—Using the information determined in Steps 1 and 2, one can write a separate superposition equation for each discontinuity point, expressing the corresponding applied normal force at each point in terms of the unknown, normal displacements of all discontinuity points. These simultaneous equations, when solved, will yield the magnitude of the normal displacements of all discontinuity points in the beam or cylinder.

Step No. 4.—

(a) The end shears and moments, for each case solved in Step 2 involving a unit displacement at a particular point, are multiplied by the displacement of that particular point as found in Step 3. Using superposition, all resulting end moments and shears obtained in this manner are added algebraically to those found in Step 1; thus, the final end moments and shears for each segment of the beam or cylinder are known.

(b) One can now write the general equations for the normal displacement, slope, moment, and shear along each segment using Eqs. 3, 4, 5, and 6, respectively. The constants of integration A, B, F, and G appearing in these equations are determined by superposition, using the final end moments and shears found in Step 4(a) along with the basic integration constants, found in Table 1, which were determined for the unit loading conditions shown at the head of that table.

To illustrate this step, consider a beam segment A B as shown in Fig. 3. Consider also that the end moments M_A and M_B and that the shears V_A and V_B are the final values determined in Step 4(a). The constants of integration A, B, F, and G for this segment may now be expressed in terms of these known end moments and shears and the appropirate constants in Table 1 as follows:

$$\begin{Bmatrix} A \\ B \\ F \\ G \end{Bmatrix} = \begin{bmatrix} A_1 & A_2 & A_3 & A_4 \\ B_1 & B_2 & B_3 & B_4 \\ F_1 & F_2 & F_3 & F_4 \\ G_1 & G_2 & G_3 & G_4 \end{bmatrix} \begin{Bmatrix} M_A \\ V_A\,L \\ M_B \\ V_B\,L \end{Bmatrix} \frac{L^2}{E\,I} \quad \ldots\ldots\ldots (9)$$

For the positive loading shown in segment A B in Fig. 3, the particular solution $w_p(x)$ appearing in Eq. 3 and its derivatives may be expressed as follows:

TABLE 1.—INTEGRATION CONSTANTS

βL	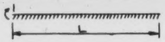				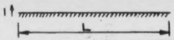				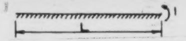				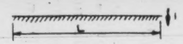			
	A_1	B_1	F_1	G_1	A_2	B_2	F_2	G_2	A_3	B_3	F_3	G_3	A_4	B_4	F_4	G_4
0.05	-227957	-239957	251957	-239957	-112157	-119957	128157	-119957	228057	240057	-252057	240057	-115957	-119957	123957	-119957
0.10	-675155	-749855	825155	-750355	-326355	-373855	426355	-373855	675155	750155	-825155	750155	-350055	-375055	400155	-375055
0.15	-839654	-986654	113655	-988854	-398854	-490154	596354	-490154	839554	987654	-113655	987654	-444454	-493854	543254	-493854
0.20	-187554	-233854	281354	-235054	-875053	-115654	150054	-115654	187554	234454	-281254	234454	-101654	-117254	132854	-117254
0.25	-576353	-764453	960453	-772453	-264053	-376153	520153	-376153	575953	767953	-959853	767953	-320053	-384053	448053	-384053
0.30	-216353	-306253	401653	-311753	-972652	-149753	220753	-149753	216053	308653	-401153	308553	-123453	-154353	185253	-154353
0.35	-930652	-141053	193153	-145153	-410352	-685252	107753	-685252	927452	142753	-192753	142753	-547252	-713852	880352	-713852
0.40	-441552	-719152	102853	-750452	-190752	-347052	581452	-347052	438852	731652	-102453	731652	-268452	-366052	463652	-366052
0.45	-225352	-396252	591752	-420952	-952551	-189852	339252	-189852	223052	405752	-588552	405852	-142152	-203052	264052	-203052
0.50	-121652	-231952	362152	-251952	-502151	-110352	210352	-110352	119552	239452	-359252	239452	-798851	-119852	159852	-119852
0.55	-684951	-142452	232952	-159052	-275751	-672451	137052	-672451	666351	148452	-230252	148452	-470951	-743751	101752	-743751
0.60	-398751	-910551	156152	-104952	-156051	-426651	928651	-426651	382051	959251	-153652	959251	-288451	-481051	673551	-481051
0.65	-237951	-601551	108352	-719851	-901550	-279751	651351	-279751	222851	641551	-106052	641551	-182351	-322051	461751	-322051
0.70	-144551	-408551	774551	-510551	-527150	-188551	470251	-188551	130851	441751	-752551	441751	-118351	-222051	325851	-222051
0.75	-887650	-284051	568151	-372951	-309050	-130151	347951	-130151	762850	311851	-547351	311851	-783450	-157051	235751	-157051
0.80	-547550	-201451	426251	-279551	-179450	-916650	263051	-916650	433250	224951	-406451	224951	-528050	-113551	174251	-113551
0.85	-336550	-145351	326251	-214551	-101550	-657050	202571	-657050	231350	165351	-307451	165351	-360750	-836150	131151	-836150
0.90	-203850	-106451	254251	-168251	-542149	-478150	158851	-478150	106950	123551	-236251	123551	-249050	-626550	100451	-626550
0.95	-119850	-789750	201451	-134451	-255449	-352650	126351	-352650	302749	935750	-184151	935750	-173250	-476550	779950	-476550
1.00	-664649	-592550	161951	-109251	-829048	-263050	101851	-263050	-164849	718250	-145351	718250	-120950	-367350	613850	-367350
1.05	-326349	-448950	131951	-902450	188848	-198250	830350	-198250	-443149	557450	-115951	557450	-843949	-286550	488750	-286550
1.10	-114049	-343050	108851	-756250	765848	-150750	684850	-150750	-600949	436950	-933950	436950	-586849	-225950	393150	-225950
1.15	166148	-264050	907850	-642150	106849	-115550	570550	-115550	-681649	345450	-759050	345450	-404049	-179850	319250	-179850
1.20	939948	-204650	765750	-551850	120049	-891549	479650	-891549	-713349	275250	-621750	275250	-273249	-144450	261450	-144450
1.25	136849	-159350	652450	-479350	122749	-692149	406750	-692149	-713949	220750	-512750	220750	-179249	-116850	215750	-116850
1.30	157249	-124750	561050	-420650	119349	-540149	347550	-540149	-695449	178050	-425550	178050	-111549	-952049	179250	-952049
1.35	163349	-979949	486750	-372350	112449	-423449	299150	-423449	-665549	144250	-355050	144250	-627448	-780749	149950	-780749
1.40	160549	-772549	425750	-332450	103749	-333249	259250	-333249	-629249	117450	-297750	117450	-276848	-643949	126050	-643949
1.45	152349	-610749	375250	-298950	942048	-263149	226050	-263149	-589949	958149	-250650	958149	-263347	-533849	106550	-533849
1.50	141149	-483749	333150	-270650	846848	-208349	198350	-208349	-549749	784049	-211850	784049	150648	-444649	904249	-444649
1.55	128449	-383849	297750	-246550	754948	-165249	174950	-165249	-509949	642649	-179550	642649	273548	-371849	770949	-371849
1.60	115449	-304849	267850	-225850	668748	-131349	155050	-131349	-471549	527249	-152650	527249	356448	-312149	659849	-312149
1.65	102549	-242249	242450	-207950	589248	-104549	138150	-104549	-434849	432449	-130050	432449	409848	-262849	566649	-262849
1.70	902848	-192549	220550	-192350	516948	-831848	123650	-831848	-400249	354349	-110950	354349	441648	-221949	488049	-221949
1.75	788748	-153049	201750	-178650	451748	-662448	111150	-662448	-367849	289749	-947149	289749	457348	-187949	421449	-187949
1.80	684048	-121549	185550	-166550	393548	-527448	100250	-527448	-337649	236049	-809749	236049	461348	-159349	364849	-159349
1.85	589348	-963548	171350	-155750	341848	-419748	907849	-419748	-309649	191449	-692349	191449	456848	-135449	316549	-135449
1.90	504348	-763248	158850	-146150	296048	-333548	825349	-333548	-283649	154149	-591949	154149	446348	-115249	275049	-115249
1.95	428848	-603448	147850	-137550	255748	-264748	752849	-264748	-259649	123049	-505649	123049	431548	-981148	239449	-981148

2.00	362248	-476248	138150	-129850	220448	-209648	689049	-209648	-237549	969248	-431349	969248	413848	-836048	208649	-836048
2.05	303848	-375048	129550	-122750	189448	-165648	632449	-165648	-217149	751048	-367349	751048	394348	-712648	182049	-712648
2.10	252948	-294648	121850	-116350	162448	-130448	582249	-130448	-198349	568448	-311949	568448	373748	-607448	158849	-607448
2.15	208848	-230948	114950	-110850	138948	-102348	537449	-102348	-180949	415548	-264049	415548	352648	-517448	138749	-517448
2.20	170948	-180648	108650	-105150	118548	-798847	497449	-798847	-165049	287748	-222549	287748	331548	-440448	121249	-440448
2.25	138448	-141048	103050	-100250	100848	-620847	461549	-620847	-150349	181248	-186649	181248	310648	-374348	105949	-374348
2.30	110748	-110048	978249	-956249	855647	-479747	429149	-479747	-136849	926447	-155449	926447	290248	-317648	925448	-317648
2.35	873047	-857647	931349	-914049	724147	-368247	399949	-368247	-124449	193847	-128349	193847	270548	-268948	808248	-268948
2.40	676347	-669847	888249	-874849	610947	-280447	373449	-280447	-113049	-409047	-104849	-409047	251548	-226948	705448	-226948
2.45	512147	-525047	848649	-838249	513947	-211747	349449	-211747	-102549	-901147	-845148	-901147	233448	-190948	615148	-190948
2.50	376347	-414247	812049	-804149	430947	-158147	327549	-158147	-929148	-129948	-669348	-129948	216148	-159848	535848	-159848
2.55	264947	-330047	778249	-772249	360047	-116747	307549	-116747	-840648	-161648	-517348	-161648	199848	-133148	466148	-133148
2.60	174547	-266747	746749	-742349	299847	-848446	289249	-848446	-759548	-186548	-386448	-186548	184448	-110248	404748	-110248
2.65	102047	-219447	717449	-714249	248647	-606446	272449	-606446	-685048	-205648	-273948	-205648	169948	-904647	350848	-904647
2.70	447146	-184447	690049	-687749	205447	-424446	256949	-424446	-616848	-219748	-177448	-219748	156248	-735447	303348	-735447
2.75	266344	-158947	664349	-662749	169047	-289346	242749	-289346	-554248	-229548	-952147	-229548	143548	-590447	261648	-590447
2.80	-334746	-140347	640249	-639249	138347	-190846	229549	-190846	-497048	-235848	-254347	-235848	131648	-466547	224948	-466547
2.85	-582846	-126947	617549	-616849	112747	-120446	217449	-120446	-444748	-239148	334147	-239148	120448	-360847	192648	-360847
2.90	-757246	-117247	596149	-595749	913346	-715445	206149	-715445	-396948	-239848	826647	-239848	110148	-270947	164348	-270947
2.95	-872146	-110247	575949	-575649	735946	-389245	195649	-389245	-353348	-238448	123548	-238448	100548	-194747	139448	-194747
3.00	-939046	-104947	556749	-556649	589246	-183845	185849	-183845	-313548	-235248	157048	-235248	915947	-130547	117748	-130547
3.10	-965846	-973646	521349	-521349	369746	-118344	168249	-118344	-244448	-224948	205348	-224948	757147	-315046	820147	-315046
3.20	-902046	-913146	489249	-489249	224346	-173444	152849	-173444	-187448	-210748	234048	-210748	621847	363746	549147	-363746
3.30	-789546	-851946	460149	-450049	130446	-944644	139349	-944644	-140848	-194348	247848	-194348	507347	810746	345147	810746
3.40	-658046	-784146	434449	-433349	717045	-185545	127349	-185545	-102948	-176848	250748	-176848	410847	108647	193547	108647
3.50	-526146	-709646	409149	-408949	364645	-262345	116749	-262345	-723647	-159048	245548	-159048	330047	123747	826046	123747
3.60	-404546	-630546	386749	-386449	164845	-314045	107249	-314045	-480247	-141448	234948	-141448	262747	129847	324245	129847
3.70	-299046	-550246	366049	-365849	608744	-339445	987848	-339445	-288347	-124648	220548	-124648	207147	129547	-518646	129547
3.80	-211546	-471546	347049	-346749	144344	-342045	911948	-342045	-139447	-108848	203848	-108848	161347	124947	-884546	124947
3.90	-141946	-397246	329449	-329149	362442	-327245	843648	-327245	-258046	-942247	185948	-942247	123947	117547	-111147	117547
4.00	-885545	-329146	313149	-312849	270443	-300645	781948	-300645	588246	-808547	167648	-808547	935646	108447	-123347	108447
4.10	-492045	-268246	297949	-297749	117744	-267245	726048	-267245	119947	-687647	149548	-687647	691346	984846	-127847	984846
4.20	-213845	-215346	283949	-283749	220644	-230845	675448	-230845	162147	-579547	132148	-579547	496246	882846	-126947	882846
4.30	-276344	-170146	270849	-270649	307744	-194645	629348	-194645	189147	-483747	115748	-483747	342046	782446	-122347	782446
4.40	884344	-132346	258549	-258449	367344	-160345	587348	-160345	204347	-399647	100348	-399647	221446	686246	-115147	686246
4.50	152145	-101346	247149	-247049	398344	-129545	549048	-129545	210447	-326247	862847	-326247	128446	596246	-106447	596246
4.60	179845	-764145	236549	-236449	403444	-102545	513948	-102545	209447	-262847	735147	-262847	578345	513346	-968946	513346
4.70	182745	-566645	226849	-226449	388644	-797044	481848	-797044	203447	-208547	620447	-208547	535644	438246	-871046	438246
4.80	170545	-413345	217149	-217149	359744	-607944	452348	-607944	193647	-162447	518347	-162447	-326245	370846	-774246	370846
4.90	149945	-296445	208349	-208349	322144	-455144	425148	-455044	181347	-123547	428347	-123547	-590845	311046	-681146	311046
5.00	125545	-208545	200149	-200049	280444	-334044	400148	-334044	167547	-910346	349547	-910346	-764945	258546	-593546	258546
5.10	101145	-144045	192349	-192249	238244	-240244	377048	-240244	152847	-642346	281347	-642346	-868945	212846	-512546	212846
5.20	780144	-975244	184949	-184949	197944	-169044	355748	-169044	137947	-423446	222647	-423446	-919345	173346	-438646	173346
5.30	583544	-649144	178049	-178049	160944	-115944	335948	-115944	123247	-247046	172647	-247046	-929545	139546	-372046	139546
5.40	408144	-422344	171549	-171549	128344	-773743	317648	-773743	109047	-107046	130447	-107046	-910445	110846	-312746	110846
5.50	275444	-275444	165349	-165349	100444	-499743	300548	-499743	955346	209844	951146	209844	-870445	866645	-260446	866645
5.60	171944	-179344	159449	-159449	770643	-310343	284748	-310343	829546	850745	659346	850745	-816645	664645	-214646	664645
5.70	920343	-118644	153949	-153949	580043	-183443	270048	-183443	713446	146246	420946	146246	-754145	497545	-174946	497545
5.80	327243	-825243	148649	-148649	428243	-101443	256348	-101443	607646	189446	228746	189446	-687045	360545	-140846	360545
5.90	-996341	-617743	143649	-143649	309543	-510542	243548	-510542	512146	217846	764045	217846	-618645	249445	-111746	249445

TABLE 1.—*Continued*

βL	A_1	B_1	F_1	G_1	A_2	B_2	F_2	G_2	A_3	B_3	F_3	G_3	A_4	B_4	F_4	G_4
6.00	-264243	-535943	138949	-138949	218543	-222342	231548	-222742	426846	234446	-419745	234446	-550945	160345	-871645	160345
6.10	-395043	-480643	134449	-134449	150443	-739641	220348	-739641	351246	241446	-131646	241446	-485845	900044	-665845	900044
6.20	-494643	-453443	130149	-130149	100743	-122441	209848	-122841	285046	241146	-197346	241146	-424345	353844	-495045	353844
6.30	-700843	-439243	126049	-126049	651642	-350939	200048	-350939	227446	235246	-243046	235246	-367145	-617443	-354845	-617443
6.40	-426943	-423043	122149	-122149	404442	-146241	190748	-146241	177846	225146	-272446	225146	-314845	-369444	-240945	-369444
6.50	-352543	-407243	118349	-118349	238542	-383041	182148	-383041	135546	212046	-288646	212046	-267345	-588844	-149545	-588844
6.60	-292243	-379943	114849	-114849	132342	-605641	173948	-605641	997345	197046	-294346	197046	-224845	-737144	-774044	-737144
6.70	-240143	-349243	111449	-111449	653541	-826841	166248	-826841	698645	180946	-291946	180946	-187145	-828544	-214244	-828544
6.80	-182943	-313643	108149	-108149	273741	-978341	159048	-978341	452045	164246	-283246	164246	-154045	-875144	-210544	-875144
6.90	-138843	-285443	105049	-105049	887040	-102542	152248	-102542	251145	147646	-270046	147646	-125145	-887344	523344	-887344
7.00	-922542	-246943	102049	-102049	115740	-104442	145848	-104442	901844	131346	-253546	131346	-100245	-873344	744544	-873344
7.10	-577542	-209343	991948	-991948	183739	-101042	139748	-101042	-363544	115746	-235046	115746	-789144	-840344	891544	-840344
7.20	-432042	-176743	964548	-964548	250640	-936341	134048	-936341	-133445	101046	-215346	101046	-608444	-793844	979144	-793844
7.30	-174242	-154643	938348	-938348	628040	-853141	128548	-853141	-205645	872545	-195146	872545	-456844	-738444	102045	-738444
7.40	-245541	-125243	913148	-913148	782640	-688441	123448	-688441	-256845	746445	-175046	746445	-330844	-677844	102545	-677844
7.50	281241	-913942	888948	-888948	109441	-600341	118548	-600341	-290745	631645	-155446	631645	-227244	-614944	100345	-614944
7.60	102142	-775842	865748	-865748	134841	-514541	113948	-514541	-310545	528245	-136746	528245	-143244	-551744	960244	-551744
7.70	105842	-528842	843348	-843348	152641	-433341	109548	-433341	-318845	435945	-119146	435945	-760643	-490144	904144	-490144
7.80	-487441	-172042	821848	-821848	162841	-358341	105448	-358341	-318145	354445	-102746	354445	-232943	-431144	838944	-431144
7.90	135942	-363642	801248	-801248	166141	-290841	101448	-290841	-310445	283045	-876545	283045	173043	-375644	768544	-375644
8.00	195942	-264842	781348	-781348	127141	-204441	976647	-204441	-297445	221245	-739745	221245	476743	-324144	695944	-324144
8.10	190342	-229642	762148	-762148	123441	-160641	940847	-160641	-280745	168045	-616745	168045	695543	-277044	623544	-277044
8.20	-205941	-411841	743648	-743648	116441	-123141	906847	-123141	-261445	122945	-507145	122945	844743	-234344	553144	-234344
8.30	-262041	-524041	725848	-725848	107141	-918140	874547	-918140	-240545	849244	-410445	849244	937543	-196144	485944	-196144
8.40	143842	-845941	708648	-708648	744040	-608240	843647	-608240	-218945	534344	-325845	534344	985143	-162144	422744	-162144
8.50	-166541	0000	692048	-692048	662040	-429940	814247	-429940	-197245	276744	-252545	276744	997343	-132344	364344	-132344
8.60	370741	0000	676048	-676048	577140	-289240	786147	-289240	-175945	693043	-189745	693043	982343	-106344	310844	-106344
8.70	-252941	-252941	660648	-660648	358340	-189040	759347	-189040	-155345	-942843	-136545	-942843	947043	-838643	262444	-838643
8.80	176841	0000	645748	-645748	302040	-117840	733747	-117840	-135945	-220144	-918444	-220144	897043	-646943	219144	-646943
8.90	255341	-127641	631248	-631248	249840	-653239	709347	-653239	-117645	-313744	-549044	-313744	837243	-484743	180644	-484743
9.00	0000	961440	617348	-617348	202840	-279939	685947	-279939	-100845	-380144	-247844	-380144	771243	-348843	146944	-348843
9.10	0000	-770840	603848	-603848	161640	-254138	663547	-254138	-854144	-423844	-645542	-423844	702243	-236443	117544	-236443
9.20	-686341	686340	590748	-590748	765439	-175039	642147	-175039	-714944	-448844	182744	-448844	632543	-144643	921743	-144643
9.30	-229842	153241	578148	-578148	575739	-722138	621647	-722138	-590244	-458644	327144	-458644	563943	-707342	705343	-707342
9.40	240242	240241	565948	-565948	421939	-104638	602047	-104638	-479644	-456444	433244	-456444	497843	-123442	522543	-123442
9.50	-495342	0000	554048	-554048	300439	226438	583247	226438	-382444	-444744	507044	-444744	435343	328042	369743	328042
9.60	0000	267641	542548	-542548	206939	366236	565147	366238	-297844	-425944	554044	-425944	376943	667342	243543	667343
9.70	538641	269341	531448	-531448	136739	386238	547847	386238	-224944	-401944	578944	-401944	323143	912442	140643	912442
9.80	0000	-251141	520648	-520648	857138	337638	531247	337638	-162844	-374444	586044	-374444	274143	108043	581742	108043
9.90	0000	126741	510248	-510248	497938	256238	515347	256238	-110544	-344744	578944	-344744	229943	118343	-669141	118343
10.00	0000	-671940	500048	-500048	255138	165438	500047	165438	-669843	-314044	560944	-314044	190543	123543	-565242	123543

$$w_p(x) = -\frac{1}{k_f}\left[\left(1 - \frac{x}{L}\right) p_A + \frac{x}{L}\, p_B\right] \quad \ldots\ldots\ldots \quad (10a)$$

$$w_p'(x) = -\frac{1}{k_f\, L}\left[(p_B - p_A)\right] \quad \ldots\ldots\ldots\ldots \quad (10b)$$

and

$$w_p''(x) = w_p'''(x) = 0 \quad \ldots\ldots\ldots\ldots\ldots \quad (10c)$$

In the case of a cylinder, D is substituted for E I in Eqs. 9, and E h/r^2 is substituted for k_f in Eqs. 10. Having the constants of integration as defined by Eqs. 9 and the particular solution to the differential equation with its derivatives as given by Eqs. 10, the normal displacements, slopes, moments, and shears are completely defined in the interval A B as used in this illustration. The trigometric relations shown in Table 2, which appear in Eqs. 3, 4, 5, and 6, have been tabulated to simplify the use of these equations.

The general method of analysis, as outlined in Steps 1-4, can be carried out quite rapidly using the basic data plotted in Figs. 4 through 14. All curves have been plotted over a range of β L between 0 and 10. Also shown in these figures are the approximate relationships for obtaining the ordinates for values of β L greater than 10.

The stiffness and carry-over factors to be used in the iteration procedure are given in Figs. 4, 5, and 6. The fixed-end moments and shears for the case of a unit displacement, as required in Steps 2(a) and 2(e), are presented in Figs. 7, 8, and 9. The fixed-end moments and shears required in Step 1(a) for uniform and triangular loadings are given in Figs. 10 through 14.

Three problems have been completely solved in the following section to illustrate the generality of the method of analysis. Example 1 illustrates its use on a combined footing, Example 2 illustrates its use when stresses in a cylinder are produced by axisymmetrical temperature changes, and Example 3 illustrates its use for the case of axisymmetrical loading on a cylinder. The general method presented herein can also account for partial restraint against both normal displacement and rotation at various points along the beam or cylinder.

SAMPLE PROBLEMS

Example 1.—A combined footing 26 ft long, 48 in. wide, and 24 in. deep is loaded by two concentrated loads, as shown in Fig. 15. The foundation stiffness k_f is assumed constant. This is required to determine the foundation pressures and the bending-moment diagram for the footing.

Step No. 1.—The fixed-end moments and shears are zero.

Step No. 2.—The stiffness coefficients are determined as shown in Fig. 16.

TABLE 2

$A = e^{x} \sin x$ $B = e^{x} \cos x$ $C = e^{-x} \sin x$ $D = e^{-x} \cos x$

X	A	B	C	D	X	A	B	C	D	X	A	B	C	D
0.05	525449	104951	475449	950050	2.30	743751	664551	-747649	668049	6.10	812152	-438353	408547	-220548
0.10	110350	109951	903349	900350	2.35	746051	736851	-678549	670149	6.20	409452	-491053	168647	-202248
0.15	173650	114851	128650	851050	2.40	744551	812851	-612749	668949	6.30	915651	544453	308746	183648
0.20	242650	119751	162650	802450	2.45	739051	892551	-550349	664649	6.40	701452	597753	193647	165048
0.25	317650	124451	192650	754550	2.50	729051	975951	-491249	657649	6.50	143053	649553	323447	146848
0.30	398950	128951	218950	707750	2.55	714251	106352	-435449	648149	6.60	229053	698553	423847	129248
0.35	486550	133351	241650	661950	2.60	694051	115352	-382849	636449	6.70	328953	742853	498347	112548
0.40	580950	137451	261050	617450	2.65	668151	124752	-333449	622849	6.80	443653	780553	550347	968347
0.45	682150	141251	277350	574150	2.70	635951	134552	-287249	607549	6.90	573953	809453	582947	822047
0.50	790450	144651	290750	532250	2.75	597051	144552	-243949	590849	7.00	720453	826753	599047	687447
0.55	905950	147751	301550	491850	2.80	550851	154952	-203749	572949	7.10	883453	829653	601447	564847
0.60	102851	150351	309850	452950	2.85	496951	165552	-166249	554049	7.20	106354	814853	592547	454147
0.65	115951	152451	315950	415550	2.90	434851	176452	-131649	534249	7.30	125854	778753	574547	355347
0.70	129751	154051	319950	379850	2.95	363851	187552	-996648	513849	7.40	147054	717453	549347	268047
0.75	144351	154851	321950	345650	3.00	283451	198852	-702548	492849	7.50	169554	626753	518747	191747
0.80	159651	155051	322350	313050	3.10	923050	221752	-187348	450149	7.60	193454	502053	484347	125747
0.85	175751	154451	321150	282050	3.20	143251	-244952	-237948	-406949	7.70	218254	338753	447447	694546
0.90	192651	152851	318450	252750	3.30	427651	-267752	-581848	-364249	7.80	243754	131653	409147	221046
0.95	210351	150451	314550	224950	3.40	765751	-289652	-852848	-322649	7.90	269454	124053	-370347	170546
1.00	228751	146851	309550	198750	3.50	116152	-310152	-105949	-282749	8.00	294954	433753	-331847	488046

1.05	247851	142151	303550	174150	3.60	161952	-328152	-120949	-245049	8.10	319554	802353	-294347	739246
1.10	267751	136251	296650	150950	3.70	214352	-343052	-130949	-209649	8.20	342554	123454	-258347	931546
1.15	288251	129051	289050	129350	3.80	273552	-353552	-136849	-176949	8.30	363054	173554	-224247	107247
1.20	309451	120351	280750	109150	3.90	339752	-358652	-139249	-146949	8.40	380054	230954	-192147	116747
1.25	331251	110051	271850	903449	4.00	413252	-356852	-138649	-119749	8.50	392454	295854	-162447	122447
1.30	353551	981550	262650	729049	4.10	493752	-346852	-135649	-952648	8.60	398854	368654	-135247	124947
1.35	376351	844850	252950	567749	4.20	581252	-326952	-130649	-735148	8.70	397954	449454	-110447	124747
1.40	399651	689250	243050	419149	4.30	675252	-295352	-124349	-543848	8.80	388054	538054	-881646	122247
1.45	423251	513750	232850	282649	4.40	775052	-250352	-116849	-377348	8.90	367354	634554	-683346	118047
1.50	447051	317050	222550	157849	4.50	879952	-189752	-108549	-234148	9.00	333954	738254	508546	112447
1.55	471051	979749	212250	441348	4.60	988552	-111552	-998848	-112748	9.10	285754	848754	-356346	105847
1.60	495051	144650	-201850	589548	4.70	109953	-136251	-909448	-112647	9.20	220554	964854	-225246	984946
1.65	519051	411950	-191450	151949	4.80	121053	-106352	819848	-720047	9.30	136154	108555	-113746	907146
1.70	542851	705250	-181150	235349	4.90	131953	-250452	731548	-138848	9.40	299453	120855	-204945	826946
1.75	566251	102551	-170950	309749	5.00	142353	-420952	646148	-191148	9.50	100354	-133255	-562545	-746446
1.80	589151	137451	-160950	375549	5.10	151853	-619952	564448	-230448	9.60	257354	-145355	-118046	-666946
1.85	611351	175251	-151150	433349	5.20	160153	-849252	487348	-258448	9.70	443454	-157055	-166546	-589746
1.90	632651	216151	-141550	483549	5.30	166753	-111053	415448	-276748	9.80	660854	-167755	-203246	-515946
1.95	652951	260151	-132150	526649	5.40	171053	-140553	349048	-286648	9.90	911854	-177255	-229546	-446146
2.00	671851	307451	-123050	563149	5.50	172653	-173453	288348	-289648	10.0	119855	-184855	-246946	-380946
2.05	689251	358151	-114250	593549	5.60	170753	-209753	233448	-286748					
2.10	704951	412251	-105750	618249	5.70	164553	-249453	184248	-279248					
2.15	718451	469851	-974849	637549	5.80	153453	-292453	140648	-268048					
2.20	729651	531151	-895849	652049	5.90	136453	-338553	102448	-254048					
2.25	738251	595951	-820049	662049	6.00	112753	-387353	692647	-238048					

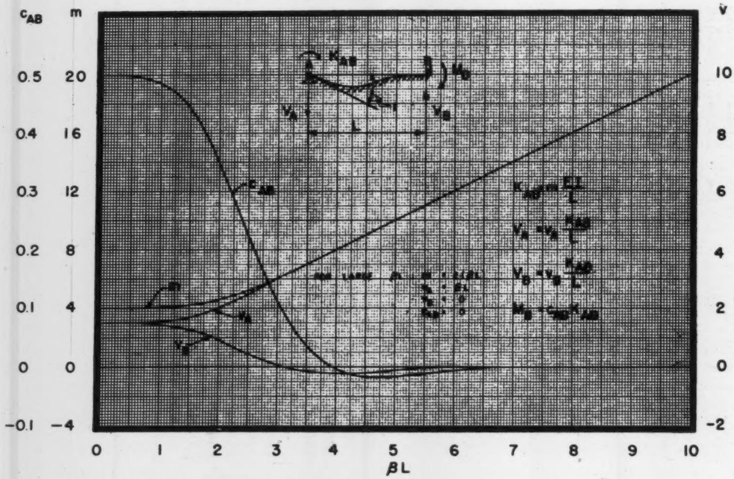

FIG. 4.—BEAM STIFFNESS IN ROTATION - FAR END FIXED

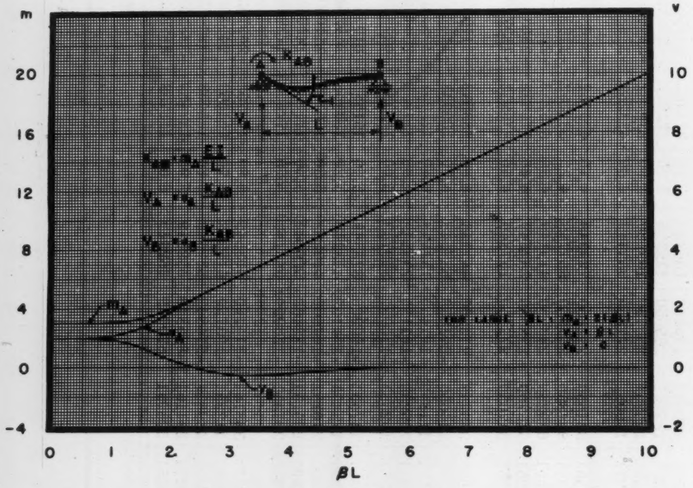

FIG. 5.—BEAM STIFFNESS IN ROTATION - FAR END HINGED

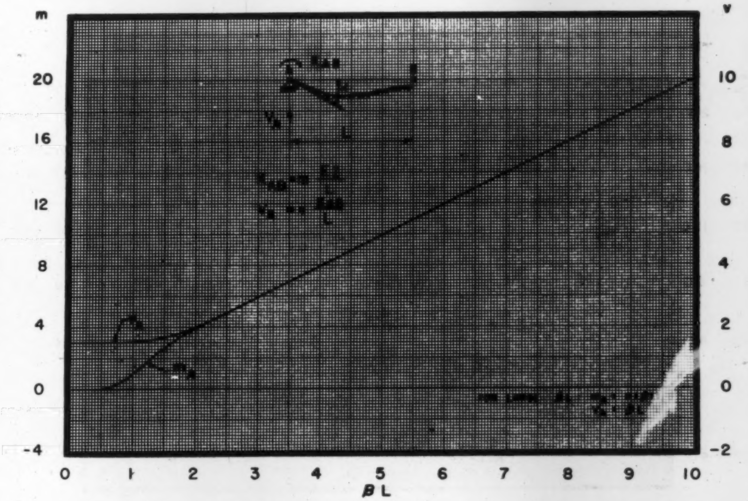

FIG. 6.—BEAM STIFFNESS IN ROTATION - FAR END FREE

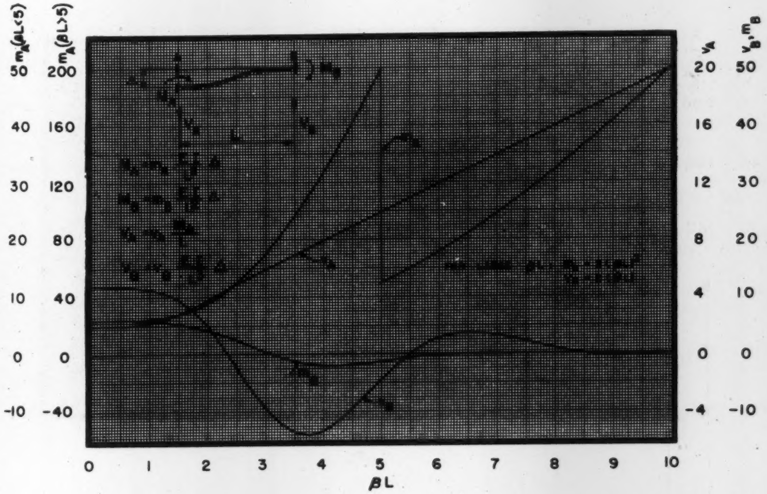

FIG. 7.—BEAM STIFFNESS IN TRANSLATION - FAR END FIXED

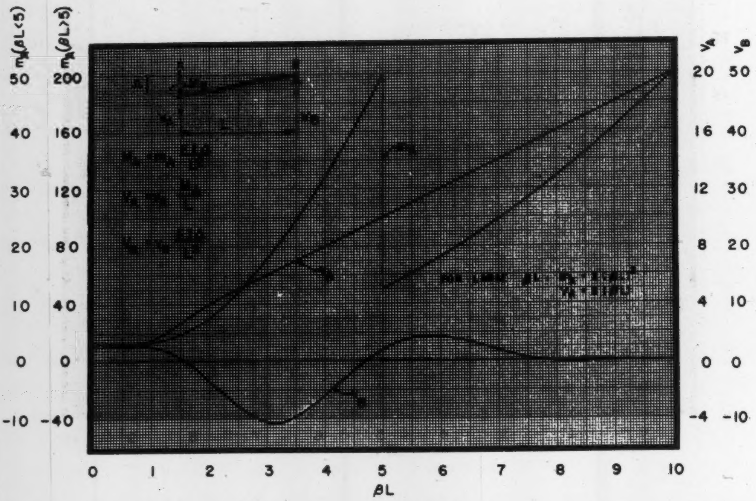

FIG. 8.—BEAM STIFFNESS IN TRANSLATION - FAR END HINGED

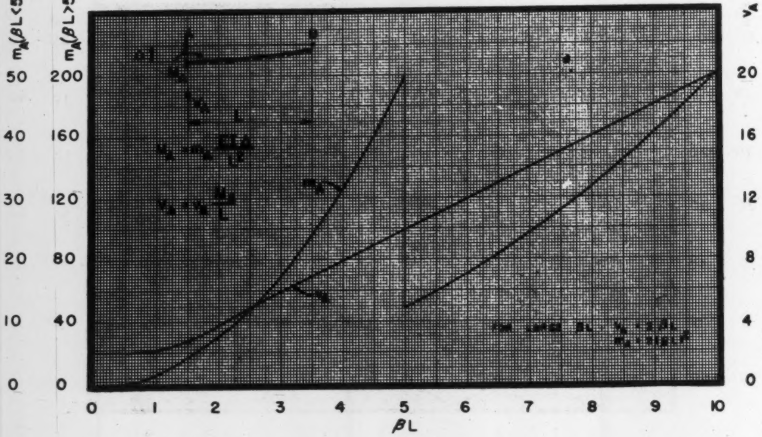

FIG. 9.—BEAM STIFFNESS IN TRANSLATION - FAR END FREE

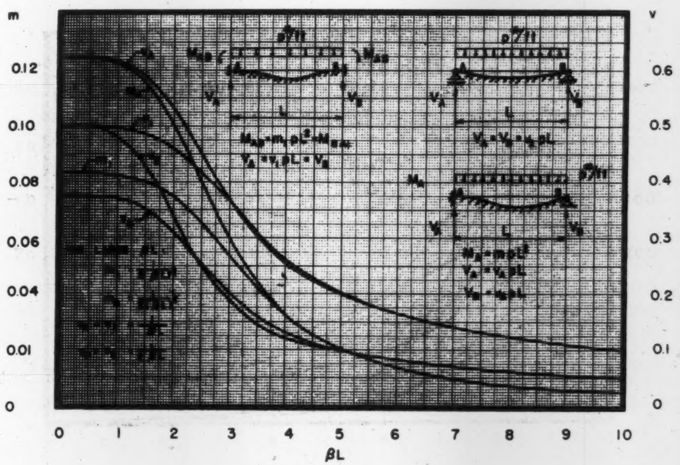

FIG. 10.—UNIFORMLY DISTRIBUTED LOADING - FIXED END MOMENTS AND REACTIONS

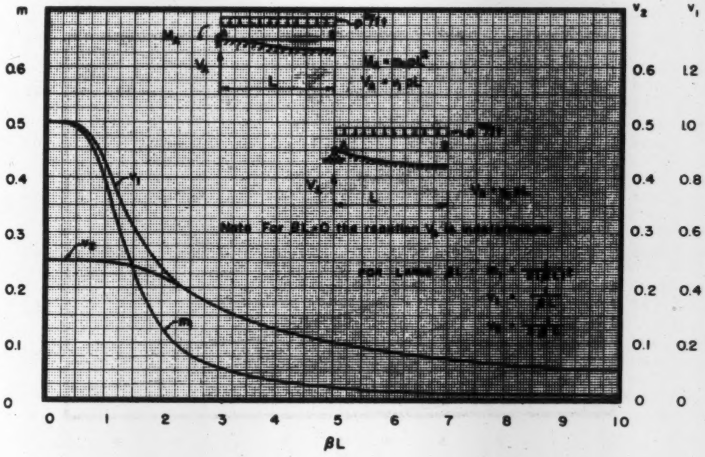

FIG. 11.—UNIFORMLY DISTRIBUTED LOADING - FIXED END MOMENTS AND REACTIONS - ONE END FREE

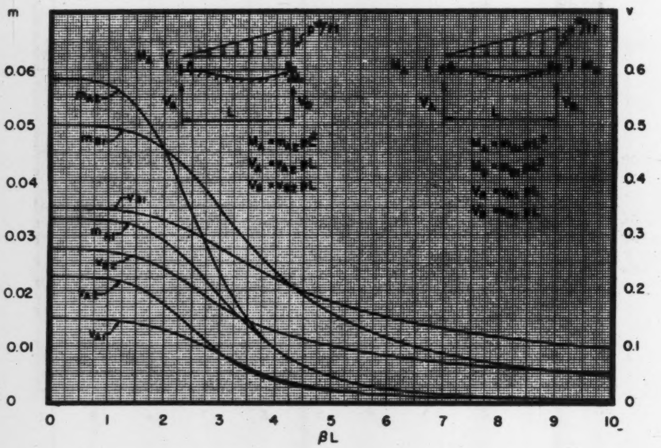

FIG. 12.—TRIANGULAR LOADING - FIXED END MOMENTS - AND REACTIONS

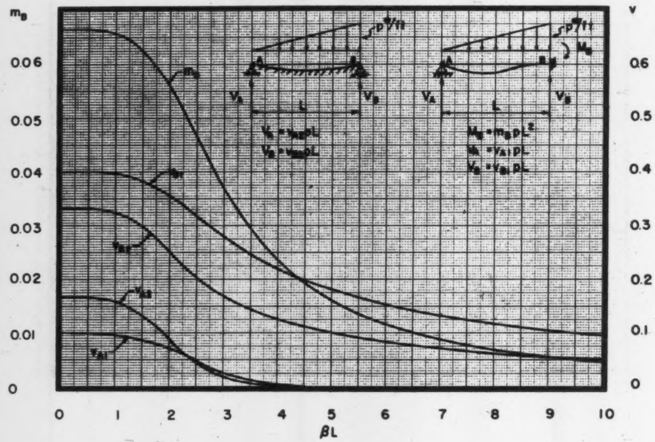

FIG. 13.—TRIANGULAR LOADING - FIXED END MOMENTS AND REACTIONS

Step No. 3.—The superposition equations are

$$0.947\ Y_B + 0.070\ Y_C = -\ \frac{160}{40}\ (0.0289)$$

and

$$0.070\ Y_B + 0.339\ Y_C = -\ \frac{80}{48}\ (0.0289)$$

from which $Y_B = -0.0928$ in. and $Y_C = - -.1225$ in.

Step No. 4.—The final end moments and shears are shown in Fig. 17. For segment B C Eqs. 9 become

$$\begin{Bmatrix} A \\ B \\ F \\ G \end{Bmatrix} = \begin{bmatrix} 0.000774 & 0.000667 & -0.0118 & 0.00261 \\ -0.000763 & -0.000324 & -0.000107 & -0.00248 \\ 0.0909 & 0.0386 & -0.0116 & 0.00756 \\ -0.0894 & -0.000324 & -0.000107 & -0.00247 \end{bmatrix} \begin{Bmatrix} 0.823 \\ -5.33 \\ 0.0303 \\ 4.07 \end{Bmatrix}$$

which leads to A = 0.0073 in., B = -0.0090 in., F = -0.101 in., and G = -0.0819 in.

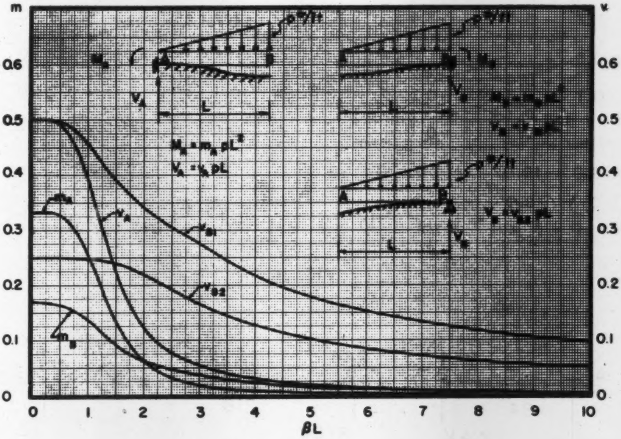

FIG. 14.—TRIANGULAR LOADING - FIXED END MOMENTS AND REACTIONS - ONE END FREE

Step No. 5.—The general equations for moment and deflection are shown in Fig. 18.

Example 2—The long cylindrical shell shown in Fig. 19 is held at a temperature T_1 in region A B and at a temperature T_2 in region C D. It is desireable to calculate the unit stresses in the transition region B C for a linear temperature change over this region. For purposes of analysis, stresses produced

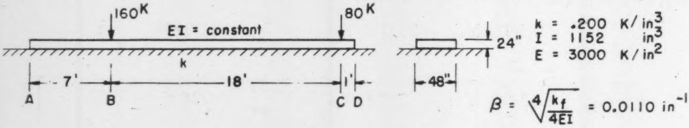

160^K
80^K
EI = constant
k
7'
18'
1'
A
B
C
D
24"
48"
k = .200 K/in^3
I = 1152 in^3
E = 3000 K/in^2

$$\beta = \sqrt[4]{\frac{k_f}{4EI}} = 0.0110 \text{ in}^{-1}$$

	βL	K		K/EI	C
BA	.925	.796	EI/L_{AB}	0.114	0
BC, CB	2.375	5.001	EI/L_{BC}	0.278	.258
CD	.132	.0005	EI/L_{CD}	0.0005	0

$\Sigma K_B = 0.392$ $\Sigma K_C = 0.278$

$DF_{BA} = 0.709$ $DF_{CB} = 0.998$

$DF_{BC} = 0.291$ $DF_{CD} = 0.002$

FIG. 15

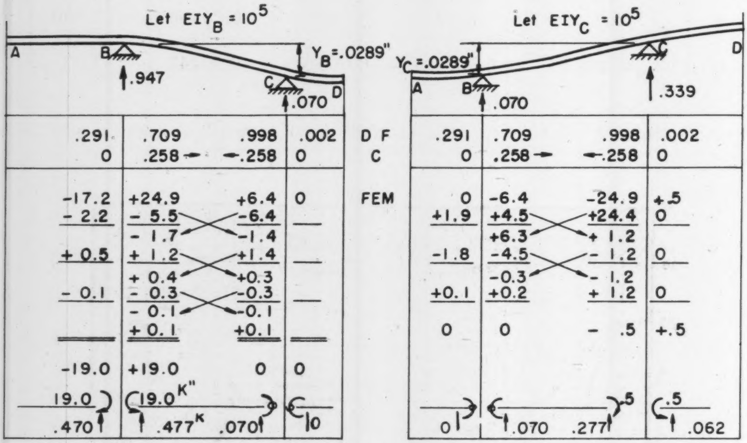

Let EIY_B = 10^5
A
B
C
D
Y_B = .0289"
.947
.070
.291
.709
.998
.002
0
.258
.258
0
-17.2
+24.9
+6.4
0
- 2.2
- 5.5
-6.4
- 1.7
-1.4
+ 0.5
+ 1.2
+1.4
+ 0.4
+0.3
- 0.1
- 0.3
-0.3
- 0.1
-0.1
+ 0.1
+0.1
-19.0
+19.0
0
0
19.0
19.0^K"
.470
.477^K
.070
0
D F
C
FEM
Let EIY_C = 10^5
Y_C = .0289"
A
B
C
D
.070
.339
.291
.709
.998
.002
0
.258
.258
0
0
-6.4
-24.9
+.5
+1.9
+4.5
+24.4
0
+6.3
+ 1.2
-1.8
-4.5
- 1.2
0
-0.3
- 1.2
+0.1
+0.2
+ 1.2
0
0
0
- .5
+.5
0
.070
.277
.5
.5
.062

FIG. 16

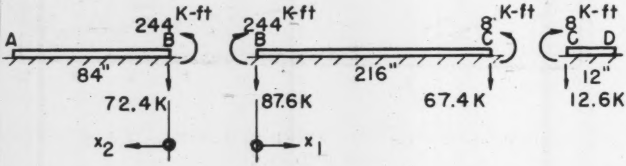

A
B
244^K-ft
244^K-ft
B
8^K-ft
C
8^K-ft
C
D
84"
216"
12"
72.4K
87.6K
67.4K
12.6K
x_2
x_1

FIG. 17

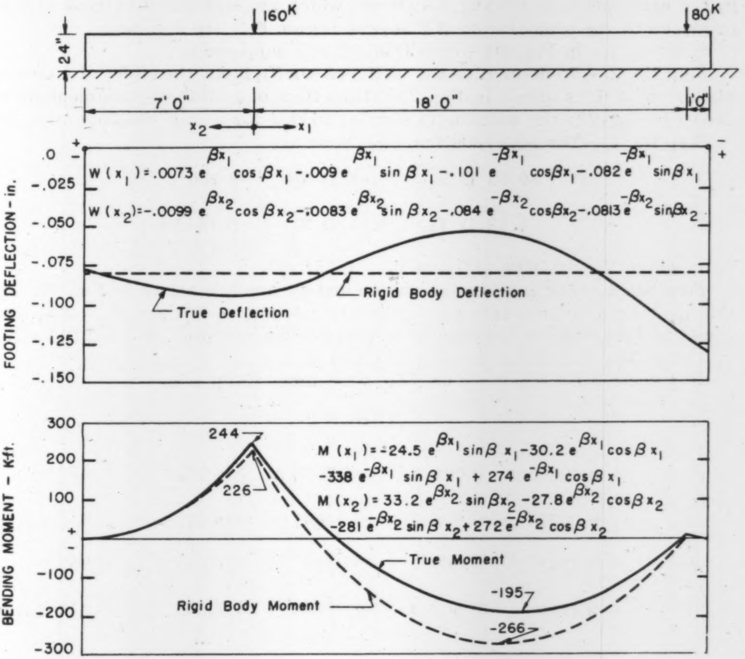

FIG. 18

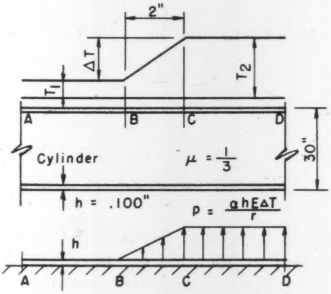
2"
ΔT
T1
T2
A
B
C
D
Cylinder
μ = 1/3
30"
h = .100"
p = αhEΔT/r
h
A
B
C
D

$$\beta = \sqrt[4]{\frac{3(1-\mu^2)}{r^2 h^2}} = 1.042$$

	βL	K^*	C
AB	Large	2.08 D (Fig. 6)	—
BC	2.08	2.32 D (Fig. 4)	.330 (Fig. 4)
CD	Large	2.08 D (Fig. 6)	—

*For Large βL $K = 2\beta D$

$\Sigma K_B = 4.40$ $\Sigma K_C = 4.40$

$DF_{BA} = .473$ $DF_{CB} = .527$

$DF_{BC} = .527$ $DF_{CD} = .473$

FIG. 19

by the axisymetrical loading, as shown, which are equivalent to those stresses produced by the temperature ΔT across region B C are obtained.

Step No. 1.—In Fig. 20, joints B and C are supported.

Step No. 2.—To determine the stiffness coefficients, the effect of a unit displacement at B is shown in Fig. 21. The effect of a unit displacement of C is shown in Fig. 22; the solution is similar to that for a unit displacement of B.

Step No. 3.—The superposition equations are

$$-9.13\ D\ Y_B + 0.42\ D\ Y_C = -0.186\ p$$

$$0.42\ D\ Y_B - 9.13\ D\ Y_C = -0.1640\ p$$

from which $Y_B = 0.0285\ p/D$ and $Y_C = 0.181\ p/I$.

Step No. 4.—The final end moments and shears are shown in Fig. 23. Since this problem is completely anti-symmetrical, $M_B = -M_C$ and $V_B = V_C$, therefore, the foregoing values should be adjusted as follows: $M_B = 0.052\ p$, $V_B = -0.014\ p$, $M_C = -0.052\ p$, and $V_C = -0.014\ p$.

For section B C ($\beta L = 2.08$), Eq. 9 becomes (Step 4(b))

TABLE 1

$$\begin{Bmatrix} A \\ B \\ F \\ G \end{Bmatrix} = \begin{bmatrix} 0.00273 & 0.00173 & -0.0206 & 0.00382 \\ -0.00327 & -0.00144 & 0.00641 & -0.00649 \\ 0.1248 & 0.0602 & -0.0334 & 0.01680 \\ -0.1189 & -0.00144 & 0.00641 & -0.00649 \end{bmatrix} \begin{Bmatrix} 0.052 \\ -0.014\ L_{BC} \\ -0.052 \\ -0.014\ L_{BC} \end{Bmatrix}$$

Find Maximum Stress at B and C.—Let ΔT represent 200 F, α equal 6.5×10^{-6} in. per in., h be 0.100 in., E equal 30×10^6 psi, and r represent 15 in. These lead to

$$p = \frac{2\ h\ E\ \Delta T}{r} = 260\ \text{psi}$$

$$M_B = -\ M_C = (0.052)\ (260) = 13.5\ \text{lb-in. per in.}$$

and

$$\sigma = \frac{6\ M}{h^2}\ 8100\ \text{psi.}$$

Example 3.—The cylinder shown in Fig. 24 has a recess between locations B and C, and is loaded axially on the recess collar at location C. In obtaining radial displacements, slopes, moments, and shears, a longitudinal strip of unit width is removed and placed on an elastic foundation whose stiffness equals

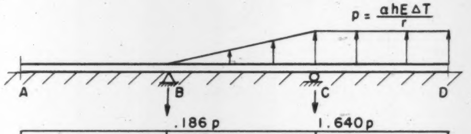

						Remarks
	.473	.527	.527	.473		DF ; Figs 4, 6
	0	.330	.330	0		C ; Fig. 4
0	0	-.114 p	+.180p	-.460p		FEM; Figs. 11, 12 (Step 1a)
	+.054	+.060	+.148	+.132		
		+.049	+.020			
	-.023	-.026	-.010	-.010		Iteration Procedure (Step 1b)
		-.003	-.009			
	+.001	+.002	+.005	+.004		
		+.002	+.001			
	-.001	-.001	-.001			
0	+.031p	-.031p	+.334p	-.334p	0	End Moments
	.031p .032p ↓	.031p ↓ .154p	.334p .811p ↓	.334p ↓ .829p		End Shears (Step 1c) Figs. 5, 6, 11, 12

FIG. 20

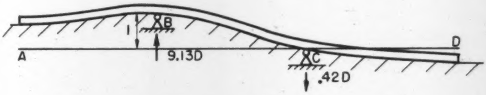

				Remarks
.473	.527	.527	.473	DF
0	.330	.330	0	C
-2.18 D	+2.40 D	+1.00 D	0	FEM; Fig. 7, 9 (Step 2a)
-0.11	-0.11	- .53	-.47	
	- .17	- .04		Iteration Procedure (Step 2b)
+ .08	+ .09	+ .02	+.02	
	+ .01	+ .03		
	- .01	- .02	-.01	
-2.21 D	+2.21 D	+ .46 D	-.46 D	End Moments
2.21 D A 4.57 D ↑	2.21 D B ↑ 4.56 D	.46 D C .06D ↑	.46 D D ↓ .48 D	End Shears (Step 2c) Figs. 5, 6, 7, 9

FIG. 21

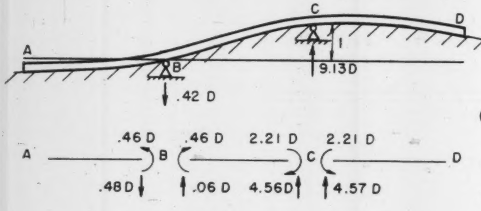
A
B
C
D
1
9.13D
.42 D
.46 D
.46 D
2.21 D
2.21 D
.48 D
.06 D
4.56D
4.57 D

(Step 2e)

$k_{BB} = +9.13D \quad k_{CB} = -.42D$

$k_{BC} = -\ .42D \quad k_{CC} = 9.13D$

$-9.13\,D\,Y_B + .42\,D\,Y_C = -\,.186p \qquad Y_B = +.0285\,\frac{p}{D}$

$+.42\,D\,Y_B - 9.13\,D\,Y_C = -1.640p \qquad Y_C = +.1810\,\frac{p}{D}$

FIG. 22

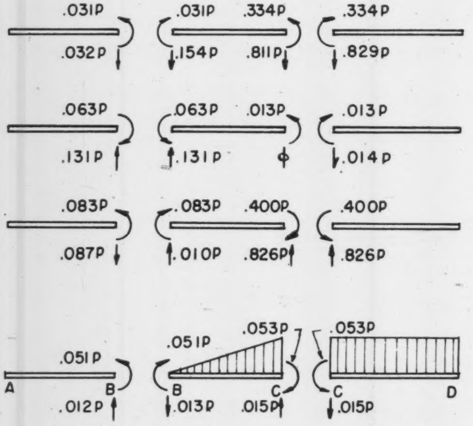
.031P
.031P
.334P
.334P
.032P
.154P
.811P
.829P
Step No. 1
.063P
.063P
.013P
.013P
.131P
.131P
ϕ
.014P
.0285 P/D (Step No. 2a)
.083P
.083P
.400P
.400P
.087P
.010P
.826P
.826P
.181 P/D (Step No. 2b)
.051P
.051P
.053P
.053P
A
B
B
C
C
D
.012P
.013P
.015P
.015P
Final End Moments And Shears Equal Sum of Above Three Cases. (Step 4a)

FIG. 23

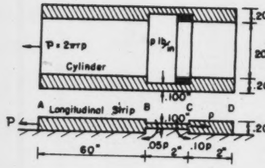
P = 2πrp
p lb/in
Cylinder
.200"
20"
.200"
.100"
A
Longitudinal Strip
B
C
D
P
.100"
p
.200"
60"
.05p
2"
.10p
2"

	t	L	r	β	βL	D	K	C
AB	.200	60	10	.901	54.00	$8D_b$	$14.40D_b$	-
BC	.100	2	10	1.275	2.55	D_b	$2.65D_b$	.21
CD	.200	2	10	.901	1.80	$8D_b$	$13.80D_b$	-

$K_B = 17.05 \quad DF_{BA} = .845 \quad DF_{BC} = .155$

$K_C = 16.45 \quad DF_{CB} = .161 \quad DF_{CD} = .839$

$\mu = 1/3$

FIG. 24

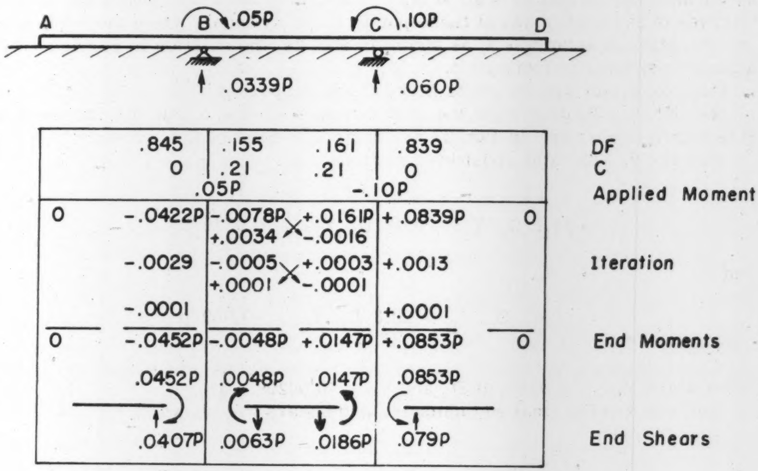

	.845	.155	.161	.839		DF
	0	.21	.21	0		C
		.05P	-.10P			Applied Moment
0	-.0422P	-.0078P +.0034	+.0161P -.0016	+.0839P	0	
	-.0029	-.0005 +.0001	+.0003 -.0001	+.0013		Iteration
	-.0001			+.0001		
0	-.0452P	-.0048P	+.0147P	+.0853P	0	End Moments
	.0452P	.0048P	.0147P	.0853P		
	.0407P	.0063P	.0186P	.079P		End Shears

FIG. 25

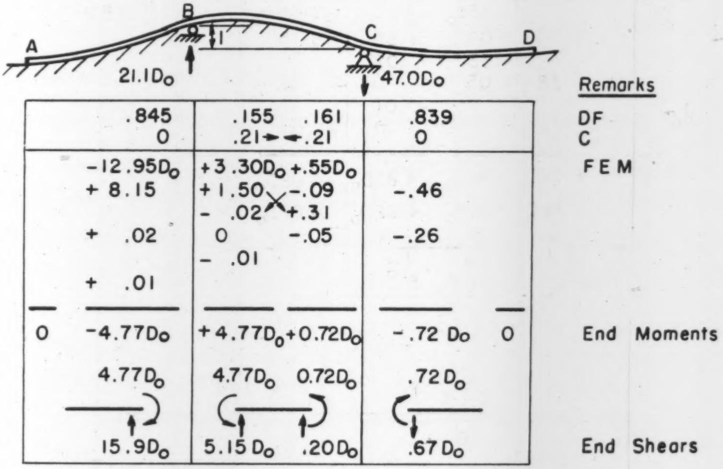

						Remarks
	.845	.155	.161	.839		DF
	0	.21 →	← .21	0		C
	$-12.95D_o$	$+3.30D_o$	$+.55D_o$			FEM
	+8.15	+1.50 - .02	-.09 +.31	-.46		
	+ .02	0 - .01	-.05	-.26		
	+ .01					
0	$-4.77D_o$	$+4.77D_o$	$+0.72D_o$	$-.72\ D_o$	0	End Moments
	$4.77D_o$	$4.77D_o$	$0.72D_o$	$.72D_o$		
	$15.9D_o$	$5.15\ D_o$	$.20D_o$	$.67D_o$		End Shears

FIG. 26

the hoop stiffness of the cylinder. In this solution, the axis of all segments of the strip are assumed to coincide; therefore, it is necessary to load the strip with concentrated moments at points B and C in order to account for the eccentricities of the axial loads at these points in the cylinder. Once the loading on the unit strip is established, as shown in Fig. 24, the solution is carried out in a manner similar to Example 1.

Step No. 1.—In Fig. 25 joints B and C are supported.

Step No. 2.—To determine the stiffness coefficients, a unit displacement of B is shown in Fig. 26. In Fig. 27 a unit displacement of C is shown.

Step No. 3.—The superposition equations are

$$21.1\ D_o\ Y_B - 0.48\ D_o\ Y_C = -0.0339\ p$$

and

$$-0.47\ D_o\ Y_B + 20.3\ D_o\ Y_C = -0.060\ p$$

from which $Y_B = -0.00167\ p/D_o$ and $Y_C = -0.00299\ p/D_o$.

Step No. 4.—The final end moments and shears are shown in Fig. 28.

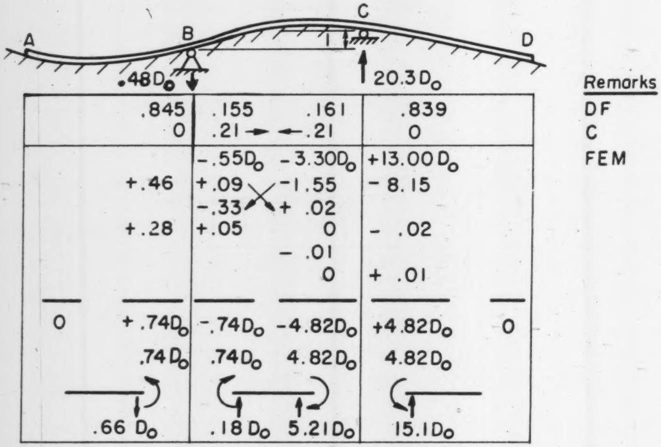
A
B
C
D
1
.48D₀
20.3D₀
Remarks
DF
C
FEM
.845
0
.155
.21
.161
.21
.839
0
-.55D₀
-3.30D₀
+13.00D₀
+.46
+.09
-1.55
-8.15
-.33
+.02
+.28
+.05
0
-.02
-.01
0
+.01
0
+.74D₀
-.74D₀
-4.82D₀
+4.82D₀
0
.74D₀
.74D₀
4.82D₀
4.82D₀
.66 D₀
.18 D₀
5.21D₀
15.1D₀

FIG. 27

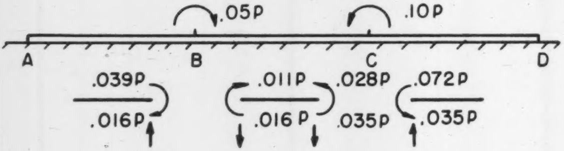
.05P
.10P
A
B
C
D
.039P
.016P
.011P
.016 P
.028P
.035P
.072P
.035P

FIG. 28

TABLES

The location of the decimal points in Tables 1 and 2 is given by subtracting 50 from the last two digits of each tabular value. If this difference is zero the decimal point is located in front of the first digit of the number. However, if the difference is +n, the decimal is moved n digits to the right and if the difference is -n, the decimal is moved n digits to the left. For example, the tabular value -1555446 is equal to -.00001555 and the tabular value 358151 is equal to 3.581.

FIGURES

In all figures the flexural rigidity term E I (for beams) should be replaced by the flexural rigidity D when applying to plates.

ACKNOWLEDGMENTS

The author wishes to express his appreciation to the Ernest O. Lawrence Radiation Laboratory, Livermore, Calif. for the assistance provided in carrying out the digital computer work required for this paper and also for the assistance provided in preparing the tables and figures included herein.

APPENDIX I.—ADDITIONAL REFERENCES

---

1. "Beams on Elastic Foundation," by M. Hetinyi, The Univ. of Michigan Press, Ann Arbor, Mich., 1946.
2. "Analysis of Finite Beams on Elastic Foundations," by D. C. Gazis. *Proceedings* ASCE, No. ST 4, July, 1958.
3. "Influence Lines for Pressure Distribution Under a Finite Beam on Elastic Foundation," by K. C. Ray, *Journal*, A. C. I., December, 1958.
4. "Analysis of Continuous Conical Shells of Rotational Symmetry by Method of Successive Approximations," by G. Oravas. Internatl. Assn. for Bridge and Structural Engrg. Publications, Vol. 14, 1954, p. 195.

APPENDIX II.—NOTATION

A, B, F, G = Constants of integration;
C = carry over factor;
$D = Eh^3/12(1 - \mu^2)$ = flexural rigidity of cylinder per unit width;
DF = distribution factor;
E = Young's modulus;
$e = 2.718$ = Naperian base;
FEM = fixed-end moment;

h = cylinder wall thickness;
I = moment of inertia of beam;
K = stiffness factor;
k = stiffness influence coefficient;
k_f = foundation stiffness;
L = length of beam or cylinder segment;
M = moment per unit width of cylinder; beam moment;
p = radial loading per unit area for cylinder; load per unit length for beam;
r = cylinder radius;
T = temperature;
V = shear per unit width for cylinder; beam shear;
x = longitudinal distance along beam or cylinder from discontinuity point;
w = radial displacement of cylinder wall; beam deflection;
w_p, w_p', w_p'', w_p''' = particular solution to differential equation and its derivatives;
α = coefficient of thermal expansion;
θ = slope of cylinder wall relative to axis; beam slope;
μ = Poisson's ratio;

$$\beta = \sqrt[4]{\frac{3(1-\mu^2)}{r^2 h^2}}$$ = for cylinder; and

$$\beta = \sqrt[4]{\frac{k_f}{4 E I}}$$ = for beam.

DISCUSSION

R. S. ALWAR.[4]—An interesting iterative procedure for the evaluation of stresses in beams on elastic foundations with discontinuous loadings has been suggested.

If the differential equation for the deflection curve of the beam on an elastic foundation is solved by the classical method, the number of simultaneous equations to be dealt with would be 4 n, where n is the number of discontinuities in loading. This, as the author himself has pointed out, is quite cumbersome. It is rather unfortunate that Penzien has not mentioned in his introduction the existence and utility of the operational methods in solving such discontinuity problems. With this method, the number of simultaneous equations to be dealt with is only two, whatever the number of discontinuities. A paper on the application of the operational method to simple beam problems by William T. Thompson is available.[5] Recently the writer[6] applied the operational technique to problems of beams on elastic foundations in which beams with arbitrary discontinuous loading was also considered.

---

[4] Research Fellow, Civ. and Hydr. Engrg. Sect., Indian Inst. of Science, Bangalore-12, India.

[5] Journal of the Franklin Inst., 1949.

[6] "Solution of Problems in Beams on Elastic Foundations by the Method of LaPlace Transformation," by R. S. Alwar, Journal, Institution of Engineers, India, Vol. XL, No. 12, Part 1, August, 1960.

By applying the Laplace transformation, the ordinary differential equation is reduced to a simpler form, usually a linear algebraic equation. This simple equation is then solved for a transition function from which the desired solution to the original differential equation is obtained by the use of inverse Laplace transforms.

In addition the load functions that are used in the transformation method provide, in the case of beams with arbitrary discontinuous loading, a very convenient tool for arriving at the solution, in a continuous form, and in a single process, for deflection, moment, and foundation reaction at any point in the beam.

There is one more point of particular interest and that is in contrast to the 4 n simultaneous equations, involved in the classical method, which Penzien has referred to, this method needs the solution of only two simultaneous equations, whatever the number of discontinuities.

JOSEPH PENZIEN,[5] M. ASCE.—The Laplace transform method of solving differential equations is, of course, well known and has many advantages in solving certain types of initial-value problems. However if all initial values are not known, this method can become rather cumbersome.

The great advantage derived from using the unit step function, the impulse function, and the unit doublet when dealing with discontinuous functions is also well known and is discussed in many of our modern day textbooks.

As pointed out by Alwar, these techniques can be used to solve the problem of a beam on an elastic foundation having a discontinuous loading. The advantages and disadvantages of this method over that suggested by the author are subject to one's own personal preference that is influenced a great deal by one's background. No doubt, a person having a great deal of experience using Laplace transforms would prefer the Laplace transform approach to this problem. However, a person unfamiliar with Laplace transform methods but experienced with moment-distribution techniques would prefer the writer's suggested approach.

It might be well to point out that for many beams on elastic foundations, the interaction from one discontinuity point to adjacent discontinuity points is negligible. Thus, the problem can be reduced to one having a single discontinuity that does not require iteration. Problems of this type are extremely simple to solve using the basic data presented by the author.

The basic data presented in curve form in the original paper have been made available in tabular form. These data are tabulated for values of β L at very close intervals and are accurate to four significant figures, thus greatly aiding in obtaining accurate solutions. These tables can be obtained from the writer.

---

[5] Assoc. Prof. of Civ. Engrg., Univ. of California, Berkeley, Calif.

AMERICAN SOCIETY OF CIVIL ENGINEERS
Founded November 5, 1852
TRANSACTIONS

Paper No. 3262

GENERALIZATION OF THE SUCCESSIVE APPROXIMATIONS METHOD

By Panagiotis D. Moliotis,[1] M. ASCE

With Discussion by Messrs. Pering-Fei Gou; and Panagiotis D. Moliotis

SYNOPSIS

This study concerns the analysis of rigid frames, whose joints are not just points but small undeformed areas, by the method of successive approximations.

INTRODUCTION

The stresses in the members of a framework are usually computed with the assumption that the connections between members are points to which they meet and are connected together by rigid or pinned joints.

In reality, however, joints are small areas to which the various members of a framework are connected.

Fig. 1(a) shows a typical rigid joint k, in which k is not in reality a point but the shaded area aa' - bb'. Consider this area as suffering no deformation, because the moments of inertia in the directions 1-1 and 2-2 are large compared with those of the sections of members 1-1 and 2-2. In the case of reinforced concrete structures, after computing the bending moments of the various members meeting at joint k, the bending moments are determined at the sections of the faces aa', bb', ab, and a'b'. From these values, the required dimensions of the sections and reinforcement of the members are obtained. Thus, the area of joint k suffers no deformation.

In Fig. 1(b), the joint k is the wall of reservoir. In this case, due to the dimensions of the wall, joint k can safely be considered as an area suffering no deformation.

Note.—Published essentially as printed here, in October, 1958, in the Journal of the Structural Division, as Proceedings Paper 1816. Positions and titles given are those in effect when the paper or discussion was approved for publication in Transactions.

[1] Dir. Civ. Engrg., National Technical Univ., Athens, Greece.

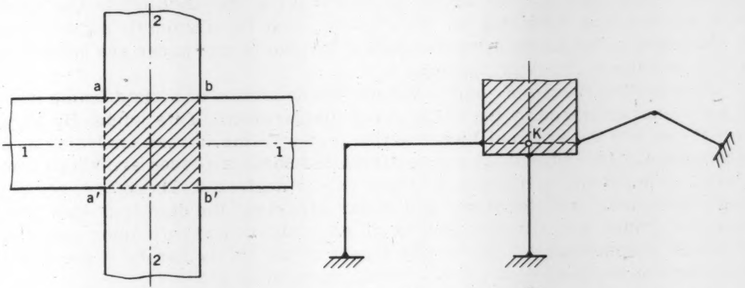

(a) (b)

FIG. 1

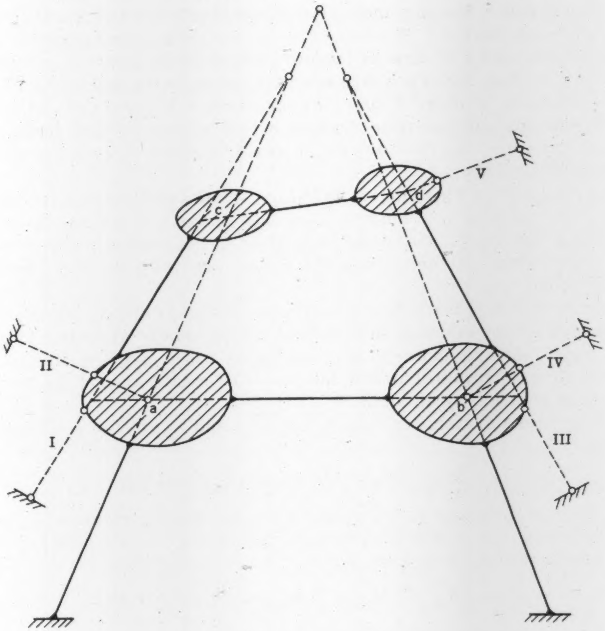
c
d
V
II
a
I
IV
b
III

FIG. 2

The stress analysis of rigid frames with straight members, can be made by the successive approximation method making the assumption that joints are small areas suffering no deformation, that is, absolutely rigid bodies.

Notation.—The letter symbols adopted for use in this paper are assembled for convenience of use in Appendix II.

Elastic Movement of Frame.—The elastic deflection of a rigid frame under load is characterized by the rotation and displacement of its joints. By knowing these and the external forces acting on the frame, stress analysis can be performed. Also deflections due to direct and shear stresses are small compared to those due to bending, and they can be neglected. Therefore, neglecting deflections due to direct and shear stresses, the displacements of the various joints are not independent of each other, and by making use of the "virtual displacement," the displacement of all joints can be expressed as functions of the displacement of a certain number of joints.

If a rigid frame is converted into a pin-jointed frame by replacing rigid joints by pinned ones, the resulting formation will, as a rule, be capable of suffering geometrical displacement. This resulting formation can be made a just-stiff frame by the addition of a certain number of pin-jointed bars (roller restraints), as seen in Fig. 2. The number of bars required for this purpose gives the degree of the elastic freedom of the original rigid frame.

Sign Convention.—Bending moments at sections by the joints are considered positive when clockwise.[2] Shearing forces are considered positive when the shearing couple tends to turn an infinite portion of the beam clockwise. Normal forces are considered positive when they produce tension to the members.

Stress Analysis of Rigid Frames by the Method of Successive Approximations.—Stress analysis of rigid frames of the classical case (joints-points) is carried out either in two[3] or one stages.[2] The new factors for both cases are given subsequently.

Stress Analysis in Two Stages. 1st Stage.—It is assumed that the joints are not deflected and that the bending moments shear and normal forces acting on the joints are those of a member built-in at both ends. The new distribuion and carry-over factors, when the joints are not allowed to deflect are then determined.

Reactions on Joints When Fixed.—Assume that all joints are fixed and therefore, rotation is not allowed. In this case, all members are built-in at either end and exert bending moment $\overline{M}_{ai}$, shearing force $\overline{Q}_{ai}$, and normal forces, $\overline{N}_{ai}$. Due to these systems of forces, the joint will rotate around the instantaneous center of rotation by an angle θ_a (Fig. 3).

Replacing these systems of forces $\overline{M}_{ai}$, $\overline{Q}_{ai}$, and $\overline{N}_{ai}$ by the equivalent ones, results in

$$\overline{M}'_{ai} = \overline{M}_{ai} + \overline{Q}_{ai}\ d_{ai} \qquad \overline{Q}_{ai} \text{ and } \overline{N}_{ai} \quad \dots\dots\dots\dots (1)$$

It is obvious that joint a will suffer the same elastic rotation θ_a by either of the preceding two systems of forces. Therefore, in this case, the bending moment which acts on joint a is

$$\overline{M}'_a = \Sigma\, \overline{M}'_{ai} = \Sigma\, \overline{M}_{ai} + \Sigma\, Q_{ai}\ d_{ai} + M_a \quad \dots\dots\dots (2)$$

in which M_a represents any existing external couple on the joint.

---

[2] "A General Method of Analysis of Rigid Frames," by Panagiotis D. Moliotis, Transactions, ASCE, Vol. 122, 1957, p. 850.

[3] "Continuous Frames of Reinforced Concrete," by Hardy Cross and Newlin Morgan, New York, 1949.

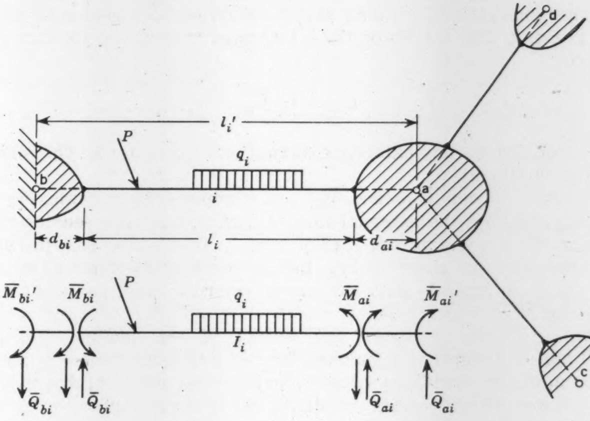
d
l_i'
P
q_i
b
a
i
d_{bi}
l_i
d_{ai}
$\overline{M}_{bi}'$
$\overline{M}_{bi}$
P
q_i
$\overline{M}_{ai}$
$\overline{M}_{ai}'$
I_i
c
$\overline{Q}_{bi}$
$\overline{Q}_{bi}$
$\overline{Q}_{ai}$
$\overline{Q}_{ai}$

FIG. 3

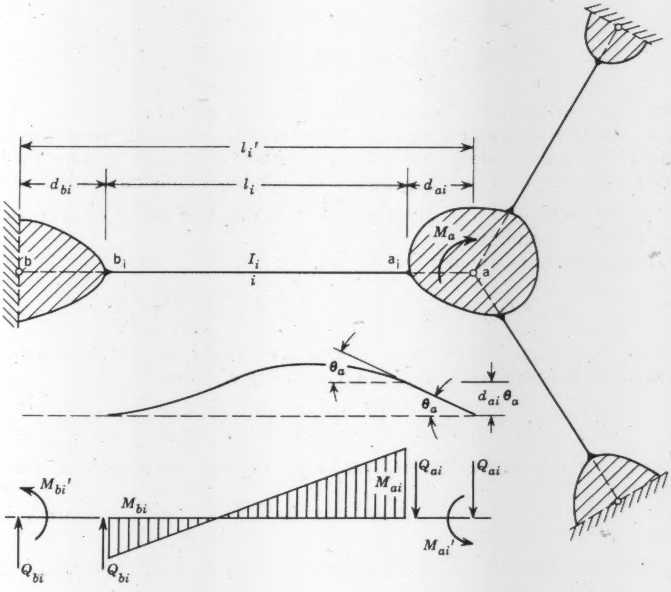
l_i'
d_{bi}
l_i
d_{ai}
M_a
b
b_i
I_i
a_i
a
i
θ_a
θ_a
$d_{ai}\,\theta_a$
M_{bi}'
M_{bi}
M_{ai}
Q_{ai}
Q_{ai}
M_{ai}'
Q_{bi}
Q_{bi}

FIG. 4

The fixing moment of joint a is equal and opposite to $\overline{M}'_a$ acting on joint a, as computed in Eq. 2. The forces on the joints used to compute the fixing forces F_1^o . . . . are

$$\overline{P}_a = \Sigma_i \overline{Q}_{ki} + \Sigma_i \overline{N}_{ki} + P_a \quad \dots\dots\dots\dots\dots \quad (3)$$

in which P_a represents any existing external force on joint a. The summation in Eq. 3 is geometrical.

The shearing forces $\overline{Q}_{ai}$ and $\overline{Q}_{bi}$ are computed by considering bending moments $\overline{M}_{ai}$ and $\overline{M}_{bi}$, the external load of span l_i, and also bending moments $\overline{M}'_{ai}$, $\overline{M}'_{bi}$ and the same external load of span l'_i. In other words, the shearing forces of the built-in span l_i are taken as being the same as those of an imaginary built-in span l'_i with the same external load, and end fixing moments $\overline{M}'_{ai}$ and $\overline{M}'_{bi}$ (Fig. 3).

Distribution Factors.—Under the action of the bending moment M_a, joint a will suffer a rotation θ_a around the instantaneous center of rotation a. The section a_i of any member i will turn through and angle θ_a due to the rotation of joint a and will therefore be displaced at right angles to its axis by a distance $\theta_a \times d_{ai}$ (Fig. 4). The section b_i will suffer no rotation or displacement because joint b remains fixed.

Bending moments are given by

$$M_{ai} = \left(a_{ai} + u_{bi} \frac{d_{ai}}{l_i}\right) \theta_a \quad \dots\dots\dots\dots\dots \quad (4a)$$

and

$$M_{bi} = \left(\mu_i \; a_{ai} + u_{bi} \frac{d_{ai}}{l_i}\right) \theta_a \quad \dots\dots\dots\dots\dots \quad (4b)$$

in which a_{ai} represents the bending moment which should be applied on section a_i to obtain rotation of it equal to unity, that is, the factor of stiffness to rotation of member i, μ_i denotes the carry-over factor of member i for the rotation of the section only, and u_{ai}, u_{bi} are the bending moments at the sections a_i and b_i of member i for a ration $\frac{\theta_{ai}}{l_i} = 1$, that is, "factor of stiffness to displacement" of member i.[2]

Shearing forces are given by

$$Q_{ai} = Q_{bi} = \left[a_{ai} \left(1 + \mu_i\right) + \left(u_{ai} + u_{bi}\right) \frac{d_{ai}}{l_i}\right] \frac{\theta a}{l_i} \quad \dots\dots \quad (5)$$

Joint a is in equilibrium under bending moments M_{ai}, M_a and shearing forces Q_{ai}. Bending moment, M'_{ai} is given by the equation

$$M'_{ai} = M_{ai} + Q_{ai} \; d_{ai} \quad \dots\dots\dots\dots\dots \quad (6)$$

If in Eq. 6 the values for M_{ai} and Q_{ai} are replaced from Eqs. 4 and 5,

$$M'_{ai} = b_{ai} \; \theta_a \quad \dots\dots\dots\dots\dots\dots \quad (7)$$

in which

$$b_{ai} = a_{ai} \left[1 + \left(1 + \mu_i\right) \frac{d_{ai}}{l_i}\right] + u_{ai} \frac{d_{ai}}{l_i} \left(1 + \frac{d_{ai}}{l_i}\right) + u_{bi} \left(\frac{d_{ai}}{l_i}\right)^2 \quad \dots \quad (8)$$

The equilibrium of joint a is expressed by

$$M_a + \Sigma M'_{ai} = 0 \quad \dots\dots\dots\dots (9)$$

and by replacing the values for M'_{ai} from Eq. 7

$$\theta_a = \left(-M_a\right) \frac{1}{\Sigma b_{ai}} \quad \dots\dots\dots\dots (10)$$

From Eqs. 7 and 10

$$M'_{ai} = (-M)\,k_{ai} \quad \dots\dots\dots\dots (11)$$

in which

$$k_{ai} = \frac{b_{ai}}{\Sigma b_{ai}} \quad \dots\dots\dots\dots (12a)$$

The factor k_{ai} is the new "factor of distribution" for the case of rigid frames examined. The factor b_{ai} is the new index of stiffness of the member and Σb_{ai} is the new index of stiffness of joint a. If in Eq. 9 the value for M'_{ai} is replaced from Eq. 11,

$$\Sigma k_{ai} = +1 \quad \dots\dots\dots\dots (12b)$$

Special Cases - Straight Members With Constant Moments of Inertia.—The factors b_{ai} for the case of straight members of constant moment of inertia have the following values:

(a) Member built-in at both ends

$$a_{ai} = \frac{4\,E\,I_i}{l_i},\ \mu_i = +\frac{1}{2},\ u_{ai} = u_{bi} = \frac{6\,E\,I_i}{l_i} \quad \dots\dots\dots\dots (13a)$$

and

$$b_{ai} = \frac{4\,E\,I_i}{l_i}\left[1 + 3\,\frac{d_{ai}}{l_i} + 3\left(\frac{d_{ai}}{l_i}\right)^2\right] \quad \dots\dots\dots\dots (13b)$$

(b) Member built-in at one end - Pin joint at section b_i (Fig. 5)

$$a_{ai} = \frac{3\,E\,I_i}{l_i} \quad \mu_i = 0 \quad u_{ai} = \frac{3\,E\,I_i}{l_i} \quad u_{bi} = 0 \quad \dots\dots\dots\dots (14a)$$

and

$$b_{ai} = \frac{3\,E\,I_i}{l_i}\left[1 + 2\,\frac{d_{ai}}{l_i} + \left(\frac{d_{ai}}{l_i}\right)^2\right] \quad \dots\dots\dots\dots (14b)$$

(c) Member built-in at one end - Pin joint at section a_i (Fig. 5)

$$a_{ai} = 0 \quad \mu_i = 0 \quad u_{ai} = 0 \quad u_{bi} = \frac{3\,E\,I_i}{l_i} \quad \dots\dots\dots\dots (15a)$$

and

$$b_{ai} = \frac{3\,E\,I_i}{l_i}\left(\frac{d_{ai}}{l_i}\right)^2 \quad \dots\dots\dots\dots (15b)$$

Carry-Over Factors.—The bending moment M'_{ai} is expressed in terms of the computed bending moment M'_{ai}

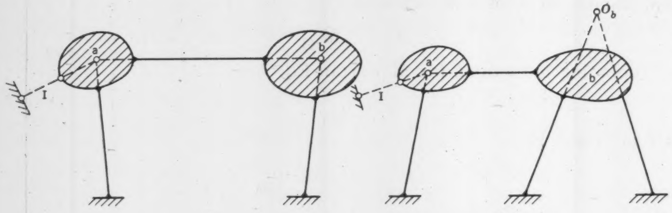

(a) (b)

FIG. 5

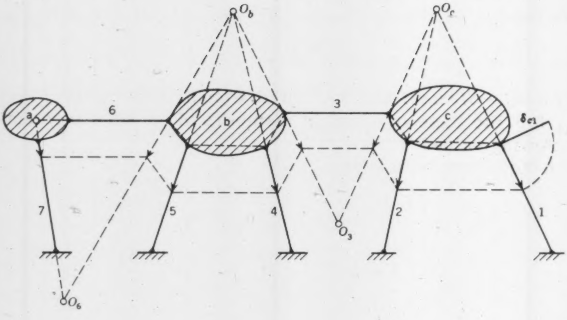
O_b
O_c
a
6
b
3
c
δ_{c1}
7
5
4
O_3
2
1
O_6

FIG. 6

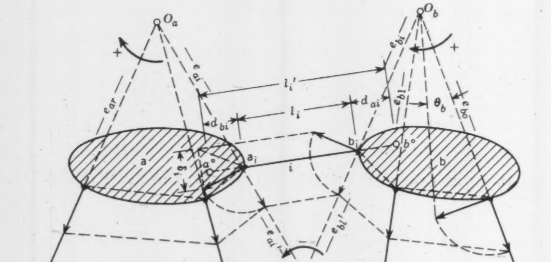
O_a
+
e_{ar}
e_{ai}
l_i'
l_i
d_{bi}
d_{ai}
O_b
+
e_{bi}
e_{bl}
θ_b
e_{b0}
a
a°
a_i
g_i
i
b_i
b°
b
e_{ai}
e_{bl}'
O_i
r
1
0

FIG. 7

$$M'_{bi} = M_{bi} + Q_{bi}\, d_{bi} \tag{16}$$

and by replacing the values for M_{bi} and Q_{bi} from Eqs. 4 and 5

$$M'_{bi} = \left(\mu_i\, a_{ai} + u_{bi}\,\frac{d_{ai}}{l_i}\right)\theta_a + \left[a_{ai}\left(1 + \mu_i\right) + \left(u_{ai} + u_{bi}\right)\frac{d_{ai}}{l_i}\right]\frac{d_{bi}}{l_i}\,\theta_a \tag{17}$$

and replacing the value for the angle θ_a result in

$$M'_{bi} = \mu_{ab}\; M'_{ai} \tag{18}$$

in which

$$\mu_{ab} = \frac{a_{ai}\left[\mu_i + \left(1 + \mu_i\right)\dfrac{d_{bi}}{l_i}\right] + u_{ai}\,\dfrac{d_{ai}}{l_i}\,\dfrac{d_{bi}}{l_i} + u_{bi}\left(1 + \dfrac{d_{bi}}{l_i}\right)\dfrac{d_{ai}}{l_i}}{b_{ai}} \tag{19}$$

which gives the required carry-over factor of member i from joint a to joint b.

Special Cases - Straight Members with Constant Moments of Inertia.—

(a) Member built-in at both ends

$$\mu_{ab} = \frac{1}{2}\;\frac{1 + 3\,\dfrac{d_{ai} + d_{bi}}{l_i} + 6\,\dfrac{d_{ai}\;d_{bi}}{l_i^{\,2}}}{1 + 3\,\dfrac{d_{ai}}{l_i} + 3\left(\dfrac{d_{ai}}{l_i}\right)^2} \tag{20}$$

(b) Member built-in at one end. Pin joint at section b_i

$$\mu_{ab} = \frac{\dfrac{d_{bi}}{l_i}\left(1 + \dfrac{d_{ai}}{l_i}\right)}{1 + 2\,\dfrac{d_{ai}}{l_i} + \left(\dfrac{d_{ai}}{l_i}\right)^2} \tag{21}$$

(c) Member built-in at one end. Pin-joints at section a_i

$$\mu_{ab} = \frac{1 + \dfrac{d_{bi}}{l_i}}{\dfrac{d_{ai}}{l_i}} \tag{22}$$

Computation of Bending Moments M'_{ai}.—The bending moments M'_{ai} of the rigid frame are computed by successive approximation as in the classical case.

For the computation of bending moments M_{ai}, the shearing forces Q_{ai} are first determined. These are obtained from

$$Q_{ai} = Q^{\circ}_{ai} + \frac{M'_{ai} + M_{bi}}{l_i} \tag{23}$$

in which Q°_{ai} is the shearing force for the freely supported span l_i. Having obtained the value of shearing force Q_{ai}, bending moments M_{ai} are computed from

$$M_{ai} = M'_{ai} - Q_{ai}\ d_{ai} \qquad (24)$$

In Eq. 24, bending moment M_{ai} and shearing force Q_{ai} are entered with their appropriate signs.

Second Stage.—Having computed the bending moments M'_{ai} of the 1st stage, the shearing and normal forces Q_{ai} and N_{ai} are determined. With these values and any other existing external forces on the joints, the fixing forces F of the 1st stage are computed. The stress condition of the 2nd stage is the stress condition of the rigid frame acted on by the forces on the joints Q_{ai}, N_{ai} and P_a or by an equivalent loading by forces Z equal and opposite to the fixing forces F of the 1st stage.

All the joints or members of the frame will be displaced together should only one roller restraint be removed.[2] These joints and members are called "group of condisplaced joints" and "group of condisplaced members." Number each roller restraint by I, II, III . . . .

The solution of the 2nd stage in the classical case of frame is obtained by computing the "partial stress condition" of the frame of a simple elastic freedom and obtaining a system offlinear equations of the same number as the degree of elastic freedom of the frame with the help of the "convertion factors" x. The required "stress condition" of the 2nd stage is obtained by the addition of the partial stress conditions of simple elastic freedom, having multiplied them by the respective "convertion factors."[3]

When computing the preceding "partial stress conditions" by the method of successive approximation, the fixing moments are determined with the supposition that the joints of the frame can be displaced without rotating. The relative displacements of the joints are obtained by the help of the virtual displacement diagrams.[2]

Virtual Displacement Diagrams.—From solid mechanics it is known that any solid, moving in a plane, can have the possibility of two displacements and one rotation in the plane of the frame. The movements of the joints depend, therefore, on the number of members which connect the joint with the ground or other rigidly fixed neighboring joints [Fig. 5 (a) and (b)]. Thus, by the addition of the member I joints a and b of Fig. 5 (a), have the possibility of rotation only.

Joints of double elastic freedom are those having the possibility of displacement and rotation. Joints a and b of Fig. 5(a) and joint a of Fig. 5(b) are of "double elastic freedom."

Joints of "single elastic freedom" are those joints which can only rotate around an instantaneous center 0. In the rigid frame of Fig. 6, joints b and c are of a "single elastic freedom," and joint a of "double elastic freedom." By the addition of member I pinned at both ends, a can rotate whereas b and c can neither rotate nor be displaced.

For any movement δ_{c1}, the movement of any point of the joints of the frame can be computed by making use of the diagrams of virtual displacement.

Fixing Moments of 2nd Stage.—In the classical case of rigid frames, that is, when joints are taken as points, in order to compute the fixing moments of the 2nd stage, it is achieved that joints do not rate. Using the diagrams of virtual displacement, the relative displacement between two adjacent joints in the direction perpendicular to the member, joining the joints under consideration, is computed. By using these relative displacements of the ends of the members, the fixing moments at all sections by the joints of the rigid frame are computed.

In this case, and in the 2nd stage, it is believed that joints of "double elastic freedom" do not rotate during displacement, and joints of "single elastic freedom" rotate around the instantaneous center of rotation of the joint.

Thus, when member I is removed (Fig. 6), joint a is displaced without rotation, and joints b and c rotate around their instantaneous centers of rotation O_b and O_c.

The fixing moments of a member, connecting joints of "single elastic freedom," are computed subsequently. The equations given are general. Special cases of joints of double elastic freedom, one joint of single elastic freedom, and one of the double elastic freedom are also considered.

Joints of Single Elastic Freedom.—In Fig. 7, we have joints a and b of single elastic freedom connected together by member i, and moments M_{ai} and M_{bi} at sections a_i and b_i as well as the moments at a° and b°, distances d_{ai} and d_{bi} from the sections a_i and b_i. We also have a displacement δ_1 of the point of the "imaginary" pin-jointed member of joint b.

Using the diagram of virtual displacement, and in connection with the displacement placement δ_1, the rotations θ_b, θ_a, and θ_i of joints b, a, and member i, respectively, are computed by using

$$\theta_b = \rho_b \ \delta_1, \ \ \theta_a = \rho_a \ \delta_1, \ \ \theta_i = \rho_i \ \delta_1 \ \ldots\ldots\ldots\ldots (25)$$

in which

$$\rho_b = \pm \frac{1}{e_{bo}}, \ \ \rho_a = \pm \frac{1}{e_{bo}} \frac{e_{bi}}{e'_{bi}} \frac{e'_{ai}}{e_{ai}}, \ \ \rho_i = \pm \frac{1}{e_{bo}} \frac{e_{bi}}{e'_{bi}} \ \ldots\ldots (26)$$

In Eq. 26, constants are either positive or negative depending on whether the rotation θ around the instataneous centers O_a, O_b, and O_i are clockwise or counter-clockwise.

Displacements δ_{bi}, δ_i, and δ_{ai} and $\delta_r = \delta_{ar}$ (Fig. 9) are found from

$$\delta_{bi} = c_{bi} \ \delta_1, \ \ \delta_1 = c_i \ \delta_1, \ \ \delta_{ai} = c_{ai} \ \delta_1, \ \ \delta_r = \delta_{ar} = c_{ar} \ \delta_1 \ \ldots (27a)$$

in which

$$c_{bi} = \pm \rho_b \ e_{bi}, \ \ c_i = \pm \rho_i \ l_i, \ \ c_{ai} = \pm \rho_a \ e_{ai}, \ \ c_r = \pm \rho_a \ e_{ar} \ \ldots (27b)$$

Special cases.—

a. Members 0,1 . . . which are connected to joint b are parallel. In this case, the constants ρ and c take the values

$$\rho_b = 0, \ \ \rho_a = \pm \frac{1}{e'_{bi}} \frac{e'_{ai}}{e_{ai}}, \ \ \rho_i = \pm \frac{1}{e'_{bi}} \ \ldots\ldots\ldots\ldots (28a)$$

and

$$c_{bi} = \pm 1, \ \ c_i = \pm \rho_i \ l_i, \ \ c_{ai} = \pm \rho_a \ e_{ai}, \ \ c_r = \pm \rho_a \ e_{ar} \ \ldots\ldots (28b)$$

b. The members connected to the joints a and b, when taken as a total, are parallel

$$\rho_b = 0 \quad \rho_i = 0 \quad \rho_a = 0 \quad \ldots\ldots\ldots\ldots\ldots (28c)$$

and

$$c_{bi} = \pm 1 \quad c_i = 0 \quad c_{ai} = \pm 1 \quad c_r = \pm 1 \quad \ldots\ldots\ldots\ldots (28d)$$

Computations of Moments M_{ai} and M_{bi}.— Sections a_i and b_i (Fig. 7), due to the joints a and b by θ_a and θ_b, will rotate themselves, in accordance with the rules of solid mechanics, by the same angles θ_a and θ_b and in the same direction.

Using Eqs. 29 we compute the moments M_{ai} and M_{bi}

$$M_{ai} = -\left(a_{ai}\ \theta_a + \mu_i\ a_{bi}\ \theta_b\right) + u_{ai}\ \frac{\delta_i}{l_i} \quad \ldots\ldots\ldots (29a)$$

and

$$M_{bi} = -\ \left(\mu_i\ a_{ai}\ \theta_a + a_{bi}\ \theta_b\right) + u_{bi}\ \frac{\delta_i}{l_i} \quad \ldots\ldots\ldots (29b)$$

In Eqs. 29, the moments due to the rotations by θ_a and θ_b are entered with negative signs because a clockwise rotation of the sections by θ_a and θ_b causes negative moments to the sections a_i and b_i. Substituting the values for θ_a, θ_b, and δ_i from Eqs. 25 and 27a in Eqs. 29,

$$M_{ai} = u^{\circ}_{ai}\ \frac{\delta_I}{l_i} \quad \ldots\ldots\ldots\ldots\ldots\ldots (30a)$$

and

$$M_{bi} = u^{\circ}_{bi}\ \frac{\delta_I}{l_i} \quad \ldots\ldots\ldots\ldots\ldots\ldots (30b)$$

in which

$$u^{\circ}_{ai} = u_{ai}\left[-\left(\frac{a_{ai}}{u_{ai}}\ \rho_a + \mu_i\ \frac{a_{bi}}{u_{ai}}\ \rho_b\right) l_i + c_i\right] \quad \ldots\ldots\ldots (31a)$$

and

$$u^{\circ}_{bi} = u_{bi}\left[-\left(\mu_i\ \frac{a_{ai}}{u_{bi}}\ \rho_a + \frac{a_{bi}}{u_{bi}}\ \rho_b\right) l_i + c_i\right] \quad \ldots\ldots\ldots (31b)$$

The shearing forces are given by

$$Q_i = Q_{ai} = Q_{bi} = \frac{u^{\circ}_{ai} + u^{\circ}_{bi}}{l_i}\ \frac{\delta_I}{l_i} \quad \ldots\ldots\ldots\ldots\ldots (32)$$

For straight members with constant moment of inertia, Eq. 31 takes the following form:

1. **Member built-in at both ends.**

$$u_{ai} = u_{bi} = \frac{6\,E\,I_i}{l_i} \quad a_{ai} = a_{bi} = \frac{4\,E\,I_i}{l_i} \quad \mu_i = +\frac{1}{2} \;\dots\dots\;(33a)$$

$$u^{\circ}_{ai} = \left[-\left(2\;\rho_a + \rho_b\right)\frac{l_i}{3} + c_i\right]\frac{6\,E\,I_i}{l_i} \;\dots\dots\dots\dots\;(33b)$$

and

$$u^{\circ}_{bi} = \left[-\left(\rho_a + 2\;\rho_b\right)\frac{l_i}{3} + c_i\right]\frac{6\,E\,I_i}{l_i} \;\dots\dots\dots\dots\;(33c)$$

2. **Member built-in at one end - Pinned at section.**

$$u_{ai} = \frac{3\,E\,I_i}{l_i},\;\; u_{bi} = 0,\;\; a_{ai} = \frac{3\,E\,I_i}{l_i},\;\; a_{bi} = 0,\;\; \mu_i = 0 \;\dots\dots\;(34a)$$

$$u^{\circ}_{ai} = \left(-\,\rho_a\;\,l_i + c_i\right)\frac{3\,E\,I_i}{l_i} \;\dots\dots\dots\dots\dots\dots\;(34b)$$

and

$$u^{\circ}_{bi} = 0 \;\dots\dots\dots\dots\dots\dots\dots\dots\dots\dots\;(34c)$$

3. **Member built-in at one end - Pinned at section.**

$$u^{\circ}_{ai} = 0 \;\dots\dots\dots\dots\dots\dots\dots\dots\dots\dots\;(35a)$$

and

$$u^{\circ}_{bi} = \left(-\,\rho_b\;\,l_i + c_i\right)\frac{3\,E\,I_i}{l_i} \;\dots\dots\dots\dots\dots\dots\;(35b)$$

Computation of Moments M'_{ai} and M'_{bi}.—The moments M'_{ai} and M'_{bi} are given by

$$M'_{ai} = M_{ai} + Q_{ai}\;\,d_{ai} \;\dots\dots\dots\dots\dots\dots\dots\;(36a)$$

and

$$M'_{bi} = M_{bi} + Q_{bi}\;\,d_{bi} \;\dots\dots\dots\dots\dots\dots\dots\;(36b)$$

If in Eq. 36 the values for M_{ai} and M_{bi} are substituted from Eqs. 30 and Q_{ai}, and Q_{bi} from Eq. 32, Eqs. 37 are

$$M'_{ai} = \bar{u}_{ai}\;\frac{\delta_I}{l_i} \;\dots\dots\dots\dots\dots\dots\dots\dots\;(37a)$$

and

$$M'_{bi} = \bar{u}_{bi}\;\frac{\delta_I}{l_i} \;\dots\dots\dots\dots\dots\dots\dots\dots\;(37b)$$

in which

$$\bar{u}_{ai} = u^{\circ}_{ai}\left(1 + \frac{d_{ai}}{l_i}\right) + u^{\circ}_{bi}\;\frac{d_{ai}}{l_i} \;\dots\dots\dots\dots\;(38a)$$

and

$$\bar{u}_{bi} = u^{\circ}_{ai}\;\frac{d_{bi}}{l_i} + u^{\circ}_{bi}\left(1 + \frac{d_{bi}}{l_i}\right) \dots\dots\dots\dots\;(38b)$$

Comparing Eqs. 30 and 37, the conclusion canbe drawn that Eqs. 37 are the general form of Eqs. 30 because when $d_{ai} = d_{bi} = 0$, by substituting these values in Eqs. 37. Eqs. 30 are obtained that is, the moments M_{ai}, and M_{bi} at sections a_i and b_i.

In accordance with the preceding, M_{ai} and M_{bi} are computed using Eqs. 37, for $d_{ai} = d_{bi} = 0$

$$\bar{u}_{ai} = u^{\circ}_{ai} \quad \text{(39a)}$$

and

$$\bar{u}_{bi} = u^{\circ}_{bi} \quad \text{(39b)}$$

Joints of "Double Elastic Freedom."—Joints a and b of Fig. 8 are of "double elastic feedom" and are connected together by the member i which has an instantaneous center of rotation O_i. The diagram of virtual displacement has been drawn for a given displacement δ_b. Angle θ_i can be expressed in terms of δ_b (for infinitely small displacements) by

$$\theta_i = \frac{\delta_b}{e^{\circ}_{bi}} \quad \text{(40)}$$

From Fig. 8 we obtain

$$\delta_a = c_a \ \delta_b, \quad \delta_i = c_i \ \delta_b, \quad n_i = \frac{h_i}{e^{\circ}_{bi}} \ \delta_b \quad \text{(41)}$$

in which

$$c_a = \frac{e^{\circ}_{ai}}{e^{\circ}_{bi}}, \quad c_i = \frac{l'_i}{e^{\circ}_{bi}} \quad \text{(42)}$$

Joints a and b do not rotate when displaced. By making this supposition, sections a_i and b_i will take the positions a'_i and b'_i (Fig. 8). The relative displacement of sections a_i and b_i normal to the direction of the member is that computed δ_i.

The difference of the constant c_i for joints of a single and double elastic freedom results from the fact that in the first case the span l_i is considered, and in the second, the span l'_i.

The moments M'_{ai}, M'_{bi}, M_{ai}, and M_{bi} are computed by making use of Eqs. 37 and 30 in which the factors $\bar{u}_{ai}$, $\bar{u}_{bi}$, u°_{ai}, and u°_{bi} take the following values: For, $\rho_a = \rho_b = 0$, we have (Eqs. 33 and 38)

$$u^{\circ}_{ai} = c_i \ u_{ai} \quad \text{(43a)}$$

$$u^{\circ}_{bi} = c_i \ u_{bi} \quad \text{(43b)}$$

$$\bar{u}_{ai} = \left[u_{ai}\left(1 + \frac{d_{ai}}{l_i}\right) + u_{bi} \ \frac{d_{ai}}{l_i}\right] c_i \quad \text{(44a)}$$

and

$$\bar{u}_{bi} = \left[u_{ai} \ \frac{d_{bi}}{l_i} + \left(1 + \frac{d_{bi}}{l_i}\right) u_{bi}\right] c_i \quad \text{(44b)}$$

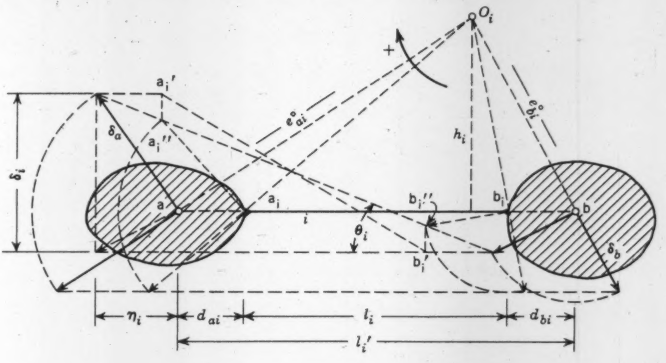
O_i
+
a_i'
δ_a
a_i''
e°_{ai}
e°_{bi}
h_i
δ_i
a
a_i
i
θ_i
b_i''
b_i
b
b_i'
δ_b
η_i
d_{ai}
l_i
d_{bi}
l_i'

FIG. 8

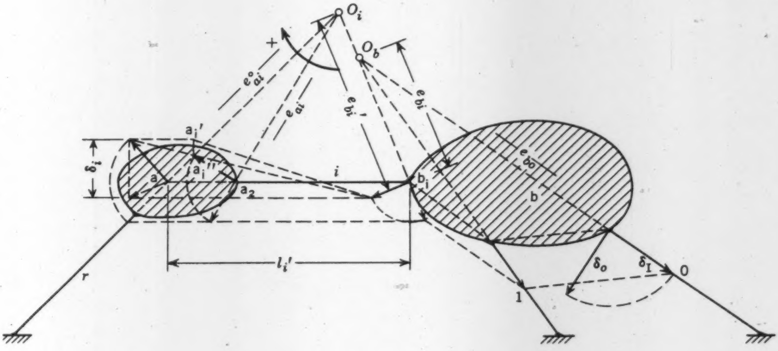
O_i
+
O_b
e°_{ai}
e_{ai}
e_{bi}'
e_{bi}
a_i'
δ_i
a
a_i''
a_2
i
b_i
e_{bo}
b
l_i'
r
δ_o
δ_I
0
1

FIG. 9

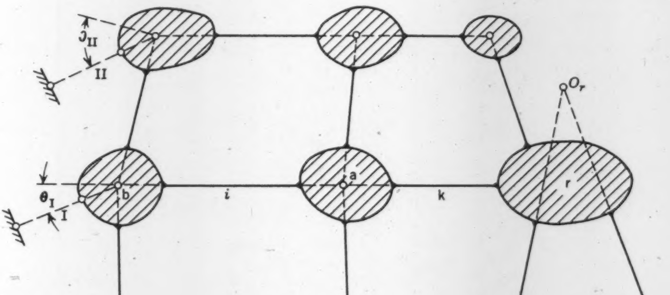
ϑ_{II}
II
O_r
θ_I
I
b
i
a
k
r

FIG. 10

In the case of straight members of constant moment of inertia, Eqs. 43 and 44 take the forms:

1. Member built-in at both ends

$$u^{\circ}_{ai} = u^{\circ}_{bi} = \frac{6\ E\ I_i}{l_i}\ c_i \tag{45a}$$

$$\overline{u}_{ai} = \frac{6\ E\ I_i}{l_i}\left(1 + 2\ \frac{d_{ai}}{l_i}\right)c_i \tag{45b}$$

and

$$\overline{u}_{bi} = \frac{6\ E\ I_i}{l_i}\left(1 + 2\ \frac{d_{bi}}{l_i}\right)c_i \tag{45c}$$

2. Member built-in at one end - Pinned at b_i

$$u^{\circ}_{ai} = \frac{3\ E\ I_i}{l_i}\ c_i \quad u^{\circ}_{bi} = 0 \tag{46a}$$

$$\overline{u}_{ai} = \frac{3\ E\ I_i}{l_i}\left(1 + \frac{d_{ai}}{l_i}\right) c_i \tag{46b}$$

and

$$\overline{u}_{bi} = \frac{3\ E\ I_i}{l_i}\ \frac{d_{bi}}{l_i}\ c_i \tag{46c}$$

Joint a of Double Elastic Freedom - Joint b of Single Elastic Freedom.— In this case (Fig. 9)

$$\theta_b = \rho_b\ \delta_I, \quad \theta_a = 0, \quad \theta_i = \rho_i\ \delta_I \tag{47}$$

in which

$$\rho_b = \pm\ \frac{1}{e_{bo}}, \quad \rho_i = \pm\ \frac{1}{e_{bo}}\ \frac{e_{bi}}{e'_{bi}} \tag{48}$$

The displacements are given by

$$\delta_{bi} = c_{bi}\ \delta_I, \quad \delta_i = c_i\ \delta_I \tag{49a}$$

and

$$\delta_a = c_a\ \delta_I, \quad \delta_r = \delta_{ar} = c_{ar}\ \delta_I \tag{49b}$$

in which

$$c_{bi} = \pm\ \rho_b\ e_{bi} \qquad c_i = \pm\ \rho_i\ l'_i \tag{50a}$$

and

$$c_a = \pm\ e^{\circ}_{ai}\ \rho_i \qquad c_r = c_{ra} = \pm\ e_{ar}\ \rho_i \tag{50b}$$

The moments M_{ai}, M_{bi}, and M'_{ai} are computed by using Eqs. 30 and 37 in which the factors u°_{ai}, u°_{bi}, and $\overline{u}_{ai}$ take the values for $\rho_a = 0$ (Eqs. 31 and 38)

$$u^{\circ}_{ai} = u_{ai}\left(-\ \mu_i\ \frac{a_{bi}}{u_{ai}}\ \rho_b\ l_i + c_i\right) \tag{51a}$$

$$u^{\circ}_{bi} = u_{bi}\left(-\ \frac{d_{bi}}{u_{bi}}\ \rho_b\ l_i + c_i\right) \tag{51b}$$

$$\overline{u}_{ai} = u^{\circ}_{ai}\left(1 + \frac{d_{ai}}{l_i}\right) + u^{\circ}_{bi}\ \frac{d_{ai}}{l_i} \tag{52a}$$

and

$$\bar{u}_{bi} = u^{\circ}_{bi} \ldots\ldots\ldots\ldots\ldots \text{(52b)}$$

For straight members with constant moment of inertia

1. Member built-in at both ends

$$u^{\circ}_{ai} = \frac{6\,E\,I_i}{l_i}\left(-\rho_b \frac{l_i}{3} + c_i\right) \ldots\ldots\ldots\ldots \text{(53a)}$$

and

$$u^{\circ}_{bi} = \frac{6\,E\,I_i}{l_i}\left(-2\,\rho_b \frac{l_i}{3} + c_i\right) \ldots\ldots\ldots\ldots \text{(53b)}$$

2. Member built-in at one end - Pinned at b_i

$$u^{\circ}_{ai} = u_{ai} \quad c_i = \frac{3\,E\,I_i}{l_i} \, c_i \ldots\ldots\ldots\ldots \text{(53c)}$$

and

$$u^{\circ}_{bi} = 0 \ldots\ldots\ldots\ldots\ldots \text{(53d)}$$

3. Member built-in at one end - Pinned at a_i

$$u^{\circ}_{ai} = 0 \ldots\ldots\ldots\ldots\ldots \text{(54a)}$$

$$u^{\circ}_{bi} = \frac{3\,E\,I_i}{l_i}\left(-\rho_b \, l_i + c_i\right) \ldots\ldots\ldots\ldots \text{(54b)}$$

Fixing Forces of 2nd Stage.—The fixing forces of the second stage are computed in a more simple way by the principle of virtual works.

We denote the diagrams of virtual displacement obtained by the removal of each of the imaginary pin-jointed members (roller restraints) I and II, etc., by the general symbols (Π^{I}), (Π^{II}), etc., respectively.

Also by δ^{I}_{i}, δ^{II}_{i}, etc., c^{I}_{i}, and c^{II}_{i}, etc., we denote displacements δ and constants c of the respective member, for the removal of I and II, etc.

The displacements δ^{I}_{i} and δ^{II}_{i}, etc., and the constants c^{I}_{i} and c^{II}_{i}, etc., are computed with the help of the virtual displacement diagrams (Π^{I}), (Π^{II}) in conjunction with the geometry of the figure and the respective displacements δ_{I}, and δ_{II}, etc.

Also θ^{I}_{a}, θ^{II}_{a}, etc., ρ^{I}_{a} and ρ^{II}_{a}, etc., denotes the rotations θ and the constants ρ of the joints of single elastic freedom.

If we now detach the members of the frame by taking sections close to the joints, and apply to the joints forces Q^{I}_{ai}, N^{I}_{ai}, F^{I}_{I}, and F^{II}_{I}, etc., and the moments M^{I}_{ai} for joints of single elastic freedom, or M^{I}_{ai} for joints of double elastic freedom, each joint will be in equilibrium under these system of forces. The equilibrium of the joints (taken as a whole) can be expressed by the principle of virtual works.

Applying the principle of virtual works, for example, for the stress condition which has resulted by the removal of the imaginary member I and (virtual) deformation of the geometrical one, which is taken from the diagram of virtual displacement (Π^{I}), results in[2]

$$F^{I}_{I}\,\delta_{I} + \Sigma_a\,\theta_a\,\Sigma_k\,M^{I}_{ak} - \Sigma_i\,Q^{I}_{i}\,\delta^{I}_{i} = 0 \ldots\ldots\ldots\ldots \text{(55)}$$

in which $Q_i^I = Q_{ai}^I = Q_{bi}^I$, Σ_a is the summation extending to all joints of single elastic freedom, and Σ_k is the summation extending to all members of the group of condisplaced members I.

The sign of the third additive in Eq. 55 is minus because positive shearing force and positive displacement δ_i^I result in negative work.

The work done by the forces F_{II}^I and F_{III}^I, is equal to zero, because the displacements of the points of application of II and III, etc., on the joints are normal to the directions of the imaginary pinned members I and II, etc.

The forces N_i^I do not appear in Eq. 55 because the work done by them, being equal and opposite, cancels each other.

Also the moments M_{ai}^I at the joints of double elastic freedom taken at each joint, give work equal to zero.

If in Eq. 54 we substitute the values for θ_a^I and δ_i^I as a function of δ_I

$$F_I^I = \Sigma_i \ c_i^I \ Q_i^I - \Sigma_a \ \rho_a^I \ \Sigma_k \ M_{ak}^I \ \ldots\ldots\ldots\ldots (56)$$

Using Eq. 55, the fixing forces of the 2nd stage are computed.

Stress Analysis of Rigid Frames by the Method of Successive Approximations in One Stage.[3]—In the case of stress analysis of rigid frames by the method of successive approximations in one stage only, after the fixed end moments and reactions for joints suffering neither displacement nor rotation are computed, we successively free the joints of double elastic freedom allowing rotation. Using the distribution and carry-over factors, the moments are computed. By the help of the restraining factors,[2] which will be computed subsequently, we compute the fixing forces F_I^a and F_{II}^a, which are developed at the imaginary pin-jointed members, due to allowing the joints to rotate.

After the successive freeing to rotation the joints of the frame, and the computation of the fixing forces, we successively remove the imaginary pinned members, applying at their points of connection, equal and opposite forces to the computed fixing forces. In this case we consider that joints of double elastic freedom are displaced without rotation and joints of single elastic freedom rotate around the instantaneous center of rotation of the joint. With the help of the distribution factors, due to displacement and shear carry-over, which shall be worked out subsequently, compute the moments at the joints of the rigid frame and the fixing forces at the imaginary pinned members. The preceding work is repeated successively, and thus the stress analysis of the rigid frame is obtained by successive approximations in one stage.[2]

Restraining Factors.—In the stress analysis of (Fig. 10), none of the joints of double elastic freedom rotate except joint a on which M_a acts.

To generalize the equation, moments are denoted with the general symbol $\left(M_{ai}^a\right)'$, in which $\left(M_{ai}^a\right)' = M_{ai}^a$ for joints of single elastic freedom and $\left(M_{ai}^a\right)' = M_{ai}^{a\,\prime}$ for joints of double elastic freedom. Lengths of members l_i are also denoted by the general symbol $\left(l_i\right)'$, in which $\left(l_i\right)' = l_i$ for member joining joints of single elastic freedom, $\left(l_i\right)' = l_i + d_{ai} + d_{bi}$ for joints of double elastic freedom, and $\left(l_i\right)' = l_i + d_{ai}$ for joint a of double elastic freedom and joint b of single elastic freedom. Moments $\left(M^a_{ai}\right)'$ and $\left(M^a_{bi}\right)'$ are computed from Eqs. 57 (Fig. 16)

$$\left(M^a_{ai}\right)' = \left(-\ M_a\right)\ K_{ai} \quad \text{(57a)}$$

and

$$\left(M^a_{bi}\right)' = \left(-\ M_a\right)\ K_{ai}\ \mu_{ab} \quad \text{(57b)}$$

The shearing force is given by

$$Q^a_{ai} = Q^a_{bi} = Q^a_i = \left(-\ M_a\right)\ \frac{K_{ai}\left(1 + \mu_{ab}\right)}{\left(l_i\right)'} \quad \text{(58)}$$

The computation of the fixing force F^a_I is given subsequently. The remaining F^a_{II} and F^a_{III} are computed in a similar way as F^a_I.

If the equilibrium of the forces on the joints M^a_{ai}, Q^a_i, N^a_i, and F^a_I, F^a_{II} (taken as a whole) is expressed by the principle of virtual works, taking as virtual deformation the $\left(\Pi^I\right)$, Eq. 59 results (Fig. 10)

$$F^a_I\ \delta_I \cos\theta_I - \Sigma_i\ Q^I_i\ \delta^I_i + \Sigma_r\ M^a_{rk}\ \theta^I_r = 0 \quad \text{(59)}$$

The moment M^a_{rk}, as a function of the factor of distribution, due to rotation k_{ar} and the carry-over factor μ_{ar}, is given by

$$M^a_{rk} = \left(-\ M_a\right)\mu_{ar}\ K_{ak} \quad \text{(60)}$$

If in Eq. 59 we replace δ^I_i and θ^I_i as functions of δ_I, and the values for Q^a_i and M^a_{rk} are substituted from Eqs. 58 and 60,

$$F^a_I = \left(-\ M_a\right)\delta_{aI}. \quad \text{(61)}$$

in which

$$\sigma_{aI} = \frac{1}{\cos\theta_I}\left[\Sigma_i\ \frac{K_{ai}\left(1 + \mu_{ab}\right)c^I_i}{\left(l_i\right)'} - \Sigma_r\ \rho^I_r\ \Sigma_k\ \mu_{ak}\ K_{ak}\right] \quad \text{(62a)}$$

The summation Σ_r extends to the joints r of single elastic freedom next to the joint under consideration (Fig. 10).

For $\theta_I = 0$

$$\sigma_{aI} = \Sigma_i\ \frac{K_{ai}\left(1 + \mu_{ab}\right)c^I_i}{\left(l_i\right)'} - \Sigma_r\ \rho^I_r\ \Sigma_k\ \mu_{ak}\ K_{ak} \quad \text{(62b)}$$

In Eqs. 62 the restraining factors of the joints of double elastic freedom of the rigid frame are obtained. The dimensions of the "restraining factor" are 1 per length.

Distribution Factors Due to Displacement.—After the removal of the imaginary pinned member, for example I, we apply a force equal to - F_I on the joint at the point of connections, that is, equal and opposite to the computed fixing force at position I

$$F_I = F^\circ_I + F^a_I + F^b_I + \ldots. \quad \text{(63)}$$

in which F°_I is the fixing force at position I for the case of perfectly rigid joints (neither rotation nor displacement allowed) of the frame.

Because of the force $-F_I$, the joints of the rigid frame will be displaced. We assume that during this displacement, joints of double elastic freedom will not rotate, and those of single elastic freedom will rotate around the instantaneous center of rotation.

Due to the displacement of the joints of the rigid frame, forces Q^I_i, N^I_i, and moments $\left(M^I_{ai}\right)'$ will develop at the sections next to the joints.

The moments $\left(M^I_{ai}\right)'$ and $\left(M^I_{bi}\right)'$ are given by Eqs. 37

$$\left(M^I_{ai}\right)' = \bar{u}^I_{ai} \frac{\delta_I}{l_i} \qquad \dots\dots\dots\dots\dots\dots (64a)$$

and

$$\left(M^I_{bi}\right)' = \bar{u}^I_{bi} \frac{\delta_I}{l_i} \qquad \dots\dots\dots\dots\dots\dots (64b)$$

The shear forces are given by

$$Q^I_i = Q^I_{ai} = Q^I_{bi} = \frac{\bar{u}^I_{ai} + \bar{u}^I_{bi}}{\left(l_i\right)'} \frac{\delta_I}{l_i} \qquad \dots\dots\dots\dots (65)$$

If the equilibrium of the forces acting on the joint of the rigid frame is expressed by the "principle of virtual works" taking as "virtual deformation," the elastic one given by the diagram of virtual displacement $\left(\Pi^I\right)$, Eq. 66 results

$$\left(-F_I\right) \delta_I \cos\theta_I - \Sigma_i \; Q^I_i \; \delta^I_i + \Sigma_r \; \theta^I_r \; \Sigma_k \left(M^I_{rk}\right)' = 0 \; \dots\dots (66)$$

in which Σ_i denotes the summation extending to all member i of group I, and Σ_r represents the summation extending to all joints r of single elastic freedom of group I.

If in Eq. 66 the values for Q^I_r, and $\left(M^I_{rk}\right)'$ from Eqs. 64 and 65 are replaced, and δ^I_i and θ^I_r are expressed as functions of the displacement δ^I, Eq. 67 results

$$\delta_I = \left(-F_I\right) \frac{\cos\theta_I}{\Sigma_i \; \frac{\bar{u}^I_{ai} + \bar{u}^I_{bi}}{\left(l_i\right)'} \; \frac{c^I_i}{l_i} - \Sigma_r \; \rho^I_r \; \Sigma_k \; \frac{\bar{u}^I_{rk}}{l_k}} \; \dots\dots (67)$$

Combining Eqs. 64 and 67

$$\left(M^I_{ai}\right)' = \left(-F_I\right) \bar{q}^I_{ai} \qquad \dots\dots\dots\dots\dots\dots (68)$$

in which

$$\bar{q}^I_{ai} = \frac{\dfrac{\bar{u}^I_{ai}}{l_i}}{\Sigma_i \; \dfrac{\bar{u}^I_{ai} + \bar{u}^I_{bi}}{\left(l_i\right)'} \; \dfrac{c^I_i}{l_i} - \Sigma_r \; \rho^I_r \; \Sigma_k \; \dfrac{\bar{u}^I_{rk}}{l_k}} \cos\theta_I \; \dots\dots (69a)$$

In the case of angle $\theta_I = 0$, Eq. 69(a) becomes

$$\bar{q}^{I}_{ai} = \frac{\dfrac{\bar{u}^{I}_{ai}}{l_i}}{\Sigma_i \dfrac{\bar{u}^{I}_{ai} + \bar{u}^{I}_{bi}}{(l_i)'} \dfrac{c^{I}_{i}}{l_i} - \Sigma_r \rho^{I}_{r} \Sigma_k \dfrac{\bar{u}^{I}_{rk}}{l_k}} \quad \ldots\ldots (69b)$$

Eqs. 69 (a) and 69 (b) give us the distribution factors due to displacement.

Check.—The shearing forces as function of the moments $\left(M^{I}_{ai}\right)'$ are given by

$$Q^{I}_{i} = \left(-F_I\right) \frac{\bar{q}^{I}_{ai} + \bar{q}^{I}_{bi}}{(l_i)'} \ldots\ldots\ldots\ldots\ldots\ldots (70)$$

Applying the principle of virtual works for the computed, shearing forces, normal forces, and moments of group I, due to $-F_I$ and virtual deformation of the geometrical one given by the diagram of virtual displacement $\left(\Pi^{I}\right)$, we obtain

$$\left(-F_I\right) \delta_I \cos \theta_I - \Sigma_i \left(-F_I\right) \frac{\bar{q}^{I}_{ai} + \bar{q}^{I}_{bi}}{(l_i)'} \delta^{I}_{i} + \Sigma_r \theta^{I}_{r} \Sigma_k \bar{q}^{I}_{rk} \left(-F_I\right) = 0 \ldots (71)$$

If in Eq. 71, the values for δ^{I}_{i} and θ^{I}_{r} are placed in terms of the displacement δ_i and the constants c^{I}_{i} and ρ^{I}_{r}, we have

$$\Sigma_i \frac{\bar{q}^{I}_{ai} + \bar{q}^{I}_{bi}}{(l_i)'} c^{I}_{i} - \Sigma_r \rho^{I}_{r} \Sigma_k \bar{q}^{I}_{rk} = \cos \theta_i \ldots\ldots\ldots (72)$$

When angle $\theta_I = 0$, Eq. 72 becomes

$$\Sigma_i \frac{\bar{q}^{I}_{ai} + \bar{q}^{I}_{bi}}{(l_i)'} c^{I}_{i} - \Sigma_r \rho^{I}_{r} \Sigma_k \bar{q}^{I}_{rk} = 1 \ldots\ldots\ldots\ldots (73)$$

Remarks.—The factors $\bar{u}^{I}_{ai}$ take the following forms depending on whether the joint is of single or double elastic freedom.

1. For joints of single elastic freedom $\left(M^{I}_{ai}\right)' = M^{I}_{ai}$ and $\bar{u}^{I}_{ai} = u^{\circ}_{ai}$ (Eq. 31).
2. For joints of double elastic freedom $\left(M^{I}_{ai}\right)' = M^{I'}_{ai}$, $\bar{u}_{ai} = u^{\circ}_{ai}\left(1 + \dfrac{d_{ai}}{l_i}\right) + u^{\circ}_{bi} \dfrac{d_{ai}}{l_i}$, and $\bar{u}_{bi} = u^{\circ}_{ai} \dfrac{d_{bi}}{l_i} + u^{\circ}_{bi}\left(1 + \dfrac{d_{bi}}{l_i}\right)$ (Eq. 38).

Shear Carry-over Factors.—In the rigid frame, besides the pinned member I, II and III exist also. Due to the removal of I and application to the joint where I is connected of force $-F_I$, fixing forces F^{I}_{II} and F^{I}_{III} are developed on the remaining members II and III, of which we require the value in terms of $-F_I$.

The computation of the fixing force F^{I}_{II} is given subsequently.

If the equilibrium of the forces acting on the joint is expressed by the principle of virtual works, taking as virtual deformation that given by the diagram of virtual displacement $\left(\Pi^{II}\right)$ Eq. 74 results

$$F^{I}_{II}\cos\theta_{II}\,\delta_{II} - \Sigma_i\,Q^{I}_{i}\,\delta^{II}_{i} + \Sigma_r\,\theta^{II}_{I}\,\Sigma_k\left(M^{I}_{rk}\right)' \;\ldots\ldots.(74)$$

If in Eq. 74, the displacements δ^{II}_{i} and θ^{II}_{i} are expressed in terms of the constants c^{II}_{i}, ρ^{II}_{r}, and displacement δ_{II}, and solved with regard to F^{I}_{II}, Eq. 75 results

$$F^{I}_{II} = \frac{\Sigma_i\,Q^{I}_{i}\,c^{II}_{i} - \Sigma_r\,\rho^{II}_{r}\,\Sigma_k\left(M^{I}_{rk}\right)'}{\cos\theta_{II}} \ldots\ldots\ldots\ldots.(75)$$

The shearing forces Q^{I}_{i} and moments $\left(M^{I}_{rk}\right)'$ are given by

$$Q^{I}_{i} = \frac{\bar{q}^{I}_{ai} + \bar{q}^{I}_{bi}}{l_i}\left(-F_I\right) \ldots\ldots\ldots\ldots\ldots\ldots.(76)$$

and

$$\left(M^{I}_{rk}\right)' = \left(-F_I\right)\bar{q}^{I}_{rk} \;\ldots\ldots\ldots\ldots\ldots\ldots.(77)$$

If in Eq. 75 the values for Q^{I}_{i} and $\left(M^{I}_{rk}\right)'$ are replaced by Eqs. 76 and 77, Eq. 78 is

$$F^{I}_{II} = \left(-F_I\right)m^{I}_{II} \ldots\ldots\ldots\ldots\ldots\ldots\ldots\ldots.(78)$$

in which

$$m^{I}_{II} = \frac{1}{\cos\theta_{II}}\left[\Sigma_i\left(\bar{q}^{I}_{ai} + \bar{q}^{I}_{bi}\right)\frac{c^{II}_{i}}{\left(l_i\right)'} - \Sigma_r\,\rho^{II}_{r}\,\Sigma_k\,\bar{q}^{I}_{rk}\right] \ldots\ldots.(79)$$

For the case of angle $\theta_{II} = 0$, Eq. 79 becomes

$$m^{I}_{II} = \Sigma_i\left(\bar{q}^{I}_{ai} + \bar{q}^{I}_{bi}\right)\frac{c^{II}_{i}}{\left(l_i\right)'} - \Sigma_r\,\rho^{II}_{r}\,\Sigma_k\,\bar{q}^{I}_{rk} \ldots\ldots\ldots\ldots.(80)$$

in which Σ_k is the summation extending to members k connected to joint r of single elastic freedom.

Layout of the Work of Successive Approximation.—The layout of the work of successive approximations is given again in Appendix I in table form (4th example) as in the case where joints are taken as points.[2] The final total moments are obtained by adding up all values, in the squares, of the bending moments at the sections by the joints of the members of the rigid frame.

CONCLUSIONS

The present study constitutes the general form of the method of successive approximation for rigid frames whose joints are not points or infinitely small areas, an assumption which is made in all up-to-day classical methods of stress analysis of rigid frames, but areas of limited dimensions, which at the analysis of the rigid frame, are taken as solid areas suffering no deformation.

It can be said that the equations given, both for the analysis in one stage or two stages, constitute the generalized form of the method of successive approximation. The equations known today for the analysis of rigid frames can be considered as a special case of the generalized ones.

Besides the theoretical interest of this study, in certain cases either due to the interposition of partition or due to large dimensions of sections of certain members of the rigid frame, it is possible to have types of rigid frames for which the joints cannot be considered as being either points or infinitely small areas. The stress analysis of such types of frames by the method suggested is in the author's opinion, simple and rapid.

In order to make the application of this method clearer, four examples are given in Appendix I.

APPENDIX I.—EXAMPLES

Example No. 1 (Fig. 11)

Moments M_{ai}

$$\overline{M}_{a1} = -\overline{M}_{b1} = \frac{2000 \times 5.5^2}{12} = 5050 \text{ kg m} \quad \overline{M}_{b2} = -\overline{M}_{c2} = \frac{2000 \times 6.5^2}{12}$$
$$= 7080 \text{ kg m}$$

$$\overline{M}_{c3} = -\overline{M}_{k3} = \frac{2000 \times 5^2}{12} = 4160 \text{ kg m}$$

Shearing forces

$$Q^\circ_{a1} = -Q^\circ_{b1} = \frac{2000 \times 5.5}{2} = 5500 \text{ kg} \quad Q^\circ_{b2} = -Q^\circ_{c2} = \frac{2000 \times 6.5}{2} = 6500 \text{ kg}$$

$$\overline{Q}_{a1} = -\overline{Q}_{b1} = Q^\circ_{a1} = -Q^\circ_{b1} \quad \overline{Q}_{b2} = -\overline{Q}_{c2} = Q^\circ_{b2} = -Q^\circ_{c2}$$

$$Q^\circ_{c3} = \frac{2000 \times 5}{2} = 5000 \text{ kg} \quad \overline{Q}_{c3} = Q^\circ_{c3}$$

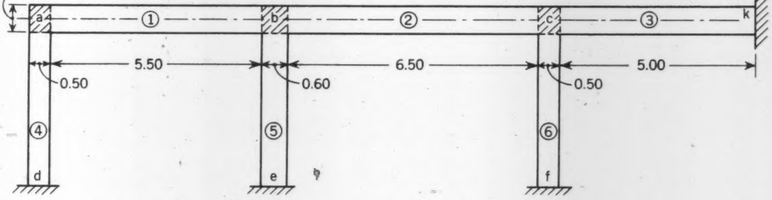

FIG. 11

Fixed-end moments

$\overline{M}'_{a1} = 5050 + 5500 \times 0.25 = 6425$ kg m $\quad \overline{M}'_{b1} = -5050 - 0.30 \times 5500$
$= -6700$ kg m

$\overline{M}'_{b2} = +7080 + 0.30 \times 6500 = +9030$ kg m $\quad \overline{M}'_{c2} = -7080 - 0.25 \times 6500$
$= -8700$ kg m

$\overline{M}'_{c3} = +4160 + 0.25 \times 5000 = +5410$

Distribution factors

$I_1 = I_2 = I_3 = 2.75\, I_4 \quad I_5 = 1.6\, I_4 \quad I_6 = I_4$

$d_{a1} = 0.25 \quad d_{a4} = 0.35 \quad d_{b1} = 0.30 \quad d_{b2} = 0.30 \quad d_{b5} = 0.35 \quad d_{c2} = 0.25$
$d_{c3} = 0.25 \quad d_{c6} = 0.35$

$\frac{d_{a1}}{l_1} = \frac{0.25}{5.5} = 0.045 \quad \frac{d_{a4}}{l_4} = \frac{0.35}{4.00} = 0.087 \quad \frac{d_{b1}}{l_1} = \frac{0.30}{5.5} = 0.054 \quad \frac{d_{b2}}{l_2} = \frac{0.30}{6.5} = 0.046$

$\frac{d_{b5}}{l_5} = \frac{0.35}{4.00} = 0.087 \quad \frac{d_{c2}}{l_2} = \frac{0.25}{6.5} = 0.038 \quad \frac{d_{c3}}{l_3} = \frac{0.25}{5.00} = 0.05 \quad \frac{d_{c6}}{l_6} = \frac{0.35}{4.00} = 0.087$

In solving b_{ai}, neglect the quantity $\left(\frac{d_{ai}}{l_i}\right)^2$ as being small

Joint a:

$$b_{a1} = \frac{4\,E\,2.75\,I}{5.50}(1 + 3 \times 0.045) = 2.27\,E\,I \quad K_{a1} = \frac{2.27}{3.531} = 0.643$$

$$b_{a4} = \frac{4\,E\,I}{4.00}(1 + 3 \times 0.087) = \frac{1.261\,E\,I}{3.531\,E\,I} \quad K_{a4} = \frac{1.261}{3.531} = \frac{0.357}{1.000}$$

Joint b:

$$b_{b1} = \frac{4\,E\,2.75\,I}{5.50}(1 + 3 \times 0.054) = 2.33\,E\,I \quad K_{b1} = \frac{2.33}{6.27} = 0.372$$

$$b_{b2} = \frac{4\,E\,2.75\,I}{6.5}(1 + 3 \times 0.046) = 1.92\,E\,I \quad K_{b2} = \frac{1.92}{6.27} = 0.306$$

$$b_{b5} = \frac{4\,E\,1.6\,I}{4.00}(1 + 3 \times 0.087) = \frac{2.02\,E\,I}{6.27\,E\,I} \quad K_{b5} = \frac{2.02}{6.27} = \frac{0.322}{1.000}$$

Joint c:

$$b_{c2} = \frac{4\,E\,2.75\,I}{6.5}(1 + 3 \times 0.038) = 1.89\,E\,I \quad K_{c2} = \frac{1.89}{5.68} = 0.332$$

$$b_{c3} = \frac{4\,E\,2.75\,I}{5.00}(1 + 3 \times 0.05) = 2.53\,E\,I \quad K_{c3} = \frac{2.53}{5.68} = 0.446$$

$$b_{c6} = \frac{4\,E\,I}{4}(1 + 3 \times 0.087) = \frac{1.26\,E\,I}{5.68\,E\,I} \quad K_{c6} = \frac{1.26}{5.68} = \frac{0.222}{1.000}$$

Carry-over factors:

$$\mu_{ab} = \frac{1}{2}\,\frac{1 + \dfrac{0.25 + 0.30}{5.5}\;3 + 6\;\dfrac{0.25 \times 0.30}{5.5^2}}{1.135} = 0.580$$

$$\mu_{ad} = \frac{1}{2}\,\frac{1 + 3\;\dfrac{0.35}{4}}{1.261} \cong 0.500$$

$$\mu_{ba} = \frac{1}{2}\,\frac{1 + 3\,\dfrac{0.25 + 0.30}{5.5} + 6\;\dfrac{0.25 \times 0.30}{5.5^2}}{1.138} = 0.558$$

$$\mu_{bc} = \frac{1}{2}\,\frac{1 + 3\dfrac{0.30 \times 0.25}{6.5} + 6 \cdot \dfrac{0.25 \times 0.30}{6.5^2}}{1.138} = 0.558$$

$$\mu_{be} = \frac{1}{2}\,\frac{1 + 3\;\dfrac{0.35}{4}}{1.261} \cong 0.500$$

$$\mu_{cb} = \frac{1}{2}\,\frac{1 + 3\;\dfrac{0.30 + 0.25}{6.5} + 6\;\dfrac{0.25 \times 0.30}{6.5^2}}{1.114} = 0.568$$

$$\mu_{ck} = \frac{1}{2}\,\frac{1 + \dfrac{0.25}{5}\;3}{1.15} \cong 0.500$$

$$\mu_{cf} = \frac{1}{2}\,\frac{1 + 3\;\dfrac{0.35}{4}}{1.261} \cong 0.500$$

The successive approximations and the values of M'_{ai} are given in Table 1.
Shearing forces:

$$Q_{a1} = 5500 + \frac{2254 - 9277}{5.95} = 4320 \qquad Q_{b1} = 5500 + \frac{2254 - 9277}{5.95} = -6680$$

$$Q_{b2} = 6500 + \frac{9468 - 7674}{7.05} = 6754 \qquad Q_{c2} = -6500 + \frac{9468 - 7674}{7.05} = -6246$$

$$Q_{c3} = 5000 + \frac{6921 - 3405}{5.25} = 5670 \qquad Q_{a4} = \frac{-2254 - 1128}{4.35} = -795$$

$$Q_{b5} = \frac{-191 - 95}{4.35} = -47 \qquad Q_{c6} = \frac{753 + 376}{4.35} = +266$$

Total moments:

$$M_{a1} = 2254 - 4320 \times 0.25 = +1174 \qquad M_{b1} = -9277 + 6680 \times 0.30 = -6277 \text{ kg m}$$

$$M_{b2} = 9468 - 6754 \times 0.25 = 7783 \text{ kg m} \qquad M_{c2} = -7674 + 6246 \times 0.25 = -6144 \text{ kg m}$$

$$M_{c3} = +6921 - 5670 \times 0.25 = 5501 \text{ kg m}$$

Example No. 2 (Fig. 12)
Distribution factors

TABLE 1

	d	a		b			c			e	f	k
	4	4	1	1	5	2	2	6	3	5	6	3
K_{ai}	—	0.357	0.643	0.372	0.322	0.306	0.332	0.222	0.446	—	—	—
μ_{ab}		ad 0.500	ab 0.580	ba 0.565	be 0.500	bc 0.558	cb 0.568	cf 0.500	ck 0.500			
			+6425	-6700		+9030	-8700		+5410			-4160
	-1148	-2295	-4130	-2400								
			+ 15	+ 26	+ 23	+ 21	+ 12			+ 12		
						+ 620	+1090	+ 728	+1460		+364	+730
			-130	-230	-200	-190	-106			-100		
	+ 20	+ 41	+ 74	+ 43								
				- 16	-14	-13	-7			-7		
							+37	+ 25	+ 51		+ 12	+ 25
M_{ai}	-1128	-2254	+2254	-9277	- 191	+9468	-7674	+ 753	+6921	- 95	+ 376	-3405

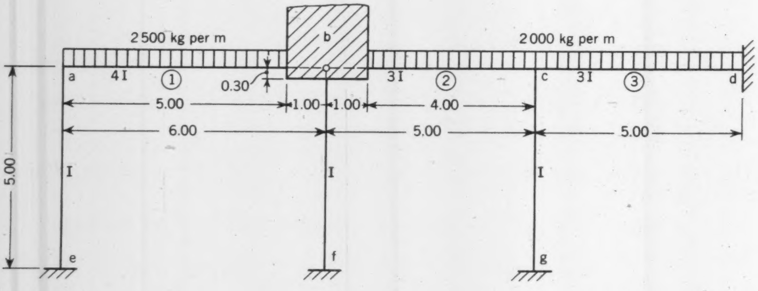

FIG. 12

Joint a:

$$b_{a1} = \frac{4\ E\ 4\ I}{5.50} = 2.91\ E\ I \qquad K_{a1} = \frac{2.91}{3.71} = 0.785$$

$$b_{a4} = \frac{4\ E\ I}{5.00} = \frac{0.80\ E\ I}{3.71\ E\ I} \qquad K_{a4} = \frac{0.80}{3.71} = \frac{0.215}{1.000}$$

Joint b:

$$b_{a1} = \frac{4\ E\ 4\ I}{5.5}\left[1 + 3\,\frac{1}{5.5} + 3\left(\frac{1}{5.5}\right)^2\right] = 4.78\ E\ I \qquad K_{b1} = \frac{4.78}{11.60} = 0.412$$

$$b_{b2} = \frac{4\ E\ 3\ I}{4.00}\left[1 + 3\,\frac{1}{4} + 3\left(\frac{1}{4}\right)^2\right] = 5.81\ E\ I \qquad K_{b2} = \frac{5.81}{11.60} = 0.501$$

$$b_{b5} = \frac{4\ E\ I}{4.70}\left(1 + 3\,\frac{0.30}{4.70}\right) = \frac{1.01\ E\ I}{11.60\ E\ I} \qquad K_{b5} = \frac{1.01}{11.60} = \frac{0.087}{1.000}$$

Joint c:

$$b_{c2} = \frac{4\ E\ 3\ I}{4.00} = 3\ E\ I \qquad K_{c2} = \frac{3.00}{6.20} = 0.485$$

$$b_{c3} = \frac{4\ E\ 3\ I}{5.00} = 2.40\ E\ I \qquad K_{c3} = \frac{2.40}{6.20} = 0.386$$

$$b_{c6} = \frac{4\ E\ I}{5.00} = \frac{0.80\ E\ I}{6.20\ E\ I} \qquad K_{c6} = \frac{0.80}{6.20} = \frac{0.129}{1.000}$$

Moments $\overline{M}_{a1}$

$$\overline{M}_{a1} = -\ \overline{M}_{b1} = \frac{2500 \times 5.5^2}{12} = 6300\ \text{kg} \qquad \overline{M}_{b2} = -\ \overline{M}_{c2} = \frac{2000 \times 4^2}{12} = 2660\ \text{kg}$$

$$\overline{M}_{c3} = -\ \overline{M}_{d3} = \frac{2000 \times 5^2}{12} = 4160\ \text{kg}$$

Shearing forces:

$$\overline{Q}_{b1} = Q^{\circ}_{b1} = -\ \frac{2500 \times 5.5}{2} = -\ 6880\ \text{kg}$$

$$\overline{Q}_{b2} = Q^{\circ}_{b2} = +\ \frac{2000 \times 4.0}{2} = +\ 4000\ \text{kg}$$

Fixed-end moments:

$$\overline{M}'_{a1} = +\ 6300\ \text{kg} \qquad \overline{M}'_{b1} = -\ 6300 - 6880 \times 1.0 = -\ 13180\ \text{kg}$$

$$\overline{M}'_{b2} = +\ 2660 + 4000 \times 1 = 6660\ \text{kg} \qquad \overline{M}'_{c2} = -\ 2660\ \text{kg}$$

$$\overline{M}'_{c3} = -\ \overline{M}'_{d3} = 4160\ \text{kg}$$

Carry-over factors:

$$\mu_{ab} = \frac{1}{2}\left(1 + 3\ \frac{1}{5.5}\right) = 0.773 \qquad \mu_{ae} = 0.500$$

$$\mu_{ba} = \frac{1}{2}\ \frac{\left(1 + 3\frac{1}{5.5}\right)}{1.644} = 0.470 \qquad \mu_{bf} = \frac{1}{2}\ \frac{\left(1 + 3\ \frac{0.30}{4.70}\right)}{1.191} \cong 0.500$$

$$\mu_{bc} = \frac{1}{2}\ \frac{\left(1 + 3\ \frac{1}{4.00}\right)}{1.938} = 0.452 \qquad \mu_{cg} = 0.500$$

$$\mu_{cb} = \frac{1}{2}\left(1 + \frac{3}{4}\right) = 0.875 \qquad \mu_{ed} = 0.500$$

For moments M'_{a1} (Table 2)
Shearing forces:

$$Q_{b1} = -\ 6880 + \frac{1925 - 12895}{6.50} = -\ 8570\ \text{kg}$$

$$Q_{b2} = +\ 4000 + \frac{11680 - 1761}{5.00} = 5980\ \text{kg}$$

TABLE 2

	e	a		b			c			d	f	g
	4	4	1	1	5	2	2	6	3	3	5	6
K	—	0.215	0.785	0.412	0.087	0.501	0.485	0.129	0.386	—	—	—
μ_{ab}	—	ae 0.500	ab 0.773	ba 0.470	bf 0.500	bc 0.452	cb 0.875	cg 0.500	cd 0.500	—	—	—
			+6300	-13180		+6660	-2660		+4160	-4160		
	-675	-1350	-4950	-3830								
			+2000	+4260	+900	+5190	+2350				+450	
	-215	-430	-1570	-1210		-1640	-1870	-500	-1480	-740		-250
			+550	+1170	+250	+1430	+645				+125	
	-59	-118	-432	-334		-274	-313	-83	-249	-125		-42
			+127	+250	+53	+305	+138				+27	
	-28	-27	-100	-77		-59	-67	-18	-53	-26		-9
				+56	+12	+68	+31				+5	
							-15	-4	-12	-6		-2
M_{xi}	-977	-1925	+1925	-12895	+1215	+11680	-1761	-605	+2366	-5057	+607	-303

Total moments:

$M_{a1} = 1925 \quad M_{b1} = -12895 + 8570 \times 1.0 = -4115$ kg

$M_{b2} = +11690 - 5980 \times 1.0 = -5700$ kg $\quad M_{c2} = -1761$ kg

$M_{c3} = +2366$ kg $\quad M_{d3} = -5057$ kg

Example No. 3 (Fig. 13)

$$l_o = \sqrt{4^2 + 2^2} = 4.47 \text{ m} \quad l_2 = l_3 = \sqrt{8^2 + 2^2} = 8.22 \text{ m}$$

1st Stage
Active moments

$$\overline{M}_{a2} = \overline{M}_{b2} = \frac{2 \times 8^2}{12} = 10.65 \text{ tm} \quad \overline{M}_{b3} = -\overline{M}_{c3} = +10.65 \text{ tm}$$

$$\overline{M}_{c5} = -\overline{M}_{d5} = \frac{2 \times 6^2}{12} = 6 \text{ tm}$$

Distribution factors
Joint b:

$K_{b2} = 0.500 \quad K_{b3} = 0.500$

Joint c:

$$a_{c3} = \frac{4 \text{ E } 5 \text{ I}_o}{8.22} = 2.44 \text{ E I}_o \quad K_{c3} = \frac{2.44}{5.44} = 0.448$$

$$a_{c4} = \frac{4 \text{ E I}_o}{4.00} = 1.00 \text{ E I}_o \quad K_{c4} = \frac{1.00}{5.44} = 0.184$$

$$a_{c5} = \frac{4 \text{ E } 3 \text{ I}_o}{6} = \frac{2.00 \text{ E I}_o}{5.44 \text{ E I}_o} \quad K_{c5} = \frac{2.00}{5.44} = 0.368$$

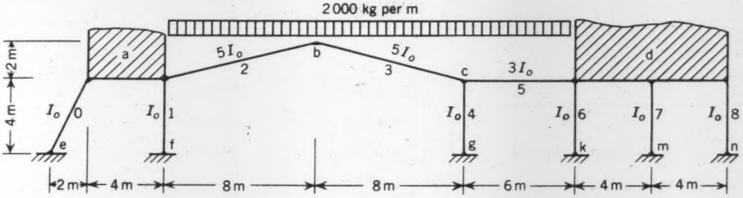
2000 kg per m
a
$5I_o$
b
$5I_o$
2
3
c
$3I_o$
5
d
2 m
4 m
I_o
0
I_o
1
I_o
4
I_o
6
I_o
7
I_o
8
e
f
g
k
m
n
2m
4m
8m
8m
6m
4m
4m

FIG. 13

Carry-over factors: $\mu = \pm \frac{1}{2}$

The moments of the 1st stage are given in Table 3.
Restraining forces of 1st stage (Fig. 16).

$$V_a = 16 + \frac{10.375 - 8.714}{16} = 16.104 \text{ t}$$

Moments relative to b: $2\text{ H} + 10.375 - 11.199 - 16.104 \times 8 + 16 \times 4 = 0$

$$\text{H} = 32.82 \text{ t}$$

Moments relative to 0_a:

$$8.94\ F_I = 32.82 \times 8 + 10.375 \qquad \overrightarrow{F_I} = 30.56 \text{ t}$$

$$\overleftarrow{F_{II}} = -\ 32.91 + \frac{0.908 + 0.454}{4} = -\ 32.47 \text{ t}$$

2nd stage:
Virtual displacement diagrams
a. For removal of imaginary roller restraint I (Fig. 14)

$$\theta_a^I = -\frac{1}{8.94}\ \delta_I = -\ 0.112\ \delta_I \qquad \rho_a^I = -\ 0.112 \qquad \delta_{a1}^I = \delta_1^I = \frac{8.00}{8.94}\ \delta_I = 0.895\ \delta_I$$

$$c_1^I = 0.895 \qquad \rho_2^I = -\frac{1}{8.94}\ \frac{8.00}{4.00} = -\ 0.224 \qquad c_2^I = -\ 0.224 \times 8.22 = -\ 1.84$$

$$\delta_2^I = -\ 1.84\ \delta_I \qquad c_3^I = +\ 1.84 \qquad \delta_3^I = +\ 1.84\ \delta_I$$

$$c_4^I = c_5^I = c_6^I = c_7^I = c_8^I = 0$$

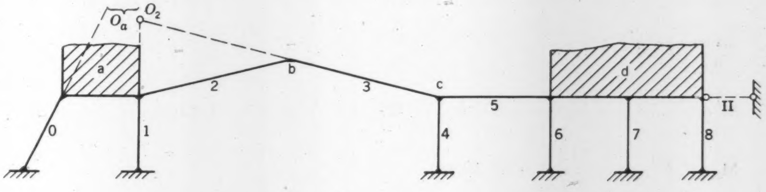
O_a
O_2
a
b
2
3
c
5
d
II
0
1
4
6
7
8

FIG. 14

TABLE 3

	a	b		c			d	g
	2	2	3	3	4	5	5	4
K_{ai}	—	0.500	0.500	0.448	0.184	0.368	—	—
	+10650	-10650	+10650	-10650		+6000	-6000	
			+ 1040	+ 2080	+ 860	+1710	+855	+430
	-260	-520	-520	-260				
			+ 58	+ 116	+48	+96	+48	+24
	-15	-29	-29					
M_{ai}	+10375	-11199	+11199	-8714	+908	+7806	-5097	+454

Computation of u°_{ai} and u°_{bi}

General formulas:

$$u^\circ_{ai} = \left[- \left(2\,\rho_a + \rho_b\right) \frac{l_i}{3} + c_i \right] \frac{6\,E\,I_i}{l_i}$$

$$u^\circ_{bi} = \left[- \left(\rho_a + 2\,\rho_b\right) \frac{l_i}{3} + c_i \right] \frac{6\,E\,I_i}{l_i}$$

$$6\,E\,I_o = 100 \text{ tm}$$

$$u^\circ_{ao} = \left(2 \times 0.112 \times \frac{4.47}{3} + 1\right) \frac{6\,E\,I_o}{4.47} = 29.8 \text{ tm} \quad u^\circ_{eo} = \left(0.112 \times \frac{4.47}{3} + 1\right) \frac{6\,E\,I_o}{4.47} = 26.10 \text{ tm}$$

$$u^\circ_{a1} = \left(2 \times 0.112 \times \frac{4.00}{3} + 0.895\right) \frac{6\,E\,I_o}{4} = 29.8 \text{ tm} \quad u^\circ_{f1} = \left(0.112 \times \frac{4}{3} + 0895\right) \frac{6\,E\,I_o}{4} = 26.10 \text{ tm}$$

$$u^\circ_{a2} = \left(2 \times 0.112 \times \frac{8.22}{3} - 1.84\right) \frac{6\,E\,5\,I_o}{8.22} = -\,74.6 \text{ tm}$$

$$u^\circ_{b2} = \left(0.112 \times \frac{8.22}{3} - 1.84\right) \frac{6\,E\,5\,I_o}{8.22} = -\,93.4 \text{ tm}$$

$$u^\circ_{b3} = u^\circ_{c3} = 1.84\ \frac{6\,E\,5\,I_o}{8.22} = 112.0 \text{ tm}$$

$$\overline{M}^I_{ao} = 29.8\,\frac{1}{4.47} = 6.66 \text{ tm} \qquad \overline{M}^I_{eo} = 26.1\,\frac{1}{4.47} = 5.83 \text{ tm}$$

$$\overline{M}^I_{a1} = 29.8\,\frac{1}{4} = 7.45 \text{ tm} \qquad \overline{M}^I_{f1} = 26.1\,\frac{1}{4} = 6.53 \text{ tm}$$

$$\overline{M}^I_{a2} = -\,74.6\ \frac{1}{8.22} = -\,9.07 \text{ tm} \qquad \overline{M}^I_{b3} = -\,\frac{93.4}{8.22} = -\,11.35 \text{ tm}$$

$$\overline{M}^I_{b3} = \overline{M}^I_{c3} = +\,\frac{112}{822} = +\,13.60 \text{ tm}$$

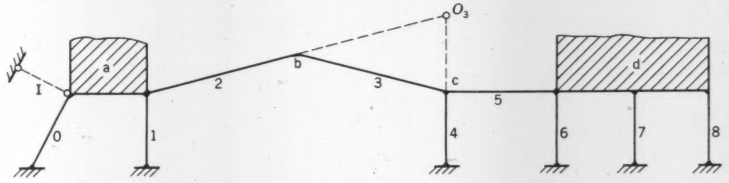
O_3
a
I
0
1
2
b
3
c
4
5
d
6
7
8

FIG. 15

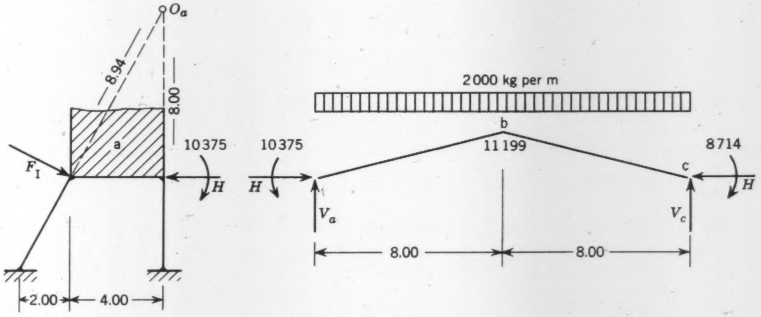
O_a
8.94
8.00
a
F_I
10375
H
2.00
4.00
2000 kg per m
b
11199
10375
H
V_a
8714
c
H
V_c
8.00
8.00

FIG. 16

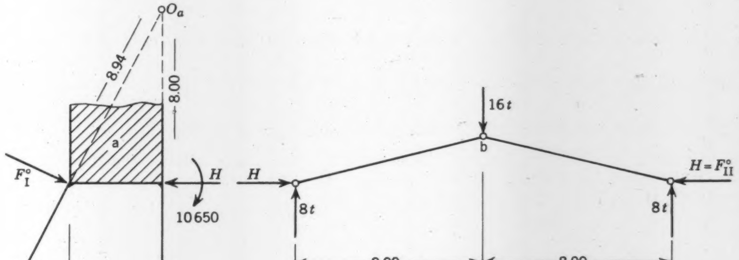
O_a
8.94
8.00
a
F_I°
H
10650
2.00
4.00
16t
b
H
8t
$H = F_{II}^\circ$
8t
8.00
8.00

FIG. 17

TABLE 4

	a	b		c			d	g
	2	2	3	3	4	5	5	4
K_{ai}	—	0.500	0.500	0.448	0.184	0.368	—	—
	-9070	-11350	+13600	+13600				
			- 3050	- 6100	-2500	-5000	-2500	-1250
	+ 200	+ 400	+ 400	+ 200				
			- 45	- 90	- 37	- 73	- 36	- 19
	+ 11	+ 22	+ 23	+ 12				
				- 6	- 2	- 4		
M_{ai}	-8859	-10928	+10928	+7616	-2539	-5077	-2536	-1269

The moments for removal of the imaginary roller restraint I are given in Table 4.

Restraining forces - Shear forces

$M^I_{ao} = +6660$ kg m $M^I_{eo} = +5830$ kg m $M^I_{a1} = 7450$ kg m

$M^I_{f1} = +6530$ kg m $M^I_{a2} = -8859$ kg m $M^I_{b2} = -10928$ kg m

$M^I_{b3} = +10928$ kg m $M^I_{c3} = +7616$ kg m $M^I_{c4} = -2539$ kg m $M^I_{g4} = -1268$ kg m

$M^I_{c5} = -5077$ kg m $M^I_{d5} = -2536$ kg m $M^I_{d6} = M^I_{k6} = M^I_{d7} = M^I_{m7} = M^I_{d8} = M^I_{n8} = 0$

$$Q^I_o = \frac{6660 + 5830}{4.47} = 2800 \text{ kg} \qquad Q^I_1 = \frac{7450 + 6530}{4.00} = 3490 \text{ kg}$$

$$Q^I_2 = \frac{-8859 - 10928}{8.22} = -2400 \text{ kg} \qquad Q^I_3 = \frac{7616 + 10928}{8.22} = 2260 \text{ kg}$$

$$Q^I_4 = \frac{-2539 - 1269}{4} = -950 \text{ kg}$$

$$F^I_I = 2800 + 0.895 \times 3490 + 2400 \times 1.84 + 2260 \times 1.84 + 0.112(6660 + 7450 - 8859)$$

$$F^I_I = 15.19 \text{ t}$$

$$F^I_{II} = -2400 \times 2.065 - 2260 \times 2.055 - 0.950 \times 1 = -10.53 \text{ t}$$

For removal of imaginary roller restraint II (Fig. 15)

$$\delta^{II}_4 = \delta^{II}_6 = \delta^{II}_7 = \delta^{II}_8 = 1 \qquad c^{II}_4 = c^{II}_6 = c^{II}_7 = c^{II}_8 = +1 \qquad \theta^{II}_a = 0$$

$$e_{c3} = 4.00 \text{ m} \qquad e_{b3} = 16.44 \text{ m} \qquad \rho^{II}_d = 0$$

$$\delta_3 = -\frac{8.22}{4.00}\,\delta_{II} = -2.055\,\delta_{II} \qquad c^{II}_3 = -2.055 \qquad \theta^{II}_a = 0$$

$$\rho^{II}_a = 0 \qquad c^{II}_2 = +2.055 \qquad c^{II}_o = c^{II}_1 = c^{II}_5 = 0$$

$$6\ E\ I_o = 100\ \text{tm}$$

$$\overline{M}^{II}_{c4} = \overline{M}^{II}_{g4} = \overline{M}^{II}_{d6} = \overline{M}^{II}_{d7} = \overline{M}^{II}_{m7} = \overline{M}^{II}_{d8} = \overline{M}^{II}_{n8} = \frac{6\ E\ I_o}{4}\ \frac{1}{4} = 6250\ \text{kg m}$$

$$\overline{M}^{II}_{a2} = \overline{M}^{II}_{b2} = \frac{6\ E\ 5\ I_o}{8.22}\ \frac{2.055}{8.22} = 15200\ \text{kg m}$$

$$\overline{M}^{II}_{b3} = \overline{M}^{II}_{c3} = -\ 15200\ \text{kg m}$$

The moments for the removal of the imaginary pinned member II are given in Table 5.

Moments:

$$M^{II}_{ao} = M^{II}_{eo} = M^{II}_{a1} = M^{II}_{f1} = 0 \qquad M^{II}_{a2} = +\ 14672 \qquad M^{II}_{b2} = +\ 14144\ \text{kg m}$$

$$M^{II}_{b3} = -\ 14144 \qquad M^{II}_{c3} = -\ 11491 \qquad M^{II}_{c4} = +\ 7997 \qquad M^{II}_{g4} = +\ 7124\ \text{kg m}$$

$$M^{II}_{c5} = +\ 3494 \qquad M^{II}_{d5} = 1747\ \text{kg m}$$

$$M^{II}_{d6} = M^{II}_{k6} = M^{II}_{d7} = M^{II}_{m7} = M^{II}_{d8} = M^{II}_{n8} = 6250\ \text{kg m}$$

Shear forces:

$$Q^{II}_2 = \frac{14672 + 14144}{8.22} = 3510\ \text{kg} \qquad Q^{II}_3 = \frac{-\ 14144\ -\ 11491}{8.22} = -\ 3120\ \text{kg}$$

$$Q^{II}_4 = \frac{7997 + 7124}{4} = 3780\ \text{kg} \qquad Q^{II}_5 = \frac{3494 + 1749}{6} = 873\ \text{kg}$$

$$Q^{II}_6 = Q^{II}_7 = Q^{II}_8 = \frac{6250 + 6250}{4} = 3125\ \text{kg}$$

Restraining forces:

$$F^{II}_{I} = -\ 1.84 \times 3.510 - 1.84 \times 3.120 + 0.112 \times 14.672 = -\ 10.54\ \text{t}$$

$$F^{II}_{II} = 3.510 \times 2.055 + 3.120 \times 2.055 + 3.780 + 3 \times 3.125 = 26.84\ \text{t}$$

TABLE 5

	a	b		c			d	g
	2	2	3	3	4	5	5	4
K_{ai}	—	0.500	0.500	0.448	0.184	0.368	—	—
	+15200	+15200	-15200	-15200	+6250			+6250
			+ 2000	+ 4000	+1650	+3300	+1650	+ 825
	-500	-1000	-1000	-500				
			+ 112	+224	+92	+184	+92	+46
	- 28	-56	-56	-28				
				+13	+5	+10	+5	+3
M_{ai}	+14672	+14144	-14144	-11491	+7997	+3494	+1747	+7124

Convertion factors:

$$+ 15.19 x_1 - 10.54 x_2 + 30.56 = 0$$

$$- 10.53 x_1 + 26.84 x_2 - 32.47 = 0$$

$$x_1 = - 1.62 \qquad x_2 = 0.570$$

Total moments:

$$M_{ao} = - 6660 \times 1.62 = - 10780 \text{ kg m} \qquad M_{eo} = - 5830 \times 1.62 = - 9450 \text{ kg m}$$

$$M_{a1} = - 7450 \times 1.62 = - 12050 \text{ kg m} \qquad M_{f1} = - 6530 \times 1.62 = - 10580 \text{ kg m}$$

$$M_{a2} = + 8859 \times 1.62 + 14672 \times 0.57 + 10375 = + 33085 \text{ kg m}$$

$$M_{b2} = + 10928 \times 1.62 + 14144 \times 0.57 - 11199 = + 14561 \text{ kg m}$$

$$M_{b3} = - 10.928 \times 1.62 - 14144 \times 0.57 + 11199 = - 14561 \text{ kg m}$$

$$M_{c3} = - 7616 \times 1.62 - 11491 \times 0.57 - 8714 = - 27574 \text{ kg m}$$

$$M_{c4} = + 2539 \times 1.62 + 7997 \times 0.57 + 908 = + 9578 \text{ kg m}$$

$$M_{g4} = 1268 \times 1.62 + 7124 \times 0.57 + 454 = + 6564 \text{ kg m}$$

$$M_{c5} = 5077 \times 1.62 + 3494 \times 0.57 + 7806 = + 18006 \text{ kg m}$$

$$M_{d5} = 2536 \times 1.62 + 1747 \times 0.57 - 5097 = + 7 \text{ kg m}$$

$$M_{d6} = M_{k6} = M_{d7} = M_{m7} = M_{d8} = M_{n8} = 6250 \times 0.57 = 3560 \text{ kg m}$$

Example No. 4.—The rigid frame of Example 3 is worked out again by the one stage method.

Constants of diagrams of virtual displacement

Group I:

$$c_o^I = + 1 \qquad c_1^I = 0.895 \qquad c_2^I = - 1.84 \qquad c_3^I = + 1.84 \qquad \rho_a^I = - 0.112 \qquad \rho_a^I = 0$$

$$c_5^I = 0 \qquad c_4^I = c_6^I = c_7^I = c_8^I = 0$$

Group II:

$$c_o^{II} = 0 \qquad c_1^{II} = 0 \qquad c_2^{II} = + 2.055 \qquad c_3^{II} = - 2.055 \qquad \rho_a^{II} = 0 \qquad \rho_d^{II} = 0$$

$$c_5^{II} = 0 \qquad c_4^{II} = c_6^{II} = c_7^{II} = c_8^{II} = + 1$$

Distribution factors due to rotation:

Joint b:

$$K_{b2} = 0.500$$

$$K_{b3} = 0.500$$

Joint c:

$$K_{c3} = 0.448$$

$$K_{c4} = 0.184$$

$$K_{c5} = 0.368$$

Carry-over factors: $\mu = + \frac{1}{2}$

Restraining factors:

For the case of the rigid frame all members have

$$\left(M_{ai}\right)' = M_{ai} \text{ and } \left(l_i\right)' = l_i$$

General formula:

$$\sigma_{a1} = \Sigma_i \frac{3}{2} K_{ai} \frac{c_i^I}{l_i} - \Sigma_r \rho_r^I \Sigma \frac{K_{ar}}{2}$$

Group I:

$$\sigma_{bI} = -\frac{1.84}{8.22} \frac{3}{2} \times 0.500 + \frac{1.84}{8.22} \frac{3}{2} 0.500 - (-0.112) \frac{0.500}{2} = +0.028$$

$$\sigma_{cI} = \frac{1.84}{8.22} \times \frac{3}{2} \times 0.448 = +0.150$$

Group II:

$$\sigma_{bII} = + \frac{2.055}{8.22} \times 0.500 \times \frac{3}{2} - \frac{2.055}{8.22} \times 0.500 \times \frac{3}{2} = 0$$

$$\sigma_{cII} = - \frac{2.055}{8.22} \times 0.448 \times \frac{3}{2} + \frac{1}{4} \times 0.184 \frac{3}{2} = -0.099$$

Distribution factors due to displacement:

Group I:

Computed $\bar{u}_{ai}^I$: In the case examined: $\bar{u}_{ai}^I = u_{ai}^{\circ}$

$$u_{ao}^{\circ I} = \left(2 \times 0.112 \times \frac{4.47}{3} + 6\right) \frac{6\,E\,I_o}{4.47} = 1.790\,E\,I_o$$

$$u_{eo}^{\circ I} = \left(0.112 \times \frac{4.47}{3} + 1\right) \frac{6\,E\,I_o}{4.47} = 1.565\,E\,I_o$$

$$u_{a1}^{\circ I} = \left(2 \times 0.112 \times \frac{4.00}{3} + 0.895\right) \frac{6\,E\,I_o}{4.00} = 1.790\,E\,I_o$$

$$u_{f1}^{\circ I} = \left(0.112 \times \frac{4.00}{3} + 0.895\right) \frac{6\,E\,I_o}{4.00} = 1.565\,E\,I_o$$

$$u_{a2}^{\circ I} = \left(2 \times 0.112 \times \frac{8.22}{3} - 1.84\right) \frac{6\,E\,5\,I_o}{8.22} = -4.48\,E\,I_o$$

$$u_{b2}^{\circ I} = \left(0.112 \times \frac{8.22}{3} - 1.84\right) \frac{6\,E\,5\,I_o}{8.22} = -5.60\,E\,I_o$$

$$u_{b3}^{\circ I} = 1.84 \times \frac{6\,E\,5\,I_o}{8.22} = 6.72\,E\,I_o = u_{c3}^{\circ I}$$

$$\frac{u_{ao}^{\circ I} + u_{eo}^{\circ I}}{l_o} \frac{c_o^I}{l_o} = \frac{1.790 + 1.565}{4.47} \frac{1}{4.47}\,E\,I_o = +0.168\,E\,I_o$$

$$\frac{u_{a1}^{\circ I} + u_{f1}^{\circ I}}{l_i} \frac{c_1^I}{l_i} = \frac{1.790 + 1.565}{4.00} \frac{0.895}{4.00}\,E\,I_o = +0.187\,E\,I_o$$

$$\frac{u_{a2}^{\circ I} + u_{b2}^{\circ I}}{l_2} \frac{c_2^I}{l_2} = \frac{4.48 + 5.60}{8.22} \frac{1.84}{8.22}\,E\,I_o = +0.275\,E\,I_o$$

$$\frac{u_{b3}^{\circ I} + u_{c3}^{\circ I}}{l_3} \frac{c_3^I}{l_3} = \frac{6.72 + 6.72}{8.22} \frac{1.84}{8.22}\,E\,I_o = \begin{array}{c}\underline{+0.367\,E\,I_o} \\ 0.997\,E\,I_o\end{array}$$

$$\Sigma_r \rho_r^I \Sigma \frac{u_{rk}^{\circ I}}{l_k} = -0.112 \left(\frac{1.79\,E\,I_o}{4.47} + \frac{1.79\,E\,I_o}{4} - \frac{4.48\,E\,I_o}{8.22}\right) = -0.031\,E\,I_o$$

TABLE 6

	e	f	a			b		c		
	0	1	0	1	2	2	3	3	4	5
K_{ai}	—	—	—	—	—	0.500	0.500	0.448	0.184	0.368
σ_{aI}			—			+0.028		+0.150		
σ_{aII}			—			+0.000		-0.090		
$\bar{q}^{I}_{ai}$	+0.341	+0.382	+0.390	+0.436	-0.531	-0.664	+0.795	+0.795	—	—
$\bar{q}^{II}_{ai}$	—	—	—	—	+0.548	+0.548	-0.548	-0.548	+0.225	—
					+10650	-10650	+10650	-10650		+6000
							+1040	+2080	+860	+1710
					-260	-520	-520	-8570	+860	+7710
						-11170	+11170	260		
	-10400	-11620	-11870	-13300	+16180	+20200	-24200	-24200		
					+6160	+6160	-6160	-6160	+2530	
					+1000	+2000	+2000	+1000		
						+28360	-28360	+12120	+4990	+9980
							+6060	-17500	+7520	+9980
	+242	+272	+278	+310	-378	-472	+566	+566		
					+1610	+1610	-1610	-1610	+662	
					-1538	-3077	-3077	-1538		
						-1939	+1939	+860	+352	+708
							+430	-1722	+1014	+708
	+390	+437	+447	+500	-608	-760	+910	+910		
					+534	+534	-534	-534	+219	
					-145	-290	-290	-145		
						-516	+516	-202	-83	-165
							-101	+29	+136	-165
	+171	+191	+195	+218	-266	-342	+398	+398		
					+170	+170	-170	+70		
					+11	+22	+23	+11		
						-150	+150	-138	-57	-114
							-69	+101	+13	-114
	+60	+68	+69	+77	-94	-117	+141	+141		
					+52	+52	-52	-52	+22	
						+23	+22	+11		
						-42	+42	-55	-22	-45
								+45	+0.00	-45
M_{ai}	-9537	-10652	-10881	-12195	+33078	+14543	-14543	-27617	+9543	+18074

TABLE 6.—*CONTINUED*

d				g	k	m	n	F_I	F_{II}
5	6	7	8	4	6	7	8	$m_I{}^I$	$m_{II}{}^I$
—	—	—	—	—	—	—	—	—	-0.697
—				—	—	—	—	$m_I{}^{II}$	$m_{II}{}^{II}$
—				—	—	—	—	-0.430	—
—	—	—	—	—	—	—	—		
—	0.225	0.225	0.225	0.225	0.225	0.225	0.225		
-6000								+29800	-32000
+ 855								+ 698	- 418
				+ 430				- 29	—
								+30469	+21200
								- 4830	- 11218
	+2530	+2530	+2530	+2530	+2530	+2530	+2530		
								+ 108	—
+4990				+2495				+ 4060	- 2440
								- 712	- 498
	+ 662	+ 662	+ 662	+ 662	+ 662	+ 662	+ 662	- 1260	- 2938
								- 172	—
+ 354				+ 176				+ 288	- 173
								- 1144	- 800
	+ 219	+ 219	+ 219	+ 219	+ 219	+ 219	+ 219	- 418	- 973
								- 16	—
- 82				- 41				- 68	+ 40
								- 502	- 350
	+ 70	+ 70	+ 70	+ 70	+ 70	+ 70	+ 70	- 132	- 310
								+ 1	—
- 72				- 28				- 46	+ 28
								- 177	- 123
	+ 22	+ 22	+ 22	+ 22	+ 22	+ 22	+ 22		- 95
+ 45	+3503	+3503	+3503	+6535	+3503	+3503	+3503		

$$\Sigma_i \frac{u^{\circ I}_{ai} + u^{\circ I}_{bi}}{l_i} \frac{c^I_i}{l_i} - \Sigma_r \rho^I_r \Sigma \frac{u^{\circ I}_{rk}}{l_k} = (+\,0.997 + 0.031)\; E\, I_o = +\,1.028\; E\, I_o$$

$$\bar{q}^I_{ao} = \frac{\frac{1.79}{4.47}}{1.028} = +\,0.390 \quad \bar{q}^I_{eo} = \frac{\frac{1.565}{4.47}}{1.028} = +\,0.341 \quad \bar{q}^I_{a1} = \frac{\frac{1.79}{4.00}}{1.028} = +\,0.436$$

$$\bar{q}^I_{f1} = \frac{\frac{1.565}{4.00}}{1.028} = +\,0.382 \quad \bar{q}^I_{a2} = -\frac{\frac{4.48}{8.22}}{1.028} = -\,0.531 \quad \bar{q}^I_{b2} = \frac{-\frac{5.60}{8.22}}{1.028} = -\,0.664$$

$$\bar{q}^I_{b3} = \bar{q}^I_{c3} = \frac{\frac{6.72}{8.22}}{1.028} = 0.795 \quad \bar{q}^I_{c4} = \bar{q}^I_{f4} = \bar{q}^I_{c5} = \bar{q}^I_{d5} = \bar{q}^I_{d6} = \bar{q}^I_{k6} = \bar{q}^I_{d7} = \bar{q}^I_{m7}$$

$$= \bar{q}^I_{d8} = \bar{q}^I_{m8} = 0$$

Check:

$$\frac{0.390 + 0.341}{4} \times 1 + \frac{0.436 + 0.382}{4} \times 0.895 + \frac{0.531 + 0.664}{8.22} \times 1.84$$

$$+ \frac{0.795 + 0.795}{8.22} \times 1.84 - (-0.112)(0.390 + 0.436 - 0.531)$$

$$= +\,1.004$$

Group II:

$$u^{\circ II}_{ao} = u^{\circ II}_{co} = 0 \quad u^{\circ II}_{a1} = u^{\circ II}_{f1} = 0 \quad u^{\circ II}_{o2} = u^{\circ II}_{b2} = \frac{6\; E\; 5\; I_o}{8.22} \times 2.055 = 7.50\; E\, I_o$$

$$u^{\circ II}_{b3} = u^{\circ II}_{c3} = \frac{6\; E\; 5\; I_o}{8.22}\; (-\,2.055) = -\,7.50\; E\, I_o \quad u^{\circ II}_{c5} = u^{\circ II}_{a5} = 0$$

$$u^{\circ II}_{c4} = u^{\circ II}_{g4} = \frac{6\; E\, I_o}{4} \times 1.0 = 1.50\; E\, I_o$$

$$u^{\circ II}_{d6} = u^{\circ II}_{k6} = u^{\circ II}_{d7} = u^{\circ II}_{m7} = u^{\circ II}_{d8} = u^{\circ II}_{n8} = 1.50\; E\, I_o$$

$$\frac{u^{\circ II}_{a2} + u^{\circ II}_{b2}}{l_2} \frac{c^{II}_2}{l_2} = \frac{2 \times 7.50\; E\, I_o}{8.22} \; \frac{2.055}{8.22} = 0.458\; E\, I_o$$

$$\frac{u^{\circ II}_{b3} + u^{\circ II}_{c3}}{l_3} \frac{c^{II}_3}{l_3} = -\,\frac{2 \times 7.50\; E\, I_o}{8.22} \times \frac{(-\,2.055)}{8.22} = 0.458\; E\, I_o$$

$$\frac{u^{\circ II}_{c4} + u^{\circ II}_{g4}}{l_4} \frac{c^{II}_4}{l_4} = \frac{2 \times 1.50\; E\, I_o}{4.00} \times \frac{1}{4.00} = 0.1875\; E\, I_o$$

$$\Sigma_i \frac{u^{\circ II}_{ai} + u^{\circ II}_{bi}}{l_i} \frac{c^{II}_i}{l_i} - \Sigma_r \rho^{II}_r \Sigma_k \frac{u^{\circ II}_{rk}}{l_k} = (2 \times 0.458 + 4 \times 0.1875)\; E\, I_o$$

$$= 1.666\; E\, I_o$$

$$\bar{q}^{II}_{ao} = \bar{q}^{II}_{eo} = \bar{q}^{II}_{a1} = \bar{q}^{II}_{f1} = 0$$

$$\bar{q}^{II}_{a2} = \bar{q}^{II}_{b2} = \frac{\frac{7.50}{8.22}}{1.666} = 0.548 \qquad \bar{q}^{II}_{b3} = \bar{q}^{II}_{c3} = -0.548$$

$$\bar{q}^{II}_{c4} = \bar{q}^{II}_{g4} = \frac{\frac{1.50}{4.00}}{1.666} = 0.225 \qquad \bar{q}^{II}_{d6} = \bar{q}^{II}_{k6} = \bar{q}^{II}_{d7} = \bar{q}^{II}_{m7} = \bar{q}^{II}_{d8} = \bar{q}^{II}_{n8} = 0.225$$

Check:

$$4 \times \frac{0.548}{8.22} \times 2.055 + 8 \times \frac{0.225}{4.00} \times 1 = 0.998$$

Shear carry-over factors:

General formula: $m^{I}_{II} = \Sigma_i \left(\bar{q}^{I}_{ki} + \bar{q}^{I}_{bi}\right) \frac{c_i^{II}}{l_i} - \Sigma_r\, \rho^{II}_r\, \Sigma_k\, \bar{q}^{I}_{rk}$

$$m^{I}_{II} = (-0.531 - 0.664)\ \frac{2.055}{8.22} - \frac{2 \times 0.795}{8.22} \times 2.055 = -0.697$$

$$m^{II}_{I} = -\ \frac{2 \times 1.84 \times 0.548}{8.22} - \frac{0.548 \times 1.84 \times 2}{8.22} - (-0.112) \times 0.548 = -0.430$$

Fixing forces: (Fig. 17)

$$\overline{M}_{a2} = -\ \overline{M}_{b2} = -\ 10650 \text{ kg m} \quad \overline{M}_{b3} = -\ \overline{M}_{c3} = 10650 \text{ kg m} \quad \overline{M}_{c5} = -\ \overline{M}_{d5} = 6000 \text{ kg m}$$

$$2\text{ H} = 8 \times 8 \qquad \text{H} = 32 \text{ t} \qquad F^{\circ}_{I} = \frac{32 \times 8 + 10.65}{8.94} = 29.80 \text{ t}$$

$$F^{\circ}_{II} = -\ 32.00 \text{ t}$$

The successive approximations and the arrangement of the operations is tabulated in Table 6.

APPENDIX II.—NOTATION

The following symbols are adopted for use in the paper and for the guidance of discussers:

a = Factor of stiffness to rotation;

b = new factor of stiffness to rotation;

E = modulus of elasticity;

F = fixing forces of the 1st stage;

I = moment of inertia;

k = factor of distribution;

l = length;

m = shear carry-over factor;

N = normal force;

P = forces or loads;

Q = shearing force;

u = factor of stiffness to displacement;

δ = displacement;

θ = rotation;

μ = carry-over factor;

μ_{ab} = carry-over factor from joint a to joint b; and

σ = restraining factor.

DISCUSSION

PERING-FEI GOU.[4]—Moliotis has derived a general formula to express the new index of stiffness and formulas expressing the carry-over factor for such frames whose joints of the frames are a small undeformed area. Those formulas can also be derived by the well known slope-deflection equation. The derivations are given subsequently.

Derivation of the Index of Stiffness.—In Fig. 18 the bending moments are given by the slope-deflection equations

$$M_a = 2 \, E \, K \left(2 \, \theta_a + \theta_b + 3 \, \frac{d_a \, \theta_a}{l}\right) \ldots \ldots \ldots \ldots (81)$$

and

$$M_b = 2 \, E \, K \left(2 \, \theta_b + \theta_a + 3 \, \frac{d_a \, \theta_a}{l}\right) \ldots \ldots \ldots \ldots (82)$$

Member AB is in equilibrium, then

$$Q_a = Q_b = \frac{1}{l} \left(M_a + M_b\right) = 2 \, E \, K \left[\frac{\theta_a}{l} \left(3 + 6 \, \frac{d_a}{l}\right) + 3 \, \frac{\theta_b}{l}\right] \ldots . (83)$$

Member AA′ is in equilibrium too, then

$$M_a' = M_a + Q_a \, d_a \ldots \ldots \ldots \ldots \ldots \ldots (84)$$

---

[4] Asst. Civ. Engrg. Dept., Chen Kung Univ., Taiwan, Taiwan Free China.

Substitute Eqs. 81 and 83 into Eq. 84 results in

$$M'_a = 2\ E\ K \left[2 + 6\ \frac{d_a}{l} + 6 \left(\frac{d_a}{l}\right)^2\right] \theta_a + 2\ E\ K\ \left[1 + 3\ \frac{d_a}{l}\right] \theta_b \quad . . . . (85)$$

By the definition of stiffness (that is a moment which, when applied at the pin end of a beam will cause there unit rotation when the far end is fixed against rotation) then we let θ_b equal to zero and θ_a equal to 1. Therefore

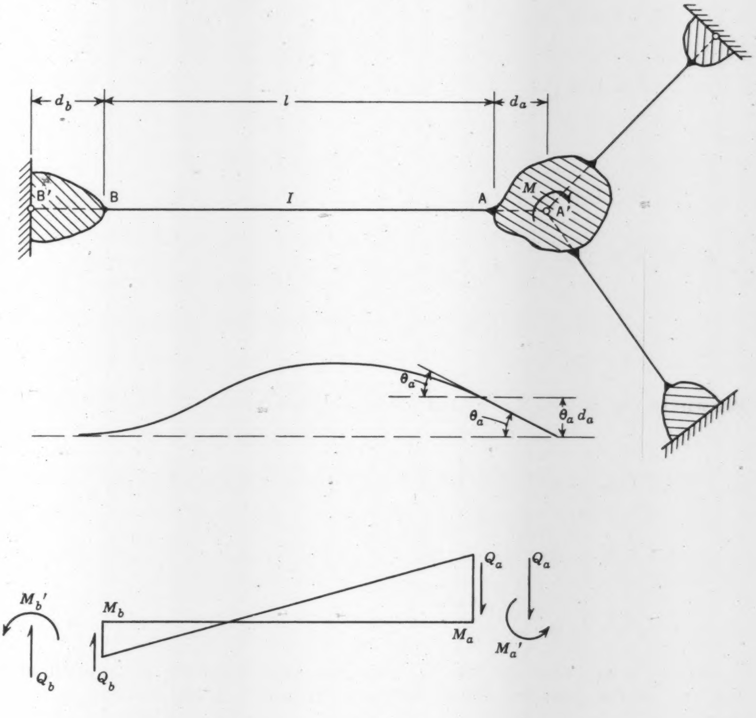

FIG. 18

$$S_a = 4\ E\ K \left[1 + 3\ \frac{d_a}{l} + 3\left(\frac{d_a}{l}\right)^2\right] . . . . (86)$$

If $d_a = 0$, then $S = 4\ E\ K$. That is the general expression of stiffness under the assumption that the joints of the ridge frame are point connections.

Eq. 86 is identical with Eq. 13.

Special Case

(a) $M_b = 0$ That is the case which the joint B is a pin. Then

$$\theta_b = -\frac{1}{2}\left(1 + 3\frac{d_a}{l}\right)\theta_a \quad \dots\dots\dots\dots\dots\dots \quad (87)$$

Substitute Eq. 87 into Eq. 85 and let $\theta_a = 1$, then

$$S = 2\,E\,K\left[2 + 6\frac{d_a}{l} + 6\left(\frac{d_a}{l}\right)^2 - \frac{1}{2} - 3\frac{d_a}{l} - \frac{9}{2}\left(\frac{d_a}{l}\right)^2\right]$$

$$= 2\,E\,K\left[1.5 + 3\frac{d_a}{l} + 1.5\left(\frac{d_a}{l}\right)^2\right]$$

and

$$= 3\,E\,K\left(1 + 2\frac{d_a}{l} + \frac{d_a^2}{l^2}\right) \quad \dots\dots\dots\dots\dots\dots \quad (88)$$

(b) $M_a = 0$ Then

$$\theta_a = -\frac{\theta_b}{-2 + \dfrac{3\,d_a}{l}} \quad \dots\dots\dots\dots\dots\dots \quad (89)$$

Substitute Eq. 89 into Eq. 35 and let $\theta_a = 1$, results in

$$S = 2\,E\,K\left[2 + 6\frac{d_a}{l} + 6\left(\frac{d_a}{l}\right)^2\right] - 2\,E\,K\left[2 + 9\frac{d_a}{l} + 9\left(\frac{d_a}{l}\right)^2\right]$$

$$= 2\,E\,K\left[-3\left(\frac{d_a}{l}\right) - 3\left(\frac{d_a}{l}\right)^2\right]$$

$$= -6\,E\,K\left[\left(\frac{d_a}{l}\right) + \left(\frac{d_a}{l}\right)^2\right] \quad \dots\dots\dots\dots\dots\dots \quad (90)$$

(c) $\theta_a = \theta_b$ That is, the member rotates through the same angle at the far end as the near end and in the same direction. In Eq. 85 let $\theta_a = \theta_b = 1$, then

$$S = 2\,E\,K\left[2 + 6\frac{d_a}{l} + 6\left(\frac{d_a}{l}\right)^2\right] + 2\,E\,K\left[1 + 3\frac{d_a}{l}\right]$$

$$= 6\,E\,K\left[1 + 3\left(\frac{d_a}{l}\right) + 2\left(\frac{d_a}{l}\right)^2\right] \quad \dots\dots\dots\dots\dots\dots \quad (91)$$

In $d_a = 0$, then $S = 6\,E\,K$. This is the modified stiffness of those rigid frames whose joints are point connection.

(d) $\theta_a = -\theta_b$. That is the case which the member of a frame rotates through the same angle at the far end as at the near end, but in the opposite direction. Or in other words, it is the case of symmetrical condition. In Eq. 85, let $\theta_a = -\theta_b = 1$, then

$$S = 2\,E\,K\left[2 + 6\left(\frac{d_a}{l}\right) + 6\left(\frac{d}{l}\right)^2 - 2\,E\,K\left[1 + 3\left(\frac{d_a}{l}\right)\right]\right.$$

$$= 2\,E\,K\left[1 + 3\left(\frac{d_a}{l}\right) + 6\left(\frac{d_a}{l}\right)^2\right] \quad \ldots\ldots\ldots\ldots\ldots\ldots (92)$$

Eq. 92 is the modified stiffness of a symmetrical condition of point joint rigid frame, if $d_a = 0$.

Derivation of Carry-Over Factors

$$M_b' = M_{ba} + Q_b\,d_b$$

$$= 2\,E\,K\left(2\,\theta_b + \theta_a + 3\,\frac{d_a\,\theta_a}{l}\right) + 2\,E\,K\left(3\,\theta_a + 6\,\frac{d_a\,\theta_a}{l} + 3\,\theta_b\right)\frac{d_b}{l}$$

$$= 2\,E\,K\left[\left(1 + 3\,\frac{d_b}{l}\right)\theta_a + \left(2 + 3\,\frac{d_b}{l}\right)\theta_b + 3\left(1 + 2\,\frac{d_b}{l}\right)\frac{d_a\,\theta_a}{l}\right] \quad \ldots (93)$$

By the definition of carry-over factor

$$M_b' = \mu_{ab}\,M_a' \quad \ldots\ldots\ldots\ldots\ldots\ldots\ldots (94)$$

Substitute Eqs. 93 and 85 for M and M, respectively, in Eq. 94

$$\mu_{ab} = \frac{\left[\left(1 + 3\,\frac{d_b}{l}\right)\theta_a + \left(2 + 3\,\frac{d_b}{l}\right)\theta_b + 3\left(1 + 2\,\frac{d_b}{l}\right)\frac{d_a\,\theta_a}{l}\right]}{2\left[1 + 3\,\frac{d_a}{l} + 3\left(\frac{d_a}{l}\right)^2\right]\theta_a + \left[1 + 3\,\frac{d_a}{l}\right]\theta_b} \quad \ldots (95)$$

Eq. 95 is the general expression of carry-over factor and it is practically equal to the Eq. 19.

Special Cases.—

(a) $\theta_b = 0$ This is the case which section B is fixed end

$$\mu_{ab} = \frac{1}{2}\,\frac{1 + 3\,\frac{d_a + d_b}{l} + 6\,\frac{d_a\,d_b}{l^2}}{1 + 3\,\frac{d_a}{l} + 3\left(\frac{d_a}{l}\right)^2} \quad \ldots\ldots\ldots\ldots (96)$$

(b) $M_b = 0$ That is the case which the section B is a pin-joint. Substitute θ_b of Eq. 87 for θ_b in Eq. 95, then

$$\mu_{ab} = \frac{1.5\,\frac{d_b}{l} + 1.5\,\frac{d_a\,d_b}{l^2}}{1.5 + 3\,\frac{d_a}{l} + 1.5\left(\frac{d_a}{l}\right)^2} = \frac{\frac{d_b}{l}\left(1 + \frac{d_a}{l}\right)}{1 + 2\,\frac{d_a}{l} + \left(\frac{d_a}{l}\right)^2} \quad \ldots\ldots (97)$$

(c) $M_a = 0$ That is member built-in at one end, pin-joint at Section A. From Eqs. 89 and 95

$$\mu_{ab} = \frac{\left(1 + 3\ \frac{d_b}{l}\right) - \left[4 + 6\ \frac{d_a}{l} + 6\ \frac{d_b}{l} + 9\ \frac{d_a\ d_b}{l^2}\right] + \left[3\ \frac{d_a}{l} + 6\ \frac{d_a\ d_b}{l^2}\right]}{2 + 6\ \frac{d_a}{l} + 6\left(\frac{d_a}{l}\right)^2 - \left[2 + 9\left(\frac{d_a}{l}\right) + 9\left(\frac{d_a}{l}\right)^2\right]}$$

$$= \frac{1 + \frac{d_a + d_b}{l} + \frac{d_a\ d_b}{l^2}}{\frac{d_a}{l}\left[1 + \left(\frac{d_a}{l}\right)\right]} = \frac{1 + \frac{d_b}{l}}{\frac{d_a}{l}} \quad \ldots\ldots\ldots\ldots\ldots\ldots\ldots (98)$$

(d) $\theta_a = \theta_b$ Eq. 95 can be changed into Eq. 99

$$\mu_{ab} = \frac{\left[3 + 6\ \frac{d_b}{l} + 3\ \frac{d_a}{l} + 6\ \frac{d_a\ d_b}{l}\right]}{\left[3 + 9\ \frac{d_a}{l} + 6\left(\frac{d_a}{l}\right)^2\right]} = \frac{1 + 2\left(\frac{d_b}{l}\right)}{1 + 2\left(\frac{d_a}{l}\right)} \quad \ldots\ldots (99)$$

(e) $\theta_a = -\ \theta_b$ Then

$$\mu_{ab} = \frac{1 + 3\ \frac{d_b}{l} - 2 - 3\ \frac{d_b}{l} + 3\ \frac{d_a}{l} + 6\ \frac{d_a\ d_b}{l^2}}{1 + 3\ \frac{d_a}{l} + 6\left(\frac{d_a}{l}\right)^2}$$

$$= \frac{-\ 1 + 3\ \frac{d_a}{l} + 6\ \frac{d_a\ d_b}{l^2}}{1 + 3\ \frac{d_a}{l} + 6\left(\frac{d_a}{l}\right)^2} \quad \ldots\ldots\ldots\ldots\ldots\ldots (100)$$

PANGIOTIS D. MOLIOTIS,[5] **M. ASCE.**—Pering-Fei Gou gives a different and interesting method of computing distribution and carry-over factors using the slope-deflection equations.

In computing distribution and carry-over factors, an identical route was followed as that used in the classical case of computing the factors in framed structures with point joints and not small undeformed areas.

It is considered more advisable to follow this route because the writer is of the opinion that it will be easier for the reader to follow a similar method for computing the distribution and carry-over factors than that used in the classical case.

The goal of this study is to compute framed structures, whose joints are not points, but small undeformed areas, by the method of successive approximations which facilitates designing for engineers.

---

[5] Dir. Civ. Engrg., National Technical Univ., Athens, Greece.

AMERICAN SOCIETY OF CIVIL ENGINEERS
Founded November 5, 1852
TRANSACTIONS

Paper No. 3263

RESEARCH ON FIRE RESISTANCE OF PRESTRESSED CONCRETE

By Hubert Woods[1]

With Discussion by Messrs. V. Paschkis; and Hubert Woods

SYNOPSIS

Most of the engineering information available on the fire endurance of concrete is of an empirical nature. A science of design for fire endurance, comparable to the existing science of design for mechanical loads, has not yet been developed.

With the strikingly rapid increase in use of prestressed concrete, the need for research facilities devoted specifically to concrete became pressing. Such facilities have been provided, as described, in the new Fire Research Center of Portland Cement Association (PCA).

The research program there comprises two separate but intimately related parts; there are tests with large furnaces and small-scale basic research on properties of concrete and steel at high temperatures. A long range objective is to assist in the development of reliable predictive methods.

In the lighter prestressed flexural elements, the concrete cover over the steel, and the mass or cross-sectional area are both important to fire endurance. Research in the Netherlands has resulted in recommendations that take both factors into account.

Note.—Published essentially as printed here, in November, 1960, in the Journal of the Structural Division, as Proceedings Paper 2640. Positions and titles given are those in effect when the paper or discussion was approved for publication in Transactions.

[1] Dir. of Research, Portland Cement Assoc. Research and Development Lab., Skokie, Ill.

At present, prestressed members can be designed to have any reasonable fire endurance period. More work needs to be done to achieve the ultimate in lightness and economy.

INTRODUCTION

Prestressed concrete was well known and widely used in Europe long before it had any considerable use in the United States. It is therefore natural that European research and development work on prestressed concrete should have been, until recently, considerably advanced over that in the United States. This is particularly true with respect to investigations on fire resistance of prestressed concrete. Much of the significant work on this subject has been done in Europe, particularly in England and in the Netherlands. Unfortunately, some code authorities in the United States are either unaware of that work, or seem unwilling to accept it. A good deal of it is applicable to types of elements of construction used in this country, although some of it is not.

Most of the engineering information now available on the fire endurance of concrete, or to speak more accurately, on the fire endurance of building elements made of concrete (prestressed or conventionally reinforced), is of a purely empirical nature. This information has been developed over the years by relatively few agencies who have commonly found themselves so pressed for commercial fire "ratings" and other "ad hoc" information, that little time and money have been available for research. In consequence, there has not been a science of design developed for fire endurance comparable to the existing science of design for mechanical loads.

NEW RESEARCH FACILITIES PROVIDED

In view of these circumstances, and with the strikingly rapid increase in the use of prestressed concrete structural members in this country, the need for adequate fire research facilities in the United States, specifically devoted to concrete, became very pressing. Aware of this need, the Portland Cement Association, in 1957, started construction of a unique fire research laboratory to house the necessary personnel and equipment. This laboratory, known as the Fire Research Center, is shown in Fig. 1. The interior arrangement is shown in Fig. 2. The frontal two-story wing contains a fundamental research laboratory, furnace control and recording equipment, a shop, and offices.

The first full-scale furnace installed was a beam furnace shown in Fig. 3. This has a firebox 40 ft long and 6 ft 4 in. wide. The furnace is provided with outboard hydraulic hold-down systems at the ends, for use in studies of the effects of continuity, and when so used can accommodate beams 60 ft long. Live load is applied by other hydraulic cylinders at the top. The furnace is gas fired, and can be programmed to follow various time-temperature curves. At present, the standard ASTM curve is being used.

All control functions and all recording of temperatures of furnace and of steel or concrete in specimens, and of all strains, deflections, and loads, are centralized in the control room shown in Fig. 4. The recording and control equipment in this room can also be used with any of several other furnaces to be

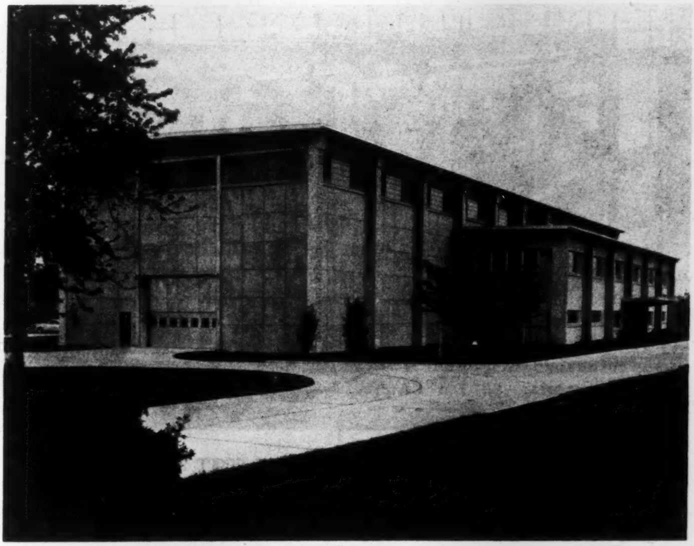

FIG. 1.—FIRE RESEARCH CENTER

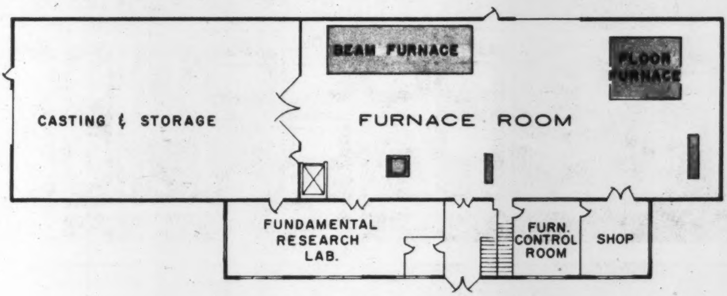
BEAM FURNACE
FLOOR FURNACE
CASTING & STORAGE
FURNACE ROOM
FUNDAMENTAL RESEARCH LAB.
FURN. CONTROL ROOM
SHOP

FIRST FLOOR PLAN

FIG. 2.—INTERIOR ARRANGEMENT OF THE FIRE RESEARCH CENTER

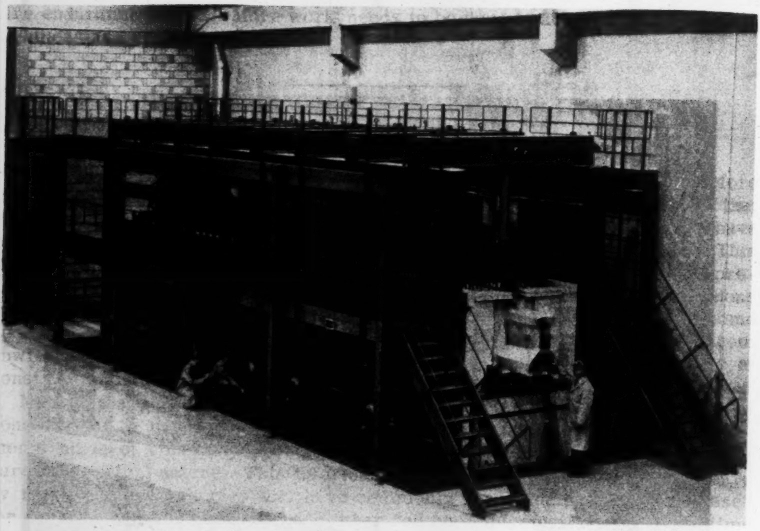

FIG. 3.—BEAM FURNACE

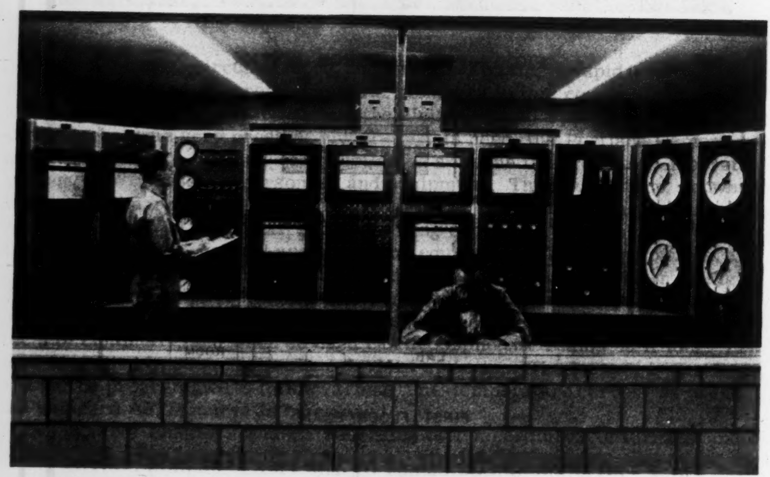

FIG. 4.—CONTROL ROOM

provided. One of these additional furnaces, now under construction, is a floor furnace for specimens 14 ft by 18 ft. A unique feature of this floor furnace is the provision of means for applying known amounts of edge restraint and edge moment to elements under test.

EDGE RESTRAINT

The present standard fire testing procedure is not specific regarding the amount of edge restraint, if any, to be applied to floor or roof sections under test. It merely says, in effect, that if the assembly to be tested represents a form of construction that restrains structural elements, then that assembly will be surrounded by a restraining frame that simulates such restraint. However, there seems to be no information as to how much edge restraint is actually imposed on a floor section in a building during a fire. It seems evident that the edge restraint would depend greatly upon the nature and size of the building in which it is located, and on its specific position in the building.

Nevertheless, it has long been common practice, in fire testing floor sections, to surround them with a very heavy steel restraining frame, resulting in a large but unknown restraint. The specific effect of this restraint upon the observed fire endurance of elements under test is not known, but could be highly significant. It was this consideration that led to the provision of hydraulic edge restraint means, in the floor furnace described, so that the matter can be investigated.

FIRE TEST OF A PRESTRESSED BEAM

The beam furnace (Fig. 3) has been in use for some months. The first beam to be tested was a heavy duty prestressed bridge beam 43 ft 6 in. long. This beam is not an exceptionally large one as prestressed beams go, but it probably is the largest so far to be tested for fire endurance. A cross-section of this beam is shown in Fig. 5. There are twenty one 7/16 in. diam strands; the seven 7/16 in. diam harped strands are indicated in the shaded zone. In the furnace, it was loaded with a 92,000 lb design load distributed equally over eight equally-spaced points, and subjected to the standard ASTM firing schedule shown in Fig. 6. After firing for 4 hr 31 min at which time the furnace temperature was 2050° F, the fire was shut off, principally because there was no reason for continuing it further. The beam was still intact and carrying full load. Initial deflection due to dead and live loads before firing was 0.3 in. When the firing was stopped, the deflection was 6.35 in. Twenty-four hours later it was 5.25 in. A close-up view of the beam after test, but still in the furnace, is shown in Fig. 7. This shows that a small amount of concrete had spalled off the lower corners, exposing one of the strands. The vertical pipe near the center is one of a number of thermocouple tubes used in furnace control.

In view of the excellent fire endurance of this beam, it was subsequently subjected to an ultimate structural load test to determine the beam's residual strength. The beam failed at a total live load of 117,700 lb distributed over 12 equally-spaced load points, by the crushing of concrete in the upper flange.

Center deflection at failure, due to fire test and application of ultimate load, was 10 in.

IMPORTANCE OF MASS AND COVER

The remarkable performance of this beam no doubt depended largely on its great mass, and hence its capacity for absorbing heat. Research in this country and abroad has shown that the mass or cross-sectional area of beams, and the amount of cover over steel strands, are both of great importance to their fire endurance. The reason why both cross section and cover are important is simple; both affect the rate of heating of the prestressed strands, and it is commonly the loss of prestress in these strands at elevated temperature that is directly responsible for failure of the element. In the Netherlands, recommendations which take both factors into account are emphasized and are shown[2] in Table 1.

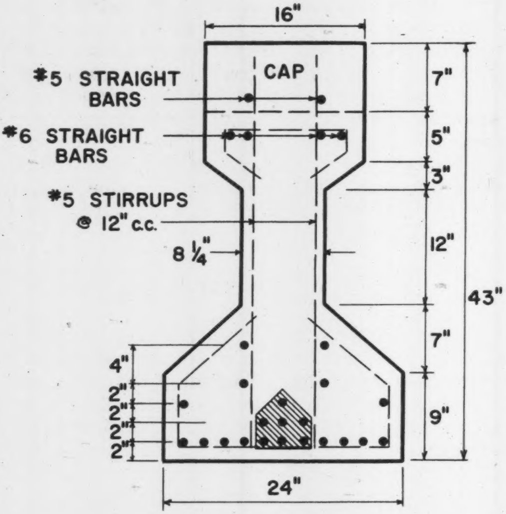

FIG. 5.—CROSS-SECTION AT THE CENTER LINE

PROPERTIES OF PRESTRESSING STEEL AT ELEVATED TEMPERATURE

The high tensile strength wire, ordinarily used for prestressing, is relatively more sensitive to high temperature than is ordinary steel. Fig. 8 shows[3] some of the significant properties of currently used prestressing steel as influenced by elevated temperature. Fig. 8 (a) shows the lowered strength as temperature is raised, the strength being reduced by 50% at about 705° F. Fig. 8 (b) shows the elongation, or creep, of the wire during one hour at the indicated temperatures when the stress is maintained at 50% of original ultimate strength. In addition to the effects of temperature on strength and creep of high tensile strength wires, it has been observed that the modulus of elasticity decreases with temperature, so that at about 575° F the modulus may be 80% of its value at room temperature. The combined result of these several effects is to induce virtually complete loss of prestress at a wire temperature of about 800° F, though the wire strength is still about half that at room temperature.

---

[2] Adapted from "Fire Tests of Prestressed Concrete Beams," Commissie Voor Utivoering van Research . . . C.U.R., Rapport 13, Netherlands, January, 1958. In Dutch.

[3] "Steel Wire for Prestressed Concrete," by W. O. Everling, presented at First National Prestressed Concrete Short Course, St. Petersburg, Fla., October, 1955.

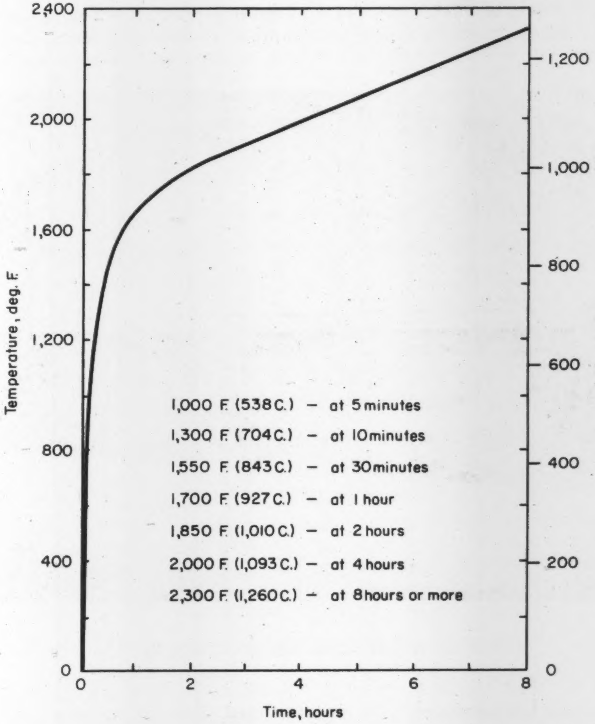

FIG. 6.—STANDARD TIME-TEMPERATURE CURVE

PREDICTION OF FIRE ENDURANCE

From an analytical point of view, the problem of predicting the fire endurance of a prestressed concrete element resolves itself, in the first place, into that of predicting the time required for the prestressing wires or cables to reach the critical temperature of 800° F. If the temperature of the gases to which the element is exposed were known, as well as the surface coefficient of heat transfer, the conductivity and specific heat of the concrete, and of any insulating coating that might be used, and if the element were a simple geometric shape such as a semi-infinite flat slab in which the heat flow was uni-directional, then it might appear that a solution could be had using mathematical methods already worked out for heat flow. However, the surface coefficients are not known, and the conductivity and specific heat of concrete are not constants, but change with temperature and are inadequately known.

It can, therefore, be seen that even the simplest practical case is not simple analytically. Other practical cases, for example, a beam with bottom and sides exposed to high temperature, present additional difficulties because the heat flow is bi-directional rather than uni-directional; and if the beam does not have a regular cross section, further difficulties of a geometric nature will be met. These considerations are presented to suggest some of the reasons why complete analytical solutions have not been reached.

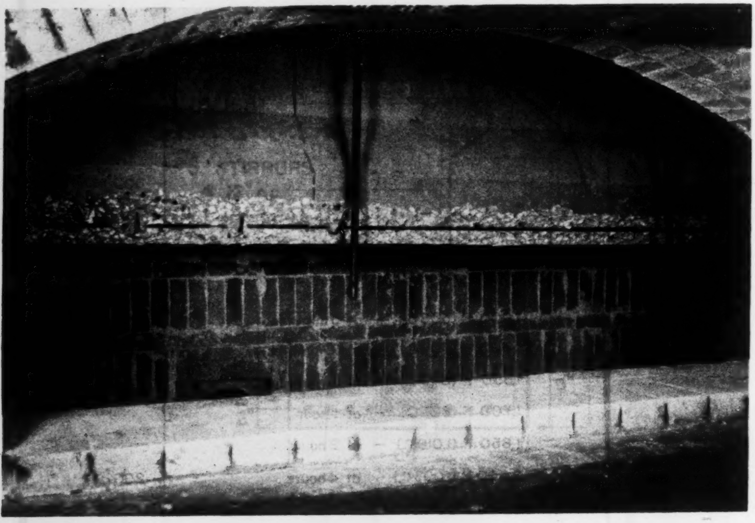

FIG. 7.—BEAM STILL INSIDE FURNACE

NEED FOR BASIC RESEARCH

With building construction and new building methods and materials playing such an important role in our economy, the volume of required fire test work has grown tremendously. With present standard methods, such work is very slow and costly. More rapid and less expensive methods and approaches must be developed. This need is providing an impetus for fundamental research in this field, looking toward a much improved science of design. Specifically, the needs are (1) acceptably reliable analytical solutions for predicting fire endurance and (2) reliable small-scale methods for fire testing to confirm predictions and substitute, at least in part, for the costly full-scale testing now required. It is not to be expected that such developments will completely eliminate the need for full-scale tests, but they will minimize the need for them.

Some progress has been made; Clarke[4,5] has applied heat-flow principles to slabs and other geometric shapes with some degree of success. Robertson and Gross[6] and Lawson and McGuire[7] have used electric network analogs in which voltage represents temperature, electrical resistance represents thermal resistivity, electrical capacitance represents heat capacity, and so on. The use of physical models suggests itself. This is a powerful approach that will eventually contribute greatly to a reduction of time and cost in research and in the engineering estimation of fire endurance. However, "scaling" laws have not been developed to the point of confidence in their application, and, indeed, are not likely to be so developed, or accepted, until a much better basic understanding of the full-size case is in hand. Nevertheless, models are now being used to save time and cost in studying the effect of certain variables and in gaining a better understanding of the heating process, even though the results cannot always be applied quantitatively and directly to the full-size case.

TABLE 1.—RECOMMENDED COVER AND CROSS-SECTIONAL AREA FOR PRESTRESSED CONCRETE BEAMS FOR VARIOUS FIRE ENDURANCE PERIODS

Required endurance time, in hours	Depth of cover required, in inches				
	Cross sectional area, in square inches				
	16-32	32-78	78-160	160-320	Over 320
1/2	1.2	0.8	0.8	0.8	0.8
1	-	2.0	1.6	1.2	1.2
1 1/2	-	-	2.4	1.6	1.2
2	-	-	-	2.4	2.0
3	-	-	-	-	3.2
4	-	-	-	-	4.0?

PRESENT STANDARD TEST METHODS

The attention of investigators over the world is being focused on the adequacy and realism of current methods of testing and specifying the fire endurance of building elements. Several specific points are at issue.

---

[4] "The Estimation of the Fire Endurance of Floors, Columns, and Beams," by J. H. Clarke, Technical Record No. B.S. 44/153/1/226, unpublished report, Experimental Bldg. Sta., Commonwealth of Australia, June, 1958.

[5] "Method of Assessing Probable Fire Endurance of Load-Bearing Columns," by J. H. Clarke, Journal, ACI, Vol. 31, No. 12, June, 1960, p. 1223.

[6] "An Electrical Analog Method for Transient Heat-Flow Analysis," by A. F. Robertson and Daniel Gross, Journal of Research, N. B. S., Vol. 61, No. 2, August, 1958, p. 105.

[7] "The Solution of Transient Heat Flow Problems by Analogous Electric Networks, by D. I. Lawson and J. H. McGuire, Proceedings, Inst. of Mech. Engrg., A, 167, 1952, p. 275.

Fire Severity.—The standard ASTM time-temperature curve (Fig. 6), that is in use in many countries, requires a continuously rising temperature up to eight hours. This is not at all characteristic of the great majority of fires in buildings in which the temperature starts to decline well before eight hours. This discrepancy between the present standard time-temperature curve and most real fires is particularly marked in buildings constructed of noncombustible materials. In such cases, the only fuel available to sustain a fire is the combustible material stored in the building, and the quantity of such material ranges from very little, in some occupancies, up to a maximum in others. The present testing procedure takes no account of the nature of the occupancy of the building, that is, the amount of combustible material, or fuel, that is, or may be, present.

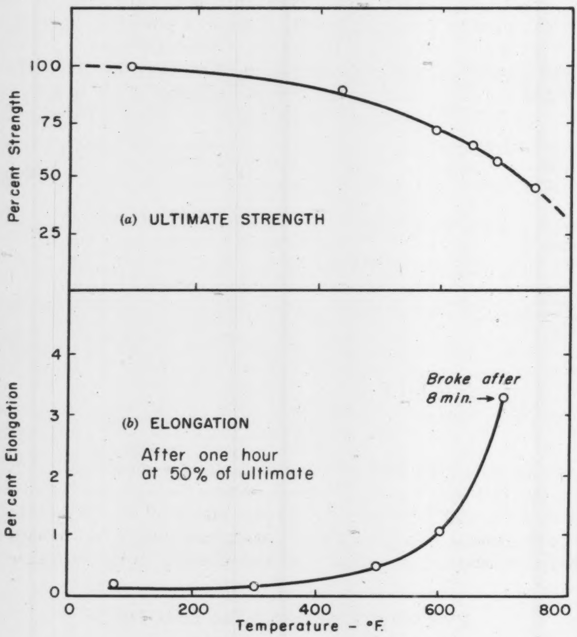

FIG. 8.—PROPERTIES OF PRESTRESSING STEEL AT ELEVATED TEMPERATURES

Early consideration should be given to a change in the testing procedure by adopting a "fire-load exposure" or limited heat input, in place of the present arbitrary time-temperature curve.

Criteria of Failure.—(1) At present, a floor construction undergoing a standard fire test is deemed to have failed if it collapses, if holes or cracks develop in it of a size to pass sufficient flame or hot gas to ignite cotton waste, or if the unexposed face (that is, the face away from the fire) increases in temperature by 250° F. Generally, the beginning temperature in a building would be about

70° F, so when the temperature of the unexposed face reaches 320° F, for example, the fire endurance period is deemed to have ended. This limitation is imposed with the thought of preventing spread of fire by ignition of combustibles stored on a floor under which there is a fire. However, the requirement is unrealistic and unnecessarily severe, and thus arbitrarily penalizes certain constructions. A British fire authority has stated privately that, in investigations of thousands of fires in London, no case of ignition and fire spread from temperature rise of the unexposed surface was uncovered.

(2) There is at present no generally accepted criterion of failure of a beam in a fire test other than failure to sustain the design load. Does this mean actual collapse? It would seem better to define the end point in some other and more definite way, perhaps by a limiting deflection stated in terms of the span.

An ASTM Committee (E-5) is currently studying these and other problems connected with fire testing of elements of construction. A number of agencies, including several in the United States and Canada, in England, the Netherlands, Russia, Japan, and Australia are active in fire research and fire testing. Some of these agencies are vitally interested in the basic problems previously discussed and are doing significant work on them.

PRESENT PROGRAM AT PCA

The current program of research at the new laboratory of the PCA has two primary aspects that are intimately related.

1. Fundamental research is being conducted on the properties of concrete and concrete materials at elevated temperatures; of importance in this connection are thermal properties and elastic properties. Knowledge of such properties will be essential in model studies and in contributing to the improvement of analytical approaches for predicting performance of structural concrete elements. It is also required in arriving at a better understanding of some aspects of the observed behavior of concrete elements subjected to fire, such as the spalling that sometimes occurs.

2. At present, work in large scale fire research is concerned with flexural elements of prestressed concrete. The following matters are being or will be investigated:

A. Effect of concrete thickness over prestressing steel;

B. Influence of aggregate type and moisture condition of concrete at time of testing;

C. Method of prestressing - pretensioning and post-tensioning;

D. Effect of cross-sectional shape and size (mass);

E. Effect of partial prestressing and supplementary mild steel reinforcing;

F. Exploratory study of influence of continuous design on fire resistance of prestressed concrete beams; and

G. Supplementary investigations.

Part A is now in progress using I-beams. Concrete cover is 1 in., 2 in., and 3 in. Aggregates are sand and gravel for half the beams and expanded shale for the others. Part B will use I-beams with 2 in. minimum cover over the steel. Aggregates will include sand and gravel, crushed limestone and natural sand, expanded shale, clay, or slate, and slag. Two moisture contents will be employed: that corresponding to the present 70% relative humidity recommended by ASTM Committee E-5, and that corresponding to 50% relative humidity. The results of these researches will be reported from time to time in the technical press.

CONCLUSIONS

It may be observed that prestressed concrete structural elements can be produced to have any reasonably required fire endurance period. This is clearly shown by work already carried out by other investigators and exemplified in Table 1. It is, however, evident that to approach the ultimate in lightness and economy consistent with fire safety will require much more study.

DISCUSSION

V. PASCHKIS.[8]—The author describes the expense and complication of the very elegant direct fire resistance tests that he performed and then calls for less expensive methods. The electric network analog work of which Mr. Woods speaks was pioneered at Columbia University, and, as far as the writer knows, the computer available at Columbia is the largest available in the western world (the Russians have published the availability of such a computer with 20,000 nodes; the Columbia computer has 600 nodes).[9]

As Mr. Woods explains, success or failure of a structure depends on whether the wires or cables reach a critical temperature of 800° F. A versatile computer such as the one at Columbia permits the determination of which of the several properties, heat-transfer coefficient, conductivity, specific heat, and density of the concrete, and what geometry (degree of covering of the wire) contributes most to an extension of the time to reach this critical temperature. Such a determination can be made even if the thermal properties, including the heat-transfer coefficient, are not known accurately. On the computer it is possible to vary the several variables over a wide range and thus to determine which is controlling. Then, if necessary, efforts can be made to determine these few controlling parameters more accurately.

The author suggests, as an alternate method of investigation, the use of small-scale models and states that the "scaling laws" have not been developed. If the small-scale model is to be subjected to the actual fire and loading, the scaling has to include both the mechanical strength and the thermal process. The scaling regarding the thermal process is understood, but is difficult. Assuming that the model can be made of the same material, having the same thermal properties as the original system, equal temperatures will be achieved under consideration of the following simple relationship between time scale and length scale: the ratio of time to reach a given temperature at a given point in the original system to that in the model system equals the square of the ratio of the original length dimension to the length dimension in the scale model.

---

[8] Prof. of Mech. Engrg., Dir., Heat and Mass Flow Analyzer Lab., Columbia Univ., New York, N. Y.

[9] "Mathematical Machines and Their Significance for Science and the National Economy," by V. I. Loskutov, Priborostroenniye, Instrument Construction, No. 11, 1958, pp. 8-12.

However, for this simple rule to apply, the heat-transfer coefficients have to be changed in such a manner that the characteristic figure m remains constant. This figure is defined as

$$m = \frac{k}{h\,L} \quad \ldots\ldots\ldots\ldots\ldots\ldots\ldots (1)$$

in which h is the heat transfer coefficient, expressed, for example, in Btu/ft^2, hr, F; k represents the thermal conductivity of the concrete, expressed in Btu/ft, hr, F° and L is the length. The value of h in the scale model must be changed proportionally to the change in geometric size. This, given a certain flame temperature, is exceedingly difficult to achieve, so much so that the writer would question the probability of achieving a satisfactory scale model approach, if the value h is important.

Again, to determine whether h is important, the analog computation, as indicated previously, would be inexpensive and helpful.

HUBERT WOODS.[10]—The necessarily brief statement by the writer regarding the possible use of small-scale models and of computers in fire research has been usefully augmented by Paschkis. He has specified some of the basic difficulties encountered with models. Principally because of such difficulties, the writer's use of models has been confined to studies in which complete similitude with the full-scale case is not necessary. These small-scale studies continue to be very useful.

For the more complex problem of an analytical approach to the full-scale case, analog computers or digital computers or both may prove extremely valuable. To use either kind of computer requires that the problem be reduced to mathematical statements capable of solution. This is not easy, but several agencies are giving attention to it.

---

[10] Dir. of Research, Portland Cement Assoc. Research and Development Lab., Skokie, Ill.

AMERICAN SOCIETY OF CIVIL ENGINEERS
Founded November 5, 1852
TRANSACTIONS

Paper No. 3264

PROPERTIES OF STEEL AND CONCRETE AND THE BEHAVIOR OF STRUCTURES

By George Winter,[1] F. ASCE

With Discussion by Messrs. Ralph L. Barnett; Lester H. Gabriel; Henry J. Cowan; Oliver G. Julian; A. Zaslavsky; Paul Zia; and George Winter

SYNOPSIS

A vast amount of new information on performance of structural materials under load is in the process of affecting, in a far-reaching manner, many established design procedures, and of creating new methods to replace outmoded approaches. At the present rate of development few engineers manage to familiarize themselves in detail with the results of pertinent research. Yet most of these new departures cannot be understood without such familiarity. The aim of this paper is to review, broadly, the basic features of these new findings on materials performance and structural behavior. They relate not only to plastic or inelastic materials properties, but also to brittle fracture, fatigue, residual stresses, creep, strength under combined stress, actual versus specified strength, and the like. Each of these features is presented not by itself, but in relation to overall performance of structures of the civil engineering type. None of the quoted research is of the writer's creation, and the only originality that can be claimed is one of presentation and interpretation.

Note.—Published essentially as printed here, in February, 1960, in the Journal of the Structural Division, as Proceedings Paper 2384. Positions and titles given are those in effect when the paper or discussion was approved for publication in Transactions.

[1] Prof., and Head, Dept. of Structural Engrg., Cornell Univ., Ithaca, N. Y.

INTRODUCTION

In his early training every structural engineer has become acquainted with the basic tools of his art in a course known as "Strength of Materials". This designation is as complete a misnomer as one will ever find in technical literature. In fact, most of the subject matter of "Strength of Materials" has little connection either with strength or with materials. It might more appropriately be called "Stresses and Deformations of Ideally Elastic Members." This describes, in brief, that conventional approach to structural design which has dominated established engineering practice until very recently. It consists, in essence, of computing stresses at design loads on the basis of assumed elasticity, and in implying that these stresses, in a manner rarely stated explicitly, have some relation to the strength and performance of the structure.

The revolution now under way in many fields of structural engineering is not correctly described by the juxtaposition of the terms "plastic" and "elastic." It is much more aptly characterized by the concepts of "strength" versus "stress." This revolution, in short, consists in the recognition that to be optimal in regard to safety and economy, design must be based on rational methods for predicting the actual strength of the structure (so that design loads can be held below that strength by an adequate margin), supplemented by means of predicting performance at service loads (so that impairment of serviceability by excessive deformation, vibration, etc., can be prevented.) Wherever it is the plastic properties of a material which govern the strength of a structure, "plastic analysis or design" is in the process of replacing the conventional "elastic" methods. Where other features determine strength and performance, attention is increasingly focused on them.

Among these other features are: Brittle fracture of normally ductile materials; the strength, brittle or ductile, of materials subject to bi- and triaxial conditions of stress; creep as it affects not so much the strength as the serviceability of some types of structures; fatigue of structures subject to large numbers of not necessarily cyclic load repetitions. In addition, increasing attention is being paid to the actual properties of structural materials "as received" (as distinct from their stipulated, nominal minimum properties) and on the statistical distribution of these actual properties as a guide for a realistic assessment of structural safety. The methods evolving from all these tendencies differ increasingly from the conventional approach of comparing an elastically computed stress with a stipulated fraction of a specified, nominal materials property.

And yet, the supercilious disparagement of conventional "elastic design," fashionable among some of the more enthusiastic exponents of the "plastic" methods, is misplaced and unjustified. The Eiffel Tower, the Golden Gate Bridge, the Empire State Building, the Sando Bridge in Sweden, the flowering of shell construction, the rigid framing of modern power stations, harbor sheds, and hangars, are living monuments to the power of elastic theory as a scientific basis for the art of design and construction. It has long been part of this art to temper the formal results of elastic computation by judgment, rational or intuitive, in order to reflect more realistically experience with actual performance. Much of what we are trying to do now is merely to incorporate into the science of design in an explicit and rational manner those very same features; to take them out of the realm of the qualitative and intuitive, and to put them on a sounder, quantitative, and scientific basis. No matter how far we go in this direction, an element of the art will always remain part of structural engineering.

It is the intent of the writer to review the most important of these developments. The tremendous scope of the relevant material imposes the character of this brief review which, of necessity, is one in breadth rather than in depth.

STEEL

Stress-Strain Curve.—Much of the information on structural performance of ductile metals is contained in the stress-strain diagram. Only to the extent that the stress-strain curve becomes known and reproducible is it possible to develop design procedures of high accuracy and reliability. For some structural metals, such as aluminum alloys, control and predictability of stress-strain curves has been achieved only lately.(1)[1] For others, such as stainless steel Type 301, otherwise a structural metal of high quality, the fact that adequate control of the effective stress-strain curve seems not yet in hand appears to represent the main difficulty in developing reliable design procedures.(2)

In contrast, for tension-test specimens of mild structural carbon steels the general character of the stress-strain curve has long been known to be that of Fig. 1. In view of the extreme elongations preceeding fracture, it is only the initial portion of the curve which is of primary structural interest (Fig. 1(b)). For most simple applications it is sufficiently accurate to replace this portion by the idealized elasto-plastic diagram of Fig. 1(c). However, in connection with inelastic buckling of steel members, which is of particular importance for plastic steel design, the initial strain-hardening range and the strain-hardening modulus for that range, E_{st}, have become increasingly consequential and have been extensively investigated.(3)

Yield Point.—The single, most important structural property of a mild steel is its yield point. Except where buckling enters the picture, allowable stresses in conventional design depend almost exclusively on this property. Likewise, carrying capacity as defined in plastic design is generally directly proportional to the yield point, again barring the influence of buckling. It is essential, therefore, that this quantity be well defined and be known with an adequate degree of certainty.

Routinely, yield points are determined in mill tests on specimens cut from the webs (for I-shaped sections). These tests are made at relatively high strain rates and by ASTM definition the yield point is customarily determined by the "drop of the beam or halt of the gage" method. By the nature of this method it is the upper yield point which is so determined. However, this upper yield point is an unstable phenomenon and structural strength is generally governed by the stable, lower yield point. Here, then, is one influence which makes for

---

[1] Numerals in parentheses refer to corresponding items in the Appendix.

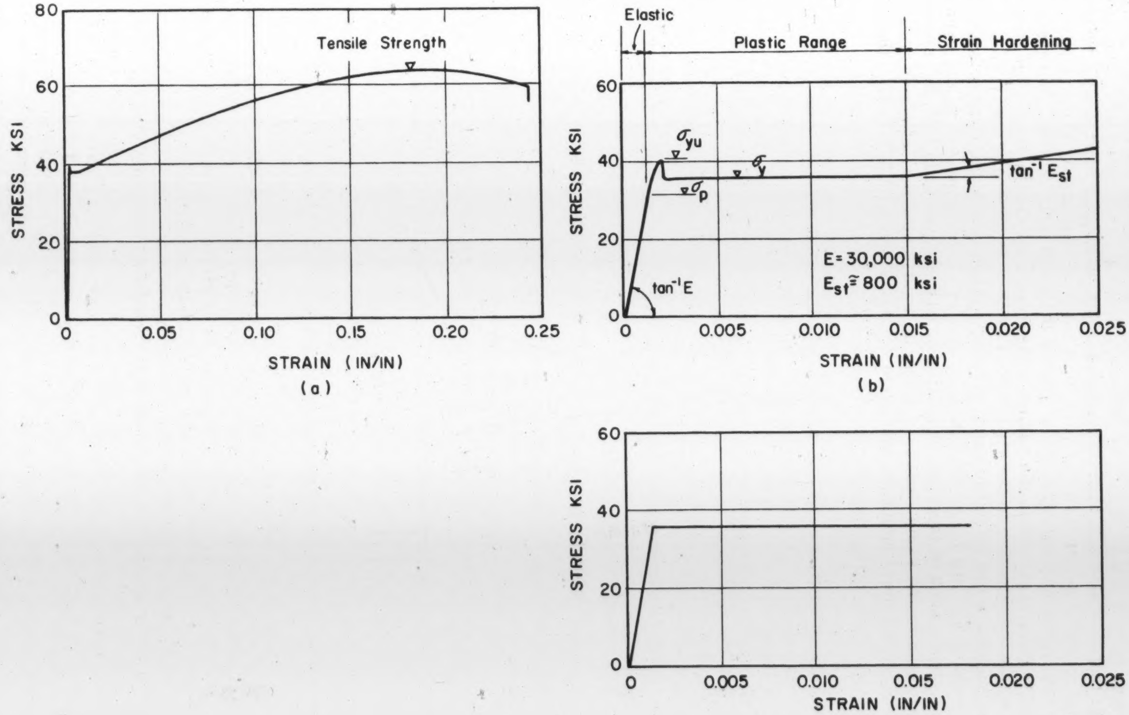

(a)

(b)

(c)

FIG. 1.—STRESS-STRAIN CURVE OF STRUCTURAL STEEL

the fact that the actual value of this structurally important porperty is below that given in mill tests. A further influence, tending in the same direction, is the fact that the relatively high strain rates (rates of loading) used in mill tests are significantly faster than the very slow rates of essentially static loading which take place in most structures. Since the yield point of steel increases with increasing strain rate, the values measured in mill tests are higher than those which are effective in the structure. Lastly, it is generally observed that if specimens are cut from the thicker flanges rather than the thinner webs, their yield points are lower than those of the web specimens which are used for mill tests. Each of these several influences rarely exceeds 10%, but since they all tend in the same direction it can be said that actual effective yield points of rolled steel members are from 5% to as much as 30% below those indicated by mill tests.(4) It follows that mill tests should show yield points about 20% larger than the stipulated values on which strength calculations are based, or, conversely, that for computations of strength a yield value should be used which is about 20% below that indicated by mill tests.

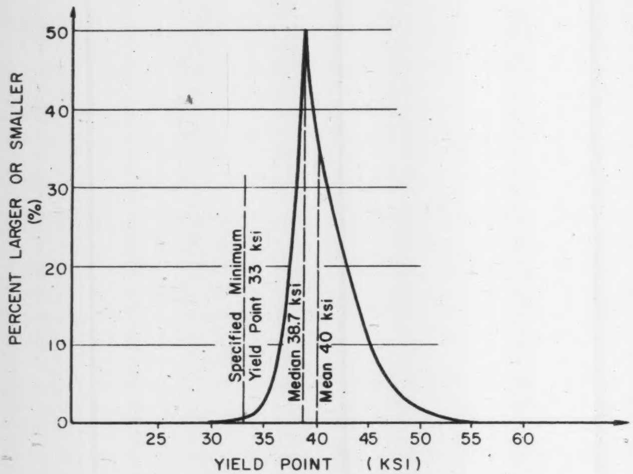

FIG. 2.—PROBABILITY CURVE OF MILL TESTS FOR STEEL (ASTM A-7)

Steel mills conduct their operations in such a manner that only a negligible fraction of their steels will fail to meet the specified minimum yield point as determined by mill test. To ensure this, production is so arranged that the average yield stress is considerably above the specified minimum. The probability curve of Fig. 2 reflects this clearly. It shows results of 3,974 mill tests representing 33,000 tons of structural steel (ASTM A-7) on nine projects between 1938 and 1951.(5) For this steel the specified minimum yield point is 33 ksi. It is seen that the median mill test value was 38.7 ksi, with a mean value of 40 ksi, and that less than 2% of the mill tests failed to meet the 33-ksi requirement. However, if one considers that the structurally effective actual yield point is on the average only about 80% of that indicated by mill test, then, in order to ensure that the actual yield point be at least 33 ksi, the mill tests should show not less than about 41 ksi. It is seen that this is in the range of the mean rather than the minimum values of large samples of actual mill tests. It follows that about half of the steel rolled to ASTM A-7 requirements seems to have structurally effective, static yield points less than 33 ksi, even though only a negligible fraction will fail to pass the mill-test requirements. The amount of this deficiency will seldom exceed 15% although it does reach about 25% in small fractions of the total sample. It follows that if plastic design continues to be based on the specified minimum yield point, and if this yield point continues to be determined by present mill-test procedures, then the discrepancies which have been discussed represent one of the features which need to be taken care of in the safety factor.

The investigations which have led to this improved knowledge of the actual yield-strength properties of structural steels are an example of a general tendency of recent origin. This is the tendency toward a more rational approach to the entire question of structural safety, and to safety factors in particular. The attempt is to reduce the amount of "judgment" and increase the factual and quantitative basis on which safety and load factors are determined. While it is unlikely that it will ever be possible to deal with safety entirely on a statistical-probabilistic basis, it is evident that if information such as the one just cited on yield strength is available, it can be incorporated in the safety factor explicitly and numerically. Thereby it decreases that area of general uncertainty which must be covered by an undefined amount of reserve strength and which had led to the ironical term "factor of ignorance."

Residual Stresses.—The information discussed previously was obtained from materials tests carried out on coupons cut from rolled sections. Until relatively recently it was generally assumed that such coupon tests correctly reflected the behavior of the steel in the member. It has now been learned that residual stresses which are present in hot-rolled shapes as well as in members fabricated by welding, have a decisive influence on buckling strength. There is no such agreement, as yet, on the possible influence of residual stresses on brittle fracture and on fatigue strength, but it seems likely that they will be found to play some role in these fields.

Residual stresses in steel members arise from two sources—from differential cooling and from cold working, such as cold straightening. From the very nature of these processes there is a sizeable degree of randomness involved in the magnitude as well as in the distribution of residual stresses. However, at least in rolled shapes, the cooling stresses are by now quite well known both as to order of magnitude and types of distribution.(6)

It is easily realized that if a hot-rolled member cools down from the partially plastic state, those portions which cool first and are fully solidified while other portions are still hot, partially plastic, and contracting, will contain residual compression stresses when the member is fully cooled. Conversely, those portions which cool last find their tendency to contract counteracted by those adjacent portions which are at lower temperature; they are, therefore, subject to residual tension stresses, when fully cooled. In view of this, it is easily understood that the distribution of residual stresses in wide-flange shapes varies between the two extremes shown in Fig. 3. In the stocky, thick-walled, approximately square sections generally used for columns (Fig. 3(a)) the flange tips cool first, the web lags behind the outer portions of the flanges, and the junctions of web and flange are the last to cool. This leads to high residual compression stresses in the outer parts of the flanges, and to residual tension stresses throughout the web. Conversely, in deep and relatively thin sections as they are mostly used for beams (Fig. 3(b)) cooling begins in the central portion of the web as well as at the flange tips, while the last parts to cool, as before, are the web-flange junctions. Correspondingly, high residual compression stresses appear in the web as well as in the outer flange portions, while residual tension is restricted to the inner portions of the flanges and the immediately adjacent parts of the webs. Very extensive measurements on large numbers of specimens have shown that a good average value for the maximum residual compression stresses is 13 ksi, with individual values occasionally reaching as much as 20 ksi. There seems to be evidence that these same values apply not only to low carbon, but also to high-strength, low-alloy steels.

It is well known that under ductile conditions internal, residual stresses do not influence the static strength of members, no matter what their magnitude

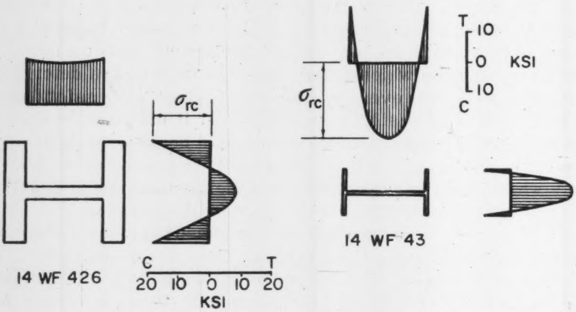

HEAVY COLUMN SECTION
(a)

LIGHT BEAM SECTION
(b)

FIG. 3.—RESIDUAL STRESSES IN ROLLED SHAPES

and distribution. This is so because residual stresses are of necessity self-equilibrating, that is, have zero force and zero moment resultant. Therefore they neither add to nor subtract from moments and forces caused by external loads. However, they can be a factor in reducing resistance to brittle fracture and to fatigue. In addition, they change the load-deformation characteristics of the member and, therefore, can decisively affect its buckling strength.

If a short piece of the column shape of Fig. 3(a) is concentrically compressed, the applied uniform stress P/A superposes on the residual stresses. Yielding will start at the flange tips when the applied plus the residual stress equals the yield point:

$$\frac{P}{A} + \sigma_{rc} = \sigma_y \text{. . . . .} \quad (1)$$

As the load is further increased, yielding spreads inward and additional load is resisted only by that shrinking part of the cross-sectional area which is still elastic. It is easily verified by elementary computation that the resulting load-deformation diagram is curved. If one plots it in the form of a stress-strain diagram, it has the shape of Fig. 4(a). On this same figure is drawn the simplified (elasto-plastic (see Fig. 1)) stress-strain diagram which would be measured if no residual stresses were present. It is seen that their effect is to produce in the steel member an "artificial" proportional limit

$$\sigma_p = \sigma_y - \sigma_{rc} \quad \ldots\ldots\ldots\ldots \quad (2)$$

equal to that applied stress, P/A, at which yielding starts in the flange tips.

On the other hand it is known that when a column is concentrically compressed to a stress beyond the proportional limit it buckles at the load

$$P_{cr} = \frac{\pi^2 E_t I}{L^2} \quad \ldots\ldots\ldots\ldots \quad (3)$$

or at the stress

$$\sigma_{cr} = \frac{\pi^2 E_t}{(L/r)^2} \quad \ldots\ldots\ldots\ldots \quad (4)$$

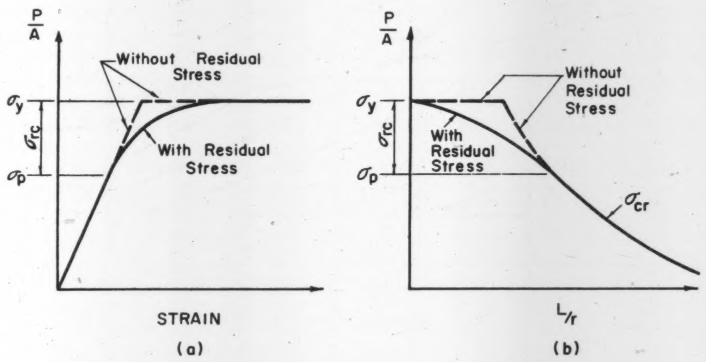

FIG. 4.—INFLUENCE OF RESIDUAL STRESS σ_{rc} ON COLUMN STRENGTH

in which E_t is the slope of the tangent to the stress-strain curve (dashed line in Fig. 4(a)). Eq. (4) is plotted on Fig. 4(b) together with that curve which would result if no residual stresses were present. It is seen that in the practically most important range (up to about L/r = 120 in steel) the presence of residual stresses reduces the buckling strength of columns very significantly.(6,7) The same holds true for lateral buckling of beams and, to a lesser extent, for local buckling of compressed flanges and webs.(3)

This large influence of residual stresses on buckling strength calls for adequate information on their magnitude also for members other than hot-rolled shapes. In regard to members fabricated by welding there are some indications that residual stresses may be even larger than in rolled shapes. Corresponding investigations are now under way at Lehigh University.

Brittle Fracture.—Ductile metals, and particularly steel, under certain conditions will fracture in a brittle manner, suddenly, and without any warning by preceeding plastic deformation or distortion. A considerable number of more or less catastrophic failures, not only of ships, but also of bridges, storage and pressure vessels, and other structures have been traced to this cause.

The nature of brittle fracture is most easily understood in the following manner: Two types of strengths can be distinguished in ductile materials, namely that stress which will cause sliding (yielding) through a shear-type displacement, and that stress which will cause separation (cleavage) by a sudden break without noticeable plastic deformation. If the yield strength is lower than the cleavage strength then, as the structure is loaded, yielding will occur long before cleavage fracture and ordinary, ductile behavior is obtained. The important point is that neither the yield strength nor the cleavage strength of a material are constant but change in different ways depending on a variety of influences. Among these, temperature is one of the chief factors and the nature of brittle fracture is most easily visualized by a plot of the two types of strength versus temperature.

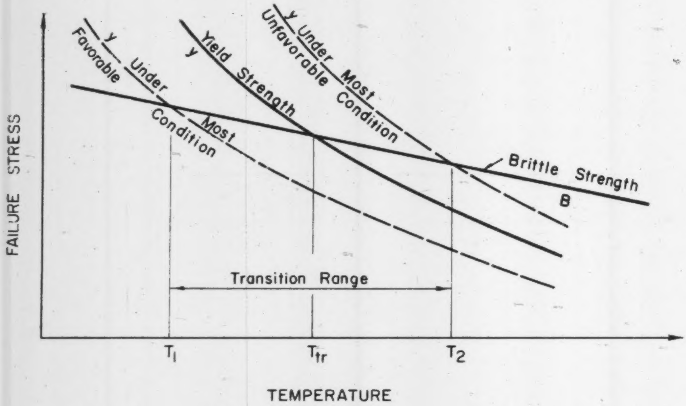

FIG. 5.—SCHEMATIC EXPLANATION OF BRITTLE FRACTURE

The solid curves of Fig. 5 show, schematically, the manner in which the ductile yield strength Y and the brittle cleavage strength B depend on temperature. It is seen that both decrease with increasing temperature, but that Y decreases at a much faster rate than B. If a structure subject to increasing load is at a temperature larger than that marked T_{tr}, then, as the load is increased the stress will reach the yield strength Y before it can attain the cleavage strength B. Consequently, yielding will start and the structure will behave in a desirable, ductile manner. Conversely, if the service temperature is lower than T_{tr} then, with increasing load, the cleavage strength B will be reached first, and sudden, brittle fracture without prior yielding will ensue. For this reason T_{tr} is known as the transition temperature, below which behavior is brittle and above which it is ductile.

Temperature, however, is not the only variable. While the cleavage strength is relatively insensitive to other influences, the yield strength, particularly of steels, depends on a number of factors. It is the greater the higher the strain rate, the larger the carbon content, the coarser the grain, the higher such stress concentrations as may exist, and it is also increased by the presence of triaxial tension stresses, such as residual stresses from welding.(8) On the other hand, the yield strength is the lower the finer the grain size, the higher the manganese and the lower the carbon content, the slower the strain rate, and the more uniform and nearly uni-axial the stress field.(9) Assuming, for simplicity, that the brittle strength on the other hand, is not influenced at all by these factors (which is only an approximation), it is seen that even for a single steel of given chemical composition the yield strength can vary over a wide range depending on the degree of simultaneous effect of the various enumerated factors. This is shown schematically by the two dashed curves in Fig. 5. The left one of these indicates the magnitude of Y under the most favorable conditions (small grain size, low strain rate, etc.), the right one under the most unfavorable conditions (high stress concentration, large triaxial tensions, etc.). Then T_1 is the "nil ductility temperature" at or below which fracture is always brittle; T_2 is the "nil brittleness temperature" at or above which the fracture is always ductile. The range T_1 - T_2 is known as the transition range. At temperatures in that range, which comprises the service temperatures of most ordinary structures, fracture can be either brittle or ductile depending on the degree of unfavorable effect of the various enumerated influences.

From the foregoing it is evident that brittle fractures can occur at average stresses sizeably below the conventional yield point if stress concentrations are present, since these have a two-fold effect: They produce a peak stress k-times the average stress (k = stress-concentration factor) and at the same time they raise the yield strength at the root of the stress raiser. Hence if, at that root, the yield strength Y is higher than the brittle strength B, the stress concentration cannot be relieved by plastic flow. If at the same time the peak stress at the root exceeds B, then a brittle fracture starts at that root, even though the average stress is below the yield stress of the metal proper. Once started, such a crack will generally, though not always, propagate because very little energy is needed to keep a brittle fracture going, and because the speed of the crack propagation produces a high strain rate which, by itself, is an unfavorable influence.

It is seen from this much simplified description that the importance of brittle fracture is by no means restricted to impact conditions. In fact, a number of ships have suffered brittle failure while at rest in harbor, and a number of bridges while free of any significant live load. It is also seen that in welded construction, particularly, a really high degree of safety against brittle fracture can be achieved only through a combination of (a) very careful detailing (to reduce to a minimum all stress concentrations), (b) a maximum of weld inspection (to detect and eliminate weld flaws), (c) appropriate weld layout and welding procedure, including preheating and postheating (to reduce triaxial tensions) and (d) the use of special steels of low notch sensitivity (several of which have recently been introduced). All these measures are costly and for this reason can be used only to a limited degree in the usual civil engineering structures.

It is not certain to what extent this situation has relevance to the newly developed methods of plastic steel design, particularly of outdoor structures.

Evidently, the premises of plastic design are satisfied only if sizeable plastic deformations at yield-stress level can actually take place before cleavage fracture occurs. Laboratory tests on full-size frames at indoor temperatures seem to indicate no danger of premature brittle fracture (that is, of brittle fracture prior to the formation of the last yield hinge). However, it should not be forgotten that fabrication, welding, and testing of these frames have been carried out under optimum laboratory conditions. Also, the structures tested were essentially two dimensional, with no framing members connected by welding at right angles to the plane of the structure. Actually, stress concentrations and tri-axial tension are likely to be worst at those many points of actual structures where members in three mutually perpendicular directions are joined. Experienced welding engineers, therefore, have expressed doubt "whether there is always a predictable amount of plastic action or reserve strength in structural steel" and that, unless and until this is proved "the possibility that here may be no *(or insufficient)* plastic action must be recognized and the designs of structures planned accordingly" (Mr. F. H. Dill, quoted in (10)). This quotation is not intended to cast doubt on the soundness of plastic design in most situations. It is intended to indicate an area where influence of material's behavior of one kind on a design method based on behavior of another kind may need further investigation and safeguards.

Fatigue.—The nature of fatigue and the multitude of factors which influence fatigue life are a matter of such complexity and scope that even an abbreviated treatment within the frame of this paper would be meaningless. The problem is of extreme importance in the case of machinery and generally of structures subject to large numbers of wide stress fluctuations or reversals, of uniform or nearly uniform peak intensity. It is evident that most civil engineering structures do not answer this description. For this reason the writer will restrict his remarks on fatigue to a few suggestions regarding the relevance of fatigue to buildings and bridges.

Laboratory fatigue tests on structural members and connections, carried out between fixed limits of either complete reversal or of zero-maximum-zero cycles often show alarmingly low fatigue strength. This is particularly true for many types of welded connections. With the more general availability of laboratory pulsators, the fatigue testing of entire structures, or at least structural subassemblies, has become possible. In fact, in certain European countries the writer has observed a tendency summarily to substitute fatigue testing by pulsators for static testing, even for such assemblies which, in actual use, would never be subject to fatigue loading of any severity, such as roof and floor structures. Such testing is certainly spectacular in showing up places of high stress concentration and the like, but its relevance to actual structural performance does not seem to have been established.

R. Weck has summarized his judgment as follows:(11)

> "The risk of fatigue failure is entirely absent in buildings unless there are travelling cranes. Even then the number of times the crane is used to full capacity may not be large enough to affect the gantry. Wind loading is variable and produces stress fluctuations but neither their number nor their magnitude is large enough for fatigue failure to result. (However) wind may lead to fatigue failure if certain parts of a structure are excited to resonance vibrations by the action of the wind. In highway bridges those stresses due to live load which occur a very large number of times are generally only fractions of the full design stress and in

> general will not result in fatigue failure—although this depends on detail design—whereas the full design stress is not reached frequently enough during the life of the structure to cause trouble. The situation in railway bridges is very different."

The statement on highway bridges, based on European conditions, may need some modification in the United States in the direction of greater caution, in view of the higher frequency of heavy truck loads in our highway traffic as compared to that in Europe.

There is a fundamental difference between the fatigue regime of such things as crankshafts, connecting rods, cranes, presses, aircraft structures, etc. on the one hand and buildings, highway bridges, and the like on the other. In the former most stress cycles are of maximum or near maximum intensity and, therefore, fatigue tests of the ordinary kind are reasonably representative. In the latter, while large numbers of stress cycles may occur, only a small fraction of them will be of, or near, maximum intensity. The application to such structures of test results obtained with cycling between fixed stress limits is, therefore, misleading and excessively conservative.

The experimental exploration of fatigue strength under the kind of variable cycling which actually occurs in structures is only in its infancy. The difficulty of reproducing in the laboratory cycling of a nature statistically similar to that even in a railway bridge are considerable, and become almost insuperable for other more random types of loading, such as wind. The authors of one of the few extensive investigations in this field(12) summarize: "From the limited number of tests it may be concluded that the variations in maximum cyclic stress obtained in railway bridges may be expected to provide a life markedly greater than one would expect to obtain on the basis of the maximum applied stresses." They estimate this increase in life to be "possibly equivalent to a decrease of approximately 2,000 - 3,000 psi in the maximum stress in constant-cycle loading." Since maximum-stress cycling is more nearly approached in railroad bridges than in practically any other structures including most cranes (with the exception of certain cranes in steel mills whose loads vary within narrow limits), these experimental results tend to confirm what was quoted in regard to low fatigue danger in buildings and bridges.

There are situations, however, where a combination of fatigue and brittle fracture may result in serious consequences when each of these occurrences, by itself, would not have been cause for alarm. Fatigue cracks are initially of microscopic proportions. At the slow rate of cycling prevalent in most structures (as distinct from high-speed machinery) they progress very slowly and may take many months and even years to reach such proportions that they will fail the member. With normal inspection and maintenance they are usually detected and corrected in time. However, if such minute fatigue cracking occurs below the transition temperature, these very cracks can become the source of a brittle fracture which is likely to propagate with the high speed characteristic of this phenomenon, and may lead to immediate failure. It is fortunate that the same measures of detailing, weld control, inspection, etc., which reduce danger of brittle fracture also tend to increase fatigue life. The possibility that a fatigue crack may "trigger" a brittle fracture emphasizes, however, that special precautions are advisable, particularly by using steels of low notch sensitivity in addition to careful detailing, when structures which are exposed to low service temperatures are also subject to significant stress cycling.

Plastic Design.—It is not the writer's intent to discuss in detail any of the phases of plastic design. A remark or two may be appropriate, however, to the extent that they fit the general tenor of this paper with its emphasis on the influence of materials' properties on structural performance.

There is no doubt that some degree of ductility is essential to the safety and proper functioning of any steel structure, no matter whether designed elastically, plastically, or by guess. Equally, there is no doubt that a larger amount of ductility is necessary for plastically designed structures to attain their planned carrying capacity. This is so because, as mentioned previously, there must be enough ductility at all locations of plastic hinges so that the hinges which form first can undergo, without fracture, those often very large amounts of local plastic rotation which will make it possible for the last hinge to form. No such demands on plastic deformation underlie elastic design. As has been pointed out, numerous tests of full-size frames under laboratory conditions have shown that the requisite amount of ductility appears to be present for the full plastic strength to develop. One possible reservation in regard to this feature was presented under the heading "Steel: Brittle Fracture." Another concerns the following:

By far the majority of tests on plastic theory have been made on rolled shapes, or on structures fabricated from rolled shapes. For the method to be universal and applicable to structures of large size, its validity for fabricated structures may need further exploration. There has been recent evidence(12) that customary ways of preparing fabricated edges may reduce ductility practically to zero at temperatures as high as 40° F to 80° F. This refers particularly to sheared edges, to a somewhat lesser extent to manually flame-cut edges, and to arc strikes on edges. In this respect, rimmed ASTM A-7 steel proved considerably worse than semi-killed steel of the same designation, and structural silicon steel (ASTM A-94) as well as a low-alloy, high-tensile steel (ASTM A-242) proved to be about as unfavorable as the rimmed A-7 steel. Except for the semi-killed A-7 steel, brittle fractures in static tensile tests at the above, relatively high temperatures were obtained at stresses equal to and sometimes somewhat below the yield point of the material, particularly for sheared edges. It is clear that if, in fabricated construction, such edges were permitted to occur at yield-hinge locations, the attainment of the necessary plastic rotation prior to possible fracture would be in serious doubt. This is but one more illustration of the fact that the more design is based on actual strength rather than on nominal stress, the more important becomes information on structural performance of the material and development of adequate safeguards.

Even though it may be necessary to surround plastic design with more refined safeguards than are necessary for conventional procedures, there is no doubt that it represents impressive progress in three respects: (a) It enables the designer to utilize hitherto hidden plastic strength reserves, and thereby to design more economically. (b) It has furnished the designer and researcher with a deeper understanding of actual, as compared to idealized, structural performance. (c) It has added a new degree of freedom to structural design whose full possibilities will evolve only gradually with increasing usage. It is on this last feature that the writer wishes to dwell briefly.

When dealing with elastic continuous structures, the designer has only limited scope in shaping the structure for optimum performance and economy. A fixed-ended, uniformly loaded elastic beam of constant section has end moments which are twice as large as the span moment, and hence most of the beam is understressed. If the designer wishes to improve the situation by reinforcing the ends he will find that, in the process, he has further increased the end moments at the expense of the span moment, in view of the added rigidity of the outer, reinforced portions. The stresses are likely to be as uneconomically distributed as before. In fact, it appears to be true that one cannot produce an elastic indeterminate structure of economically optimal stress distribution. This is illustrated by the simple, indeterminate system of Fig. 6. Economically optimal stress distribution would mean that the stresses in all three bars be equal. The elementary analysis in Fig. 6 shows that this is possible only for $\alpha = 0$, that is, when the indeterminate structure transforms into the determinate one which consists of one single bar. This example and that of the fixed beam illustrate the degree to which, for elastic conditions, the designer is hamstrung in his endeavor to optimize the shape of his structure.

In contrast, in plastic design, the designer is entirely free to dictate to the structure the manner in which he wishes it to perform. For the elementary model in Fig. 6, optimum plastic stress distribution results automatically since the structure will fail by unrestricted yielding only when the yield stress is attained in all three bars. This illustrates the economy of plastic design. In addition, however, if for some reason the designer wishes to impose the condition that, at failure, the force in each of bars 2 be one-half of that of bar 1, all he has to do is to make the area of the former one-half of the area of the latter. Or, for the previous case of the fixed-ended beam, if he wants the support moments at failure to be one-half of the span moment (possibly because the restraining structures cannot resist more than this amount), all he has to do is to shape the beam so that the plastic section modulus at the supports is one-half that at the center. To state it generally, the plastic method enables the designer to dictate to the structure the precise manner in which he wants it to resist the external forces, to tell the structure how much of the total static moment he wants to be resisted at one section, and how much at another. It is this which makes the plastic method primarily one of design, while the elastic method with its limited freedom of action is primarily one of analysis.

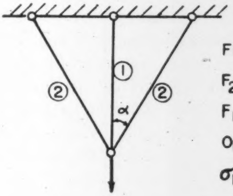

ELASTIC	PLASTIC
From Deformation Compatibility	From Yield Condition
$F_2 = F_1 \frac{A_2}{A_1} \cos^2\alpha$	$F_1 = A_1 \sigma_y$
$F_1 = A_1 \sigma_1$; $F_2 = A_2 \sigma_2$	$F_2 = A_2 \sigma_y$
Optimum Design With	$\sigma_1 = \sigma_2 = \sigma_y$
$\sigma_1 = \sigma_2$ Impossible	Automatic, Regardless
Except When $\alpha = 0$	Of α

FIG. 6.—"OPTIMUM DESIGN" OF INDETERMINATE STRUCTURES

It is likely that this new freedom of shaping structures optimally, in regard to economy in some cases, in regard to aesthetics in others, will be appreciated only gradually as designers, through use, become aware of the new potentialities of this approach.

CONCRETE AND REINFORCED CONCRETE

In comparison with steel, concrete is a much more complex and less predictable material. This is due to two entirely independent causes. From the fundamental viewpoint of materials behavior, the high degree of heterogeneity of concrete, the difference in basic properties of its various constituents (coarse and fine aggregate and hardened cement paste), the pronounced effects of creep and shrinkage, and the fact that the tensile strength is a small fraction of the compressive strength, represent some of the causes why the understanding and prediction of performance of concrete under load has not attained the same degree of development as for steel and for other ductile materials. From the practical viewpoint the fact that concrete on the whole is produced under less controlled conditions and that its final properties depend to a greater degree on job operations than is true for steel (placing, curing, etc.) adds to the lesser degree of predictability which still prevails in regard to many features of concrete behavior. (It should be noted, though, that recent investigations into the true effective properties of steel, as discussed previously in regard to yield strength, residual stress, brittle fracture, etc., have shown that these properties, too, exhibit greater scattering and dependence on fabrication operations than had previously been suspected.)

The difficulties are compounded in reinforced concrete by the complex mode of interaction of the two constituent materials and by the variety of ways in which they can be combined to form structural members. The fact that our understanding is still lagging in regard to some of the basic features of reinforced concrete, such as its behavior in shear and diagonal tension, in torsion and combined torsion and bending, its long-time deflections under load, etc. is by no means amazing. On the contrary, it should be a matter of some pride that, in spite of these fundamental complexities, such features as the strength in compression, in bending, and in combinations of compressing and bending, have been brought under very satisfactory control while in regard to the enumerated, more complex, features, methods have established themselves which, though admittedly crude and lacking of rigour, have proven themselves as adequate design tools.

Cylinder Strength.—The single, most important structural property of concrete is its cylinder strength. Wherever, in reinforced concrete, the carrying capacity is governed by the concrete rather than the steel, it is strongly dependent on, and in most cases directly proportional to, cylinder strength. In addition, and in contrast to steel, the deformation characteristics of concrete structures (modulus of elasticity, etc.) are also very largely dependent on cylinder strength. The degree to which actual cylinder strength in the finished structure corresponds to the value on which the design has been based is, therefore, of the utmost importance.

Figs. 7(a) and (b), represent, respectively, 861 tests of 33,300 cu yd and 296 tests of 3300 cu yd, exhibit the influence of good versus poor concrete quality control.(5) For the concrete of Fig. 7(a) the desired minimum strength was 3.8 ksi, for Fig. 7(b) 4.3 ksi. while the actual mean strengths were 5.2 ksi and 5.8 ksi., respectively, a spread of 35 to 40%. For the well-controlled concretes of Fig. 7(a) the percentage of cylinders which tested below the design strength of 3.8 ksi is a fraction of a percentage. In contrast, more than 15% of the cylinders of Fig. 7(b) failed to meet the stipulated minimum strength in spite of the wide spread between the actual mean and the stipulated minimum strength,

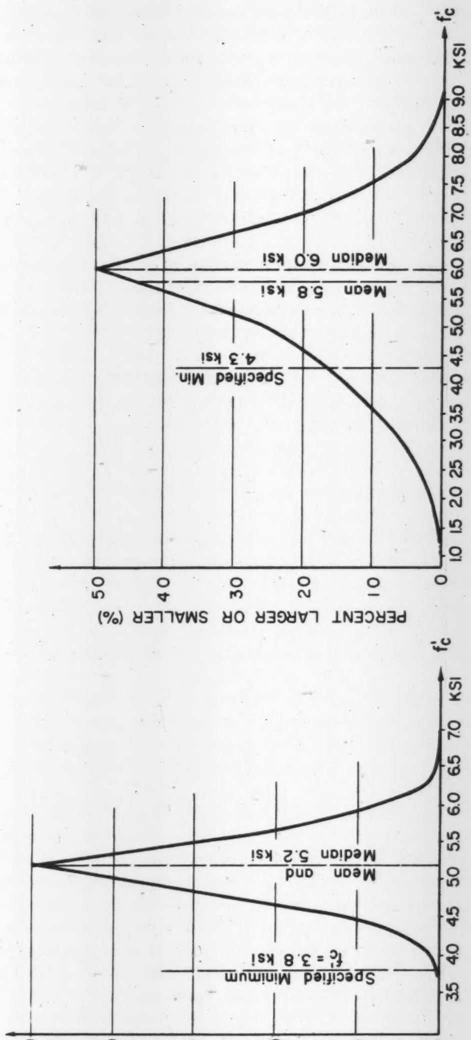

(a) GOOD CONTROL

(b) POOR CONTROL

FIG. 7.—PROBABILITY CURVES FOR CONCRETE CYLINDER STRENGTH

and some of the cylinders tested as low as one-half of the desired value. These statistical data emphasize strongly that only the combination of careful concrete control with a sufficiently wide spread between the desired minimum strength and the mean strength for which the mix is designed will assure adequate quality. Some codes require that the water-cement ratio be so chosen as to result in a strength 15% above the desired design strength. In view of the foregoing information there may be some doubt whether this spread is sufficient.

Tensile Strength.—Since reinforced concrete structures are so arranged that the strength of concrete in direct tension is rarely of practical significance, not much attention has been paid to this property. A further reason for this neglect may be found in the experimental difficulty of determining concrete tensile strength by test.

However, the strength under combined stress of a material like concrete, such as in shear, in torsion, or in a combination of these with bending, can be analyzed only if, in addition to the compressive strength, at least the tensile strength is known. This is immediately evident from Mohr's strength theory which, while not necessarily the most exact, is probably the simplest of the various strength theories applicable to a material of the nature of concrete. Lack of information on this property, therefore, seriously hampers attempts toward a deeper understanding of concrete performance.

The statement can often be found that the tensile strength is some reasonably constant fraction, such as 1/10, of the cylinder strength. It has recently been maintained(13) that this ratio can vary within the wide limits of 1/8 to 1/30 and that its most frequent range is between 1/10 to 1/16. It seems likely, therefore, that the tensile strength is a separate property of any given concrete and is not uniquely defined by some definite relation to the cylinder strength. The possible practical importance of this situation will be discussed subsequently in connection with combined stress.

Stress-Strain Curve.—Until recently, strain measurements during cylinder tests have represented the primary source of information on stress-strain curves of concrete. Such tests give adequate data at relatively low stresses (within the working range). There was considerable doubt, however, whether these data were representative of actual concrete behavior at near-ultimate stresses, that is, in the region which matters most for strength determinations. The doubts were two-fold: (a) It was suggested by C. S. Whitney that the sudden failure of test cylinders may frequently be precipitated by the elastic properties of the testing machine, rather than those of the material; (b) it was dubious to what extent the shape of the curve obtained from cylinder tests was representative of the stress distribution in the compression zone of a member subject to bending or eccentric compression. Both these questions are of decisive importance for a rigorous underpinning of ultimate strength design.

In very recent years, independently and almost simultaneously, satisfactory light was shed on these questions by evidence obtained by ingenious test methods in Germany(14) and in the United States.(15) These investigations showed that: (1) In cylinder tests the stress-strain curve upon reaching ultimate strength is indeed cut short by the properties of the testing machine, particularly for higher strength concretes. (2) The distribution of concrete stresses over the compression zone of flexural members is, in fact, closely similar to the stress-strain curve in concentric compression. (3) Most important, the shapes of the stress-strain curves of concretes of various strengths are of the character shown on Fig. 8.(15)

It is seen that concrete behaves reasonably elastically in the range of moderate stresses. There is, however, marked departure from linearity at near-ultimate stresses. In this respect concrete behaves quite differently from decidedly brittle materials, such as cast iron or glass, and can be said to possess a certain amount of ductility. This ductility, however, is seen to decrease with increasing cylinder strength. There is a certain paradox in the fact that recent tendencies to use ever higher concrete strengths coincide with simultaneous tendencies toward utilization of the ductility of concrete in ultimate strength design. It is probable that the tendency toward the very high concrete strengths is caused by the fallacious premium which the straight-line theory places on the use of such concretes in flexural members. With broader acceptance of ultimate strength design a more realistic attitude toward concrete strength is likely to establish itself.

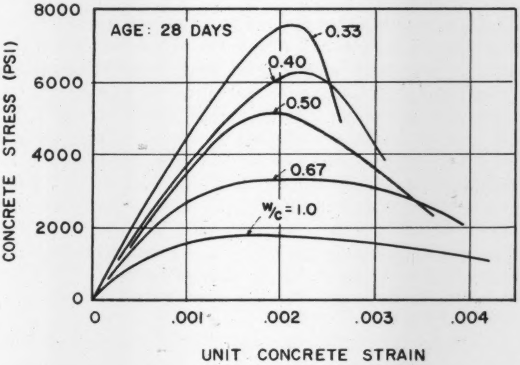

FIG. 8.—STRESS-STRAIN CURVES FOR CONCRETE

A very remarkable feature of the stress-strain curve of concrete is that it shows a descending branch after the maximum stress has been reached. The fact that its shape, in this respect, is not very different from that of certain ductile metals is deceptive. In the latter, such as in aluminum alloys, steel, etc., the descending branch pertains only to the nominal stress, referred to the original area. Since, in this region of large, ductile strains, the reduction of area is considerable, a plot of true stress versus strain invariably shows an ascending curve right up to fracture. In concrete, in contrast, in view of the relatively very small strains, no significant change of area occurs with increasing stress so that the conventional stress-strain curve differs very little from that of true stress. It seems that no other structural material possesses this descending branch, with the possible exception of timber under certain conditions. It is suspected(15,16) that this branch is caused by progressive, irreversible microcracking so that, with further increasing strain, a progressively smaller number of uncracked particles is called upon to resist the load.

The total duration of the loading process for each of the tests performed by E. Hognestad, et al(15) was about 15 min. This demonstrates that the shape of these curves is not a consequence of creep, as is sometimes stated, at least not within the normal meaning of the term creep, but represents correctly the performance of concrete at reasonably high rates of loading.

An important feature of these curves is the fact that their peaks occur, that is, the maximum stresses are reached, at strains of the order of 0.0020 to 0.0025, for all tested mix proportions and cylinder strengths. Column design has long been based on the assumption, proved in many tests, that the strength of a short, concentric column is simply the sum of the yield strength of the reinforcement plus the crushing strength of the concrete. This situation is evidently possible only if the concrete will not crush or substantially enter the descending branch of the curve before the steel has reached its yield point. Since, in steel, an elastic strain of 0.001 corresponds to a stress of 30 ksi, it is seen that column reinforcement with yield points up to 60 ksi to 75 ksi will indeed reach these yield points before the concrete starts weakening, as is assumed in present column formulas. This may not be true, however, for steels of significantly higher yield strength. The same situation may hold for compression reinforcement in flexural members. This may put a limit on the efficiency of steels of very high strength for compression reinforcement.

The descending branch of the stress-strain curve comes into play primarily in beams with very high reinforcement ratios, when strength is governed by crushing of the concrete. While such high ratios are rare, the possibility that in this range the integrity of the concrete is impaired by microcracking remains a somewhat disturbing feature. It could conceivably affect structural safety in the case of repeated applications of near-ultimate loads, and may warrant additional investigation.

Flexural Strength of Reinforced Concrete.—Flexural failure ultimately consists in the crushing of the concrete compression zone. If this crushing is preceded by yielding of the steel (for low steel ratios), then the ultimate moment at which crushing occurs differs very little from that at which yielding begins. For this reason the ultimate moment of beams which fail in tension can be computed with high accuracy, provided the reinforcing steel has a horizontal yield plateau.

If crushing takes place while the steel stress is still below the yield point (high steel ratios), the ultimate moment cannot be predicted with any comparable precision. The best that can be done is to calculate a reliable lower limit (see Fig. 4, Ref. 17). It has been proposed that for this situation the maximum concrete strain at the outer compression fiber be taken as a failure criterion. It is seen from Fig. 9(18) that ultimate strength cannot be computed from a maximum strain criterion. That is, there seems to be little prospect in establishing that concrete will crush at a certain, predictable magnitude of the strain at the extreme fiber since tests have failed to indicate reasonable correlation between strain and strength. Fortunately, with standard-strength reinforcement, the steel ratios at which strength is governed by concrete crushing prior to steel yielding are so high as to be rarely of interest. This is not so when high-strength reinforcement is used. In addition, certain high-strength steels which are coming into use both in Europe and, lately, in the United States, do not have a flat yield plateau but enter strain hardening immediately upon reaching the yield strength. In that case, even for low steel ratios, the flexural strength cannot be computed by the usual methods of ultimate strength theory and the only statement that can be made is that the strength of such beams is larger (by up to 40%) than computed by assuming the steel to possess a flat yield plateau.(19)

It is seen, then, that in view of the complex nature of concrete, the strength of flexural reinforced concrete members so far is calculable with precision only for the simplest of situations (under-reinforced beams with flat-yielding steel). It is fortunate that this is, by far, the most frequent situation, and it is equally fortunate that for all other situations, if not the strength itself, then at least a reliable lower limit can be easily computed. Investigations are under way both in the United States and in Germany which attempt to develop a basically different approach to ultimate flexural strength, based on the concept that internal stresses readjust themselves to maximize the resisting moment. In the meantime, however, there are arguments in favor of limiting the maximum admissible strain even though there appears to be no reliable correlation between it and flexural strength. If that strain is limited, for low and medium strength concretes, to 0.003 or possibly to 0.0025, and to somewhat smaller values when f_c' exceeds about 4500 psi (Fig. 8), one would thereby eliminate from utilization the descending branch of the stress-strain curve. If this branch were actually caused by irreversible microcracking, this may be a desirable measure.

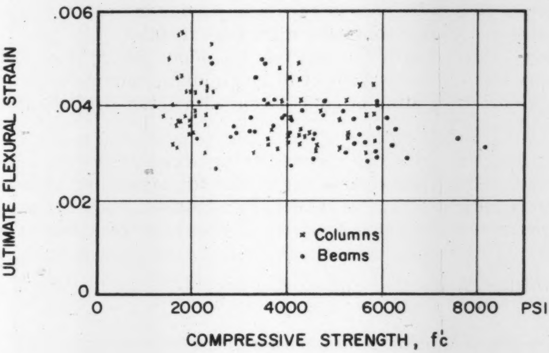

FIG. 9.—ULTIMATE STRENGTH AT FAILURE OF REINFORCED CONCRETE MEMBERS

Failure under Combined Stresses.—The difficulties cited in predicting strength for the essentially uniaxial conditions of flexural compression are compounded in the case of combined stress, that is, of stresses acting in two or three directions. The shear strength of beams and the strength of members in combined bending and torsion (with and without transverse shear) are but two examples of such biaxial, combined stress. They emphasize the importance of developing a method for predicting failure under these conditions, and several promising attempts have been made on this problem in recent years. The matter must be looked at in two different ways: For one, it is a problem of basic, pure research in which an answer is sought for which only one criterion exists, namely that it be reliable, regardless of possible complexity. The other is the fact that in order to be of engineering use, the information obtained in this fundamental manner must be capable of sufficient simplification to permit use in routine design. In both these respects the problem of concrete failure under combined stress is still in its initial stages.

Of the various, customary strength theories, the simplest which could be applied to a material of the type of concrete is that of Coulomb (identical with Mohr's theory with straight envelopes). It regards failure as a sliding on inclined planes and postulates that the resistance to such sliding consists of two parts: the internal cohesion, and the sliding friction. The latter, in turn, depends on the coefficient of internal friction and on the normal stress on the plane of sliding. H. J. Cowan(20) maintains that two types of concrete failure must be distinguished. He suggests that crushing failure is governed by Coulomb's theory, but that cleavage failure (tension cracking) is directly caused by the maximum principal tension stress (Rankine theory). On this basis he shows reasonable agreement with a moderate number of tests on beams in combined bending and torsion. While it is known that the Coulomb-Mohr theory is fundamentally deficient in that it neglects the influence of the intermediate, principal stress, this deficiency is rarely important in ordinary type members where stresses are usually biaxial rather than triaxial.

D. McHenry and J. Karni(21) find that the Mohr theory does not correlate well with their tests of tubes subject to longitudinal compression and circumferential tension. They attempt correlation with octahedral shear and normal stresses, but conclude:

> "At the present stage of our knowledge the accumulation of test data is perhaps more important than is the search for simplified criteria. The present data indicate that the relationship between the principal stresses for tension-compression failure is rather complex and is not well defined."

At the same time B. Bresler and K. S. Pister(22) observe, very much to the point

> "that strength of concrete is a function of the state of stress and can not be predicted by limitations of tensile, compressive and shearing stresses independently of each other".

It is evident, therefore that "the search for simplified criteria" is of great practical importance, since without them design for shear, torsion, and other combinations must remain on the unreliable basis of considering "the stresses independently of each other." In analyzing the results of their tests of tubes submitted to compression and shear (torsion), Bresler and Pister attempt to relate their results to the octahedral normal stress and to a slight modification of the octahedral shear stress, and they extend their method to the problem of the shear strength of beams without web reinforcement, under strictly specified, restrictive conditions.

These various approaches have in common the fact that they attempt to relate the strength of concrete under combined stress to a single property of the material, usually the cylinder strength or some modification thereof. In a doctoral dissertation prepared under the writer's supervision, S. A. Guralnick(13) maintains that the strength of concrete under combined stress can be understood only if at least two properties are known, the tensile as well as the compressive strength, and that these two properties are largely independent of each other. This has been discussed previously. To illustrate: Cowan's method is based on the assumption that the ratio of tension to compression strength is about 1 to 9 while Bresler and Pister's criterion would result in a tensile strength of $f_c'/13.2$; at the same time even the limited test evidence by McHenry and Karni shows a spread of measured tensile strength from $f_c'/11$ to $f_c'/17$. It stands to reason that strength hypotheses which do not account for this variability are not likely to be reliable. Guralnick utilizes the Coulomb-Mohr approach to derive relatively simple interaction-type criteria and applies them to results of only such tests for which the compressive and tensile strength of the particular concrete was known by independent tests. The reasonable correlation which he obtains may be regarded as one further contribution to the urgent problem of combined strength of concrete, whose satisfactory solution is not yet at hand.

Shear Strength of Beams.—The most important type of failure in concrete structures which is caused by combined stress is that usually designated as "shear failure." This occurrence is, generally, of a "brittle" character, that is, it takes place without warning and leads to immediate and total collapse. This is in contrast to the gradual way in which under-reinforced beams fail in flexure, or spiral-reinforced columns in compression. It is the reason why it is advocated that in ultimate strength design a larger margin be provided against shear than against flexural failure, so that structures so designed would give due warning of distress.

An unusually large amount of research on shear strength, within the past 10 yr, has to a considerable extent clarified the mechanism of shear failure in a qualitative manner. At the same time it seems that none of the quantitative conclusions, some of them in the form of very elaborate equations, possess sufficient generality to be applicable, with confidence, outside the range of variables of the tests from which they were derived. One of the reasons for this, apart from the basic complexity of shear strength, particularly in the presence of web reinforcement, is probably the fact that no attempt was made by these investigators to analyze shear failure as involving strength under combined stress. The necessity for this latter approach was pointed out by P. M. Ferguson.(23)

Shear failure in beams without web reinforcement proceeds in two stages: First, a "diagonal tension crack" forms, caused by the inclined tension and compression stresses which prevail in the uncracked section. The correct determination of that state of stress, and of that shear force which will cause such a crack to form is, therefore, clearly a matter of combined stress. Once such a crack is formed, the external shear is resisted only by the remaining uncracked concrete on top of the tip of the crack. Final failure occurs when this concrete is destroyed by the combined action of the flexural compression and the shear (Fig. 10(a)). This, evidently, is again a matter of failure of concrete under combined stress.

In beams with web reinforcement an additional stage is interposed between these two. That is, after a diagonal crack has formed, resistance is provided jointly by the stirrups crossed by the crack and the remaining, uncracked compression concrete (Fig. 10(b)). When the stirrups have reached their yield point, the effects of any additional load increase must be resisted by the remaining compression concrete, so that final failure, again, is caused by combined stress in this part of the beam. The foregoing represents a possibly oversimplified description of the mechanism of shear failure.

The writer knows of only two attempts to apply conditions of strength under combined stress to the problem of shear in beams.(13,22) Both these attempts show reasonable correlation with a limited number of beam tests. Neither of them pretends to have furnished more than the beginnings of a basic solution of the problem of shear strength. There is a school of thought which maintains that, in view of the brittle character of shear failure, ultimate strength design for shear should not be based on actual collapse but on the immediately preceeding stage, described previously. That is, for beams without web reinforcement, design would be based on that load which causes the first diagonal crack, and for beams with web reinforcement, on that load which causes the web reinforcement to yield. It is clear that this more conservative approach, likewise, cannot avoid the nature of the problem as one of combined stress.

If this is the state of our knowledge on shear strength (as of 1959), it might be asked how it is possible that we have been designing, for these many years, concrete structures which appear to be reasonably safe in shear. The answer is that our present shear-design procedures are based on certain simplified concepts in combination with test evidence and experience. They result in safety factors which range widely between the limits of about 2.5 to 7 and more.

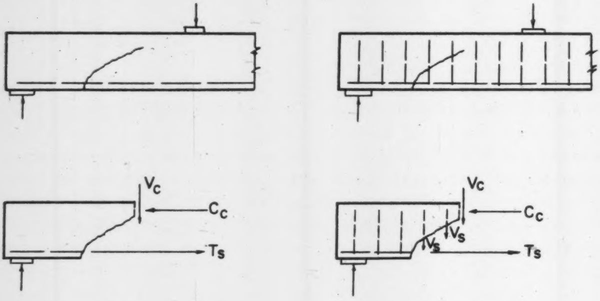

(a) (b)

FIG. 10.—"SHEAR FAILURE" MECHANISM OF REINFORCED CONCRETE BEAMS (SCHEMATIC)

Occasionally safety factors have fallen sharply below these limits and have resulted in actual structural distress or failures which were traced to shear weakness. This means that present procedures are normally adequate, but by a margin which is rarely known with any reasonable accuracy. Correspondingly, shear designs in many cases are uneconomical while others, fortunately in a much smaller number of cases, are not adequately safe.

Time Effects.—Under normal temperatures, steel is insensitive to loads of long duration so that the only time effects of importance to the structural designer are those connected with high strain or load rates. In contrast, concrete under stress continues to deform or creep for a long time at a decreasing rate; it stabilizes only after months or years. Considerable attention has been paid recently to creep in view of its importance in the design of dams, arches, and prestressed concrete. Based on extensive experimental evidence, a number of empirical formulas have been developed which describe the observed relationships between creep, stress, and time.(24)

Since concrete is subject to creep and reinforcing steel is not, it is evident that sustained loading causes a redistribution of internal stresses in reinforced concrete members. In fact, when the first extensive evidence was obtained, in the 1930's, that the stresses and the strength of columns do not conform to elastic relationships, it was thought by many that this was due to stress redistribution caused by creep. It is evident that this is not so. For one thing, the duration of most column tests from which this evidence was obtained was one of hours or fractions thereof, rather than months. For another, the concrete stress-strain curves of Fig. 8 with their pronounced inelastic portions were obtained at a steady strain rate which resulted in failure within the short time of about 15 min. Possibly the most spectacular evidence to the effect that plastic or inelastic action of concrete is not dependent on creep is presented by some column tests.(25) Ten columns of different types were tested to failure within less than 6 min each, and their ultimate loads compared with the basic formula for inelastic or plastic column strength,

$$P_{ult} = 0.85\, f'_c\, A_c + f_y\, A_s \quad \ldots\ldots\ldots\ldots\ldots \quad (5)$$

The average ratio of measured to computed ultimate load was 1.02, which indicates that inelastic action establishes itself completely, for strength purposes, within less time than the very short duration of these tests. (The writer is aware of the theoretical difficulties in clearly distinguishing between creep and plastic or inelastic action at high stresses. From a practical design viewpoint he would like to draw the line between the duration of short-time live loads in ordinary structures, a matter of minutes, and either dead or long-time live loads, a matter of months or years.)

The reverse question, which is of considerable practical consequence, is this: In view of the internal stress redistribution caused by creep, is the strength of reinforced concrete members in structures under sustained loading less than that obtained in the usual laboratory tests under relatively fast loading? In this respect two types of sustained loading must be distinguished. (1) A member or structure carries, for a long period, the full design load and is then loaded to failure at a reasonably rapid rate. This is the case of primary practical interest for the normal structure which is essentially used and loaded as designed, but which may be subject to short-time catastrophic overloads, such as by earthquakes, hurricanes, dropping loads, or the like. (2) A member or structure carries near-ultimate loads indefinitely or until these high, sustained loads cause collapse. In actual structures this case would be of interest only when, in design, long-time loads have been underestimated by a factor approaching 2, or when a structure is irresponsibly misused, such as the use of a former office building for heavy warehousing.

Test evidence shows(26) that columns subject to sustained loads of type 1, above, develop the same strength as columns of the same age failed under short-time loading. In regard to the much severer sustained loading of type 2, tests indicate for concentric(27) and for eccentric(28) columns that the sustained-load strength is rarely less than about 90% of the short-time capacity. In regard to beams, evidence is not too ample. Those tests which have been made(29,30) seem to indicate that for beams without and with compression reinforcement the long-time strength under the severer sustained loading of type 2 is indistinguishable from the short-loading strength of identical members of the same age. It seems, therefore, that creep does not present a significant problem in reducing strength under sustained load and that, consequently, design can continue to be based on the ample test evidence of the short-time strength of reinforced concrete members.

That effect of creep, therefore, which is of primary practical importance is the long-continued increase in deflection under constant, sustained load. These additional deflections can be sizeable, particularly in shallow members, where they can amount to two and more times the value of the instantaneous deflections obtained when loads are first applied.(29,31) Present tendencies are toward the use of shallower members, facilitated by the introduction of ultimate strength design and of high-strength reinforcing steels. In this connection it becomes increasingly important to develop design tools for preventing long-time deflections from becoming excessive. It appears that accurate methods for predicting long-time deflections have not yet been developed. For the time being, reasonable estimates can be obtained if the moment of inertia of the transformed cracked section is used, using for the modulus of elasticity of the concrete one-third to one-fourth of the customary value for short-time loading.

At the opposite end of the range of time effects is that of the properties of concrete at very high rates of strain, that is, when loads increase very rapidly from low values to their maximum or when the structure is subject to impact. Such evidence as exists(32) shows, fortunately, that crushing strength increases significantly with increasing strain rates (up to 80% in the reported tests), that the stress-strain curve in dynamic loading shows the same development of an inelastic range prior to failure as in static loading, and that the energy absorption capacity at high strain rates is certainly not lower, and frequently considerably higher than under static conditions. It seems to follow from this that if members are designed with full utilization of the inelastic properties of concrete (ultimate strength design), they will not fail under high strain rates at loads which are lower than those calculated by ultimate strength theory, even though the test evidence on which this theory is based was obtained at relatively slow loading.

Another time effect, to whose investigation and control too little attention has been paid recently, is shrinkage. In connection with the introduction of higher strength steels and other new developments (limit design, etc.) much effort has been and is being spent on investigating cracking of concrete as it is caused by tension stresses in flexure, shear, and combinations thereof. It so happens that these stress cracks are almost the only type that will occur in laboratory specimens of the usual, unrestrained kind. On the other hand, observation of existing structures shows, as a rule, that much more extensive and obnoxious cracking is caused by shrinkage than by stress. In addition to cracking, shrinkage also can cause warping and deflection of unsymmetrically reinforced members (since shrinkage will be resisted where steel is located, such as on the tension side of beams, but will proceed relatively unhindered on the compression side unless compression reinforcement is used). These deformations can attain sizeable and objectionable proportions, particularly in shallow members. Finally, sizeable internal tension forces due to shrinkage can develop in structures if adequate provisions for relieving restraint (shrinkage joints which work) are not made. These stresses have been known to add to those caused by loads in a manner which can result in serious distress and even failure.

Ultimate Strength Design and Limit Design.—Ultimate strength design is now an accepted procedure in several parts of the world and, since 1956, has been a permissible alternate method in the United States. The term has come to mean the utilization in design of the ultimate strength of individual reinforced concrete sections, as distinct from the load capacity of entire structures composed of members having such sections. This method is based on the more complete utilization of the actual properties of both steel and concrete, in contrast to the idealized elastic behavior on which the conventional straight-line theory is based. Historically, ultimate strength design developed rather in the inverse order, that is, phenomenologically. Tests of reinforced concrete members (beams, columns, etc.) showed that they did not behave as predicted by straight-line theory. From this it was evident that inelastic properties, though not fully known, must influence strength decisively. Methods were developed which would more closely reflect actual behavior of structural members based primarily on tests of members and then on some rather crude working hypotheses in regard to inelastic materials properties. Only recently has considerable light been shed on this basic materials performance, and refinements are now being made in ultimate strength design based on this better understanding of the fundamentals.

In addition to the actual strength of sections it has been found that the inelastic behavior of both steel and concrete leads to a redistribution of moments at high loads in indeterminate reinforced concrete structures in a manner analogous to that utilized in plastic design of steel structures. The corresponding design method of reinforced concrete structures is coming to be known as limit design.(33) The differences between plastic design of steel structures and the developing methods of limit design of reinforced concrete structures are largely a consequence of the different performance under load of these two materials. Thus, the usable plastic rotation capacity of rolled-steel shapes usually far exceeds that required for the development of adequate plastic hinges (questions of local buckling being beyond the scope of this paper). In reinforced concrete the moment-curvature relationship, beyond the limit of elastic action, is non-linear, similarly as in steel. However, in contrast to hinges in steel, undesirable consequences of various kinds may accompany plastic rotations in reinforced concrete unless adequate safeguards are provided.

For members with low steel ratios such plastic rotation is primarily caused by yielding of the reinforcement. This yielding, however, is likely to be accompanied by large-scale tension cracking. If such cracking occurs only at high (near-ultimate) loads it may be harmless in regard to serviceability of the structure. Yet, if plastic rotation leads to excessive cracking at service loads (at or slightly in excess of the design load) it may be thoroughly objectionable. From this viewpoint it is deplorable that in many valuable investigations on moment redistribution little detailed information has been obtained, or published, on crack formation.

On the other hand, for members with medium and high steel ratios, plastic rotation is necessarily accompanied by relatively large concrete strains. To what extent such large strains are admissible is still a matter of some dispute, even as far as a single loading to failure is concerned. Previously the possibility has been mentioned herein that part of the inelastic strain of concrete at high stress may be caused by irreversible microcracking. If such microcracking develops at plastic hinges, the question of repeated applications of near-ultimate loads assumes more importance in regard to structures designed by limit-design procedures than it has in structures whose moments and shears have been calculated by elastic analysis. In this respect one might conceivably speak of a shake-down problem in reinforced concrete structures in a different sense from that in steel structures. In the latter, shake-down implies the consecutive application of different load patterns, in which case the structure may or may not "shake-down" to a stable condition (in most cases it does). In reinforced concrete a shake-down problem may exist not only for successive application of different load patterns but even for repeated applications of the same loading.

These possibilities are mentioned not in order to cast doubt in advance on the possible advantages and merits of limit design in reinforced concrete. They are discussed, merely, to indicate that, in view of the greater complexity of the pertinent materials, it is likely that limit design in reinforced concrete will take different forms and will have to be surrounded with more elaborate safeguards than plastic design in steel.

Limit design, therefore, represents a prime example of the fact that thorough knowledge of the performance of materials under load, in all its various aspects, is the chief prerequisite for improving design methods. It has been the aim of this broad review to facilitate acquaintance with the present state of our knowledge in this field, so that newly developing design methods can be utilized with understanding and discretion.

APPENDIX.—BIBLIOGRAPHY

1. "Specifications for Structures of Aluminum Alloy 6061-T6," and "Specifications for Structures of Aluminum Alloy 2014-T6," 2nd and 3rd Progress Reports, Committee on Design in Lightweight Structural Alloys, Proc. Paper No. 970, and Proc. Paper No. 971, ASCE, Vol. 82, No. ST3, 1956.
2. "Buckling Strength of Type 301 Stainless Steel Plates and Columns," Amer. Iron and Steel Inst. Yearbook, 1958.
3. "On Inelastic Buckling in Steel," by G. Haaijer and B. Thurlimann, Proc. Paper No. 1581, ASCE, Vol. 84, No. EM2, 1958.
4. "Material Properties of Structural Steel," by Lambert Tall, Lehigh Univ. Fritz Engrg. Lab. Report No. 220A.28A, 1958.
5. "Synopsis of First Progress Report of Committee on Safety Factors," by O. G. Julian, Proc. Paper No. 1316, ASCE, Vol. 83, No. ST4, 1957.
6. "The Influence of Residual Stresses on the Strength of Structural Members," by R. L. Ketter, Welding Research Council Bulletin No. 44, 1958.
7. "Residual Stress and the Compressive Strength of Steel," by A. W. Huber and L. S. Beedle, Welding Journal, Welding Research Supplement, Vol. XIX, 1954, p. 589.
8. "Brittle Fracture in Welded Bridges," by P. P. Bijlaard, Engineering-News Record, McGraw-Hill Book Co., Inc., New York, April 26, 1951.
9. "Control of Steel Construction to Avoid Brittle Fracture," M. E. Shank, Editor, Welding Research Council, 1957.

10. "An Evaluation of Plastic Analysis as Applied to Structural Design," by B. G. Johnston, C. H. Yang, and L. S. Beedle, Welding Journal, Welding Research Supplement, Vol. XVIII, 1953, p. 224.

11. "Fatigue of Welded Structures," by R. Weck, The Structural Engineer, London, Vol. XXXII, 1954, pp. 115 and 274.

12. "The Effect of Fabricated Edge Conditions on Brittle Fracture of Structural Steels," by L. A. Harris and N. M. Newmark, Univ. of Illinois Structural Research Series No. 144, 1958.

13. "Some Basic Aspects of the Shear Strength of Reinforced Concrete Beams," by S. A. Guralnick, Cornell Univ. Ph. D. dissertation, 1958.

14. "Versuche zur Festigkeit der Biegedruckzone," by H. Rüsch, Deutscher Ausschuss für Eisenbeton, Heft 120, Berlin, 1955.

15. "Concrete Stress Distribution in Ultimate Strength Design," by E. Hognestad, N. W. Hanson, and D. McHenry, Proceedings, ACI, Vol. 52, 1955-56, pp. 455 and 1305.

16. "The Inelastic Behavior of Structures," by A. M. Freudenthal, John Wiley and Sons, Inc., New York, 1950.

17. Report of ASCE-ACI Joint Committee on Ultimate Strength Design, Proc. Paper No. 809, 1955.

18. "Confirmation of Inelastic Stress Distribution in Concrete," by E. Hognestad, Proc. Paper No. 1189, ASCE, Vol. 83, No. ST2, 1957.

19. "An Investigation of High-Strength Deformed Steel Bars for Concrete Reinforcement," by S. A. Guralnick, Cornell Univ., School for Engrg., Report No. TSR 4730-7146, Part I, 1957, Part II, 1958.

20. "The Strength of Plain, Reinforced and Prestressed Concrete under the Action of Combined Stresses with Particular Reference to the Combined Bending and Torsion of Rectangular Sections;" and "Experiments on the Strength of Reinforced and Prestressed Concrete Beams and of Concrete-Encased Steel Joists in Combined Bending and Torsion," by H. J. Cowan, Magazine of Concrete Research, London, Vol. 5, December, 1953, and Vol. 7, March, 1955.

21. "Strength of Concrete Under Combined Tensile and Compressive Stress," by D. McHenry and J. Karni, Proceedings, ACI, Vol. 54, 1958, p. 829.

22. "Strength of Concrete Under Combined Stress," by B. Bresler and K. S. Pister, Proceedings, ACI, Vol. 55, 1958, p. 321.

23. "Some Implications of Recent Diagonal Tension Tests," by Ph. M. Ferguson, Proceedings, ACI, Vol. 53, 1956, p. 157.

24. "Creep of Plain and Reinforced Concrete," by G. P. Fluck and G. W. Washa, Proceedings, ACI, Vol. 54, 1958, p. 879.

25. "Concrete Beams and Columns with Bundled Reinforcement," by N. W. Hanson and H. Reiffenstuhl, Proc. Paper No. 1818, ASCE, Vol. 84, No. ST6, 1958.

26. "Fourth Progress Report on Column Tests," made at the Univ. of Illinois, by F. E. Richart and G. C. Staehle, Proceedings, ACI, Vol. 28, 1932, p. 279.

27. "Reinforced Concrete Column Investigation," by F. E. Richart, *Proceedings,* ACI, Vol. 29, 1933, p. 275.

28. "Sustained Load Strength of Eccentrically Loaded Short Reinforced Concrete Columns," by I. M. Viest, R. C. Elstner, and E. Hognestad, *Proceedings,* ACI, Vol. 52, 1956, p. 727.

29. "Effect of Sustained Overload on the Strength and Plastic Flow of Reinforced Concrete Beams," by G. W. Washa and P. G. Fluck, *Proceedings,* ACI, Vol. 50, 1953, p. 65.

30. "Under-Reinforced Concrete Beams Under Long-Term Load," by A. H. Sawyer and J. E. Stephens, *Proceedings,* ACI, Vol. 54, 1957, p. 21.

31. "Plastic Flow of Thin Reinforced Concrete Slabs," by G. W. Washa, *Proceedings,* ACI, Vol. 44, 1947, p. 237.

32. "Effect of Strain Rate on the Compressive Strength and Elastic Properties of Concrete," by D. Watstein, *Proceedings,* ACI, Vol. 49, 1953, p. 729.

33. "Review of Limit Design of Structural Concrete," by C. W. Yu and E. Hognestad, *Proc. Paper No. 1878,* ASCE, Vol. 84, No. ST8, 1958.

34. "On the Absolute Minimum Weight Design of Framed Structures," by Jacques Heyman, Div. of Applied Mathematics, Brown Univ., Tech. Report 36, May, 1958.

35. "Beams of Uniform Strength Subjected to Uniformly Distributed Loading," by W. A. Gross and J. P. Li, *Journal of Applied Mathematics,* Vol. 24, No. 1, March, 1957, p. 105.

36. "Building Code Requirements for Reinforced Concrete," *Proceedings,* ACI, pp. 318-356.

37. "Reinforced Concrete Fundamentals," by Phil M. Ferguson, John Wiley and Sons, Inc., New York, 1958, p. 10.

38. "Plastic Design of Steel Frames," by L. S. Beedle, John Wiley and Sons, Inc., New York, 1958, p. 3.

39. "Compression, Flexure and Tension Tests of Plain Concrete," by H. F. Gonnerman and E. C. Shuman, *Proceedings,* ASTM, Vol. 28, Part II, 1928, p. 527.

40. "High-Strength Deformed Steel Bars for Concrete Reinforcement," by S. A. Guralnick, *Proceedings,* ACI, Vol. 32, September, 1960, p. 241.

41. "High-Strength Reinforcing Steels for Concrete Bridges," by E. Hognestad and G. Winter, *Proceedings,* Highway Research Bd., Vol. 39, 1960, p. 103.

42. "Instantaneous and Long-Time Deflections of Reinforced Concrete Beams," by W. W. Yu and G. Winter, *Proceedings,* ACI, Vol. 32, 1960, p. 29.

43. *Elementary Structural Analysis,* by John B. Wilbur and Charles H. Norris, McGraw-Hill Book Co., Inc., New York, 2nd Edition.

44. Discussion by George Winter of "Theory of Limit Design," by J. A. Vanden Broek, *Transactions,* ASCE, Vol. 105, 1940, p. 673.

45. "Concepts of Structural Safety," by C. B. Brown, *Proceedings,* ASCE, Vol. 86, No. ST12, December, 1960, p. 39.

DISCUSSION

RALPH L. BARNETT,[3] **A.M. ASCE.**—In the writer's opinion, the broadness of Mr. Winter's treatment precludes sufficient attention to detail and as a result may lead the uninitiated to misconceptions or, worse, lull him into a dangerous state of security. Typical examples of such shortcomings are found in the section on plastic design. Specifically, let us consider in a cursory manner the so-called "optimum design" of Fig. 6.

Assume that the material of the truss is elastic-perfectly plastic, that deflections are not important, that the loading shown is statically applied, and that no other loadings are admitted. Presuming that by optimum design the author refers to minimum weight design, it is clear that this condition is achieved when $\alpha = 0$, regardless of whether plastic or elastic methods are used. Furthermore, both methods produce exactly the same structure in this case. When α is a fixed acute angle, the author concludes that $\sigma_1 = \sigma_2$ is impossible for the elastic design. This conclusion is incorrect if we allow the unloaded truss to sustain a non-zero stress field, that is, if we admit the possibility of prestressing. The ultimate strength of the prestressed elastic truss can be made exactly the same as that of a similar plastic truss. For the prestressed elastic design, the bar stresses are linearly related to the external load. This desirable property is not obtained with the plastic design. In addition, the stiffness of the prestressed elastic truss is greater at full load than that of the plastic truss. In the design of a prestressed elastic truss the designer may, as in the case of a plastic design, impose the condition that, at failure, the force in each of the bars (34) be some fraction of that in the bar (35).

The author also leaves the impression that one cannot produce a variable-section, fixed-ended, elastic beam of constant maximum fiber stress. This is not the case however (34), (35).

The author makes the general statement that "the plastic method enables the designer to dictate to the structure the precise manner in which he wants it to resist the external forces. . . ." Certainly, the author realizes that this statement is an oversimplification, but the uninitiated engineers might take it literally. The example shown in Fig. 11 dramatically points out the dangers of such an interpretation.

For the truss geometry shown in Fig. 11, the relationship between the strains is,

$$\epsilon_2 = \frac{\sqrt{65 + 2\,\epsilon_1 + \epsilon_1^{2}} - \sqrt{65}}{\sqrt{65}} \Bigg|_{\epsilon_1 = 0.25} = 0.00432 \qquad \text{. . . . . (6)}$$

where the subscripts refer to members in Fig. 11. When ϵ_1 equals the breaking strain, 0.25 in per in, $\epsilon_2 = 0.00432$ in per in. Consequently, bar 1 fractures before either of bars 2 has come close to developing its yield stress σ_{ys}. Direct application of the plastic method assumes, of course, that the bars may all achieve their yield stress at the same time. Incidentally, the prestressed elastic truss can be designed so that all bars are simultaneously stressed to their yield. If, in this example, we admit infinite ductility, we might investigate the deflection under the yield load, that is, under the load that just brings either of bars 2 to its yield stress. This deflection is given by

---

[3] Assoc. Research Engr. Armour Research Foundation of Illinois Inst. of Tech., Chicago, Ill.

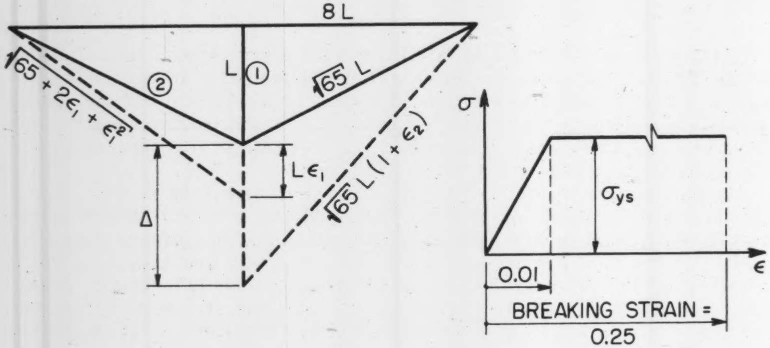

FIG. 11.—ELASTIC-PERFECTLY PLASTIC TRUSS

$$\Delta = L \left\{ \sqrt{\left[\sqrt{65}\ (1+\epsilon_2)\right]^2 - 64} - 1 \right\}_{\epsilon_2 = 0.01} = 0.5187\ L \ldots\ldots (7)$$

Such a deflection would generally be considered unacceptable; consequently, the plastic method has once again furnished too little information about the structural behavior.

The writer would like to point out that his criticism is directed primarily to this type of paper rather than the specific presentation. Even this further elaboration on a small portion of Mr. Winter's paper does not adequately introduce the reader to the limitations or potentialities of plastic design.

LESTER H. GABRIEL,[4] M. ASCE.—The author quite rightly points to the fact that the material testing procedures in common use and the interpretations placed thereon are an attempt to make explicit some of the more significant variables of a design model thought to apply.

In a design model (method), the consequences of the design are, of necessity, a function of not only the explicit factors of material composition, stress, strain, modulus of elasticity, yield point, etc., but also of many (perhaps hundreds or even thousands) of neglected factors. A good design method will satisfy the following:

---

[4] Asst. Prof. of Civ. Engrg., Sacramento State College, Sacramento, Calif.

(1) The variables of the properties of the material that have a significant effect will be well understood and properly evaluated so that the explicit factors will properly influence the design procedures.

(2) All the major factors of influence will have been made explicit and properly evaluated so that those many factors which are considered negligible and omitted are in fact negligible and act as a chance variable. If negligible factors of influence act as something other than a chance variable then the total effect of the negligible factors may be quite significant.

(3) The design method itself will be subject to test and the consequences thereof will reflect on the value of the method. If the results of the tests fail to satisfy the constraints of the design method, then the entire method itself must be scrutinized for erroneous assumptions; that is the explicit factors, the negligible factors that are assumed to act as a chance variable, and the test instruments themselves (the maintained hypotheses).

To those initiated in the area of reinforced concrete design by the elastic analysis method, it is immediately apparent just how important is the modulus of elasticity of concrete (E_c). In fact E_c and n, the ratio of the modulii of steel to concrete, underly the very substance of the method of the transformed section for elastic design. The ACI Building Code (36) calls for $n = 30{,}000/f'_c$ which in turn, gives E_c a value of $1{,}000\ f'_c$. This is the well known secant modulus and the design methods of present and past accept this estimate of one very significant factor of the many explicit factors of the design method.

The fact that it is known that the secant modulus estimate of $E_c = 1{,}000\ f'_c$ is low for moderate strength concrete and high for high strength concrete, (37) coupled with the fact that any kind of variability in E_c is ignored in the classical design methods, puts this variability in E_c in the group of neglected factors. The fact that the variability in E_c does not present itself as a chance variable but rather a function of f'_c itself, leads to a bias in the design method. How then does this one type of variation (which is not subject to chance alone) effect the strength of the structure? How does it effect the apparent factor of safety? How do variations of other factors in the design model, both explicit and neglected, effect the strength of the structure or the apparent factor of safety?

The writer wishes to lend support to the author's statements

> "The attempt is to reduce the amount of judgment and increase the factual and quantitative basis on which safety and load factors are determined. While it is unlikely that it will ever be possible to deal with safety entirely on a statistical-probabilistic basis, -------, it (information) can be incorporated in the safety factor explicitly and numerically."

This writer feels very strongly that now—when new methods of design and analysis are bursting forth, when older methods are being re-examined, and when the philosophy of the action of structures under load (s) and all the design methods related thereto are being explored anew—is the time to attempt to include probabilistic estimates of variability as a parameter of the methods themselves. This would lead to (1) more significant testing and test procedures, (2) a realization on the part of the designer that variability does exist and must be considered in the design, and (3) a more sophisticated concept of safety factor or load factor in terms of probability of failure and the related consequences.

Once a design method is developed and accepted as a "modus operendii" of the design profession, it becomes exceedingly difficult to effect changes. It is with anxiety that this writer has followed the development of plastic design so that the margin of safety of design "is not less than that provided against failure of a simply supported beam according to usual past practice" (39).

This writer believes that the structural engineering profession has arrived at that degree of sophistication whereby notions of factor of safety or margin of safety that describe a vague condition of expected strength without describing some estimate of likelihood of failure are grievously wrong. Variations of all kinds must be considered and be part of the thinking of the developers of design methods. To develop new methods so they are as safe as old methods is a step backwards because of the time lag it generates in the eventual definition of factor of safety as an estimate of the probabilities of failure or success.

HENRY J. COWAN,[5] **M. ASCE.**—Mr. Winter is to be congratulated on an outstandingly lucid paper. The writer agrees with most of the author's comments. He would, however, like to correct a small error in reference to his own work. After discussion of this work, the author states: These various approaches have in common the fact that they attempt to relate the strength of concrete under continued stress to a single property, usually the cylinder strength. . ." The criterion for failure under combined stresses used by the writer, as the author states correctly, in an earlier passage, is a dual criterion, in which the primary tension failure is governed by the maximum stress theory, and the primary compression failure by the Mohr theory (with the Coulomb straight line criterion serving as a good approximation within the range considered.) The compressive strength and the tensile strength of the concrete are, therefore, determined by two independent series of tests.

In the writer's investigation, referred to by Mr. Winter, it was the aim to keep the quality of the concrete uniform throughout the investigation, to determine the compressive strength of the concrete for each reinforced test specimen from concurrent cylinder tests, and to determine the average tensile strength for the entire series from torsion tests on plain concrete. In actual fact, there was some variation in concrete quality due to the fact that the program of tests was undertaken at a time of severe fuel restrictions in England, so that it was impossible to heat the laboratory in winter, on weekends, and holidays and this produced a seasonal variation of strength. In consequence, the tensile strength for the individual specimens was derived from the average strength of the series and from the individual cylinder tests by assuming that the tensile strength was proportional to $\sqrt[3]{(\text{compressive strength})^2}$.

While the approximate character of this correction may have affected the interpretation of the data, it in no way alters the failure criterion, which is based on two independent quantities, the tensile strength and the compressive strength.

OLIVER G. JULIAN,[6] **F. ASCE.**—The author has presented an excellent, cogent summary of currently developed technical features of structural engineering as applied to steel and concrete. It is noted that it was presented to introduce a symposium on plasticity in structural design. The intent of this discussion is to confirm and emphasize certain points that the writer considers of particular importance.

---

[5] Prof. and Head, Dept. of Architectural Science, Univ. of Sydney, Australia.

[6] Head of Structural Div., Jackson and Moreland, Inc. Engrs., Boston, Mass.

Under the section on the yield point of steel, the author states that "it is unlikely that it will ever be possible to deal with safety entirely on a statistical - probability basis." The writer has considerable sympathy with this point of view, with emphasis on the word "entirely." However, he feels compelled to add that apparently the greatest impediment to the use of such an approach is lack of knowledge by many regarding the elements of the mathematics involved, and reluctance to admit or recognize, that no matter how conservatively a structure is designed, there is in the nature of things some probability of its failure. This probability may be extremely small, say 10^{-4} or 10^{-6}, however, it is finite (not zero)(5).

It should be borne in mind that in addition to the variations in the quality of material (such as yield point) mentioned by the author, the strength of a structure depends on variations in quality of workmanship (accuracy of fabrication and erection), errors in design, and perhaps other variations. In probability studies, the combined effect of such variations is usually measured by the vectorial sum of the individual coefficients of variation. For example, if the individual coefficients are as follows: material as delivered on the job 0.124; workmanship on job 0.050; and errors in design 0.050; the combined coefficient of variation is $\sqrt{(.124)^2 + (.05)^2 + (.05)^2} = .143$.

The writer wholeheartedly endorses the author's statement to the effect that the revolution now underway in structural engineering may be aptly characterized as the strength concept versus the stress concept. However, although in many cases the value of intensity of stress may be of no practical importance, in many cases it is of prime importance because (1) it may in some cases govern the usefulness of the structure as measured by deformations and deflections, and (2) in other cases it may govern its strength with respect to collapse or unduly shorten its useful life. As a matter of fact, we have been using the principles of so called "plastic design" for many decades while giving lip service to the theory of elasticity.

The writer wishes to emphasize that we need both concepts. One cannot rationally design structures using the strength concept without having a working knowledge of the stress concept including what is commonly miscalled "strength of materials" and the theories of elasticity and elastic stability. In addition, it is of course necessary to know the pertinent values of the properties of the materials and their probable variations. We should be cautious not to oversimplify procedures for plastic design to a degree that will, in many cases, produce structures which, although safe with respect to collapse, will be unserviceable on account of excessive deformations and deflections or be unsightly, and, in many cases, may be dangerous or have an unduly limited useful life. As pointed out and illustrated by the author, "it may be necessary to surround plastic design with more refined safeguards than are necessary for conventional procedures."

The writer is well acquainted with the background of Figs. 7(a) and 7(b). For more detailed and pertinent information than is given on these Figs., reference may be made to the writer's Figs. 3 and 4, Table I and the accompanying text as referenced by the author (5). It appears desirable to state here that the coefficients of variation associated with Figs. 7(a) and 7(b) are 0.104 and 0.263 respectively. It will be noted that the mean strength (5.2 ksi) of the concrete represented by Fig. 7(a) is 1.4 ksi, that is, 37% greater than 3.8 ksi which is designated as the specified minimum strength. Such a margin is considered unwarranted. The writer's practice is to aim the mean strength of concrete as placed on the job (not of laboratory trial mixes) 18% higher than the minimum specified. Then, if the coefficient of variations closely approximates that associated with Fig. 7(a), at least 90% of the test cylinders may be expected to exceed the minimum specified strength.

One of the intangibles associated with concrete control is cooperation by the owner. Good concrete control is relatively expensive. It may approximate $3.00 per cu yd on a typical power house job where the placing of concrete is of necessity intermittent. This includes services of two control engineers, one at the proportioning plant and one at the location where the concrete is placed, and the services of a commercial laboratory to make and report the results of tests. It is not unusual to consider the cost of adequate control excessive and not worthwhile. The notion that concrete is a "fool-proof" material, which can be proportioned, mixed, transported, placed, and not cured without engineering supervision supplemented by tests of all materials and the concrete as placed, is all too prevalent.

Regarding the tensile strength of concrete, values of which are quoted by the author as fractions varying between 1/8 and 1/30 of the cylinder strengths, it appears to the writer that a far better gage for this important property is

$$f'_t = k\sqrt{f'_c} \quad \ldots\ldots\ldots\ldots\ldots\ldots \quad (8)$$

in which f'_t is the tensile strength, f'_c refers to the compressive cylinder strength (both strengths being in pounds per square inch), and k is a parameter having the dimensions $\text{lbs}^{\frac{1}{2}}\ \text{in.}^{-1}$.

From such test data as he has reviewed, the writer judges that a conservative value for k is 3. However, it apparently varies between wide limits from $2\frac{1}{2}$ to 5, dependent upon conditions. The author's statement to the effect that lack of information regarding the tensile strength of concrete seriously hampers attempts toward deeper understanding of concrete performance, is very much to the point. It is hoped that it will encourage research regarding this important property.

An expression similar in form to Eq. 8 appears suitable and desirable for bond strength. In this case, the writer is not in a position to even suggest a value for k, especially for the larger sized bars such as 14S and 18S.

An important property of concrete not covered explicitly by the author is Young's modulus, E_c, and its variations with time, exposure, and loading conditions. This parameter is of particular importance when considering buckling problems and in computing deflections. It is currently customary to take the value of E_c for short time loading as 1,000 times the compressive cylinder strength f'_c. Although this value may be a fair approximation in case $f'_c \approx$ 2,500 psi, it does not appear to be suitable for use in connection with the higher strength concretes. A preferable expression suggested to the writer by I. M. Viest, M. ASCE is

$$E_c \approx 50{,}000\sqrt{f'_c} \quad \ldots\ldots\ldots\ldots\ldots\ldots \quad (9)$$

in which E_c and f'_c are in psi and the constant has the dimensions $\text{lbs}^{\frac{1}{2}}\ \text{in.}^{-1}$. For a long time loading, this value should be reduced between 10% and 75%, dependent upon conditions, in order to obtain the effective values.

If the concrete is maintained in a continuously moist condition, there may be considerable increase in the value of f'_c which will be reflected in the value of E_c. However, this will probably be more than offset by the effect of creep so that a reduction of 10% will be in order. On the other hand, if the concrete is dried out, shrinkage as well as creep must be considered. There will be a negligible increase in the value of f'_c and a reduction of 75% will be in order.

It is noted that this latter reduction is in line with the greatest reduction noted by the author in discussing computations of deflections. The reductions stated above are for members subjected to continuous application of load. They should not be used in connection with that portion of the live loading which is applied only for short intervals.

The value of E_c suitable for use in computing the critical loads for combination columns, such as those consisting of steel pipe filled with concrete, is indeed debatable. The value currently employed by the writer is 440 f'_c. If f'_c = 4,200 psi this implies a 43% reduction from the value given above for short time loading.

The suspicion expressed by the author, that the descending branch of the stress-strain curve for concrete is caused by progressive irreversible microcracking is most plausible. It apparently solves an enigma of long standing, namely, how is it possible, in sound material, for the stress to be other than maximum at the location of maximum strain. As indicated by the author, it is questionable if the descending branch of the stress-strain curve should be considered as effective. If it is not so considered, the compressive strain of the concrete, according to Fig. 8, should be limited to roughly 0.002, which approximates the yield strain of steel having a yield strength of 60 ksi. The use of steels of higher yield strength may cause greater strains than it is possible to develop in the concrete and, therefore, as pointed out by the author, put a limit on their efficiency for compressive reinforcement. The advisability of their use for tensile reinforcement is also somewhat questionable as it may lead to undesirable deflections.

In the sections on failure under combined stresses and shear strength of beams the author presents an especially noteworthy and clear general view regarding the shear strength of beams. The quotation from Bresler and Pister (22) reading,

> "that strength of concrete is a function of the state of stress and cannot be predicted by limitations of tensile, compressive and shearing stresses independently of each other."

although axiomatic (at least to those acquainted with elementary strength of materials), cannot be emphasized too strongly.

It is indeed unfortunate that although strength theories such as Coulomb's and Mohr's apparently apply failry well to concrete subjected to compression, they do not apply to concrete subjected to tension for which Rankine's theory appears to apply. This seriously complicates problems involving combined stress such as the shear strength of concrete beams. Other complexities are introduced by shrinkage and temperature effects which are all too often neglected.

In spite of these complexities we have for many decades been designing beams by limiting the computed shearing stress (as a measure of diagonal tension) to a fractional part of f'_c and totally disregarding the quotation previously given (22). The fractional parts of f'_c specified have, in some cases, proved to be other than lower limits of the involved strength.

On account of the sudden nature of shear failures, the complexity of the problem, the large variation in reported test results, and the small relative differences in costs (when considered as a percentage of the cost of the finished concrete frame), the writer believes we should be sure to be on the conservative side with respect to shear strength of concrete structures. Salient points regarding the writer's practice are:

1. Limit the unit working shearing stress v_c for members without web reinforcing to $1\sqrt{f'_c}$. This expression is the same as that given previously for the ultimate strength of concrete in tension except for the inclusion of a "factor of ignorance" of 3.

2. If the unit working shearing stress exceeds $1\sqrt{f'_c}$ assume that the entire shearing force at a section is resisted by adequate web reinforcing stressed at not more than 20,000 psi. (This for new billet-steel with a minimum specified yield strength of 40,000 psi).

A. ZASLAVSKY.[7]—This comprehensive and authoritative review by Winter covers a topical subject of great practical importance. The writer would like to add the following remarks:

1. The term "Strength of Materials" is certainly a misnomer; so are "Resistance of Materials" as used in French, Italian, Russian, and so forth, and "Theory of Strength" as used in German.

2. The author suggests that the latest developments in structural design are characterized by "strength" vs. "stress" rather than by "plastic" vs. "elastic." This is correct; the writer wonders, however, whether (in limit desing) it is not, in the last resort, "strain" vs. "stress," as ultimate strength is actually defined by a limiting deformation (strain) criterion even if expressed in terms of strength (stresses). For instance, the appearance of a plastic hinge in a simple steel beam does not exhaust the beam's carrying capacity, there is still the strain hardening reserve available. But because of the large deflections (strains) involved, the plastic hinge stage is defined as the ultimate strength stage. Another example is the Austrian Code for plastic design of reinforced concrete where the critical moment is defined not as the one causing crushing of the concrete, but rather as the one producing a certain critical limiting compressive strain (or, alternatively, the beginning of the steel's yielding); this is in line with author's remarks.

In this connection one may also define the buckling load as the longitudinal load producing very large transverse deflections when its eccentricity approaches zero.

Finally strain (deformation) could serve as a common criterion for both the critical ("collapse") stage of the structure and its working stage where deflections and cracks are characterized by strain, and allowable working stresses could be expressed by "allowable strains."

3. Referring to the author's Fig. 6, it is a very good example for showing the optimum design possibility $\sigma_1 = \sigma_2 = \sigma_y$ by the plastic method, while in the elastic range: $\sigma_1 = \sigma_2/\cos^2 \sigma_2$ independently of the section ratio A_1/A_2. But the example of the fixed-ended beam is of a different nature, since the elastic bending moment diagram does depend on the section's variation along the beam. It is theoretically possible, by appropriate strengthening of the ends, to achieve an elastic bending moment diagram where the yield stress (or working stress) will appear simultaneously at the extreme fibers of both ends and of the midspan sections. In such a beam, no moment redistribution takes place in the

---

[7] Senior Lecturer, Technion, Israel Inst. of Tech., Haifa, Israel.

plastic range since all the plastic hinges will from simultaneously and in this case results by both methods will differ by the shape factor only (just as in a statically determinate beam).

4. Under the heading "Steel: Residual Stresses," the statement introducing Eq. 3 is not quite clear, because buckling may also take place under (average) stresses well below the proportional limit.

5. Under the heading "Steel: Plastic Design," (in the 10th line under Fig. 6) it might be clearer if the term "static moment" were replaced by "bending moment."

PAUL ZIA,[8] M. ASCE.—Mr. Winter has made an excellent presentation of the recent findings on performance of steel and concrete and their effects on structural behavior. On the subject of failure of concrete under combined stresses, the author made references to the efforts of Cowan (20), McHenry and Karni (21), Bresler and Pister (22) in searching for simplified failure criteria. In this discussion, the writer would like to present a modification to Cowan's criterion which he proposed in his recent study of torsion of prestressed concrete members. (The result of this study is to be published by the ACI Journal).

The modified Cowan's criterion is shown in Fig. 12 in the form of a failure envelope. The construction of this envelope depends on two distinct properties of concrete, namely, the compressive strength f'_c and the torsional strength τ_0. It is seen that this envelope is, in essence, a close approximation of Mohr's generalized failure envelope. Fig. 13 shows the considerable difference among the various strength theories expressed in the form of interaction curves. To test the validity of the proposed criterion, the test data from various sources are plotted in Fig. 14 in terms of the principal stresses. These test data are seen to have very reasonable correlation with the theory, considering the divergence of the types of test specimens. Fig. 15 is a design aid, prepared according to the proposed criterion, from which one may readily determine the apparent torsional strength of concrete subjected to various magnitudes of compressive stress.

Regarding the tensile strength of concrete, the writer agrees with Mr. Winter that it is not a constant fraction of the cylinder strength. The writer, however, suggests the following relationship:

$$f'_t = 0.68 \left(f'_c\right)^{3/4} \quad \ldots\ldots\ldots\ldots\ldots \quad (11)$$

This relationship is based upon the extensive test results of H. F. Gonnerman and E. C. Shuman (39) and is shown in Fig. 16.

---

[8] Asst. Prof. Civ. Engrg., Univ. of Florida, Gainesville, Fla.

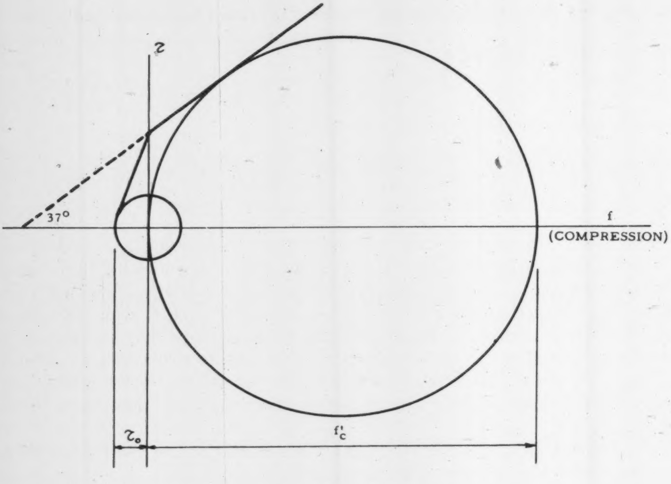
τ
37°
f
(COMPRESSION)
τ_o
f'_c

FIG. 12.—MODIFIED COWAN'S THEORY OF FAILURE

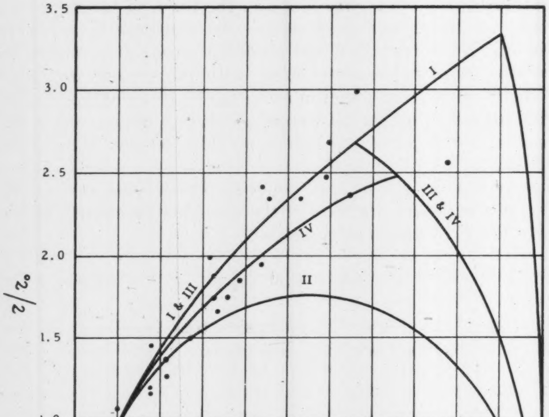

FIG. 13.—INTERACTION CURVES FOR $\tau_o = 0.10 f'_c$

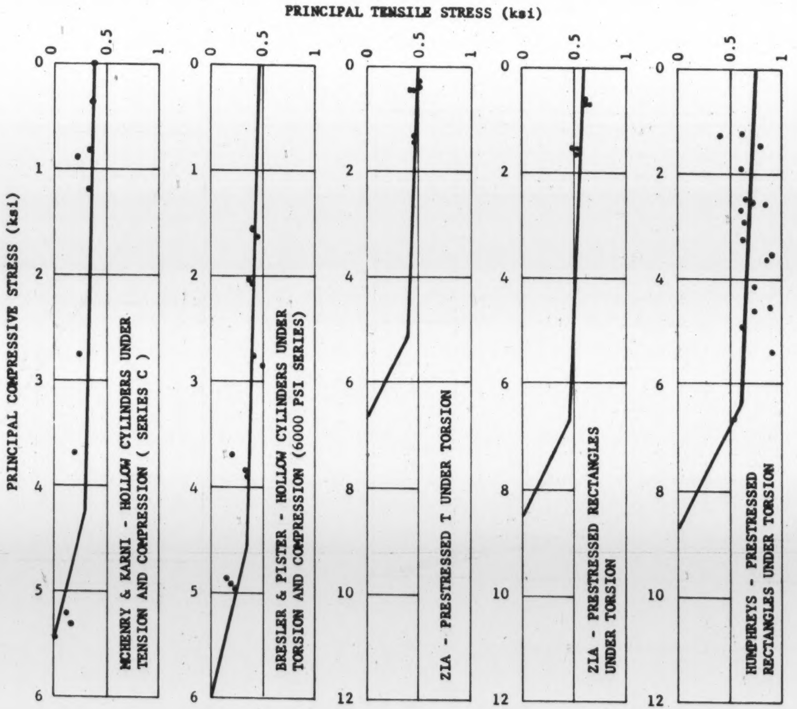

FIG. 14.—COMPARISON OF MODIFIED COWAN'S THEORY WITH EXPERIMENTAL DATA

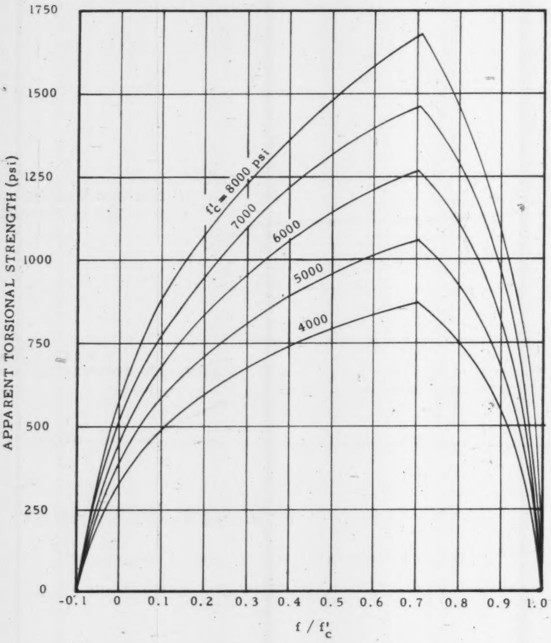

FIG. 15.—APPARENT TORSIONAL STRENGTH VERSUS f/f'_c

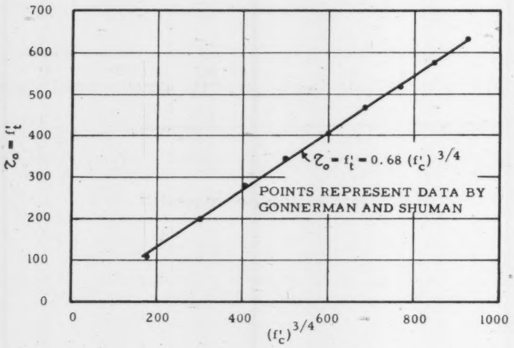

FIG. 16.—RELATIONSHIP BETWEEN TENSILE AND COMPRESSIVE STRENGTH OF CONCRETE

GEORGE WINTER,[9] F. ASCE.—The writer is most gratified by the extensive discussion this paper has received. Many of these comments not only support, but importantly supplement the content of the paper. Taken together with a number of communications received in personal correspondence, one obtains the impression that a service to the profession is being performed by reviews of this type. Barnett, however, is of the contrary opinion and implies that, "this type of paper" may actually be misleading because, in view of its very broadness, it precludes sufficient attention to detail. The writer was careful to point out that, of necessity, this was a review in breadth rather than in depth. A paper such as this is not addressed to the research worker whose business it is to be familiar with the literature. It is intended to assist the busy practicing engineer by acquainting him with recent research findings and with some of their implications. A bibliography of thirty-three items should suffice to lead one to a deeper acquaintance with any one of the discussed topics. It is not believed that any responsible engineer would rely in his work merely on the abbreviated information of such a review without broadening that information by referring, at least, to the source material given in that same paper.

Because comments on several topics have been received by more than one contributor, it may be of advantage to discuss individually the topics rather than the contributions.

Tensile Strength of Concrete.—In the paper the opinion had been advanced, in conformity with S. A. Guralnick, M. ASCE (13), that for a rational approach to a variety of strength problems in reinforced concrete it is necessary to know not only the compression strength f'_c, but also the tensile strength f'_t. It was further suggested that these two properties are not uniquely related. Cowan, Julian, and Zia all agree with the first of these propositions, and Cowan also agrees that "the compressive strength and the tensile strength are, therefore, (to be) determined by two independent series of tests." The probability that f'_c and f'_t are largely independent properties is underlined by the fact that the three aforementioned contributors propose that f'_t may be assumed to be proportional to ${f'_c}^{2/3}$, ${f'_c}^{1/2}$, and ${f'_c}^{3/4}$, respectively. This divergence reinforces the writer's suspicion that the tensile strength depends, at least in part, on other parameters of the constituent materials of concrete than does the compression strength. Studies on fundamental behavior of concrete by the writer and his collaborators, now (1961) under way at Cornell University, suggest, in a very preliminary manner, that the tensile strength of concrete may largely depend, among other factors, on the strength of bond between aggregate and paste (and thereby on surface condition and mineralogical nature of aggregate), in addition to tensile strength of the paste, and on microcracking produced by shrinkage (as explained subsequently). Compression strength, on the other hand, can be expected to depend less on these factors and more on the compression and, possibly, the shear strength of paste and aggregate.

Indirect support for the importance of the tensile strength is furnished by the fact, communicated to the writer in a letter by E. Rosenblueth, M. ASCE, that in the new Mexican concrete design code the allowable shear and bond stresses will be made proportional to $\sqrt{f_c'}$ rather than f_c'. The particular shear stress value of $0.94\sqrt{f_c'}$ mentioned by Rosenblueth, incidentally, is almost identical with the value $1.0\sqrt{f_c'}$ suggested by Julian. It is of interest to note that the forthcoming new edition of the A.C.I. Building Code, in all probability, will also relate allowable and ultimate shear stresses to $\sqrt{f_c'}$ rather than to f_c'.

---

[9] Prof. and Head, Dept. of Structural Engrg., Cornell Univ., Ithaca, N.Y.

Microcracking of Concrete.—To some extent the writer shares Julian's misgivings in regard to utilizing concrete strains in excess of about 0.002 and agrees with the implications that this seems to call for caution in the utilization of yield points in excess of about 60,000 psi, particularly for compression reinforcement. It should be said, though, that in extensive tests at Cornell University on beams with steel yield points up to 90,000 psi and more no particular difficulties have been encountered (40). In these tests, however, compression reinforcement played only a minor role. Limited experience with Kam 60 steel in Sweden (86,000 psi yield strength) also did not seem to indicate difficulties traceable to microcracking (41).

In regard to such microcracking, the aforementioned investigations at Cornell University, very much in their beginning stages, suggest that significant microcracking exists in concrete before any loading is applied. The cause for this appears to be shrinkage and possibly other factors, and it is the varying degree of this microcracking of virgin concrete that may play a role in the variability of the tensile strength. Under load, and particularly at higher stresses, microcracking not only of greater extent but of a different kind appears to develop and it may be this type that is primarily responsible for the descending branch of the stress-strain curve. However, after only about one year's investigation this information is of an extremely tentative nature and no practical conclusions whatever should be drawn from it. It is merely mentioned as a further illustration to the effect that a more rational understanding of structural behavior must be founded on deeper knowledge of the nature of material.

Instantaneous and Creep Deformations of Concrete.—Gabriel and Julian suggest that the customary value for the short-time modulus of concrete, $1{,}000\ f_c'$ is not satisfactory for the entire range of concrete strengths now being utilized, and the latter suggests $50{,}000\sqrt{f_c'}$ as a better approximation. Another expression that has been advanced is $1{,}800{,}000 + 460\ f_c'$. Rosenblueth has stated that in the new Mexican code E_c will be assumed proportional to $\sqrt{f_c'}$.

In regard to long-time deflections, that become increasingly important with the introduction of higher strength materials and consequent shallower members, Julian suggests a reduction of the short-time modulus of 10% to 75%, and Rosenblueth states that a reduction of 75% will be used in the Mexican Code. An extensive, though purely phenomenological investigation of concrete deflections, recently performed by the writer and one of his collaborators (42), suggests that the usage of an effective concrete modulus may not be the best and most practical means of estimating long-time deflections, that such an effective modulus would not bear any easily definable relation to the short-time modulus, and that better practical methods can be devised. In particular, working backward from deflection measurements in sustained-load beam tests, it was found that if effective moduli are used for estimating final long-time deflections, an effective modulus of 350,000 psi appears reasonable for $f_c' = 2{,}000$ psi, and a modulus of 400,000 psi for $f_c' = 5{,}000$ psi. It is seen that these two values bear no recognizable relation to the short-time moduli of these two concretes. The difficulty may possibly stem from the impractibility of separating long-time deflections due to creep from those due to shrinkage.

Strength versus Stress.—In the introduction to the paper the point was made that it is the present trend in structural engineering to deemphasize the concept of stress in favor of that of strength. It was pointed out that strength may depend on plastic properties, but may also depend on others, of which examples were given (brittle fracture, fatigue). A more exact formulation would have been to say that actual strength is being emphasized at the expense of the hitherto prevailing formal criterion of maximum stress computed on the basis of elasticity, particularly in such cases in which these elastic stresses are no realistic measure of strength.

The writer quite agrees with Julian that this does not imply that stresses have lost their significance as a measure of structural performance. On the contrary, in situations such as fatigue or brittle fracture, and for all materials that are essentially brittle in nature, the magnitude of elastically computed stresses continues to be the best available measure of strength. The main point that should be made here is that in such situations the conventional way of considering each individual stress by itself, rather than analyzing an entire biaxial or triaxial stress situation, may show very little correlation with strength performance. The various attempts to analyze the strength of concrete members under complex stress conditions that have been mentioned in the paper and that are supplemented by the investigation communicated in Zia's interesting contribution, are illustrations of this situation.

Deformations.—Zaslavsky and Julian, with evident justification, have pointed out that one of the most important final criteria of performance is deformation under load. There is no disagreement with this truism and with the necessity of accounting for deformation, particularly in connection with the newer, non-elastic design methods. The reason for not emphasizing this aspect resides in the scope of the paper. It has been its sole purpose to relate material properties and performance to structural behavior and primarily to strength. In this connection those material properties that have been discussed are of relatively secondary importance in regard to deformations, because deflections at design loads will generally be in the elastic range; the exception is creep deformations which have been touched on.

The writer is not sure that Zaslavsky's suggestion to regard strain as a strength criterion is altogether promising. The accepted meaning of strain is that of unit strain, that is, of local relative deformation. It is true that the integral effect of these local deformations results in the overall deformations of the structure. It is equally true that these overall deformations are very essential performance criteria and cannot be allowed to become excessive. This does not mean, however, that highly localized strains cannot be allowed to assume values that are large multiples of those average strains that would be regarded as permissible. Such large localized strains occur regularly and without ill effect in most welded connections and in many other details, provided ductility is preserved. However, the same magnitudes of strain at the roots of notches and under triaxial conditions, may have the most catastrophic consequences. It would seem, therefore, that unit strain per se is not generally a useful performance criterion, while its integrated effect, the overall deformation, is indeed essential.

Plastic Design.—By means of the simple, indeterminate truss of Fig. 6 the writer had tried to illustrate a frequently overlooked fact, namely that under elastic conditions it is in many cases impossible to design an indeterminate structure in such a manner that all its members are used to capacity. The same structure illustrates that under plastic conditions this economical condition obtains automatically. Barnett has attempted to cast doubt on this peculiarity of plastic behavior by analyzing the deformation of a structure of the same type, but with dimensions so contrived as to make the application of plastic theory invalid. Had Mr. Barnett drawn Fig. 11 to scale, as is done in Fig. 17, the unrealistic nature of his argument would have been apparent. It is always possible, by inventing special and usually unrealistic situations, to reduce ad absurdum the validity of a method that is perfectly serviceable under normal and practical conditions. In addition, however, an oversight in decimals seems to have occurred in Barnett's numerical computations. The yield strain of mild steel is not 0.01 but approximately 0.001. Consequently, Barnett's own data, if corrected, show that when bars 2 attain the yield strain, bar 1 would reach only about one-fourth of its breaking strain. That is, plastic maximizing of resistance will occur even in Barnett's extreme example. Likewise, the actual deflection corresponding to the correct value of 0.001 is only about one-tenth of Mr. Barnett's value, that is, about 6% of the length of the vertical bar instead of the 52% determined by Barnett. It should be noted that this is the deflection at incipient failure rather than at design load. Correspondingly, Barnett's "dramatic illustration" of the writer's presumed oversimplification appears to be based on an incorrect calculation

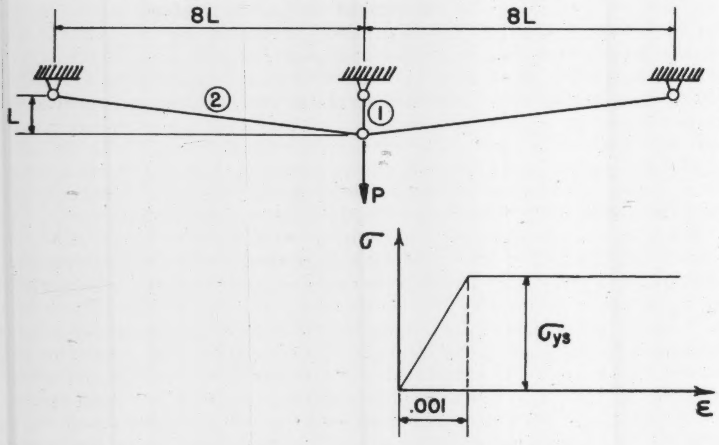

FIG. 17

applied to an unrealistic model. In this connection it may be of some interest to note that Norris and Wilbur, in the second edition of their textbook (published subsequent to the writer's paper) use the very same structure of Fig. 6, but with reasonable proportions (Fig. 13), to demonstrate this same fact of plastic maximization of strength accompanied by negligible deformations(43).

Quite apart from these discrepancies, Barnett's conclusion that "the plastic method once again furnished too little information on structural behavior" seems to rest on the misconception that plastic design specifically excludes any analysis of deformations. The writer, in his discussion of a pioneering paper in this field (44), stated that

> "Any design theory that does not provide the means for determining deformations corresponding to any given load up to ultimate is incomplete and questionable."

In that same contribution the writer then proceeded to develop a method of deformation analysis for plastic bending. Since that time simple and practical methods have been established for such analysis, and any experienced designer will recognize situations in which plastic-design computations should be supplemented by deformation analysis.

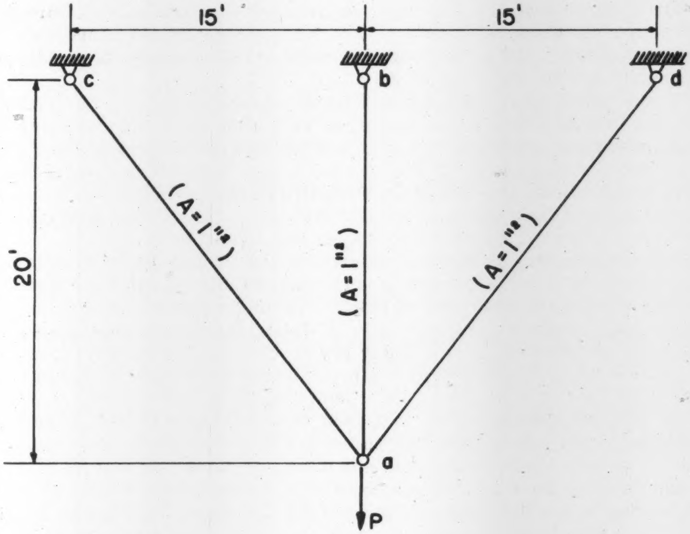

FIG. 18

Barnett also seems to juxtapose the principle of prestressing to that of plastic design and states, with regard to Fig. 6, that

> "in the design of a prestressed, elastic truss the designer may, as in the case of a plastic design, impose the condition that, at failure, the force in each of the bars 2 be some fraction of that in bar 1."

To be sure, this can be achieved by prestressing, but then the additional cost of prestressing merely results in the same condition that plastic action brings about automatically and without such additional cost. Incidentally, the optimizing condition of this and similar situations is not that of achieving certain ratios between bar forces, as implied by Barnett, but of producing a structure in which all members reach their capacity simultaneously, that is not necessarily the same thing. For the rest, the concepts of prestressing are clearly outside the scope of the paper.

On the other hand, the writer stands corrected by both Zaslavsky and Barnett: Contrary to his statement, it is indeed possible to compute for a fixed-ended beam an optimum shape in which the elastic extreme fiber stress is of constant magnitude. It may not be beside the point to remark that for ordinary structural practice such an artificial shape is not exactly an economical solution. For minimum-weight structures rather than minimum-cost structures, however, members so shaped may indeed be practical.

Structural Safety.—Structural safety and the proper ways of achieving it is a matter of broad implications and considerable complexity. The writer has only touched on it in order to indicate its interrelationship with questions of material properties. He agrees with Julian that safety provisions should rationally be based on an acceptably low probability of structural failure. He also agrees with Gabriel that such a procedure is preferable to that of simply making the "safety factor" in plastic design equal to that theretofore prevailing for simple beams elastically designed. The writer is not quite as optimistic as Julian in his expectation that such a purely probabilistic approach is capable of actual achievement. For one thing, for many relevant factors, even though they are basically of a probabilistic nature, adequate statistical data are lacking and will be lacking for some time to come. The "factor of ignorance" of 3 that Julian proposes to apply to such an extensively explored area as shear strength of beams without web reinforcement is an example in point. For another, the writer believes that a number of important factors, such as social consequences of failures, are basically of a non-probabilistic nature (45).

This is the reason why he stated his expectation that "it is unlikely that it will ever be possible to deal with safety entirely on a statistical-probabilistic basis." Needless to say, he agrees with Julian that the farther one can go in that direction, the better. In this connection it may be of interest to state that the safety provisions in the next edition (probably in 1962) of the ACI Building Code probably will be based on the concept of an acceptably low probability of failure, achieved by taking account as rationally as possible of sources of understrength and of overload. The very efforts that are and have been going into the development of these provisions have confirmed the writer's belief in the following: The area in which that intangible something known as engineering judgment continues to prevail can and should be reduced by more rational methods, but one should not even pretend or expect to be able to eliminate it completely.

AMERICAN SOCIETY OF CIVIL ENGINEERS

Founded November 5, 1852

TRANSACTIONS

Paper No. 3265

REVIEW OF RESEARCH ON COMPOSITE STEEL–CONCRETE BEAMS

By Ivan M. Viest[1], F. ASCE

With Discussion by Messrs. W. J. Jurkovich; J. C. Chapman;
and Ivan M. Viest

SYNOPSIS

Investigations of composite beams carried out in the period 1920 to 1958 in the United States and abroad included both experimental and theoretical studies. Tests of specimens with and without mechanical connectors are summarized, specimens briefly described, and major results cited. Presentation of theoretical studies emphasizes the basic assumptions of both elastic and ultimate strength theories.

INTRODUCTION

In 1922, the Dominion Bridge Company of Canada conducted tests of two floor panels, each consisting of two steel I-beams encased in concrete and a concrete slab. In reporting on the results of these tests, H. M. MacKay, P. Gillespie, and C. Leluau(2)[2] wrote:

> ". . . While such beams have hitherto been designed on the assumption that the entire load . . . is carried by the steel, it was thought that the steel and concrete might really act together so as to form a composite beam . . ."

Note.—Published essentially as printed here, in June, 1960, in the Journal of the Structural Division as Proceedings Paper 2496. Positions and titles given are those in effect when the paper or discussion was approved for publication in Transactions.

[1] Bridge Research Engr., AASHO Road Test, Ottawa, Ill.

[2] Numerals in parentheses refer to corresponding items in the Appendix.

At about the same time, tests of composite beams were carried out, also, in the United States(3) and in England(5). All of them indicated good interaction between the two materials. Thus, the starting point was provided for a chain of laboratory studies which have continued to this day.

The early studies were concerned with encased beams in which the interaction between the steel and concrete was provided primarily by bond. However, as the practice moved gradually away from full encasement toward a slab supported on the top of the steel beams, the investigators began to place more emphasis on mechanical connection between the concrete and the steel.

Today, test results are available for over 250 composite beams made of steel I-beams and concrete slabs. Included are T-beams made with one rolled beam, double T-beams made with two rolled beams, multiple T-beams, rectangular concrete beams containing one fully encased steel beam, and rectangular concrete slabs containing two or more rolled sections. Simply supported beams, beams framed into girders or column stubs, and continuous beams were tested. Results are also available for about 250 push-out specimens utilized in shear tests of mechanical connectors and for a few other miscellaneous specimens.

In addition to the simple beam, slab and push-out specimens, tests were also conducted on a number of laboratory models of bridge decks and building floors, and on numerous actual structures(6)(8)(41)(46). This paper, however, reviews only the tests of beams and other simple specimens.

SPECIMENS WITHOUT SHEAR CONNECTORS

The early investigators of composite beams were concerned primarily with the interaction between the steel rolled shapes and the surrounding concrete resulting from natural bond between the two materials. Experiments carried out and reported in Canada, England, continental Europe, and the United States are summarized in Table 1.

Canadian Tests.—The first Canadian tests were reported by MacKay, Gillespie and Leluau in 1923(2). Two specimens were tested with uniform loading applied in several increments. Each specimen was made up of two rolled beams framing into steel girders. The beams, fully encased in concrete, supported a reinforced concrete slab cast monolithically with the concrete encasements of the beams. Maximum steel stresses reached in the test of the heavier loaded specimen were less than 22,000 psi. Both strains and deflections indicated good interaction between the steel beams and the slab. The authors concluded that in the type of construction considered, the concrete and steel act together; and that within practical limits such composite beams may be designed by methods analogous to those used in the design of reinforced concrete T-beams. They have cautioned, however, that the stability and endurance of this form of construction depend on bond between the concrete and steel and that the safe limits of bond stress have not been determined.

The early tests of double T-beams were followed by a single test reported by Gillespie and R. C. Leslie(3a), and by a series of tests reported by MacKay in 1927(4). MacKay aimed at determining the strength of bond and the effects of continuity. The bond strength was investigated with seven simply supported T-beams, four with fully encased I-beams, two with only the top flange encased and one with bond absent on the top flange of a fully encased I-beam. The tests were made with two symmetrically located concentrated loads usually placed very close to the supports. The beams were tested to yielding of the steel or to bond failure. The study of continuity consisted of tests of six fully encased beams connected to transverse girders. The slab was reinforced with varying amounts of reinforcing bars and was subjected to negative moment. Bond failures occurred in the two partially encased beams at horizontal shearing stresses of 400 psi to 500 psi and in the beam with bond absent on the top flange at a horizontal shearing stress of at least 750 psi. On the basis of these tests MacKay recommended a working bond stress of 240 psi for fully encased beams and the use of reinforcing bars in the negative moment regions in an amount equal to the area of the steel beam flange.

TABLE 1.—SPECIMENS WITHOUT SHEAR CONNECTORS

Author of Investigation	Carried Out In		Reference	Number of Specimens Tested				Type of Loading
	Country	Year[a]		T-beams	TT-beams	Push-outs	Others[b]	
(1)	(2)	(3)	(4)	(5)	(6)	(7)	(8)	(9)
MacKay, et al.	Canada	1922	2		2			static and vibratory
Truscon Steel Co.[c]	USA	1921-23	3	5	3			static
Nat. Phys. Lab.	England	1922-23	5				14	
Gillespie, et al	Canada	1924	3[a]	1				static
MacKay	Canada	1927	4	6			6	static
Caughey	USA	1929	5	6				static
Stüssi	Switzerland	1932	9		6			static
Cambournac	France	1932	7				3	static
Baes	Belgium	1932	10	2			2	static
Gruening	Germany	1937	14				4	vibratory
Young	Canada	1937	23	4				static
Young, et al.	Canada	1938	23	1				static
Batho, et al.	England	1939	16	25				static
Lapsins[c]	USA	1953	42	4				static
			Total	54	11	0	29	

[a] Date of publication given where date of investigation not available. [b] Includes slab specimens and specimens with more than two steel beams. [c] Specimens with improved bond.

Further Canadian tests, carried out by Young, Morrison and Sager, were reported by R. C. Manning(23). The tests included six T-beams, four partially encased and two with slab resting on the top flange (no encasement). One of the two latter beams had mechanical connectors (square bars) welded on one half of the span, the other had flexible I-connectors throughout the span. One of the four partially encased beams was continuous over three spans; at two interior and one exterior support, the steel beam framed into columns and near the other exterior support, the beam was provided with square bar mechanical connectors. The conclusion was reached that, so long as the bond between the concrete and the steel was not definitely broken, the composite beams behaved in substantial correspondence with the theory of composite beams (assuming complete interaction between the slab and the beam). Furthermore, mechanical connectors were found to provide an excellent security against an early bond failure.

British Tests.—An early interest in composite action between rolled steel beams and the concrete encasement was manifested in England through publication of tables and design methods between 1910 and 1920. According to R. A. Caughey(5), this interest was followed by tests of 14 floor specimens at the National Physical Laboratory in 1922-1923. These tests of slab specimens reinforced with two to four rolled beams indicated definite presence of composite action.

The most comprehensive experimental study of composite beams relying primarily on natural bond was reported by C. Batho, S. D. Lash, and R. H. H. Kirkham(16). The tests included 27 composite simple beams and 3 reinforced concrete beams incorporated for comparative purposes. Of the composite beams, 18 had the steel I-beam fully encased in the concrete section while nine had only top flange encased in concrete; one of each type was provided with mechanical connectors (clip angles). Twelve composite beams were simply supported and tested with concentrated loads at the third-points applied in several increments to failure. Fifteen specimens, framed into simply supported column stubs; eleven of them were subjected to about 250 days of sustained loading usually followed by a test to failure.

The investigators concluded that the theory for reinforced concrete is applicable to composite beams as long as bond is present. All beams without special provisions for anchoring steel to concrete failed by diagonal tension after slippage between the steel section and the concrete encasement. The addition of angle connectors increased the ultimate strength.

In general, composite beams were found to possess great reserve strength after yielding when end connections provided sufficient anchorage. The column stubs apparently provided an excellent anchorage for fully encased beams, but did not prevent failure by slip in partially encased beams.

For beams without mechanical connectors or end anchorages, the authors recommended an allowable bond stress of 60 psi when the steel beam is fully encased and 50 psi when the steel beam is only partially encased.

Tests in Continental Europe.—Stüssi, Cambournac and Baes reported tests of composite beams and slabs without shear connectors in early 1930's. L. Baes(10) tested two composite T-beams with fully encased steel sections and two slabs supported on four steel beams. L. Cambournac(7) tested three heavy concrete slabs reinforced with four to five steel beams and F. Stüssi(9) tested six double T-beams with rolled steel beams encased almost to the top of the bottom flange.

Stüssi's tests included two variables: the width of the slab and the presence or absence of preloading the steel beams prior to casting the slab. The beams were tested with concentrated loads applied at the third-points in several increments to failure. Slip between the beams and slabs was noted; the beams failed at between 80% and 100% of the theoretical fully plastic capacity. The author concluded that the preloading had no effect on the ultimate capacity and suggested the designing of composite beams on the basis of their ultimate moment capacity. He also recommended the use of mechanical shear connectors or, in the absence of mechanical connectors, a 20% reduction of the calculated fully plastic ultimate moment.

The effect of vibration on the interaction between the steel and concrete was investigated by G. Gruening through tests of four slabs supported on fully encased steel beams(14). Oscillating loads, equal to a fraction of the applied static load, were increased in several increments. Higher oscillating loads caused bond failures.

Tests in the United States.—In contrast to the Canadian and European tests, the first composite beams tested in the United States had natural bond augmented by mechanical means. The tests, carried out at Purdue University, at the University of Nebraska, at the Massachusetts Institute of Technology, and at the Truscon Steel Company, were reported in 1923(3). All test beams were made of rolled beams with prongs sheared in the edges of the top flange and bent upward to project into the concrete slab. Six out of the eight specimens tested failed in flexural compression in the slab after yielding of the steel beams, one failed in bond and one test was discontinued before failure. Good interaction at working loads and high overload capacities were observed.

Tests of six composite T-beams were reported, in 1929, by Caughey(5). On the basis of these tests and of a historical review of tests reported in the literature prior to 1929, Caughey concluded that composite beams may be designed safely on the basis of "elementary principles of design" and recommended an allowable bond stress of $0.03f_c'$ (or 60 psi for 2000 psi concrete); in case of higher bond stresses he suggested the provision of angles riveted to the top flange to carry the horizontal shear in excess of the allowable bond stress(12).

An interesting method of augmenting the natural bond was employed in recent tests by V. Lapsins (42), who tested four T-beams with slab resting on the top of the steel beams. The top flange in contact with the slab was roughened by chiseling out small projections spaced at about 1/4 in. Slip between the beams and the slab was absent practically up to failure. The specimens failed abruptly by separation of the slab from the beams at loads lower than those carried by companion specimens with mechanical connectors.

SPECIMENS WITH SHEAR CONNECTORS

Tests of beams without shear connectors have shown that natural bond can be completely relied on providing composite action only in fully encased beams subjected primarily to static loads and containing end details which constitute effective end anchorages. In partially encased beams and in all beams subjected to large fluctuating loads, the bond is not, generally, fully reliable. The early investigations have indicated further that the weakness of bond may be remedied by mechanical connectors attached to the top flange of the steel beam and embedded in the concrete of the slab.

Systematic studies of specimens with mechanical connectors began in the 1930's. After 1940, practically all investigations of composite action utilized mechanical connectors. With few exceptions, in these studies the encasement of the steel section was entirely missing so that the concrete slab was in contact only with the outside surface of one flange of the steel beam.

Specimens with Spiral Connectors.—The first systematic studies with mechanical connectors were made in Switzerland in connection with the development of the so-called Alpha System. In this method of construction, the transfer of horizontal shear from the concrete slab to the steel beam was assured by a round bar formed into a helix. The helix, called spiral connector, was welded to the top flange of the steel section at the points of contact along the length of the beam. A summary of the tests with spiral connectors is given in Table 2.

Static tests of eight specimens with spiral connectors, carried out by A. Voellmy and Brunner of the Swiss Federal Institute for Testing Materials, were reported by M. Roš(11), in 1933. The tests involved two double T-beams tested with two concentrated loads, four T-beams subjected to axial loads applied at different eccentricities, and two special specimens devised for determination of the shear transfer capacity of the spirals. The last specimens consisted of a short section of a steel I-beam and two concrete slabs, one connected to each beam flange with a spiral. The specimens were supported on the ends of the slabs and the load was applied axially to the steel beam. The load was transferred from the beam to the slab by shear. This type of specimen was used extensively in later tests of mechanical connectors and is referred to as the push-out specimen.

TABLE 2.—SPECIMENS WITH SPIRAL SHEAR CONNECTORS

Author of Investigation (1)	Carried Out In		Reference (4)	Number of Specimens Tested				Type of Loading (9)
	Country (2)	Year[a] (3)		T-beams (5)	TT-beams (6)	Push-outs (7)	Others[b] (8)	
Voellmy	Switzerland	1933	11			2		static
Voellmy	Switzerland	1933	11		2			static
Brunner	Switzerland	1933	11				4	static
Voellmy	Switzerland	1935	21	2				shrinkage
Voellmy	Switzerland	1935	22	2				static
Voellmy	Switzerland	1935	13	5		36		static and fatigue
Columbia Univ.	USA	1937	15		4			static
Lehigh Univ.	USA	1943	19			4		static
Mains	USA	1943	18	4				static
Viest	USA	1956	55			6		static
			Total	13	6	48	4	

[a] Date of publication given where date of investigation not available. [b] T-specimens tested as columns.

Roš reported the existence of complete interaction between the slabs and the steel sections up to the failure of bond. However, even after the failure of bond, the composite beams and columns continued to deform essentially as units. The beams failed in flexure by exceeding the yield point of the steel beams and the columns failed by buckling. No evidence of inadequate connection between the concrete and the steel was noted. On the basis of these results, the author recommended to design the beams with spiral connectors according to the methods used for reinforced concrete beams.

Voellmy continued the studies of composite beams and spiral connectors in 1935-1936 with tests of 9 beams and 36 push-out specimens. Two T-beams, identical except for the strength of concrete, were built for observation of shrinkage stresses in an outdoor exposure(22). The effect of preloading was studied by tests to failure of two fully encased beams(21); the two beams were essentially identical, but one had an initial maximum dead load stress of ± 6,150 psi, while the bottom flange of the other beam was stressed initially to 24,160 psi by a combination of dead load effects and the residual effects of a weight hanging from the beam during casting and hardening of the concrete. The remaining five beams and the 36 push-out specimens were tested to determine the behavior of spiral connectors(13); four beams were tested with repeated loading, the other specimens with static loads to failure. The tests of push-out specimens included the following variables: two diameters of the spiral bar, two diameters of the spiral, five values of the pitch of the spiral and two levels of the strength of concrete.

The shrinkage measurements indicated that the maximum unit contraction at the top of the slab was of the order or 0.0003 and the maximum unit contraction of the steel section was of the order of 0.0002. Elongations of the steel section occurred only on the first day after casting the slab. The time dependent strains included the effects of temperature changes which seemed to explain the major portion of the measured strains. The time dependent strains in the steel beams corrected for the effects of temperature changes were less than 0.0001.

The second study(21) has shown that the initial bending stresses in the steel beam did not influence the static load-carrying capacity of a composite beam. On the other hand, the load deformation characteristics of the two beams differed.

On the basis of the static tests of push-out specimens, Voellmy concluded that spiral connectors came into action after the breaking of natural bond at bond stresses between 180 psi and 430 psi. The shear was transmitted from the slab to the spiral partly by direct bearing on the welds and partly by bending of the spiral. The bending stresses determined the beginning of the plastic deformation of the spiral. Assuming that the spiral bar acts as a beam on elastic foundations, Voellmy derived a mathematic model for static load capacity of a spiral and has shown with the aid of the push-out test data that this capacity depended only on the diameter of the spiral bar and on the strength of concrete. Static test of one T-beam indicated that the formula for the capacity of spiral connectors is conservative(13).

On the basis of the four repeated load tests, Voellmy suggested that the fatigue strength was determined primarily by the maximum stress in the spiral bar caused either by a combination of normal and shearing stresses or by a combination of normal and bending stresses. Taking the first alternative and assuming that one half of the total force per weld is transmitted by tension in the bar on one side of the weld and the other half is transmitted by compression in the bar on the other side of the weld, a tentative formula was derived for the fatigue resistance of the spiral. The formula was found conservative in comparison with the test data, but Voellmy cautioned that further fatigue tests were needed to check the validity of the dynamic formula(13).

Further studies of spiral connectors involved static tests of simply supported beams and of push-out specimens. In 1937, the staff of the Columbia University conducted tests of four double T-beams(15). The dimensions of the beams, slabs, spirals and the span length were different for each specimen. A center support was provided during casting and hardening of the slab in two specimens. All specimens were tested with two concentrated loads past yielding the steel beams. In two specimens, breaking of the spiral and some welds was observed after the beams have yielded. The data was inconclusive concerning the effects of shoring.

Comparative tests of spiral, one type of rigid and two types of flexible connectors were carried out in 1943, at the Fritz Engineering Laboratory, at Lehigh University(19). Sixteen push-out specimens, four with spirals, four with flexible angles, four with flexible channels and four with stiff H-sections were included. The strength of concrete and the number of connectors were also varied. Failures in the concrete, the connectors and the welds were observed; the flexible angles, providing no anchorage against separation of the slabs from the steel beams, failed by pulling out of the concrete.

Another study of the effect of shoring was made by R. M. Mains(18) who tested simply supported T-beams, two built with the forms for the slab suspended from the steel section and two with temporary supports along the span. The beams were loaded with concentrated loads increased in increments until the maximum load capacity of the beams was reached. In terms of the loads at first yielding, the beams supported during placement and curing of concrete had about 15% greater capacity than the beams with forms suspended from the steel section. Differences were observed, also, in the ultimate loads but comparisons with computed fully plastic capacities suggest that the temporary supports had little, if any effect on the ultimate load-carrying capacity.

To obtain data comparable to those available for stud and channel connectors, I. M. Viest(55) carried out tests of six push-out specimens with spiral connectors. The experiment differed from all earlier studies in that the spiral was welded with only one weld on each flange of the I beam and that in half of the tests the load was intermittently released to zero to permit measurements of residual deformations. The diameter of the spiral bar was the only independent variable included in the study. The capacity of the spiral was compared with the capacity of stud connectors on the basis of "critical" loads defined as the loads causing a residual slip of 0.003 in. It is of interest that the maximum load carried by the spiral connected by one weld was about ten percent higher than the average maximum load per weld obtained from the tests of push-out specimens with spirals connected to the steel beam with four welds (19) and 18% higher than the average maximum load per weld obtained from specimens with six welds(19). The critical loads were found in good agreement with Voellmy's formula for static capacity of spiral connectors(60).

Specimens with Stiff Connectors and Hooks.—After the early studies of spiral connectors, the European investigators turned their attention to two new types: connectors made from reinforcing bars in the form of hooks or loops and stiff connectors made from rectangular steel bars or from rolled shapes welded to the steel beams in such a manner as to offer the largest resistance to bending. The two types of connectors were often combined, with the stiff connector assigned the function of preventing slip and the hook or loop assigned the function of preventing lifting of the slab. The test data are summarized in Table 3.

In connection with the design of a composite bridge, the Swiss Federal Institute for Testing Materials tested one T-beam with T-connectors in 1935(20). The beam was subjected to fatigue loading followed by a static test to failure. It failed by the crushing of concrete after yielding spread through the full depth of the steel section.

Another early beam test of stiff connectors, reported by R. C. Manning(23), utilized square bars welded across the beam flange. The bars were provided only on one half of the span; the other half was left without connectors. The test was included in the discussion of Canadian tests of beams without shear connectors.

TABLE 3.—SPECIMENS WITH HOOKS AND STIFF CONNECTORS

Author of Investigation	Carried Out In		Reference	Number of Specimens Tested				Type of Loading
	Country	Year[a]		T-beams	TT-beams	Push-outs	Others[b]	
(1)	(2)	(3)	(4)	(5)	(6)	(7)	(8)	(9)
EMPA	Switzerland	1935	20	1				static and fatigue
Graf	Germany	1939-40	34	4				static
Meier-Leibnitz	Germany	1940	17	3				static
Lehigh Univ.	USA	1943	19			4		static
Roš	Switzerland	1944	20	5		25		static and fatigue
Siess, et al.	USA	1942-48	39			8		static
Viest, et al.	USA	1947-50	40			3		static
Fuchs	Germany	1950	31				2	static
Graf	Germany	1950	32			14		static
Graf	Germany	1951	35	6		8	3	static, fatigue and shrinkage
Lapsins	USA	1953	42	4				static
			Total	23	0	62	5	

[a] Date of publication given where date of investigation not available. [b] Includes bare connectors and negative moment sections with prestressed slab.

O. Graf(35) and Meier-Leibnitz(17) investigated two-span continuous beams with the slab anchored by inclined hooks. The beams were first subjected to several applications of load and then tested statically to failure. Graf's first two beams were provided with hooks only; slip between the slab and the steel beam occurred at very low loads. The next specimen had the top flange grooved transversely in addition to being provided with hooks. The grooves prevented slippage until shear failure in concrete made them ineffective. In the fourth specimen, shear connection was provided by a combination of hooks, grooves and two angles, one welded at each end of the beam.

Meier-Leibnitz tested three beams with hooked bars as shear connectors. In addition, one angle was welded at each end of the beam; and, in one beam, vertical plate and angles on end were used in the middle third. In two beams concentrated allowable loads were applied 80 times at each third point, then twice that load was applied 100 times and then the loads were increased until a static failure took place. One beam was tested with static loading only. One beam withstood the repeated loading without any noticeable change in the degree of interaction between the beam and the slab; the same beam retained complete composite action up to static ultimate load. In the other beam, the repetitions of load caused a pronounced decrease in composite action and its static ultimate capacity was considerably lower than that of the first beam. The third beam, having shear connection about the same as the second beam, developed only a slightly higher static ultimate capacity than the second beam.

An investigation of stiff connectors made with tees and angles welded on end, some combined with hooked bars attached to the connectors, was reported by Roš in 1944(20). The investigation included static tests of 21 push-out specimens and two T-beams, and fatigue tests of four push-out specimens and three T-beams. The static failure of push-out specimens occurred by crushing of concrete under the connectors at computed pressures of about 3.5 times the prism strength of concrete. The static failure of the T-beams occurred by crushing of the slab after the steel beams yielded through their full depth. The fatigue specimens, both T-beams and push-outs, failed by cracking at the welds of shear connectors.

The author concluded that the high pressures exerted by the connectors on the adjacent concrete were possible because of a triaxial state of stress; that full degree of interaction existed in the T-beams until the failure of bond; that the T-beams developed their fully-plastic moment capacity; and that good concrete and very good welds are needed when fatigue loading is involved. In the recommendations for design, the author proposed to design the connectors on the basis of an allowable pressure on concrete assuming uniform distribution on the vertical face of the connector. Allowable pressures of 55% and 75% of the prism strength of concrete were recommended for bridges and buildings, respectively.

The second extensive investigation of stiff connectors was reported by Graf (32)(35). Graf's study, including 22 push-out specimens, 6 T-beams and 3 sets of bare connectors, employed stiff connectors combined with bar anchorages. In the first part of the study, the stiff connectors were primarily square bars welded across the beam flange; the anchorages were primarily loops made from round bars. In the second portion of the investigation, the connectors were made primarily from flat bars. All push-out specimens were subjected to static tests to failure. The load was intermittently released to permit observation of residual slips. All specimens failed by the crushing of the concrete behind the connectors at pressures equal to between 1.7 times and 3.2 times the cube strength of concrete. The specimens with bar connectors failed at higher pressures than those with tees on end. The highest pressures were sustained by connectors made entirely of one continuous flat bar. The investigator concluded that the stiff portion of the connector becomes active immediately at the first application of the load while the anchorage loop or hook is activated only after some deformation has taken place. Graf observed that in the design it is necessary to consider both the capacity and the deformation characteristics of the connectors. He recommended to design stiff connectors on the basis of an allowable pressure on concrete equal to one half the cube strength.

In the report of the second part of the investigation(35), Graf presented also the results of three static tests of bare connectors, and described the plans for tests of beams to investigate the effects of fatigue, creep and shoring.

Roš(20) and Graf(32) studied experimentally the relative performance of push-out specimens with shear connectors at one and more cross-sections of the steel beam. Ros placed identical connectors at one, two and three cross sections, Graf at one and two cross sections. The capacity and stiffness per connector were found to decrease with increasing number of cross sections. To obtain data independent of the make-up of the push-out specimens, both investigators made their further studies on push-out specimens with connectors attached at one beam cross section only.

Similar connectors to those investigated by Graf were used by D. Fuchs(31) in his tests of two double T-beams with prestressed slabs. The connectors were welded to plates wider than the beam flange placed in the position before casting the slab, but welded to the beams only after the slab has been prestressed. The beam was tested with static loads to failure; the slab was located on the tension flange of the steel beam. Very good interaction between the slab and the steel beam was observed up to failure, although after tensile cracking of the concrete only the slab reinforcement was effective in resisting stresses.

Only a few tests of stiff connectors were carried out in the United States, mostly for exploratory or comparative purposes. Four push-out specimens with connectors made of short H-section welded on an angle were made at Lehigh University(19) as a part of the comparative study discussed in connection with tests of spiral connectors. Eight small-scale push-out specimens with channels, angles and tees on end and three full-size push-out specimens with square bars welded across the flange were tested as a part of an extensive study of flexible connectors at the University of Illinois(39)(40). Finally, four small-scale T-beams with angles on end were tested at the State University of Iowa(42). All specimens were tested with static loads to failure. The push-out specimens failed by crushing of concrete; bearing pressures in excess of 3 times the cylinder strength of concrete were reported for the specimens with square bars in spite of the absence of anchorages against separation of the slab. The T-beams failed in shear along the edges of the connectors.

Specimens with Flexible Connectors.—While European practice turned toward stiff connectors combined with hooks, American engineers showed preference for flexible connectors requiring less fabrication. The experimental investigations included flexible connectors made from rolled shapes, the majority of tests being made with channels, and on flexible stud connectors. The channels had one flange welded to the beam; the other provided anchorage against lifting of the slab. The tests of flexible connectors are summarized in Table 4.

Flexible connectors were used on a few T-beams in tests reported by C. Batho, S. D. Lash, and R. H. H. Kirkham, in 1939(16), Manning(23), F. Leonhardt(34), and Meier-Leibnitz(17), although none of these tests were directed toward studies of flexible connectors. The English tests(16) included angles, the Canadian tests(23) included I-sections and the German(17)(34) tests included angles and plates as an addition to hooks.

Push-out tests of flexible connectors were first reported in 1943(19). Carried out at Lehigh University, they included channel and angle connectors; the tests are described in the discussion of spiral connectors.

Two extensive investigations of channel shear connectors were carried out at the University of Illinois, in the 1940's. The first study(39) included static tests of 64 push-out specimens, static tests of three T-beams, and fatigue tests of 85 T-beams. The T-beams and a majority of the push-out specimens were made with flexible channel connectors; other push-out specimens had stiff connectors made from rolled shapes and flexible connectors made from straight and bent plates. All specimens were small-scale models. The second study(40) included four T-beams and 43 push-out specimens. The T-beams and 39 push-out specimens had flexible channel connectors; flexible plate connectors were used in one and rigid square bar connectors in three push-out specimens. Two of the T-beams were built with a temporary support at midspan during casting and curing of the slab. All specimens were of full size and were tested with static loads. In both studies, all push-out specimens were built with connectors placed only at one cross-section of the steel beam.

TABLE 4.—SPECIMENS WITH FLEXIBLE CONNECTORS

Author of Investigation (1)	Carried Out In		Reference (4)	Number of Specimens Tested				Type of Loading (9)
	Country (2)	Year[a] (3)		T-beams (5)	TT-beams (6)	Push-outs (7)	Others[b] (8)	
Batho, et al.	England	1939	16	2				static
Morrison, et al.	Canada	1940	23	1				static
Lehigh Univ.	USA	1943	19			8		static
Siess, et al.	USA	1942-48	39	88		56		static and fatigue
Viest, et al.	USA	1947-50	40	4		43		static
Viest	USA	1954-57	56			22		static
Sinclair	USA	1955	54				14	fatigue
Casillas, et al.	USA	1955-56	53				26	static
Thürlimann	USA	1957	59		1			fatigue
Thürlimann	USA	1958	61			10		static and fatigue
			Total	95	1	139	40	

[a] Date of publication given where date of investigation not available. [b] Includes bare connectors and plate-reinforced concrete beams.

It was found in the small scale experiments that, from the standpoint of load-slip characteristics, the rigid shear connectors were superior to the flexible types. However, the differences were much less than could be expected from the very large differences in the stiffness of the two types. Furthermore, the beam tests have shown that the flexible connectors can provide an entirely adequate shear connection. Among the several types of flexible connectors, the channel with one flange welded to the beam appeared to be superior to the connectors made from bent or straight plates.

The small-scale composite T-beams tested in fatigue failed in the shear connection. The failure occurred usually by fracture of the connector web on a line through the fillet closest to the beam. The failure was progressive, beginning with the end connectors and progressing toward the load at midspan. However, the overall effects of fatigue failure were not evident until several shear connectors had fractured. No evidence was found of an endurance limit up to 10,000,000 cycles. Although provisions were made to prevent the formation of natural bond in fatigue specimens, in a few T-beams the bond between the slab and the beam was effective during a part or even full duration of the repeated load test. The fatigue strength of these beams was increased appreciably over that of the beams without bond; there was no failure of shear connectors in beams bonded throughout the test.

The small-scale and particularly the full-size tests have shown the composite concrete and steel T-beam a very tough structure with large reserve strength and ductility beyond the load causing first yielding. Although after failure of bond some slip between the slab and the I-beam was found an inherent characteristic of composite steel and concrete T-beams, in all but two beams the slip was so small that, for all practical purposes, the beams could be considered as having complete interaction. The tests indicated further that even though connectors near the load have yielded, a shear connection composed of channel connectors developed the fully plastic flexural capacity of the T-beam as long as the connectors located at the ends of the beam did not yield before the ultimate load was reached. The fully plastic flexural capacity was reached or exceeded in all but two beams. The two beams, one small-scale and one full-size, had much weaker shear connections than the other beams; in the full-size beam the connectors began to yield simultaneously with the steel beam. No appreciable difference between the beams built with and without temporary supports was noted.

The flexible channel connector was found to act as a flexible dowel. The major portion of the total load was transmitted by the flange welded to the beam and only a smaller portion was transmitted through the web. Maximum stress in the channel connector occurred at the fillet adjacent to the welded flange. Maximum pressure on the concrete behind the connector occurred at the same flange. Semi-empirical formulas, derived on the basis of the dowel concept, related the maximum stress and pressure to connector width, flange and web thickness, and to the strength of concrete.

The tests of push-out specimens with channel shear connectors have shown further that the slips permitted by the connector have a recoverable and a non-recoverable portion. The non-recoverable, or residual slip remained small until the maximum stress in the channel connector reached the yield point of the steel; beyond this load, the residual slip increased rapidly.

Studies of stud connectors began in 1954. Carried out at the University of Illinois, and at Lehigh University, they included static and fatigue tests of push-out specimens, fatigue and static tests of one double T-beam, fatigue tests of bare studs and static tests of plate-reinforced concrete beams. The Illinois studies(52)(53)(54)(56) used straight studs with upset head of diameters ranging from 0.5 in. to 1.25 in.; in push-out specimens with all connectors placed at one cross section of the steel beam. The Lehigh studies(59)(61) used 0.5 in. diameter bent studs and, to a lesser extent, 0.75 in. diameter straight studs with upset head; in push-out specimens, the studs were located at two cross sections.

The static tests of push-out specimens(52)(56) have shown that a steel stud is suitable for use as a shear connector and that the behavior of a stud connector is similar to that of a flexible channel connector. The useful capacity of stud connectors was evaluated on the basis of residual slip curves as the load corresponding to a marked change in the rate of increase of the residual slip. For specimens exhibiting gradual change in the rate of residual slip increase, the useful capacity was taken as the load corresponding to the residual slip of 0.003 in. The useful capacity was found to be a function of the diameter and height of the stud and of the strength of concrete.

In the tests of plate-reinforced concrete beams(53) essentially complete interaction between the steel plate and the concrete topping existed up to loads closely approximating the useful loads determined from the static tests of push-out specimens(52). Furthermore, the tests furnished extensive data on the strength of bond between the hot rolled steel plate and the concrete. First slip between the plate and the concrete was observed at bond stresses ranging from 69 psi to 200 psi.

In the first investigation reported by B. Thürlimann(59) two rolled steel beams, one with 0.5-in. diameter bent studs and the other with 0.75-in. diameter straight studs, supported a common slab. This double T-beam was subjected to more than 1,500,000 cycles of loads equal to between 1.0 and 1.5 times the design load. No distress was noted during the fatigue tests; slip measurements indicated the presence of natural bond throughout the fatigue tests. In the static tests that followed, the beam failed by crushing at a load approximately equal to the computed fully plastic capacity. The second investigation reported by Thürlimann(61) provided push-out test data on the fatigue strength and on static load-slip characteristics for studs of the types used in the test of the double T-beam. On the basis of these two studies, Thürlimann recommended a design procedure for 0.5-in. diameter bent stud connectors.

THEORETICAL STUDIES

Most of the theories of the behavior and strength of composite steel and concrete beams followed the theories developed for reinforced concrete. Theoretical treatments covered both the elastic and the failure conditions.

After the experimental studies have shown the absence of complete interaction between the concrete slab and the steel section in beams with mechanical connectors, new theories were presented accounting for the slip between the two elements. These latter treatments were limited to the elastic range of behavior.

Elastic Theories.—The First English treatise on the theory of composite concrete and steel beams was published by E. S. Andrews in 1912(1). Considering flexural stresses only, Andrews presented equations for computation of stresses in the steel section and in a rectangular concrete encasement. The equations were based on the theory of transformed section assuming that concrete was not able to resist tensile stresses. The theory involved the implicit assumptions of straight-line stress distribution and of the absence of slip between the steel section and the concrete encasement.

The transformed section theory was compared with tests of composite beams by MacKay, Gillespie, and Leluau(2). In addition to considering the conditions after the concrete has cracked, they examined, also, the case of uncracked concrete; both flexural and bond stresses were considered.

Practically all experimental studies of composite beams have shown that the transformed section theory is applicable as long as bond between the steel and concrete is unbroken. The tests of beams with mechanical connectors have shown, also, that the transformed section theory gives an excellent approximation even after bond failure if the connection has an appropriately high stiffness. The transformed section theory has been generally accepted for design purposes.

The tests of composite T-beams with mechanical connectors have shown also that, in the absence of natural bond, some slip between the slab and the beam is an inherent characteristic of such beams; that is, that the interaction between the slab and the steel beam is incomplete. Several elastic theories, considering the effects of slip on stresses and deflections, were developed and published(24)(26)(27)(37)(51).

Stüssi's solution(24) involves a system of linear equations, the number of equations being equal to the number of mechanical connectors. The system is written with the aid of a finite difference equation based on the following assumptions (in addition to the usual assumptions of the theory of elasticity):

1. The magnitude of slip permitted by a shear connector is directly proportional to the load transmitted; and
2. The component elements deflect alike at the locations of the shear connectors.

The difference equation is given for two and three element beams made of the same material and for two element beams, with each element made of different material. The difference equation is good for any type of loading. The solution of the system of simultaneous equations gives the longitudinal forces transmitted by individual shear connectors.

In his study of composite timber structures, H. Granholm(26) derived differential equations for beams symmetrical about the horizontal axis composed of two or three elements made of the same material. The equation is based on the following assumptions concerning the connection:

a. The shear connection is continuous;

b. The slip is directly proportional to the shearing stress at the contact surfaces; and

c. The component elements have equal deflections at every point of contact.

The differential equation may be solved for slip and for deflection. Finite and trignometric solutions are given. The finite solution is presented for the case of a simple beam loaded with concentrated load at midspan or with uniform loading, a cantilever loaded with a concentrated load at the end or with uniform loading, a beam built in at both ends and loaded with uniform loading, and for a uniformly loaded beam with one end built in and the other end freely supported. Expressions are given for deflection, shearing stress at the junction between the elements and for slip.

In connection with the extensive studies of composite steel and concrete beams, shear connectors and scale model bridges at the University of Illinois, N. M. Newmark(37)(39) derived a differential equation for a beam composed of two elements made of different materials. It is assumed that

(1) the shear connection is continuous,

(2) the magnitude of slip is directly proportional to the load transmitted, and

(3) the component elements have equal deflections at every point of contact.

The axial force introduced by the shear connection is the unknown of the differential equation. Finite solutions of the axial force, the shearing force at the junction of the two elements, slip, strains and deflections are given for simply supported beams loaded with a concentrated load.

Ultimate Strength Theories.—The ultimate strength theories for concrete and steel composite beams may be classified into two general categories: those based solely on the statical equilibrium of internal forces and those considering the distribution of strains in addition to the statical equilibrium of internal forces.

Theories of the first type are based on the assumption that at the maximum flexural capacity each element of the cross section has reached the fully plastic state of stress(47). The advantage of this type of theories lies in their simplicity. In general, they represent a lower limit to the actual capacity, since no account is made of the excess strength resulting from strain hardening of the steel. However, in case of the presence of large slips or if the area of concrete available to resist compression is very small, the fully plastic state of stress may not be developed and, thus, the theory may overestimate the actual capacity.

A theory of the second type was first proposed by Stüssi(9), who assumed continuous linear strain distribution through the full depth of the composite cross section. Relating the strain to the stress through the use of stress-strain relationship from simple tension and compression tests, theories of this type are capable to account for the effects of strain hardening and of concrete failures prior to full plasticizing of the steel section. Furthermore, they may be used for computation of deformations at all levels of loading up to the ultimate load(40). However, their basic assumption, implying the absence of slip at ultimate load, is not fulfilled.

Both approaches have been used repeatedly(9)(20)(21)(31)(40)(44)(47)(59), particularly in connection with experimental investigations. Although several of the methods used differed from those described in the preceding paragraphs, the differences were of minor character.

Deformational Stresses.—The elastic theories described already were developed for computation of deformations and stresses caused by loads. However, the differences in temperature characteristics of the steel and concrete and the long-time instability of concrete result in additional deformation and stresses. These stresses are similar to those caused by temporary supports: experimental investigations as well as theory indicate that such stresses have no effect on the ultimate flexural capacity. However, they alter the stress conditions at lower loads.

In addition to the experimental investigations already described, several theoretical studies were carried out particularly in the last decade. Theoretical investigations of creep and shrinkage were reported by C. P. Siess (28), Fröhlich(25)(30, B. Fritz(29), M. Esslinger(38), K. Klöppel(36), W. Wrycza (48) and others. Studies of the effects of temperature were reported by K. Hirschfeld(33). A particularly thorough treatment of the subject of deformational stresses was presented by K. Sattler(43), and a more recent general discussion of the subject was prepared by R. David and G. G. Meyerhoff(58).

CURRENT DEVELOPMENTS

The more than 500 tests discussed in this paper and summarized in Table 5, were aimed at determination of the behavior of composite beams at working loads, of the ultimate capacity of composite beams and of the deformation and strength characteristics of the connection between the concrete slab and the steel beam. The tests have proved that it is feasible to utilize the concrete slab in the design of main members as a participating element. The data were instrumental in a general adoption of composite steel and concrete beams which is manifested by the existence of several national codes(45)(49)(50)(57). All four of these codes are based on working load conditions utilizing essentially the same allowable stresses as those used in the design of steel and reinforced concrete structures.

Perhaps the most significant of the recent developments is an increased attention given to the large reserve capacity beyond first yielding. The existence of this reserve strength is recognized in the AASHO Specifications(57) which base the design of shear connectors on the conditions prevailing at ultimate load. However, no advantage has been taken so far of the reserve strength in the design of beams. It can be expected that the current attention to this problem will lead to ultimate load, or plastic, design of composite beams.

TABLE 5.—SUMMARY OF TESTS

Type of Connectors Used	Number of Specimens Tested			
	T-beams	TT-beams	Push-outs	Others
(1)	(2)	(3)	(4)	(5)
None	54	11	0	29
Spirals	13	6	48	4
Hooks and stiff	23	0	62	5
Flexible	95	1	139	40
Total	185	18	249	78

A second development deserving a brief mention are the current attempt to improve the natural bond through the use of epoxy resins. A number of exploratory studies are in progress in the United States. If successful, this development may lead to the utilization of composite construction in the designs of light beams for which the currently used methods are often uneconomical.

Finally, developmental studies and applications are increasing in the field of composite prestressed concrete slabs on the tension flange of the steel beams. Probably the most natural application of this principle may be found in the negative moment region of continuous highway bridges, where prestressing could be beneficial particularly through prevention of tensile cracking and often accompanying seepage of water. Furthermore, a prestressed concrete slab acting compositely with the tension flange of steel beams may be used to increase the stiffness of the steel beam at working load. This solution may become important in connection with the use of high-strength steels for rolled beams. It may also be used to augment the resilience and the ultimate capacity in beams subjected to exceptional instantaneous dynamic loadings.

APPENDIX.—BIBLIOGRAPHY

---

1. E. S. Andrews, "Elementary Principles of Reinforced Concrete Construction," Scott, Greenwood and Sons, England, 1912.

2. H. M. MacKay, P. Gillespie and C. Leluau, "Report on the Strength of Steel I-Beams Haunched with Concrete," Engineering Journal, Eng. Inst. of Canada, Vol. 6, No. 8, pp. 365-369, 1923.

3. "Load Tests," Truscon Steel Co., Youngstown, Ohio, 1923.

3a. P. Gillespie and R. C. Leslie, "Steel I-Beam Haunched in Concrete," Bulletin No. 5, Section 2, University of Toronto, 1925.

4. H. M. MacKay, "Steel I-Beams Haunched with Concrete," Engineering and Contracting, Chicago, Vol. 66, No. 2, pp. 53-57, 1927.

5. R. A. Caughey, "Composite Beams of Concrete and Structural Steel," Proceeding, 41st Annual Meeting, Iowa Engineering Society, pp. 96-104, 1929.

6. C. C. Whittier, "Tests of Steel Floor Framing Encased in Concrete, Part II," Journal, Western Society of Engineers, Vol. 35, No. 3, pp. 171-225, 1930.

7. L. Cambournac, "Poutrelles en acier enrobees de beton" Publications, Int. Assoc. for Bridge and Struct. Eng., 1st Vol., pp. 25-34, 1932.

8. F. Campus, "Charpente metallique rivee at enrobee de l'Institut de Chemie et de Metallurgie de l'Universite de Liege," Final Report, First Congress Paris, Int. Assoc. for Bridge and Struct. Engrs., pp. 529-543, 1932.

9. F. Stüssi, Profilträger, kombiniert mit Beton oder Eisenbeton, auf Biegung beansprucht," Final Report, First Congress, Paris, Int. Assoc. Bridge and Struct. Engrs., pp. 579-595, 1932.

10. L. Baes, "Poutrelles Metalliques Enrobees," L'Ossature Metallique, Bruxelles, Vol. 2, No. 1, pp. 1-16, 1933.

11. M. Roš, "Les constructions acier-beton, systeme Alpha," L'Ossature Metallique, Bruxelles, Vol. 3, No. 4, pp. 195-208, 1934.

12. R. A. Caughey, "Reinforced Concrete," D. Van Nostrand Co., New York, 1936.

13. A. Voellmy, "Strength of Alpha Composite Sections under Static and Dynamic Stresses," Unpublished report, Swiss Federal Mat. Test. Lab., EMPA, Zurich, 1936.

14. G. Gruening, "Versuche zur Bestimmung der Verbundwirkung con Eisenbeton und Massivdecken mit darin einbetonierten Walzträgern bei schwingenden Beanspruchungen," Deutscher Ausschuss für Eisenbeton, Berlin, No. 84, 1937.

15. "Tests Made on Four Floor Panels Designed According to the Alpha System," Porete Mfg. Co., North Arlington, N. J., 1937.

16. C.. Batho, S. D. Lash and R. H. H. Kirkham, "The Properties of Composite Beams, Consisting of Steel Joists Encased in Concrete, under Direct and Sustained Loading," Journal, I. C. E., Vol. 11, No. 4, pp. 61-114, 1939.

17. Maier-Leibnitz, "Versuche über das Zusammenwirken von I-Trägern mit Eisenbetondecken," Die Bautechnik, Berlin, Vol. 19, No. 25, pp. 265-270, 1941.

18. R. M. Mains, "Report of Tests of Composite Steel-Concrete Beams," unpublished report, Fritz Engineering Laboratory, Lehigh University, May 1943.

19. "Report of Tests of Composite Steel and Concrete Blocks," unpublished report, Fritz Engineering Laboratory, Lehigh University, 1943.

20. M. Roš, "Träger in Verbundbauweise," Report No. 149, Swiss Federal Mat. Test. Lab., EMPA, Zurich, 1944.

21. A. Voellmy, "Tests to Investigate the Influence of Initial Bending Stresses on the Carrying Capacity of Composite Beams," Porete Mfg. Co., North Arlington, N. J., 1945.

22. A. Voellmy, "Shrinkage Tests on Two Composite Beams," Porete Mfg. Co., North Arlington, N. J., 1945.

23. R. C. Manning, "Combined Action of Concrete Slabs and Supporting Structural Steel Beams," Engineering Journal, Eng. Inst. of Canada, Vol. 99, No. 3, pp. 149-153, 1946.

24. F. Stüssi, "Zusammengesetzte Vollwandträger," Publications, Int. Assoc. for Bridge and Struct. Engrs., Vol. VIII, pp. 249-69, 1947.

25. H. Fröhlich, "Einfluss des Kriechen auf Verbundträger," Der Bauingenieur, Berlin, Vol. 24, No. 10, pp. 300-307, 1949.

26. H. Granholm, "On Composite Beams and Columns with Particular Regard to Nailed Timber Structures," Transactions No. 88, Chalmers Univ. of Tech., Gothenburg, 1949.

27. K. Jaeger, "Die Verbundwirkung zwischen Strahlträger und Stahlbetonplatte," Oesterreichische Ingenieru-Archiv, Wien, Vol. 2, No. 4, pp. 295-311, 1949.

28. C. P. Siess, "Composite Construction for I-Beam Bridges," Transactions, ASCE, Vol. 114, pp. 1023-1045, 1949.

29. B. Fritz, "Vereinfachtes Berechnungsverfahren für Stahlträger mit einer Betondruckplatte bei Berücksichtigung des Kriechens und Schwindens," Die Bautechnik, Berlin, Vol. 27, No. 2, pp. 37-42, 1950.

30. H. Fröhlich, "Theorie der Stahlverbund-Tragwerke," Der Bauingenieur, Berlin, Vol. 25, No. 3, pp. 80-87, 1950.

31. D. Fuchs, "Versuche mit Spannbeton-Verbundträgern," Der Bauingenieur, Berlin, Vol. 25, No. 8, pp. 289-294, 1950.

32. O. Graf, "Versuche über den Verschiebewiderstand von Dübeln für Verbundträger," Der Bauingenieur, Berlin, Vol. 25, No. 8, pp. 297-303, 1950.

33. K. Hirschfeld, "Der Temperatureinfluss bei der Verbund-Bauweise," Der Bauingenieur, Berlin, Vol. 25, No. 8, pp. 305-306, 1950.

34. F. Leonhardt, "Gedanken zur baulichen Durchbildung von Durchlaufträgern in Verbund-Bauweise," Der Bauingenieur, Berlin, Vol. 25, No. 8, pp. 284-286, 1950.

35. O. Graf, "Ueber Versuche mit Verbundträgern," Abhandlungen aus dem Stahlbau, Heft 10, Stahl-Tagung Karlsruhe, pp. 74-90, 1951.

36. K. Klöppel, "Die Theorie der Stahlverbundbauweise in statisch unbestimmten Systemen unter Berücksichtigung des Kriecheinfluesses," Der Stahlbau Berlin, Vol. 20, No. 2, pp. 17-23, 1951.

37. N. M. Newmark, C. P. Siess and I. M. Viest, "Tests and Analysis of Composite Beams with Incomplete Interaction," Proceedings, Society for Experimental Stress Analysis, Vol. 9, No. 1, pp. 75-92, 1951.

38. M. Esslinger, "Schwinden und Kriechen bei Verbundträgern," Der Bauingenieur, Berlin, Vol. 27, No. 1, pp. 20-26, 1951.

39. C. P. Siess, I. M. Viest and N. M. Newmark, "Studies of Slab and Beam Highway Bridges, Part III - Small-scale Tests of Shear Connectors and Composite T-Beams," Bulletin 396, Univ. of Illinois Engrg. Experiment Sta., 1952.

40. I. M. Viest, C. P. Siess, J. H. Appleton and N. M. Newmark, "Studies of Slab and Beam Highway Bridges - Part IV: Full Scale Tests of Channel Shear Connectors and Composite T-beams," Bulletin 405, Univ. of Illinois Engrg. Experiment Sta., 1952.

41. "Distribution of Load Stresses in Highway Bridges," Research Report 14-B, Highway Research Board, Washington, D. C., 1952.

42. V. Lapsins, "A Comparative Study of Composite Action in Structural Steel and Concrete Beams," thesis presented to the State Univ. of Iowa, in Ames, Iowa, in 1953, in partial fulfilment of the requirements for the degree of Master of Science.

43. K. Sattler, "Theorie der Verbundkonstruktionen," Wilhelm Ernst and Sohn, Berlin, 1953.

44. K. Sattler, "Die Fliesssicherheit von Vollband-Verbundkonstruktionen," Die Bautechnik, Berlin, Vol. 30, No. 6, pp. 153-160, 1953.

45. "National Building Code of Canada, Section 4.7.1.8," National Research Council, Ottawa, Canada, 1953.

46. N. M. Newmark and C. P. Siess, "Research on Highway Bridge Floors," Proceedings, Highway Research Board, Vol. 33, pp. 30-53, 1954.

47. I. M. Viest and C. P. Siess, "Design of Channel Shear Connectors for Composite I-beam Bridges," Public Roads, Vol. 28, No. 1, pp. 9-16, 1954.

48. W. Wrycza, "Verbundbauweise mit und ohne Vorspannung unter Berücksichtigung des Schwind und Kriecheneinflusses auf die statisch unbestimmten Systeme," Die Bautechnik, Berlin, Vol. 31, No. 8, pp. 241-246, No. 9, pp. 295-302, 1954.

49. "Verbundträger-Hochbau. Richtlinien für die Ausbildung und Bemessung. DIN 4239." Der Bauingenieur, Berlin, Vol. 29, No. 9, pp. 355-358, 1954.

50. "Verbundträger-Strassenbrucken. Richtlinien für die Berechnung und Ausbildung. DIN 1078." Die Bautechnik, Berlin, Vol. 31, No. 2, pp. 46-48, 1954.

51. A. Hoischen, "Verbundträger mit elastischer und unterbrochenen Verdübelung," Der Bauingenieur, Berlin, Vol. 29, No. 7, pp. 242-244, 1954.

52. I. M. Viest, "Investigation of Stud Shear Connectors for Composite Concrete and Steel T-Beams," Journal, A. C. I., Vol. 27, No. 8, pp. 875-891, 1956.

53. J. Casillas G de L., N. Khachaturian and C. P. Siess, "Studies of Reinforced Concrete Beams and Slabs Reinforced with Steel Plates," Civil Engineering Studies, Structural Research Series No. 134, Univ. of Ill., 1957.

54. G. M. Sinclair, "Fatigue Strength of 3/4 inch Welded Stud Shear Connectors," Engineering Test Data, Nelson Stud Welding, Lorain, Ohio.

55. I. M. Viest, "Tests of Spiral Shear Connectors," Engineering Test Data, Nelson Stud Welding, Lorain, Ohio.

56. I. M. Viest, "Tests of Stud Shear Connectors, Parts I, II, III and IV," Engineering Test Data, Nelson Stud Welding, Lorain, Ohio.

57. "Standard Specifications for Highway Bridges. Div. I, Sec. 9," The American Association of State Highway Officials, Washington, D. C., 1957.

58. R. David and G. G. Meyerhof, "Composite Construction of Bridges Using Steel and Concrete," Engineering Journal, Engrg. Inst. of Canada, Vol. 41, No. 5, pp. 41-47, 1958.

59. B. Thürlimann, "Composite Beams with Stud Shear Connectors," Bulletin 174, Highway Research Board, Washington, D. C., pp. 18-38, 1958.

60. I. M. Viest, R. S. Fountain and C. P. Siess, "Development of the New AASHO Specifications for Composite Steel and Concrete Bridges," Bulletin 174, Highway Research Board, Washington, D. C., pp. 1-17, 1959.

61. B. Thürlimann, "Fatigue and Static Strength of Stud Shear Connectors," Journal, A. C. I., Vol. 30, No. 12, pp. 1287-1302, 1959.

62. V. Lapsins, "A Comparative Study of Composite Action in Structural Steel and Concrete Beams," 1953.

63. C. L. Freyermuth, Jr., "Tests of Shear Connectors in Composite Steel and Concrete Beams," 1958.

64. R. K. Desai and B. A. Punjai, "Comparative Tests of Shear Connectors with Epoxy Resin," 1961.

DISCUSSION

W. J. JURKOVICH,[3] M. ASCE.—Mr. Viest states that "A second development deserving a brief mention is the current attempts to improve the natural bond

---

[3] Senior Bridge Engr., Calif. Div. of Highways, Sacramento, Calif.

TABLE 6.—COMPOSITE BEAM TESTS AT IMPERIAL COLLEGE

Description	No. of Specimens	Date	Reference[a,b]
(a) Full Scale Beam Tests (6.in. slab)			
12 x 6 I section with bottom flange plate. 7/8 in. welded studs with heads.	1	1957	1
Cased castellated beam with bottom flange plate. Welded studs without heads.	1	1957	-
12 x 6 I section. Welded tee connectors with hoops.	1	1960	-
12 x 6 I section. 3/4 in. welded studs with heads.	5	1960	-
12 x 6 I section. 1/2 in. welded studs with heads.	1	1960	-
12 x 6 I section. 3/4 in. welded studs with right-angle bend.	1	1960	-
(b) Full Scale Push-Out Tests			
7/8 in. welded studs with heads. 1, 2 and 3 pairs per flange.	8	1956	1
7/8 in. welded studs without heads. 1, 2 and 3 pairs per flange.	6	1956	1
3/4 in. welded studs with heads 1 pair per flange.	3	1960	-
Welded tee connectors with hoops, one connector per flange.	1	1960	-
3/4 in. welded studs with right-angle bend. One pair per flange.	2	1960	-
(c) Small Scale Beam Tests			
2 in. x 1 in. I section cased and uncased with and without 1/8 in. diameter welded studs. 7/8 in. slab.	6	1957	2
4 in. x 1 3/4 in. I sections. 1/4 in. and 3/16 in. welded studs with heads and right-angle bends. 1 1/2 in. slab.	10	1959	2
4 in. x 1 3/4 in. I sections. 3/16 in. welded studs with heads and right-angle bends. 1 1/2 in slab.	11	1960	-
(d) Small Scale Push-Out Tests			
7/64 in. welded studs with heads. 1, 2 and 3 pairs per flange. 3/4 in. slab.	8	1957	2
1/4 in. and 3/16 in. welded studs with heads, with right-angle bends and with inclined bends. In pairs and in tandem. 1 1/2 in. slab.	27	1959	2
3/16 in. diameter studs with heads and right-angle bends.	4	1960	-

[a] "Behaviour of building frames of composite construction," by K. C. F. Wong, Ph.D. Thesis, University of London, 1957.

[b] "Interaction between steel beams and a concrete floor slab," by A. O. Adekola, Ph. D. Thesis, University of London, 1959.

through the use of epoxy resins." Brief mention is all that these attempts deserve presently, as far as the preliminary tests made by the California Division of Highways-Materials and Research Laboratory reveal.

The tests consisted of jacking against a 12 in. x 12 in..x 6 in. block that was cast on the flange of a steel beam. Epoxy resin was applied to the flange before casting the block. The shear stress at failure was 100 psi. Failure was in the concrete about 1/2 in. to 1/4 in. above the steel flange. No "tie downs" were used in the test and as a result, no mechanical resistance to uplift existed. Without question, mechanical "tie downs" are required for any method used to provide composite action.

Plans are being made (August, 1960) to run a full scale test using 2 1/2 in. round studs at 24 in. centers and epoxy applied to 50% of the flange before casting the deck slab. No preparation of the flange, such as sandblasting, will be done. The test will be made to determine if composite action can be maintained to ultimate load. It is expected that these tests may deserve more than a brief mention in the future.

J. C. CHAPMAN.[4]—Congratulations are in order for this excellent and valuable review. This paper will be welcomed by all practicing engineers and research workers, since all too few papers of this kind are written.

There is always a tendency to plan a research program without taking complete account of all the related investigations which have been made, largely because of the very considerable effort which is required to do so. Viest has now made the effort for us, and we should all be very grateful.

The list in Table 6 brings the record up to date in respect to tests which have, so far, been made at Imperial College. Non-destructive tests have also been made on two composite building structures. The work is continuing.

IVAN M. VIEST,[5] F. ASCE.—Further research on composite beams is in progress at the California Division of Highways and at Imperial College, according to the discussers. It is hoped that the results, particularly from the very extensive investigations outlined by Chapman, will soon become available.

In addition to these two investigations, studies of various aspects of composite design are being conducted at several other institutions. The use of epoxy resins, discussed by Jurkovich, is also being investigated through beam tests at the University of Arizona. The relationship between the fully plastic strength of the shear connection and the ultimate strength of a composite beam is being studied at Lehigh University. The effect of stud shear connectors on the fatigue strength of a steel beam in the region of negative moment is being investigated at the University of Illinois, and the effectiveness of various types of connectors on the magnitude of slip is the subject of an intermittent series of studies in progress at the State University of Iowa.

The results of the investigations completed thus far at the State University of Iowa have been reported (62)(63)(64). No data have been published, as yet, from the other studies; however, the wide range of investigated subjects suggests that important improvements in the design of composite beams will soon be forthcoming.

---

[4] Civ. Engrg., Dept., Imperial College, England.

[5] Bridge Research Engr., Assho Rd. Test, Ottawa, Ill.

AMERICAN SOCIETY OF CIVIL ENGINEERS
Founded November 5, 1852
TRANSACTIONS

Paper No. 3269

WIND FORCES ON STRUCTURES

Final Report

Task Committee on Wind Forces
Committee on Loads and Stresses
Structural Division

FOREWORD

The purpose of this report is to assemble, correlate, and summarize existing information on the factors that determine wind forces on structures. It is intended to be a compact source of information in a form that will be of practical use to civil engineers. No new research is presented, but an evaluation of existing data in the accompanying comprehensive form has probably not been published previously.

This report is the result of a combined effort by all members of the Task Committee extending over a period of several years. A preliminary report was published as Proceedings Papers 1707 through 1712 in the July 1958 issue of the Journal of the Structural Division. Subsequent issues contained discussion that was taken into account in the preparation of this Final Report.

I. INTRODUCTION AND HISTORY

The technical literature of the past 150 yr (since the early 1800's) contains many references to structural failures caused by wind. Many of these have been bridge failures and perhaps the earliest reported was that of the Dryburgh Abbey suspension bridge in Scotland in 1818. This began a long history of difficulty with suspension bridges primarily caused by the dynamic effects of the wind. It is interesting to note that an eyewitness to the failure, in 1836, of the Brighton Chain Pier Bridge (Brighton, England) described a catastrophic motion identical to that which destroyed the Wheeling Bridge (Wheeling, W. Va.) in 1854, and the Tacoma Narrows Bridge (Tacoma, Wash.) in 1940. It is apparent that the art of designing against wind had made little progress during this period.

Failures have not been confined to suspension bridges. Perhaps the most tragic failure due to wind was that of the Tay Bridge in Scotland in 1879 that resulted in the deaths of seventy-five persons. The inquiry into the failure developed the fact that the effect of wind had not been considered and no provision had been made to resist overturning of the structure. Similar overturning failures occurred on the Smith Avenue Bridge (St. Paul, Minn.) in 1904 and the Chester Bridge (Chester, Ill.) over the Mississippi River in 1944. The latter two were apparently the result of tornadoes. Difficulties have also been encountered with oscillation of the hangers on arch bridges.

There are also numerous examples of building failures due to wind. Many of these have occurred during erection, which may indicate a carelessness on the part of engineers with regard to the effects of wind. One of the more recent examples is the collapse of the Union Carbide Building in Toronto, Canada in 1958.

Although civil engineers have had difficulties in designing structures to resist wind, they have made many efforts to understand the problem better and, as a result, considerable data have accumulated. Experiments date back to Galileo (101)[1] and Newton (102) and are continuing at the present time (1961). The history of the investigations preceding 1894 has been fully covered by W. H. Bixby (105) and more briefly outlined by Robins Fleming (110). The more pertinent data covering engineering applications were outlined by W. Watters Pagon, F. ASCE (112). More recent additions to the fund of knowledge have resulted indirectly from the development of aircraft. The wind tunnel provides a facility for measuring the forces resulting from the wind and advances in the field of fluid mechanics permit a rational interpretation of wind-tunnel tests. Structural as well as aeronautical engineers are indebted to the research of the National Advisory Committee for Aeronautics, now (1961) the National Aeronautics and Space Administration (NASA).

The early experiments of N. V. Duchemin (104) and John Smeaton (103) formed the basis for generally accepted formulas for wind forces on structures. Those of B. Baker (105) in connection with the Firth of Forth Bridge in Scotland had an important influence on bridge specifications. Wind-tunnel tests started with those of A. G. Eiffel (107) on flat plates. These were followed by tests on various shapes (108).

Tests on models of buildings began with those of J. O. V. Irminger and C. Nøkkentved (405) in 1895. These were followed by others, notably by H. L. Dryden and G. C. Hill (402). Other noteworthy investigations are those made in connection with the Empire State Building (New York, N. Y.) that included both model and field experiments (411)(422). A former committee of ASCE prepared an extensive report on wind bracing in steel buildings that also recommended design wind loads (423). More recent investigations include those at the Iowa Institute of Hydraulic Research, Ames (434).

For open-frame structures, the tests on simple shapes were followed by tests on models of trusses and complete bridges by Ludwig Prandtl and A. Betz (108) and by O. Flachsbart and H. Winter (111). The research following the failure of the Tacoma Narrows Bridge has contributed to the knowledge of both aerodynamic and aerostatic forces (113). More recent tests on complete bridge models were conducted at the David Taylor Model Basin, Washington, D. C. for the Highway Research Board (506) and at the Massachusetts Institute of Technology, Cambridge (507)(509).

---

[1] Numerals in parentheses refer to corresponding items in Appendix I.

The greatest contributions in the field of meteorology have been the observations and analyses of the Weather Bureau, United States Department of Commerce (USWB). Other investigations have provided data on the nature of the wind—such as gust velocities, velocity variation with height, and similar phenomena (208)(213).

Despite the failures that have occurred and despite the data that have been accumulated, civil engineers still use general wind loadings for designs that do not apply specifically to the form being considered and do not provide accuracy consistent with existing knowledge of wind forces. In view of the advances made in structural theory, and the use of more refined design methods by structural engineers, the accuracy of the determination of forces on structures has become more important.

The wind forces on any structure, or on any element thereof, result from the differential pressures on such elements caused by the obstruction to the free flow of the wind. Therefore, these forces are functions of the velocity of the wind and of the orientation, area, and shape of the elements. Data as to the nature of the wind come from the science of meteorology; that covering the resistance of objects to the flow of the wind from the science of fluid mechanics.

The determination of wind forces on a structure is basically a dynamic problem. However, it has been usual practice to treat such forces as static loads. This approach is satisfactory, provided that the relationship between the time variation of the wind and the natural frequencies of the structure is such as to cause an essentially static response. However, even in such cases, the engineer should be cognizant of the dynamic character of the problem.

II. NATURE OF THE WIND

INTRODUCTION

The wind possesses kinetic energy by virtue of the velocity and mass of the moving air. If an obstacle is placed in the path of the wind so that the moving air is stopped or is deflected from its path, then all or part of the kinetic energy of each filament of moving air is transformed into the potential energy of pressure. The intensity of pressure at any point depends on the shape of the obstacle, the angle of incidence of the wind, and the velocity and density of the air.

If the air were always quiet, it would not be necessary for engineers to consider wind forces when designing structures. They would need to consider only the static pressure due to the weight of the air. However, the air is seldom quiet but flows, sometimes with great violence, under the influence of forces generated by heat from the sun, and the centrifugal forces resulting from the earth's rotation. The wind may be defined as motion of the air caused by gravity, by deflective forces due to the earth's rotation, and by centrifugal forces due to the curvature of the wind path. These forces are opposed by others arising from friction and viscosity. The air never flows with a perfectly smooth and streamline motion, but always with horizontal and vertical fluctuations which, when sudden and relatively brief, are called gusts. The masses of air involved in gustiness may simultaneously, and in the same area, cover a wide range of sizes from very small to very large.

This part of the report deals only with the wind velocities that should be considered by structural engineers, based on present (1961) information. It does not deal with the shape factors that may be appropriate for various structures because these will be evaluated subsequently; brief recommendations are given for gust factors.

ORIGIN OF STRONG WINDS

Statistical studies of the records of wind observations in different parts of the United States show that the probability of strong wind is not the same in all geographical areas. The nature of the storms in which strong winds occur is better understood now than when radar and aircraft were not available for meteorological investigation. There is still much to be learned about the frequency of strong winds and the variation of wind velocity with height, but engineers cannot wait for perfect information; they must proceed on existing knowledge and its implications.

Wind forces acting on structures are significantly large only during strong winds and these occur only during storms. In this report, therefore, only tropical cyclones, extratropical cyclones, and tornadoes are discussed because these are the storms that include the wind forces that are of interest to the structural engineer in his designs.

General Circulation of the Atmosphere.—The general circulation of the atmosphere is the term applied to the average movements of the atmosphere which, in the middle latitudes of the northern hemisphere are from west to east, and in the tropical latitudes, and sometimes in the polar latitudes, are from east to west. There is a popular impression that this is a predominantly regular condition of flow that is occasionally disturbed by storms or other local deviations that are not a necessary part of the general circulation. It is also thought that the warm air of the tropical regions rises with a drift toward the poles and that the cold air of the polar regions sinks and drifts toward the tropics, and that these meridional movements are likewise predominantly regular. But these oversimplified views are not those which prevail (as of 1961) among meteorologists and physicists.

It is true that in the tropics more heat is received from the sun than is lost through long-wave radiation into outer space, and that in the polar regions the reverse is true. It is also true that the dynamic balance requires a transfer of angular momentum vertically and horizontally within the atmosphere, and that the transfer of kinetic energy is continually taking place. But this dynamic balance, thermal and mechanical, is much too complex to be achieved by streamline flow. It requires a turbulent system in which the progression of the cyclones and anticyclones of the middle latitudes, for example, are cells of the necessary system of turbulence. If the velocities of the winds that occur at a particular location are averaged over a long period, as, for example, a month, or a season, the average thus obtained may be said to represent the general circulation of the atmosphere at that location. But to the structural engineer the high velocities of the passing storms are of greater importance. A short analysis is therefore given herewith of those components of the general circulation that give rise to strong winds, namely extratropical cyclones, tropical cyclones, and tornadoes.

Extratropical Cyclones.—A cyclone is best described by reference to a synoptic weather map, where the isobars are lines of equal barometric pressure, that, in the United States, is expressed in inches of mercury reduced to sea-level conditions; the wind direction is shown by arrows. The circulation is spirally inward in a counterclockwise sense around a cyclone, and is spirally outward in a clockwise sense around an anticyclone.

As a cold air mass advances it is retarded by friction caused by the ground. The retardation is transmitted upward by the eddy viscosity of the air, and the upper cold front, to a height of several thousand feet, runs ahead of the cold front at the ground. The intervening vertical distance is filled with warm air over warm ground and because the cold, dry air aloft is heavier than the warm air below, there is created a condition of instability in which vertical mixing of the air takes place. High wind velocities are apt to occur in this region because parcels of the fast-moving upper air sink and reach the ground before losing all of their excess forward momentum, or because the heavy fast-moving upper air falls forward in a manner similar to breakers on an ocean beach.

At the warm front the warm air ordinarily advances over the cold air at a slower rate than at the cold front and under conditions that promote stability and a tendency to stagnation of the air. There is, therefore, little or no wind of interest to the structural engineer in this region.

The extratropical cyclones and anticyclones form a continuous procession in the middle latitudes, moving along paths that are approximately west to east. They cross the United States at a rate of about 2 cyclones per week. Each cyclone is usually accompanied by an anticyclone but this pairing is far from regular. The synoptic weather maps will frequently show an irregular cluster of cyclones that may merge into a larger cyclone as they move across the United States; the same thing is true of the anticyclones. The shape of the anticyclones is not always regular and their relation to the preceding and succeeding cyclones is indefinite. Nevertheless, the procession is a continuous phenomenon, especially in the winter and early spring. Some extratropical cyclones persist around the world. Some originate as hurricanes (tropical cyclones) that have moved northward from the tropics, as will be discussed subsequently. Most of the storm winds to which structures in the middle latitudes are subjected occur in the southwest quadrant of passing cyclonic storms in the winter or early spring.

Unfortunately, in some parts of the United States, there has long been a tendency to confuse the word "cyclone" and "tornado." Tornadoes and hurricanes are cyclonic storms, but most cyclones are neither tornadoes nor hurricanes, which is fortunate indeed.

Tropical Cyclones.—The continental areas of the United States are affected chiefly by those hurricanes (tropical cyclones) that originate in the Atlantic Ocean as far east as the Cape Verde Islands (213) and in the Western Caribbean. There are also hurricanes that originate in the Pacific Ocean off the coast of Mexico and Southern California, but these storms move out to sea without affecting the United States. The number of hurricanes that have reached the United States from 1887 to 1956 is 143 with an average of 2 per yr and a range from 0 to 6 per yr (212).

The hurricane (tropical cyclone) is radically different from the extratropical cyclone in several respects, and the assumption that any portion of the storm possesses a steady state dynamic condition in a closed system is not tenable without a great deal of additional information. It must be recognized also that, due to the limited number of stations on the coastal areas, and particularly the limited number of vessels at sea that can make adequate reports, the spacing and curvature of the isobars may be drawn only with considerable chance of error. There must be considerable doubt that the same relationship prevails between the gradient wind and the surface pressure gradients, as that which exists in the extratropical cyclones.

A hurricane has been likened to a heat engine (209) that is constantly receiving energy from the water vapor that is being carried aloft from the tropical ocean. Energy is released in vast quantities when the vapor is condensed and falls in torrential rains. It is not impossible, therefore, that heat energy in great quantities becomes available at relatively low elevations, and is, at least in part, transformed into the mechanical energy of wind velocity.

The theories of the V. W. Ekman (201) and C. G. Rossby (202) spirals are not appropriate for studying the variation of wind velocities with height in mature hurricanes, partly for the foregoing reasons and also because of the rather narrow spiral rain bands that characterize the structure of typical hurricanes and typhoons. The spiral bands are said to merge into a continuous ring as they approach the central eye of the storm and it is in this portion of the storm that the strongest winds occur. In Deppermann's typhoon model (214) the maximum peripheral wind velocities occur about 30 miles from the center of the eye and decrease rapidly both toward and away from the eye:

> "In intense immature storms, velocities increase until a few minutes before the calm, but in the mature and decaying stages the highest winds may occur as much as two hours before and one hour after the central calm. * * * In the large Cape Verde storms, the diameter of hurricane winds may exceed 100 miles by the time the storm has reached the western Atlantic."

For the structural engineer it is especially interesting to note that current (1961) information regarding mature hurricanes seems to locate the most severe and dangerous turbulence below the main cloud formation, probably below 1,000 ft. It has been stated that this type of turbulence may become excessive at 500 ft with winds over 80 knots (92 mph) and that it tends to disappear rapidly as the altitude increases. These observations are important to the structural engineer who must form some estimate of the variation of wind velocity with height near the ground. In the absence of detailed quantitative measurements, made at heights that are important to structures located in the coastal areas that have experienced mature hurricanes, such qualitative observations provide useful background material. It may be hoped that quantitative observations will be made using some of the higher towers in southern coastal areas. Observations made at the Brookhaven National Laboratories, Brookhaven, N. Y., supply good information regarding the variation of wind velocity with height during decaying hurricanes (215) in coastal areas.

Tornadoes.—Tornadoes have the most violent wind velocities that occur in the United States. Their occurrence is widespread in the eastern half of the country. Sometimes they are even found "embedded" in southern hurricanes. Fortunately, the path of an individual tornado covers a relatively small area and although about 700 were reported in the United States during 1954, the probability of occurrence in a highly populated area, as in a city, is small. The peripheral wind velocities are frequently estimated to be in excess of 300 mph, based on the damage done. This is a dynamic pressure (velocity pressure) of 230 psf, corresponding to an average design pressure, on a square flat plate of 260 psf.

No pretense is ever made that structures are designed to withstand such velocities. Nevertheless, it is sometimes a cause of amazement to engineers that structures, apparently in the direct path of a tornado have, if well designed and well built, suffered only minor damage. Severe damage to good buildings, when it occurs, seems to result from the explosive release of air pressure within buildings when the very low pressure within the funnel suddenly envelopes them on the outside.

No further consideration will be given herein to the subject of tornadoes, because there is no demand for the inclusion of their effects in specifications.

THE GRADIENT WIND

There is some height at which the influence of ground friction, transmitted upward through eddy viscosity, has a negligible effect on the velocity of the wind as it responds to the pressure gradient. At this height the pressure gradient is said to be dynamically balanced against two components arising from centrifugal force—one due to the rotation of the earth and the other due to the curvature of the wind path. The wind velocity computed on this basis is termed the "gradient wind." There must be a transition from the surface velocity to the gradient velocity and this is referred to as the variation of wind velocity with height.

VARIATION OF WIND VELOCITY WITH HEIGHT

The factors entering into the variation of wind velocity with height are the pressure gradient, the mass density of the air, the angular velocity of the earth's rotation, the geographic latitude at which observations are made, the curvature of the wind path, and the coefficient of eddy viscosity of the air. The equations expressing the relations of these variables have been derived by Ekman (201) and the resulting graphical representation (208) is known as the Ekman Spiral. If the theory of the "mixing length" is used instead of the coefficient of eddy viscosity, the Rossby (202) spiral is obtained. In this report the theory of the Ekman Spiral will be used as a theoretical model in presenting the results of observations in extratropical cyclones.

WIND VELOCITIES IN THE UNITED STATES

Wind codes must be based on knowledge of the probability of occurrence of high wind velocities obtained from the statistical analysis of wind velocity records. The most voluminous records of this kind are taken from the observations at the first-order stations of the USWB. These data are not homogeneous, however, because the stations have been located, until recent years, in cities where the height of the instruments and the degree of exposure were constantly changing with the erection of new, tall buildings, and where the air flow was sometimes distorted by the buildings upon which the instruments were mounted. In recent years the stations have been moved to airports where a more uniform degree of exposure exists. Therefore, the proper interpretation of these long-time records required expert and painstaking study.

It is desirable that code recommendations be based on some standard of reference, such as air flow in level open country, and that the influence of local shielding and unusual topography be evaluated by the designer in each individual case.

Figs. 1(a) and (b) are maps of the United States that were prepared by H. C. S. Thom (216). Fig. 1 shows contour lines, each of which gives the velocity of the fastest mile of wind after the observed velocity has been reduced by the one-seventh-power law to a height of 30 ft above the ground. The contour lines were based on an average of about 15 yr of USWB records at 141 airport stations throughout the United States.

The wind records were extrapolated by means of statistical analysis to velocities having a 50-yr probable period of recurrence in Figs. 1(a) and a 100-yr probable period in Fig. 1(b). On the average for the United States the 100-yr wind is 1.08 times the 50-yr wind and the 200-yr wind is 1.16 times the 50-yr wind (216). It should be noted that these are "probable" values and that, over a long period of time there may occur a 50-yr interval which may include one or more basic winds, having statistically a "probable period of recurrence" of 100 yr. Nevertheless, this method gives the designing engineer a "conservative" and a "more conservative" basis for choosing the wind velocity that is appropriate in the design of each type of structure, taking into account the wind sensitivity of the structure, and the hazard to life and property that would accompany a failure of the structure. Wind sensitivity depends on the importance of wind loading as compared to the importance of all other kinds of loading in their effect on the strength and stability of the structure.

Within any given year there is a 2% probability that the 50-yr wind will be exceeded. This does not mean that there is a 2% chance of failure of the structure in any given year, because it is also necessary to consider the probabilities involved in the quality control of the structure. In determining the overall "safety factors" there are many other variables, some of which cannot (as of 1961) be examined statistically, but the subject of safety factors (217)(218) is not within the scope of this report.

STORM OBSERVATIONS

Wind forces acting on structures are significantly large only during strong winds, and these occur only during storms. It is essential to know the type of storms during which the observations were made because the variation of wind velocity with height will be influenced by the type of storm and the terrain, (or water area) over which the wind has passed. Long-time averages that include heterogeneous meteorological conditions can be very misleading. For example, at one end of the possible range is the temperature inversion, during which the wind velocities are light, the atmosphere is so stable that there is little vertical mixing, and the coefficient of eddy viscosity is correspondingly small. In that case there is little friction between the horizontal layers, and the velocity changes rapidly with height. It is not valid to use the rapid change of velocity with height that occurs in an inversion, when one is considering the variation of storm winds with height. Storm observations should not be mixed with heterogeneous observations, nor inland observations with coastal observations. Extratropical storms should be studied separately from hurricanes, and mature hurricanes separately from decaying ones (215).

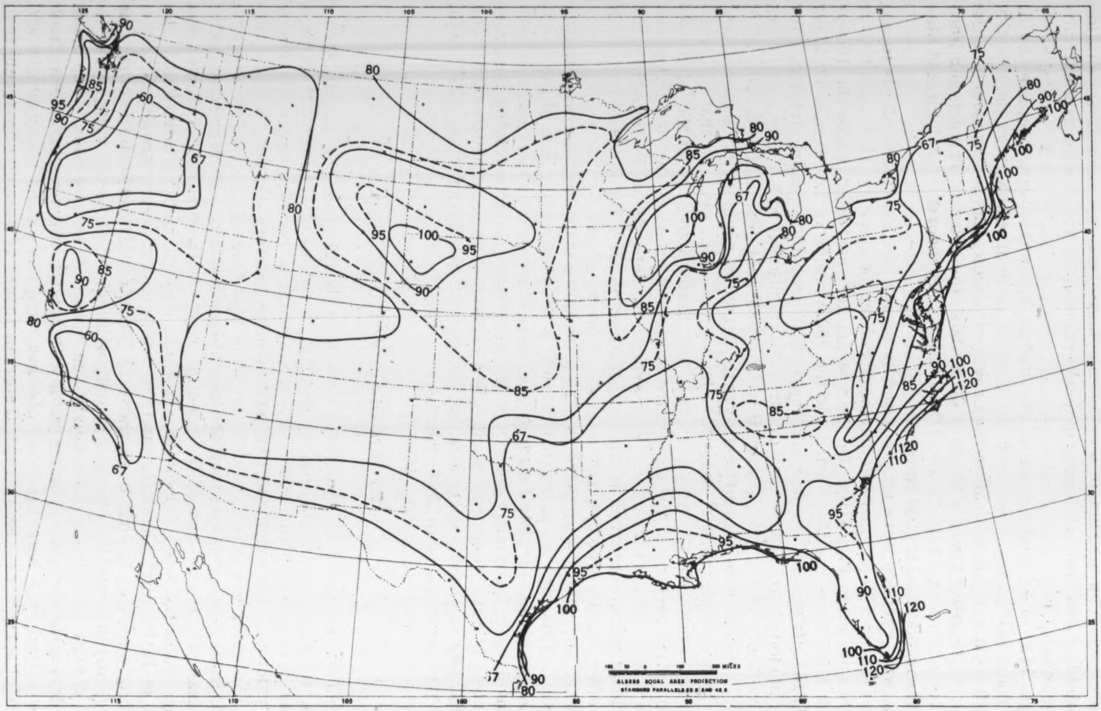
ALBERS EQUAL AREA PROJECTION
STANDARD PARALLELS 29.5 AND 45.5
MILES

FIG. 1(a).—CONTOURS SHOWING FASTEST MILE OF WIND, IN MILES PER HOUR, 30 FT ABOVE GROUND, 50 YR PERIOD OF RECURRENCE

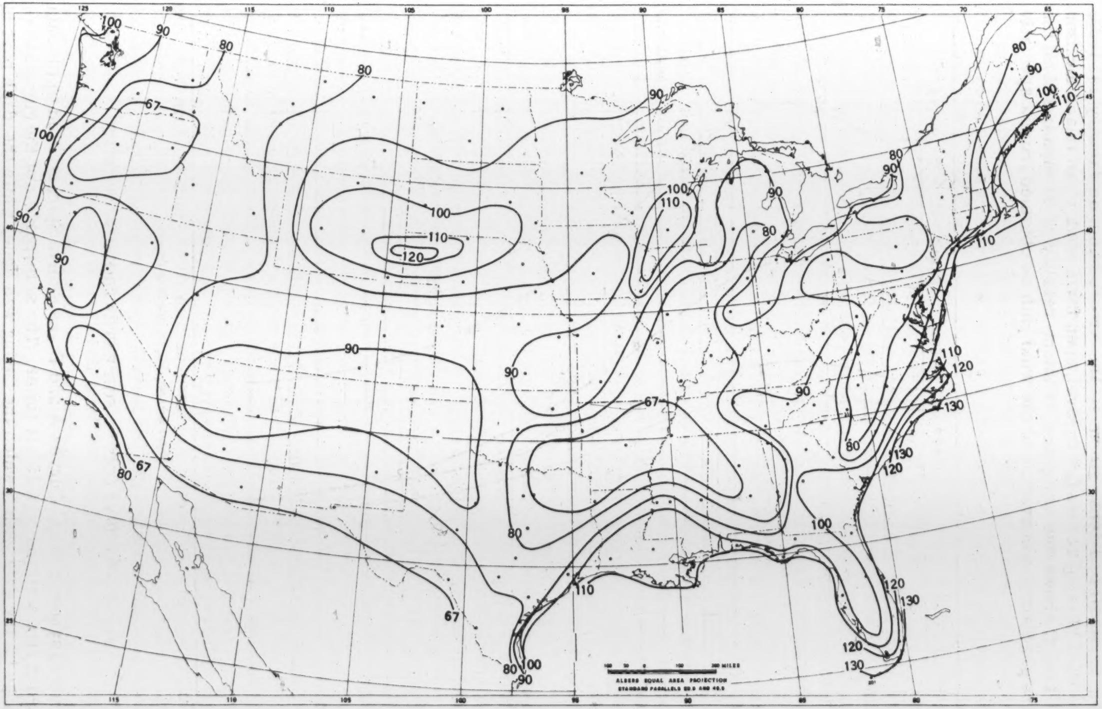
100
90
80
80
67
100
90
90
100
110
120
90
90
100
110
90
80
90
80
67
90
80
67
80
67
110
80
100
90
80
90
100
110
110
120
130
80
130
120
100
120
130
120
130
ALBERS EQUAL AREA PROJECTION
STANDARD PARALLELS 29.5 AND 45.5
MILES

FIG. 1(b).—CONTOURS SHOWING FASTEST MILE OF WIND, IN MILES PER HOUR, 30 FT ABOVE GROUND, 100 YR PERIOD OF RECURRENCE

Extratropical Cyclones.—Curves A and B in Fig. 2 are based on data taken during a moderately intense storm at Ann Arbor, Mich. on January 19, 1933, with the wind blowing across fairly level, open farm land, at an inland location (208). Line C shows the computed gradient velocity of 63 mph based on the pressure gradient and curvature of the wind path as obtained from a specially constructed synoptic map. Curves A and B are Ekman Spirals fitted to the data obtained at five stations on a 250-ft tower. The solid portion of the curve shows the range of the data within which the fitting was done, while the dash part is extrapolated toward the gradient level. Curve A is for the fastest 5 min during

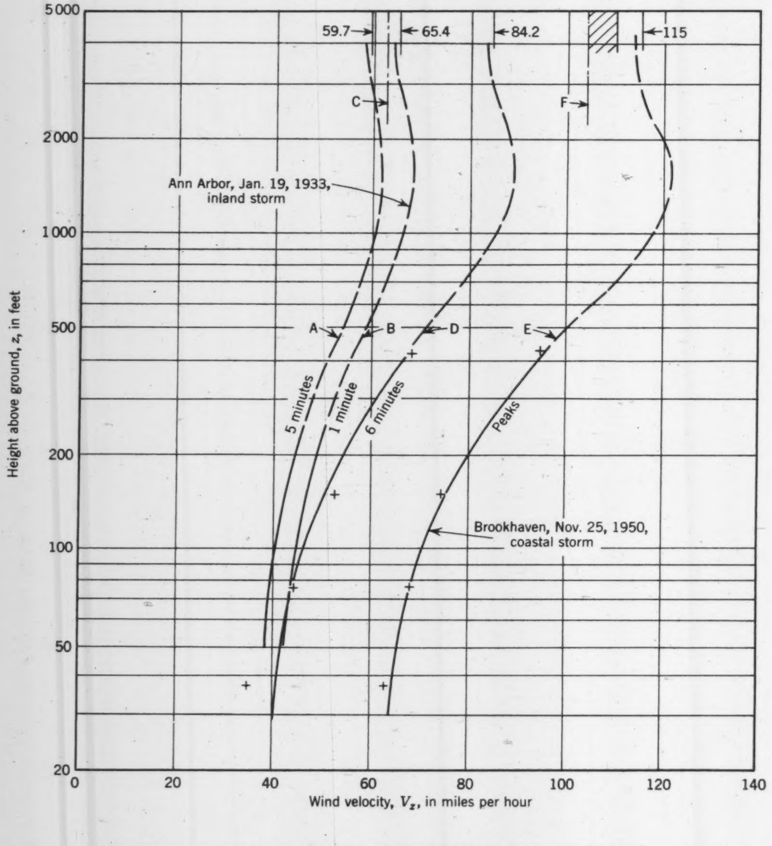

FIG. 2.—WIND VELOCITY FOR EXTRATROPICAL STORMS

the storm, and Curve B is for the fastest 1 min that, incidentally, occurred during the same 5-min period. In each case the extrapolated value of the gradient wind is shown for comparison with the computed value.

The Ekman Spiral postulates steady state dynamic conditions within the portion of the storm under consideration. If one accepts the theory of the Ekman Spiral as applied to gusts, it will be seen that the time required for the establishment of conditions suitable for the application of this theory is somewhere between 1 min and 5 min.

Curves D and E are based on data taken at the Brookhaven Laboratories during the very intense extratropical storm of November 25, 1950. The wind was blowing over the ocean from the east and occasionally from the northwest. The station is located several miles inland from the coast, but it is definitely in a coastal area. The intervening countryside is slightly rolling with moderate small-tree growth. The observations were made with aerovanes mounted on a 410-ft tower. The points to which the curves are fitted are shown with "plus" marks.

Line F shows the gradient wind velocity computed from the spacing and curvature of the isobars as shown in a special pamphlet for that storm (207). The range of computed values for the gradient wind velocity was from 104 mph to 110 mph, depending on whether the curvature of the wind path was based on the curvature of the isobars or on the wind direction as indicated by the arrows. Curve D is an Ekman Spiral fitted to the maximum 6-min average velocities at the four Brookhaven tower stations. The maximum velocities shown in Fig. 2 are not coincidental for all stations, as were the data for Curves A and B, but they are the highest values that were observed at each station during the storm. The observations differed in time by as much as 2.5 hr.

Curve E is an Ekman Spiral fitted to the "peaks" of this storm and extrapolated by dash lines to the gradient level. Although the fit of the spiral to the observed velocities is very good, the accompanying value of gradient velocity is not in perfect agreement with the computed value. The period of time necessary to establish conditions appropriate for the application of the Ekman Spiral theory to these observations, lies somewhere between the period of the "peaks" and the period of 6 min. This agrees with the observations in the previous storm when the appropriate period appeared to lie between 1 min and 5 min.

It should be noted in the application of the Ekman Spiral that not only are steady state dynamic conditions assumed, but also that this implies that the portion of the storm under observation is a closed system, or at least that the addition of energy to this system from an outside source is just exactly sufficient to balance the loss of energy through friction and viscosity. During the early stages in the growth of an extratropical cyclone it is probably true that the system is gaining energy from outside sources sufficient to promote its development, and that during the mature stages of the cyclone the steady state conditions may be approximated. During the later stages when the cyclone is decaying, the loss of energy undoubtedly exceeds the gain from sources outside the system. Under these conditions one would expect the theory of the Ekman Spiral to fit the data best during the mature stages of the extratropical cyclone.

Both the storm at Ann Arbor and the one at Brookhaven are extratropical cyclones of continental origin. The center of the first storm traveled completely across the United States and out over the St. Lawrence Gulf in approximately a west-to-east direction. The second storm was very complicated; its center originated in northeastern Tennessee, traveled south into Georgia, east through the Carolinas, and north into the northern portion of Virginia. Here the low pressure area divided and the western portion traveled into the Ohio and Lake Erie regions where it executed a complete loop in the course of about 30 hr. It traveled through Pennsylvania and into New York State where it became very intense. The velocities in the second storm, in which the wind passed over the ocean and into the coastal areas, increased more rapidly with height than in the first storm where the winds passed over level farm land (215).

Notation.—The letter symbols adopted for use herein are defined where they first appear, in the illustrations or in the text, and are arranged alphabetically, for convenience of reference, in Appendix II.

Hurricanes.—The basic wind velocities (fastest mile of wind at 30 ft above the surface) shown in Figs. 1(a) and (b) include an analysis of existing records of both extratropical and tropical (hurricane) winds. These basic winds must be used as a starting point before determining the variation of wind velocity with height, regardless of whether the structure under consideration is located in an area that is classified as inland or coastal, and regardless of whether the storm should be classified as an extratropical or a tropical (hurricane) cyclone.

The variation of wind velocity with height requires that a distinction be made between these classes of storms and locations. In the case of coastal areas during hurricanes, the variation of wind velocity with height is a subject on which adequately controlled observations are few indeed and in which code recommendations must therefore be based on inferences drawn from what little data are available (215).

Storm winds approaching a coast line have a velocity profile that is compatible with the pressure gradient, the curvature of the wind path, the roughness of the water surface, and other items that affect air movements. As the wind passes the coast line there are two main influences that are responsible for slowing down its velocity. First, it encounters an increased frictional drag that generates an increase of turbulence and this, in turn, diffuses the drag upwards. Second, the supply of water vapor is no longer available from the ocean and, consequently, can no longer provide a source of energy wherein water vapor is condensed into cloud droplets with the accompanying release of latent heat. The greater the distance that the wind moves inland from the coast line, the greater will be the height to which the increased turbulence will be effective in modifying the wind profile. It can be concluded that in coastal areas, such as Brookhaven, the rapid increase of wind velocities with height need not be continued beyond 600 ft, more than which a constant velocity may be used.

The Brookhaven data for hurricanes Carol and Edna are plotted in Fig. 3 together with the curves for the 6-min winds and the peaks of the storm of November 25, 1950. Three 0.3-power curves are shown for comparison; they seem to indicate that the exponent 0.3 gives a conservative estimate of the variation of wind velocity with height during these three Brookhaven storms.

Data for the fastest mile of wind recorded at Miami, Fla., by five hurricanes between 1945 and 1950 are also shown in Fig. 3. They were recorded, respectively, at the City Office of the Weather Bureau where the anemometers were 229 ft and 249 ft above the street, and at the Airport Station 5 miles away where the anemometer was 50 ft above the ground. The variation of wind velocity with height, z, is very erratic, the ratios of V_z to V_{50} being 1.01, 1.14, 1.26, 1.30 and 1.53 and the corresponding values of x (the exponent) being 0.0, 0.082, 0.083, 0.085, and 0.28. Only the largest of the exponents compares at all closely with those obtained at Brookhaven, as shown by the appropriate curves for the corresponding basic winds (V_{30}) in Fig. 3. R. C. Gentry points out (219) that

> "These data unfortunately cannot be used satisfactorily for determining the variation of the wind with height because of the different exposure of the two stations and the distance between them (approximately 5 miles)."

It might also be added that in each pair the readings are not coincidental, that the two stations are in different parts of the transition zone for winds blowing from the ocean, and that the anemometer at the City Office is mounted on a tall office building that affects the wind differently for different wind directions.

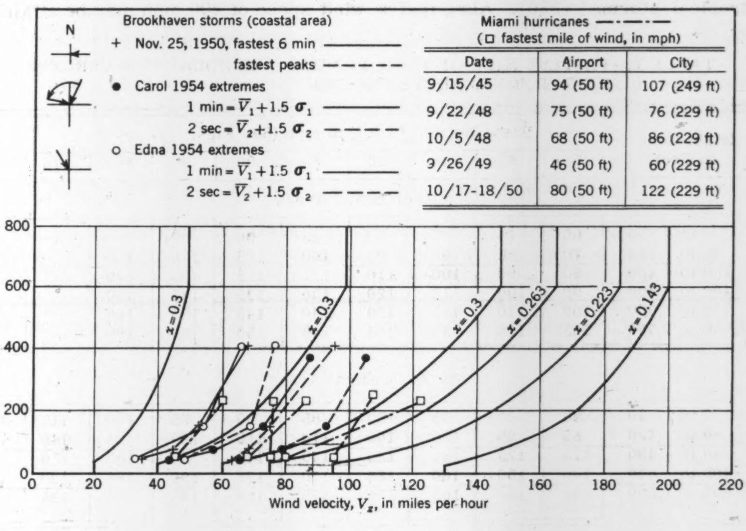

Date	Airport	City
9/15/45	94 (50 ft)	107 (249 ft)
9/22/48	75 (50 ft)	76 (229 ft)
10/5/48	68 (50 ft)	86 (229 ft)
9/26/49	46 (50 ft)	60 (229 ft)
10/17-18/50	80 (50 ft)	122 (229 ft)

FIG. 3.—WIND VELOCITY FOR COASTAL AREAS

All of this emphasizes the difficulty of obtaining reliable quantitative information regarding the variation of wind velocity with height at any situation except where anemometers are mounted on an exposed tower. In these five hurricanes the increase of maximum wind speed with 179-ft increase of height varied from 1% to 53%, and only one storm in five gave a wind profile comparable to the storms at Brookhaven. Although both Miami and Brookhaven are in transition zones of coastal areas, one is likely to experience mature hurricanes, the other hurricanes in the decaying stage.

Fig. 1(a) assigns a basic wind velocity of 75 mph to 90 mph to the Long Island area (fastest mile at 30-ft level, with a 50-yr period of recurrence). This is far greater than the extreme 1-min winds shown in Fig. 3 for Carol and Edna at the 37-ft level and even exceeds the extreme 2-sec peaks for this level. This indicates that, in this coastal area, even stronger winds must be expected by the structural engineer than those observed during Carol and Edna. Two questions arise:

1. Should the very rapid increase of wind velocity with height ($x = 0.3$), shown by these two hurricanes in their decaying stages and by the one intense extratropical storm, be used for future guidance in this coastal area when the specified basic wind (75 mph to 90 mph) is twice as great as the basic velocities accompanying the observations (Carol = 43.8 mph)?
2. Should it be used in those coastal areas that may be visited by hurricanes during their mature stages?

Herbert Riehl states that "no one knows how high wind speeds can rise in tropical storms" (220). Also, that a wind speed of 200 mph may be attained "over the sea and at a few hundred feet above the ground" in a very small area. He also quotes L. A. Hughes to the effect that an average of 90 knots (103 mph) was observed near the center of 28 storms during 84 reconnaissance flights of the United States Navy near the 1,000-ft level (221). This average value should be increased by two factors of at least 1.3 each; one to obtain the extreme storm and the other to obtain the fastest mile of wind within that storm. This would give a "fastest mile of wind" of at least 175 mph at the 1,000-ft level.

TABLE 1.—FASTEST MILE OF WIND, IN MILES PER HOUR, FOR VARIOUS HEIGHT ZONES ABOVE GROUND

Height Zone, in Feet	Basic Wind Velocity, in mph (See Figs. 1(a) and (b))									
	60	67	75	80	85	90	95	100	115	130
(a) For Inland Areas										
0 to 50	60	70	75	80	85	90	95	100		
50 to 150	70	80	90	95	100	105	110	120		
150 to 400	80	90	100	110	115	125	130	140		
400 to 700	90	100	115	120	130	135	145	150		
700 to 1,000	100	110	125	130	140	145	155	160		
1,000 to 1,500	105	115	130	135	145	150	160	165		
(b) For Coastal Areas										
0 to 50	60	70	75	80	85	90	95	100	115	130
50 to 150	85	95	100	105	110	115	120	125	140	150
150 to 400	115	125	130	135	140	145	150	155	170	180
400 to 600	140	150	160	165	170	175	180	185	190	195
600 to 1,500	150	160	165	170	175	180	185	190	195	200

Fig. 1(a) does not specify basic velocities in excess of 120 mph, but even this value would require the fastest mile of wind at 600 ft to be taken at 295 mph if the 0.3 exponent were used. Also, for the benefit of engineers who may feel the need of still higher basic winds in unusual situations, as in Fig. 1(b), basic winds as high as 130 mph are included in Table 1(b). The accompanying wind speed at 600 ft would need to be 320 mph if 0.3 were used as an exponent.

The velocities of 295 mph and 320 mph at the 600-ft level are believed to be excessive, but there appear to be no well-controlled observations in mature hurricanes, such as those which were made on the tower at Brookhaven for the two decaying hurricanes. Consequently, a prudent compromise between recklessness and extravagant conservatism requires a careful consideration of any relevant material from which reasonable inferences may be drawn.

Coastal Areas.—The answers to the two questions posed previously will be adopted as follows:

1. In coastal areas where the basic wind $V_{30} \leqq 60$mph, the variation of wind velocity with height

$$V_z = V_{30} \left[\frac{z}{30}\right]^{0.3} \quad \ldots\ldots\ldots\ldots\ldots\ldots \quad (1)$$

will be adopted for heights up to the 600-ft level, higher than which a constant velocity will be used.

2. In coastal areas where the basic wind $V_{30} \geqq 60$ mph, variable exponents will be adopted such that V_z is never greater than 200 mph at 600 ft in Table 1(b):

$$V_z = V_{30} \left[\frac{z}{30}\right]^{x} \quad \ldots\ldots\ldots\ldots\ldots\ldots \quad (2)$$

in which x varies from 0.3 when V_{30} = 60 mph to 0.143 when V_{30} = 130 mph. Curves are shown in Fig. 3 for some of the intermediate values of x.

In the present (1961) state of information it seems undesirable to try to distinguish between the wind velocities which, in coastal areas, are appropriate for structures located at the coast line and those located farther inland. It is recommended that coastal areas be considered to extend at least 30 miles inland from a well-defined coast line (222).

For all situations which, in the judgment of the engineer, deserve the classification of "coastal area," the wind velocities shown in Table 1(b) should be used together with the "basic velocities" shown in Figs. 1(a) or (b). Special analysis should be made for promontories and in areas where the coast line is precipitous.

Inland Areas.—For all inland areas Table 1(a) should be used together with Figs. 1(a) or (b). These values are minimum and should be increased where higher basic velocities have been recorded locally, or are likely to occur, due to mountains, gorges, or for other unusual reasons.

There is a considerable decrease in the density of the air at locations high above sea level and consequently there is a reduction in the dynamic pressure (velocity pressure) as compared to the same wind speed and temperature at sea level. If, however, the fastest mile of wind, for which the contours of Figs. 1(a) and (b) are drawn, should occur at a temperature greatly below that of the standard atmosphere (59°F), the loss in density due to elevation may be completely compensated by the increase in density due to lower temperature. For example, G. N. Brekke gives (222) a table which shows that, at 4,000 ft-elevation and at standard temperature, there is a decrease of 14% in the density compared to sea-level elevation, but if the temperature were reduced to -10°F there would be no over-all reduction in density of the atmosphere. Consequently, it is recommended that the engineer make no reduction in wind pressure based on reduced density at high elevations unless he has investigated the probability that the fastest mile of wind used in the design may be coincident with a significant reduction of temperature.

SUMMARY OF RECOMMENDATIONS

The scope of these recommendations has been limited to those general considerations that are common to most problems in the selection of appropriate wind velocities for the design of bridges, buildings, towers, and similar structures. It has been assumed that highly specialized problems will receive the attention of engineers with competence to make or direct the necessary modifications or additions to the recommendations.

1. All recommendations herein are based on conditions in open, level country as a standard of reference, and the influence of shielding, or of deflections and channelling due to unusual topography or to large obstructions shall be evaluated by the engineer in each individual case.

2. The "effective ground" (that is, the height in open, level country or its equivalent) at which minor obstructions are unimportant, and which approximates the height of anemometers now (1961) in use by the USWB in the first-order stations at airports, shall be taken at 30 ft.

3. Basic wind velocity shall be defined as the fastest-mile-of-wind, reduced to a height of 30 ft, as shown in Figs. 1(a) and (b) for the various geographical areas of the United States. Fig. 1(a) shows the basic winds that have a statistically derived probable period of recurrence of 50 yr and Fig. 1(b) a probable period of recurrence of 100 yr.

4. A basic wind velocity with a 50-yr period of recurrence (Fig. 1(a)) may be used for all permanent structures except those that, in the judgment of the engineer, have a high degree of wind sensitivity and an unusually high degree of hazard of life and property in case of failure. In the latter case a 100-yr period of recurrence should be used (Fig. 1(b)). In the case of temporary structures, such as those used during construction only, basic winds having velocities equal to three-quarters of the velocities shown in Fig. 1(a) may be used at the discretion of the engineer.

In connection with the foregoing recommendations, it should be noted that the selection of design wind velocities is directly related to the selection of allowable stresses and design procedures because these combine to determine the over-all factor of safety. These recommended velocities are believed to be reasonable for use in conjunction with the allowable stresses given by most codes. However, the determination of loads for a particular structure should be a part of the engineer's responsibility.

5. In special locations such as on promontories, on mountains, in gorges, or for other unusual reasons, where records or experience indicate that the basic velocities given in Figs. 1(a) or (b) are inadequate, higher basic velocities may be used at the discretion of the engineer.

6. Table 1(a) shall be used in inland areas to obtain the variation of wind velocity with height after Fig. 1(a) or (b) has been used to obtain the minimum basic wind velocity for that area. For each basic wind velocity, a stepped approximation to the one-seventh-power law has been used in Table 1(a) to a height of 1,000 ft, above which a constant velocity has been used.

7. Table 1(b) shall be used in coastal areas to obtain the variation of wind velocity with height after Fig. 1(a) or (b) has been used to obtain the minimum basic wind velocity for that area. For each basic wind velocity, a stepped approximation to a power law has been used for the variation of wind velocity with height. The power law up to a height of 600 ft is as follows: (a) Where the basic wind velocity is equal to or less than 60 mph, an exponent of 0.3; (b) where the basic wind velocity is greater than 60 mph, an exponent varying from 0.3 to 0.143 at 130 mph. Above 600 ft a constant velocity is used in each case. Coastal areas shall be considered to extend at least 30 miles inland from a well-defined coast line along the oceans, great lakes, or other large bodies of water.

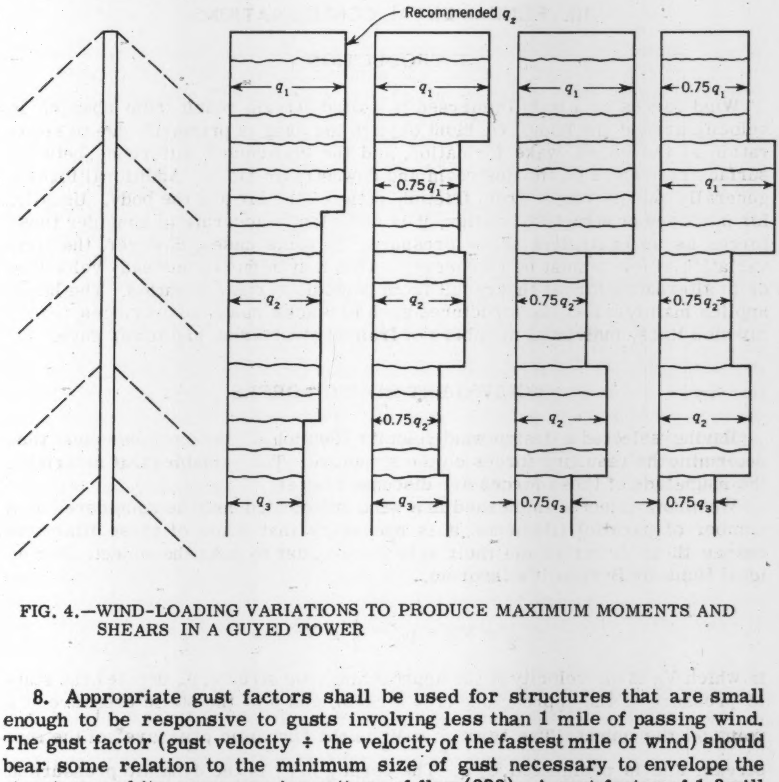

FIG. 4.—WIND-LOADING VARIATIONS TO PRODUCE MAXIMUM MOMENTS AND SHEARS IN A GUYED TOWER

8. Appropriate gust factors shall be used for structures that are small enough to be responsive to gusts involving less than 1 mile of passing wind. The gust factor (gust velocity ÷ the velocity of the fastest mile of wind) should bear some relation to the minimum size of gust necessary to envelope the structure and its accompanying pattern of flow (223). A gust factor of 1.3 will allow for gusts of approximately one-second duration (224) that, in a 90-mph basic wind, would have a length downwind of about 130 ft. This will be adequate for sign boards and small residences. A gust factor of 1.1 will allow for gusts of approximately 10-seconds duration that, in a 90-mph basic wind, would have a length downwind of about 1,300 ft; this factor is adequate for structures having a horizontal dimension, transverse to the wind, of about 125 ft.

9. Guyed towers shall be designed for the moving load effects of aerial jets (208) and descending gust fronts, as indicated in Fig. 4. In Fig. 4

$$q_z = \frac{1}{2} \rho V_z^2 \quad \ldots\ldots\ldots\ldots\ldots\ldots\ldots \quad (3)$$

in which q_z is the dynamic pressure of the free stream at height z and ρ denotes density of the air.

10. In those geographical areas where ice storms may be followed by strong winds, at least a $\frac{1}{2}$ inch thickness of ice shall be assumed on all structural members.

III. FUNDAMENTAL CONSIDERATIONS

INTRODUCTION

Wind forces on a body immersed in a wind stream result from changes in velocity around the body. On blunt objects the drag is primarily due to separation at the edges, wake formation, and the consequent difference between surface pressures on the upstream and downstream faces. Additional forces, generally minor, result from friction between the air and the body. Usually, for purposes of structural design, it is sufficiently accurate to consider these forces as an equivalent static pressure. In some cases, however, the time variation of force must be considered. This may be due to unsteady velocities or to alternating forces that result from periodic vortex formation. The latter applies mainly to flexible structures such as stacks, suspension bridges, transmission lines, individual members of framed structures, and tower guys.

EQUIVALENT STATIC FORCES

Having selected a design wind velocity (Section II) the engineer must then determine the resulting forces on the structure. The variables that determine the magnitude of these forces are discussed herein.

When any object is immersed in a wind stream that may be considered as a number of parallel filaments, it is necessary that some of these filaments change their direction and their velocity in order to pass the object. For an ideal fluid, by Bernoulli's theorem,

$$\frac{1}{2} \rho V_o^2 + p_o = \frac{1}{2} \rho V^2 + p$$

in which V_o is the velocity of the approaching free stream, p_o denotes the static pressure of the approaching free stream, and p is the static pressure at a point on the object. The term $\frac{1}{2} \rho V_o^2$ is the "dynamic pressure" of the free stream and is designated by q. The term $\frac{1}{2} \rho V^2$ is the dynamic pressure at some point on the object. Thus the sum of the dynamic and static pressures is a constant at all points. If the dynamic pressure changes by a certain amount, the static pressure must change by the same amount but in the opposite direction. Where the velocity becomes zero, as at the center of the front of a plate, the increase in static pressure must equal the dynamic pressure in the approaching stream. At the edges and in the lee of the plate, the velocity becomes greater than that of the stream and a negative pressure is developed (that is, less than atmospheric pressure). These changes in pressure produce drag or net force on the object. In addition, there are friction forces, but these are generally small for structural elements.

It is convenient to resolve the wind effect into two force components and a moment and to use dimensionless coefficients to define the magnitude of the forces. Thus,

Drag (force parallel to wind) $= C_D \; q \; A$

Lift (force normal to wind) $= C_L \; q \; A$

Moment arm $= C_{CP} \, h$

in which C_D is the drag coefficient, C_L represents the lift coefficient, C_{CP} is the eccentricity coefficient, A denotes the exposed area, and h is some convenient dimension. The moment arm is the distance from some reference point to the center of pressure and the moment is the distance times the resultant force. Except for symmetrical situations, the center of pressure is not usually at the centroid of the exposed area. The values of the coefficients must be determined experimentally because the science of fluid mechanics has not developed to the point at which theoretical determinations can be made, except perhaps in the simplest of cases.

The magnitude of the foregoing coefficients depends on (a) the geometrical form of the object, (b) its orientation in the wind stream, (c) friction effects, and (d), to a limited extent, the size of the object.

Geometrical Form.—An object that is "streamlined" symmetrically with the direction of the wind, produces little change in the velocity of any of the wind filaments; hence, the principal effects arise from friction; the drag is small and the lift (neglecting the effects of alternating vortices) is zero. An air foil is so shaped that at its top the velocity is high, resulting in a reduction of pressure—thereby producing a large lift. As compared to streamlined objects, greater velocity changes are involved when the object is "blunt" with sharp corners and, consequently, higher drag coefficients result. The wind forces on any object are affected as conditions change the pattern and velocity of the wind.

If the thin rectangular plate in Fig. 5(a) is infinitely long, that is, the aspect ratio (λ = ratio of length, L, to width, b) is infinite, the wind can escape only over the two edges and the pressure distributions are as shown. The summation of pressures on the two faces equals the total drag, that in this case is 1.98 q A or $C_D = 1.98$.

For a square plate, that is, $\lambda = 1$, the wind can escape around all four sides, with the result that the suction on the rear, and hence, the drag, is reduced. The variation of drag coefficient with aspect ratio is shown in Table 2(a). It should be noted that a relatively high aspect ratio is required for a substantial increase in drag greater than that for a square plate.

For a circular disk the air flow is uniform around the periphery. Consequently the drag coefficient is reduced, as compared with a square plate, to 1.11.

When a rectangular plate is placed on the ground (Fig. 5(b)) the air can no longer flow around the bottom edge. This has little effect on the front face pressures but reduces the rear suction considerably, especially in the case of

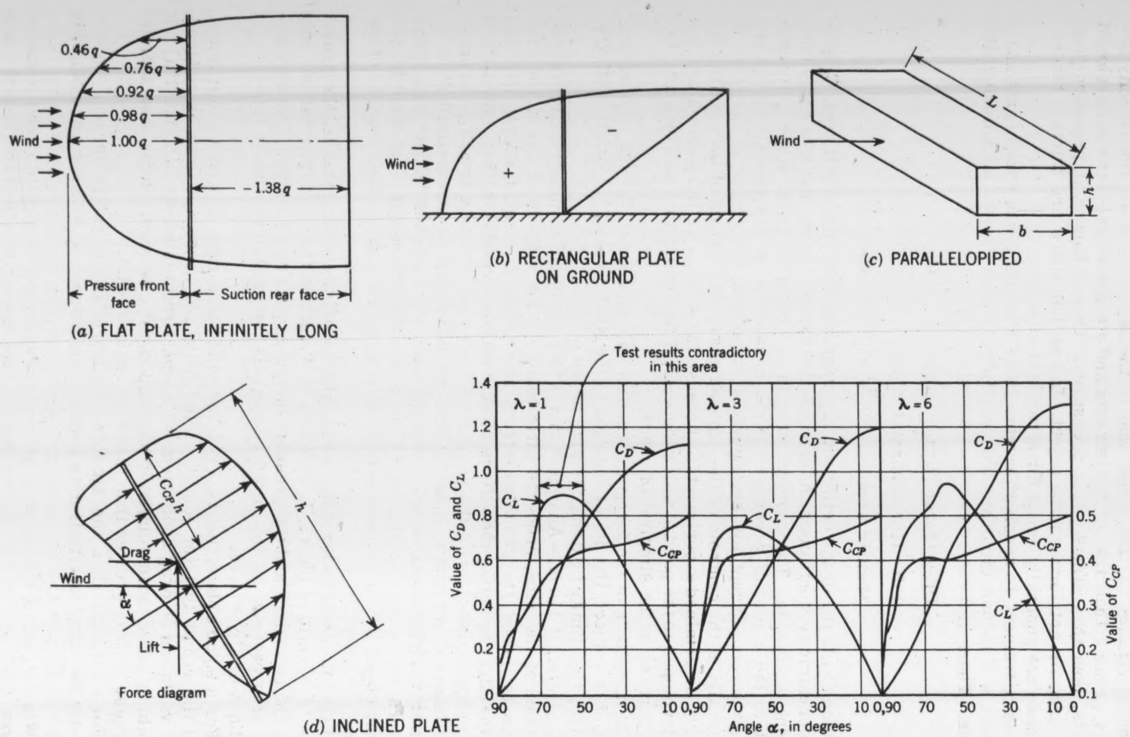

(a) FLAT PLATE, INFINITELY LONG

(b) RECTANGULAR PLATE ON GROUND

(c) PARALLELOPIPED

(d) INCLINED PLATE

FIG. 5.—WIND PRESSURES ON ELEMENTARY BODIES

long plates. As a result, the aspect ratio has little effect in this case and the drag coefficient is nearly the same as for a square, freely suspended plate. It should be noted, however, that the drag in this case depends on the degree of development of the boundary layer upstream that depends, in turn, on the ground-surface condition. Consequently, the pressure distribution may, in some cases, be quite different from that shown in Fig. 5(b).

In all cases the suction on the rear is the larger factor in the total drag. When, for any reason, this suction is reduced, the effect on the drag is appreciable. As an example, consider the parallelopiped in Fig. 5(c). As the width, b, increases relative to the height, the object becomes more "streamlined" and the drag coefficient decreases.

If the plate is perforated the drag becomes a function of the solidity ratio, ϕ, or the ratio of solid to enclosed area, as well as the aspect ratio (see Section V).

Drag and lift coefficients for several typical structural shapes are given in Table 3. Extensive data on the drag of elemental shapes are available (112) (311) (315).

TABLE 2.—DRAG COEFFICIENTS

	(a) Flat Plate in Normal Wind[a]							(b) Rectangular Plate on Ground[a]			(c) Parallelopiped[b]		
	Value of λ										Value of b/h		
	1.0	2.0	5.0	10	20	40	∞	1.0	10	∞	0.1	1.0	6.0
Pressure, front face	0.76						0.60	0.38		0.60			
Suction, rear face	0.36						1.38	0.72		0.60			
Value of C_D	1.12	1.19	1.20	1.23	1.42	1.66	1.98	1.10	1.20	1.20	1.95	2.03	0.90

[a] From reference 111. [b] From reference 303.

When two plates or lattice structures form the obstruction, the leeward plate is "shielded" by the windward one. When the spacing is infinite, it is evident that the case is two separate plates. The degree of shielding is a function of the spacing between the structures, the solidity ratio and the angle of attack, either horizontal, vertical, or both (see Section V).

Orientation of the Object in the Wind Stream.—In general the wind does not strike an immersed object perpendicular to any of its axes. Even for a structure near the ground the wind may have a vertical angle of attack, possibly as much as 20° from the horizontal. The horizontal angle (yaw) may be of any amount.

Fig. 5 (d) shows a plate inclined to the wind. For aspect ratios of 1, 3, and 6 the variation of pressure coefficients with the angle of attack is given. The pressure distributions on the two faces are, of course, not uniform and the center of pressure is not at the plate centroid. Similar information for various structures is given in Sections IV and V.

Friction Forces.—In the examples given previously, the forces were a result of the change of surface pressure. Additional forces result from friction be-

TABLE 3.—DRAG COEFFICIENTS FOR STRUCTURAL SHAPES WITH $\lambda = \infty$ (111)

Profile and wind direction	C_D	C_L
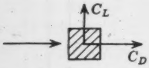	2.03	0
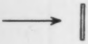	1.96 2.01	0
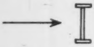	2.04	0
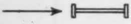	1.81	0
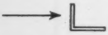	2.0	0.3
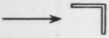	1.83	2.07
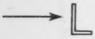	1.99	−0.09
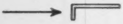	1.62	−0.48
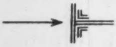	2.01	0
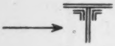	1.99	−1.19
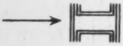	2.19	0

tween the air and the immersed object. Obviously, this friction varies with the surface roughness of the immersed body, but, for most civil engineering structures, this is of less consequence than the shape of the body, so that it becomes possible to consider the effect of Reynolds number, **R**, only.

The Reynolds number is the ratio of the inertial force to the viscous force which a fluid stream exerts on an object. The inertial force is the product of dynamic pressure and area, and the viscous force is the viscous drag or friction between the fluid and the object.

$$\mathbf{R} = \frac{\rho V^2/h}{\mu V/h^2} = \frac{V\,h}{\mu/\rho} = \frac{V\,h}{\nu} \quad \ldots\ldots\ldots\ldots\ldots \quad (5)$$

in which ν is the kinematic viscosity, h is a characteristic dimension of the object, and μ is the dynamic viscosity. For standard air (density = 0.002378 slugs, temperature = 59°F) **R** = 6380 V h where V is in feet per second and h is in feet. There are only minor variations with changes from these conditions.

The variations of drag coefficient with **R** for some elementary objects are shown in Fig. 6. Some comments on Fig. 6 are:

a. Experimental data are lacking for **R** much greater than 10^6. For comparison, a circular stack of 20-ft diameter with a velocity of 60 mph has an **R**-value of 11.3×10^6. There is little reason to believe that there is material change in the drag coefficient above **R** = 10^6.

b. The drag coefficients for streamlined objects (such as cylinders, tanks, and so forth) show a large decrease at the critical **R** of about 0.5×10^6.

c. No such change occurs for bodies with sharp corners such as bridges and buildings. In these cases, the boundary layer is forced to separate from the body at the sharp corner instead of separating at variable distances behind the leading edge. Hence, **R** has little effect on "blunt" objects. An exception to this is the drop in coefficients for flat plates in the range **R** = 1,000 to 3,000 that may have some effect in tests on small models at low velocities.

Effect of Size of Object.—Most tests have been made on comparatively small models. Pagon (112) cites examples in which there was a moderate increase in drag coefficients with increase in dimensions, even for blunt objects. For example, for large squares C_D becomes 1.28 in place of 1.12 as shown in Table 2(a). The difference is small compared with the other uncertainties of wind forces and may be merely the result of experimental error.

UNSTEADY WIND FORCES

Structures may be subject to wind-induced oscillations of large amplitude and involving severe stresses when damping is small and one or more of the following conditions exist:

a. The structure, or structural component, is relatively flexible or flexibly supported;

b. an exciting force is produced by the wind; and

c. the cross section of the structure, or structural component, is such as to promote the discharge of vortices or to exhibit unstable lift or moment characteristics; or

d. the structure, or structural component, is free to oscillate in a bending mode and a torsional mode simultaneously. Under this condition the two modes may couple in a motion compounded from both modes and appear as an eccentric torsion in which the center of rotation has moved upwind by an amount determined by the relative strength of the bending mode; and the coupled frequency lies between that in torsion and in bending. This type of motion that is known as flutter may, under some conditions, become quite violent, reaching a catastrophic amplitude in a few cycles of oscillation.

When the source of excitation takes the form of a gust the change in wind velocity seldom causes a significant oscillation because the time is usually long with respect to the natural frequency of the structure. A possible exception arises with free standing multiple tall stacks in line. It has been noted that the first stack in line may be at rest whereas the second in line may show strong motion. Considerations of gusts in selecting the basic design wind velocity have been discussed (Section II).

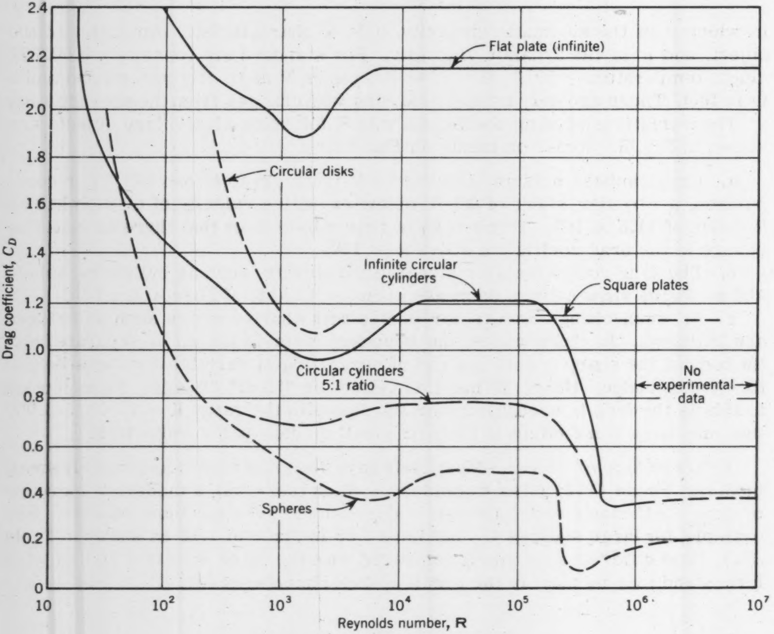

FIG. 6.—DRAG COEFFICIENTS FOR SPHERES AND LONG CYLINDERS (112)

Vortex formations may cause periodic alternating forces perpendicular to the wind direction resulting in vibration of the structure. This phenomenon has been repeatedly observed on cylindrical objects. Of particular interest to the civil engineer is the case of vibrating stacks.

Certain cross sections develop negative slopes over certain portions of the lift or moment curves plotted against angle of attack of the wind; and even though the wind may show an angle of attack in one direction the lift or moment effect may act in the opposite direction. This condition may cause disastrous motion on certain types of plate girder stiffened suspension bridges (see Section VI).

IV. ENCLOSED STRUCTURES

INTRODUCTION

Recognizing that the civil engineer needs to know more about the aerodynamic characteristics of structures, this section analyzes the work of past and present (1961) investigators and correlates data relating to shape or drag coefficients for various building forms. Included is a table from the Swiss Building Code that contains the latest and most extensive data published. This section should assist the civil engineer in establishing more logical design criteria for proper economy and safety in buildings.

A review of many building codes and specifications for the structural design of buildings reveals that surprisingly little interest is taken in the proper application of wind forces even though there are experimental data available on which to build a consistent theory and which will correlate much of the observed phenomena. For example, building codes usually specify a certain number of pounds per square foot with no reference to the wind velocity implied or building shape assumed. Furthermore, the pressure given is not a real pressure but rather a value that, when multiplied by the projected area in elevation, is intended to give the total force on the building. This force is the result of pressure on the windward and suction on the leeward side. It seems reasonable to expect the modern engineer to use more refined methods. Fortunately, some of the more recent building code revisions are taking steps in this direction.

In order to establish a logical basis for design, an examination of all available research data, to 1936, was made by Subcommittee 31 of ASCE (419). The results of this study were subsequently incorporated into a final report of the Subcommittee (423) that recommended actual pressures and suctions to be used in design rather than shape coefficients that could be used after the design velocity had been selected. It is believed that it would be more helpful to the civil engineer to start with appropriate shape coefficients for structures so that consistent design loads could be obtained for areas subjected to winds that may be greater than the averages established for the country as a whole. For the eastern coast and the southeast section of the United States, where winds of hurricane velocity are common, it is believed that a more detailed knowledge of the aerodynamic characteristics of structures would be most useful in arriving at logical criteria for design. At the same time engineers should be cognizant of economy in design of structures and proper factors of safety.

USE OF COEFFICIENTS

The local pressure at any point on the surface of a building is equal to the dynamic pressure (q) times the pressure coefficient, Cp. If one desires the total force on a building use may be made of a shape or drag coefficient, C_D, that, when multiplied by q gives the average force per unit of elevation area.

Dynamic pressure is the product of one-half the air density and the square of the resultant design velocity, the units being self-consistent, and represents the kinetic energy per unit volume of moving air. For standard air (0.07651 lb per cu ft, corresponding to 15°C at 760 mm of mercury) and velocity V expressed in miles per hour, the dynamic pressure in pounds per square foot is given by

$$q = 0.002558\ V^2 \qquad (6)$$

As an example of the use of coefficients, for the external forces on buildings with plane surfaces normal to the wind the total combined average pressure on the outside of the windward and leeward faces of an average building may be 1.3 q of which 0.8 q is the pressure on the windward wall and 0.5 q the suction on the leeward wall (423). The value 1.3 represents the shape coefficient for a typical building with vertical walls normal to the wind direction. Therefore,

$$p = q \times C_D = q \times 1.3 = 0.0033\ V^2 \qquad (7)$$

in which p is an average pressure that, when multiplied by the projected elevation area, gives the total force on the building. On the basis of Eq. 7 the wind velocity corresponding to a total wind pressure of 20 psf is 77.8 miles per hour. The dynamic pressure for this velocity is 15.5 psf.

It should be noted that the values given above for average wall pressures are the net forces on the walls only in the case in which the building is airtight. Such a condition will rarely arise. Normally, air leakage due to small openings around windows, doors, skylights, and eaves will give rise to a net internal pressure or suction depending on whether the openings are chiefly in the windward or leeward surfaces. Where openings are of substantial size, such as hangars, the internal wind pressure may be of considerable magnitude. In the design of roof and walls the pressure coefficients should include the summation of internal and external pressures for the particular geometric configuration of the structure.

Experimental values of average and local pressure and shape coefficients are available for a variety of building configurations. Some of these are presented and discussed herein. Although the number of possible building shapes is obviously infinite, it is feasible, on the basis of the available coefficients, to make reasonable predictions of wind force on most structures.

AVERAGE PRESSURE COEFFICIENTS

It is possible to draw some general conclusions regarding pressure coefficients for common building types of typical proportions; these are summarized herewith. For more unusual shapes the test data described in a later part of this section will be helpful.

Flat-Topped Buildings.—Consider first a box-shaped building with the wind direction perpendicular to one of the sides. The average coefficient for the front face is about 0.9 regardless of building proportions. The rear suction, however, depends on the ratio of the various dimensions. For example, considering a building that is square in plan, the suction coefficient is about 0.3 if the height-width ratio is 1/4, about 0.5 for a ratio of unity and about 0.6 if the ratio is 2.5 or greater. An increase in the length of the building (perpendicular to the wind) has about the same effect as an increase in height. The side walls experience a suction of about 0.8 q for most proportions. The roof suction is generally larger on the windward side but the average coefficient for the entire roof is about -0.5 for a height-width ratio of 1/4 and -0.8 for a ratio of 2.5 or larger.

If the wind is not perpendicular to a face or if the plan shape of the building is rectangular the test data described subsequently will be useful.

Gabled Roofs.—Many investigations have been made of the wind forces on typical gabled-roof buildings. Some of these are summarized herewith and shown in Fig. 7.

ASCE Subcommittee 31 recommended (419) average pressure coefficients as follows: On the windward wall, 0.8, and on the leeward wall, -0.5; on the leeward slope, -0.6, and on the windward slope a value varying with the pitch as shown in Fig. 7. These values are obviously averages because no consideration was given to the proportions of the building.

The Danish Building Code recommends (427) the following: On the windward wall, 1.0, and on the leeward wall, -0.2; on the leeward slope, -0.2, and on the windward slope a linear variation with pitch as shown in Fig. 7. It will be noted that the negative pressures are considerably less than those recommended elsewhere. However, the additional requirement is given that all walls and roofs shall be anchored to resist a suction of -0.8 q. Again, no reference is made to the proportions of the building.

The Swiss Building Code recommends (438) the following: For the windward wall, 0.9, and for the leeward wall, -0.5; for the leeward slope, -0.7, and for the windward slope, the variation with pitch shown in Fig. 7. Recognizing the effect of the dimensions of the building, the Swiss Code recommends the foregoing values only within the following limits: Ratio of wall height to building depth (parallel to wind direction), 0.67 to 1.5, and ratio of building width (perpendicular to wind) to depth, 0.4 to 2.5.

Also shown in Fig. 7, as a matter of historical interest, is the Duchemin formula that for many years was used as the pressure on the windward slope. This formula assumed positive pressures for all roof angles and neglected suction on the leeward slope. The more recent data as indicated by the three recommendations noted previously show appreciable suction on the leeward slope and also on the windward slope for small roof pitches.

Of the data given previously the Swiss Code is probably the most accurate because it is based on the most recent and extensive series of tests; however, it is reasonably close to the earlier ASCE recommendation. All of the coefficients are averages for the various wall or roof areas. More detailed local pressure coefficients are given in the test results described subsequently in this section.

Rounded Roofs.—The situation with regard to arched roofs is more complex. Perhaps the most general information is that contained in the Subcommittee 31 Report (419) that is shown graphically in Figs. 8 and 9. Pressure coefficients are given for four segments of circular arches: The center half and the leeward and windward quarters. (Subcommittee 31 used variable segments depending on the rise-span ratio but in the Final Report (423) these were changed to the simpler procedure given herein.) These are given as a func-

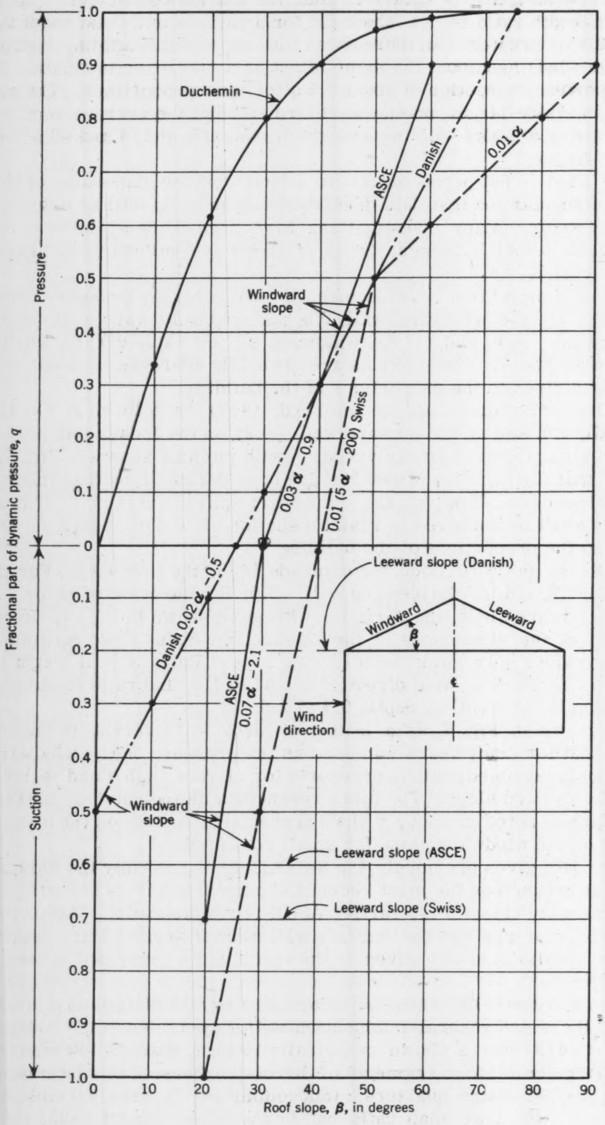

FIG. 7.—EXTERNAL COEFFICIENTS FOR WIND PRESSURES AND SUCTIONS ON SYMMETRICAL GABLE ROOFS

tion of the rise-span ratio, r. Fig. 8 is for an arch springing from the ground and Fig. 9 for one supported above ground, for example, on vertical walls. In the latter case the vertical-wall coefficients could reasonably be taken as 0.8 on the front and -0.5 on the rear. Note that in Fig. 9 alternate values of pressure and suction are given for the windward segment and for r = 0.25 and 0.30. Also note that in all cases suction occurs over a major portion of the roof.

These recommendations for rounded roofs are obviously rather approximate. However, they appear reasonable in view of more recent tests (438) (434). An important factor not considered in Fig. 9 is the height above ground.

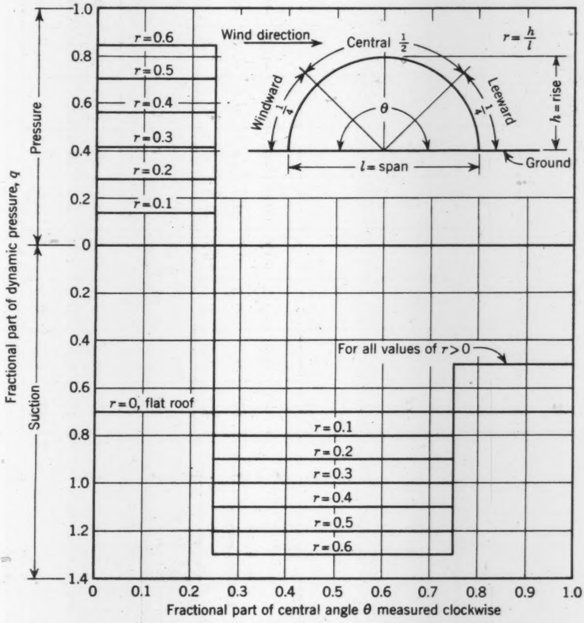

FIG. 8.—WIND PRESSURE DISTRIBUTION ON ROUNDED ROOFS STARTING FROM GROUND LEVEL

In general, roof suction increases or pressure decreases, especially on the windward segment, with increasing height of the supports above ground. These data are for a transverse wind. If the wind is parallel to the arch axis the roof pressures are similar to those on a flat-roofed building.

DETAILED TEST RESULTS

The recommendations from various sources given previously are obviously of limited use. They do not consider oblique wind directions, the variation of pressure over the surfaces or buildings of unusual shape. In many cases it is

TABLE 4 (a).—WIND PRESSURE COEFFICIENTS FOR HOUSES AND CLOSED HALLS

Structure	α	External Pressure Coefficient, C_{pe}								Internal Pressure Coefficient, C_{pi}			
										Openings uniformly distributed	Openings Mainly on Side		
		A	B	C	D	E	F	G	H		A	B	C
House Roofs 0° to 10°, h:b:L = 1:1:1 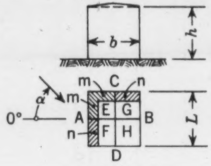 h b m C n α m 0° A E G B n F H L D	0°	0.9	-0.5	-0.6	-0.6	-0.7	-0.7	-0.5	-0.5	±0.2	0.8	-0.4	-0.5
	15°	0.8	-0.5	-0.7	-0.5	-0.7	-0.6	-0.5	-0.6	±0.2	0.7	-0.4	-0.6
	45°	0.5	-0.5	0.5	-0.5	-0.8	-0.5	-0.5	-0.4	±0.2	0.4	-0.4	0.4
	45°	For m, C^*_{pe} = -1.2; for n, C^*_{pe} = -0.8											
House h:b:L = 2.5:2:5 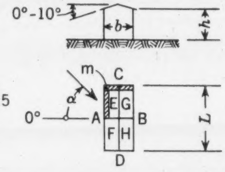 0°-10° b h m C α 0° A E G B F H L D	0°	0.9	-0.5	-0.7	-0.7	-0.6	-0.6	-0.5	-0.5	±0.2	0.8	-0.4	-0.6
	45°	0.6	-0.5	0.4	-0.5	-0.9	-0.7	-0.6	-0.7	±0.2	0.5	-0.4	0.3
	90°	-0.5	-0.5	0.9	-0.4	-0.8	-0.2	-0.8	-0.2	±0.2	-0.4	-0.4	0.8
	45°	For m, C^*_{pe} = -1.5											

House $h:b:L = 2.5:2:5$	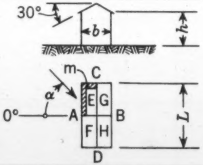 30° b h m C α 0° A E G F H B D L	0°	0.9	-0.5	-0.7	-0.7	-0.6	-0.6	-0.5	-0.5	±0.2	0.8	-0.4	-0.6
		45°	0.6	-0.5	0.4	-0.4	-0.4	-0.5	-0.6	-0.7	±0.2	0.5	-0.4	0.3
		90°	-0.5	-0.5	0.9	-0.4	-0.7	-0.2	-0.7	-0.2	±0.2	-0.4	-0.4	0.8
		45°	For m, $C^*_{pe} = -1.2$											
House $h:b:L = 2.5:2:5$	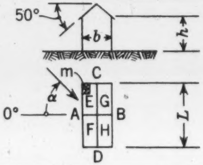 50° b h m C α 0° A E G F H B D L	0°	0.9	-0.5	-0.8	-0.8	0.3	0.3	-0.6	-0.6	±0.2	0.8	-0.4	-0.7
		45°	0.6	-0.5	0.4	-0.4	0.3	-0.1	-0.5	-0.6	±0.2	0.5	-0.4	0.3
		90°	-0.5	-0.5	0.9	-0.4	-0.8	-0.2	-0.8	-0.2	±0.2	-0.4	-0.4	0.8
		75°	For m, $C^*_{pe} = -1.2$											
Closed hall Roofs 0° to 3°, $h:b:L = 1:4:4$	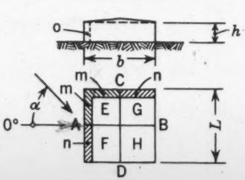 o h b m C n m α 0° A E G F H B n D L	0°	0.9	-0.3	-0.4	-0.4	-0.8	-0.8	-0.3	-0.3	±0.2	0.8	-0.2	-0.3
		15°	0.8	-0.3	-0.1	-0.5	-0.7	-0.8	-0.2	-0.3	±0.2	0.7	-0.3	-0.2
		45°	0.5	-0.4	0.5	-0.4	-0.9	-0.6	-0.6	-0.3	±0.2	0.4	-0.4	0.4
		15°	For o, side C, $C^*_{pe} = -0.8$											
		45°	For m, $C^*_{pe} = -2.0$; n, $C^*_{pe} = -1.0$											
Closed hall $h:b:L = 1:8:16$	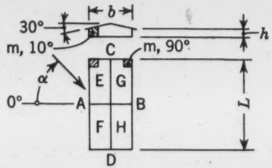 b 30° m, 10° h C m, 90° α 0° A E G F H B D L	0°	0.8	-0.5	-0.5	-0.5	0.2	0.2	-0.6	-0.6	±0.2	0.7	-0.4	-0.4
		45°	0.5	-0.5	0.4	-0.3	0.1	-0.1	-0.8	-0.5	±0.2	0.4	-0.4	0.3
		90°	-0.3	-0.3	0.9	-0.3	-0.5	-0.1	-0.5	-0.1	±0.2	-0.2	-0.2	0.8
		10° and 90°	For m, $C^*_{pe} = -1.0$											

TABLE 4 (b).—WIND PRESSURE COEFFICIENTS FOR OPEN AND CLOSED BUILDINGS

Structure	α	External Pressure Coefficient, C_{pe}									
		A	B	C	D	E	F	G	H	J	K
Building open on one side Roof 30°, $h{:}b{:}L = 1{:}2{:}4$ 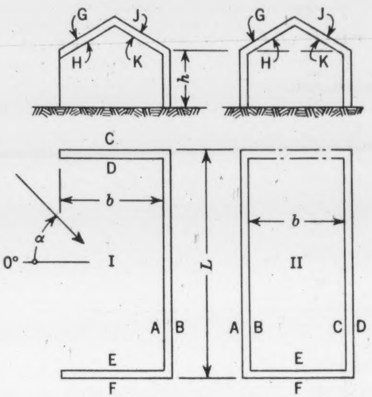 G J H K h G J H K C D b α 0° I A B E F L b II A B C D E F		(I) One long wall open									
	0°	0.8	-0.5	-0.7	0.8	0.8	-0.7	-0.3	0.8	-0.4	0.8
	45°	0.7	-0.6	0.4	0.6	0.8	-0.4	-0.2	0.6	-0.7	0.7
	60°	0.3	-0.7	0.7	0.3	0.4	-0.4	-0.3	0.2	-0.6	0.2
	180°	-0.5	0.9	-0.8	-0.5	-0.5	-0.8	-0.4	-0.5	-0.2	-0.5
		(II) One end wall open									
	0°	0.9	-0.7	-0.7	-0.4	-0.7	-0.8	-0.2	-0.7	-0.4	-0.7
	45°	0.5	0.7	0.8	-0.5	0.7	-0.4	-0.3	0.7	-0.6	0.8
	60°	0.1	0.9	0.9	-0.6	0.9	-0.4	-0.3	0.9	-0.7	0.9
	90°	-0.5	0.8	0.8	-0.5	0.8	-0.3	-0.4	0.8	-0.4	0.8

Buildings open on two sides Roofs 30°, $h:b:L = 1:2:4$ 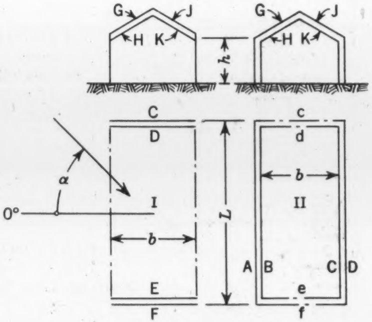 G J H K h C D c d α 0° I II b L A B C D E F e f		(I) Two long walls open													
	0°			-0.2	-0.7	-0.7	-0.2	0.4	-0.9	-0.5	-0.8				
	45°			0.5	-0.4	0.5	-0.4	0	-0.3	-0.6	0				
	60°			0.7	-0.6	0.5	-0.4	-0.3	-0.1	-0.7	-0.3				
		(II) Two end walls open													
	0°	0.9	-0.7	-0.7	-0.4			-0.2	-0.7	-0.4	-0.7				
	45°	0.5	-0.4	-0.1	-0.8			-0.3	-0.4	-0.8	-0.3				
	60°	0.3	-0.2	0.1	-0.5			-0.3	-0.1	-0.8	0.1				
	60°	End Det, c = 0.7, d = -0.6; End Det e = 0.6, f = -0.8													
·Closed buildings with roof vents Roofs 20° $h:b:L = 1:4:8$ 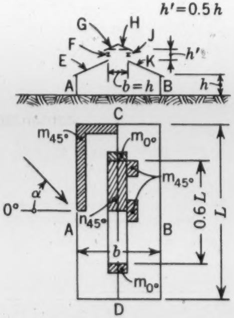 $h' = 0.5h$ G H F J E K h' A $b = h$ B h C $m_{45°}$ $m_{0°}$ $m_{45°}$ α 0° A $n_{45°}$ B 0.6L L b $m_{0°}$ D												Internal Pressure Coefficient, C_{pi}, with Vents			
												F & J open	F & J closed	F only open	J only open
	0°	0.8	-0.5	-0.7	-0.7	-0.2	0.6	-1.0	-0.6	-0.5	-0.6	-0.2	±0.2	0.5	-0.4
	45°	0.4	-0.5	0.4	-0.5	-0.3	0.2	-1.3	-1.4	-1.0	-0.7	-0.5	±0.2	0.1	-0.9
	90°	-0.4	-0.4	0.8	-0.3	-0.4	-0.2	-0.3	-0.3	-0.2	-0.4	-0.3	±0.2	-0.2	-0.2
	0° and 45°	For m, $C^*_{pe} = -1.2$; n, $C^*_{pe} = -2.4$													

TABLE 4 (c).—WIND PRESSURE COEFFICIENTS FOR TALL BUILDINGS, ROOFS, AND PASSAGEWAYS

Structure	α	External Pressure Coefficient, C_{pe}								Internal Pressure Coefficient, C_{pi}				
		A	B	C	D	E	F	G	H	Openings uniformly distributed	Openings Mainly in			
											A	B	C	Roof EF
Tall buildings closed Roofs 0° to 15° h:b:L=2.5:1:1 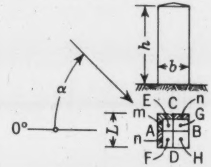 h b α 0° E C n m G L n A B F D H	0°	0.9	-0.6	-0.7	-0.7	-0.8	-0.8	-0.8	-0.8	±0.2	0.8	-0.5	-0.6	
	15°	0.8	-0.5	-0.9	-0.6	-0.8	-0.8	-0.7	-0.7	±0.2	0.7	-0.5	-0.8	
	45°	0.5	-0.5	0.5	-0.5	-0.8	-0.7	-0.7	-0.5	±0.2	0.4	-0.4	0.4	
	45°	For m, C^*_{pe} = -1.0; n, C^*_{pe} = -0.8												
Tall buildings closed h:b:L=2:1:2 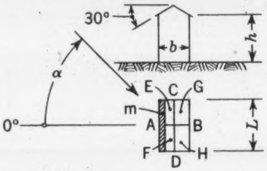 30° b h α 0° E C G m A B L F D H	0°	0.9	-0.5	-0.8	-0.8	-1.0	-1.0	-0.5	-0.5	±0.2	0.8	-0.4	-0.7	
	45°	0.6	-0.5	0.4	-0.4	-0.3	-0.4	-0.5	-0.6	±0.2	0.5	-0.4	0.3	
	90°	-0.6	-0.6	0.9	-0.4	-0.7	-0.5	-0.7	-0.5	±0.2	-0.5	-0.5	0.8	
	0°	For m, C^*_{pe} = -1.2												

Shed roof $h{:}b{:}L = 1{:}2.4{:}12$ 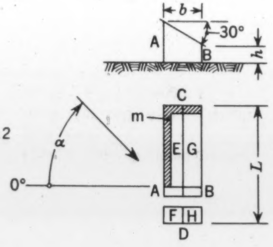 b 30° A B h C m E G α 0° A B L F H D	0°	0.9	-0.5	-0.6	-0.6	-0.5	-0.5	-0.5	-0.5	±0.2	0.8	-0.4	-0.5	-0.4
	45°	0.5	-0.6	0.4	-0.4	-1.2	-0.7	-1.1	-0.7	±0.2	0.4	-0.5	0.3	-0.8
	90°	-0.4	-0.3	0.9	-0.2	-0.3	0	-0.3	0	±0.2	-0.2	-0.1	0.8	0
	180°	-0.4	0.8	-0.7	-0.7	0.1	0.1	0.2	0.2	±0.2	-0.3	0.7	-0.6	0
	45°	For m, $C^*_{pe} = -1.4$												
Peaked roof $h{:}b{:}L = 1{:}1{:}5$ 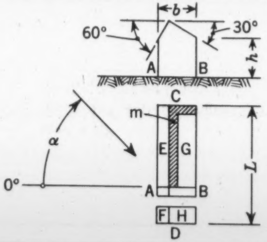 b 60° 30° A B h C m E G α 0° A B L F H D	0°	0.9	-0.5	-0.6	-0.6	0.6	0.6	-0.5	-0.5	±0.2	0.8	-0.4	-0.5	0.5
	45°	0.5	-0.8	0.4	-0.5	0.2	-0.1	-1.0	-0.8	±0.2	0.4	-0.7	0.3	0
	90°	-0.4	-0.4	0.9	-0.3	-0.4	0	-0.4	0	±0.2	-0.1	-0.1	0.8	-0.1
	180°	-0.5	0.9	-0.6	-0.6	-0.5	-0.5	-0.1	-0.1	±0.2	-0.4	0.8	-0.5	-0.4
	45°	For m, $C^*_{pe} = -1.3$												
Closed connecting passage between large walls $h{:}b{:}L = 1{:}1{:}10$ 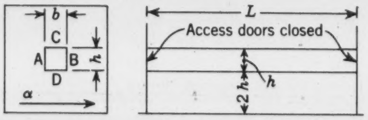 b C A B D h α L Access doors closed h 2 h	0°	0.8	-1.2	-1.4	-1.5					-0.5	0.7	-1.1	-1.3	

TABLE 4 (d).—WIND PRESSURE COEFFICIENTS FOR SHELTER ROOFS

Structure	α	External Pressure Coefficient, C_{pe}							
						End Surfaces			
		A	B	C	D	J	K	L	M
Roof +30° $\alpha = 0°\text{-}45°$, A-D full length $\alpha = 90°$, A-D part length L' 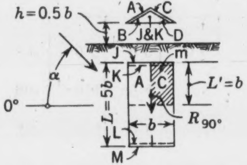 $h = 0.5\,b$ A C B J&K D J m α 0° K A C $L = 5b$ $L' = b$ $R_{90°}$ L b M	0°	0.6	-1.0	-0.5	-0.9				
	45°	0.1	-0.3	-0.6	-0.3				
	90°	-0.3	-0.4	-0.3	-0.4	0.8	-0.4	0.3	-0.3
	45°	For m, $C^*_{pe,top} = -1.0$; $C_{pe,bottom} = -0.2$							
	90°	Tangential acting friction, R = 0.05 q : L : b							
Effect of trains or stored material Roof +30° $\alpha = 0°\text{-}45°\text{-}180°$, A-D full length $\alpha = 90°$, A-D part length L' 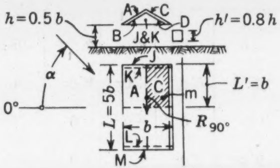 $h = 0.5\,b$ A C D $h' = 0.8\,h$ B J&K J α 0° K A C m $L = 5b$ $L' = b$ $R_{90°}$ b L M	0°	0.1	0.8	-0.7	0.9				
	45°	-0.1	0.5	-0.8	0.5				
	90°	-0.4	-0.5	-0.4	-0.5				
	180°	-0.3	-0.6	0.4	-0.6				
	45°	For m, $C^*_{pe,top} = -1.5$; $C_{pe,bottom} = 0.5$							
	90°	End surface friction load, see above							

Roof +10° α=0°-45°, A-D full length α=90°, A-D part length *L′*	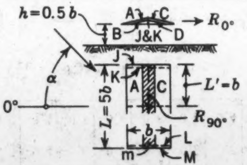	0°	-1.0	0.3	-0.5	0.2				
		45°	-0.3	0.1	-0.3	0.1				
		90°	-0.3	0	-0.3	0	0.8	-0.6	0.3	-0.4
		0°	For m, $C^*_{pe,top}$ = -1.0; $C^*_{pe,bottom}$ = 0.4							
		0° and 90°	Tangential acting friction, R = 0.1 q : L : b							
Effect of trains or stored material Roof +10° α=0°-45°-180°, A-D full length α=90°, A-D part length *L′*	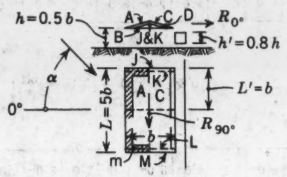	0°	-1.3	0.8	-0.6	0.7				
		45°	-0.5	0.4	-0.3	0.3				
		90°	-0.3	0	-0.3	0				
		180°	-0.4	-0.3	-0.6	-0.3				
		0°	For m, $C^*_{pe,top}$ = -1.6; $C^*_{pe,bottom}$ = 0.9							
		0° and 180°	End surface friction load, see above							
Roof −10° α=0°-45°, A-D full length α=90°, A-D part length *L′*	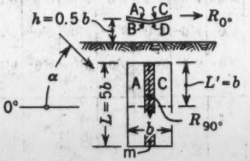	0°	0.3	-0.7	0.2	-0.9				
		45°	0	-0.2	0.1	-0.3				
		90°	-0.1	0.1	-0.1	0.1				
		0°	For m, $C^*_{pe,top}$ = 0.4; $C^*_{pe,bottom}$ = -1.5							
		0° and 90°	Tangential acting friction, R = 0.1 q : L : b							
Effect of trains or stored material Roof −10° α=0°-45°-180°, A-D full length α=90°, A-D part length *L′*	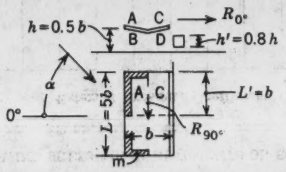	0°	-0.7	0.8	-0.6	0.6				
		45°	-0.4	0.3	-0.2	0.2				
		90°	-0.1	0.1	-0.1	0.1				
		180°	-0.4	-0.2	-0.6	-0.3				
		0°	For m, $C^*_{pe,top}$ = -1.1; $C^*_{pe,bottom}$ = 0.9							
		0° and 180°	Tangential acting friction, R = 0.1 q : L : b							

TABLE 4 (e).—WIND PRESSURE COEFFICIENTS ON ROOFS AND GRANDSTANDS

	α	External Pressure Coefficient, C_{pe}																Internal Pressure Coefficient, C_{pi}			
		A	B	C	D	E	F	G	H	J	K	L	M	N	O	P	Q	Openings uniformly distributed	Openings mainly in A	B	C
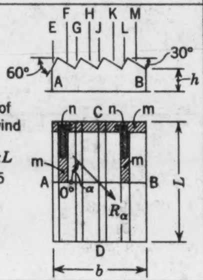 Sawtooth roof Friction in wind direction $R_\alpha = 0.1\, q{:}b{:}L$ $h{:}b{:}L = 1{:}4{:}5$	0°	0.9	-0.3	-0.4	-0.4	0.6	-0.6	-0.6	-0.5	-0.5	-0.4	-0.3	-0.3					±0.2	0.8	-0.2	-0.3
	45°	0.5	-0.4	0.5	-0.3	0.2	-0.8	-0.5	-0.4	-0.2	-0.4	-0.2	-0.5					±0.2	0.4	-0.3	0.4
	90°	-0.4	-0.4	0.9	-0.3	-0.3	-0.4	-0.4	-0.4	-0.4	-0.4	-0.4	-0.3					±0.2	-0.3	-0.3	0.8
	180°	-0.3	0.9	-0.3	-0.3	-0.2	-0.3	-0.3	-0.4	-0.4	-0.6	-0.6	-0.1					±0.2	-0.2	0.8	-0.2
	0° and 180°	For m, $C_{pe}^{*} = -1.3$; n, $C_{p3}^{*} = -2.0$																			
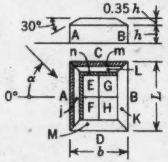 Flat roof $h{:}b{:}L = 1{:}3{:}4$	0°	0.9	-0.5	-0.6	-0.6	-0.8	-0.8	-0.4	-0.4	-1.0	-0.4	-0.5	-0.5					±0.2	0.8	-0.4	-0.5
	45°	0.5	-0.5	0.5	-0.4	-0.6	-0.5	-0.5	-0.5	-0.5	-0.5	-0.5	-0.5					±0.2	0.4	-0.4	0.4
	90°	-0.5	-0.5	0.9	-0.4	-0.8	-0.4	-0.8	-0.4	-0.4	-0.4	-1.0	-0.4					±0.2	-0.4	-0.4	0.8
	0° and 90°	For m, $C_{pe}^{*} = -1.1$; n, $C_{pe}^{*} = -1.5$																			

E
F
G
H
J
K
L
M
60°
30°
A
B
h
n
C
n
m
m
m
A
B
0°
α
R_α
L
D
b

0.35 h
30°
A
B
h
n
C
m
L
α
0°
A
E
G
F
H
B
j
K
M
D
b
L

																		Openings uniformly distributed with windows and doors closed	Openings mainly in		
																			A with window Y open	C with all gates open	C with only gate X open
Hanger arch roof Smooth surface $h:b:L = 1:12:12$ $r = 5/6b$ $Y = 0.1b$ $X = 0.1b$ 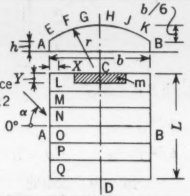 b/6 E F G H J K A B h r X C b Y L M N O P Q m α 0° A B L D	0°	0.7	-0.2	-0.3	-0.3	-0.1	-0.5	-0.8	-0.8	-0.4	-0.1							±0.2	0.4	-0.1	-1.5
	30°	0.6	-0.3	0.2	-0.4	-0.1	-0.4	-0.7	-0.9	-0.7	-0.4							±0.2	0.7	0.6	0.7
	90°	-0.3	-0.3	0.9	-0.3							-0.8	-0.7	-0.5	-0.3	-0.1	-0.1	±0.2	-1.0	0.8	0.4
	30°	For m, $C^*_{pe} = -1.8$ with $C^*_{pe,min} = -2.5$																			
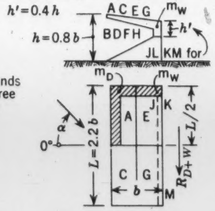 h′=0.4h h=0.8b ACEG BDFH m_w h′ JL KM for m_D m_w A E J K C G α 0° L=2.2b L/2 R_D+W b M Grandstands open three sides Roof 5°		C_{pe} at top and bottom of roof								C_{pe} at front and back of wall											
	0°	-1.0	0.9	-1.0	0.9	-0.7	0.9	-0.7	0.9	0.9	-0.5	0.9	-0.5								
	45°	-1.0	0.7	-0.7	0.4	-0.5	0.8	-0.5	0.3	0.8	-0.6	0.4	-0.4								
	135°	-0.4	-1.1	-0.7	-1.0	-0.9	-1.1	-0.9	-1.0	-1.1	0.6	-1.0	0.4								
	180°	-0.6	-0.3	-0.6	-0.3	-0.6	-0.3	-0.6	-0.3	-0.3	0.9	-0.3	0.9								
	45°	For m_D, $C^*_{pe,top} = -2.0$; $C^*_{pe,bottom} = 1.0$																			
	60°	For m_W, $C^*_{pe,k} = -1.0$; $C^*_{pe,j} = 1.0$																			
	90°	Tangential acting friction, $R_D = 0.1\ q:b:L$; $R_W = 0.1\ q:h:L$																			
Smooth closed reservoir 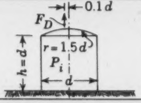 0.1d F_D r=1.5d P_i h=d d		$F_D = (P_i - P_a)\ A$ in which P_i = working pressure, $A = \frac{\pi}{4} d^2$, $P_a = C_{pe}\ q$, and $C_{pe} = -1.0$																			

TABLE 4 (f).—WIND PRESSURE COEFFICIENTS FOR RESERVOIRS, STACKS, MASTS, POLES, ROPES, AND WIRES

Structure	α	Sphere	Value of h/d		
			1	7	25
			Value of L/d		
			2	14	50
		Value of C_{pe}			
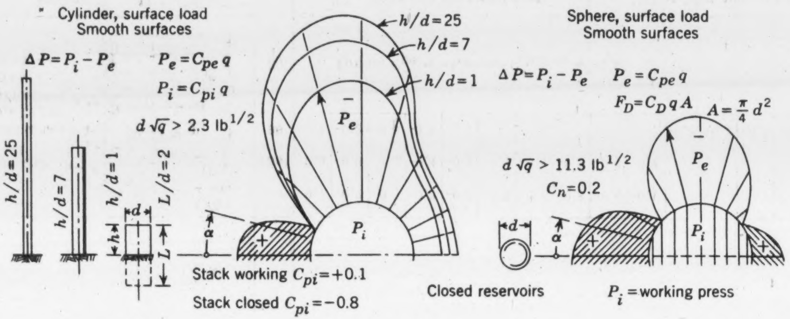 Cylinder, surface load Smooth surfaces $\Delta P = P_i - P_e$ $P_e = C_{pe}\,q$ $P_i = C_{pi}\,q$ $d\sqrt{q} > 2.3\ \mathrm{lb}^{1/2}$ h/d=25 h/d=7 h/d=1 L/d=2 d h L α P_e P_i + − Stack working $C_{pi} = +0.1$ Stack closed $C_{pi} = -0.8$ Sphere, surface load Smooth surfaces $\Delta P = P_i - P_e$ $P_e = C_{pe}\,q$ $F_D = C_D\,q\,A$ $A = \frac{\pi}{4}d^2$ $d\sqrt{q} > 11.3\ \mathrm{lb}^{1/2}$ $C_n = 0.2$ Closed reservoirs P_i = working press	0°	1.0	1.0	1.0	1.0
	15°	0.9	0.8	0.8	0.8
	30°	0.5	0.1	0.1	0.1
	45°	-0.1	-0.7	-0.8	-0.9
	60°	-0.7	-1.2	-1.7	-1.9
	75°	-1.1	-1.6	-2.2	-2.5
	90°	-1.2	-1.7	-2.2	-2.6
	105°	-1.0	-1.2	-1.7	-1.9
	120°	-0.6	-0.7	-0.8	-0.9
	135°	-0.2	-0.5	-0.6	-0.7
	150°	0.1	-0.4	-0.5	-0.6
	165°	0.3	-0.4	-0.5	-0.6
	180°	0.4	-0.4	-0.5	-0.6

Structure	Cross Section	Description	Value of C_D		
Upright cylinder $F_D = C_D q A$ $d\sqrt{q} > 2.3 \text{ lb}^{1/2}$ $A = dh$ 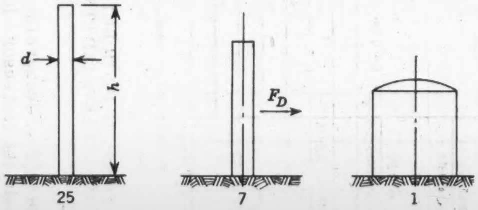 $h/d =$	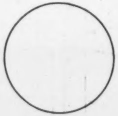	Smooth surface; metal, timber, concrete	0.45	0.5	0.55
	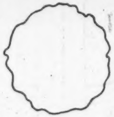	Rough surface; round ribs, h = 2% d	0.7	0.8	0.9
	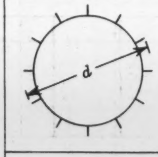	Very rough surface; sharp ribs, h = 8% d	0.8	1.0	1.2
	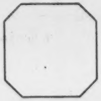	Smooth, rough surface; sharp edges	1.0	1.2	1.4

advisable for the engineer to take advantage of the many test results available. Perhaps the earliest tests on building forms were those by Irminger and Nøkkentved (405). The most extensive tests conducted in the United States are probably those conducted at the Iowa Institute of Hydraulic Research (434). These are very useful in that they not only consider a variety of building shapes but also give contours of pressure for the external surfaces.

The most extensive series of tests conducted to date (as of 1961) and the most useful from the engineer's viewpoint are those conducted by J. Ackeret of the Institute for Aerodynamics of Zurich. These have since been included in the Swiss Building Code (438). Because the Committee believes this to be the best information available, the test results for building forms are reproduced, through the courtesy of Ackeret, in Table 4. Each set of data is for a particular building model. The values given are local pressure coefficients for various parts of the building surface and for various wind directions. Also given are coefficients for internal pressure depending on the location of openings. The total force in any direction can, of course, be obtained by summing the pressures on the appropriate surfaces. The pressure coefficients given for m and n take into account the large local pressures that occur near roof edges.

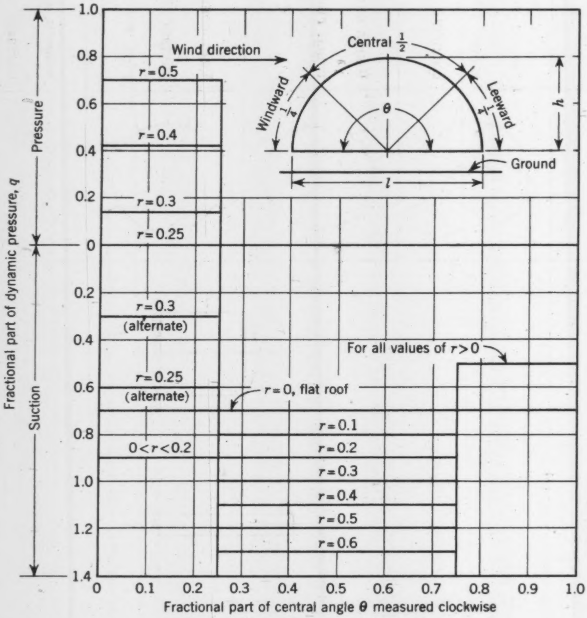

FIG. 9.—WIND PRESSURE DISTRIBUTION ON ROUNDED ROOFS RESTING ON ELEVATED STRUCTURES

They should be used in the design of local elements but not for over-all roof loading.

SUMMARY

With the test data available (including both that reproduced here and that given in the references) and the information on wind velocities given in Section II the engineer should be able to make reasonable predictions of wind forces on most building forms. It is not necessary, therefore, to rely on the rather crude approximations contained in many building codes.

V. PLATE GIRDERS AND TRUSSES

INTRODUCTION

In contrast to the preceding section (Section IV) on enclosed structures (primarily buildings), this section deals with open structures such as bridges, towers, or other exposed frameworks. For purposes of discussion open structures may be divided into two classes: (a) Large sheet areas such as plate girders or sign boards that have a large surface exposed to the wind but small depth, and (b) trusses such as those in bridges and towers. When placed in pairs and combined with a road deck classes (a) and (b) may be considered to include plate girder and truss bridges.

Of general interest in the consideration of such structures are the effects of aspect ratio, Reynolds number, solidity ratio, and shielding. Aspect ratio, or ratio of length to width, is of particular importance in connection with class (a). As discussed in Section III and shown in Table 2(a), the drag coefficient varies from 1.12 for a square plate to 1.98 for an infinitely long plate; the same is true for a plate girder with flanges. It should be noted that a plate may, in effect, be considered infinitely long if flow is prevented around the ends. For example, the plate girders of a deck bridge should normally be considered infinite in length because flow around the ends is prevented by the abutments. The aspect ratio of a truss is generally less important. This is true because there is some flow through the structure and the flow pattern around the edges of the total enclosed area is of less importance. In this case the aspect ratio of the individual truss members is a more significant parameter.

In general, the effect of the Reynolds number may be ignored with regard to the open-type structures considered in this section, that is, the drag coefficient may be assumed constant and independent of wind velocity. This is true because such structures are generally comprised of members having sharp edges (see Section III). A possible exception would be a truss made up of pipe or solid round members.

The solidity ratio, ϕ, defined as the solid elevation area divided by the total enclosed elevation area, is obviously a parameter of importance. A truss with $\phi = 1$ becomes a plate girder and the drag coefficients for the two elements are identical. On the other hand, the drag on a truss with very small solidity ratio is merely the sum of the drags on the individual members, that are essentially independent of each other. Between these extremes the flow through the openings in the element is accelerated and contracted into "jets." This obviously affects the drag on the total element and also that on other elements downstream.

For a structure consisting of a combination of trusses and plates, or both, the effect of the shielding of one member by another is appreciable. For example, the drag on the leeward truss of a bridge must be less than that on the windward truss to a degree that depends on the spacing. Each upwind member causes a "shadow" or widening wake with lessened velocity and a member lying within this wake would have reduced drag. In this connection the wind direction is obviously important. With zero angles of attack and yaw each upwind member shields its downwind counterpart but with small values of these angles the downwind members are more exposed. The amount of shielding also depends on the solidity ratio (511).

SINGLE GIRDERS AND TRUSSES

As noted previously a plate girder with flanges may be considered to be a flat plate. Therefore the drag coefficient depends only on the aspect ratio as modified by the presence of abutments or other obstructions at the boundaries.

The drag on a single truss depends on the aspect ratio of the individual members. For small solidity ratios (less than 0.15) the coefficient (based on the solid area) approaches 2.0 because, in this case, the truss members must be long and narrow with flow prevented around the ends—that implies an infinite aspect ratio. In this connection it should be noted that truss members for which the depth and width are normally of the same order have essentially the same drag coefficient as flat plates. For large solidity ratios (greater than 0.9) the coefficient approaches that for a solid plate having the same over-all aspect ratio. Between these two extremes the coefficient is less easily determined because the effective aspect ratio of the members is uncertain and the drag on the gusset plates is significant. Most tests (111) (507) (506) (512) for common truss solidity ratios indicate coefficients between 1.6 and 1.7. The actual arrangement of members does not appear significant.

Pagon suggests, (511) as a conservative approximation, that the drag coefficient based on the total enclosed area be taken as $1.8\,\phi$ up to $\phi = 0.6$ and thereafter a linear interpolation to the value at $\phi = 1.0$ corresponding to the aspect ratio for the entire enclosed area. Pagon also suggests (511) a more refined procedure based on an effective solidity that is greater than the true solidity due to the contraction of flow through the openings.

The foregoing applies to a wind direction perpendicular to the plate or truss. As the direction departs from the normal, the drag in that direction decreases although the difference is not important for small angles. For design purposes one would normally be concerned with a wind acting perpendicular to an area.

PAIRS OF GIRDERS OR TRUSSES

When two elements are placed in line with the wind the total drag depends on the spacing of the elements. If the spacing is zero or very small the drag is the same as on a single element, whereas if the spacing were infinite the total force would be twice as much as on a single member.

Fig. 10 contains some experimental results relating the total drag coefficient to the spacing of elements. Curves A, B, and C are for solid plates, the first being for circular disks and the latter two for rectangular plates. At zero spacing the coefficient plotted is that for a single plate of the same shape. At small

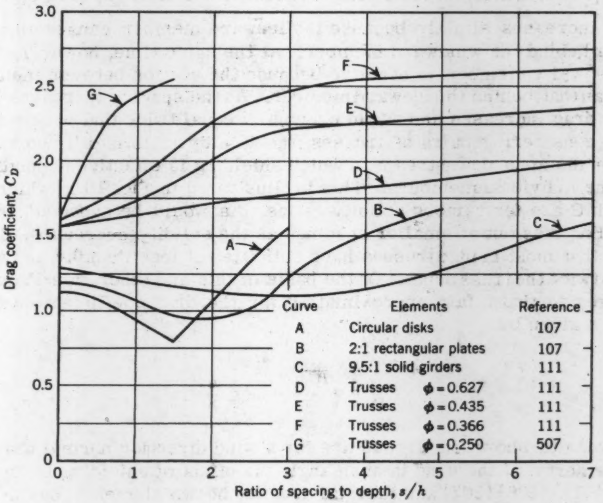

FIG. 10.—EFFECT OF SPACING ON THE DRAG OF PAIRS OF ELEMENTS

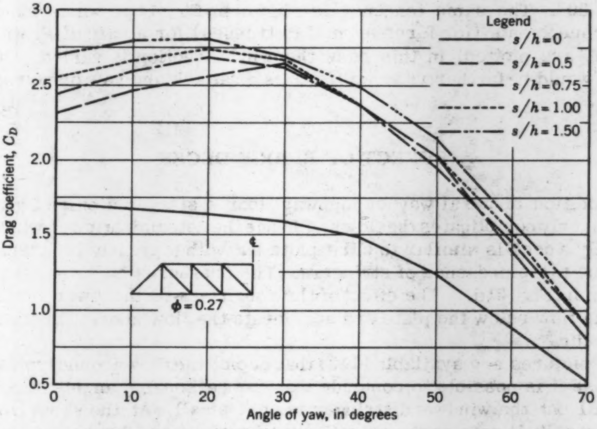

FIG. 11.—EFFECT OF YAW ON PAIRS OF TRUSSES (512)

spacing $\left(\frac{s}{h}\text{ less than } 2\right)$ the total drag decreases. Actually the drag on the front member increases slightly because the leeward member causes an increase in suction behind the windward member. At the same time, however, the drag on the leeward member is negative because the suction between members is larger than that behind the leeward member. As the spacing increases further, the total drag increases and would eventually equal twice that at zero spacing.

When considering pairs of trusses, the solidity ratio is of importance because the distance downstream in which shielding is effective depends on the size of the individual members. This is illustrated in Fig. 10 in which curves D through G are for various solidity ratios. As would be expected, the effect of shielding dies out at smaller spacings as the solidity decreases. It should be noted that most bridge trusses have solidities of less than 0.4 and spacings less than twice the truss depth. On the basis of this and other data Pagon (513) has suggested that a fair approximation for the drag coefficient on a pair of trusses is given by

$$C_D = \sqrt{\frac{1.7}{\phi}} + \log \frac{s}{h} \quad \ldots\ldots\ldots\ldots\ldots\ldots (8)$$

The results shown in Fig. 10 are for a wind direction normal to the plane of the elements. If the wind is at an angle the effect of shielding is, of course, reduced (111) (506) (507) and the total drag on the two elements may be greatly increased. The general effect is thus to reduce the importance of spacing above a certain critical minimum. It has been shown (507) that for a particular Warren truss ($\phi = 0.25$) the difference in total drag coefficient between $s/h = 0.27$ and $s/h = 1.22$ is 40% for a normal wind but only 15% for an angle of attack of 20°. The same tendency is shown in Fig. 11 in which experimental drag coefficients (for force normal to trusses) for a pair of Pratt trusses ($\phi = 0.27$) are plotted; in this case the wind direction is varied. Of course shielding would be further reduced if angles of attack and yaw occurred simultaneously.

EFFECT OF BRIDGE DECKS

The addition of a railway or highway floor system to a pair of girders or trusses clearly complicates the flow and hence the determination of wind forces. Essentially a deck is similar to a flat plate but with a greatly roughened lower surface due to the presence of stringers. The pressures on a smooth flat plate are shown in Fig. 5(d). The effect of the roughness on the lower surface is to retard the flow below the plate and accelerate the flow above. In general this produces lift.

Smoke pictures are available (113) that depict the flow around typical decks. From these it is possible to conclude that for reasonable angles of attack the drag on all but the windward stringer is very small. At the same time there is, of course, little drag on the smooth upper surface and, hence, the total horizontal force is almost entirely a function of the frontal elevation area. These conclusions must be modified if there are openings in the deck between stringers. Each opening becomes an "escape vent" that tends to deflect the horizontal wind velocity, thus producing additional drag.

The most important effect of the bridge deck is the modification of the flow pattern around the main trusses or girders. The drag on the leeward element is obviously affected but, in addition, the pressures behind the front element, and hence the drag on that element, are also modified. Because of the obvious uncertainties it is difficult to predict the wind forces on a given bridge section. Wind-tunnel test data are available for a variety of bridge sections. However, these indicate that the drag coefficient is very sensitive to the spatial arrangement of roadway deck, sidewalks, railways, and so forth, and where wind forces are important, special wind-tunnel tests are advisable.

PLATE GIRDER BRIDGES

Reports have been made (509)(610)(506)(113) of wind-tunnel tests on deck and through bridge sections consisting of girders in various numbers together with both open and closed decks. Typical of these results are those plotted in Fig. 12 (509). Two bridge types are shown: A two-girder through railway bridge with open floor, and a two-girder deck highway bridge with solid floor. The highway bridge also has a sidewalk projection with railing outside the girders. The results are plotted as horizontal drag coefficient (based on frontal area) versus s/h. The angle of attack, α, is positive when the wind has an upward component.

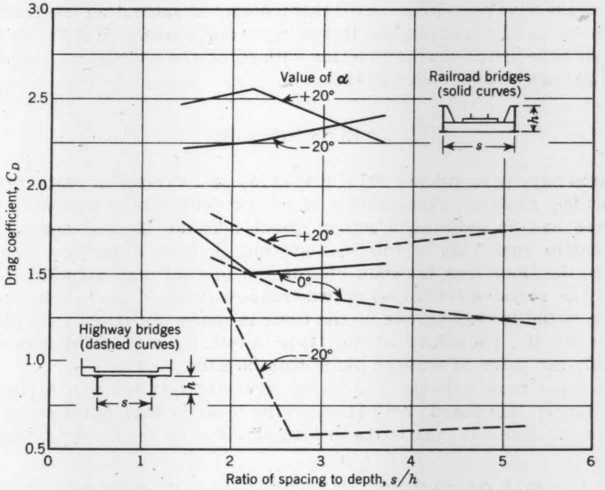

FIG. 12.—DRAG COEFFICIENTS FOR PLATE GIRDER BRIDGES (509)

It may be observed in Fig. 12 that there is no systematic variation in drag with the s/h ratio. The presence of the floor system disrupts the orderly increase with s/h that occurs with pairs of girders alone.

The difference in drag between the two types of bridges shown in Fig. 12 is not great for zero angle of attack (horizontal wind). As expected, the open-floor railway bridge has slightly greater drag because the leeward girder is more exposed. However, for angles of attack other than zero the difference is more pronounced. The railway bridge shows a considerable increase in drag with angle of attack and it makes little difference whether the angle is plus or minus. On the other hand, the drag on the highway bridge increases only slightly for positive angle of attack and actually decreases for a negative angle. This occurs because the deck shields the girders when the wind has a downward component and in no case is flow permitted between girders. This result is, of course, affected by the sidewalk projection on these models.

Results for three-girder and four-girder bridges are also available (509). These indicate that there is no appreciable increase in drag as the number of girders is increased. Results are also given for deck railway and through highway bridges. Comparisons with current design specifications indicate that these are probably conservative.

Tests have also been made (610) that indicate greater drag on girder bridges with open or partly open decks. However, as discussed in Section VI, the open-deck spans have better characteristics with regard to oscillation, that is important in the case of suspended spans.

TRUSS BRIDGES

Reports have been made (507)(506)(113) of a variety of tests on complete truss bridge models. The addition of a floor deck (open or closed) to a pair of trusses has, in general, a minor effect because the trusses have a depth much greater than that of the floor system; in fact, it has been shown (507) that when the floor lies between chords (as in a through structure) the total drag may be reduced from that of two trusses alone. This is true because the shielding of the leeward truss by the floor is more important than the drag on the floor itself. Therefore, if the floor is thus positioned the data discussed previously for pairs of trusses alone may be used.

If for some reason the floor is displaced vertically from the chords, the drag is, of course, increased, both because the floor is less shielded by the front truss and because the rear truss is less shielded by the floor (507).

EFFECT OF ANGLES OF ATTACK AND YAW ON BRIDGES

The effect of angle of attack (vertical angle) on the horizontal drag for girder bridges is appreciable, as shown in Fig. 12 and as discussed previously. The effect on truss bridges is due to a reduced shielding of the leeward truss that is only slightly affected by the floor system. Therefore, the foregoing discussion for pairs of trusses would apply. Perhaps the most difficult problem is the selection of a proper design value for the angle of attack. This is very uncertain because it depends, to a large extent, on local topography, although certain types of storms produce vertical wind components. It is probable that values in excess of ±15° should not be considered for design.

The effect of angle of yaw (horizontal angle) is not appreciable on girder bridges but is on truss bridges, again because of reduced shielding of the leeward truss. In the latter case yaw is not as important as angle of attack because yaw does not reduce shielding on the horizontal chords. Results are available (506) for angles of attack and yaw in combination that, intuitively, is the situation producing maximum drag.

LIFT AND OVERTURNING MOMENT ON BRIDGES

Data have been obtained (506) (507) on lift forces and moments for both girder and truss spans. The two effects should be considered together since lift, although seldom of importance by itself, is of primary importance with regard to overturning. For railway or other open-deck bridges, lift forces are small (even with angle of attack) and the overturning moment may be computed simply as the effect of the horizontal force acting at the centroid of the elevation area. For solid-deck bridges, however, the lift is appreciable, increasing with width of deck. With upward angle of attack the effect on the overturning moment becomes significant.

TRUSSED TOWERS

Perhaps the most complete discussion of wind forces on towers was presented by E. Cohen, F. ASCE, and H. Perrin, M. ASCE (510). After a study of available test data it was suggested that the following expressions for drag coefficient be used: for square towers,

$$C_D = 4 - 5\,\phi \ldots\ldots\ldots\ldots\ldots\ldots \text{(9a)}$$

and for triangular towers,

$$C_D = 3.65 - 4.65\,\phi \ldots\ldots\ldots\ldots\ldots \text{(9b)}$$

Pagon (511) has suggested the formula

$$C_D = \sqrt{\frac{3}{2\,\phi}} \ldots\ldots\ldots\ldots\ldots\ldots \text{(10)}$$

for square towers which does not differ greatly from the Cohen-Perrin value in the significant range of ϕ. All of these expressions are for a wind normal to one face. For square towers it has been suggested that C_D be multiplied by $(1.1 + 0.4\,\phi)$ to allow for yaw (510).

For towers made up of round members there are little data available but the opinion is generally held that the drag coefficients for such structures may be taken as two-thirds that for structures having angular members.

SUMMARY

Drag coefficients for open structures consisting of combinations of structural elements in various spatial configurations can reliably be determined only by wind-tunnel tests. However, considerable data are available and a designer is often able to find test results for a structure sufficiently similar to the one under consideration. It should be noted, however, that apparently minor variations in configuration may have major effects on the wind forces. Therefore, in cases in which wind loads are of primary importance, wind-tunnel tests are advisable.

VI. STRUCTURES SUBJECT TO OSCILLATION IN WIND

INTRODUCTION

The dynamic effect of wind on modern structures has received ever-increasing attention since the dramatic collapse of the Tacoma Narrows Bridge in 1940. Prior to this period the prevailing design practice depended wholly on static wind loads based on an arbitrary force constant, that generally ignored the shape of the structure and the actual value of the wind velocity and direction at the site.

Increasingly, the civil engineering profession has been forced to consider the possibility of wind-induced dynamic response on certain types of flexible structures that had formerly been designed solely on the basis of static considerations.

The notable contribution (112) of Pagon, provided a firm basis for the solution of the problem of wind effects on structures, but did not receive the attention it deserved.

The problem of the dynamic effect of wind on modern structures may be divided into four principal categories, depending on the shape and flexibility of the structure. All of these categories fall under the general classification of self-excited oscillations:

1. High-frequency oscillations may be excited on slender structures such as transmission and telephone lines, tower guys, and some types of girder-stiffened suspension bridges as a result of resonance (generally subharmonic) between the rate of vortex shedding and some natural frequency of the structure.
2. Cylindrical bodies (The term "cylinder" is used throughout to denote a body whose cross-sectional shape is the same at every section along the span) showing a negative slope over certain portions of the curve of the lift force plotted against angle of attack of the wind may oscillate in a bending mode (Fig. 13(a)). Sleet-coated transmission lines and some types of girder-stiffened suspension bridges fall in this classification. If the structure is free to oscillate in torsion, a negative slope, when moments are plotted against angle of attack, will indicate the possibility of torsional instability (Fig. 13(b)).
3. Thin flat plates placed horizontally in a horizontal wind, or the deck of a girder-stiffened suspension bridge, may be subject to flutter if the natural frequencies in bending and torsion are not too dissimilar. The wind force causes a lift that acts eccentrically, thus inducing a twisting moment. The coupling of these two modes may result in a motion that is catastrophic.
4. There have been some occasions in which a buffeting action has developed on a structure due to the effect of some other structure relatively close upwind. Such a condition has been reported on multiple tall stacks in line.

SELF-EXCITED OSCILLATIONS

Experience has indicated that the most significant manifestations of wind-induced oscillation fall in the classification of "self-excited" motion that may

be described by the following statement (609):

> **In a self-excited oscillation the alternating force that sustains the motion is created or controlled by the motion itself; if the motion stops, the alternating force disappears (609).**

In the case of vortex excitation of structures or structural components that are free to oscillate in one or more bending or torsional modes, the following criteria may be stated (614).

a. While the structure is at rest the vortex frequency is controlled by the wind.

b. At certain discrete wind velocities, designated as "critical velocities," the vortex frequency will either coincide with, or be a multiple of one of the frequencies of motion of the structure; such a coincidence results in self-excited oscillation.

c. Beyond the critical wind velocities the oscillating structure and not the wind velocity controls the vortex frequency. In such cases the range of oscillation extends over certain finite ranges of wind velocity. The lower limit of each range is a critical velocity. The upper limit is not as well defined as the critical velocity. However, between the upper limit and the next critical velocity the structure is practically at rest.

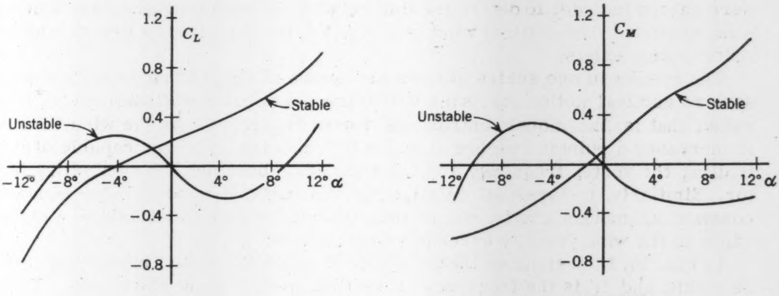

(*a*) LIFT (*b*) MOMENT

FIG. 13.—STATIC LIFT AND MOMENT GRAPHS

When the vortex frequency coincides with a natural frequency of the structure, harmonic excitation results. If the vortex frequency is some multiple of a natural frequency of the structure, the resulting excitation is subharmonic.

In very flexible structures, such as girder-stiffened suspension bridges, some of the lower bending modes may develop twice, but at the same frequency. The first appearance will be harmonically excited, whereas the second appearance will be of subharmonic origin. The torsional mode also shows two appearances at the same frequency. The first is harmonic and the second is subharmonic. However, the second appearance may be catastrophic and suppresses the development of any but the lower two or three bending modes.

Under conditions of very low damping, which can only be obtained in the laboratory, more than two appearances of a torsional mode may develop for certain cross-sectional shapes (614).

EXPERIMENTAL VERIFICATION OF VORTEX EXCITATION

The pioneering investigation of the aerodynamic stability of a suspension bridge was made by Theodore von Kármán, Hon. M. ASCE, and Louis Dunn at the California Institute of Technology, Pasadena, Calif., in 1942 (614). The rigid, spring-supported model used in these tests was a highly idealized H. section (Fig. 14) similar to the suspended structure of the original Tacoma Narrows Bridge.

Vortex frequencies at the windward girder were measured by means of a hot-wire anemometer with the model held stationary in the wind, and also when the model was allowed to oscillate.

If the oscillations are a result of vortex shedding, it also follows that a linear relationship will exist between the frequencies and the velocities at which motion starts. A number of tests were conducted in which the spring constants were varied in order to determine this relation between frequency and critical wind velocity. The critical wind velocity, V_c, is that velocity beyond which a finite motion exists.

The results of one series of tests are shown in Fig. 15 that indicate that as soon as vertical motion starts the vortex frequency has a well-defined constant value; that is, the model controls the vortex frequency. As the wind velocity is increased a point is reached at which the model is no longer capable of controlling the vortex frequency and the wind again becomes the controlling factor. Similarly, in torsional oscillations the vortex frequency also becomes constant as motion starts, but in this instance it shifts suddenly to a higher value as the wind velocity exceeds certain limits.

In Fig. 16, f_0 designates the frequency at which the model moves vertically as a unit, and f_1 is the frequency of vertical motion about the z-axis. These two motions are known as the "fundamental" mode and the "single-noded" mode, respectively.

The first appearance of the three modes was relatively weak. At higher wind velocities the cycle of mode development was repeated with a greatly increased amplitude in the vertical mode and a catastrophic second appearance of the torsional mode.

The critical wind velocity as a function of frequency is shown in Fig. 17. It is seen that a linear relationship exists for each of the two values of critical wind velocity. Also, the test points indicate that the first critical velocity is just half of the second.

Later investigations at the University of Washington, involving a 50-scale flexible model of the original Tacoma Narrows Bridge, confirmed the relationships discussed herewith. These tests also duplicated faithfully all of the modes of motion observed on the original bridge, including the final catastrophic motion that destroyed this structure on November 7, 1940 (614).

MECHANISM OF VORTEX SHEDDING

Circular Cylinders.—Cylinders of circular cross section are of special interest and have been the subject of considerable attention in recent years. Above

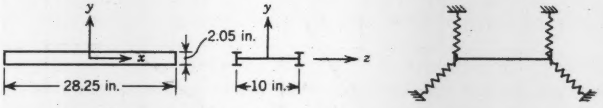
y
x
2.05 in.
28.25 in.
y
z
10 in.

FIG. 14.—IDEALIZED SUSPENDED STRUCTURE

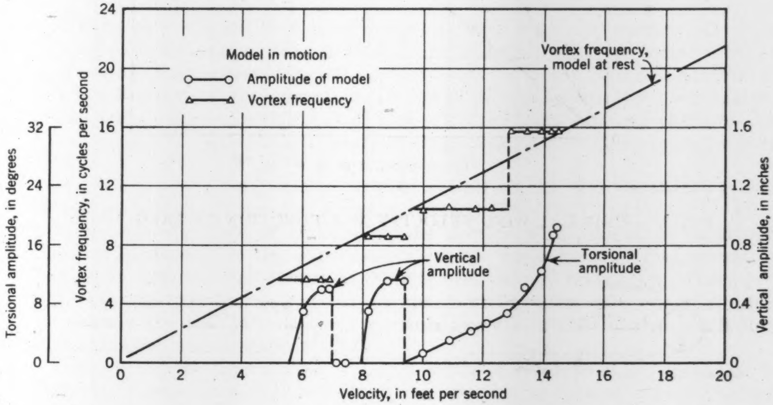

FIG. 15.—TEST RESULTS

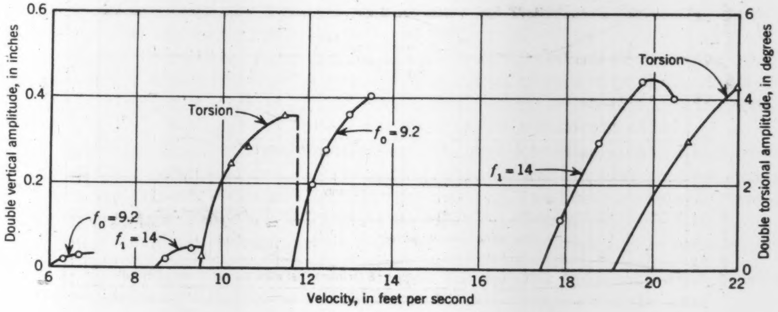

FIG. 16.—THREE MODES OF AMPLITUDE RESPONSE

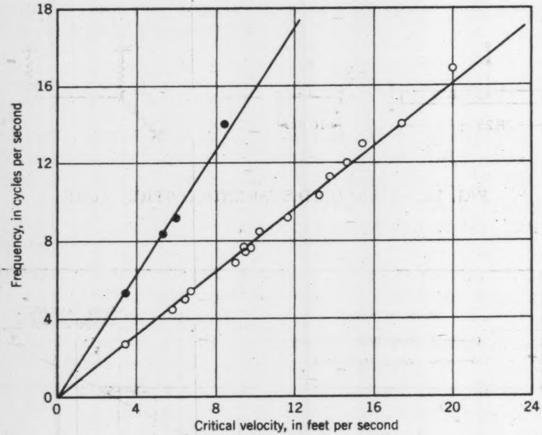

FIG. 17.—CRITICAL WIND VELOCITY AS A FUNCTION OF FREQUENCY

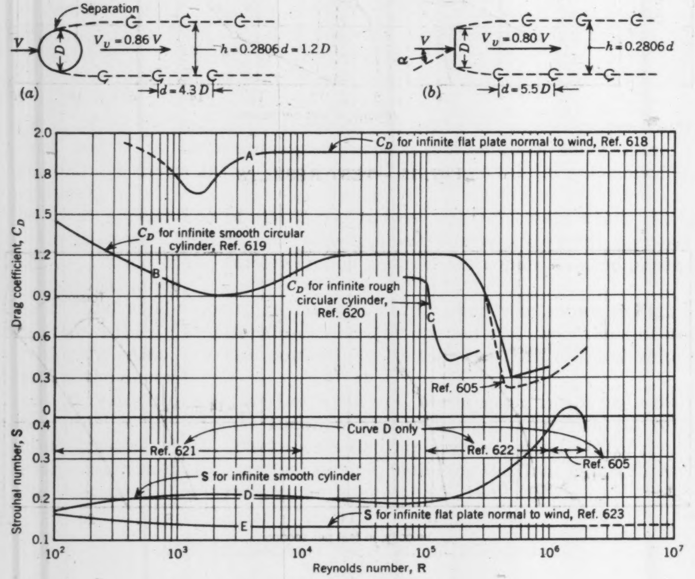

FIG. 18.—REYNOLDS NUMBER VERSUS DRAG COEFFICIENT AND STROUHAL NUMBER

$R \approx 25{,}000$ the wake becomes turbulent at the point of separation. In this range the vortex shedding is periodic but the velocities fluctuate in an irregular manner due to trubulence in the flow. As a result the magnitudes of the oscillating lift forces are somewhat random, and become more so with increasing Reynolds numbers (633).

The idealized vortex street in Fig. 18(a) is that theorized by von Kármán and may be considered as reasonably accurate for six or seven diameters downstream (618). The data in Fig. 18(a) and curve B are applicable up to $R \approx 3 \times 10^5$ where the flow changes from laminar to turbulent and the separation points move downwind on the cylinder. At this critical point there is a sharp drop in the drag coefficient, an abrupt rise in the Strouhal number S (curve D), and the wake narrows with regular vortex formation no longer visible.

The value $R \approx 3 \times 10^5$ is known as the critical Reynolds number (curve B) and values below this number are called subcritical, whereas higher numbers are termed supercritical. In the supercritical range the Strouhal number increases sharply, but the phenomenon is aperiodic and its efficiency is impaired. The Strouhal number, which is $\overline{0}.20$ at $R \approx 2 \times 10^5$, has climbed (615) to 0.43 at $R \approx 1.5 \times 10^6$. The effect of surface roughness on a circular cylinder (635) is shown in curve C, Fig. 18.

In recent years a significant number of tall stacks have oscillated in wind and some have suffered catastrophic damage (605)(624)(625)(626). All of these structures were of circular cross section with diameters up to 18 ft. They all oscillated in the supercritical range but generally in an erratic or spasmodic manner, and always at their lowest natural frequency. Their performance indicates that in spite of the aperiodic shedding of vortices at values of $R \approx 11 \times 10^6$ the "processes in the wake are essentially unchanged at Reynolds numbers above critical" (619).

Cylinders with Sharp Edges.—When a cylinder involves sharp edges that fix the point of detachment of the vortex, the regular process of vortex shedding is independent of Reynolds number above $R \approx 10^3$, as shown in Fig. 18, curve E, for a flat plate normal to the wind. The Strouhal number for a variety of shapes of structural interest is shown in Table 5.

The effect of wind impinging on a flat plate at an angle (Fig. 18(b)) was investigated by A. Fage and F. C. Johansen (603). It was found that $d/\bar{D} \sin \alpha$ remained substantially constant with an average value of 5.32, as the angle of incidence α was varied between 30° and 90°.

Effect of Rounding Sharp Edges.—In general the effect of rounding sharp edges on a cylinder tends to promote a subcritical region of R, but until the ratio of corner radius to transverse measurement between edges exceeds a value of 0.20, the effect of corner rounding is not significant (615).

Modifying Wind-Excited Oscillation.—Many of the situations in which wind-induced oscillations are of a serious character involve circular cross sections. It will be instructive to examine three devices that have been developed, two of which have been found to be effective on existing structures.

Prior to these developments only two effective devices have been known:

1. Alteration of the design to increase the natural frequency thus raising the critical wind velocity to a level beyond that anticipated at the site.
2. Increasing the effective damping through the installation of mechanical damping devices that act to reduce the amplitude.

TABLE 5.—STROUHAL NUMBER FOR A VARIETY OF SHAPES

Wind	Profile dimensions, in mm	Value of S	Wind	Profile dimensions, in mm	Value of S
→	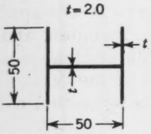	0.120	↓	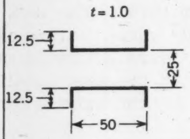 t = 1.0 12.5 25 12.5 50	0.147
↓		0.137			
→	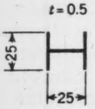	0.120	↓	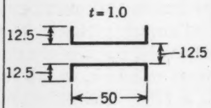 t = 1.0 12.5 12.5 12.5 50	0.150
↓	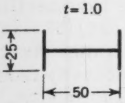	0.144	←	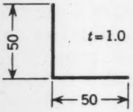	0.145
			↑		0.142
			↙		0.147
↓	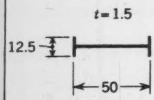	0.145	←	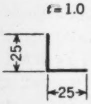	0.131
			↑		0.134
			↙		0.137
↓	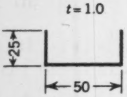	0.140	→	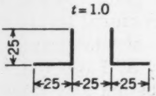 t = 1.0 25 25 25 25	0.121
↑		0.153	↓		0.143
↓	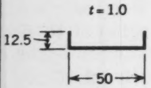	0.145	→	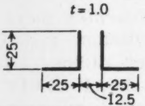 t = 1.0 25 25 25 12.5	0.135
↑		0.168			
→	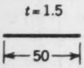	0.156	→	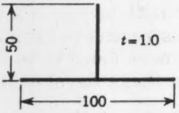	0.160
↓		0.145			
Cylinder 11800 < R < 19100	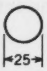	0.200	→	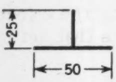	0.114
			↑		0.145

In practice both of these methods are generally unsatisfactory because gains are likely to be quite limited. This is especially true where an increase in damping is involved, because significant gains may only be achieved through elaborate auxiliary systems that are practical only on free-standing structures such as tall stacks.

In 1956, P. Price revealed the results of an extensive investigation at Stanford University, Stanford, Calif., using a perforated circular shroud that surrounded a circular cylindrical member (629). Wind-tunnel tests proved the shroud to be an effective vibration supressor at subcritical and transitional values of Reynolds number (up to **R** = 4 x 10^5).

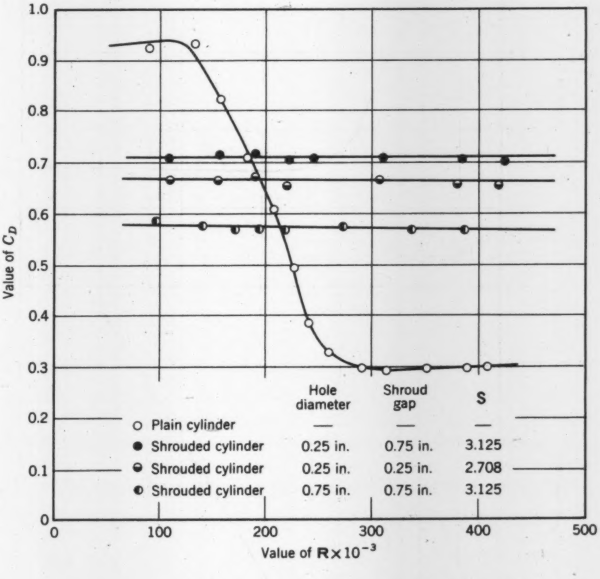

FIG. 19.—CYLINDER DRAG COEFFICIENT VERSUS REYNOLDS NUMBER WITH DIAMETER OF 6 IN.

Fig. 19 shows the marked effect of three shroud designs applied to a 6-in. circular cylinder, with various combinations of shroud gap and perforation hole diameter. A striking feature regarding the effect of the shroud lies in the fact that the drag was drastically reduced in the transitional range of Reynolds number and that for each of the three shrouds mentioned the drag coefficient remained constant into the supercritical range up to the limit of the wind velocity available.

Fig. 20 shows a plot of double amplitude y_2 versus dynamic pressure q for the plain cylinder. At q = 4 a double amplitude of about 0.039 in. was observed.

This amplitude fell off to 0.017 in. at q = 8 and thereafter increased at a uniform rate to a double amplitude of 0.069 in. at q = 20.

Either of the three shrouds mentioned in Fig. 19 proved to be effective in suppressing vortex excitation at subcritical, transitional, and supercritical Reynolds numbers. The shroud virtually eliminated periodic oscillation of a stiff model at transitional and supercritical Reynolds numbers.

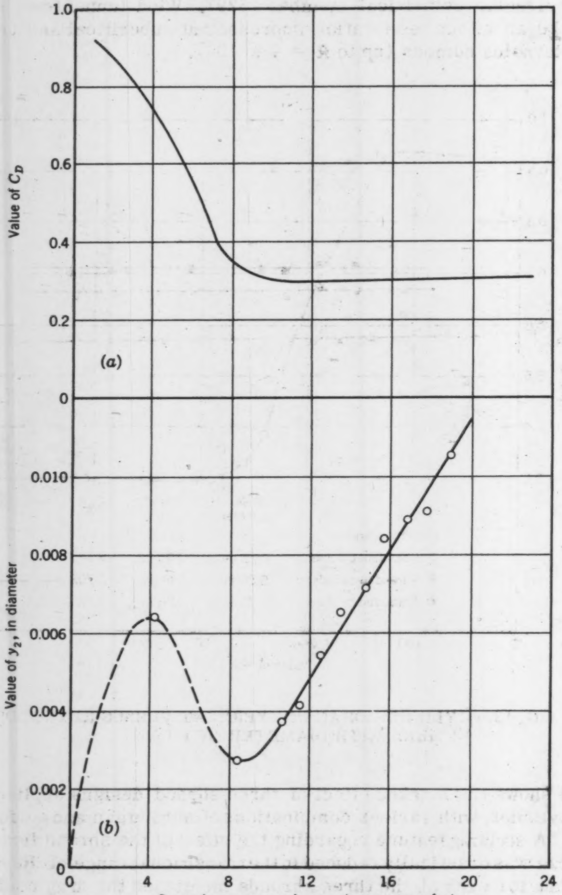

FIG. 20.—DRAG COEFFICIENT AND TIP DOUBLE AMPLITUDE VERSUS DYNAMIC PRESSURE

In 1957, C. Scruton and D. E. J. Walshe published (631) the results of an experimental investigation at the National Physical Laboratory, (Teddington, England), that accomplished the same result as that achieved by Price, but in a manner that promises to be more universally acceptable on all sizes and lengths of members of circular cross section, and is applicable to tapered members.

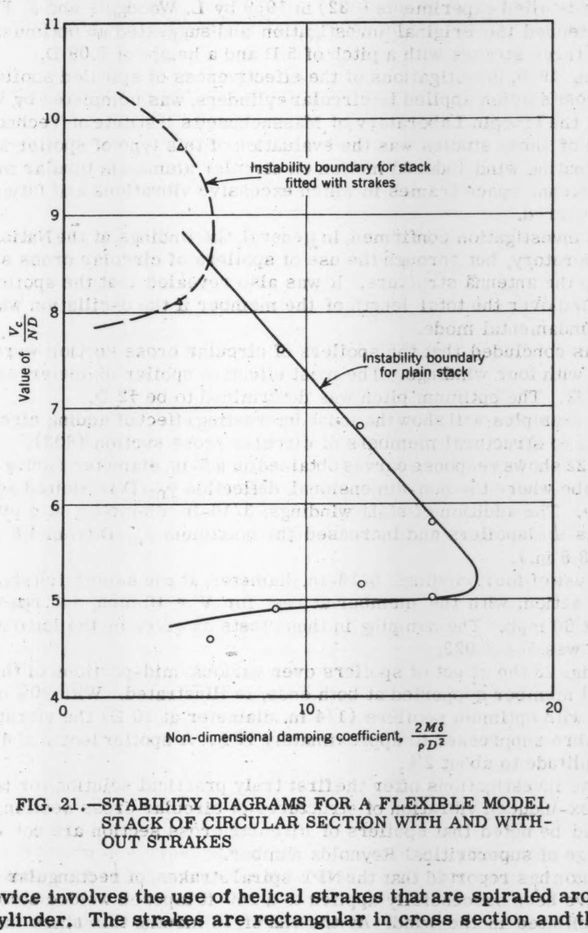

FIG. 21.—STABILITY DIAGRAMS FOR A FLEXIBLE MODEL STACK OF CIRCULAR SECTION WITH AND WITHOUT STRAKES

This device involves the use of helical strakes that are spiraled around the circular cylinder. The strakes are rectangular in cross section and their efficiency is dependent on their number, height, and pitch.

A $4\frac{1}{4}$-in. diameter aluminum tube, 61 in. long, was spring-mounted horizontally in a wind tunnel with freedom to oscillate in a vertical direction only.

The strakes were made of $\frac{1}{4}$-in. wide rubber of various heights. With three equally spaced spiraled strakes of pitch 15 D and height 0.12 D the oscillations under wind were only barely discernible. The maximum amplitude found with the plain stack was 0.75 D; with the stack fitted with strakes it was only 0.05 D. Fig. 21 shows the boundary of instability for a bare tube as compared with a tube fitted with strakes. In Fig. 21, M represents mass per unit length.

More detailed experiments (632) in 1959 by L. Woodgate and J. F. M. Maybrey extended the original investigation and suggested an optimum arrangement of three strakes with a pitch of 5 D and a height of 0.09 D.

During 1959, investigations of the effectiveness of spiraled spoilers of circular cross section applied to circular cylinders, was completed by W. Weaver (633) at the Lincoln Laboratory of Massachusetts Institute of Technology. The purpose of these studies was the evaluation of this type of spoiler as a means of eliminating wind-induced motion on circular aluminum tubular members of radar antenna space frames in which excessive vibrations and fatigue failures have occurred.

This investigation confirmed, in general, the findings at the National Physical Laboratory, but through the use of spoilers of circular cross section that make up the antenna structure. It was also revealed that the spoiler need not be applied over the total length of the member if the oscillation was confined to the fundamental mode.

It was concluded that the spoilers of circular cross section were most effective with four windings. The most effective spoiler diameter was found to be 3 D/32. The optimum pitch was determined to be 12 D.

Two examples will show the most interesting effect of adding circular spiral windings to structural members of circular cross section (633).

Fig. 22 shows response curves obtained on a 5-in. diameter spring-supported rigid tube where the non-dimensional deflection y_m/D is plotted against wind velocity. The addition of eight windings, 3/16-in. diameter, at a pitch of 12 D acted as antispoilers and increased the maximum y_m/D from 4.6 to 5.76 (23 in. to 28.8 in.).

The use of four windings, 5/16-in. diameter, at the same pitch showed strong spoiler action, with the member at rest for V = 10 mph, and reaching $y_m/D = 0.3$ at 60 mph. The damping in these tests as given by the logarithmic decrement was $\delta = 0.022$.

In Fig. 23 the effect of spoilers over various mid-portions of the span of a flexural member supported at both ends, is illustrated. With 20% of the length served with optimum spoilers (1/4 in. diameter at 10 D) the vibration amplitudes were suppressed to approximately 10%. A spoiler length of 40% reduced the amplitude to about 2%.

These investigations offer the first truly practical solution for the problem of vortex-induced vibration of structures of circular cross section. However, it should be noted that spoilers of circular cross section are not effective in the range of supercritical Reynolds number.

Scruton has reported that the NPL spiral strakes, of rectangular cross section, have been successfully applied to a 250-ft tapered welded steel stack that had oscillated in the wind. At the end of 18 months this stack had shown no further oscillation. It would appear that the spiral spoilers of rectangular cross section are effective at supercritical Reynolds numbers as a result of the sharp edges presented by the spiraled strakes.

BUFFETING OSCILLATION

Oscillation due to buffeting may develop when a structure lies in the wake of an obstruction that sheds a vortex trail in a more or less regular fashion. The obstruction may arise from the topography of the region, but most frequently takes the form of another structure, or on complex structures one element of the structure may become the source of a buffeting action on another downwind portion.

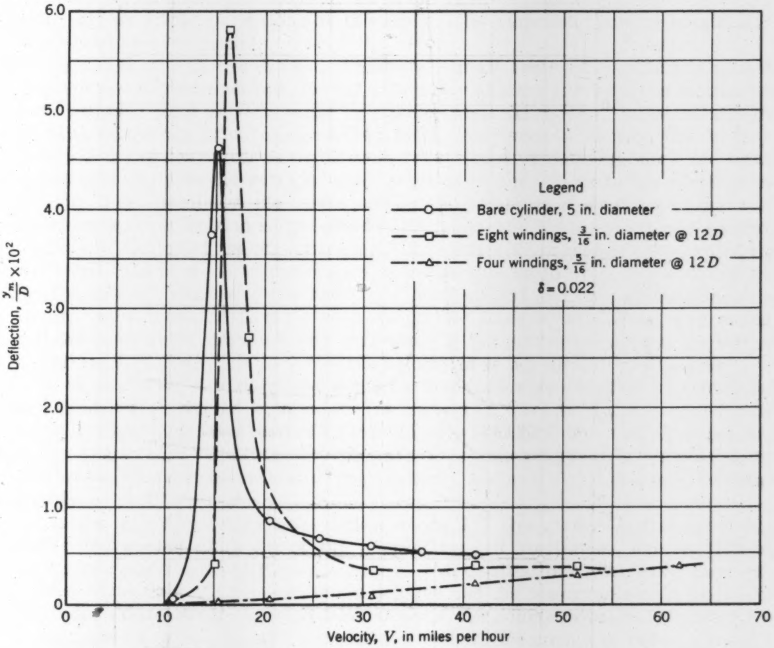

FIG. 22.—RESPONSE OF A 5-IN. DIAMETER SPRING-SUPPORTED CYLINDER WITH BOTH SPOILERS AND ANTI-SPOILERS ATTACHED

The buffeting action is generally irregular, resulting in short bursts of amplitude and has rarely been catastrophic except in the case of some aircraft components.

One interesting manifestation of this phenomenon occurred in connection with two tall stacks 11 ft in diameter, spaced 48 ft apart (605). When the wind blew at an angle of 16° to the alinement of the stacks and at a velocity of 53 mph, the downwind stack swayed in a direction transverse to the wind whereas the upwind stack remained at rest. The rate of vortex shedding was almost exactly equal to the natural frequency of the stack, but the amplitude of vibration was small due to relatively high damping because the stacks were supported on a roof structure.

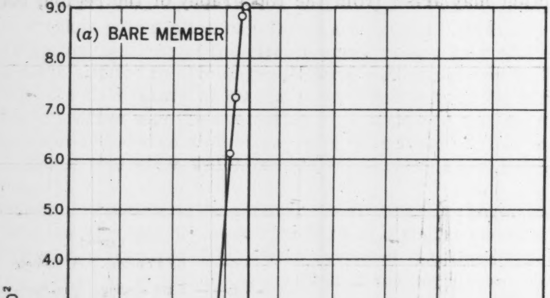

FIG. 23.—RESPONSE OF 4-IN. DIAMETER FLEXURAL CYLINDER WITH SPOILERS OVER VARIOUS PROPORTIONS OF THE MEMBER

Evidently, due to the stack spacing, a vortex discharged from stack No. 1 could reach the opposite side of stack No. 2 just as a vortex was detached from this stack. The effective vortex from stack No. 1, being of opposite rotation from that discharged from stack No. 2, caused a neutralizing effect. This would result in an effective vortex discharge from only one side of the stack and consequently generated a periodic force.

FACTORS WHICH CONTROL SUSPENSION BRIDGE BEHAVIOR IN THE WIND

The aerodynamic forces that act on a bridge in the wind depend only on the velocity and direction of the wind and the size, shape, and motion of the bridge (623). Properties of the bridge, including its elastic forces and its mass and motion, can be computed and reduced to model scale, and wind conditions bracketing all probable conditions at the site can be imposed upon an elastically-supported section model.

Behavior of a Girder-Stiffened Section.—In all tests of oscillating models of girder-stiffened sections, except extremely shallow girders, the motion has been either a pure vertical mode or a pure torsional mode at substantially the natural frequency of vibration (614)(623). For such a section the V/(fb)-ratios and the character of oscillation (restricted or catastrophic) are influenced primarily by the ratio, h/b, of the depth of the girder to the width of the bridge. (The dominant characteristic of the behavior of a bridge in the wind is the consistent relationship between the frequency N [in cycles per second] of the oscillation of the structure and the velocity V [in feet per second] of the wind that causes it. It is convenient to divide this ratio by b, the width of the bridge, in feet, rendering the ratio non-dimensional and thus applicable to the bridge or its model.) Details such as girder flanges, stringers, and curbs, and the position of the deck with reference to the girders also have important modifying influences. This influence of details is not always predictable.

It is characteristic of girder sections that they may oscillate at restricted amplitudes at moderate wind velocities and with a variety of successive modes and corresponding frequencies as the velocity changes. In general, depending on the shape, both vertical and torsional modes may reappear at higher velocities (but at their characteristic frequencies), and some of these may be catastrophic.

As the h/b ratio decreases below about 1/7 the girder-stiffened section shows increasing evidence of the coupled type of oscillation, namely flutter.

Behavior of Truss-Stiffened Sections.—All oscillations that have been observed on models of truss-stiffened bridges and the observed small motion of the Golden Gate Bridge as well have been of the couple type (611). Often the mode appears to be almost a pure torsion but the frequency is reduced toward that of the corresponding vertical mode. In many cases (including all of the catastrophic motions observed) the vertical mode component has sufficient amplitude to shift the axis of rotation considerably to the windward from the center line of the structure. In some cases the axis of rotation has been practically at the windward truss or even well beyond it.

It is characteristic that coupled types of oscillation occur at considerably higher velocities than do the pure vertical and torsional types of the girder sections. It is apparent also that the aerodynamic forces on the truss-stiffened section are determined primarily by the deck and truss members adjacent thereto. In model tests the removal of the bottom chord and web members of a deck truss section has affected the motion only slightly. These members are beneficial aerodynamically in that they add a little to the aerodynamic damping.

Because coupled motion requires a blending of vertical and torsional motions in a manner to be mutually exciting under wind action, it depends upon the elastic factors affecting the relative frequencies of the vertical and torsional modes. The use of lateral systems in the planes of the top and bottom chords increases the torsional stiffness and thus may so widely separate the vertical and torsional frequencies that the critical velocity of coupling and flutter falls beyond any probable wind velocity.

ACKNOWLEDGMENTS

In addition to the task committee members, many former members made valuable contributions to the effort represented herewith. These included C. H. Gronquist, F. ASCE, G. E. Howe (deceased), F. A. Reichert, S. Mitchell, F. ASCE, and J. Karol, F. ASCE.

Respectfully submitted

E. Cohen
F. B. Farquharson
J. J. Kozak
H. G. Lorsch
W. W. Pagon
E. P. Segner, Jr.
R. H. Sherlock
T. W. Singell
H. C. S. Thom
G. B. Woodruff
J. M. Biggs, Chairman
Task Committee on Wind Forces
Committee on Loads and Stresses
Structural Division, ASCE

APPENDIX I.—BIBLIOGRAPHY

---

1. HISTORY

101. "Discorsi a Due Nuove Scienze," by Galileo, Bologna, 1655.

102. "Philosophiae Naturalis Principia Mathematica," by Sir Issac Newton, 1687.

103. "An Experimental Investigation Concerning the Natural Powers of Water and Wind," by John Smeaton, Philosophical Transactions, Royal Soc., 1759.

104. "Recherches Experimentales sur les Lois de la Resistance des Fluides," by N. V. Duchemin, Memorial de l'Artillerie, Vol. 5, 1842, p. 65.

105. "The Forth Bridge," by B. Baker, Engineering, Vol. 38, August, 1884, p. 213.

106. "Wind Pressure in Engineering Construction," by W. H. Bixby, Engineering News-Record, Vol. 33, 1895, p. 175.

107. "Nouvelles Recherches sur la Resistance de l'Air et la Pression du Vent sur les Hangars de Dirigeables," by A. G. Eiffel, Paris, 1914, Trans. by J. C. Hunsaker, Houghton-Mifflin Co., New York.

108. "Ergebnisse der Aerodynamischen Versuchsanstalt (A VA) zu Geottingen," by Ludwig Prandtl and A. Betz, Vol. I, 1920; Vol. II, 1923; by O. Flachsbart, Vol. III, 1927; Vol. IV, 1932, Berlin.

109. "Wind Pressure on Structures," by H. L. Dryden and G. C. Hill, Sci. Paper 523, Natl. Bur. Stds., 1926.

110. "Wind Stresses in Buildings," by Robins Fleming, John Wiley and Sons, Inc., New York, N. Y., 1930.

111. "Modellversuche ueber die Belastung von Gitterfachwerken durch Windkraefte," by O. Flachsbart and H. Winter, Der Stahlbau, No. 9, p. 65; No. 10, 1934, p. 73; No. 8, 1935, p. 65; Trans. by Sandia Corp. AFSWP-464.

112. "Aerodynamics and the Civil Engineer," by W. W. Pagon, Engineering News-Record, Vol. 112, 1934, p. 348; Vol. 113, 1934, pp. 41, 456, 814; Vol. 114, 1935, pp. 582, 665, 742; Vol. 115, 1935, p. 601.

113. "Aerodynamic Stability of Suspension Bridges," by F. B. Farquharson, Univ. of Washington Bulletin No. 116, Part I, 1949; Part II, 1950, by F. C. Smith and G. S. Vincent; Part III, 1952, by F. B. Farquharson; Part IV, 1954, by F. B. Farquharson; Part V, 1954, by G. S. Vincent, Seattle, Wash.

2. NATURE OF THE WIND

201. "On the Influence of the Earth's Rotation on Ocean Currents," by V. W. Ekman, Arkiv. Mat. Astr. Fysik, 1905.

202. "A Generalization of the Theory of the Mixing Length with Applications to Atmospheric and Oceanic Turbulence," by C. G. Rossby, Meteorological Papers, Vol. I, No. 4, Mass. Inst. of Tech., Cambridge, Mass., 1932, p. 33.

203. "Hurricanes," by I. R. Tannehill, Princeton Univ. Press, Princeton, N. J., 1938.

204. "Atmosphaerische Turbulenz," by H. Lettau, Akad. Verlagsges, Leipzig, 1939.

205. "Effective Gust Structure at Low Altitudes," by Philip Donely, NACA, TR 692, 1940.

206. "Physics of the Air," by W. J. Humphreys, 3rd Ed., McGraw-Hill Book Co. Inc., New York, 1940.

207. "Report on the Storm of November 25, 1950," by Earnest J. Christie, Weather Bur. Office, New York, N. Y., December, 1950.

208. "Variation of Wind Velocity and Gusts with Height," by R. H. Sherlock, Transactions, ASCE, Vol. 118, 1953, p. 463.

209. "Hurricanes," by R. H. Simpson, Scientific American, Vol. 190, No. 6, June, 1954, p. 34.

210. "Wind Velocities During Hurricanes," by R. C. Gentry, Transactions, ASCE, Vol. 120, 1955, p. 169.

211. "A Comparison of Six Great Florida Hurricanes," by D. C. Bunting, Weatherwise, Vol. 8, No. 3, June, 1955, pp. 64-67, 78-79, 82.

212. "Hurricanes and Tropical Storms 1887-1956," Weatherwise, Vol. 10, No. 4, August, 1957, pp. 132, 133, 139.

213. "Where Hurricanes Begin," by W. H. Haggard, Weatherwise, Vol. 12, No. 4, August, 1959, pp. 145-150.

214. "Compendium of Meteorology; Tropical Cyclones," by G. E. Dunn, Amer. Meteorological Soc., Boston, Mass., 1951, pp. 887-889.

215. Closure to "Nature of the Wind," by R. H. Sherlock, Proceedings, ASCE, Vol. 86, No. ST7, July, 1960, Fig. 11.

216. "Distributions of Extreme Winds in the United States," by H. C. S. Thom, Proceedings, ASCE, Vol. 86, No. ST4, April, 1960, Figs. 2, 3, 4.

217. "The Safety of Structures," by A. M. Freudenthal, Transactions, ASCE, Vol. 112, 1947, p. 125.

218. "Synopsis of First Progress Report of Committee on Factors of Safety," by O. G. Julian, Proc. Paper No. 1316, ASCE, Vol. 83, No. ST4, July, 1957; Discussion by T. Au, Proc. Paper No. 1442, ASCE, Vol. 83, No. ST6, November, 1957; Milos Vorlicek, Jan Suchy, Ernest Basler, Rene E. Walther, Proc. Paper No. 1522, ASCE, Vol. 84, No. ST1, January, 1958; E. Ruble, Raymond Archibald, Proceedings, ASCE, Vol. 86, No. ST2, February, 1959; Closure, by O. G. Julian, Proceedings, ASCE, Vol. 86, No. ST2, February, 1959.

219. Discussion by R. C. Gentry of "Nature of the Wind," by R. H. Sherlock, Proceedings, ASCE, Vol. 85, No. ST3, March, 1959.

220. "Tropical Meteorology," by Herbert Riehl, McGraw-Hill Book Co. Inc., New York, 1954, p. 288.

221. "On the Low-Level Wind Structure of Tropical Storms," by L. A. Hughes, Journal of Meteorology, Vol. 9, 1952, p. 422.

222. "Wind Pressures in Various Areas of the United States," by G. N. Brekke, Building Materials and Structures Report 152, Natl. Bur. of Stds., April, 1959, pp. 4, 7.

223. "Gust Factors for the Design of Buildings," by R. H. Sherlock, Publications Vol. 8, Internatl. Assoc. for Bridge and Structural Engrg., Zurich, Switzerland, 1947, Fig. 11.

224. Ibid., Fig. 19.

225. "Dallas Tornado of April 2, 1957," by S. G. Bigler and E. P. Segner, Jr., Raw Data Report No. 2, Dept. of Oceanography and Meteorology, Agric. and Mech. College of Texas, College Station, Tex., August, 1957.

3. FUNDAMENTAL CONSIDERATIONS

301. "Aerodynamics," by L. J. Briggs and H. L. Dryden, International Critical Tables, Vol. I, 1926, pp. 402-411.

302. "Turbulent Flow," by L. Prandtl, NACA TM 435, 1927.

303. "On the Flow of Air Behind an Inclined Flat Plate of Infinite Span," by A. Fage and F. C. Johansen, R. and M. 1104, British A. R. C., 1927; and Proceedings, Royal Soc., Vol. 116, No. 773, Series A, September, 1927, pp. 170-197.

304. "The Structure of Vortex Sheets," by A. Fage and F. C. Johansen, R. and M. 1143, British A. R. C., 1927; and Philosophical Magazine, Vol. 5, No. 28, Series 7, February, 1928, pp. 417-441.

305. "Applied Hydro- and Aeromechanics," by L. Prandtl and O. G. Tietjens, Trans. by J. P. Den Hartog, McGraw-Hill Book Co. Inc., New York, 1934.

306. "Aerodynamic Theory," Ed. by W. F. Durand, Springer, Berlin, 1934-5.

307. "Variation of the Wind-Pressure Distribution on Sharp-Edged Bodies," by Chr. Nϕkkentved, Laboratorium for Bygningasstatik, Denmark Tekniske Hϕjskole, 1936, and SC-4204 (TR).

308. "Modern Developments in Fluid Dynamics," Ed. by S. Goldstein, Oxford, England, 1938.

309. "Vibrations Produced by Wind," by Chr. Nϕkkentved, Dansk Selskab for Bygningsstatik, Copenhagen, Denmark, 1941.

310. "Hydrodynamics," by H. Lamb, 6th Ed., Dover, New York, 1946.

311. "L'Action, du Vent sur les Constructions," by L. Blanjean, Ossature Metallique, No. 2, February, 1949.

312. "On the Drag and Shedding Frequency of Two-Dimensional Bluff Bodies," by A. Roshko, NACA TN 3169, Washington, July, 1954.

313. "Vortex Formation and Resistance in Periodic Motion," by J. S. McNown and G. H. Keulegan, Proceedings, ASCE, Vol. 85, No. EM1, January, 1959.

314. "Vortex Systems in Wakes," by L. Rosenhead, Advances in Applied Mechanics, Vol. III, Academic Press, New York, pp. 185-195.

315. "Fluid-Dynamic Drag," by S. F. Hoerner, published by the author, Midland Park, N. J., 1958.

4. FORCES ON ENCLOSED STRUCTURES

401. "Windloads on Buildings," by A. Smith, Journal of the Western Society of Engineers, 1912, 1914.

402. "Wind Pressures on Structures," by H. L. Dryden and G. C. Hill, Sci. Paper 523, Natl. Bur. Stds., 1926.

403. "Wind Pressure on Circular Cylinders and Chimneys," by H. L. Dryden and G. C. Hill, Research Paper No. 221, Natl. Bur. Stds., 1930.

404. "Wind Pressure on Engineering Structures," by R. Katzmayr, Oesterr. Ing. Arch. Verein, Vienna, Vol. 82, No. 21-22, 1930, p. 175; No. 23-24, p. 191.

405. "Wind Pressures on Buildings," by J. O. V. Irminger and C. Nφkkentved, Copenhagen, Denmark, 1930, 1936.

406. "Wind Pressures on a Model of a Mill Building," by H. L. Dryden and G. C. Hill, U. S. Bur. Stds. Research Paper No. 301, 1931.

407. "Wind Loads on Airship Hangars," by H. Sylvester, 6th Natl. Aeronautical Meeting of ASME, 1932.

408. "Wind Pressure on Buildings," by Chr. Nφkkentved, Publ. Int. Assoc. Bridge and Structural Engrg., Vol. I, 1932, p. 365; Vol. II, 1934, p. 257, Zurich, Switzerland.

409. "Wind Pressure on a Model of the Empire State Building," by H. L. Dryden and G. C. Hill, Research Paper No. 545, Natl. Bur. Stds., 1933.

410. "Wind Pressure on Buildings," by A. Bailey, *Journal*, Inst. Civ. Engrs., Select. Engrg. Paper No. 139, 1933.

411. "Influence of Neighboring Structures on the Wind Pressure on Tall Buildings," by C. L. Harris, Pa. State Coll. Engrg. Experiment Sta. Ser. Bull. No. 43, 1934, also Natl. Bur. Stds., *Journal of Research*, Vol. 12, No. 1, 1934, p. 103.

412. "L'Action du Vent Sur Les Constructions," by F. Biron, Science et Indust. Constr., Vol. 18, No. 16, 1934, p. 131.

413. "L'Action du Vent Sur Les Batiments et Constructions," by R. Pris, Trav. Architect. Construct., Vol. 20, 1936, p. 71.

414. "Wind Pressure Distribution on Sharp-Edged Bodies," by H. Sylvester, *Bygningsstatiske Meddelelser*, Vol. 8, 1936, p. 41.

415. "L'Azione del Vente sulle Costruzioni," by Renato Giovannozzi, *Aerotecnica*, Vol. 16, 1936, p. 413.

416. "The Effect of Wind Loads on Frames With Semi-Rigid Connections," by J. F. Baker and E. F. Williams, Final Report, Steel Struct. Res. Comm., London, England, 1936.

417. "Der Winddruck auf Schornsteine mit Kreisquerschnitt," by J. Ackeret, *Schweiz. Bauzeitung*, Vol. 108, 1936, p. 25.

418. "Wind Pressures on the Akron Airship Dock," by K. Arnstein and W. Klemperer, *Journal of the Aeronautical Sciences*, Vol. 3, 1936, p. 88.

419. "Wind-Bracing in Steel Buildings," Fifth Progress Report, Sub-Committee No. 31, Committee on Steel, Structural Division, *Proceedings*, ASCE Vol. 62, March, 1936, p. 397.

420. "Aerodynamics of the Perisphere and Trylon at the World's Fair," by A. Klemin, E. B. Schaefer and L. H. Burer, Jr., Transactions, ASCE, Vol. 104, 1939, p. 1449.

421. "The Big Storm," Ed. by L. H. Tyler, The City Printing Co., New Haven, Conn., 1938.

422. "Wind Forces on a Tall Building," by J. C. Rathbun, Transactions, ASCE, Vol. 105, 1940, p. 1.

423. "Wind Bracing in Steel Buildings," Final Report, ASCE Sub-Committee No. 31, Committee on Steel, Transactions, ASCE, Vol. 105, 1940, p. 1713.

424. "Wind Pressure on Buildings Including Effects of Adjacent Buildings," by A. Bailey and N. D. G. Vincent, Journal, Inst. Civ. Engrs., Vol. 20, 1943, p. 243.

425. "Wind Loads on Buildings," by H. Ferrington, Structural Engineer, Vol. 21, 1943, p. 497; Vol. 22, 1944, p. 15.

426. "Aerodynamic Characteristics of Circular Arch Roof Structures," by J. H. Cissel and L. M. Legatski, Eng. Res. Prof. M-518, Univ. of Mich., Ann Arbor Mich., 1944.

427. Normer for Bygningskonstruktioner 1. Belastningsforskrifter, June, 1948 (Danish Standard).

428. "Protection of Small Buildings Against High Velocity Winds," by R. A. Thompson, Bull. 28, Fla. Engrg. and Industrial Experiment Sta., Gainesville, Fla., 1949.

429. "L'Action du Vent Sur Les Constructions," by L. Blanjean, Ossature Metallique, Brussels, Belgium, February, 1949.

430. "Wind Loads on Structures," by Michael R. Horne, Journal, Inst. Civ. Engrs., Vol. 33, January, 1950, p. 155.

431. "Wind Stresses in Semi-Rigid Connections of Steel Framework," by B. Sourochnikoff, Transactions, ASCE, Vol. 115, 1950, p. 382.

432. "Wind-Load Standards in Europe," by John W. T. Van Erp, Proc. Sepaate No. 42, ASCE, Vol. 76, November, 1950.

433. "Lateral Forces of Earthquake and Wind," by Arthur W. Anderson, et al, Proc. Separate No. 66, ASCE, Vol. 77, April, 1951.

434. "Wind Tunnel Studies of Pressure Distribution on Elementary Building Forms," by N. Chien, Y. Feng, H. Wang, and T. Liao, Iowa Inst. of Hydr. Research, State Univ. of Iowa, Ames, Iowa, 1951.

435. "Wind Pressure on Elementary Building Forms Evaluated by Model Tests," by J. W. Howe, Civil Engineering, May, 1952, p. 42.

436. "Determining Basic Wind Loads," by George F. Collins, Proc. Paper No. 825, ASCE, Vol. 81, November, 1955.

437. "Minimum Design Loads in Building and Structures," Amer. Stds. Assoc., A58.1, 1955.

438. Schweizerischer Ingenieur und Architekten Verein, Technische Normen No. 160, 1956.

5. FORCES ON PLATE GIRDERS AND TRUSSES

501. "Application of the Theory of Free Jets," by A. Betz and R. Peterson, Natl. Adv. Comm. for Aeronautics, TN667 (translation).

502. "Winddruck auf Fachwerktuerme von quadratischem Querschnitt," by R. Katzmayr and H. Seitz, Bauingenieur, Vol. 15, 1934, pp. 215-221.

503. "Experiments on a Static Model of a Section of the Severn Bridge," by D. H. Williams, H. L. Nixon, and W. C. Skelton, Natl. Physical Lab., England, Aero/209.

504. "Tests of Plate Girder Bridges in the Duplex Wind Tunnel," by D. H. Williams, H. L. Nixon, and W. C. Skelton, Natl. Physical Lab., England, Aero/216.

505. "Empirical Formulas for the Tunnel Blockage Correction for Wind Force Measurements on Lattice Structures, and some Wind Load Coefficients for Lattices Masts," by C. Scruton, Natl. Physical Lab., NPL/Aero/355. Permission has been given to publish this unpublished data with this note: "The date in NPL/Aero/355 was obtained in behalf of the British Insulated Callender's Construction Co., Ltd., and is now published by permission of the Director, National Physical Laboratory, England."

506. "Investigation of Wind Forces on Highway Bridges," by G. S. Vincent, Highway Research Board Special Report 10, No. 272, 1953.

507. "Wind Loads on Truss Bridges," by J. M. Biggs, Transactions, ASCE, Vol. 119, 1954, p. 879.

508. "Wind-Induced Vibrations of a Pipe-Line Suspension Bridge and its Cure," by R. C. Baird, Transactions, ASME, Vol. 77, No. 6, August, 1955.

509. "Wind Loads on Girder Bridges," by J. M. Biggs, S. Namyet, and J. Adachi, Transactions, ASCE, Vol. 121, 1956, p. 101.

510. "Design of Multi-Level Guyed Towers; Wind Loading," by Edward Cohen and Henri Perrin, Proc. Paper No. 1355, ASCE, Vol. 83, No. ST5, September, 1957.

511. "Wind Forces on Structures: Plate Girders and Trusses," by W. Watters Pagon, Proc. Paper No. 1711, ASCE, Vol. 84, No. ST4, July. 1958.

512. "Wind Resistance of Lattice Girder Bridges," Inst. of Civ. Engrs., London, England, 1948.

513. Closure to "Wind Forces on Structures: Plate Girders and Trusses," by W. Watters Pagon, Proceedings, ASCE, Vol. 85, No. ST7, September, 1959.

6. STRUCTURES SUBJECT TO OSCILLATION

601. "Uber eine besondere Art der Tonerregung," by V. Strouhal, Ann. der Physik, Vol. 5, 1878.

602. "Uber den Mechanismus des Flussigkeits und Luftwiederstandes," by Theodore von Kármán and H. Rubach, Phys. Zeits., Vol. 13, 1912.

603. "The Flow of Air About an Inclined Flat Plate of Infinite Span," by A. Fage and F. C. Johansen, Proceedings, Royal Soc., Vol. A116, London, England, 1927.

604. "The Effects of Turbulence and Surface Roughness on the Drag of Circular Cylinders," by A. Fage and J. W. Warsap, British ARC, R and M No. 1283, 1929.

605. "Vibration Problems in Tall Stacks Solved by Aerodynamics," by W. Watters Pagon, Engineering News-Record, July 12, 1934.

606. "Laboratory Studies of Conductor Vibrations," by Joseph S. Carroll, Transactions, AIEE, Vol. 55, 1936, p. 543.

607. "Rigidity and Aerodynamic Stability of Suspension Bridges," by D. B. Steinman, Transactions, ASCE, Vol. 110, 1945, p. 439.

608. "Problems of Aerodynamic and Hydrodynamic Stability," by D. B. Steinman, Bulletin 31, Univ. of Iowa Studies in Engrg., Iowa City, Iowa, 1947.

609. "Mechanical Vibrations," by J. P. Den Hartog, McGraw-Hill Book Co. Inc., New York, 1947.

610. "Wind Tunnel Tests of Suspension Bridge Section Models," by F. J. Maher, D. Frederick, E. R. Estes, and D. B. Steinman, Bulletin, Va. Polytech. Inst. Engrg. Experiment Sta., Vol. 41, No. 6, Series No. 69, 1948.

611. "Dynamic Instability of Truss-Stiffened Suspension Bridges under Wind Action," by F. Bleich, Transactions, ASCE, Vol. 114, 1949.

612. "Aerodynamic Theory of Bridge Oscillations," by D. B. Steinman, Transactions, ASCE, Vol. 115, 1950, p. 1180.

613. "The Mathematical Theory of Vibration in Suspension Bridges," by Fredrich Bleich, C. B. McCullough, R. Rosecrans, and George S. Vincent, Bur. of Pub. Rds., 1950.

614. "Aerodynamic Stability of Suspension Bridges," by F. B. Farquharson, Univ. of Washington Engrg. Experiment Sta. Bulletin, 116, Part III, 1952.

615. "Low Speed Drag of Cylinders of Various Shapes," by N. K. Delany and N. E. Sorenson, NACA TN 3038, November, 1953.

616. "The Investigation of Models of the Original Tacoma Narrows Bridge under the Action of Wind," by F. B. Farquharson, Univ. of Washington Engrg. Experiment Sta. Bulletin 116, Part IV, 1954.

617. "Extended Studies," by G. S. Vincent, Univ. of Washington Engrg. Experiment Sta. Bulletin 116, Part V, 1954.

618. "An Introduction to the Theory of Aeroelasticity," by V. C. Fung, John Wiley and Sons, Inc., New York, 1955.

619. "On the Wake and Drag of Bluff Bodies," by A. Roshko, Journal of the Aeronautical Sciences, Vol. 22, No. 2, February, 1955.

620. "Wind Effects on Bridges and Other Flexible Structures," Notes on Applied Science, No. 11, Natl. Physical Lab., England, 1955.

621. "Aerodynamic Buffeting of Bridges," by C. Scruton, The Engineer, Vol. 199, May 13, 1955, pp. 654-667.

622. "Wind-Induced Vibrations of a Pipeline Suspension Bridge, and Its Cure," by R. C. Baird, ASME Paper No. 54-PET-12, July, 1955.

623. "Aerodynamic Stability of Bridges," Report of the Advisory Board on the Investigations of Suspension Bridges, Transactions, ASCE, Vol. 120, 1955, p. 721.

624. "Factors Influencing the Dynamic Behavior of Tall Stacks under the Action of Wind," by M. S. Ozker and J. C. Smith, Transactions, ASME, Vol. 78, No. 6, 1956.

625. "Vibrations of Steel Stacks," by W. L. Dickey and G. B. Woodruff, Transactions, ASCE, Vol. 121, 1956.

626. "Resonant Vibrations of Steel Stacks," by E. A. Dockstader, W. F. Swiger, and E. Ireland, Transactions, ASCE, Vol. 121, 1956.

627. "Progress Report on the Investigation of Galloping Transmission Line Conductors," by A. T. Edwards and A. Madeyski, Transactions, AIEE Paper No. 55-213, 1956.

628. "Wind Tunnel Investigation of Conductor Vibration with Use of Rigid Models," by F. B. Farquharson and Robert E. McHugh, Jr., Power Apparatus and Systems, AIEE, October, 1956, pp. 871-878.

629. "Suppression of the Fluid-Induced Vibration of Circular Cylinders," by Peter Price, Proc. Paper No. 1030, ASCE, Vol. 82, No. EM3, July 1956.

630. "Wind Induced Vibration of Cylindrical Structures," by Joseph Penzien, Proc. Paper No. 1141, ASCE, Vol. 83, No. EM1, January, 1957.

631. "A Means for Avoiding Wind Excited Oscillations of Structures with Circular or Nearly Circular Cross Sections," by C. Scruton and D. E. J. Walshe, NPL/Aero/335, October, 1957.

632. "Further Experiments on the Use of Helical Strakes for Avoiding Wind Excited Oscillations of Structure with Circular or Near Circular Cross Section," by L. Woodgate and J. F. M. Mabrey, NPL/Aero/381, June, 1959.

633. "Experimental Investigation of Wind-Induced Vibration in Antenna Members," by W. Weaver, Group Report No. 75-4 Lincoln Lab., Mass. Inst. of Tech., Cambridge, Mass., August 26, 1959.

634. "Effect of Flow Incidence and Reynolds Number as Low-Speed Aerodynamic Characteristics of Several Noncircular Cylinders with Application to Directional Stability and Spinning," by Edward C. Paulhamus, NASA, TR R-29, 1959.

635. "ARC Reports and Memoranda," by A. Fage and J. W. Warsap, No. 1283, 1930.

APPENDIX II.—NOTATION

The following letter symbols conform essentially with "American Standard Letter Symbols for Structural Analysis" (ASA Z10.8-1949), prepared by a committee of the American Standards Association, with Society representation, and approved by the Association in 1949:

A = exposed area;

b = width;

C = coefficient;

C_{CP} = eccentricity coefficient;

C_D = drag coefficient;

C_L = lift coefficient;

C_P = pressure coefficient;

C_{Pe} = external pressure coefficient;

C_{Pi} = internal pressure coefficient;

D = diameter;

d = distance between vortexes;

f = frequency;

f_0 = frequency at which model moves vertically as a unit;

f_1 = frequency of vertical motion about the z-axis;

h = height or depth;

L = length;

l = span;

M = mass per unit length;

p = static pressure at a point;

p_o = static pressure of the approaching free stream;

q = dynamic pressure of the free stream;

q_z = dynamic pressure of the free stream at height z;

R = Reynolds number;

r = rise-span ratio;

S = Strouhal number;

s = spacing;

V = wind velocity;

V_c = critical wind velocity;

V_o = wind velocity of the approaching free stream;

V_z = wind velocity at height z;

V_{30} = wind velocity at height of 30 ft;

V_{50} = wind velocity at height of 50 ft;

x = exponent in Eq. 2;

y = deflection;

y_m = deflection of tube;

y_2 = double amplitude;

z = elevation;

α = angle of attack of wind on object;

δ = logarithmic decrement;

θ = central angle;

λ = length-width ratio, or aspect ratio;

μ = dynamic viscosity;

ν = kinematic viscosity;

ρ = density of air; and

ϕ = solidity ratio.

AMERICAN SOCIETY OF CIVIL ENGINEERS
Founded November 5, 1852
TRANSACTIONS

Paper No. 3270

FOUNDATION INSTALLATION-REQUIRING RECHARGING OF GROUND WATER

By James D. Parsons,[1] F. ASCE

SYNOPSIS

Ground water, at the site described herein, provided partial support, through buoyancy, for the five 14-story structures constructed. However, when the ground water was lowered to permit the new foundations to be installed in the dry, special precautions had to be taken to safeguard the adjacent existing structures. The soil conditions prevailing, the foundation treatment adopted, the proximity of existing adjacent structures, and the ground water conditions all have an important bearing on the requirements of the diffusion system described herein. This system was developed to maintain normal ground water levels in the adjacent areas during the construction period.

INTRODUCTION

In the installation of foundations for structures, it is not infrequent that all or part of such installations are located below ground-water level and, as a result, dewatering is required to permit the work to be carried out in the dry. In lowering the ground water for this purpose, however, it is essential to consider the effect of such operations on adjacent structures; occasionally, the added requirement of maintaining ground water at normal levels in the immediately adjacent areas, in order to protect existing adjacent structures, presents itself. The complications that may arise in accomplishing the latter

---

Note.—Published essentially as printed here, in September, 1959, in the Journal of the Construction Division, as Proceedings Paper 2141. Positions and titles given are those in effect when the paper or discussion was approved for publication in Transactions.

[1] Assoc. Partner, Moran, Proctor, Mueser and Rutledge, Cons. Engrs., New York, N. Y.

requirement can be serious, and are often costly. The appropriate solution depends, to a large degree, on the prevailing soil conditions. The installation described presents a novel approach that was developed to overcome a particularly difficult foundation condition.

GENERAL CONDITIONS

The site involved was selected by the New York City Housing Authority (NYCHA) for the construction of five 14-story middle income apartments to be known as "Coney Island Houses." The project is three blocks in area, located immediately adjacent to the boardwalk at Coney Island, and approximately 150 ft from the ocean. The buildings, oriented as shown in Fig. 1 are among the largest and heaviest in the area, and because of the foundation conditions prevailing had to be supported on heavy, buoyed, reinforced concrete boxes founded at about el -10. This elevation is approximately 10 ft below mean sea level. To permit the foundations to be installed in the dry, required lowering the ground water to below el -12 and to accomplish this the contractor elected to install wellpoints, 6 ft on centers, around the periphery of the three block area. Two intermediate lines were also installed across the project between the north and south main lines to permit flexibility in pumping the construction area. (See Fig. 1.)

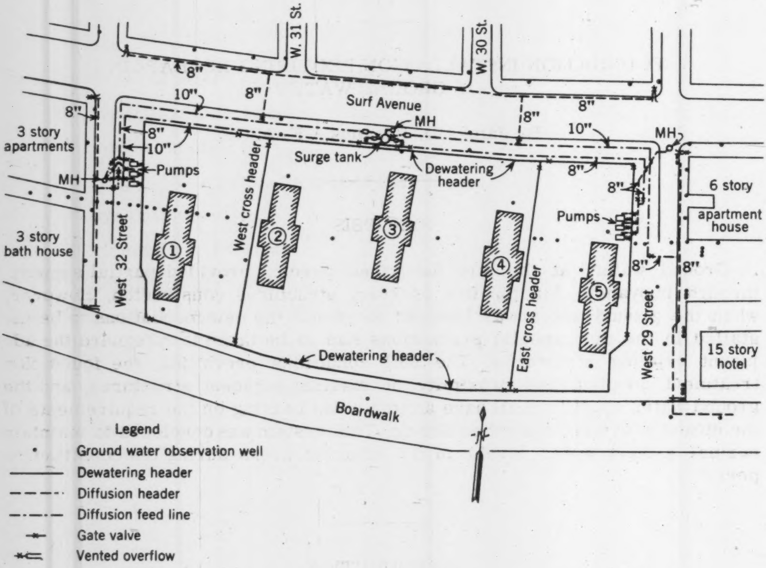
W. 31 St.
W. 30 St.
8"
10"
8"
Surf Avenue
MH
8"
8"
10"
MH
8"
3 story apartments
8"
10"
Surge tank
Dewatering header
Pumps
MH
8"
8"
West cross header
6 story
apartment house
Pumps
3 story bath house
West 32 Street
①
②
③
④
⑤
8"
8"
East cross header
West 29 Street
15 story hotel
Dewatering header
Boardwalk
Legend
Ground water observation well
Dewatering header
Diffusion header
Diffusion feed line
Gate valve
Vented overflow

FIG. 1.—SITE PLAN AND LAYOUT OF DEWATERING AND DIFFUSION SYSTEM

Immediately across 29th St, on the east side of the project, is a 15-story former hotel and a 6-story apartment house, the foundation conditions under each of which necessitated the maintenance of normal ground water conditions in their area. Each of these buildings is only approximately 110 ft from project building No. 5. In addition, in a number of the smaller surrounding buildings on the other sides of the project across Surf Ave. and 32nd St evidence of earlier settlement distress was noted and the influence of lowering the ground water on their performance was a matter of concern.

SOIL AND FOUNDATION CONDITIONS

Numerous borings of the dry sample, undisturbed and continuous sample types, had been made throughout the area of the site and in adjacent areas, and the principal soil formations encountered were included in the longitudinal geological sections shown in Fig. 3. Except for the upper sand layer, the individual formations are uniform in thickness and character within the area. The upper sand layer, that prevails between, approximates el +6 and -55, was found, however, to contain occasional thin discontinuous layers or lenses of organic silt (mud) up to 2 ft in thickness and, consequently, in the five NYCHA buildings numerous continuous sample borings were required to establish the integrity of this upper sand layer for the support of the buildings at the locations selected.

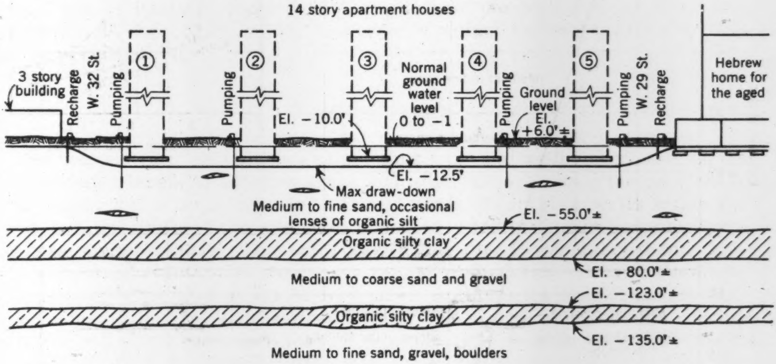
14 story apartment houses
3 story building
Recharge
W. 32 St.
Pumping
①
Pumping
②
El. −10.0'
③
Normal ground water level 0 to −1
④
Pumping
Ground level El. +6.0'±
⑤
Pumping
W. 29 St.
Recharge
Hebrew home for the aged
El. −12.5'
Max draw-down
Medium to fine sand, occasional lenses of organic silt
El. −55.0'±
Organic silty clay
El. −80.0'±
Medium to coarse sand and gravel
El. −123.0'±
Organic silty clay
El. −135.0'±
Medium to fine sand, gravel, boulders

FIG. 2.—LONGITUDINAL SECTION THROUGH PROJECT

The settlements in a number of the adjacent existing structures were believed to be due principally to the presence of these organic silt layers, and the lowering of the ground water would unquestionably induce further settlements in these buildings. To avoid possible claims for damage that might result, it was considered essential to avoid lowering the ground water in the adjacent areas.

Of principal concern in connection with the foundation requirements for the five new buildings constructed, was the presence of the two organic silt beds, shown in Fig. 2, between el -55 to -80 and -123 and -135. Exhaustive laboratory analyses of undisturbed samples recovered from these beds

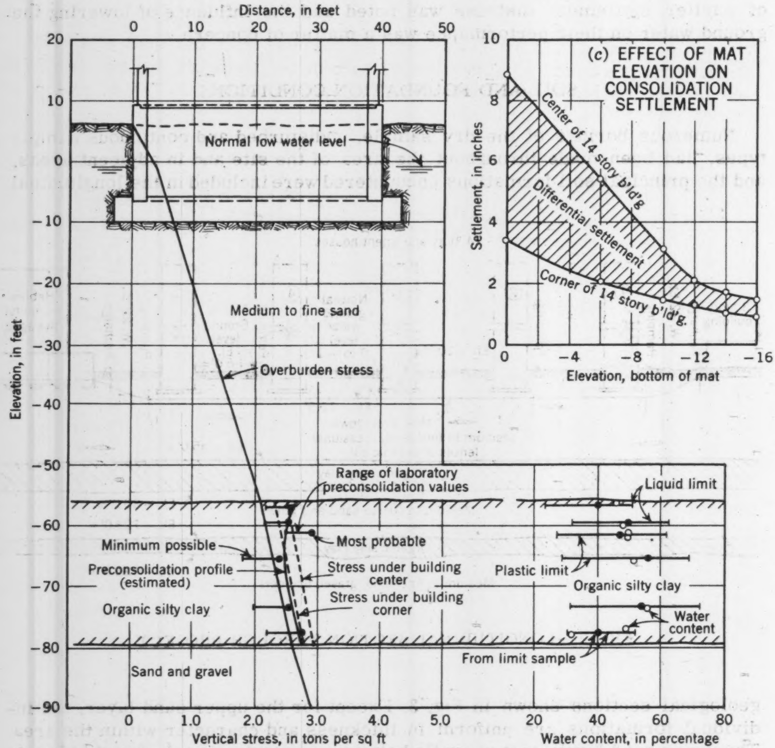

(*a*) DISTRIBUTION OF STRESSES IN ORGANIC SILT FORMATION UNDER 14 STORY BUILDING

(*b*) WATER CONTENT AND ATTERBERG LIMITS OF ORGANIC SILT FORMATION

FIG. 3

demonstrated that they have been preconsolidated in the past by the weight of an overriding sand dune to approximately 1/4 tons in excess of the present existing overburden. The estimated distribution of preconsolidation stresses in the upper silt bed are shown in Fig. 3.

Fourteen-story buildings, if supported on piles or on footings founded at or above normal ground water level would stress these beds well in excess of the maximum stresses to which they have been exposed in the past and, because of the excessively high settlements to be expected they could not be so supported. The influence of foundation level on the ultimate settlements anticipated, based on a uniform distribution of loading, is shown in Fig. 3(c). The buildings, therefore, had to be either reduced in height and weight or supported on buoyed reinforced boxes founded at el -10 or lower to provide, through buoyancy, the necessary reduction in weight on the underlying silt beds. The latter method was selected because the number of additional apartment units afforded by the higher structures were needed. The resulting wellpoint system was provided by the contractor to permit these foundations to be installed in the dry.

The estimated existing stresses in the organic silt bed under the former hotel, that is supported on spread footings in the upper sand layer, were computed and found to be close to the maximum preconsolidation stresses in this bed. Thus, it became evident that a drawdown of the ground water under this building with the accompanying increase in weight on the organic silt could not be permitted.

PUMPING TEST

To demonstrate the influence of pumping from the wellpoint system on the ground water levels in adjacent areas and to permit evaluating the problem in this connection, a large number of ground water observation wells within and outside of the limits of the site were installed, a test program, pumping from the west cross-header of the system only (see Fig. 1) was carried out. Continuous pumping from this line for a period of about two weeks, maintaining a drawdown of from -9 to -11 at the header, provided the drawdown information indicated in Fig. 4. The drawdown in this period, along an axis roughly parallel with the beach, extended back some 1000 ft from the single line of wellpoints operated, demonstrating that if pumping were carried out from the full wellpoint system that had been installed, a very large area would be affected. Towards the ocean, the radius of influence, of course, would be less but in the direction of Surf Avenue a greater influence could be expected.

A drawdown to -8 or -9 under the 15-story hotel and 6-story apartment building at a distance of roughly 90 ft from the east header was estimated on the basis of this evidence. Therefore, the need for providing facilities to prevent this drawdown under the existing buildings was evident.

DIFFUSION TEST

A number of methods for maintaining the ground water at normal levels outside of the limits of the site during the drawdown period, including the driving of steel sheeting through the upper sand bed into the underlying silt layer and the pumping of water back into the ground by means of a diffusion system located around the periphery of the site, were considered. Cost estimates indicated that the latter method would provide a savings over the other methods and studies for its development were undertaken.

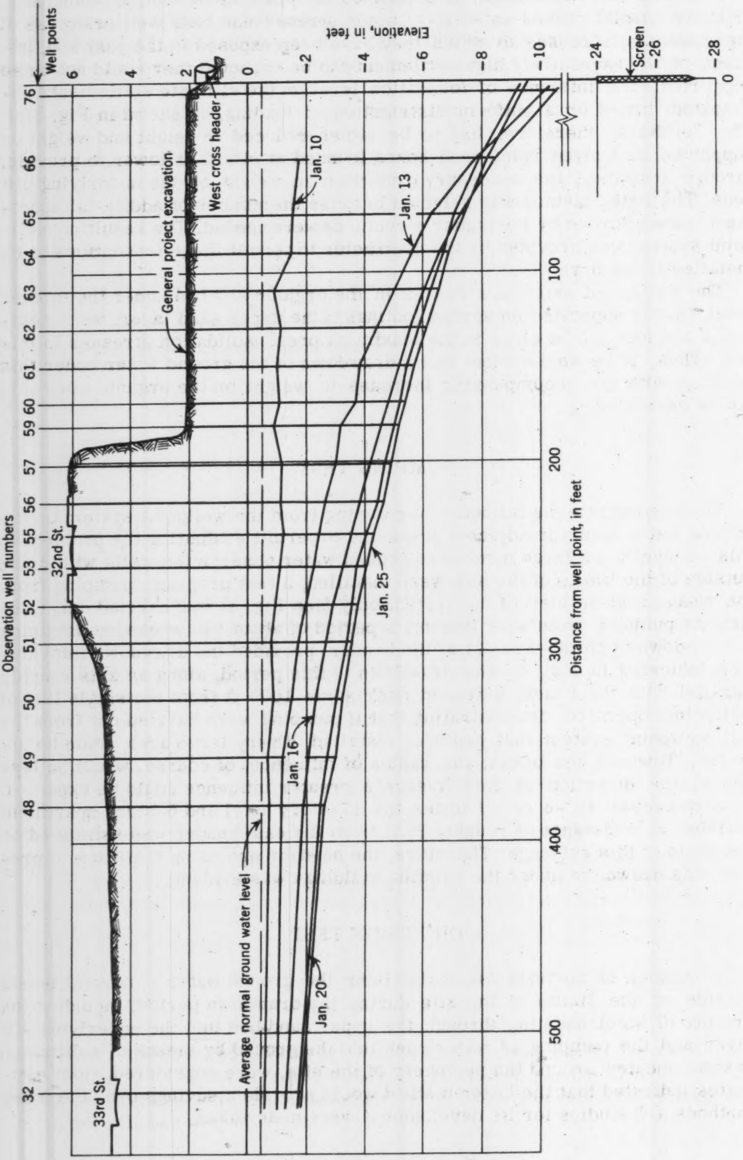

FIG. 4.—WATER LEVELS DURING PUMPING TEST

In view of the limited evidence available regarding the applicability of diffusion methods for installations of comparable size and nature it was decided to first install, as a test section, a 200 ft portion of the anticipated ultimate diffusion system located on the east side of W. 29th St for a test run. This test section, however, was in the most critical area because it was located immediately adjacent to the hotel and apartment house. (Fig. 1) Pumping during this test was from a 100 ft section of the wellpoint system located immediately across 29th St. The discharge was pumped back into the ground across the street through the diffusion test section.

The diffusion system, as first installed, was much like an ordinary wellpoint system with header pipe, swing joints, riser pipes, and wellpoint assembly. Even the diffusion points were fabricated similar to standard dewatering wellpoints except that the points themselves were capped at the bottom and the ball check valve and jet holes were omitted. Also, instead of utilizing screens approximately 3 ft in length, as ordinarily provided in wellpoint installations, the diffusion points were made up with 8-ft-3-in. screens to provide adequate discharge area. The diffusion wellpoints in the test section were jetted into position on 4 ft centers, with the screens located between el -1 to -9. While the 4 ft spacing was first felt to be closer than necessary, it was used in order to more readily permit experimentation.

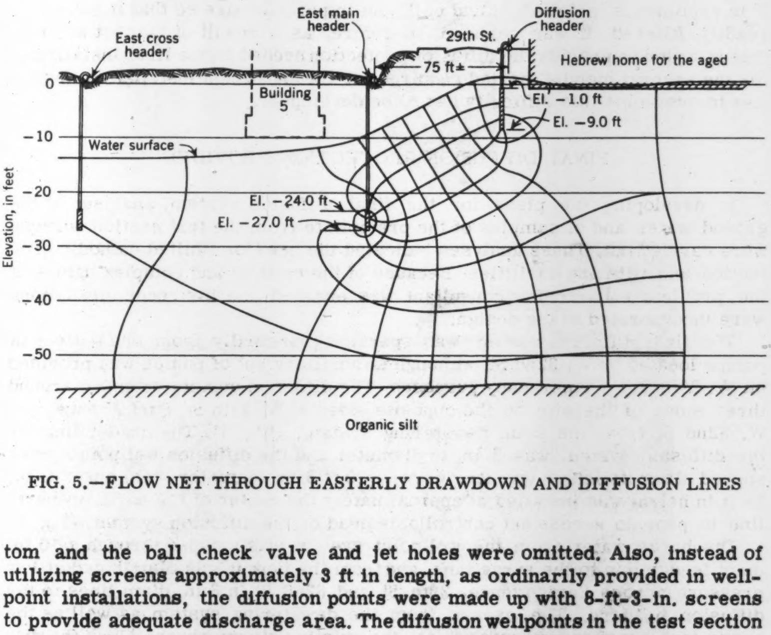

FIG. 5.—FLOW NET THROUGH EASTERLY DRAWDOWN AND DIFFUSION LINES

Before operating the test section, detail surveys of all of the existing buildings in the area were carried out, and settlement points on them were established for periodic observations during the pumping period. Provisions were also made to obtain hourly ground water level in the early stages in each of the 135 observation wells (see Fig. 1) that were established in the area for control purposes.

The test section was operated for a period of about two weeks and, by careful control of the wellpoint pumping and discharge pressures in the diffusion system, the desired drawdown conditions shown in Fig. 5 were readily attained. This flow net is drawn perpendicular to the lines of dewatering and diffusion points, through several wells in the area of the test section, and closely approximates the conditions anticipated by earlier studies. Normal, or slightly above normal, ground water conditions were maintained for a major part of the test period outside the limits of the site; however, during the latter stages, the pressure in the diffusion line had to be substantially increased and, in some instances even with the higher pressures, it was found that the discharge was almost negligible. This was found to be due to the accumulation, predominately, of a precipitate of ferrous hydroxide $Fe[(OH)_2]$ or active rust in the diffusion points, that may have resulted, in part, from insufficient prior clearing of the lines. This compound forms, for a large degree, from the galvanic action between the various metals in the system. It is voluminous, gelatinous, and colloidal in particle size so that it cannot be readily filtered. It was realized, therefore, as a result of the test section, that in order to provide the diffusion protection needed in the final installation for the several months' period required for the foundation installation, facilities to overcome this difficulty had to be developed.

FINAL DIFFUSION PROTECTION PROVIDED

In developing the plans for the final diffusion system, analyses of the ground water and of samples of the precipitate from the test section screens were carried out. These analyses indicated the need for limited cathodic protection and filtering facilities. Because of the critical and complex nature of the problem a corrosion consultant was engaged and his recommendations were incorporated in the design.

The final diffusion system was operated principally from one battery of pumps located on W. 32nd St, although an auxiliary set of pumps was provided on W. 29th St for emergency purposes. The diffusion system extended around three sides of the site on the opposite sides of W. 29th St, Surf Avenue, and W. 32nd St from the main dewatering system, (Fig. 1). The header line for the diffusion system was 8 in. in diameter and the diffusion wellpoints were spaced along its length on 4 ft centers. A 10 ft 6 in. diameter steel surge tank, 25 ft in height was installed at approximately the center of the north property line to provide a constant controllable head on the diffusion system. (Fig. 6)

Discharge water from the wellpoint system was pumped through a 10 in. diam feeder line to the surge tank, and from the tank it was distributed at low pressure across Surf Avenue, 29th St and 32nd St in 8 in. diam lines to the diffusion headers. The excess from the dewatering system as well as the surge tank overflow was wasted into the existing storm sewer. Along the diffusion header and feeder lines were installed gate valves, piezometers, and pressure gages to further regulate the pressures. The maximum pressure in the diffusion header at the ends of the lines was maintained at 3 psi by 7 ft high vented overflow loops (Fig. 7) and the pressure drop between the surge tank and the ends was 7 psi. In the 1600 ft of diffusion system installed there were approximately 400 diffusion points. The main dewatering system, on the other hand, that was roughly 2400 ft in length had an equal number of wellpoints. In the two cross-headers there were about seventy additional points.

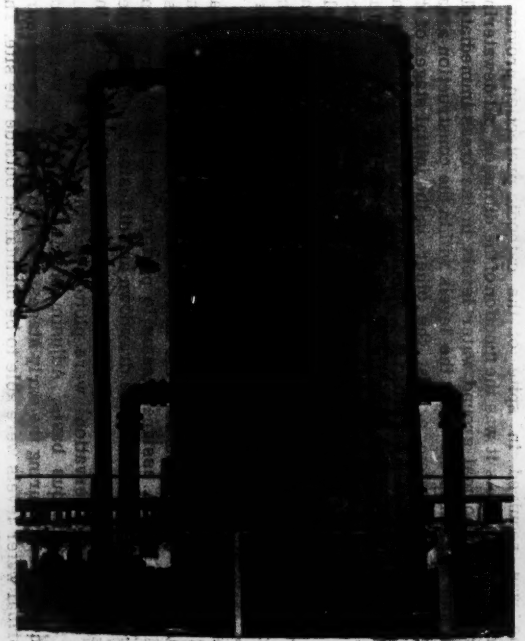

FIG. 6.—DIFFUSION SYSTEM SURGE TANK

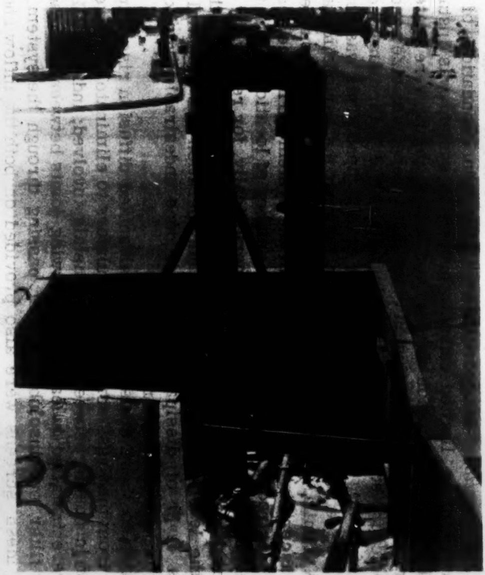

FIG. 7.—VENTED OVERFLOW LOOP

As in the test section, the diffusion wells were jetted into position with their screens located between roughly el -1 and -9. The dewatering point screens, on the other hand, were between el -24 and -27 as shown in Fig. 5.

Cathodic Protection.—In accordance with the recommendations of the corrosion consultant, a limited cathodic protection system was installed, the inside walls of the diffusion feeder and header piping were coated with a special vinyl paint, and the diffusion riser pipes were galvanized and coated. The cathodic protection involved the installation of 1 in. diam zinc rods at intervals of from 4 ft to 6 ft along the header pipes. This was considered necessary to retard the galvanic action between the various metals in the system. A similar cathodic protection was provided in the surge tank. In order to ascertain the degree of zinc in the system during the operations, reference electrodes were installed at a number of locations along the lines and potentiometer readings were taken periodically, for review, by the corrosion consultant. A study of the potentiometer readings permitted the monitoring of the level of zinc dissipation. This operation was essential because too high a level of dissipation could produce undesirable hydroxides that might clog the diffusion filters.

In addition to these measures, the galvanized diffusion riser pipes were separated from the brass screens by insulators to eliminate the development of an electric couple between the two metals involved; individual 100 mesh screens were installed in each of the swing joints between the headers and risers to filter out insoluble matter passing through the system. (Fig. 8) Large 50 mesh screens were also provided on both the inflow and outflow sides of the surge tanks as shown in Figs. 9 and 10(a). Frequent cleaning of all screens was required in spite of the cathodic protection provided.

Operation of System.—As it was the function of the diffusion and dewatering systems to maintain normal ground water levels in the areas immediately surrounding the site while lowering the levels within the construction area, the balancing of one system against the other in the initial stages of its operation, was of principal concern. Of particular significance in this connection was the fact that the quantity of water diffused into the ground is principally a function of the pressure in the water at the diffusion wells. Such pressures, in all cases, had to be limited to those associated with the development of a quick condition in the soil that surrounded the points. Flooding or a quick condition, however, could be readily detected when it occurred and throttling of the swing joint valve at the location permitted immediate correction.

The system was balanced in the initial stage so that the surge tank was maintained full, up to the overflow pipe with the feeder and diffusion line valves adjusted so that pressures in the diffusion header lines averaged less than 3 psi. The NYCHA assigned teams to perform constant observations during the early stages to record the drawdown and diffusion levels indicated in the 135 observation wells established within and outside the limits of the site (Fig. 1). These observations were plotted and the ground water levels contoured on a continuous basis. Adjustments in the system were made several times each day during the early stages, and with an average pressure of 3 psi normal water levels were able to be maintained outside the site. The water pumped by the wellpoint dewatering system was initially 6000 gpm, and was ultimately reduced to about 4500 gpm in the final stages of which roughly 3000 gpm were diffused into the ground and the rest wasted.

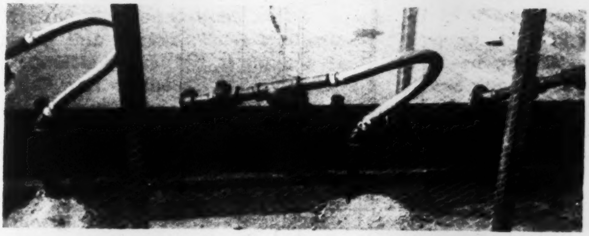

FIG. 8.—INDIVIDUAL 100 MESH FILTER

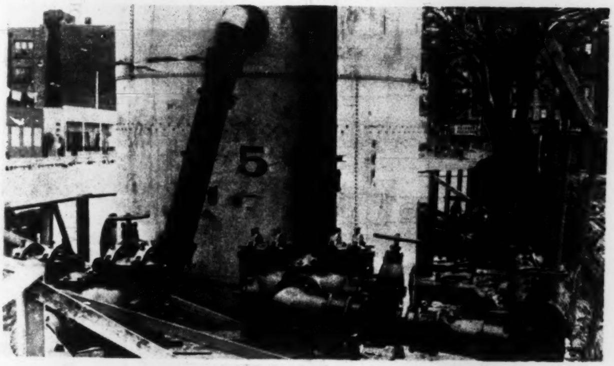

FIG. 9.—GIANT FILTERS AT SURGE TANK

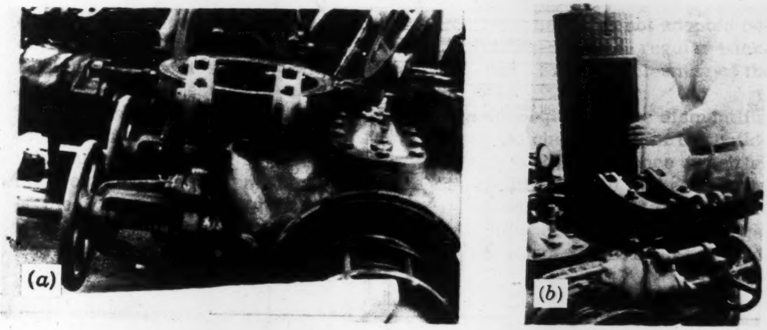

FIG. 10.—GIANT FILTER

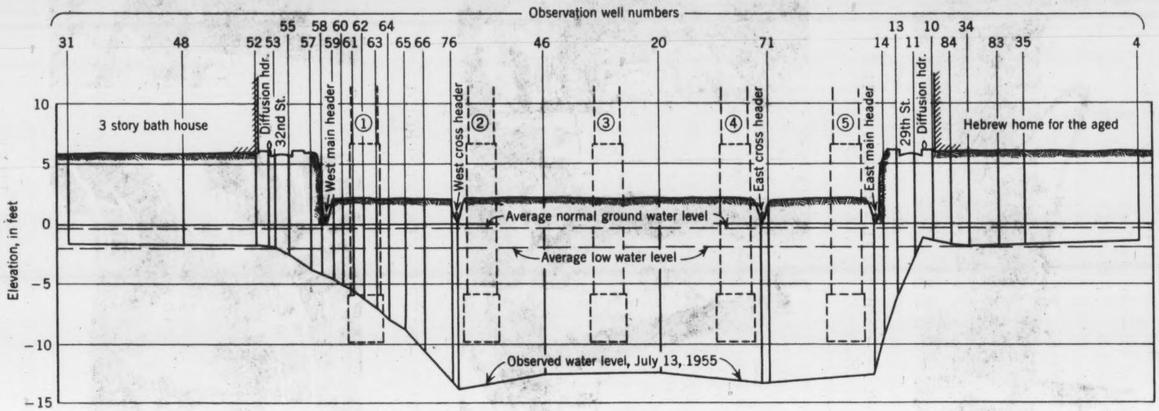

FIG. 11.—MAXIMUM DRAWDOWN AND DIFFUSION WATER LEVELS DURING FOUNDATION INSTALLATION

The full system shown in Fig. 1 was operated between late June through September, and the foundations of the five buildings constructed were installed during this period. While a maximum drawdown to el -12.5 over the entire site was not required at any one time, this drawdown was maintained over a major part of the area during the later stages when work on four of the foundations was being carried out simultaneously. The drawdown curve for this period is shown in Fig. 11. Note the normal levels maintained outside the limits of the site. An aerial view of the site showing each of the several building foundations in varying stages of construction during pumping is shown in Fig. 12.

While the final diffusion system provided the protection needed under the existing adjacent structures it was not completely devoid of operating difficulties because, after a limited period of operation, new gelatinous substances began to again collect at the filters. In spite of the fact that chemical and biochemical analyses of the material indicated the possibility of a multiplication of bacteria in the system, antibacteriological treatment was not adopted because of the limited period of operation remaining; instead, regular backflushing of the diffusion wells was carried out. Frequent cleaning of the filters also was required.

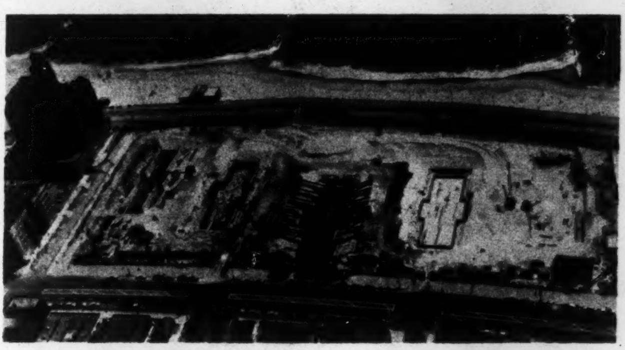

FIG. 12.—BUILDING SITE

After the completion of the foundations, and subsequent to the dismantling of the diffusion and dewatering systems, a detailed check of all of the buildings surrounding the site was again made; this showed no evidence of settlement or movement and no damage to the buildings attributable to the lowering of the water table. During and subsequent to the construction of these buildings, settlement observations were carried out on each of the five buildings. The settlements have been noted to be within the predicted limits computed.

CONCLUSIONS

The diffusion system described is believed to be the first of its type to be developed. While it definitely served its purpose and shows great promise of providing a valuable and practical solution to problems of a similar nature, in any specific case, the soil and ground water conditions must first be adequately determined before its applicability can be established.

ACKNOWLEDGMENTS

The dewatering and recharging operations described in this paper were carried out at the site of Coney Island Houses of the NYCHA and the observations reported on were obtained by the NYCHA staff on the project. Moran, Proctor, Mueser, and Rutledge, Consulting Engineers, advised the NYCHA on all phases of the foundation work and provided field supervision during the dewatering and diffusion operations. Structural engineers were Di Stasio and Van Buren. The design and installation of the dewatering and diffusion systems was carried out by the Griffin Wellpoint Corp.